A Colour Atlas of

HAEMATOLOGICAL CYTOLOGY

Second Edition

F.G.J. HAYHOE • R.J. FLEMANS

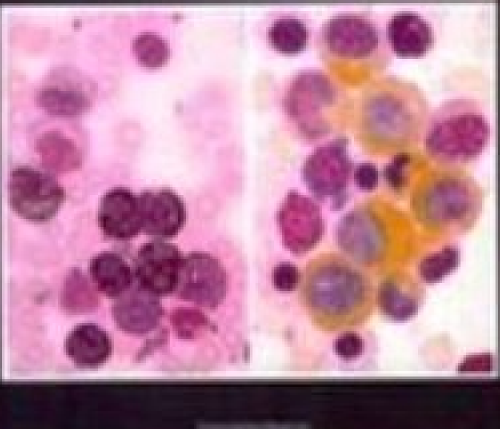

Contents

Part 1

The red cells and their precursors

Normal forms and abnormal variants

The nomenclature of red-cell precursors is confusing. The earliest recognizable member of the red-cell series, the proerythroblast, has the cytoplasmic basophilia, the nucleolated and moderately leptochromatic nucleus and the large cell size generally characteristic of primitive cells. It gives rise to a sequence of nucleated cells, the erythroblasts, which progressively develop increasingly pachychromatic nuclei, lose their nucleoli and their cytoplasmic basophilia and acquire a rising haemoglobin content. This sequence is subject to an arbitrary division into stages, the commonest division being into three:

1. The basophilic or early erythroblast, or normoblast A
2. The polychromatic or intermediate erythroblast, or normoblast B
3. The orthochromatic or late erythroblast, or normoblast C.

There are objections to the use of many of these terms, but they are all so firmly entrenched in common usage that they must be accepted. When authors use different or more elaborate staging and nomenclature they usually define their terminology, but those who use any of the synonyms above expect them to be understood without further explanation.

The proerythroblast is not itself the functional stem cell serving as a self-maintaining progenitor of the normoblast series, but is derived from an earlier functional myeloid stem cell of unidentified morphology, having pluripotential capacity for giving rise to cells of erythroid, granulocytic, monocytic and megakaryocyte-platelet lines.

Kinetic studies with radio-isotopically labelled cells suggest that four cell cycles culminating in mitoses occur during development from proerythroblast to late normoblast, three at the proerythroblast and early basophilic normoblast stages, and the last at the polychromatic intermediate normoblast stage. Nests of erythroblasts of different stages of maturity commonly occur in apposition around a centrally situated reticulo-endothelial cell. Transfer of iron may be effected in one or other direction, and the central macrophage is often rich in stainable free iron. Late normoblasts do not undergo a further cell cycle but lose their nuclei by extrusion and give rise to marrow reticulocytes.

Reticulocytes spend up to two days in the bone marrow before being released into the peripheral blood. There they make up normally less than 1% of the red-cell population and within another one to two days lose the remnants of cytoplasmic basophilia which give them their characteristic staining properties, and become orthochromatic mature red cells.

Mature red cells survive some 120 days before destruction. They are normally circular and fairly uniform in diameter, but are readily distorted by external pressure, as from neighbouring cells in a smear. Their structure as biconcave discs leads to weaker eosinophil staining at the centre than at the periphery, a feature which is least prominent at the tail of a blood smear where the cells are most spread out and flattened. In the body of the smear it becomes more conspicuous and this normal phenomenon must be appreciated and distinguished from hypochromia.

Abnormal variants: nucleated precursors

The chief cytological variants involving alteration in morphology rather than numbers or relative proportions of erythroblasts are as follows:

Macronormoblasts. Cells having the general nuclear and cytoplasmic morphology of normoblasts but an increased average cell diameter. They occur especially in states of active erythroblastic hyperplasia without haematinic defects, such as haemolytic anaemias, but may be seen also in the early stages of disorders that subsequently become megaloblastic.

Megaloblasts. The essential morphological change in megaloblasts as compared with normoblasts lies in the more open chromatin pattern of the nucleus at all stages of development. There is often a degree of haemoglobinization of the cytoplasm which appears excessive for the state of nuclear maturation, and later megaloblasts may appear fully orthochromic. Megaloblasts are larger than normoblasts of comparable maturity. They may show mitotic irregularities, with multipolar mitoses, sometimes asymmetrical, producing unequal daughter cells. Cytokinesis may not occur and giant cells with two or more nuclei, sometimes unequal in size, result. Chromosomes or fragments of chromatin may become separated from the spindle and constitute

accessory small nuclear masses. These 'Howell-Jolly bodies' may remain in the red cells after the main bulk of nuclear material has been extruded. Rosette formation, with several chromatin masses linked by bridges, may follow a halt of the mitotic process in metaphase.

Megaloblasts are present in the marrow in states of B_{12} and folic acid deficiency, the commonest of which are Addisonian pernicious anaemia and conditions of gastro-intestinal malabsorption due either to disease or to gastric or intestinal resections. The folic acid deficiency of pregnancy may lead to megaloblastic anaemia. Megaloblasts are seen also in some cases of refractory sideroblastic anaemia and in erythraemic myelosis. They may be seen in acute leukaemias, especially following treatment with antimetabolites.

Micronormoblasts. Small normoblasts with a tendency to ragged cytoplasmic outline and irregular staining are found in states of iron deficiency. The changes are most evident in intermediate and late normoblasts, which also show defective haemoglobinization.

Sideroblasts. Normoblasts containing free, non-haemoglobin, iron are best detected by the use of Prussian blue staining, but occasionally coarse accumulations of free iron may be visible in Romanowsky preparations.

Bizarre cytological variants. Gross mitotic and nuclear abnormalities, of the same kind as described under megaloblasts but much more extreme in degree, occur in erythraemic myelosis.

Reticulocytes

Blood normally contains less than 1% of reticulocytes and an increase in numbers indicates a heightened output of young red cells from the bone marrow. This may occur during the correction by increased marrow activity of any anaemic state, whether spontaneously (as after an acute haemorrhage) or following treatment (as in pernicious anaemia after B_{12} or iron deficiency anaemia after iron). Reticulocytosis is especially prominent in haemolytic anaemias, where great erythropoietic activity attempts to compensate for the shortened life span of peripheral erythrocytes.

In Romanowsky preparations reticulocytes may sometimes be detected as polychromatic cells, with a blue or purple tinge, or much less often may show a scattering of fine blue 'basophilic stipples'. They are best recognized, however, by the use of supravital staining with brilliant cresyl blue, which reveals a network of fine filaments and dots. Reticulocytes are often a little larger in diameter than mature red cells.

Mature red cells

Red cells may differ from normal in their appearance in stained films by variations in size (anisocytosis, microcytosis, macrocytosis), in shape (poikilocytosis, elliptocytosis, sickle cell formation, crescent formation, crenation) and in depth of staining (hypochromia, anisochromia, spherocytosis, target cell formation). They may also undergo fragmentation (schistocytosis) or contain abnormal inclusions, such as the residual chromatin material of the Howell-Jolly bodies.

All these abnormalities may be seen in varying degree and frequency and several of them may occur together in the same smear.

Disorders involving chiefly the red-cell series, and their associated main cytological features

Megaloblastic anaemias. These disorders are characterized by striking erythroblastic abnormalities arising from deficiencies of either vitamin B_{12} or folic acid. The underlying biochemical defect involves a slowing of DNA synthesis in the S phase of the cell cycle, due principally to defective formation of thymidylate, which is normally dependent on both B_{12} and folate as cofactors in its synthesis. Nuclear division is thus retarded, and the pattern of nuclear chromatin disposition and nuclear–cytoplasmic synchronization in development is affected, with the results illustrated in **39–69**. In fact, the changes of megaloblastosis, with increase in cell size and opening of the nuclear chromatin network, are detectable in most proliferating cells, such as those of the gut mucosa, and including granulocyte and platelet precursors in the bone marrow.

The findings in bone marrow aspirates and biopsies include high cellularity, the hyperplasia involving mainly the red-cell series, with myeloid–erythroid (M:E) ratio commonly 1:1 or even 1:2 – compared with the normal range of 5–20:1. There is a shift to the left in red-cell precursors, with an increased proportion of large proerythroblasts and early basophilic erythroblasts, numerous mitotic figures – often showing Howell-Jolly bodies – and the typical premature haemoglobinization best seen in intermediate erythroblasts. Giant myelocytes and metamyelocytes can be found, as can multinucleated polymorphs (**74**), and parallel changes involving asynchrony of nuclear–cytoplasmic maturation, with granular cytoplasm and relatively primitive nuclear structure, sometimes in mitosis, occur in promegakaryocytes, while nuclear hypersegmentation may be conspicuous in mature megakaryocytes. Macrophages usually show an increased load of haemosiderin, with the fast turnover pattern of small particles, resulting from the considerable component of ineffective erythropoiesis and consequent intramedullary breakdown of non-viable red-cell precursors.

The peripheral blood findings include a more or less severe anaemia with normochromic but markedly macrocytic erythrocytes, the mean cell volume (MCV) usually exceeding 115 femtolitres (fl) and reaching as high as 150fl. The mean cell haemoglobin (MCH) is raised above 32 picograms (pg), but the mean cell haemoglobin concentration (MCHC) is normal, not over 36%. Anisocytosis and poikilocytosis appear early in the course of the anaemia and become increasingly severe, large ovalocytes being particularly characteristic, but other shapes, including tear-drop poikilocytes, may also be seen (**70–73**). The red cells may occasionally show basophilic stippling (**126**) and Howell-Jolly nuclear fragments (**146**), but reticulocytes are not usually increased and may be depressed. As the anaemia

progresses, occasional late erythroblasts with residual megaloblastic features appear in the circulation.

Leucopenia around $2–4\times10^9/1$ is usual in megaloblastic anaemias, perhaps especially in pernicious anaemia, with neutropenia and a relative lymphocytosis. The neutrophils show a shift to the right with increased nuclear lobulation, most cells having four lobes and some hypersegmented cells having five or six. Neutrophils may also manifest cellular gigantism – these exceptionally large cells are known as macropolycytes. Platelets may be present in normal numbers, but thrombocytopenia is more common and is sometimes severe, while giant platelets and occasional megakaryocyte fragments provide further evidence of megaloblastic dysthrombopoiesis.

Haemolytic anaemias. Excessive destruction of red cells arises from two very broad groups of causes, intrinsic and extrinsic. In the first group are defects of the cell constitution, ranging from hereditary spherocytosis (HS), enzyme defects such as pyruvate kinase (PK) and glucose-6-phosphate dehydrogenase (G6PD) deficiencies, and paroxysmal nocturnal haemoglobinuria (PNH), to haemoglobinopathies such as the thalassaemias and sickle cell disease. The second group includes acquired auto-immune haemolytic anaemias (AIHA) due to warm lytic antibodies active at the red-cell surface; cold haemagglutinin disease (CHAD) due to high titre agglutinating antibodies, usually with anti-I specificity; and haemolysis secondary to toxins, foreign antibodies as in mismatched transfusions, and circulatory impediments such as occur in microangiopathy, thrombotic thrombocytopenic purpura (TTP), renal glomerular disease, disseminated intravascular coagulation (DIC) and artificial vascular prostheses.

All these conditions share features in common, arising from the increased breakdown of red cells, with resulting raised levels of serum bilirubin and disappearance of haptoglobins, and attempts at compensatory marrow erythropoietic hyperplasia, with normoblastic proliferation, a reduced M:E ratio, and an outpouring of reticulocytes, sometimes accompanied by late normoblasts, into the peripheral blood. The intense normoblastic hyperplasia, with obliteration of fat spaces and 100% cellularity in trephine sections, from a severe haemolytic anaemia due to PK deficiency, is shown in **19** and **20**, and a less marked but substantial erythroid component in sections from a case of AIHA secondary to non-Hodgkin's lymphoma (NHL) is shown in **21** and **22**.

The anaemia of haemolytic disease is usually normochromic and neither macrocytic nor microcytic, although anisocytosis and poikilocytosis are common. Neutrophil leucocytosis may be seen, especially in acute haemolytic reactions, but the count is often normal. Apart from the acquired haemolytic processes associated with microangiopathy, TTP and DIC, where there is severe thrombocytopenia, platelet levels show no consistent trend. The chief morphological findings of differential diagnostic value among this wide range of diseases are therefore to be found in the circulating erythrocytes themselves, although they are rarely pathognomonic and need confirmation or supplementation by appropriate immunological studies, enzymology, or haemoglobin electrophoresis, as the case may be. Nevertheless, red-cell morphology can offer some useful pointers.

Spherocytes (**135–137**), apparent in stained blood smears as small, deeply stained red cells, are always present in HS and commonly detectable in AIHA.

Elliptocytes (**138**) forming more than 5% of the red-cell population are virtually confined to hereditary elliptocytosis, but a few markedly oval or cigar-shaped red cells may be found whenever gross anisocytosis is present, as in severe megaloblastic or iron deficiency anaemia and in thalassaemia, and a localized elliptocytotic appearance may be produced in some areas of a smear as a spreading artefact (**139**).

Echinocytes or 'burr cells', erythrocytes with numerous surface undulations or spicules (**141**), may be produced by exposure of normal 'discocytes' to an alkaline pH or to various echinocytogenic factors such as bile acids, lysolecithins and fatty acids. Although the change is reversible, it is associated with a tendency to sphering and subsequent haemolysis. In pathological states, echinocytes occur especially in uraemia, chronic liver disease, and acutely in severe burns and toxic infections.

Acanthocytes or 'spur cells', erythrocytes with sharp spiny irregular projections (**143**), are also associated with a haemolytic tendency, and occur in hereditary acanthocytosis or congenital abetalipoproteinaemia, and may develop in liver disease or after splenectomy.

Stomatocytes, cup-shaped erythrocytes which in stained smears show an elongated slit of central pallor instead of the normal circular area (**128** and **158**), are found conspicuously in hereditary stomatocytosis, and not infrequently in haemolytic anaemias with altered membrane permeability. A few may usually be found in normal blood smears, and their numbers may be increased in hepatic cirrhosis and in many generalized neoplastic states.

Drepanocytes or sickle cells (**155**) are characteristic of haemoglobin S disease, being produced by the crystallization of reduced HbS within the cell.

Codocytes or target cells, bell-shaped erythrocytes with a striking target appearance in stained smears (**150**, **151** and **153**), are especially prominent in thalassaemia, but are found also in other haemoglobinopathies, such as HbC and HbSC disease.

Leptocytes, or thin flat erythrocytes (**150**), occur in the same conditions as target cells, and also in liver or gall bladder disease with biliary obstruction, and after splenectomy.

Schistocytes, red cells with irregularly fragmented shapes due mostly to mechanical damage (**134**, **152**, **163** and **164**), are found especially in microangiopathic haemolytic anaemia and the related states of DIC, TTP and microvascular nephropathy.

Heinz bodies (**160**) may be demonstrable in the red cells in supravitally stained preparations of blood from patients with haemolytic anaemias due to G6PD deficiency, unstable haemoglobins, chemical damage or thalassaemia. They are sometimes removed by the spleen and therefore are particularly conspicuous after splenectomy.

Haemoglobin H inclusions, which stain with supravital cresyl blue after prolonged exposure (**162**), are found in the red cells of alpha-thalassaemia.

Apart from these various pointers, the differential diagnosis between haemolytic disorders is not greatly assisted by morphological features present in the peripheral blood, and the only contributory differential finding in the bone marrow, where normoblastic or macronormoblastic hyperplasia is the common rule, is the existence of strong periodic acid-Schiff (PAS) positivity in the erythroblasts of beta-thalassaemia major and to a lesser extent in those of beta-thalassaemia minor. Other haemolytic states only rarely show any erythroblastic PAS positivity, although this was a feature of foetal haemolytic disease, now fortunately preventable and therefore uncommon where there are adequate medical services.

Aplastic and hypoplastic anaemias. Despite the titular emphasis on anaemia, these diseases are usually pancytopenias, with accompanying neutropenia and thrombocytopenia, all becoming progressively more severe as the disease advances, and associated with failure of myelopoiesis. The bone marrow is poorly cellular, with a predominance of fatty spaces and a reactive or inflammatory infiltrate ranging from a few residual islands of lymphocytes and plasma cells to widespread diffuse lymphoplasmacytosis. Marrow aspirates are generally acellular, and firm diagnosis requires trephine biopsy. Typical appearances at different stages of disease are shown in **24–27**.

The anaemia itself is usually normocytic and normochromic with little anisocytosis or poikilocytosis, and reticulocytes are scanty.

Pure red-cell aplasia, without concomitant decrease of granulocytes and platelets, and with a cellular marrow devoid of red-cell precursors, occurs only rarely.

Primary and secondary polycythaemias. Polycythaemia rubra vera (PRV) or primary proliferative polycythaemia is characterized by high haemoglobin, haematocrit and red-cell count, a raised red-cell mass, normal arterial oxygen saturation, commonly significant splenomegaly, and usually elevated total leucocyte and platelet counts. It is thus a pancytosis, and the high peripheral blood figures reflect a chronic neoplastic myeloproliferative state involving all cell series in the bone marrow (**28** and **29**), where fat spaces are much reduced in trephine sections and trilineage hyperplasia may approach 100% cellularity. Cytogenetic studies in the stable phase of PRV reveal non-random chromosomal abnormalities in many patients, trisomy 8, trisomy 9, 5q– and, especially, 20q– being the most common, thus confirming the clonal neoplastic nature of the disease. Morphologically, there are few changes from normal, with erythropoiesis normoblastic and erythrocytes normochromic and normocytic, and with both granulopoiesis and thrombopoiesis regular and cytologically typical, apart from an occasional increase in basophils and a few giant platelets, at least during the main course of the disease. The one abnormal cytochemical feature almost invariably found is a raised leucocyte alkaline phosphatase (LAP) score.

A late transition to a myelofibrotic state occurs in around 15–20% of PRV cases, and when this change takes place the marrow sections show, of course, increasing reticulin and fibrosis (as in **30**), and the peripheral red cells manifest anisocytosis and teardrop poikilocytosis. Terminal transformation to a preleukaemic myelodysplastic state or to frank acute myeloid leukaemia (AML) may also occur.

Secondary polycythaemia or erythraemia resembles PRV in having raised haemoglobin, haematocrit, erythrocyte count and red-cell mass, but differs in the absence of leucocytosis and thrombocytosis, and, when due to chronic cardiovascular or pulmonary disease, in showing decreased arterial oxygen saturation. Morphologically, erythroid hyperplasia predominates in the bone marrow, without parallel increase in other lineages, and the overall cellularity of sections is generally less marked than in PRV, as exemplified in **23**.

Congenital dyserythropoietic anaemias (CDAs). This group of relatively uncommon disorders is of particular interest to the cytologist because the dyserythropoietic abnormalities manifest in the erythroblasts are so striking and bizarre. There are three main varieties of CDA. Type I affects the later basophilic and intermediate erythroblasts predominantly, with megaloblastoid features and spongy chromatin patterns sometimes giving an appearance of irregularity in the nuclear membranes, and with occasional internuclear chromatin bridges. Type II, the commonest form, affects later erythroblasts especially, with conspicuous multinuclearity and with double nuclear membranes seen by electron microscopy. In this type of CDA the erythrocytes are susceptible to haemolysis in an acid medium, hence the alternative name, HEMPAS – hereditary erythroblastic multinuclearity with positive acidified serum test. Type III is characterized by giant erythroblasts, up to 70 microns in diameter, with either numerous separated nuclei or a single multiploid lobulated nucleus.

Examples of all these variants of CDA and their main cytological and cytochemical features are illustrated in **78–88**.

Erythraemic myelosis and erythroleukaemia. Although an acute neoplastic state with vast preponderance of erythroblasts has long been recognized as erythraemic myelosis or Di Guglielmo's disease, it is probable that this occurs rarely if ever as a purely monolineage disorder, but that it is almost always, if not always, a bilineage or trilineage disease from the start, with involvement to a greater or less extent of the granulocytic/monocytic line and the megakaryocytic line. The name 'erythroleukaemia' is therefore strictly more correct in all cases, although erythraemic myelosis is still commonly used for cases where the erythroid component is clearly dominant.

Cytogenetic abnormalities are found in the majority of cases, including the commonest AML alteration, trisomy 8 (8+), and defects of 5 and 7, but multiple numerical and structural aberrations are usual. The cytology of the neoplastic erythroblasts in the bone

marrow and in the blood, where they may be numerous, varies from relatively normal to grossly bizarre (**89–95**). Cytochemically, they usually show conspicuous PAS positivity (**98–102**), and often strong localized acid phosphatase reactions (**103** and **104**).

Refractory sideroblastic anaemias (RSAs). These disorders are characterized by an overload of iron in the bone marrow (**112**), and by hypercellular micronormoblastic or occasionally megalobastic erythropoiesis. Coarse siderotic granules, demonstrable by the Prussian blue stain, are found arranged in a ring around the nucleus of many erythroblasts. The appearance is most striking and involves the highest proportion of erythroblasts in cases of primary acquired RSA, a neoplastic myelodysplastic state which may transform to AML. Examples of the cytology and of ringed sideroblasts are shown in **113–116**. In hereditary RSA and in acquired cases secondary to agents such as isoniazid, cycloserine, chloramphenicol, alcohol and lead, there are generally fewer sideroblasts, and only intermediate and late erythroblasts are affected.

PAS positivity is found in a proportion of the erythroblasts in some cases of RSA, although the reaction is usually much weaker than in erythraemic erythroblasts (**118**).

Anaemia of blood loss and iron deficiency. Acute blood loss insufficient to produce cardiovascular collapse results in haemodilution and the development, over a period of 24 hours or so, of an anaemia which is normochromic and normocytic, but usually associated with some increase in reticulocytes and a parallel rise in leucocyte and platelet counts as marrow activity is stimulated.

Chronic blood loss leads to the development of iron deficiency anaemia, and is the commonest cause by far of this disorder, characterized by falling haemoglobin with initially microcytic and later hypochromic red cells with increasing central pallor and progressive anisocytosis and poikilocytosis (**132** and **133**). The red-cell indices, MCV, MCH and MCHC, all become decreased. The leucocyte count tends to be low or normal, while the platelet count is often raised. Until iron treatment is started the reticulocyte count is low and there is no peripheral polychromasia. Erythropoiesis in the bone marrow is hyperplastic, but with abnormal cytology, the erythroblasts being small, poorly haemoglobinized, and often with irregular and ragged outlines (**106** and **107**). They may contain PAS-positive material (**108**). The marrow is notably devoid of free iron whether in macrophages or extra-cellularly in particles and flecks (**111**), and there are virtually no sideroblasts or siderocytes.

These cytological features are really diagnostic, but confirmation is given by the finding of low serum iron and raised total iron-binding capacity (TIBC), with decreased saturation and a low serum ferritin level. Other microcytic hypochromic anaemias generally have clear distinguishing features; the anaemia of chronic disorders, for example, shows an increase of large-particle free iron in the marrow, decreases in both serum iron and TIBC, and normal or raised ferritin, while thalassaemia and HbC and HbSC diseases show conspicuous target cells and increased marrow iron.

Leucoerythroblastic anaemia (myelophthisic anaemia, myeloid metaplasia). This complex form of anaemia – with the appearance of both erythroblasts and granulocyte precursors in the peripheral blood, and with moderately severe anisocytosis and poikilocytosis, the latter often including dacryocytes – arises when the marrow is infiltrated with metastatic tumour cells or other foreign tissue. Megakaryocyte fragments may be seen in the blood, and platelet morphology is frequently abnormal with distorted or giant forms.

Bone marrow aspirates or trephine biopsies reveal the nature of the infiltrate. Examples of causative invasion are illustrated and described in Part 4, but the resulting red-cell morphology generally resembles that shown in **131**.

1

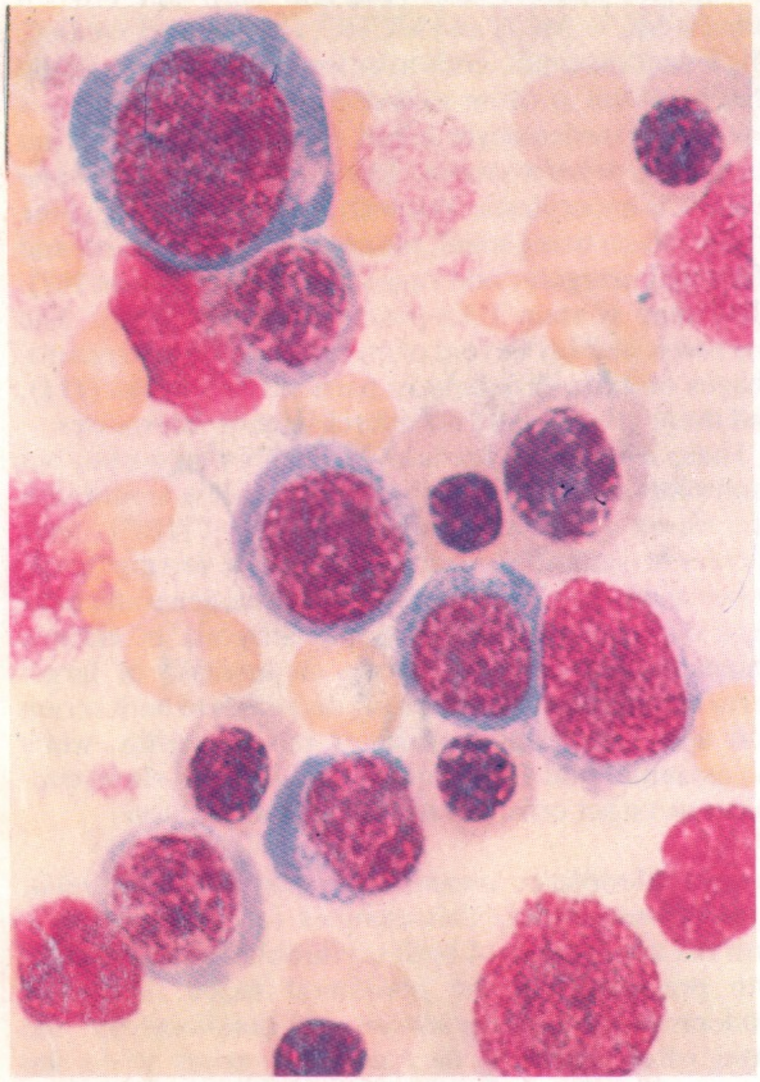

2

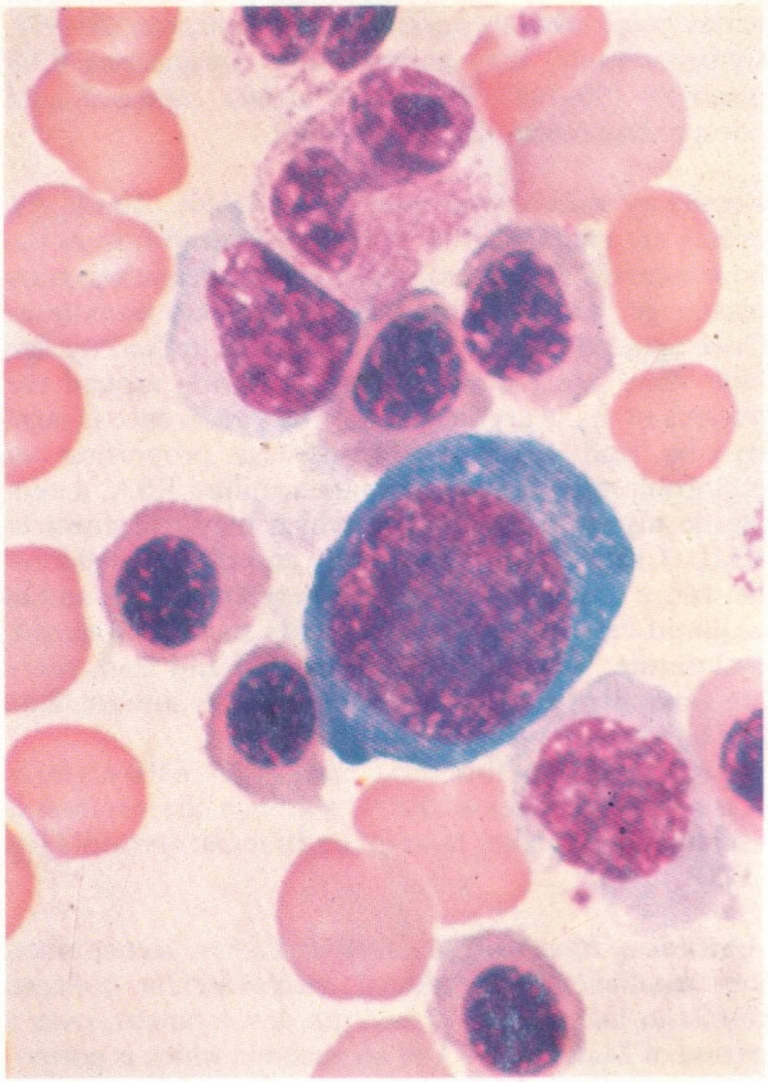

1–12. *Romanowsky stains of bone marrow aspirates.*

1. A sequence from proerythroblast through early, intermediate and late normoblasts to non-nucleated red cells. The gradual progression in nuclear and cytoplasmic maturation shown here indicates the artificial nature of the arbitrary division into stages.

2. A proerythroblast and six intermediate-to-late normoblasts. The proerythroblast has deeply basophilic cytoplasm with a paler area to one side of the nucleus, commonly seen at this cell stage, as in the proerythroblasts in **1** and **3**, and probably representing the Golgi region. The nucleus has several poorly defined nucleoli, recognizable as bluer areas in the centre. The normoblasts have pachychromatic nuclei and cytoplasmic haemoglobinization, giving a polychromatic-to-orthochromatic colour in comparison with the fully haemoglobinized and orthochromatic colour of the neighbouring erythrocytes. The field also contains two lymphocytes and an eosinophil polymorph.

3. A proerythroblast and two early normoblasts.

3

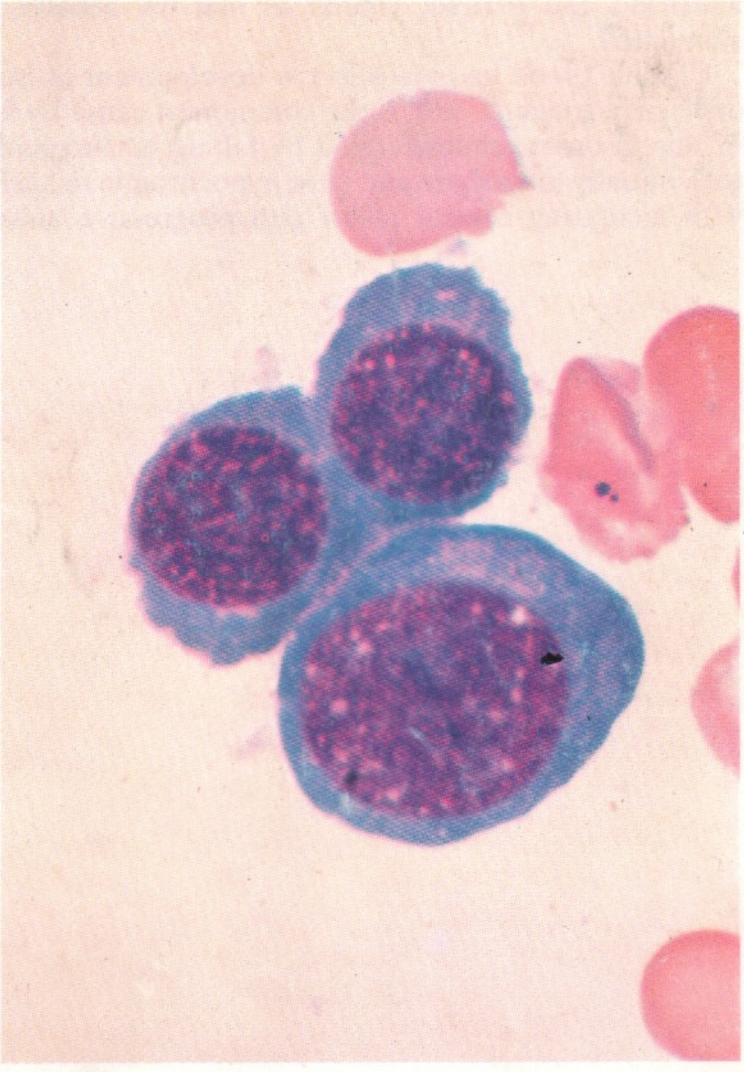

4

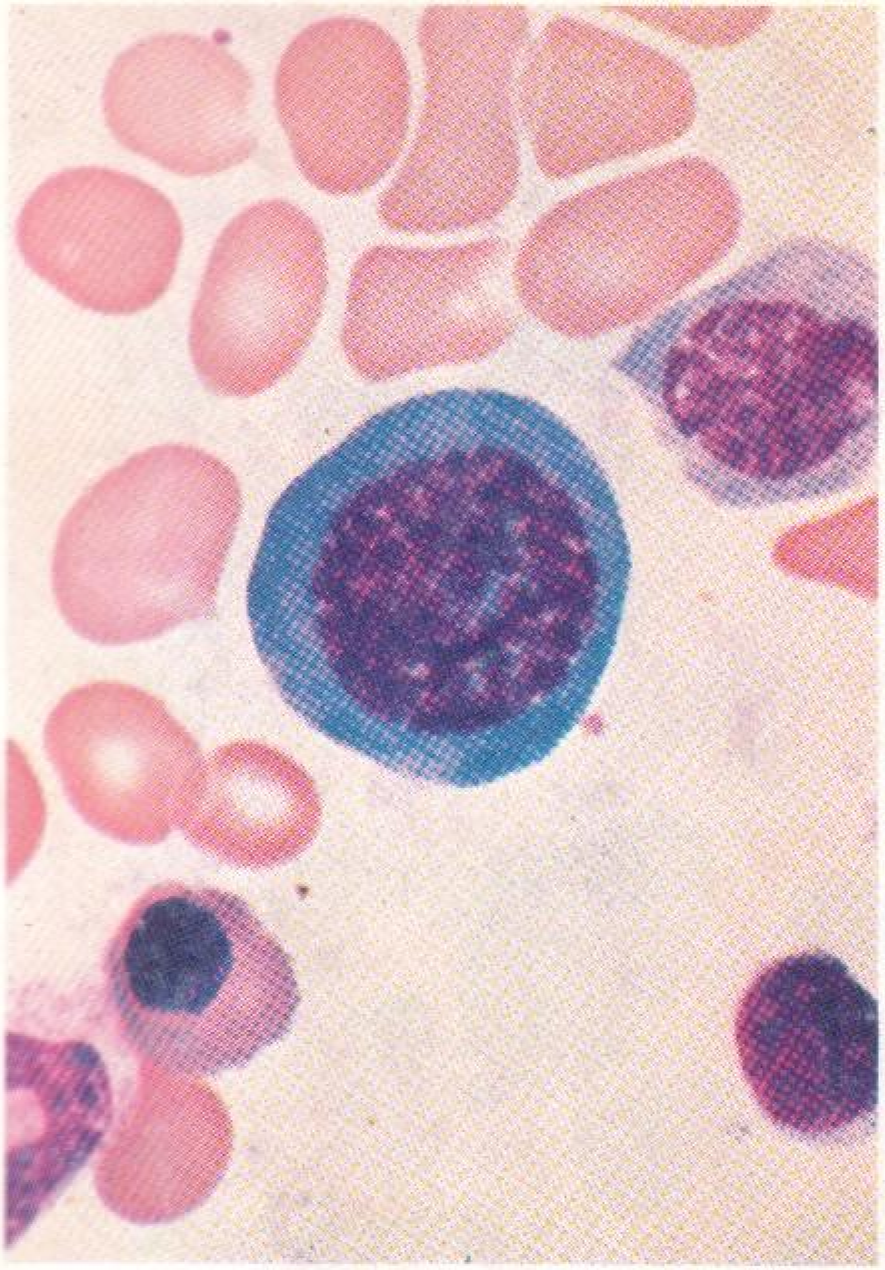

5

6

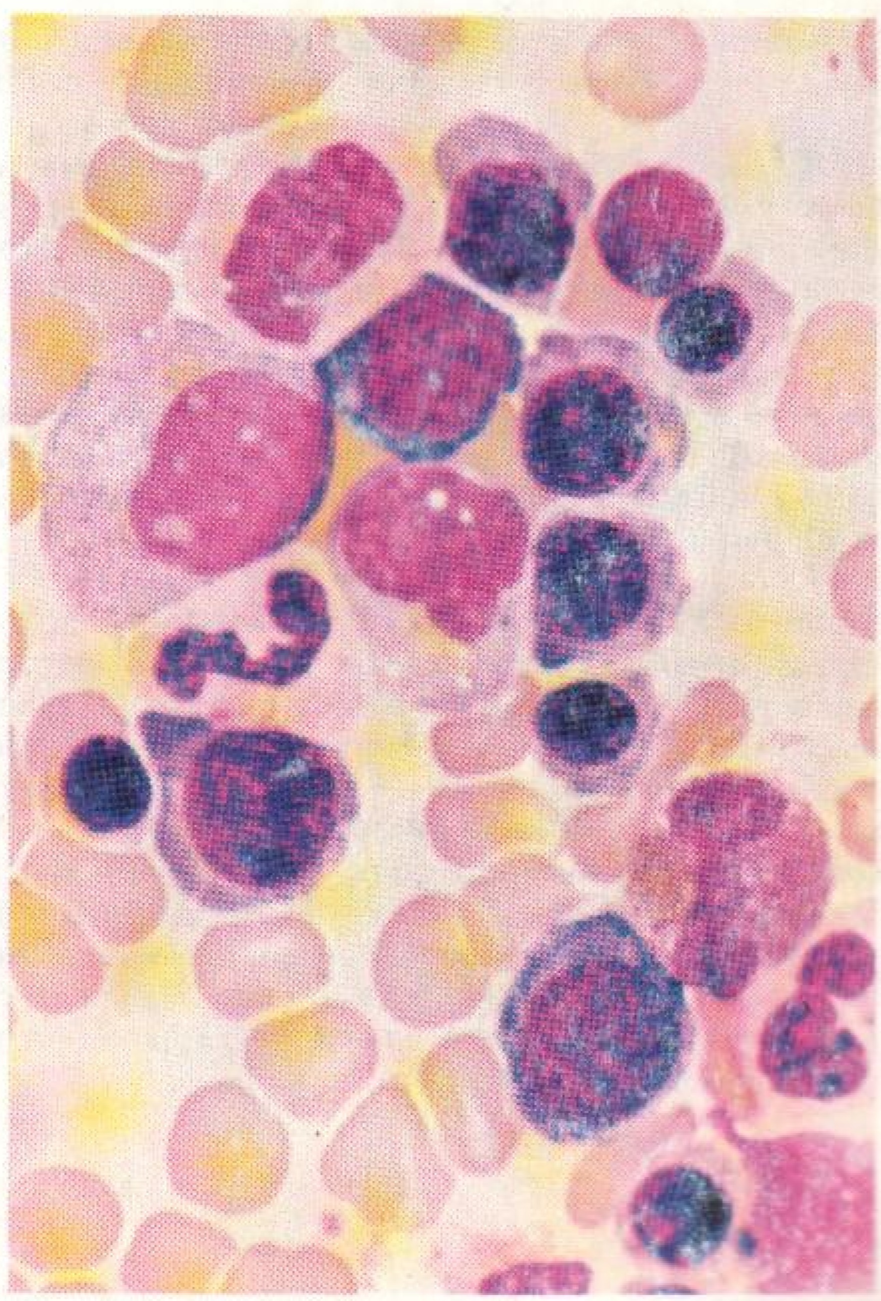

4. A proerythroblast in early prophase of mitosis. The nuclear chromatin is beginning to condense into distinct chromosomes and the integrity of the nuclear membrane is disrupting, showing areas of cytoplasm through the centre of the chromatin mass. Below are a late normoblast and a lymphocyte, and above is a cell of uncertain nature, possibly a poorly granular myelocyte.

5. A proerythroblast, a late normoblast and an early normoblast or proerythroblast in mitosis (metaphase).

6. A group of normoblasts with accompanying granulocytes for comparison. The ten normoblasts range from early basophilic to late orthochromatic stages, illustrating the reduction in size, progressive nuclear condensation and increasing cytoplasmic haemoglobinization that occur with maturation. The granulocytes include an eosinophil, two neutrophil stab cells, an early neutrophil myelocyte and two metamyelocytes. The immature granulocytes have lighter nuclei than the erythroblasts, and pale, weakly granular cytoplasm.

7

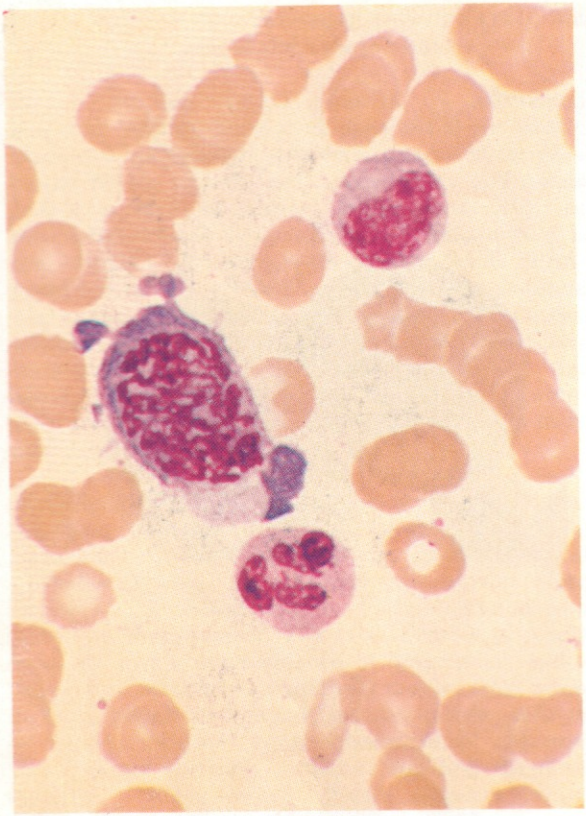

8

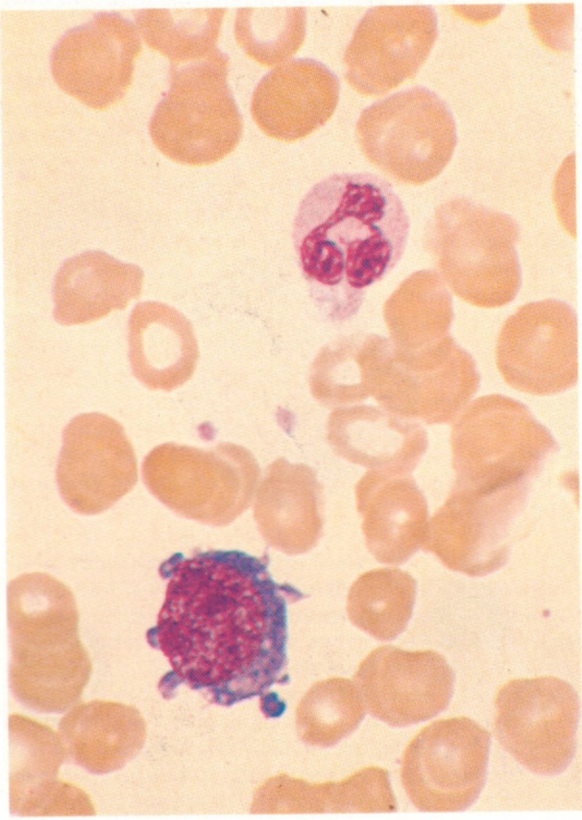

9

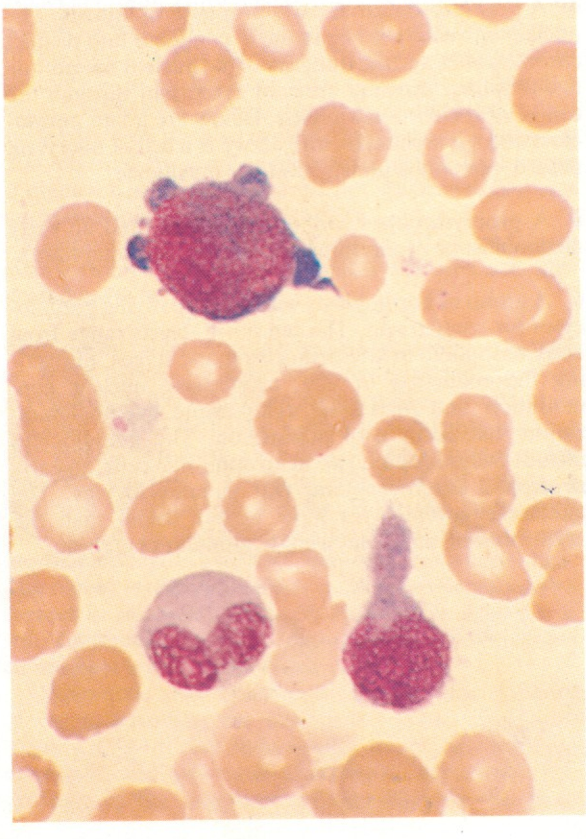

7. Another example of prophase of mitosis in a proerythroblast. There is evidence of abnormality in the irregular loss of cytoplasmic basophilia and in the separation of fragments of cytoplasm by an exaggerated process of budding or exocytosis. The mature red cells show rouleaux formation. The cell below the proerythroblast is a normal neutrophil polymorph, but the one above is a weakly granular mature neutrophil with a single nuclear lobe – an example of pseudo Pelger-Huët phenomenon – suggesting that granulopoiesis is also dysplastic. This marrow aspirate is in fact from a patient with a refractory anaemia and dysmyelopoiesis – a myelodysplastic state (MDS).

8 and **9**. Two further fields from the same marrow aspirate, both showing the dimorphic red-cell picture commonly found in MDS, with a mixture of either macrocytic or normocytic normochromic cells and microcytic hypochromic ones. Each field also contains a proerythroblast or early basophilic normoblast with conspicuous cytoplasmic budding – an exaggeration of a feature often shown less markedly by normal early red-cell precursors. In **8** there is a neutrophil with fragmenting cytoplasm, and in **9** a pseudo Pelger-Huët polymorph and an early myelocyte with a hand-mirror distortion of trailing cytoplasm.

plasma cell

10

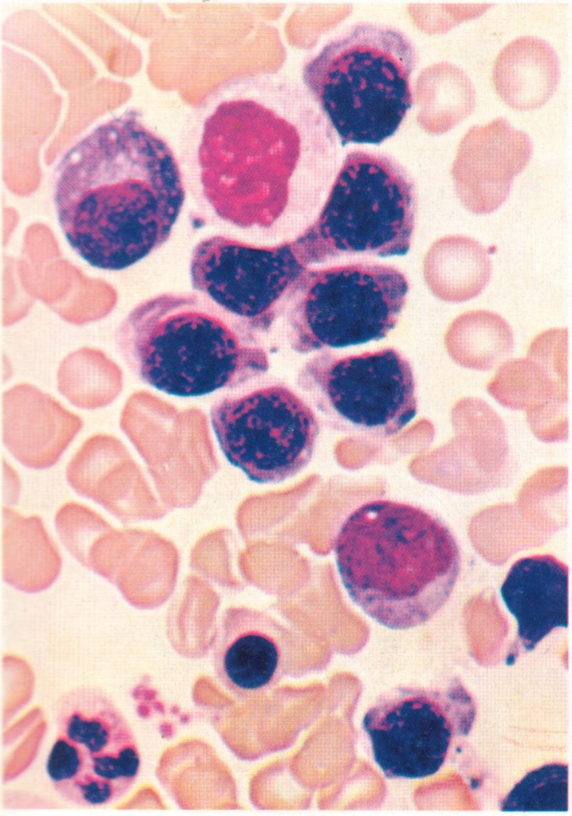

11

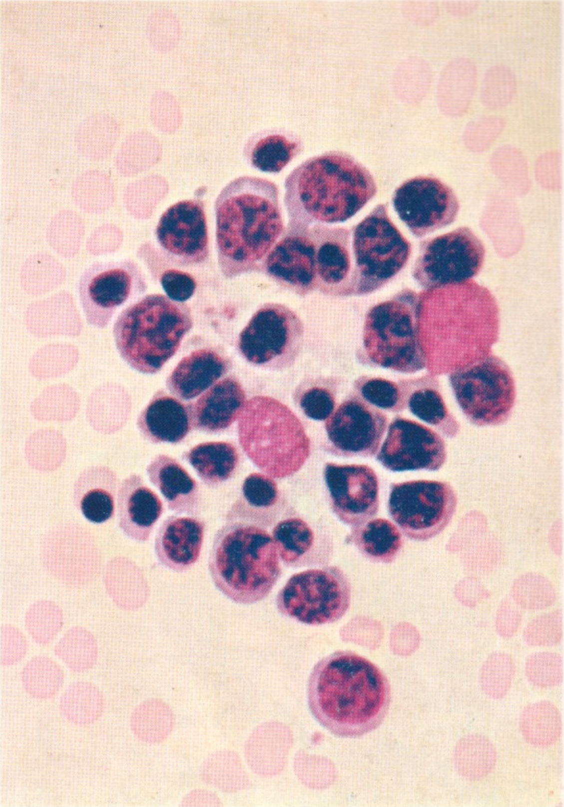

12

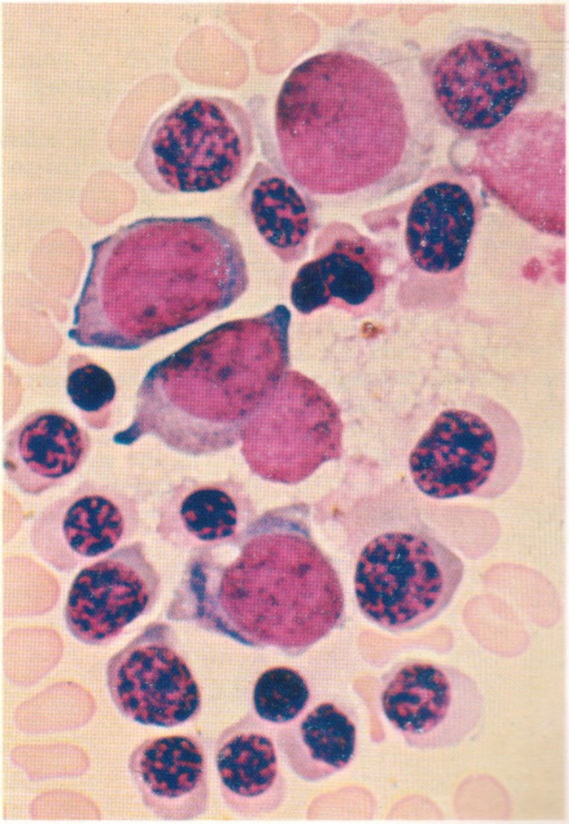

Macrophage

10. A group of normoblasts with two granulocyte precursors and a plasma cell, for comparison. The plasma cell is at the upper left of the field and differs in appearance from the early and intermediate normoblasts by the more marked eccentricity of its nucleus and the greater amount of cytoplasm. Nevertheless, these cell types may often be difficult to distinguish, since the nuclear chromatin patterns tend to be similarly coarse, and normoblast nuclei are often eccentric, as shown in **11** and **12**.

11 and **12**. Nests of normoblasts around a central macrophage. These erythroblast islands are a common feature in normal bone marrow, serving the purpose of iron exchange between the macrophage and the surrounding erythroblasts. There are probably two macrophages in the island shown in **11**, their cytoplasm being filmy and with indistinct outlines, but their nuclei recognizable in the central area and at the right-hand edge of the cell clump by their light reddish-purple staining and leptochromatic density, as compared with the purple-black colour and pachychromatic density of the normoblast nuclei. The macrophages in both these two fields contain one or two large iron particles, staining an orange colour in these Romanowsky preparations, but less grossly particulate free iron is not visible without special staining, as in **14** and **15**.

13

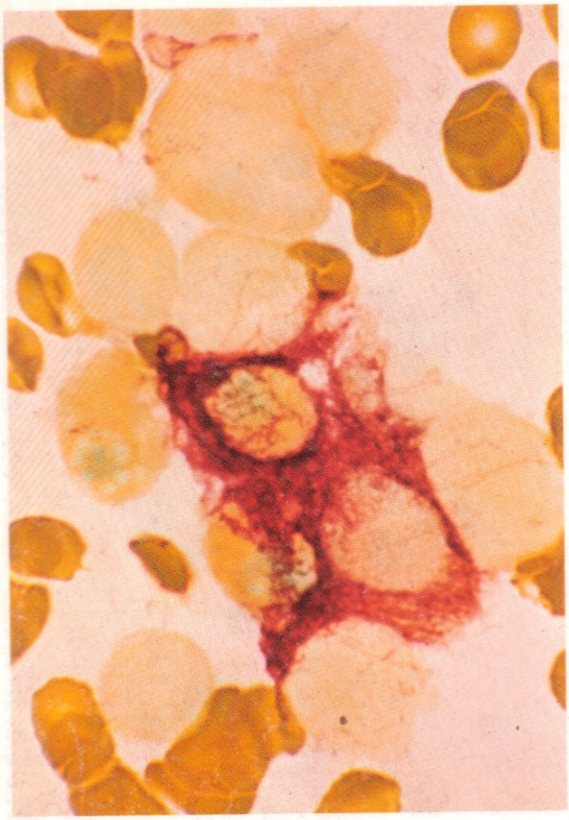

14

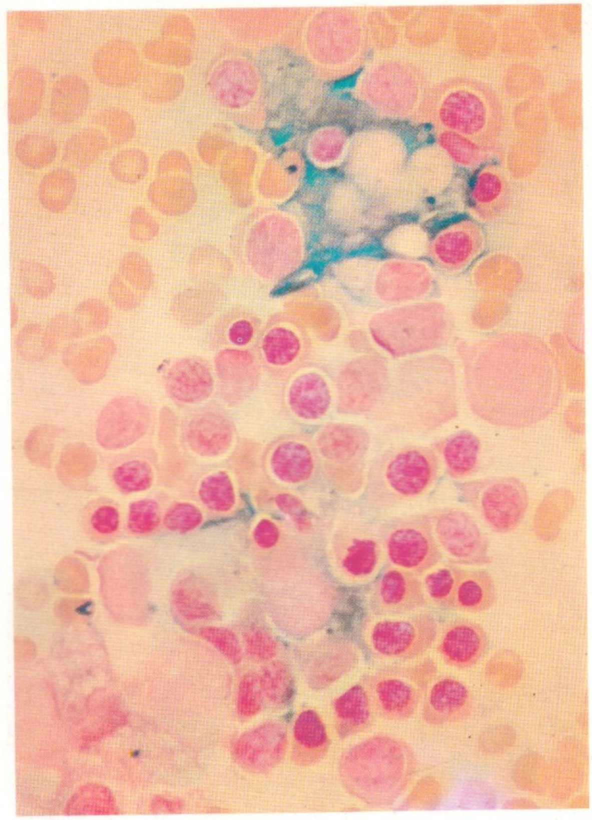

15

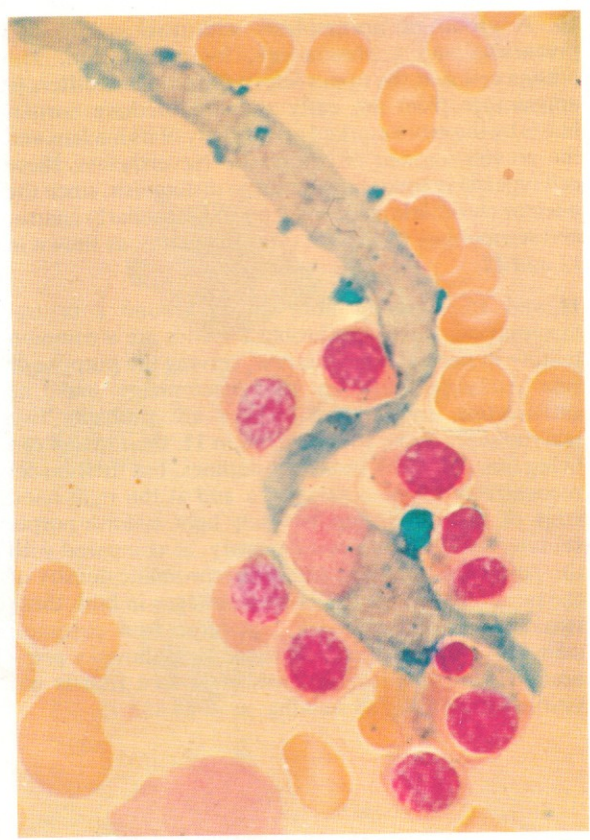

13. Normoblasts around a macrophage – alkaline phosphatase reaction. The strong positivity of the macrophage spills over to give threads of positive reaction over the surface of contiguous normoblasts.

14 and **15**. Nests of normoblasts around a central macrophage – Prussian blue stain for free iron. The iron-containing cytoplasm of the macrophage extends as a long broad tail across the field in **15**. The central macrophages often contain a few remnants of ingested cellular fragments, and in the upper island of **14** these are more striking than usual, with three or four ghost areas probably representing the sites of ingested erythrocytes, and the encircled nucleus of a late normoblast. The lower island in the same field shows the macrophage cytoplasm extending around and between the neighbouring late normoblasts, but not convincingly ingesting them. If multiple red cells and normoblasts were in fact being engulfed, the existence of the pathological state of malignant histiocytosis would have to be considered.

16

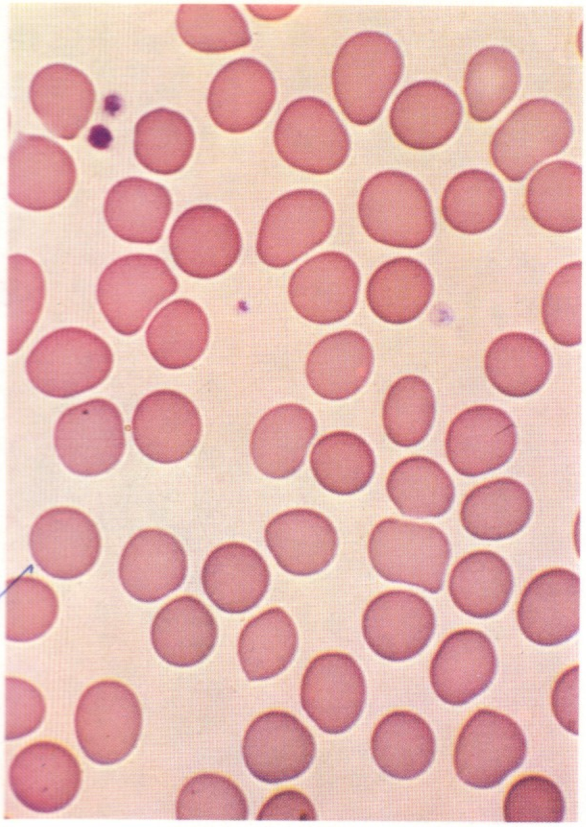

17

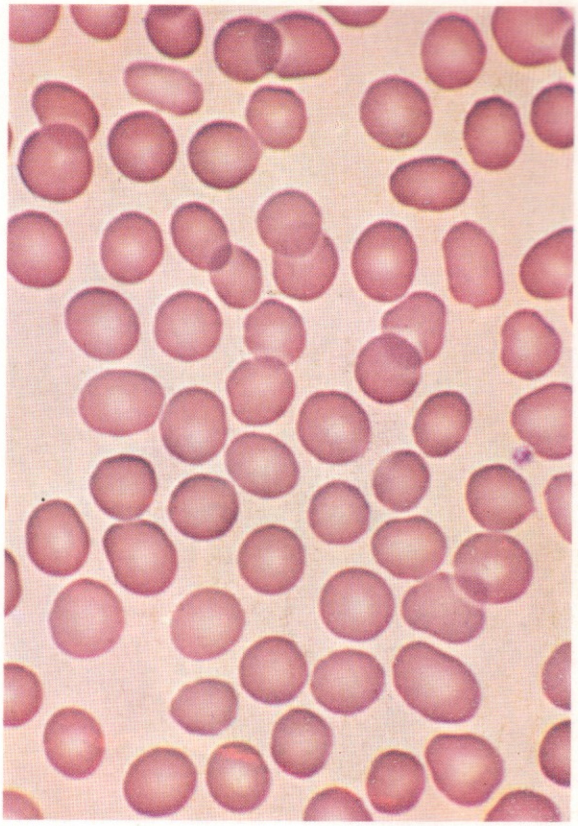

16. Normal mature red cells, from the tail of a blood smear. Minor variations in size and depth of staining are seen, together with occasional pressure distortion of shape.

17. Normal mature red cells from the body of a blood smear. There is a greater tendency here for cells to overlap one another, and the weaker staining of the central area is more evident.

18. Mixture of normal adult and cord blood red cells – Kleihauer reaction. The HbF-containing cord cells remain unlysed, while the HbA-containing adult cells show haemolysis. Acid and alkali resistance less marked than that of cord cells but greater than that of normal red cells may be shown by the red cells in hereditary persistence of HbF and in some thalassaemias.

18

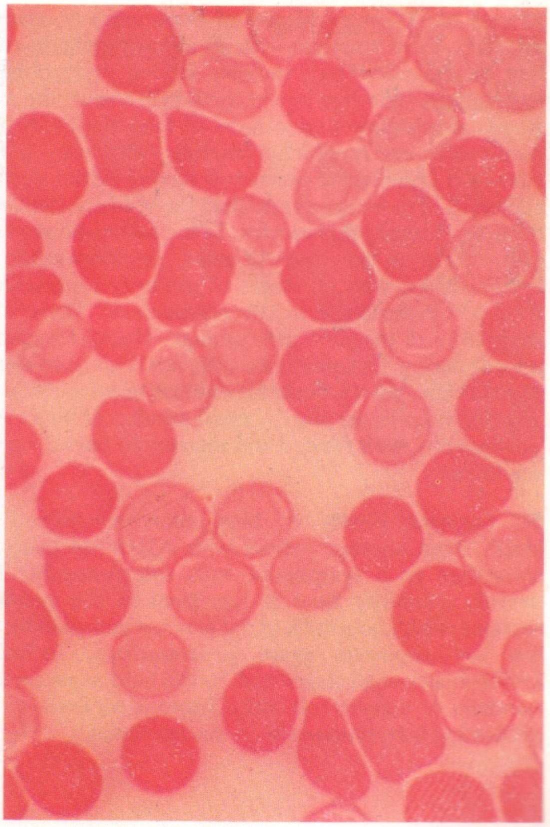

19

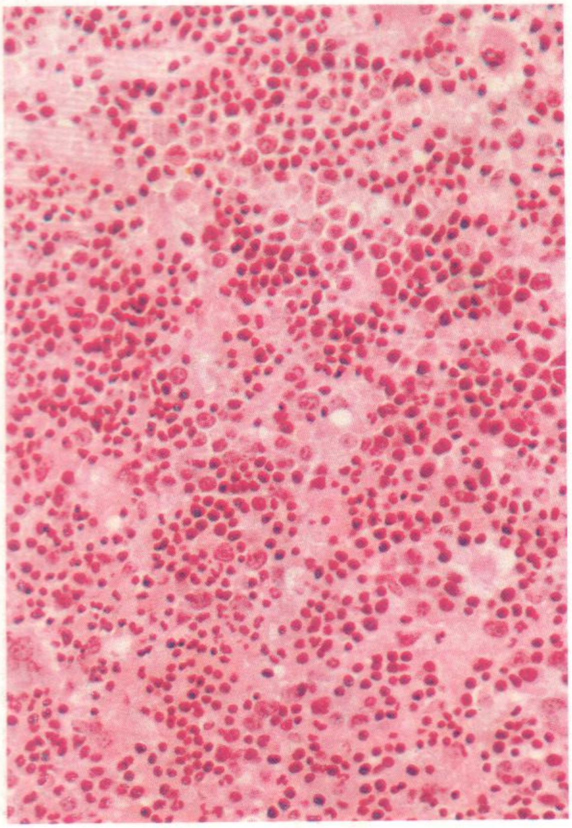

20

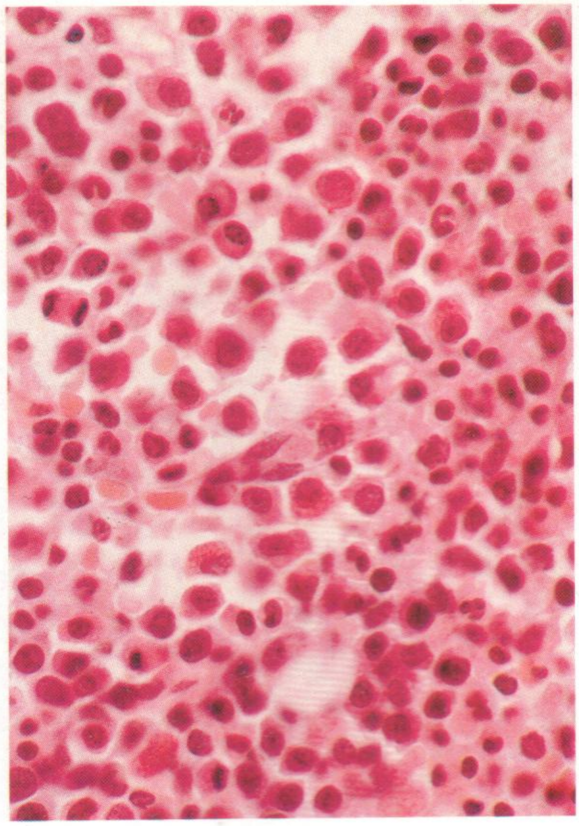

21

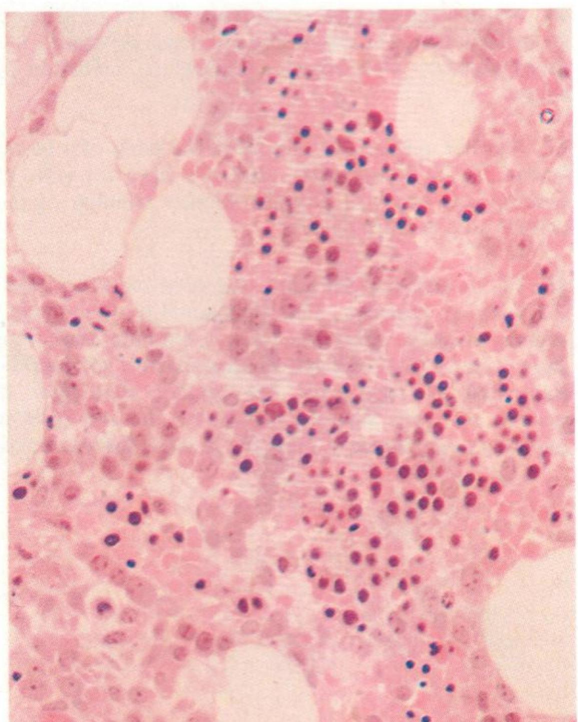

19 and **20**. Trephine biopsy of bone marrow, stained by H&E, from a patient with an auto-immune haemolytic anaemia (AIHA), showing intense erythroblastic hyperplasia. The low-power view (**19**) shows the substantially complete replacement of fatty spaces by predominantly erythropoietic marrow, with only a few clumps of granulocyte precursors having lighter nuclear staining and more cytoplasm than the erythroblasts, and three or four megakaryocytes. In the higher-power field (**20**), there is an overwhelming preponderance of erythroblasts, with all stages of maturity represented, from proerythroblasts to late normoblasts. There is no suggestion of megaloblastic change. Nuclei frequently appear eccentric, sometimes sufficiently so as to mimic plasma cells, but it is doubtful whether there are actually any plasma cells present. A small number of neutrophil polymorphs, with twisted and segmented nuclei, can be made out.

21. Trephine biopsy of bone marrow, stained by H&E, from another patient with AIHA, in this case secondary to a lymphoma with splenomegaly. The overall cellularity here is less than in the previous sections, with about 40% of the marrow occupied by fat, but erythropoiesis again predominates, including erythroblasts of all stages and, in this field, considerable numbers of mature red cells. There is no evidence of infiltrating lymphoma cells in this specimen.

22

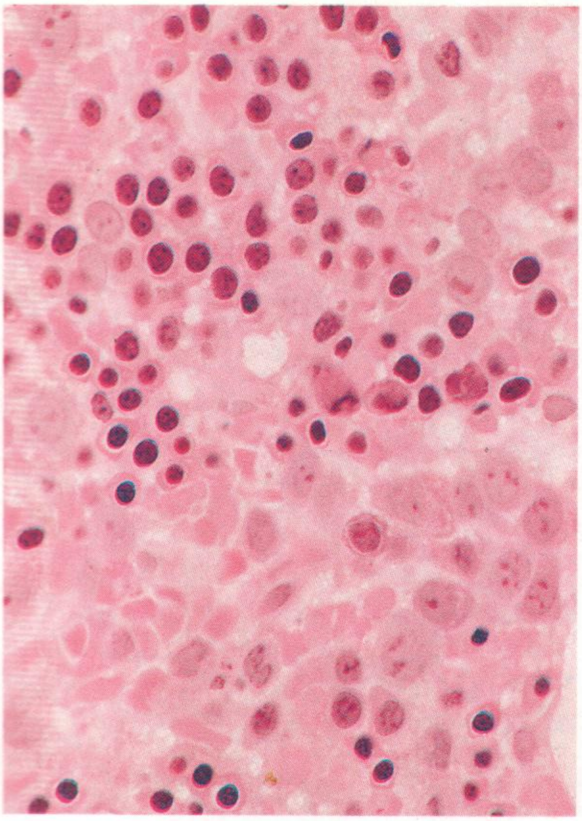

23

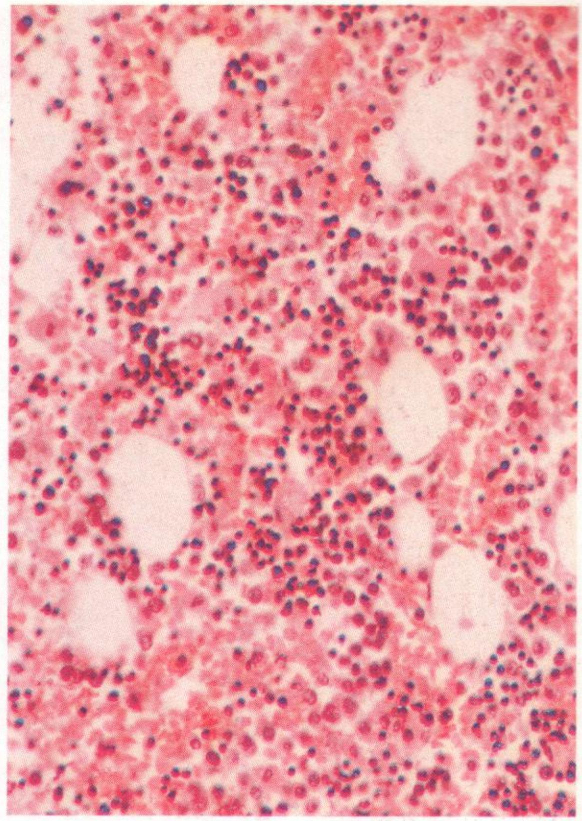

24

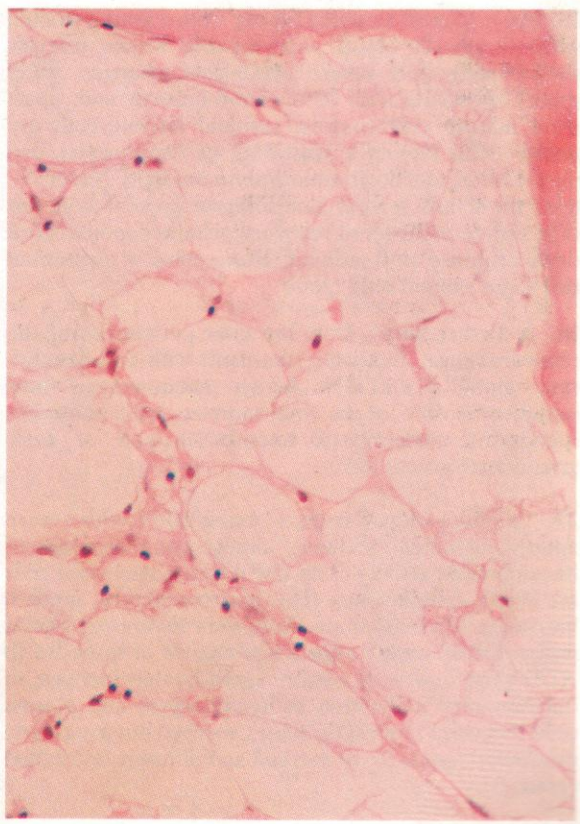

22. A higher-power view of part of the field shown in **21** where virtually all of the cells can be clearly identified as of the erythroid series. The large proerythroblasts with leptochromatic nuclei and conspicuous nucleoli are particularly well shown.

23. H&E-stained section of marrow trephine biopsy from a patient with polycythaemia (or more properly erythraemia) secondary to chronic lung disease. The marrow shows increased cellularity, with reduction in fat spaces and a predominance of erythropoiesis, and with other cell series present in reduced amount. Contrary to the usual finding in polycythaemia rubra vera (PRV), there is no increase in megakaryocytes. There is congestion of sinuses and considerable haemorrhage.

24. In complete contrast to the previous hyperplastic sections, this trephine biopsy of iliac crest marrow from a young woman with a drug-induced severe aplastic anaemia shows loss of virtually all haemopoietic tissue, with only a few residual lymphocytes distributed among the extensive fat spaces, and little to suggest any reactive or inflammatory increase in perivascular lymphocytes and plasma cells – thus grade 0 histology. This non-reactive marrow picture may indicate a reduced likelihood of response to anti-lymphocyte globulin or other immunosuppressive therapy.

25

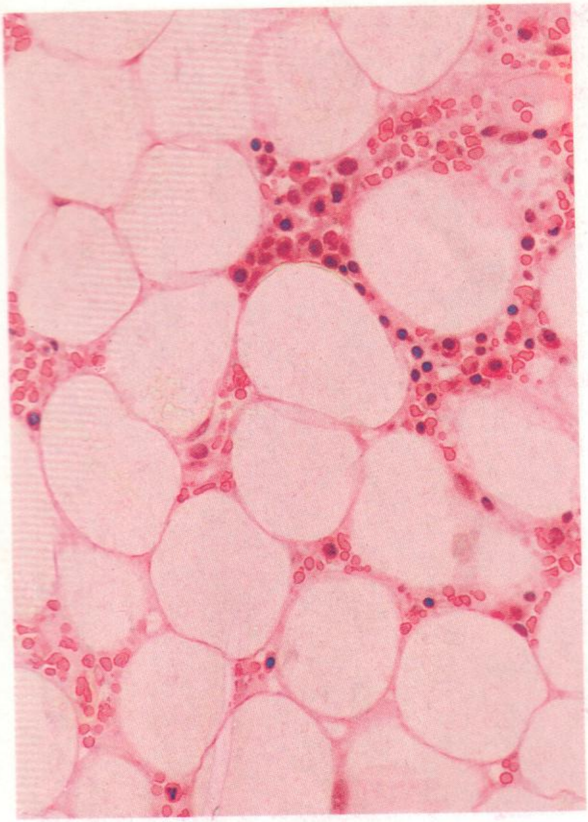

26

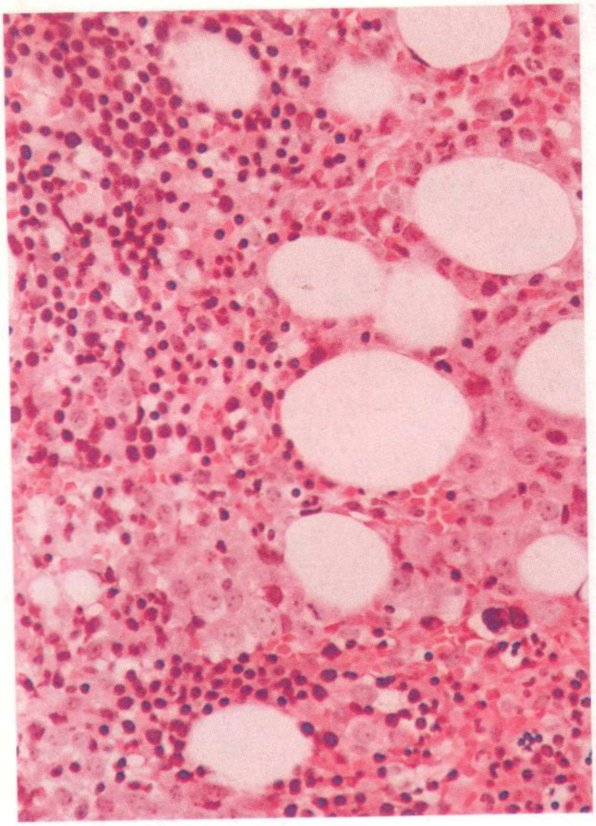

27

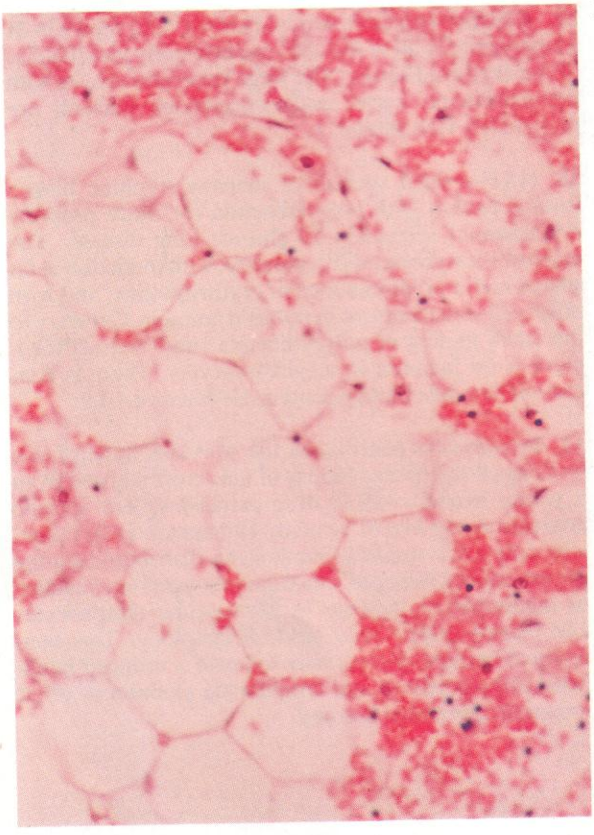

25. An iliac crest trephine biopsy from a young woman with peripheral blood pancytopenia whose marrow shows moderately severe hypoplastic changes. Fatty spaces constitute over 90% of the marrow and, apart from mature erythrocytes, residual haemic cells are scanty, with merely a scattering of lymphocytes and plasma cells, and no granulocytes in this field. Nevertheless, there are several normoblasts present and this offers some prospect of recovery, whether spontaneous or in response to treatment. Bone marrow aspirate at this stage yielded only blood.

26. A further biopsy from the same patient during the recovery phase, following treatment with anti-lymphocyte globulin (ALG). Active haemopoiesis now occupies 70–80% of the total marrow, with numerous islands of normoblastic hyperplasia and of early granulocyte precursors.

27. Trephine biopsy from a young adult with severe aplastic anaemia, showing almost complete loss of haemopoietic activity. The few residual nucleated cells are chiefly lymphocytes. This marrow picture, grade 0 histology, when associated with very severe peripheral pancytopenia, may indicate less chance of response to ALG than one with a more considerable increase in inflammatory infiltration by lymphocytes and plasma cells – whether modest (grade 1), marked but irregularly distributed (grade 2), or marked and diffusely distributed (grade 3).

28

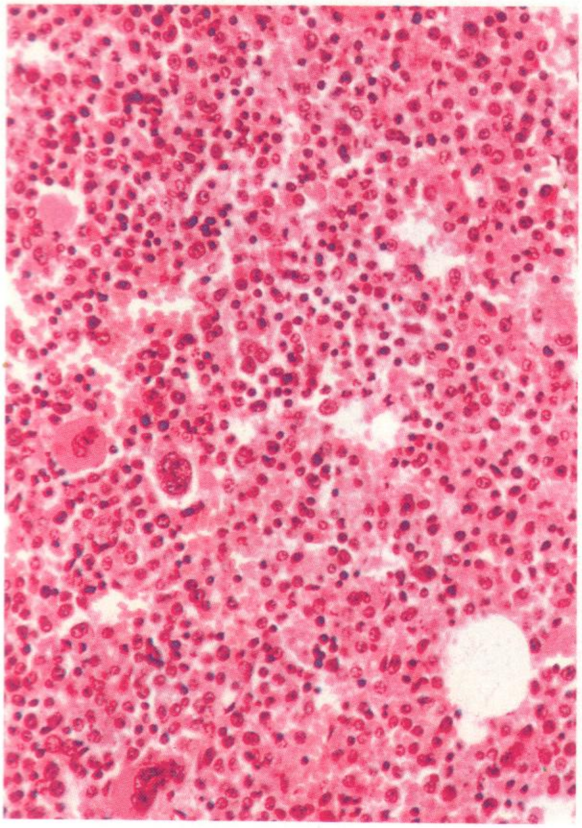

29

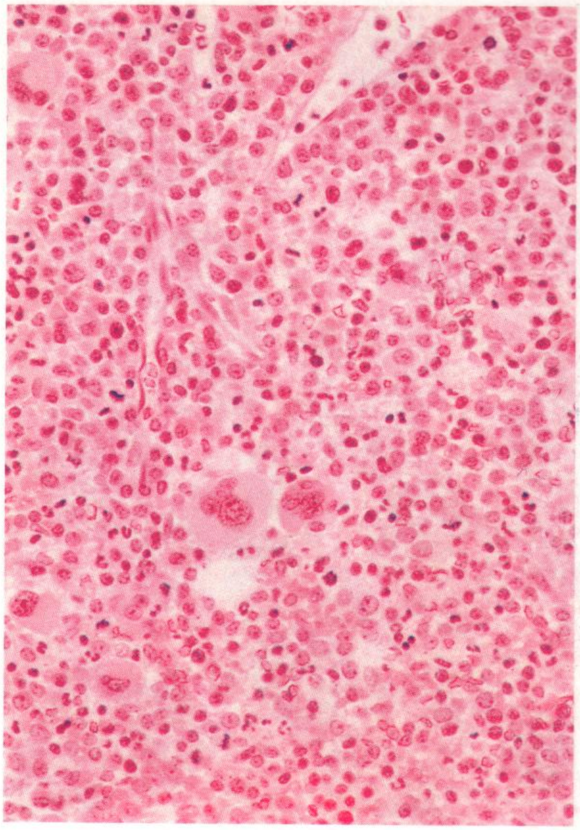

28 and **29**. Respectively thick (6-micron) and thin (2-micron) sections of iliac crest trephine biopsy from a patient with PRV in a stable erythrocytotic phase. Both show overall increased cellularity with trilineage involvement – erythroid, granulocytic and megakaryocytic. In **28** the black nuclei of the thickly sectioned normoblasts allow their relative proportions to be assessed easily, and the megakaryocytosis can be readily appreciated, while in **29** the finer details of cytology in the thinner section permit more accurate identification of individual cells.

30

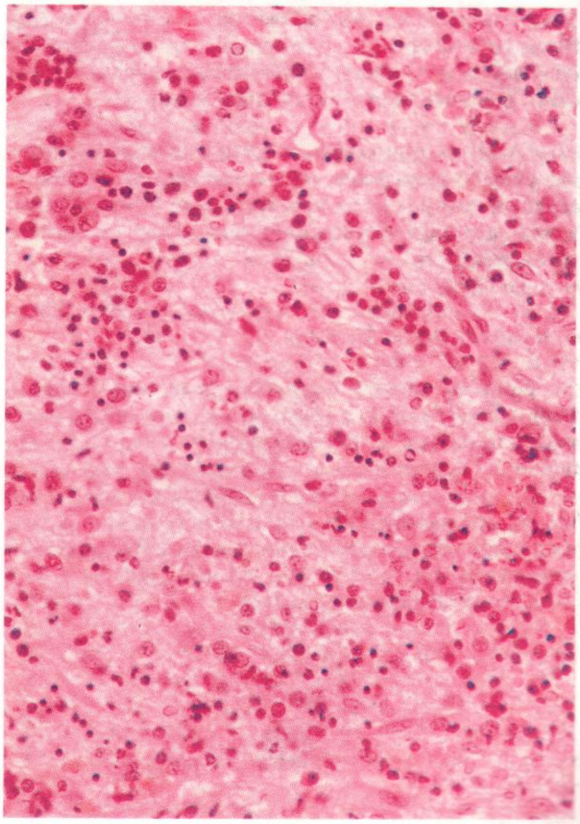

30. Section of marrow trephine biopsy from a patient with long-standing PRV, now moving into a phase of myelofibrosis, as occurs in about 15–20% of cases. The section shows persistence of trilineage hyperplasia, but there is now a strong component of fibroblastic proliferation, and the picture is becoming indistinguishable from that of idiopathic myelofibrosis (IMF) or agnogenic myeloid metaplasia (AMM). At this stage the raised haemoglobin and red-cell count tend to fall towards normal, while splenomegaly increases, and teardrop poikilocytes appear in the blood. Attempts to aspirate marrow are likely to yield a dry tap.

31 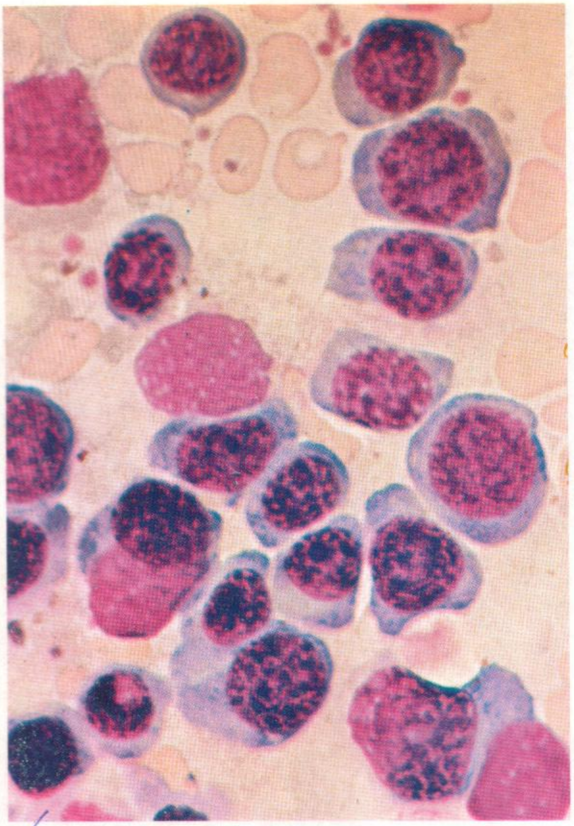

32 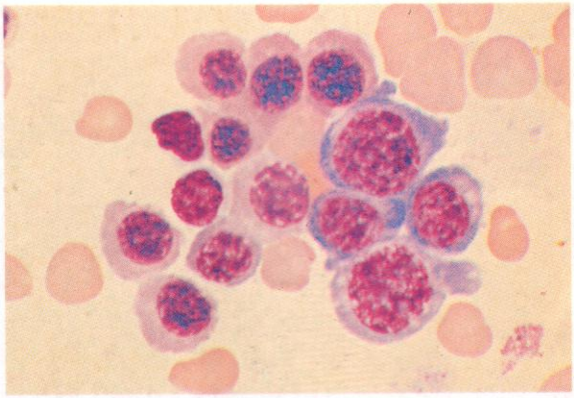

33 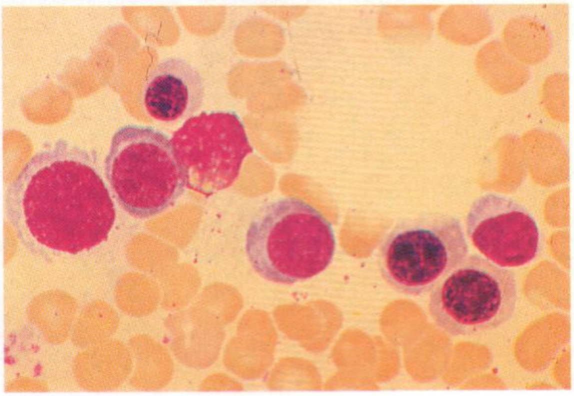

34 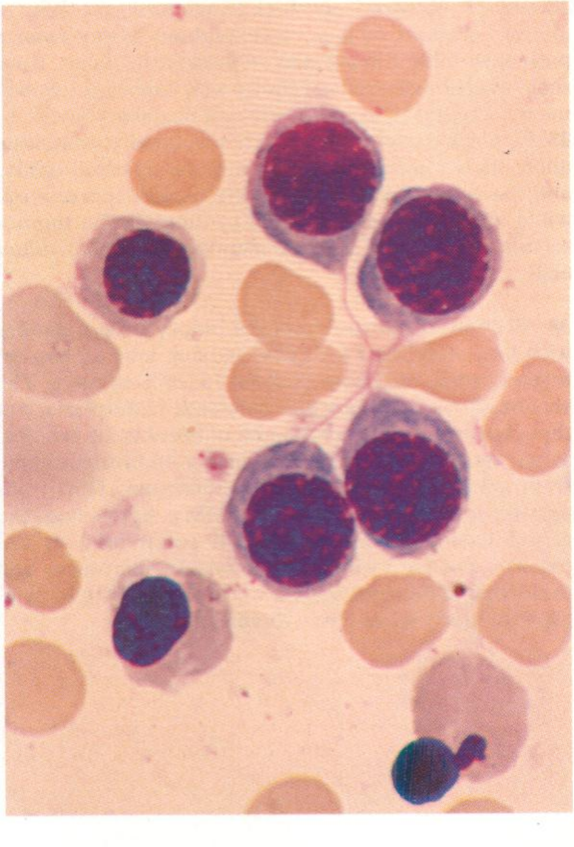

31. A group of early basophilic macronormoblasts. This type of erythropoiesis occurs especially in haemolytic anaemias, as in the patient with hereditary spherocytosis (HS), from whom this aspirate was taken.

32. Early and intermediate macronormoblasts, showing cytoplasmic maturation with accumulation of haemoglobin in some cells to a degree more advanced than would normally accompany their state of nuclear maturation.

33. Macronormoblasts, from early to late stages. There is a lymphocyte on the right.

34. A group of four basophilic normoblasts derived from a single cell as a result of two recent successive mitotic divisions, with the cytoplasm of each pair still linked by fine threads of cell membrane, and with a further cross-looping of the threads. To the left are two intermediate-to-late normoblasts with dense nuclear chromatin and polychromatic, partially haemoglobinized cytoplasm, and at the bottom right is a late normoblast shedding its nucleus.

35

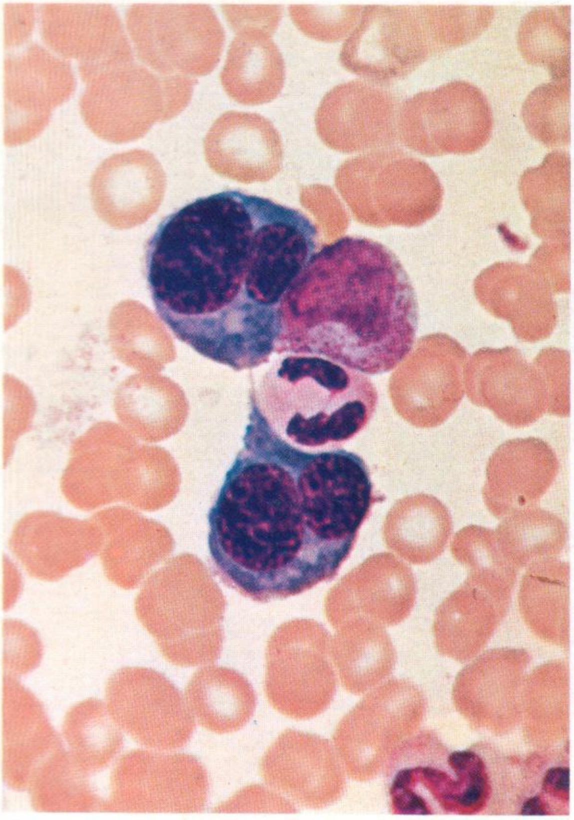

36

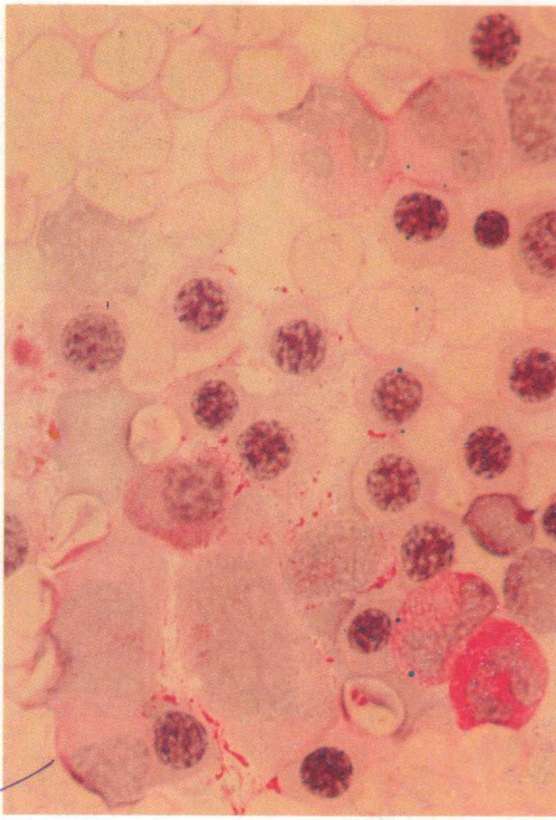

35. Late telophase of mitotic division in a macronormoblast, with daughter cells each containing two unequal nuclear masses. A mature neutrophil and a myelocyte are also present.

36. Periodic acid-Schiff (PAS) reaction on a normal bone marrow aspirate, showing an erythroblastic island around a macrophage. The macrophage nucleus, with an open chromatin network, is in the midline a third of the way from the bottom, and its cytoplasm, with a scattering of PAS-positive granules especially towards the margins, spreads out between the cells clustering around. Among these are 14 erythroblasts, all PAS-negative, as are four others in the top-right corner. Across the lower part of the field are several granulocytes, with a group of immature cells on the left, and a stab cell and a mature segmented neutrophil on the right. These show the typical increasing PAS positivity with increasing cell maturity. A single plasma cell just above the promyelocyte shows moderately intense PAS positivity.

37

37. Macronormoblastic hyperplasia in foetal haemolytic disease, stained by the PAS reaction. Normal erythroblasts are PAS-negative, but positive material is found in foetal haemolytic disease, thalassaemia, iron deficiency anaemia, refractory sideroblastic anaemia and erythraemic myelosis or erythroleukaemia. Here, two late erythroblasts show moderately heavy positive stippling.

38

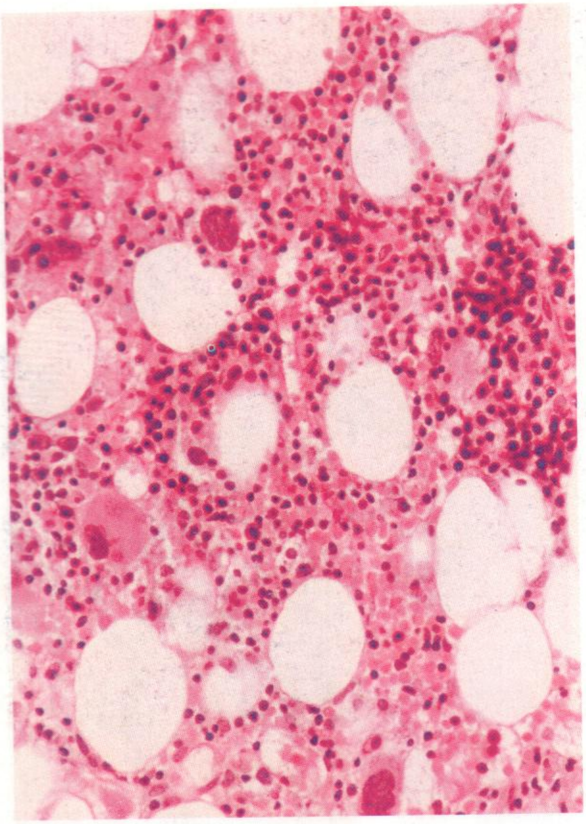

39

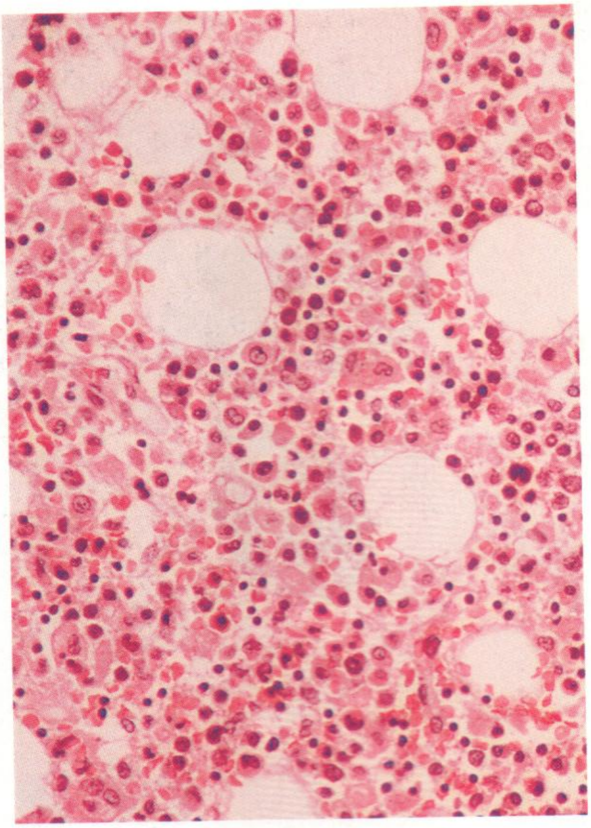

40

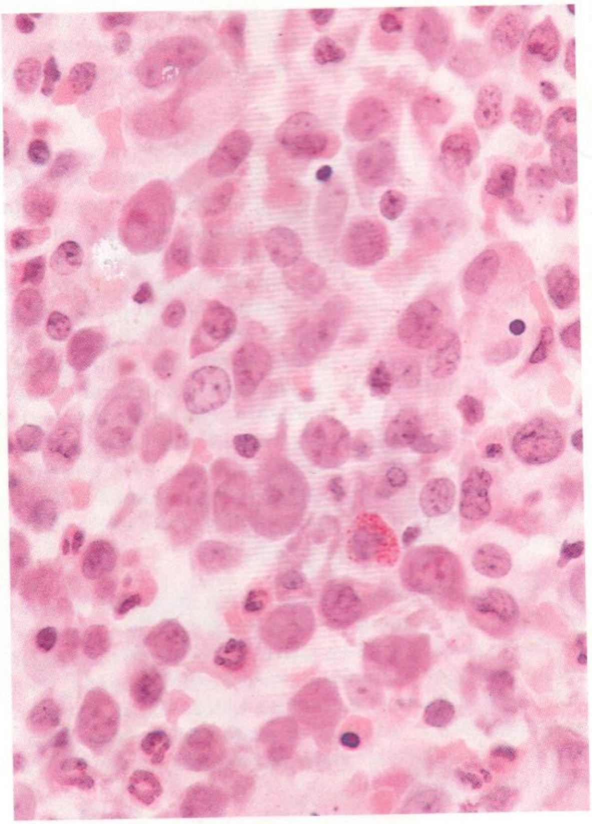

38. Haemorrhage and hyperplastic areas of erythropoietic activity, together with an increase in megakaryocytes, in a trephine biopsy of bone marrow from an elderly patient with idiopathic (auto-immune) thrombocytopenic purpura (ITP). Two of the megakaryocytes are immature, with single unlobed nuclei, as is common in this disorder. There is no overall marrow hyperplasia in this specimen, and a normal proportion of fat spaces remains.

39 and **40**. Respectively low- and high-power fields from a marrow biopsy section taken from a patient with B_{12} deficiency secondary to intrinsic factor deficiency – pernicious anaemia. The first field (**39**) gives a good impression of the moderate degree of hyperplasia, with no great diminution in fat spaces in this case, but with a predominance of erythropoiesis. In the second (**40**), the shift to the left in erythroblasts is apparent, with numerous nucleolated proerythroblasts, and a suggestion of megaloblastic change can be appreciated. Nevertheless, the histological detail is much inferior to the cytological detail evident in smear preparations from aspirated marrow, as shown in the illustrations that follow.

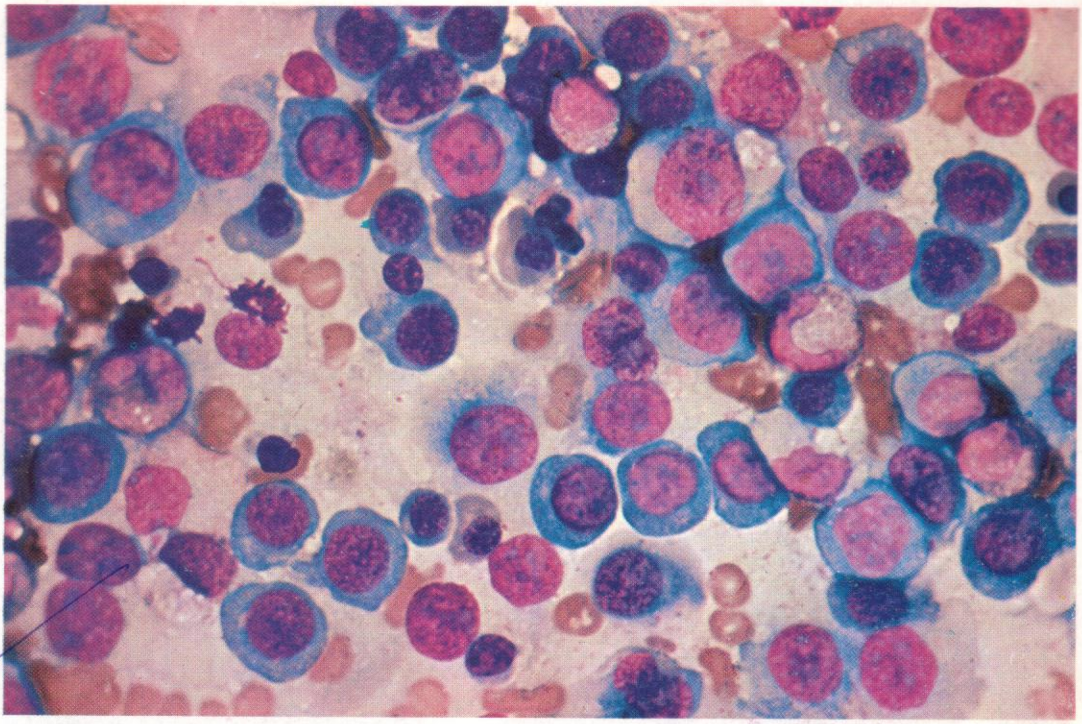

41

41. A general view of a marrow smear from a patient with pernicious anaemia. Erythroblasts greatly predominate, and erythropoiesis is megaloblastic. Early stages in the sequence from proerythroblast onwards are particularly common.

42. Proerythroblasts (nucleolated) and early and intermediate megaloblasts. While the nuclear pattern of proerythroblasts in pernicious anaemia and other megaloblastic anaemias is not distinctively different from that of normal proerythroblasts, there is a tendency for cytoplasm to be more abundant and nucleoli larger and more conspicuous. The field contains a late megaloblast of large size and having an irregular pycnotic nucleus. There is also a separated fragment of polychromatic megaloblast cytoplasm.

42

43
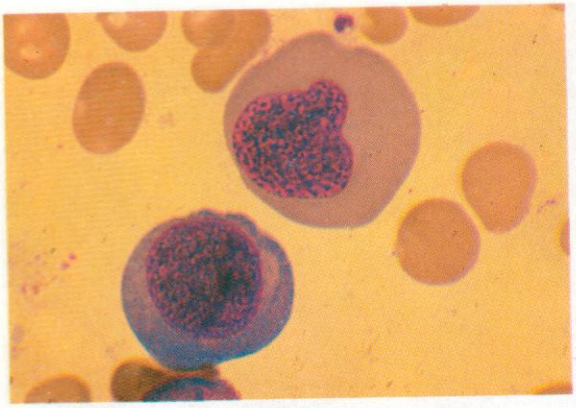

44
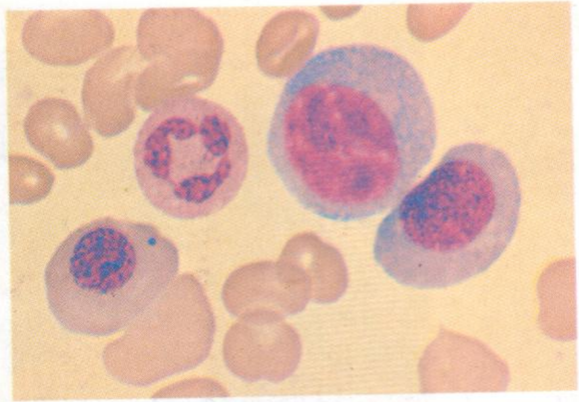

45


46
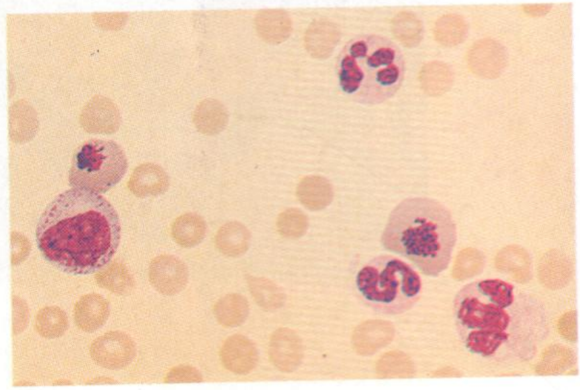

47
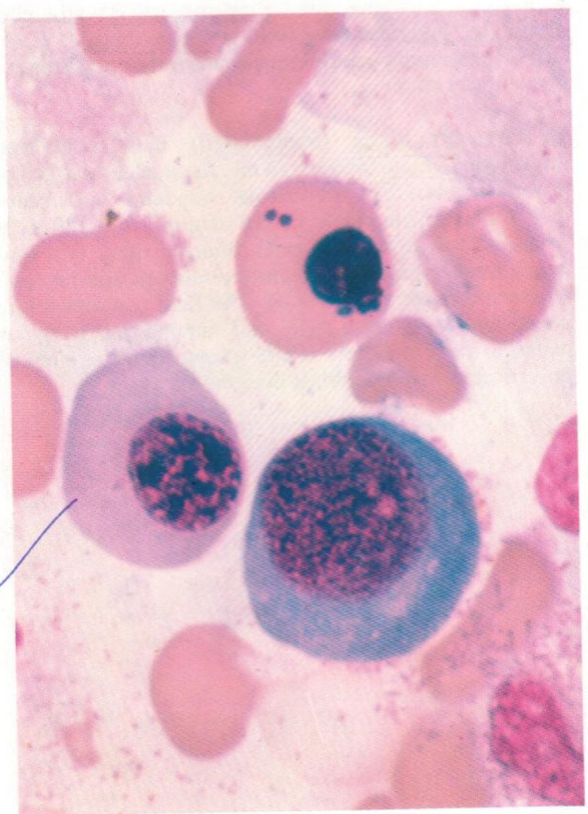

43. An early megaloblast with nucleolar traces and deep cytoplasmic basophilia, and an intermediate megaloblast of gigantic size.

44. A mature neutrophil with a proerythroblast, an early-to-intermediate megaloblast and a late megaloblast. This last cell has not quite reached the stage of complete nuclear pycnosis, but contains a Howell-Jolly body.

45 and **46**. Two fields from a peripheral blood buffy coat smear from a patient with chronic myeloid leukaemia (CML) treated with the antimetabolite hydroxyurea. In **45** two basophils and two neutrophil stab cells accompany two large intermediate megaloblasts, and in **46** are shown a stab cell, two neutrophil polymorphs, a metamyelocyte and two late megaloblasts, widely separated but with incomplete nuclear reconstitution after a preceding mitosis.

47. Early, intermediate and late megaloblasts, the last containing two Howell-Jolly bodies. At the nuclear margin are four additional chromatin fragments, apparently still attached to the nuclear membrane but of the same character as Howell-Jolly bodies.

48

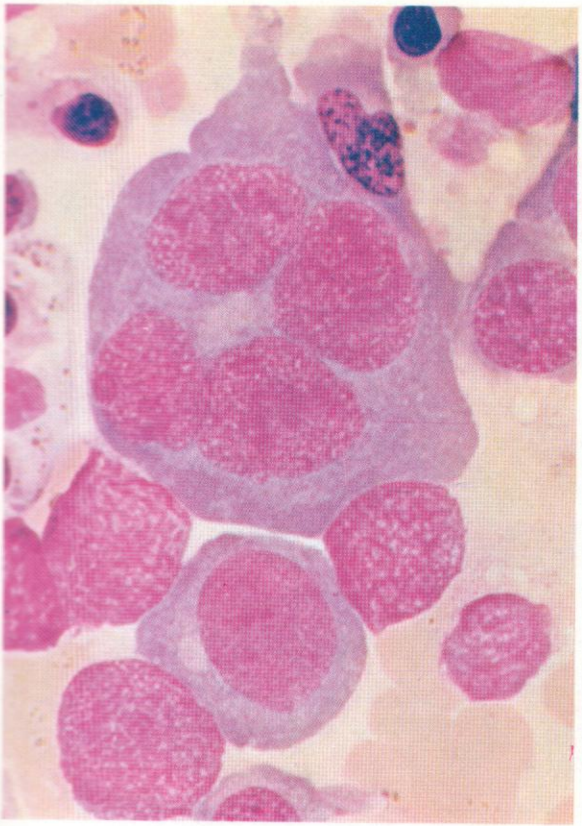

49

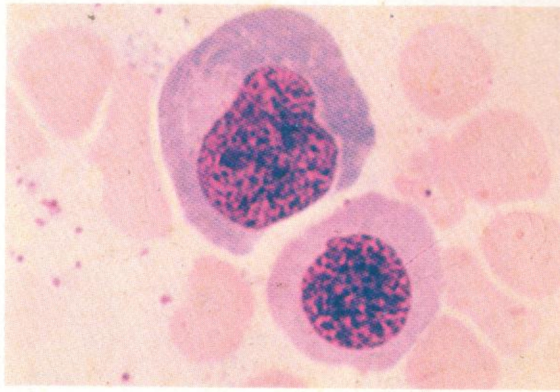

50

51

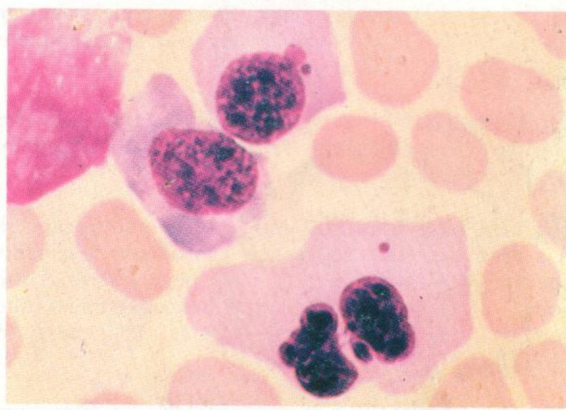

52

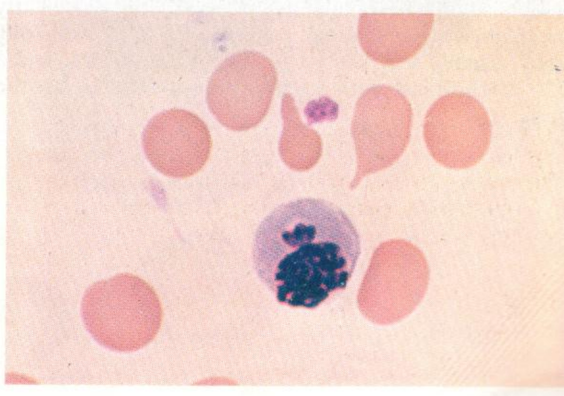

48–57. *This series of fields showing megaloblasts with extra cytological abnormalities comes from marrow or peripheral blood samples from patients with pernicious anaemia, and illustrates that gross abnormalities may be found in remediable B_{12} deficiency and are not confined to erythroleukaemias.*

48. A gigantic early megaloblast with four nuclei, probably resulting from two consecutive incomplete mitoses, with nuclear division unaccompanied by cytoplasmic division.

49. An intermediate and a late megaloblast, the former showing nuclear distortion of minor degree.

50. An intermediate megaloblast with two nuclei.

51. Late megaloblasts. One is gigantic, with two connected irregular nuclear masses and a free Howell-Jolly body.

52. An irregular nuclear mass approaching extrusion in a late megaloblast.

53

54

55

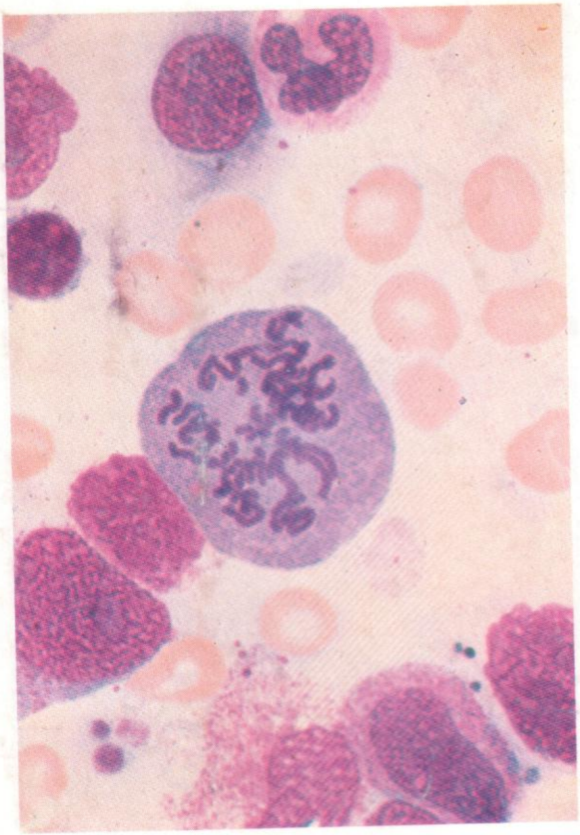

56

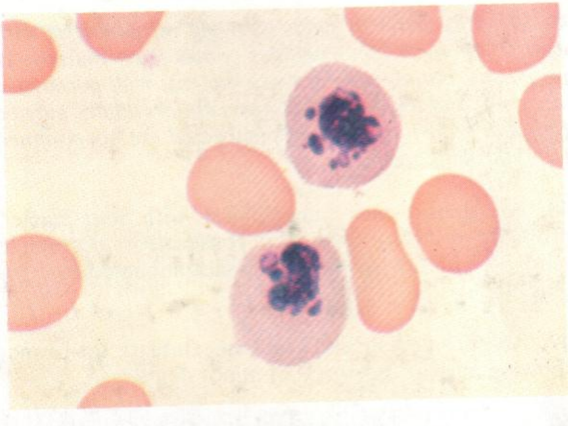

57

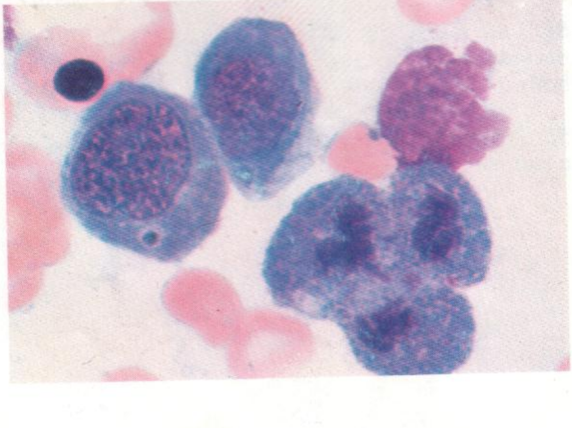

53 and **54**. Late megaloblasts showing typical nuclear rosette formation, probably arising from an incomplete mitosis with hold-up at metaphase.

55. Metaphase of mitosis in an early megaloblast. The chromosomes are notably long and thin and unusually widely scattered.

56. Telophase in late megaloblasts. The mitotic process has been defective and several chromatin fragments (perhaps whole chromatids) have been lost from the spindle and appear separate from the main bodies of the reconstituted nuclei. This illustrates the genesis of Howell-Jolly bodies.

57. An abnormal tripolar mitosis, approaching telophase, in a basophilic megaloblast. Two more early megaloblasts, one already containing a Howell-Jolly body, usually seen mostly in later megaloblasts, and a late erythroblast with pycnotic nucleus make up the field.

58

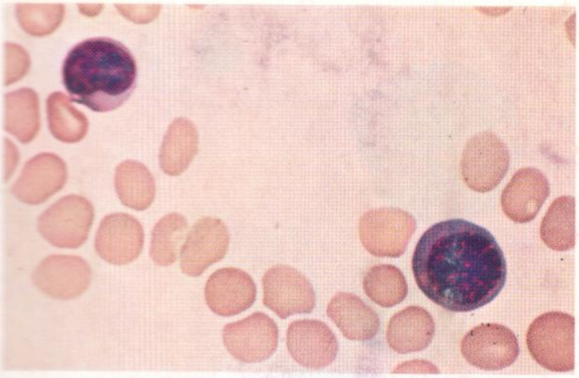

60

59

61

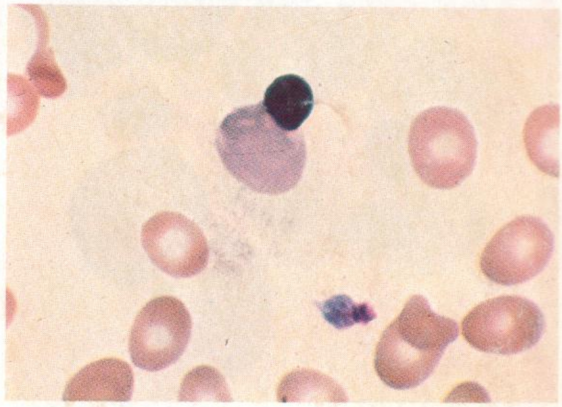

62

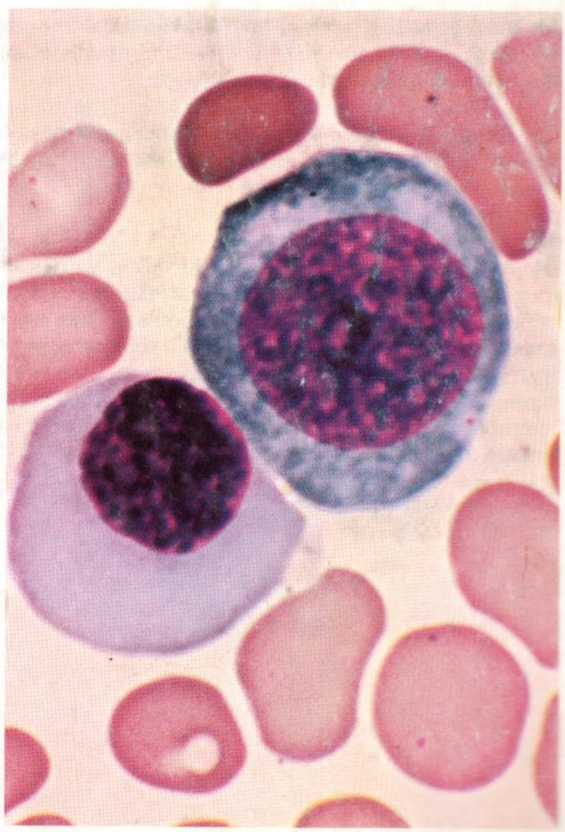

58. An intermediate megaloblast and a lymphocyte (for comparison) in the blood.

59. An intermediate megaloblast with nuclear distortion. The eccentric position of the nucleus and the persistent basophilia of the cytoplasm give a resemblance to a plasma cell.

60 and **61**. Late megaloblasts in the peripheral blood. Each shows almost complete extrusion of the pycnotic nucleus. With loss of the nucleus a polychromatic reticulocyte or young erythrocyte will remain.

62. A proerythroblast and a late megaloblast, surrounded by erythrocytes showing macrocytosis and minor anisocytosis and poikilocytosis. A few small Howell-Jolly bodies are visible in several of the mature red cells.

63

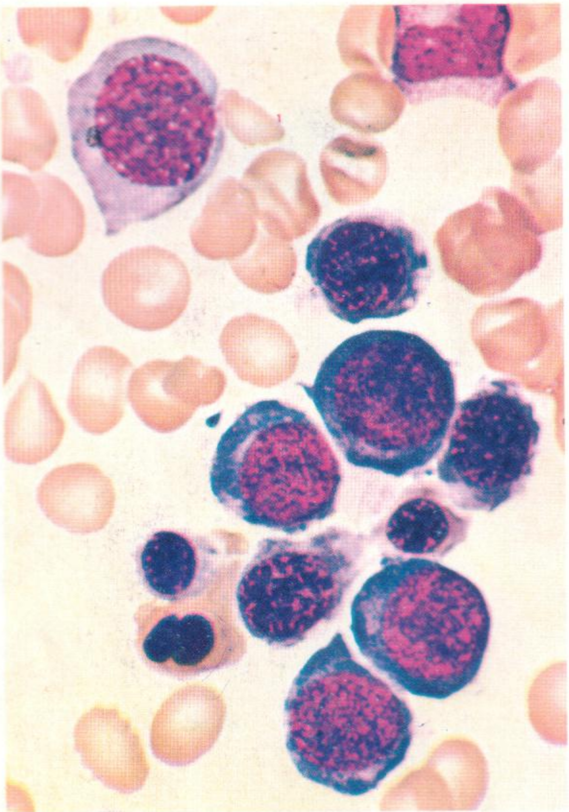

64

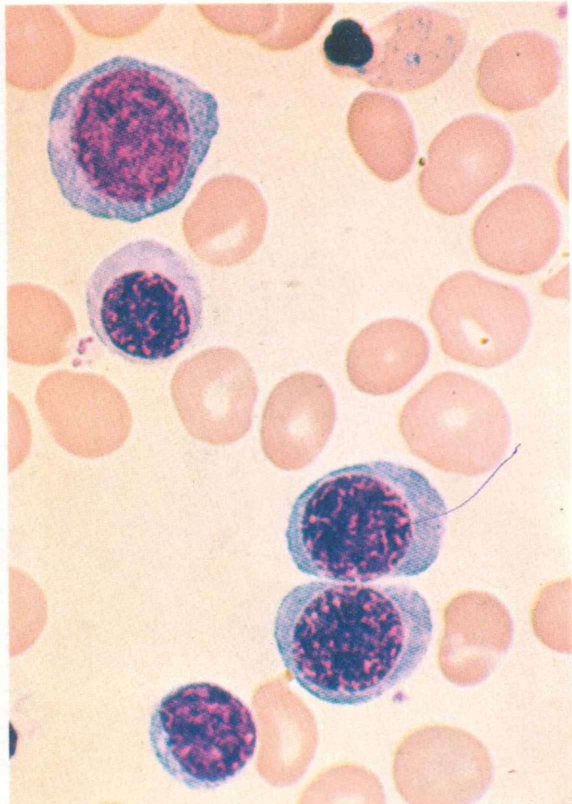

65

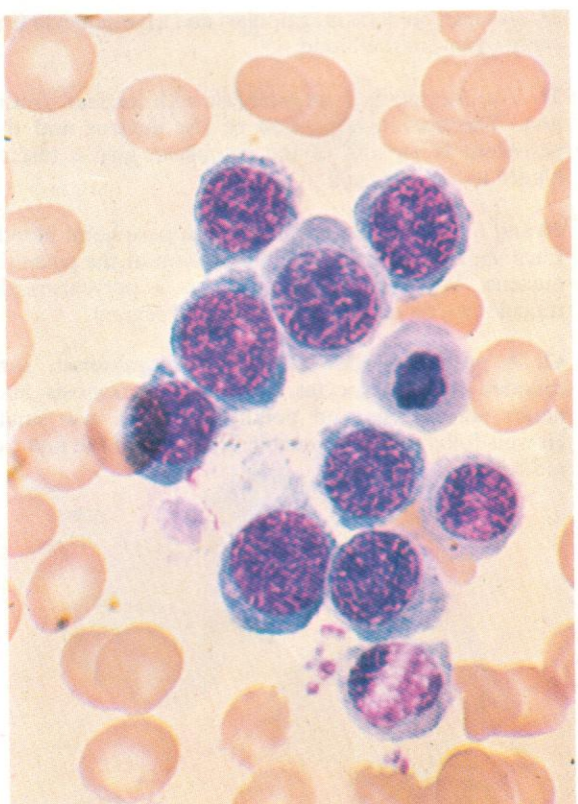

63. A range of erythroblasts with minimal megaloblastic change. The confusing terms 'intermediate' and 'transitional' megaloblasts are sometimes applied to such erythroblasts, whether early or late in the maturation sequence. A late megaloblast with densely pycnotic paired nuclei shows basophilic stippling of the orthochromatic cytoplasm. At the top of the field is a neutrophil metamyelocyte.

64 and **65**. Further groups of erythroblasts with minor megaloblastic changes. The nuclear pattern is more open than that of comparable normoblasts, but less so than in florid megaloblasts. The cell at the bottom of **64** is a lymphocyte, and the loss of nucleus from a late normoblast at the top leaves a stippled red cell. There is another lymphocyte at the bottom of the field in **65**, with several neighbouring platelets.

66

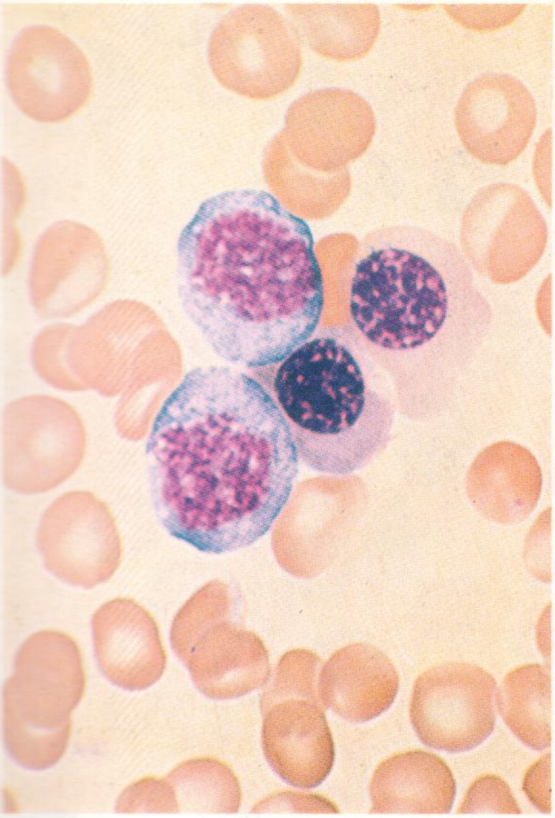

67

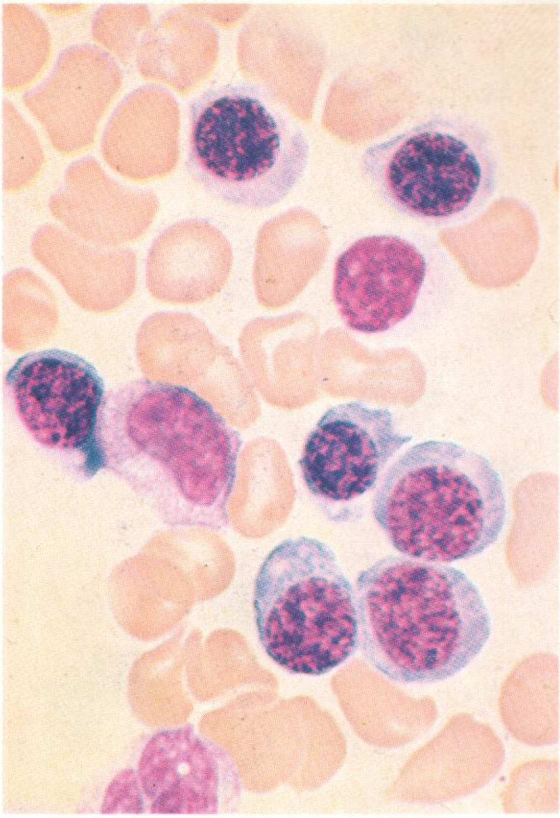

68

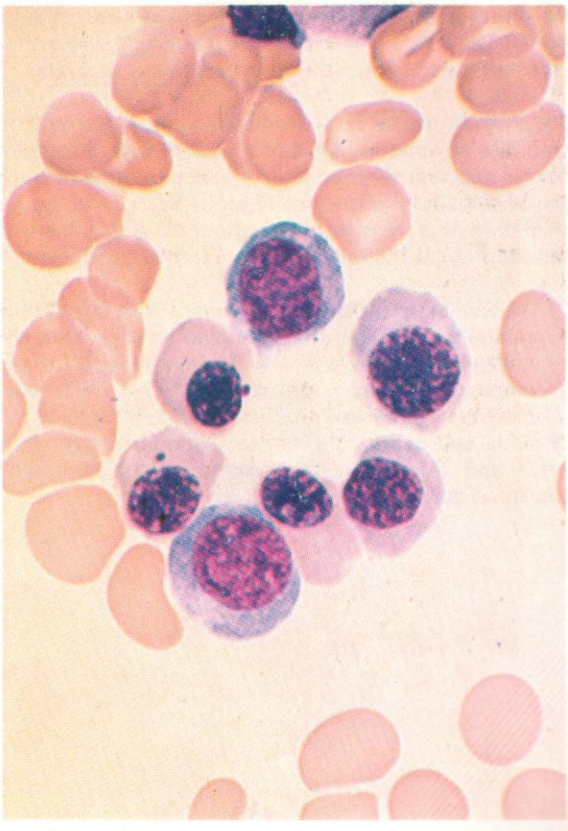

66–68. A series of fields illustrating recognizable but minor megaloblastic changes in erythroblasts from the bone marrow of a patient in an early stage of pernicious anaemia. It is interesting to note that there is already quite marked nuclear–cytoplasmic asynchrony of development, with conspicuous premature haemoglobinization accompanying moderate nuclear chromatin condensation, although the nuclear pattern does not show a floridly open and fully megaloblastic chromatin network. Mitotic abnormalities are also already occurring, with resulting Howell-Jolly bodies in two late megaloblasts in **68**.

69

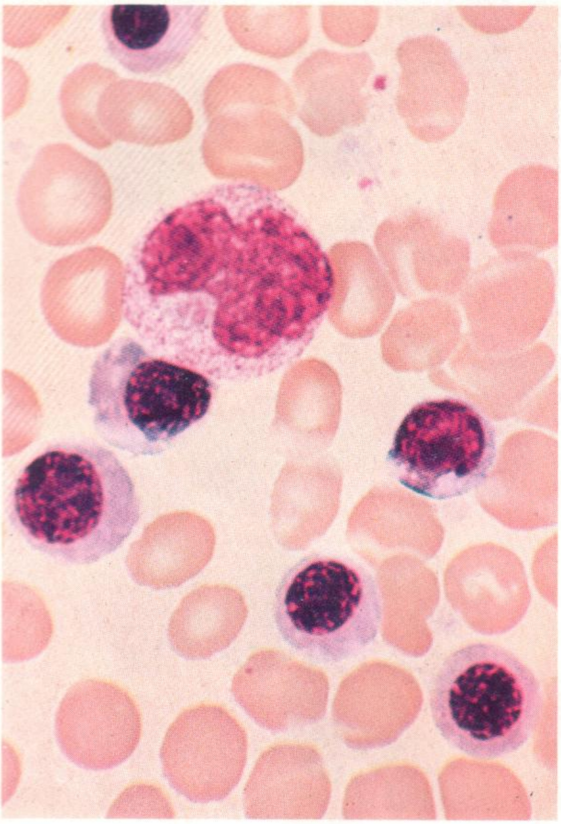

70

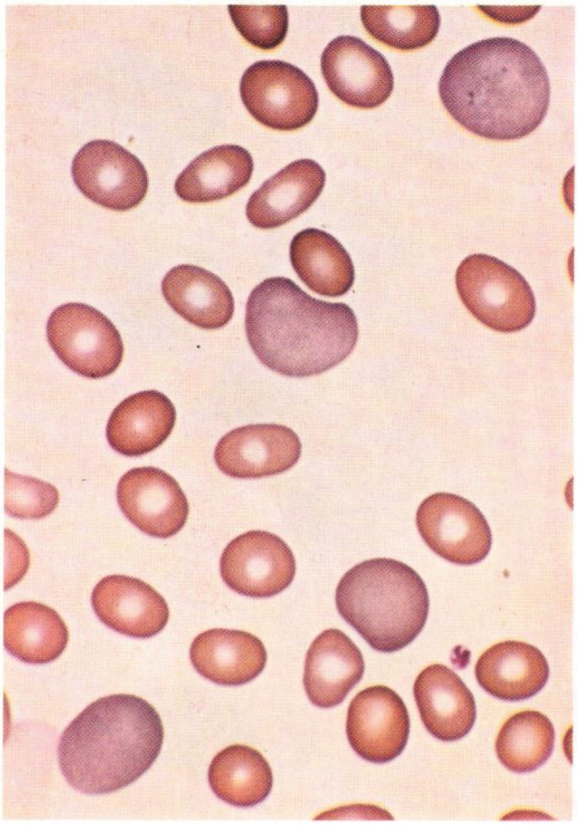

71

69. Further minor megaloblastic changes in erythroblasts. The large cell in the centre is a 'giant metamyelocyte' characteristically found in pernicious anaemia.

70. Polychromasia in a Leishman-stained preparation from the peripheral blood of a patient with a megaloblastic anaemia responding to specific treatment. Such polychromatic erythrocytes tend, as here, to be larger than more mature orthochromatic cells, and with cresyl blue supravital staining are shown to be reticulocytes.

71. A similar specimen to **70**, stained with cresyl blue supravitally. Note that the haemoglobin content of the reticulocytes appears high – an element of hypochromia accompanied the megaloblastic changes in this case. 'Dimorphic' patterns with macrocytosis and hypochromia and deficiencies of both vitamin B_{12} (or folic acid) and iron occur especially in association with intestinal malabsorption.

72

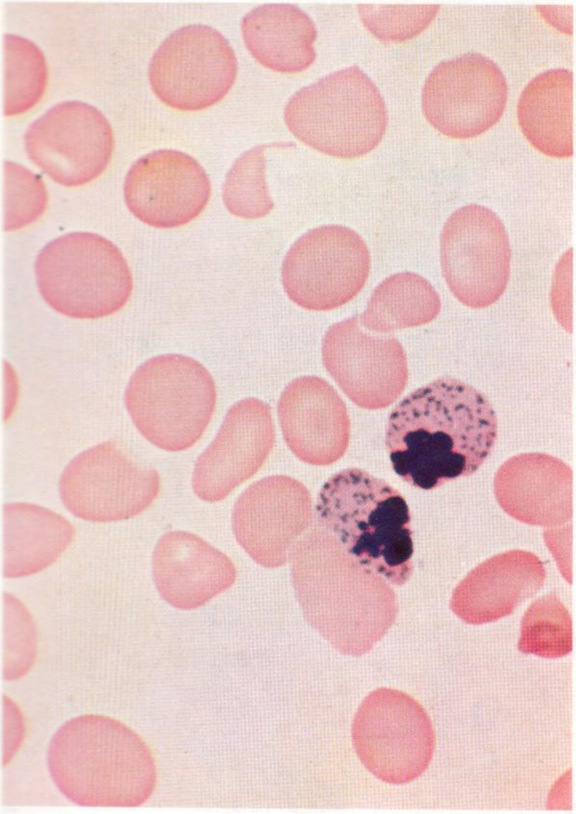

73

74

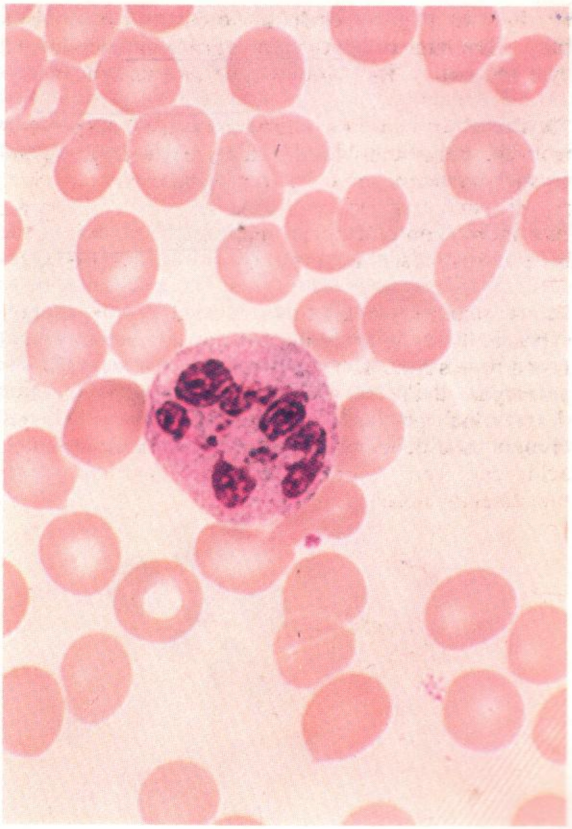

72. Peripheral blood in pernicious anaemia. There are two late megaloblasts with nuclear rosette formation and basophil stippling (another manifestation of reticulocyte material). The red cells show macrocytosis, anisocytosis and poikilocytosis.

73. Similar changes in red cells from another area in the same specimen as appeared in **72**. This field includes a late megaloblast and a multi-lobed neutrophil polymorph.

74. Another field showing macrocytosis, and minor anisocytosis and poikilocytosis, with a striking multi-lobed neutrophil polymorph.

75

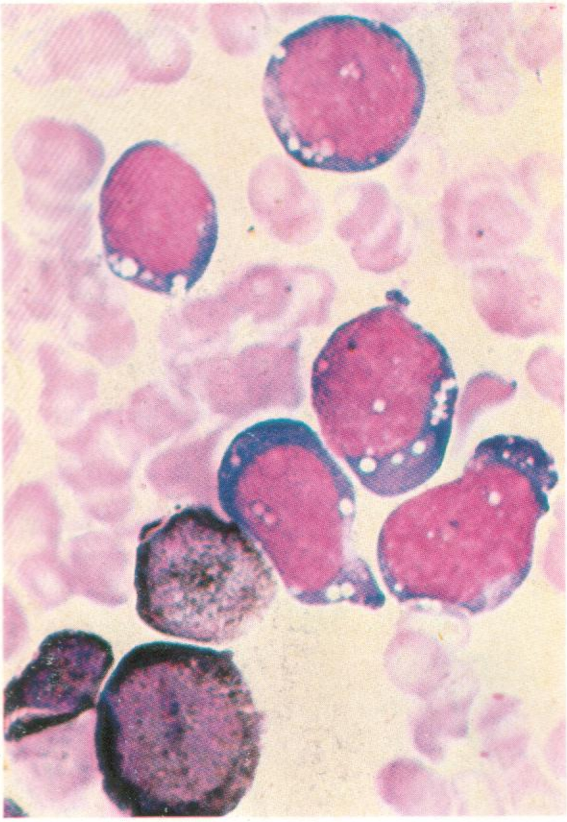

76

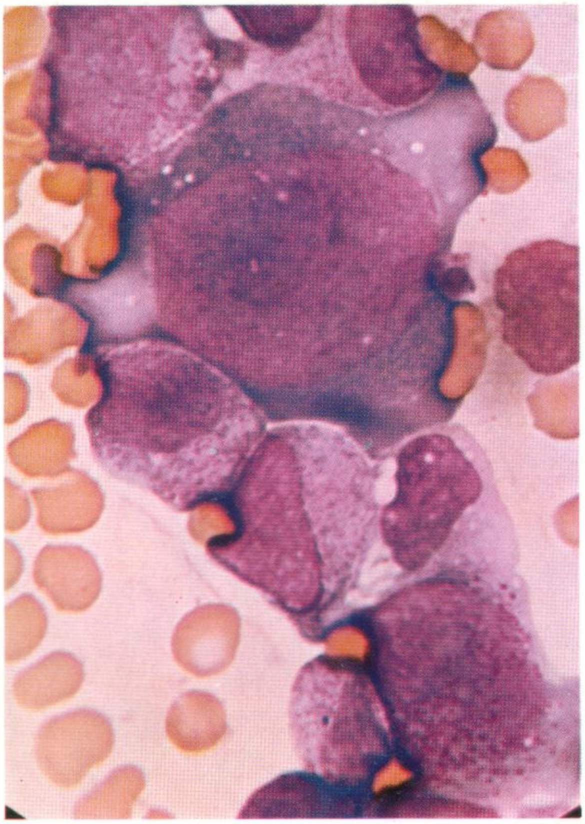

75. A bone marrow aspirate stained by Sudan black (SB), showing vacuolation in proerythroblasts following toxic reaction to chloramphenicol. The proerythroblasts are SB negative, while the sudanophilic granulocytes show no vacuolation. A similar vacuolated appearance in early red-cell precursors may result from excess alcohol exposure.

76 and **77**. Examples of giant proerythroblasts in the bone marrow of a patient with HS during the early stages of recovery from an aplastic crisis. These cells may be so large as to be mistaken for mononuclear promegakaryocytes, but there is no doubt that they are actually giant proerythroblasts, which emerge, perhaps under the influence of the parvovirus, after the temporary cessation of erythropoiesis characterizing aplastic crises of HS and thought usually to be due to that group of organisms.

77

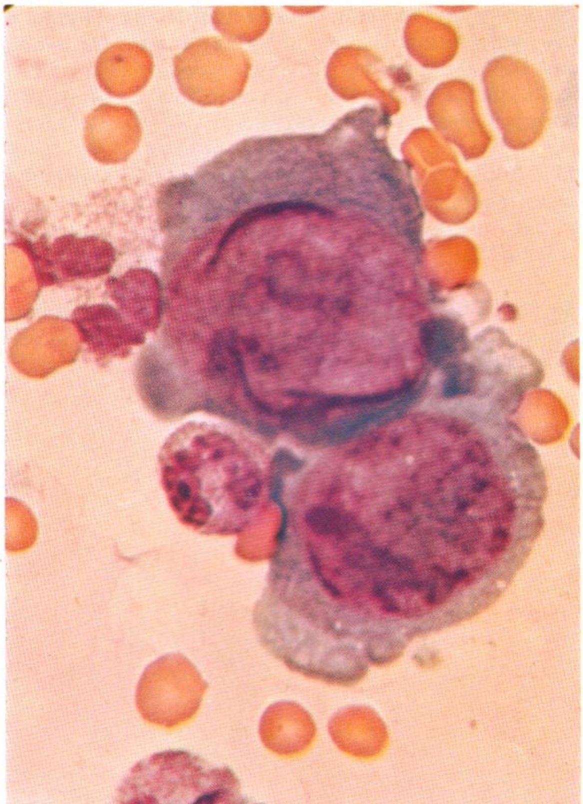

78

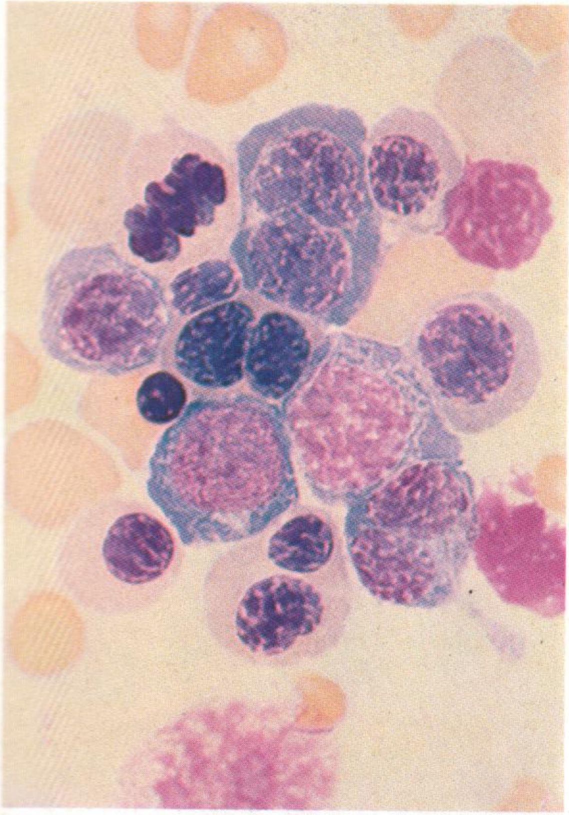

79

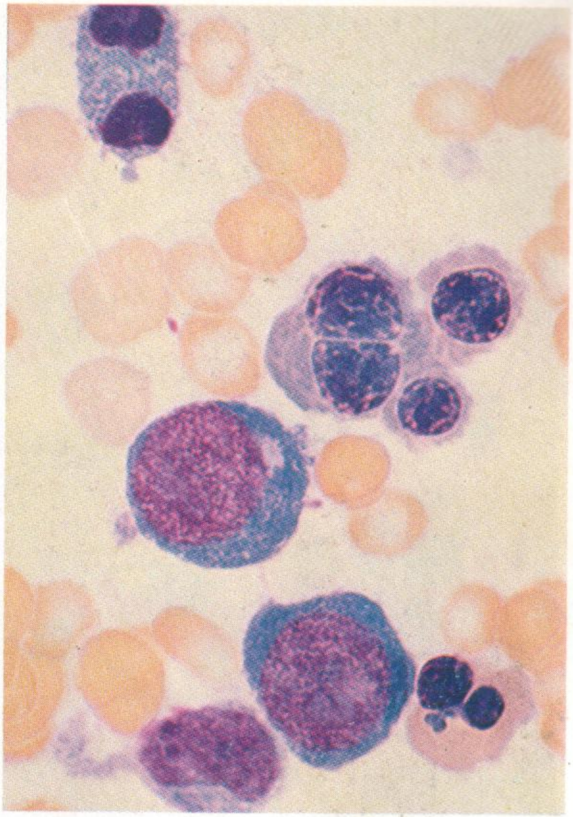

78 and **79**. Congenital dyserythropoietic anaemia (CDA), type I. Later basophilic and polychromatic erythroblasts chiefly affected; megaloblastoid changes; binucleated cells with internuclear chromatin bridges; spongy chromatin with irregular nuclear outline.

80. CDA, type II. Late erythroblasts chiefly affected; many binucleated cells. A double nuclear membrane is visible only on electron microscopy. In type II CDA (hereditary erythroblastic multinuclearity with positive acidified serum test – HEMPAS) the red cells are susceptible to acid haemolysis.

80

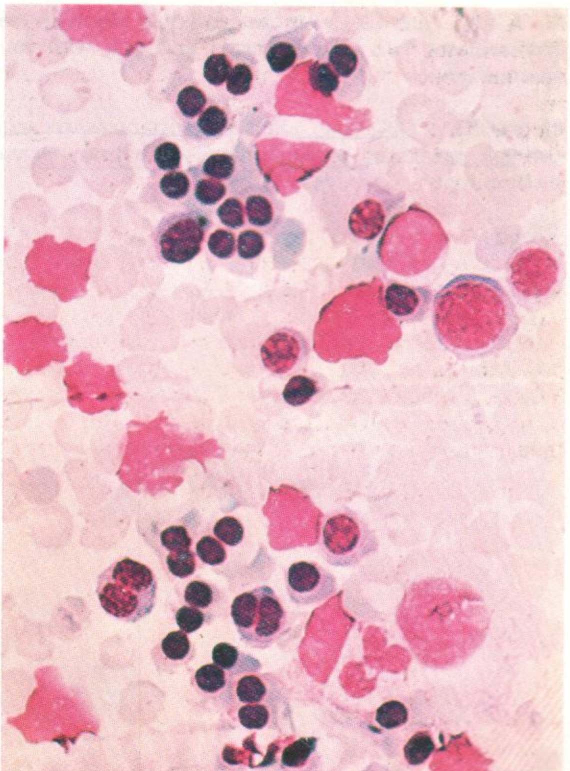

81

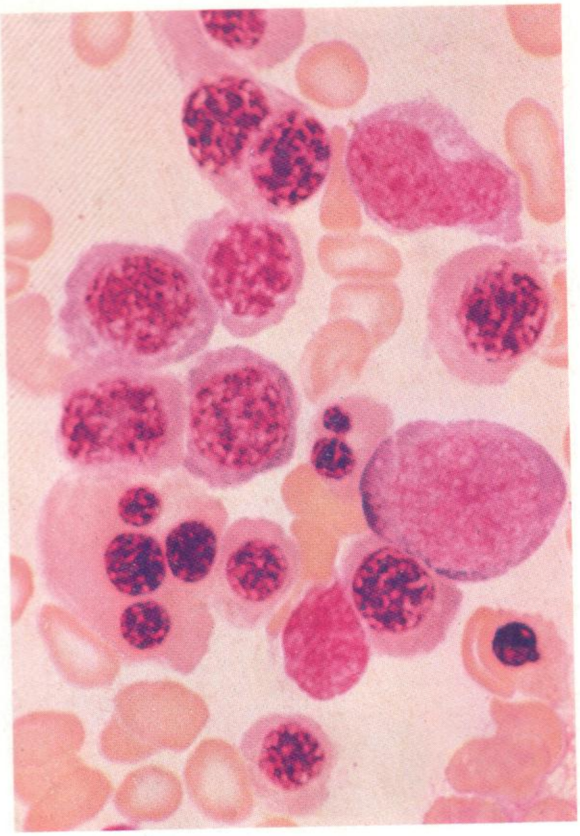

82

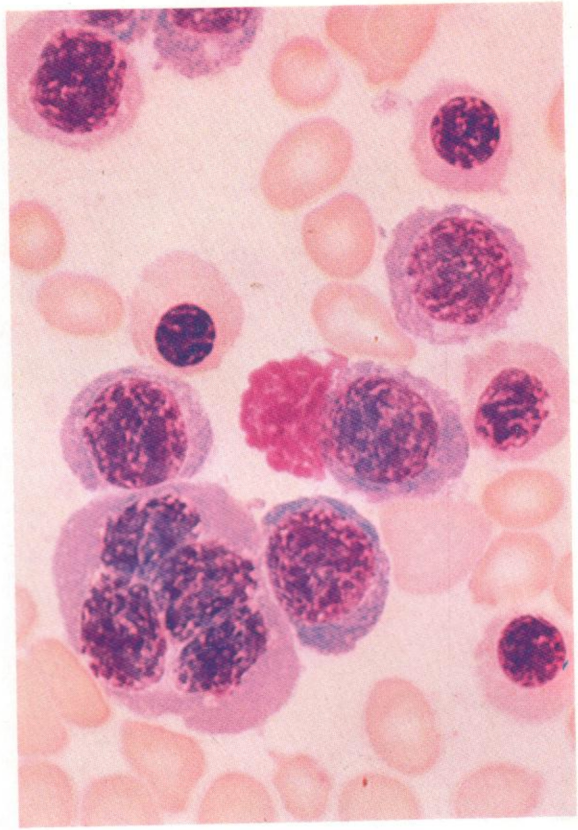

83

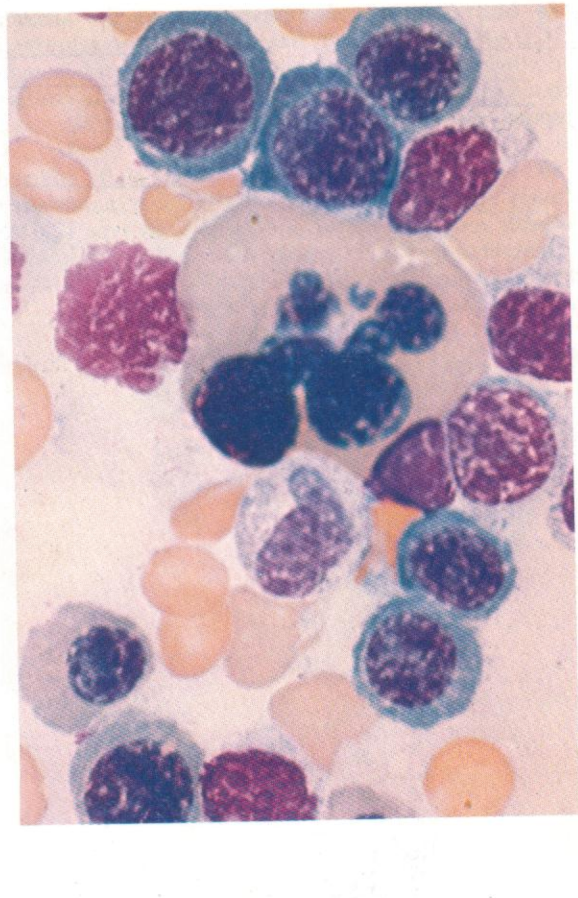

81. CDA, type II. A further example showing two erythroblasts with double nuclei and one with four unequal nuclei.

82 and **83**. CDA, type III. Giant erythroblasts with multiple nuclei or a single large lobulated nucleus predominate.

84

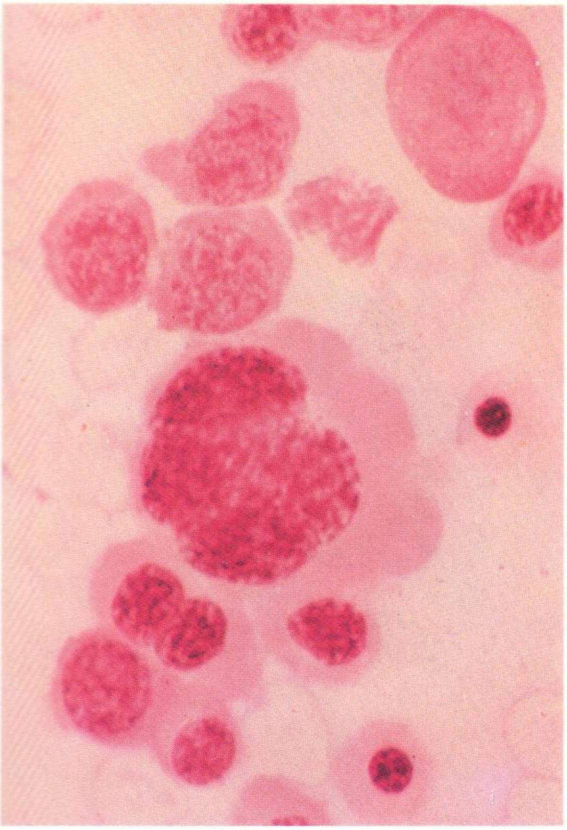

85

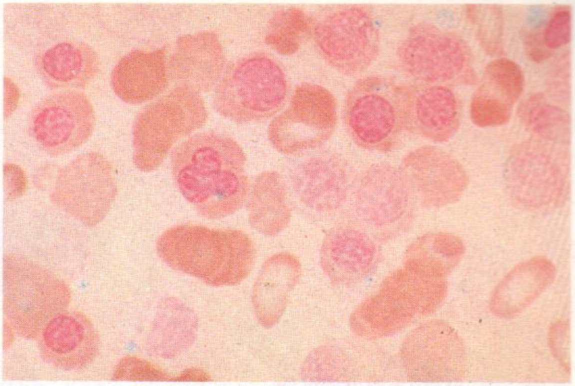

86

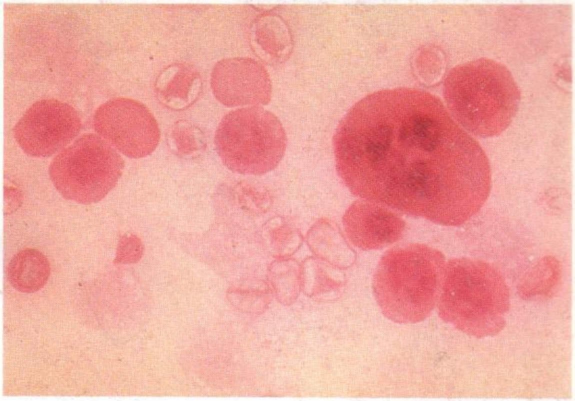

87

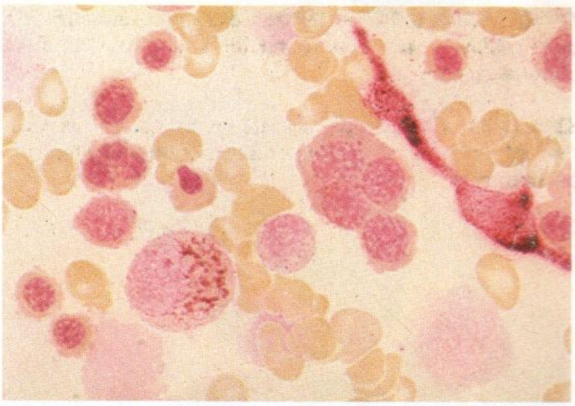

88

84–88. *Cytochemical reactions of erythroblasts in CDA. The patterns illustrated appear common to all types.*

84. PAS reaction shows weak diffuse, and some finely granular, positivity, much less than usual in erythraemic erythroblasts.

85. Prussian blue stain. Excess free iron in erythroblasts, but no ringed sideroblasts seen.

86. Kleihauer reaction. CDA erythroblasts and some erythrocytes show acid-resistant HbF.

87. Acid phosphatase: normal positivity in a macrophage and an eosinophil myelocyte. CDA erythroblasts are essentially negative, in contrast to erythraemic erythroblasts.

88. Double esterase: normal chloroacetate esterase (CE) positivity in a neutrophil stab cell: negative reaction in CDA erythroblasts, unlike the positive butyrate esterase (BE) in erythraemic erythroblasts.

89

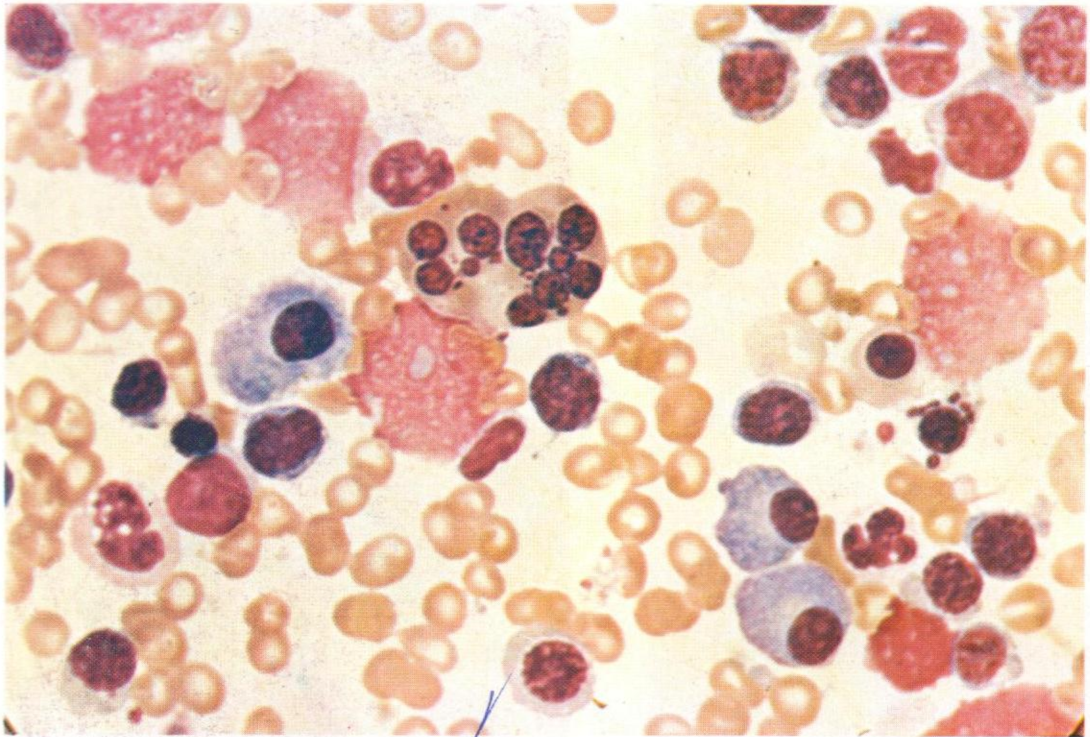

90

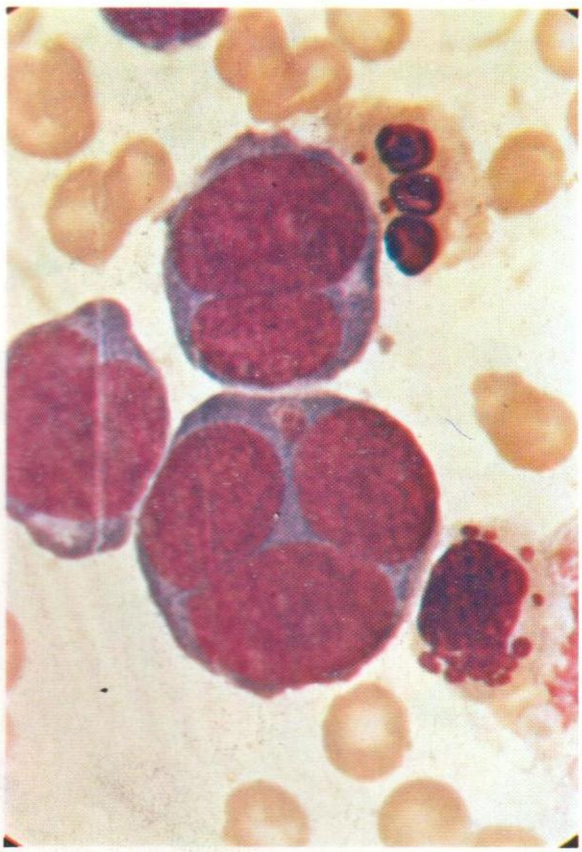

89. Bizarre nuclear abnormalities in erythroblasts from the bone marrow of a patient with erythraemic myelosis. Most cells present are erythroblasts (apart from three plasma cells) and several show multiple nuclear masses of irregular size and shape, as well as smaller Howell-Jolly bodies. At the top-right corner is a group of three cells with light-staining nuclei, possible nucleoli, and weakly basophilic cytoplasm, which may be myeloblasts, representing a relatively inconspicuous granulocyte precursor component of this predominantly erythraemic erythroleukaemia.

90. Multinucleated giant erythroblasts or proerythroblasts in erythraemic myelosis. The later erythroblasts to the right, with orthochromatic cytoplasm, show several exceptionally large nuclear fragments or Howell-Jolly bodies separated from the main nucleus.

91

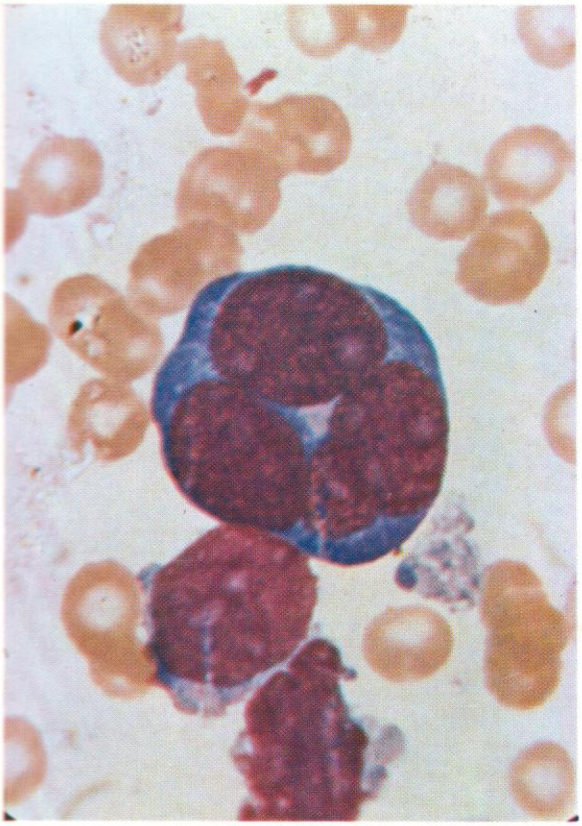

92

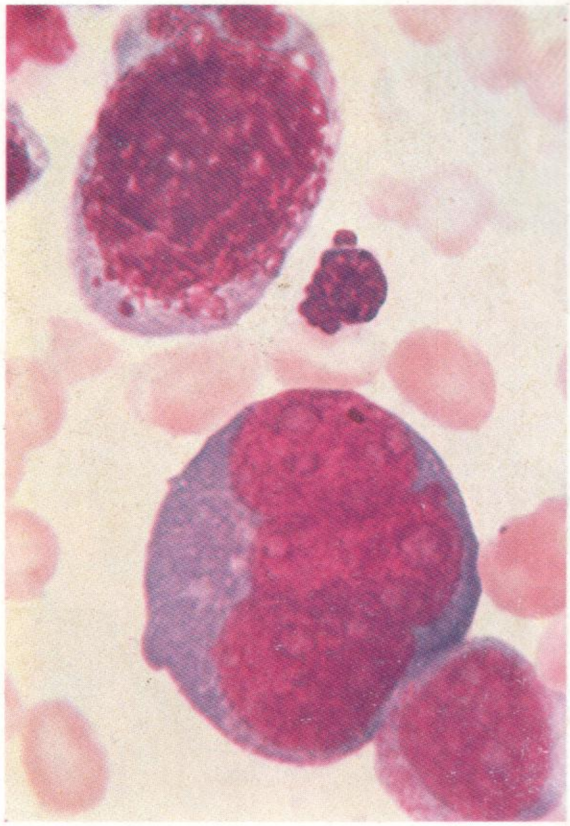

91–94. Highly abnormal erythroblasts from erythraemic myelosis.

Cellular gigantism, multiple and irregular nuclear masses and abnormal mitotic figures occur in erythroblasts at different stages of nuclear maturation and cytoplasmic haemoglobinization.

Abnormalities as striking and bizarre as these are virtually restricted to erythraemic myelosis and erythroleukaemias, but they are probably not essentially different in kind from the similar but much less frequent and prominent nuclear abnormalities illustrated earlier as occurring in the common megaloblastic anaemias, or the frequent but more regular multinuclearity of CDA.

93

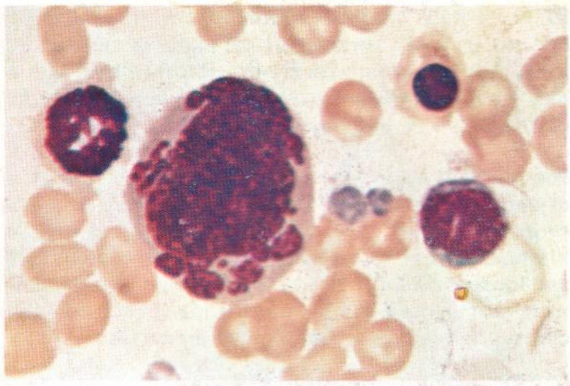

94

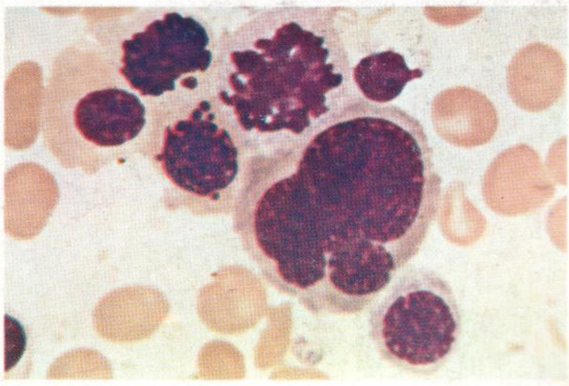

95

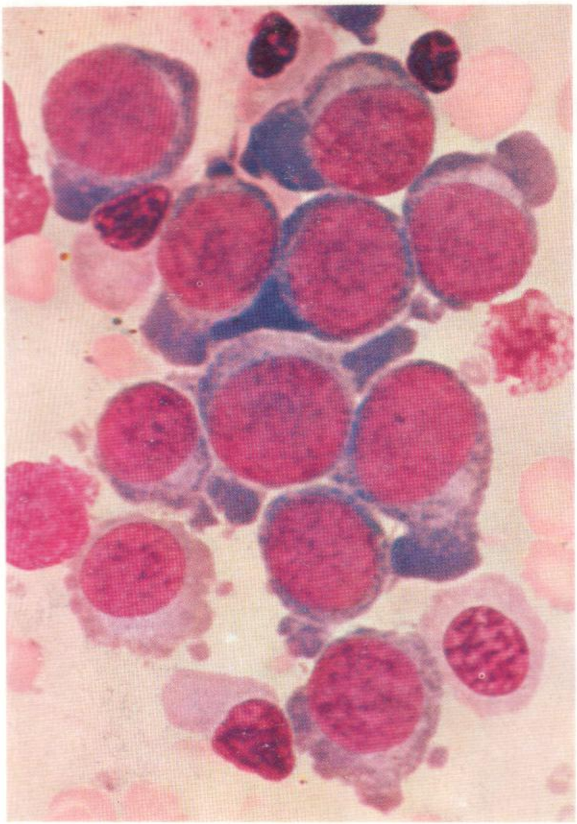

96

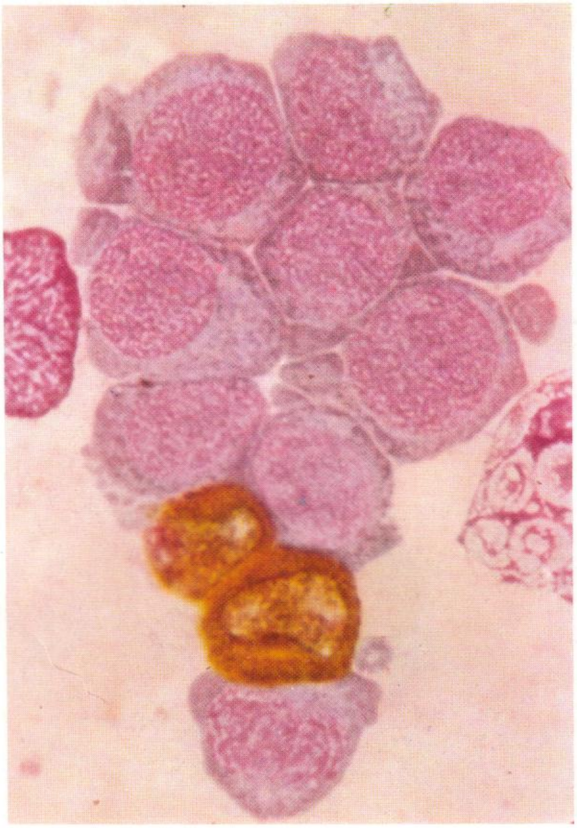

97

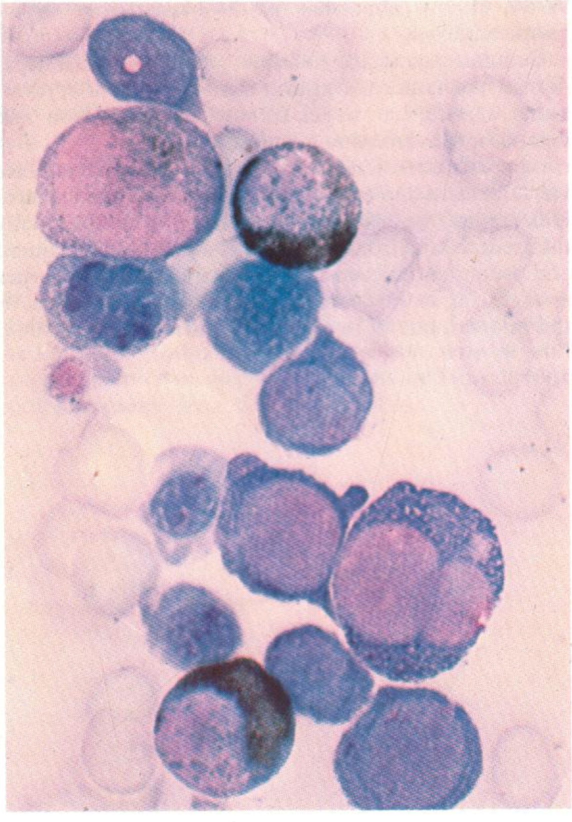

95. A group of proerythroblasts with some later erythroblasts of various stages of maturity surrounding them, from a patient with erythraemic myelosis. Mitotic abnormalities were not gross or frequent in this case, but erythroblasts vastly predominated.

96. Another example of bone marrow cytology in erythraemic myelosis. Although the cells are mostly proerythroblasts, they show a suggestion of megaloblastic change. Erythroblasts are always negative to SB and for peroxidase. This smear shows a peroxidase stain, with strong positivity in two neutrophils but a complete absence of reaction in the red-cell precursors.

97. SB stain on a further marrow aspirate from erythraemic myelosis. The erythroblasts are negative, while three granulocyte precursors show characteristic positivity.

98

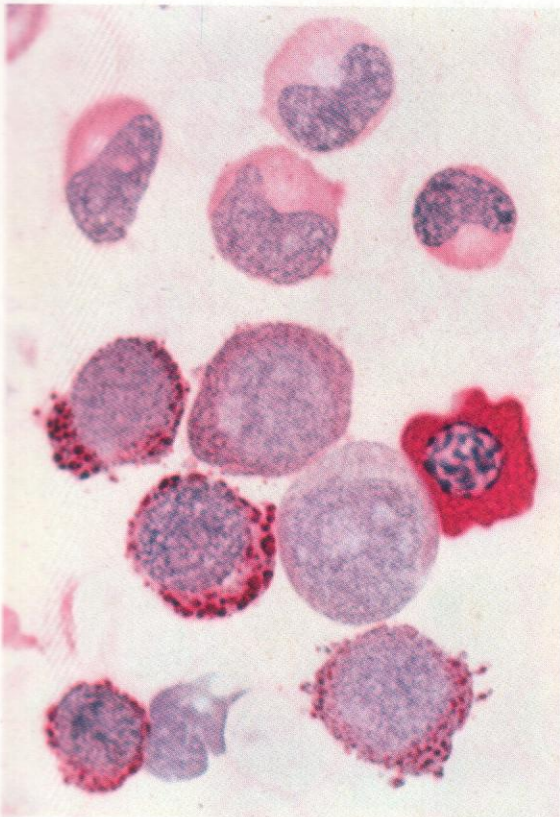

99

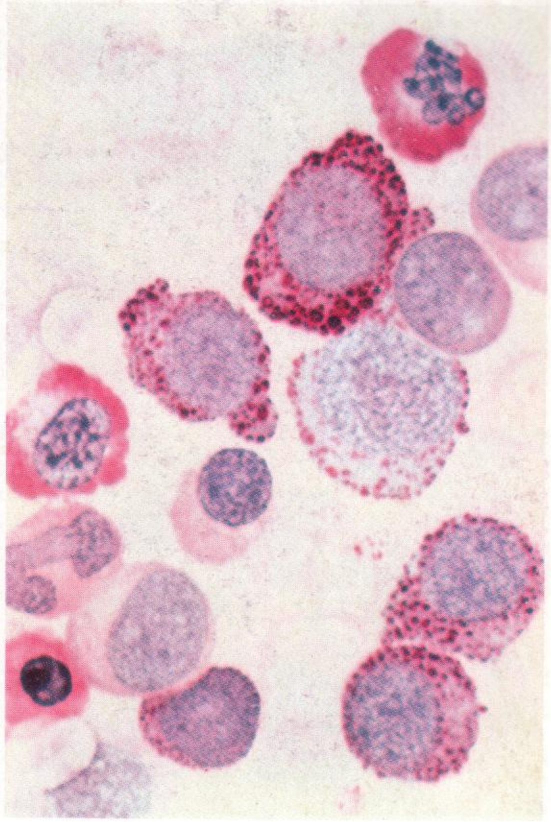

98 and **99**. Two examples of PAS positivity in erythroblasts from erythraemic myelosis. Coarse granular positivity is conspicuous in early erythroblasts, with diffuse positivity, sometimes very intense, in later erythroblasts. Both these fields contain granulocytes, four metamyelocytes at the top and a possible myeloblast next to the diffusely PAS-positive late erythroblast in **98**, and three myeloblasts or early promyelocytes and a stab cell in **99**. These cells show the expected pattern of PAS positivity for their respective stages of maturity, and their presence again demonstrates the existence of multilineage involvement in erythraemic myelosis.

100

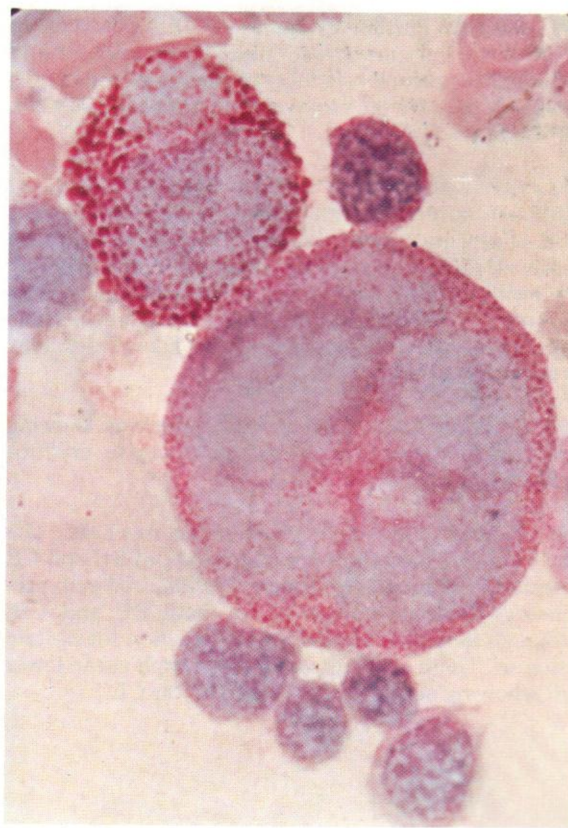

100. PAS positivity in two grossly abnormal giant erythroblasts from erythraemic myelosis.

101

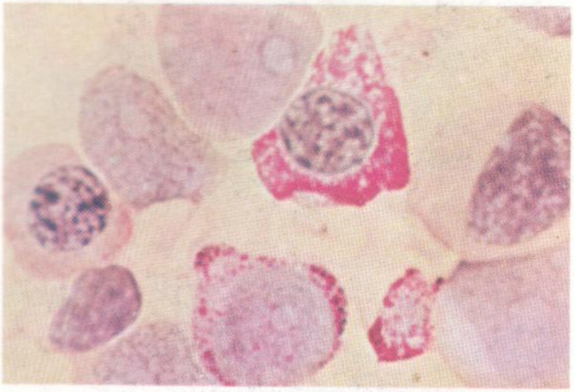

102

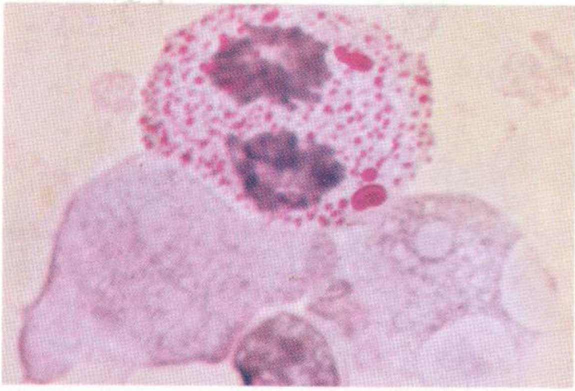

103

104

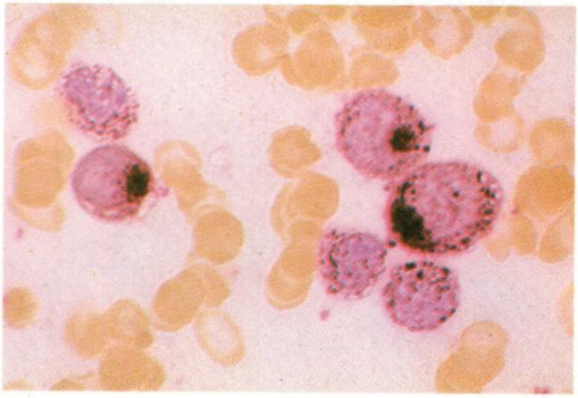

105

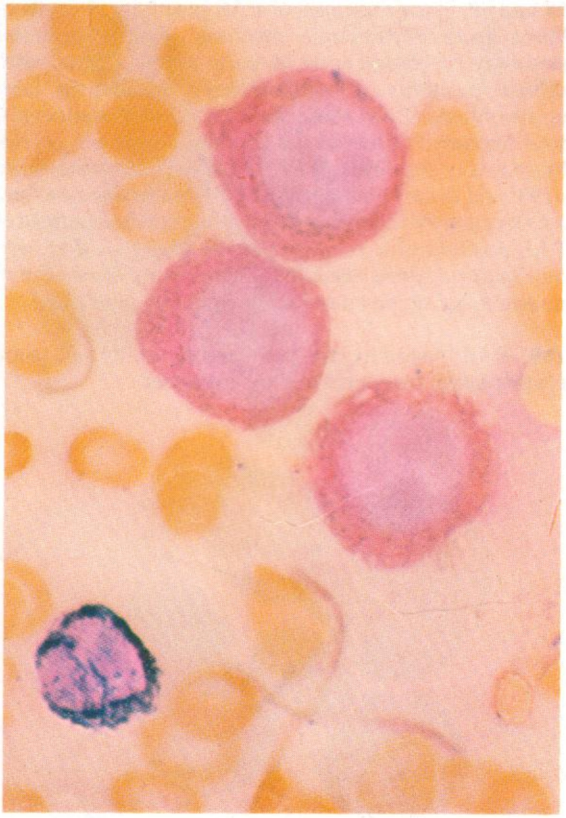

101 and **102**. Further examples of PAS positivity in erythraemic erythroblasts, one in mitosis. Early granulocyte precursors in these two fields show negative reactions, or, as in the promyelocyte in **102**, only a weak diffuse tinge of positivity.

103. Acid phosphatase in erythraemic myelosis. Although normal erythroblasts also show paranuclear acid phosphatase positivity, the reaction tends to be more marked in certain proliferative states, notably erythroleukaemias and megaloblastic anaemias. The enzyme in erythroblasts, unlike that in most other haemic cells but like the acid phosphatase enzyme in hairy cells, is tartrate resistant.

104. Another case of erythraemic myelosis showing even coarser acid phosphatase positivity in erythroblasts.

105. Double esterase in erythraemic myelosis. The early erythroblasts show a mixture of both BE and CE positivity, chiefly the former. Normal red-cell precursors are usually negative for both BE and CE, although they may exhibit a weak reaction for acetate esterase. There is a neutrophil polymorph at the lower left, showing normal strong positivity for CE.

106

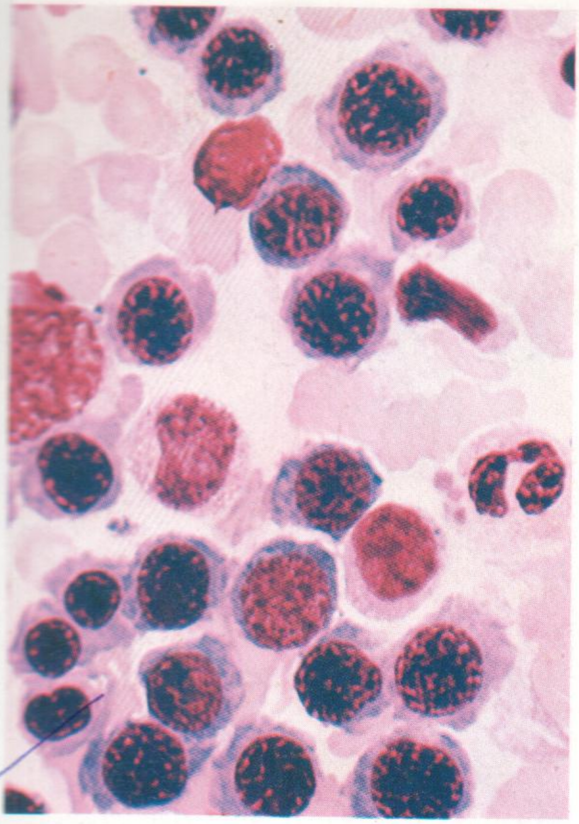

107

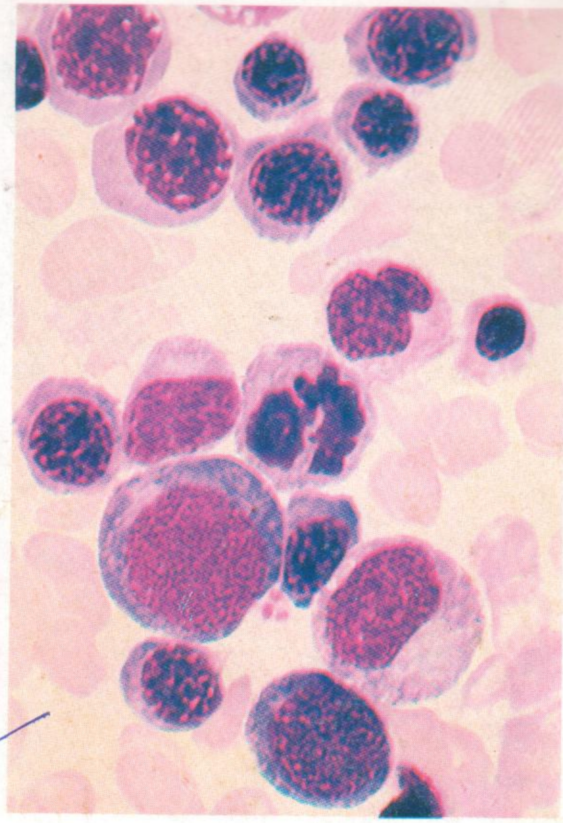

106 and **107**. Erythroblasts from the bone marrow in iron deficiency anaemia. Erythropoiesis is normoblastic, but the normoblasts tend to be small, with ragged outlines and defective haemoglobinization. The myeloid–erythroid ratio appears notably low in these fields, with few granulocytes present, but although this is often the case in iron deficiency anaemia, erythroid hyperplasia is not always conspicuous.

108. PAS positivity in the small and ragged late erythroblasts of iron deficiency anaemia. This is a frequent but not invariable finding in iron deficiency. Earlier red-cell precursors in this field show little or no positivity, while the two metamyelocytes and one stab cell present show the expected strong reactions.

108

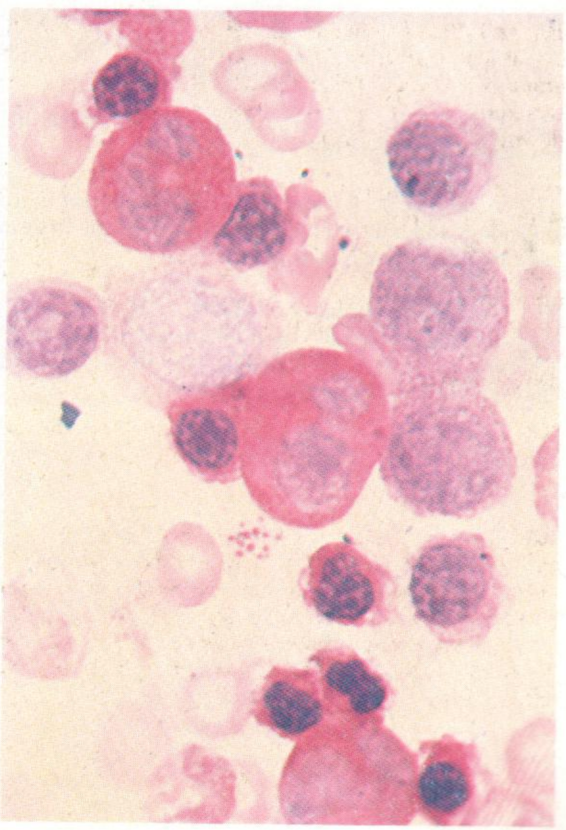

109

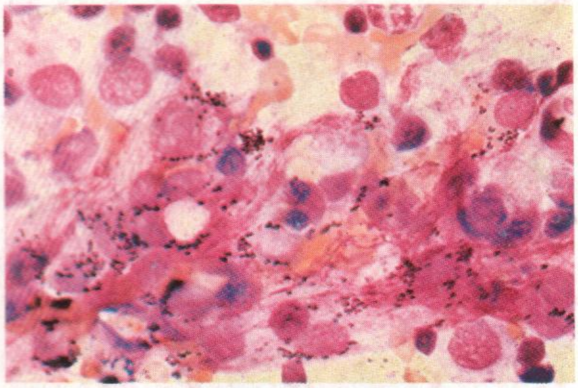

110

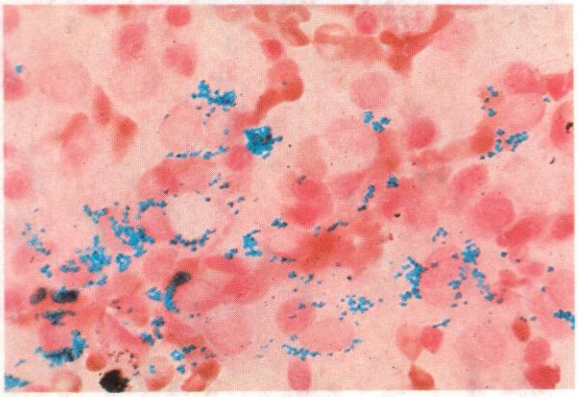

111

112

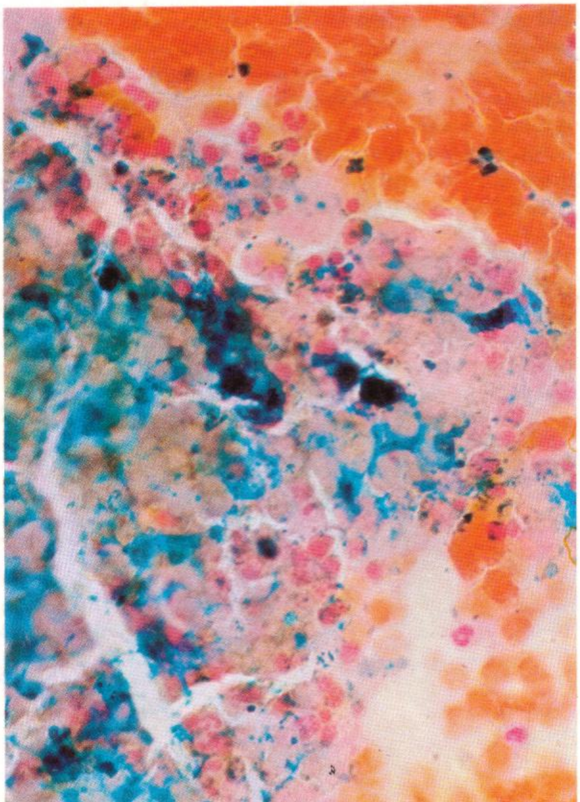

109. Leishman stain of a marrow fleck containing scattered brownish-black granules, probably mostly within reticulo-endothelial (RE) cells.

110. Consecutive free iron stain on the same field showing that the granules react for iron.

111. A cellular fleck from a bone marrow smear in iron deficiency anaemia, stained for free iron by the Prussian blue method. Free iron is absent.

112. A similar preparation from a patient with a sideroblastic anaemia and increased iron stores. (Normal subjects have stainable free iron in amounts midway between these two extremes.)

113

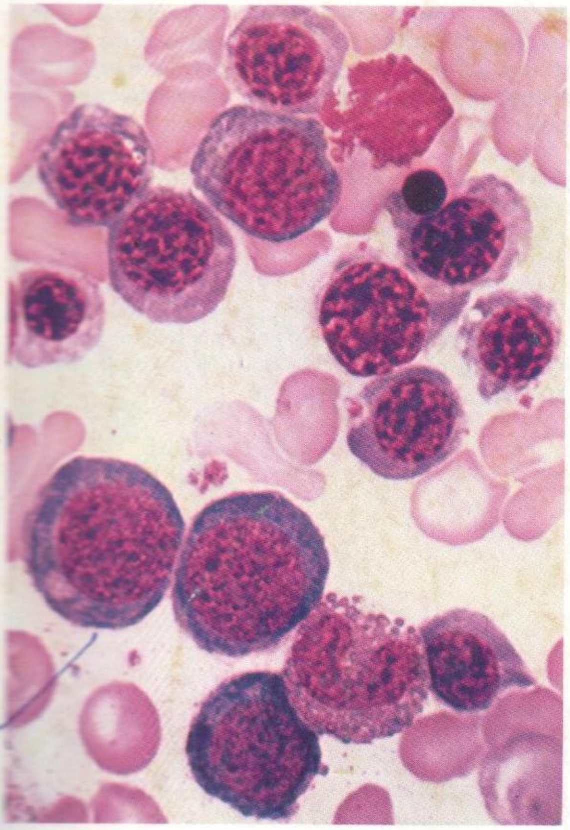

114

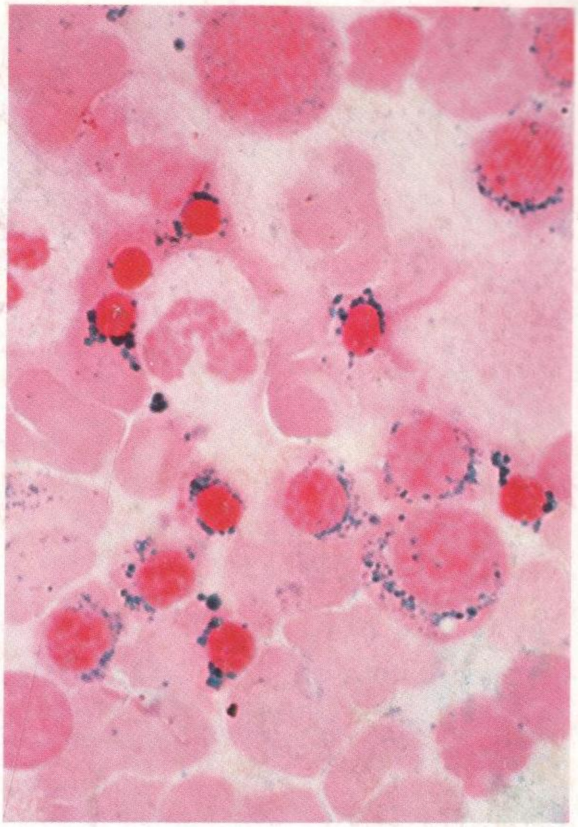

113. Leishman stain, bone marrow from a patient with sideroblastic anaemia. There is a suggestion of megaloblastic nuclear changes and irregular cytoplasmic staining in the erythroblasts.

114. A stain for free iron on the same marrow specimen, showing coarsely positive ringed sideroblasts – erythroblasts with free iron granules arranged as a continuous, or almost continuous, ring around the nucleus. This iron is chiefly concentrated in mitochondria.

115 and 116. Prussian blue stain for free iron, showing further examples of ringed sideroblasts.

115

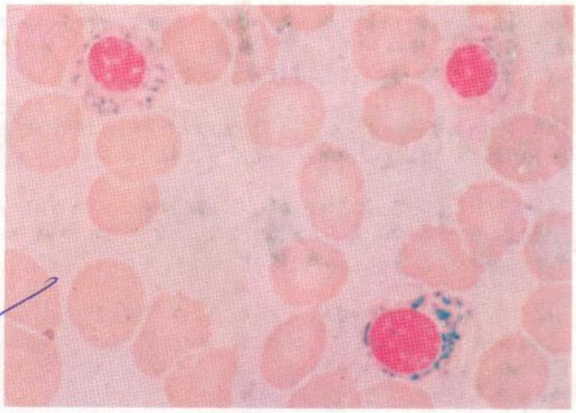

116

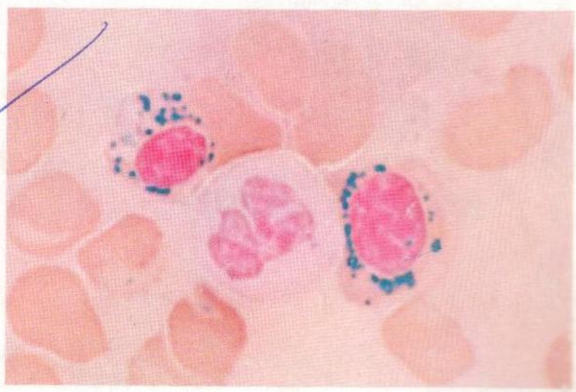

117

117. Free iron in erythroblasts (sideroblasts) with a non-ringed distribution. This example is of the 'normal' pattern of free iron distribution in erythroblasts, but the positive cells (sideroblasts) are more numerous than usual.

118. Consecutive reactions for PAS positivity and free iron in the marrow from a patient with refractory sideroblastic anaemia. There are ringed sideroblasts present and also granular PAS positivity in early erythroblasts.

Similar pictures may be seen in erythraemic myelosis, except that the iron tends to be less abundant and rarely in ringed form, and the PAS positivity is often stronger, especially in later erythroblasts.

118

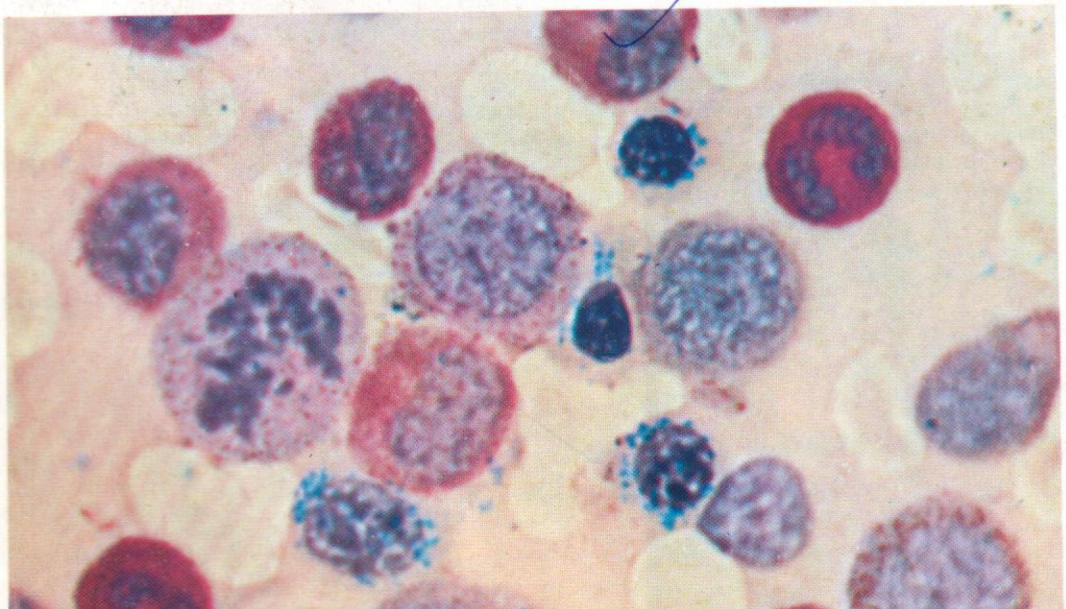

119

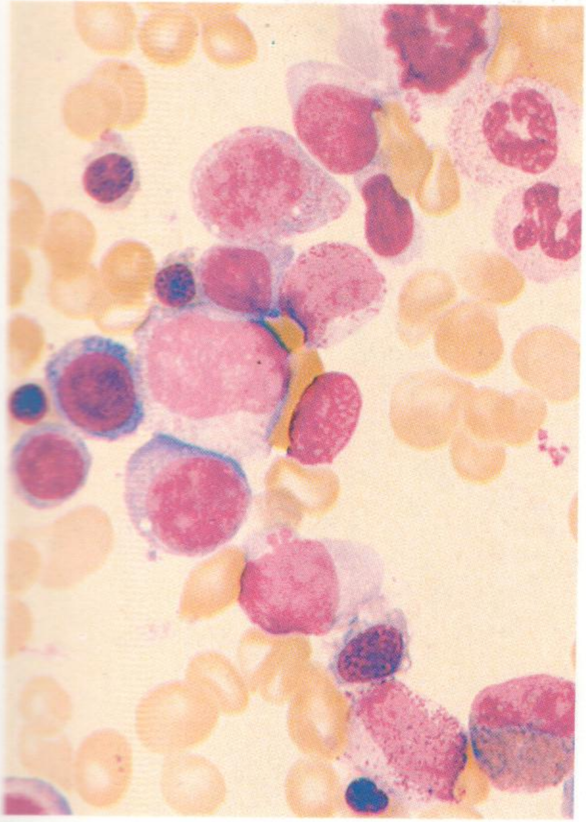

120

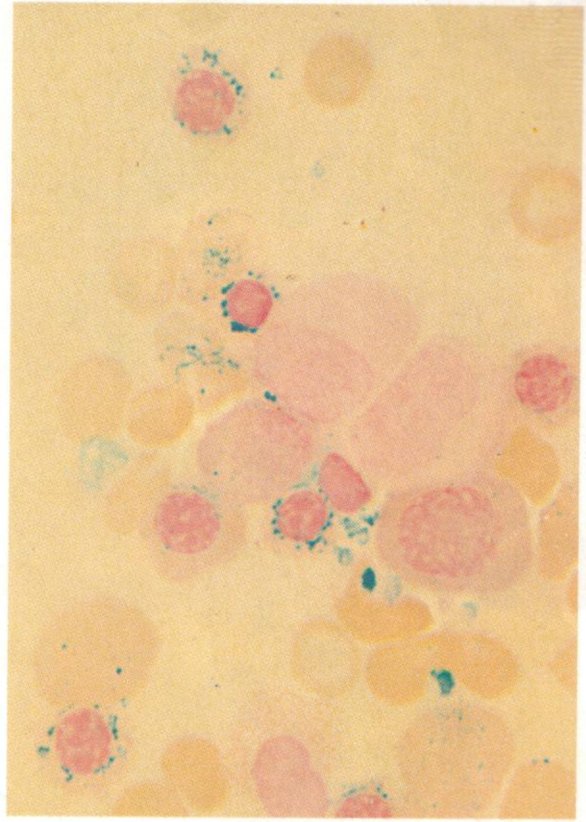

121

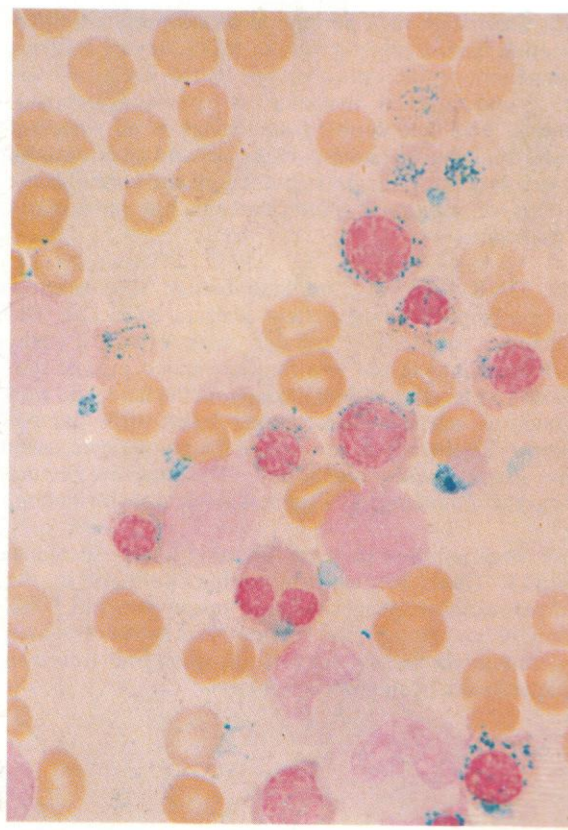

119–121. Smears of bone marrow aspirate from a patient who had presented with an apparent *de novo* acute myeloblastic leukaemia (AML), after remission had been induced by the DAT protocol of daunorubicin, cytosine arabinoside and 6-thioguanine.

The appearance in the Heyl-stained preparation (**119**) suggests return to normal haemopoiesis, with a range of apparently normal granulocyte precursors and a scattering of erythroblasts with no more than a slight degree of cytoplasmic vacuolation or staining irregularity to suggest possible dyserythropoiesis.

The Prussian blue stains for free iron (**120** and **121**), however, reveal the presence of numerous ringed sideroblasts and also siderocytes heavily loaded with particles of free (non-haem) iron. A late erythroblast is binucleated, providing further evidence of erythroid dysplasia. This cytological picture is now that of refractory sideroblastic anaemia (RSA).

The most likely explanation is that the initial AML was in fact secondary to a pre-existing MDS, and that the cytotoxic therapy has suppressed the acute leukaemic process, allowing the underlying chronic myelodysplasia to re-emerge.

122

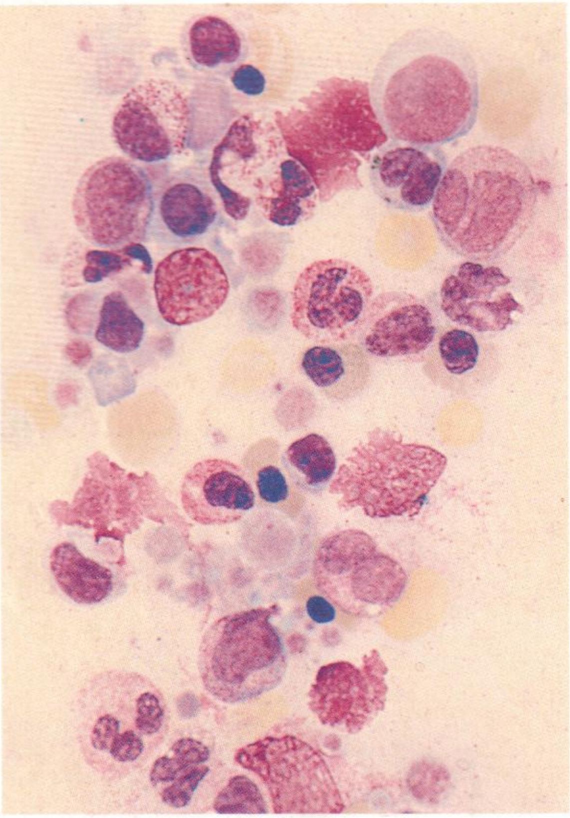

123

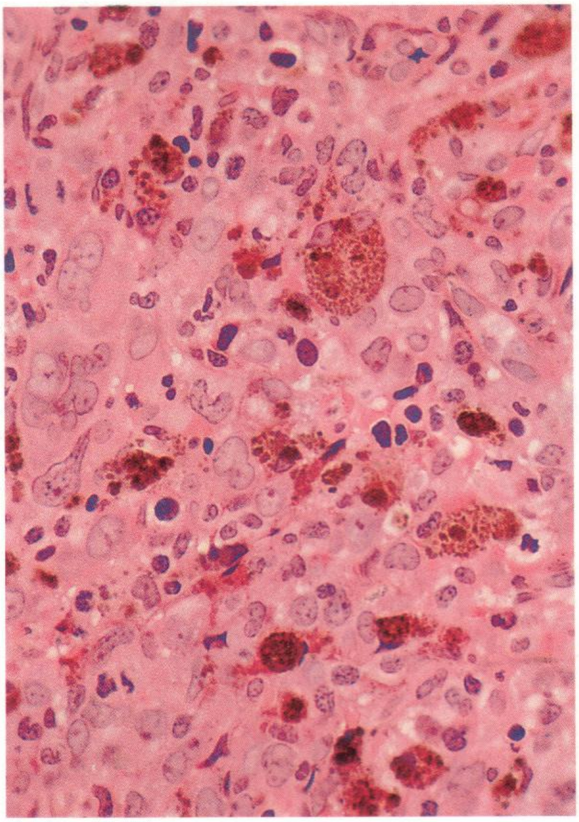

124

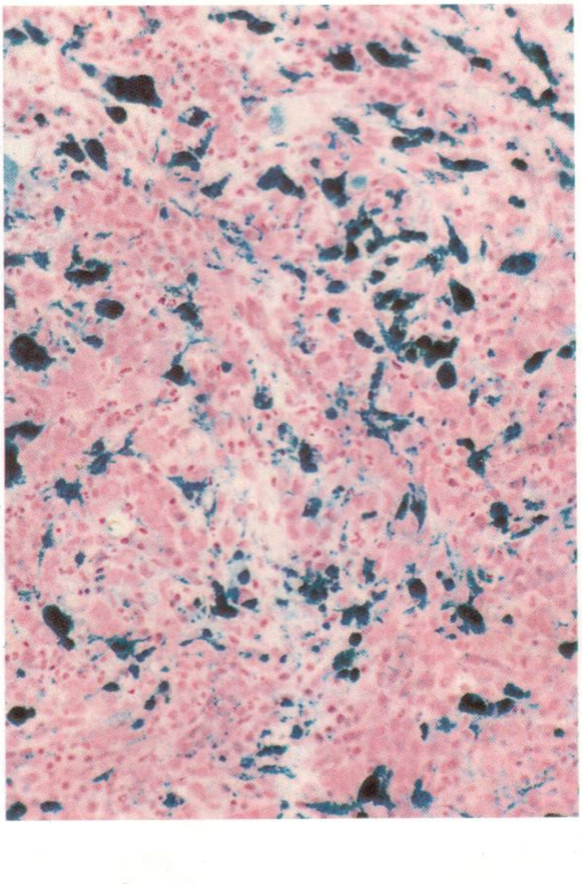

122. Heyl stain of a peripheral blood buffy coat preparation from a patient with an MDS, having a strong component of sideroblastosis but also an excess of blast cells, and marked evidence of dysmegakaryocytopoiesis. The field shows granulocytes at all stages of maturity, including several basophils and an eosinophil as well as neutrophils, and a number of late normoblasts; groups of abnormal giant platelets are particularly conspicuous.

123. H&E stain of a trephine biopsy bone marrow section from the same patient as featured in **122**. The specimen is intensely cellular, with primitive cells, including binucleated and multinucleated megakaryoblasts – widely distributed throughout the field, and with numerous macrophages heavily laden with haemosiderin. Erythroblasts and cells of the granulocyte series can also be easily recognized. This marrow picture suggests imminent trilineage leukaemic transformation.

124. Prussian blue stain on the same biopsy specimen as **123**. There is free iron as haemosiderin in the numerous macrophages, as seen in the previous H&E stain, but in addition, the erythroblasts can now be seen to contain the heavy rings of mitochondrial free iron characteristic of ringed sideroblasts.

125

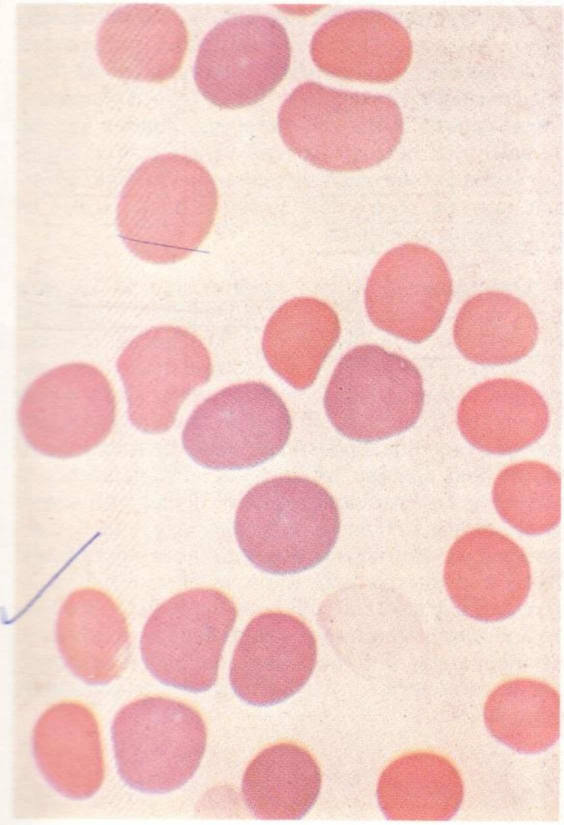

126

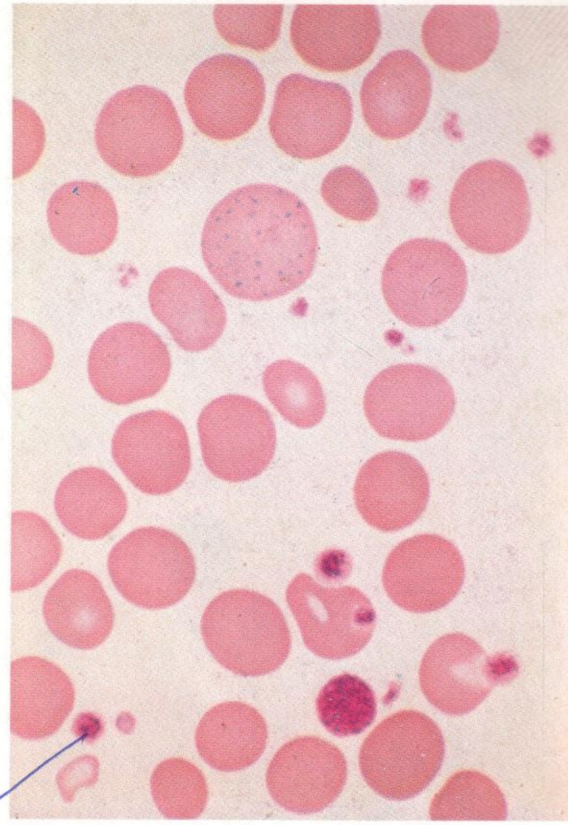

125–128. *Various appearances of reticulocytes.*

127

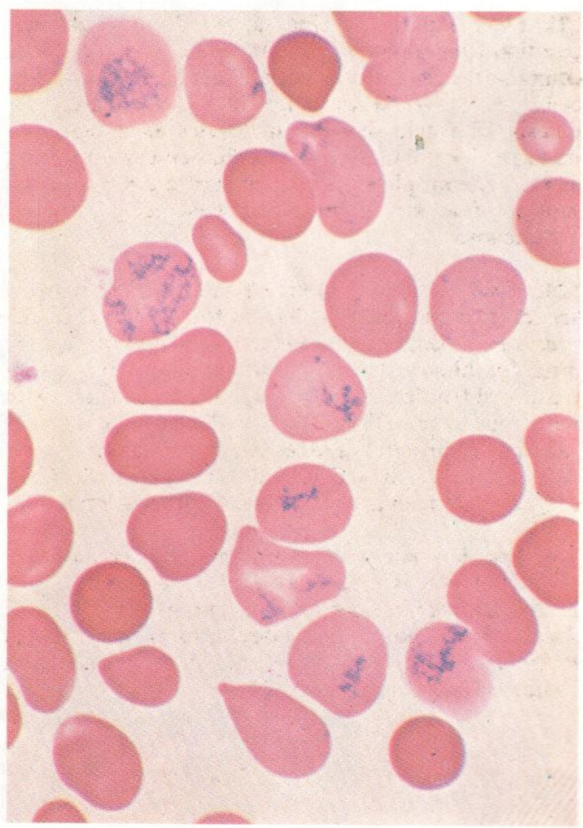

125. Polychromasia. In this Romanowsky-stained blood smear from a patient with a megaloblastic anaemia responding with a brisk reticulocytosis to B_{12}, the young red cells freshly released from the bone marrow appear a little larger than mature red cells and have a purple tinge to their non-nucleated cytoplasm. This colour results from a deficit in haemoglobin, still being synthesized, and a residuum of the earlier erythroblast cytoplasmic basophilia due to RNA.

126. Basophilic stippling. The same residual ribonucleoprotein may form discrete aggregated deposits to appear as basophilic stippling. This appearance is prominent in lead poisoning and in thalassaemias, but is also seen as a minor component of the reticulocyte response in other anaemias, as in this case of HS, with occasional small dense spherocytes contrasting with the stippled macrocyte.

127. Reticulin material after supravital brilliant cresyl blue staining with Leishman counterstain. This method of staining precipitates the residual RNA material to form a partially clumped network of blue-staining threads. Different stages of reticulocyte maturation have been recognized according to the quantity and disposition of the precipitated material, the earlier denser stages being generally restricted to the marrow.

128

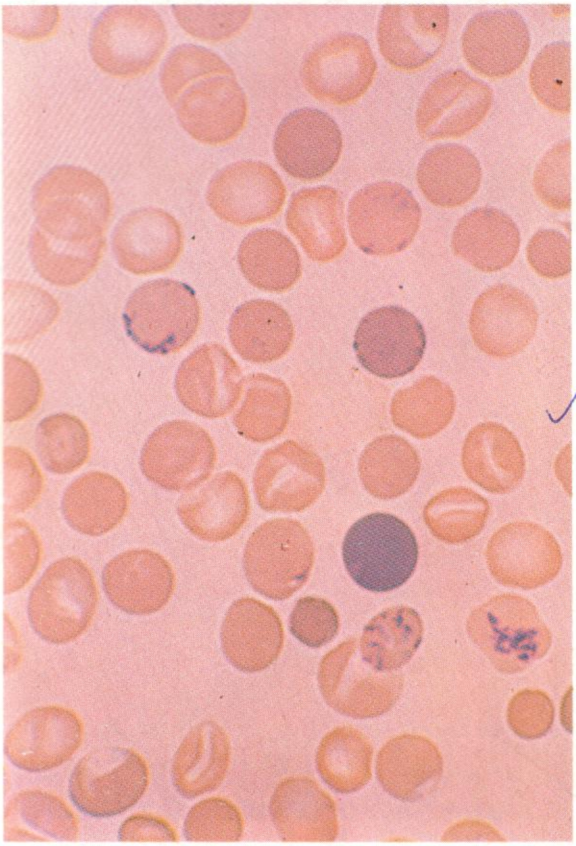

128. Reticulocytes stained supravitally, but uncounterstained. Some erythrocytes manifest a precipitated reticulin network, while several others in this field show a polychromasia with the cresyl blue dye, accompanying minimal deposit at the cell periphery. Among the red cells illustrated here are several with a central slit of pallor instead of the usual circular area – stomatocytes – which may be seen occasionally in many states of erythropoietic hyperplasia.

129. Gross reticulocytosis – approaching 80% – in a patient with haemolytic anaemia due to congenital pyruvate-kinase (PK) deficiency. This disorder involves a deficiency of the penultimate enzyme in the Embden-Meyerhof pathway of carbohydrate metabolism, which catalyses the transfer of phosphate from phosphoenol pyruvate to adenine diphosphate, with the formation of pyruvate and adenine triphosphate. PK deficiency is inherited as an autosomal recessive defect with severe lack of enzyme in homozygotes (usually, in fact, compound heterozygotes with a heterogeneous pair of allelic defects) and intermediate levels in heterozygotes. In severe deficiency the red cells have a greatly reduced life span and, despite intense erythropoietic hyperplasia in the bone marrow with the consequent high reticulocyte count illustrated here, the haemoglobin is commonly around 80 g/l.

129

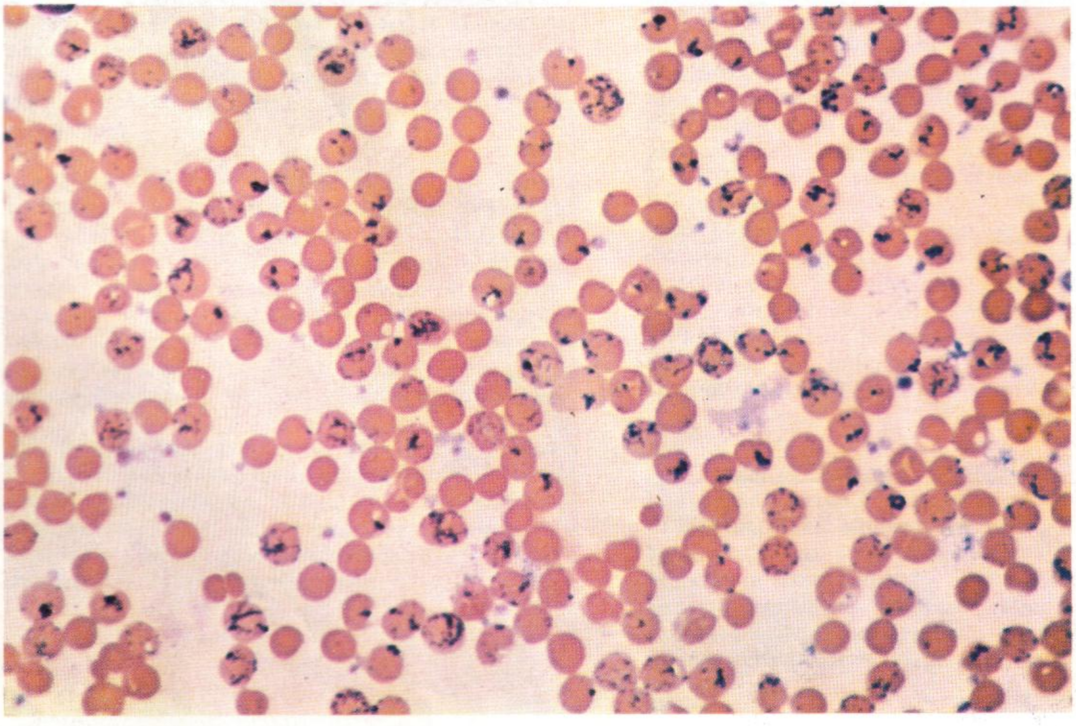

130

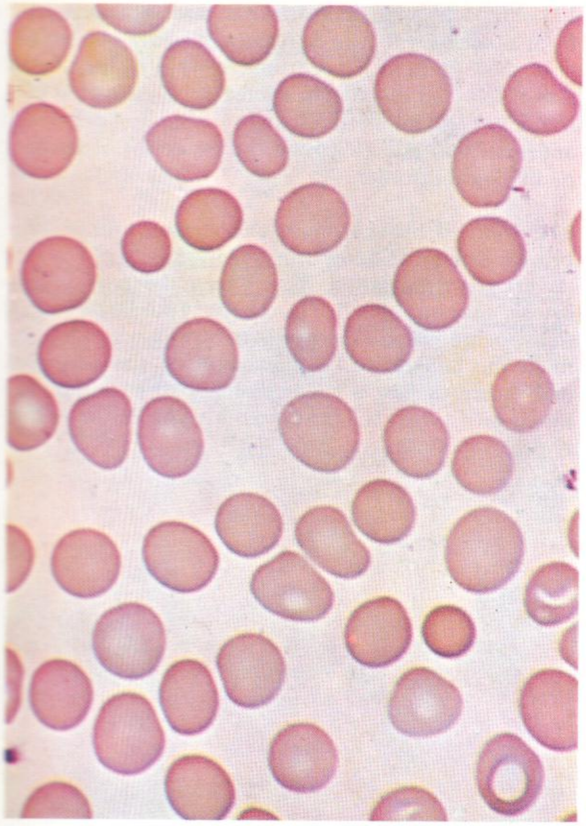

131

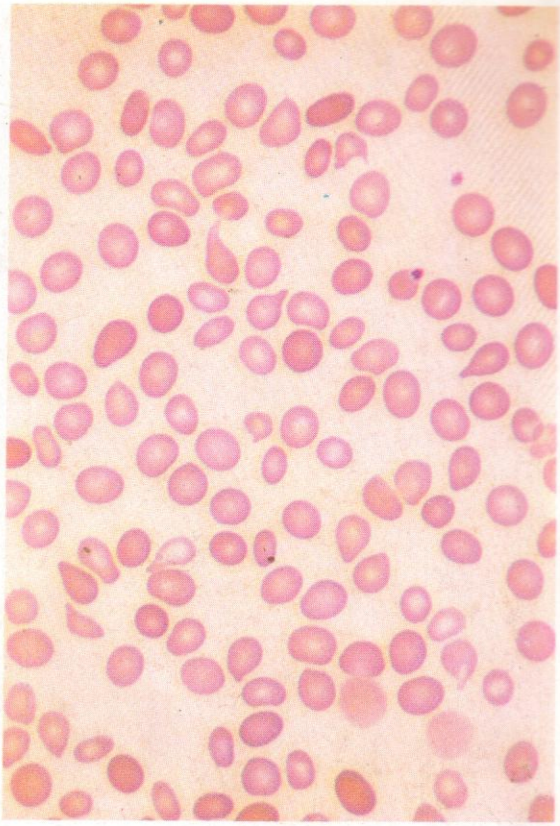

132

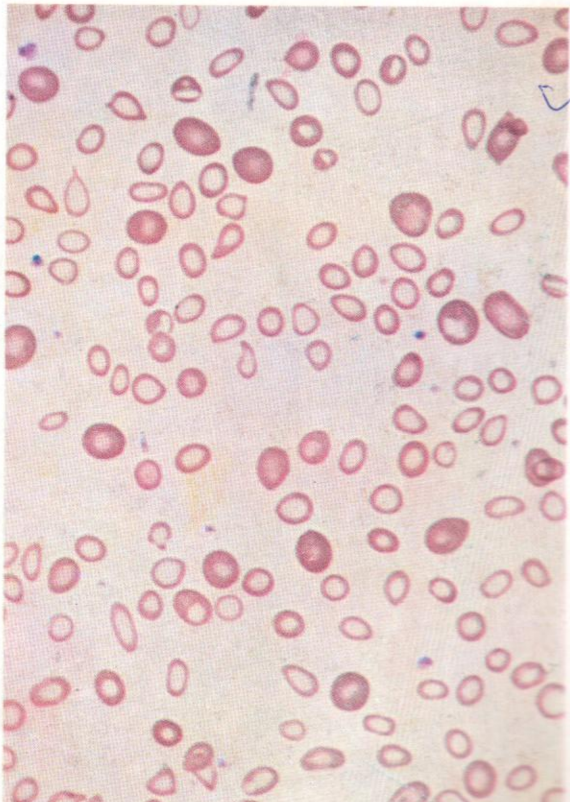

130. Anisocytosis. The red cells show variations in size. This smear illustrates minimal changes. Grosser anisocytosis is usually accompanied by other defects, such as poikilocytosis.

131. Poikilocytosis. The red cells show variations in shape. This smear also illustrates minimal changes, mostly of 'teardrop' character – dacryocytosis. Grosser poikilocytosis usually occurs together with other defects. Mild teardrop poikilocytosis of this sort may provide the first indication of emerging myelofibrosis or marrow infiltration with foreign cells as in metastatic malignancy.

132. Hypochromia and microcytosis – a general low-power view. A few cells stain normally and are of normal size (are normochromic and normocytic) but most have conspicuous central pallor (hypochromia) and small diameter (microcytosis). This is the picture of severe iron deficiency anaemia. The red-cell indices, MCV, MCH and MCHC, would all be much below normal.

133

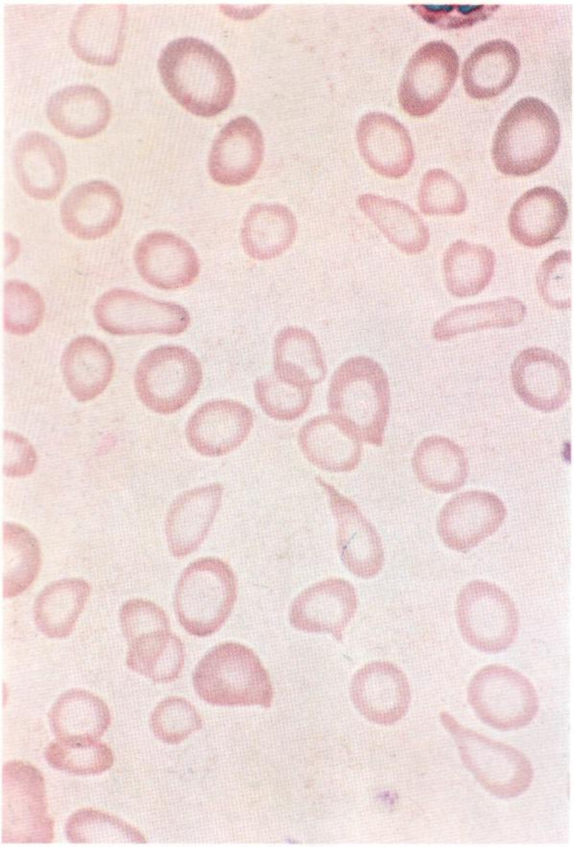

133. Hypochromia, anisocytosis and poikilocytosis; from a patient with iron deficiency anaemia. All the red cells show marked hypochromic central pallor. A few also display an elliptocytic or teardrop distortion of a frequency and kind often seen in simple iron deficiency anaemia, and not indicating the existence of another pathological disorder.

134. Marked hypochromia, anisocytosis and poikilocytosis. Where, as here, irregular fragments of red cells or very grossly distorted cells are seen, the term 'schistocytosis' may be applied. The relatively moderate degree of hypochromia and the extent of bizarre poikilocytosis make this unlikely to be an example of iron deficiency and rather suggest a haemoglobinopathy (despite the absence of target cells), or possibly one of the microangiopathic disorders.

134

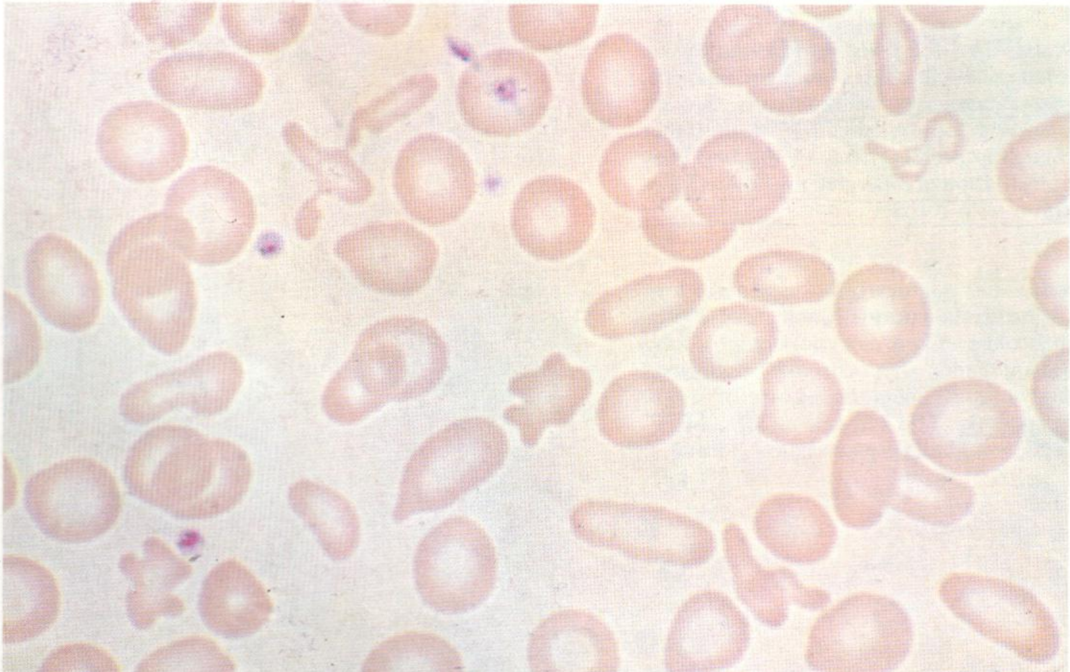

135

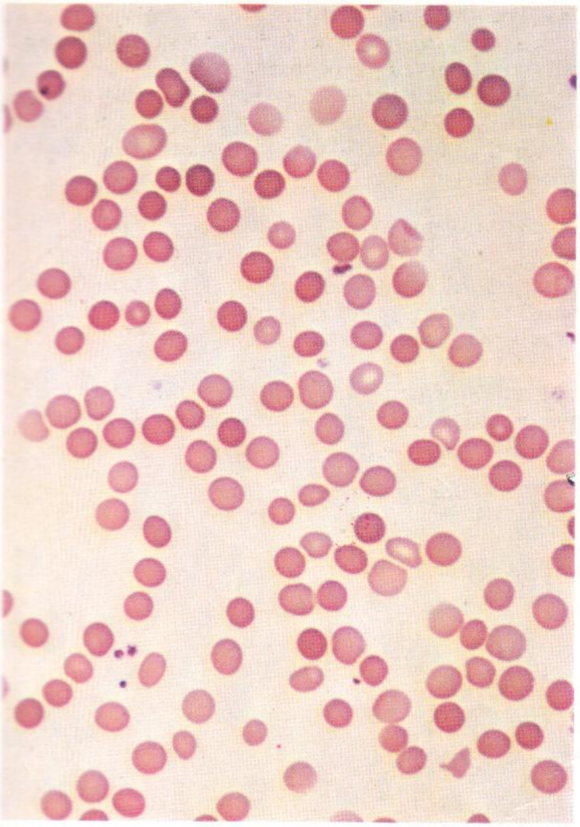

136

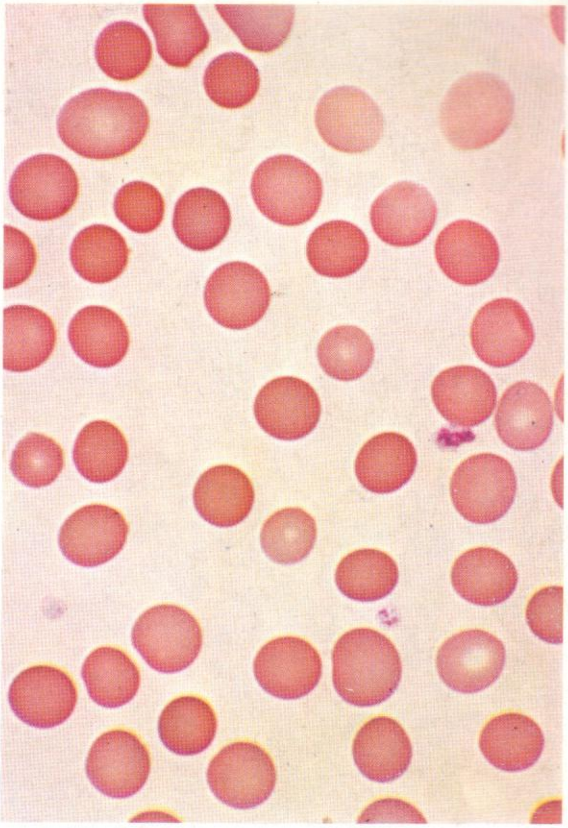

135 and **136**. Respectively low- and high-power views of spherocytes. These are red cells with more spherical shape than normal, recognizable in stained smears by their apparent small diameter and dense staining. More than half the cells in these fields are acceptable as normal; only the small, very deeply stained cells can be regarded with fair certainty as spherocytes.

137

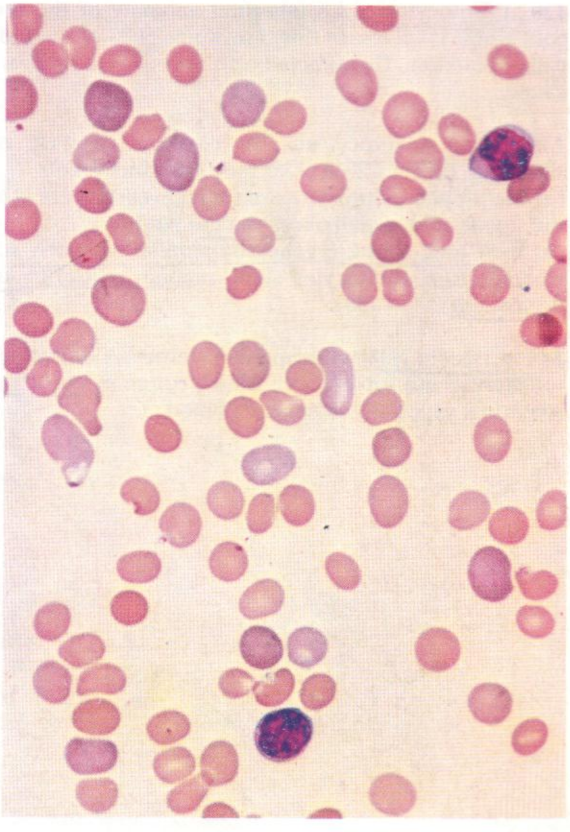

137. Anisocytosis due to a mixture of polychromatic reticulocytes and smaller spherocytes from a case of HS. Supravital staining with brilliant cresyl blue confirms that the polychromatic red cells contain residual RNA precipitable as a network, with an overall reticulocyte count around 60%.

138

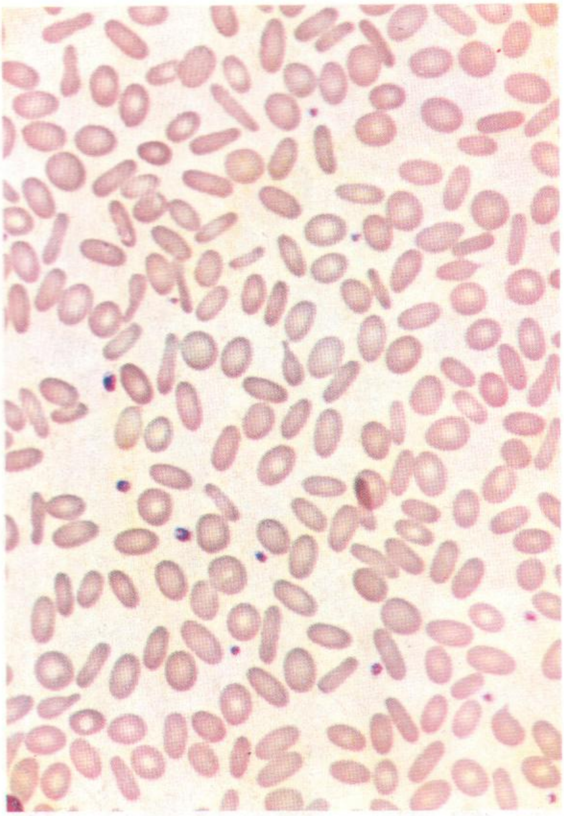

139

140

138. Elliptocytosis. An inherited anomaly of the red cells which involves, in this case, some 50% of the red-cell population. The affected cells appear oval or cigar-shaped.

139. Pseudo-elliptocytosis. A common artefact of smearing, recognizable as such by two chief points:
(a) the pseudo-elliptocytes are found in certain areas of the smear only, usually near the tail, and
(b) their long axes are generally parallel or nearly so, whereas true elliptocytes show random scattering of disposition (as in **138**).

140. Crescent cells – disrupted erythrocytes drawn out into a crescentic form. This is a fairly common artefact of smearing, especially in anaemic blood.

141

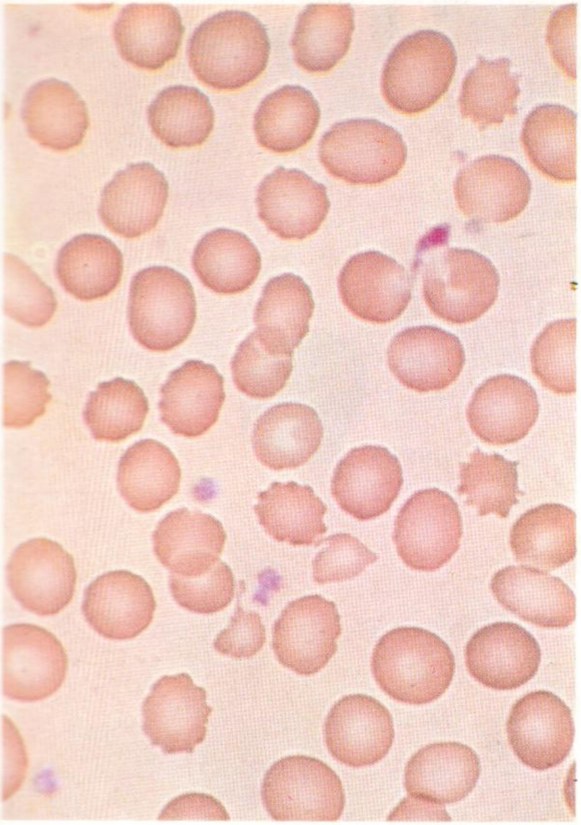

142

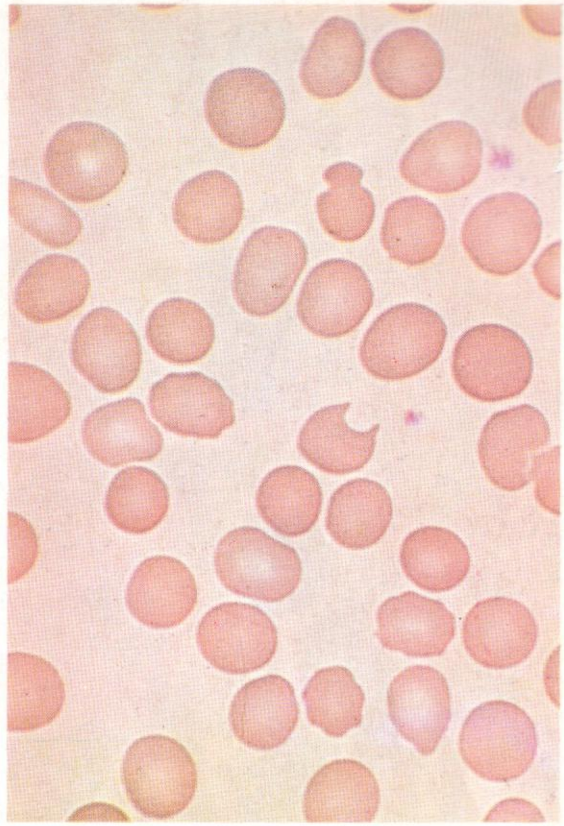

141. 'Crenation'. Crenated erythrocytes show an irregular undulation of the cell membrane in fixed smears. The appearance may be induced by exposing red cells to hypertonic saline or otherwise causing loss of fluid from the cells. *In vivo,* this defect usually accompanies other defects of size, shape and structure. When the feature is marked, as here, the term 'burr cell' or echinocyte may be applied.

142. Erythrocytes showing a tendency to crenation and also with evidence of physical damage or distortion involving the cell membrane, one red cell in the upper part of the field showing a constrictive defect so that it resembles a cottage loaf in section and a lower cell appearing to have lost a bite from the periphery. Probably both these defects result from mechanical trauma from fibrin threads.

143. So-called 'spur cells' or acanthocytes, showing some resemblance to crenated cells, but with sharper projections. They occur, often in association as here with fragmented schistocytes, particularly in uraemia and microangiopathy, but may also be seen after splenectomy and in abetalipoproteinaemia and malabsorptive states.

143

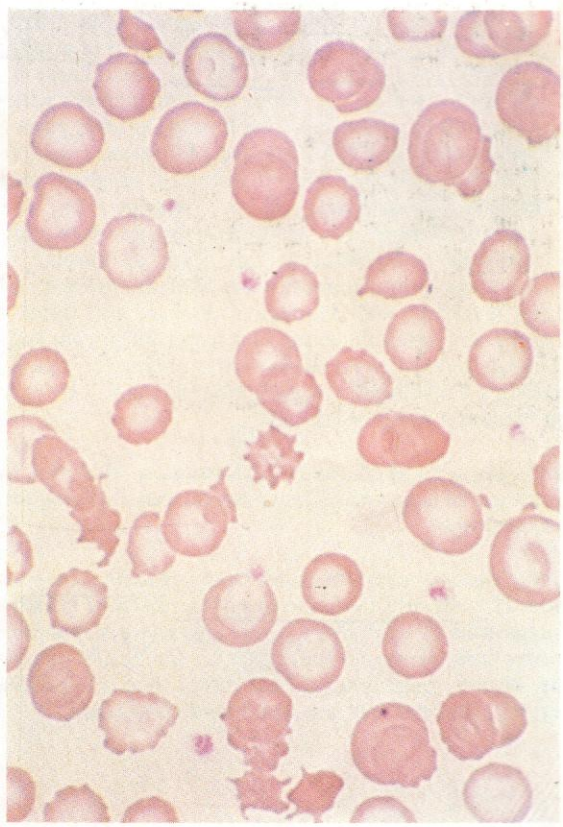

144

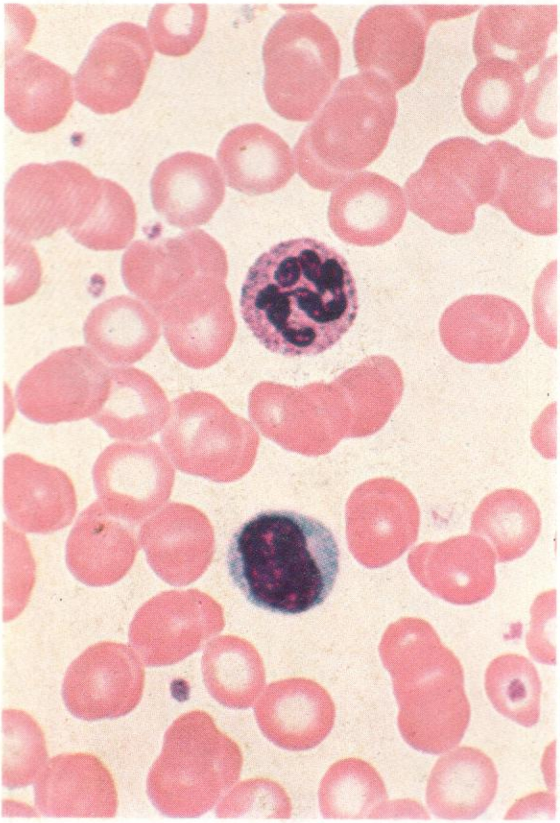

145

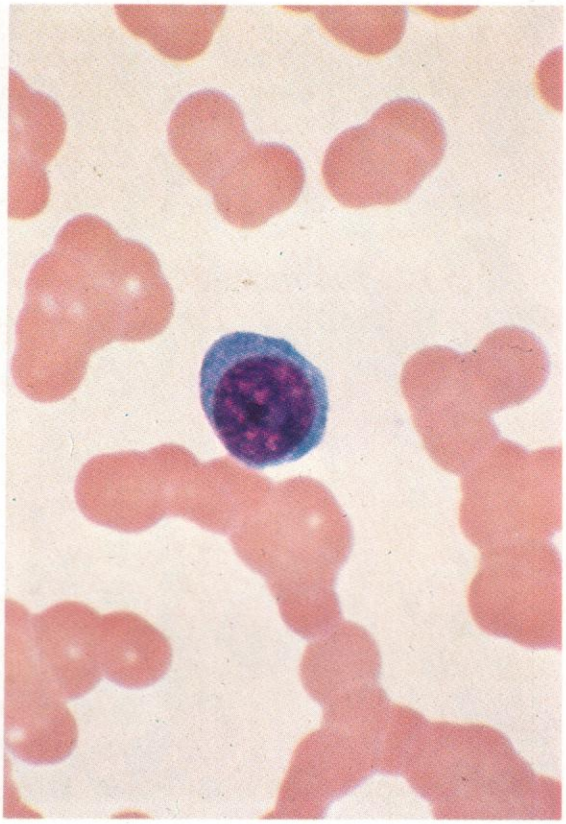

146

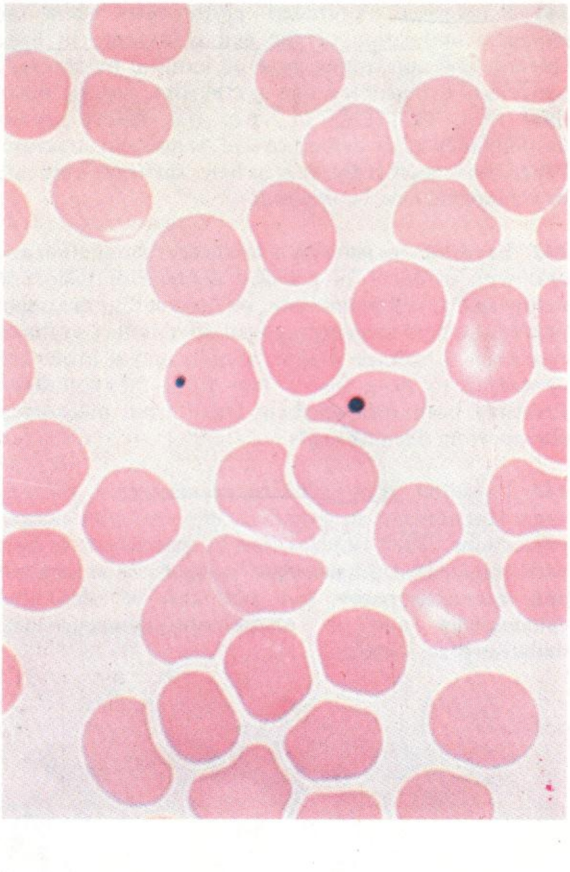

144. Moderate rouleaux formation; some hypochromia. Rouleaux are aggregations or piles of erythrocytes arranged like rolls or stacks of coins. There is a tendency for red cells to adopt this arrangement within the circulation and to manifest it in the thicker parts of blood smears, but the presence of rouleaux in areas where red cells are well distributed suggests some additional predisposing factor. Among the most important of these are conditions associated with a high erythrocyte sedimentation rate such as chronic inflammatory or malignant disease, as in the present slide from a patient with Hodgkin's disease, and states of hypergammaglobulinaemia and hyperfibrinogenaemia. The commonest cause of marked rouleaux formation is multiple myeloma, macroglobulinaemia or other monoclonal gammopathy.

145. More marked rouleaux formation; this and the presence of a plasma cell suggests the possible diagnosis of myeloma.

146. Macrocytic erythrocytes from pernicious anaemia, with Howell-Jolly bodies in two of them. There is a slight suggestion of ovalocytosis and anisocytosis, but most distortions of shape appear to be the result of compression by neighbouring cells rather than true poikilocytosis. The red cells are well haemoglobinized.

147

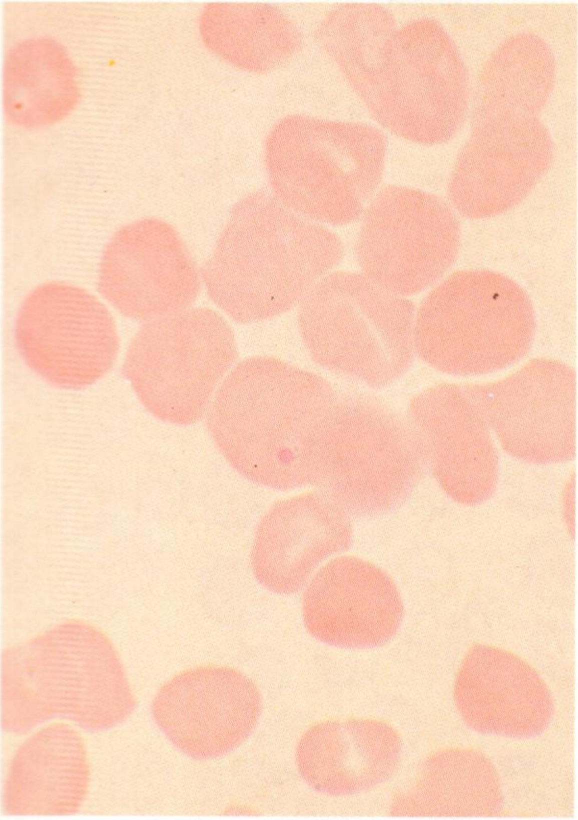

148

147. Romanowsky stain showing a Howell-Jolly body and a blue-staining siderotic granule or Pappenheimer body in the same red cell, from the peripheral blood of a patient with megaloblastic anaemia. The red cells are macrocytic, with an occasional stomatocyte.

148. A remarkable giant binucleated late erythroblast with polychromasia and coarse basophil stippling of the irregularly stained cytoplasm, in the blood of a patient with AML and megaloblastic erythropoiesis induced by a combination of purine and pyrimidine antimetabolite chemotherapy. Conspicuous basophilic stippling due to aggregates of RNA is a particular feature of erythrocyte pyrimidine-5-nucleotidase deficiency, whether congenital or acquired, as in lead or other heavy metal poisoning; its occurrence following the use of a pyrimidine analogue may indicate interference with the action of that enzyme and consequent failure to complete the breakdown of cytoplasmic RNA.

149. PAS reaction on a slide of bone marrow aspirate from a patient with glycogen storage disease, which arises as a consequence of congenital deficiency of alpha-glucosidase. Various granulocytes show substantially normal patterns of glycogen distribution, while a late normoblast in the centre of the field contains a single block of glycogen, resembling the localized PAS-positive vacuoles seen in lymphocytes in this disorder.

149

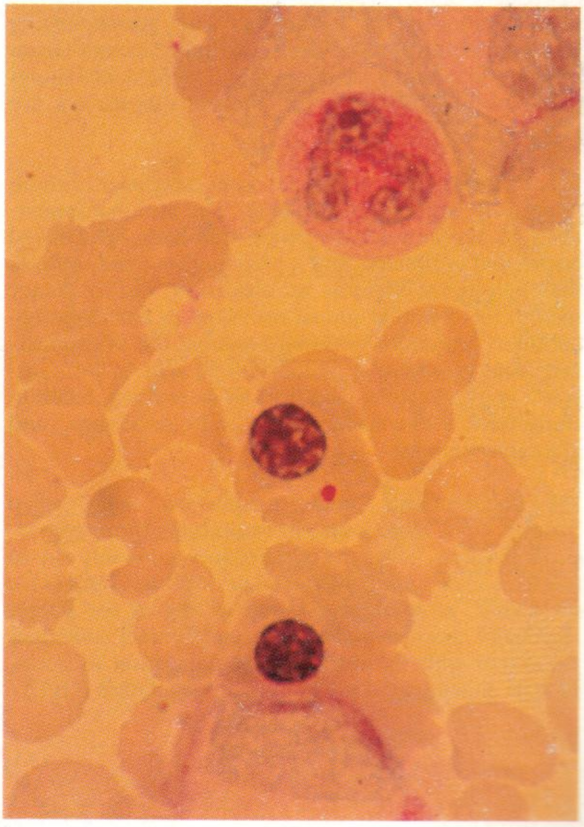

150

151

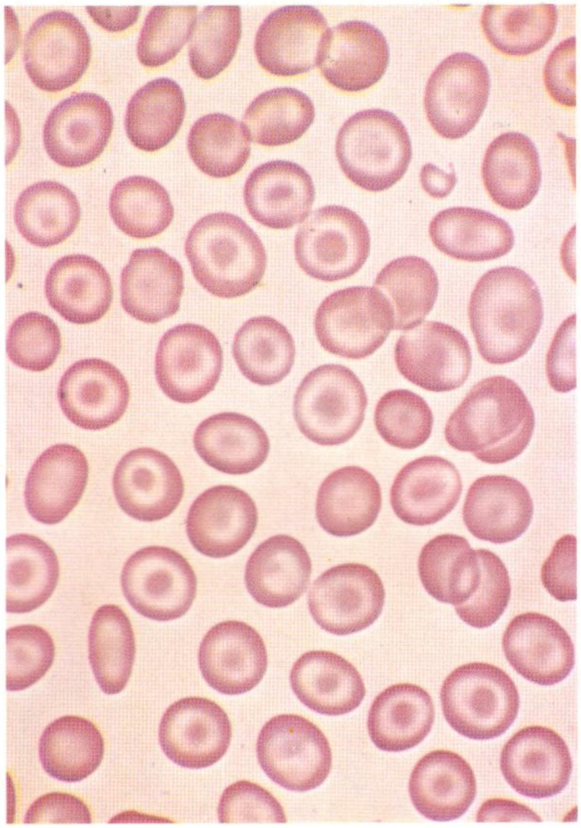

152

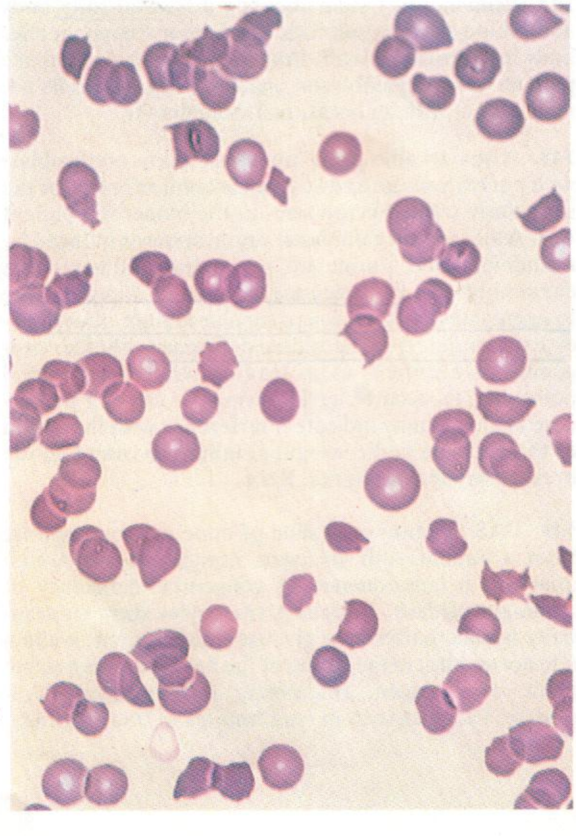

150. Target cells or codocytes, with accompanying anisocytosis and poikilocytosis, and hypochromia – from a case of beta-thalassaemia minor. The field also shows thin flat cells or leptocytes. Several elliptocytes are present.

151. Another field from the same specimen, where target cells greatly predominate. The striking appearance of these red cells, with well-haemoglobinized centre and periphery, and a pale ring between, reflects their bell-like or Mexican hat distortion. The frequency seen in this figure is almost restricted to haemoglobinopathies, especially beta-thalassaemia, but the appearance affects a smaller proportion of cells in liver disease, in obstructive jaundice, in hereditary lecithin-cholesterol acyl-transferase (LCAT) deficiency, and after splenectomy.

152. Poikilocytosis, with conspicuous sharp-angled 'helmet' cells, from a case of thrombotic thrombocytopenic purpura. This type of deformity, probably due to mechanical damage from forced passage through a fibrin meshwork, is commonly found in any of the microangiopathic haemolytic anaemias and in other conditions associated with the intravascular deposition of fibrin, such as disseminated intravascular coagulation (DIC).

Poikilocytosis c̄ helmet-cells

153

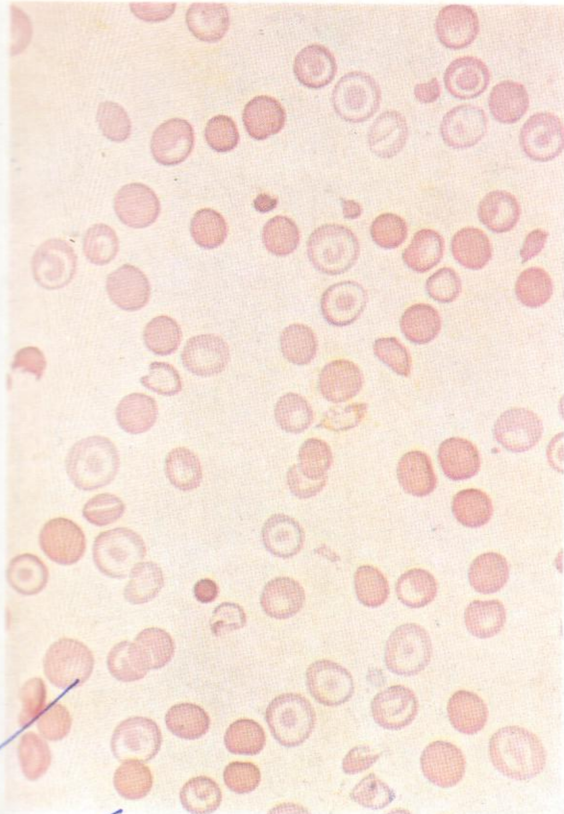

154

155

153. Target cells, macrocytes, spherocytes, schistocytes – including helmet cells – and small cell fragments, from a case of severe beta-thalassaemia.

154. Leishman-stained fresh fixed blood smear, from a patient with sickle cell disease. Elongated or sickled cells are rare, but anisocytosis and poikilocytosis, and target cells, are more common.

155. Sickle cells, drepanocytes, formed by exposing erythrocytes from a patient with sickle cell disease to the reducing action of sodium metabisulphite under a sealed coverslip. As the reduced HbS crystallizes within the cells, they all come to assume the distorted elongated sickle shape.

- Target cells – codocytes
- Tear drop cells. dacryocytes
- sickle cells – drepanocytes
-

156

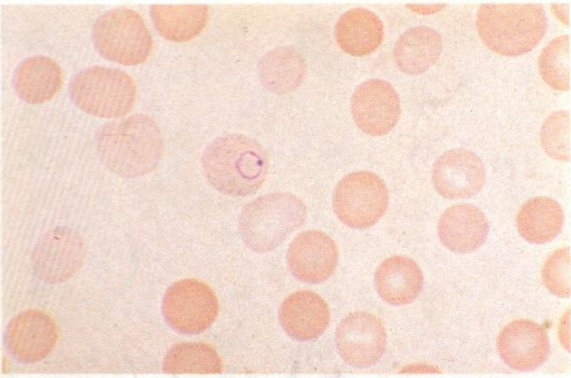

157

158

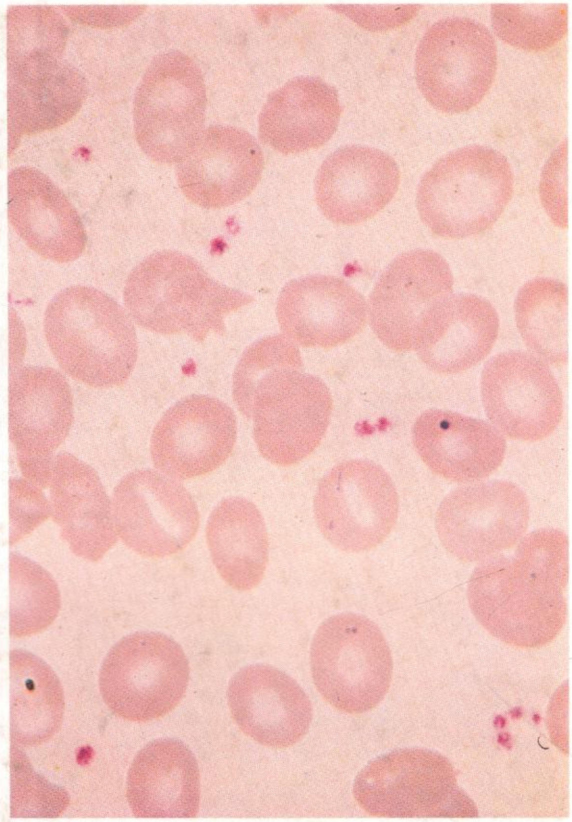

159

156 and **157**. Cabot rings, respectively round and in figure-of-eight form, in stippled red cells. They are probably an RNA or protein precipitation artefact of little diagnostic significance but should not be confused with malaria parasites.

158. Leishman-stained erythrocytes from a patient with haemolytic anaemia and increased iron stores. There is faint polychromasia present and also Howell-Jolly bodies. Granules of free iron are occasionally detectable. Several stomatocytes are present with elongated areas of central pallor.

159. Prussian blue stain for free iron on the same blood specimen as in **158**. Siderocytes (erythrocytes with free iron) are seen to be numerous.

—G6PD defi haemolytic Anaemia

160

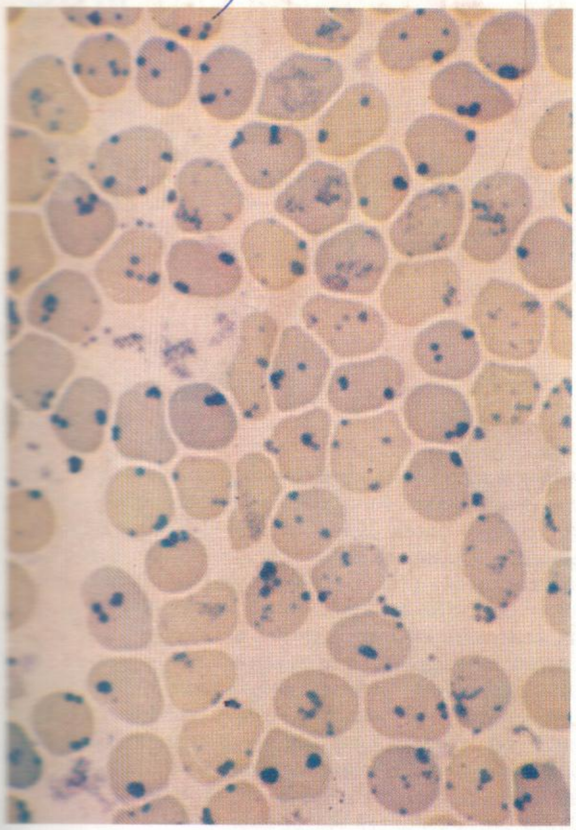

161

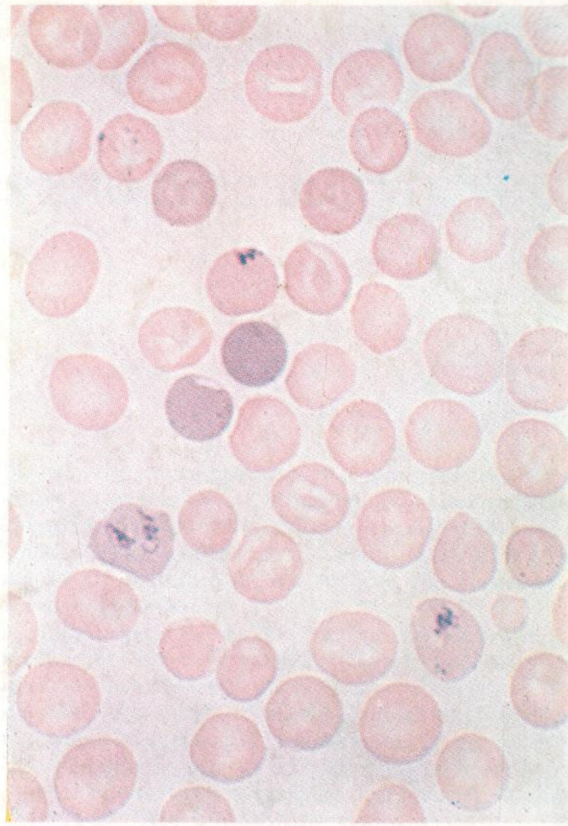

162

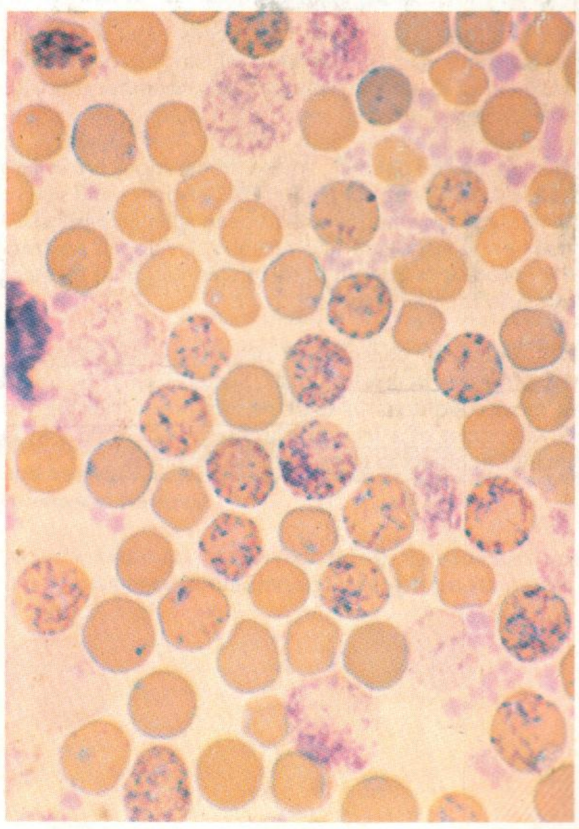

160. Heinz bodies in erythrocytes from haemolytic anaemia associated with deficiency of glucose-6-phosphate dehydrogenase. These bodies, shown here in a supravital methyl violet stain, are precipitates of denatured haemoglobin resulting from the lack of reducing enzymes. Heinz bodies appear to be firmly fixed to the cell membrane. They occur in small numbers normally, but are removed by the spleen, and thus some may be detected in most patients after splenectomy.

161. Uncounterstained preparation of red cells from alpha-thalassaemia exposed to cresyl blue stain for ten minutes – reticulocytes have taken up the stain.

162. A similar preparation from the same blood sample after an hour's exposure to stain. The multiple dotted positivity of 'golf-ball' pattern in many cells is that of haemoglobin H inclusions. A high proportion of the red cells in HbH disease contain tetramers of the beta chain which readily oxidize and precipitate as these inclusion bodies; but quite small numbers of cells with HbH can be detected by supravital staining and allow the diagnosis of alpha-thalassaemia variants with minimal HbH formation to be made.

163

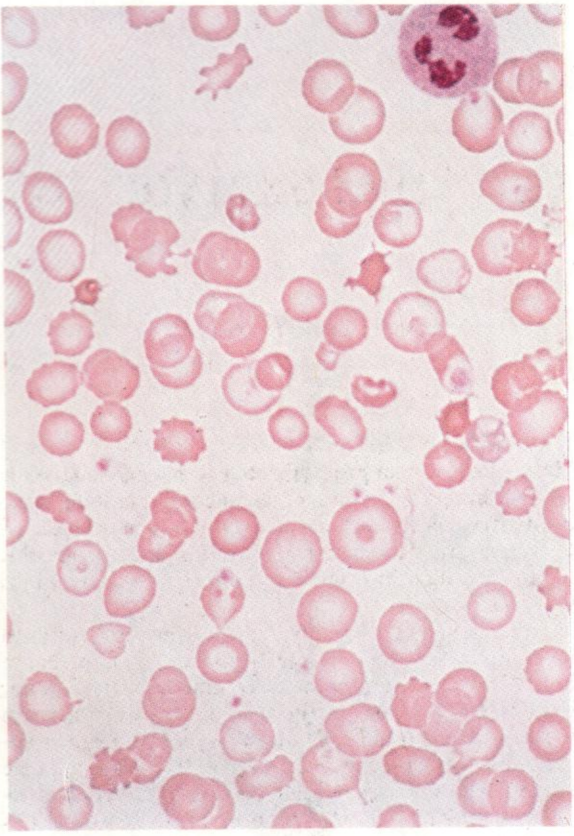

164

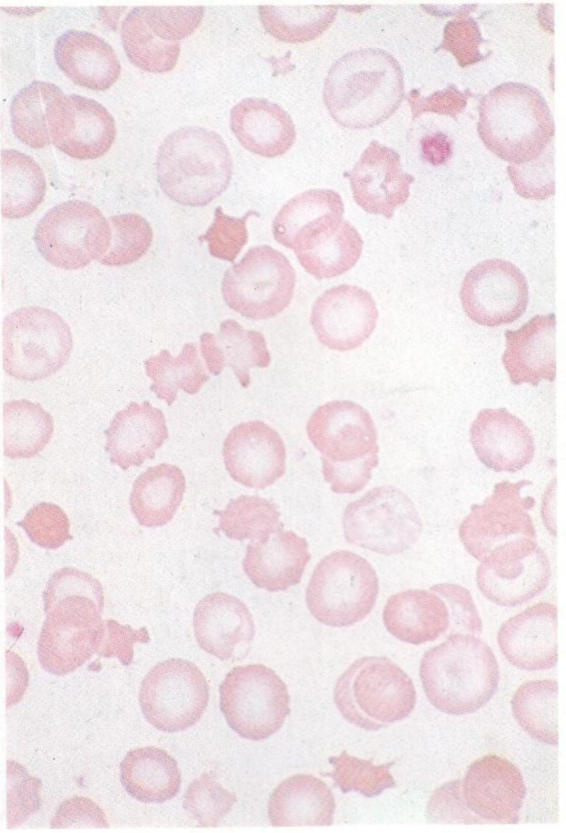

165

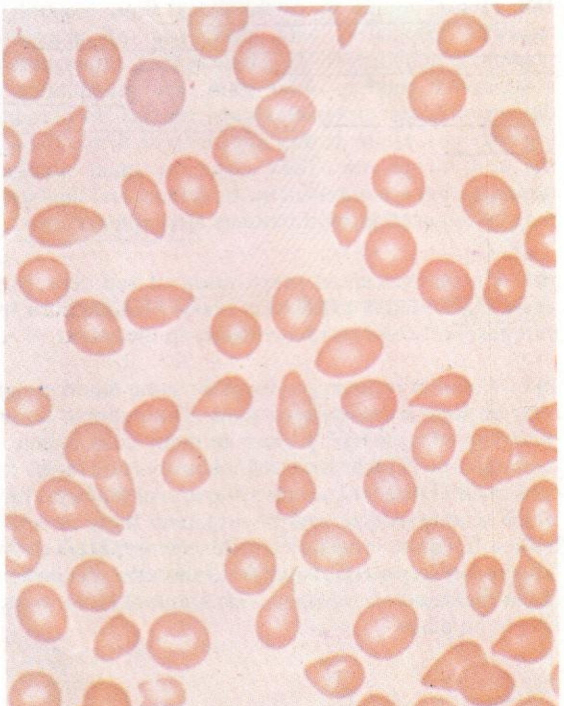

163 and **164**. Target cells, spur cells or acanthocytes with multiple sharp projections, schistocytes of irregular fragmented shape and 'sputnik' cells, acanthocytes with two or three elongated spurs. Such changes are seen in microangiopathy especially and may be conspicuous in splenectomized patients. These preparations are in fact from a patient with congenital PK deficiency and severe haemolytic anaemia, who had been splenectomized 20 years previously, and had recently developed obstructive jaundice as a result of the accumulation of pigment stones in the gall bladder.

165. Frequent conspicuous teardrop poikilocytes – dacryocytes – in myelofibrosis. Such cells may be found in most conditions of marrow infiltration causing the development of a leucoerythroblastic anaemia, and in smaller numbers in megaloblastic anaemias.

Part 2

Granulocytes, monocytes and megakaryocytes

Normal and abnormal forms

Although there probably exists a basic common progenitor or precursor cell for both myelopoiesis and lymphopoiesis, it is appropriate to group together the granulocyte, monocyte and the megakaryocyte-platelet series of cells because they share with each other and with the erythroblast series a less primitive functional stem cell in the bone marrow, and because they are frequently involved together in pathological processes.

The earliest recognizable cell of the granulocyte series is the myeloblast, which gives rise to a sequence of promyelocyte, myelocyte, metamyelocyte, stab cell and polymorph. From promyelocyte onwards 'specific' granules, neutrophil, eosinophil or basophil, become increasingly conspicuous in the cytoplasm and differentiate the common neutrophil granulocytes from the much less common eosinophils and the normally rare basophils. Mitoses may occur in immature cells up to the metamyelocyte stage, but there is now some evidence that the myelocyte may act as a secondary 'stem' cell for the granulocyte series, maintaining its own numbers and feeding cells into the maturation chain without normally requiring frequent replenishment from earlier precursors. In states of granulocyte hyperplasia and in granulocytic leukaemias this capacity is ineffective and earlier precursors derived from the primary stem cell preceding the myeloblast become more numerous.

Monocytes and their precursors – monoblasts and promonocytes – are present only in small numbers in normal marrow, and become conspicuous only in states of pathological proliferation or accumulation, notably leukaemias, and then nearly always in association with parallel involvement of the granulocyte line. The illustrations of monocyte precursors shown here are therefore mostly taken from leukaemic states.

Myeloblasts and monoblasts may be difficult to differentiate in Romanowsky-stained preparations, and may not always be easily distinguished from lymphoblasts or even from proerythroblasts in some leukaemic and erythraemic states. Cytochemical and immunocytochemical reactions will usually resolve such difficulties. Characteristic cytochemical patterns helpful in this regard are therefore included among the illustrations where appropriate.

Megakaryocytes usually present no difficulty in recognition, but their 'megakaryoblast' precursors are much smaller, and they too have similarities with other immature precursors of the myeloid series. Early but recognizable stages in the megakaryoblast-megakaryocyte line may be seen in idiopathic thrombocytopenic purpura and may occasionally be distinguished in acute myeloid leukaemia (AML); however, the earliest cells committed to this line, which are presumed by analogy to resemble the myeloblast and monoblast, cannot be certainly differentiated even by cytochemical means – although they may show peripheral periodic acid-Schiff (PAS) positivity at an early stage and also acetate esterase rather than butyrate esterase positivity, while ultrastructurally platelet peroxidase may be present and there may be immunocytochemical reactivity with antibodies to platelet glycoproteins.

The illustrations have been chosen to allow the range of appearances shown by different cell types to be appreciated and to allow frequent comparisons between cells of different lines or of different stages of maturity. The particular importance of cytochemical reactions among the cells dealt with in this section is emphasized, especially in the differentiation of the varieties of AML.

Disorders involving chiefly the granulocyte, monocyte and megakaryocyte lineages and their associated main cytological features

Acute leukaemias of myeloid origin. Leukaemias are clonal neoplastic proliferations arising from stem cells.

For the AMLs, the originating cell may be the general myeloid precursor, the CFU-GEMM, capable of giving rise to colonies *in vitro* containing granulocytes, monocytes/macrophages, erythroblasts and megakaryocytes; or perhaps the more narrowly committed granulocyte monocyte/macrophage precursor, the CFU-GM; or the corresponding erythroblast or megakaryocyte precursors, BFU-E and CFU-Meg, respectively. Pure erythroblastic or megakaryoblastic 'leukaemias' must be very rare, if they occur at all, since a predominance of these cells seems always to be accompanied by at least some neoplastic component of granulocytes and/or monocytes.

The causes of AML are still not determined, although activation or other functional change of proto-oncogenes, which normally play a controlling role in myelopoiesis, may be important in this regard, and may result from the chromosomal rearrangements that are readily demonstrable in about 50% of AML cases, and probably occur at a less easily recognized level in the remaining cases.

It is not surprising, given the complexity of bone marrow cytology, that many cytological variants of AML occur. They have been classified traditionally for the last 60 years or more according to the nature of the predominating cell in the bone marrow, and this approach formed the basis of the FAB subdivisions proposed by a group of French, American and British (FAB) haematologists in 1976, subsequently widely adopted. For AML the divisions are: M1, myeloblastic (>90% myeloblasts); M2, myeloblastic with granulocytic maturation (>10% promyelocytes or later granulocytes); M3, promyelocytic (either coarsely granular or microgranular promyelocytes predominating); M4, myelomonocytic (>20% granulocytes or precursors and >20% monocytes or precursors); M5, monocytic (M5a predominantly monoblastic, M5b with differentiation); M6, erythroleukaemia (>50% erythroblasts); and M7, megakaryoblastic (>50% megakaryoblasts). AML with minimal differentiation but positive antigenic markers may be grouped as M0.

This classification is based on arbitrary borderlines between the groups, and although broadly in conformity with the general usage of predominating cell classifications in the early 1970s it has two important defects. One concerns its failure to discriminate between monolineage (counting the progeny of the CFU-GM as of one lineage) and multilineage cases (with granulocyte/monocyte (GM) involvement but also erythroid and/or megakaryocytic). This may be of some importance in prognosis, with multilineage cases possibly surviving less well overall, although with advancing efficacy of treatment this difference may well diminish. Of greater significance, however, may be the different pathogenetic mechanisms active in producing, respectively, monolineage or multilineage disease, with either a different level of stem cell affected or a difference in stem cell expression dictated by biological controlling mechanisms. As biological activators such as colony-stimulating factors (GM-CSF etc.) come more widely into clinical use, different factors may well be found to have more appropriate use in monolineage and multilineage cases, respectively.

The second broad defect of the FAB classification is its undue reliance on Romanowsky cytology as an index of cell differentiation. Sudanophilia, often shown by maturing myeloblasts before azurophil granulation becomes evident in Romanowsky stains, is probably the best single prognostic factor in AML, apart from age.

Surface antigenic markers have not proved of great discriminatory value in AML, although positivity to the major GM markers (CD13 and/or CD33) helps to distinguish poorly differentiated AML from ALL (acute lymphoblastic leukaemia), and reactions with antibodies to glycophorin A or to platelet glycoproteins may further aid the recognition of erythroblastic or megakaryoblastic components.

Cytogenetic changes may well have pathogenetic significance and are of some prognostic value, t(8;21), t(15;17), inv(16), and trisomy 8 as an isolated defect, all having relatively good prognosis, t(v;11), monosomy 7, deletions of 7 or 5, and most multiple abnormalities, having a poor one, and other structural abnormalities having intermediate prognostic significance. However, differences of this kind tend to diminish as treatments become more effective. In any case, since some 50% of AML cases do not exhibit an obvious chromosomal abnormality, cytogenetic data do not at present provide a satisfactory basis for a general classification.

The authors have developed a simple classification of AML which takes these various considerations into account. Monolineage cases are grouped as Type I and multilineage as Type II. Each type is further split into A and B according to whether > or <50% of the leukaemic GM cells are sudanophilic. Type IA thus includes all t(8;21), inv(16) and t(15;17) cases, and may be of any FAB group from M1 to M5. Type IB, with little differentiation, includes most t(v;11), and again crosses the FAB groups widely from M1 to M5, excluding M3. Type II cases include most with poor prognosis cytogenetics, as well as FAB groups M6 and M7 and a proportion of all the remaining groups except M3.

Type I AMLs, including cases with the associated chromosomal defects listed above, are illustrated in parallel with other disorders affecting granulocytes and/or monocytes early in this section. Type II AMLs, with multiple lineage involvement, are grouped at the end of the section, with the myelodysplastic states which are mostly also clonal neoplastic disorders with multiple lineage expression.

The characteristic features of all these variants of AML are described in the respective captions to the relevant cytological and cytochemical illustrations, as are the features found in bone marrow aspirates and trephine biopsies during emerging remission or developing relapse.

Chronic myeloid leukaemia (CML). This disease is another clonal neoplastic state, probably arising in the

uncommitted pluripotential haemopoietic stem cell, but with differentiation expression initially confined to the myeloid cell lines. Some 85% of cases manifest the Ph chromosome, a short chromosome 22 resulting from a reciprocal translocation between parts of its long arm and the long arm of chromosome 9, t(9;22) (q34;q11), with the transfer of the c-abl oncogene from 9q to a site on 22q known as the breakpoint cluster region (bcr). The combined chimeric gene at this site produces an abnormal protein kinase, characteristic for CML. Most of the remaining 15% of cases with the cytological picture of CML – with a high leucocyte count and presence of granulocyte precursors in the blood, granulocytic hyperplasia of the bone marrow, frequent eosinophilia and basophilia, and a low leucocyte alkaline phosphatase (LAP) score in the neutrophils – show evidence that a morphologically inapparent translocation has occurred, with production of the bcr-abl chimeric gene, to the extent that the same abnormal protein kinase gene product as in Ph+ve CML can be detected and c-abl probes locate this oncogene at the bcr site on chromosome 22.

CML is well controlled by single agent chemotherapy, usually busulphan or hydroxyurea, for variable periods from a few months to many years, until a change in the pattern of disease happens, with malignant progression to hypoplasia, myelofibrosis, or an acute leukaemic picture, usually that of AML but occasionally ALL in type. In transformations to an AML-like state there is often an erythraemic and/or a megakaryocytic component, with a multilineage Type II cytology – although, sometimes, a more purely monolineage GM form (Type I) develops. At this stage further chromosome abnormalities are frequently found, notably one or more extra 9;22 translocations, structural anomalies of 17q, and trisomies of 8 or 19.

The haematological findings in both chronic and transformed phases of CML are illustrated in **320–374**, where characteristic features of histology, cytology and cytochemistry are further described in the captions.

Juvenile CML. This is a form of subacute neoplastic proliferation with features intermediate between the adult type of Ph+ve CML (which itself occurs in childhood, but only rarely) and a myelomonocytic acute leukaemia. This disease is not associated with t(9;22), but about 50% of cases show chromosomal abnormalities, much the commonest being monosomy 7. The cytology is illustrated in **375–383**, where additional descriptive material is included in the captions.

Myelodysplastic states (MDS) and other preleukaemic disorders. Among the conditions grouped together under the title of MDS are refractory anaemia (RA) and refractory anaemia with sideroblasts (RAS), both of which have been discussed and illustrated already in Part 1. The present section includes the remaining MDS variants, refractory anaemia with excess of blasts (RAEB), the same with a higher proportion of blasts and/or the presence of Auer rods – hence presumed to be closer to transformation to AML (RAEBt) – and, finally, chronic myelomonocytic leukaemia (CMML).

This nomenclature is that proposed by the FAB group for conditions described over many years under various names, which probably make up a broad spectrum of indolent or smouldering clonal leukaemic states, already associated with non-random cytogenetic abnormalities. The way in which these disorders evolve is erratic; transformation to a floridly leukaemic picture of multilineage (Type II) AML may occur in any of them, perhaps more commonly in RAEB and RAEBt, but many patients with MDS die from chronic anaemia, infection or haemorrhage without any such overwhelmingly blastic metamorphosis.

The histology, cytology and cytochemistry of RAEB and CMML are illustrated extensively in **560–565** and **569–594**. The distinction between RAEB and RAEBt is essentially a quantitative one, with up to 20% blasts in the marrow in the former and from 20–30% in the latter – although the presence of readily detectable Auer rods allows less blastic cases to be classed as RAEBt. Evidence of multilineage involvement in erythroblasts includes nuclear budding or rosette formation, multiple nuclei, sideroblastosis, megaloblastosis, and PAS positivity, and in megakaryocytes atypical mononuclear or multi-nuclear forms and either giant or micromegakaryocytes. Defective granularity in myelocytes and acquired Pelger-Huët nuclear anomaly in segmented cells provide evidence of dysplasia in the granulocyte series, while monocytes may show bizarre nuclear morphology especially in CMML.

Reactive changes in granulocytes and monocytes. Leucocytosis with increase in the WBC above the normal upper limit of 11×10^9/l occurs chiefly in infective and inflammatory states, with a reactive increase in neutrophils accompanied by a 'shift to the left', with a raised proportion of stab cells and polymorphs with few nuclear lobes. Occasionally, more immature precursors, metamyelocytes – or even an odd myelocyte – may be found in the peripheral blood. The neutrophils may show coarse darkly staining 'toxic' granules, and there may be bluish Döhle bodies visible in Romanowsky preparations in their cytoplasm, representing areas of hyperactive aggregated rough or smooth endoplasmic reticulum.

Leucopenias with granulocyte counts $<1.5\times10^9$/l are seen in states of primary or secondary marrow hypoplasia or aplasia, with generally defective myelopoiesis and associated anaemia and thrombocytopenia; however, selective neutropenia may occur in overwhelmingly severe infections, whether bacterial, viral, rickettsial or protozoal, and may proceed to agranulocytosis, with circulating neutrophils $<0.5\times10^9$/l. A similar selective neutropenia may result from sensitivity to certain drugs, including sulphonamides, anti-thyroid agents and some anti-convulsants.

Cytoplasmic inclusions of degenerating nuclear

material resulting from the action of an anti-nuclear factor (ANF) form a special feature of systemic lupus erythematosis (SLE), and are of cytological interest as well as providing a rapid diagnostic test, although their practical importance has been largely replaced by immunological testing for ANF. Examples are illustrated in **384** and **385**.

The reverse of the infective 'left shift' in neutrophils is seen in megaloblastic anaemias, where deficiency of B_{12} or folate leads to nuclear changes involving a 'right shift' with an increase in the average number of nuclear lobes in neutrophil polymorphs and the presence of some cells with six or more nuclear lobes, macropolycytes or hypersegmented neutrophils.

Eosinophilia, with blood levels over $0.5 \times 10^9/1$, may be seen as a familial anomaly, but occurs as a reactive phenomenon – especially in skin disorders, allergic states, and parasitic infestation – and has additionally been found with associated myalgia in patients taking dietary supplements of L-tryptophan. Basophilia, with counts over $0.2 \times 10^9/1$, may also be seen in some allergic or inflammatory states, although it is relatively uncommon.

Monocytosis, above the normal upper level of $1 \times 10^9/1$, may occur in more chronic infective states or in those due to non-pyogenic bacteria, viral or rickettsial infections and some protozoal or other parasitic infestations. A reactive monocytosis may also be seen in some auto-immune disorders and collagen diseases, and in some cases of disseminated malignancy.

Congenital anomalies and acquired parallels. Although many anomalies of leucocytes have been described, most are very uncommon; only the four most important are described and illustrated here.

The **Pelger-Huët** nuclear anomaly occurs as a rare benign familial inherited disorder (**387**), but it is seen very commonly as an acquired or 'pseudo' form in many cases of myelodysplasia and both acute (e.g. **215**) and chronic (**388**) myeloid leukaemia.

The **May-Hegglin** anomaly, like the Pelger-Huët anomaly, is a generally benign condition inherited as an autosomal dominant. It is associated with the formation of large oval or crescentic basophilic inclusions (**394** and **395**) in the cytoplasm of granulocytes and occasionally also of monocytes. These represent a special type of inclusion material rather than an aggregation of normal cytoplasmic structures, and are thus essentially different from Döhle bodies. Giant platelets may also be found in this anomaly, and there is sometimes thrombocytopenia and leucopenia.

The **Alder-Reilly** anomaly, which may occur in association with various mucopolysaccharidoses, involves the development of coarse azurophilic granules in the cytoplasm of granulocytes (**389**). The material of the granules is derived from the mucopolysaccharide and resembles basophil granules somewhat, in reacting metachromatically with toluidine blue.

The **Chédiak-Higashi-Steinbrinck** syndrome is a rare inherited disease, usually fatal in early life, with severe cytopenias and a lymphoma-like clinical picture, associated with remarkably large cytoplasmic granules in various tissue cells – including many leucocytes of blood and bone marrow, especially granulocytes (**398**). These coarse granules are probably lysosomal in nature. Pseudo-Chédiak inclusions may develop as an acquired phenomenon in some acute leukaemias, notably cases of AML with the 8;21 translocation (**211** and **213**).

Platelet disorders. While qualitative defects of platelets are best detected by platelet function tests and are not reliably recognized by changes in platelet morphology, quantitative changes – thrombocytopenias and thrombocytosis or thrombocythaemia – are associated with characteristic cytological findings, not only in terms of numbers of circulating platelets but also with regard to the cytology of megakaryocytes and the process of thrombopoiesis as observed in marrow smears and sections.

Thrombocytopenia, with reduction in circulating platelets below $150 \times 10^9/1$, arises in most instances from one or two broad causes: defective formation of platelets (as in primary or secondary aplastic or hypoplastic states, including the effects of myelotoxic chemotherapy and some less common drug sensitivities), and increased destruction of platelets in the peripheral circulation and spleen (arising generally from auto-immune sensitization of platelets, rendering them liable to phagocytosis by macrophages). The former type of thrombocytopenia is associated with a reduction or absence of megakaryocytes in the bone marrow – an amegakaryocytic thrombocytopenia – whereas, in the latter, megakaryocytes are generally plentiful and often increased in numbers, although they may appear cytologically unusual in having immature nuclear features and defective granularity, with often prominent glycogen inclusion bodies and few peripheral platelets (**467–473**).

Thrombocytosis, with counts over $500 \times 10^9/1$ occurs as a component feature of many states involving marrow hyperplasia, from iron-deficiency and haemolytic anaemias to acute infections. It may also be a feature of disseminated malignancy. This type of platelet increase is a secondary or reactive phenomenon of no great clinical significance.

A more severe and persistent increase in platelets, often to over $1000 \times 10^9/1$, occurs in essential thrombocythemia or megakaryocytic myelosis, a chronic neoplastic myeloproliferative disorder which appears to be largely confined to the megakaryocyte-platelet line. Thrombocythemia of similar degree may also be seen in multilineage proliferations, especially polycythemia vera, but also occasionally in CML. In all these conditions there is a conspicuous increase in megakaryocytes in the bone marrow, often with immature or otherwise atypical cytology (**477–482**), and clumps of aggregated platelets are frequently found in the periph-

eral blood smears, where megakaryocyte nuclei and nuclear fragments may also sometimes be present.

Megakaryoblastic proliferation in the bone marrow may be prominent in some trilineage acute leukaemias and may occasionally predominate. This occurs in some cases, apparently arising *de novo* (**488–495**), but also emerges as a form of blastic transformation or malignant progression in the terminal phases of polycythemia rubra vera (PRV) or CML (**339–348**). More mature megakaryocyte proliferation, arising in a similar fashion as either a primary or a secondary condition, appears often to stimulate the development of myelofibrotic or osteomyelosclerotic changes, probably through the production of growth factors and other biological activators of fibroblast proliferation and collagen formation.

166

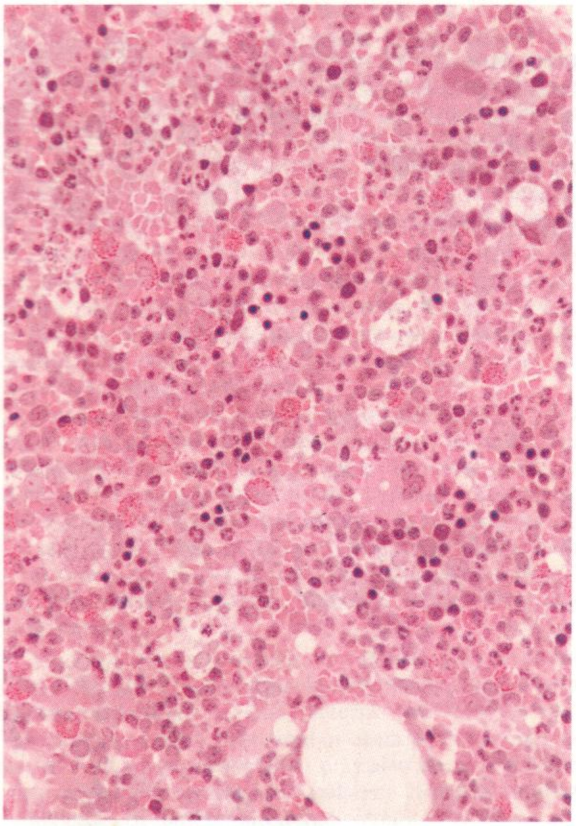

167

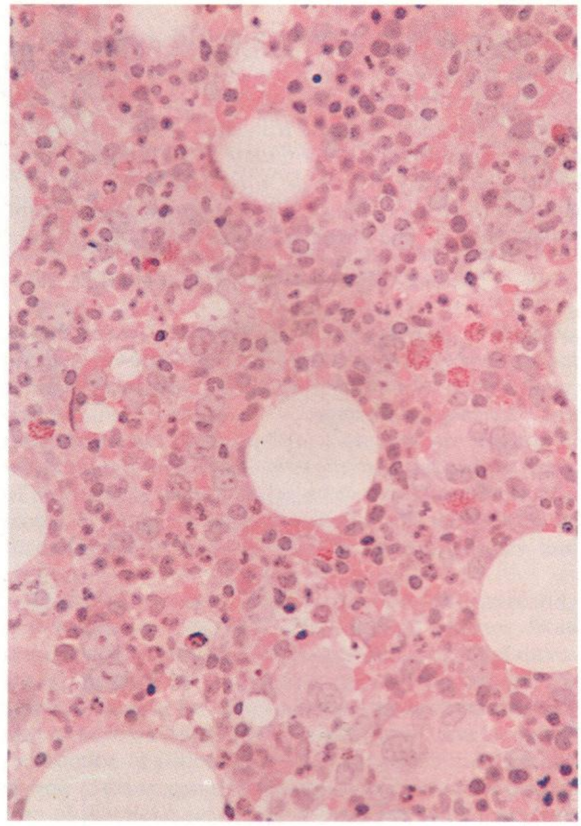

168

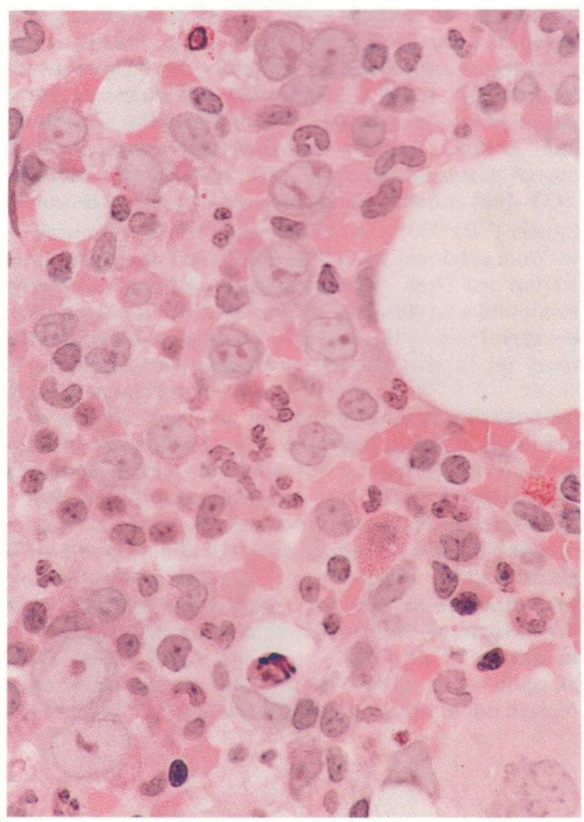

166. Trephine biopsy section of normal bone marrow from a child of two, showing some 90% overall cellularity and good representation of most normal marrow cells, including megakaryocytes, erythroblasts, and granulocytes at various stages of maturity. The granulocytes include chiefly neutrophils, with a few eosinophils, and the ratio of granulocytes to erythroblasts – the so-called myeloid–erythroid or M:E ratio – is about 3:1.

M:E 3:1

167 and **168**. Trephine biopsy section, viewed at low and higher magnification, respectively, from the bone marrow of an adult with a refractory anaemia and a cellular marrow containing a higher proportion of granulocyte precursors – M:E ratio 6:1 – and with a shift to the left, i.e. relatively more nucleolated immature cells, myeloblasts and promyelocytes, and fewer later non-nucleolated granulocytes. The diagnosis suggested by this marrow picture is one of the myelodysplastic states, refractory anaemia with excess of blasts (RAEB), further illustrated later. This figure is included here to show the extent to which the granulocyte maturation stages can be recognized in histological sections, and for comparison with the much greater cytological detail found in smears, as depicted in the succeeding figures.

169

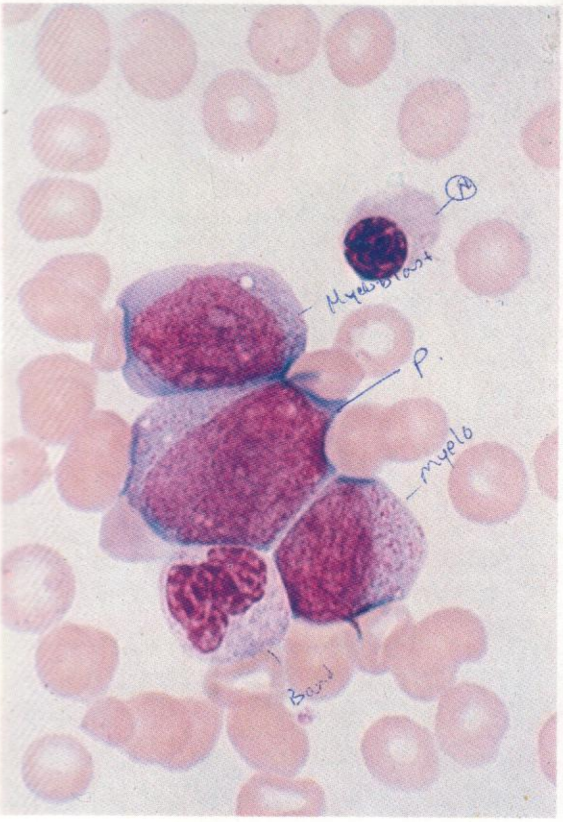

170

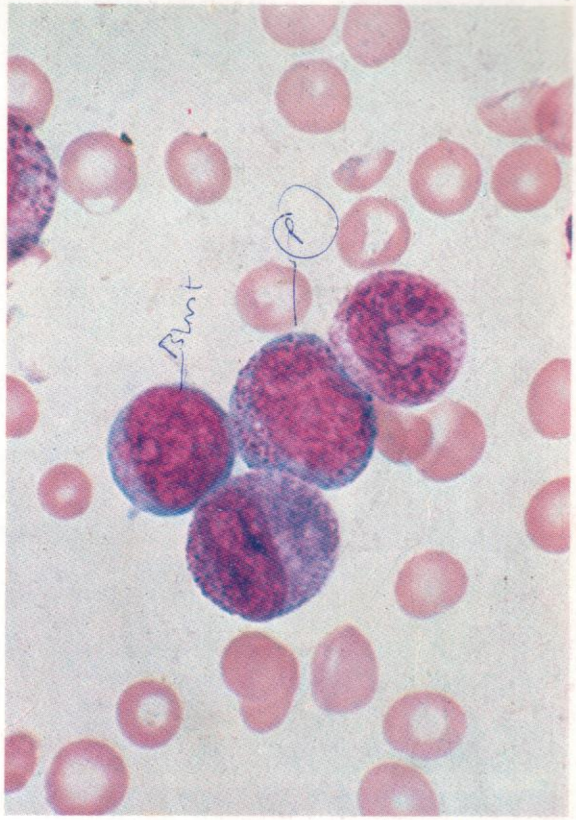

169. A myeloblast with two conspicuous nucleoli, a vacuole and a few azurophilic granules, a larger promyelocyte, a myelocyte and a stab cell of the neutrophil series, together with a late normoblast. Both the cells at the promyelocyte and early myelocyte stages show fading nucleoli and azurophil granules, the smaller and more mature myelocyte also having less sharply defined and less strongly coloured neutrophil specific granules, like those in the accompanying stab cell.

170. A sequence of granulocytes, with a myeloblast, promyelocyte, myelocyte (with neutrophil granules), and a late neutrophil metamyelocyte or early stab cell. The myeloblast, on the left of the group, has a clearly defined nucleolus within a dark ring of nucleolus-associated chromatin; the promyelocyte, in the centre, has three less distinct nucleoli visible in the upper part of the nucleus and numerous coarse azurophil granules; while the two maturing neutrophils show a denser nuclear chromatin pattern and have many specific granules. The red cells are abnormal, with anisocytosis and irregular hypochromia.

171. A promyelocyte, two myelocytes, a metamyelocyte and a stab cell, of the neutrophil series. The red cells again show anisocytosis and marked hypochromia.

171

172

173

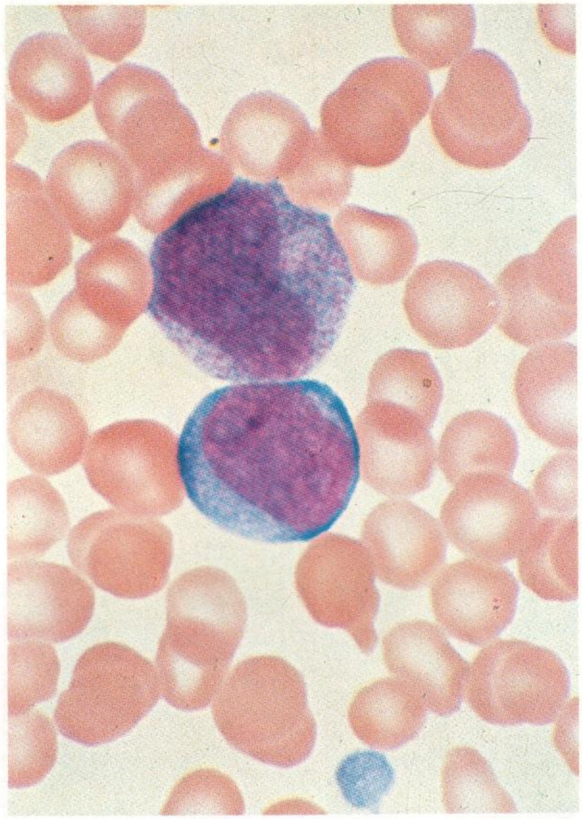

174

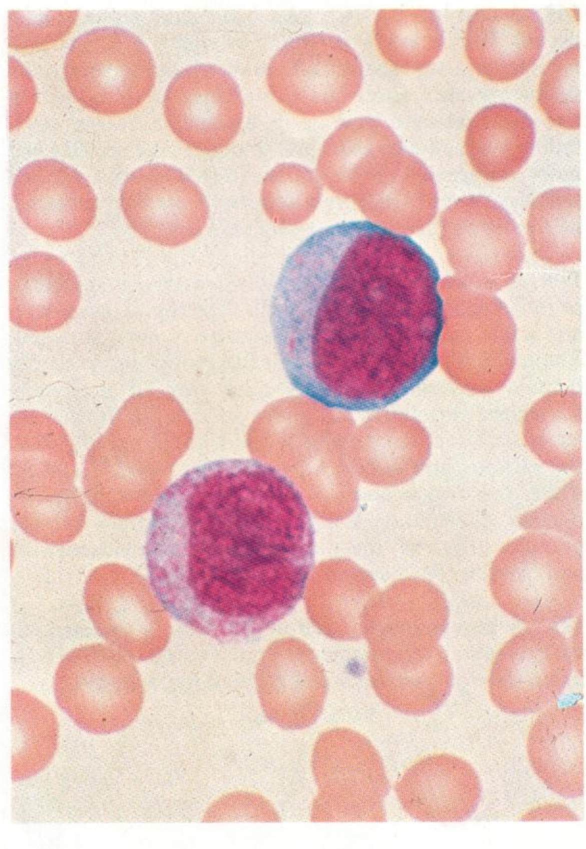

172. A myelocyte and four metamyelocytes of increasing maturity (with increasingly indented nuclei). The myelocyte is the smallest cell in this group and has the most basophilic cytoplasm, though without any detectable azurophil granules, and its nucleus has several small but fading nucleoli. Specific granules are inconspicuous in this cell but numerous in all the metamyelocytes. There is again hypochromia of the red cells and a stomatocyte with a neighbouring dacryocyte towards the upper left.

173. A myeloblast and an early neutrophil myelocyte. The cytoplasmic basophilia, due to residual RNA, and the three or four pale blue nucleoli of the myeloblast are well shown here and in **174** and **175**.

174. A myeloblast with a monocyte for comparison. The monocyte shows a coarser nuclear chromatin pattern, an absence of nucleoli, and a greyish rather than a basophilic cytoplasm.

175

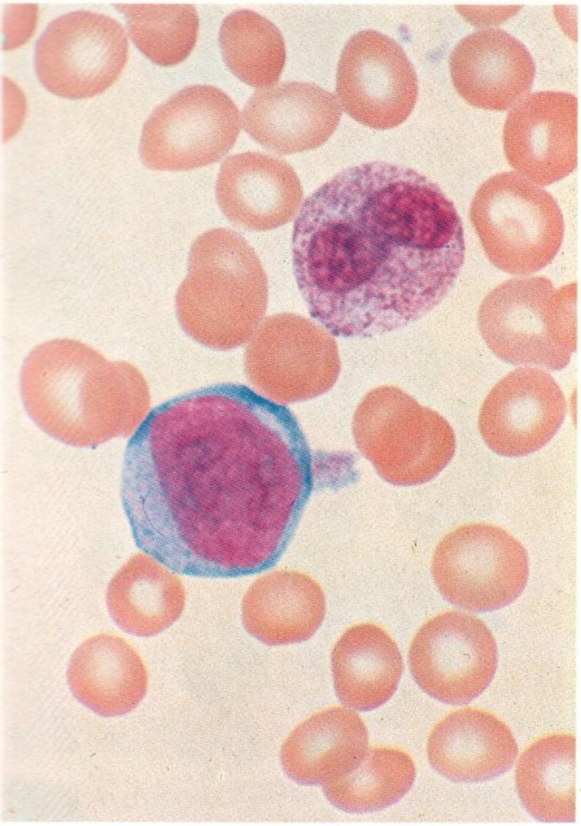

176

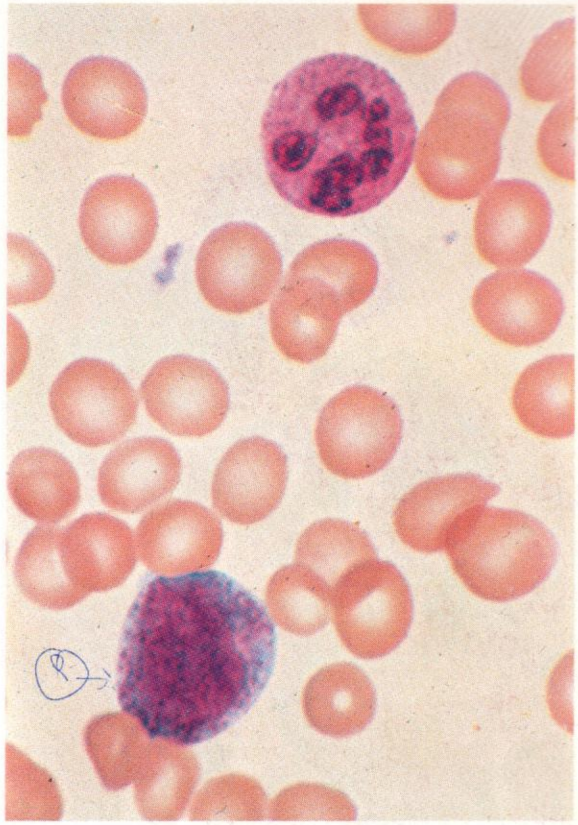

175. A myeloblast with a neutrophil stab cell. To the right of the myeloblast and impinging on its cytoplasm is a rather large platelet. Three smaller platelets are present at the top of the field.

176. Below is a promyelocyte with numerous azurophil granules in its moderately basophilic cytoplasm and a smooth leptochromatic nucleus without clearly distinguishable nucleoli, while above is a neutrophil segmented polymorph. There are three platelets present and the red cells show only slightly exaggerated central pallor, scarcely amounting to hypochromia.

177. Two myeloblasts, the smaller showing diminution of cytoplasmic basophilia and the first appearance of azurophilic granulation, a promyelocyte with coarse granularity and considerably larger size than the myeloblasts (a frequent finding), and a monocyte, for comparison.

177

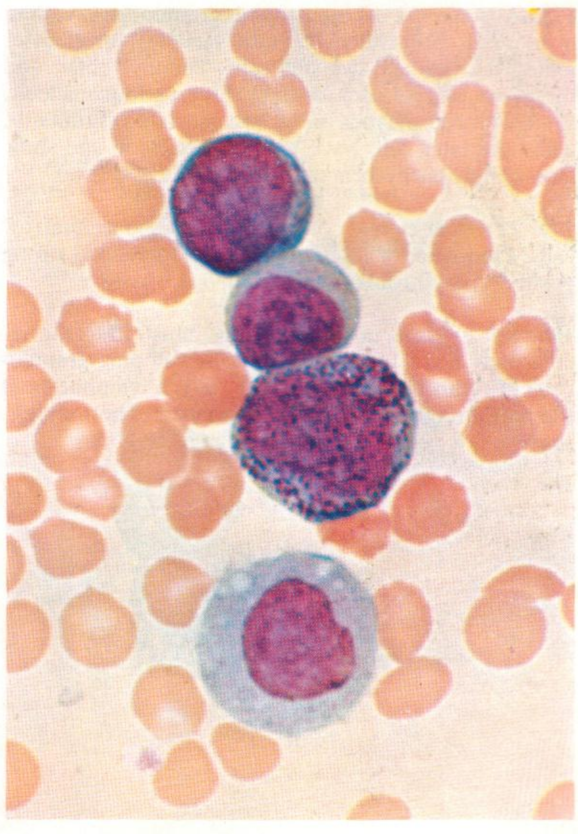

178

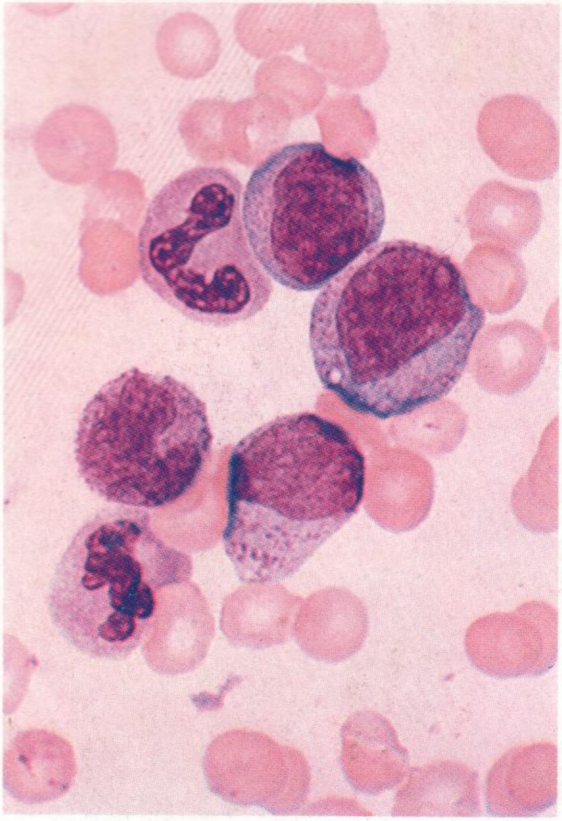

179

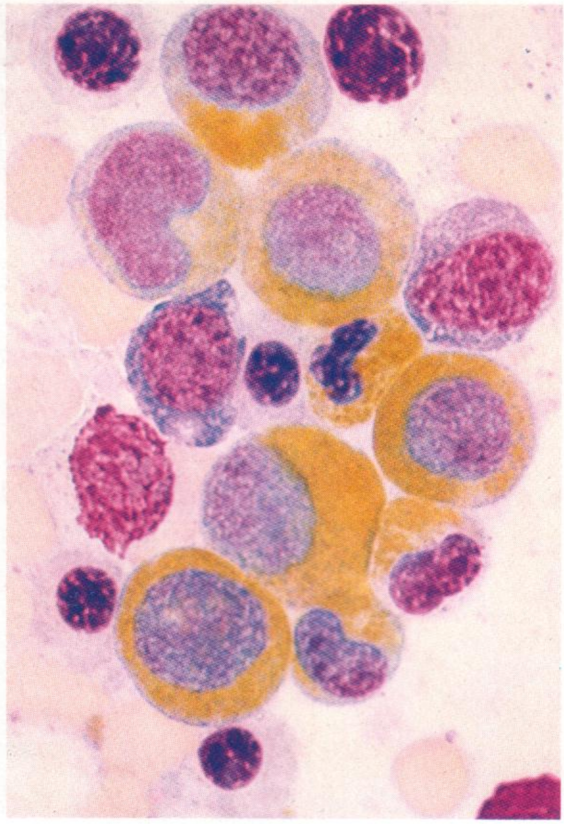

178. A sequence of neutrophil granulocytes with a myeloblast, promyelocyte (with vacuole), myelocyte, metamyelocyte and two stab cells. The myeloblast and the promyelocyte each contain three or four nucleoli, some with conspicuous nucleolus associated chromatin, while the later cells have lost their nucleoli and show increasingly pachychromatic nuclei.

179. Peroxidase reaction on normal bone marrow cells; a sequence of granulocyte precursors shows strong positivity; erythroblasts are negative.

180. SB stain on normal marrow, illustrating the increasingly heavy positivity in the developing granulocytes. Erythroblasts are negative, as is a lymphocyte at the bottom right. A vacuolated monocyte, bottom left, shows a few positive granules.

180

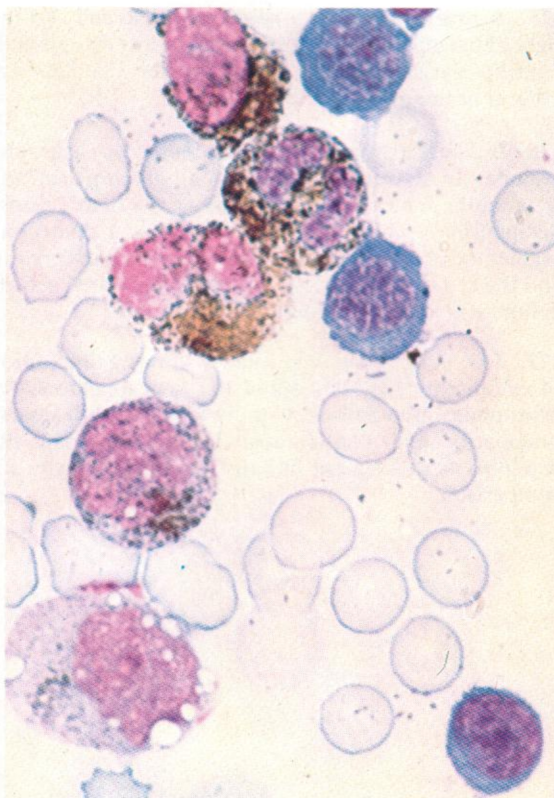

181

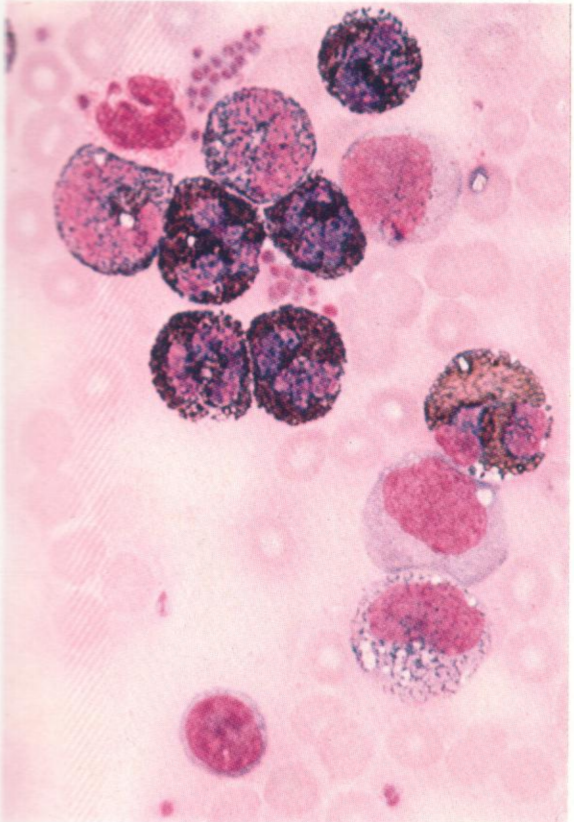

182

181. SB stain on normal buffy coat smear. The coarse positivity in neutrophil polymorphs contrasts with the weaker reactions in monocytes – one negative, one with a few fine granules and three with scattered granules, more discrete than in the neutrophils. There is an eosinophil with hollow positive granules, a negative basophil and a negative lymphocyte. Beside the basophil, at the top left of the field, is a clump of negative platelets.

182. SB stain on normal peripheral blood, illustrating the contrast between the dense and coarse positivity in mature granulocytes and the discrete scattered granule pattern of monocytes. Lymphocytes are negative.

183. SB stain on normal buffy coat showing the presence of a myeloblast, as can usually be found in normal circulating blood if carefully sought. Two negative basophils, two normally reacting neutrophil polymorphs, a monocyte and a lymphocyte complete the field.

183

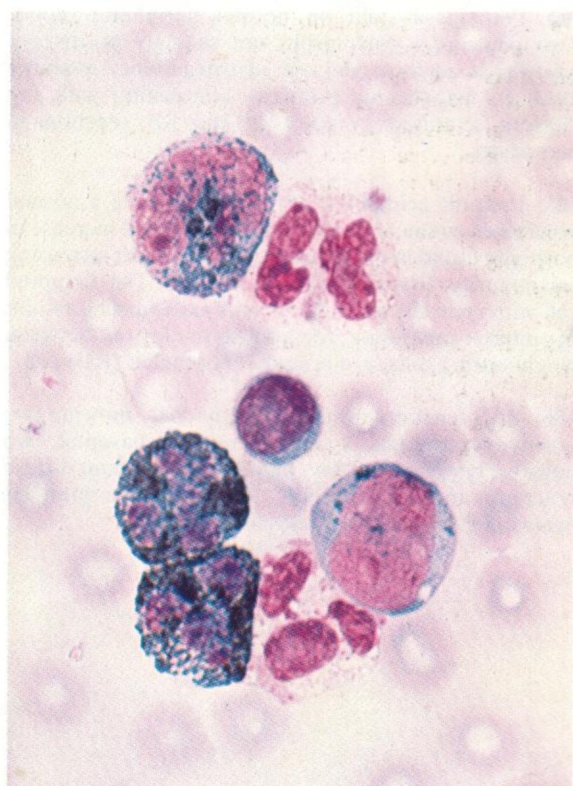

184

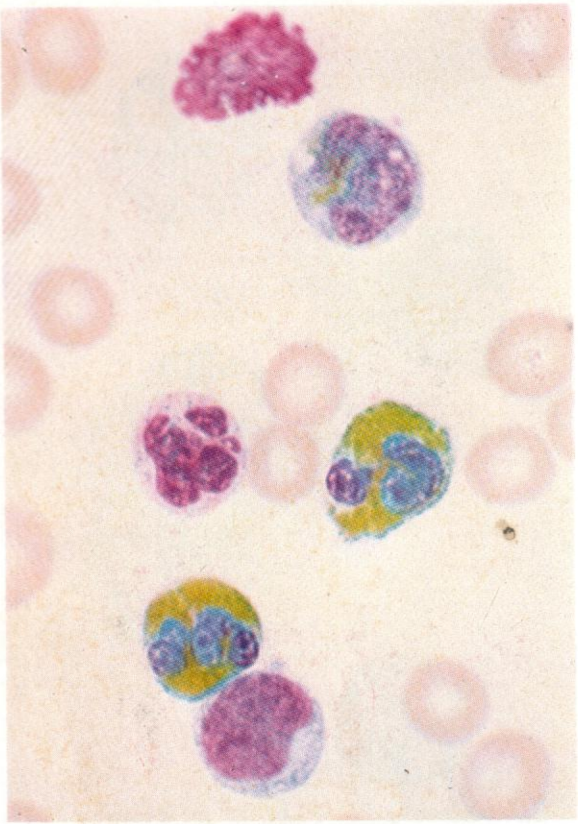

185

186

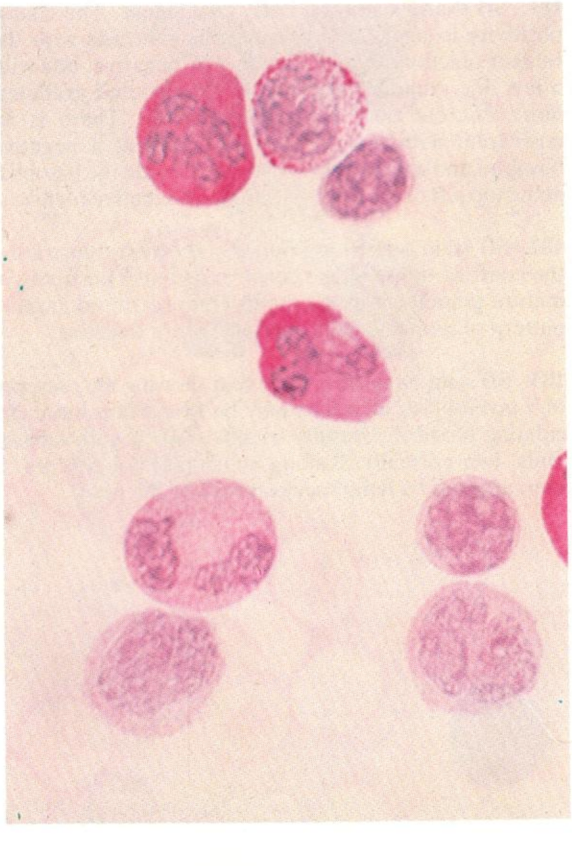

184. Peroxidase stain on normal peripheral blood. Two neutrophil polymorphs are strongly positive; a basophil is negative and one of two monocytes shows localized cytoplasmic positivity contrasting with the discrete scattered granules of the SB reaction in monocytes.

185. Periodic acid-Schiff (PAS) reaction on a normal bone marrow smear, to illustrate the gradual increase in positivity found in the granulocyte series with increasing cell maturity. Erythroblasts are negative. The disrupted cell with centrally situated nucleus and coarse granules of material containing free iron, spreading out between neighbouring cells, is a reticulo-endothelial (RE) cell.

186. PAS reaction on normal buffy coat, showing two positive neutrophils, a coarsely reacting basophil, two negative lymphocytes, two monocytes with faint diffuse reaction, and an eosinophil with negative granules against a PAS-positive background.

187

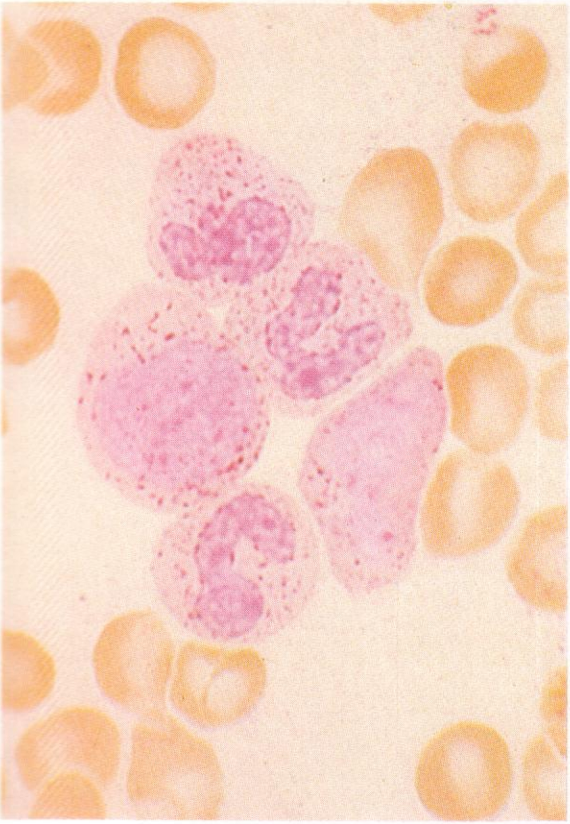

188

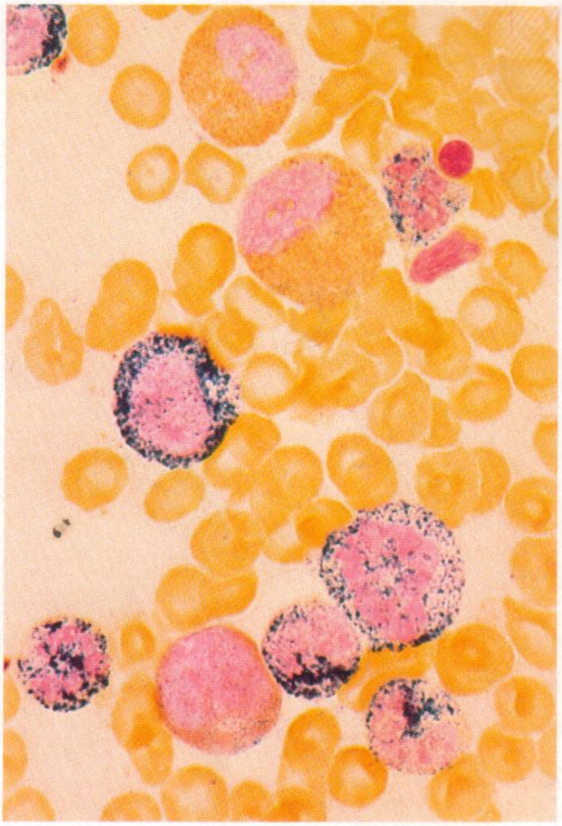

189

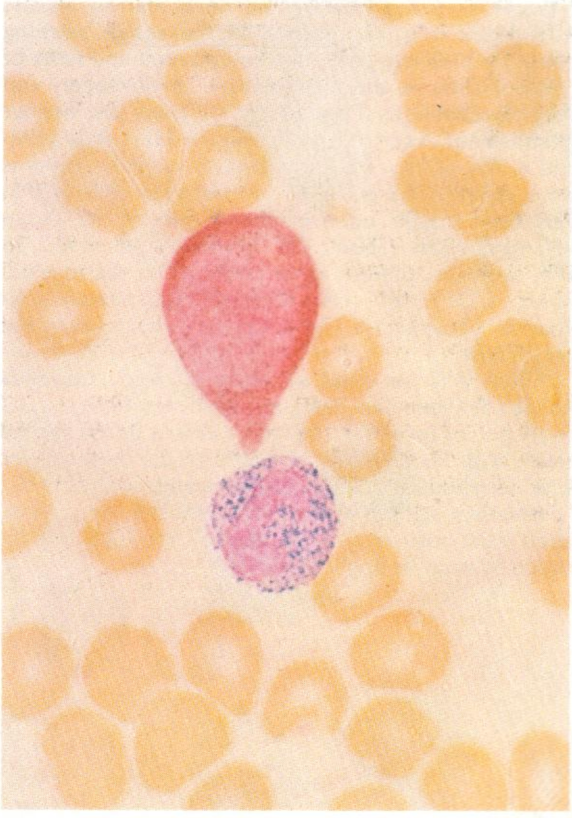

187. Acid phosphatase in granulocytes in normal marrow; myeloblast, promyelocyte, stab and two segmented neutrophils. All these granulocytes show a scattering of fine granules, probably representing the primary lysosomal azurophil granules which first appear at the late myeloblast to early promyelocyte stage and remain in the cytoplasm of later granulocytes, although diluted in concentration by division at the myelocyte stage. Acid phosphatase positivity in the normal cell series is therefore generally most conspicuous in promyelocytes.

188. Dual esterase, on normal marrow cells – seven neutrophil granulocytes, including two myelocytes, one in mitosis, all showing chloroacetate esterase (CE) positivity, two negative eosinophil myelocytes, a monocyte of mixed butyrate esterase (BE) and CE reaction, and a negative late normoblast and lymphocyte.

189. Dual esterase on normal peripheral blood, showing CE-positive polymorph and BE-positive monocyte.

190 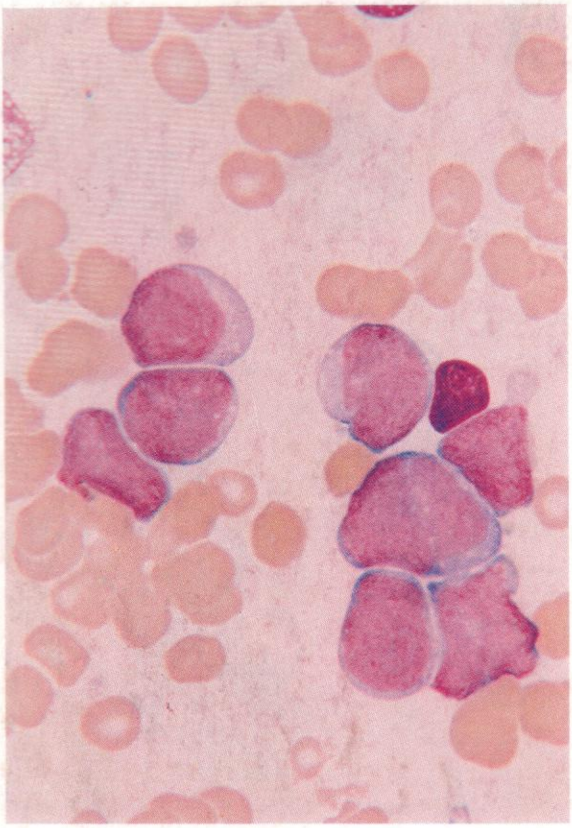

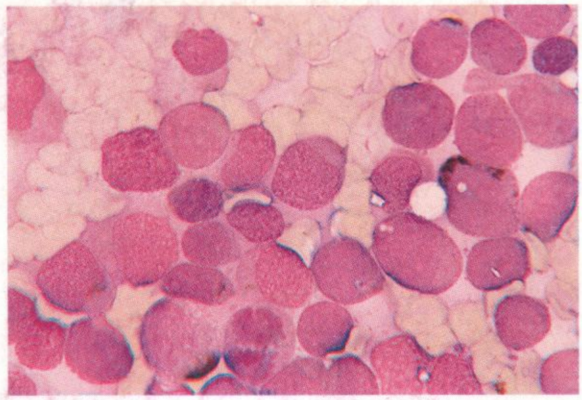 191

 192

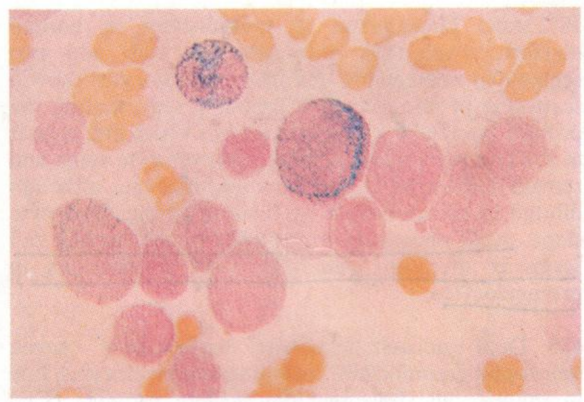 193

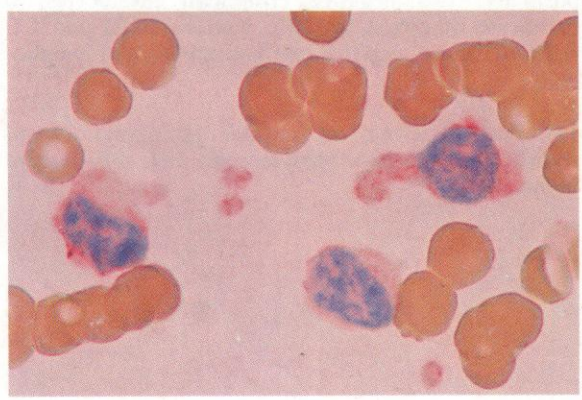 194

190–194. A series of stains on bone marrow smears from a case of acute myeloblastic leukaemia, showing relatively little evidence of differentiation and none of erythroblastic or megakaryoblastic involvement, and thus classifiable as Type IB (M1). There are neither granules nor Auer rods visible in the Heyl stain (**190**) and <10% of blast cells are SB positive (**191**). There is weak diffuse PAS positivity in most blast cells in **192**, and only a later neutrophil and one of the group of myeloblasts show CE positivity in **193**. In **194**, however, there is clear positivity to the myeloid MAb CD13 in this alkaline phosphatase-anti-alkaline phosphatase (APAAP) immunocytochemical preparation.

About 20% of cases of acute myeloid leukaemia (AML) fall into this category, and they have a relatively poorer prognosis than more clearly differentiated cases, with SB positivity in >50% of the blast cells or with Auer rods or other inclusions readily found.

When few signs of myeloid differentiation are present, apart from positive antigen markers, the FAB classification M0 may be applied.

195

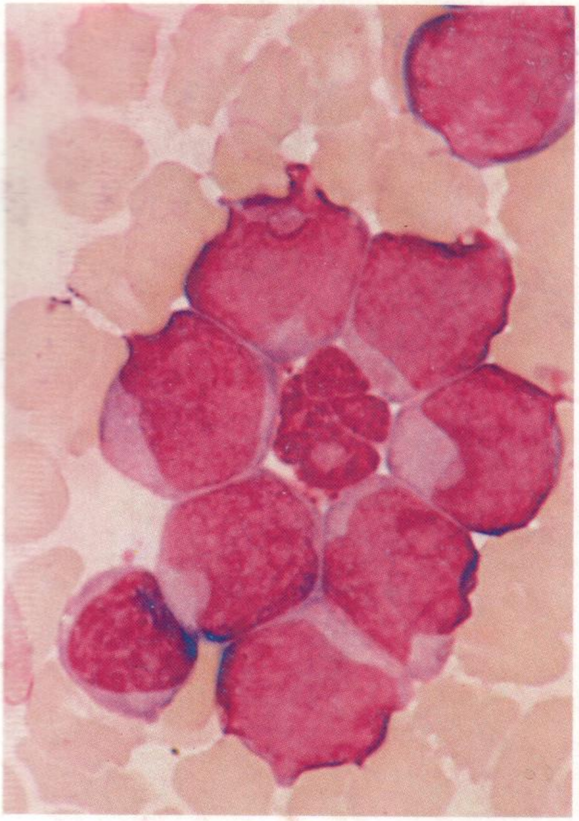

196

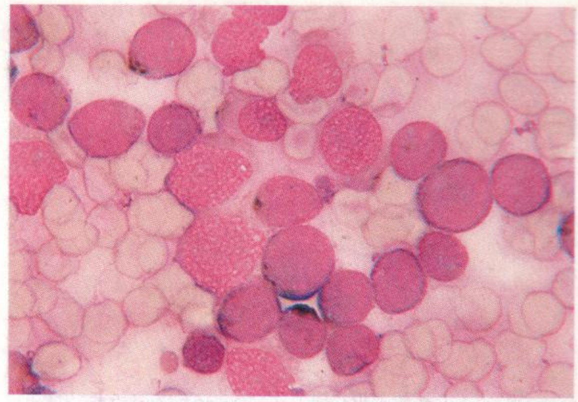

197

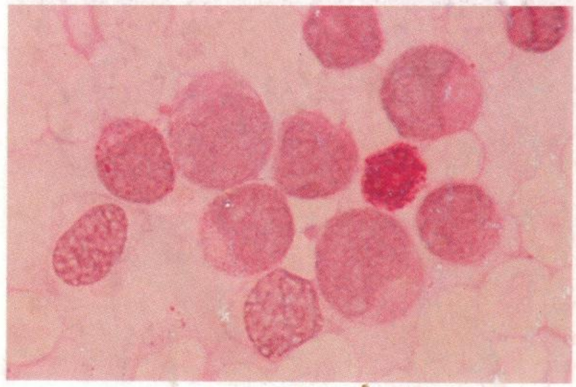

198

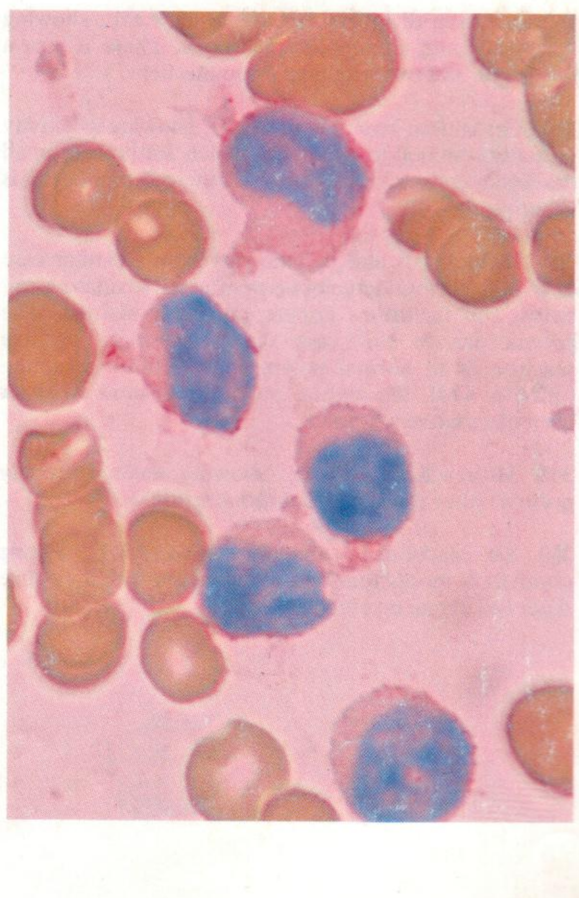

195–198. Another example of a bone marrow smear from a case of Type IB AML, again without multilineage involvement and with only poorly differentiated blast cells present, where the cytology in the Romanowsky stain (**195**) shows some indentation of nuclear membranes, and the identification of the blasts as myeloblasts rather than monoblasts (M1 rather than M5) is uncertain. The presence of localized rather than scattered SB positivity, even in only <10% of cells in **196**, suggests the former. The weak diffuse PAS reaction with an occasional positive granule (**197**) is equivocal on this issue, as is the positive surface membrane APAAP reaction to CD13 shown in **198**. Reactions to both dual esterases and the monocyte MAb CD14 were negative. The case is therefore almost certainly myeloblastic (M1) – but in terms of the Type IB classification the possible difference is unimportant, the presence of <50% SB-positive blast cells carrying a poor prognosis, whatever the precise balance between the granulocyte and monocyte precursor components of an essentially monolineage AML.

199

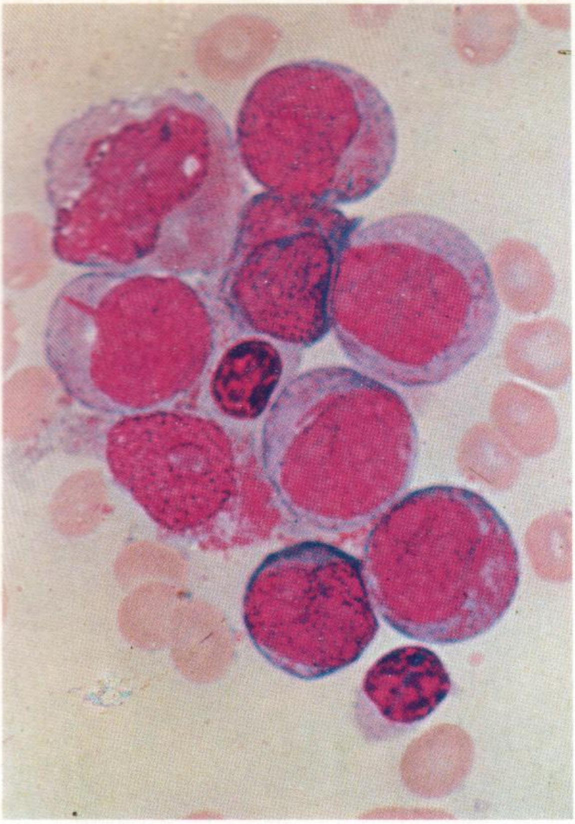

200

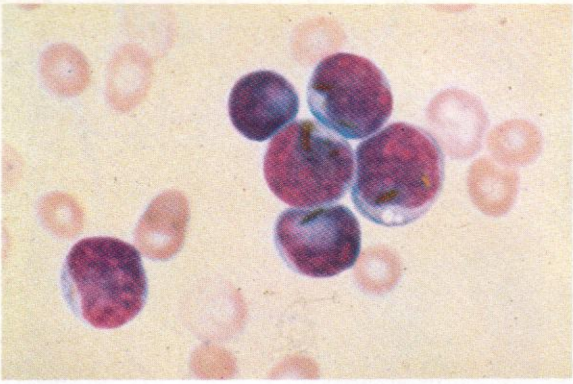

201

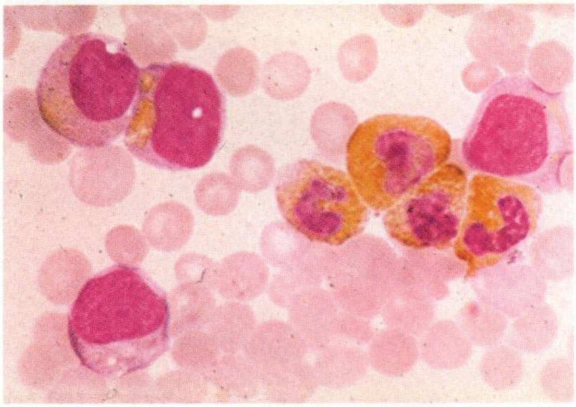

202

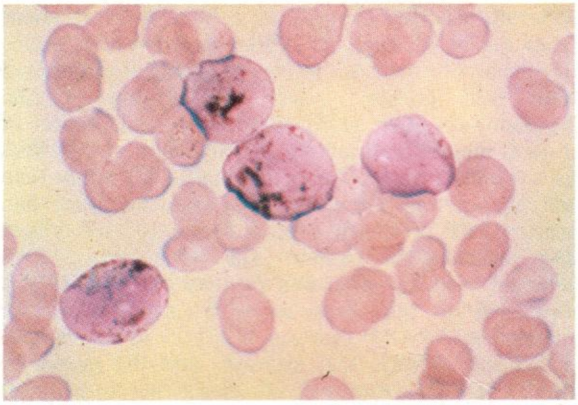

203

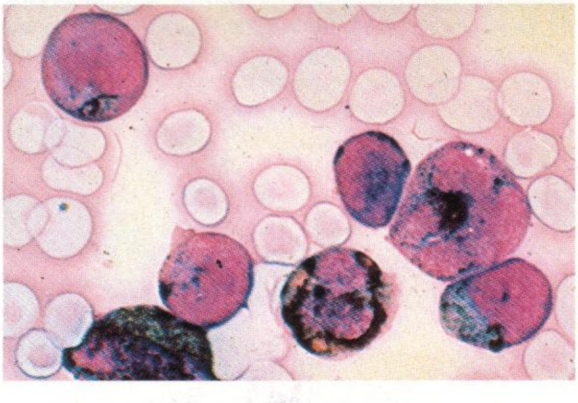

199. A group of myeloblasts from an AML, showing Auer rods and azurophilic inclusions. There is also a myelocyte and two lymphocytes in this field.

200. Peroxidase reaction in AML, showing positivity virtually confined to Auer rods which are present in all the blast cells in this field. A single lymphocyte is negative.

201. Myeloblasts and polymorphs from a similar case of AML. Several myeloblasts show peroxidase positivity, and inclusions appear positively stained. The polymorphs in this case display strongly positive reaction as in normal polymorphs – although sometimes in AML the mature polymorphs show weak or even negative reactions.

202. SB reaction in AML, showing several strongly positive Auer rods and localized reaction.

203. SB reaction in myeloblasts of AML. Strong positivity is mostly localized to cytoplasm with a positive Auer rod in one myeloblast.

204

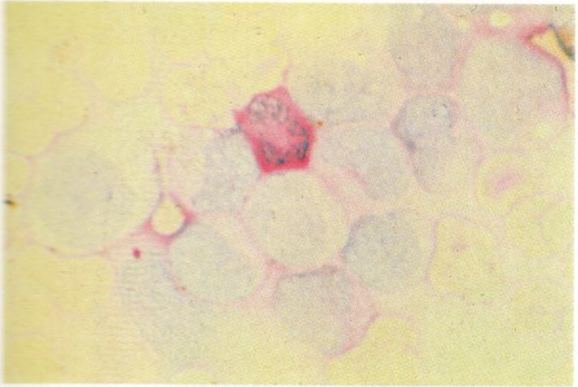

205

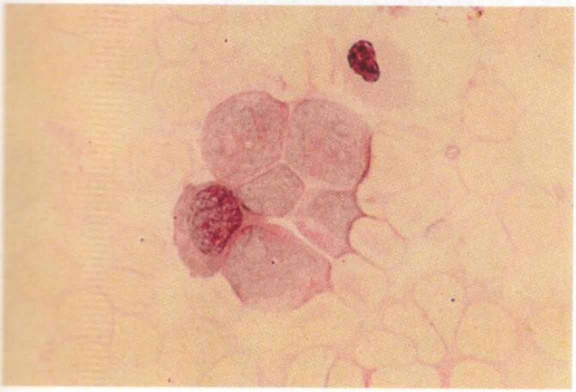

206

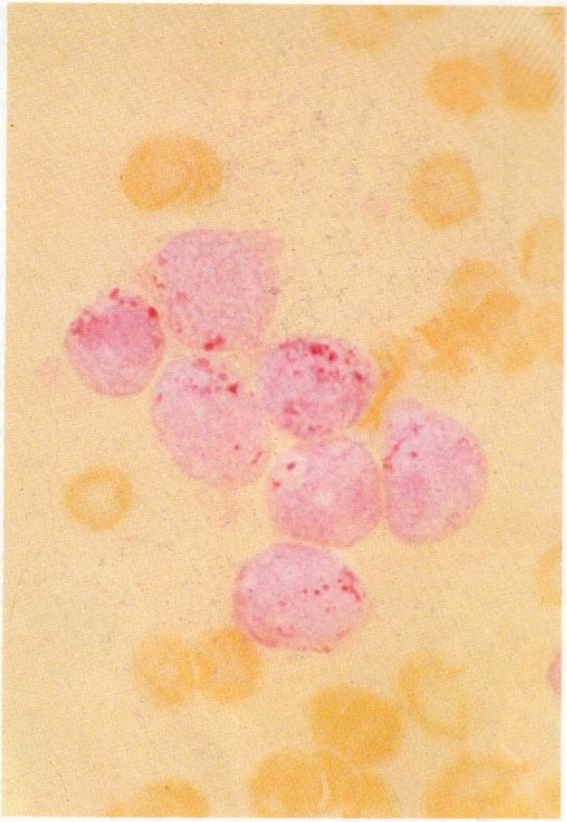

207

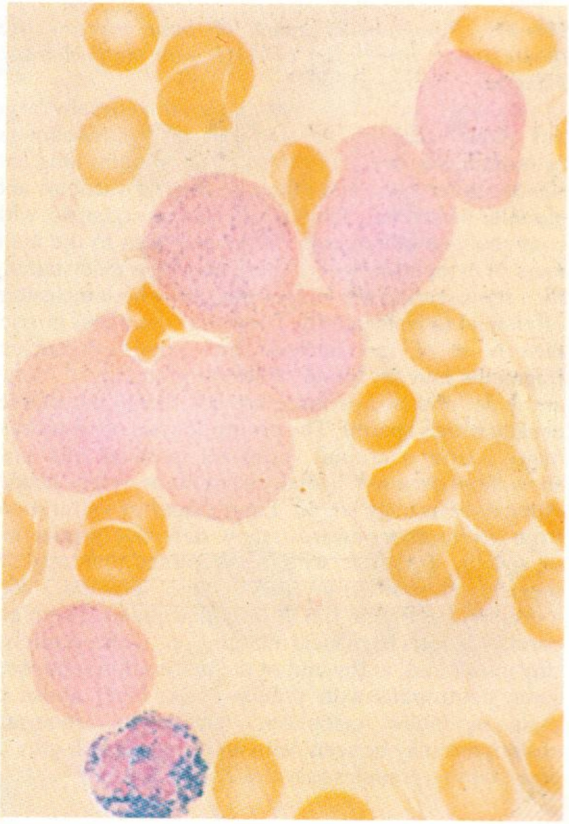

204. PAS reaction in a similar acute leukaemia. The single polymorph is normally positive, while the primitive cells give a reaction ranging from negative to a weak diffuse positive tinge over most of the cytoplasm. Sometimes fine granules are also present, but on a background of diffuse tingeing unlike the clear background seen in lymphoblasts.

205. PAS reaction in marrow cells from another case of AML. The field shows a central group of four myeloblasts and a metamyelocyte, all with diffuse to finely granular positivity, and a negative late normoblast at the upper right. One of the myeloblasts contains a weakly positive Auer rod overlying the nucleus.

206. Acid phosphatase reaction in a similar case. Moderately coarse granular positivity is present.

207. Dual esterase reaction in the same case. The myeloblasts show a weak, finely granular, scattered CE positivity. A single neutrophil polymorph shows strong CE reaction.

208

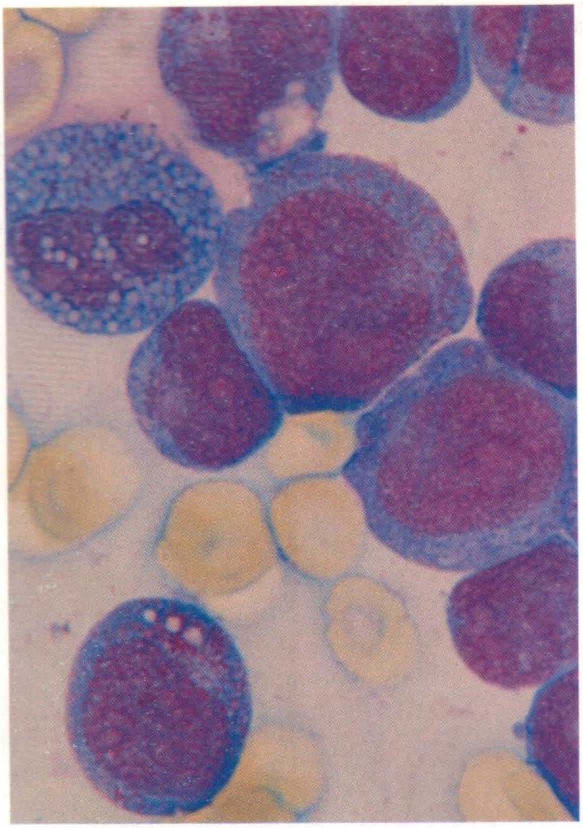

209

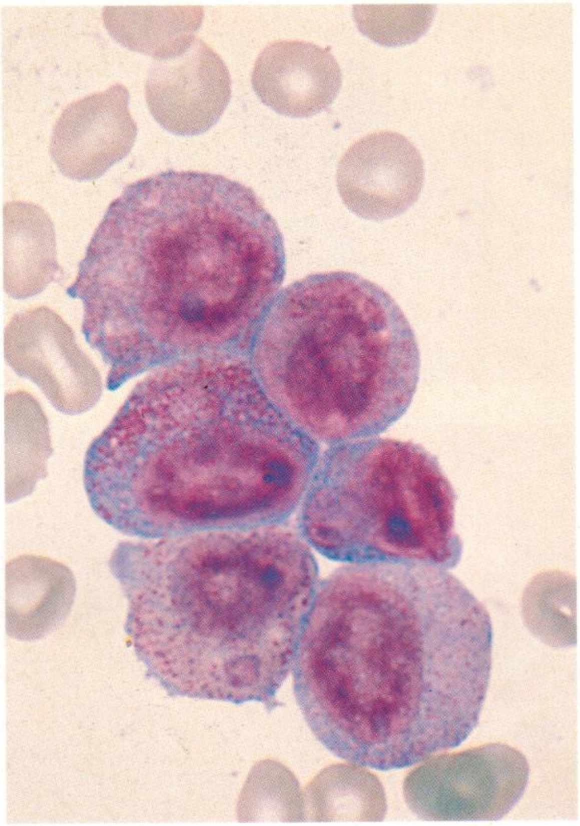

208–215. *Romanowsky stains of bone marrow and blood smears from cases of AML with the 8;21 translocation – t(8;21) (q22;q22).*

In this AML variant the blast cells are generally large but show variability in size and in the amount of cytoplasm, which is basophilic, often contains long and slender Auer rods, and may also contain vacuoles and globular inclusions. The nucleus may be eccentric, with commonly an indentation on the side next to the main mass of cytoplasm, where there may be a pale-staining area representing the Golgi body and where inclusions often tend to be localized. There are sometimes grosser distortions of the nucleus and separated nuclear fragments may be found. Nucleoli are generally large and pale, and two or three are commonly detectable, usually widely spaced. The promyelocytes often possess many coarse azurophil (primary) granules and may show large pseudo-Chediak inclusions as well as slender Auer rods, usually single. Later stages of maturation, from myelocytes onwards, show defective production of specific granules, with a cytoplasm that appears pinkish-yellow at the myelocyte stage, sometimes with a residual peripheral rim of deep basophilia. There are parallel defects in nuclear maturation, with occasional ring nuclei and, at the end of the maturation sequence, some neutrophils with pseudo-Pelger-Huët nuclei in their agranular cytoplasm. Occasional abnormal eosinophils may be seen, with atypical greenish-grey or blue-staining granules (*see also* **220**).

210

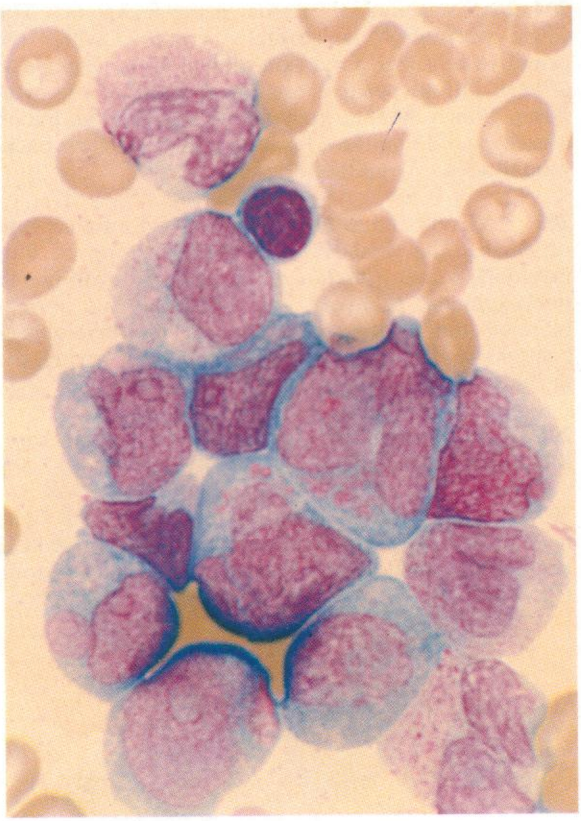

211

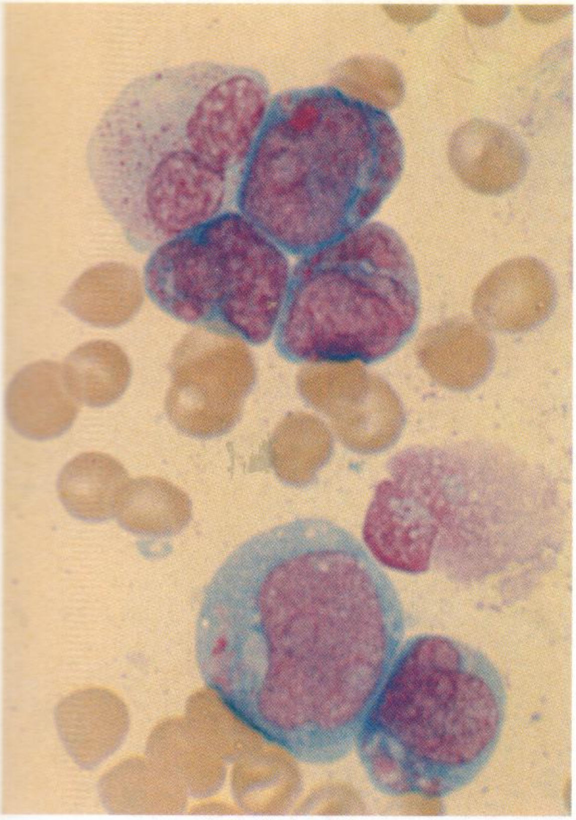

212

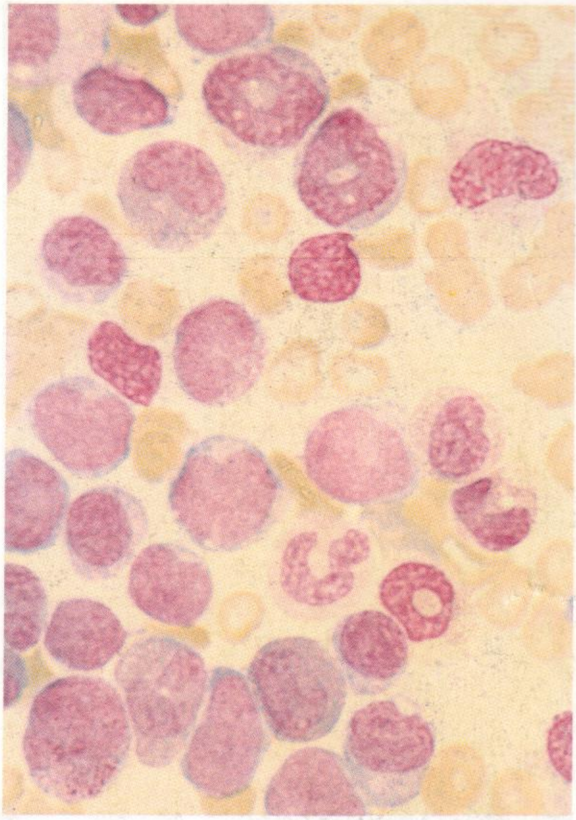

213

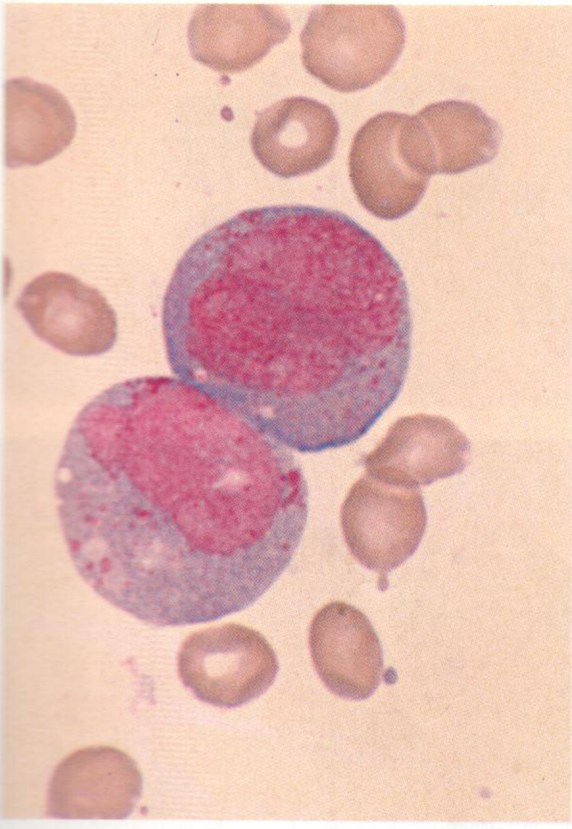

214

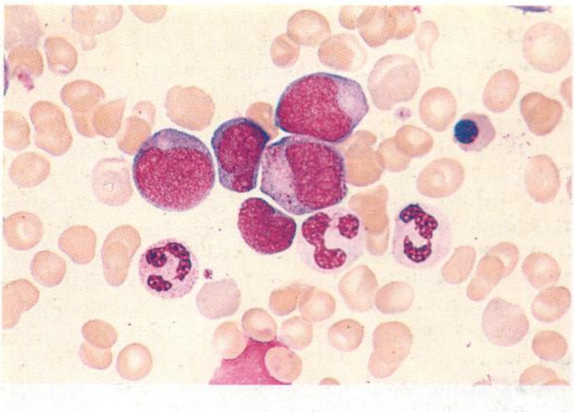

215

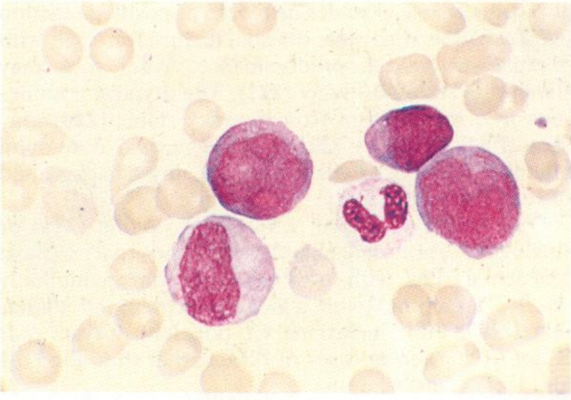

216

217

220

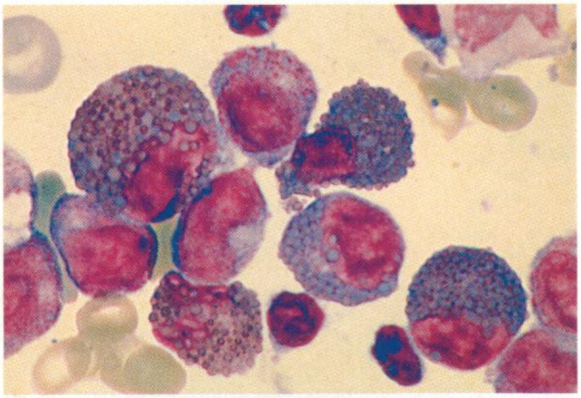

221

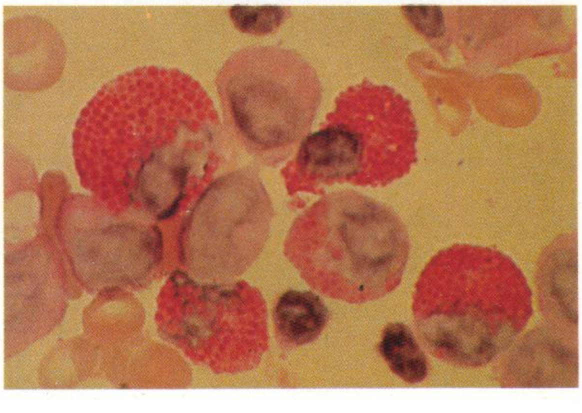

216–225. *Cytochemical reactions in cases of t(8;21).* Peroxidase and Sudan black reactions (**216–219**) always show strong localized cytoplasmic positivity in the great majority of blasts. Generally, this is concentrated at the nuclear indentation but often it involves most of the cytoplasm and, in the case of Sudan black especially, tends to obscure the frequent positively reacting Auer rods, which are therefore best seen in diaminobenzidine (DAB)–peroxidase preparations, but may occasionally be found in maturing eosinophils, too (*see* **217**). The inclusions seen in Romanowsky stains are also usually peroxidase positive and sudanophilic. Occasional negatively reacting neutrophil polymorphs may be seen.

PAS stains show the usual weak diffuse or finely granular positivity of leukaemic myeloblasts, but may also show coarse granules or blocks of positive reaction (**223**), an otherwise quite unusual feature for AML with granulocyte lineage predominance. Auer rods may sometimes stain positively (**222**). The atypical granules seen in eosinophils in Romanowsky stains (**220**) may show PAS positivity (**221**), unlike normal eosinophil granules, which are PAS-negative against a background of cytoplasmic positivity.

Dual esterase staining with either double (**224**) or single (**225**) capture agents shows CE positivity in most leukaemic cells with positive Auer rods commonly visible, sometimes with a negative core, and similar reactions in other inclusions. CE positivity of Auer rods is not often seen in cases of AML other than the 8;21 and 15;17 translocations

218

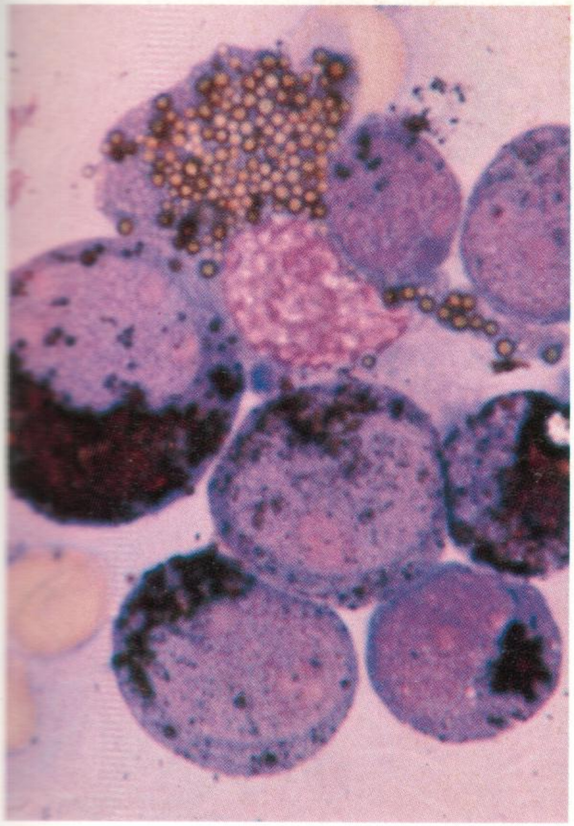

219

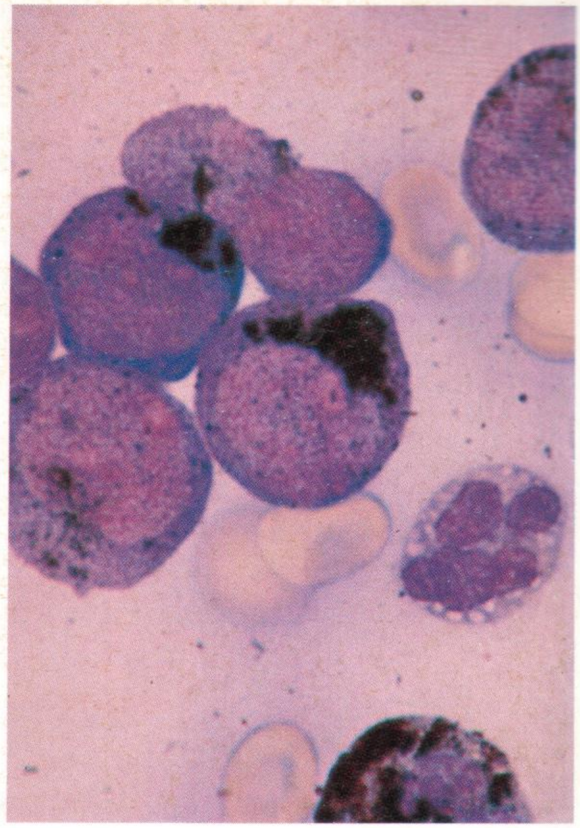

222

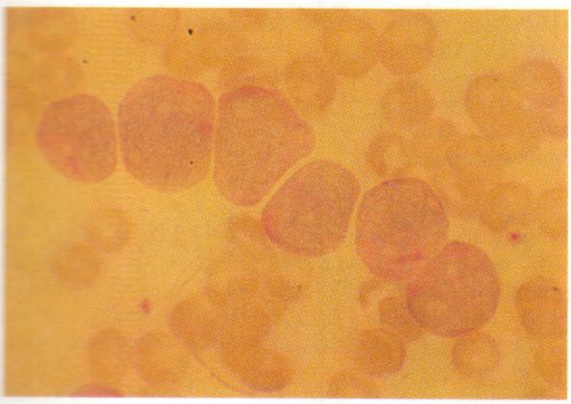

224

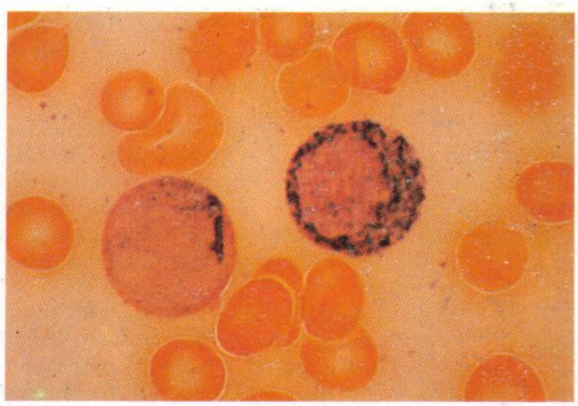

223

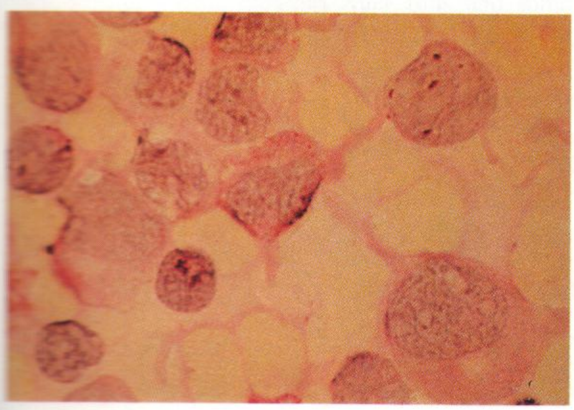

225

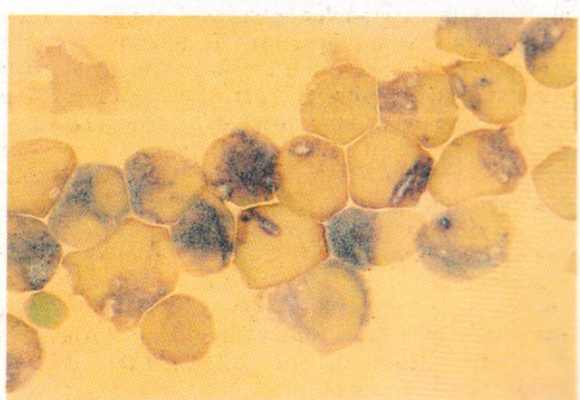

226

227

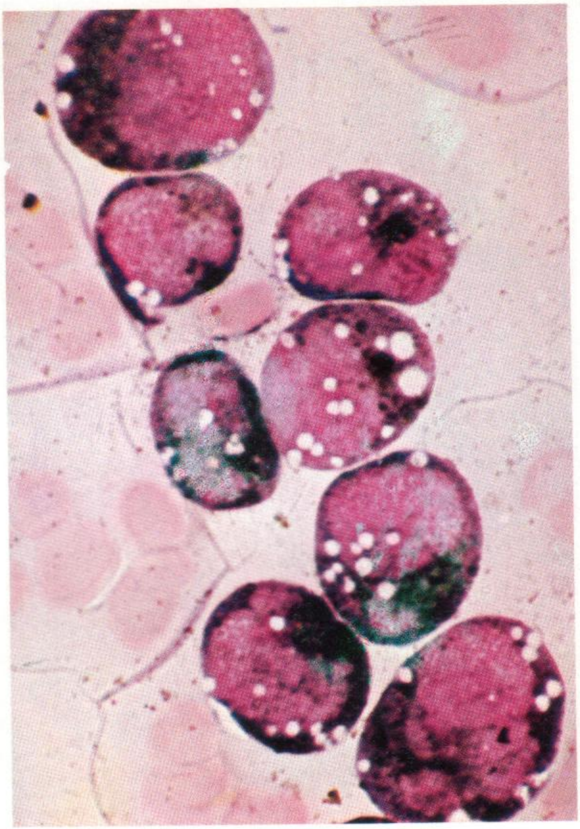

226–256. *Cytology and cytochemistry of AML cases with the 15;17 translocation, t(15;17) (q22;q21) – acute promyelocytic leukaemia (APL).*

226. An APL with early granularity in the archoplasmic zone next to the nucleus in most cells. The cells are leukaemic promyelocytes, but do not show multiple Auer rods, although there is a suggestion of the coarsely lobular nuclear changes of the type often seen in APL. Striking vacuolation was a feature of this case.

227. SB reaction in the same case. The dense cytoplasmic positivity resembles that seen in normal later granulocytes from myelocyte to polymorph. In this preparation the tendency towards nuclear indentation to produce twinned or unevenly paired lobes, a striking feature of APL, can be discerned in several cells.

228. The PAS reaction on these cells shows diffuse positivity with some increased granularity in the archoplasmic zones. This is the PAS picture of AML with promyelocytic preponderance.

229. Dual esterase reaction in the same cells, with strong CE positivity, including a CE-positive Auer rod.

228

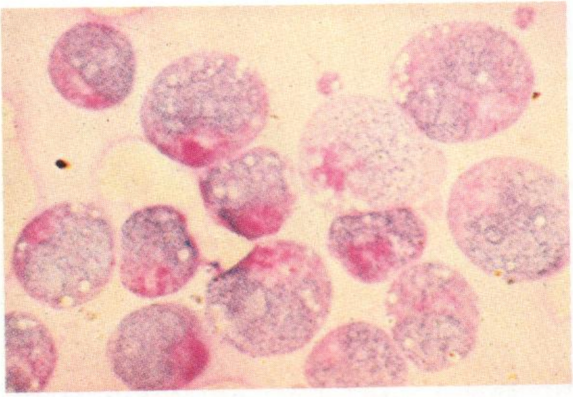

229

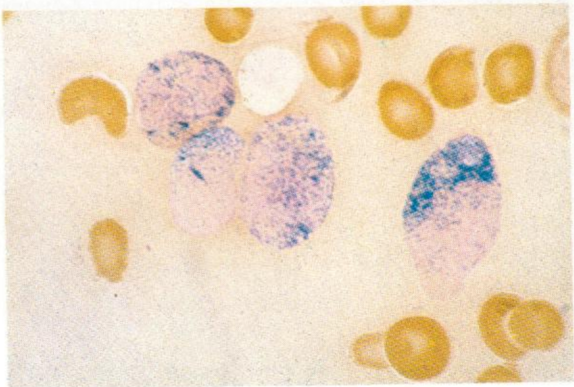

230

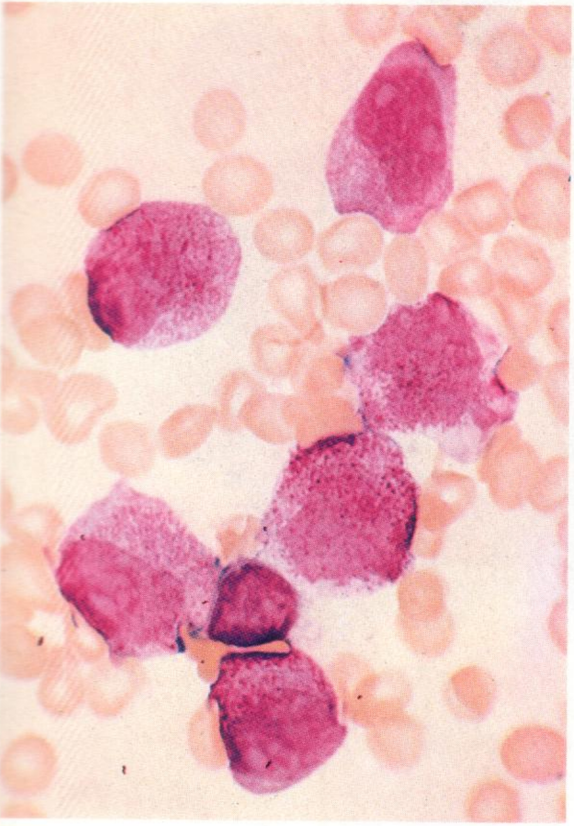

231

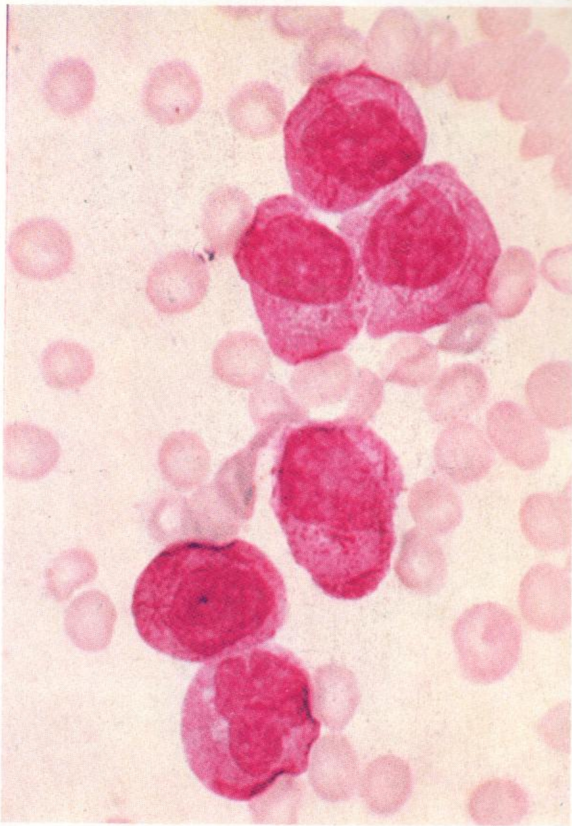

232

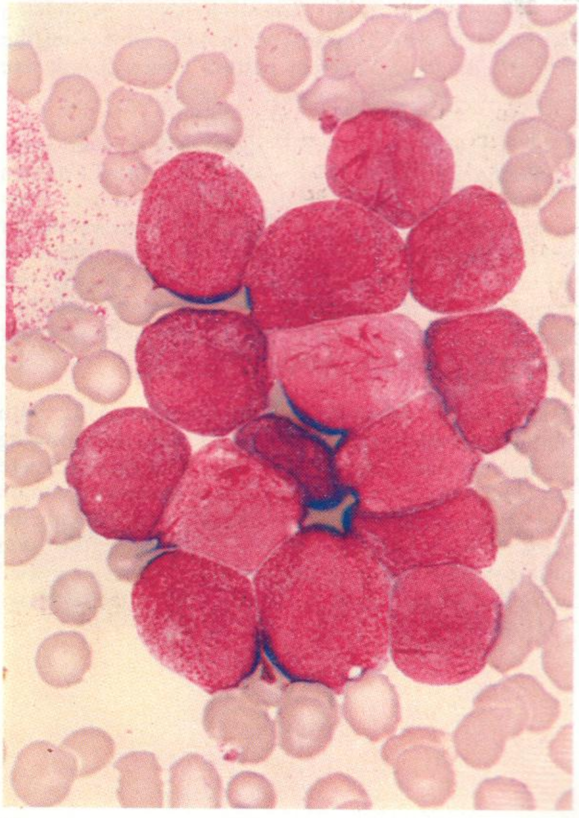

230. APL with coarse azurophil (primary) granules largely filling the cytoplasm of all the leukaemic promyelocytes. Nucleoli are conspicuous and variable in number but the overlapping or dumb-bell type of nuclear shape often seen in APL is not shown here, and Auer rods are not visible in this Leishman-stained preparation.

231. Another preparation from the same case, stained with MGG. Conspicuous multiple Auer rods are now visible in several cells. The difference in staining reaction of Auer rods in APL to Leishman and MGG stains, though not always shown, is frequently striking.

232. Another case of APL with granular promyelocytes, several having multiple Auer rods and some showing typical nuclear lobulation.

233

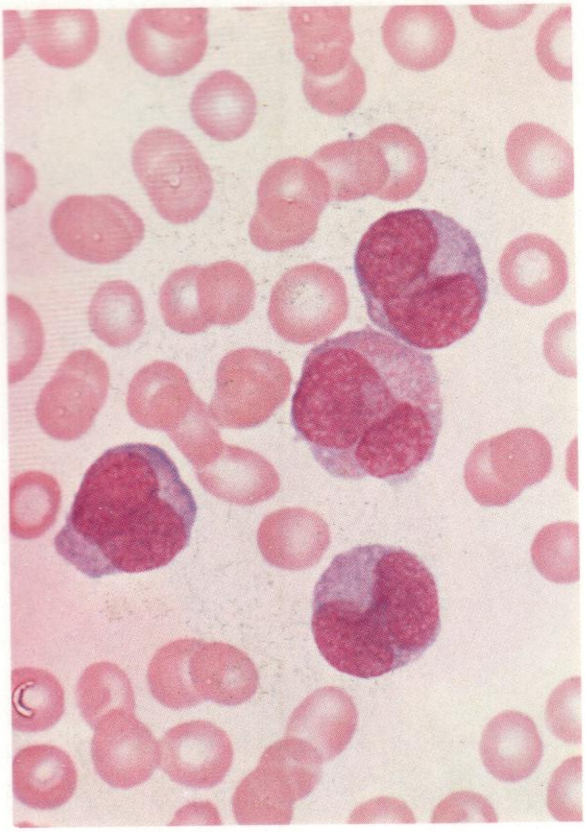

234

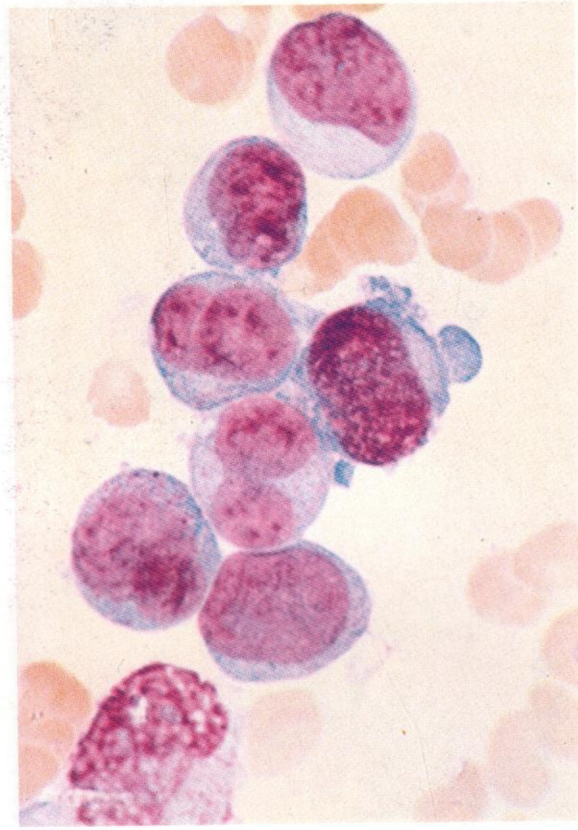

233. Myeloblasts and promyelocytes from the peripheral blood of another case of APL, all showing the virtually diagnostic nuclear pattern although only the central cell is heavily granular.

234. Another case of APL, showing few or no cytoplasmic granules and no Auer rods with either Leishman or MGG stains, but with the characteristic and diagnostic nuclear shape with dumb-bell appearance or overlapping of twinned nuclear lobes. This variant of APL is sometimes distinguished as a separate 'agranular' or 'micrognular' form, although usually – as here and in **235** – an occasional normally granular promyelocyte may be seen.

235. Another example of micrognular APL, with minimal granularity, but again with several cells showing the nuclear structure typical of APL. That these cells are not essentially different from those of the more common coarsely granular variant is indicated by their having the same chromosomal defect, the 15;17 translocation, and also by their capacity to develop coarse azurophil granulation after short periods of culture *in vitro* (*see* **236**).

235

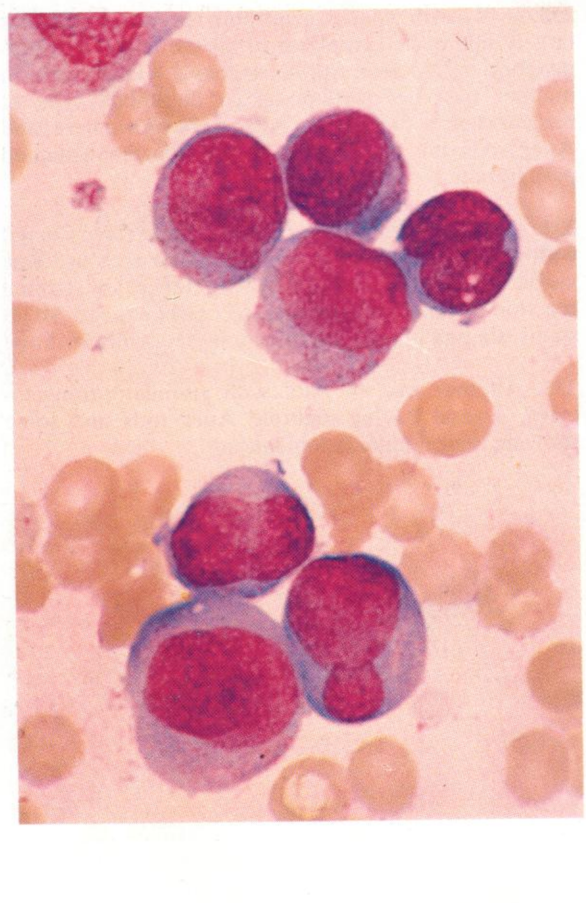

236

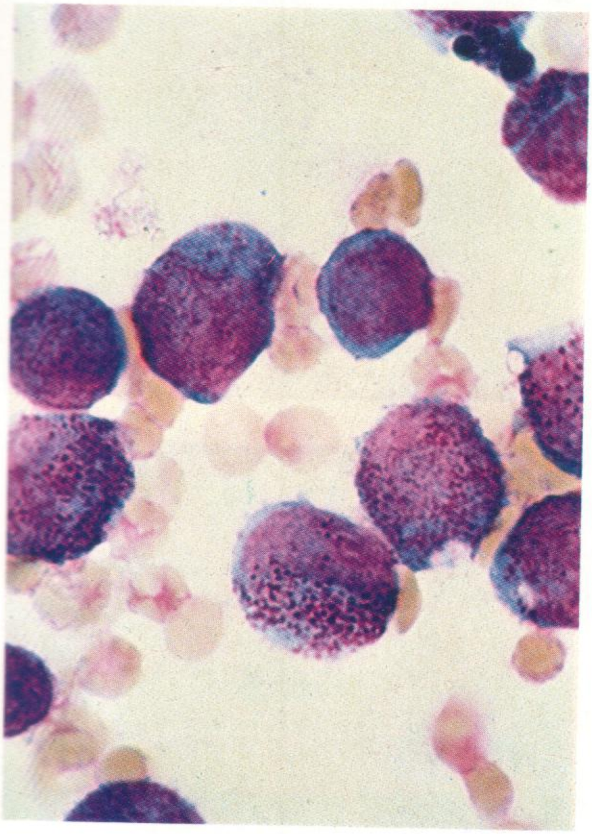

237

236. The same marrow as seen in **234**, here after 20 hours in culture; coarse azurophil granules have now appeared in the cytoplasm of all the promyelocytes.

237. A marrow from APL: SB stain showing heavy overall positivity, with positively stained Auer rods.

238. Another case of APL: SB stain of marrow cells shows similar overall positivity, but here the Auer rods, seen in the cell at the extreme right of the field, appear hollow with a sudanophilic outer coat but a negative core.

239. A similar SB preparation from another case of APL, again showing strong positivity and with both solid and hollow Auer rods visible in cells to the right and left of the field, respectively. There is also a disrupting promyelocyte shown, with scattered sudanophilic granules among which several positively reacting Auer rods can be made out. Multiple Auer rods, sometimes arranged in leashes or fasces, are diagnostically very characteristic of APL, and can often be best detected in SB stains, especially in thinner parts of the smear, where they are less likely to be obscured by heavy overall granular positivity. Here they may show up as negative rods (if they have hollow SB-negative cores), or be revealed among the scattered granules of disrupting cells.

238

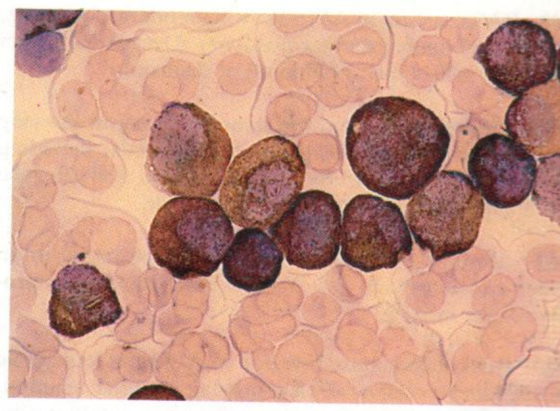

239

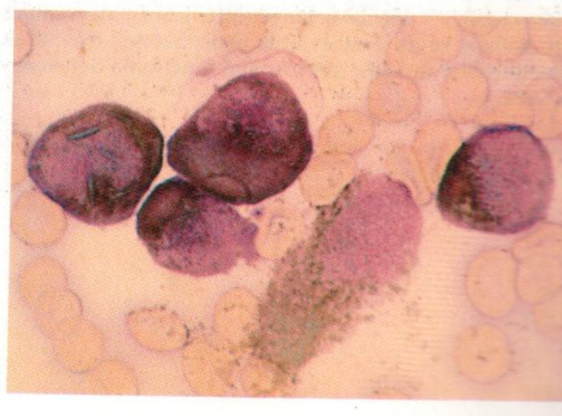

240

241

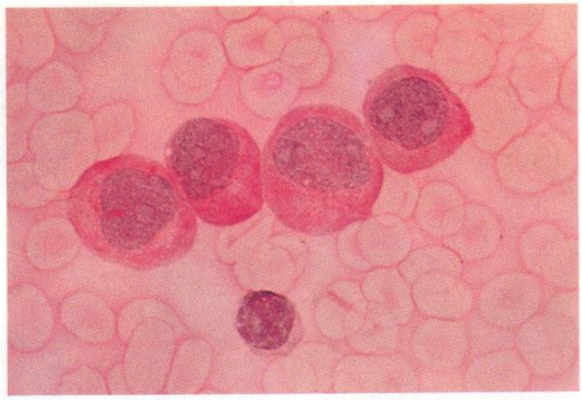

242

243

240. PAS reaction in APL, showing moderately strong, diffuse and finely granular positivity. Occasional nuclei show the APL type of twinning or distortion.

241. Another field from the same preparation showing unusually strongly PAS-positive Auer rods, including several in the cytoplasmic rim and others overlying the nucleus in the cell at the right of the field.

242. Another example of strong PAS positivity in an Auer rod overlying the nucleus in a leukaemic promyelocyte in APL.

243. Acid phosphatase reaction in APL: the leukaemic promyelocytes show only a very weak granular reaction, contrasting with the stronger reaction in a neighbouring plasma cell. As normal promyelocyte azurophil granules are usually quite rich in acid phosphatase, this weak reaction may indicate a lysosomal functional deficiency in APL.

244

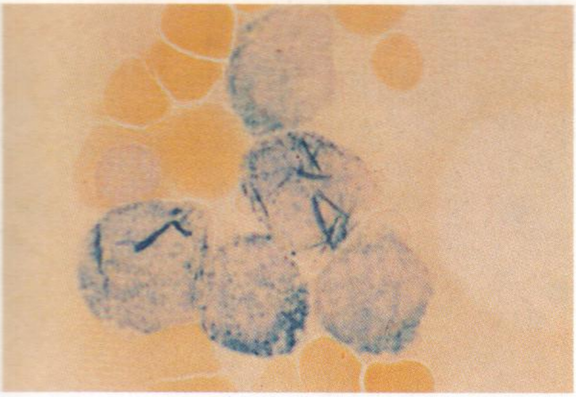

245

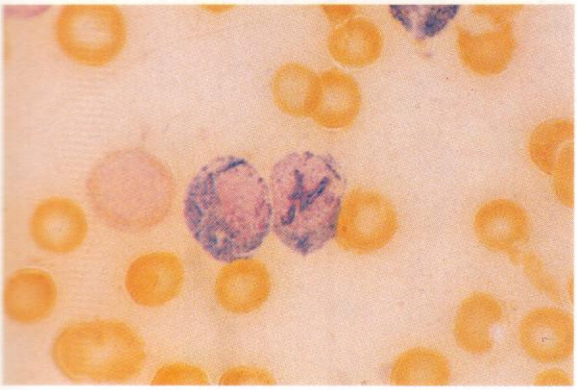

246

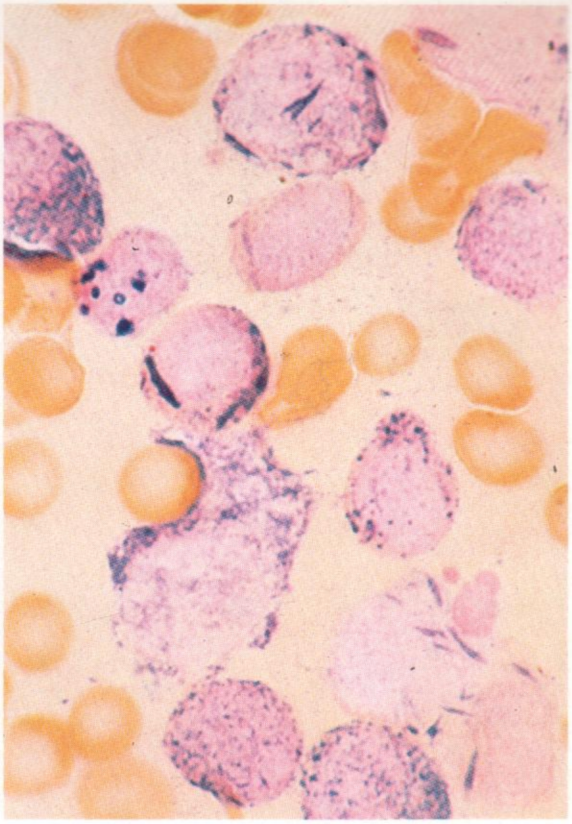

244. Dual esterase reaction in APL: there is a negative erythroblast present but all five promyelocytes exhibit strong granular CE positivity and two of them contain multiple Auer rods which are here intensely CE-positive. The strong reaction for CE, with or without negative or BE-positive central cores, is not usually seen in Auer rods except in the 15;17 and 8;21 translocations.

245. Dual esterase reaction in APL: a negative early erythroblast and two CE-positive promyelocytes containing multiple Auer rods showing CE-positive outlines but negative cores.

246. Dual esterase reaction in APL: the leukaemic cells show CE positivity with numerous strongly CE-positive Auer rods; the dense circular or ring-like CE-positive structures, some with a hollow CE-negative centre, seen especially in one of the promyelocytes, probably represent early stages in the formation of Auer rods. A sequence between these hollow rings and the more common hollow rods (as shown in **245**) can be made out.

247. A dual esterase reaction in another case of APL: the hollow rings and short Auer rods in several of the promyelocytes here display a CE-positive envelope with a BE-positive core.

247

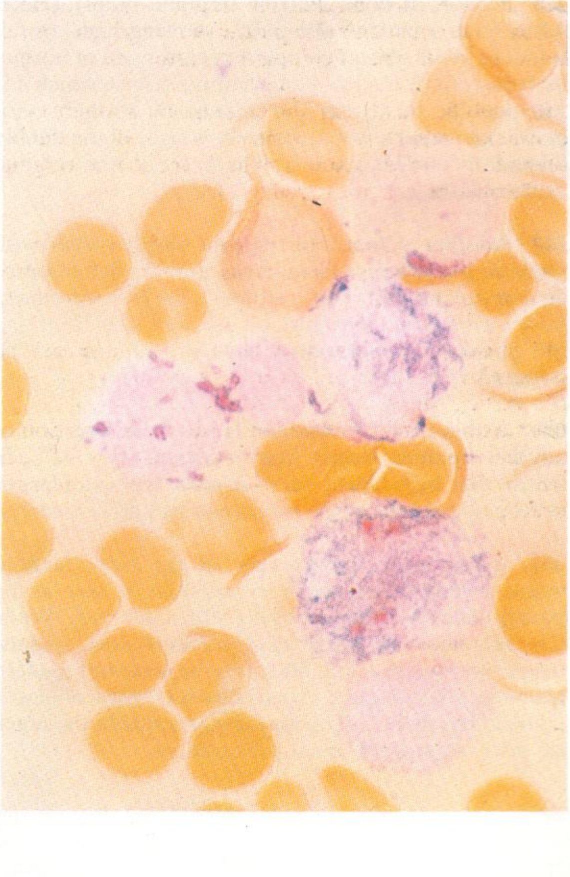

248

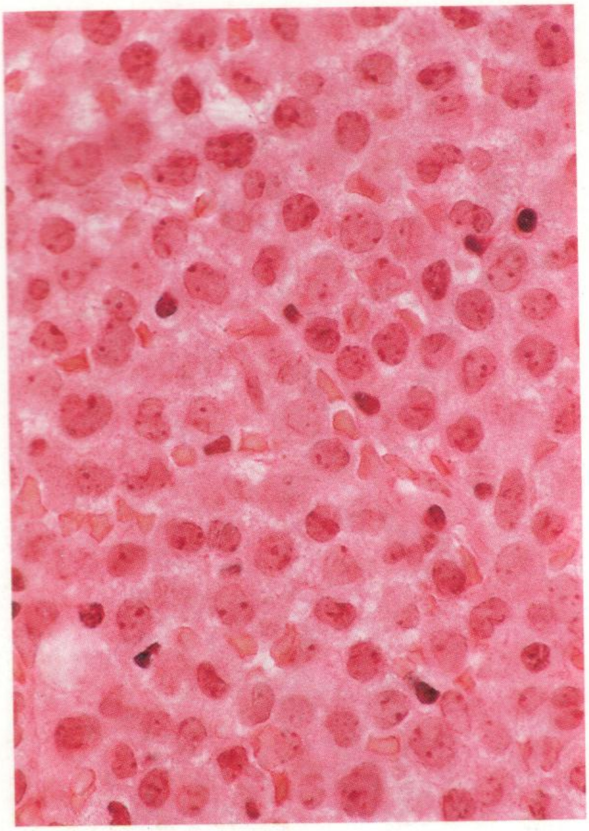

249

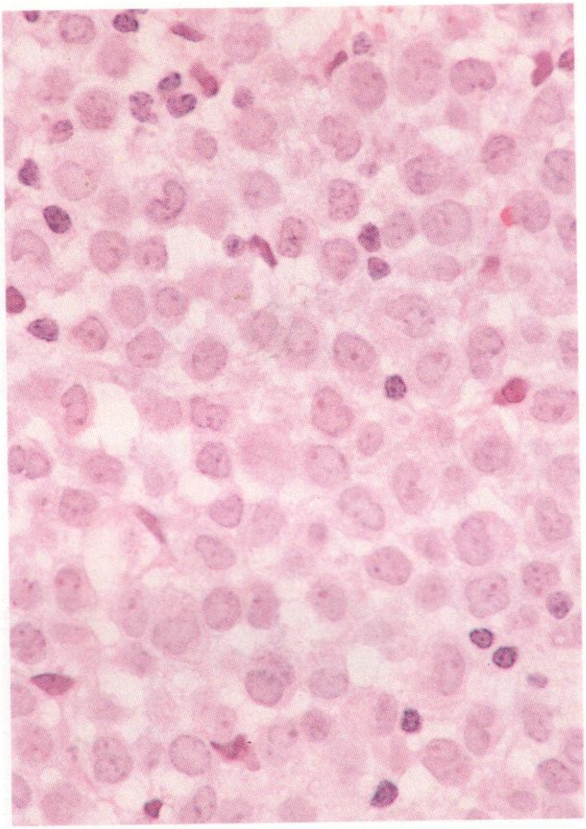

250

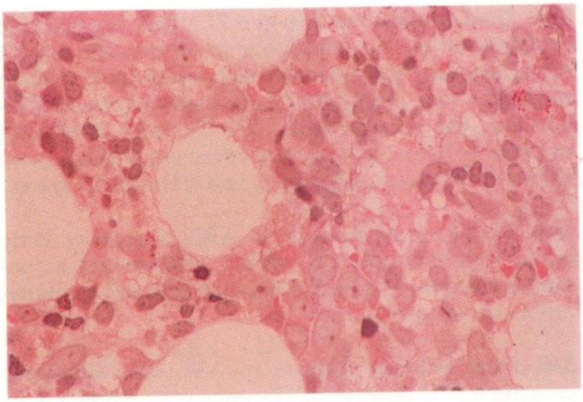

251

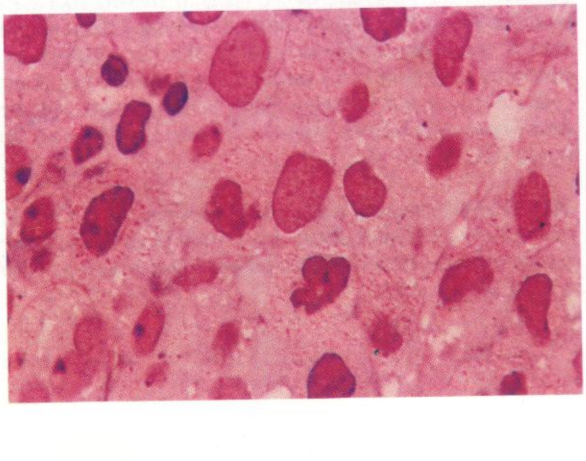

248. Section of bone marrow trephine biopsy (H&E stain) from a patient with APL, showing high overall cellularity with almost complete replacement of normal marrow cells by nucleolated primitive cells in which it is just possible to discern the granularity of their cytoplasm, and among which some show signs of the double lobulation nuclear pattern. There are a few residual erythroblasts.

249. Another section from the same biopsy stained with Giemsa, but not providing better granule definition or clearer cell differentiation, although the leptochromatic nuclei with prominent nucleoli are well visualized and the presence of occasional nuclear twinning can be detected.

250. A thin plastic-embedded H&E-stained section of another trephine biopsy from a patient with APL, in which this high-power view reveals the cytoplasmic azurophil granules of the promyelocytes more clearly.

251. A still-higher-power view of the same section, where several leashes of Auer rods can be seen in the poorly defined cytoplasm of the leukaemic cells. While this sequence of histological sections does include diagnostic material and illustrates the power of modern histological techniques, especially with the use of plastic embedding, there can be no comparison with the much superior cytology of smear preparations.

252

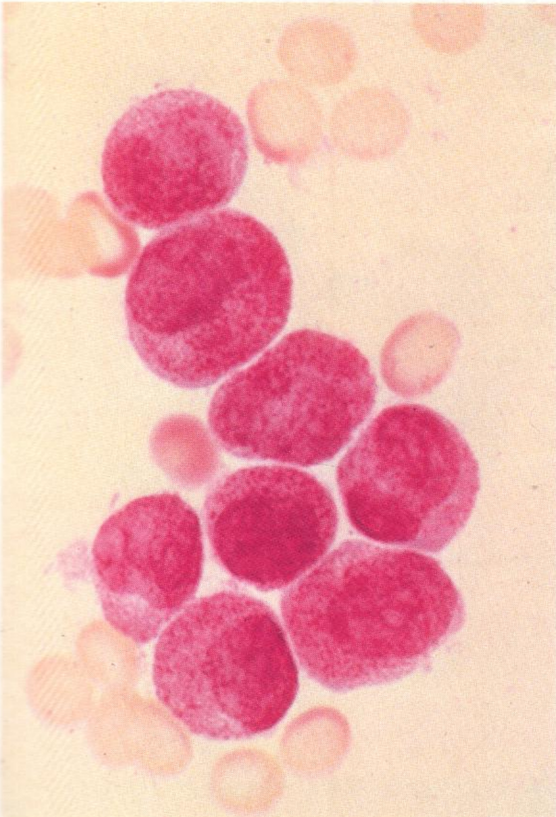

253

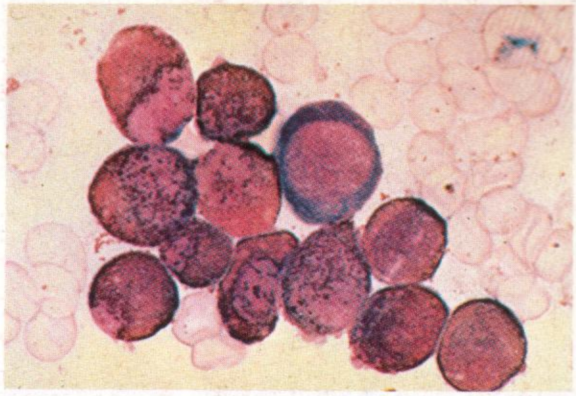

254

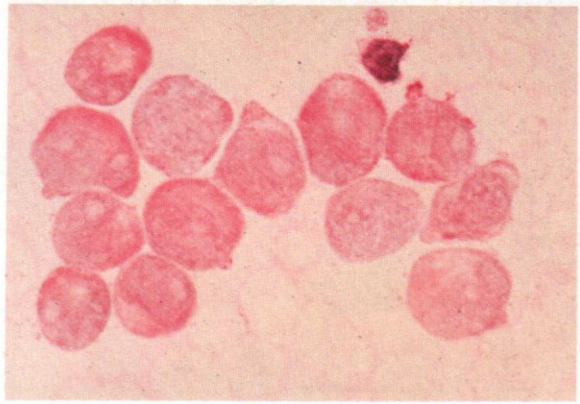

252–256. *A further APL variant.*

252. APL variant – the cells show numerous moderately coarse granules but no Auer rods were visible in either Leishman (here) or MGG stains.

253. Heavy granular SB positivity typical of promyelocytes but again no Auer rods.

254. Strong diffuse tinge of PAS positivity – the characteristic APL pattern.

255. Negative reaction or fine scattered granules only of acid phosphatase positivity.

256. Dual esterase – a remarkable mixture of strong reactions to both CE and BE, perhaps shared sometimes in the same granule (cf. **247**). A mixture of CE and BE positivity is quite commonly found in APL, either in different cells making up a dual population with respectively CE and BE positivity, or with both kinds of reaction present in the same cells. About a third of cases show this feature, but it is accompanied, as in this case, by otherwise typical promyelocytic cytochemistry and surface marker immunology and does not indicate the presence of a monocytic component.

255

256

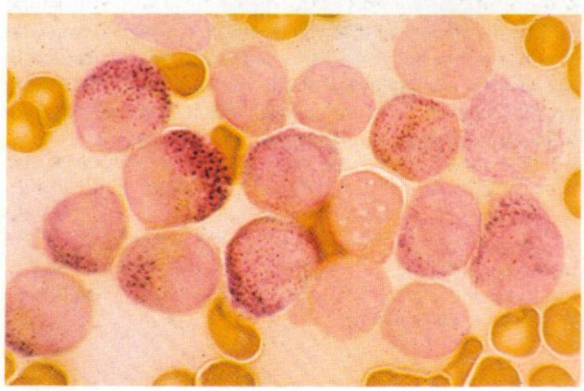

257

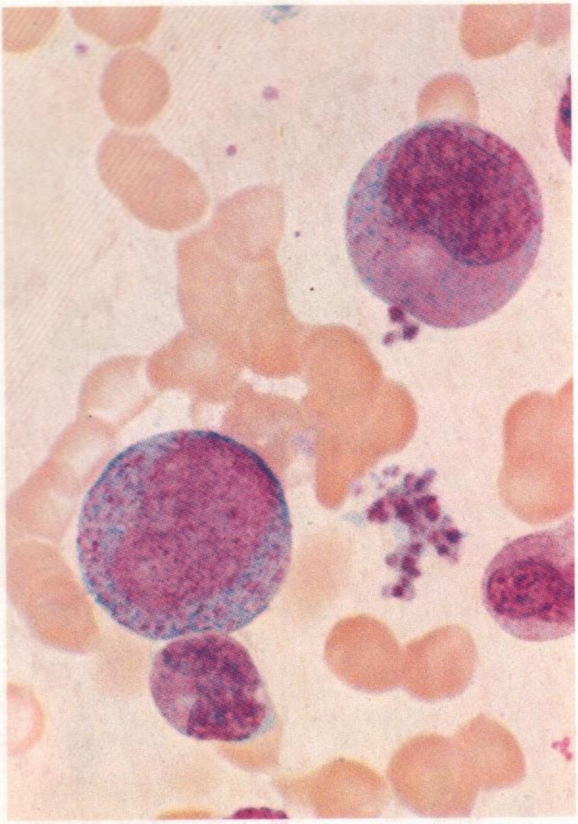

258

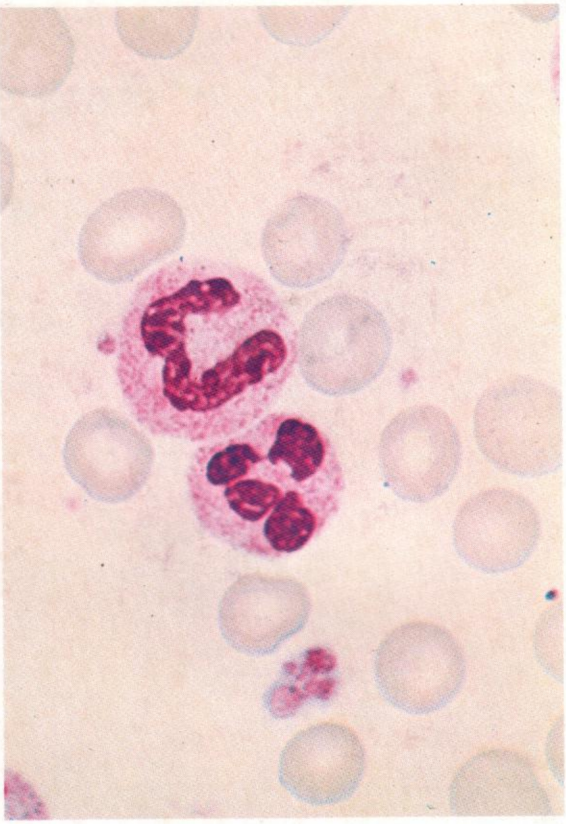

259

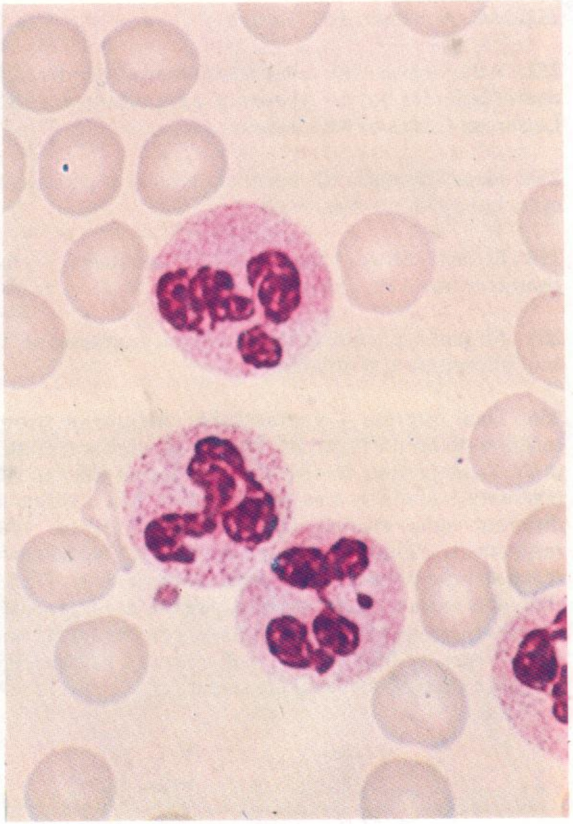

257. Exceptionally large promyelocytes, myelocytes and metamyelocytes may be encountered in the marrow of pernicious anaemia (PA) and sometimes of other megaloblastic (and rarely normoblastic) anaemias. Here are examples of giant promyelocyte and myelocyte from PA.

258. A neutrophil stab cell and a segmented cell from normal peripheral blood.

259. Three segmented neutrophil polymorphs, one showing a drumstick appendage. Two small sessile appendages, not countable as drumsticks, are visible in the upper cell. Well-separated small nuclear appendages, attached to the main nucleus by a short narrow strand, are found in female neutrophils only and represent the same inactive late-replicating X-chromosome material as is visible in the Barr bodies of buccal mucosal or other epithelial cells. They are not to be confused with the smaller protrusions, which have a broad attachment rather than a narrow stalk, and which occur quite often in the neutrophils of either sex.

260

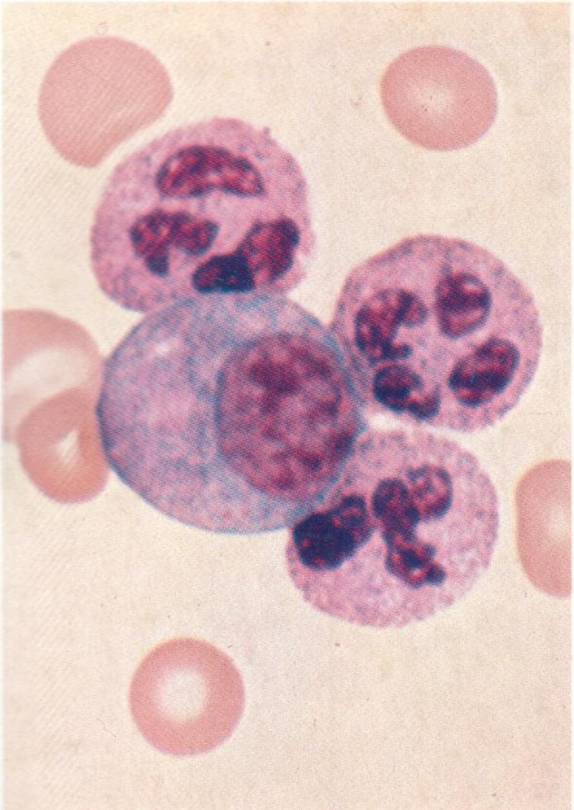

261

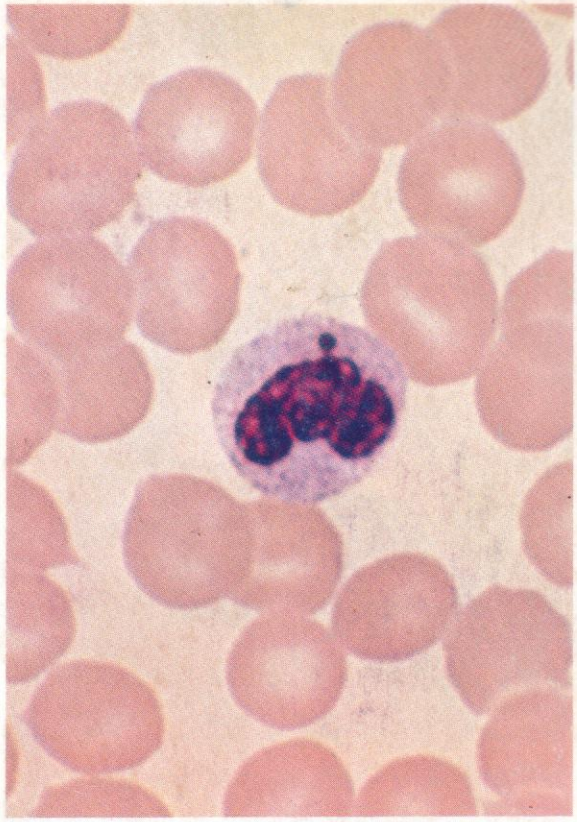

262

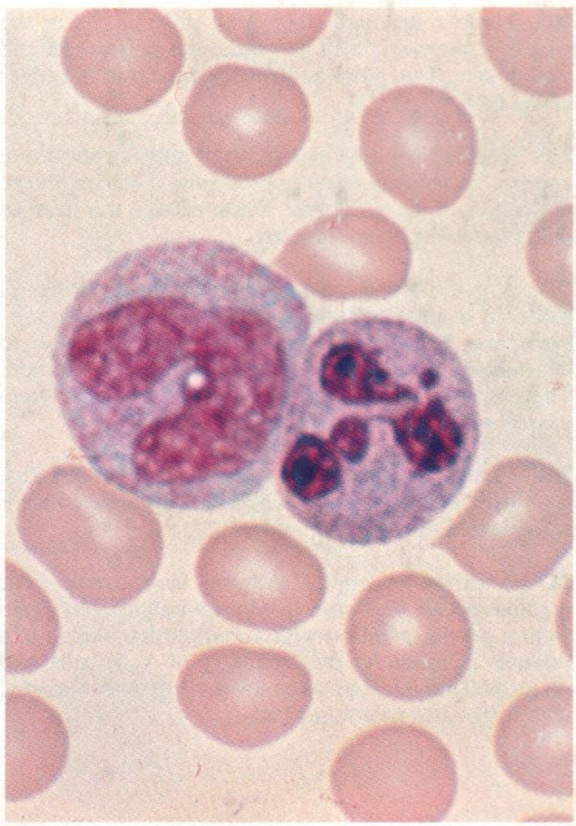

260. Three segmented neutrophil polymorphs and a myelocyte. The myelocyte still retains a degree of cytoplasmic basophilia as compared with the later neutrophils, and the nucleus – although showing the irregularly dense chromatin pattern associated with maturation – is less pachychromatic than in the case of the polymorphs.

261. A drumstick appendage attached to the nucleus of a stab cell. Although the connecting strand is a little thicker than in the typical appendage, the size is about right and the body is acceptable as a female drumstick appendage.

262. A segmented neutrophil polymorph, with drumstick appendage and a monocyte. The lighter grey staining of the monocyte cytoplasm and the more open chromatin pattern of the nucleus contrast clearly with the staining colour and intensity of the neutrophil, despite the granularity of this monocyte cytoplasm. The granules are also different, being generally finer and with a more reddish and less purple colour in the monocyte as compared with the neutrophil polymorph.

263

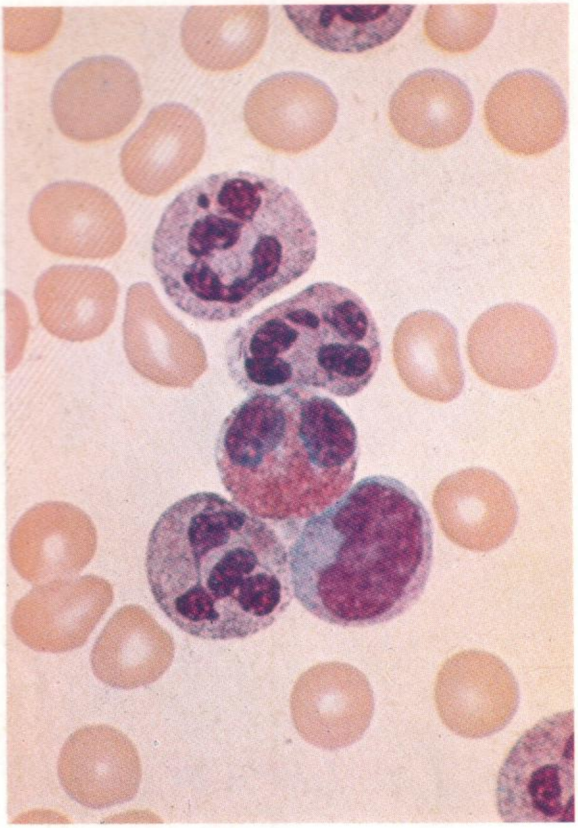

264

265

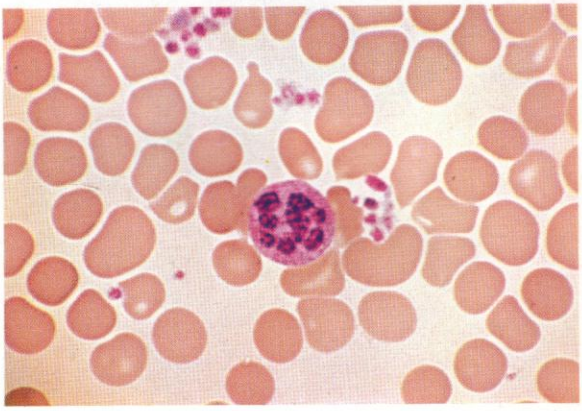

266

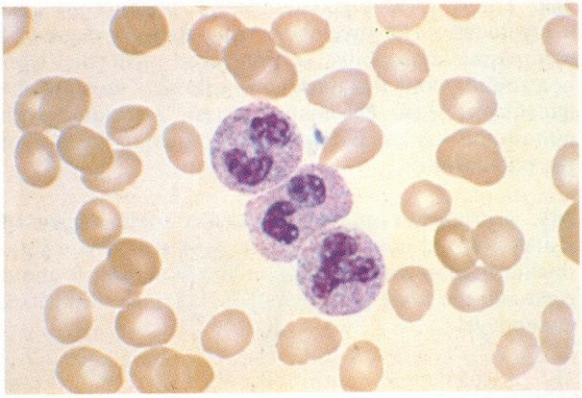

267

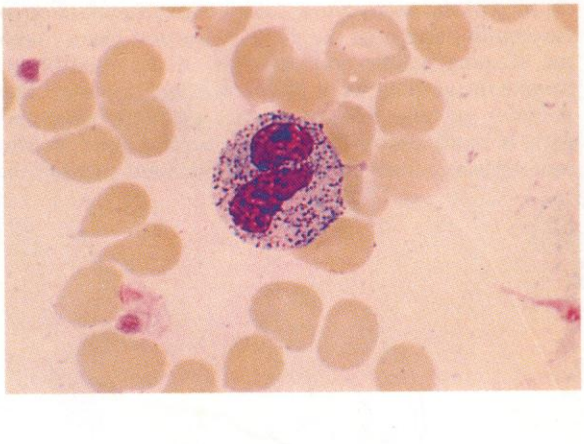

263. Three segmented neutrophil polymorphs in the centre of the field, with an eosinophil polymorph and a monocyte. Two more neutrophils appear at the edges of the field.

264. Nuclear twinning in neutrophil polymorphs; there appears to be something approaching a mirror image disposition of nuclear lobes. This specimen was from an AML following chemotherapy.

265. A multi-lobed polymorph from the peripheral blood in a megaloblastic anaemia. These macropolycytes may be found in megaloblastic states due to deficiencies of either cyanocobalamin or folic acid. There is anisocytosis and macrocytosis of the accompanying red cells visible in this field.

266. Coarse granularity in stab cells from an infective state with leucocytosis and left shift. This appearance is sometimes called toxic granularity.

267. Another neutrophil showing very coarse toxic granulation, in this case a bilobed polymorph, again from a severe infection with a marked left shift, i.e. a relative increase in the numbers of stab cells and neutrophil polymorphs with only two lobes as compared with three- and four-lobed cells.

268

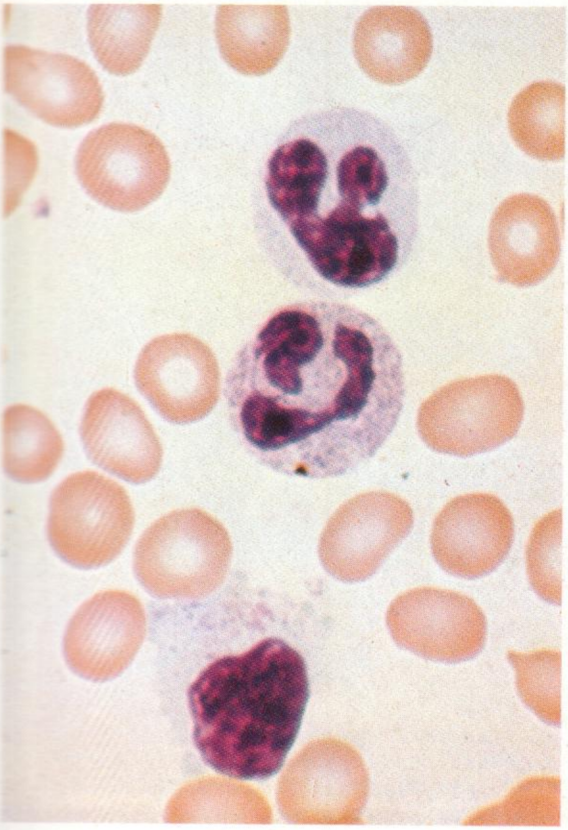

269

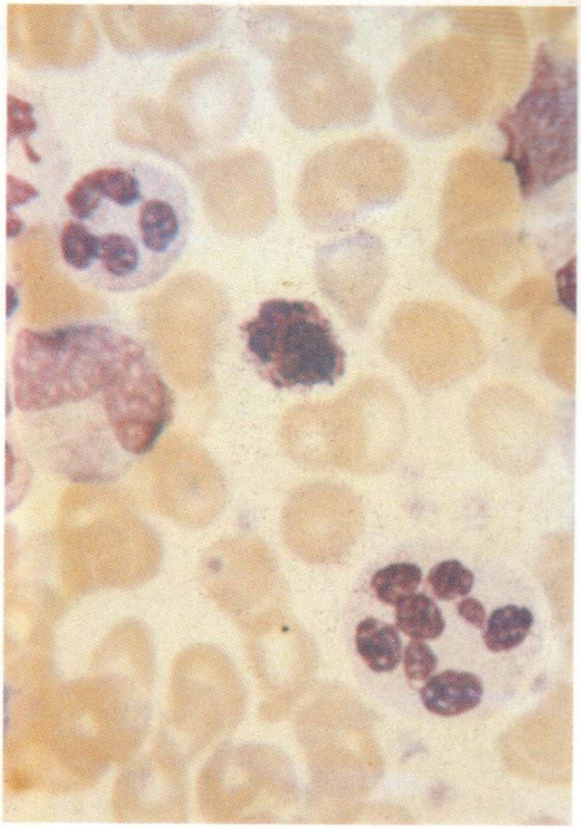

270

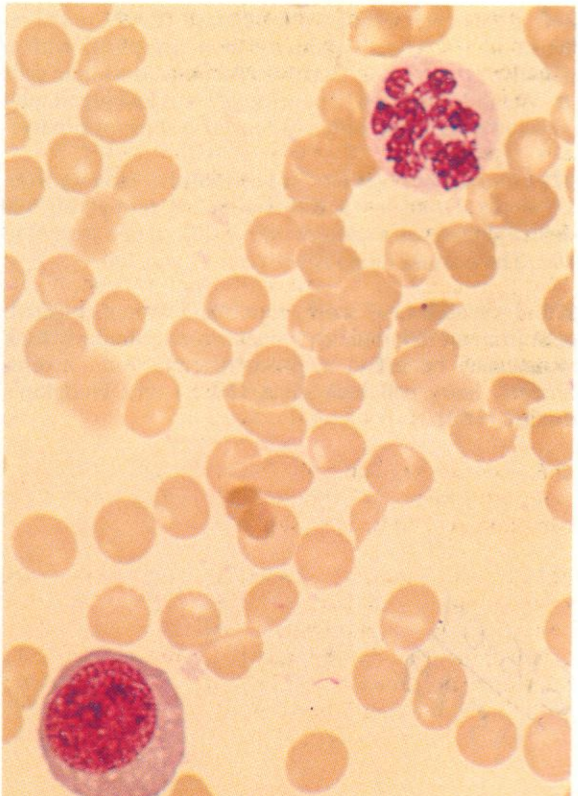

268. A normally granular and a non-granular neutrophil polymorph, together with a lymphocyte. Absence of granularity in polymorphs is most common in leukaemic states but may occasionally be seen in most anaemic or leucopenic states.

269. A poorly granular multi-lobed polymorph from the bone marrow in a case of pernicious anaemia. A second segmented cell with four nuclear lobes, a basophil polymorph and various earlier granulocytes make up the remainder of the field.

270. A smear from the buffy coat of a blood sample taken from a patient who developed severe deficiency of both B_{12} and folic acid while on parenteral nutrition in an intensive therapy unit. The field shows an early basophilic megaloblast and a multi-lobed polymorph or macropolycyte. Two red cells contain Howell-Jolly bodies.

271

272

273

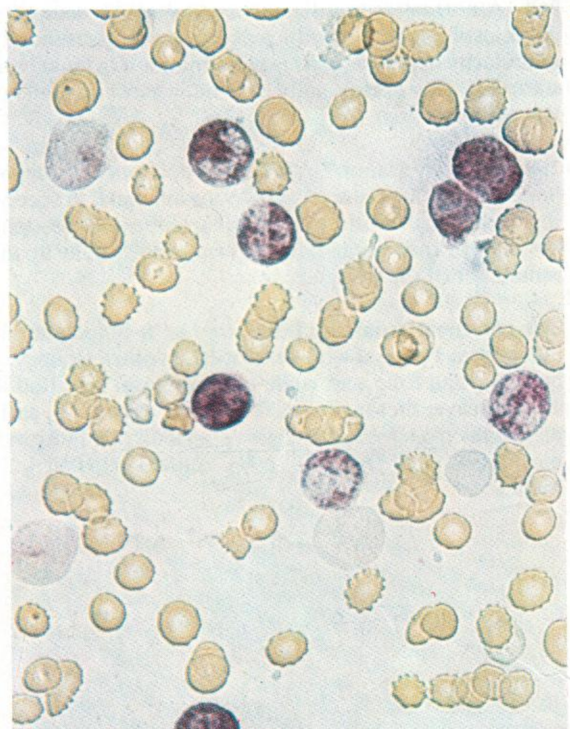

271. Leucocyte alkaline phosphatase (LAP) reaction. Weak and stronger positivity in neutrophils, with a negative lymphocyte. Positive reactions in haemic cells are virtually confined to neutrophil stabs and segmented cells, although macrophages may also show positivity.

272. Grades of positivity in polymorphs, ranging from 1 (+) to 4 (++++). Summation of ratings on 100 neutrophils gives a score with possible range from 0 to 400. The normal range is between 15 and 100.

273. Increased LAP score, with many strongly positive cells from an inflammatory leucocytosis. Similarly high scores may be found in polycythaemia vera, myelofibrosis, hairy cell leukaemia (HCL) and Hodgkin's disease (HD).

274

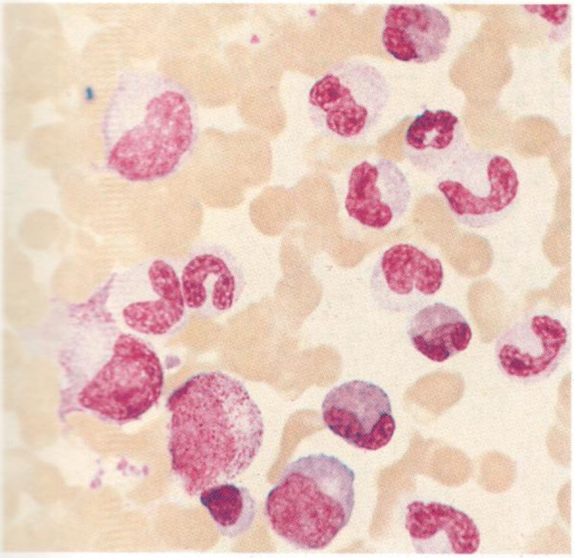

275

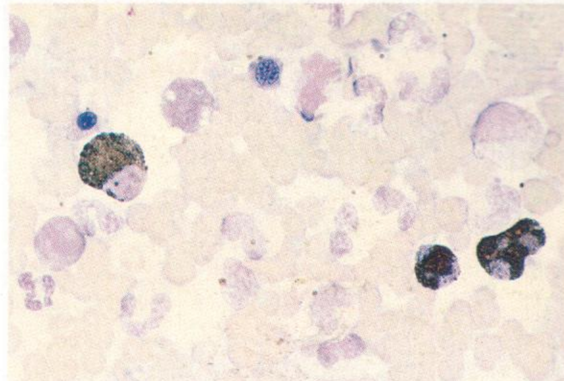

276

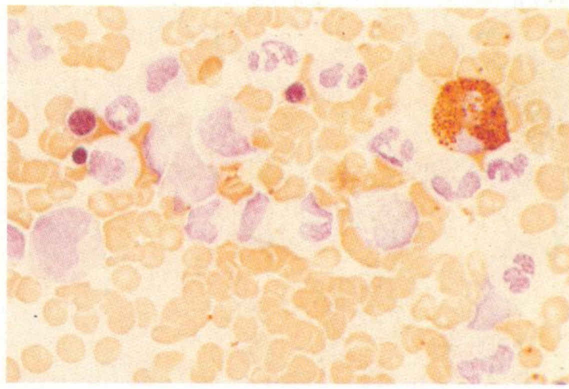

277

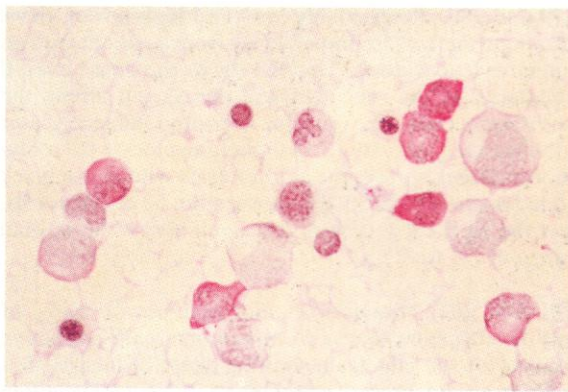

278

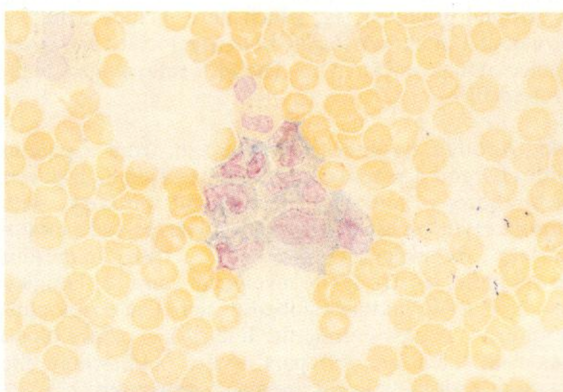

274–278. *Cytology and cytochemistry of bone marrow cells from a patient with an hereditary leucocyte defect involving enzyme deficiencies and the Pelger-Huët anomaly.*

274. Romanowsky stain illustrating various stages of granulocyte maturation and a single late normoblast at the bottom of the field. Azurophil granules are visible in the promyelocyte just above the normoblast, and specific granules are present in the three mature eosinophils, but the neutrophils show little or no granularity. All the mature granulocytes, neutrophils and eosinophils alike, show unsegmented coarsely pachychromatic nuclei with a straight or curved band or dumb bell-like structure, typical of the rare homozygous form of the Pelger-Huët anomaly. This is a benign familial disorder, inherited as an autosomal dominant. In the commoner heterozygotes the neutrophils have mostly bilobed nuclei.

An acquired form of this anomaly, which occurs quite often in myeloproliferative states and generally resembles the heterozygotic form has already been illustrated in dealing with the 8;21 translocation variant of AML (215).

275 and 276. SB and DAB-peroxidase, respectively, showing normally positive eosinophils but negative neutrophils. The deficiency of myeloperoxidase (MPO), here shown in the familial form which, like the Pelger-Huët anomaly, is inherited as an autosomal dominant, also develops commonly as an acquired feature in myeloproliferative states, especially in AML, CML, myelofibrosis and myelodysplastic states.

277. The PAS reaction is normally positive in the neutrophils.

278. Dual esterase staining reveals a reduction in expected positivity of the neutrophils for CE, although some enzyme is present.

279

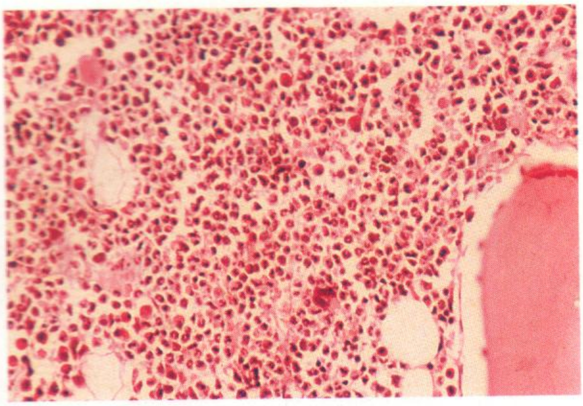

280

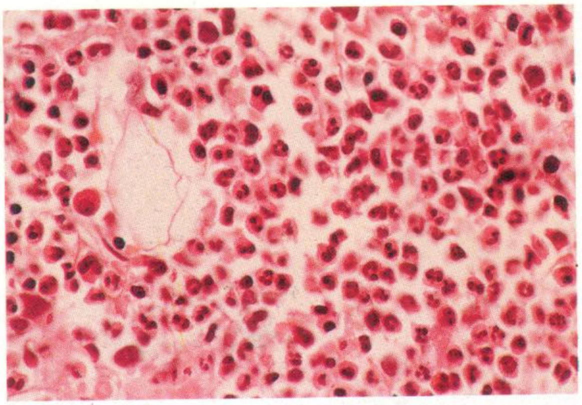

281

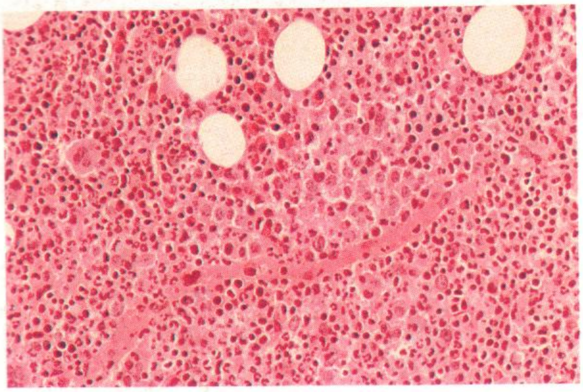

282

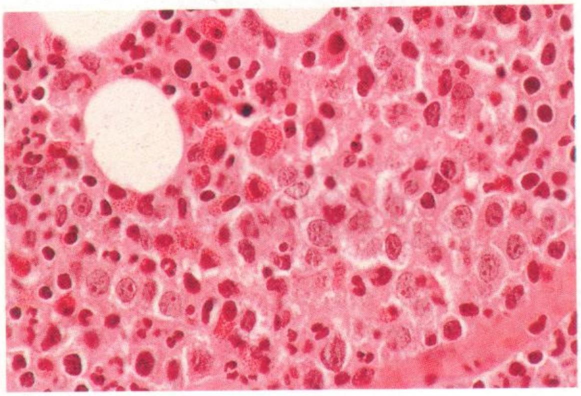

283

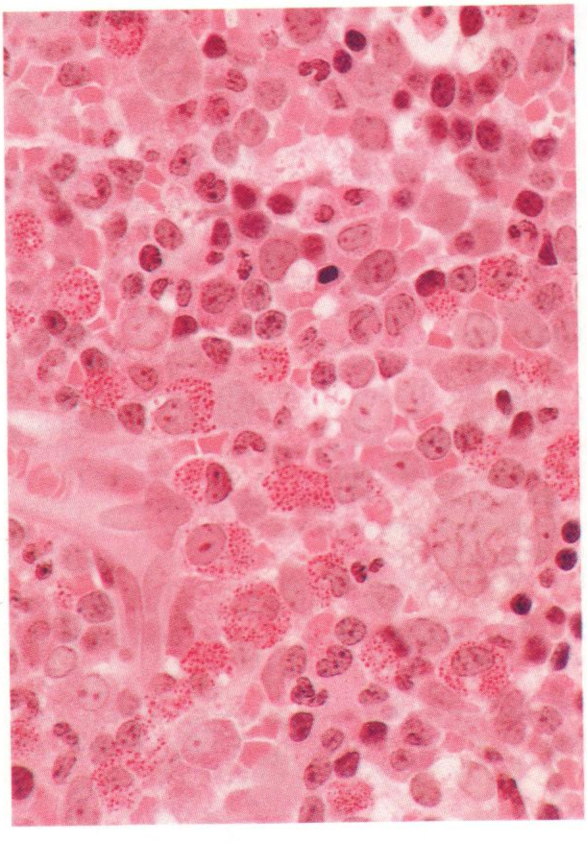

279 and **280**. Respectively low- and high-power views of a bone marrow trephine biopsy from a patient with an infective leucocytosis. The first shows the dense overall cellularity of the specimen and the second allows the constituent cells to be recognized as predominantly later granulocytes, mostly at the metamyelocyte to polymorph stages. A few late normoblasts with dense black round nuclei and minimal cytoplasm can be distinguished, but the M:E ratio is over 20:1, well above the normal range of 2:1 to 8:1.

281 and **282**. Similar low- and high-power views of another trephine biopsy from a patient with a reactive leucocytosis in HD again showing dense cellularity, but with a more mixed cytological picture, including erythroblasts and eosinophils as well as the predominating neutrophil granulocytes, which here include a higher proportion of earlier stages, both myelocytes and some nucleolated promyelocytes. The M:E ratio is again high, around 10:1.

283. Another trephine biopsy section from a patient with HD and a reactive eosinophilia. This high-power view shows a generally pleomorphic cytology, with various erythroblast and granulocyte stages and a mononuclear megakaryocyte, together with numerous eosinophils, mostly at the myelocyte stage, although a few have more mature bilobed nuclei. The eosinophils tend to be grouped along the line of a capillary blood vessel in the lower left part of the field, where the vascular endothelial cells are also conspicuous.

284

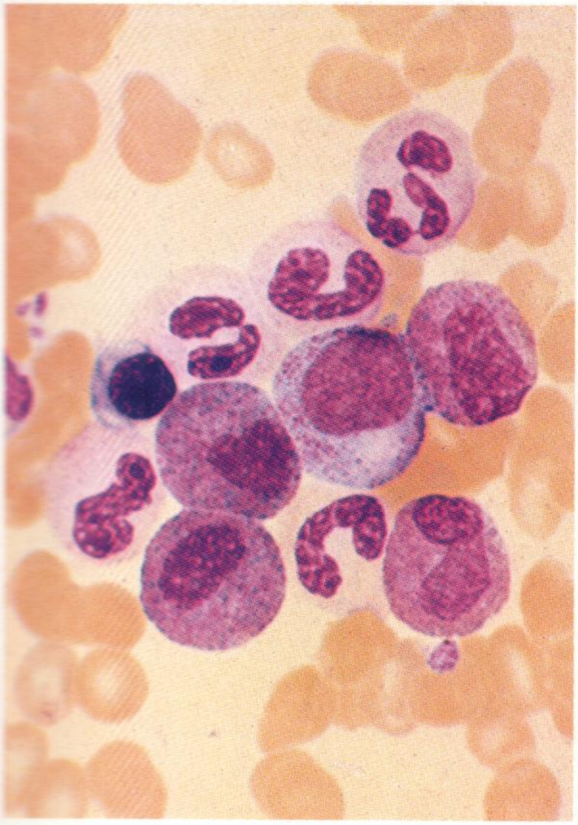

285

286

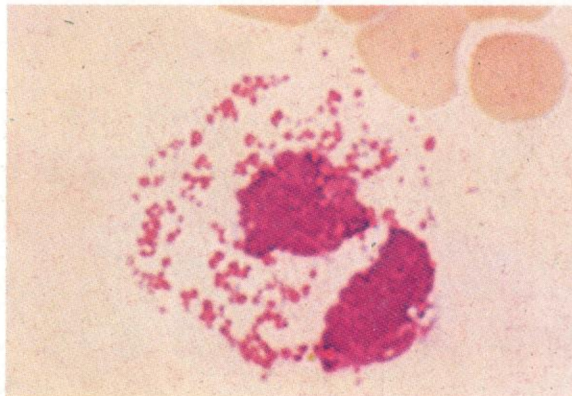

287

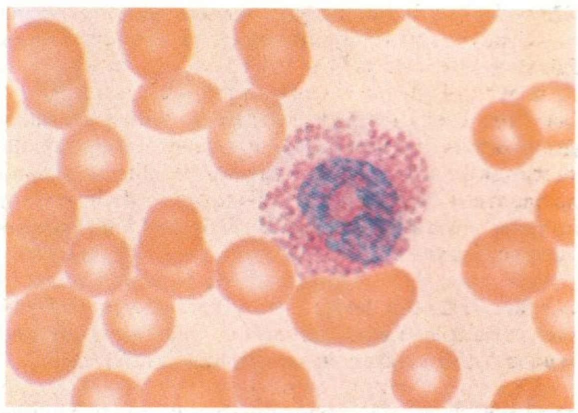

288

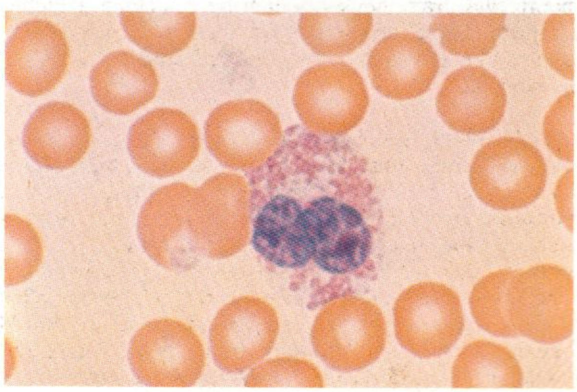

284. Eosinophil myelocytes and metamyelocyte in bone marrow. There is also a neutrophil myelocyte, various stab and segmented neutrophils, and a late normoblast.

285. A normal eosinophil polymorph, showing the characteristic 'spectacle' arrangement of the nuclear segments, which are usually two in number. The surrounding red cells show slight hypochromia and there is a single platelet overlying one of them.

286. A disrupted eosinophil. In this and the next two figures, the relatively large size of eosinophil as compared with neutrophil specific granules can be appreciated.

287 and **288**. Eosinophil polymorphs with agranular spaces in the cytoplasm. This appearance is not uncommon, but becomes most frequent and conspicuous in leukaemias. The lower cell has a typically bilobed nucleus but the upper has an annular or ring nucleus, a feature only occasionally seen in normal mature eosinophils or neutrophils although more common in some forms of AML, notably cases with 8;21 translocation (q.v.).

289 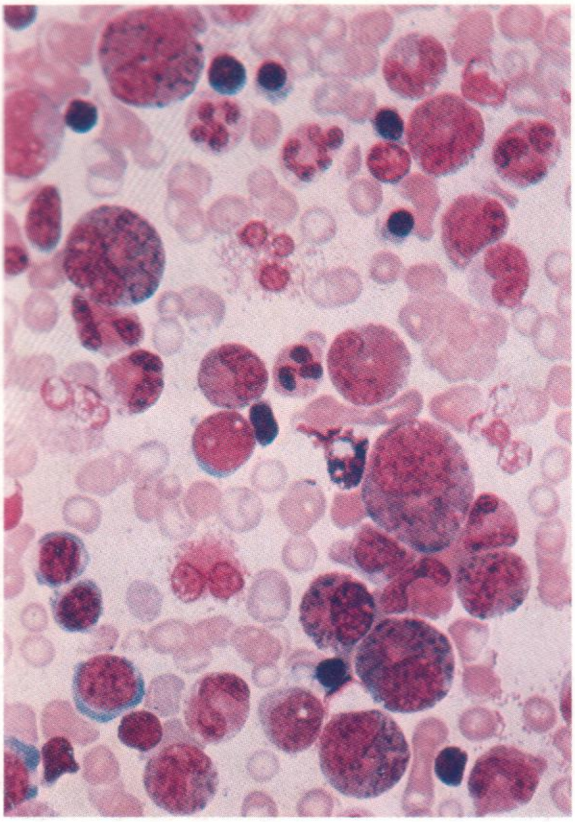

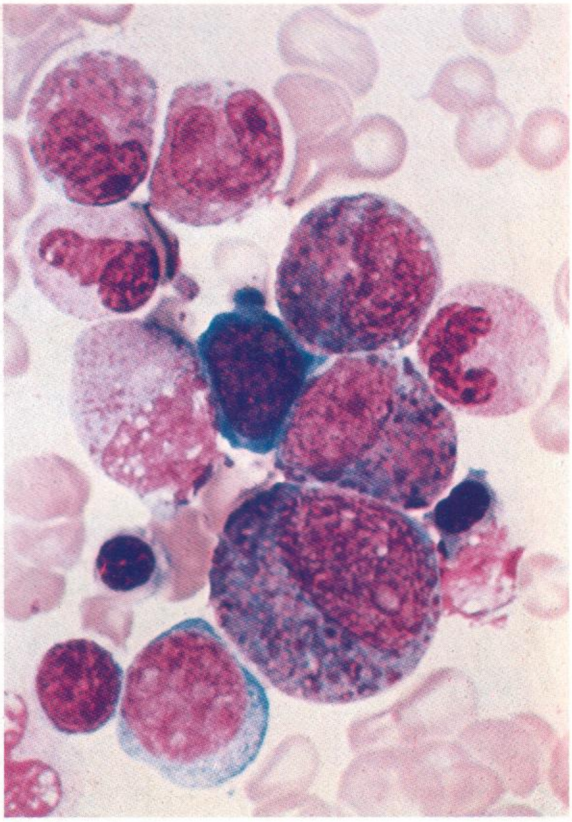 290

289. Familial eosinophilia; general view of bone marrow; all stages of maturation in the eosinophil series are present.

290. The same case: high-power view to show 'amphophil' appearances (both basophil and eosinophil-staining granules) in eosinophil promyelocyte and myelocytes. The 'basophil' granules probably represent primary eosinophil granules. This amphophil appearance of granules in eosinophils, seen here in an hereditary eosinophilia, is a striking and conspicuous feature of certain variants of AML, especially cases with chromosomal abnormalities affecting the long arm of 16, and also to a lesser extent those with 8;21 translocation.

291. Peripheral blood in the same case as in **289** and **290**. Numerous mature eosinophil polymorphs are present.

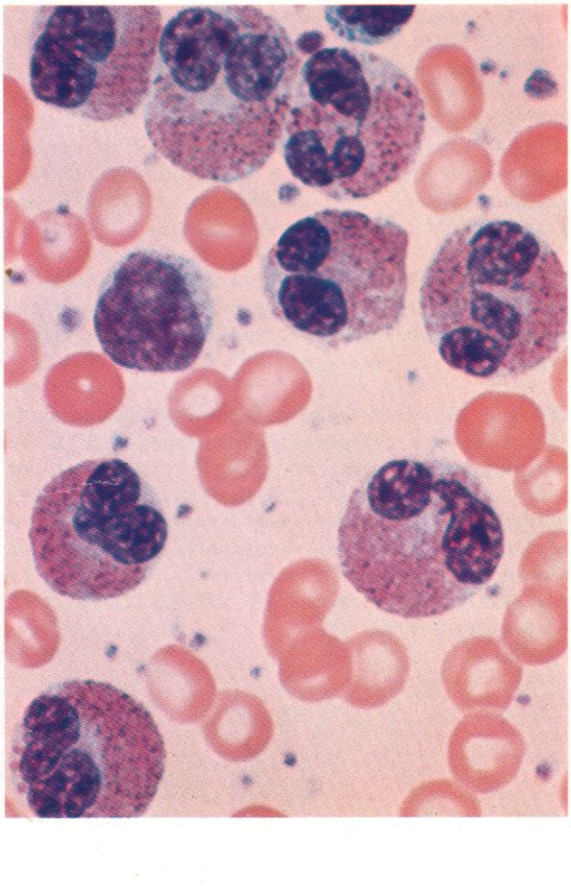 291

292

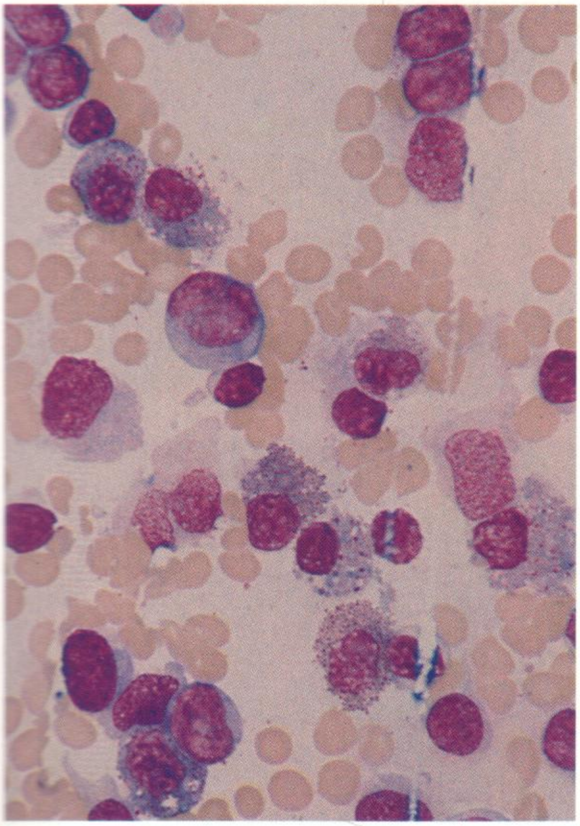

293

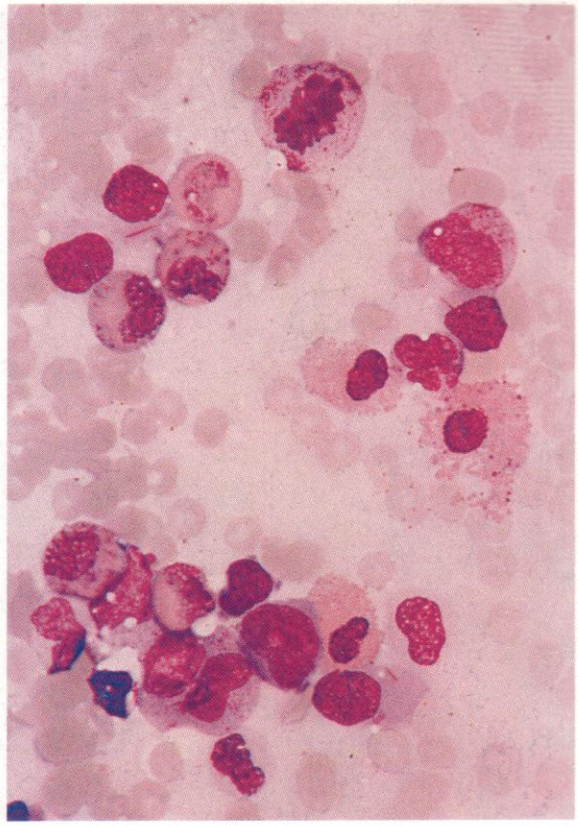

292–304. *Cytology and cytochemistry of bone marrow cells from cases of AML with abnormalities – deletions, inversions or translocations – involving the long arm of chromosome 16 – del(16)(q22), inv(16)(p13;q22), or t(16;16)(p13;q22).*

292–294. General low-power views of bone marrow aspirates from three cases of AML with chromosome 16 defects. Such cases show a highly cellular mixed population, with a predominance of blast cells, usually, but not always, including some with nuclear twisting or indentation suggesting monocytic lineage and others with promyelocytic or later granulocytic features. The cases illustrated here all show these mixed features, but about 20% of cases have more purely granulocytic precursors, and occasional cases are essentially monocytic. Among the blast cells are scattered variable numbers of eosinophils, at all stages of maturation, with frequent abnormalities of granule staining and disposition. In **292** the numerous eosinophils mostly have a blue tinge, while in **293** and **294** the colour of most granules is more normal but some cells show an admixture of darker, more basophilic, granules, illustrated in more detail in the next figures.

294

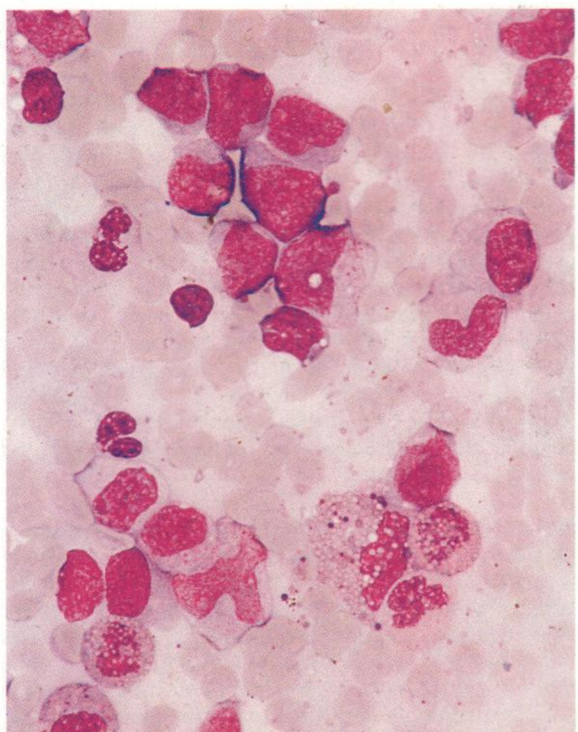

295

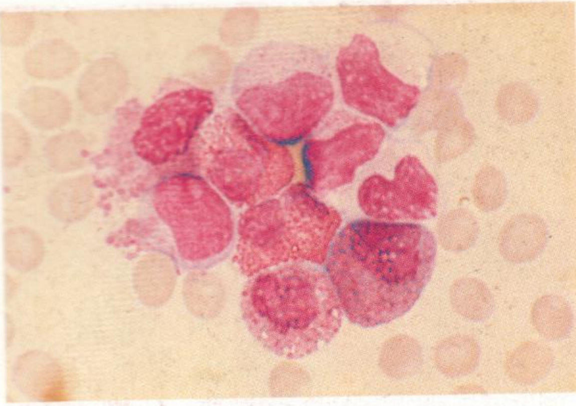

296

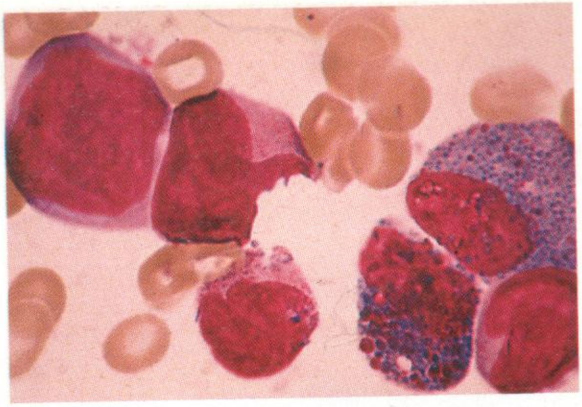

297

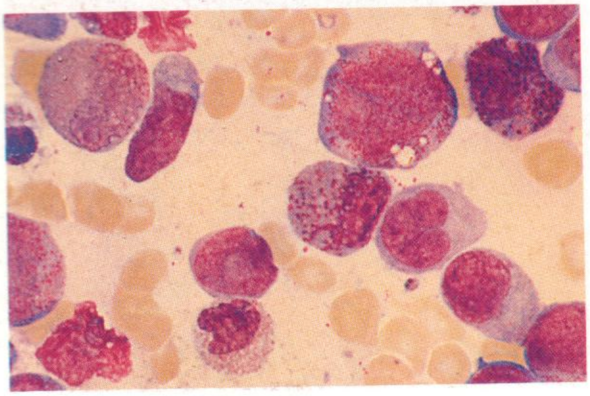

298

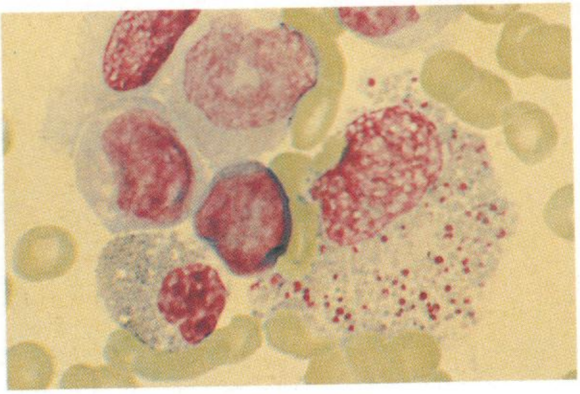

295–298. Higher-power views of the marrow cells in AML with 16q abnormalities. There are abnormal eosinophils in each field. They are least prominent in **295**, which has five eosinophils, three with normal granules, one disrupting, and the fifth with some amphophilia. The lowest cell shows lack of segmentation of its otherwise mature nucleus, a pseudo-Pelger-Huët phenomenon frequently seen in these cases. The two eosinophils in **296** are grossly abnormal, with a scattering of coarse deep red or basophilic granules and a blue-black colour replacing the normal eosin stain of the predominant granules. Similar features are shown in variable degrees in **297** and **298**, the granule colour replacing eosin ranging from blue to greenish-grey and the basophilic granules varying widely in numbers. These fields also demonstrate the variable size of blast cells and the common presence of both granulocyte and monocyte precursors.

299

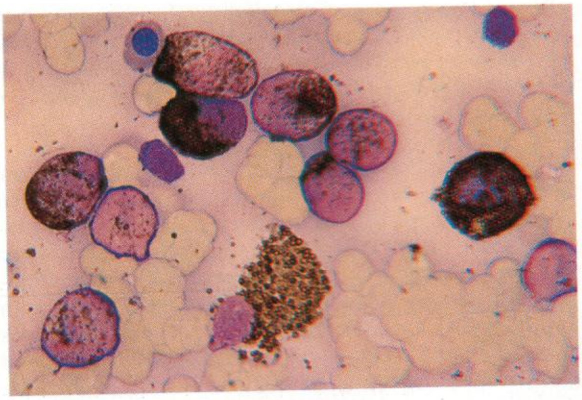

300

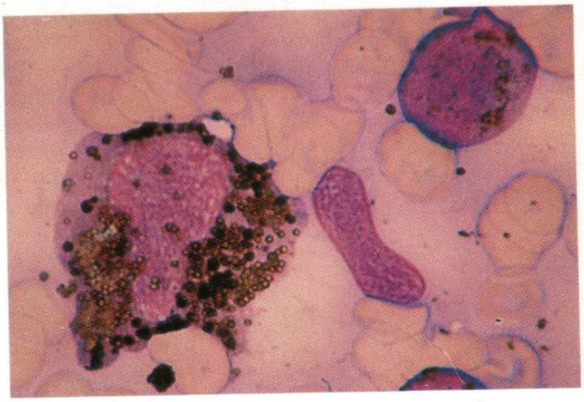

299 and **300**. Low- and high-power views of SB staining in a case of inv(16). In **299** the presence of strong localized or heavy overall positivity of the granulocytic type in six blast cells contrasts with the monocytic type of discrete scattered granules of positivity in four. In this field, and also in **300**, the eosinophil granules show a mixture of the normal reaction – positive shell with negative centre – and solid sudanophilia, the latter probably in the coarser and more basophilic abnormal granules.

301

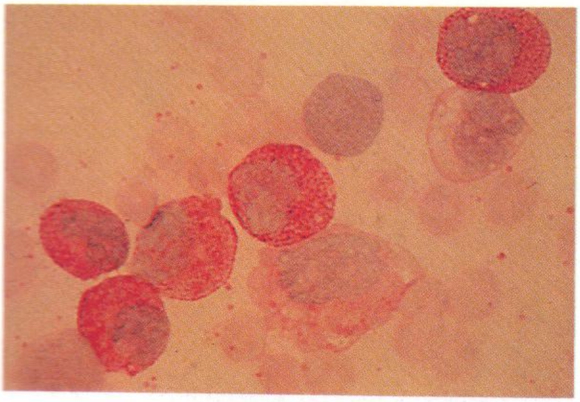

302

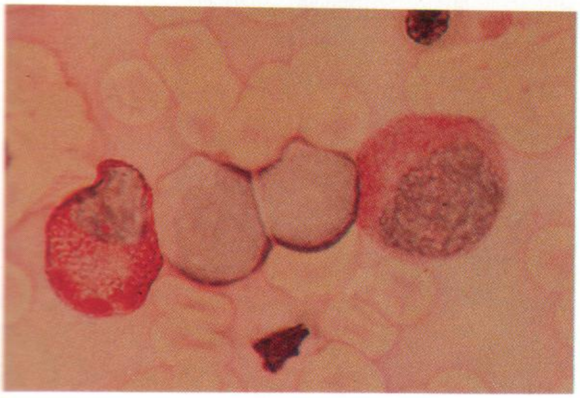

303

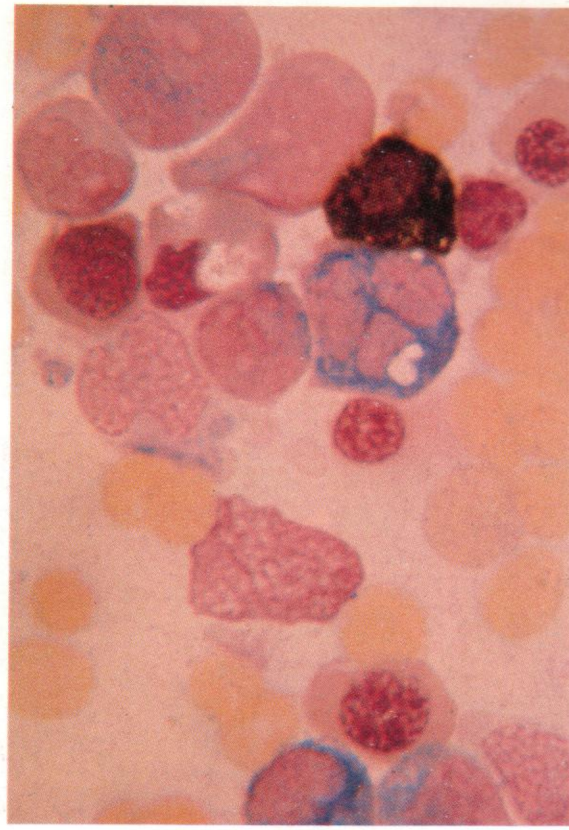

304

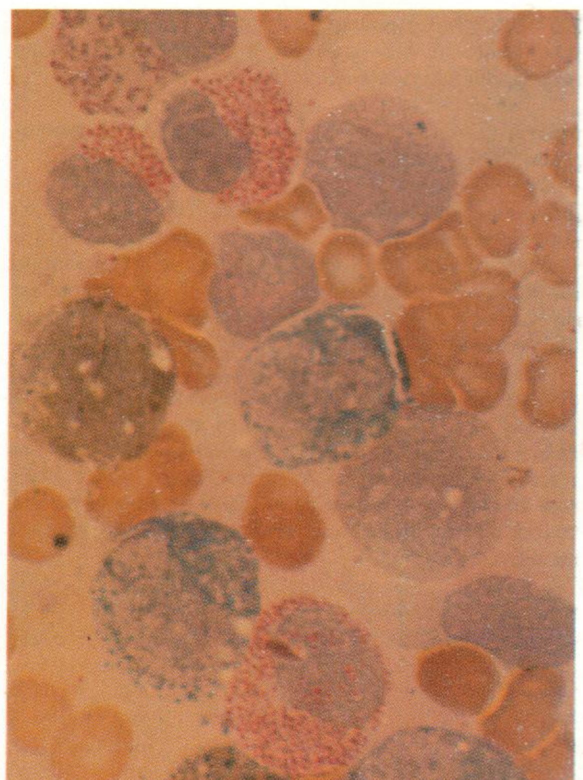

301 and **302**. PAS reactions in marrow cells from AML with inv(16), showing negative or weak finely granular and diffuse positivity in blast cells, but strong and variable positivity in the atypical eosinophils. Some granules show the usual negative reaction against a positive cytoplasmic background, while others react with a solid positivity. A disrupting early eosinophil in **301** has positive granules of this type, some being scattered widely across the whole field.

303. Dual esterase reaction in a similar case, showing negative erythroblasts, one apparently containing eosinophil granules within a vacuole, several myeloblasts or promyelocytes with weak-to-strong CE positivity, one monoblast with strong BE reaction, and two neighbouring degenerating and partially disrupted eosinophils at the centre left of the group, one with weak CE positivity in some of the coarser granules, a feature not normally seen in eosinophils.

304. Dual esterase reaction combined with Chlorazol Fast Pink (a dye reacting specifically with eosinophil granules) to show the variable pattern of CE positivity in the granules, several eosinophils showing only the Fast Pink stain but others, notably the cell at the top left, reacting also for CE. Blast cells of granulocytic and monocytic lines show respectively CE and BE positivity.

305

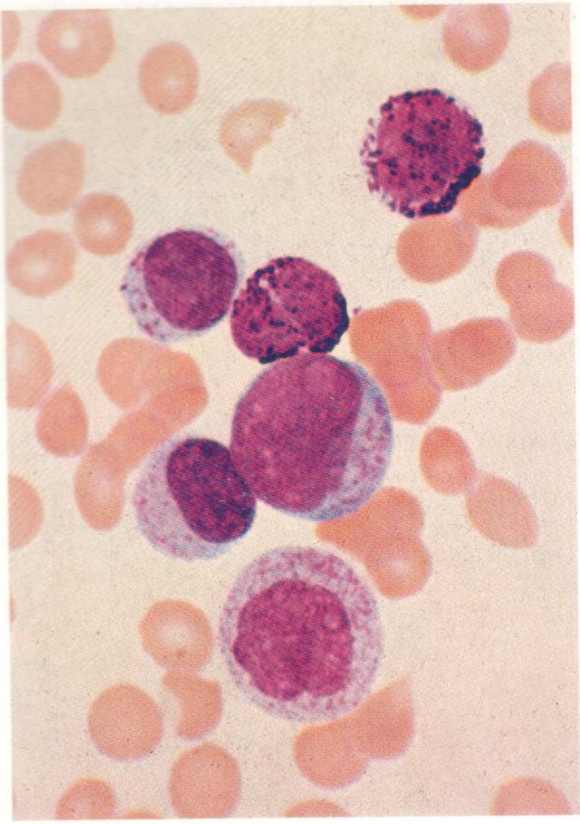

306

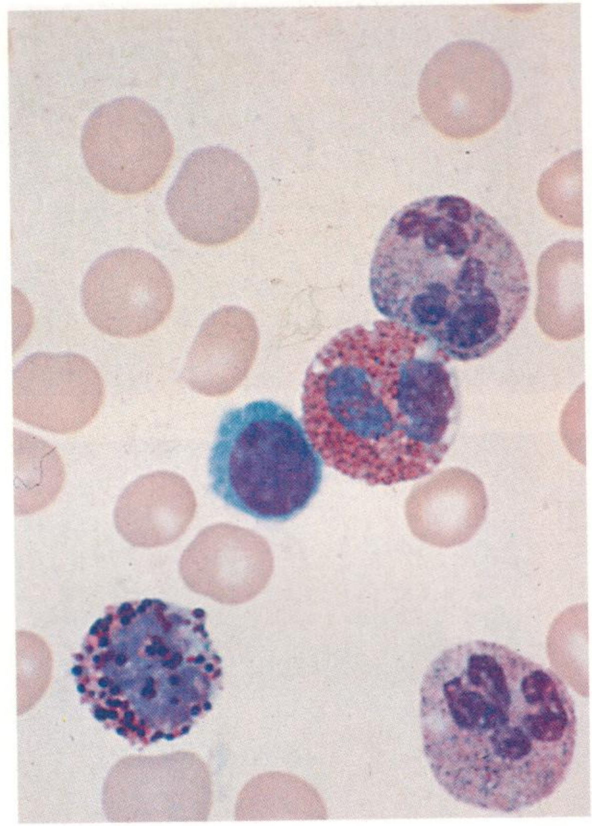

307

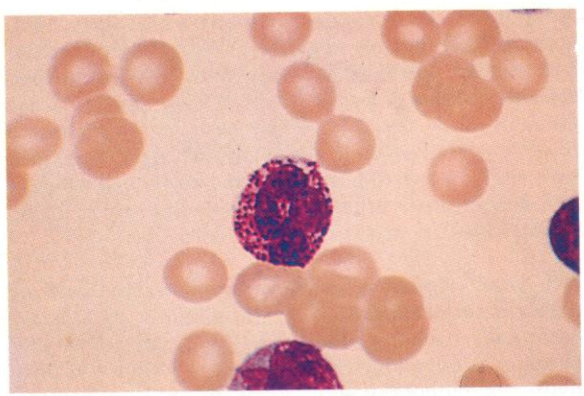

308

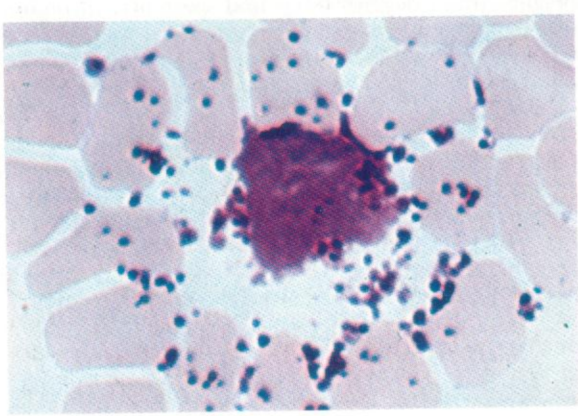

305. Basophil precursors, together with neutrophil precursors, in the blood of a patient with chronic myeloid leukaemia (CML).

306. A basophil polymorph, together with two neutrophils, an eosinophil and a lymphocyte.

307. Another basophil polymorph. These cells do not show the clear separation of nuclear lobes seen in mature polymorphs of other kinds, but overlapping lobes may be distinguished. Here, the coarse granules do not entirely obscure the nuclear structure, which can be seen to have three incompletely separated lobes.

308. A disrupted degenerating basophil, with loss of nuclear structure and scattering of granules. The individual basophil granules, scattered in this way and usually seen at the tail of the smear, vary considerably in size and shape, often being larger than normal neutrophil or eosinophil granules and sometimes having a rod shape.

309

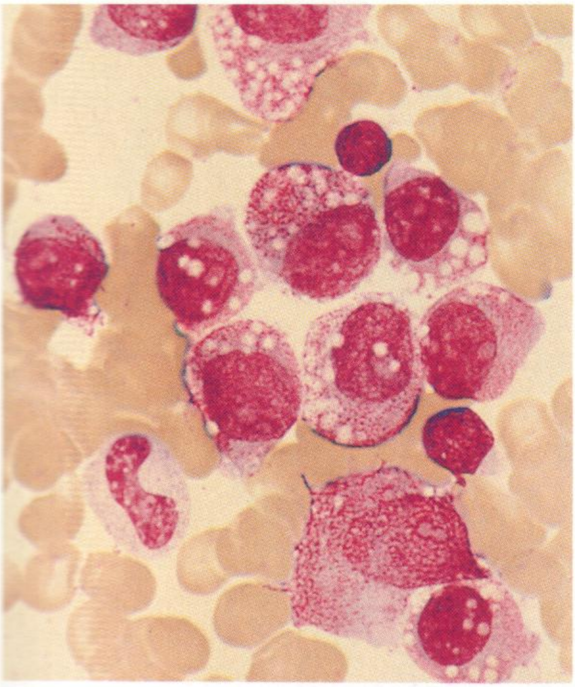

310

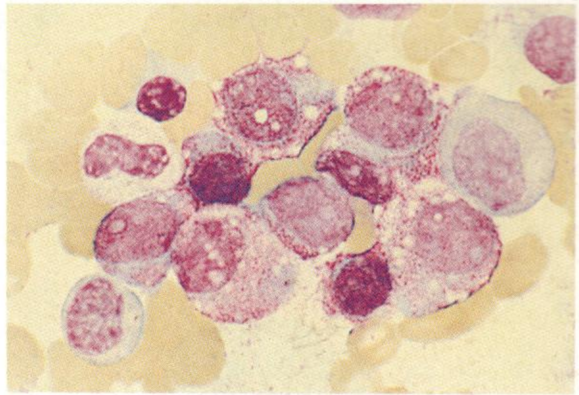

311

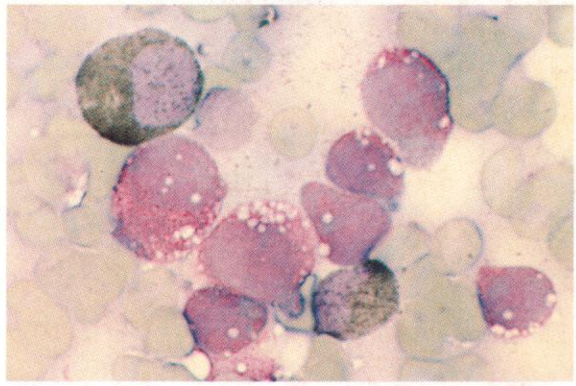

312

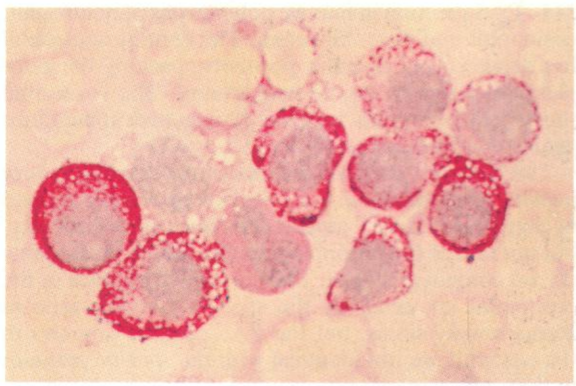

313

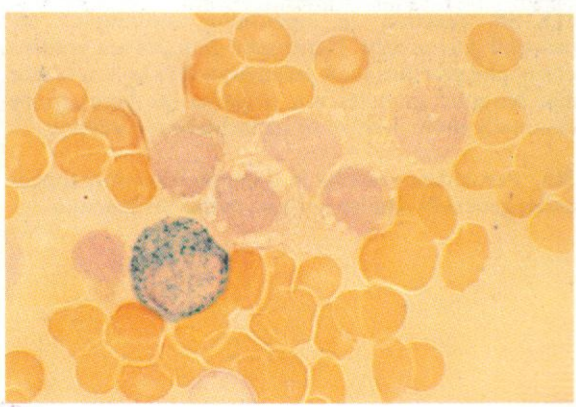

309–313. *Bone marrow smears from an unusual case of acute leukaemia with basophilia.*

309. A Romanowsky preparation showing a collection of nucleolated primitive cells with a generally low nuclear–cytoplasmic ratio, the ample cytoplasm containing numerous vacuoles and fine basophil granules. There is a neutrophil stab cell, a lymphocyte and a naked normoblast nucleus also present in this field.

310. A similar field to that in **309** but stained with toluidine blue, which reacts with the basophil granules to give a bluish-purple coloration. One blast cell here is negative, as are a neutrophil stab cell, a lymphocyte at the lower left corner, and a late normoblast.

311. A slide from the same case as in **310**, stained with SB. Two primitive cells show the usual positive reaction pattern of neutrophil precursors, while seven others give a metachromatic reaction with the dye, resulting in a reddish stain, a picture not infrequently seen in both normal and pathological basophils.

312. Another slide from this marrow stained with the PAS stain. There is one negative blast cell and a normally reacting neutrophil metamyelocyte; the remaining eight vacuolated blast cells show intense and coarsely granular positivity, characteristic of basophils.

313. The last stain from this sequence is a dual esterase reaction. Strong CE positivity is present in a single neutrophil precursor with a possible CE-positive Auer rod overlying the lower border of the nucleus, but the remaining five neighbouring vacuolated primitive cells are devoid of either CE or BE activity, as are normal basophils.

314

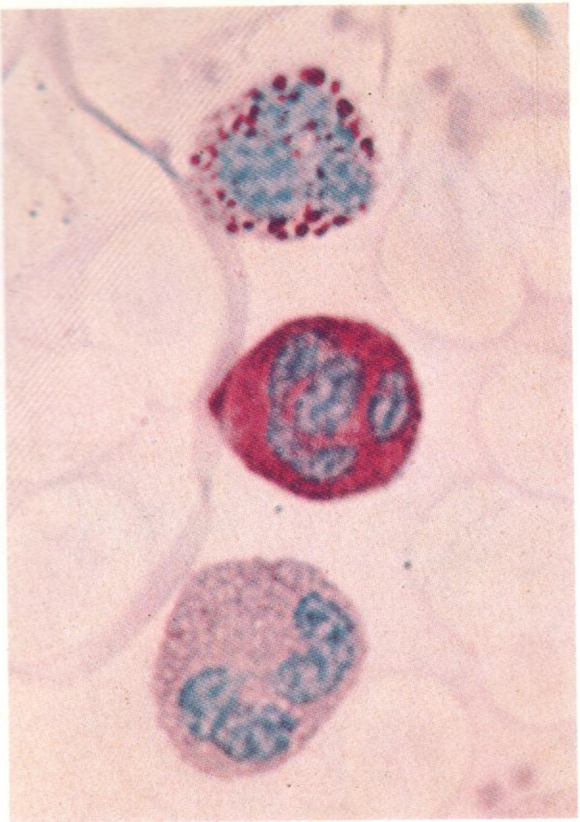

315

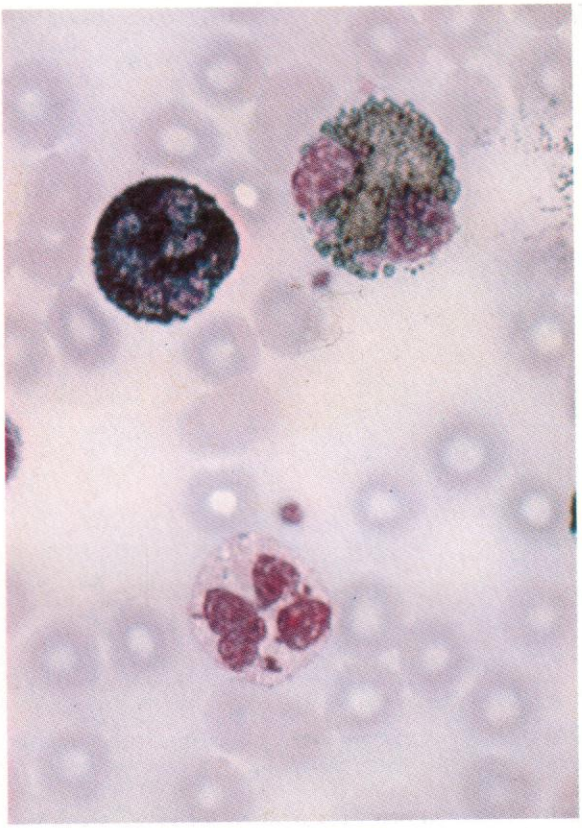

316

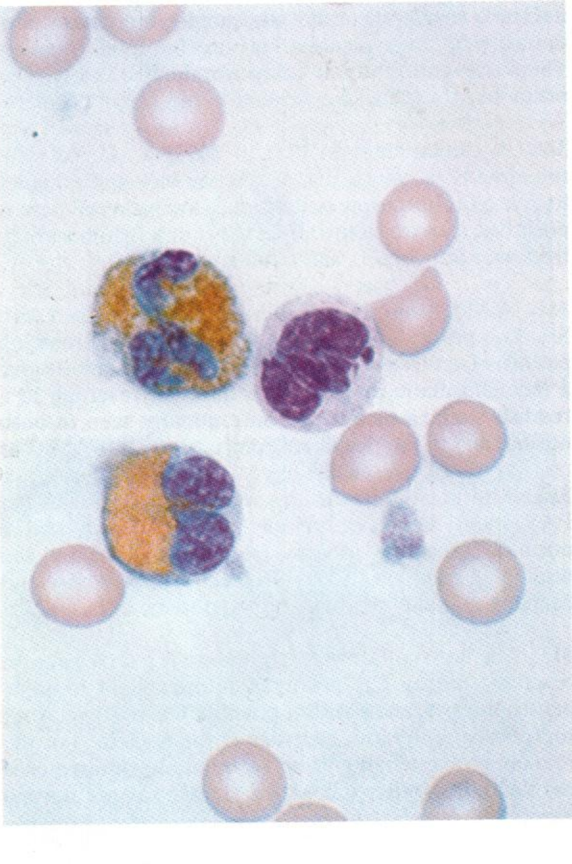

314. PAS reaction in mature polymorphs of neutrophil, eosinophil and basophil series. The central neutrophil has dense strong granular positivity, packing the cytoplasm to leave no visible background. The eosinophil shows granules with unstained, negative appearance against background positivity.

The basophil granules are discretely scattered, very heavily positive, against a negative or weakly stained background. Salivary amylase removes most positivity, but not that of the basophil granules, which presumably do not contain glycogen. The unstained granules in the eosinophil are certainly the specific granules seen in Romanowsky stains, but the PAS-positive granules in the basophil are not identical with the specific granules in that cell.

315. SB reaction in neutrophil, eosinophil and basophil polymorphs. Neutrophil granules are positive, eosinophil granules show positivity with a hollow centre, and basophil granules are negative (as here) or occasionally show positive or metachromatic staining.

316. Peroxidase reaction in a similar trio, with appearances generally similar to those in the SB reaction.

317

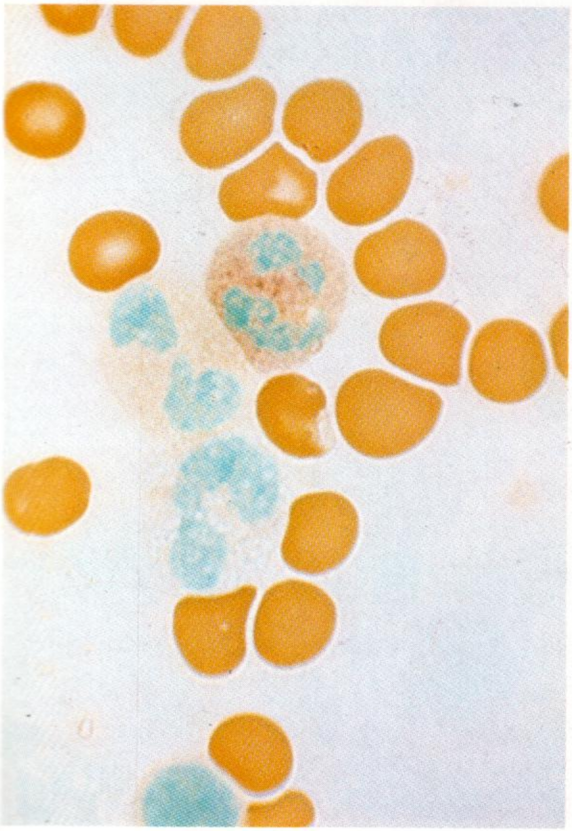

318

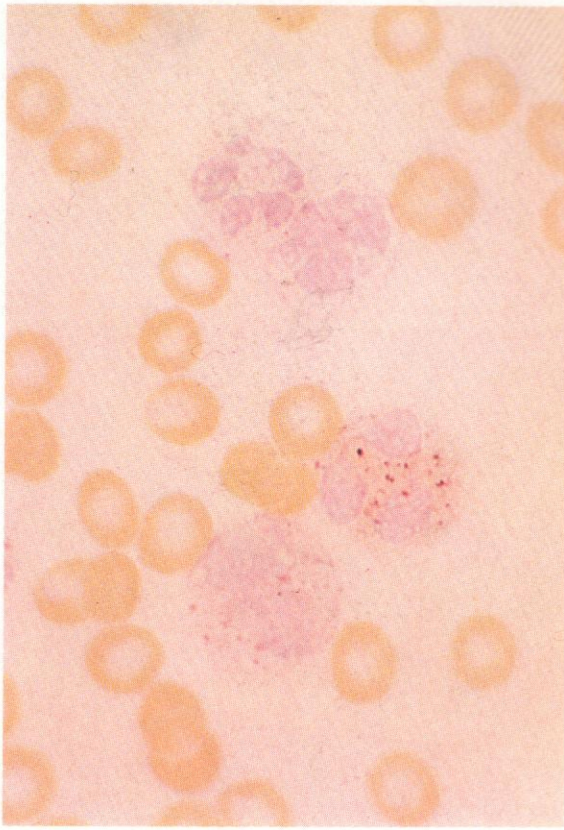

319

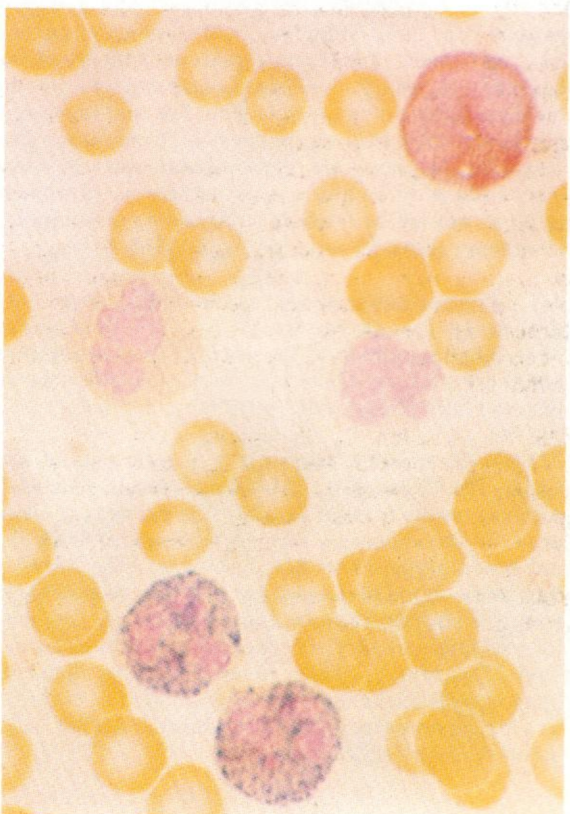

317. Alkaline phosphatase reaction in a similar cell group; only the neutrophil shows positivity. The eosinophil immediately below the neutrophil has a typical bilobed nucleus, while that of the lower basophil has incompletely separated lobes. Neither shows any alkaline phosphatase activity.

318. Acid phosphatase reaction in neutrophil, eosinophil and basophil polymorphs and a monocyte. The neutrophil and monocyte show normally positive granular reactions; the eosinophil and basophil show very little positivity with only a rare positively reacting granule.

319. Dual esterase in a group of basophil, eosinophil, two neutrophils and a monocyte. The basophil and eosinophil cells are essentially negative, while the neutrophils show typical CE positivity and the monocyte typical BE positivity.

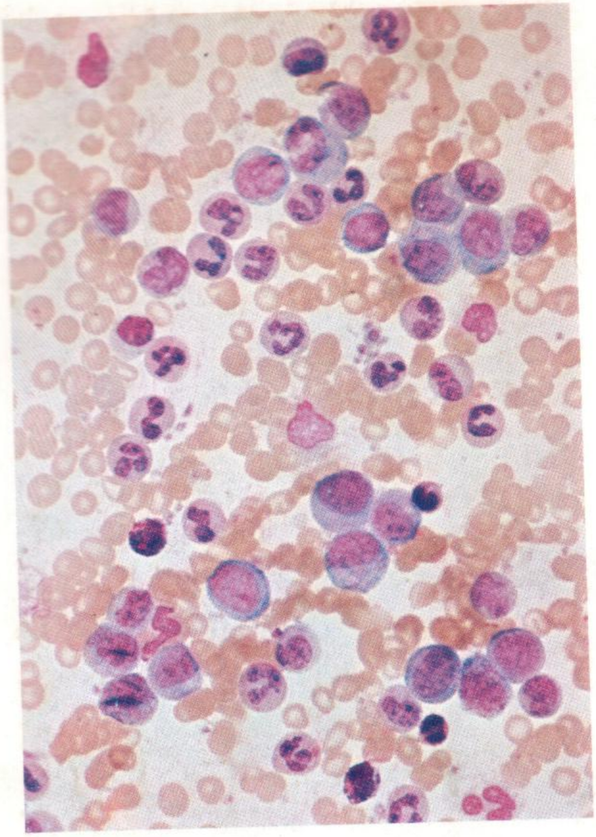

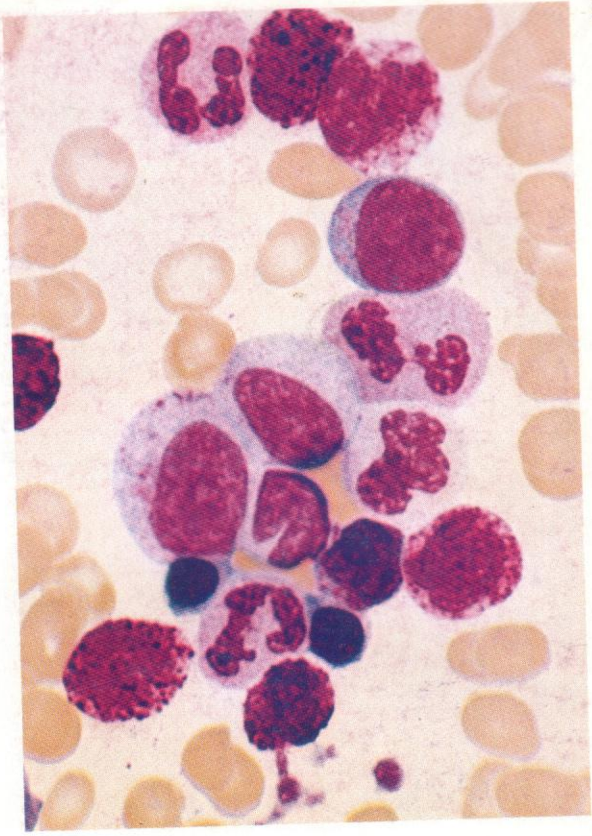

320. A low-power view of peripheral blood from a patient with CML. Granulocytes of all stages of maturation can be seen, mostly neutrophils but with occasional basophils. Although myeloblasts and promyelocytes are distinguishable, they are relatively few and much outnumbered by later granulocytes from myelocyte onwards. A peripheral blood smear with as many leucocytes of different stages of maturity as shown here is found only in CML, where the WBC at presentation is commonly above 50 and may exceed $500 \times 10^9/l$.

321. A higher-power view of another preparation showing various granulocyte precursors, including several basophils. In addition to the granulocytes, two normoblasts are present. There is a single myeloblast in the field but later granulocytes greatly predominate.

322. A chromosome spread from a male patient with CML. The Philadelphia (Ph) chromosome, seen at 12 o'clock, results from a translocation between the long arms of chromosomes 22 and 9 (usually) visible in unbanded preparations as a loss of material from the long arms of one of the small acrocentric chromosomes (no. 22). The translocation is a reciprocal one, involving the exchange of material between the two chromosomes – t(9;22) (q34;q11) – and is found in virtually all haemic marrow cells, including those of granulocytic, erythroid and megakaryocytic series, thus confirming that CML is a multilineage neoplasm.

323

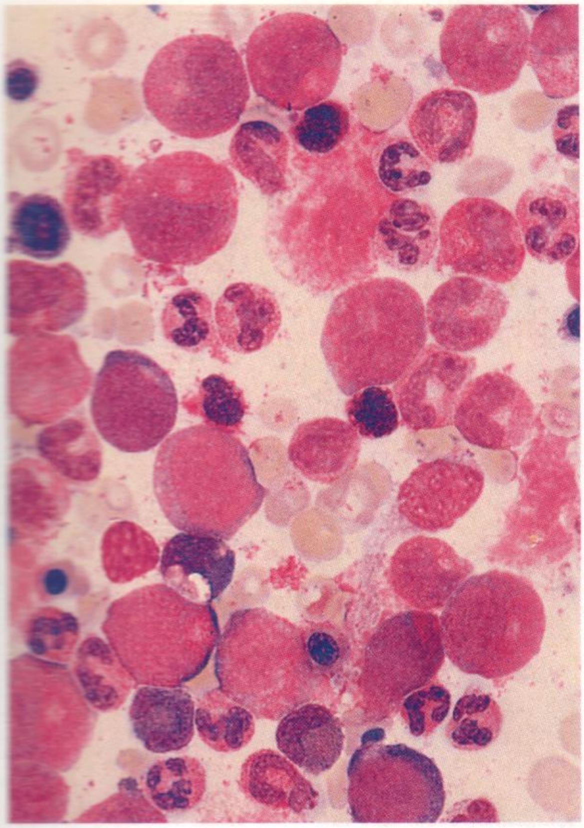

324

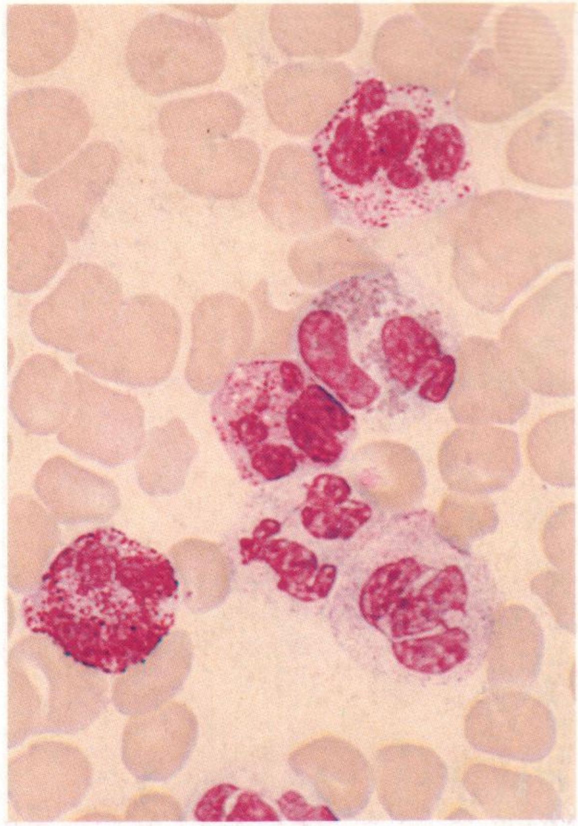

323. A low-power view of a bone marrow smear from a patient with CML, showing a cellular preparation with a high M:E ratio and preponderance of neutrophil granulocytes, with all stages of development represented. Four or five scattered erythroblasts and a proerythroblast near the bottom of the field can be seen, and an eosinophil myelocyte and polymorph, while the two small cells with deeply stained nuclei and coarse granules just distinguishable in the narrow rim of cytoplasm, situated to either side of a small centrally placed neutrophil myelocyte, are basophil polymorphs.

324. A blood smear from a patient with CML, showing different polymorph granules. A basophil is on the left and an eosinophil is to the upper right of the central group of cells; the remaining cells are all neutrophils with variable granularity, from an almost agranular example in the partly sectioned cell at the bottom, to coarse 'toxic' granularity in the polymorph at the top and that to the left of the eosinophil. Variations of this kind are not uncommon in CML.

325. Occasionally there may be an almost total absence of granules in the later neutrophils in CML, as in this peripheral blood sample, where the central promyelocyte has azurophil granules but the remaining later cells, a myelocyte, two metamyelocytes and two mature neutrophils, are devoid of specific granules. The dense nuclear chromatin but minimal segmentation of the most mature cells suggests that a pseudo-Pelger-Huët effect is also present.

325

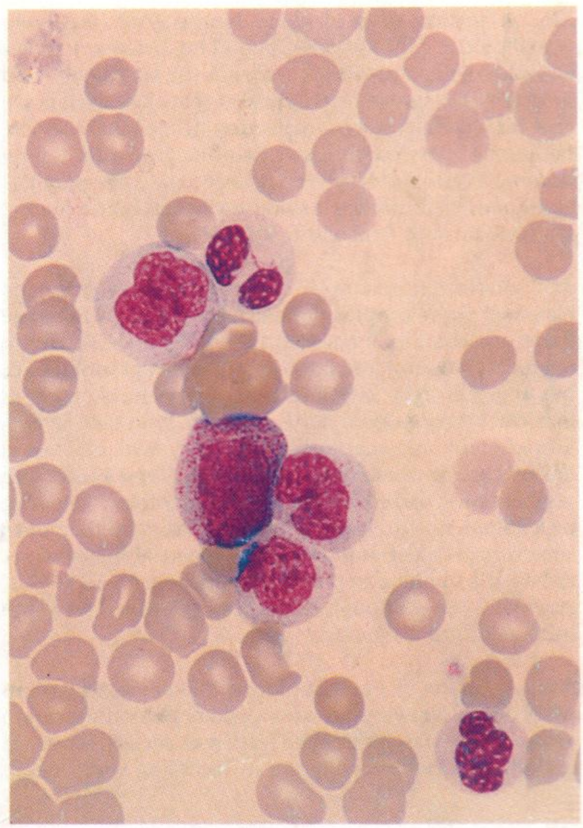

326

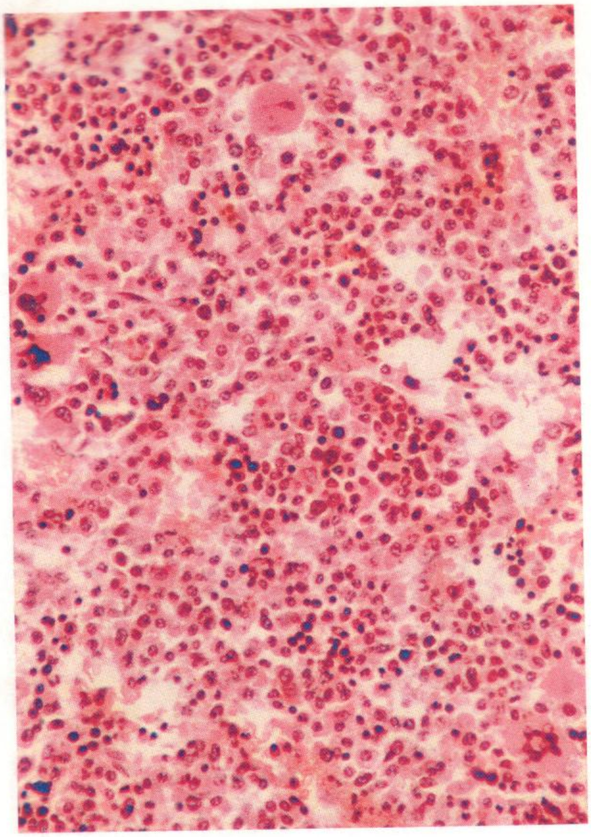

327

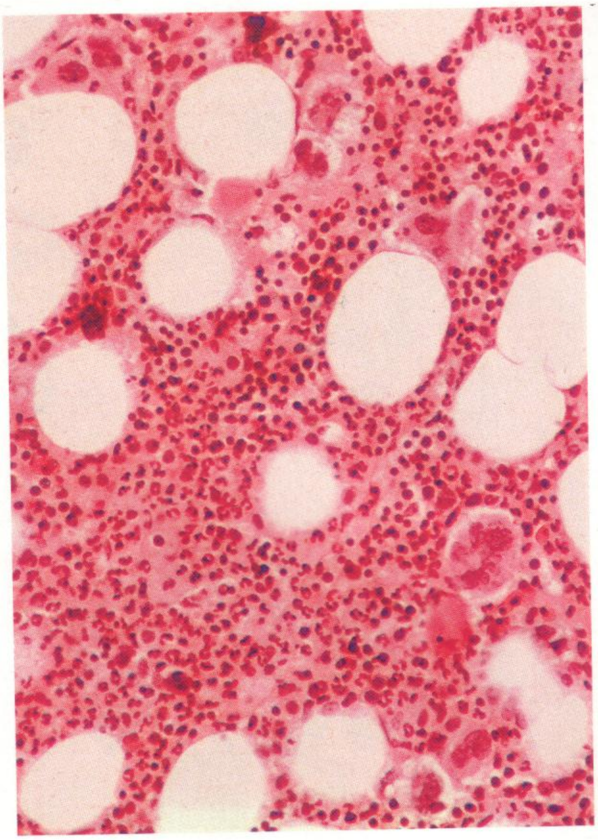

328

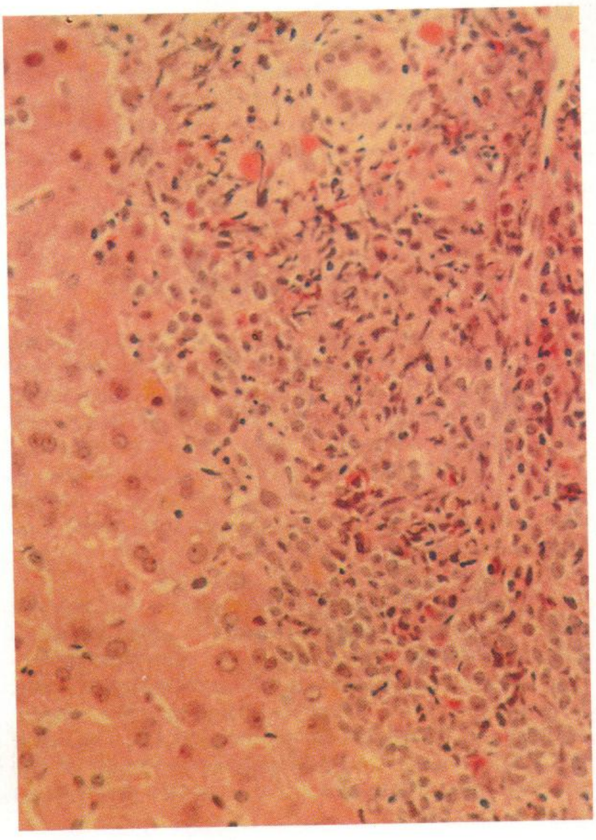

326. A section of a trephine biopsy from the bone marrow of a patient with CML. The specimen shows intense cellularity with obliteration of fat spaces, and even at this low power it is apparent that all cell series are well represented, with a scattering of megakaryocytes, numerous granulocyte precursor stages with lightly staining nuclei and ample cytoplasm, and later granulocytes and erythroblasts having pachychromatic nuclei, the former more irregular in outline.

327. A further example of bone marrow trephine histology from another patient with CML. In this case there are numerous residual fat spaces and less dense overall cellularity, and later granulocytes predominate, but there is also another feature sometimes seen in marrow biopsies from CML, namely the marked proliferation of megakaryocytes. In this field at least a dozen can be seen, with various degrees of nuclear segmentation and complexity, but most often with single or bilobed nuclei. Such cells, and even smaller ones sometimes called micromegakaryocytes, are characteristically found in trephine sections from about 80% of cases of CML, although not necessarily associated with increased thrombopoiesis.

328. A section of a needle biopsy of liver from a patient with CML, showing an area of leukaemic infiltration around a portal tract, with a dense accumulation of granulocytes compressing the surrounding liver cells.

329

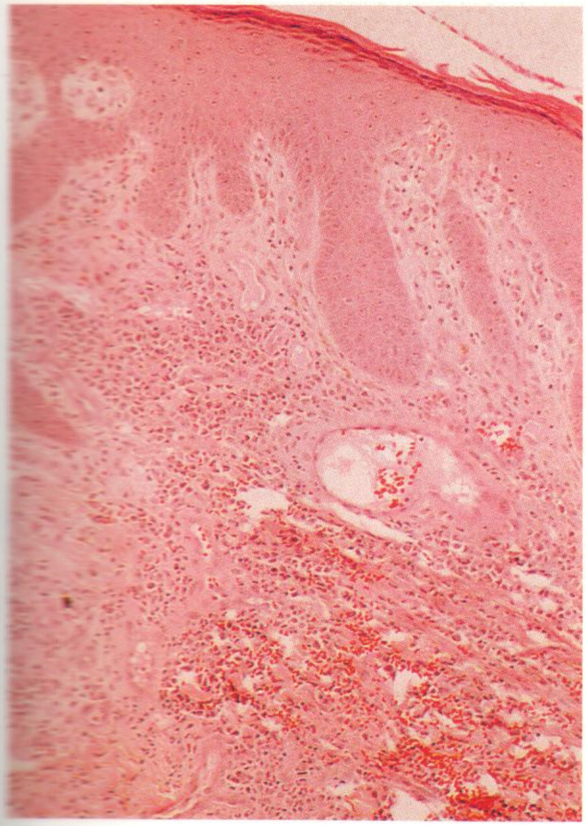

330

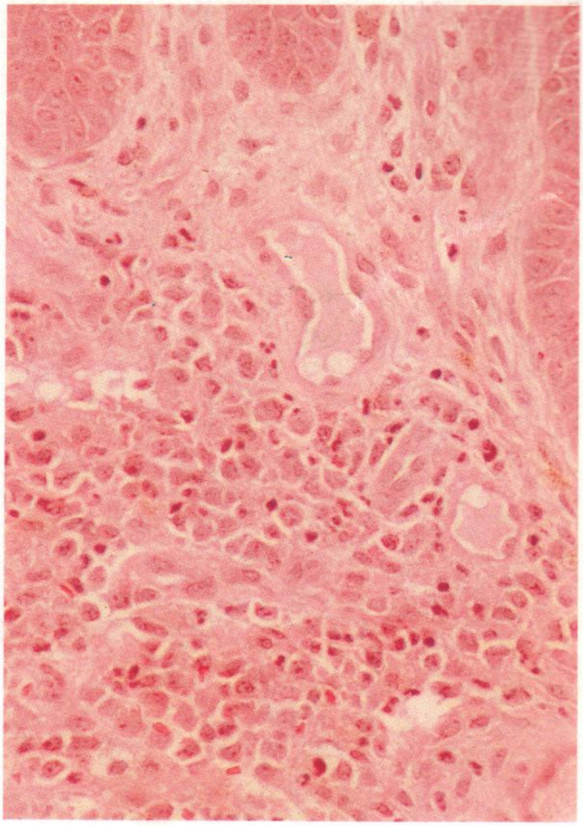

329–331. A series of views at low, intermediate and higher powers of sections made from a biopsy of skin and subcutaneous tissue taken from a patient with CML, showing a leukaemic infiltration. The first two figures are from a section stained with H&E and the third is from a Giemsa-stained section. The first field shows the epidermis above, with the infiltrate extensively involving the underlying dermis, producing vascular erosion and areas of haemorrhage. In the second field the nature of the infiltrating cells can be distinguished more clearly, with predominantly nucleolated myeloblasts and fewer later granulocytes spreading between the subcutaneous fibrous connective tissue. The third field shows the edge of the infiltrate as it reaches the epidermis, where the infiltrate of immature granulocyte precursors intermingles with collagen fibrils and macrophages laden with pigment, either free iron or possibly carbon particles. A tissue mast cell is visible towards the lower left corner.

Small and shallow skin deposits are not uncommon in CML, being sometimes numerous and widespread so as to produce a leukaemic skin rash, especially, as in the present case, at the time of general metamorphosis of the disease process from the chronic to a more acute phase. Their appearance may therefore have a poor prognostic significance. More bulky and restricted localized deposits may also occur, less commonly, at any stage of the disease, and are sometimes referred to as granulocytic sarcoma.

331

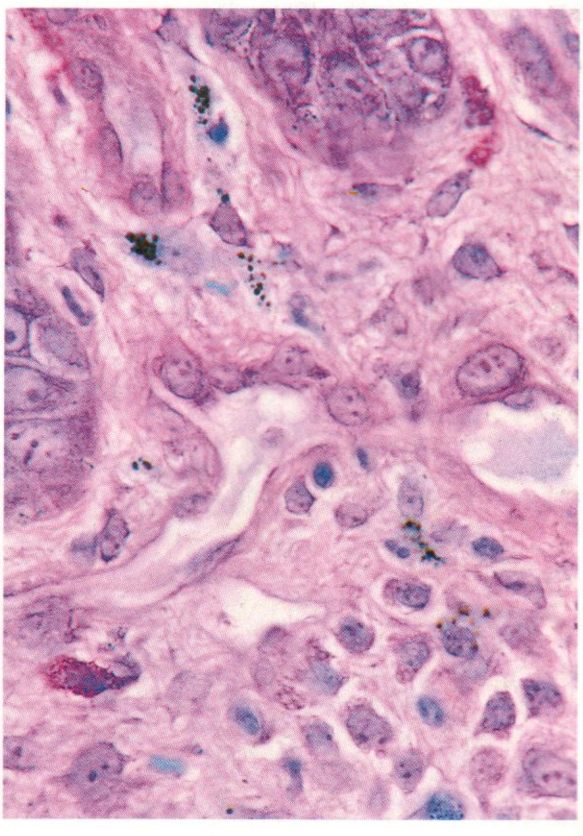

332

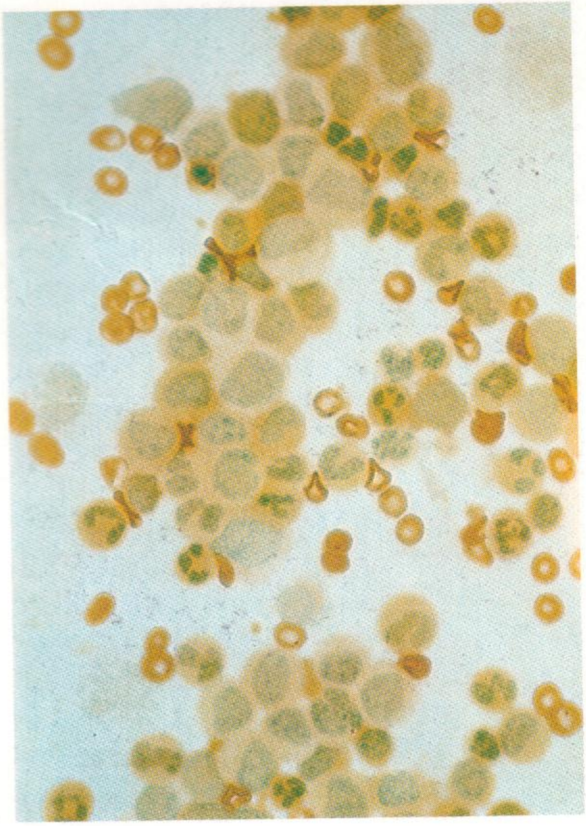

333

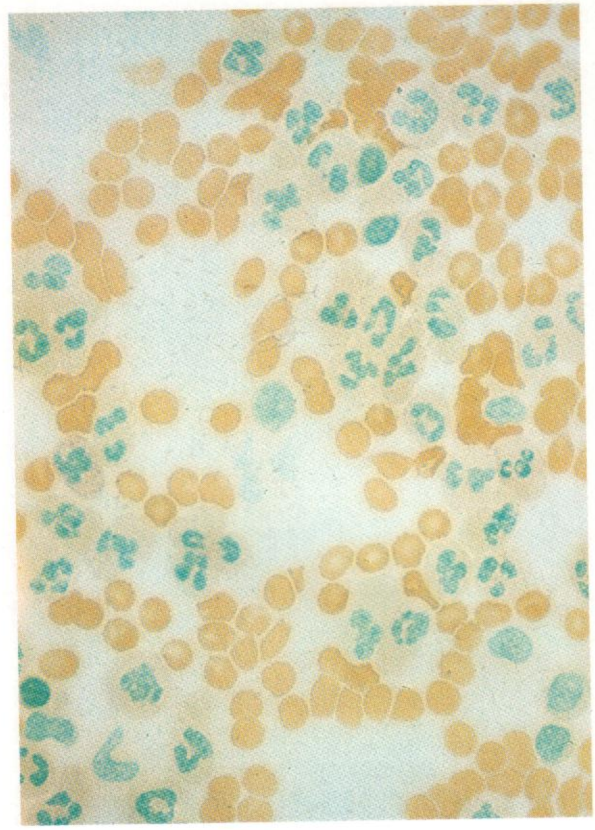

334

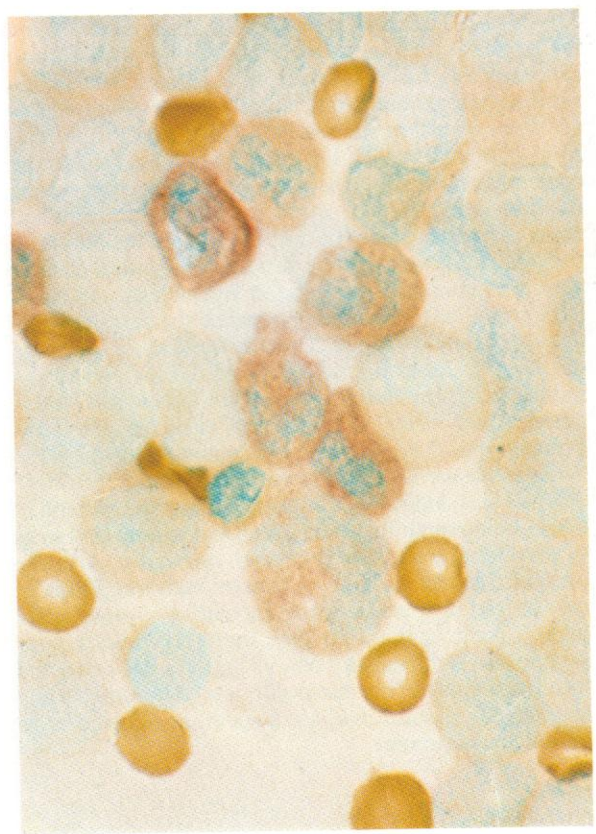

332. LAP reaction in CML. The polymorphs are virtually devoid of enzyme. This is a striking and almost uniform characteristic of neutrophils in CML.

333. Under effective treatment, when the blood picture returns quantitatively to normal, the LAP score remains low (and precursors still have the Ph chromosome), but an improvement towards the lower normal range often occurs.

This preparation shows the presence of faint positivity in some polymorphs from a buffy coat in well-controlled CML, although nearly all of the neutrophils remain quite negative.

334. When blastic crisis emerges, the LAP score usually rises sharply. This figure shows + to ++ reactions in polymorphs in a peripheral blood film from a patient at this stage of the disease. Surrounding the group of polymorphs are predominantly blast cells.

335

336

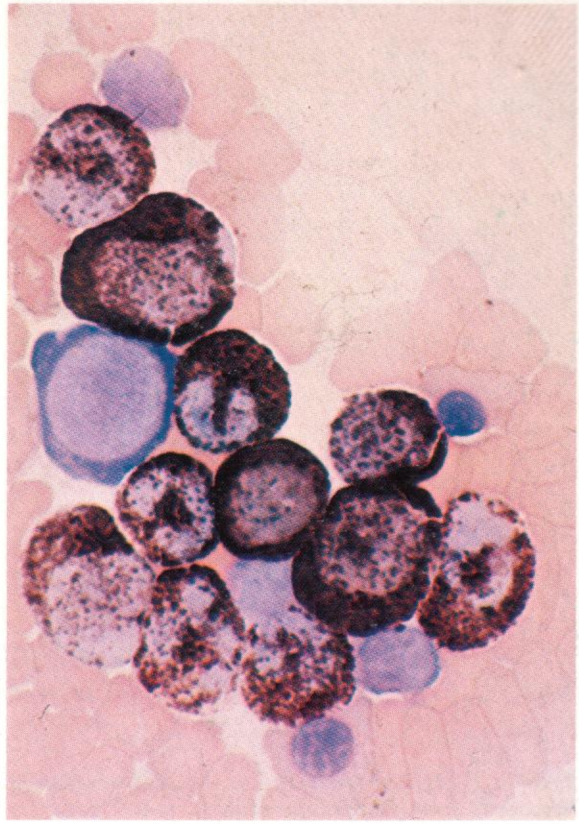

335. Peroxidase reaction in CML. Exceptionally strong positivity is the rule in polymorphs in this disease, although some peroxidase-negative cells can be found in most cases and may occasionally be numerous. The MPO-negative polymorphs may include some basophils, but others of them are certainly neutrophils.

336. SB reaction in CML. The polymorphs may react normally with strong positivity, as here, but the reaction is sometimes weaker than normal and negative polymorphs may be found, including some basophils (cf. 338), but also a proportion of the neutrophils, which may show a parallel absence of peroxidase reactivity.

337. Basophils may show a metachromatic reddish staining, as in this field from CML progressing towards myelofibrosis, which also shows typical positivity in eosinophils and neutrophils with SB.

338. A field from CML showing SB positivity in neutrophil precursors, while four basophils show varying degrees of reaction, partly metachromatic. One of the basophils is almost SB-negative.

337

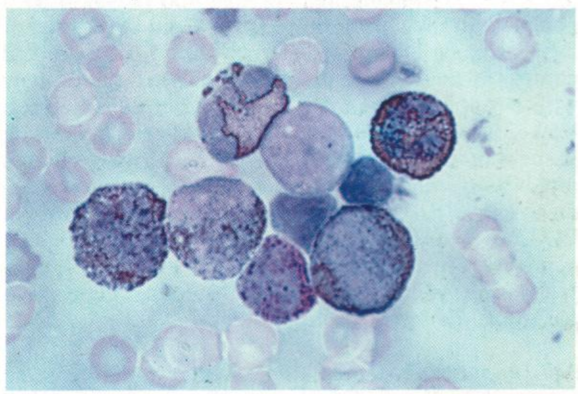

338

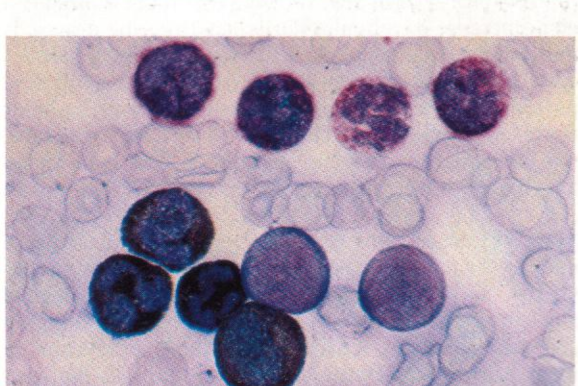

339

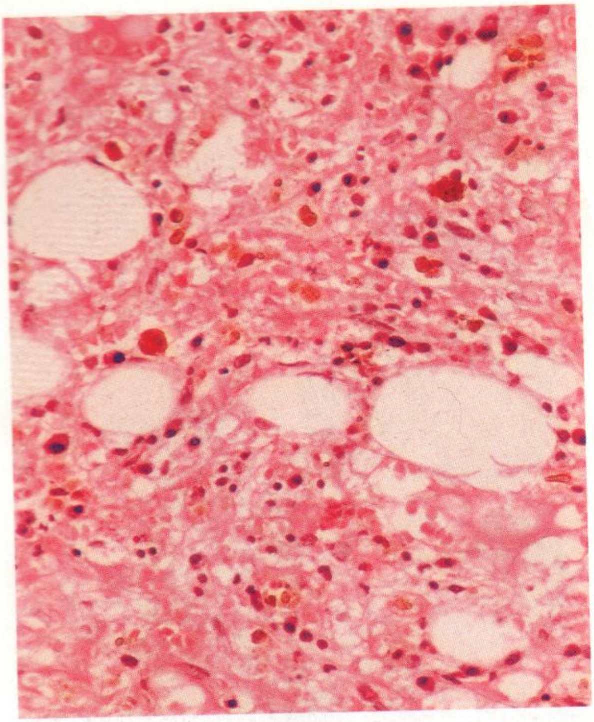

340

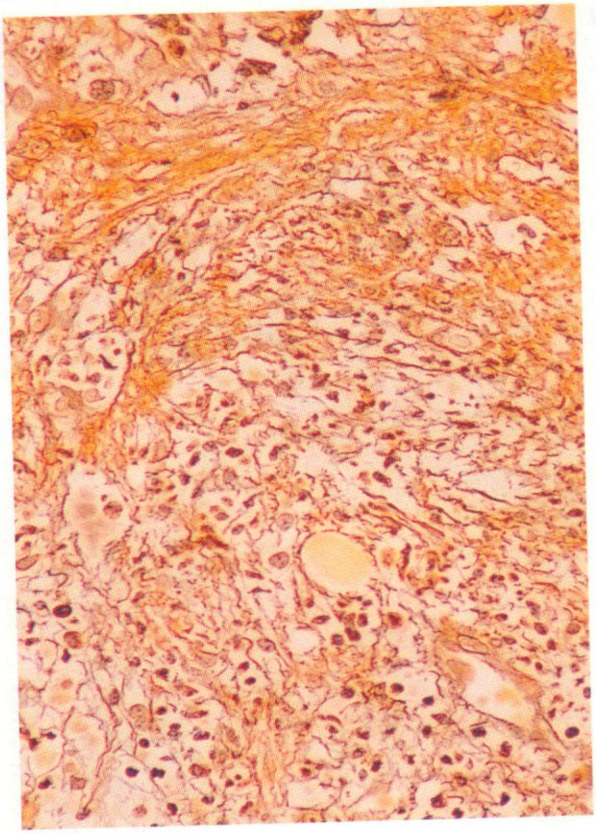

339–348. *CML progression to myelofibrosis/megakaryocytic myeloproliferative state.*

339. Section of bone marrow trephine biopsy from a patient with CML who showed progression to a phase of haemorrhagic hypoplasia after a period of prolonged control of the chronic disease by pulse chemotherapy with busulphan. The marrow is poorly cellular, with a background of necrotic and haemorrhagic supporting tissue containing a scattering of iron-laden macrophages and both lymphocytes and plasma cells, but few recognizable myeloid cells. A picture such as this may arise in CML as a consequence of myelotoxicity from unduly aggressive chemotherapy, but may also be a spontaneous phase in disease progression, generally preceding a myelofibrotic transformation.

340. A reticulin-stained thin section from the same marrow biopsy as in **339**, showing that there is already a clear increase in reticulin fibrils, and that the disease is undergoing a metamorphosis to a myelofibrotic phase. This, in turn, is commonly superseded after a variable period of weeks or months by a more floridly cellular acute leukaemic type of blood and bone marrow picture, not infrequently showing at least a transient megakaryoblastic or megakaryocytic component.

341

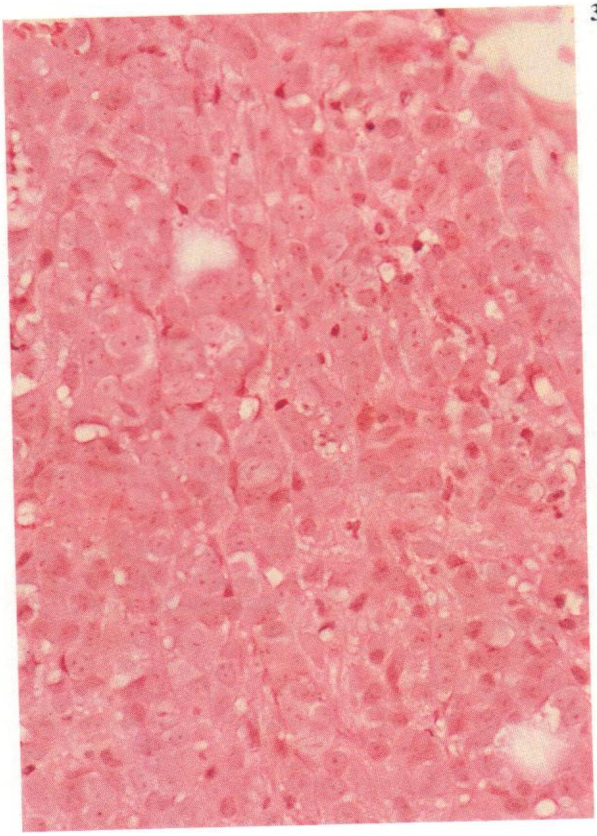

341. Section of bone marrow trephine biopsy from a patient who showed the type of transformation described in **340**, with the replacement of successive chronic leukaemic and myelofibrotic phases by a highly cellular acute transformation, the primitive cells having megakaryoblastic features, shown further in the next three fields (**342–344**).

342

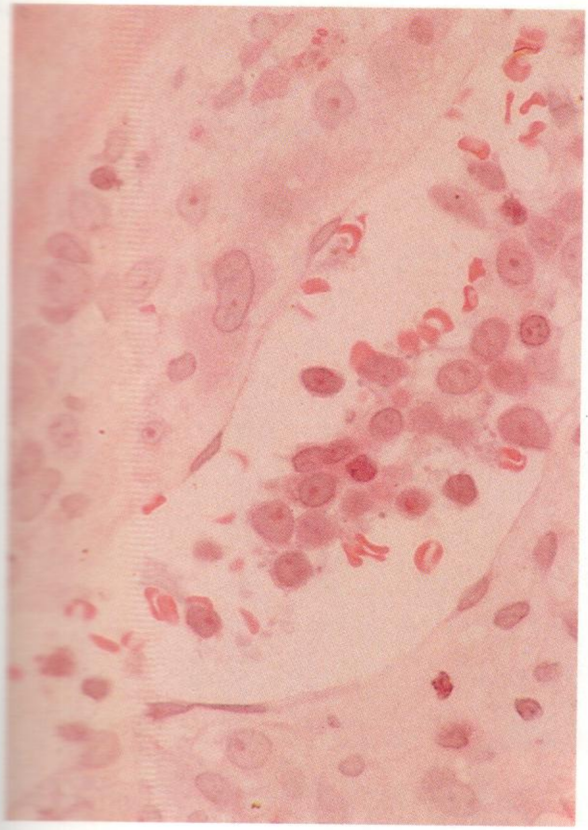

343

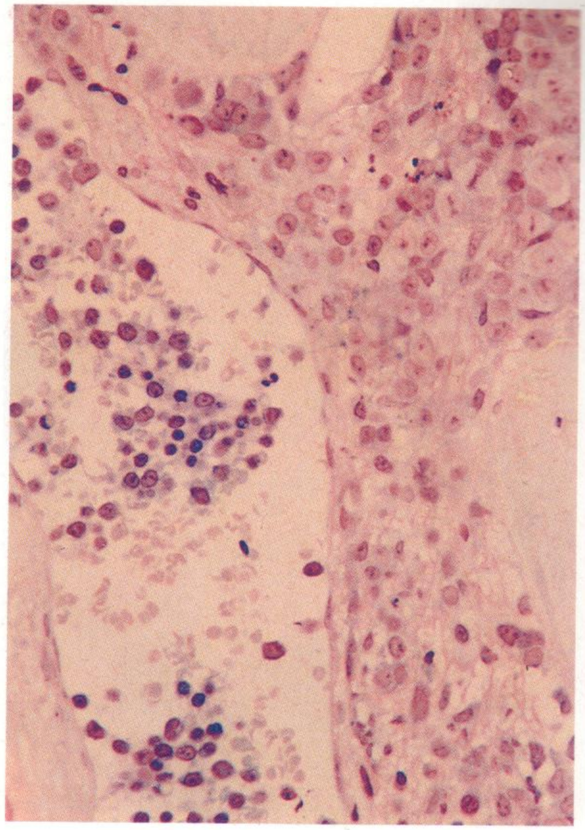

344

342–344. Thin plastic-embedded sections from the same bone marrow trephine biopsy as in **341**, stained respectively with H&E, Giemsa and the PAS reaction. In each section an area has been selected for photomicrography to show a sectioned blood vessel, with neoplastic cells both within and surrounding it. While these are undoubtedly all members of the same neoplastic clonal proliferation, their localization affects their cytological appearance, with the intramedullary blasts, despite the poor definition of their cytoplasm, having more uniformly primitive features of leptochromatic nuclear staining, with some visible nucleoli, especially in the Giemsa preparation, whereas the intravascular cells have a generally denser nuclear pattern and also show the irregular cytoplasmic outlines characteristic of megakaryoblasts and early megakaryocytes when seen in smear preparations. Although the PAS reaction when carried out on plastic sections usually gives much less striking positivity in haemic cells than is found in PAS stains on smears (cf. **346**), some peripheral cytoplasmic positivity can be discerned in the primitive cells in **344**, more obviously in the intravascular than in the intramedullary populations. The differences in cytology between the two sites may be partly a consequence of greater compression from contiguous cells in the marrow as compared with the vascular lumen, but may also represent some increase in maturity associated with passage through the vessel wall.

345

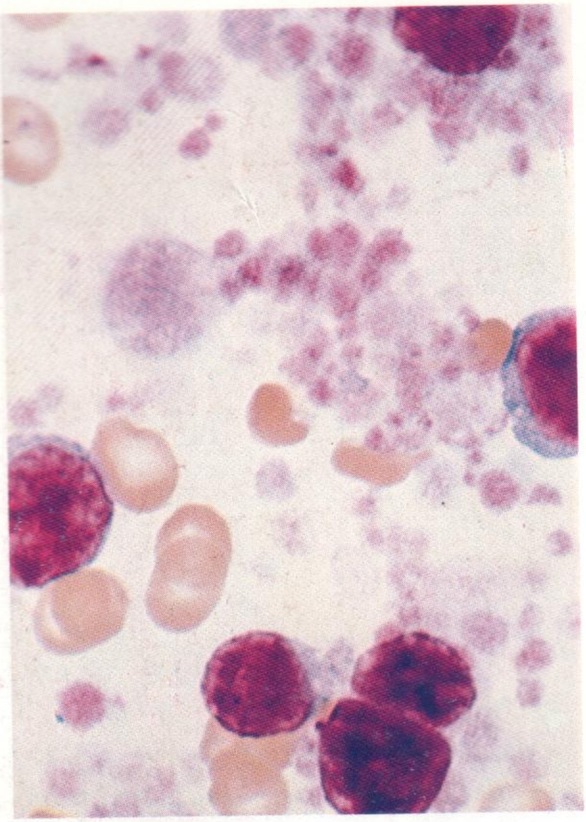

346

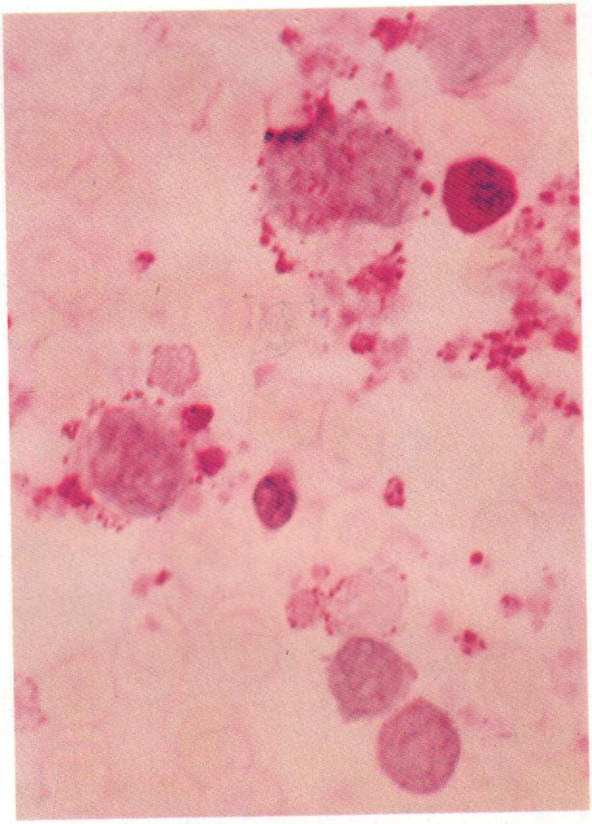

347

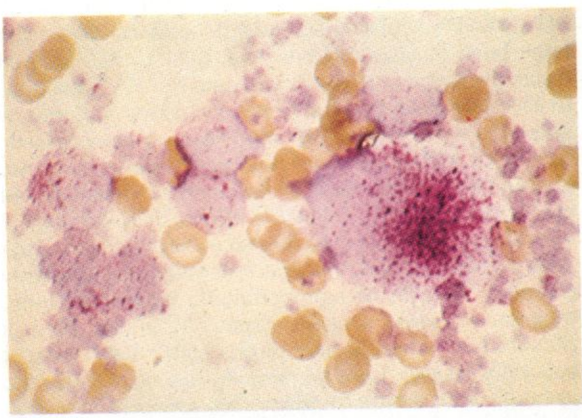

348

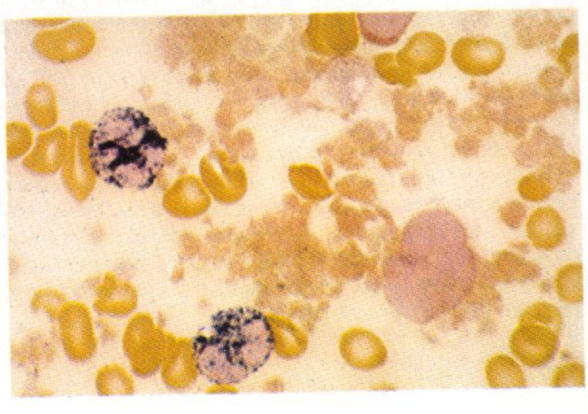

345–348. *Cytological and cytochemical details of megakaryoblastic and megakaryocytic transformation in CML as seen in smear preparations of bone marrow aspirates.*

345. Romanowsky stain shows two blast cells, to left and right, several megakaryocyte nuclei and masses of variably sized platelets.

346. PAS reaction shows the coarse positivity in platelet and megakaryocyte precursors.

347. Acid phosphatase is strongly positive in megakaryocyte precursors.

348. Dual esterase shows strong CE reaction in polymorphs but only weak BE reaction in a megakaryocyte and some platelets, and in a blast cell. A stronger reaction might be expected in cells of the megakaryocyte series if alpha naphthyl acetate rather than butyrate is used as the substrate for the esterase reaction.

349

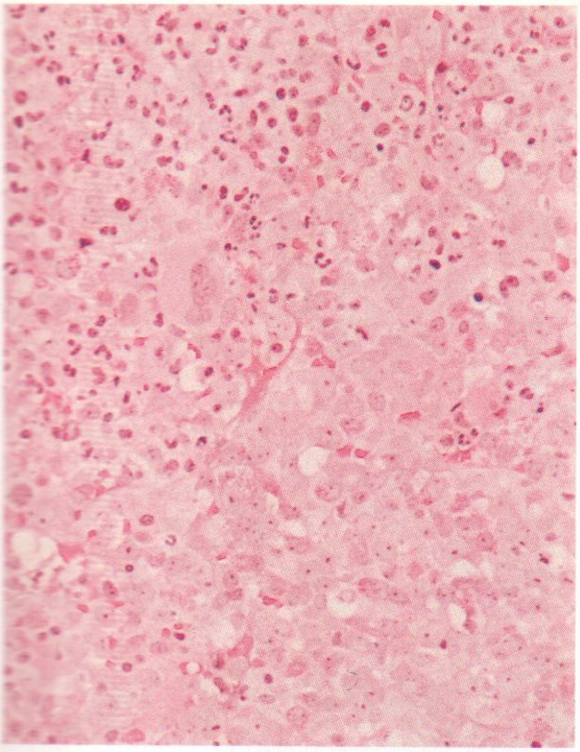

350

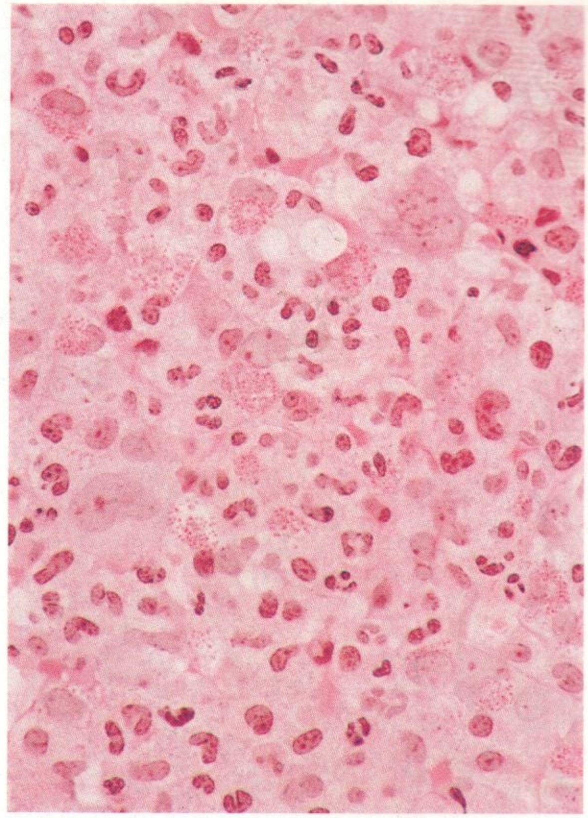

351

349–362. *CML progression to myeloblast-type crisis. Histology of plastic-embedded bone marrow trephine biopsy sections (**349–357**) and cytology and cytochemistry of smears from bone marrow aspirates (**358–362**).*

349. Low-power view of a thin section of marrow biopsy from a patient undergoing myeloblastic transformation of CML, with islands of primitive cells scattered through the marrow, among residual areas of chronic-phase cytology. In this field the lower right area contains the myeloblastic component while the upper left part shows residual chronic-phase mixed cytology. Progression of CML commonly develops with a patchy distribution of blast-cell islands, and a more reliable picture of the process may be obtained from trephine biopsies than from aspirates.

350. A higher-power view of the upper left part of **349**, showing the chronic-phase cytology with numerous neutrophil polymorphs, metamyelocytes and myelocytes, a few blast cells, occasional erythroblasts, and several megakaryocytes, including typical micromegakaryocytic forms.

351. In sharp contrast is this view, at the same increased magnification, of the lower left area of **349**, where the predominating cells are myeloblasts with fine leptochromatic nuclear chromatin containing conspicuous nucleoli (usually only one or, less often, two visible in each of the thinly sectioned cells). The few scattered cells with deeply staining nuclei are either erythroblasts or later granulocytes.

352

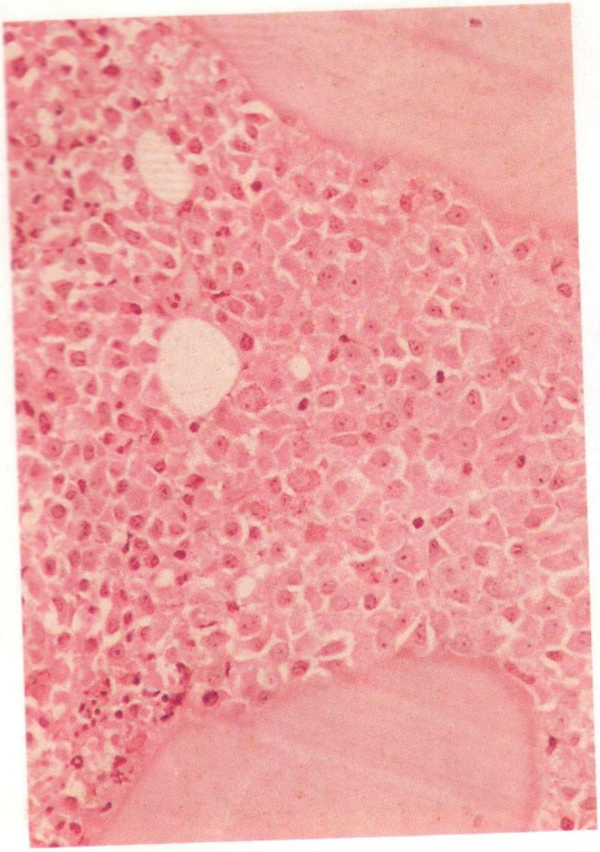

353

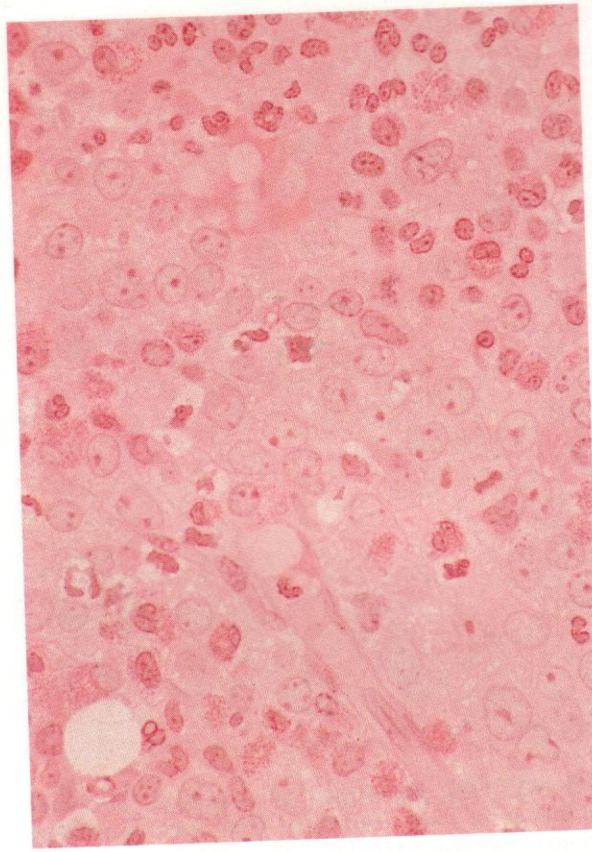

354

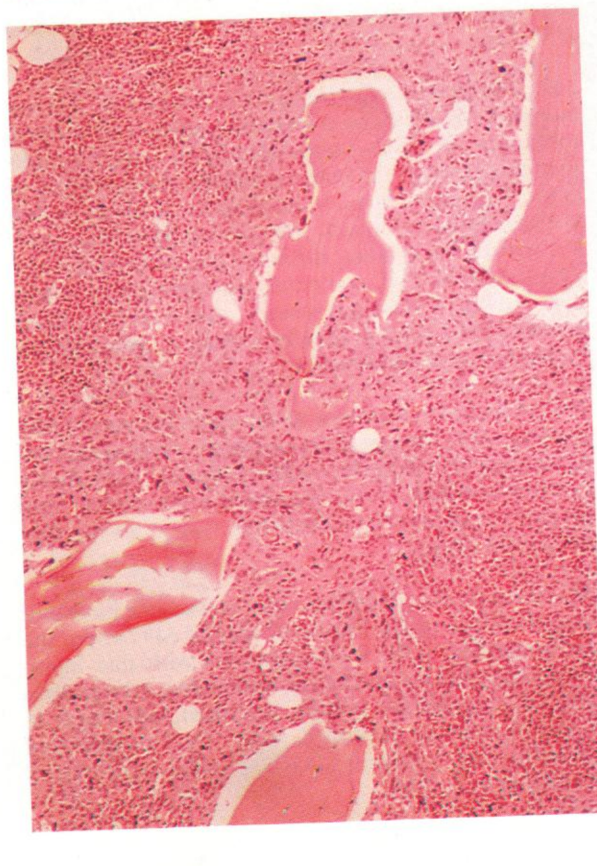

352. Another example of myeloblastic transformation developing in CML. In this thin section of plastic-embedded trephine biopsy material from the iliac crest bone marrow, the edge of a blastic nodule is on the right, between bony trabeculae above and below, with residual chronic phase cells having generally darker nuclei on the left.

353. A higher-power view of the same section as in **352**, showing a tongue of myeloblastic cytology penetrating between chronic phase cells to the upper right and lower left. The finely leptochromatic nuclear structure and nucleoli of the myeloblasts are well shown, contrasting with the darker and more polymorphic nuclear pattern of the later granulocytes of the chronic phase.

354. A similar thin section from another patient with emerging myeloblastic transformation, here illustrating the destructive trabecular erosion sometimes produced by the myeloblastic proliferation, which in this section can be seen to be concentrated around the damaged trabeculae. There are residual later granulocytes and erythroblasts from the chronic phase of the disease in the upper left and lower right corners of the field.

Increased bony destruction, associated with the onset of bone pain and the development of radiological changes, is one of the more common forms of presentation of blastic metamorphosis in CML.

355

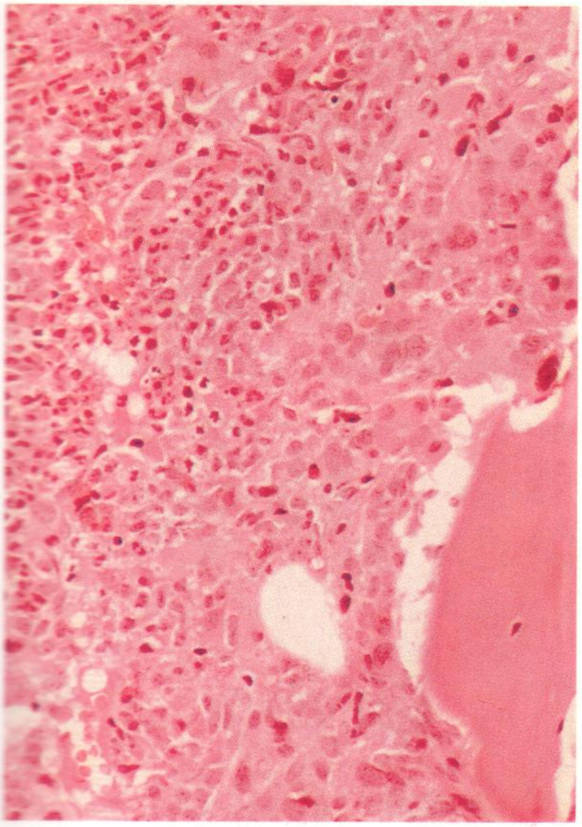

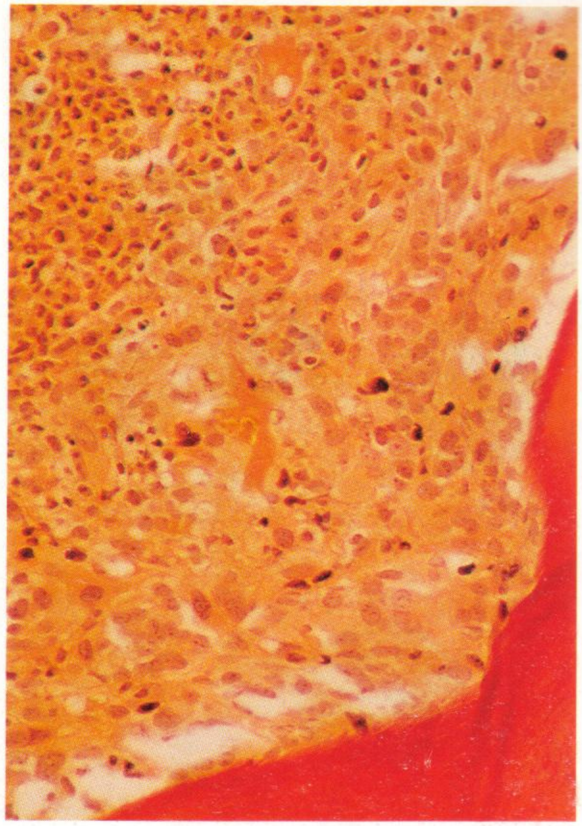

356

355–357. Three further thin sections from the same trephine biopsy as in **354**. The first (**355**) shows at higher magnification an area similar to that reproduced at low power in **354**, with a clearly visible contrast between the primitive nucleolated and leptochromatic myeloblasts along the irregularly eroded trabecular margin and the mixture of more mature cells spaced further away. The single cell with large darkly stained nucleus, directly abutting a semi-circular bony erosion at the middle of the right margin of the field, is probably a polyploid osteoclast. The second field, in **356**, from a Ponceau S-stained preparation, reveals an absence of collagenous tissue and fibroblasts from an area of myeloblastic paratrabecular proliferation very similar to that shown in the preceding two figures. The third similar field (**357**) is from a preparation stained for argyrophil reticulin fibrils; again, there is a notable absence of such fibrils in the neighbourhood of the trabeculae, where the myeloblastic proliferation is concentrated.

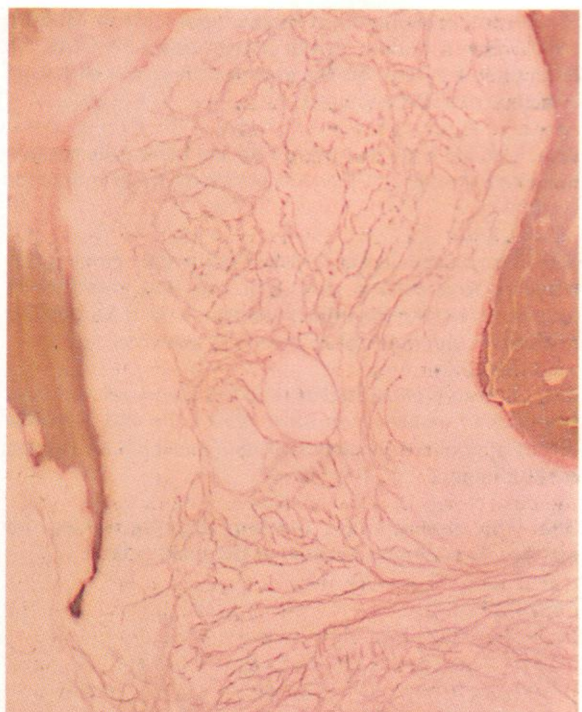

357

358

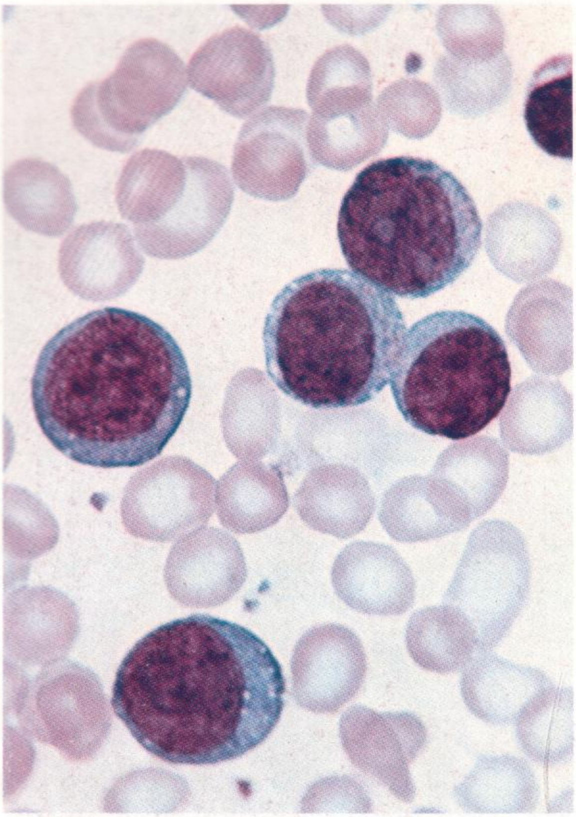

359

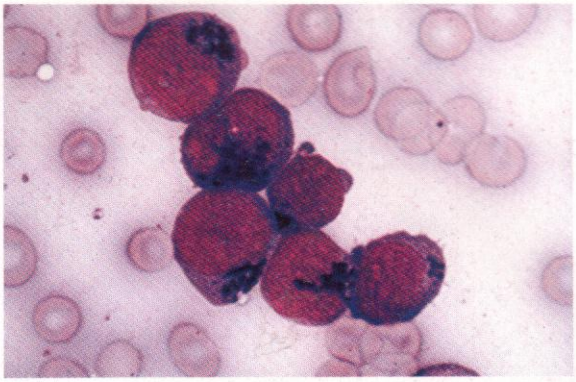

360

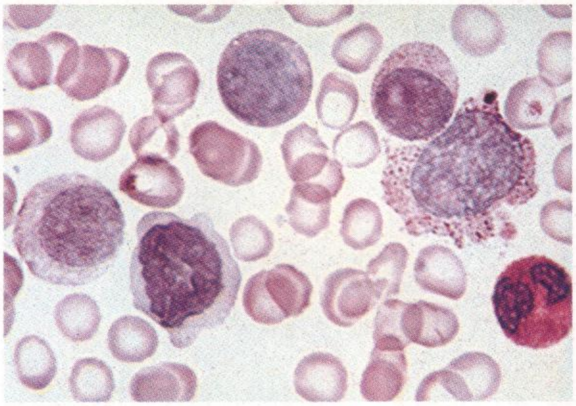

361

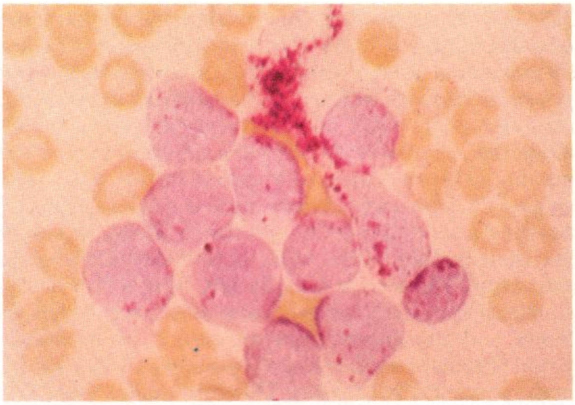

362

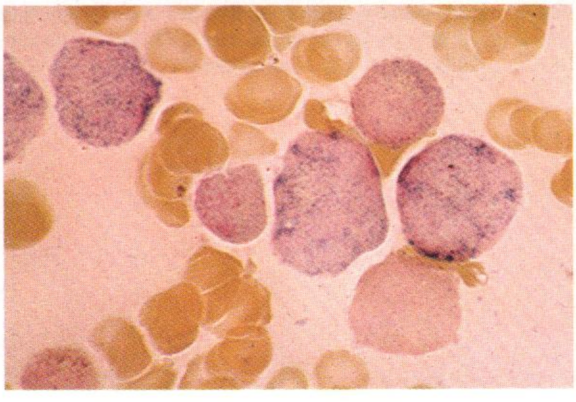

358. A smear preparation from a bone marrow aspirate taken from a patient in the blastic phase of CML. A Romanowsky stain shows a group of blast cells with little evidence of differentiation.

359. The SB stain shows that all the blast cells contain localized strong cytoplasmic positivity of granulocytic type.

360. The blast cells are largely PAS-negative or weakly reacting with diffuse positivity and fine granules. A monocyte/macrophage shows some coarse PAS-positive granules – a polymorph is normally positive.

361. The acid phosphatase reaction shows a few coarse granules of positivity in most blast cells and a trail of strongly positive granules from a partially disrupting macrophage.

362. The dual esterase reaction displays moderately strong CE positivity in most of the blast cells.

363

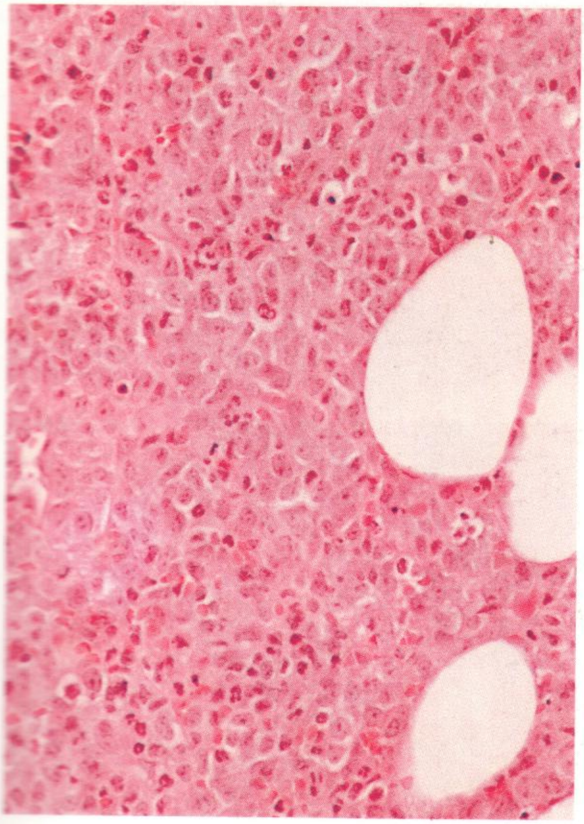

364

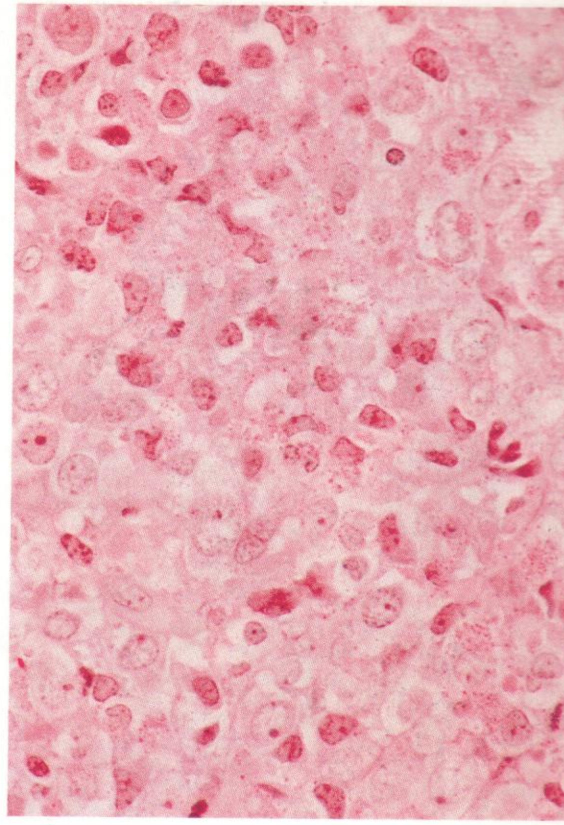

363–370. *CML progression to a lymphoblast-type crisis, with C-ALL antigenic findings. Histology of trephine biopsies (363–365) and cytology and cytochemistry of aspiration smears (366–370).*

363. A thin section showing a scattered infiltration of blast cells among residual later granulocytes of the chronic phase of CML. Although this view includes some fat spaces, the overall cellularity of the specimen is extremely dense, with closely packed cells and little to suggest a preceding stage of myelofibrosis.

364. A higher-power view of the same preparation, showing the intermingling of scattered nucleolated primitive cells with later granulocytes – myelocytes, metamyelocytes and polymorphs. Only a few late erythroblasts can be recognized. The proportion of blast cells, around 50%, exceeds that to be found during the chronic phase of CML, and indicates the emergence of blastic transformation.

365. Another example of blastic transformation of CML shown in a thin section of plastic-embedded trephine biopsy specimen of bone marrow. In this case the area shown depicts an almost complete replacement of the chronic-phase cytology by a uniform sheet of blast cells with single nucleoli and very open nuclear chromatin network. There is a mitotic figure at the lower right, a very few probable late neutrophils, and a plasma cell. The lineage of the blast cells cannot be determined from these histological preparations, but parallel aspirate cytochemistry shows them to be lymphoblasts.

365

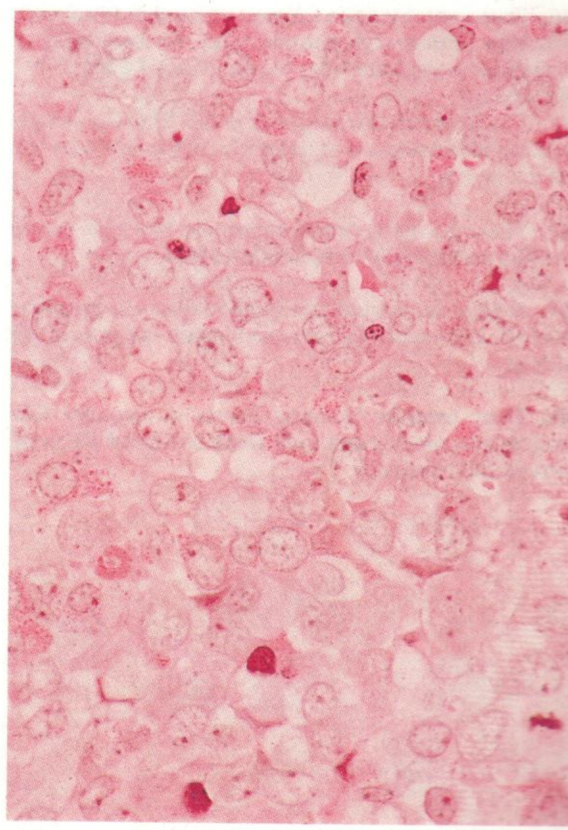

366

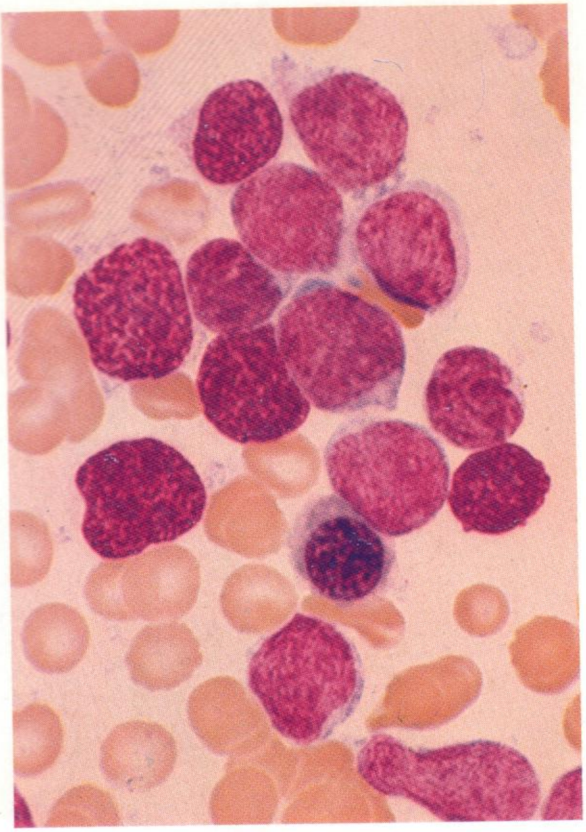

367

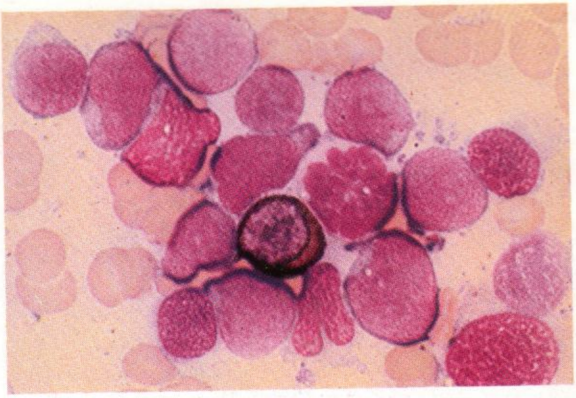

368

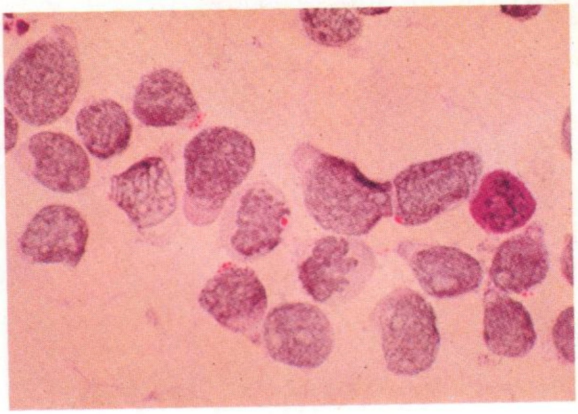

369

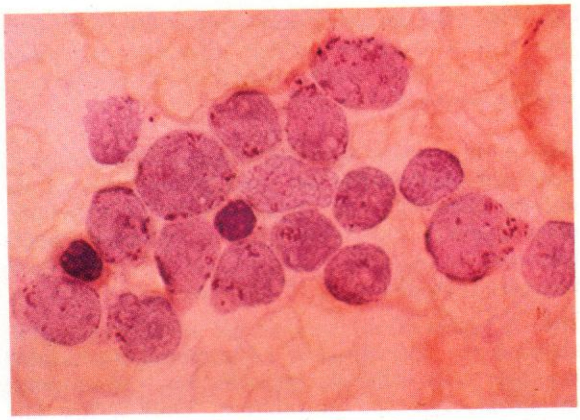

370

366. Romanowsky stain shows agranular blast cells with high nuclear–cytoplasmic ratio, in this smear of bone marrow aspirate from blastic crisis of CML.

367. The blast cells are negative to SB. There is a single sudanophilic myelocyte in the centre of the field next to a mitotic figure.

368. The PAS stain shows occasional block or coarse granular positivity of lymphoblastic type.

369. Acid phosphatase staining shows scattered positive reaction, not especially concentrated at one pole of the nucleus.

370. Dual esterase staining shows a strongly CE-positive granulocyte but only weak scattered BE positivity in the blast cells.

371

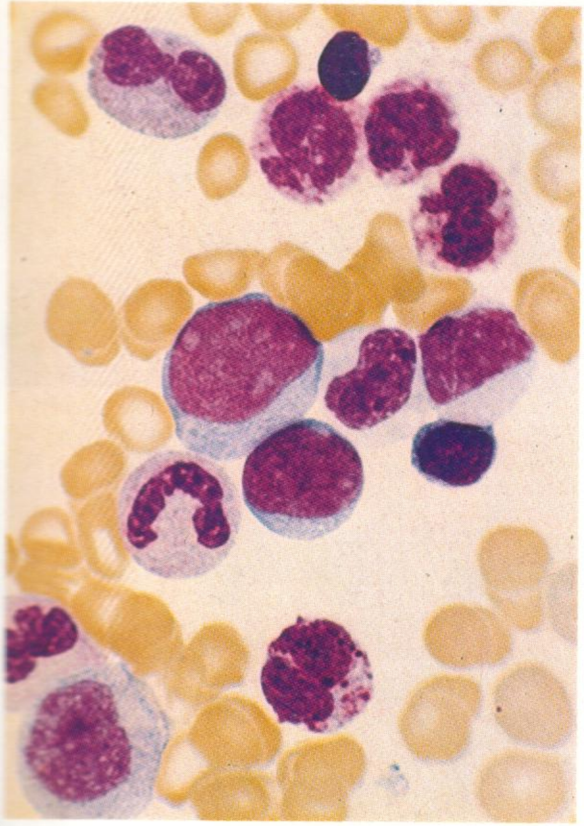

372

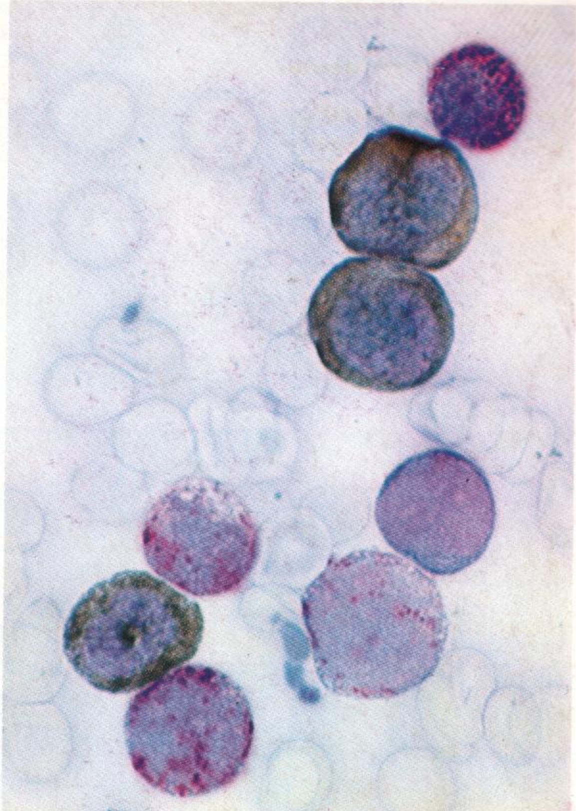

***371–374**. Basophil predominance in malignant progression of CML.*

371. Romanowsky stain shows a mixture of granulocytes and their precursors including two blast cells, myelocytes, stab cells and four basophils.

372. SB stain in the same case, showing a myeloblast, three neutrophil myelocytes with normally strong sudanophilia and four basophils from promyelocyte to polymorph with mostly reddish metachromatic staining of the basophil granules.

373. PAS reaction in the same case, showing coarse and patchy positivity in four basophils at various stages of maturity from promyelocyte onwards. Neutrophil precursors show normal diffuse tinge.

374. PAS reaction in another example of basophil predominance during malignant progression of CML. In this field there are two early neutrophil precursors at the top and a neutrophil metamyelocyte at the bottom, while all six remaining cells are of the basophil series and show varying degrees of coarse granular PAS positivity typical of that cell series.

373

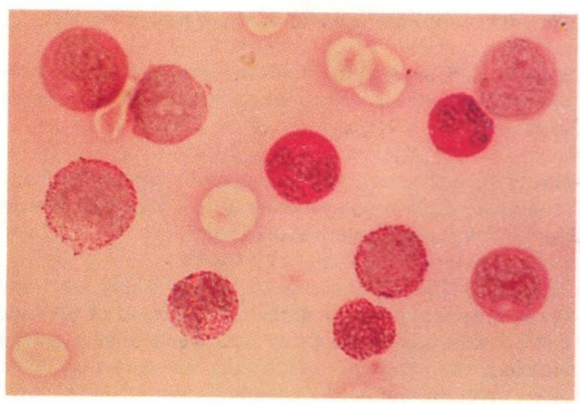

374

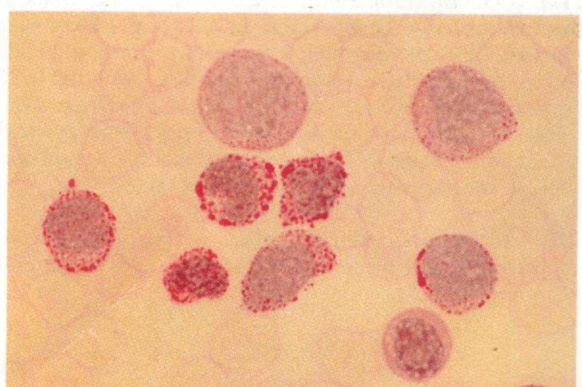

375

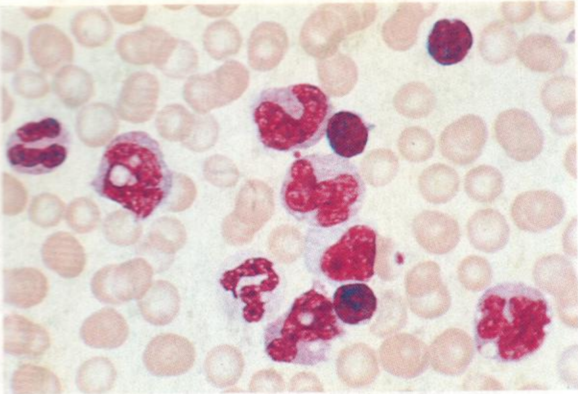

376

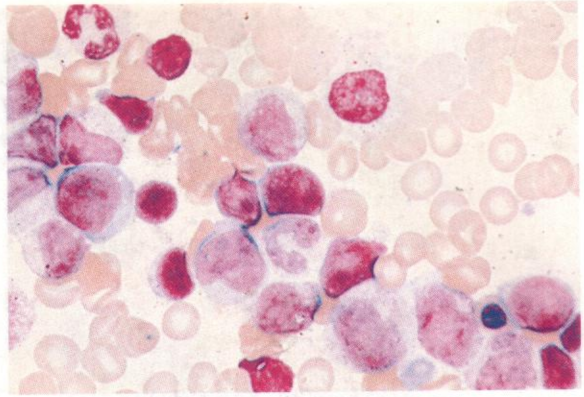

377

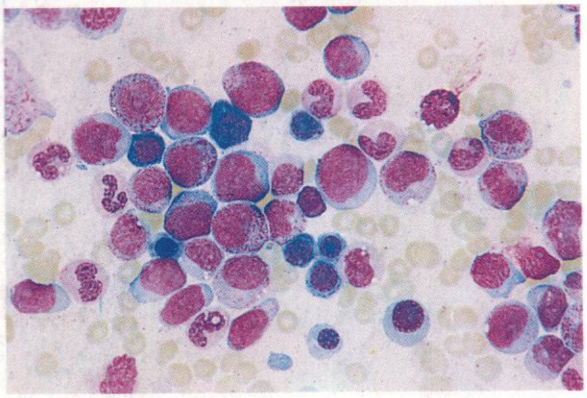

378

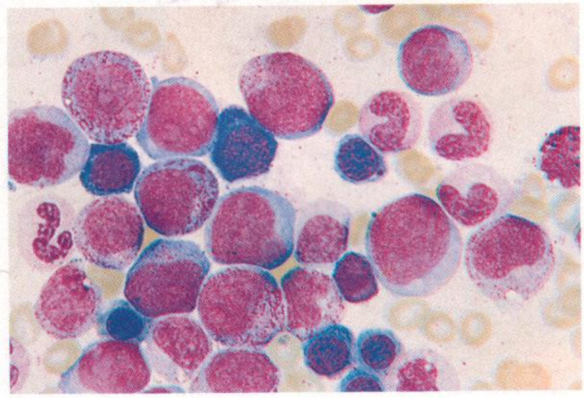

379

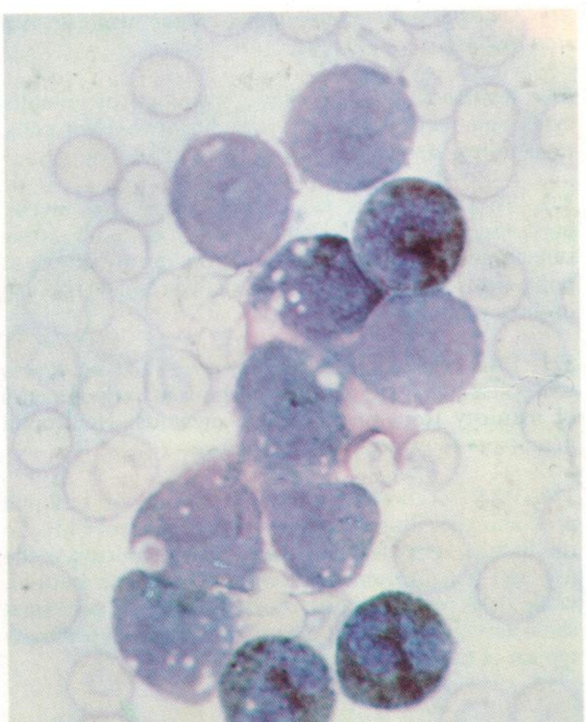

375–383. *Preparations from cases of juvenile CML.*

375. A Leishman stain of blood smear showing prominent monocytic component, several monocytes being vacuolated.

376. Leishman stain of bone marrow smear from the same patient, showing resemblance to CML, with various granulocyte precursors predominant.

377 and **378**. Romanowsky (Heyl) stains of bone marrow aspirate smears from another case of juvenile CML, showing respectively low- and higher-power views of the cytology, which falls between that of an acute myelomonocytic leukaemia (AMML) and a CML. This condition is sometimes called 'AMML of childhood' and is probably best treated as an acute leukaemia. Unlike CML proper, which does occur rarely in childhood, so-called juvenile CML does not show the 9;22 translocation, although the LAP score is usually low. There is typically a high level of HbF and low HbA_2, and the infantile ratio (3:1) of glycine to alanine at position 136 on the gamma chains of HbF is retained.

379. SB stain on blood smear: coarse positivity in neutrophils and discrete scattered granules in several monocytoid cells.

380

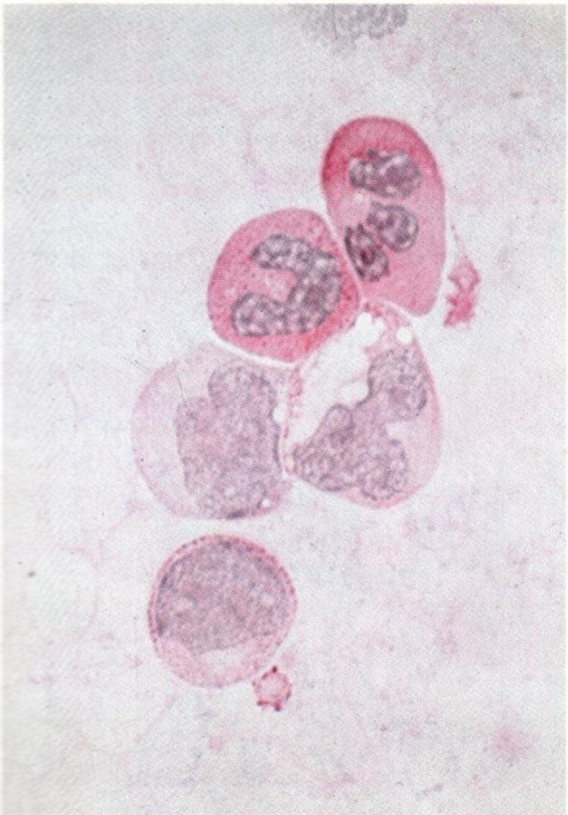

381

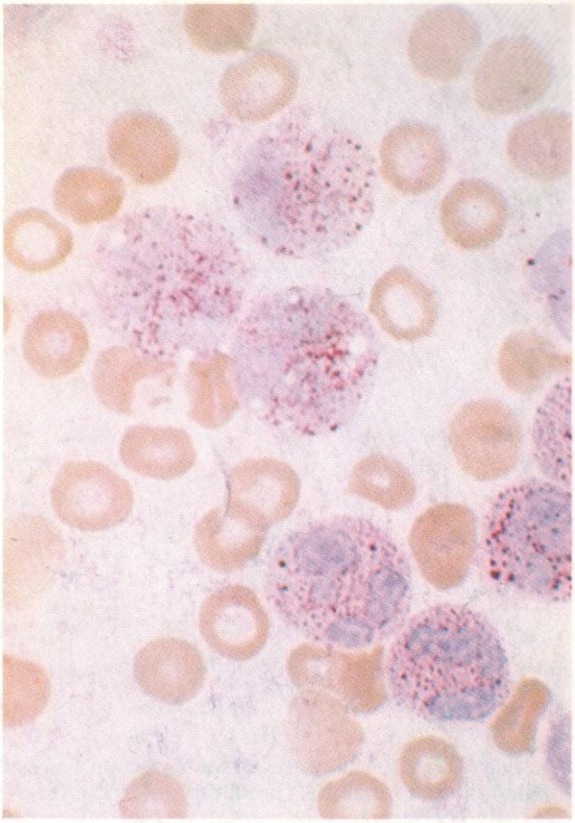

380. PAS stain on blood smear: a blast cell with monocytic PAS-positivity pattern, two vacuolated monocytes, and two neutrophil polymorphs with normal PAS reactions.

381. Acid phosphatase: three polymorphs and three monocytes in peripheral blood show moderately strong granular positivity.

382. Dual esterase: two polymorphs show CE positivity and six monocytes and precursors show moderate BE positivity.

383. Another example of the dual esterase reaction on a smear of bone marrow cells from the same case of juvenile CML as shown in **377** and **378**. The mixture of monocytic and granulocytic precursors with respectively BE and CE positivity is well shown. Several later neutrophils also show CE positivity.

382

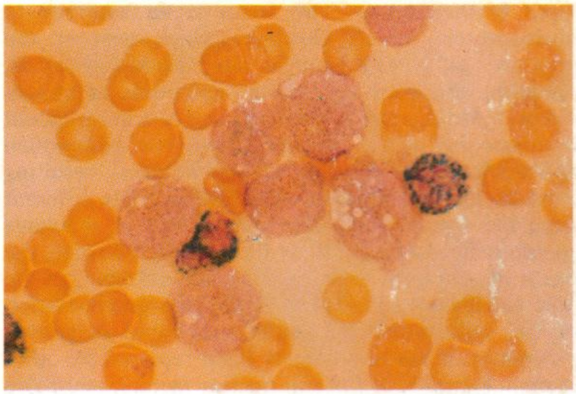

383

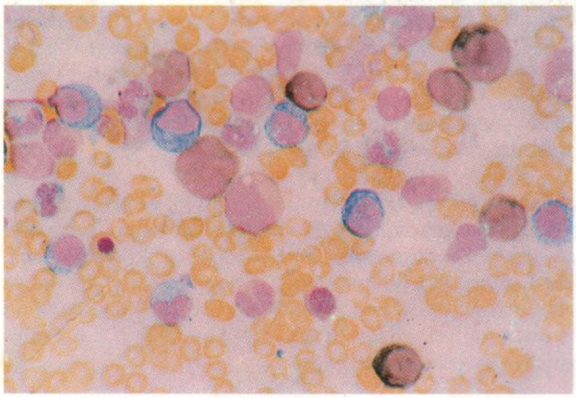

384

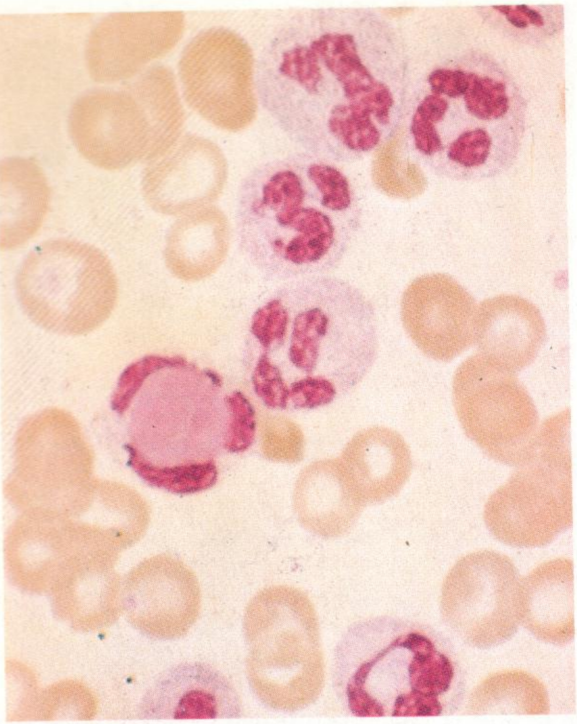

385

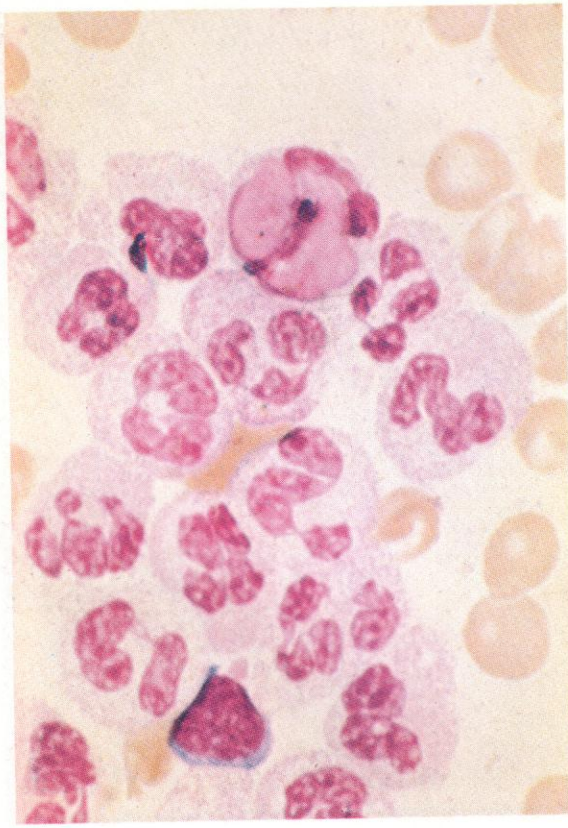

384. An 'LE' cell. The characteristic inclusion body of ingested nuclear material produced in leucocytes – especially polymorphs – as a result of the action of a factor present in the serum of patients with disseminated lupus erythematosus. The factor is an antibody to nucleoprotein, chiefly histone, which acts in the presence of complement as an opsonizing agent, rendering the sensitized nuclei susceptible to phagocytosis by neutrophil polymorphs and to a lesser extent by eosinophils and monocytes. The smooth and swollen appearance of the ingested nuclear material, resulting from the immune process, is characteristically different from the smaller and often denser nuclear remnants engulfed by polymorphs or monocytes following the death of senescent cells, as seen, for example, in the 'tart' cell illustrated in **386**. Although the demonstration of LE cells remains a useful and rapid diagnostic procedure, it has now largely been replaced by other immunological tests for anti-nuclear factors, and more specific tests for the antibodies to double-stranded DNA that especially distinguish systemic lupus erythematosus (SLE) from other collagenoses. Nevertheless, the LE cell remains a striking cytological phenomenon.

385. Another example of an LE cell with a large but partially divided inclusion.

386. A 'tart' cell, as commonly found in preparations made in the search for LE cells. The inclusion is usually, as here, in a monocyte, and consists of a cell nucleus, most often of a lymphocyte. The inclusion stains more deeply than does the LE body. These tart cells are of no known pathological significance and must be distinguished from LE cells.

386

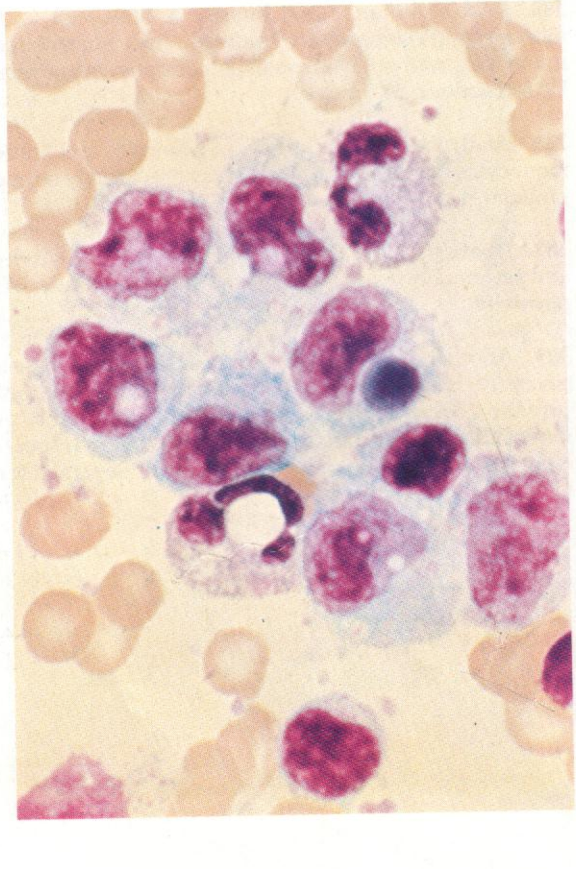

387

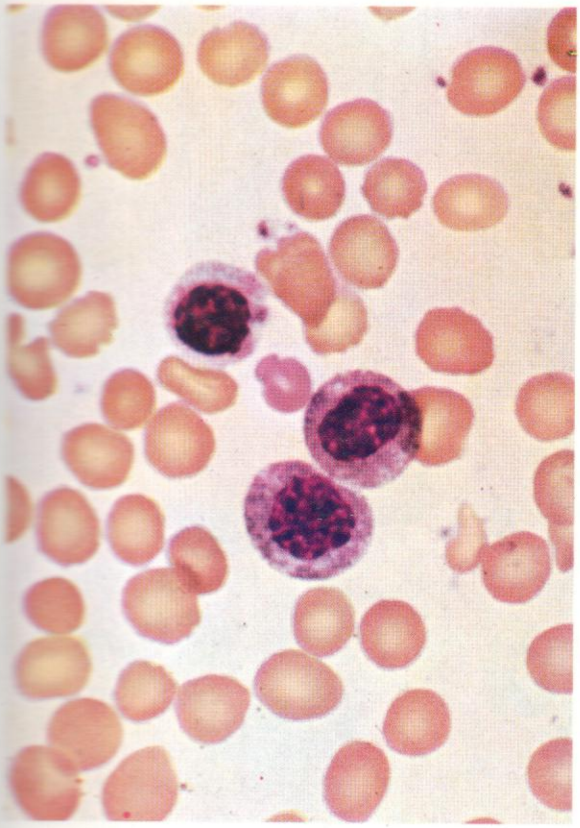

388

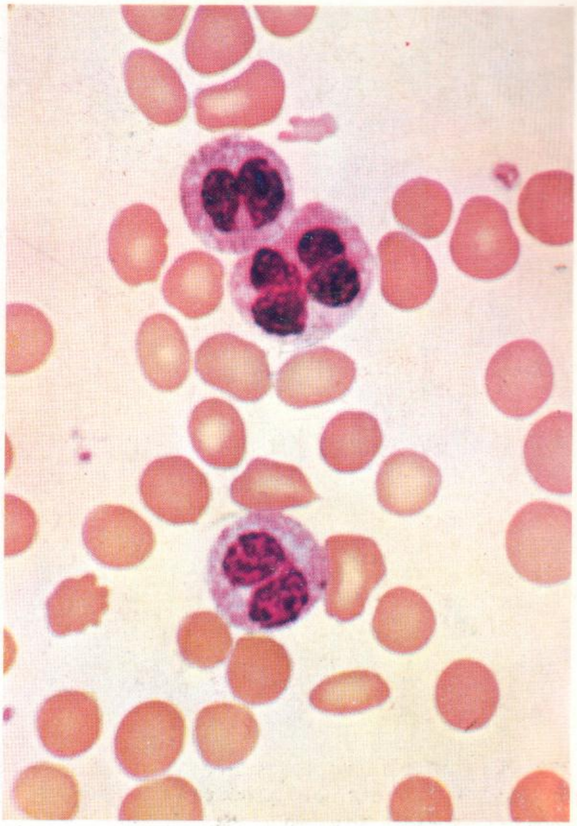

389

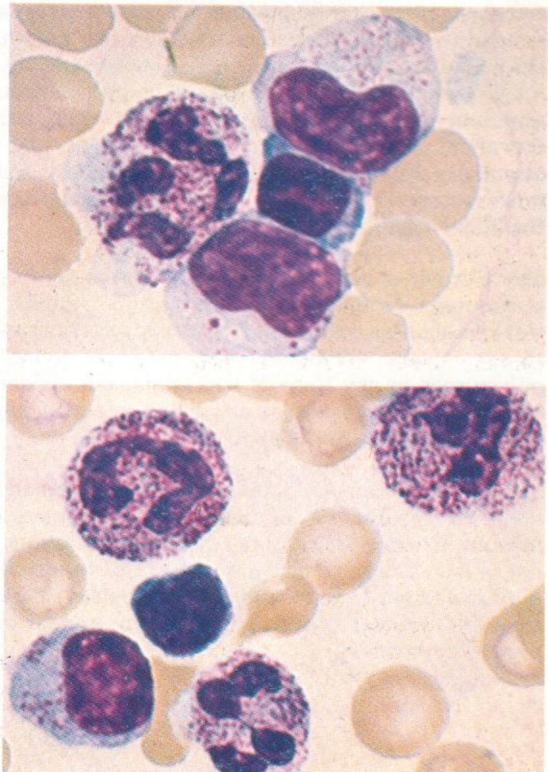

387. Pelger-Huët phenomenon. In the homozygous form the polymorphs show a single rounded dense nucleus. All the granulocytes are affected in the hereditary form of this disorder, but the change may affect some cells in myeloid leukaemia, giving a 'pseudo-Pelger' appearance.

388. Pelger-Huët phenomenon. Heterozygous form with most polymorphs showing a 'band' or bilobed nuclear structure. This appearance may occur as a familial abnormality, but may be mimicked in the 'pseudo-Pelger' polymorphs sometimes seen in acute and chronic myeloid leukaemias and in myelofibrosis.

The example illustrated here is from a patient with CML. One of the cells shows twinning of bilobed pseudo-Pelger nuclei.

389. Coarse reddish-violet granules in leucocytes in Alder's anomaly, a familial disorder of leucocyte granularity. The appearance in the neutrophils resembles the 'toxic granules' commonly seen in leucocytosis of infection (as in **390–392**), but the accompanying granules in lymphocytes, sometimes within vacuoles, and occasionally showing a 'comma' shape, are strongly suggestive of Alder's anomaly.

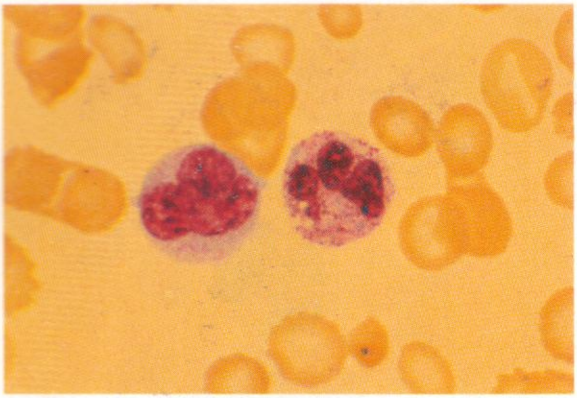

390

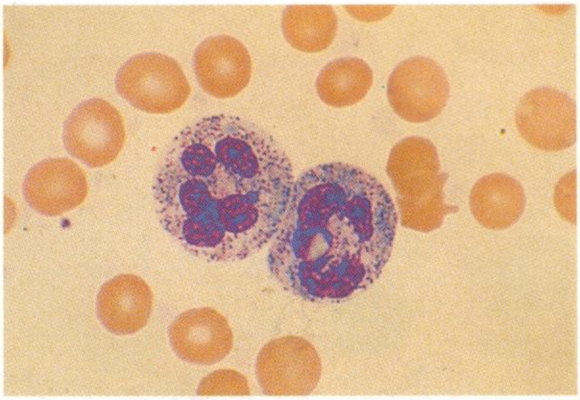

391

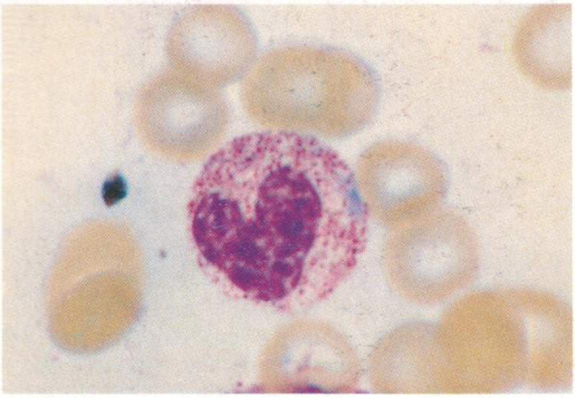

392

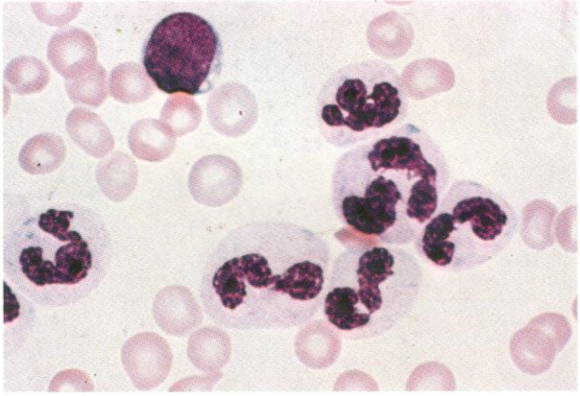

393

390–392. Examples of the blue-staining areas in the cytoplasm of neutrophil polymorphs sometimes seen in infections, especially pneumonia. They are known as Döhle bodies. The polymorphs also show some coarse toxic granularity. The Döhle bodies of infection represent areas of aggregated rough endoplasmic reticulum, as seen in the electron microscope, and are essentially different from the inclusion bodies, sometimes incorrectly given the same name, which occur in the May-Hegglin anomaly.

393. Further examples of Döhle bodies in neutrophil polymorphs. In this instance the specific granules are weak rather than coarse, and the Döhle inclusions more readily visible. Döhle bodies may be found in polymorphs in any form of leukaemia, but appear to arise as a consequence of associated infection rather than being intrinsic to the neoplastic process.

394 and **395**. Examples of the May-Hegglin anomaly, an inherited disorder with basophilic inclusions, 2–5 microns in diameter, in granulocytes. The inclusions are larger than Döhle bodies and not related to infection. Ultrastructurally, they contain particulate material including rod-like structures unlike any normal cytoplasmic component.

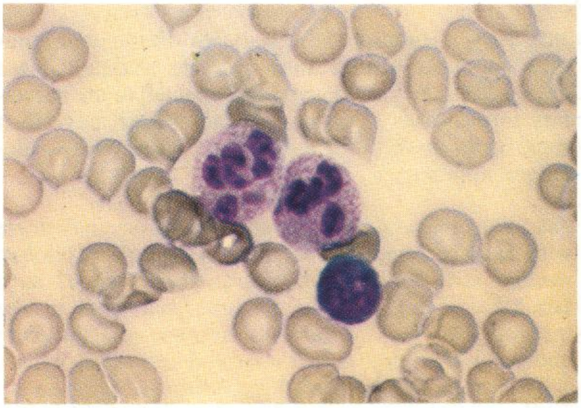

394

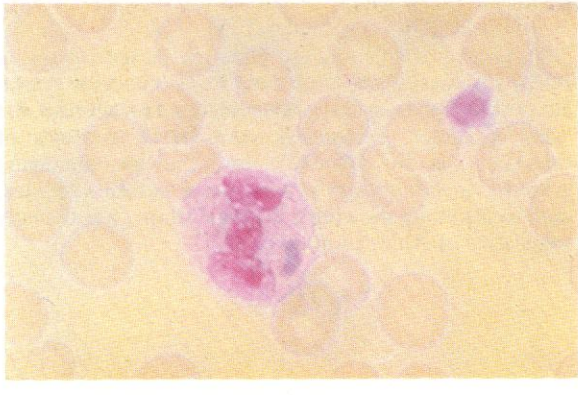

395

396

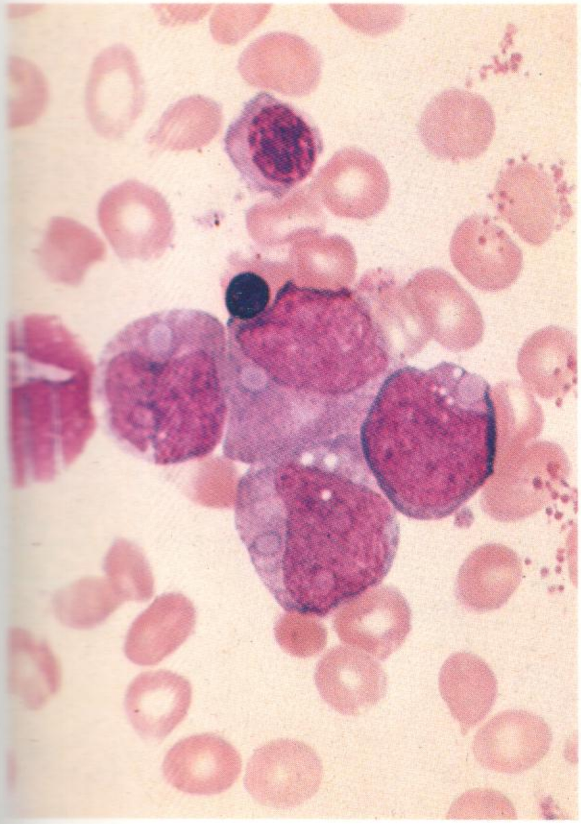

397

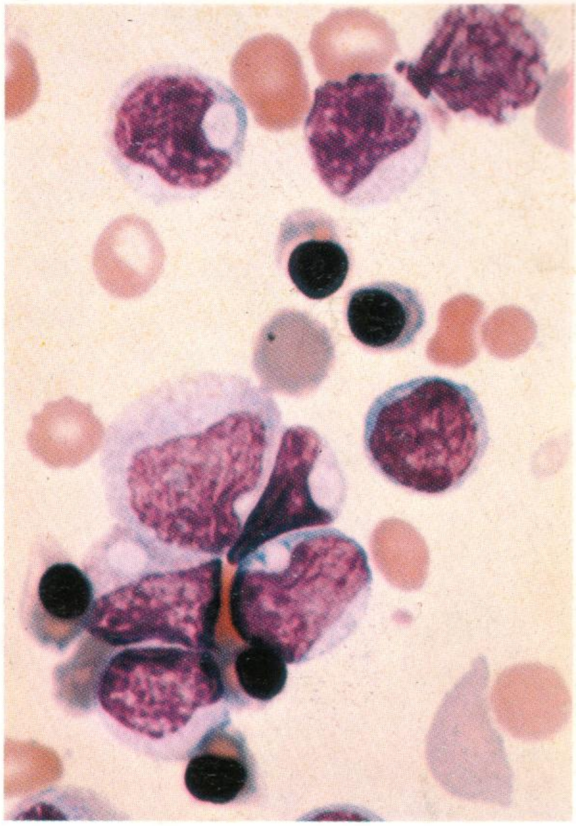

398

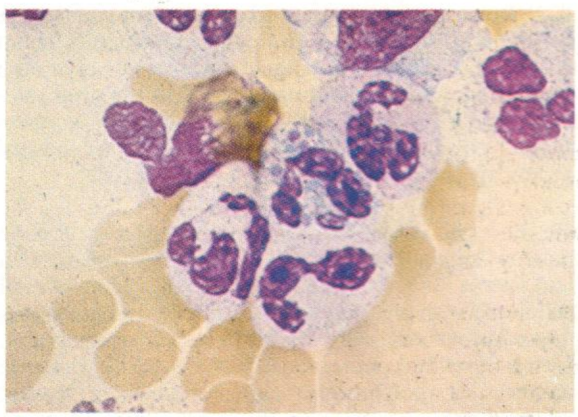

399

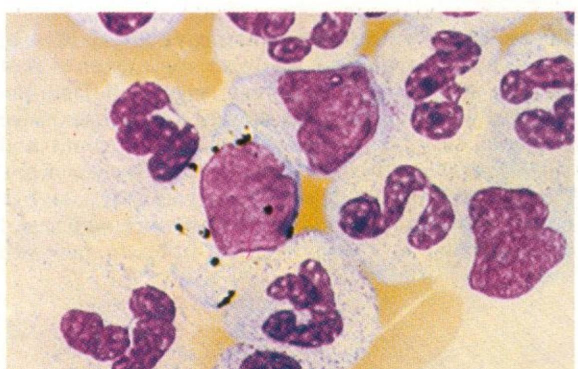

396 and 397. Further unusual inclusions, some 3–5 microns in diameter, weakly basophilic and apparently membrane-bound, in granulocyte precursors and in lymphocytes from a child with a transient pancytopenia and haemolytic syndrome. The material seems likely to be ribosomal protein.

398. Giant granulation, with both red and pale blue granules in a neutrophil polymorph. Similar giant granules in leucocytes of all kinds may be seen in the rare familial Chédiak-Higashi-Steinbrinck anomaly. These large granules are thought to be derived by the fusion of primary lysosomal azurophil granules at the promyelocyte and early myelocyte stages. There are similar inclusions to be found in many other tissues in this disease. Affected polymorphs appear hyperactive in phagocytosis but ineffective in killing and destroying ingested bacteria or other material.

399. Conspicuous inclusion particles, probably carbon, in a peripheral blood monocyte. Such material may be ingested during a period of temporary sequestration within the respiratory tract.

400

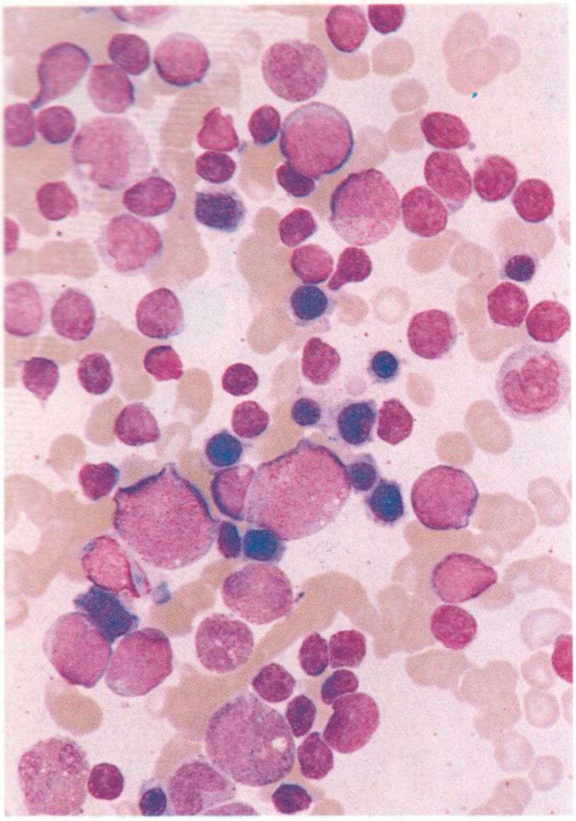

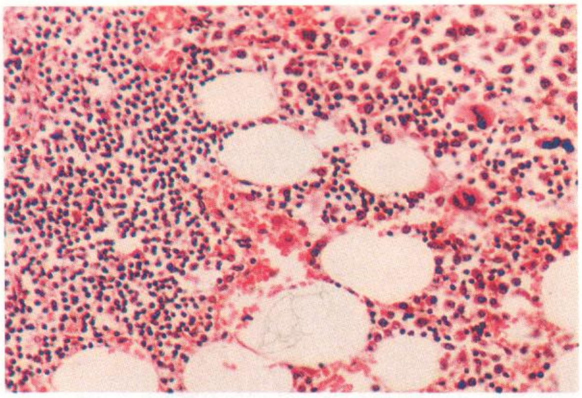

401

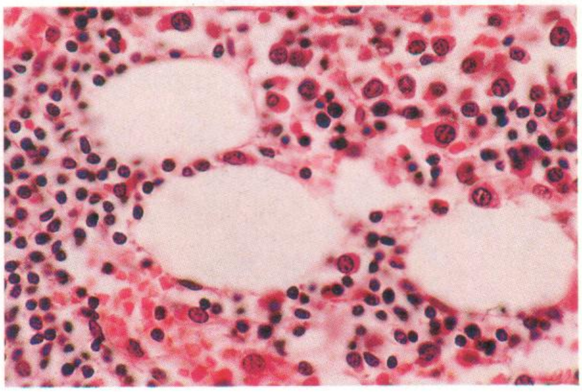

402

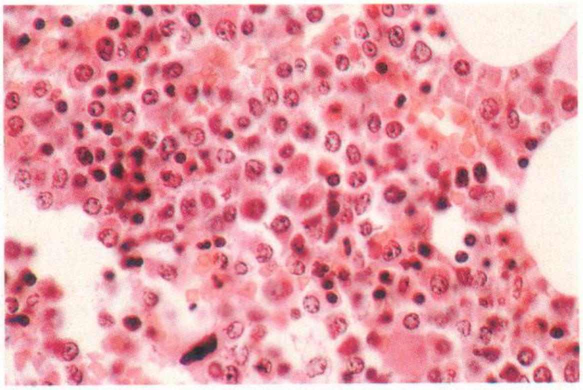

403

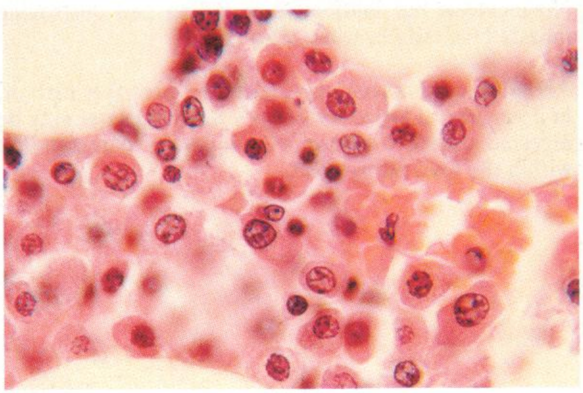

404

400. Bone marrow aspirate from a patient with severe agranulocytosis and peripheral neutrophil count $<0.5\times10^9/1$. There is not a single neutrophil polymorph to be seen, and few neutrophils beyond the promyelocyte and early myelocyte stages, although erythroblasts, eosinophils, lymphocytes and an occasional monocyte can be recognized.

401 and **402**. Low- and higher-power views of bone marrow trephine biopsy section from a patient with leukopenia due to drugs. There is adequate overall cellularity with plentiful megakaryocytes and numerous mononuclear cells, shown in **402** to include normoblasts, lymphocytes and plasma cells, but a virtually complete absence of polymorphs and recognizable earlier granulocytes.

403 and **404**. Two views at increasingly higher powers of thin sections from a bone marrow sample taken at post mortem from a young woman who died from an overwhelming streptococcal septicaemia, unresponsive to antibiotics. Her peripheral neutrophil count had fallen precipitously to $<0.2\times10^9/1$. The bone marrow shows complete absence of granulocytes at any stage of maturity, the relatively high cellularity being made up of mononuclear cells including erythroblasts but also numerous plasma cells.

405

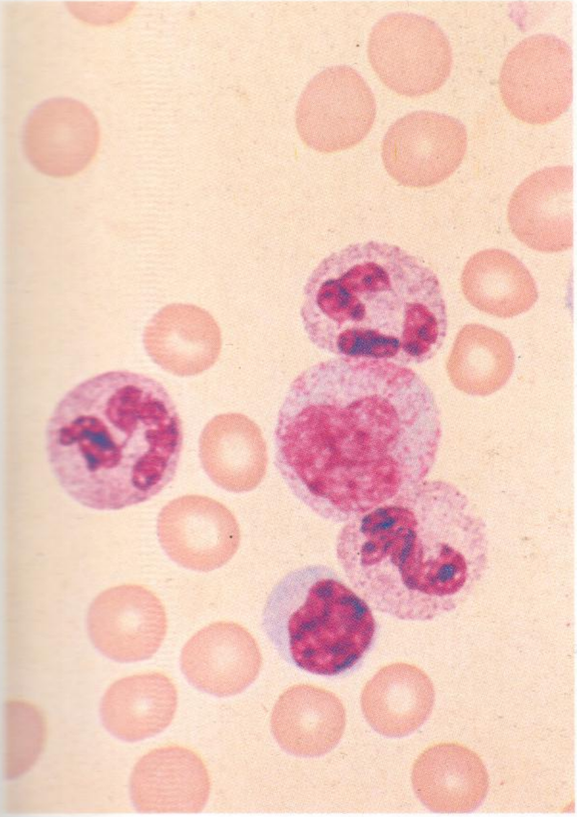

406

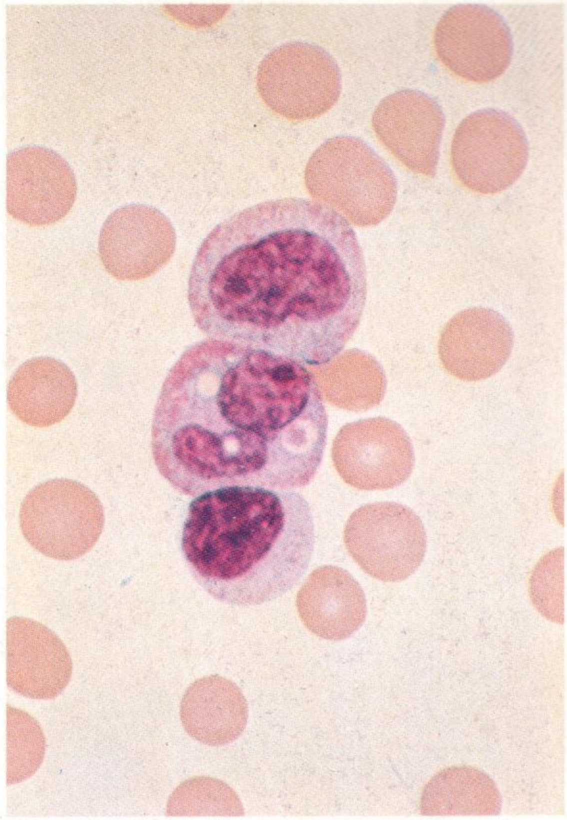

405–407. Various monocytes from normal peripheral blood.

405. A monocyte with some reddish granules in the grey cytoplasm, together with a lymphocyte, a stab cell, and two neutrophil segmented polymorphs. The extent of indentation or more gross convolution of the monocyte nucleus is quite variable. A very few monocytes with characteristic cytoplasm and nuclear chromatin pattern have oval nuclei without indentation, perhaps 20% have only minor indentation, as in the upper cell in **406**, but most monocytes in the peripheral blood show more marked nuclear bending or twisting, as in the remaining cells shown in **405–407**. Cytoplasmic granularity is also variable, from little or none to relatively coarse, weakly azurophil granules as in the central cell of **406** and the lower cell of **407**.

406. Two monocytes, one with vacuoles, and a lymphocyte. The vacuoles are probably all phagocytic, one still containing an ingested platelet and the other two having lost or already digested their contents.

407. Two monocytes and a stab cell. The monocytes show moderate cytoplasmic granularity and typical nuclear shapes.

407

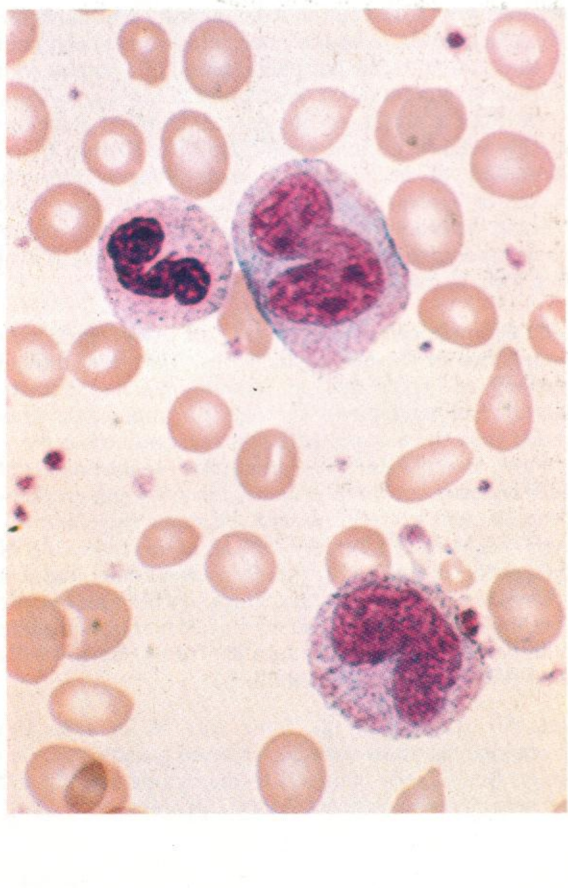

408

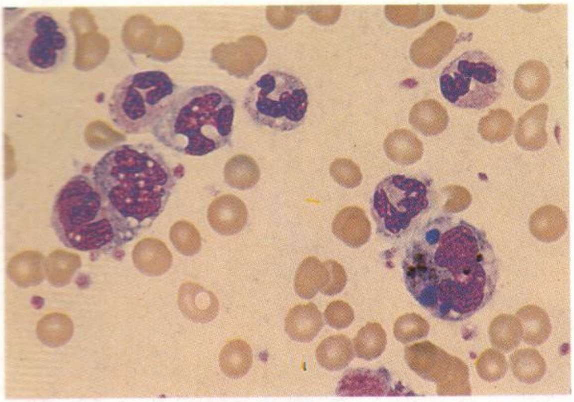

409

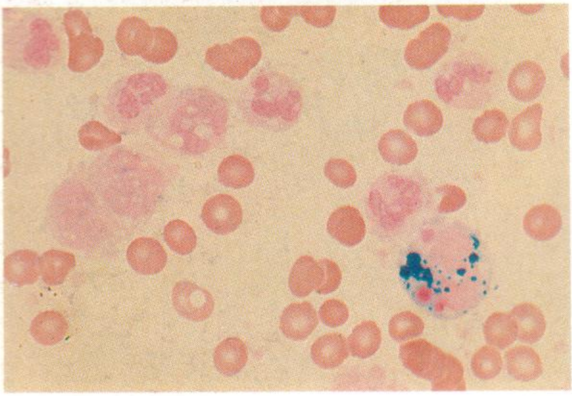

410

411

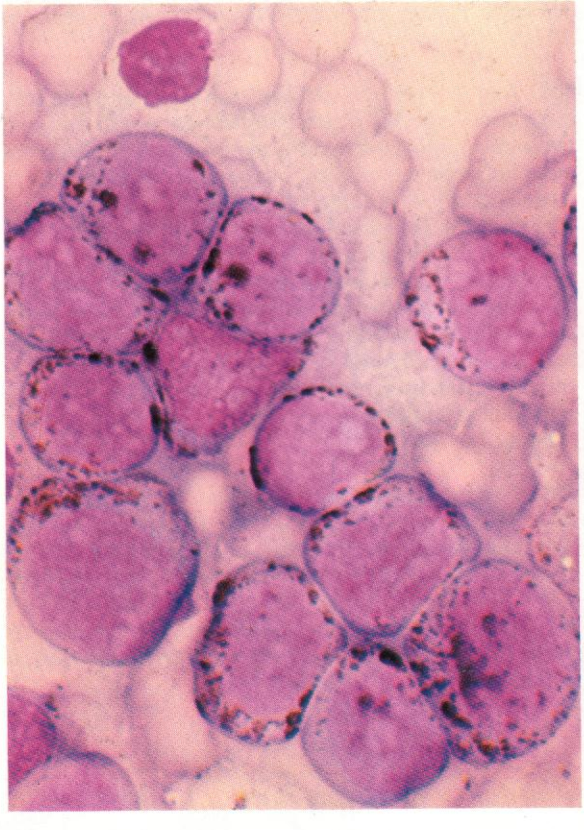

408 and **409**. Consecutive Romanowsky and duplicate Prussian blue stains on the same field, from a buffy coat smear made from the peripheral blood of a patient with chronic myelomonocytic leukaemia (CMML), to show more bizarre forms of nuclear convolution than are usually seen in normal monocytes. The further transformation of monocytes to macrophages normally occurs in tissues, but may occasionally, as here, take place in the blood. The transforming monocyte contains phagocytosed nuclear fragments and also a heavy load of free iron, as demonstrated in **409**.

410. Promonocytes from a case of AML with predominance of the monocytic series. The cells, though nucleolated, show nuclear indentations and a cytoplasmic colour tending towards the monocytic grey rather than the basophilia of less differentiated cells.

Pure 'monoblastic' or 'monocytic' leukaemias are very uncommon; there is nearly always some granulocytic element present, so that the name 'myelomonocytic' might strictly be used, but, as in this case, cells of the monocyte series may greatly predominate, and it is convenient to retain the term 'acute monocytic leukaemia' (AMonL) for such cases. When recognizable granulocytes make up less than 20% of the marrow cells the FAB classification would be M5.

411. SB staining in the same case as in **410**. The promonocytes show discrete scattered granules of positivity, here chiefly confined to the cytoplasm, but not densely clumped as in granulocyte precursors.

412

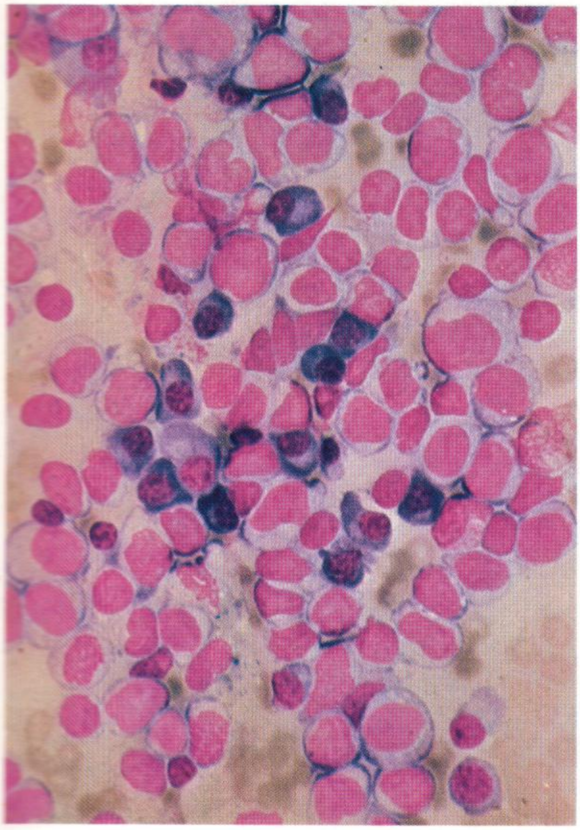

413

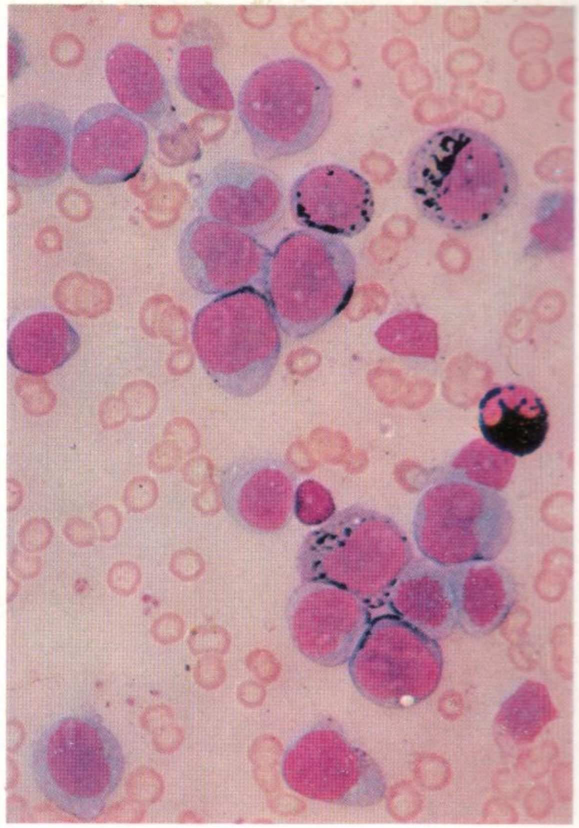

414

412. AMonL, with monocyte precursors of variable morphology and state of maturity. This field also illustrates a scattering of plasma cells. An increase in plasma cells, generally focal or patchy in distribution, is commonly observed in acute leukaemias of any kind and is also seen when other malignant processes invade the marrow.

413. SB reaction in the same case. A single strongly sudanophilic polymorph contrasts sharply with the monocyte precursors, with their reactions ranging from negative to moderately strong positivity of the discrete scattered granule type.

414. Three primitive cells from an acute leukaemia with minimal morphological signs of differentiation in Romanowsky preparation. The SB reaction, shown here, has the typical distribution of positive granules characteristic of the monocytic series. The primitive blast cells are therefore monoblasts.

415

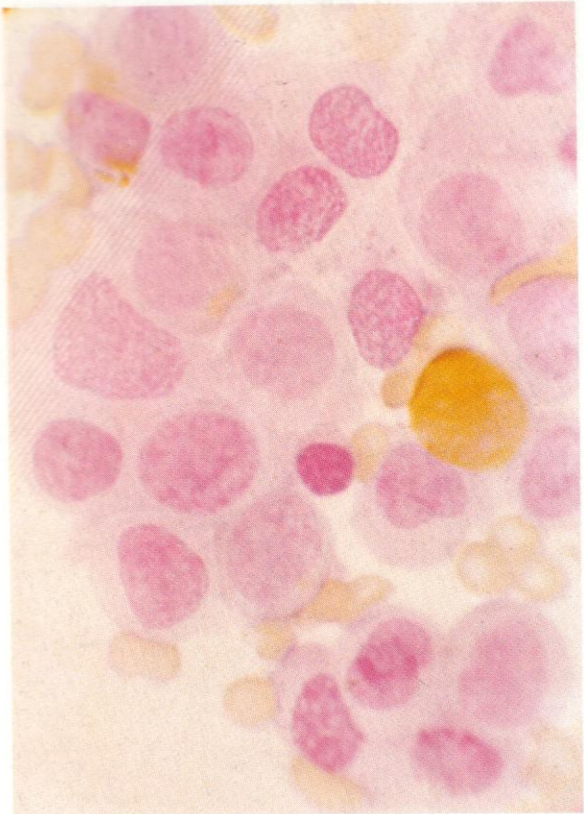

416

417

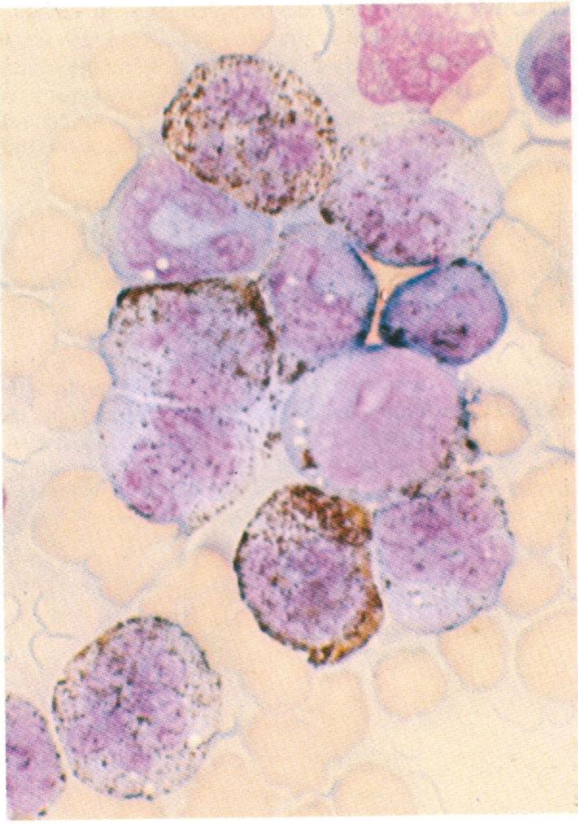

415. AMonL: peroxidase reaction. Monocytes and their precursors are generally negative for peroxidase, but may show a faint localized cytoplasmic reaction. Auer rods, as shown in the upper left corner, are strongly peroxidase-positive. Their presence confirms the myelomonocytic nature of the disease, since Auer rods probably do not occur in the monocyte line but are confined to granulocyte precursors, being derived chiefly from primary azurophil granules.

416. Another example of peroxidase staining in an AMonL. The monocytes appear rather more differentiated than in the previous example, and have a negative reaction.

417. SB reaction in the same case: the monocytes mostly show discrete scattered granules. A myeloblast with two positive Auer rods is also seen.

418

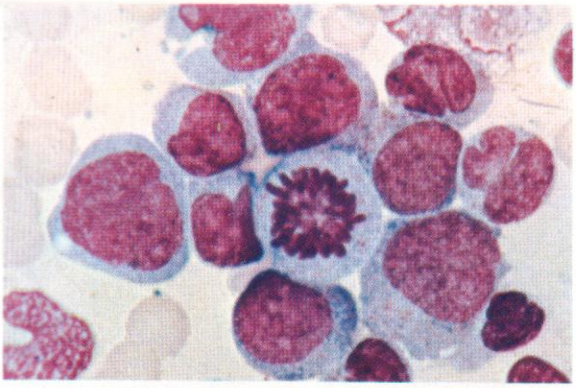

419

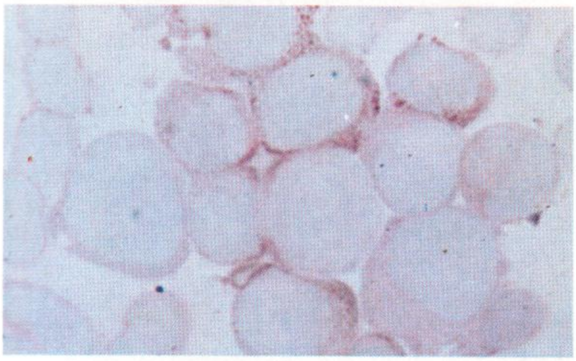

420

421

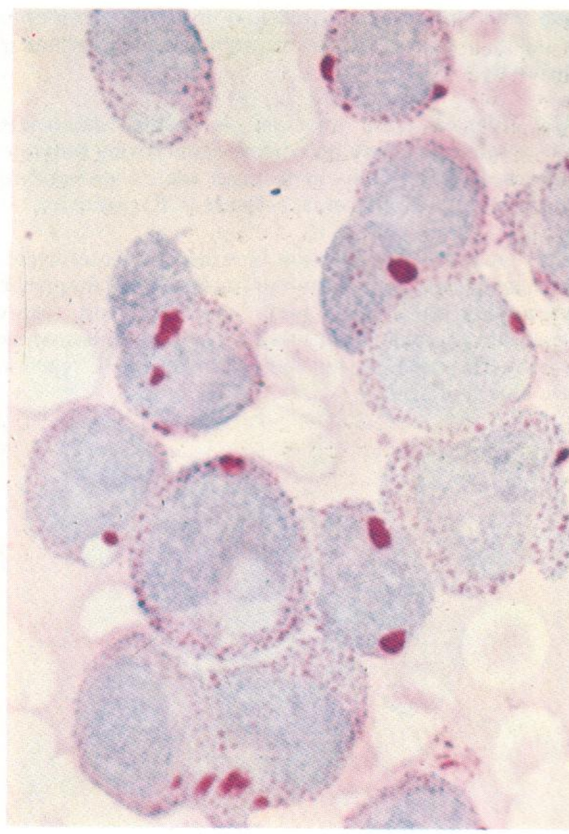

418. A group of monocyte precursors from an AMonL.

419. The same field, consecutively stained with the PAS reaction. Monocyte precursors show considerable variability in their positivity to PAS, from completely negative reactions to coarsely granular, heavy positive ones. Here the cells show a mixture of diffuse cytoplasmic staining and fine granules.

420. A series of monocytes and precursors from an AMonL, to illustrate the range of variation encountered in PAS reactivity in this cell series.

421. Very strong PAS positivity with coarse blocks in monocytes, from a further case of myelomonocytic leukaemia with predominance of well-differentiated monocytes.

422

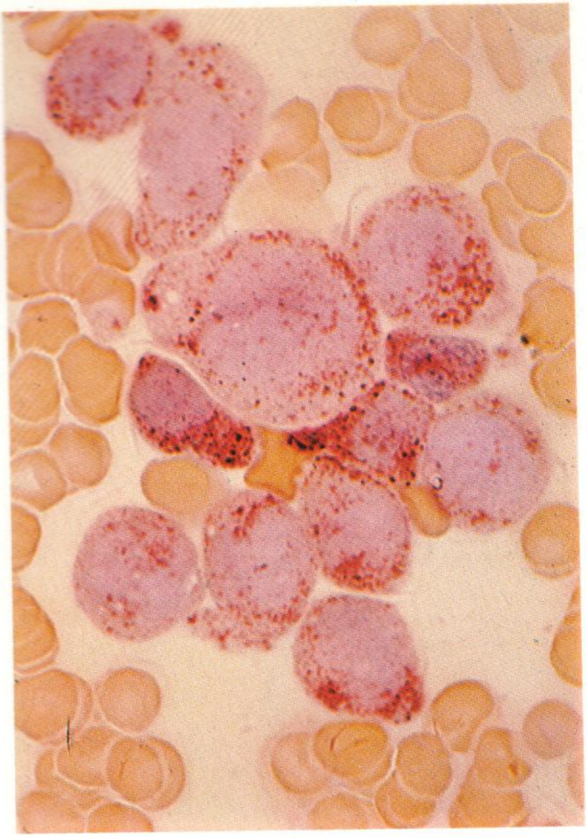

423

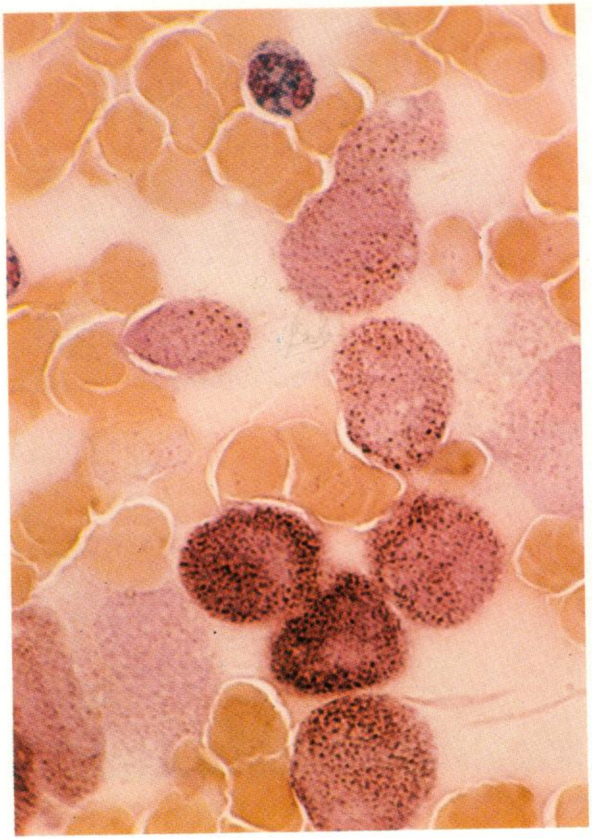

422. Acid phosphatase reaction in acute monocytic leukaemia: most cells show strong and coarsely granular positivity.

423. Dual esterase reaction in acute monocytic leukaemia: monocyte precursors show strong butyrate esterase (BE) positivity in this case, while a granulocyte shows strong chloroacetate esterase (CE) positivity.

424. Dual esterase reaction in a case of acute myelo-monocytic leukaemia. In this instance the monocyte precursors show only weak reactions with scanty scattered granular BE positivity. Two myeloblasts show chiefly CE positivity, but some granules of BE reaction are also detectable.

424

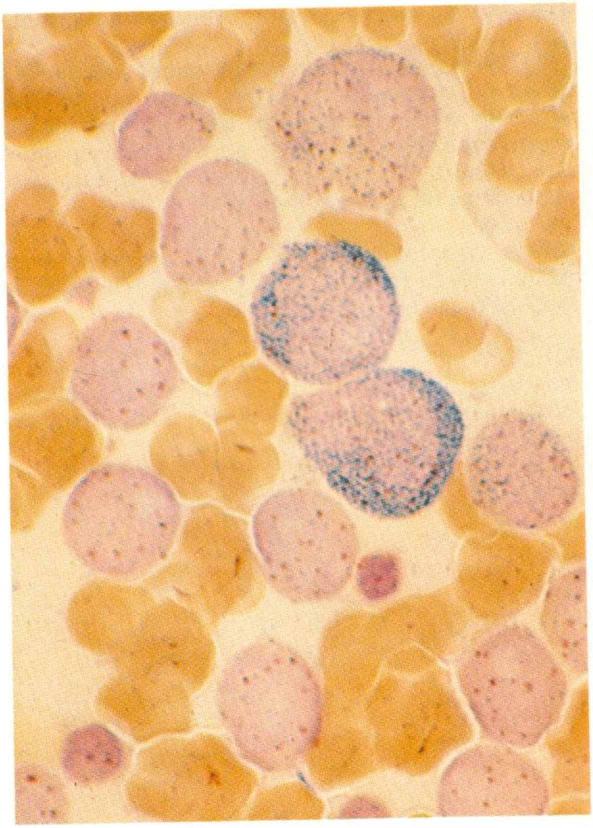

425

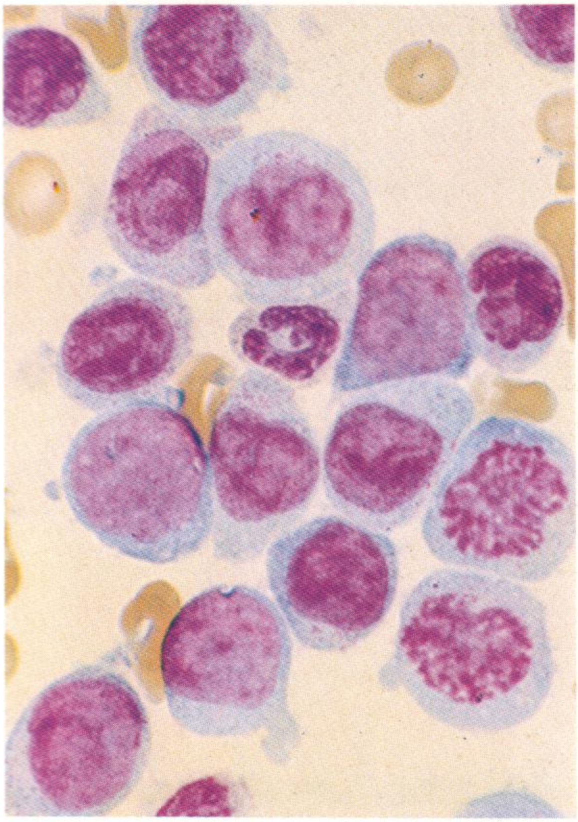

426

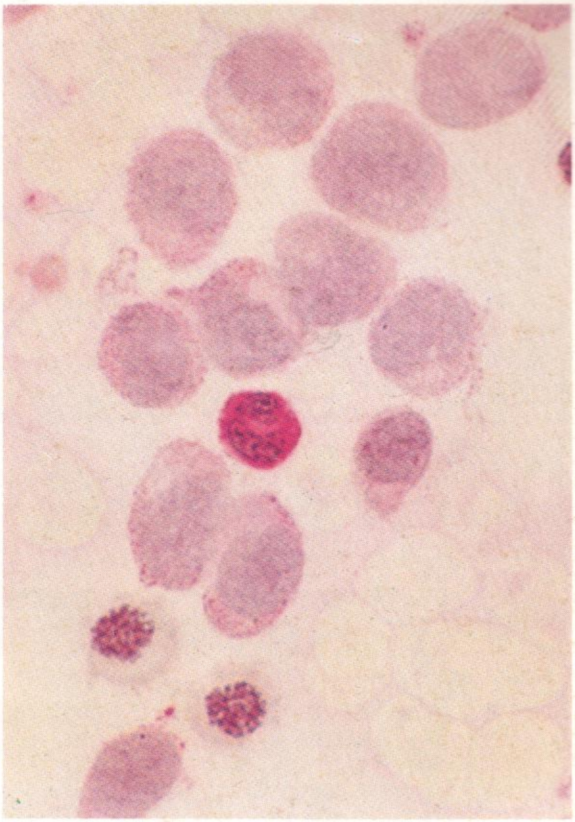

425–427. Romanowsky, PAS and dual esterase reactions on the cells of an AMML, with predominantly monocytic morphology and typically monocytic mixed diffuse and granular PAS reaction, but with weak CE rather than BE positivity in the monocytes. This is a very uncommon picture but illustrates the potential variability of monocytic esterase content.

427

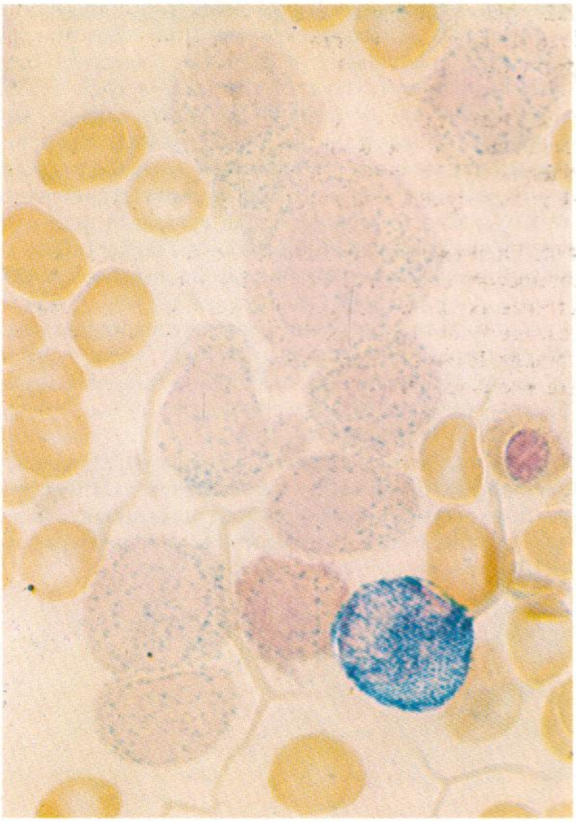

428

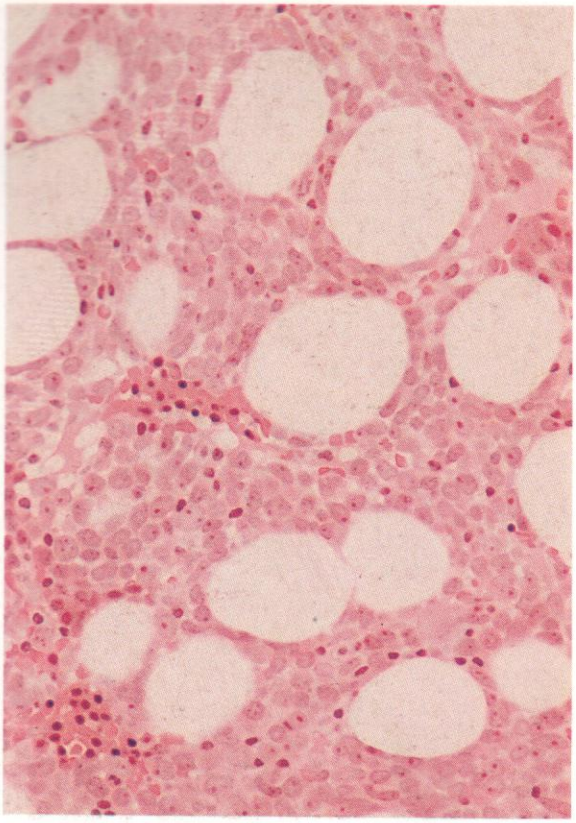

429

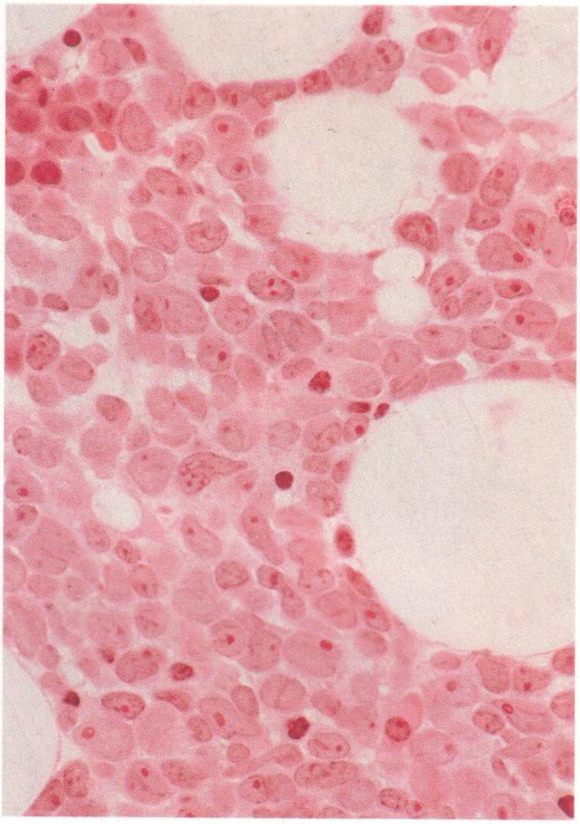

430

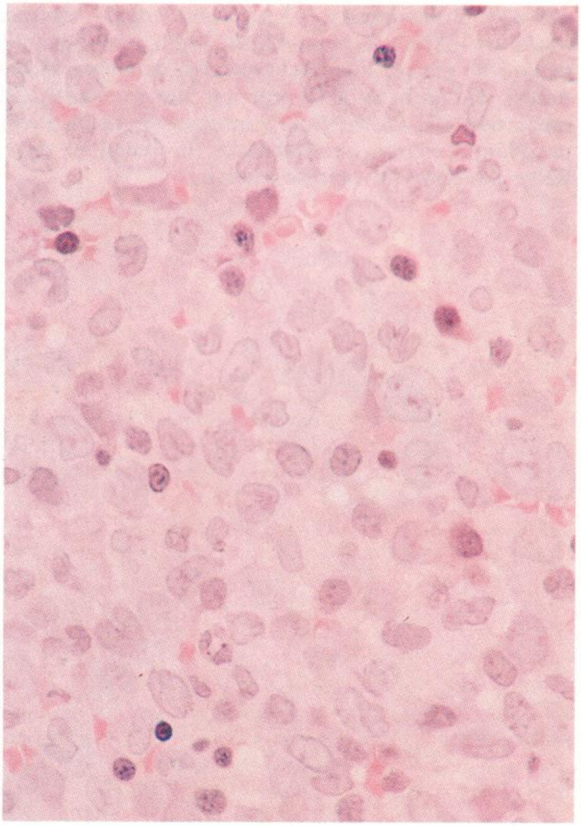

428–430. Various histological fields from thin sections of bone marrow trephine biopsies from cases of acute monocytic leukaemias. In **428** and **429**, respectively low- and higher-power views of the same section (H&E stain), considerable residual fat spaces remain, and islands of erythropoietic tissue can be distinguished; but the cellular areas are predominantly occupied by large, poorly differentiated blast cells with nuclei sufficiently widely spaced to indicate ample cytoplasm, and with several nucleoli often visible under the higher power. A suggestion of nuclear twisting can be discerned in **429**. This is a more readily recognized feature of **430**, a thinner section stained with Giemsa from another case, where there is denser cellularity with a scattering of erythroblasts having dark nuclei and eosinophilic cytoplasm – but, again, a preponderance of nucleolated primitive cells with nuclear twisting of the monocytoid type. These sections provide valuable supplementary information on overall cellularity and relative proportions of different cell types, but for cytological detail and comprehensive cytochemistry it is necessary to study smear preparations in parallel.

431

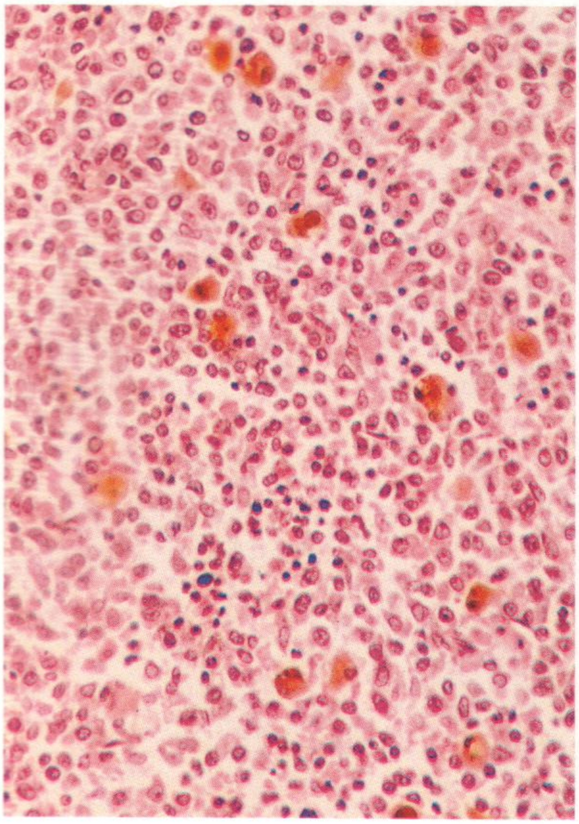

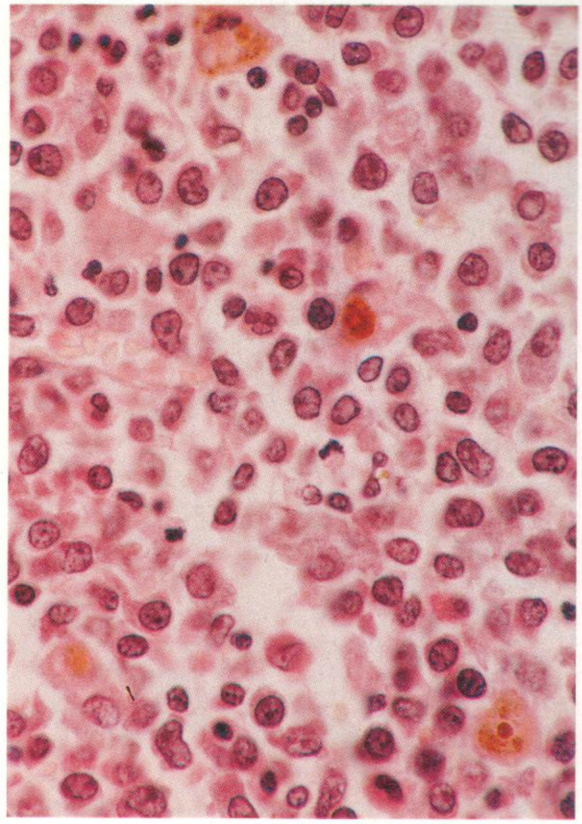

432

431–433. Sections of a trephine biopsy from a case of AML with monocytic features. In aspiration smears the cytology showed a well-differentiated monocytic pattern; this is reflected in the predominant cell appearance in these sections, where the H&E stain in **431** and **432**, at respectively low and higher magnification, shows moderately dense nuclear chromatin, occasional nuclear indentation, nucleoli, and a generally low nuclear–cytoplasmic ratio. Residual nests of erythroblastic activity are apparent in **431**, and scattered normoblasts with small dark nuclei are present in **432**, but the striking and unexpected feature in these sections, not previously noted in the marrow smears, is the conspicuous increase in macrophages, many heavily laden with haemosiderin and some containing other phagocytosed cellular material. The section appearing in **433** is of an acetate esterase stain on plastic-embedded material, with reddish positivity in a proportion of the leukaemic monocytes.

The normal sequence of monocyte development proceeds from the common granulocyte–monocyte progenitor to a committed monoblast, then promonocyte and mature monocyte, with a final potential transformation to tissue macrophage (or other related cell such as osteoclast or Langerhans cell) occurring after the monocyte has migrated from the peripheral blood into the tissues. Neoplastic disorders chiefly involving macrophages are dealt with in Part 4, but the present case shows the emergence of some differentiation to that level in an otherwise typical monocytic AML.

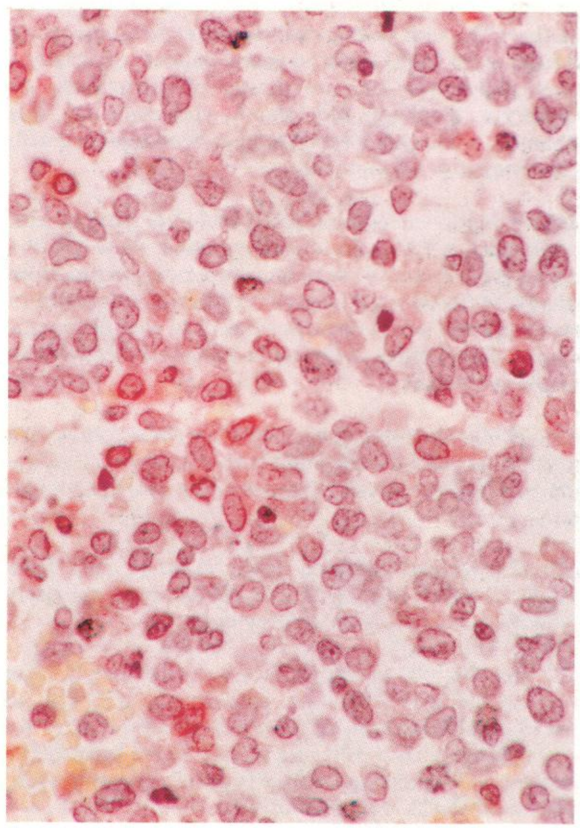

433

434
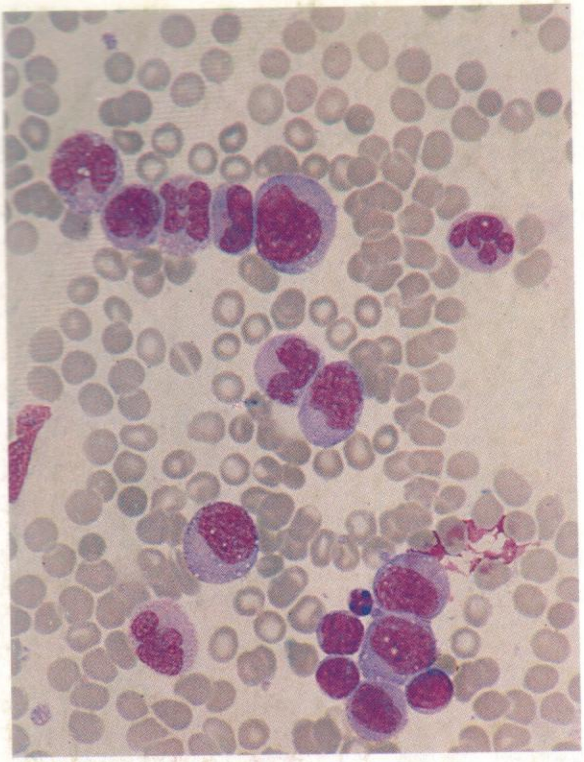


435

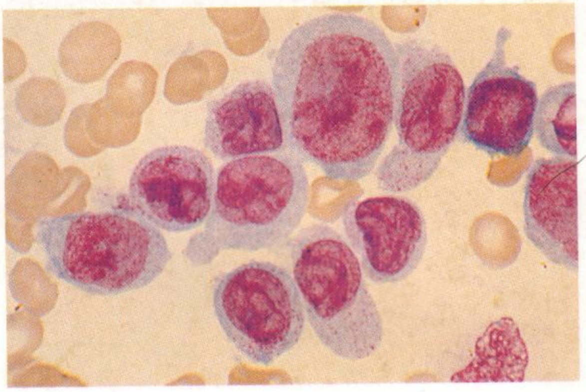
436

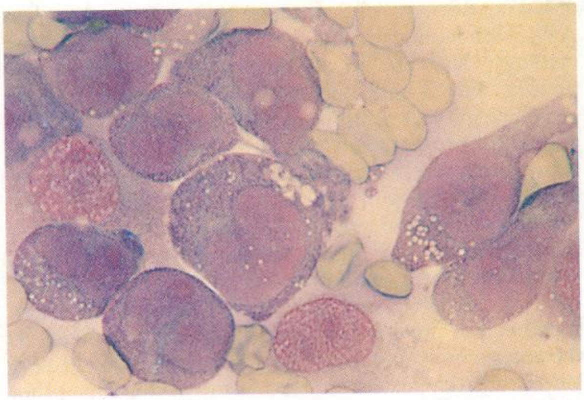
437

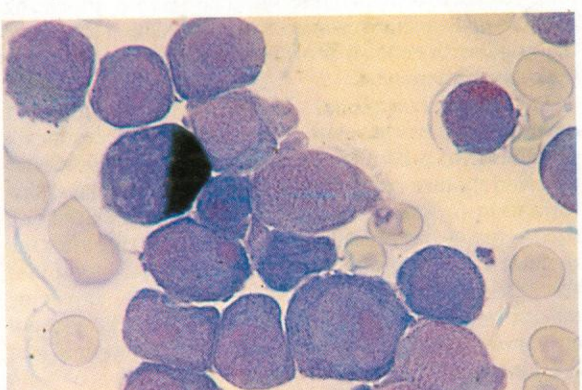
438

434–443. *Examples of cytology and cytochemistry of AML cases with abnormalities involving 11q23.*

Leukaemias with translocations or deletions involving chromosome 11q23 occur in young patients especially – often children – and are mostly of monoblastic or monocytic cytology. Myelomonocytic cases are less common, while only a very few have been reported with granulocytic predominance.

434. A blood smear from a child of nine months with AML and t(9;11). In this low-power view all the nucleated cells are of the monocyte series, ranging from small undifferentiated blasts with minimal cytoplasm (a group of three are at the lower right), to well-differentiated promonocytes with multi-lobulated nuclei and ample cytoplasm.

435. A higher-power view of the same smear, showing a good sequence of maturation stages from small monoblast to late promonocyte, again with marked lobulation.

436. Romanowsky-stained bone marrow cells from another case of AML with t(11;19) and predominantly monoblastic or promonocytic cytology.

437 and **438**. SB stains on bone marrow smears from two patients with AML and, respectively, t(11;17) and t(9;11). The leukaemic cells are SB-negative. There is a single SB-positive myelocyte in **438**. Weak or negative staining for SB and peroxidase is usually found in these defects of 11q23.

439

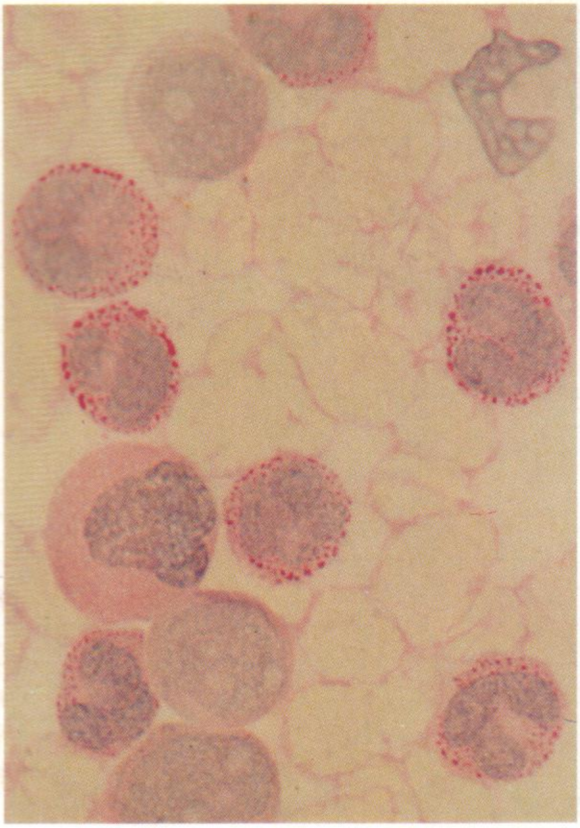

440

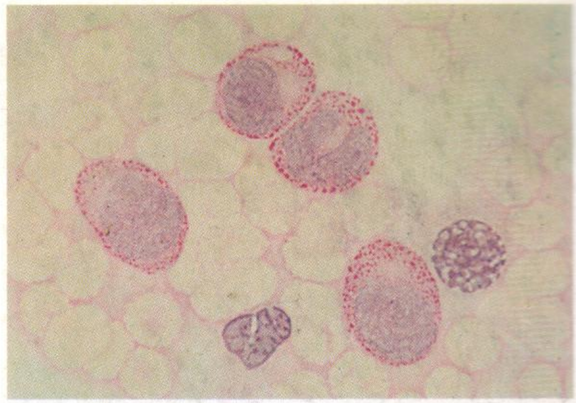

441

442

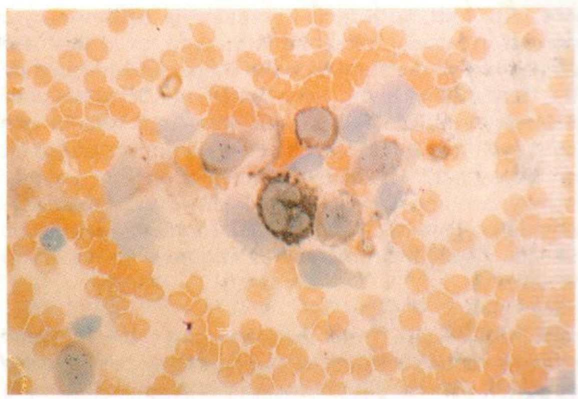

443

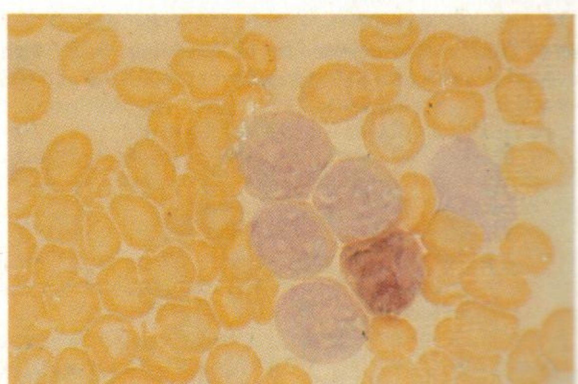

439. PAS reaction on the same specimen as in **434**. There is a negative or weak reaction in the least mature blast cells, increasing to moderately coarse granular positivity against a diffusely positive background in the more mature promonocytes.

440 and **441**. PAS reactions from two further cases of AML with t(9;11), showing a similar pattern of increasing positivity with increasing maturity, but in general conformity with the patterns of PAS reaction usually encountered in leukaemic monocytes. In **440** there is a typically monocytic pattern of positivity in the promonocytes and a negative erythroblast, and in **441** six almost negative monoblasts and one very coarsely positive promonocyte.

442 and **443**. Dual esterase reactions in t(11;17) and t(9;11), respectively. The low-power view in **442** shows the variable positivity for BE in the leukaemic cells, with generally negative blasts and more marked positivity in the most mature-looking promonocytes. The higher-power view in **443** illustrates the same pattern, with four negative monoblasts and a BE-positive promonocyte.

444

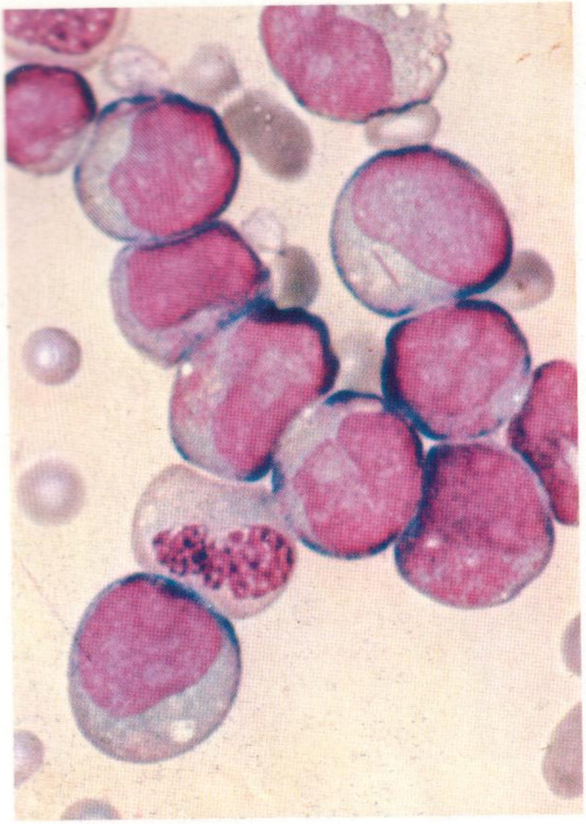

445

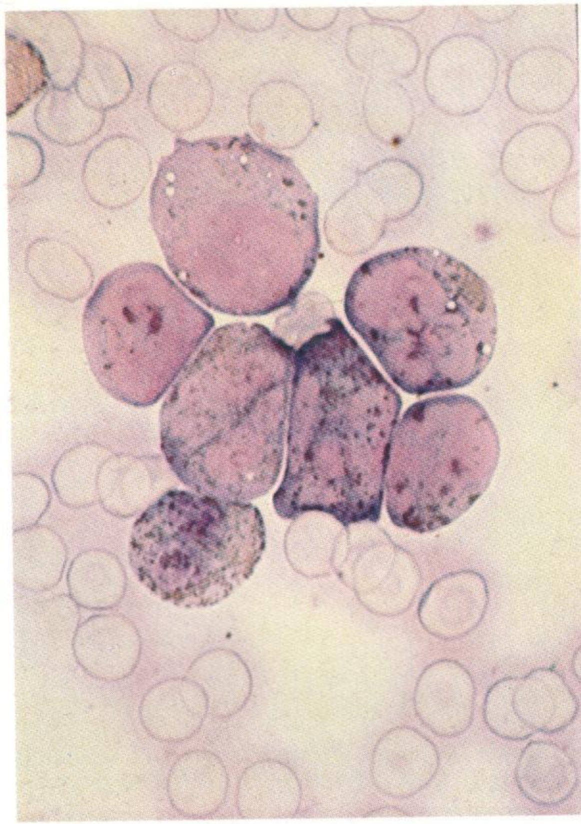

446

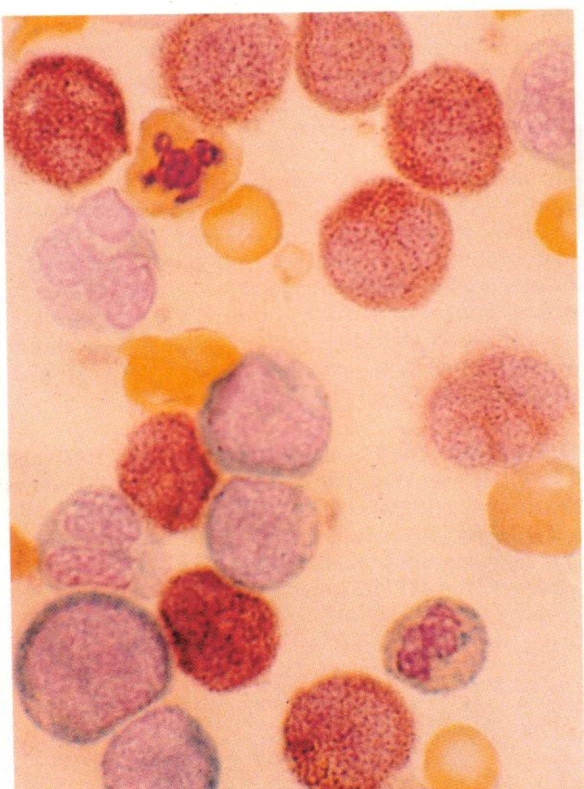

444. An AML with mixed granulocyte and monocyte precursors; when admixture is marked, as in this case (suggested by the Romanowsky stain and confirmed by the Sudan black), the term 'myelomonocytic' is conveniently applied. The conspicuous Auer rods in two blast cells and the localized accumulation of azurophil granules to the left of the nucleus in another identify myeloblasts and a promyelocyte. However, the remaining cells might be of either granulocytic or monocytic lineage, and cytochemistry is required to ascertain which.

445. SB reaction from the same case; the localized cytoplasmic positivity in the early granulocyte precursors contrasts with the discrete scattered granule pattern of the monocyte precursors.

446. Dual esterase reaction in a similar case, with typical BE reaction in the monocyte precursors and CE reaction in granulocytic precursors. An erythroblast with distorted nucleus is esterase-negative.

447

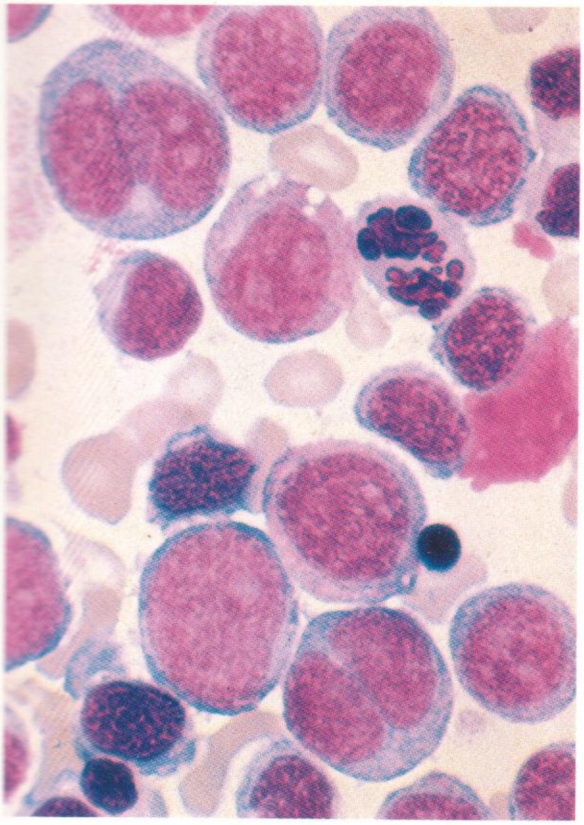

448

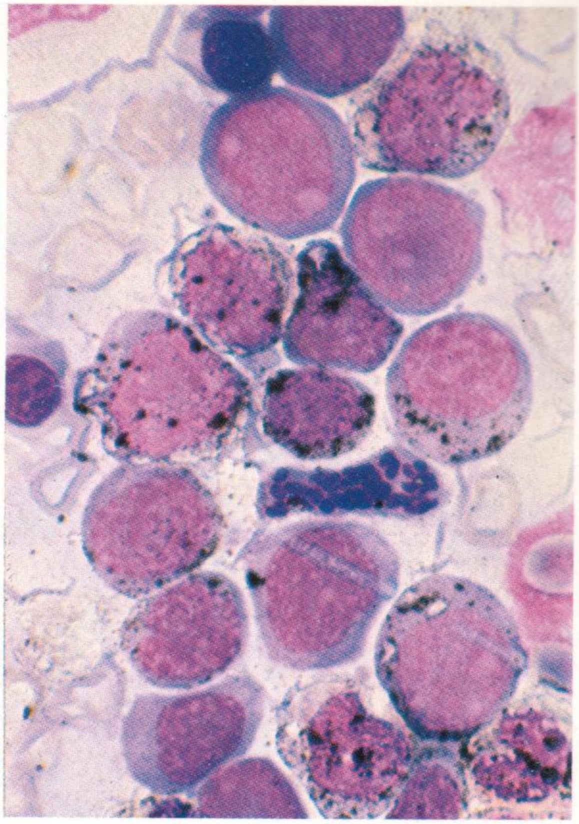

449

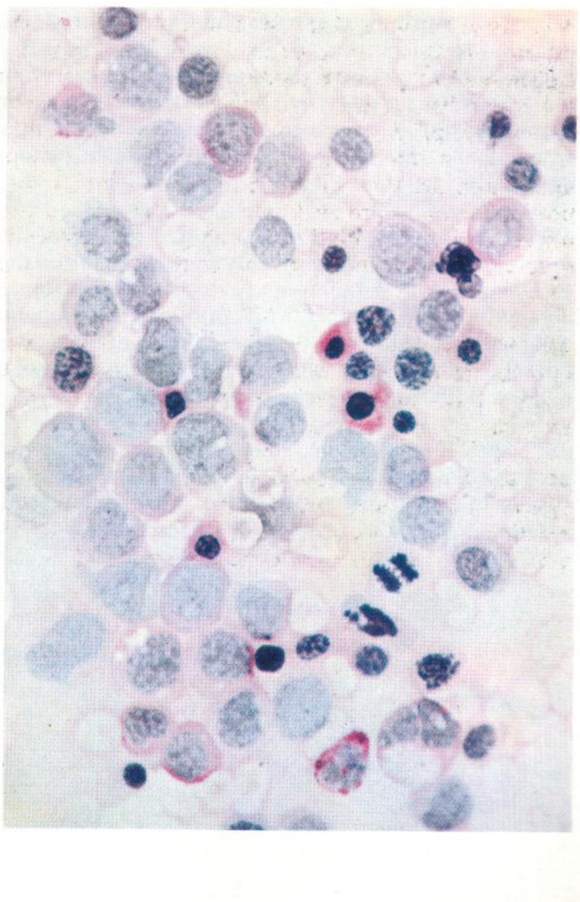

447. An AML with mixed erythroid, granulocytic and monocytic precursors – an erythro-myelo-monocytic leukaemia. Such mixed leukaemias are quite common, an observation which supports the concept of a myeloid stem cell with multiple potentialities. Such a stem cell is presumably the clonogenic leukaemic cell with multilineage expression in cases like this one, where the granulocyte and monocyte involvement is accompanied by erythroid and/or megakaryocytic neoplastic cells – demonstrable, by cytogenetic or biochemical techniques, as being of the same clonal origin. All multilineage cases are more sensibly grouped together as Type II AML (IIA with >50% SB positive blasts and IIB with less) rather than scattered among a wide range of FAB groups, M1, M2, M4, M5a or b, M6 or M7, according to precise differential counts.

448. The SB reaction helps to differentiate the negative pro-erythroblasts from the myeloblasts with dense localized positivity and the monoblasts with scattered granules.

449. A general view of a bone marrow smear from the same case as shown in the previous figures, stained by the PAS reaction. The diffuse and finely granular positivity of granulocyte precursors, increasing in intensity with increasing maturity, is shown; the strong positive reaction in some erythroblasts is very characteristic of erythraemic involvement in a mixed leukaemic process.

450

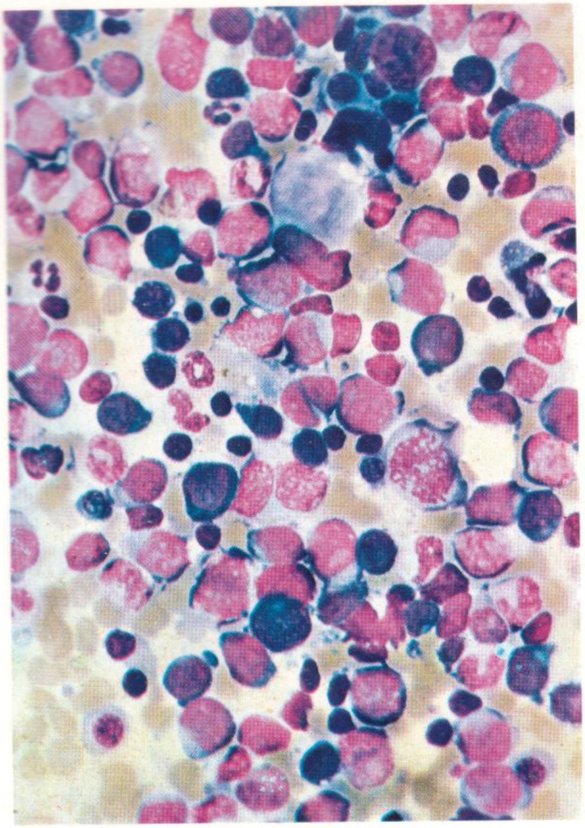

451

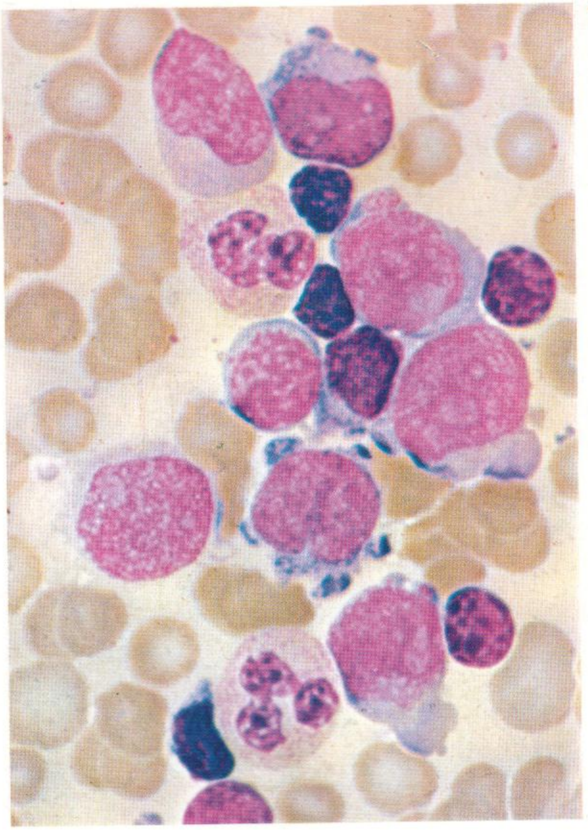

452

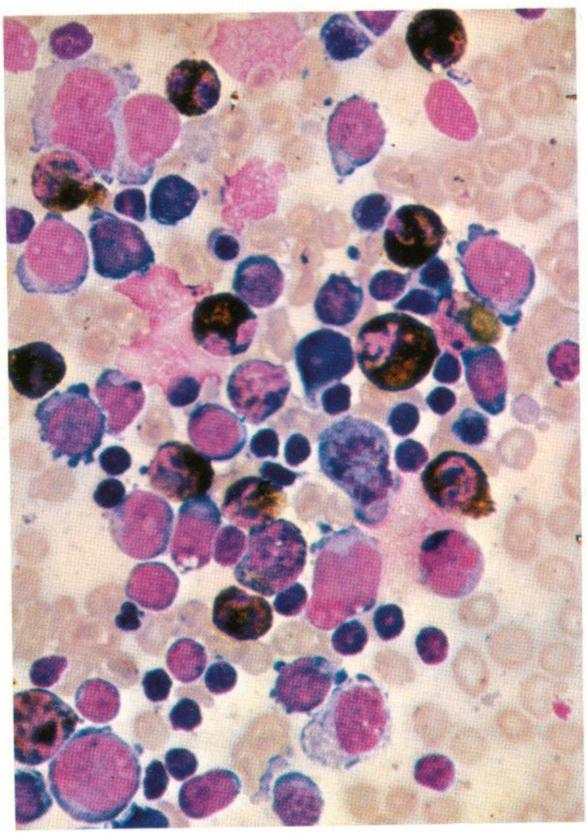

450. AML, with mixed proliferation of erythroid and granulocyte precursors – an 'erythromyeloid' leukaemia. Most cases of erythraemic myelosis have from the earliest stages some component of granulocytic or monocytic cell-line involvement, which, though it may be minimal at first, often comes to dominate the picture eventually.

451. A higher-power view of primitive cells from the same case; they are not altogether easy to classify on the Romanowsky preparations and cytochemical assistance is required. The blast cell with conspicuous peripheral cytoplasmic budding just below the centre of the field is probably a megakaryocyte precursor, thus suggesting additional lineage involvement in this case.

452. The SB reaction on a smear from the same case of erythroleukaemia as shown in the last two figures. Erythroid precursors are negative, while granulocyte precursors show typical coarse localized positivity.

453

454

453. PAS reaction in the same case. Strong positivity in red-cell precursors at different stages of maturity is conspicuous, while myeloblasts and promyelocytes show their customary negative reactions or faint diffuse tinge of the cytoplasm. At upper mid-left is another budding cell with PAS-positive fragments, again suggesting megakaryocyte line involvement.

454. Acid phosphatase reaction in mixed erythromyeloid leukaemia. Coarse positivity, especially paranuclear, in all cells present.

455. Dual esterase reaction in the same case. An early granulocyte precursor shows CE positivity and the erythroblasts have fine granular positivity of mixed BE and CE type.

455

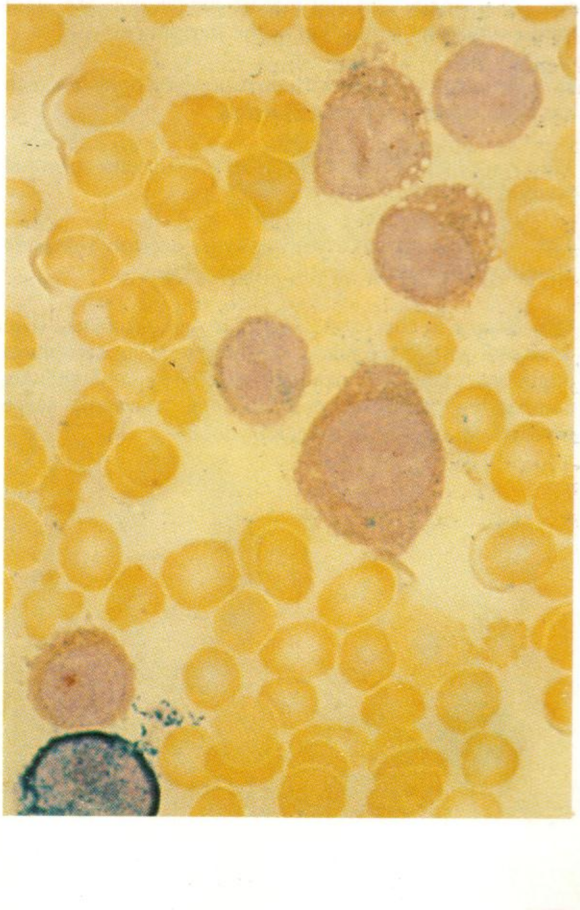

456

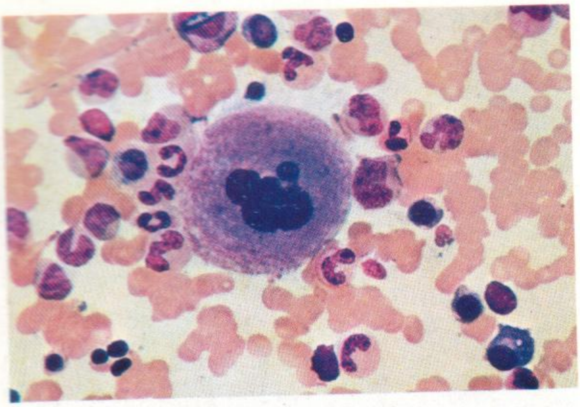

457

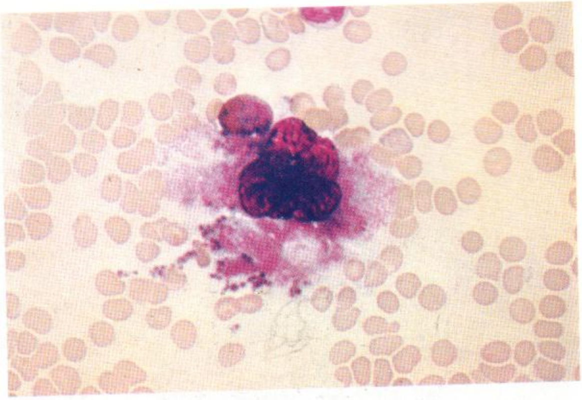

458

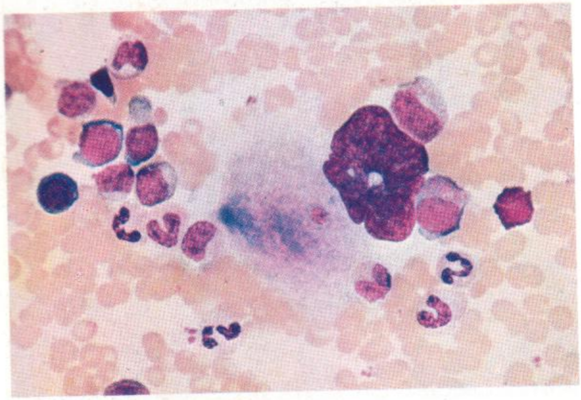

459

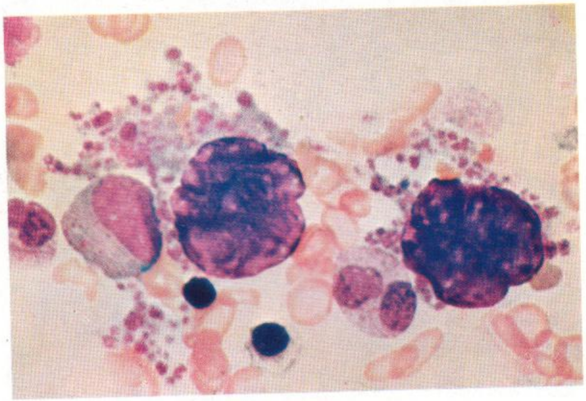

460

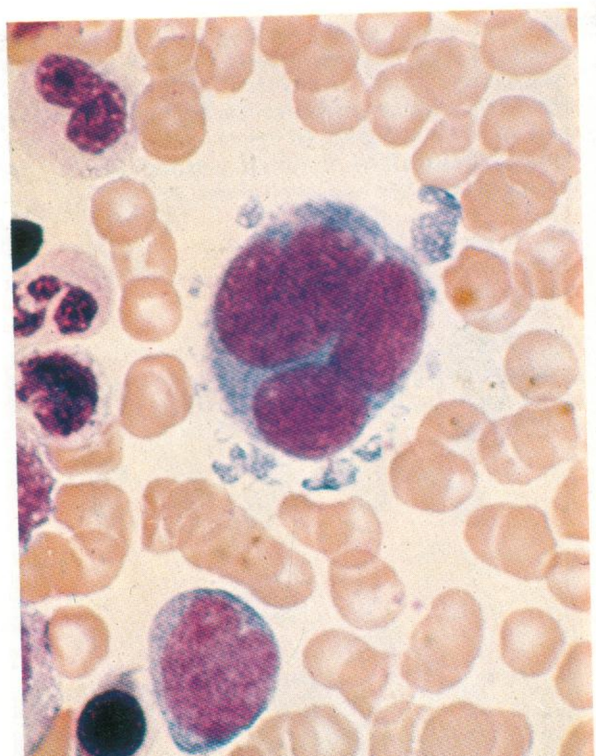

456. A normally granular mature megakaryocyte, with minimal platelet formation at the periphery.

457. A megakaryocyte with disrupting cytoplasm which has been actively forming platelets.

458. A poorly granular megakaryocyte with minimal platelet formation.

459. A pair of megakaryocytes, very actively releasing platelets, and almost devoid of cytoplasm.

460. Stages in the formation of megakaryocytes. The large cell with three nuclei and fragmenting cytoplasm might be called a 'promegakaryocyte', and the accompanying primitive cell, like an unusually large myeloblast, may be a 'megakaryoblast'.

461

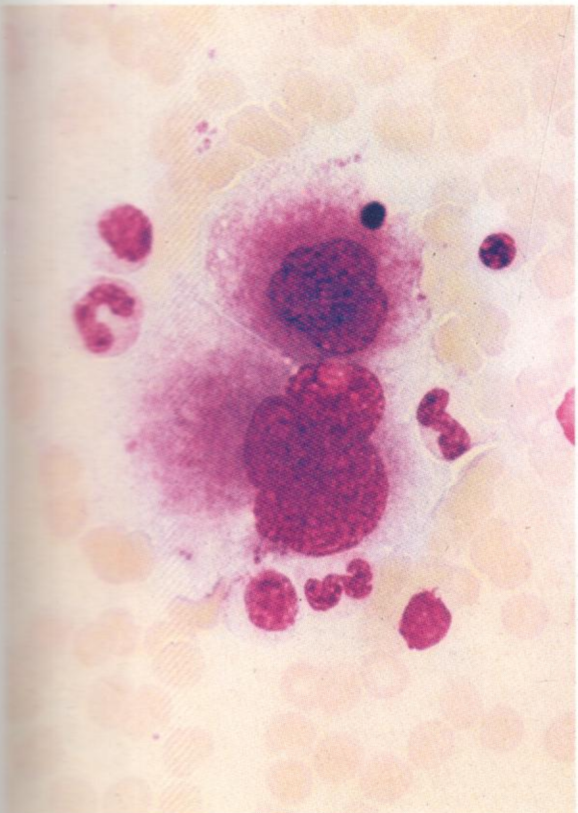

462

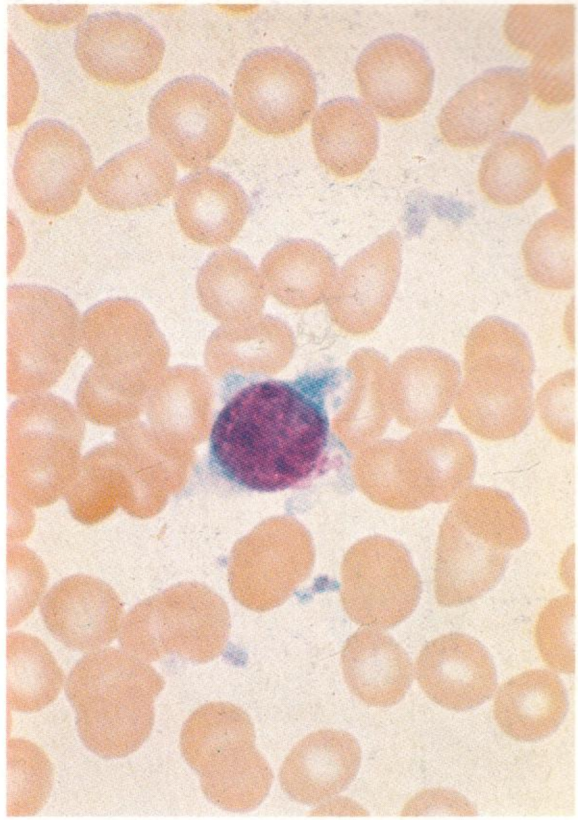

463

461. Mature megakaryocytes with strong granularity of their cytoplasm.

462. A megakaryocyte fragment in the peripheral blood (from blastic crisis in CML). This may represent a mononuclear precursor, of the megakaryoblast or promegakaryocyte stage, since there is commonly a component of the megakaryocyte line involved in blastic crisis of CML and the nuclear pattern of this cell looks primitive, but the presence of a few platelets on the right suggests greater maturity.

463. A giant platelet of snake-like form, beside various red-cell precursors in the bone marrow of a patient with iron-deficiency anaemia.

464

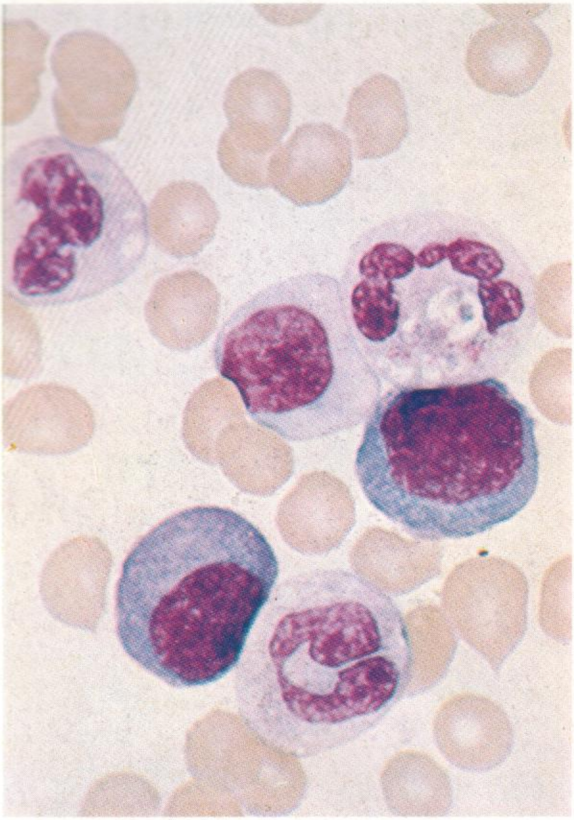

465

466

464. Phagocytosis of platelets by neutrophil polymorphs in an auto-immune disorder with circulating immunoblasts, two of which are seen in this field.

465. PAS reaction in a normal megakaryocyte. Diffuse cytoplasmic positivity, weak in intensity, is accompanied by occasional strongly positive glycogen inclusion bodies.

466. When platelet formation is active or imminent, a peripheral rim of denser positivity may also be observed. In this low-power view of normal marrow, the megakaryocyte is surrounded by other marrow cells which show the increasing positivity with greater maturity in the granulocyte series. Erythroid precursors are negative.

467

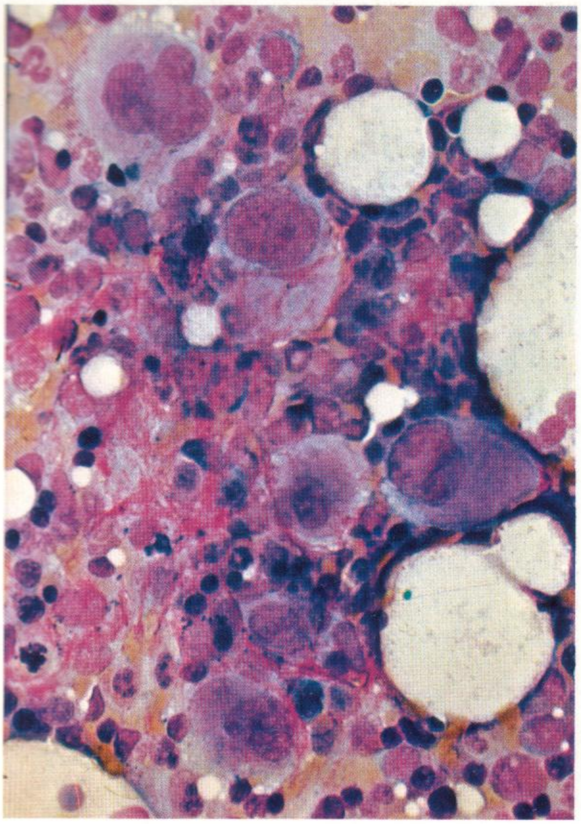

468

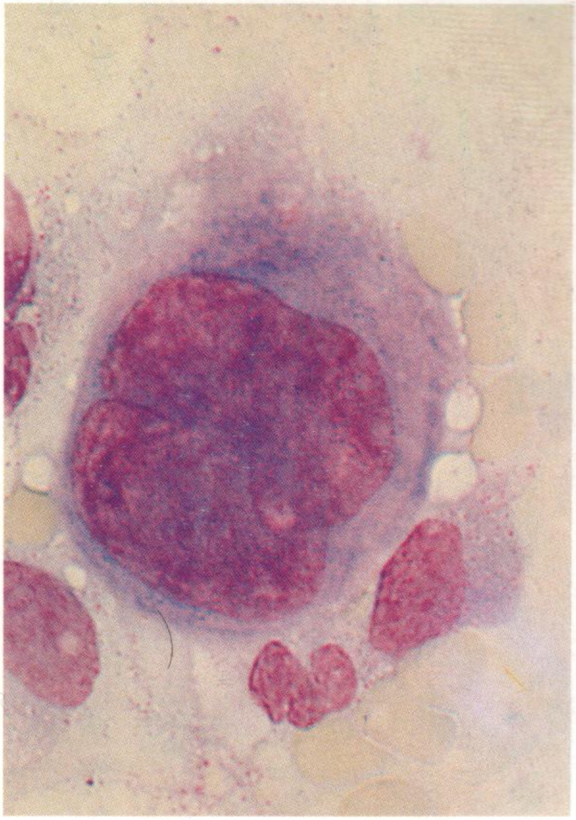

469

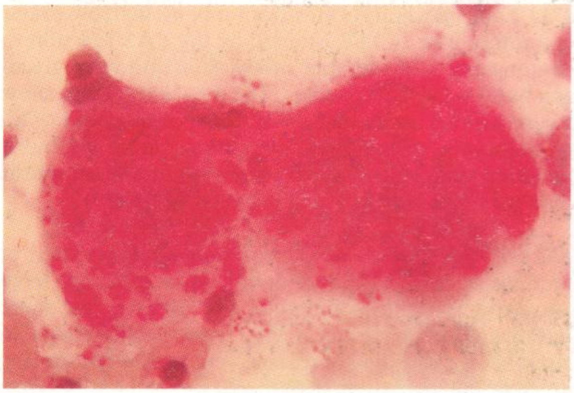

470

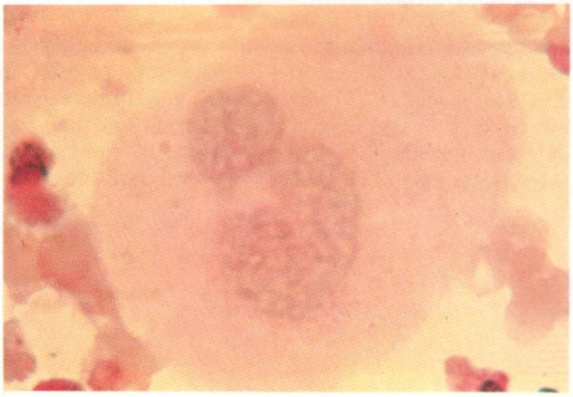

467. Numerous megakaryocytes without peripheral platelets from the marrow of a patient with chronic idiopathic thrombocytopenic purpura (ITP).

468. An immature megakaryocyte from another patient with auto-immune ITP, showing two large nuclear lobes and minimal cytoplasmic granularity or platelet accumulation at the cytoplasmic rim.

469. PAS reaction; megakaryocytes from another patient with chronic ITP show the intense accumulation of glycogen inclusion bodies sometimes seen in this disorder.

470. A megakaryocyte from the same patient as in **469** but after spenectomy (with good response), to show the disappearance of glycogen inclusion bodies in the PAS stain.

471

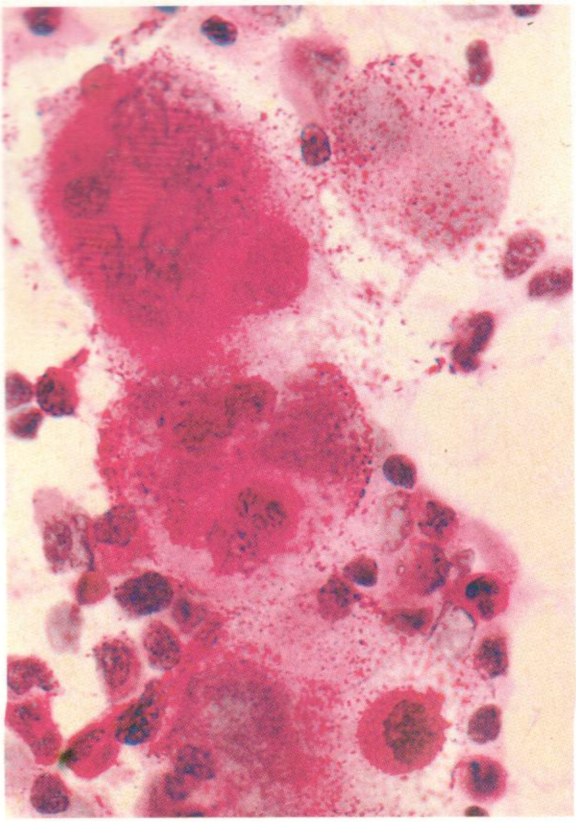

472

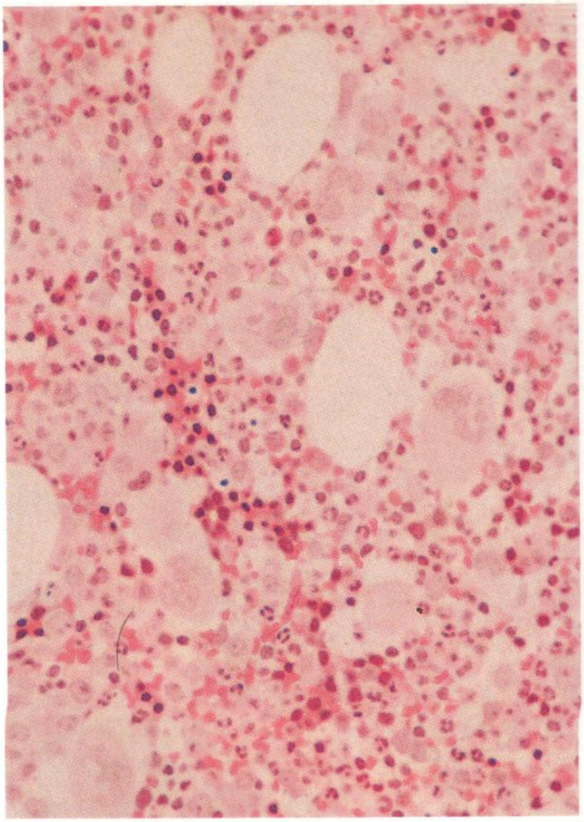

473

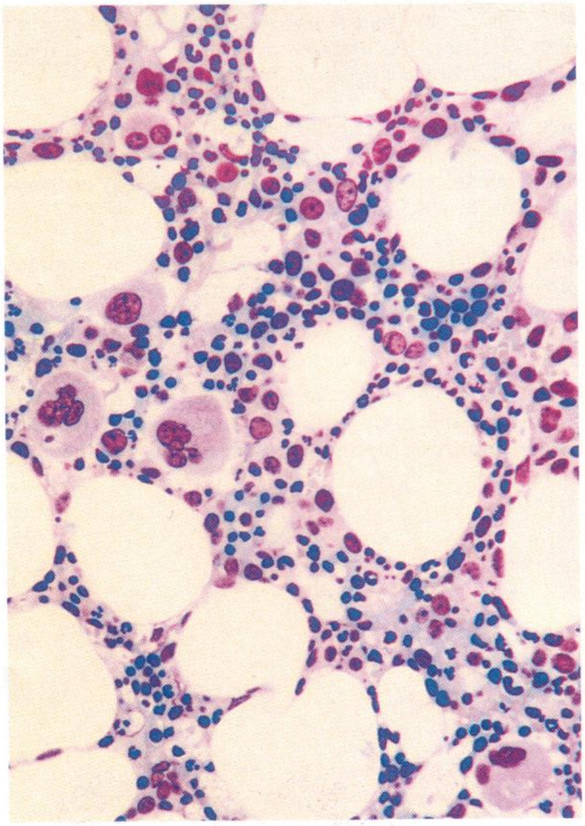

471. Four megakaryocytes from a bone marrow smear in another case of ITP, stained by the PAS reaction to demonstrate considerable cytoplasmic granular glycogen but few inclusion bodies. The megakaryocytes show a very striking accumulation of PAS-positive neutrophil granulocytes within their cytoplasm, more probably resulting from a passive incorporation or emperipolesis than an active phagocytic process (cf. **477–479**).

472 and **473**. H&E and Giemsa stains, respectively, of sections of bone marrow trephine biopsies taken from two patients with auto-immune ITP. In each case there has been sufficient blood loss from haemorrhage to stimulate erythroid hyperplasia – but without producing any marked increase in overall marrow cellularity, since fat spaces are plentiful. Megakaryocytosis is clearly evident with generally somewhat primitive, defectively lobulated nuclei and poorly granular cytoplasm in most megakaryocytes. The absence of peripheral platelets in megakaryocytes in ITP reflects their rapid release into the circulation and destruction there, rather than any defect in production, for the output of functionally active platelets in ITP is usually several times normal.

474

475

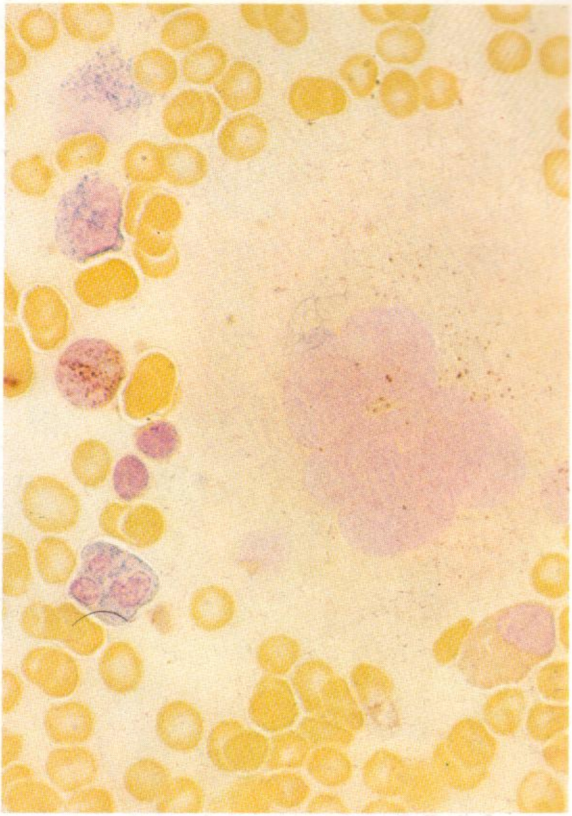

476

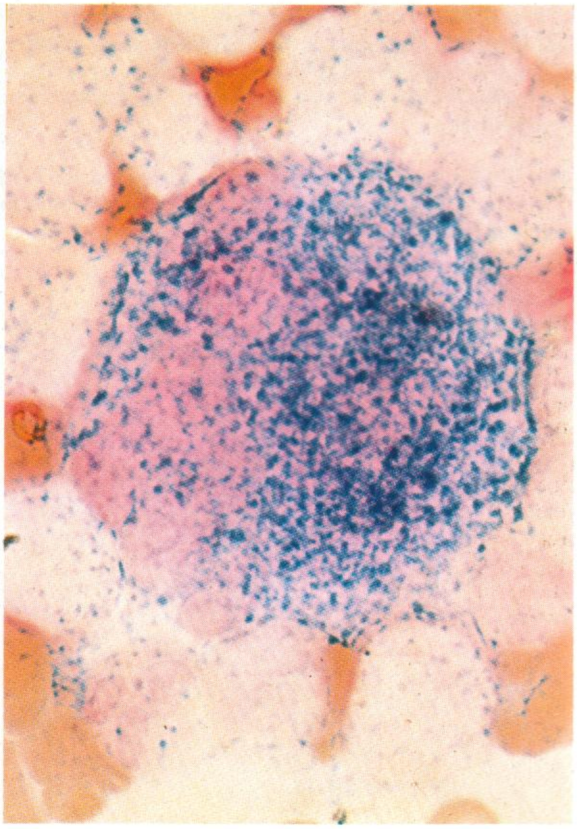

474. Acid phosphatase reaction, showing coarse granular scattered positivity in a megakaryocyte; two myelocytes show a few granules, as does a late normoblast, and a lymphocyte is negative.

475. Dual esterase reaction showing weak granular BE positivity in a megakaryocyte: three granulocytes show CE positivity, a monocyte is BE-positive, and two lymphocytes are negative.

476. α-Naphthyl acetate esterase (AE) reaction in a megakaryocyte – the positivity is much stronger and denser than with butyrate as substrate, a characteristic feature of megakaryocytes.

477

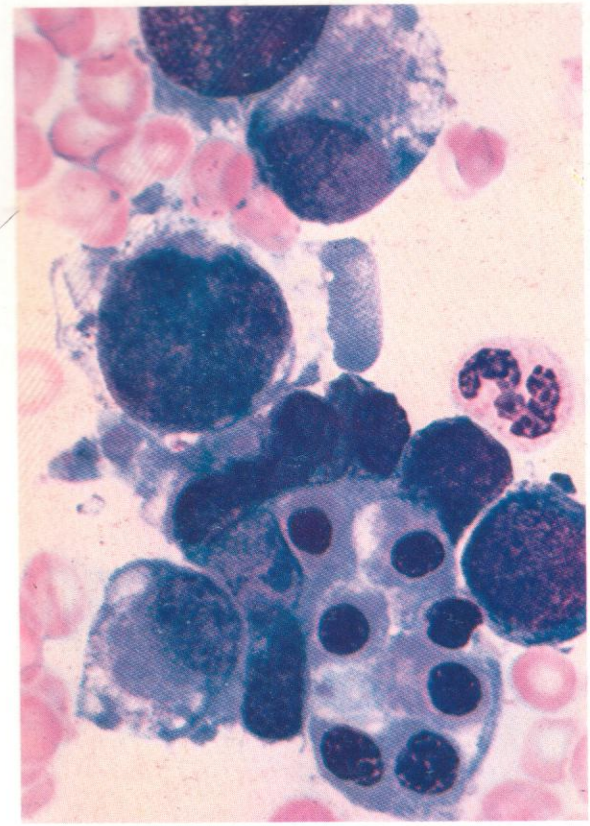

478

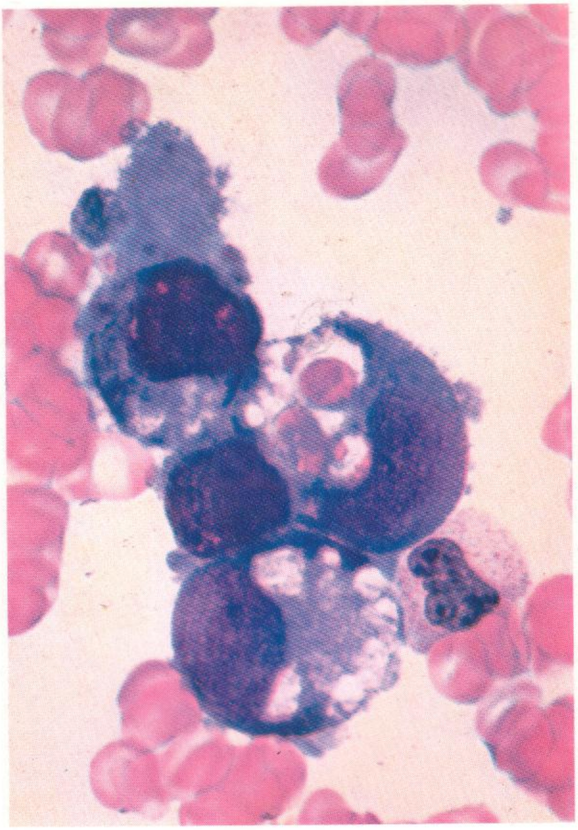

479

477 and **478**. Gross phagocytosis of an erythroblast clump by one megakaryocyte and phagocytosis of other cellular debris and red cells by other megakaryocytes in a myeloproliferative disorder with megakaryocytic hyperplasia.

479. PAS stain in the same case, showing coarse PAS positivity in two megakaryocytes, each of which contains ingested leucocytes.

480

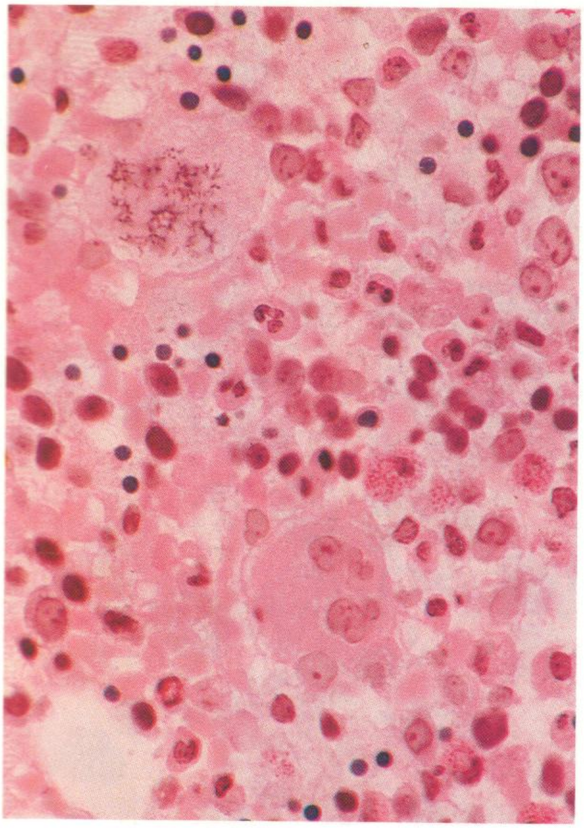

481

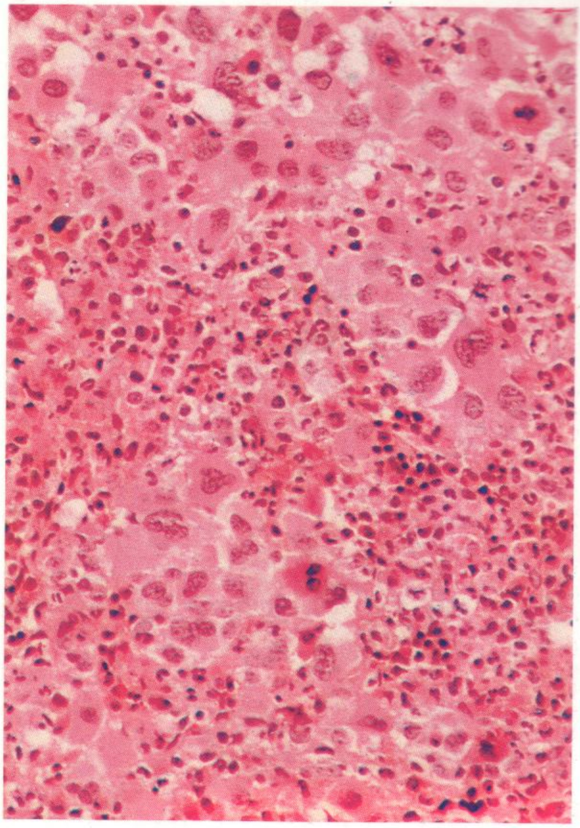

482

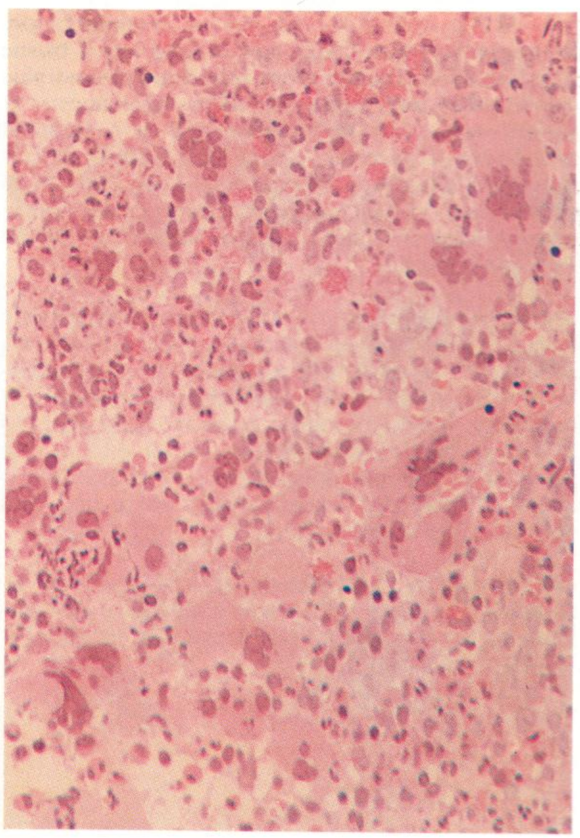

480–482. Thin sections of bone marrow trephine biopsies from three different examples of megakaryocytic hyperplasia. In **480** the background condition is hairy cell leukaemia (HCL) with a secondary infection producing only minimal neutrophil leucocytosis (reflecting the severe neutropenia common in HCL), but an attempt at megakaryocyte proliferation which resulted in some platelet increase. There are no more than a few recognizable HCs present, but there are two large megakaryocytes – the lower with several separated nuclei and the upper in polyploid mitosis with three or perhaps four separate spindles.

Gross hyperplasia involving both granulocytic and megakaryocytic lines is visible in **481**, with disappearance of fat spaces and an almost complete absence of erythroblasts. The small cells with deeply stained and often lobulated nuclei are neutrophil polymorphs; the large pale-staining cells are all megakaryocytes at various stages of maturity, most with poorly lobulated nuclei, the few with densely stained nuclear material being in various stages of mitosis. This is another example of CML with megakaryocytosis, many of these cells being classifiable as micromegakaryocytes.

The third example, **482**, is from a patient with a chronic myeloproliferative disease (CMPD) associated with a high platelet count ($>1000\times10^9/1$) and numerous mature, sometimes almost gigantic, megakaryocytes with multiple nuclear lobes and ample cytoplasm present in the bone marrow. This disorder is variously called 'essential thrombocythemia' or 'megakaryocytic myelosis' of mature cell type.

483

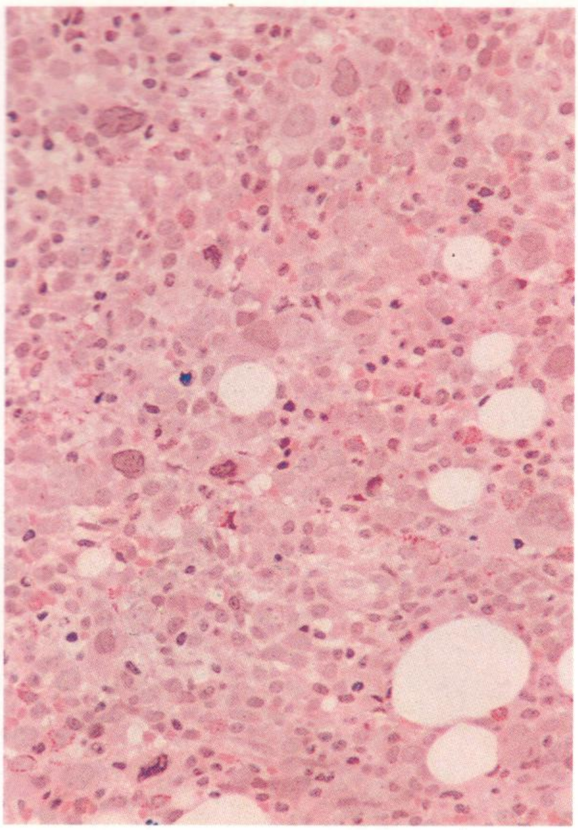

484

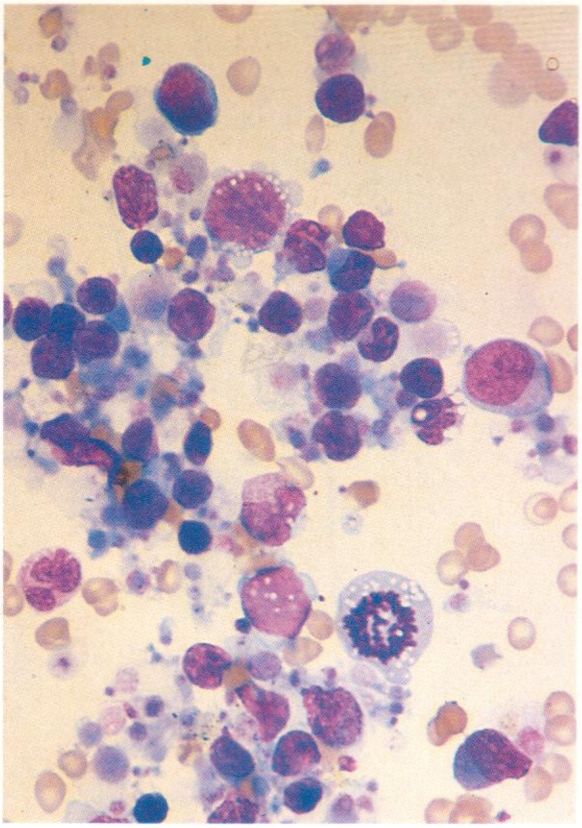

483. A thin section of bone marrow trephine biopsy from a patient with CML, now moving into a blastic transformation. There is a very mixed and pleomorphic cytological picture, with erythroblasts, granulocytes at various stages of maturation, and a substantial component of primitive-looking cells with leptochromatic and sometimes nucleolated nuclei, shown by cytochemistry and immunology of their counterparts in marrow smears (cf. **487**) to be immature cells of the megakaryocyte line.

484. Numerous megakaryocyte fragments and probable megakaryocyte precursors in the peripheral blood of a patient with an AML with megakaryocytic preponderance – the terms acute megakaryocytic myelosis or megakaryoblastic leukaemia may be applied. Large and fully developed megakaryocytes are not present, but these are multiple megakaryocyte fragments or abnormal small cells of that series, where the usual polyploidy has not occurred.

485. A further field from acute megakaryocytic myelosis. The nucleolated primitive cells have a similarity to myeloblasts, but may be 'leukaemic' megakaryoblasts.

485

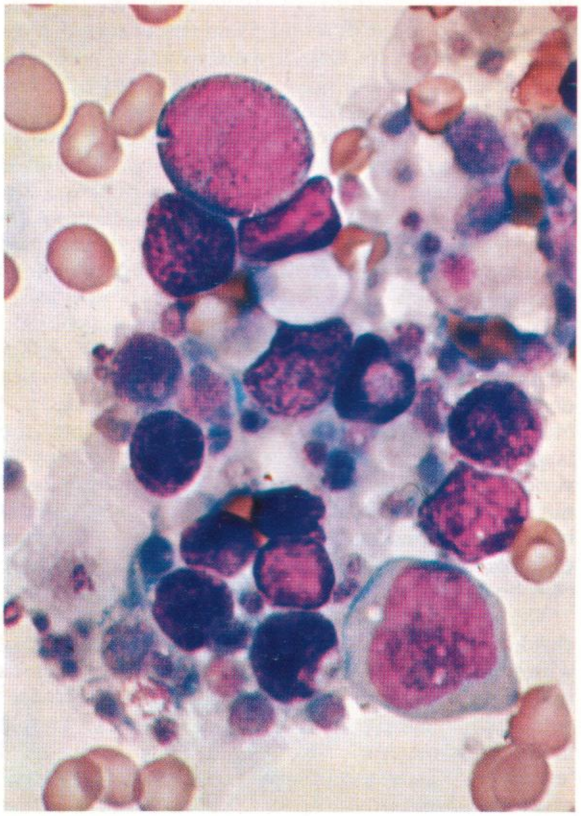

486. SB reaction in the same case. A megakaryocyte with three phagocytosed lymphocytes or erythroblasts is negative, as is the neighbouring megakaryoblast.

487. PAS reaction in acute megakaryocytic myelosis. The strong and coarse irregular positivity in the 'leukaemic' megakaryocytic cells resembles that in platelets. The diffuse tinge in certain precursors does not allow a clear distinction from myeloblasts to be made.

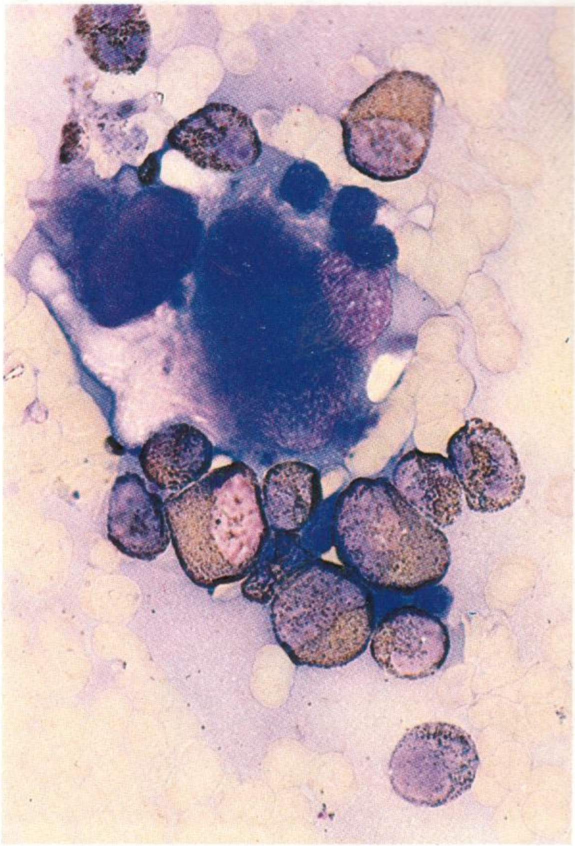

486

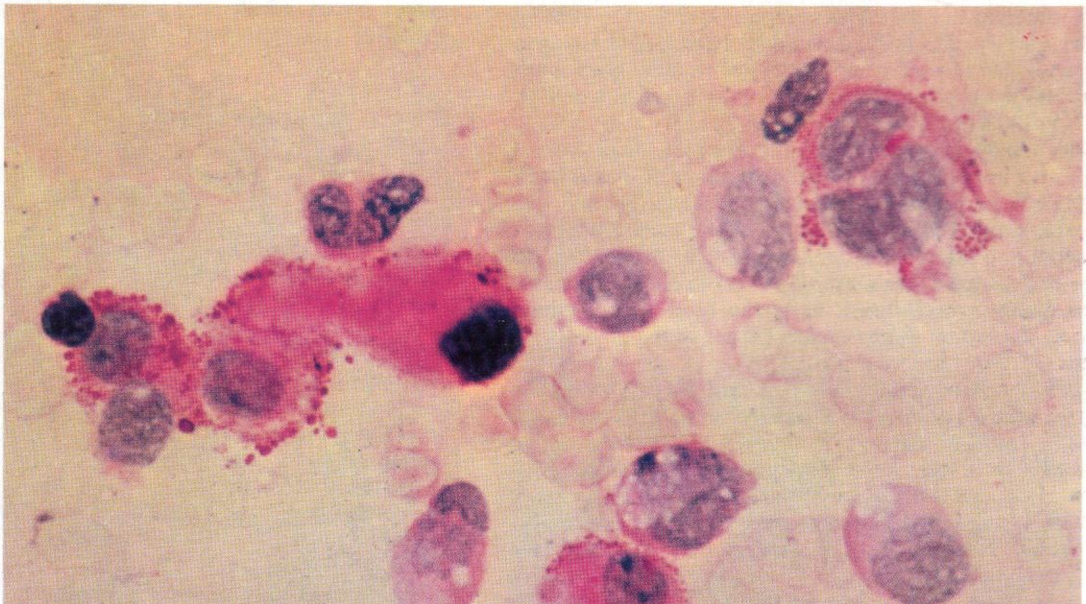

487

488

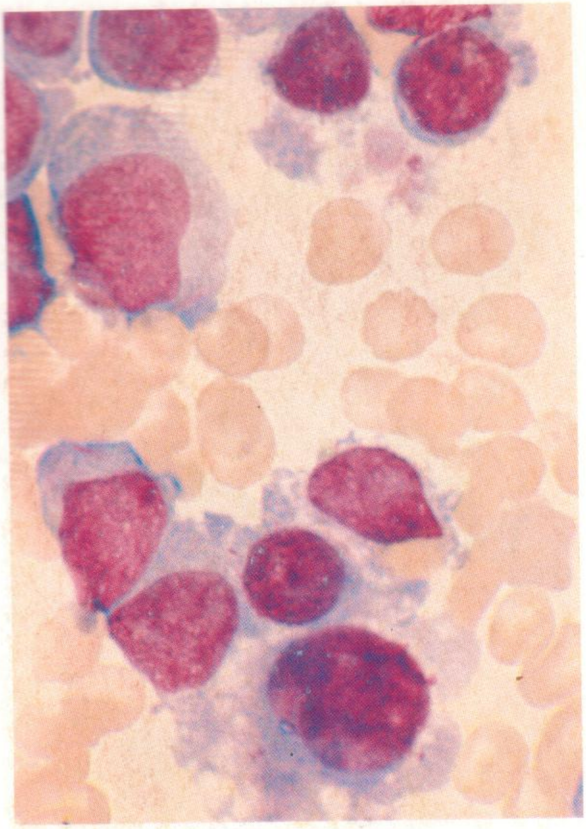

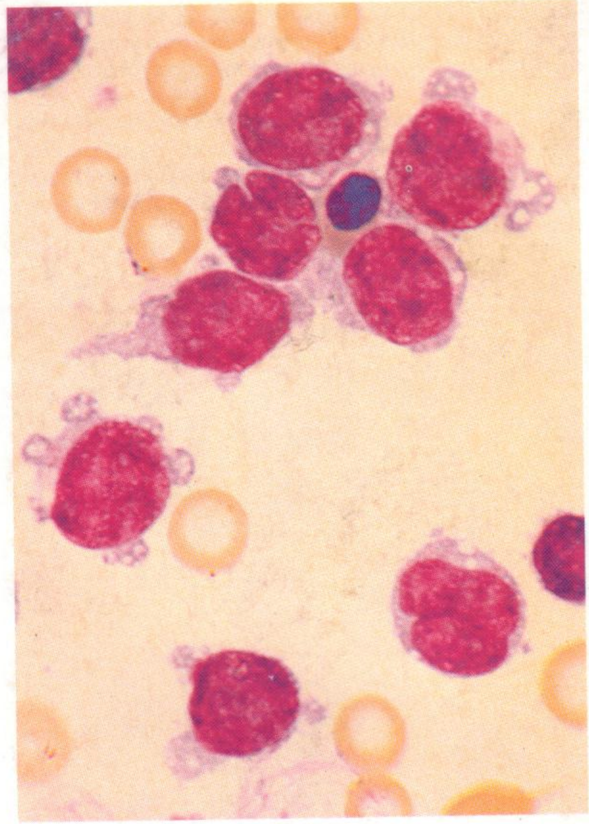

489

488–495. *Examples of the cytology and cytochemistry of multilineage (Type II) AML with chromosome abnormalities involving inversion or insertion 3;3.*

These chromosome changes are associated with an increase in megakaryoblasts and later megakaryocyte stages in the marrow, together usually with both erythroblastic and granulocytic/monocytic involvement.

488. High-power view of bone marrow smear from a case of inv(3;3), showing predominance of megakaryoblasts and promegakaryocytes, with cytoplasmic disruption in some cells and, at the upper part of the field, formation of several giant platelets. The blast at the top left of the lower cell clump contains an Auer rod, and is probably a myeloblast, as is the blast with minimal cytoplasm near the upper left corner of the field.

489. Another example of AML with inv(3;3), showing the very characteristic cytology of megakaryoblasts, with frequently irregular cytoplasmic outlines and a tendency to form buds which often contain vacuoles.

490. Although these cells are negative to myeloperoxidase staining, they do possess platelet peroxidase (PPO), best demonstrated by electron microscopy. This enzyme activity is confined to the endoplasmic reticulum and perinuclear space, as illustrated here.

490

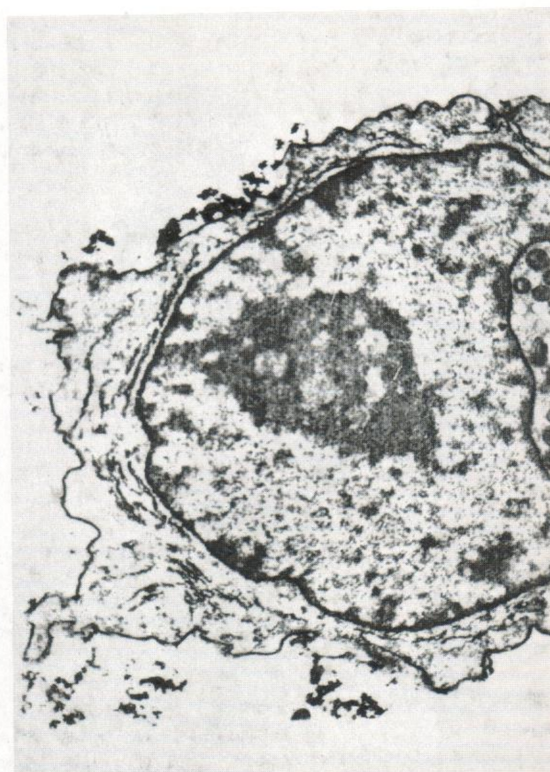

491

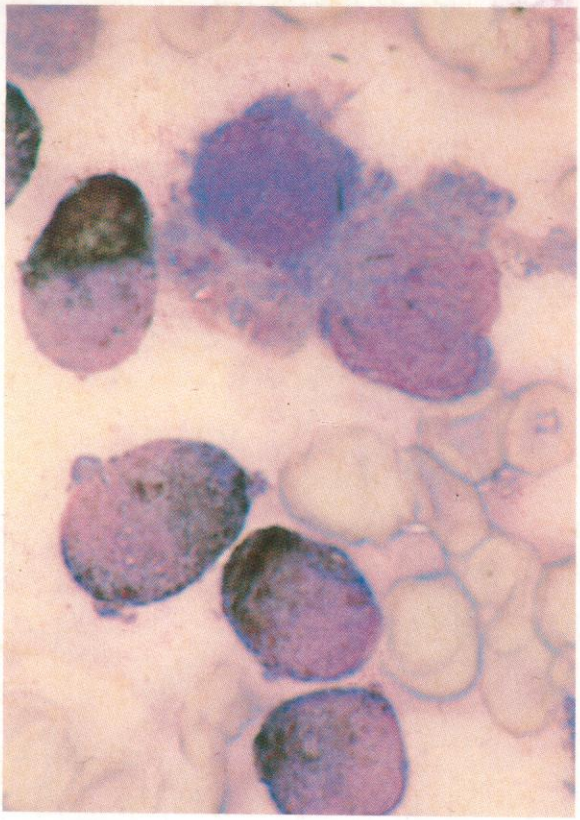

492

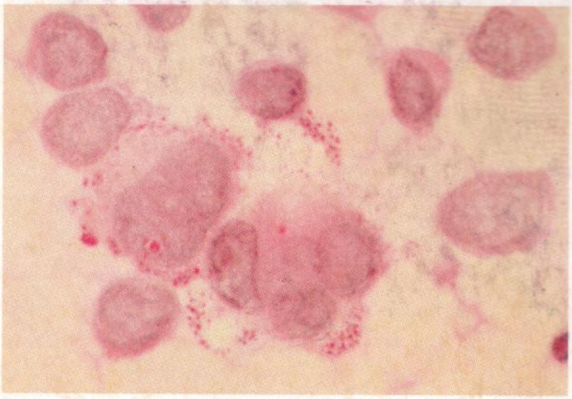

493

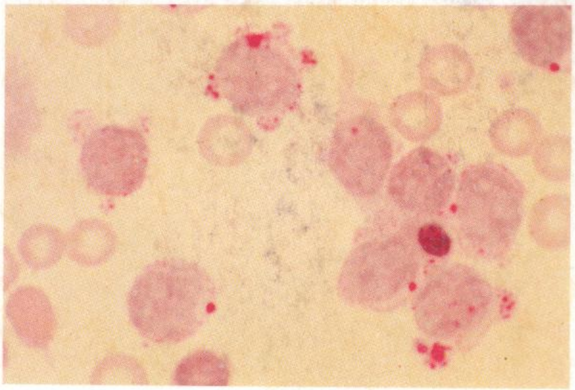

494

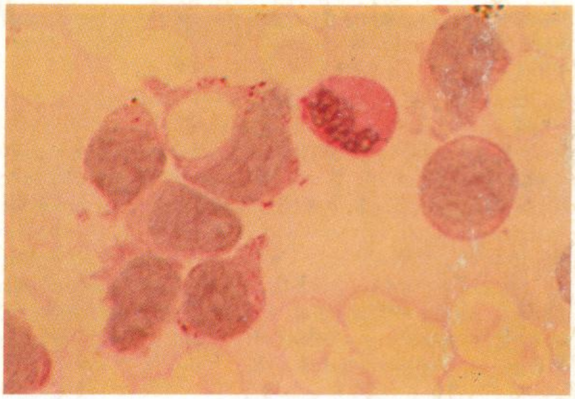

495

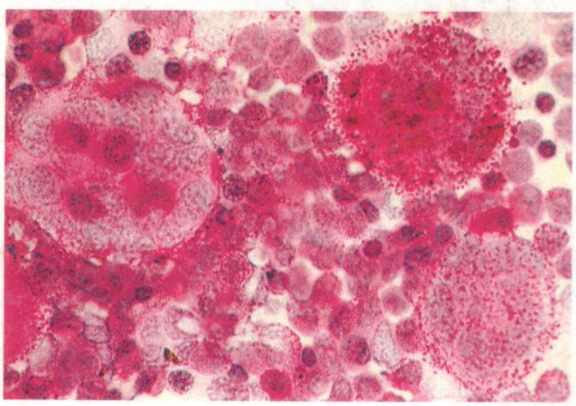

491. SB stain on the same specimen as in **488**, showing granulocyte-type positivity in several myeloblasts and negative reactions in two megakaryoblasts, except for a strongly positive Auer rod in the upper megakaryoblast and several possible but more weakly sudanophilic Auer rods in the lower one, probably resulting from phagocytosis.

492. PAS reaction on the same bone marrow as in **488** and **491**, showing mixture of granulocytic and megakaryocytic patterns of positivity.

493. PAS reaction on the same bone marrow as in **489**, where all the blast cells in the field are megakaryoblasts with coarse granular positivity, especially in the peripheral evaginations.

494. A further example of PAS staining in a case of ins(3;3), with a group of megakaryoblasts to the left, together with a pair of probable monoblasts to the right. Between the two groups is a late neutrophil with maturely condensed nuclear chromatin but an unsegmented nucleus, possibly a normal stab cell but perhaps exemplifying the pseudo-Pelger phenomenon often encountered in these cases.

495. A PAS reaction on clumped cells from another case of ins(3;3), to show both multinuclearity and gross phagocytic activity of some megakaryocytes in this form of AML. There are also several groups of PAS-positive erythroblasts present in this field.

496

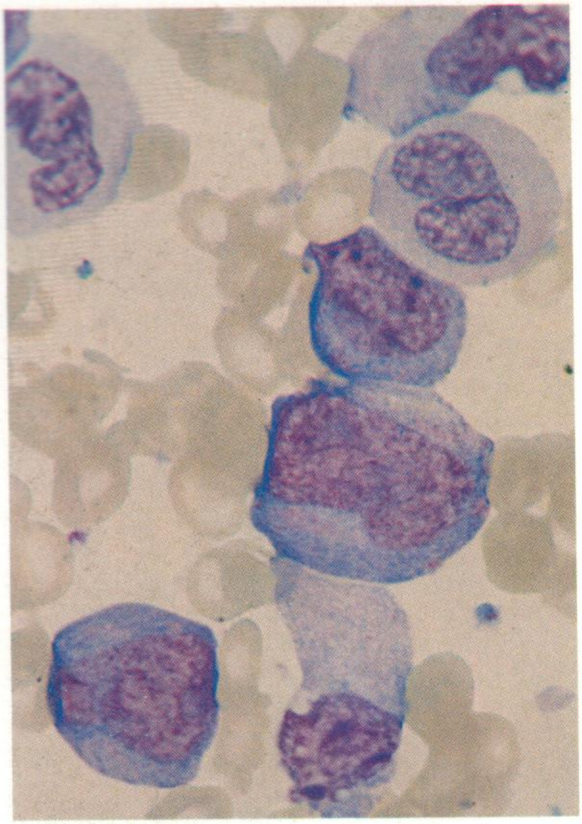

497

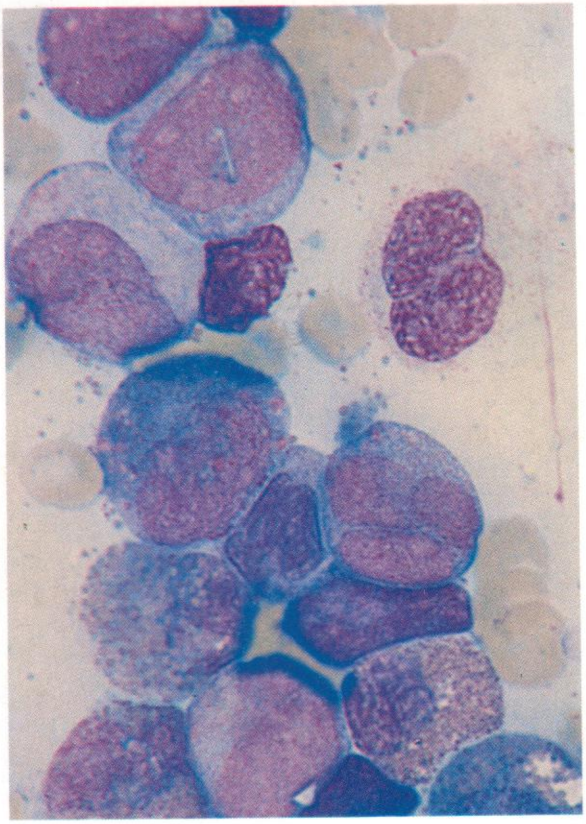

498

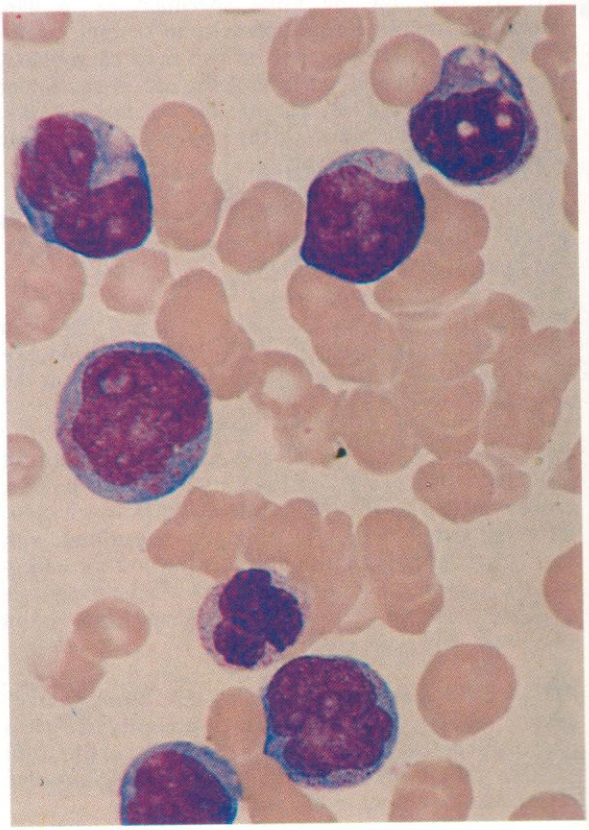

496–502. *Examples of the cytology and cytochemistry of AML with trisomy 8.*

Trisomy 8 is the commonest chromosomal abnormality found in AML, and often co-exists with other cytogenetic aberrations, perhaps chiefly as a secondary phenomenon in cases which are usually of multilineage (Type II) expression and which have a generally poor prognosis. When trisomy 8 occurs alone, as it does in about a third of all cases with this abnormality, the cytological picture is predominantly granulocytic with marked evidence of dysplastic maturation. Romanowsky stains of bone marrow smears from three different cases of trisomy 8 appear in **496–498**.

496. Typically variable maturation, with enough granularity in the more primitive cells to indicate their granulocytic rather than monocytoid lineage, but with agranular later neutrophils showing acquired Pelger-Huët nuclei.

497. Myeloblasts, one with an unstained Auer rod overlying the nucleus, defective neutrophil myelocyte granularity, and various eosinophils, some with greenish granules.

498. A more primitive blastic picture, with deep nuclear lobulation in one cell and large pinkish inclusions or vacuoles overlying the nucleus and in the cytoplasm of another. A poorly granular neutrophil polymorph is also present.

499

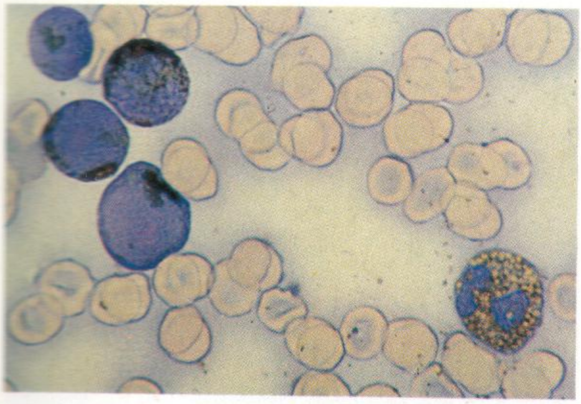

500

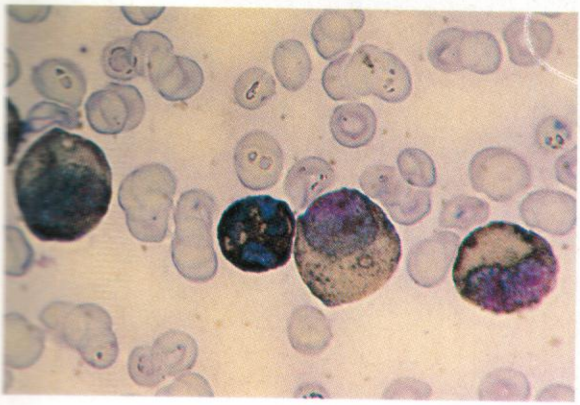

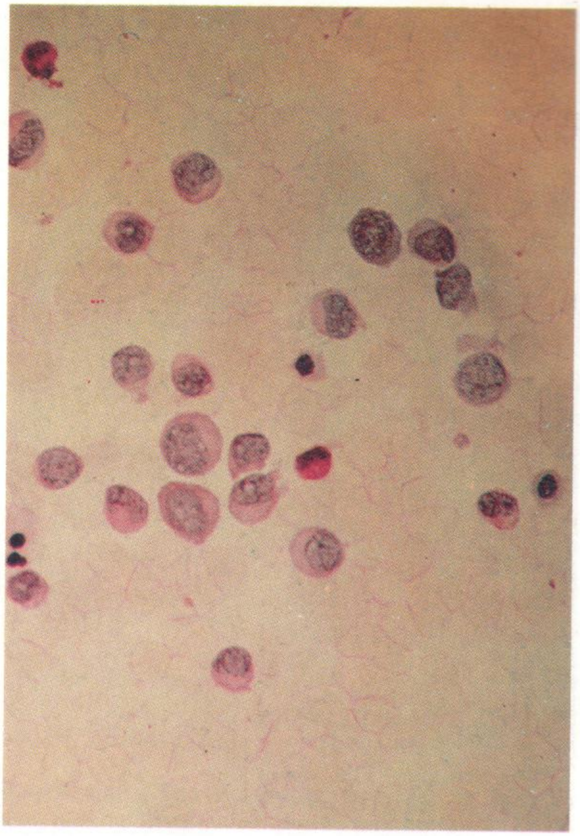

501

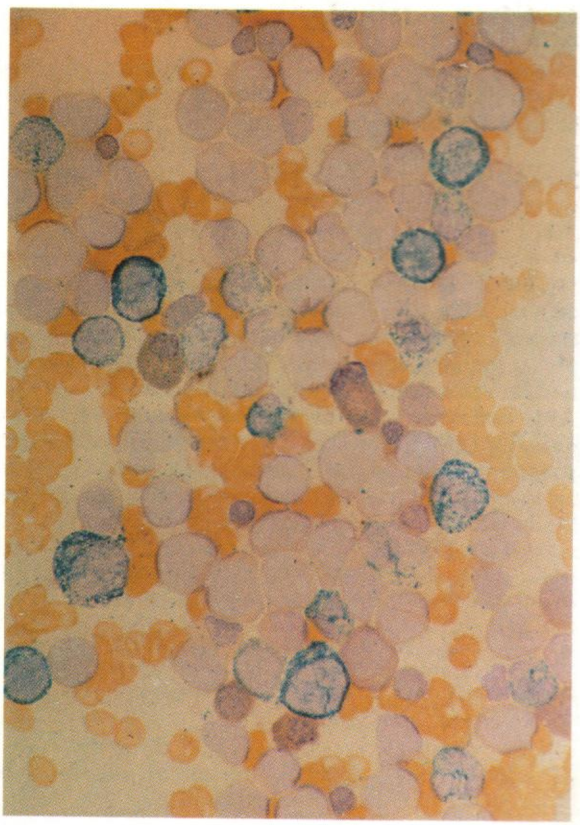

502

499. SB stain on bone marrow smear from the case illustrated in **498**, three primitive blasts showing localized cytoplasmic positivity of myeloblastic pattern – including a dense Auer rod in the lower blast and either hollow Auer rods or other inclusions in the upper cell of this group. The fourth blast cell has an overall granular sudanophilia together with strong localized positivity, more granulocytic than monocytic in pattern. A normally reacting eosinophil is in the lower right corner of the field.

500. SB stain on the bone marrow of another patient with AML and trisomy 8, illustrating the frequent finding in this condition of unexpectedly poor sudanophilia. The central densely positive cell, probably a neutrophil polymorph, shows a strong normal reaction, but the promyelocyte at the left, with an Auer rod, and both the eosinophil and neutrophil myelocytes, are very feebly positive with a greenish-brown rather than black stain.

501. PAS reaction in this form of AML generally has no unusual findings, the blast cells having negative or weak diffuse reactions, as here.

502. The dual esterase reaction shown here illustrates typical findings, with most blast cells negative but CE positivity appearing in later granulocytes from promyelocyte onwards. There is BE positivity in two plasma cells and in several erythroblasts.

503

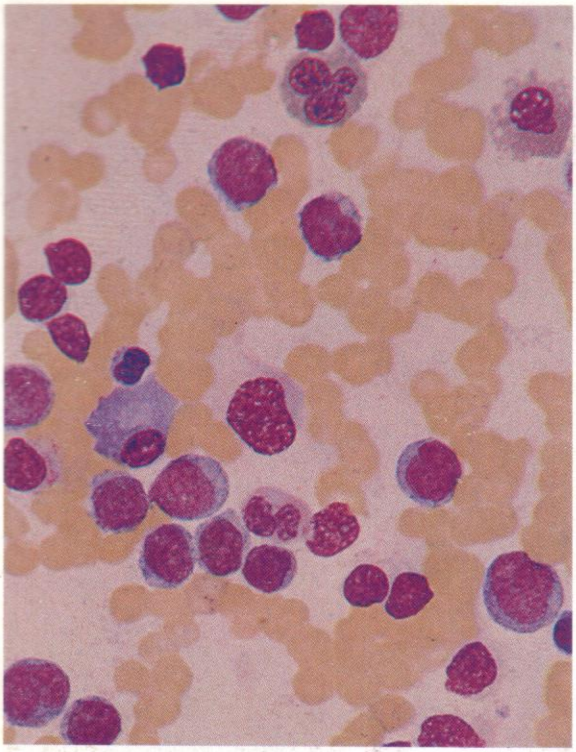

504

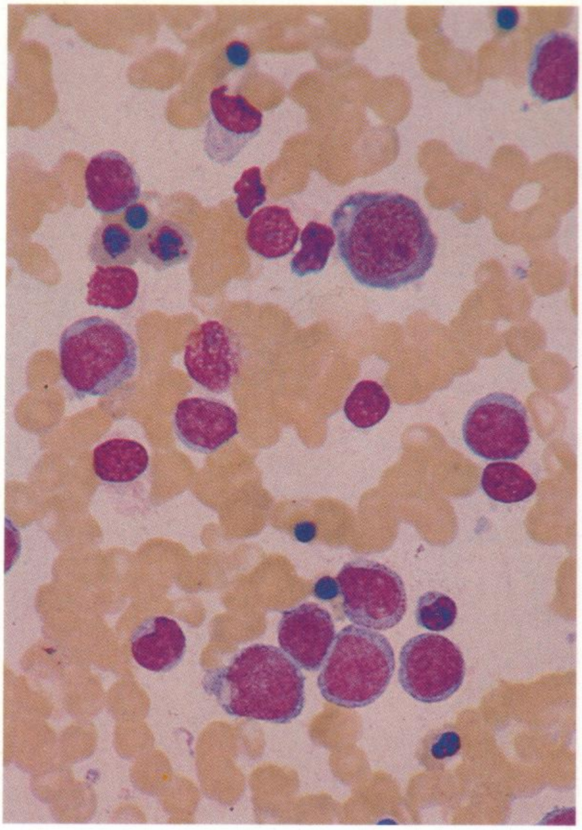

503–520. *Examples of the cytology and cytochemistry of AML associated with an interstitial deletion of the long arm of chromosome 9 between bands q13 to q22, 9q–(q13;q22)(Type IIA).*

Although most cases of 9q– have predominantly myeloblastic cytology, they show evidence of erythroid and megakaryocytic dysplasia.

503 and **504**. Typical low-power fields (Heyl stain), with blasts of variable size, dysplastic erythroblasts and, in **503**, an occasional plasma cell and eosinophil.

505–510. High-power details of the bone marrow cell cytology from several different cases of 9q– AML. In **505** there are two myeloblasts with vacuolar inclusions and a poorly granular stab cell. In **506** a myeloblast showing nuclear convolution resembling that commonly seen in APL is accompanied by two very coarsely granular eosinophils; **507** shows ten myeloblasts, two with Auer rods, and a promyelocyte, **508** an eosinophil promyelocyte with mixed granules, and four myeloblasts, **509** six blasts, one with a bilobed nucleus, another with a twisted monocytoid nucleus, one with primary granules, and one with a vacuole, and **510**, four variably sized blasts with vacuoles or small azurophilic inclusions.

511–513. DAB peroxidase reactions, with positive Auer rods, other coarse inclusions and granular positivity in most blast cells.

514. SB positivity of chunky inclusions, usually with negative cores, in vacuolated myeloblasts.

505

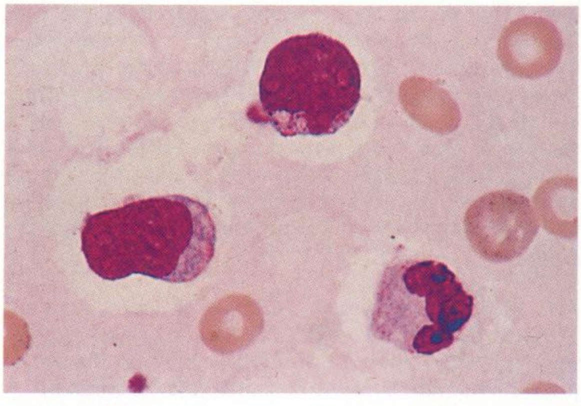

506

507

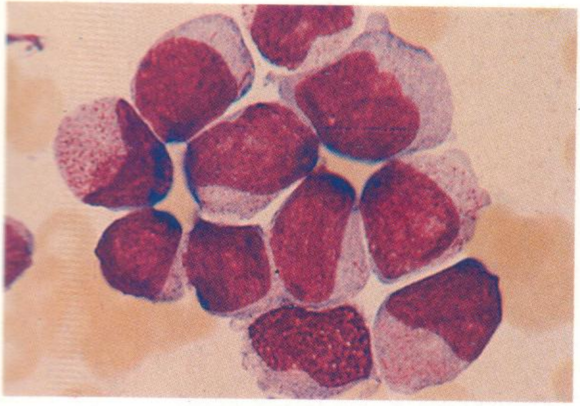

508

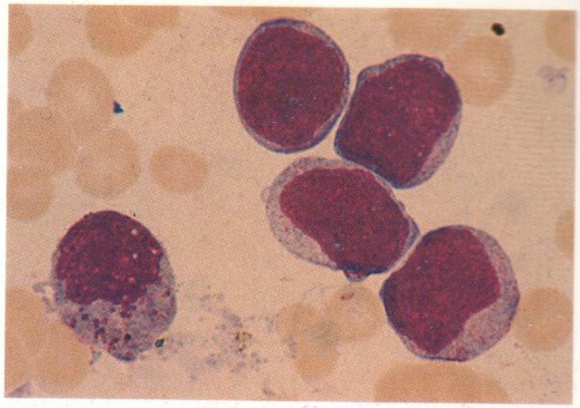

509

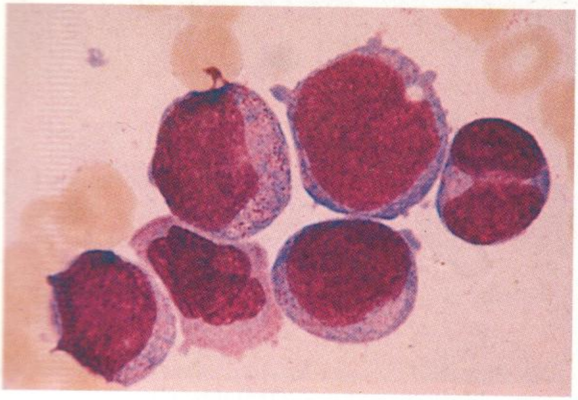

510

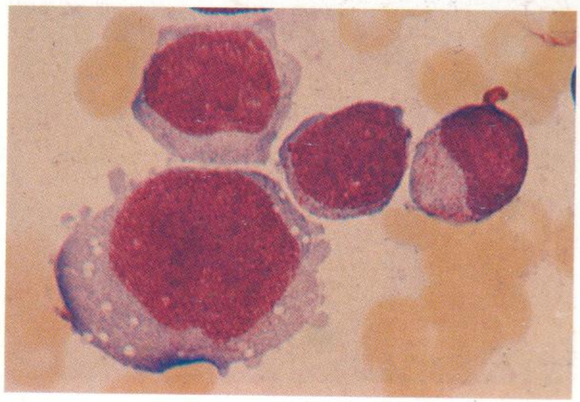

511

512

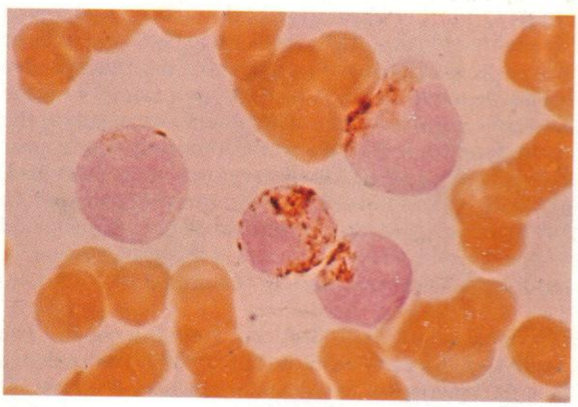

513

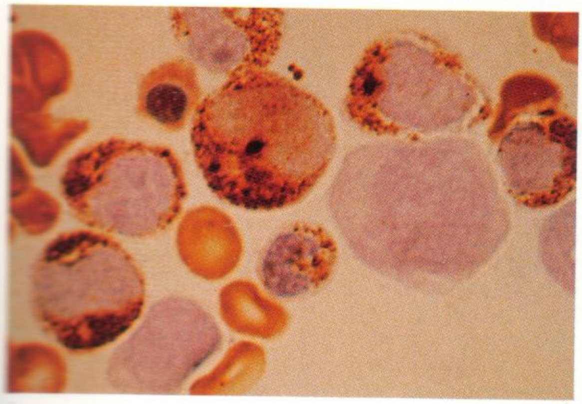

514

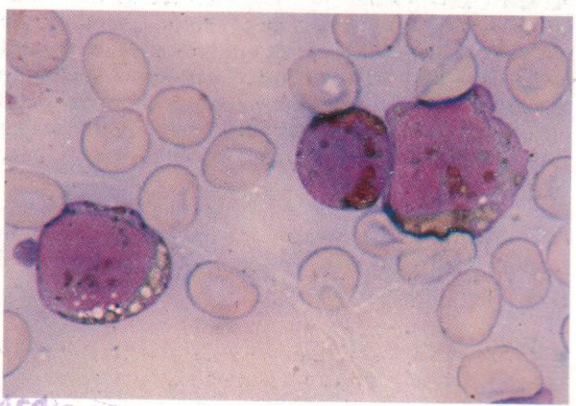

515

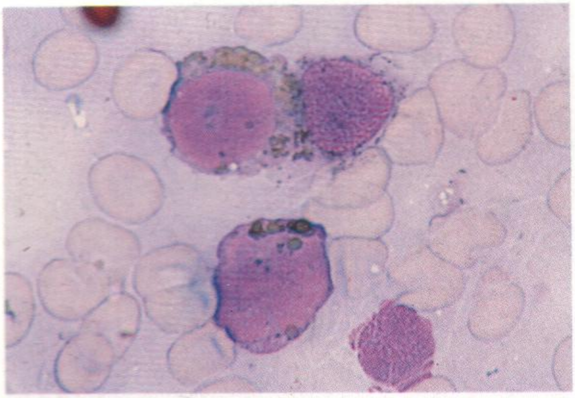

516

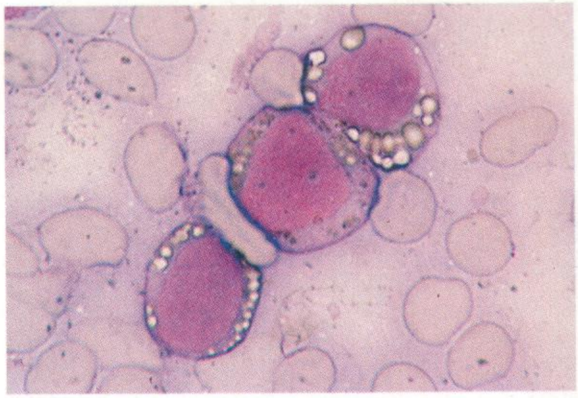

517

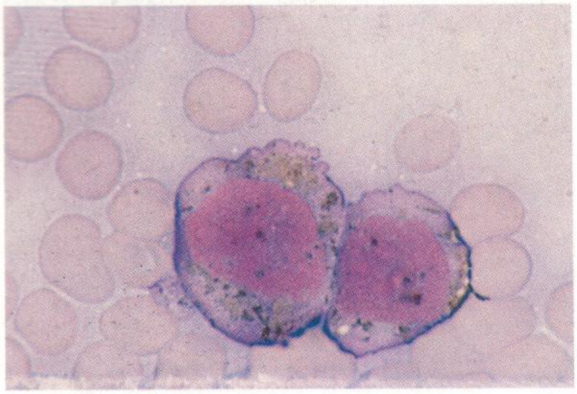

518

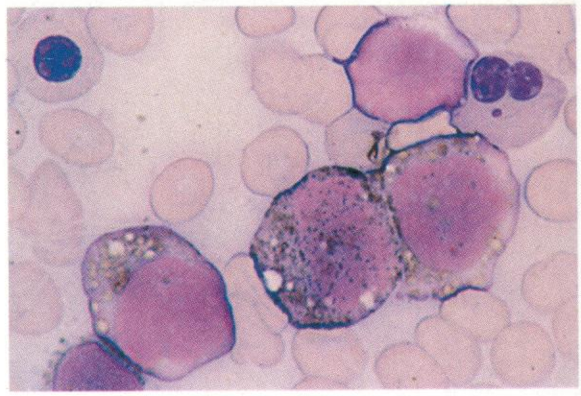

515–518. Further illustration of the striking patterns of SB positivity in 9q– AML, with very coarse granules or inclusions usually showing a positive periphery and a hollow negative centre. Conspicuous vacuoles in some blast cells manifest weak sudanophilia – especially at the circumference, as in **516** – while Auer rods may appear as needle- or spindle-shaped structures, or as short thick rods with either solid or hollow centres (**517** and **518**). In **518** there are also two erythroblasts, one binucleated with a Howell-Jolly body, and with a suggestion of residual megaloblastic nuclear features.

519

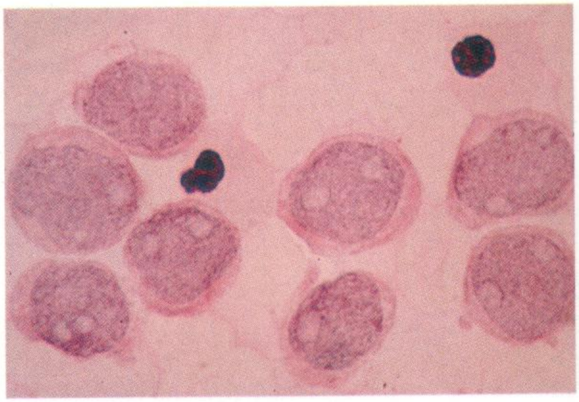

519. PAS reaction on blast cells from 9q– AML. The positivity is typically weak, as here, with no more than a faint diffuse tinge or fine granular reaction. Nucleoli are revealed very clearly in this preparation, and their disposition, when paired, at opposite poles of the nucleus is well seen. Two late erythroblasts are present in this field, both with evidence of dysplasia, one having a separated nuclear fragment or Howell-Jolly body and the other a trifoliate nucleus. Neither shows convincing PAS positivity.

520

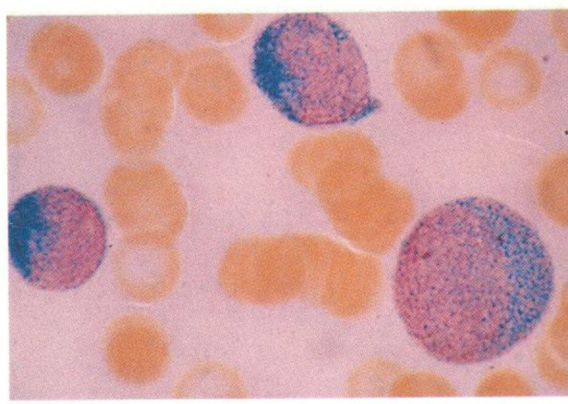

520. Dual esterase reaction in another case of 9q– AML, showing the presence of strong CE positivity in each of three blast cells, with even a possible positive Auer rod in the uppermost.

521

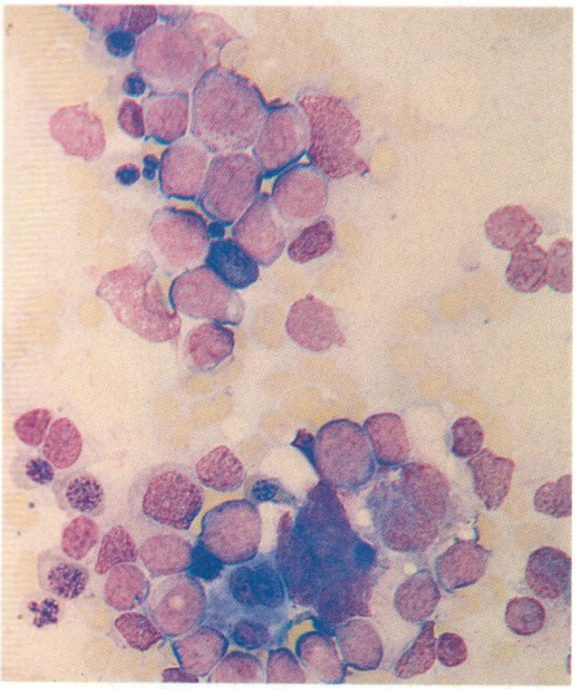

522

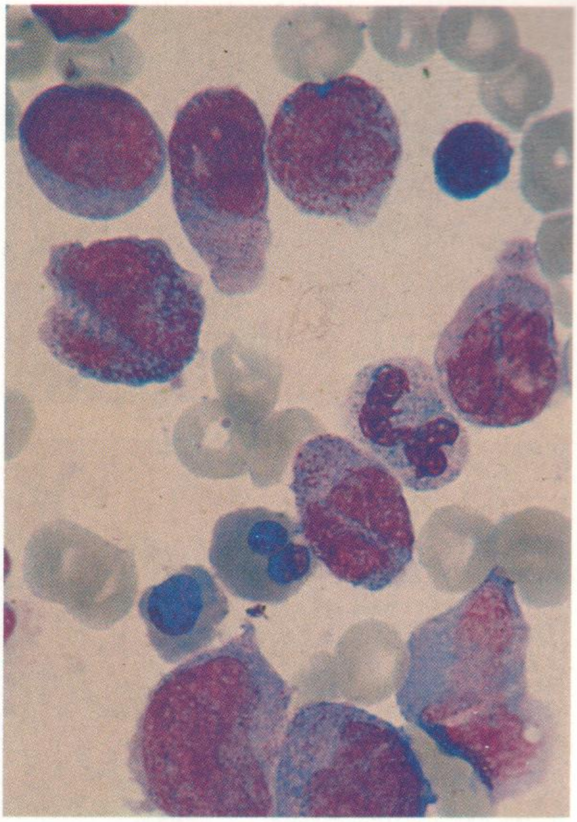

521–523. *Examples of AML associated with monosomy 7, 7q– and 5q–(Type IIA).*

These chromosome abnormalities are common in myelodysplastic states (MDS) and occur in both primary (*de novo*) and secondary AML. Monosomy 7 and 7q– are often found together with other chromosomal defects. Cases usually show dysplasia of both erythroid and megakaryocytic lines as well as either myeloblasts or monoblasts, or both. 5q– is relatively uncommon as a sole abnormality in AML but has usually been associated with a rather similar picture so far as erythroid and megakaryocytic involvement is concerned, but with mostly myeloblastic and later granulocytic cells rather than those of the monocyte line.

521. A low-power view of a bone marrow smear (Heyl stain) from a patient with AML and monosomy 7, showing blast cells with some granulocytic maturation, a group of abnormal megakaryocytes including mononuclear, binuclear and trinuclear forms, and ten erythroblasts, several of which show nuclear deformities or megaloblastic change. There is a central plasma cell.

522. An example of the bone marrow cytology in AML with 5q–, showing a predominantly myeloblastic and promyelocytic picture with a normally granular segmented neutrophil and two erythroblasts, one binucleated.

523. A smear from a case of AML with multiple chromosomal defects, including monosomy 7 and trisomy 8. There are myeloblasts with nuclear ring formation and a suggestion of both defective granularity and Pelger-Huët nuclei in later neutrophils.

523

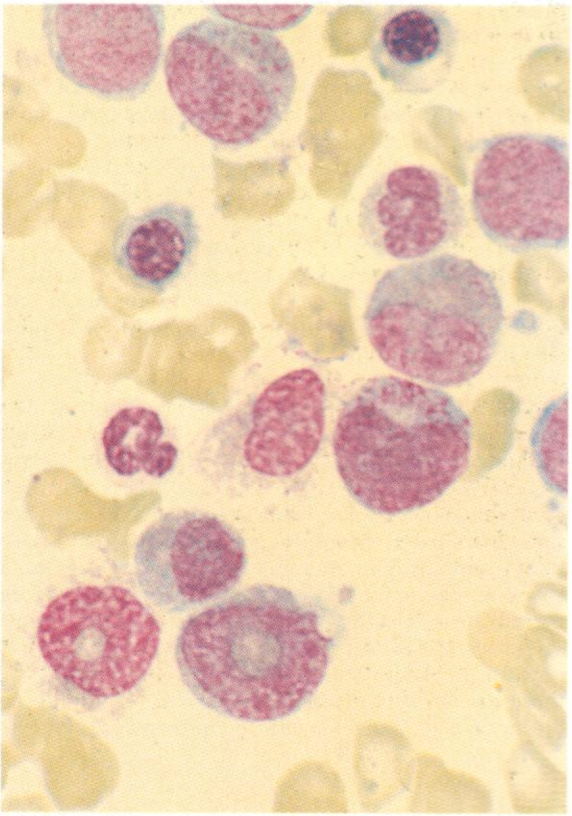

524

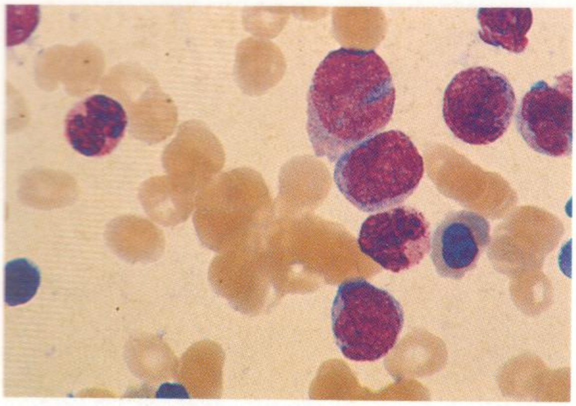

525

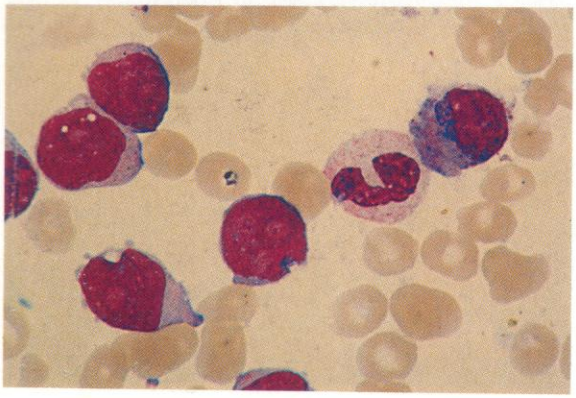

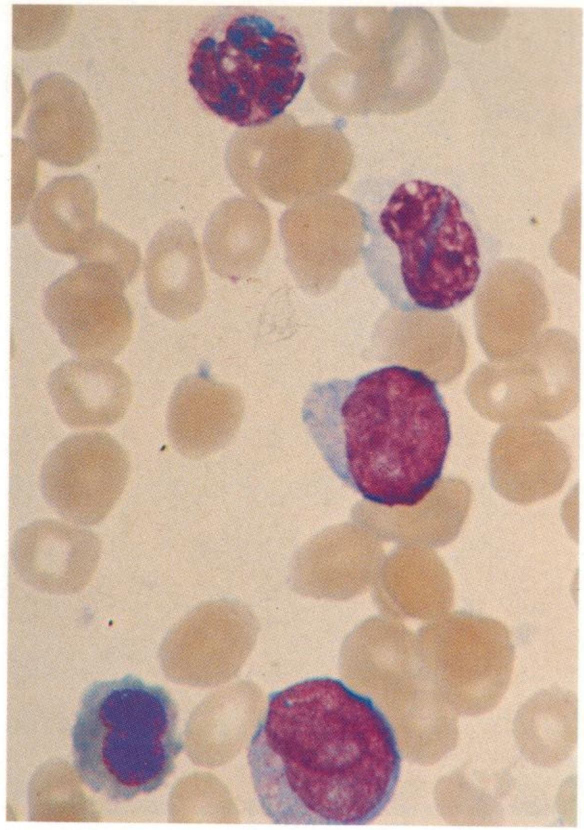

526

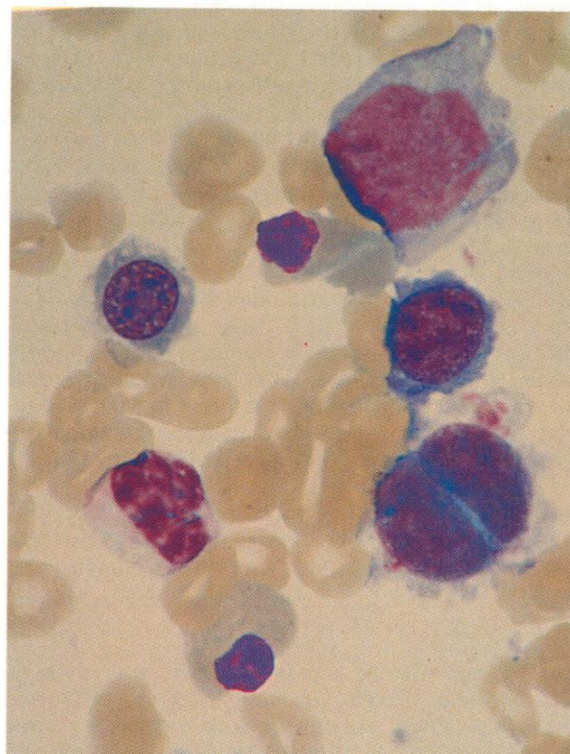

527

524–532. *Examples of the cytology and cytochemistry of AML with 6;9 translocation, t(6;9) (p23;q34).*

This chromosomal defect is usually, though not quite always, associated with a strong basophilic component, including mature basophils and numerous basophil precursors from promyelocytes onwards, and frequently with abnormally coarse or poorly staining granules or atypical nuclear forms. Cases have been classified mostly in FAB group M2, less commonly in M1, M4, or as MDS, but as there are often minor components of both erythroid and megakaryocytic involvement with dysplasia and micromegakaryocytes, most cases probably fit Type IIA.

524–527. Various fields from the bone marrow of a patient with t(6;9) AML, stained by Romanowsky dyes to illustrate these abnormalities. In **524** there are two late basophils with recognizable nuclear structure but poorly stained granules, while two of the blast cells show a suggestion of basophilic granulation. Four myeloblasts, a neutrophil stab cell and a coarsely granular basophil myelocyte can be seen in **525**, while **526** has three blast cells with little differentiation, a binucleated erythroblast and, at the top, a poorly granular basophil polymorph. There are no basophils present in **527**, but there are four erythroblasts, one with some megaloblastic change, and a binucleated micromegakaryocyte.

528

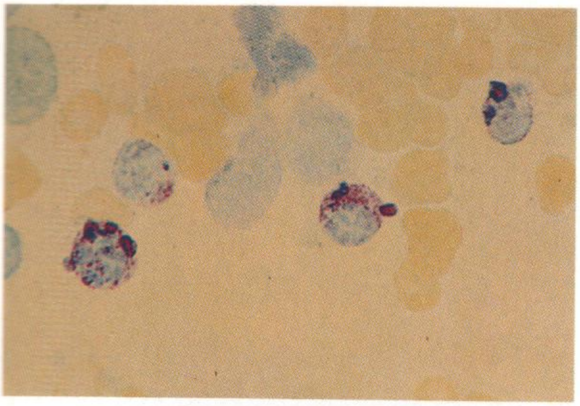

529

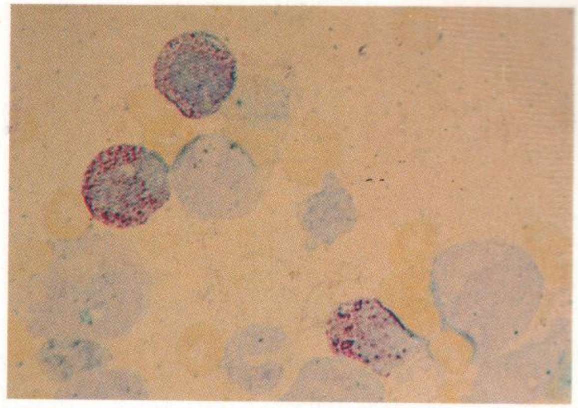

530

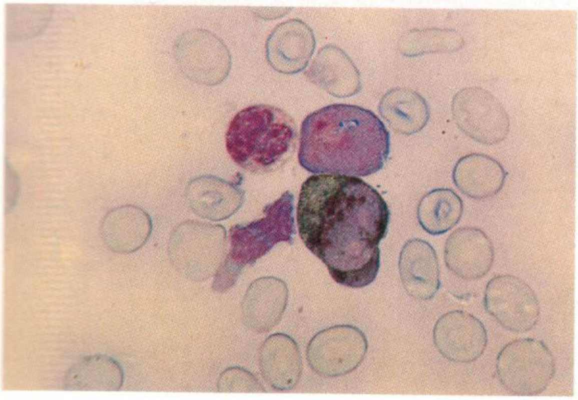

531

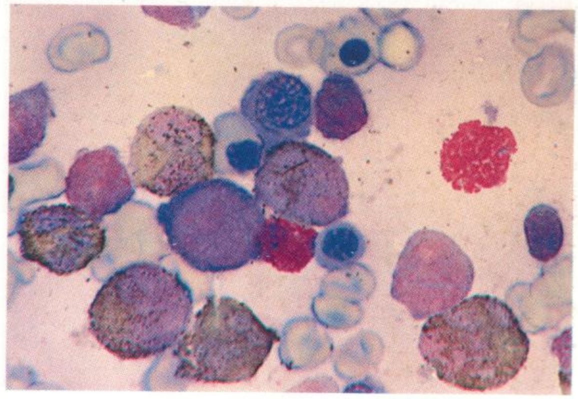

528–532. *Further fields from cytochemically stained slides of the same bone marrow aspirate as in 524–527.*

528 and **529**. Fields stained with toluidine blue, which reacts specifically with the mucopolysaccharide of basophil granules. Positively reacting cells can be picked out with ease and generally prove to be more numerous than had been thought from the Romanowsky stains. Here, the coarse granularity of more mature basophils and the finer granules in basophil myelocytes are clearly visible.

530 and **531**. SB stains, **530** showing a negatively reacting segmented basophil, a negative myeloblast and a normally positive eosinophil myelocyte, **531** a metachromatically staining basophil, normally reacting neutrophil-precursors – one with a positive Auer rod – and negative erythroblasts.

532. PAS stain on the same material, showing two erythroblasts with cytoplasmic positivity, two myeloblasts with single nucleoli and a negative or weak diffuse reaction, and a normally reacting metamyelocyte. There are no basophils in this field.

532

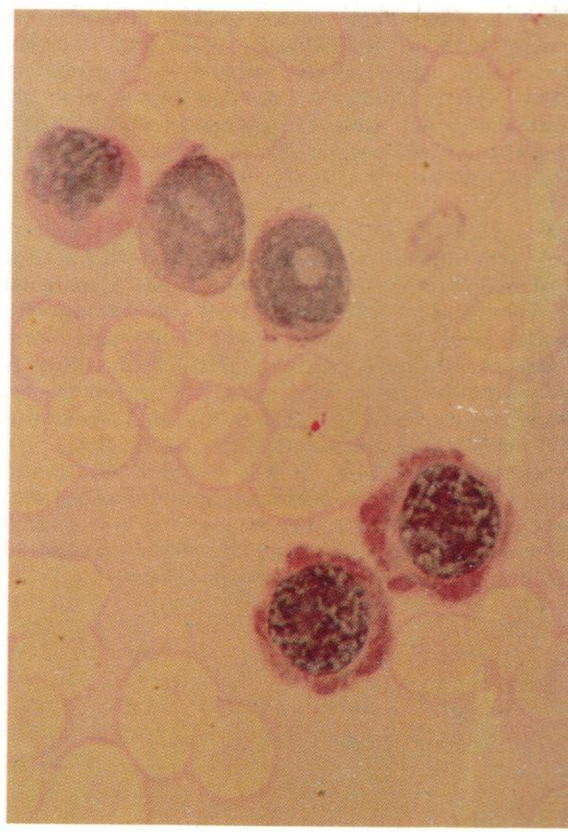

533
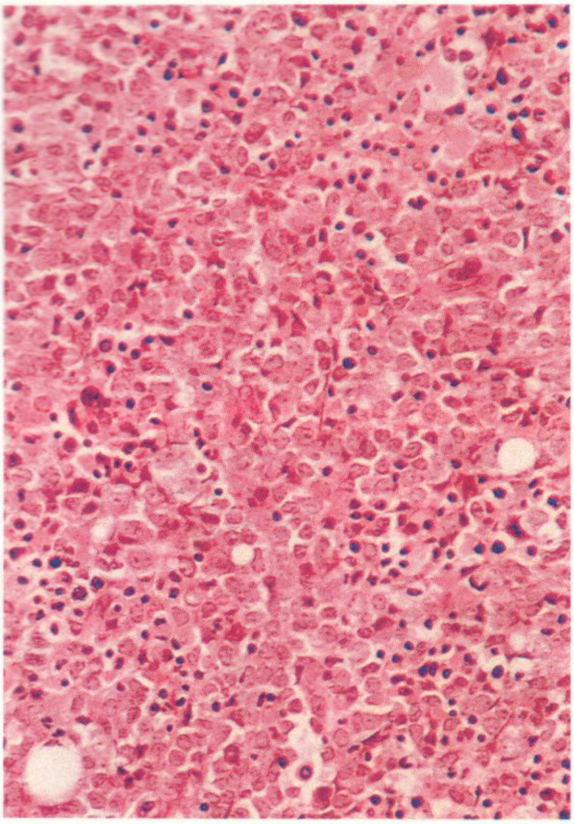

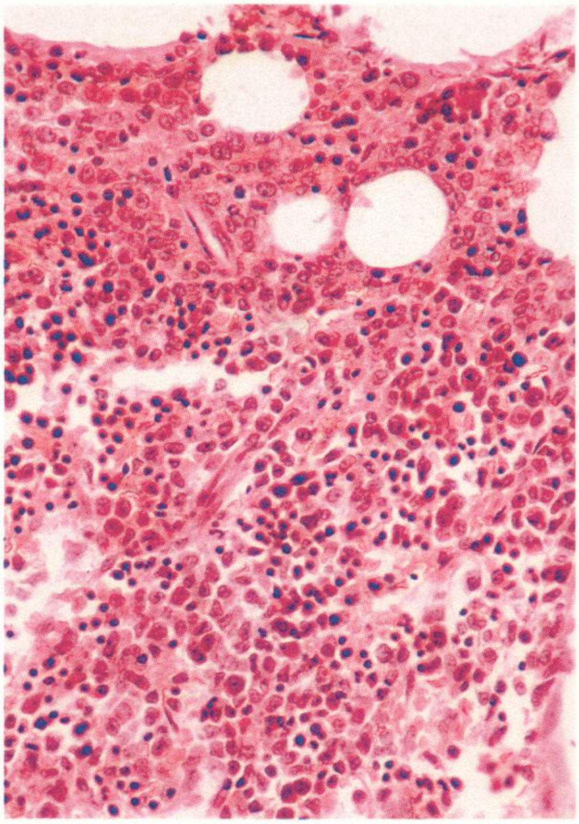
534

533. A section of bone marrow trephine biopsy from a patient with a multilineage AML and complex chromosome abnormalities, secondary to a preceding MDS. The predominant cells are blasts, probably myeloblasts, but there are islands of erythroblastic proliferation and several dysplastic megakaryocytes. Overall cellularity is high.

534 and **535**. Low- and higher-power views, respectively, of a trephine biopsy section from another patient with multilineage AML, showing again a marginal predominance of nucleolated blast cells, many with twisted monocytoid nuclei, among a substantial component of erythroblasts of different stages of maturity. A few megakaryocytes, some apparently mononuclear, can be distinguished. There is an occasional late neutrophil with dense but segmented or twisted nucleus.

Sections of this kind help to establish the overall cellularity and broad differential proportions of cell lines in cases of AML, but smear preparations are required for more accurate recognition of dysplastic changes and detailed differentiation of primitive cell types.

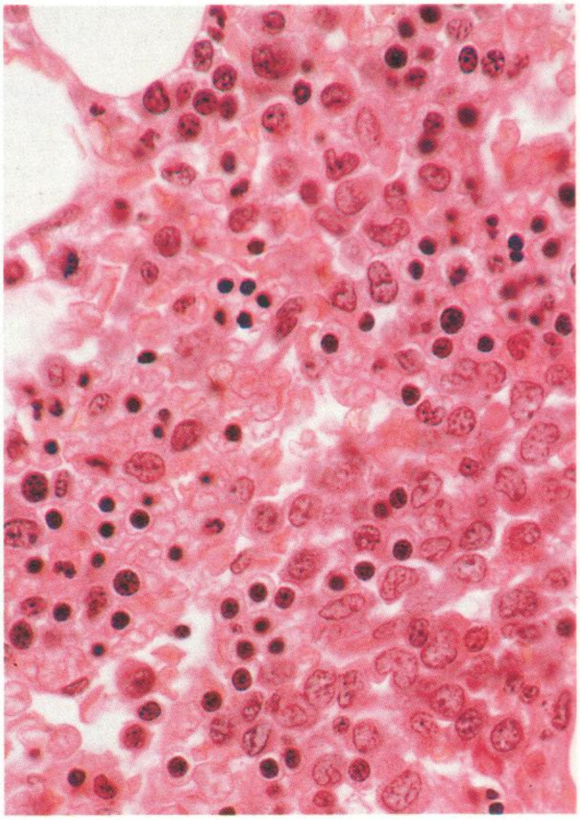
535

536

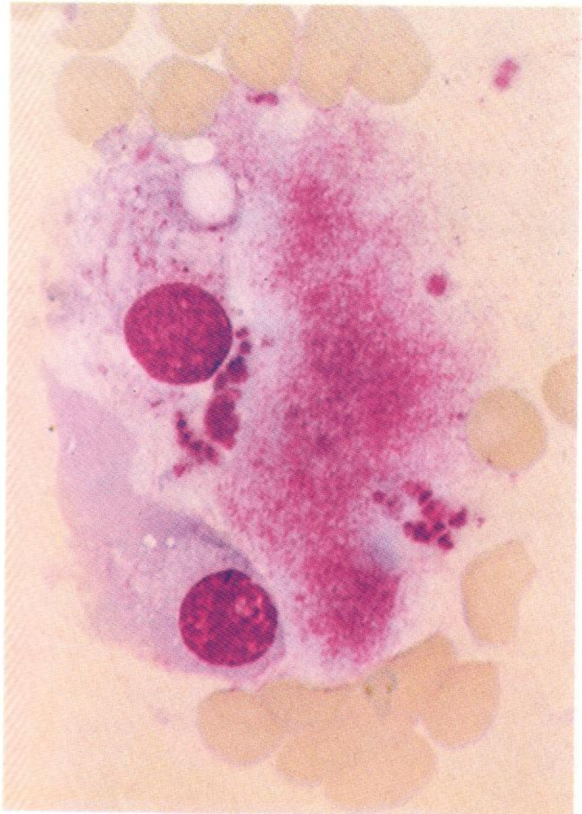

537

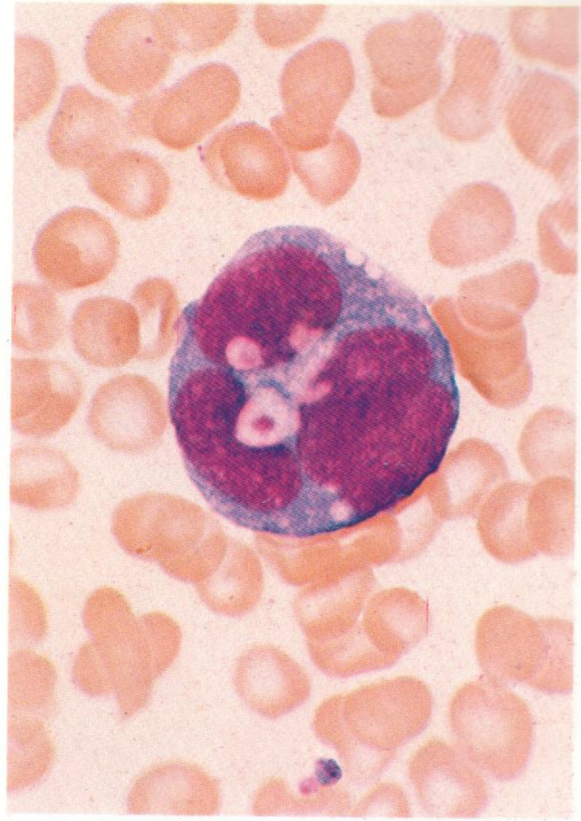

536–547. *Early cytological signs of emerging myeloid haemopoietic activity during remission development in acute leukaemia. The features illustrated are usually found in marrows which otherwise remain hypoplastic following cytotoxic therapy.*

536. A plasma cell, an RE cell (macrophage) and the granular, platelet-forming cytoplasm of a megakaryocyte.

537 and **538**. Young megakaryocytes, showing new platelet formation at sites where the primitive cytoplasmic basophilia is first lost.

538

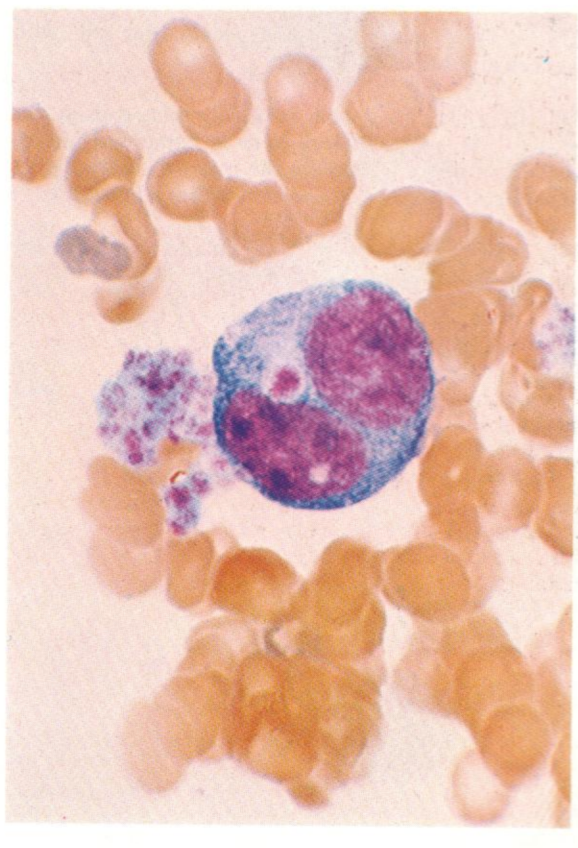

539

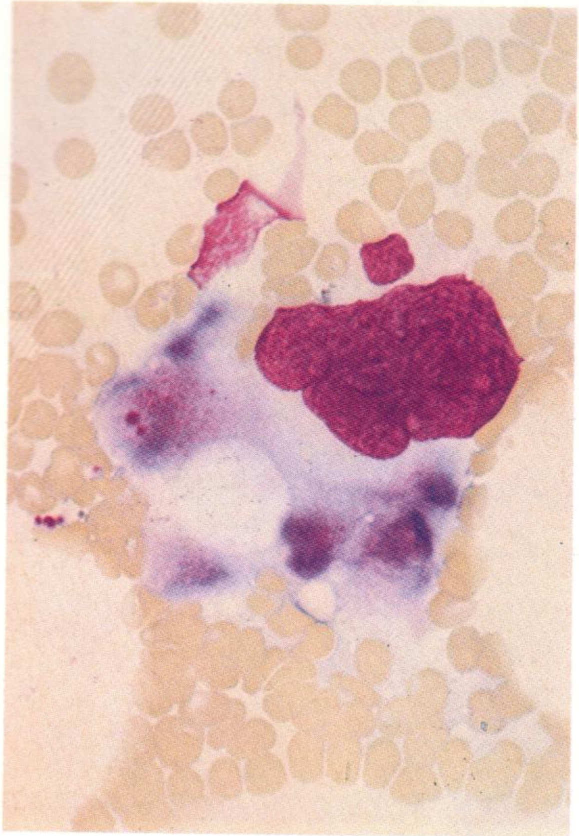

540

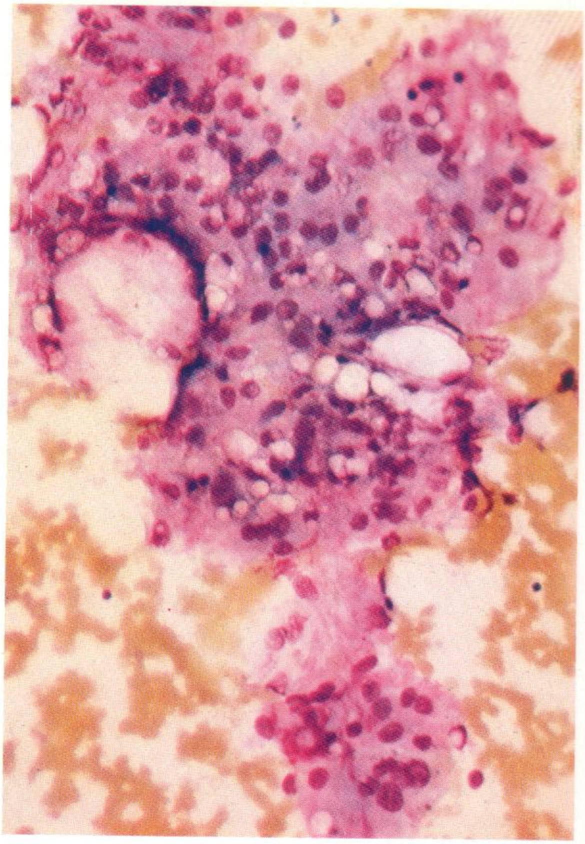

541

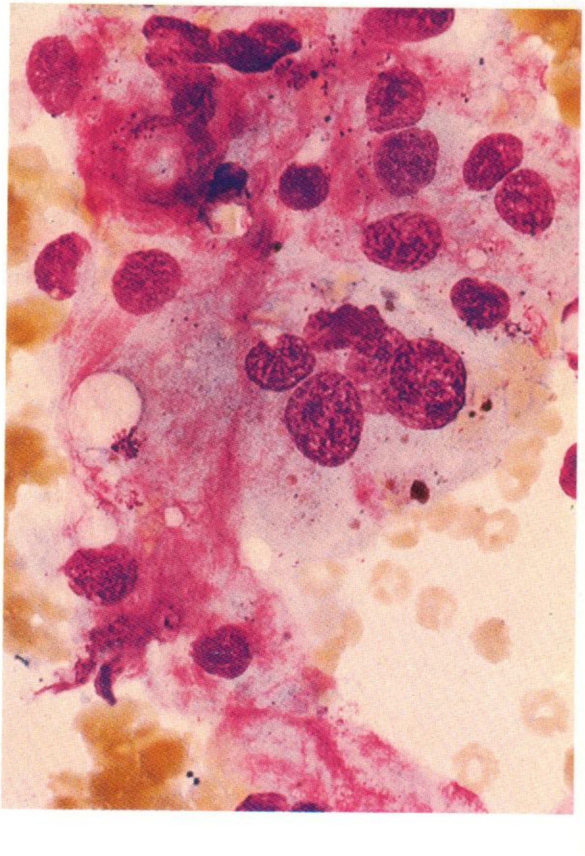

539. A more mature megakaryocyte, but still with patches of residual basophilia.

540. RE cells may appear relatively numerous at this phase – the marrow fleck here is composed almost entirely of them. Elsewhere the marrow showed gross hypoplasia, yet remission ensued within a few days.

541. A higher-power view of the cells in this fleck – the nuclear pattern is characteristic of RE cells.

542

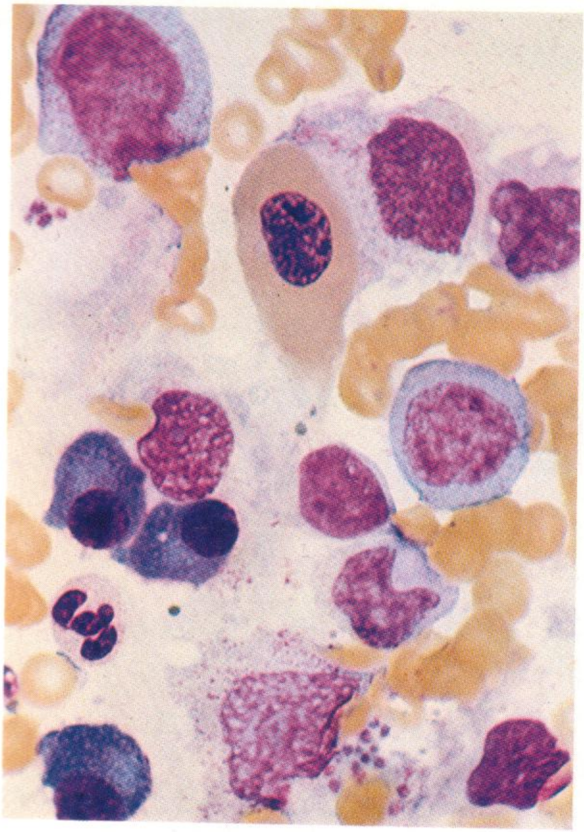

543

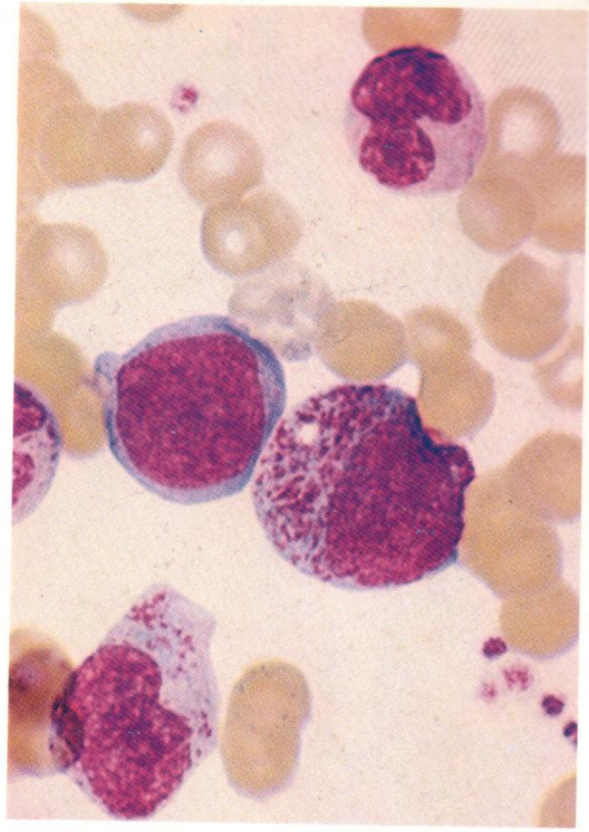

544

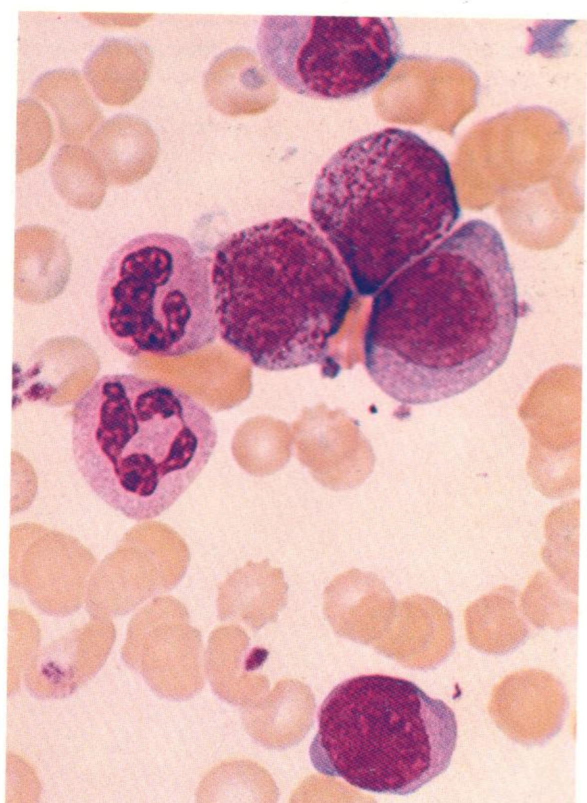

542. A group of typical remission-associated cells: plasma cells, RE cells, megakaryocyte-platelets, a single blast cell, granulocyte precursors and a giant megaloblast following antimetabolite chemotherapy.

543. A myeloblast, two coarsely granular promyelocytes (as typically found in early remission) and a metamyelocyte.

544. A similar sequence of granulocyte precursors together with stab and segmented neutrophils of normal appearance.

545

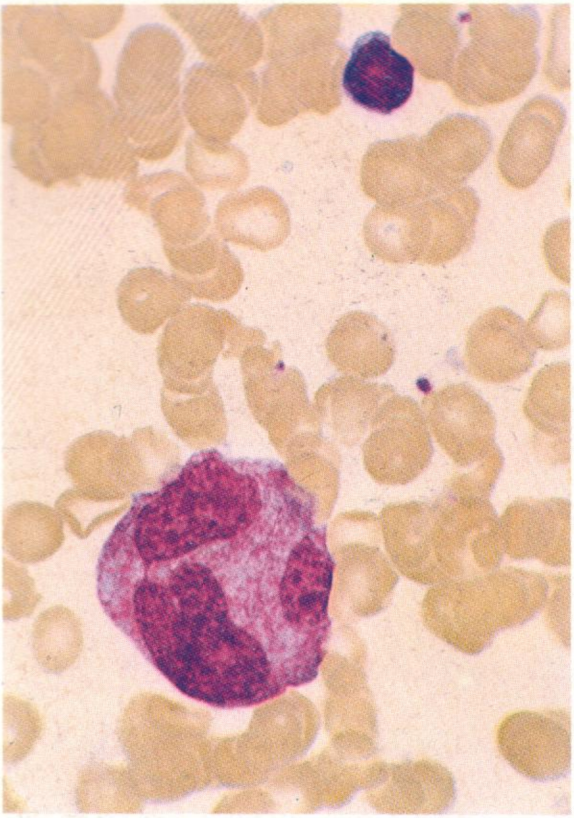

546

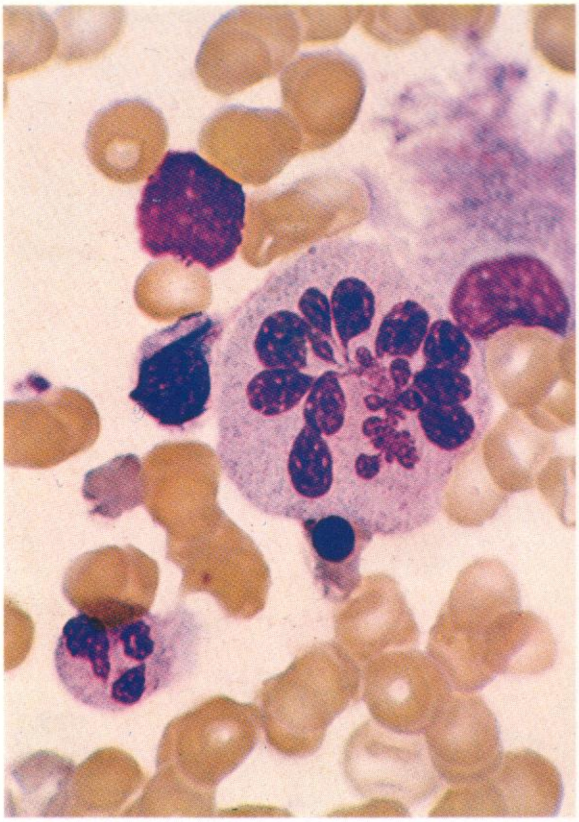

545–547. Examples of giant or multilobed neutrophil metamyelocytes or polymorphs in bone marrow aspirates taken during early stages of remission emergence in acute leukaemia. An activated lymphocyte or immunocyte approaching plasma-cell morphology is also shown in **547**. Pathological though the multilobed neutrophils appear, they do seem frequently to precede remission development.

547

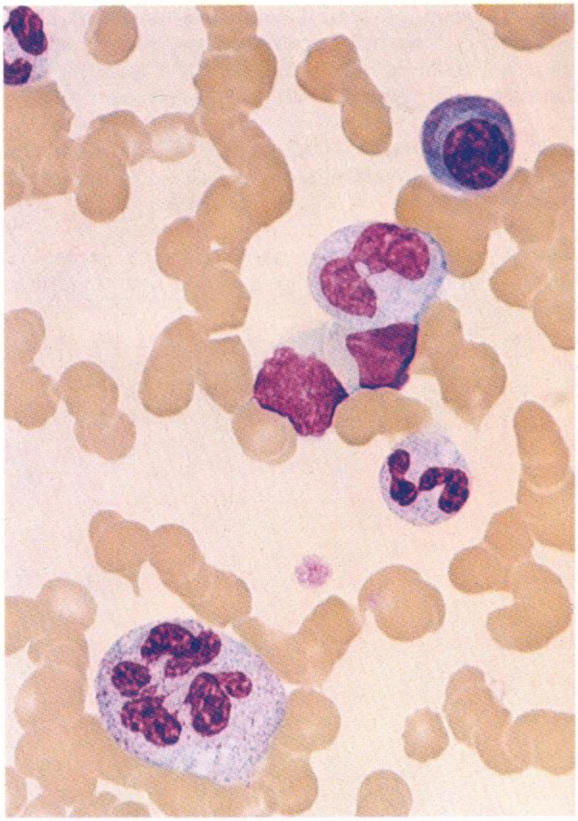

548

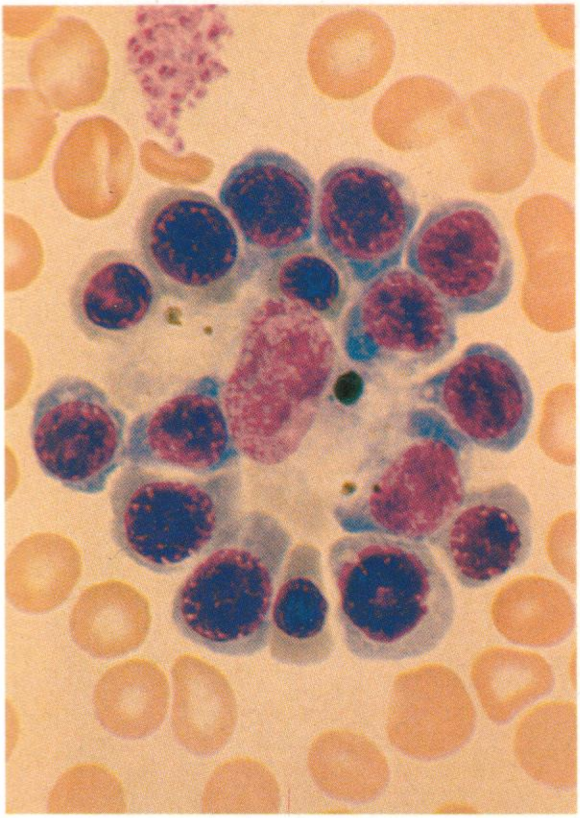

549

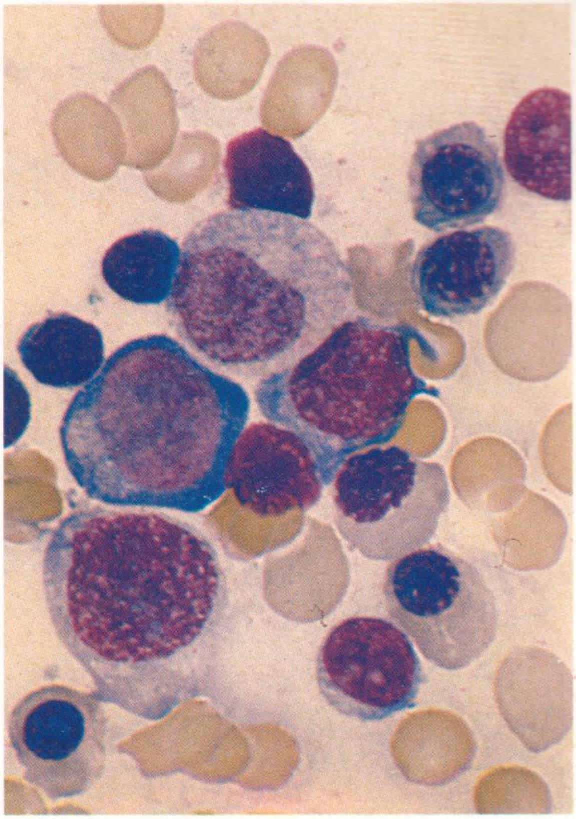

548–550. Three further illustrations of phases of emerging remission in bone marrow aspirates from patients with AML after successful induction therapy. In the first (**548**), an island of erythroblasts with cytoplasm ranging from basophilic to polychromatic surrounds a macrophage, as active erythropoiesis emerges. In the second (**549**), a single neutrophil myelocyte is present in a field containing predominantly erythroblasts, from pro-erythroblast to late normoblast. There is evident polychromasia among the red cells, no doubt reflected by a reticulocytosis in the peripheral blood. The third field (**550**) shows a range of neutrophil granulocytes, illustrating maturation stages from nucleolated myeloblast at the bottom, through promyelocyte and myelocyte, to metamyelocyte and stab cell. Four erythroblasts, a possible basophil, and a compressed lymphocyte nucleus are also present.

550

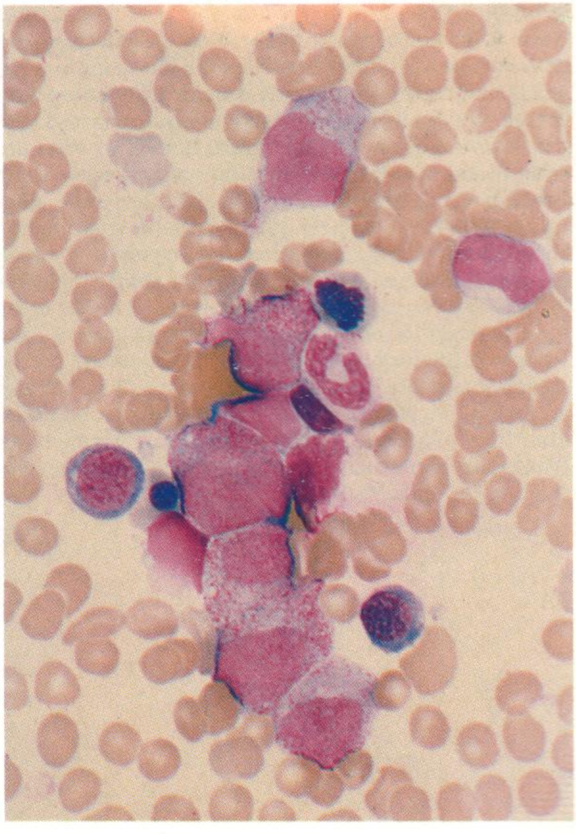

551

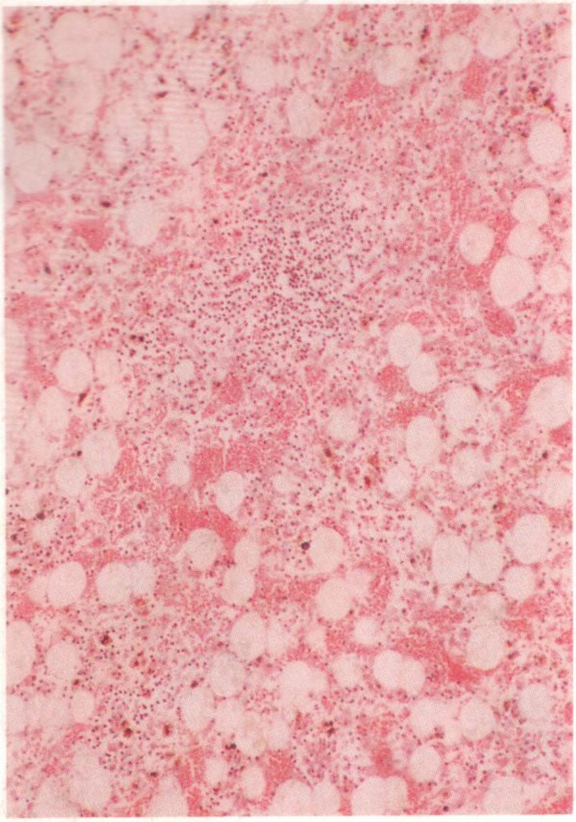

552

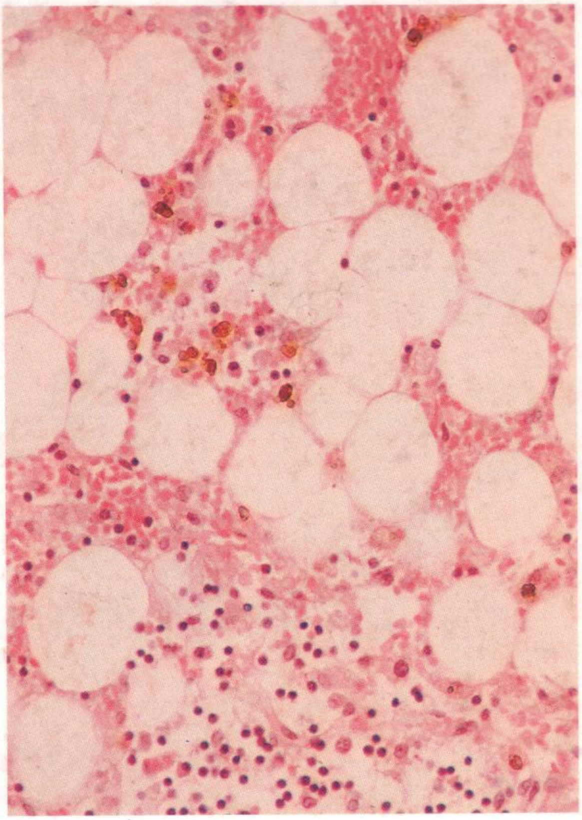

551–553. A very low-power field and two higher-power views of bone marrow trephine biopsy sections from a patient with AML after remission induction therapy. In **551** the marrow is very poorly cellular with multiple fat spaces, scattered haemorrhage and macrophages laden with haemosiderin, and a residual nodule of what are seen, in **552** (a higher magnification of part of the same field), to be lymphoid cells. This picture is one commonly found immediately after aggressive combination chemotherapy and represents the hypoplastic phase preceding emergence of remission. The third field in this group is from another biopsy taken a week later from the same patient. There is now a mixed picture present, with islands of erythroblastic activity evident among the fat spaces, especially in the upper part of the field, but also recurrent myelomonocytic blast cell proliferation elsewhere. Parallel aspiration smears confirmed this leukaemic recurrence and further induction chemotherapy was indicated.

553

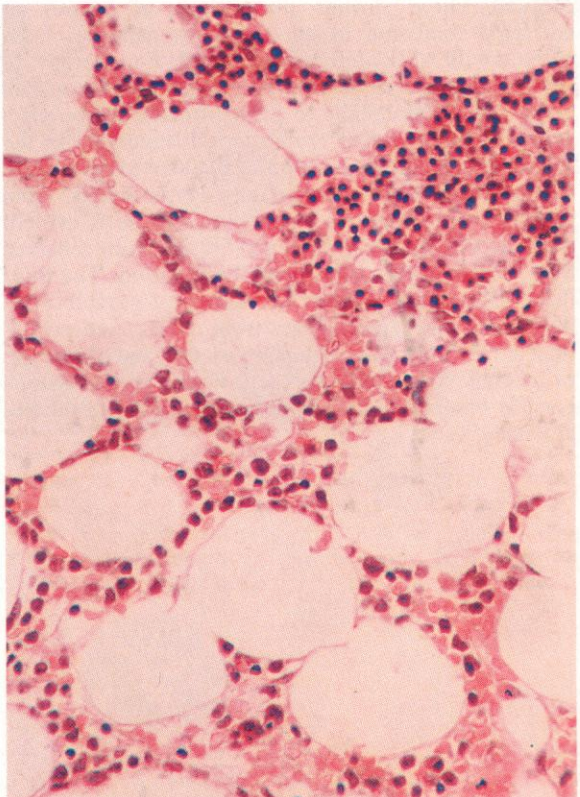

554

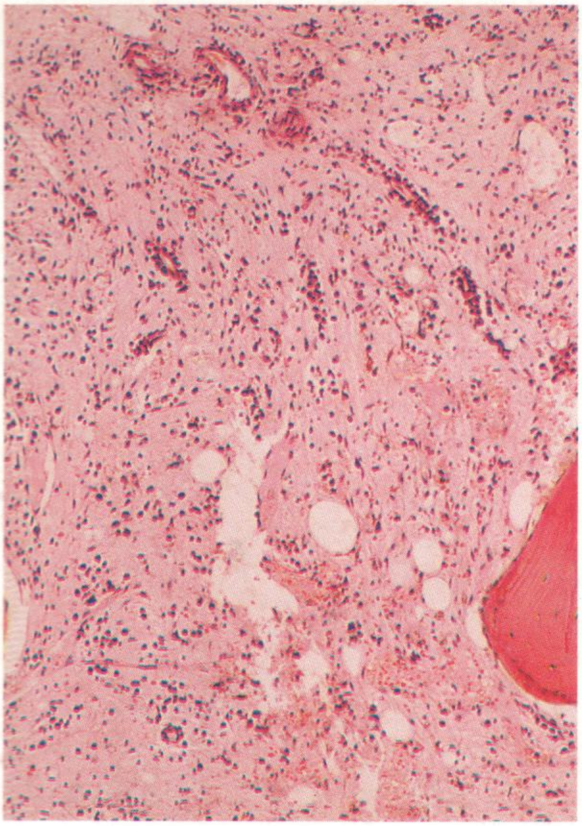

555

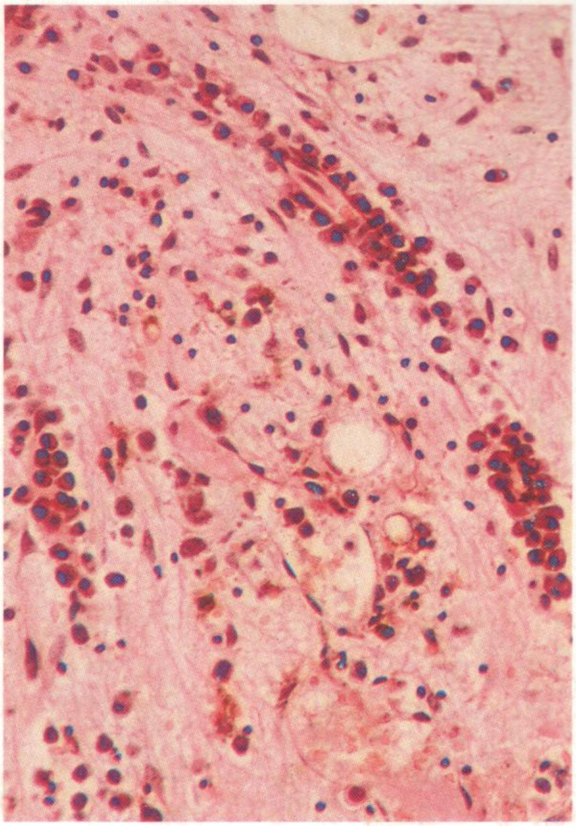

554 and **555**. Low- and higher-power views, respectively, of a bone marrow trephine biopsy section taken from a patient with secondary AML, after repeated courses of remission induction therapy were followed by a prolonged period of marrow hypoplasia and peripheral pancytopenia. At this stage the marrow under low power (**554**) shows a reticular stroma with recovering scattered cellularity and fresh cellular proliferation, especially along capillaries. The higher magnification of **555** reveals that the cytology is pleomorphic, with plasma cells along the capillaries and cells of various lineages scattered through the stroma, among them, primitive immature cells, possibly representing leukaemic recurrence, but possibly normal emergent precursors.

556

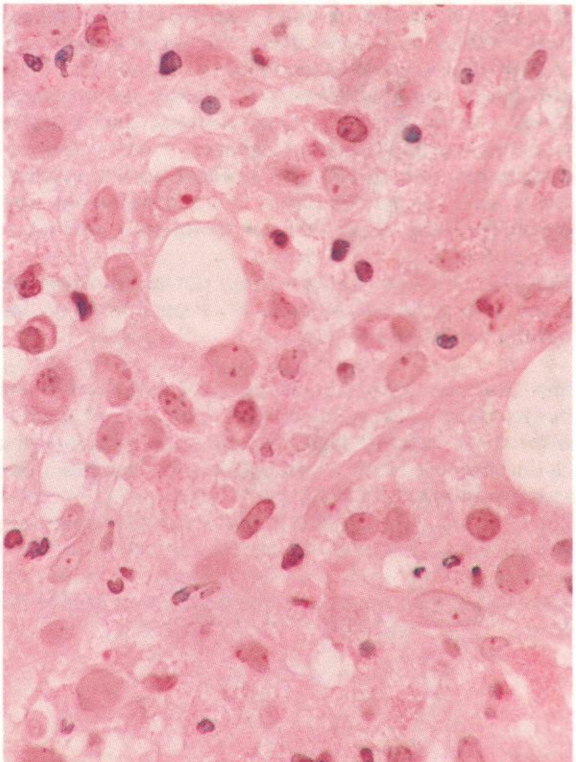

556. A further biopsy taken a week later from the same patient as in **554** and **555** resolves the question of relapse or early remission. This thin section shows a few residual plasma cells but also good maturation in the granulocyte series, with all stages from promyelocyte onwards recognizable, together with scattered erythroblastic proliferation. Clearly, remission is now emerging.

557

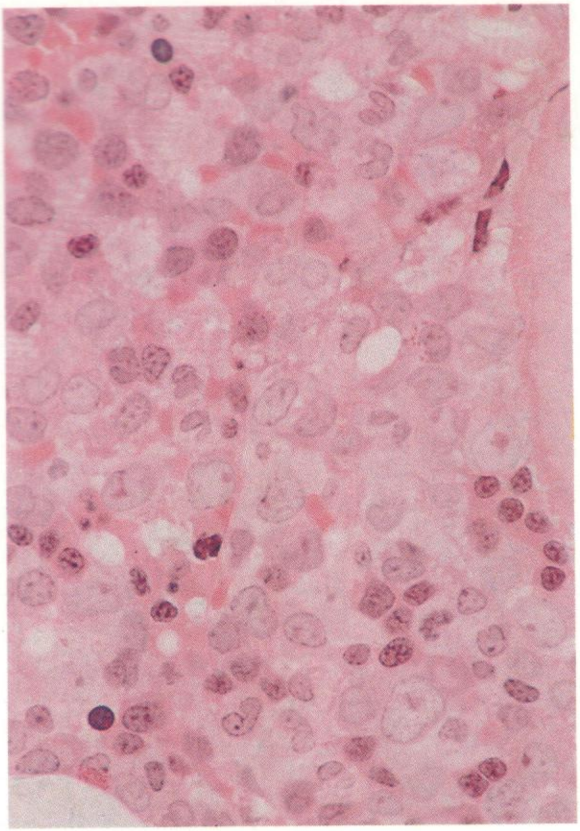

558

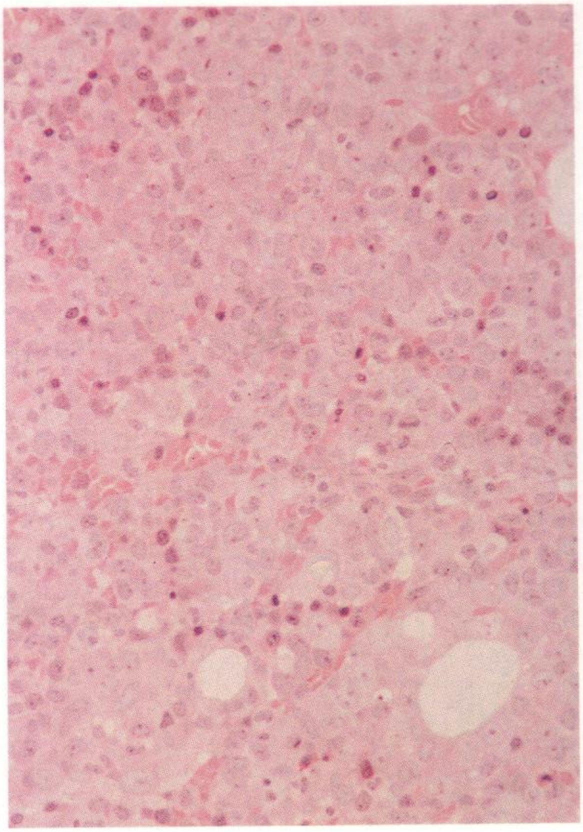

557. A thin section of bone marrow trephine biopsy from a patient with AML after induction of a temporary remission, now showing evidence of relapse. This high-power field contains about 50% lightly staining large blast cells, with conspicuous nucleoli and variable myelomonocytic nuclear shapes and nuclear–cytoplasmic ratio. There are residual normal erythroblasts and later granulocytes, but full relapse is now inevitable unless fresh intensive treatment is started.

558. Another similar field at lower power, showing here some 80% leukaemic blast cells, with fewer residual normal haemopoietic cells.

559. Another thin section from a bone marrow trephine biopsy taken from a patient with AML, after repeated courses of remission induction and consolidation chemotherapy, now followed by late relapse. The specimen shows marked post-therapy fibrosis, with fibroblasts and plasma cells prominent at the upper right part of the field, but with reduced numbers of residual normal marrow cells and with recurrent blast cells scattered among them, notably in the lower half of the field.

559

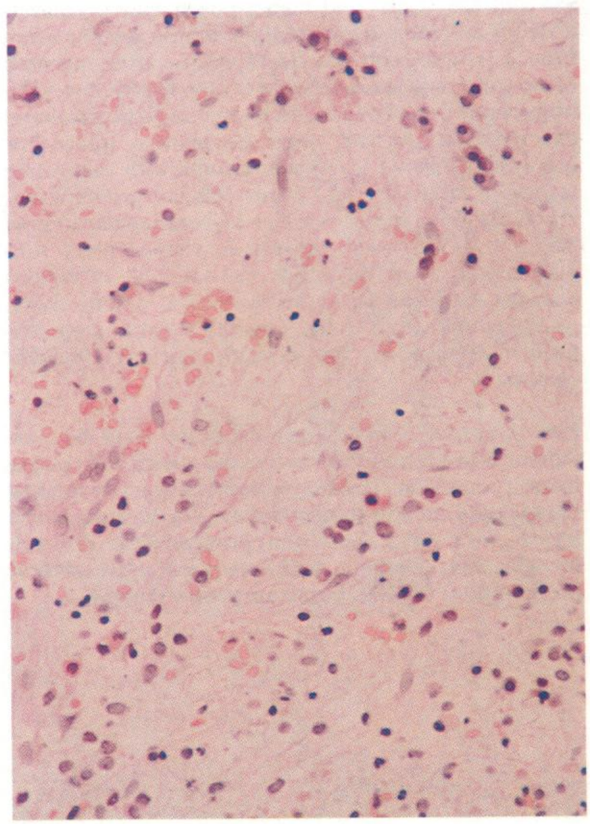

560

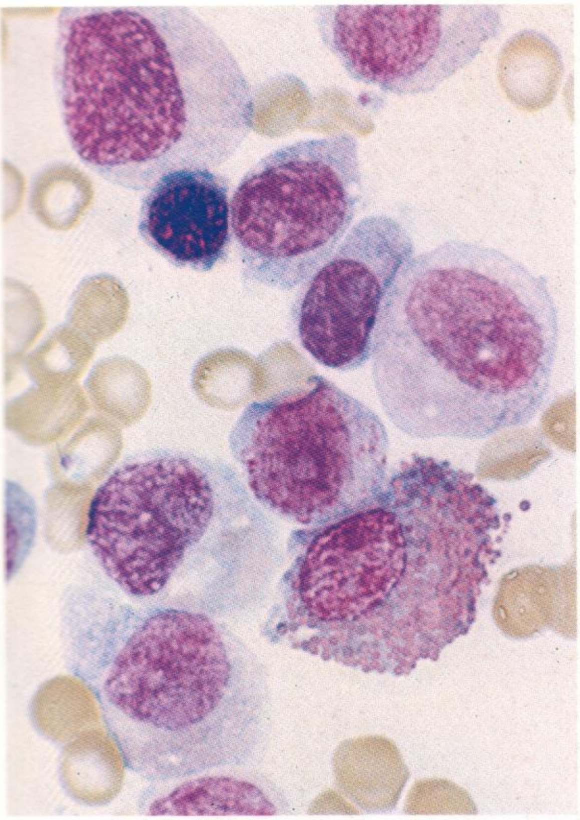

561

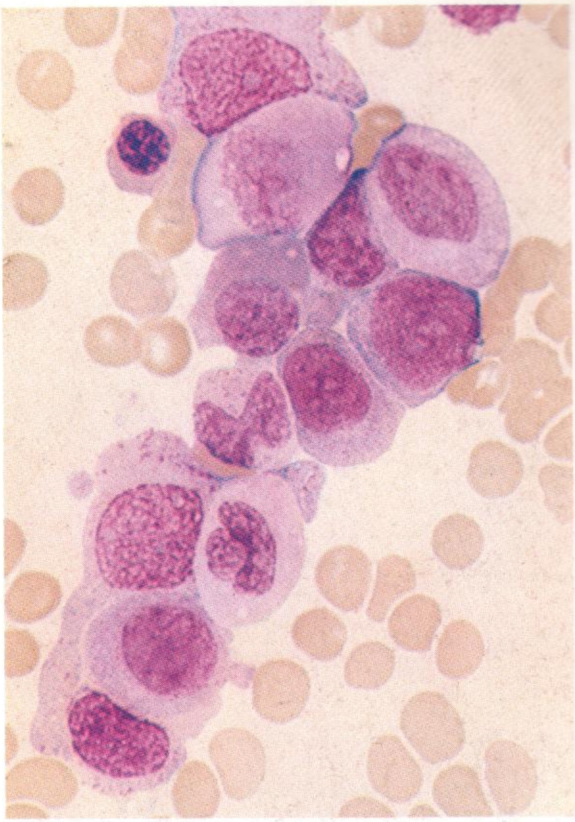

560–565. *Examples of defective granulogenesis – with a diffuse eosinophilic staining of the cytoplasm of myelocytes and few specific granules. This appearance is most often observed in preleukaemic states, including defective erythropoiesis with excess of myeloblasts, neutrophilic myelogranular dysplasia, smouldering leukaemia and all forms of myelodysplastic syndrome (MDS).*

560. A typical appearance of myelocytic cytoplasm in this condition as seen by Romanowsky staining.

561. A myeloblast, two probable premitotic promyelocytes with scattered azurophil granules and prominent nucleoli, five myelocytes with diffuse eosinophilic staining, and two later granulocytes with a more normally granular cytoplasm.

562. Further granulocytes from the same case, showing the diffuse and finely granular eosinophilic staining in several cells.

562

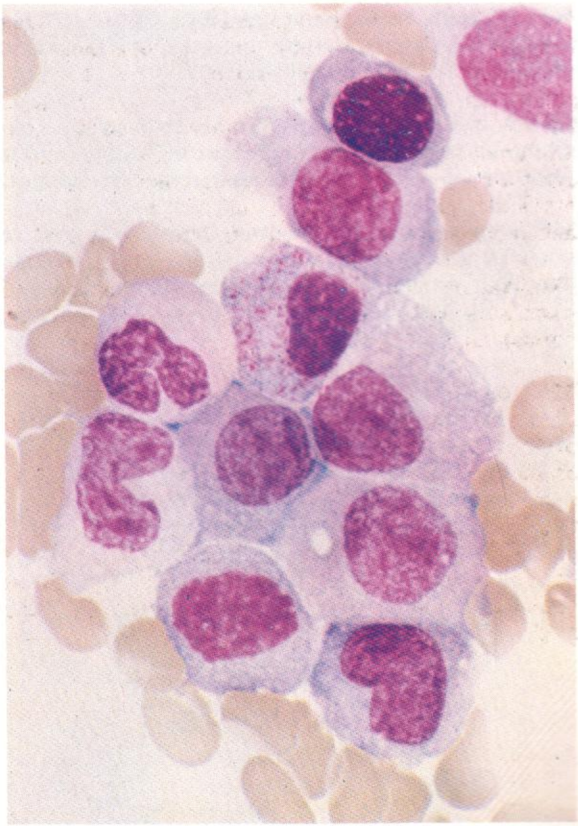

563

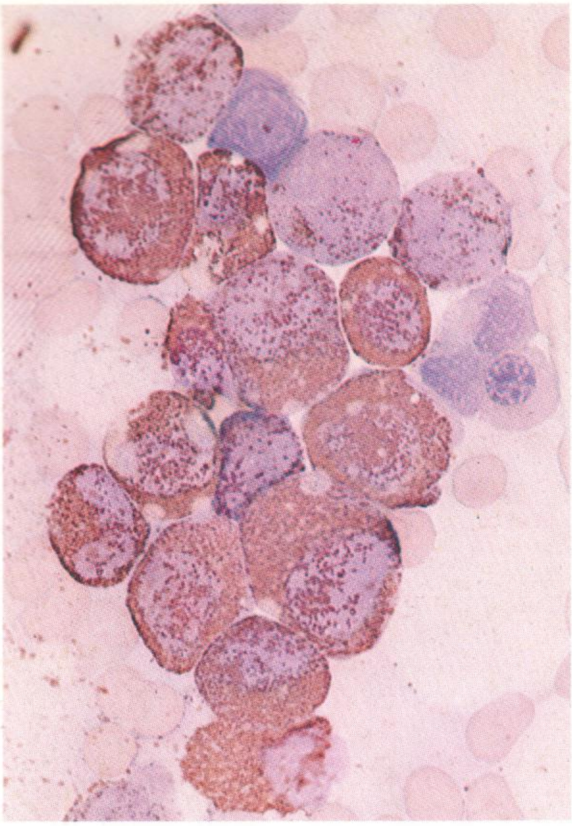

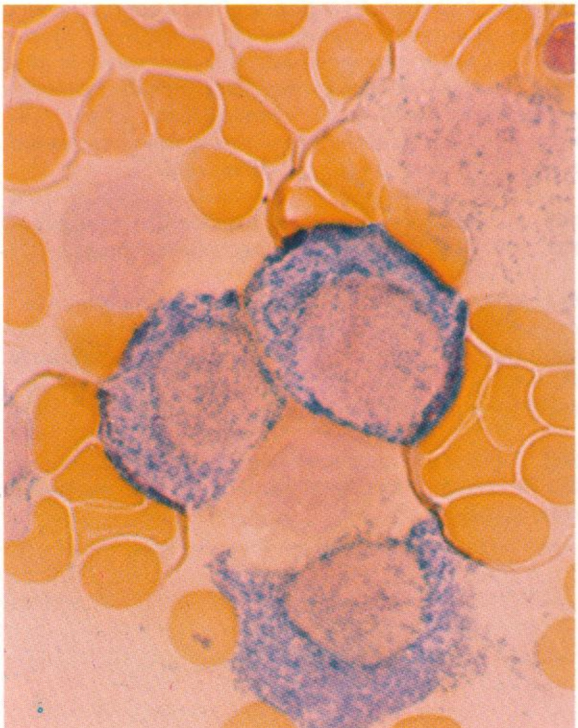

563. SB stain on the same marrow sample, showing strong sudanophilia, despite the lack of clear specific granules in the Romanowsky preparations.

564. A high-power view of the SB stain in this condition. The sudanophilic granules are of the same size as those seen in myelocytes with normal specific granules.

565. Dual esterase stain showing normal CE-positive granules in three of these unusual myelocytes, despite their poor granularity with the Romanowsky stains.

566

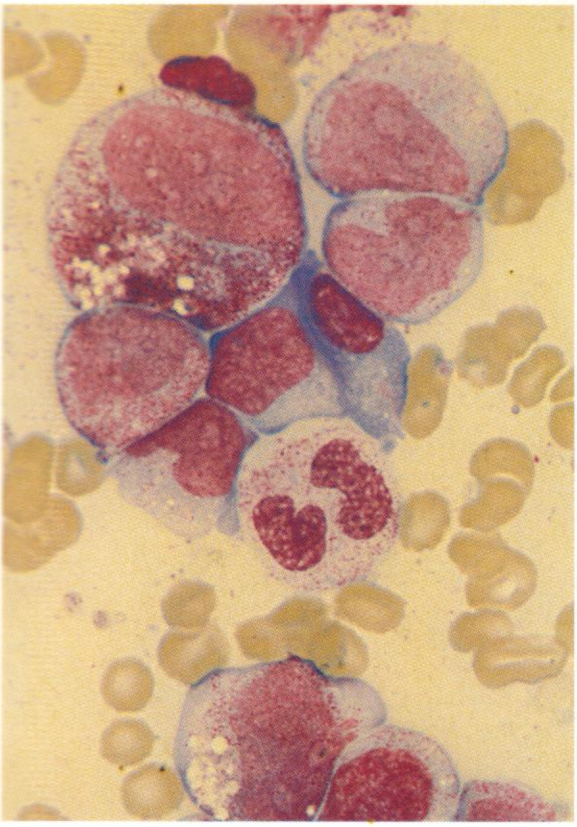

567

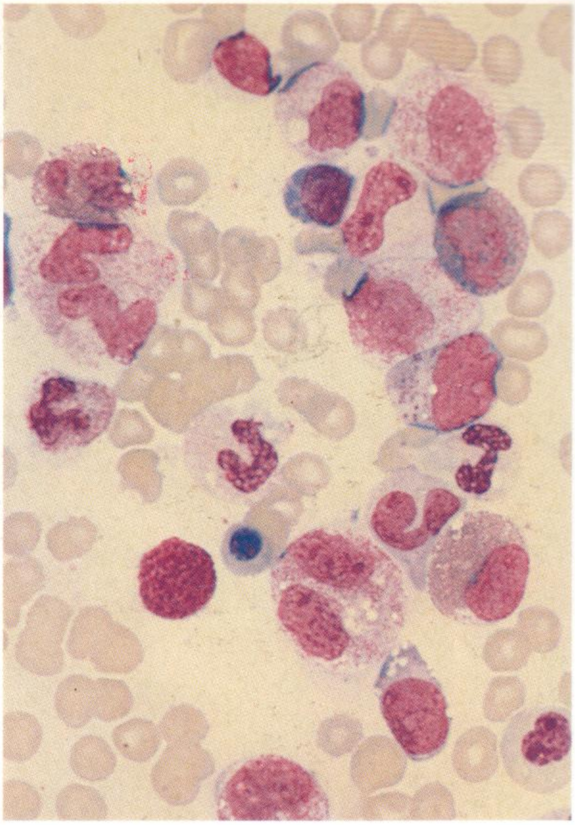

568

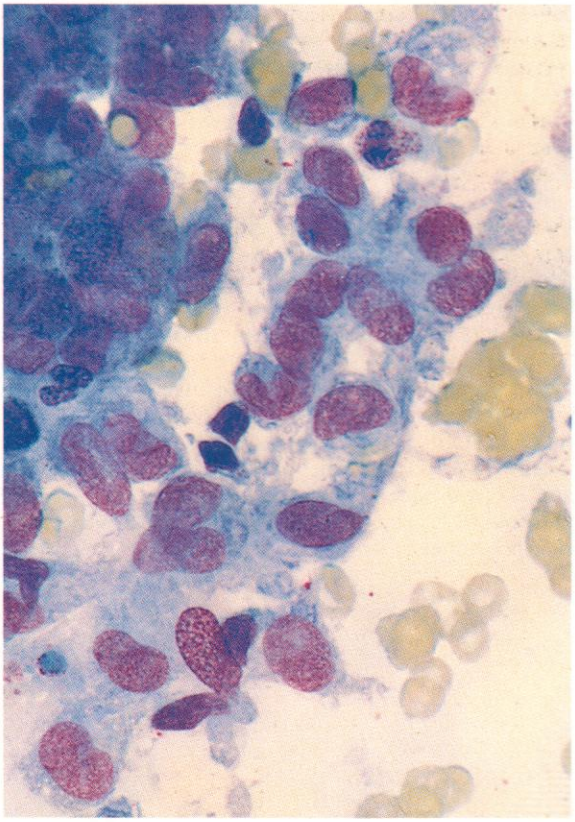

566–568. *An example of transient myeloproliferative disorder (TMD) of Down's syndrome, trisomy 21.*

Patients with Down's syndrome are at much increased risk of acute leukaemia, including a form of AML with a megakaryoblastic component. They are subject to a transient non-clonal blastic proliferation, with a strong megakaryoblastic component, which is manifest in the peripheral blood and persists for a few weeks before spontaneously disappearing without treatment. Fortunately, this transient disorder (TMD) can usually be easily distinguished from acute megakaryoblastic leukaemia (AMegL) by its earlier age incidence, <1 month as compared with >3 months, the presence of a higher proportion of blasts in the blood than in the marrow and the relatively normal levels of haemoglobin and platelets. These three fields are from the bone marrow aspirate in a neonate with TMD and blast cells in the peripheral blood. The first (**566**) has a typically variable blast cell population, with generally low nuclear–cytoplasmic ratio, vacuolation, nuclear twisting or lobulation with multiple nucleoli, a giant promyelocyte with coarse azurophil granulation, a plasma cell and a neutrophil segmented cell with nuclear twinning. The second field (**567**) shows another area to illustrate especially the varied granulocyte development, with several eosinophils as well as later neutrophils; while the third (**568**) shows the edge of a dense clump of cells of more uniform morphology consistent with megakaryoblasts, with occasional intermingled macrophages.

569

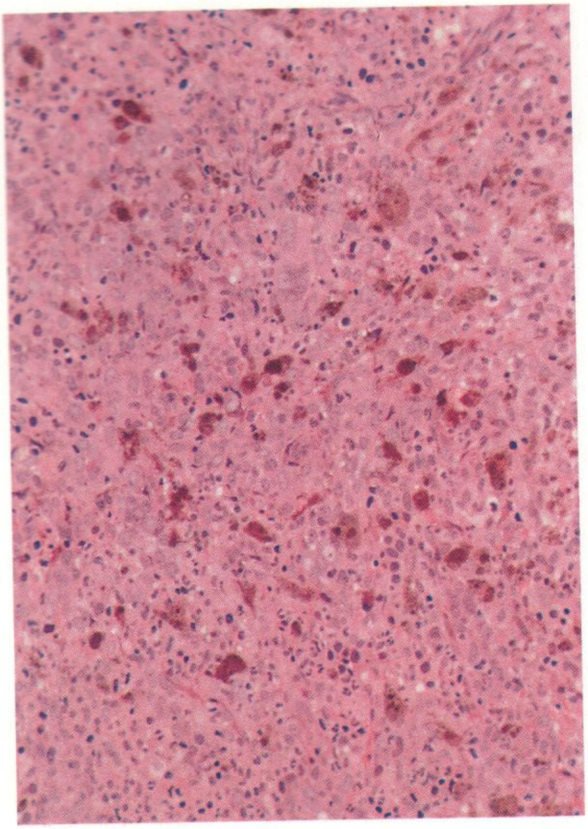

570

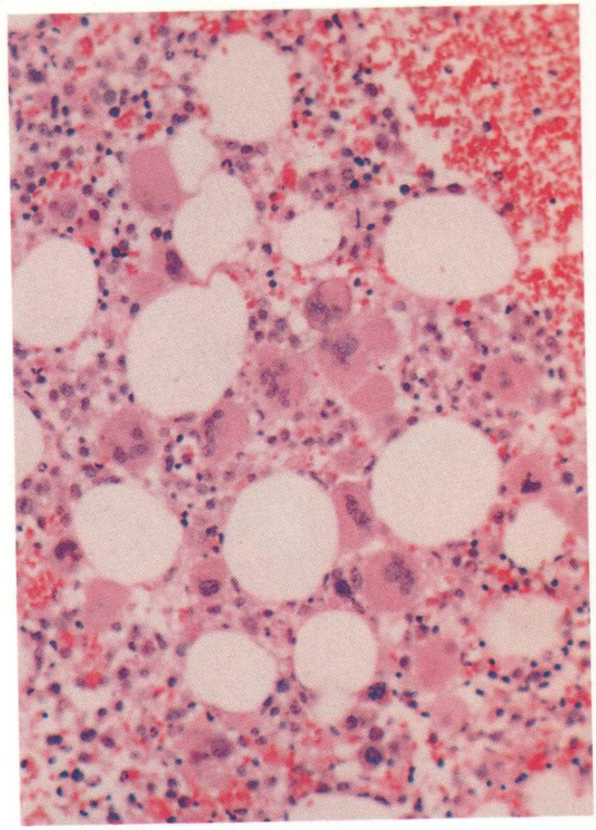

569–571. Thin sections of bone marrow trephine biopsy from a patient with an MDS involving components of refractory sideroblastic anaemia and excessive blastic proliferation together with an increase in megakaryocytes. In **569** the low-power view shows generally high cellularity with a very pleomorphic picture, including numerous scattered macrophages laden with haemosiderin and several multinucleated megakaryocytes. The higher-power view in **570** is of a neighbouring area with more residual fat spaces, where the megakaryocytic cytology is well shown, and where there are several areas of haemorrhage of the kind from which the haemosiderin in the macrophages in **569** was doubtless derived. The remaining cells in this field include granulocytes chiefly from myelocyte onwards and erythroblasts with densely stained nuclei. In the reticulin-stained preparation at still higher power illustrated in **571**, the absence of any increase in reticulin and the presence of laden macrophages, and also of nucleolated blast cells with lightly stained nuclei, are clearly evident.

571

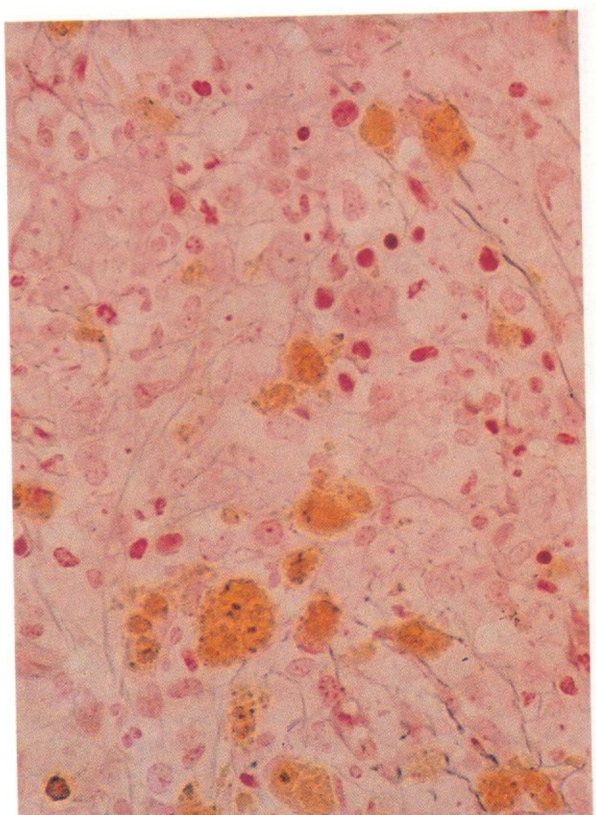

572


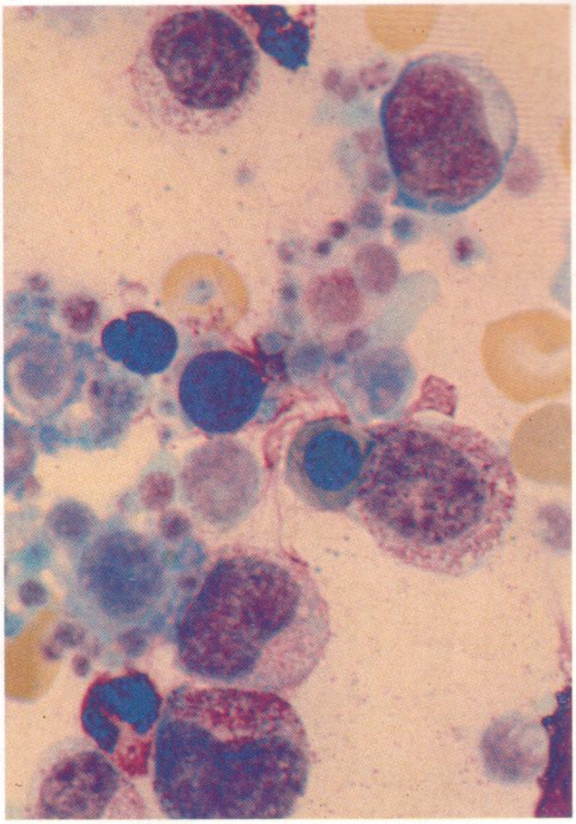
573

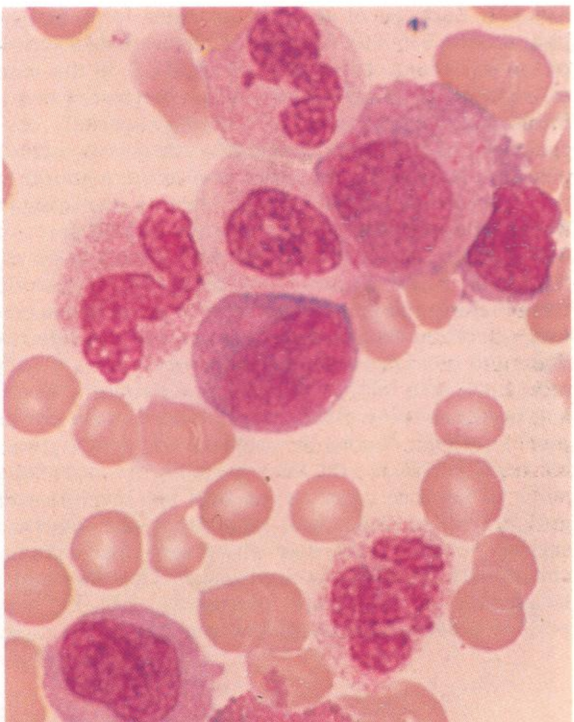
574

572. Prussian blue stain for free iron on cells in a bone marrow smear made from the same patient whose trephine sections are shown in **569–571**. The cluster of erythroblasts in this field shows a high content of free iron with occasional ringed distribution.

573. In this Romanowsky stain, a buffy coat preparation from peripheral blood – again, from the same patient – shows a myeloblast, a promyelocyte, later neutrophils, two late erythroblasts on either side of a megakaryocyte nuclear fragment, and a mass of giant platelets.

This whole sequence of slides (**569–573**), taken at the same time from one patient, illustrates the complex cytology of the multilineage myelodysplasias and the common overlap between the recognized subdivisions.

574. Another bone marrow sample from a patient with MDS, this time classified as refractory anaemia with excess blasts (RAEB). There is a shift to the left in the granulocyte series, but, as this field reveals, there is conspicuous granular dysplasia, with defective neutrophil granulation from myelocyte to polymorph, and nuclear defects ranging from pseudo-Pelger-Huët lack of segmentation (in the three upper neutrophils) to hypersegmentation in the lower polymorph.

575

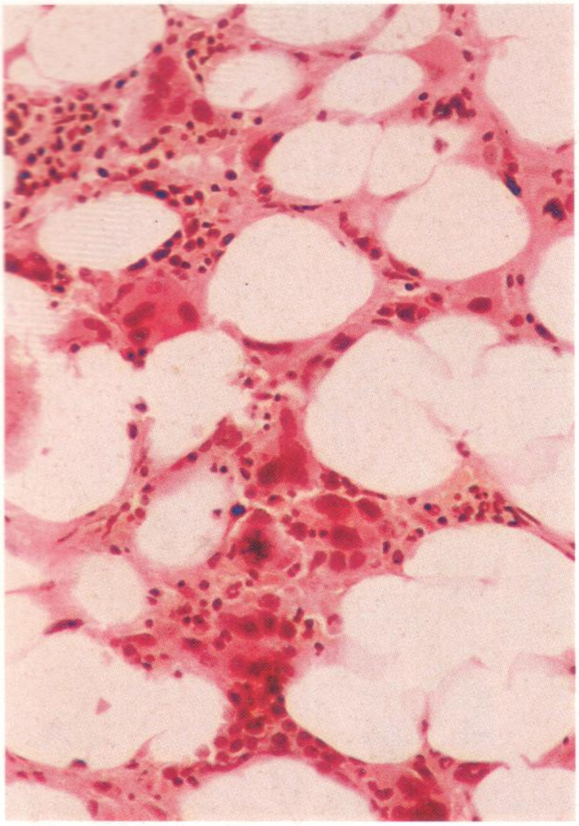

576

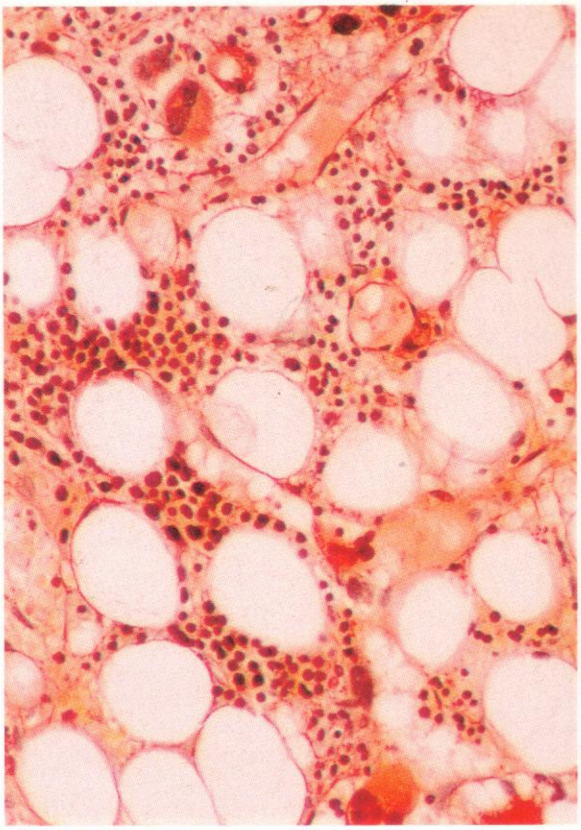

575–577. Sections of trephine biopsies from further patients with MDS. In **575** and **576**, an example is shown of the more hypocellular variant of MDS, in this case associated with marked dysmegakaryocytosis (microforms and multinucleated cells being especially conspicuous in **575**); the presence of erythroblastic islands and the absence of collagenous fibrosis are manifest in the Van Gieson stain of **576**. The section appearing in **577** is from another patient with the RAEB form of MDS, associated also with the chromosome anomaly 5q–. This defect occurs most commonly in elderly females, as in this case, and is usually found in association with refractory anaemia, dysgranulopoiesis with left shift, and a characteristic megakaryocyte picture with mononuclear or bilobed cells. Typical dysplastic megakaryocytes showing this feature are seen in the upper part of the field. Among the scattered islands of erythroblastic hyperplasia and later granulocytes occupying much of the lower part of the field are several small groups of blast cells, well away from the endosteal surfaces of bony trabeculae where early myeloid precursors are normally concentrated. This 'abnormal localization of immature precursors' (ALIP) may perhaps predicate imminent leukaemic transformation.

577

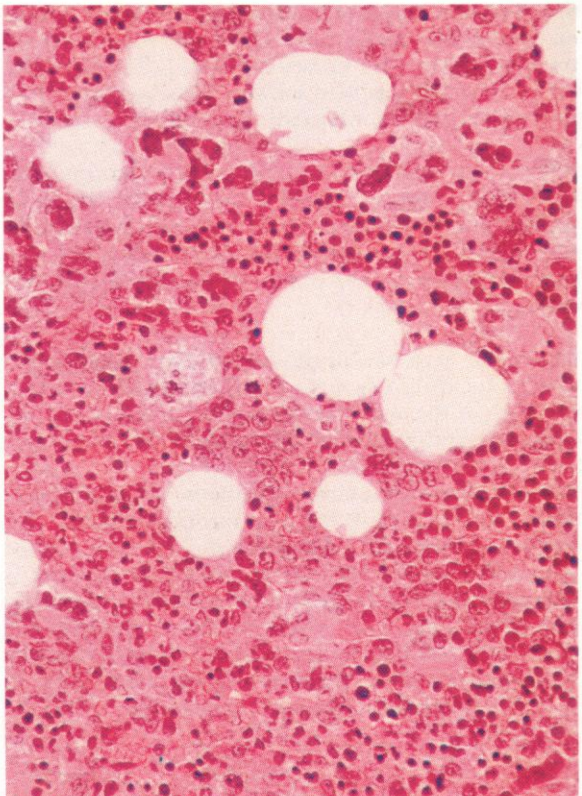

578

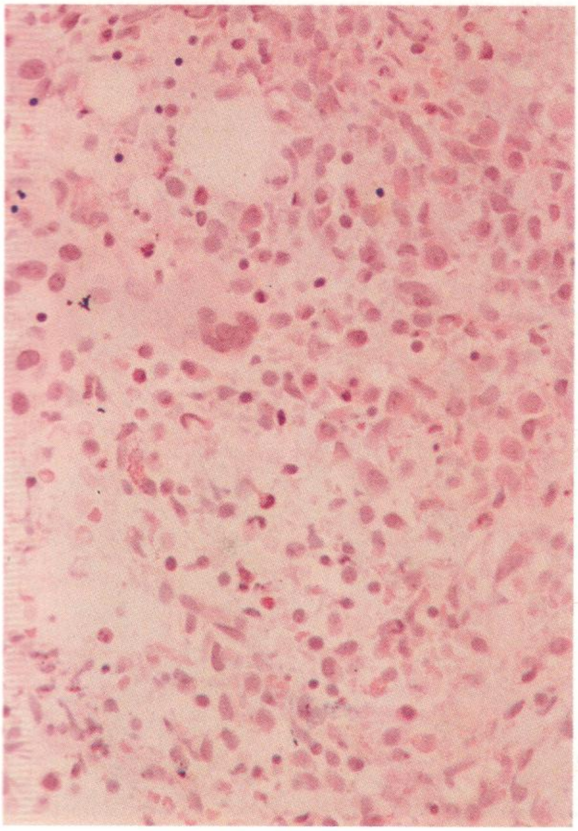

579

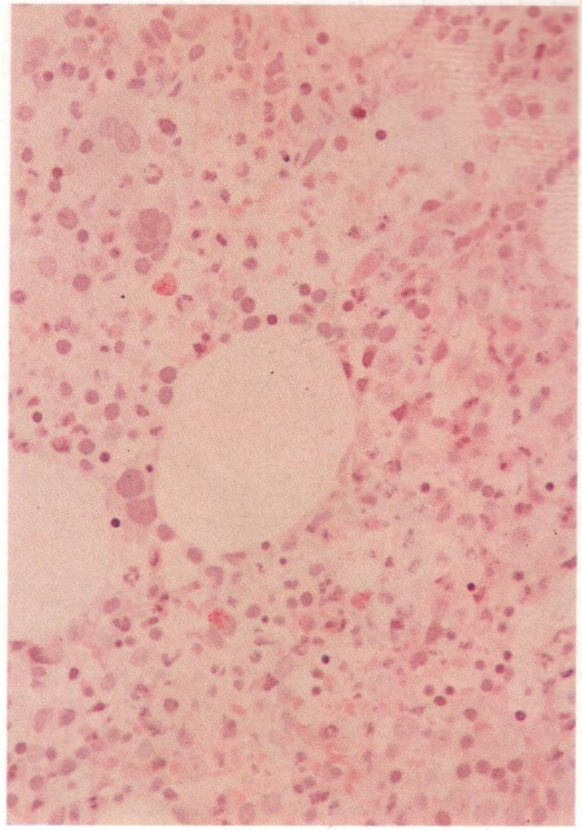

578–580. Two low-power views and a higher-power field, respectively, from a thin section of bone marrow trephine biopsy from a patient with MDS, showing RAEB with trilineage dysplasia. In **578** there is a generally pleomorphic picture with mononuclear megakaryocytes and others with multiple peripheral nuclei, an evident increase in early granulocytes – though with poorly granular cytoplasm – a few later neutrophils and eosinophils, and a scattered erythroblastic component with deeply stained compact nuclei. A broadly similar field is shown in **579**, but with several abnormal megakaryocytes having large single or double nuclei. In both these fields occasional cells with elongated nuclei suggest the presence of fibroblasts. The high-power view of **580** clearly illustrates the nucleolated myeloblasts which predominate, together with erythroblastic islands at top and bottom of the field showing some megaloblastic features, and various cells of the megakaryocyte line, including a binucleated cell at mid-centre left and a micromegakaryocyte at the right edge, a third up from the bottom.

580

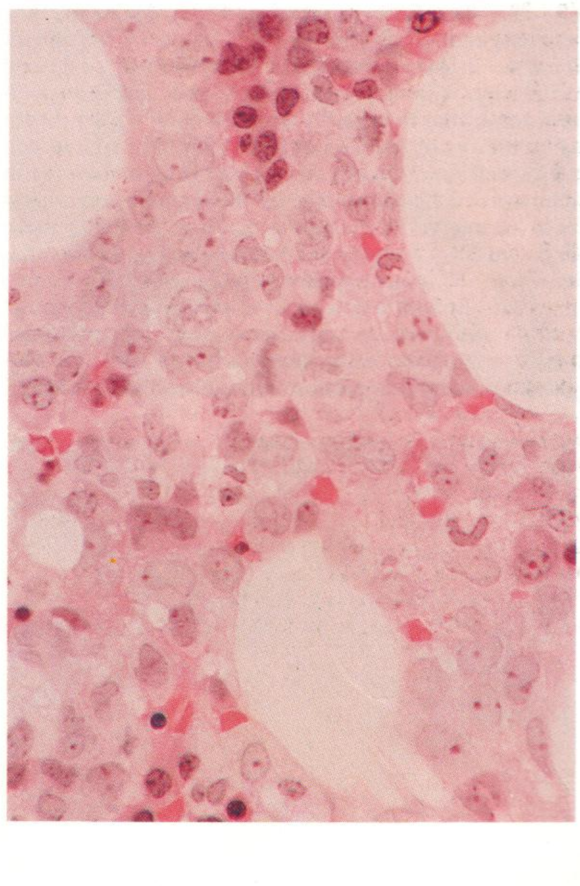

581

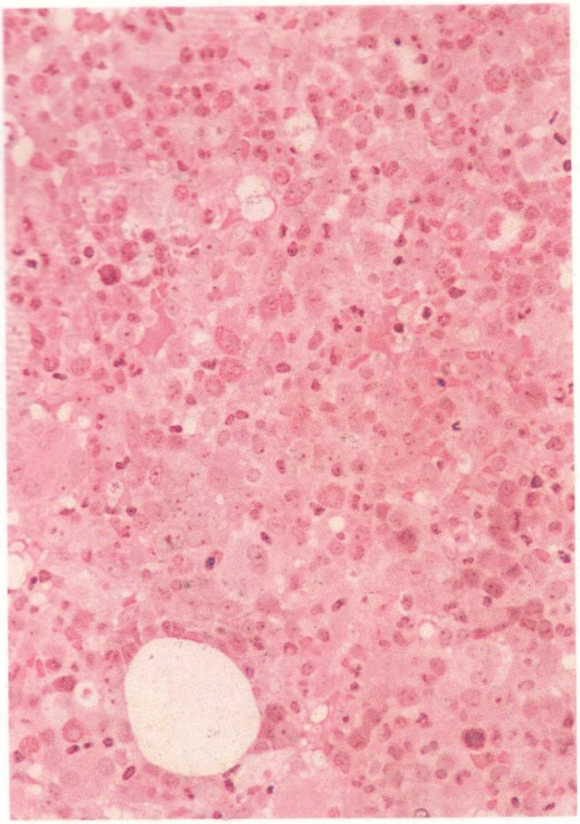

582

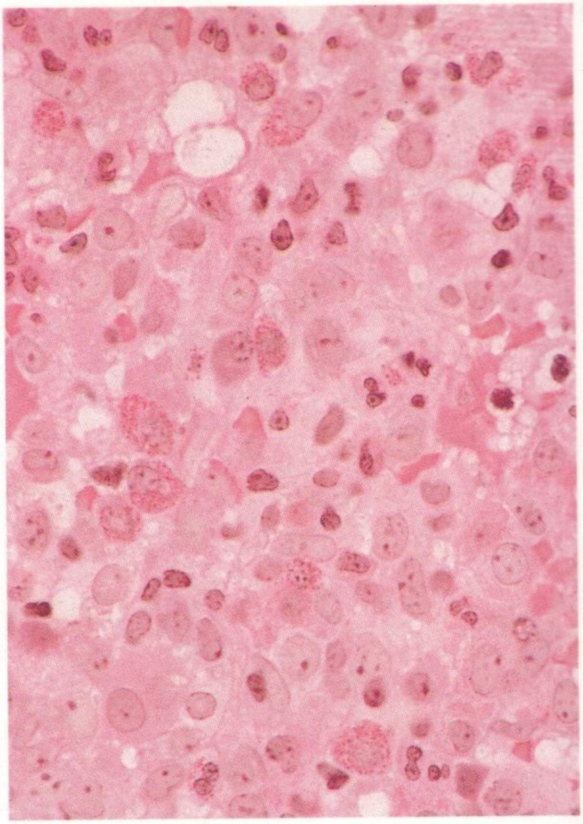

581–583. Two further examples of typical bone marrow trephine biopsy appearances in variants of MDS with increase in blasts (RAEB). Both show hyperplastic cellularity with few fat spaces and marked pleomorphism, the first case – with low- and higher-power fields shown in **581** and **582** – having all myeloid cell series well represented, but with an evident increase in immature cells, especially of the granulocyte series, both neutrophil and eosinophil, as revealed in more detail in **582**. The thicker section from another case shown in **583** is again highly cellular, with all cell series present, but with a conspicuous shift to the left in the granulocytes, with several clumps of nucleolated myeloblasts. Both these cases illustrate ALIP, possibly suggestive of early progression to florid trilineage AML.

583

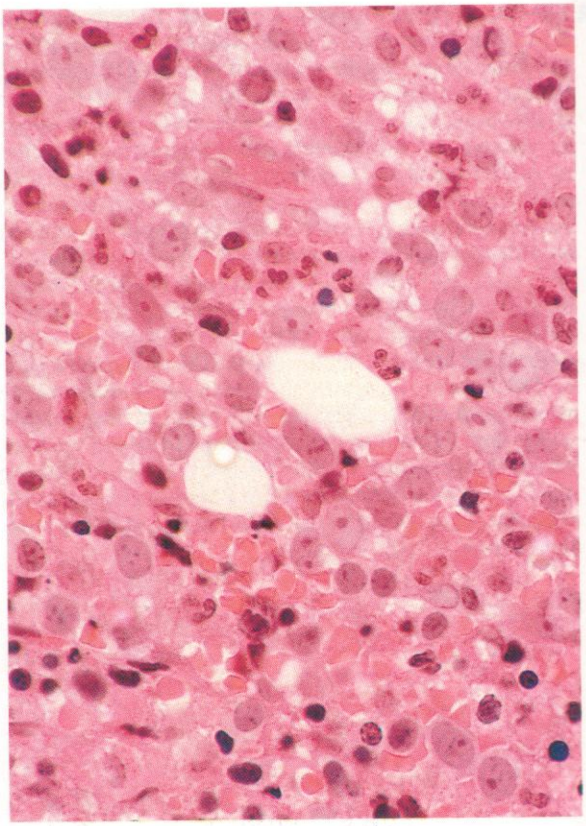

584

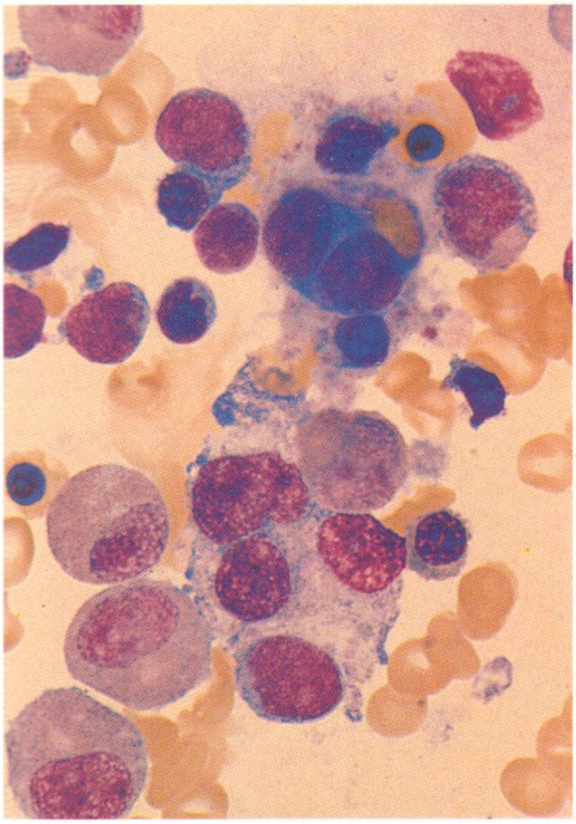

585

584–587. A succession of fields from bone marrow aspirates taken from patients with RAEB to demonstrate some of the common cytological and cytochemical features of dysplasia in the myelopoietic series seen in MDS. In **584** erythroblasts show irregular, twisted or fragmenting nuclei, there is an immature binucleated megakaryocyte with ingested red cells, and several neutrophil myelocytes show the yellow cytoplasmic colour and defective granulation often seen in myelodysplasia (cf. **561**). Figure **585** shows another slide from the same aspirate, stained with SB, where a dual population of granulocytes is apparent, with six strongly positive myelocytes or promyelocytes and three totally negative cells, a myeloblast, a promyelocyte or early myelocyte, and a neutrophil stab cell. Figures **586** and **587** are from slides of another bone marrow aspirate taken from a second patient with RAEB and stained respectively for peroxidase and with SB. In **586** a promyelocyte is strongly peroxidase-positive, while three poorly granular segmented neutrophils are quite negative. In **587** one neutrophil polymorph is normally sudanophilic, while two others show only weak scattered granular positivity.

586

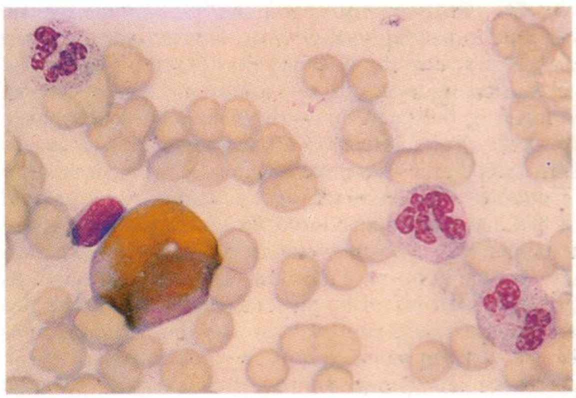

587

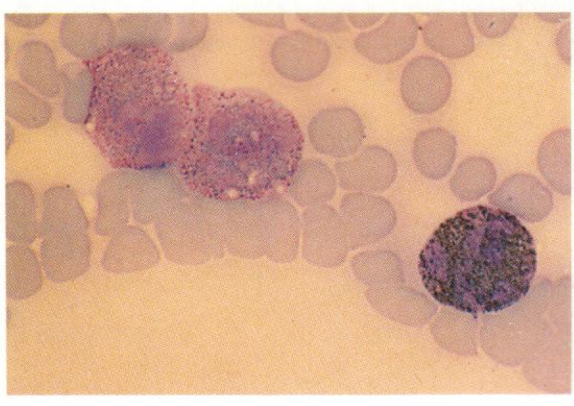

588

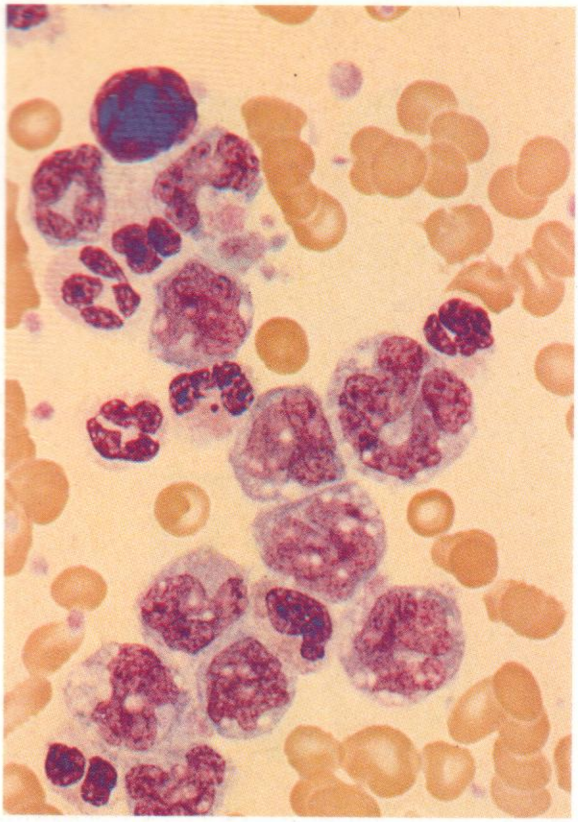

589

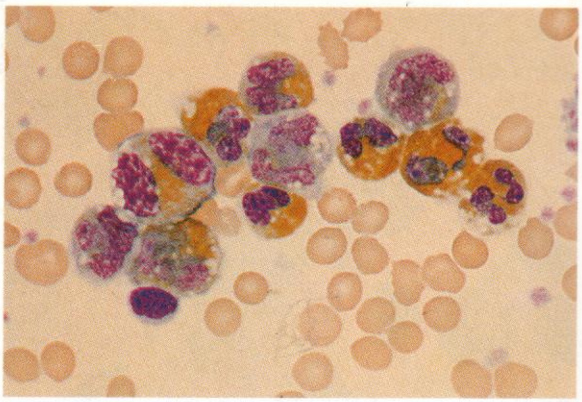

590

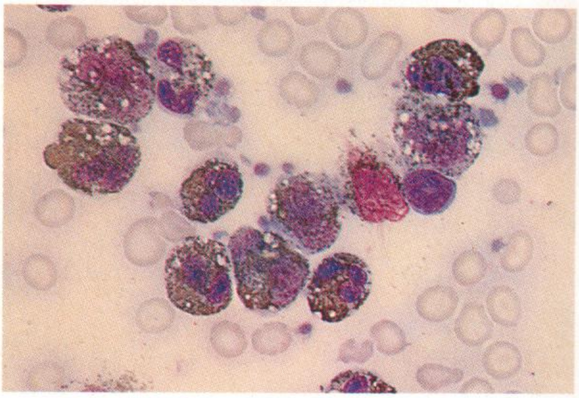

591

588–591. Buffy coat preparations from the peripheral blood of a patient with CMML, another variant often classified among the myelodysplastic states. The blood picture in this disorder shows a substantial monocytosis, commonly $5–10\times10^9/1$, and the monocytes may have markedly convoluted or hypersegmented nuclei, as illustrated here. There may also be occasional immature granulocytes in the blood, and, as at the top of the field in **588**, dysplastic megakaryocytes or naked nuclei, and irregular or giant platelets. In **589** and **590** the peroxidase content and SB reactions are revealed as generally normal for both granulocytes and monocytes in this case, although erratic staining is sometimes found, and monocytes may give negative or weak reactions. As shown in the dual esterase reaction depicted in **591**, the monocytes are usually strongly positive for BE, while neutrophils react normally for CE. There are two negatively reacting basophils in this field.

592

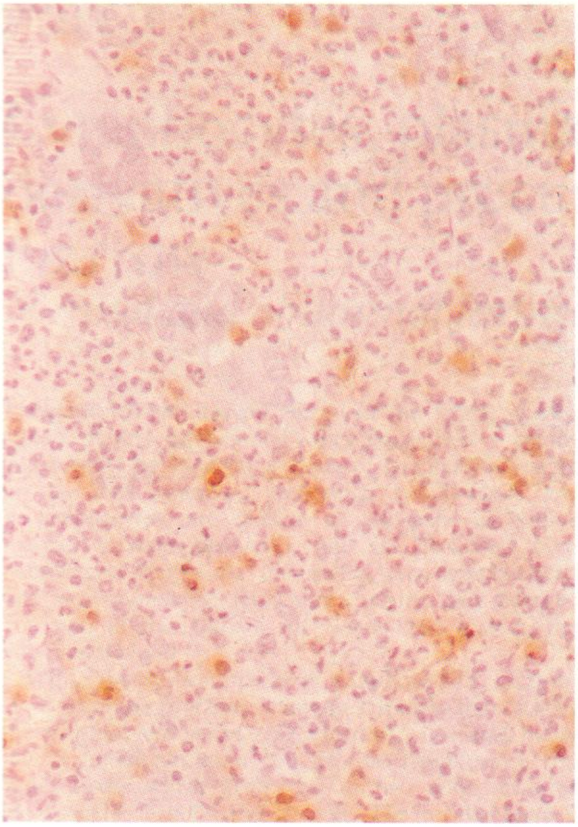

593

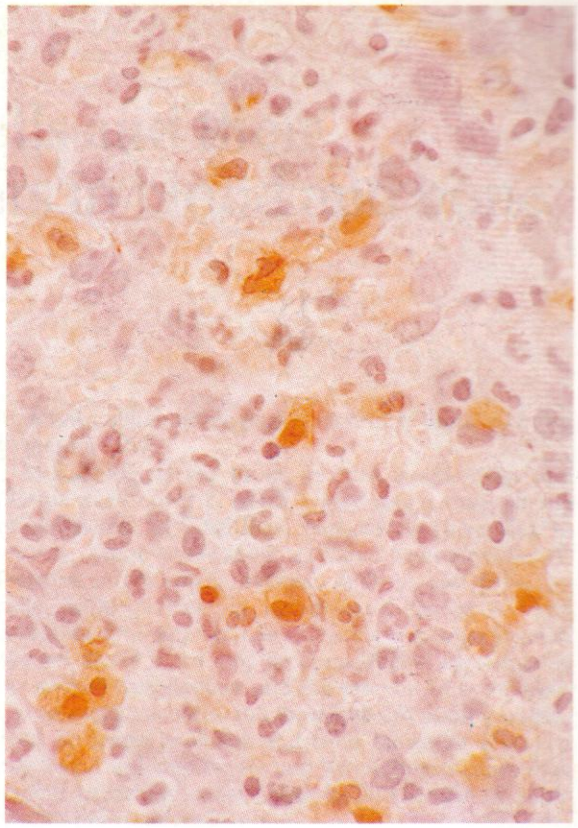

594

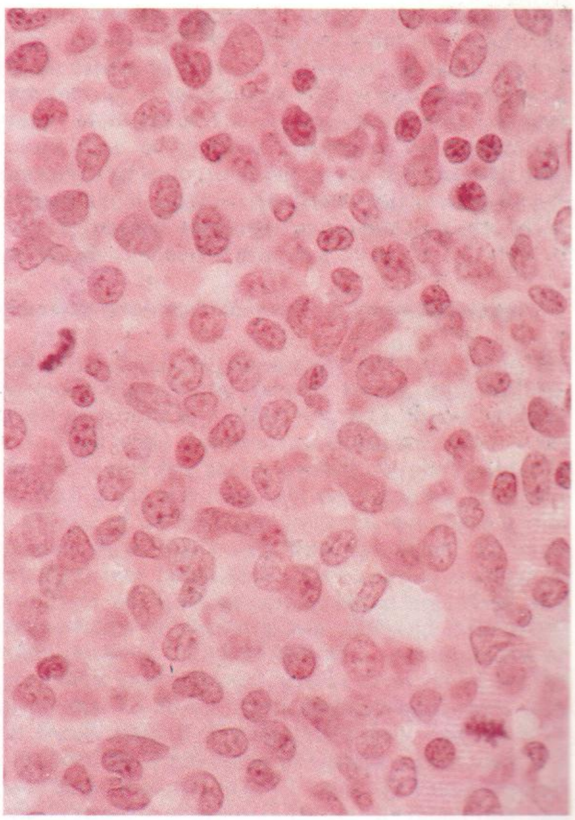

592 and **593**. The low- and higher-power views, respectively, shown here are from a bone marrow trephine biopsy taken from a patient with CMML and a similar peripheral blood picture to that illustrated in **588–591**. Monocytosis is usually evident in the marrow, but is less conspicuous than in the blood, and is accompanied by other features of MDS, including variable signs of trilineage dysplasia. The section illustrated here has been stained for the monocyte enzyme muramidase (lysozyme), which allows the monocyte component to be distinguished more clearly than is possible in simple H&E or Giemsa stains. In **592** several multinucleated megakaryocytes can be seen, and in **593** there is a pleomorphic picture with numerous granulocytes at different stages of maturation.

594. This section of a trephine biopsy is from a patient with a long-standing CMML, now transforming to a more florid acute leukaemia, with increasing numbers of blast cells in the blood. The histology shows an almost uniform replacement of marrow tissue with immature cells having promonocytic features, including relatively low nuclear–cytoplasmic ratio with poorly defined cytoplasmic outlines and occasional nuclear twisting or indentation. There are two mitotic figures visible.

Part 3

Lymphocytes, plasma cells and their derivatives and precursors in blood and bone marrow

Normal and abnormal forms

Lymphocytes are formed chiefly in the lymph glands, spleen, Peyers patches and other nodal sites – among which must be included nodules of lymphocytic nature in the bone marrow. Precursors, lymphoblasts and prolymphocytes, are difficult to recognize in normal marrow aspirates, however, and are illustrated from pathological conditions, principally acute lymphoblastic and prolymphocytic leukaemia, where they become common in the marrow and sometimes also in the peripheral blood.

While the earliest stages of lymphoid cell development from the probable common stem cell shared with the myeloid series are still uncertain, it seems likely that a functional stem cell for the lymphocytic cell series exists which gives rise to two main sorts of lymphocyte: T cells and B cells. The former have a special role in cell-mediated immune responses and may have helper (Tμ subset) or suppressor (Tγ subset) functions in relation to B-cell activity. B cells are largely responsible for humoral immune responses. These cells, and smaller groups of lymphocytes which seem to fall into different, less clear, categories are distinguishable by immunological means, but also have certain morphological and cytochemical differences which are illustrated in this section, and which are sometimes also manifest in neoplastic states.

Immunologically, T cells from the earliest stages of maturity show a capacity to form rosettes with sheep red cells, and react with the MAbs CD2, CD3 and CD7. The helper subset reacts also with CD4 and the suppressor subset with CD8. From an early stage, B-cell committed precursors show immunoglobulin gene rearrangements, expression of HLA-Dr and antigens reacting with CD19 and CD9. At a transient early phase of development they react also with CD10, and later transiently express cytoplasmic immunoglobulin (cIg) before producing surface membrane immunoglobulin (smIg). These features are all of importance in determining the stage of maturation at which neoplastic change emerges, and are especially valuable in classifying lymphoid leukaemias.

Under stimulation by phytohaemagglutinin normal T lymphocytes may undergo, *in vitro*, a process of dedifferentiation or transformation to produce primitive cells, with basophilic cytoplasm and leptochromatic nucleolated nuclei, able to divide. A similar transformation of B cells may occur following antigenic stimulation, and the primitive cells resulting may undergo further cytological transformation to give rise to plasma cells.

Morphological variations in both lymphocytes and plasma cells cover a much wider range than among granulocytes. In infections, particularly those due to viruses, lymphocytes show activated or immunoblastic features intermediate between mature and primitive cells, with increase in cytoplasmic basophilia, and sometimes the appearance of visible nucleoli. Even in normal blood there may be considerable variations in the size of lymphocytes and the amount of cytoplasm. Cytoplasmic vacuoles and inclusions are not infrequent. Fine or coarse granules and even blocks of glycogen may occur in lymphocytes and lymphoblasts, and often appear especially conspicuous in leukaemias or other lymphoproliferative states.

Plasma cells show even more abundant cytological variants, mostly connected, there is little doubt, with their production of immunoglobulins and the accumulation of part or the whole of these protein molecules in various morphological guises in the cytoplasm. Here again, the cytological variants are most conspicuous in multiple myeloma, the plasma-cell equivalent of leukaemia, but any of them may be seen occasionally in plasma cells from other conditions and even in normal marrows, and none appears to be specifically confined to myeloma.

Disorders involving chiefly cells of lymphoid lineage

Acute lymphoblastic leukaemias (ALLs). These are monoclonal neoplastic diseases arising from lymphoblastic precursors of lymphocytes. ALL makes up about 85% of all acute leukaemic cases occurring below the age of 16, and has been classified morphologically by the FAB group into three subtypes according principally to the size of the leukaemic cells: L1 cases have homogeneous small blasts with little cytoplasm, L2 cases heterogeneous larger blasts with variable amounts of cytoplasm, and L3 cases homogeneous large blasts with vacuolated basophilic cytoplasm. Although this classification does not correlate well with immunological or cytogenetic characteristics, except to an extent for the uncommon L3 group, which includes most cases with the B-cell marker of smIg production, and the 8;14 translocation, it has some prognostic significance, L2 cases doing less well than L1 cases. This may perhaps reflect the phase of proliferative activity rather than any

essential difference in cell type or origin, since cases presenting as L1 often show a change to L2 in relapse. The discriminating morphological features are nevertheless illustrated in subsequent figures and further described in their captions.

Immunologically, ALL can be subdivided into many different types, but there are five main groups: T-ALL derived from T-cell precursors (TdT+, CD3+, CD7+); 'null' ALL and C-ALL from early B-cell precursors (TdT+, CD19+ and respectively CD10– and CD10+); pre-B ALL from B precursors at a somewhat later stage (TdT+/–, cIgM+); and B-ALL from a still later stage of B-cell development (TdT–, smIg+). C-ALL makes up about 70% of childhood cases, T-ALL about 15%, null ALL about 12%, and B-ALL <2%. In adults, where only about 15% of acute leukaemias are lymphoblastic, C-ALL is relatively infrequent, comprising perhaps 40% of all cases, other early B and pre-B cases making up the difference. A small proportion of cases (<2%) with dubious or mixed reactions remain difficult to classify immunologically. Apart from the partial association of B-ALL immunology with L3 morphology, there are few distinguishing cytological features in parallel with the remaining subtypes, except for the presence of localized paranuclear dot positivity to acid phosphatase and less markedly to other acid hydrolases in T-ALL.

Cytogenetically, several non-random chromosomal abnormalities have been identified in ALL. These include t(9;22), occurring in nearly 20% of adult ALL cases, but in only about 5% of childhood cases; t(8;14) in most cases of B-ALL; t(1;19), t(v;12) and 6q– in a small proportion of early B-cell cases; t(4;11) in uncommon cases with a tendency to develop mixed lymphoblastic and monoblastic features; and t(11;14) in T-ALL. More important than these individual structural anomalies in terms of overall prognosis for the ALL group as a whole are chromosome numbers, hyperdiploidy with 50–60 chromosomes being associated with a relatively good response to treatment, diploidy and near haploidy with an intermediate one, and minor hypodiploidy or pseudodiploidy with most structural abnormalities a worse one.

Chronic lymphocytic leukaemia (CLL). This disease is rare before middle years and has an increasing incidence with rising age. There is a peripheral lymphocytosis usually over $15\times10^9/l$, with variable lymphadenopathy, splenomegaly, hepatomegaly and defects of marrow function manifest by anaemia and thrombocytopenia. The extent of these clinical features forms the basis of various staging systems, now in international use. Some 10% of patients with CLL also show a more or less severe auto-immune haemolytic anaemia with spherocytosis and a positive antiglobulin test. Hypogammaglobulinaemia is common, especially in more advanced stages of disease, and a monoclonal paraprotein may be produced, probably always in cases with a lymphoplasmacytoid component to the cytology of both peripheral blood and lymph nodes. CLL is usually a B-cell disease with CD19 positivity and at least weak expression of smIg, but a small proportion (<5%) of cases with CLL morphology and small agranular lymphocytes with non-convoluted nuclei show paranuclear focal acid phosphatase positivity, and react with the pan-T MAbs CD3 and CD7, and usually with CD4. These cases are classifiable as T-CLL and are to be distinguished from T-prolymphocytic leukaemia and also from CD8+ granular T-cell lymphocytosis, whether in an early non-malignant stage, or frankly neoplastic. They commonly show skin infiltration and a more aggressive clinical course than B-CLL.

Prolymphocytic leukaemia (PLL). This subacute and clinically intractable variant may emerge by a form of malignant progression in CLL, or may arise *de novo*, usually in association with gross splenomegaly and often also hepatomegaly. The peripheral cell count is usually very high, with prolymphocytic features of nucleolated but moderately pachychromatic nuclear chromatin and variable amounts of granular cytoplasm. Most cases of PLL show a B-cell phenotype, with stronger expression of smIg than in B-CLL, and with CD19 positivity, but up to 20% of cases have a T-cell phenotype, most often CD4+.

Hairy cell leukaemia (HCL) or leukaemic reticuloendotheliosis (LRE). This cytologically fascinating leukaemia of B-cell lineage occurs in middle years or later, four times as commonly in men as in women, and is associated with general malaise, splenomegaly, occasional abdominal lymphadenopathy, moderate anaemia, thrombocytopenia and neutropenia, and conspicuous monocytopenia. A few erythroblasts are usually to be found in the peripheral blood. The bone marrow is diffusely infiltrated with hairy cells (HCs) and also shows diffuse fibrosis, so that attempts at aspiration usually result in a dry tap. Trephine biopsies show a very characteristic picture, as illustrated in **767–772**. The HCs can be recognized and studied in blood smears or in buffy coat preparations (**748–766**); they have a striking and diagnostic cytological appearance in Romanowsky stains and have tartrate-resistant acid phosphatase (TRAP) positivity and typical PAS cytochemistry. The LAP score is notably high. Immunologically, HCs, like B-CLL cells, have receptors for C3b (CD11+) but, unlike CLL cells, not for C3d (CD21–). They express activation markers such as IL2 receptors (CD25+) and have certain relatively specific markers such as CD22 antigen, strongly present on HCs but only weakly present on a minority of normal B cells. Biochemically, the cells produce monoclonal Ig, and DNA analysis indicates the presence of clonal rearrangements of both light and heavy chain genes. All these features suggest that HCs are activated B cells, at a stage before maturation to plasma cells. HCL is of further unique interest in being the only haematological malignancy to show almost invariably a dramatic therapeutic response to the biological agent alpha-interferon.

Sézary syndrome (SS). This chronic T-cell neoplasm represents the leukaemic phase of mycosis fungoides, combining the skin infiltration, nodular and exfoliative dermatitis and epidermal Pautrier's microabscesses, with the presence of typical Sézary cells in the circulating blood. The characteristics of Sézary cells include, most importantly, a deeply convoluted or cerebriform nucleus, not always clearly manifest, although it may be suspected, in smears viewed under the light micro-

scope, but striking in electron microscopic preparations (cf. **776–788**). There is generally a high nuclear–cytoplasmic ratio, surface membrane reactivity with the pan-T MAb CD3 and usually with the helper cell marker CD4, although rarely with the suppressor cell marker CD8 instead. The cells are usually PAS-positive but rarely show localized acid phosphatase reaction. It seems likely that Sézary cells are the same as the convoluted T cells of mycosis fungoides, although the latter show some immunological differences, notably CD7 and CD25 positivity, suggesting that a possible activation effect may follow infiltration into the dermis.

Large granular lymphocytosis (LGL) and granular lymphocytic leukaemia (GLL). This chronic disorder with over 10×10^9/l large granular lymphocytes in the peripheral blood, associated with splenomegaly but little other organ involvement, may have a benign course when found as a response to various chronic infective or auto-immune conditions, but may also occur in an apparently primary neoplastic form when it is best regarded as a form of T-CLL. The large granular lymphocytes, with typically lymphocytic nuclei but with a moderately low nuclear–cytoplasmic ratio and fine scattered azurophilic granules in the cytoplasm, as illustrated in **643**, express the pan-T cell marker CD7 and are usually CD8+ve. They may have cytotoxic functions, including natural killer (NK) cell activity. They do not usually show focal paranuclear acid phosphatase positivity, but scattered granular reaction (**644**).

Adult T-cell leukaemia/lymphoma (ATL). This neoplastic disease has cytological features somewhat resembling, though more exaggerated than, those of SS, with circulating T cells having conspicuously convoluted nuclei, scattered acid phosphatase positivity, and an immunophenotype including CD3 and CD4 positivity, but unlike SS, the disease is due to infection with a retrovirus, human T-cell lymphotrophic virus 1 (HTLV1), and is largely restricted to certain areas in Japan and to Caribbeans of African descent. Clinically, the condition is associated with lymphadenopathy, hepatosplenomegaly and commonly hypercalcaemia, and generally pursues an acute aggressive course, although chronic forms exist.

Myeloma and Waldenström's macroglobulinaemia. These disorders involve a neoplastic growth of the plasma cells or lymphoplasmacytoid cells at the end of the B-cell maturation chain, with the formation and secretion of a monoclonal immunoglobulin or its component parts. In myeloma the plasma cells in any individual case are usually of a single clone (rarely biclonal), proliferating in and displacing the bone marrow and producing a specific Ig, biochemically and immunologically unique. This is usually IgG or IgA, rarely IgM and even more rarely IgD or IgE; but in about a third of cases, sometimes called Bence-Jones myeloma, only the light chain, kappa or lambda, is produced. There is associated bone destruction, due to increased osteoclastic activity, secondary to production by the neoplastic cells of an osteoclast activating factor (OAF). The histological picture in trephine biopsies is characteristic and the cytology in aspirates usually diagnostic, as illustrated in **798–830**, although individual cytological features such as multinuclearity, fragmenting cells, flaming cells, thesaurocytes, Mott cells, grape cells, cells with intranuclear or cytoplasmic inclusions and so forth are not in themselves indicative of neoplastic change, since any of them may be found in reactive plasmacytosis. An increase in plasma cells above 20% in the bone marrow, or a smaller increase with demonstrable light chain restriction, provides acceptable evidence of myeloma, confirmed when taken in conjunction with X-ray evidence of osteolytic lesions and the demonstration of a circulating monoclonal paraprotein.

Clinically, the bony destruction often leads to hypercalcaemia, and myelomatous infiltration of the kidney frequently produces renal failure and uraemia. Blood findings include a raised ESR and variable anaemia, but plasma cells are not often seen, except occasionally in buffy coat preparations, and leucocytes and platelets are generally present in normal numbers, although there may be a mild leucoerythroblastic picture with infrequent erythroblasts and myelocytes detectable. Levels of serum beta2 microglobulin become increasingly elevated with advancing disease and probably provide the best single prognostic index, although the degree of anaemia and of renal failure are also of prognostic importance.

Waldenström's macroglobulinaemia is a form of lymphoplasmacytoid immunocytoma with bone marrow involvement and production of a circulating monoclonal IgM paraprotein. As in myeloma, there is usually a high ESR and moderate-to-severe anaemia, but leucocytes and platelets are generally normal. The bone marrow shows infiltration with lymphoplasmacytoid cells and commonly an increase in macrophage iron and in tissue mast cells, manifest in both aspirates (**834–842** and **844**) and histological sections (**843** and **845–851**), where the large intranuclear inclusions known as Dutcher bodies and characteristic of this disease may also be conspicuous. Clinically, the course is generally more indolent than that of myeloma, and there is more resemblance to a low-grade non-Hodgkin's lymphoma, with lymphadenopathy and some degree of hepatosplenomegaly more often found.

Lymphoma. This malignant disease arising in lymph nodes and involving cells of more or less mature degree in the lymphocytic line, commonly extends at some stage to involve the bone marrow and to liberate abnormal lymphocytes in the peripheral blood. If the cell type is mature the disease is cytologically indistinguishable from chronic lymphocytic leukaemia (CLL), and, if very primitive, as it may be in children especially, it is equally indistinguishable from acute T- or B-cell lymphoblastic leukaemia. In some cases, however, abnormal 'lymphoma cells', unlike either mature lymphocytes or the lymphoblasts of acute leukaemia but with characteristics intermediate between the two, may be seen. These cells are usually of the B-cell line but may be of T-cell lineage and include neoplastic variants of the centrocytes, centroblasts and immunoblasts present in lymph nodes and illustrated more fully in Part 5.

The cytology and cytochemistry of all these normal and abnormal variants as seen in blood and marrow are illustrated in the following pages.

595

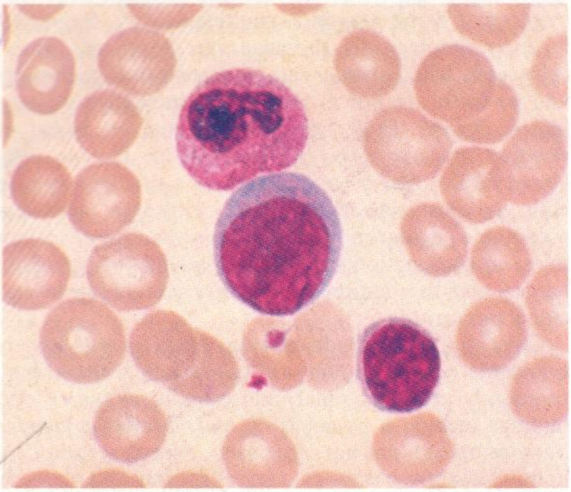

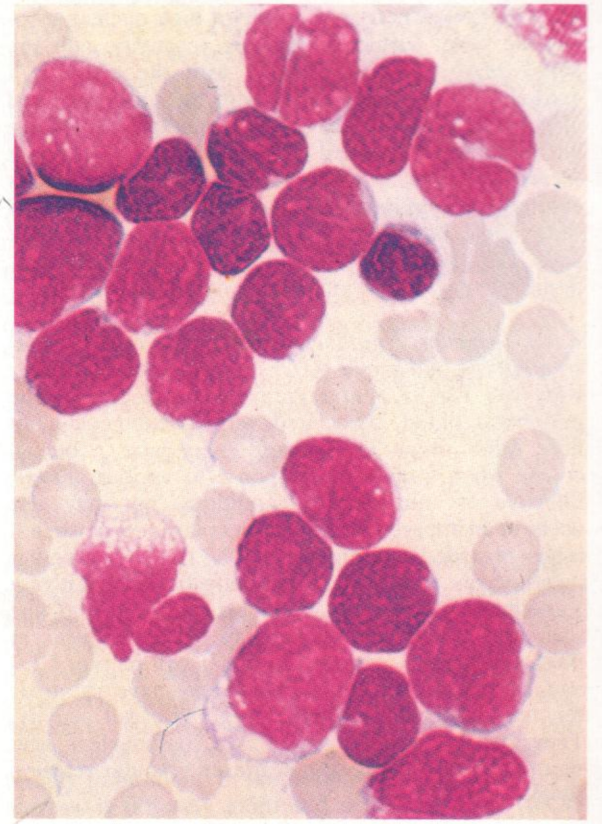

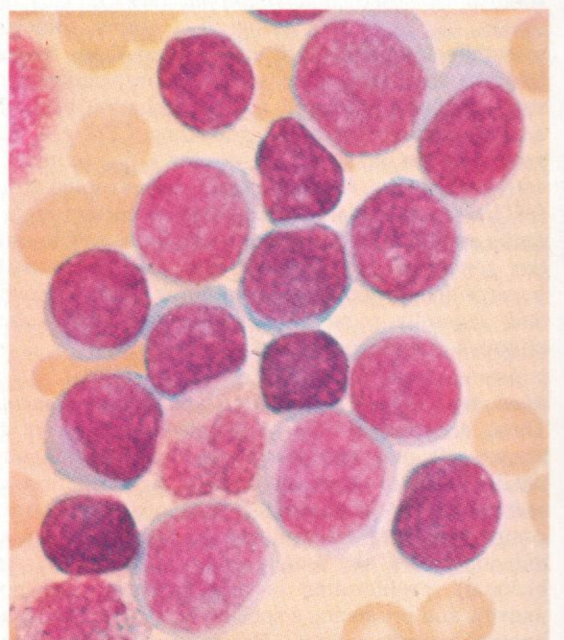

***595–639**. Acute lymphoblastic leukaemia (ALL), including examples of the range of morphology classifiable under the FAB system as L1 (small blast cells with high nuclear–cytoplasmic ratio, regular nuclear outlines apart from possible Rieder cell formation, and poorly visible nucleoli) (**596** and **598–609**), as L2 (cells generally larger, with relatively more cytoplasm, more indentations in nuclear outline and more easily visible nucleoli) (**597** and **610–612**), or as L3 (large cells with regular nuclear outlines and homogeneous nuclear chromatin with readily visible nucleoli, and with ample basophilic cytoplasm sometimes containing vacuoles) (**625–629**). Immunophenotypes correlate poorly with morphology, apart from an association between L3 and B-ALL and cytochemical paranuclear localization of acid phosphatase positivity in blasts of T-ALL.*

595. A lymphoblast with a mature lymphocyte and a stab cell, from the peripheral blood of a patient with ALL.

596. Lymphoblasts from the common type of non-T non-B acute lymphoblastic leukaemia (C-ALL), showing the high nuclear–cytoplasmic ratio and occasional nuclear cleavage – Rieder cell formation. There are a few mature lymphocytes and some intermediate 'prolymphocytes' present. Despite the nuclear cleavage this cytological picture is probably best classified as L1.

597. Another example of C-ALL. There are two granulocytic cells present – a metamyelocyte and an eosinophil myelocyte – and also some cells with denser nuclei maturing along the lymphocytic line. This field illustrates the difficulty of achieving the certain allocation of acute leukaemia to a specific type based on the appearances in Romanowsky stains alone. Cytochemical staining in this case gave the typical findings shown in the following figures and established the diagnosis unequivocally. Although the cell size is much the same as in **596**, the lower nuclear–cytoplasmic ratio and more conspicuous nucleoli conform with the criteria for L2.

598

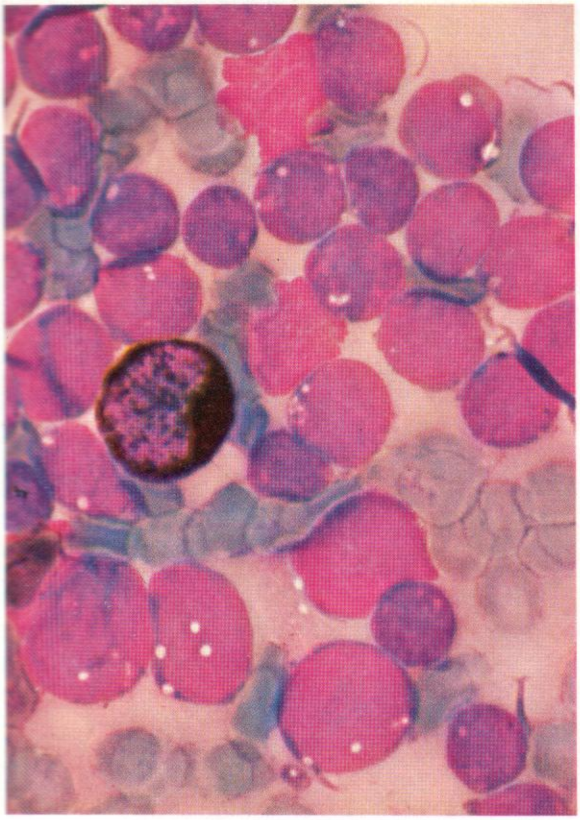

599

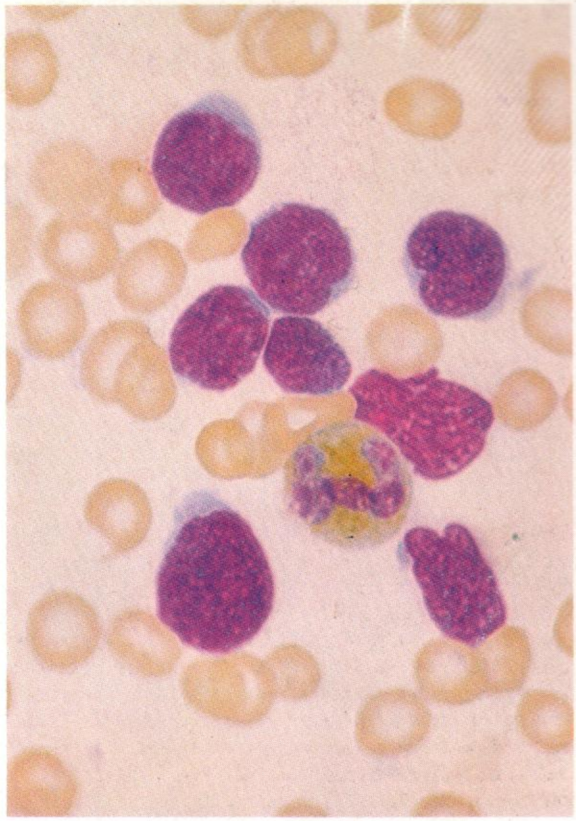

600

598. SB stain in C-ALL. There is a myelocyte with normal positivity present (for contrast), but the lymphoblasts and occasionally more mature cells of the lymphocyte line are uniformly negative. As well as the high nuclear–cytoplasmic ratio, occasional vacuolation can be seen.

599. Peroxidase reaction in C-ALL. Lymphoblasts are uniformly negative. A polymorph present is normally positive.

600. PAS stain in acute lymphoblastic leukaemia (C-ALL). The lymphoblasts mostly show numerous fine and coarse granules of positivity. Note that the erythroblasts present are negative – unlike those forming an erythraemic component in mixed myeloid leukaemias. A single myelocyte shows normal diffuse but weak PAS positivity.

601

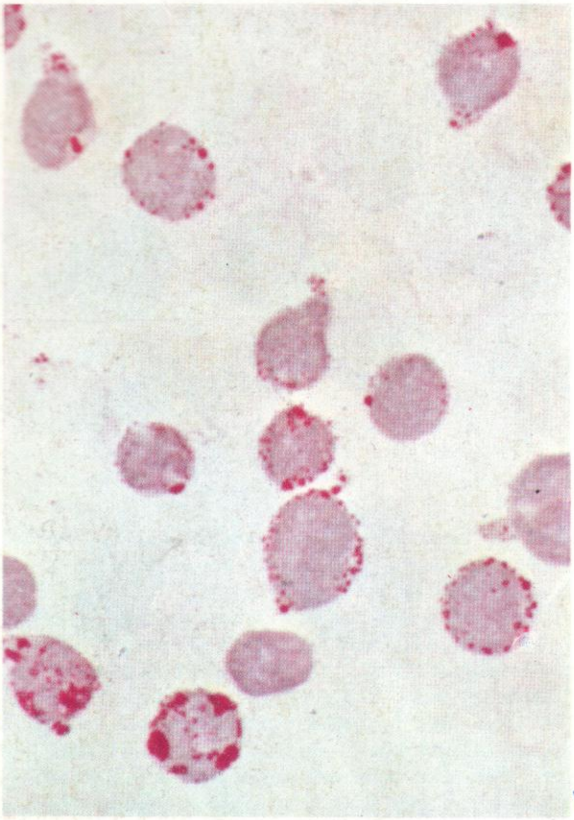

602

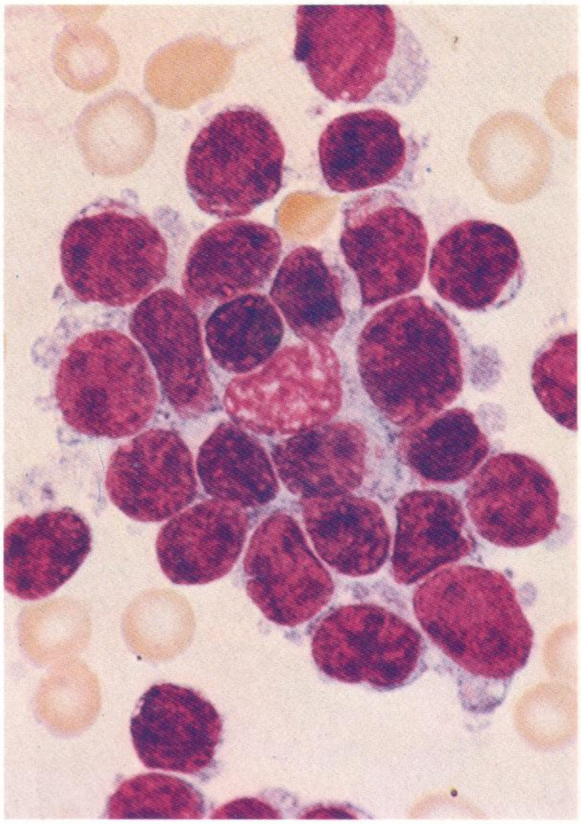

601. Another example of PAS staining in ALL. In this case some cells contain blocks in addition to coarse granules.

602. A group of lymphoblasts from C-ALL. The cytoplasm shows frequent irregularities of staining and occasional vacuoles, particularly in cytoplasmic buds.

603. The same field as above, consecutively stained with the PAS reaction. Most of the lymphoblasts contain coarse granules of PAS-positive material, often coinciding with vacuoles or areas of lighter staining within the cytoplasm and, especially, in cytoplasmic protuberances – as shown in **602**.

603

604

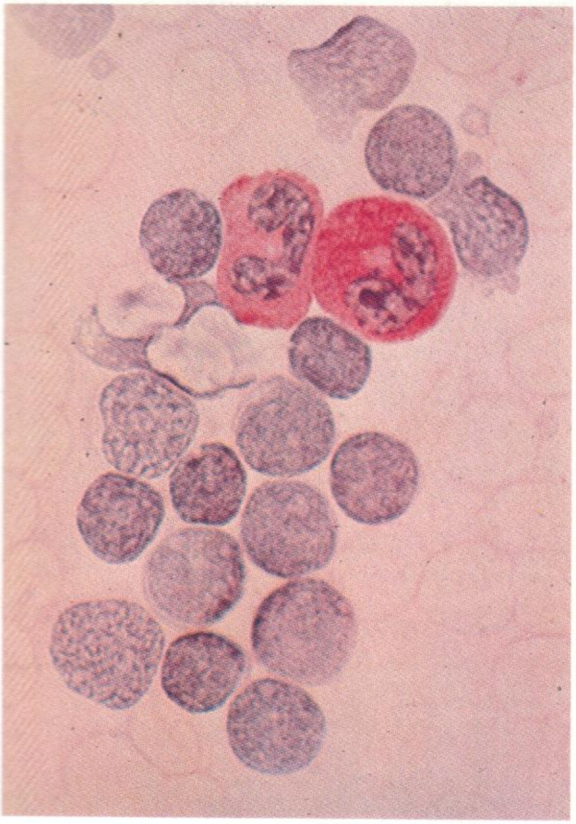

605

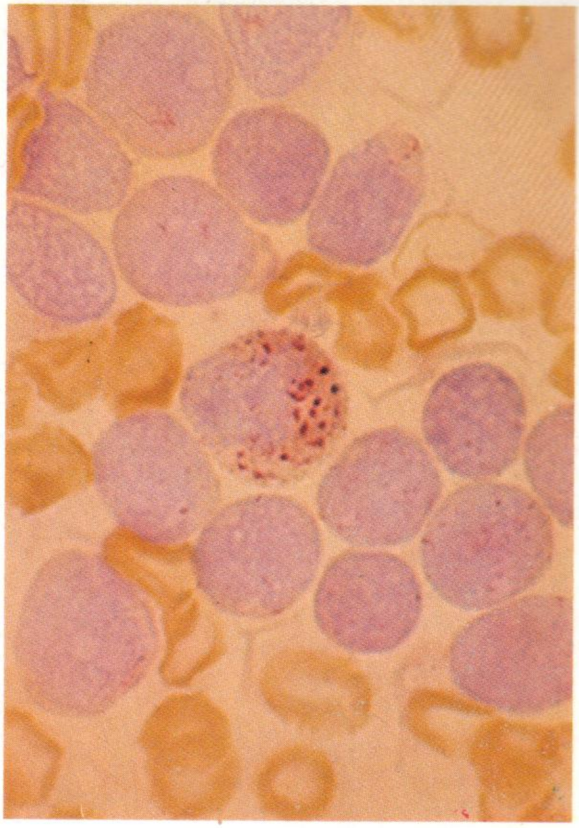

606

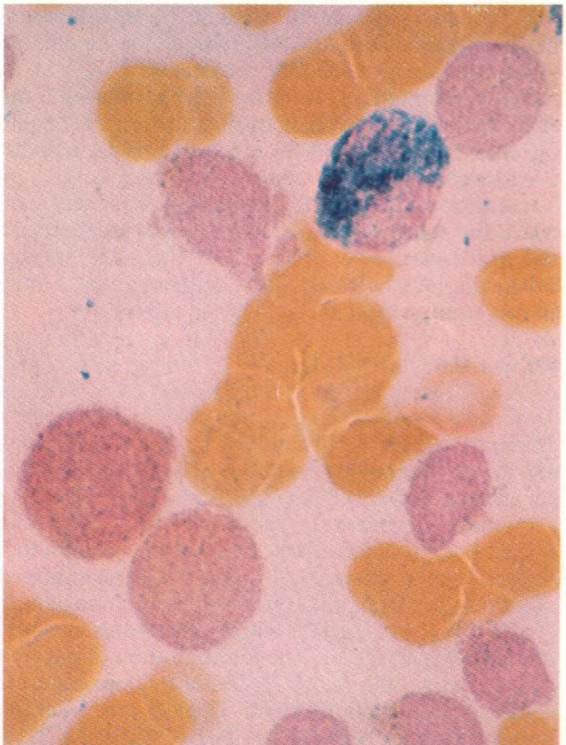

604. PAS reaction in a further case of C-ALL with minimal positivity. Even such almost entirely negative lymphoblasts commonly show some granular positivity in a very occasional cell. Weak reactions are perhaps commoner in T-cell cases, but this is not a very useful discriminatory feature since much variation exists.

605. Acid phosphatase reaction in the same case, showing little positivity, typically for C-ALL. There is a normally positive polymorph present.

606. Dual esterase reaction with weak scattered butyrate esterase (BE) positivity in lymphoblasts of C-ALL. This pattern is usual in non-B non-T cases.

607

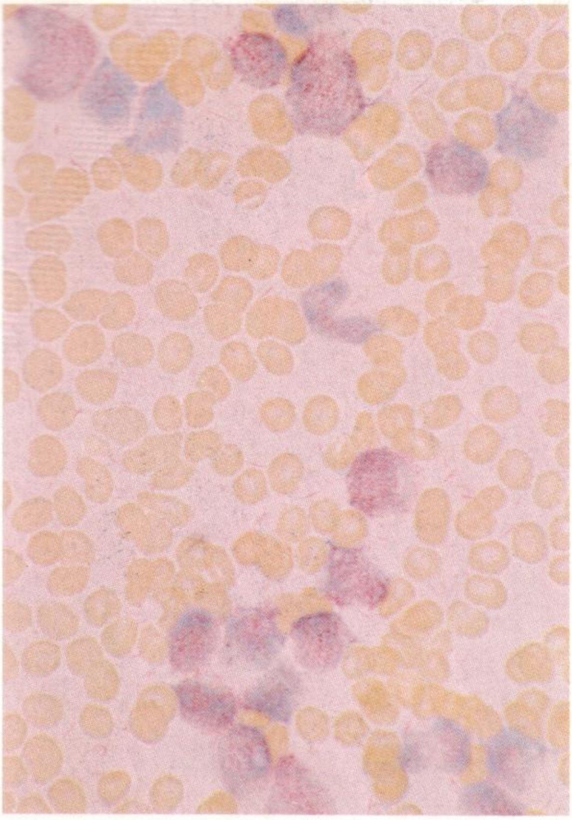

608

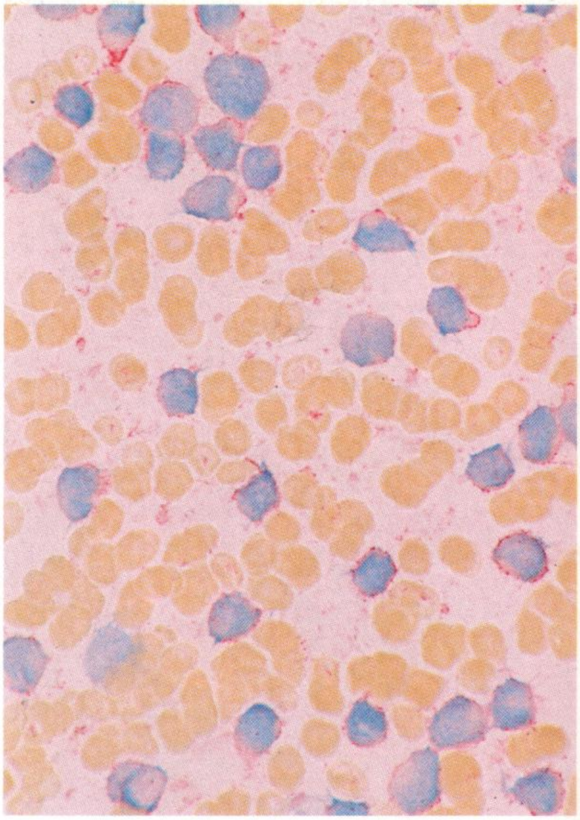

609

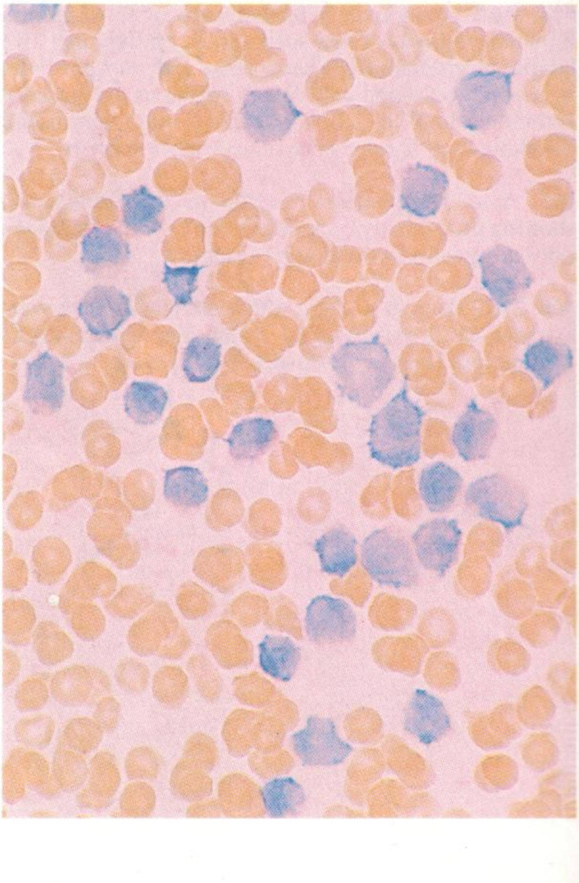

607. Immunocytochemical alkaline phosphatase-anti-alkaline phosphatase (APAAP) reaction for the presence of terminal deoxynucleotide transferase (TdT) in the nuclei of lymphoblasts from the bone marrow in a case of C-ALL. Nuclear TdT is demonstrable in the primitive cells of more than 90% of cases of ALL, including C-ALL, null ALL, most pre-B ALL, and T-ALL, but is absent from B-ALL. TdT positivity in acute leukaemic cells is not confined to ALL, however, being detectable also in the blast cells of around 20% of acute myeloid leukaemia (AML) cases, most of them with no other feature to suggest mixed phenotypic expression.

608 and **609**. Further examples of immunocytochemical APAAP reactions on lymphoblasts of C-ALL to demonstrate surface antigens of discriminative value in differential diagnosis. A positive reaction is shown in **608** to the monoclonal antibody (MAb) CD10, and a negative reaction in **609** to the myeloid MAb CD13.

Immunocytochemical reactions for cell-surface antigens are not illustrated extensively in relation to all the varieties of leukaemia because the appearances do not reveal important differences in distribution patterns of positivity, cells being simply positive or negative, whatever MAb is used. The interpretation of positivity patterns with different MAbs therefore depends essentially on the captions, with C-ALL, for example, showing typically cells that are TdT+, CD10+, CD19+ and CD3–, CD13–.

610

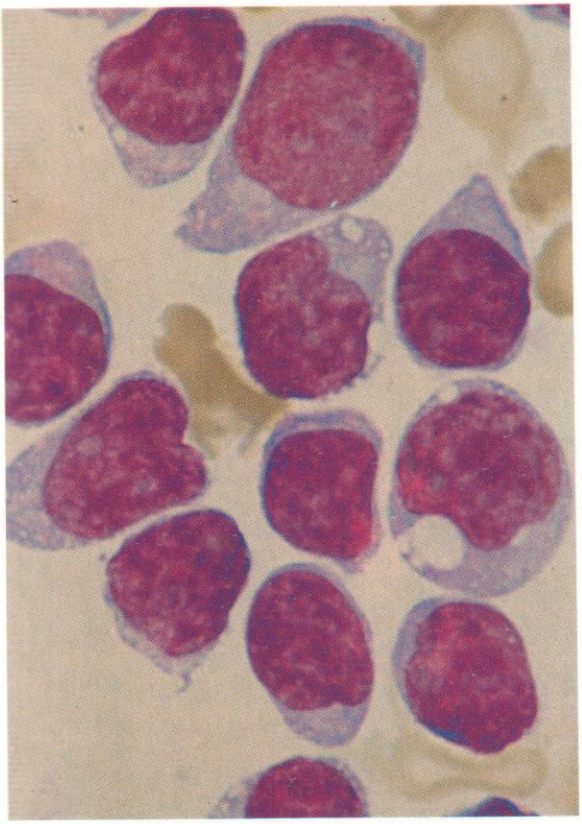

611

610. Romanowsky stain on bone marrow cells from an adult case of null ALL (TdT+, CD19+, CD10–, CD3–, CD13–), showing, more clearly than in the earlier **597**, the pattern of larger cell size, lower nuclear–cytoplasmic ratio, more easily visible nucleoli and occasional indentation of nuclear outline that is classifiable under the FAB system as the L2 variant.

This variant is seen in adults more often than in children, at least at the time of diagnosis, and carries a poorer prognosis than the more common L1 variant. There is no correlation, however, between immunological phenotype and L1 or L2 morphology, and cases initially classed as L1 may show an L2 picture at relapse.

611. SB stain on the same marrow sample, showing a positive myelocyte but negative reactions in the remaining blast cells.

612. Another example of an ALL bone marrow aspirate to illustrate the frequent difficulty in applying the FAB classification. The cells are generally large with moderate nuclear–cytoplasmic ratio, regular nuclear outlines, some conspicuous nucleoli, and moderately basophilic cytoplasm with scattered vacuoles. This appearance conforms best to L3, but immunophenotyping revealed a pattern of null ALL as in the previous case, and reclassification as L2 was thought appropriate.

612

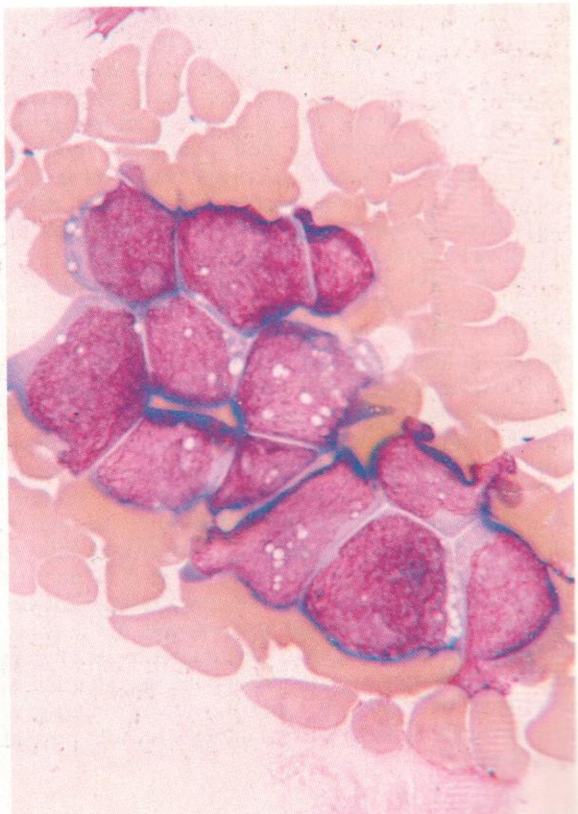

613

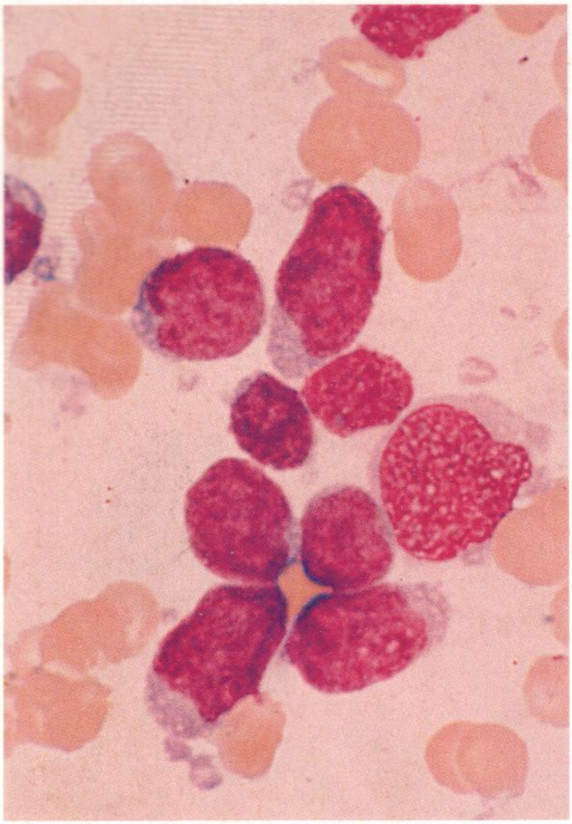

614

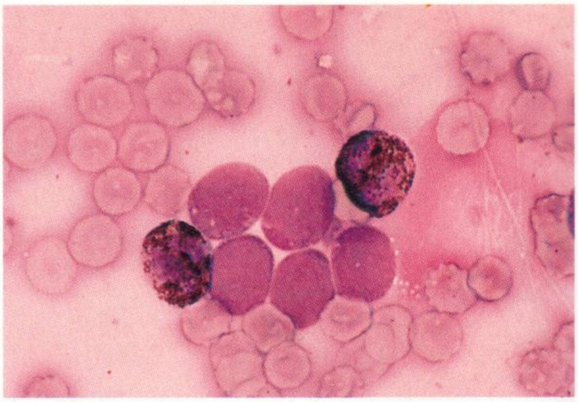

615

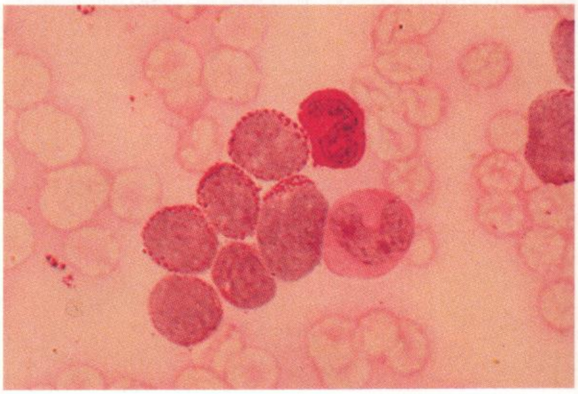

616

617

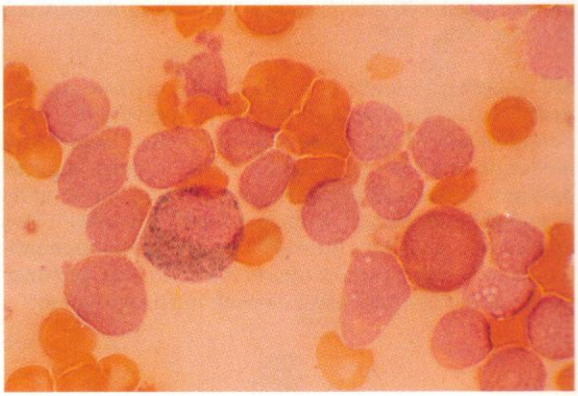

613–617. Cytology and cytochemistry of aspirated bone marrow from a case of pre-B ALL (TdT+, CD19+, CD10+, cIgM+). The Romanowsky stain in **613** shows considerable variation in cell size and irregularity of cytoplasmic outlines, with a scattering of peripheral cytoplasmic fragments, and variable nuclear–cytoplasmic ratio. Several cells show two or three small nucleoli. The cytoplasm is generally basophilic, with a suggestion of vacuole formation, and in this area the appearances would be consistent with L2 or L3.

The SB-stained field (**614**) and the remaining cytochemical stains (**615–617**) from the same preparation, however, show much more uniform cytology with smooth nuclear chromatin, regular nuclear membranes, poorly visible nucleoli, and no more than a minimal rim of cytoplasm, generally more consistent with an L1 classification. Sudanophilic granulocyte precursors are present in **614**, and a neutrophil metamyelocyte and polymorph with typical PAS positivity in **615**, although the blast cells in each of these fields have the characteristic reactions of lymphoblasts, negative to SB and with coarsely granular positivity to PAS. The acid phosphatase reaction in **616** shows scattered positivity in a neutrophil stab cell and a polymorph, but the blast cells are essentially negative. The dual esterase stain in **617** is also negative in the lymphoblasts, although a chloroacetate esterase (CE)-positive neutrophil myelocyte and a BE-positive monocyte are also present in this field.

618

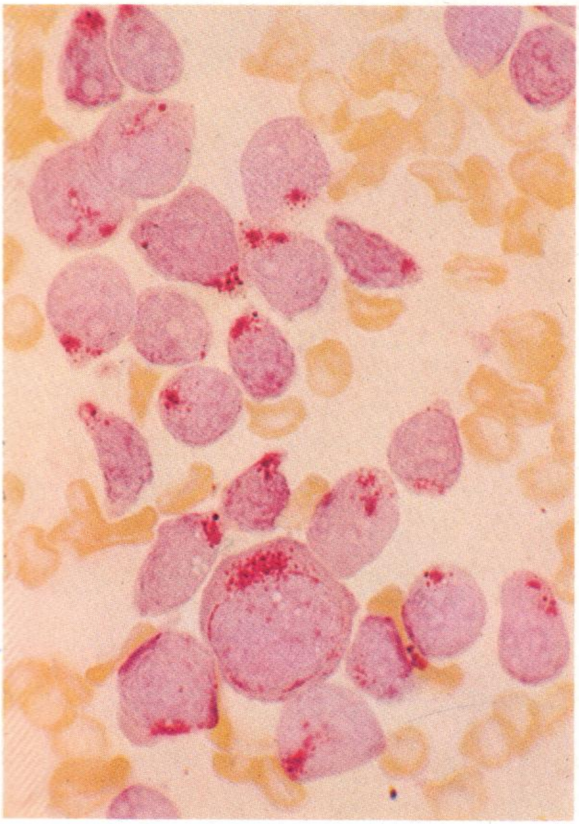

619

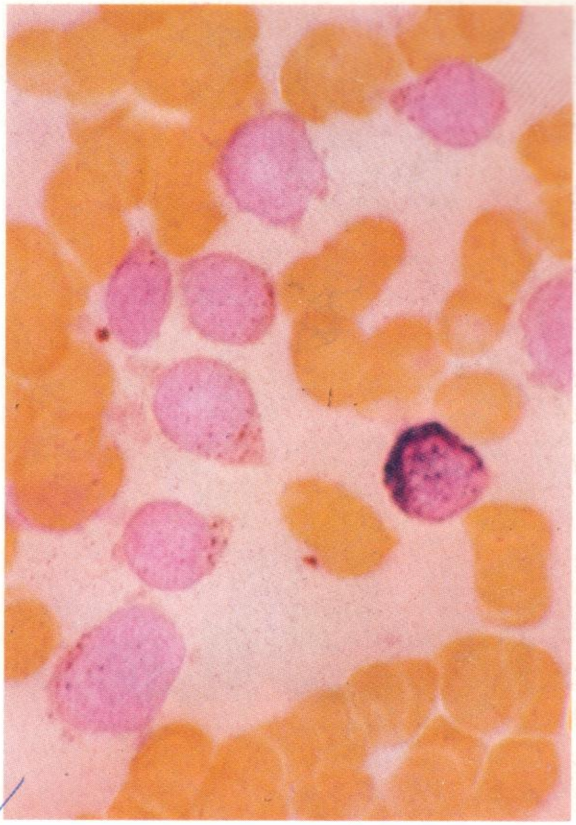

618. Acid phosphatase reaction in a T-cell ALL, showing the strong localized paranuclear positivity in most lymphoblasts characteristic of this ALL variant. Such positivity is much less commonly found in C-ALL and null-cell ALL, and is absent in only a small minority of cases of T-ALL.

619. Dual esterase reaction, showing localized BE positivity in lymphoblasts of T-cell ALL.

620. Scattered BE positivity in lymphoblasts, with a tendency to localization on one side of the nucleus (less striking than in **619**). This pattern suggests a T-cell lineage, but the cells are in fact from a C-ALL case.

620

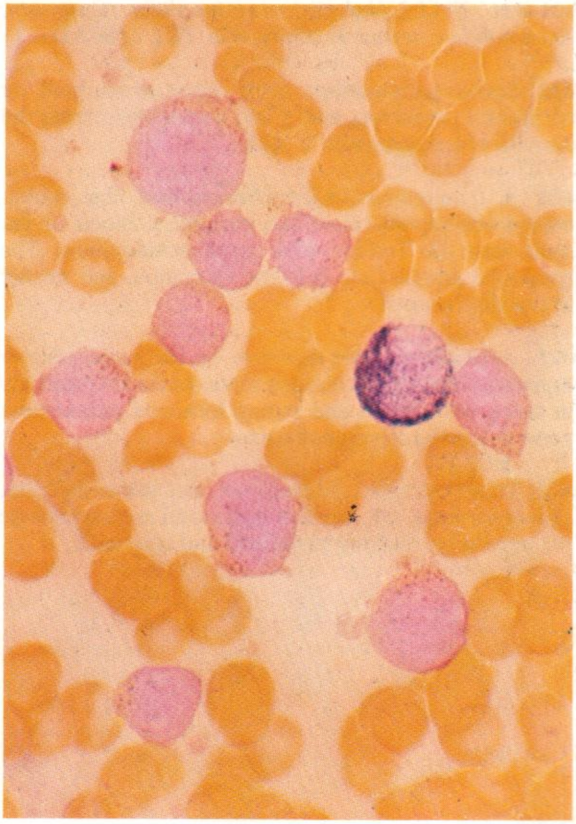

621

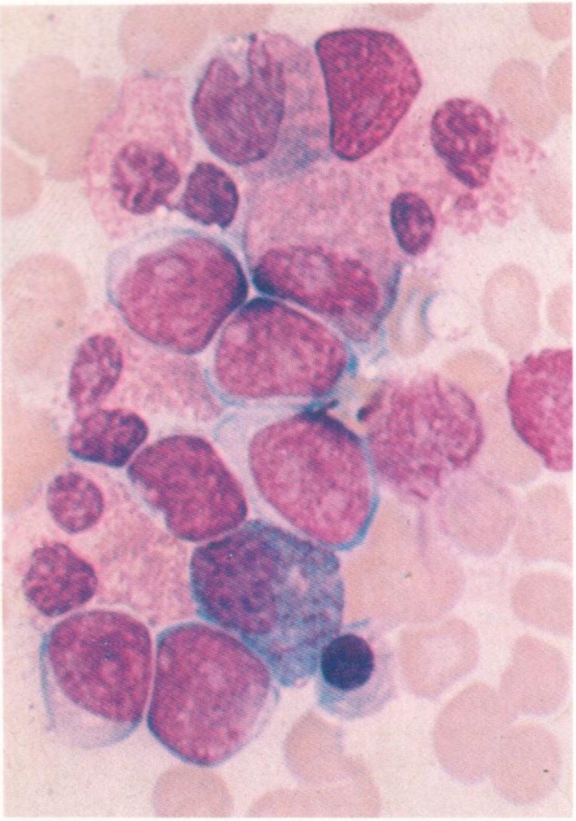

622

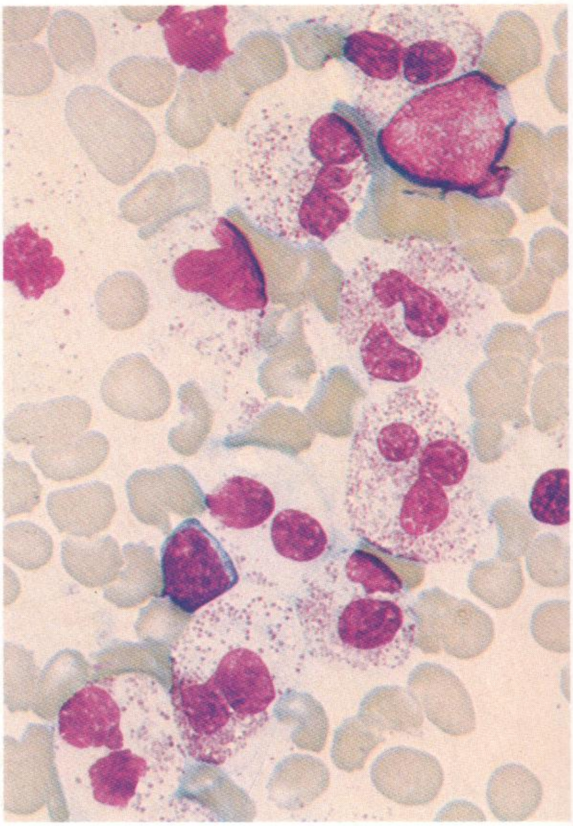

621–624. *T-ALL plus marked eosinophilia. (Curiously, eosinophilia is at least as common in ALL as in AML.)*

621. Seven lymphoblasts with seven eosinophil or eosinophil precursors and a late normoblast; from the marrow of a patient with T-ALL.

622. A lymphoblast, a lymphocyte and nine pathological eosinophils; from the peripheral blood of the same case of T-ALL with gross eosinophilia. The eosinophil granules are defective in number and smaller in size than normal.

623. Acid phosphatase reaction on the same marrow aspirate, showing scattered granules of coarse positivity in three eosinophils and strong localized paranuclear positivity in the T lymphoblasts.

624. Dual esterase reaction on the same aspirate, showing a single CE-positive neutrophil metamyelocyte but negatively reacting eosinophil and blast cells.

623

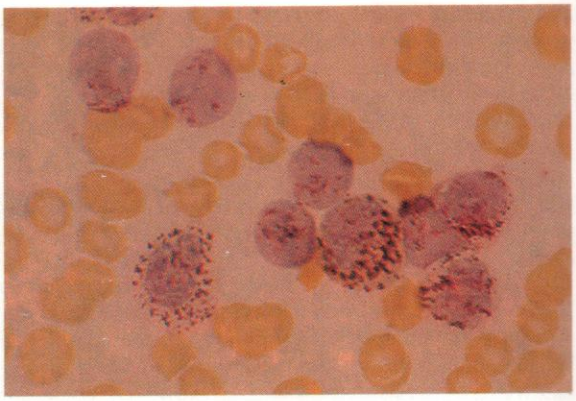

624

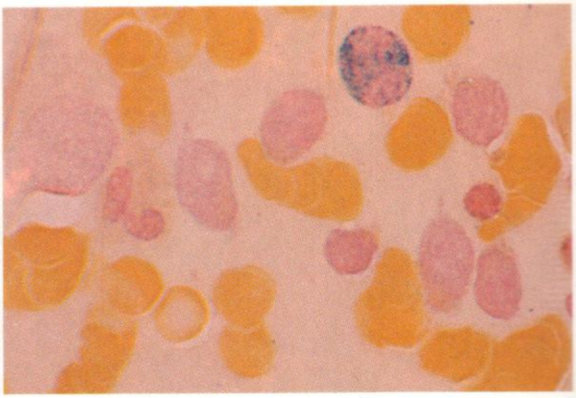

625

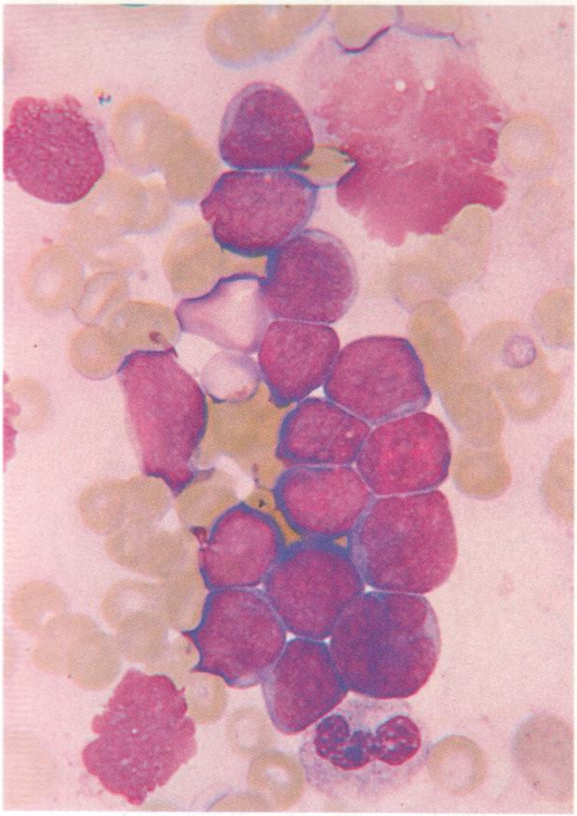

626

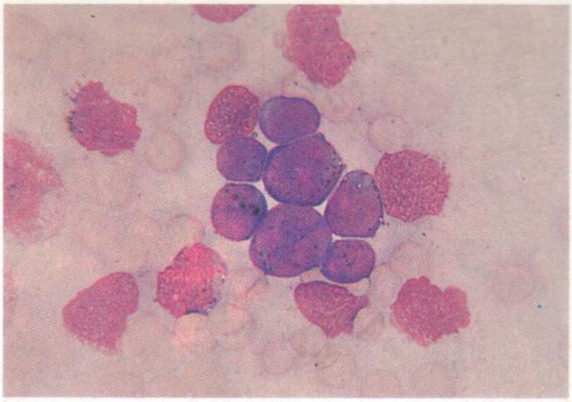

627

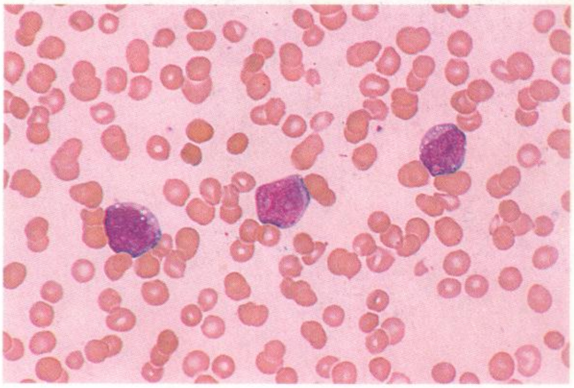

628

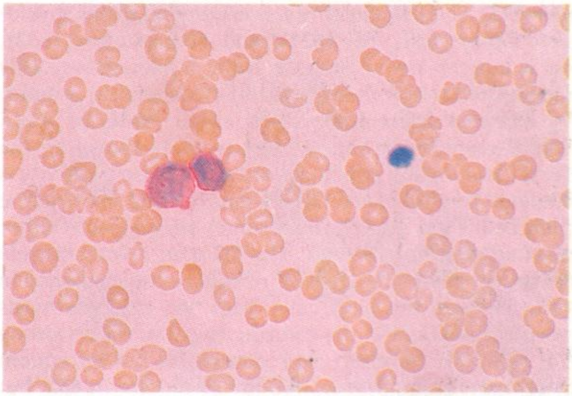

629

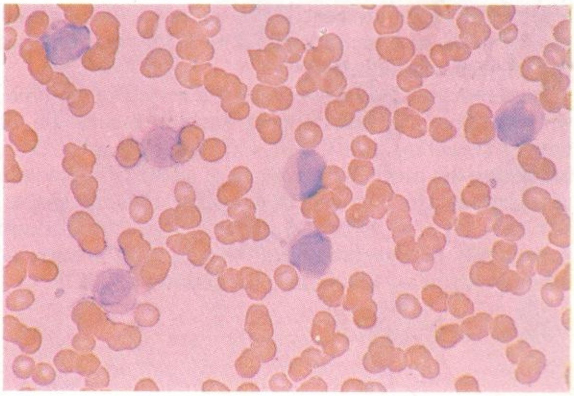

625–629. Bone marrow and blood smear preparations from an adult patient with B-ALL. The Heyl stain in **625** shows a clump of marrow cells with moderate size, visible nucleoli, somewhat irregular nuclear outlines, high nuclear–cytoplasmic ratio, and basophilic but minimal cytoplasm, difficult to classify on the FAB system. There were numerous smear cells present. The SB stain (**626**) showed the unusual pattern of coarsely granular, globular sudanophilia found in <2% of ALL cases.

The B lymphoblasts in the peripheral blood from this patient show a more typical L3 cytology than the marrow blasts, with a greater amount of basophilic vacuolated cytoplasm, as seen in **627**, while the immunocytochemical APAAP reactions show positivity to CD19 in **628** and negativity to CD10 in **629**. The cells were TdT– and smIg+.

630

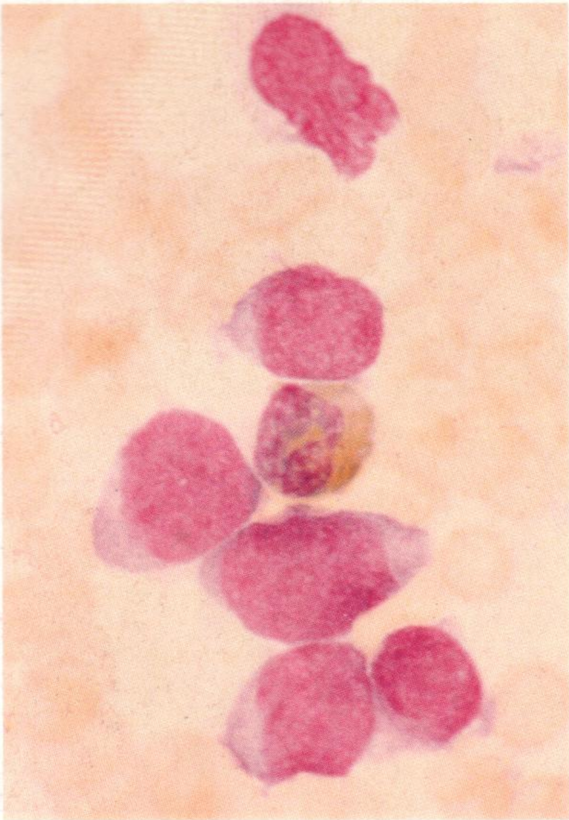

631

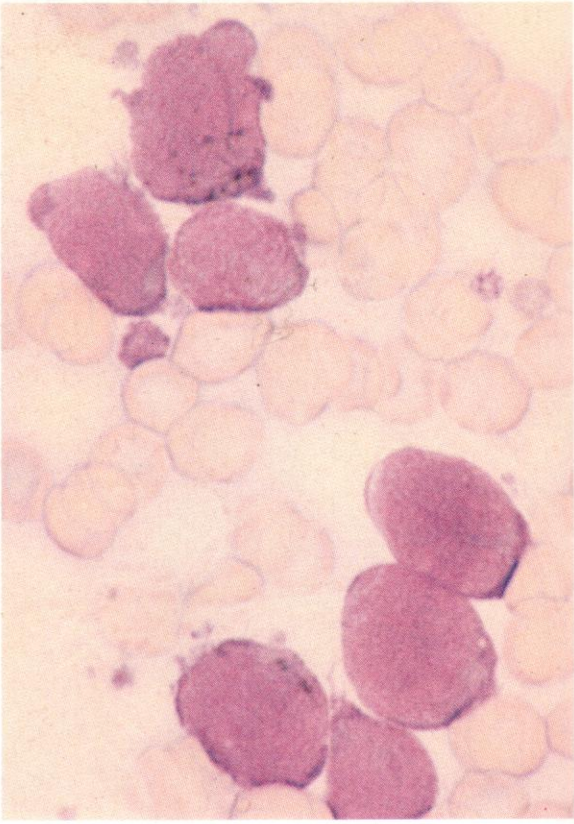

630–632. Cytochemical reactions, respectively myeloperoxidase (**630**), SB (**631**), and dual esterase (**632**), on a bone marrow aspirate from a patient variously diagnosed on morphological and cytochemical grounds by different haematologists as either AML or ALL. The Romanowsky appearances were as shown by the Heyl counterstain in **630**, where peroxidase positivity is confined to a single neutrophil stab cell and the negative blast cells show no features strongly suggestive of either myeloid or lymphoid lines. The SB stain reveals discrete scattered granular positivity of monocytic character in some 30% of the blast cells, with two of seven blasts positive in **631**, and the esterase reaction shows strong CE positivity in otherwise recognizable but infrequent neutrophil granulocytes, like the myelocyte in **632**, but quite strong BE positivity in most of the blast cells, resembling more the reaction of monoblasts than that usually seen in lymphoblasts. The PAS reaction, not shown here, was negative.

Immunocytochemistry revealed a mixed phenotype, with variable but overlapping surface expression of antigens reacting with CD10, CD19, CD13 and CD15, indicating the probable existence of an acute leukaemia of mixed lineage. Cytogenetic studies were not available, but this type of hybrid leukaemia has been found particularly in association with a 4;11 translocation or other abnormality involving a breakpoint at 11q23.

632

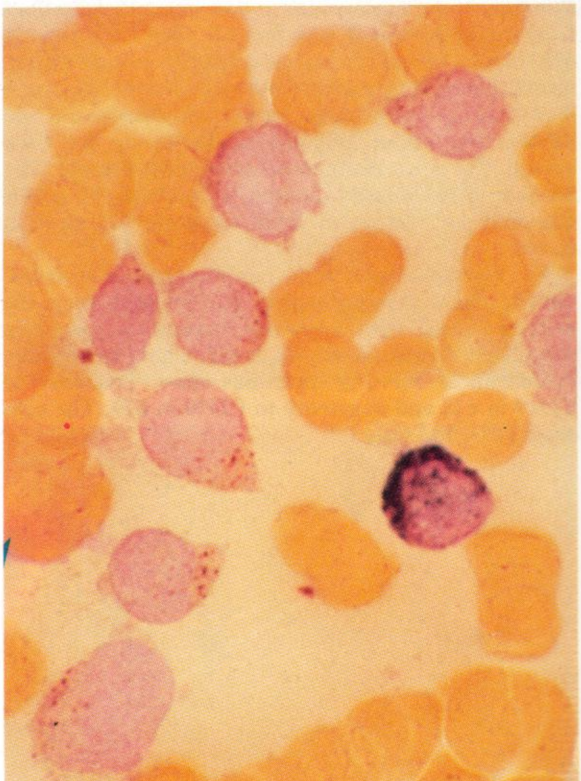

633 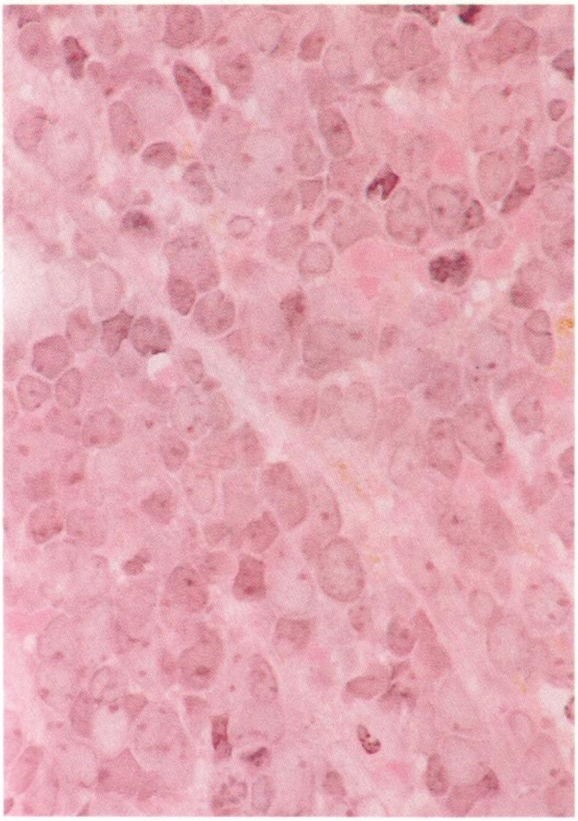

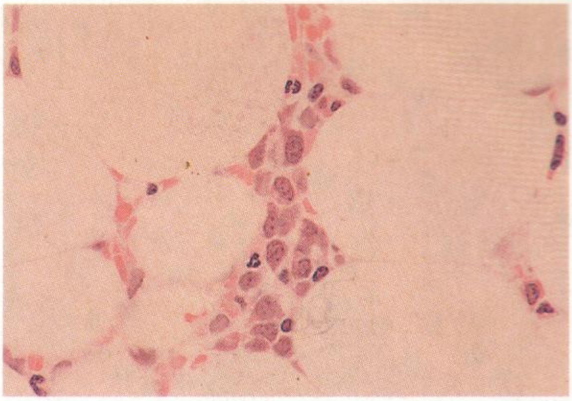 634

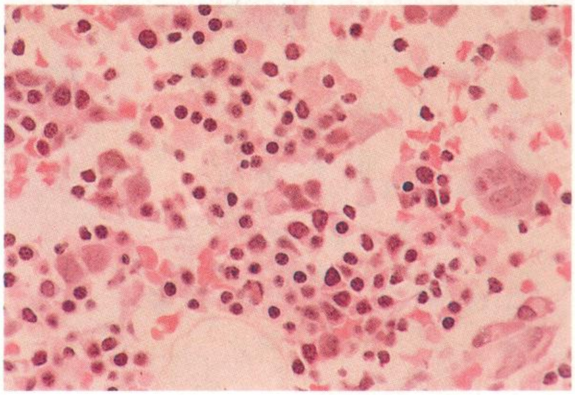 635

633–635. A sequence of bone marrow trephine biopsies from a patient with C-ALL, undergoing remission induction. In **633**, taken at the start of therapy, the specimen shows an overwhelming preponderance of primitive cells with large and leptochromatic nuclei often containing visible nucleoli. There are only a few cells of the erythroid or later granulocyte series present, with more pachychromatic nuclei. After two weeks of cytotoxic combination chemotherapy, marrow aspirates gave only a poorly cellular specimen with too few cells for differential assessment, but the trephine biopsy shown in **634** revealed a severely hypoplastic picture still containing a substantial proportion of blast cells. With the continuation of treatment, a further trephine biopsy two weeks later revealed the emergence of a remission picture with active proliferation of normal haemopoietic cells of all myeloid lines, although with erythroblasts predominating, as shown in **635**.

These fields illustrate again the important additional information to be obtained from marrow sections in acute leukaemias, especially with regard to overall cellularity and the differential composition of hypoplastic marrow during phases of attempted remission induction.

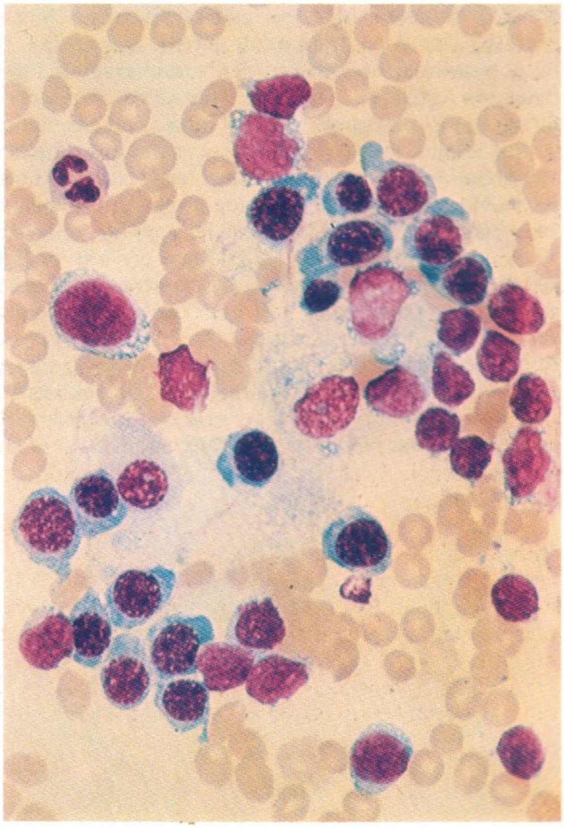 636

636. C-ALL plus normoblastic hyperplasia. The field shows some 20 blasts, 16 normoblasts and a reticulo-endothelial (RE) cell. This type of mixed cytology is seen in phases of emerging remission or relapse in ALL.

637

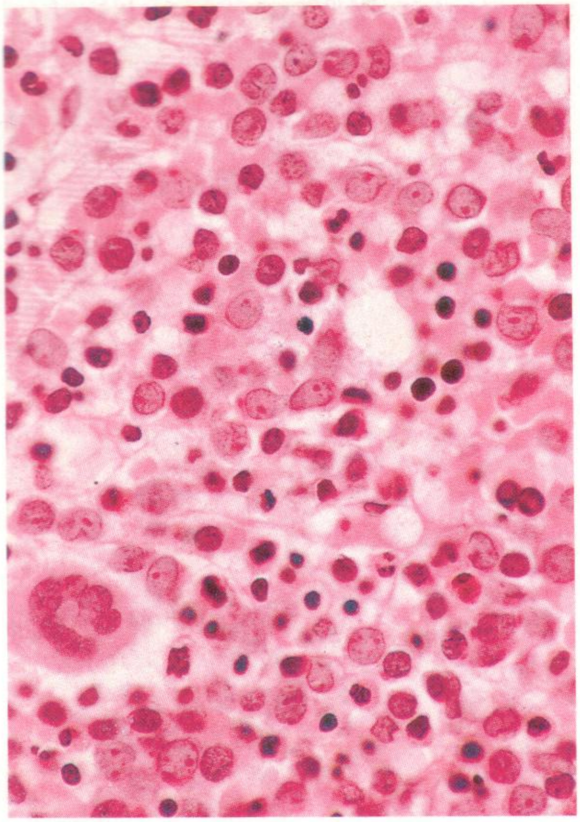

638

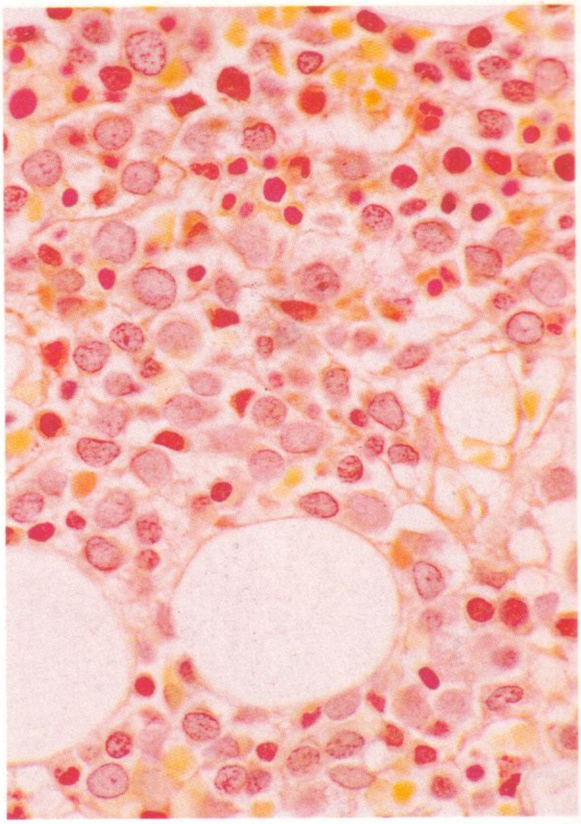

637–639. Sections of bone marrow trephine biopsy from the iliac crest of an adult patient with smIg+ B-ALL, moving from a period of chemotherapy-induced remission to relapse. The H&E-stained paraffin section shown in **637** illustrates the very mixed cell population at this stage, with a megakaryocyte at the left and numerous scattered erythroblasts and later granulocytes, but with blast cells having large leptochromatic and frequently nucleolated nuclei making up some 50% of the whole. The PAS stain in **638** reveals positively reacting neutrophil polymorphs and earlier granulocyte precursors, but the blast cells appear negative. A further H&E stain, this time of a plastic-embedded thin section, again shows the mixed cytology, with cells of different lineage readily distinguishable. The B lymphoblasts, with their pale nuclear chromatin and conspicuous nucleoli, constitute about 50% of the population.

639

640

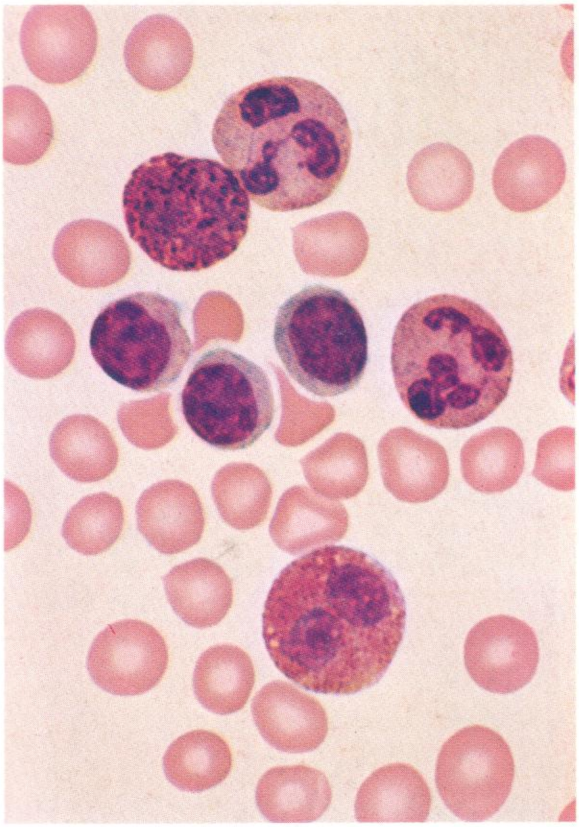

641

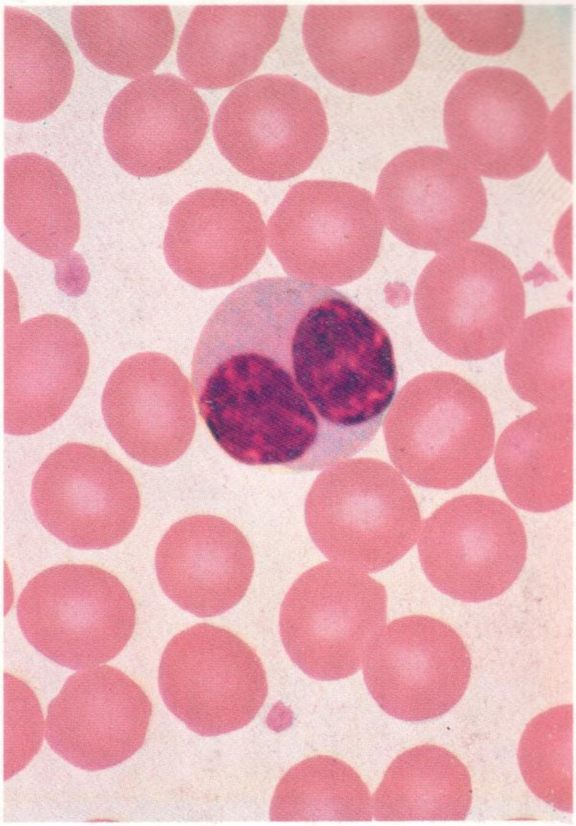

642

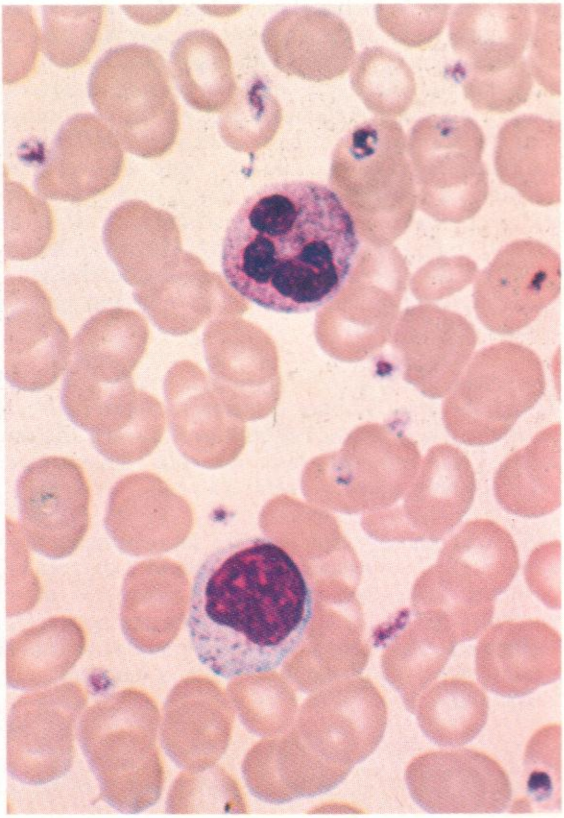

640. Three mature lymphocytes, together with a basophil, an eosinophil, and two segmented neutrophil polymorphs.

641. A binucleated lymphocyte. Such cells may rarely be seen in normal blood and are not, as at one time thought, suggestive of an irradiation effect.

642. A lymphocyte with more cytoplasm than those shown above, and with azurophil granules, possibly a suppressor T cell (Tγ). A neutrophil polymorph is also present.

643

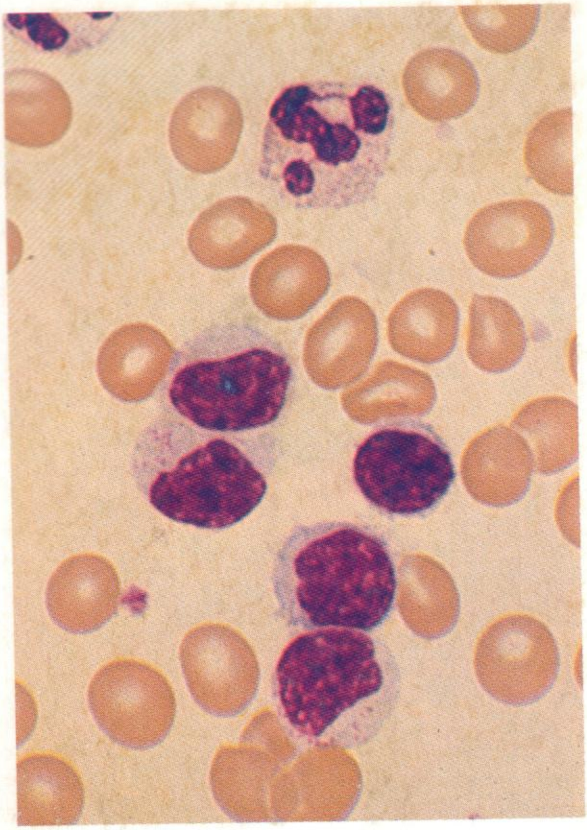

64

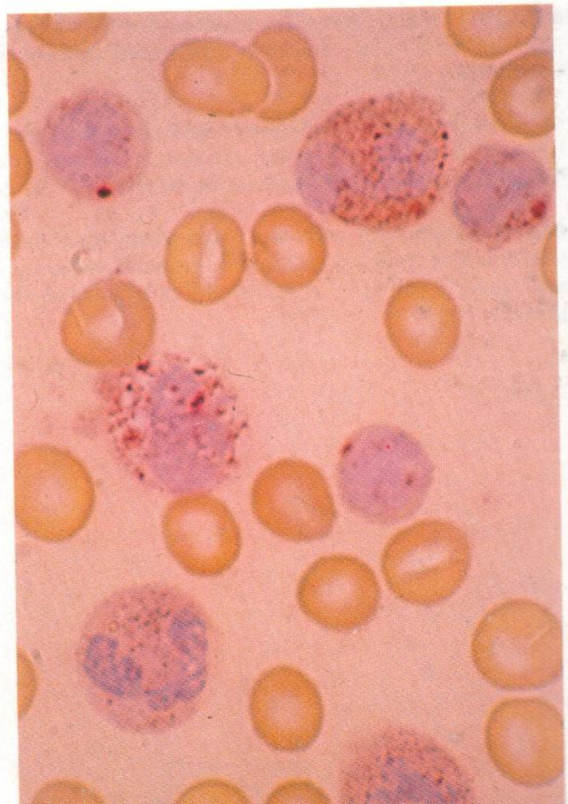

643. Variations in lymphocyte cytology in a normal buffy coat smear. One of the five lymphocytes has little cytoplasm and is probably either a B or a Tμ cell; one has some marginal hair-like processes, not infrequently seen in normal lymphocytes and not to be confused with the appearance of hairy cells (*see* **748–750**); and the remaining three lymphocytes have relatively large amounts of cytoplasm with a few scattered granules, and are probably Tγ cells. A persistent increase in cells of this cytological character, with positivity to the pan-T MAb CD7 and the suppressor subset MAb CD8, is found in large granular lymphocytosis and granular lymphocytic leukaemia.

644. Acid phosphatase reaction in buffy coat cells. Two of the three lymphocytes show localized coarse dot positivity characteristic of the Tμ cell subset; the third is larger with more cytoplasm, and with a little scattered positivity only, and is probably a Tγ cell.

645. Acid phosphatase reaction in peripheral blood lymphocytes: the proportion of cells with the localized positivity seen here in three lymphocytes closely parallels the Tμ cell proportion by surface marker techniques. This field also shows granular acid phosphatase positivity in two neutrophils, a basophil and an eosinophil.

646

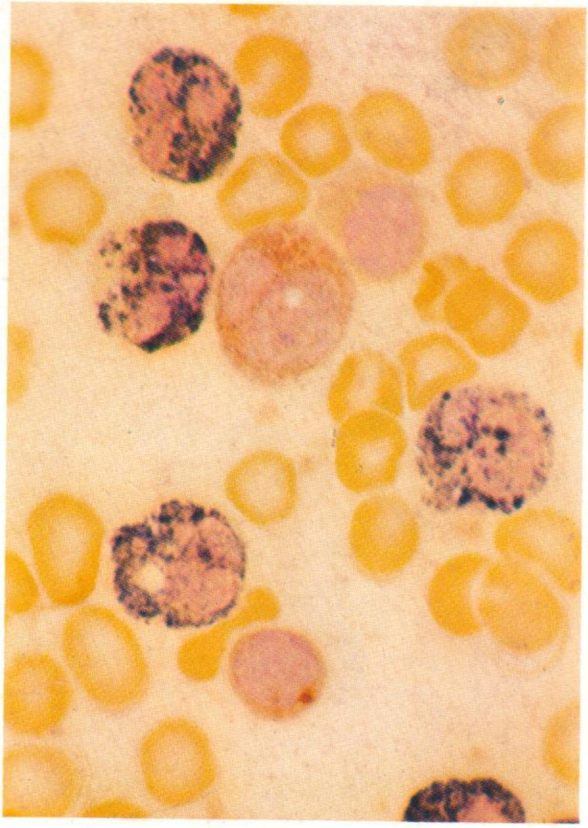

647

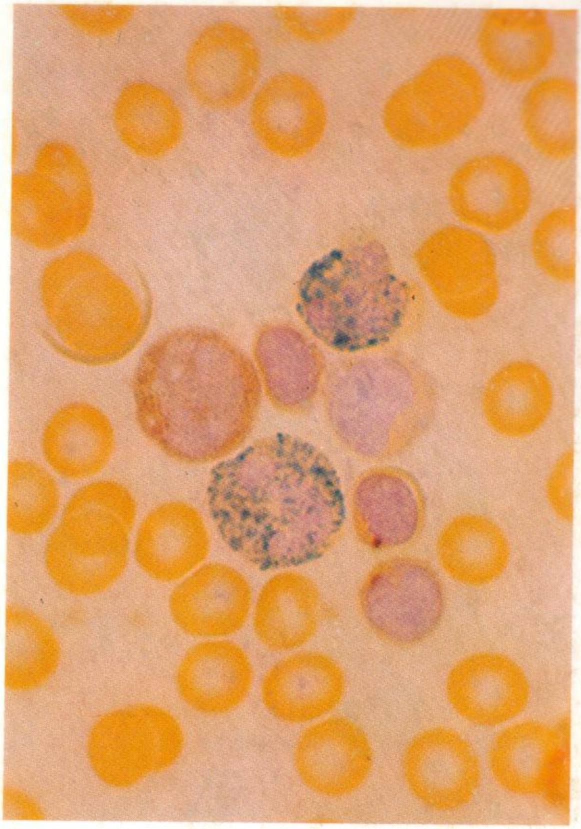

646. Dual esterase reaction. Localized T-cell positivity in one lymphocyte, probably a Tμ cell, and weak granular BE positivity in a second. This may be a null cell or perhaps a cell of the Tγ subset. There are four CE-positive polymorphs and a BE-reacting monocyte.

647. Two normally reacting (CE-positive) polymorphs, a BE-positive monocyte and four lymphocytes – two showing the localized dot-like Tμ-subset type positivity, one a small, negative, probable B cell, the other a larger lymphocyte with ample negative cytoplasm, probably of the Tγ subset.

648. A monocyte and a polymorph, together with two lymphocytes of the Tμ subset.

648

649

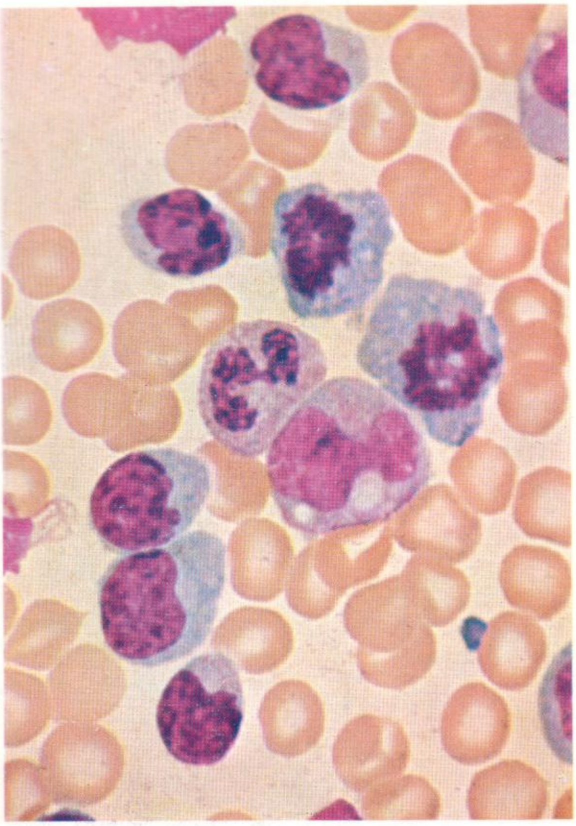

650

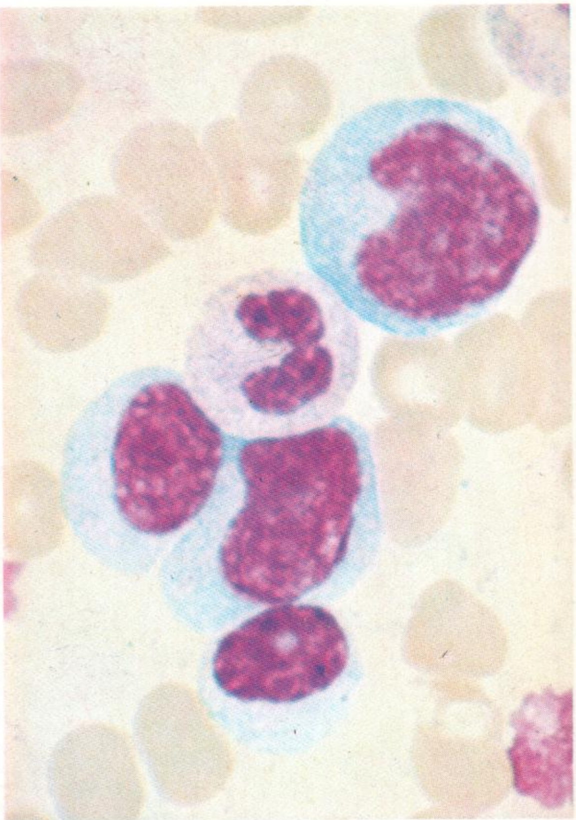

651

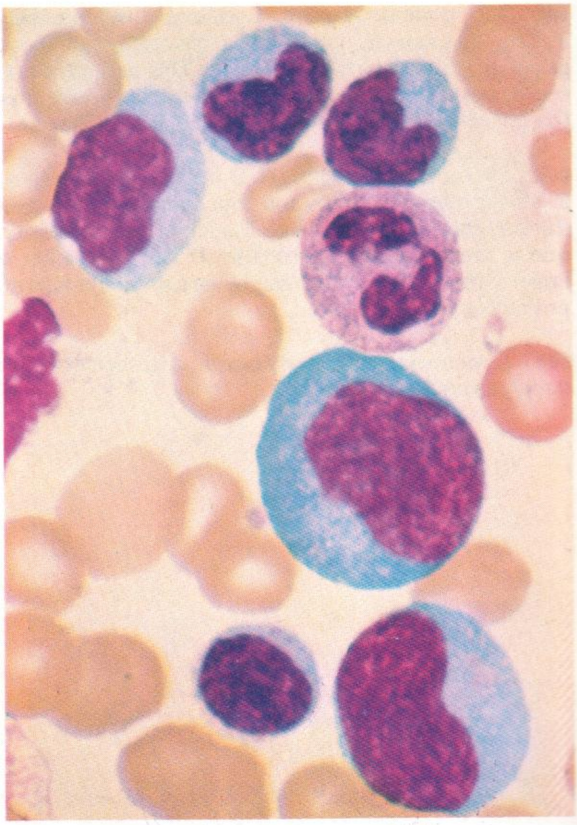

649–660. *Reactive 'immunoblasts' and 'virocytes' arising in various infective states. These activated lymphocytes are generally PAS, acid and alkaline phosphatase and esterase negative.*

649. A blood smear from a patient with infectious mononucleosis. Apart from a central monocyte (with phagocytic vacuoles) and a segmented neutrophil, the nucleated cells are all lymphocytes. The mitotic figure (in telophase) shows the increased cytoplasmic basophilia often encountered in the abnormal lymphocytes of this disease. Mitoses in mononuclear cells are very uncommon in normal peripheral blood, but are seen much more often in activated lymphocytes.

650 and **651**. Further examples, from two different patients, of the abnormal morphology of lymphocytes in infectious mononucleosis. The nuclear chromatin in the most abnormal cells is still too coarse and the cytoplasm too abundant for real confusion to exist between these cells and lymphoblasts.

652

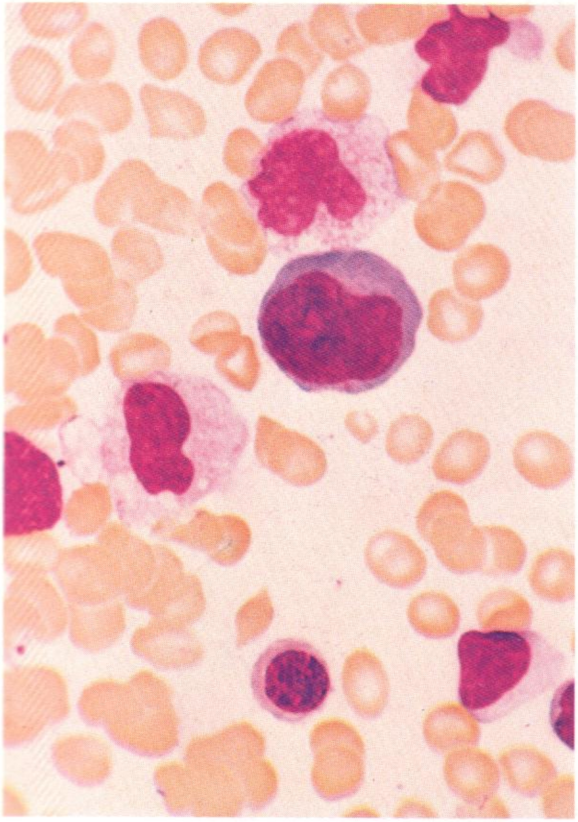

653

654

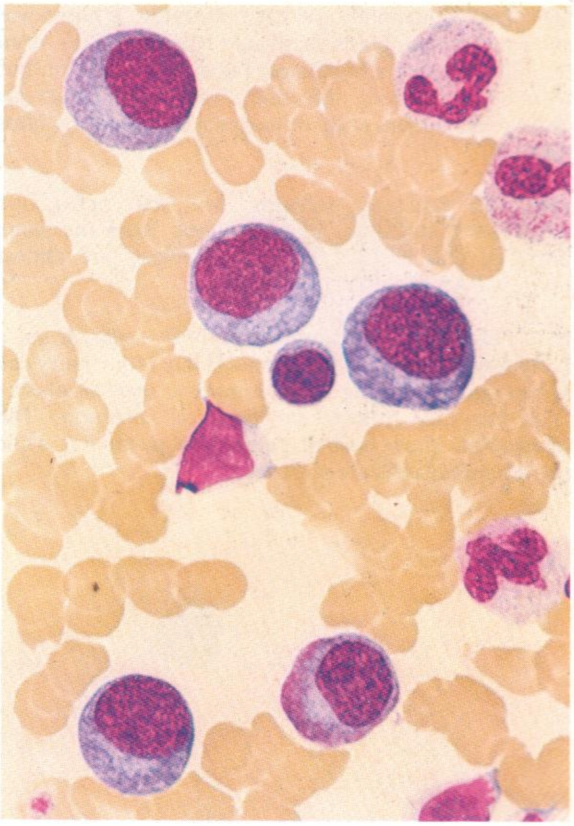

652. An immunoblast in the marrow of a patient with ALL in remission, but with a viral infection. Such cells must not be confused with leukaemic blast cells.

653. A disrupted RE cell and a binucleated immunoblast from the same case.

654. Three stabs, two lymphocytes and five immunoblasts, from an infective episode during remission emergence in AML. One of the immunoblasts shows early 'flaming' of the cytoplasm (cf. **807–809**).

655

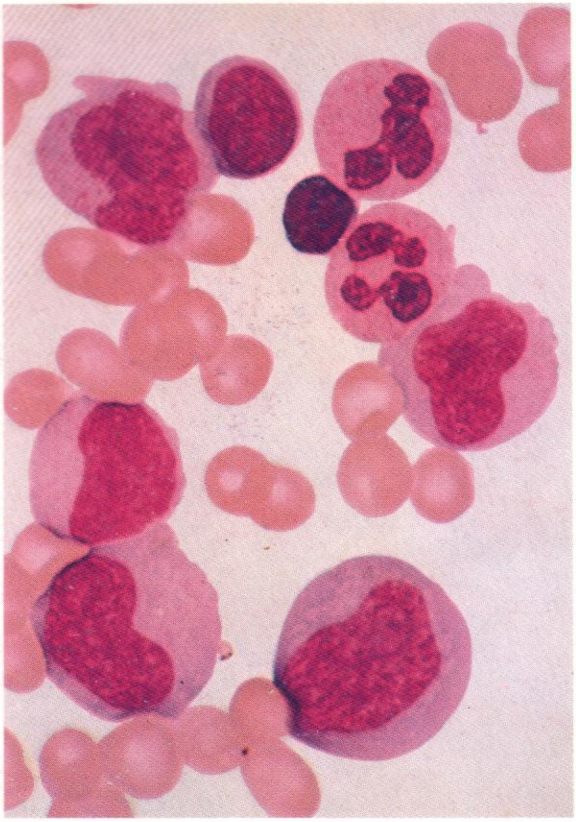

656

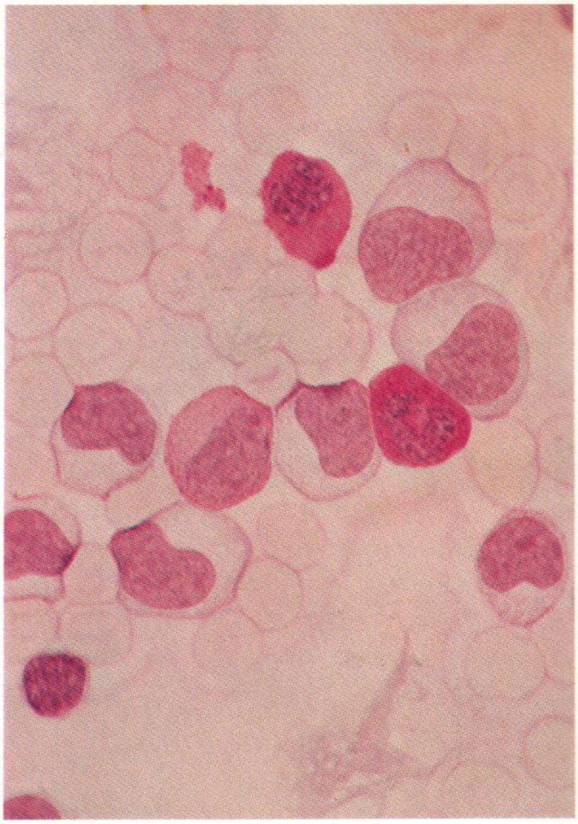

657

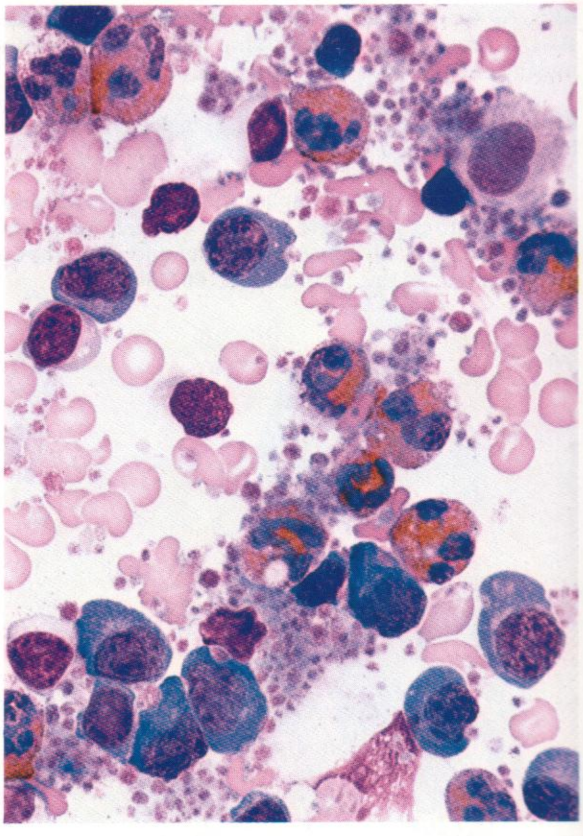

655. Two neutrophils, two lymphocytes, a monocyte and four immunoblasts (activated lymphocytes) – from the buffy coat of a leukaemic patient in remission but with a mycoplasma infection. These cells must be distinguished from early monocytes or leukaemic blast cells.

656. PAS reaction, showing two stab cells, one lymphocyte and eight immunoblasts, from the same buffy coat as in **655**. The immunoblasts are almost entirely PAS-negative.

657. Peroxidase reaction on a buffy coat from a patient with hairy cell leukaemia (HCL) (one hairy cell at top right), showing 24% of immune reactive plasma cells resulting from acute bacterial infection. The neutrophils show normal peroxidase positivity, while the remaining cells are negative.

658

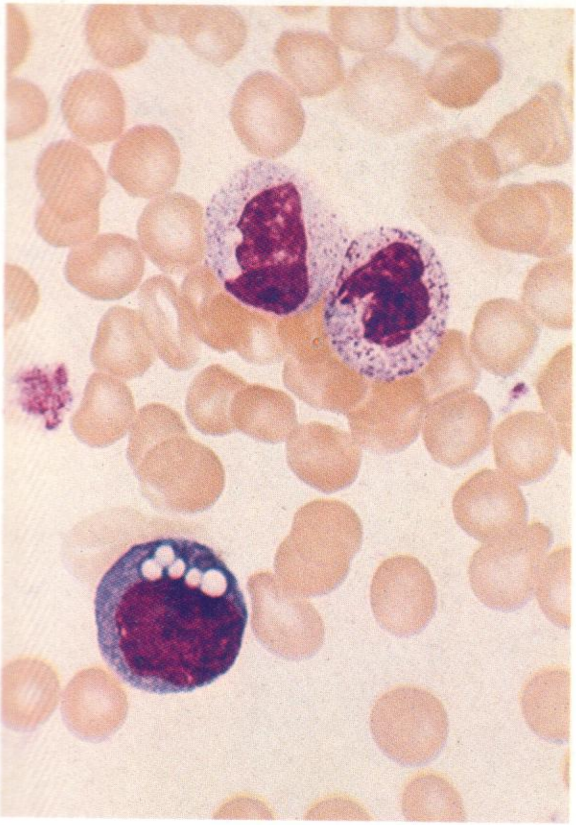

659

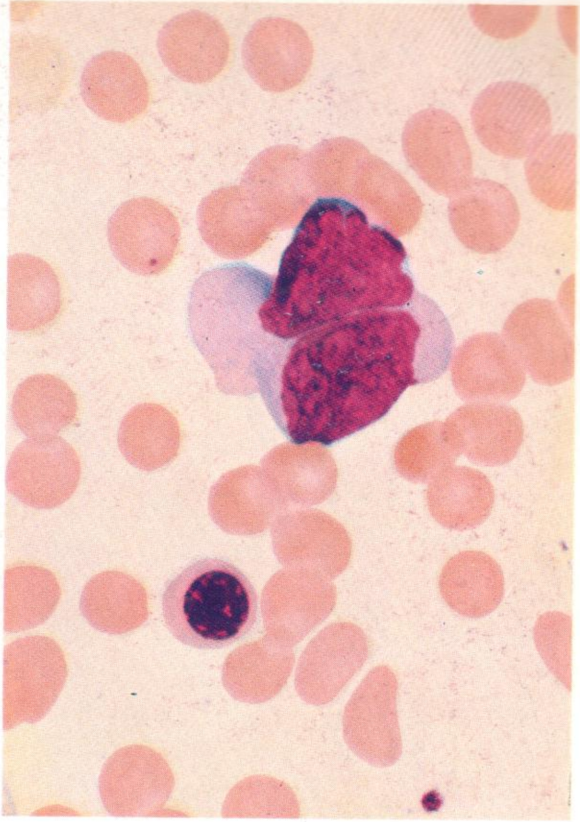

660

658. A vacuolated immunoblast and two stab cells with toxic granules, more conspicuous in one of them, from the blood of a child with a pseudomonas infection.

659. A binucleated immunoblast, showing a tendency to nuclear distortion and peripheral cytoplasmic basophilia, from a patient with a viral infection.

660. A mononuclear immunoblast with twisted nucleus and fine azurophil stippling of cytoplasm, but with basophilia at the periphery, from the same case.

661

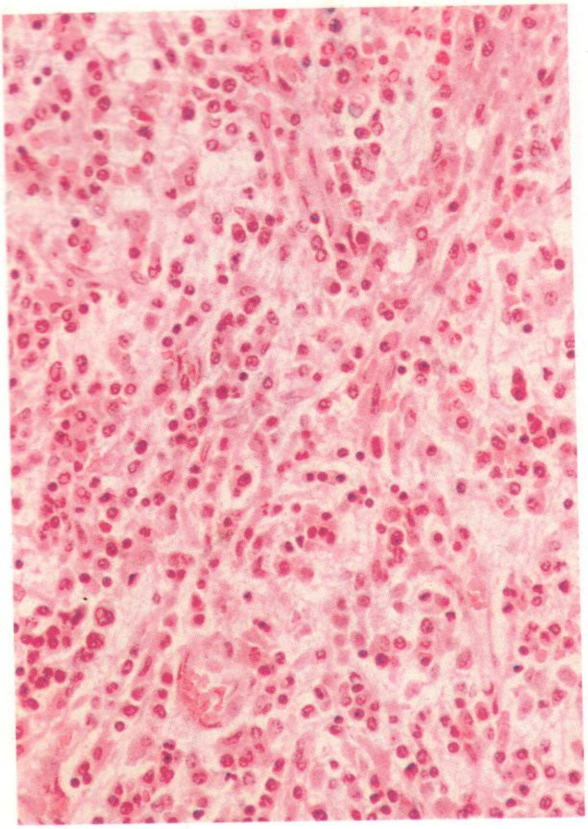

662

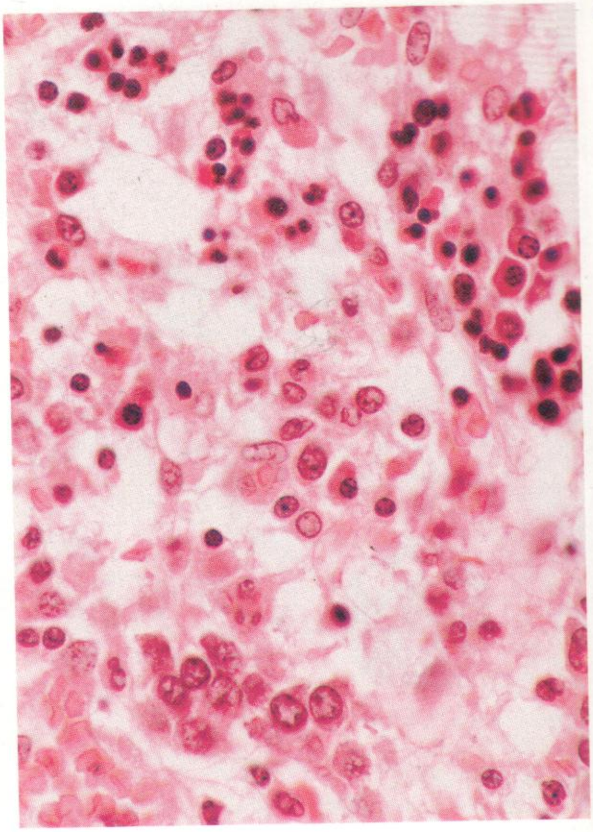

663

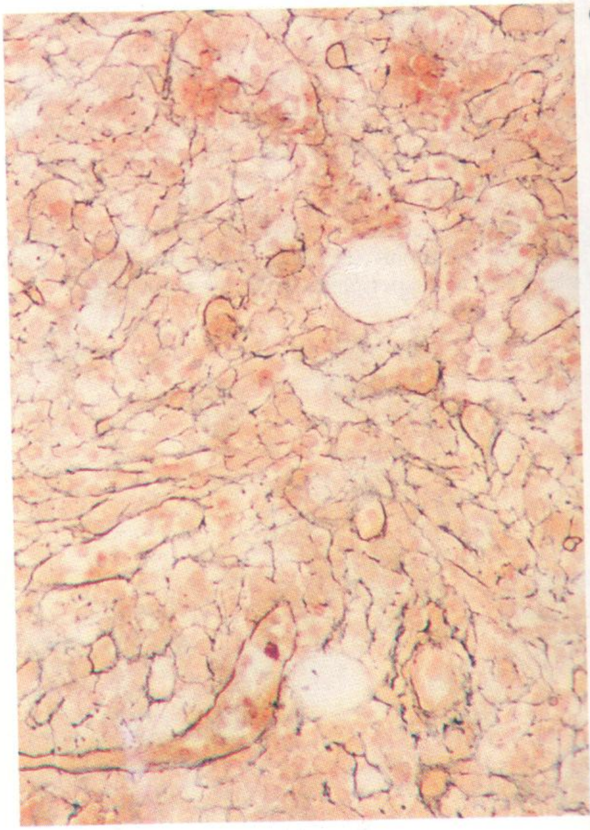

661–663. *Sections of bone marrow trephine biopsy from a patient with diffuse marrow involvement with angio-immunoblastic lymphadenopathy (AIL).*

AIL is generally regarded as a reactive process, although with a high risk of transformation to a floridly neoplastic non-Hodgkin's lymphoma (NHL). Marrow involvement may be either focal or diffuse. The low- and higher-power views shown in **661** and **662** reveal the characteristic morphological picture, with a swirling pattern of branching endothelium-lined blood vessels, an interspersed proliferation of activated lymphocytes – plasmacytoid immunoblasts and plasma cells, and an interstitial deposit of weakly staining amorphous eosinophilic material. There is often a component of haemolytic anaemia present in these cases, and the marrow may show areas of normoblastic hyperplasia, as in **662**, where there is an island of normoblastic proliferation at the upper right corner. In the low-power view of a reticulin stain in **663**, the characteristic increase in reticulin fibres and their distribution in a swirling pattern around the pseudo-vessels is well shown.

The peripheral blood in AIL often contains lymphoplasmacytoid immunoblasts and occasional mature plasma cells, and there is commonly a polyclonal dysproteinaemia.

664

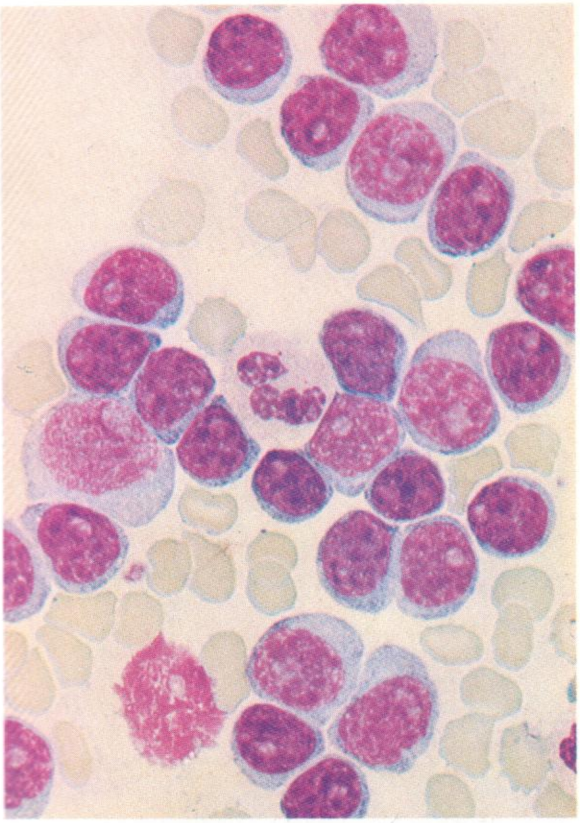

665

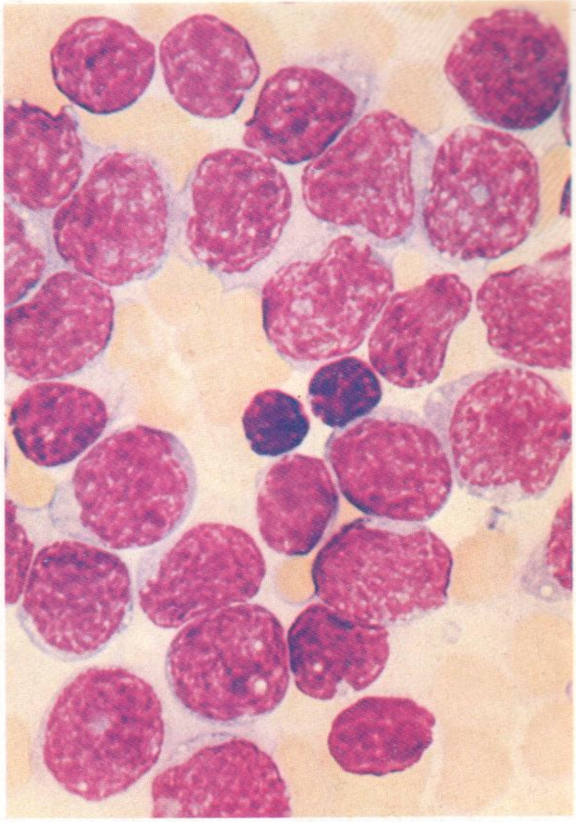

666

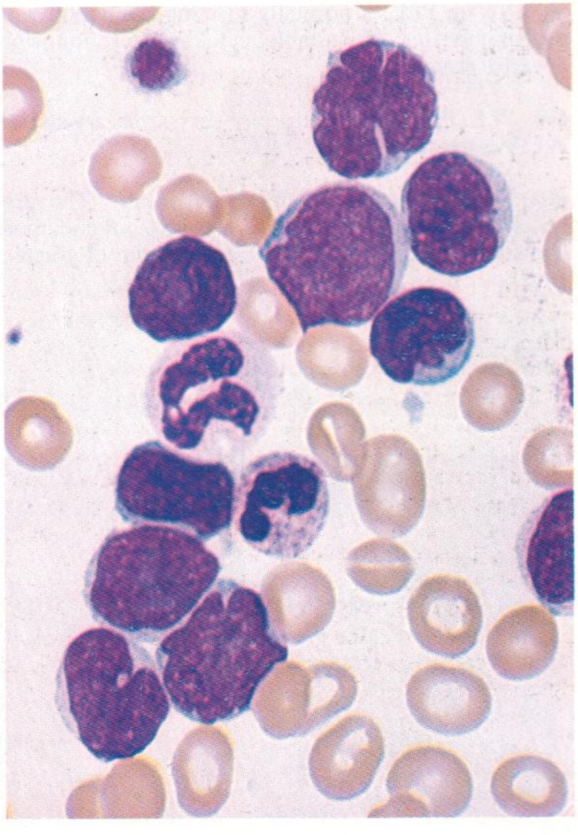

664–675. *Prolymphocytic leukaemia (PLL).*

664. PLL, Romanowsky stain: the cells show more basophilic cytoplasm and more pronounced nucleoli than is the case with lymphocytes, but have moderately pachychromatic nuclei, unlike blast cells.

665. PLL, Romanowsky stain, a T-cell case: the large cell size and moderately pachychromatic nuclear pattern, with occasional variable nucleoli, contrast sharply with the two normal lymphocytes present.

666. PLL, Leishman stain on another case; this was of B-cell origin. The nuclear cleavage and invaginations sometimes seen in PLL cells are well shown in this case.

667 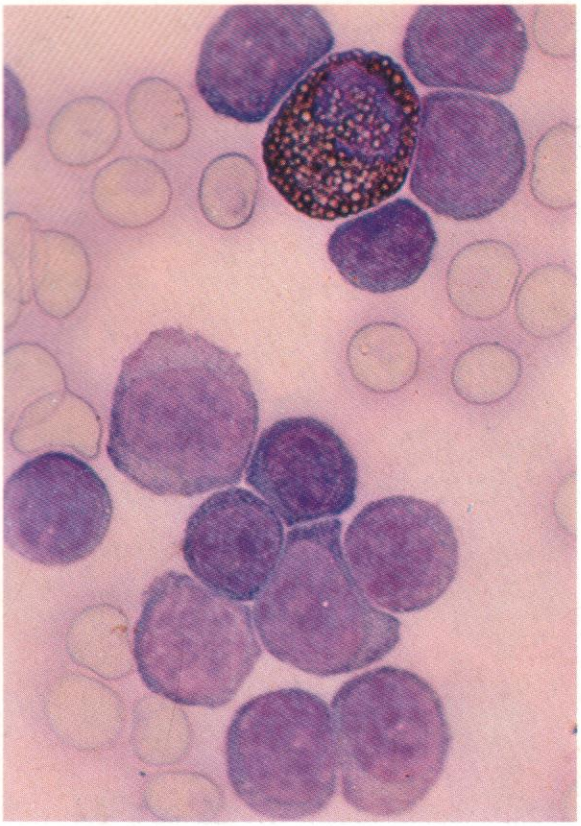

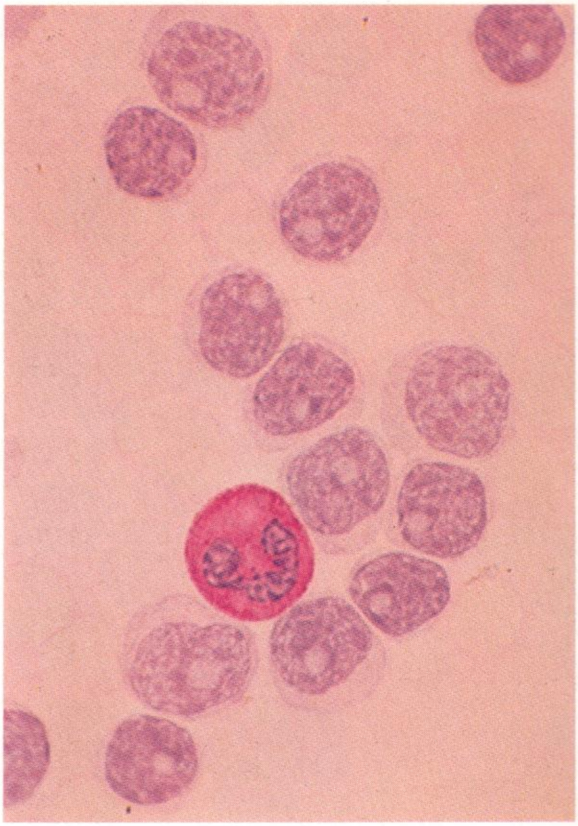 668

667. SB on PLL: a normally reacting eosinophil with prolymphocytes of variable cytology but uniformly negative reactions.

668. PLL, PAS reaction: the prolymphocytes are essentially PAS-negative in this T-cell case.

669. PAS reaction on a B-cell PLL case. The prolymphocytes are again essentially negative but one, more immature, blast cell (top right) shows a rim of granular PAS positivity.

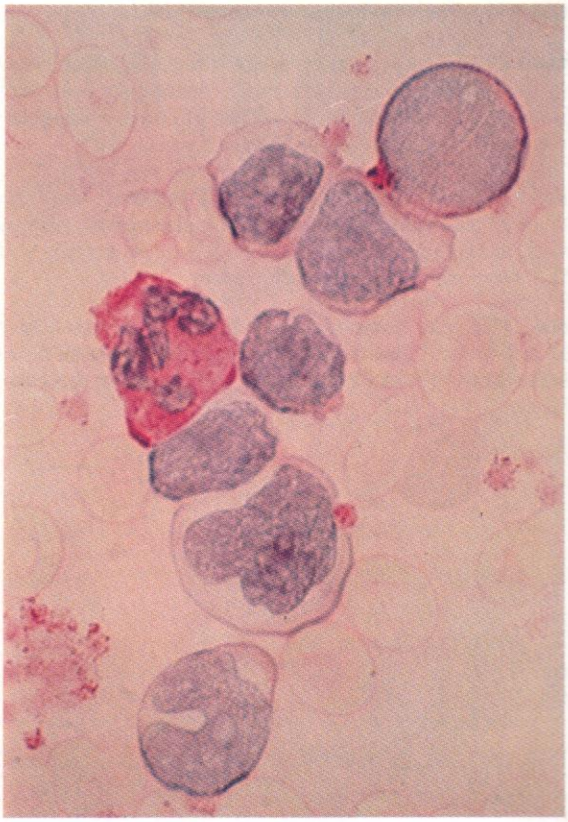 669

670

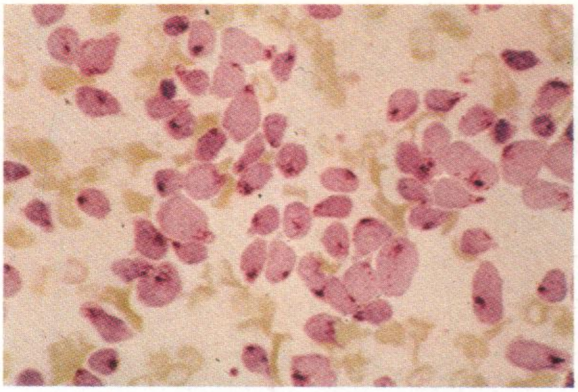

671

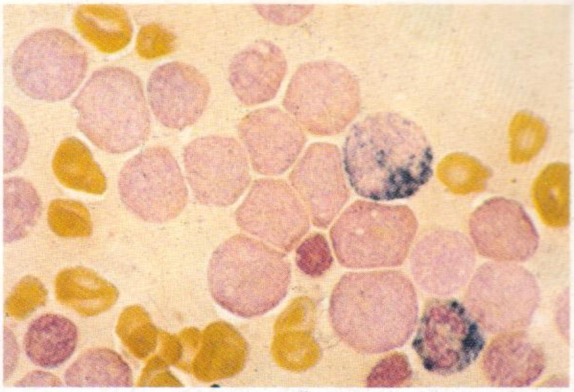

672

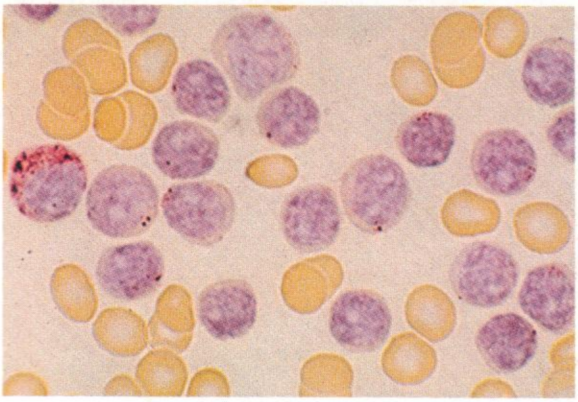

673

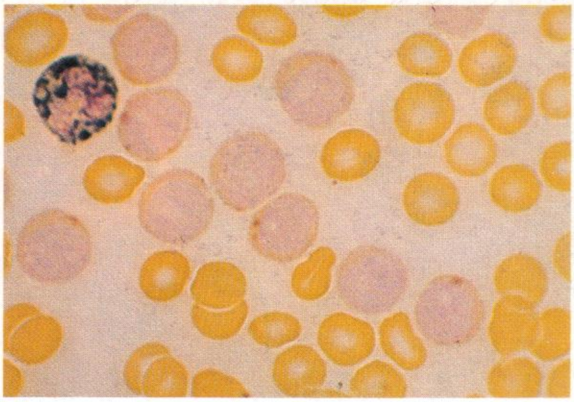

674

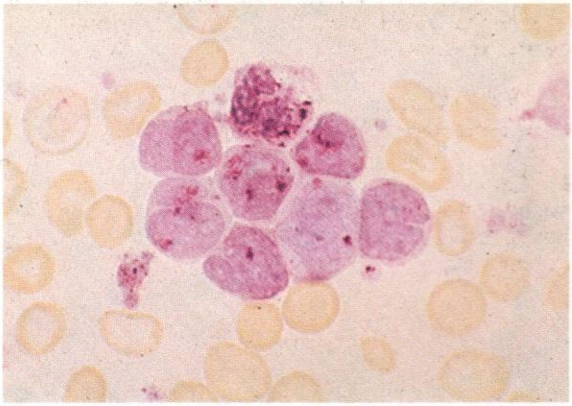

675

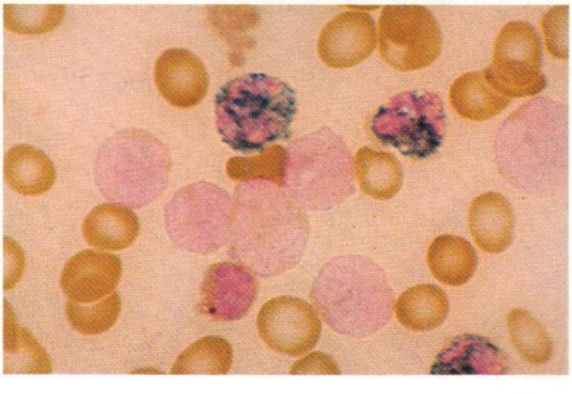

670. PLL: acid phosphatase reaction. In this T-cell case all the prolymphocytes show strong localized reaction.

671. PLL: dual esterase on the same T-cell case as illustrated in **665**, **668** and **670**. The reaction is almost negative.

672. PLL: acid phosphatase reaction. Another T-cell case showing variable positivity, about half the cells having one or two coarse granules, as often seen in mature Tμ cells.

673. Dual esterase reaction in the same case as **672**; about half the prolymphocytes showed moderately strong localized BE positivity.

674. Acid phosphatase reaction in a B-cell PLL. The field shows a normally positive polymorph and seven prolymphocytes, with occasional granules of coarse positivity scattered mostly over the nucleus rather than localized in the paranuclear zone.

675. Dual esterase on the same case as in **674**. Two CE-positive polymorphs and a BE-positive normal Tμ cell contrast with the virtually negative B prolymphocytes.

676

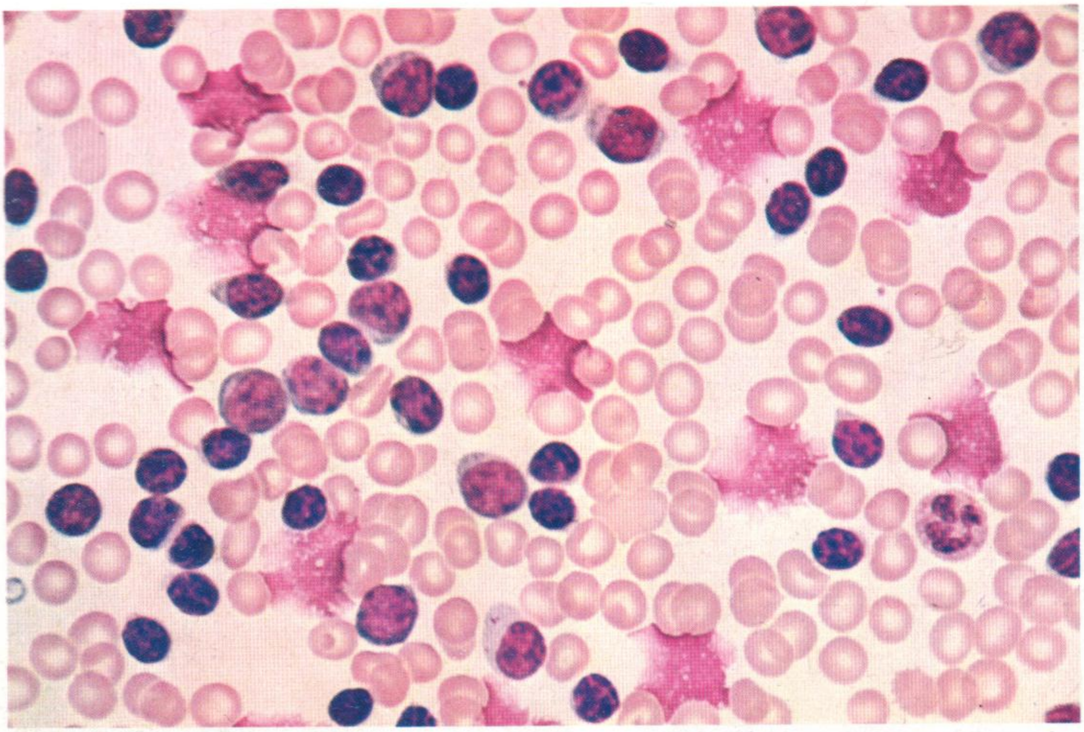

677

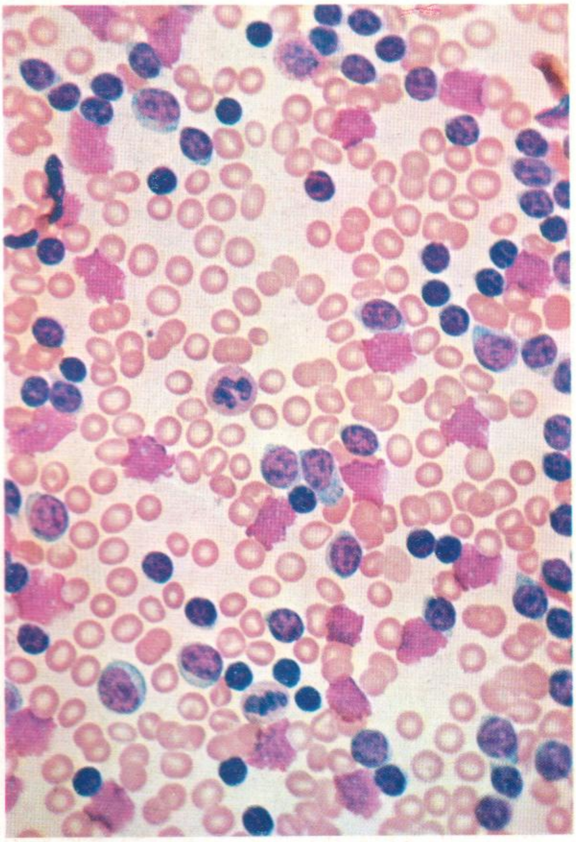

676. A general view of a peripheral blood smear from chronic lymphocytic leukaemia (CLL). The intact cells are nearly all lymphocytes, showing some variation in morphology probably in parallel with maturity. The smeared disrupted cells are typically numerous in this disease. The spread nuclear remnants are sometimes known as 'Gumprecht's shadows'.

677. Another example of the blood picture in CLL. The range of morphological variation is not great, but a few precursors – prolymphocytes or lymphoblasts – can be seen, and the smeared cells are again conspicuous.

678

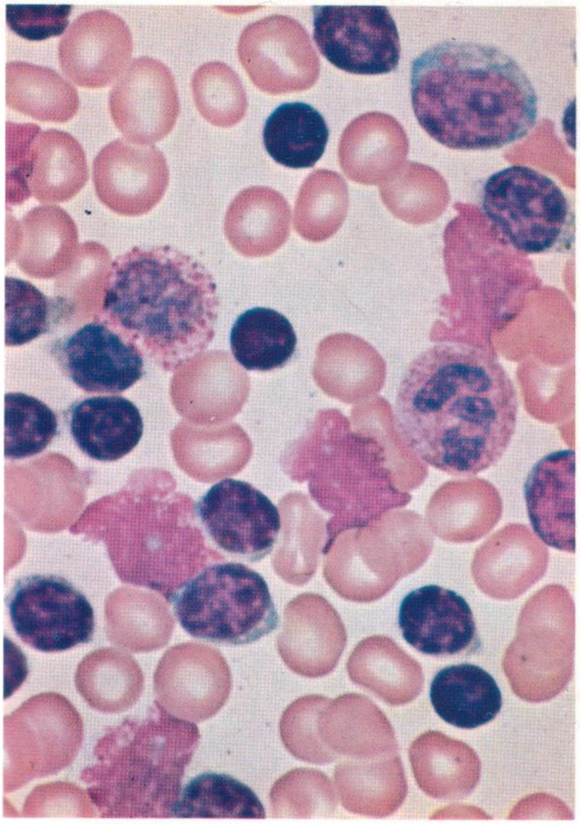

679

680

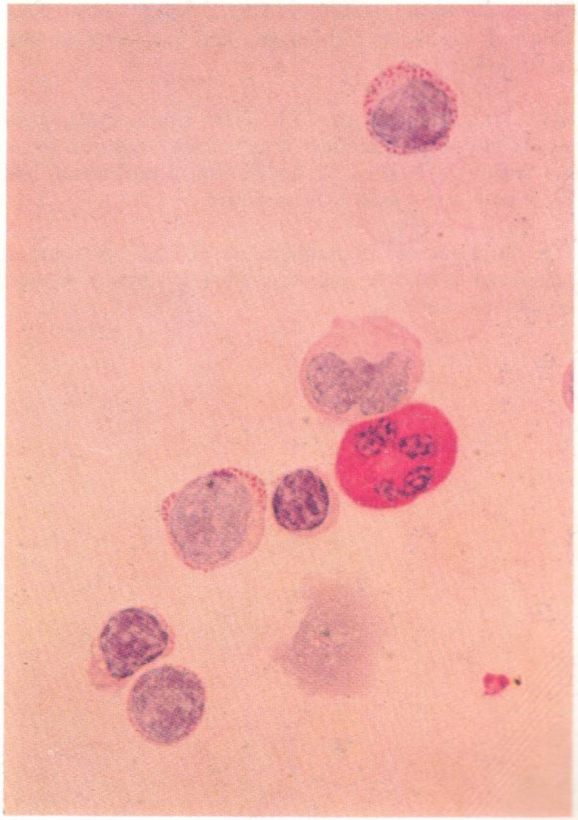

678. A high-power view of the peripheral blood in CLL. Again an occasional precursor is visible.

679. PAS reaction in CLL. The lymphocytes show a pattern of positivity like that of normal lymphocytes, but a higher proportion of cells shows positivity than in a normal specimen.

680. Another example of PAS reaction in CLL.

681

682

683

681. Acid phosphatase in CLL. Most cells show scattered positivity without marked paranuclear concentration.

682. Dual esterase in CLL. The lymphocytes show mostly negative reactions; a few have scattered weak BE positivity. Normal CE reaction in a polymorph and BE positivity in a monocyte are shown.

683. Dual esterase in another case of CLL, showing an occasional crescentic positive reaction, similar to that usually seen in HCL.

684

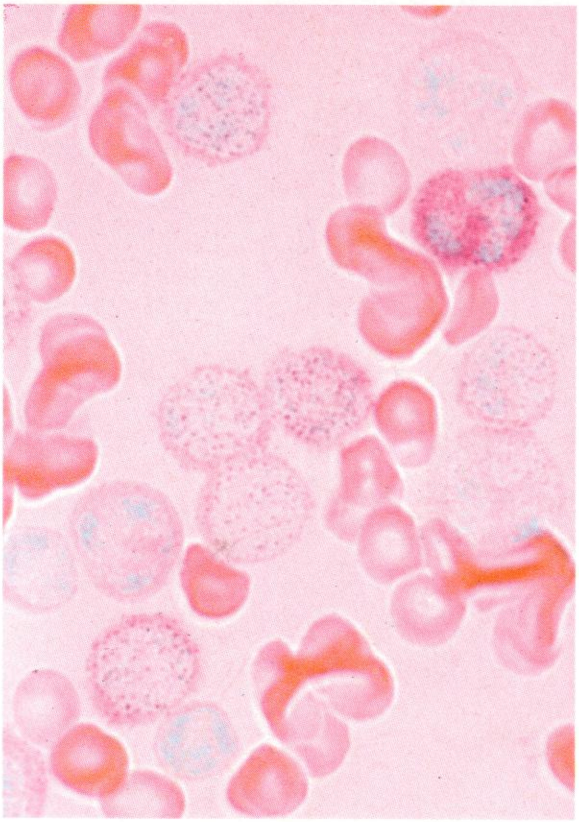

685

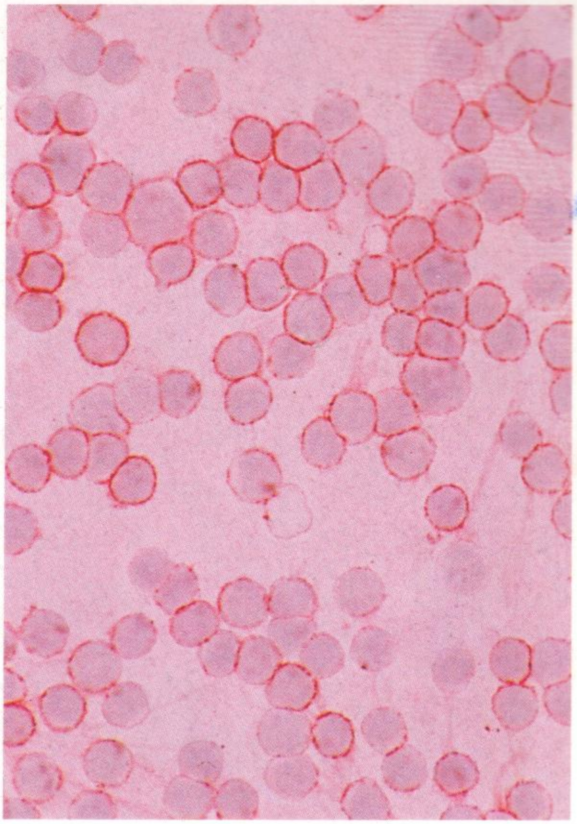

686

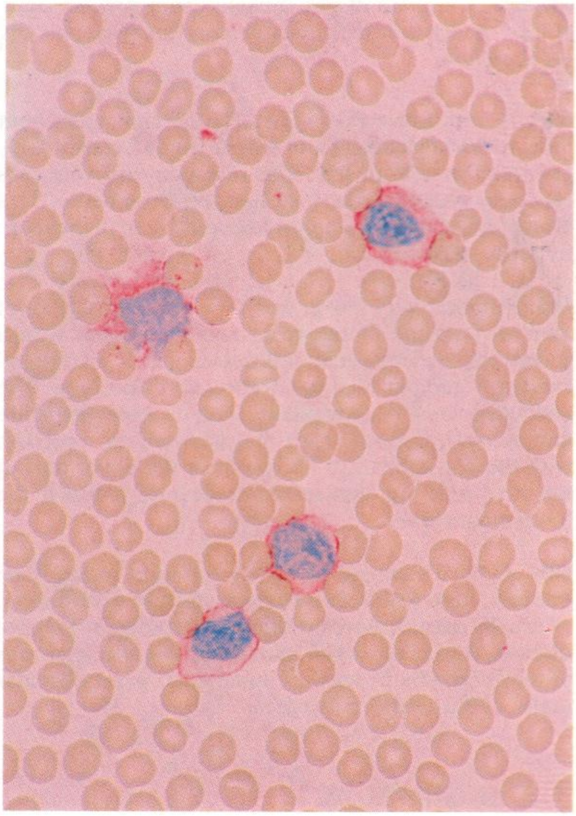

684. A buffy coat preparation from the peripheral blood of a patient with B-CLL, stained for alkaline phosphatase, showing the rare finding of positivity for this enzyme in the neoplastic lymphocytes. Four neutrophil polymorphs show from 0–2+ positivity, and most of the CLL cells show scattered positive granules. Although this finding is quite uncommon in CLL, the lymphoid cells of NHL, especially the centrocytes and centroblasts of follicular lymphomas, show it rather more often.

685. An immunocytochemical alkaline phosphatase–anti-alkaline phosphatase (APAAP) preparation of B-CLL peripheral blood buffy coat, showing a strong membrane reaction for IgM.

686. A similar APAAP reaction on peripheral blood cells from a T-CLL, showing membrane positivity to the T-cell MAb CD3.

687

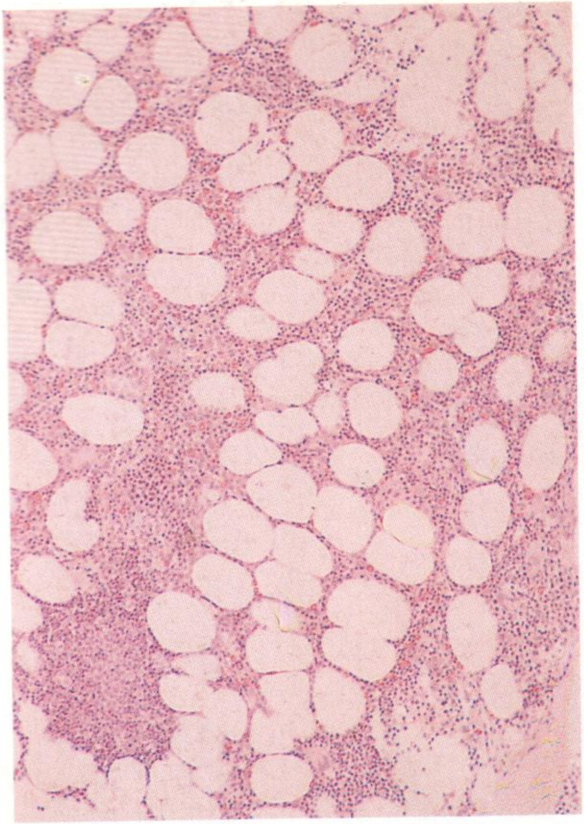

688

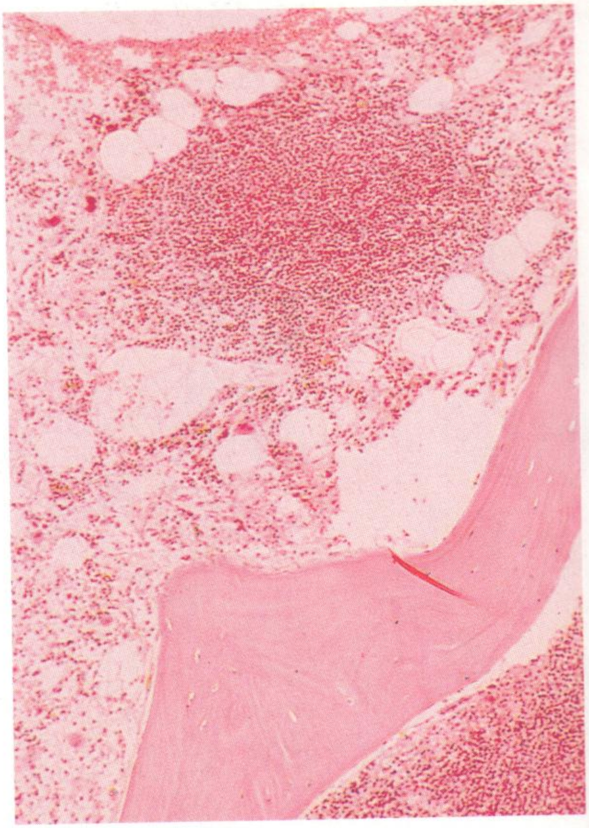

687–692. Trephine biopsy sections from various cases of CLL to illustrate the common morphological patterns of infiltration.

687. A very low-power view of a marrow with about 50% overall cellularity and with a single focus of CLL towards the bottom left. The remaining marrow cells represent essentially normal haemopoietic tissue. This type of focal involvement is commonly seen in the more indolent stages of CLL.

688. Another very low-power view of a thin section of marrow trephine biopsy from another patient with a somewhat denser nodular infiltration, partly distributed randomly and partly of paratrabecular disposition. The residual normal marrow tissue, with its looser structure and recognizable scattered megakaryocytes, contrasts with the dense focus of CLL cells in the upper part of the field and the similar paratrabecular focus at the lower right corner.

689. A third example of CLL infiltration in the bone marrow, here with a more general diffuse distribution, as usually seen in more advanced or rapidly progressive disease. Residual normal marrow in this specimen was virtually confined to the immediate paratrabecular areas, as illustrated in this field.

689

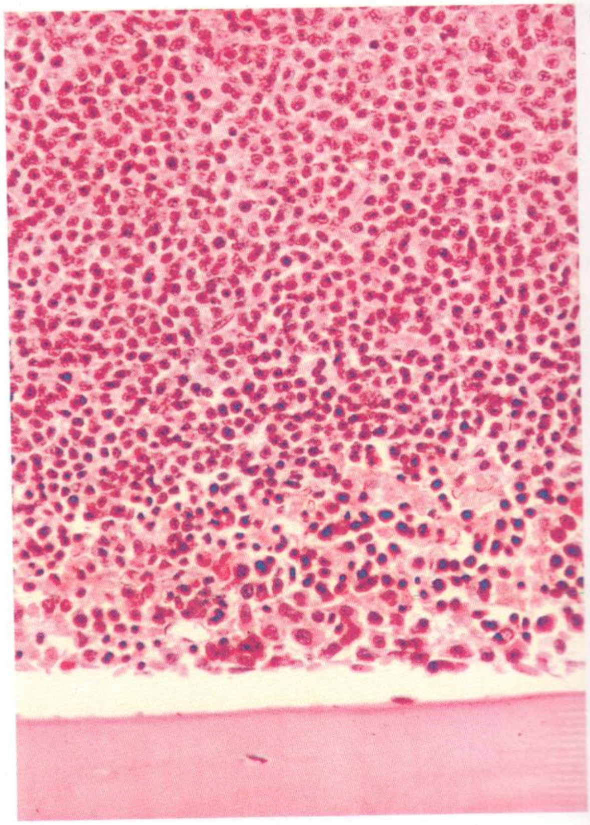

690

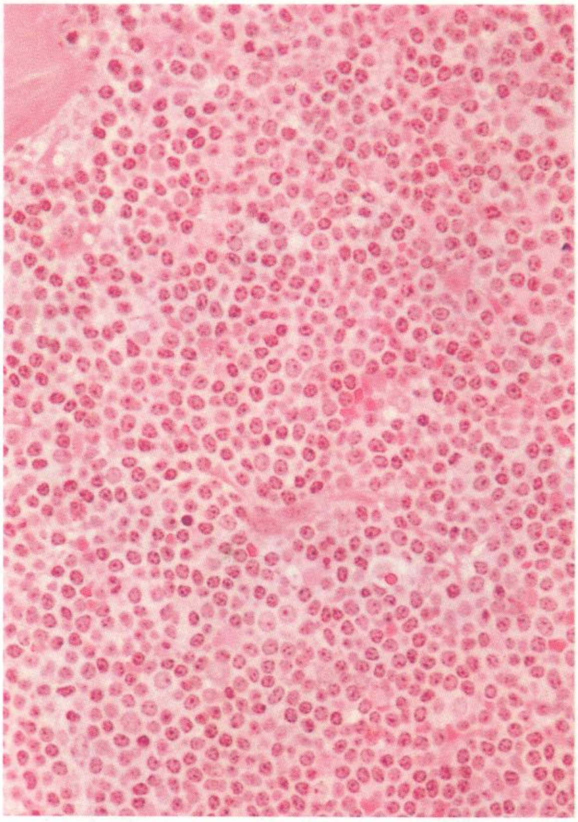

691

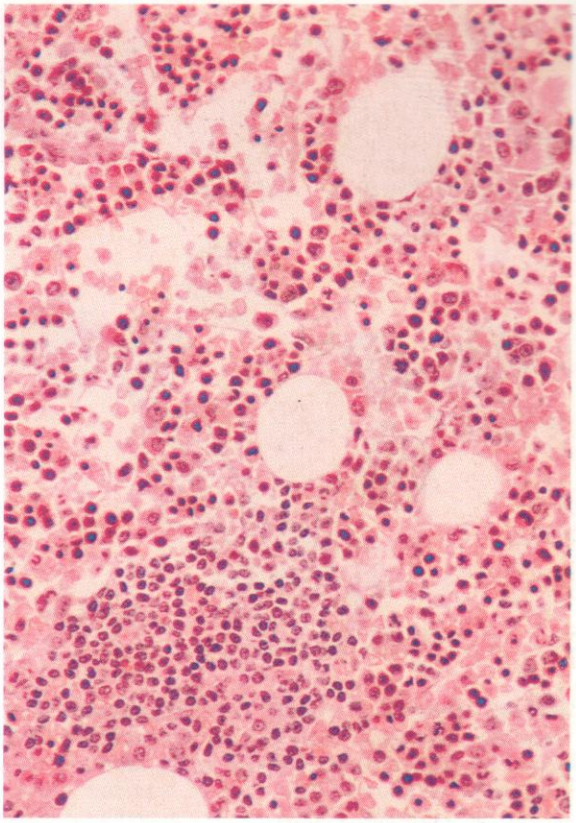

692

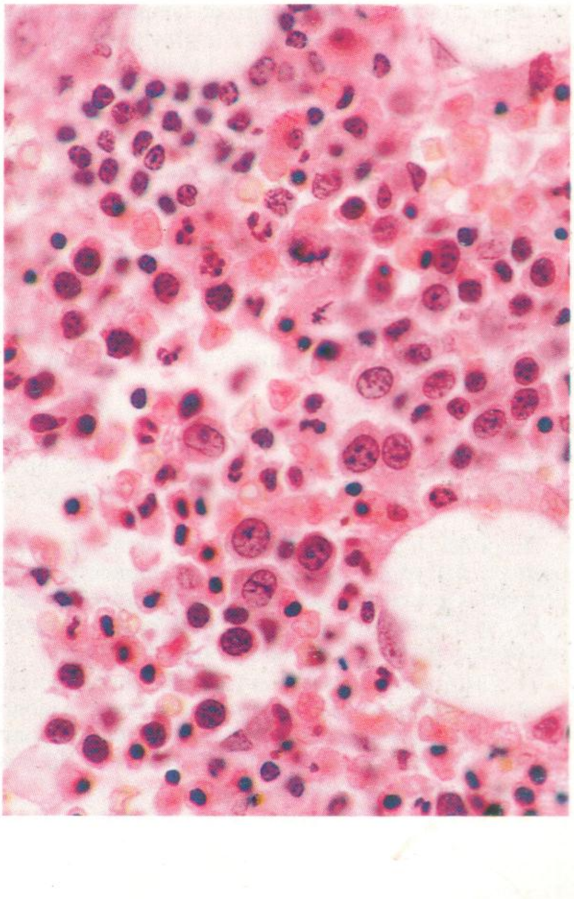

690. A high-power view of bone marrow in late CLL showing the diffuse nature of the infiltrate and its uniformity in both interstitial and paratrabecular areas, and also the overwhelming predominance of lymphocytes and the paucity of residual normal haemopoietic tissue. This type of picture is usually found at advanced stages of disease, commonly in association with marked anaemia and thrombocytopenia.

691 and **692**. Intermediate and high-power views, respectively, of a bone marrow trephine biopsy section from a patient with B-CLL and an accompanying auto-immune haemolytic anaemia. There is some generalized diffuse lymphocytic infiltration, but also a focal collection of lymphocytes at the lower left of the field in **691**, against a cellular background of gross erythroblastic hyperplasia. The higher magnification of **692** reveals more cytological detail, and shows the pleomorphic character of the interstitial cells, with lymphocytes, various granulocyte stages, and a predominance of erythroblasts, including numerous nucleolated proerythroblasts. There is a suggestion of megaloblastic change among the early erythroblasts.

693

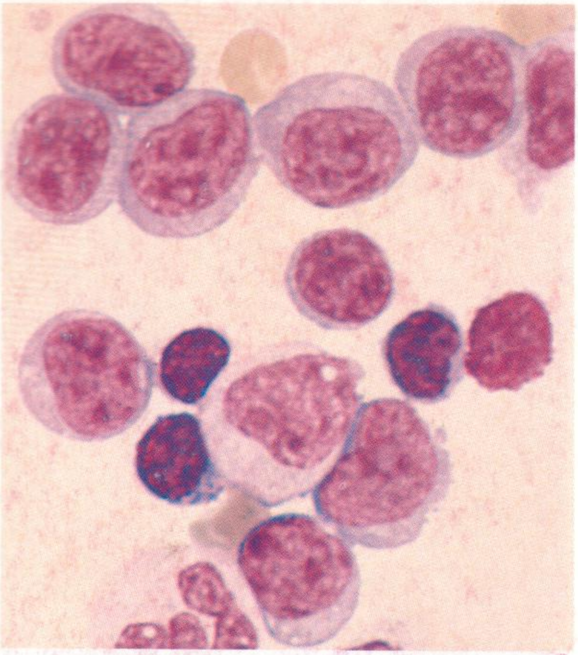

694

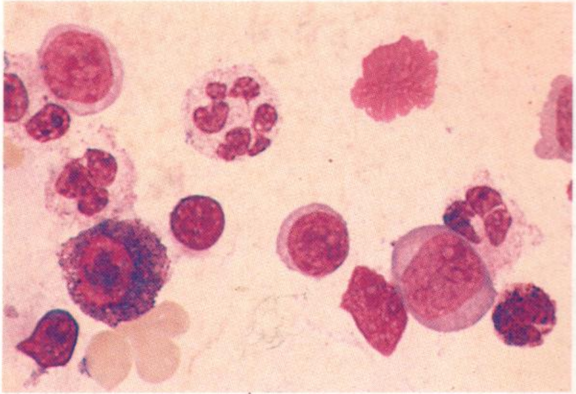

695

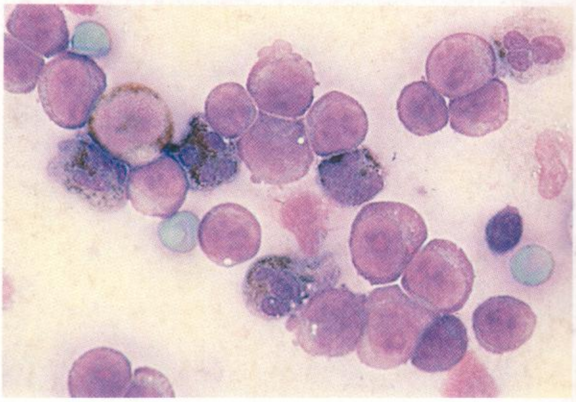

696

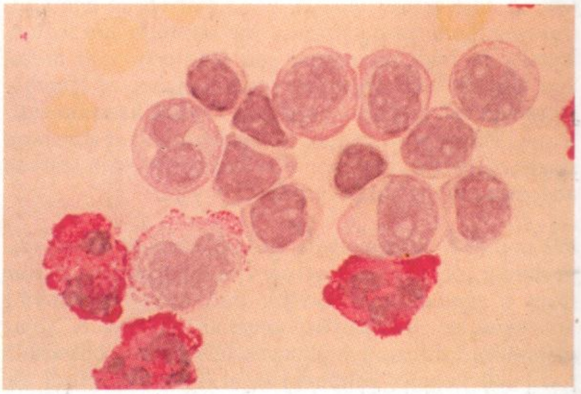

697

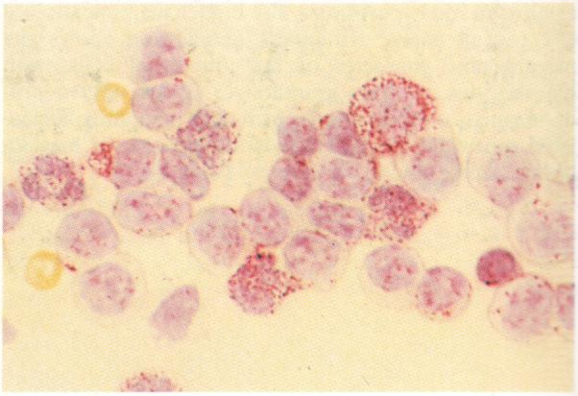

693–697. Smears of a buffy coat preparation, made from the peripheral blood of a patient with B-CLL in course of malignant progression to an immunoblastic leukaemia/lymphoma. This type of transformation – Richter's syndrome – develops as a terminal manifestation in about 5% of patients with CLL, and is usually characterized by recurrent lymphadenopathy, fever, weight loss, and resistance to previously effective chemotherapy. Immunoblasts are usually present in the peripheral blood and heavily infiltrate the marrow (*see* **698–700**).

There are three residual lymphocytes and a neutrophil polymorph in **693**, but the predominant cell population is made up of immunoblasts with basophilic cytoplasm and somewhat plasmacytoid nuclei.

Apart from the immunoblasts in the blood, there may be other unusual reactive elements, like the rare tissue mast cell appearing in **694**, where there are also several neutrophils, one of them polysegmented, and a basophil, as well as a lymphocyte and several immunoblasts of varied size.

The SB stain in **695** shows the predominating immunoblasts to be negative, the positive cells in this field including two neutrophil stab cells, a basophil to the right, and two probable monocytes towards the top left.

The PAS reaction in **696** reveals three normally positive neutrophil polymorphs, a monocyte with peripheral granular positivity, three negative lymphocytes, and nine immunoblasts with either negative reactions or no more than a faint tinge of positivity.

The acid phosphatase stain in **697** shows normal positivity in polymorphs, a stronger reaction in a monocyte, a few positive granules in most of the immunoblasts, and paranuclear dots of positivity in two T lymphocytes next to the monocyte.

698

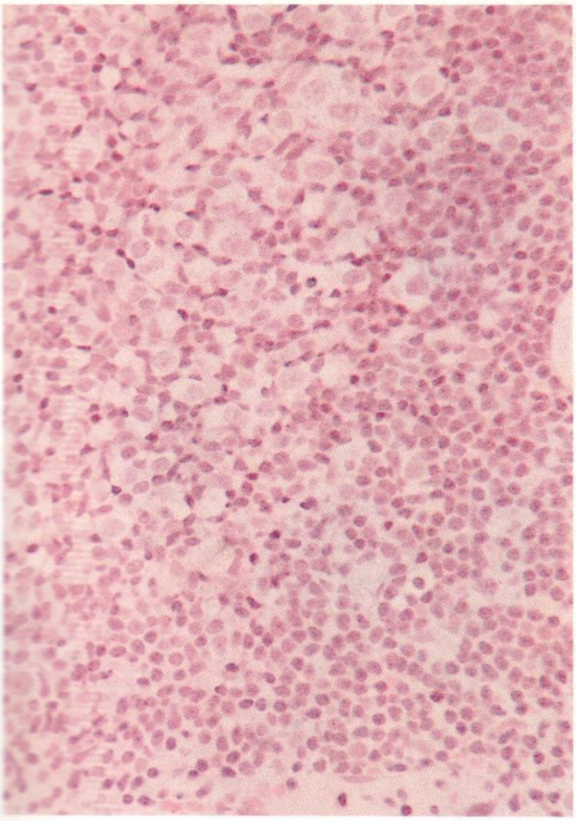

699

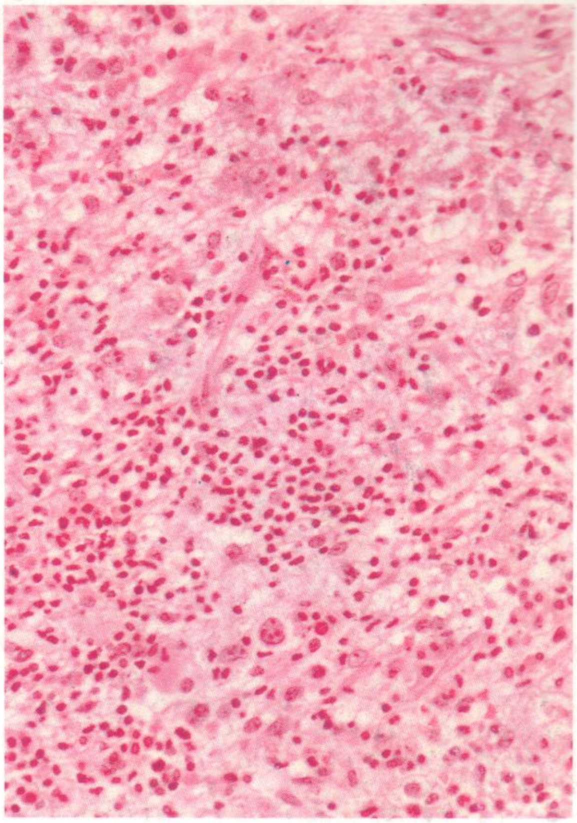

698–700. Sections of bone marrow trephine biopsy specimens taken from patients with CLL undergoing transformation to Richter's syndrome.

The field in **698** is of a junctional area with residual CLL lymphocytes at the lower right half and large cells with paler nuclei and more ample cytoplasm occupying most of the upper left half.

In **699** a low-power view of another transforming marrow sample reveals a less nodular and more diffuse pattern of infiltration with large immunoblastic cells. There is also evidence in this field of accompanying fibroblastic reaction.

In **700** a higher-power view of the same section as in **699** provides details of the cytology, including a scattering of the large cells with vesicular nuclei and generally conspicuous nucleoli among a mixed population of residual small CLL lymphocytes, occasional polymorphs and erythroblasts, capillary endothelial cells, and scanty fibroblasts. Several of the large cells possess twisted nuclei and bear a general resemblance to histiocytes, and it is not surprising that Richter's syndrome was at one time thought to represent a malignant histiocytic transformation of CLL, but both the cytology and cytochemistry of these cells in smears and the frequent demonstration that they express monoclonal surface immunoglobulin confirm that they are in fact immunoblasts.

700

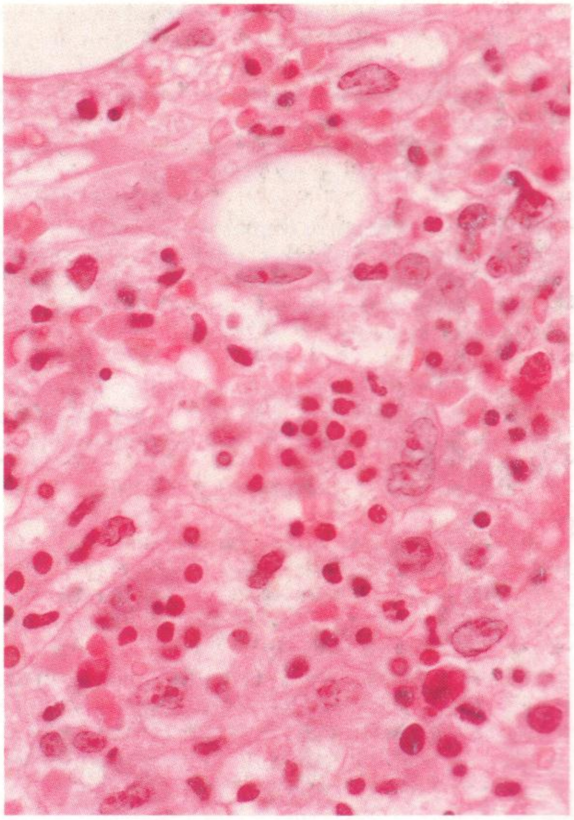

701

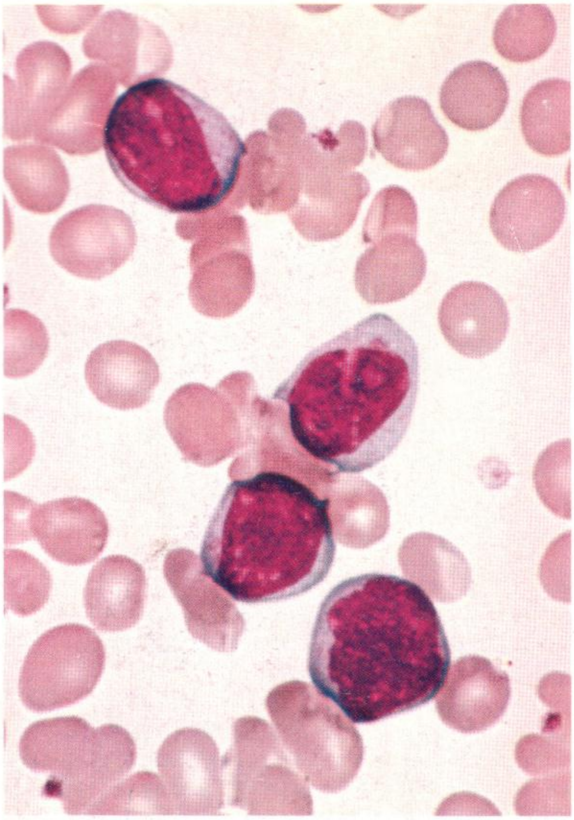

702

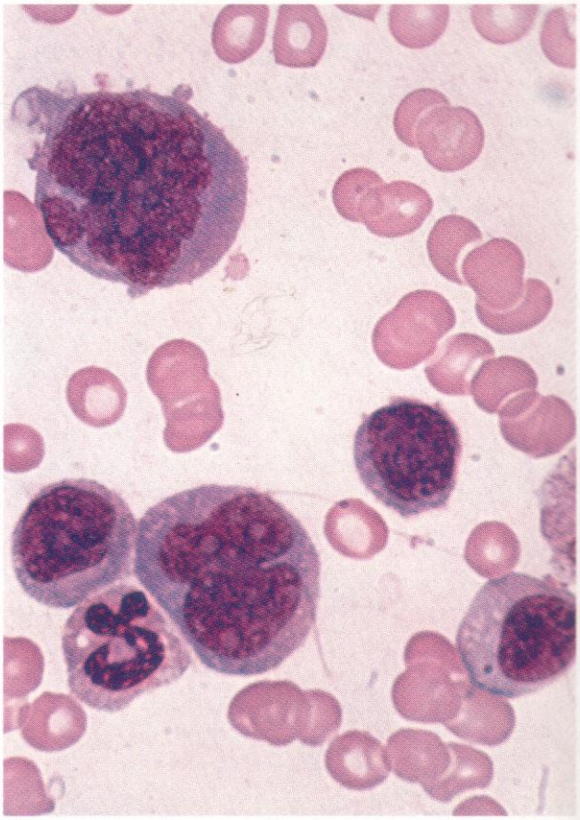

703

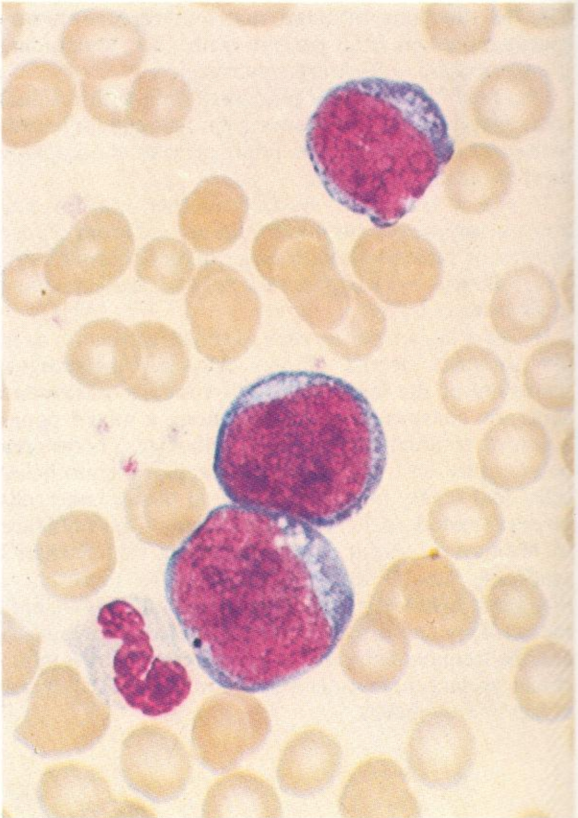

701. Four lymphoma cells from the blood of a patient with longstanding NHL recently spreading to involve bone marrow and blood. The cells resemble neither mature lymphocytes nor leukaemic lymphoblasts, but have intermediate characteristics. One cell shows a tendency to nuclear cleaving. These cells are of 'centrocytic' or 'follicular centre cell' (FCC) type.

702. Another example of lymphoma cells in the blood: this represents a leukaemic phase of a secondary centroblastic lymphoma. There are multiple small nucleoli visible in the irregular nuclei and cytoplasmic basophilia is moderate.

703. A third example of lymphoma cells in the blood – in this case the cells have deep cytoplasmic basophilia and multiple nucleoli, and are of immunoblastic character.

704

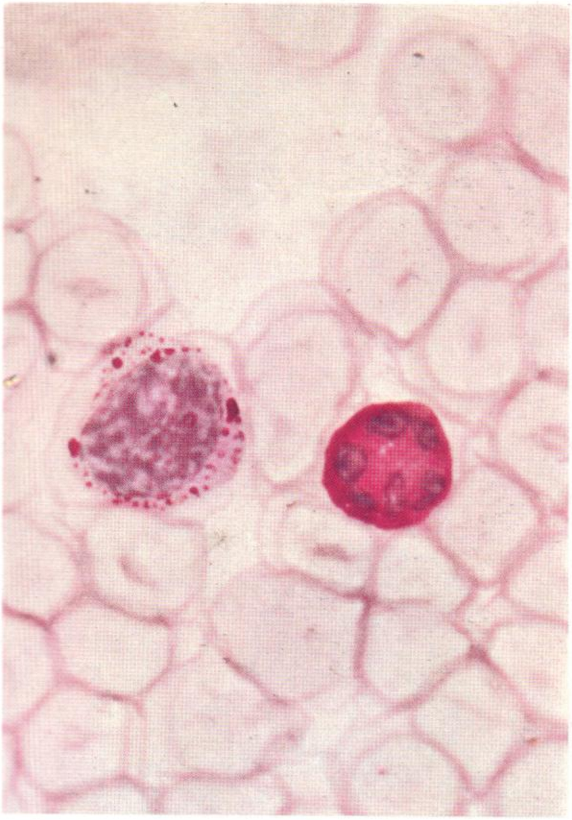

705

704. A lymphoma cell from the specimen illustrated in **701**, stained with the PAS reaction, to show coarse granules and two small blocks of positivity. A polymorph reacts normally. Centrocytes of this kind more often show PAS positivity when circulating in the leukaemic phase than do similar cells in lymph node imprints.

705. Strong PAS reaction, with rings of moderately coarse granules around the nuclei in circulating lymphoma cells, from the case illustrated in **702**. Fine and moderately coarse granular positivity is present.

706. Almost negative PAS reaction in the circulating neoplastic immunoblasts from the case illustrated in **703**.

706

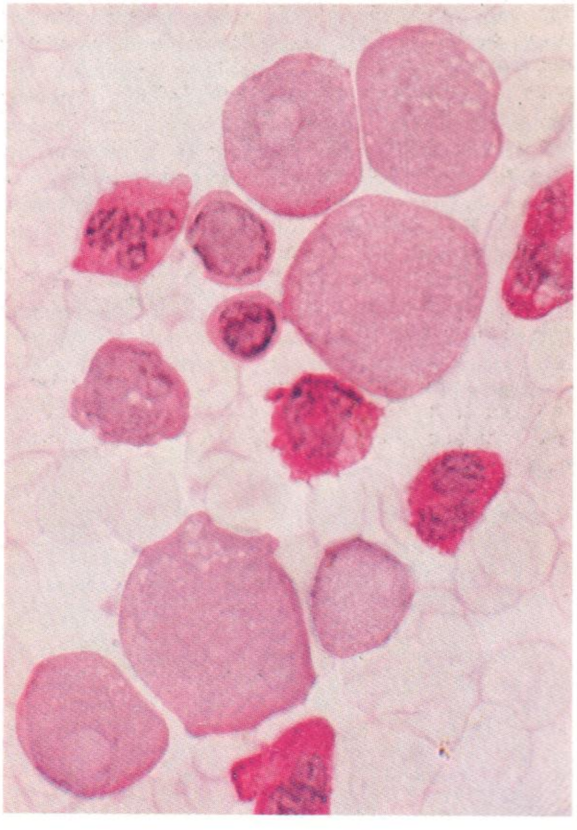

707

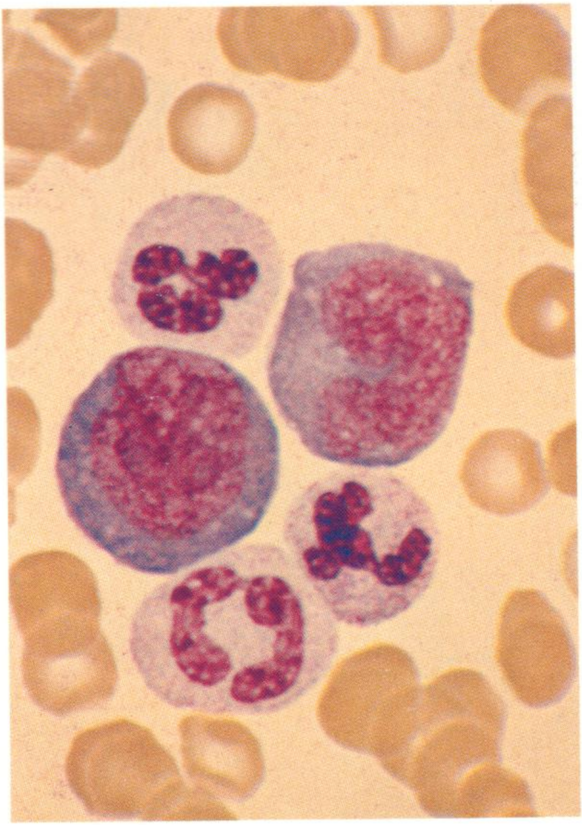

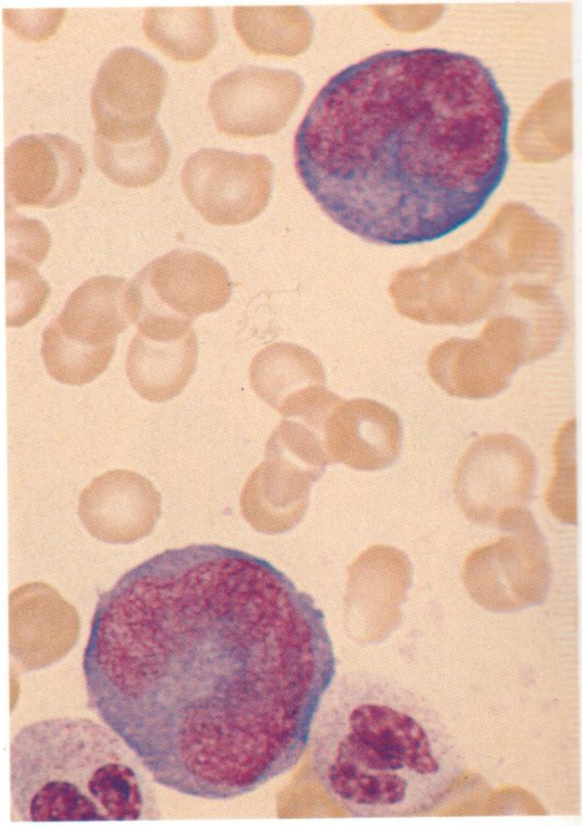

707 and **708**. Romanowsky stains on two further examples of cells from the peripheral blood of a patient in a leukaemic phase of immunoblastic lymphoma. The large cell size, deep cytoplasmic basophilia, irregular, somewhat plasmacytoid, but generally primitive, nuclear chromatin pattern, the presence of large centrally placed nucleoli in some cells, and the variability of nuclear shape from uniformly round to deeply indented, all characteristic features of malignant immunoblasts, are well shown.

709. Scattered BE positivity in three neoplastic immunoblasts, a normally BE-positive monocyte, a T lymphocyte with localized 'dot' BE positivity, and a CE-positive neutrophil.

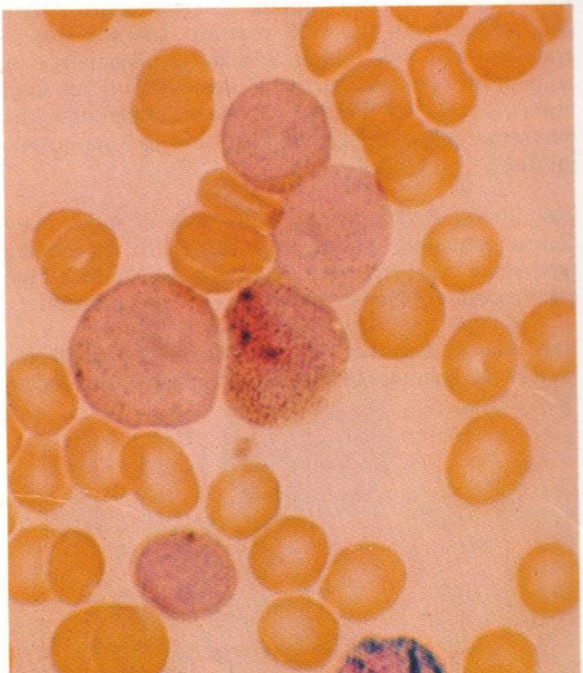

710 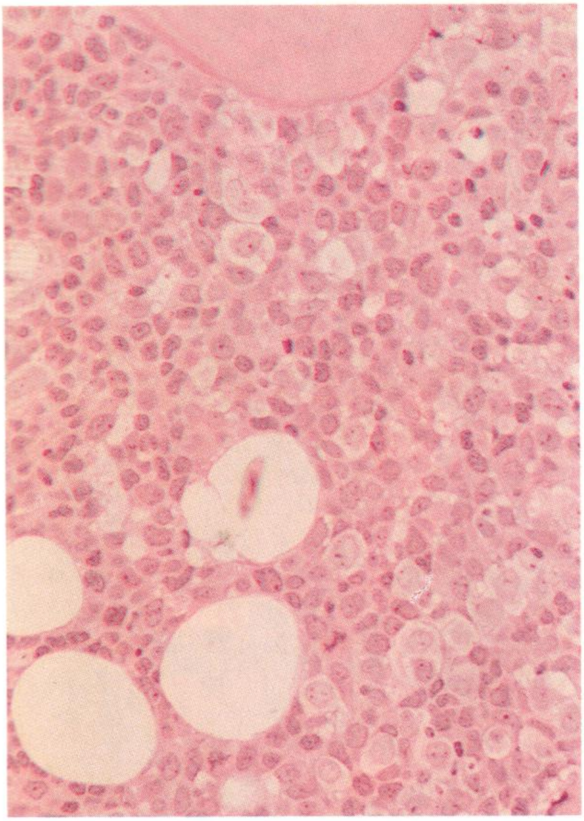

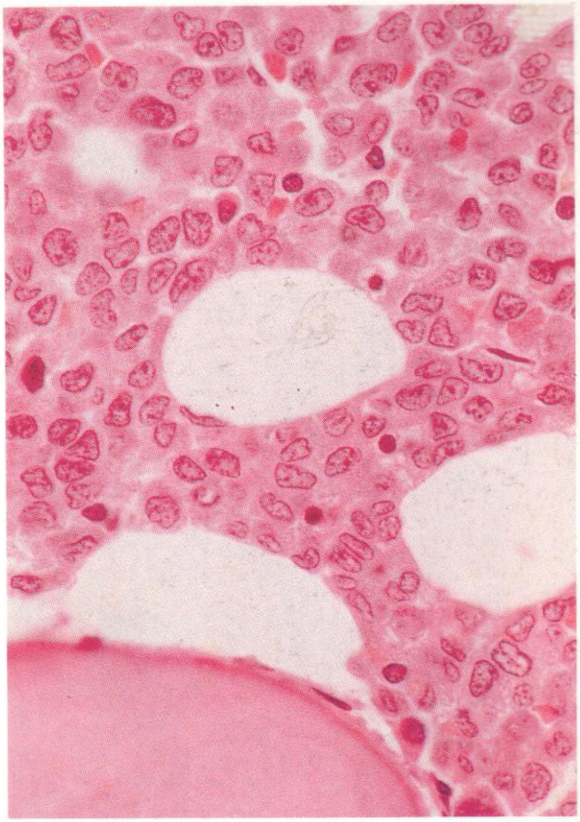 711

710. A section of bone marrow trephine biopsy from a patient with a large-cell diffuse immunoblastic lymphoma, showing extensive diffuse infiltration of the marrow parenchyma with mostly large immunoblastic cells, often having conspicuous centrally placed single nucleoli. The remaining cells with darker nuclear chromatin and less visible cytoplasm are residual haemopoietic elements of erythroid and granulocytic lines.

711. Another higher-power view of a trephine biopsy of bone marrow from a patient with a large-cell lymphoma, this time again showing diffuse infiltration but with centroblasts rather than immunoblasts. These cells generally show more twisted and indented nuclear outlines, and their nucleoli are smaller and more often multiple and near the nuclear membrane; these cytological characteristics are those of centroblasts or large-cleaved follicular centre cells.

712. A high-power view of a section of marrow trephine biopsy with centroblastic lymphomatous infiltration. The large, if somewhat variable, cell size and the irregular nuclear outlines, which give rise to the alternative name of 'large-cleaved cell', are well shown.

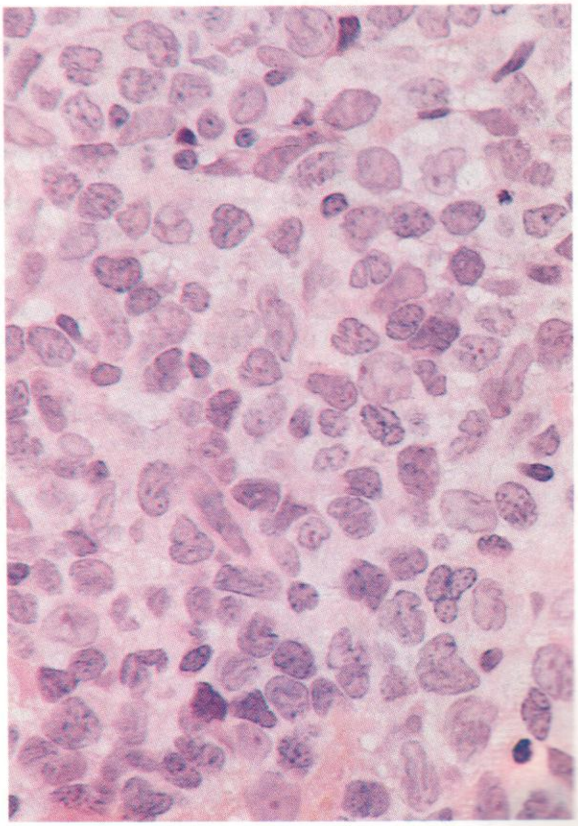 712

713

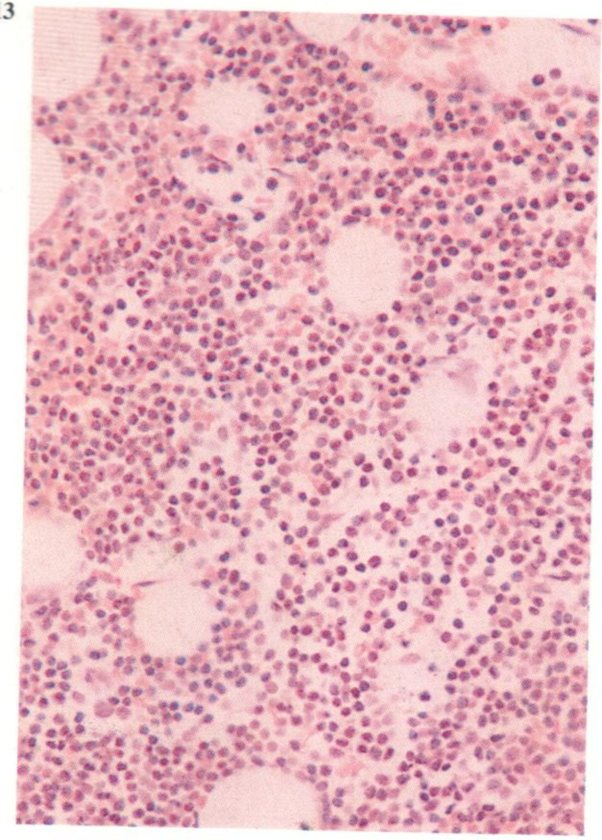

7

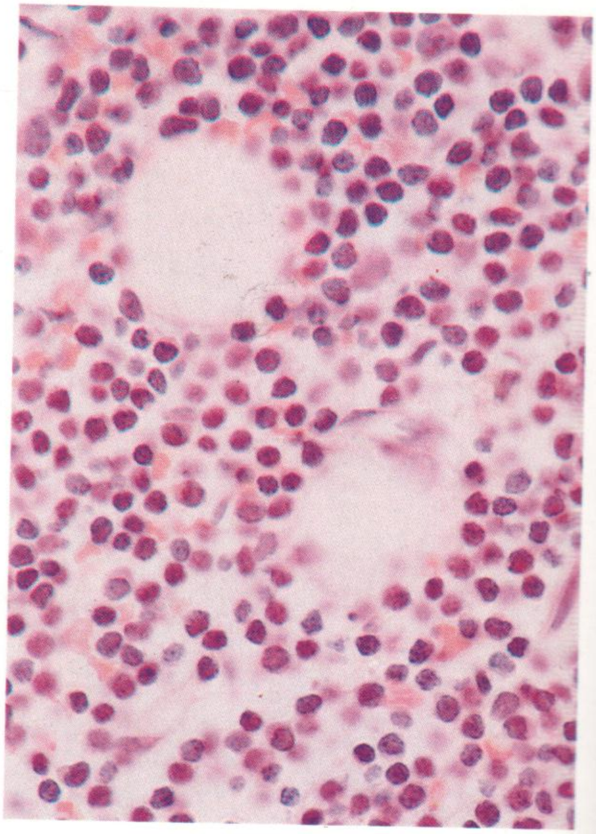

713–715. Sections of bone marrow trephine biopsies from another patient with a diffuse follicular centre cell or centrocytic lymphoma, showing response to treatment with an anti-lymphoid MAb. The respective low- and higher-power views of the pre-treatment biopsy in **713** and **714** illustrate the extensive nature of the marrow infiltration and the cytology of the cells as predominantly non-cleaved centrocytes. In **715**, the fresh biopsy taken after a short course of MAb therapy shows an entirely changed picture, with return to the normal highly pleomorphic cell mixture of normal haemopoietic tissue, including erythroblasts, granulocytes of all stages, and megakaryocytes, the only apparent abnormality being a reactive increase in eosinophils.

Trephine biopsies are essential in the assessment of response to therapy when marrow infiltration exists, since they allow the degree of residual tumour-cell persistence to be measured with much greater accuracy than is possible in aspiration biopsies.

715

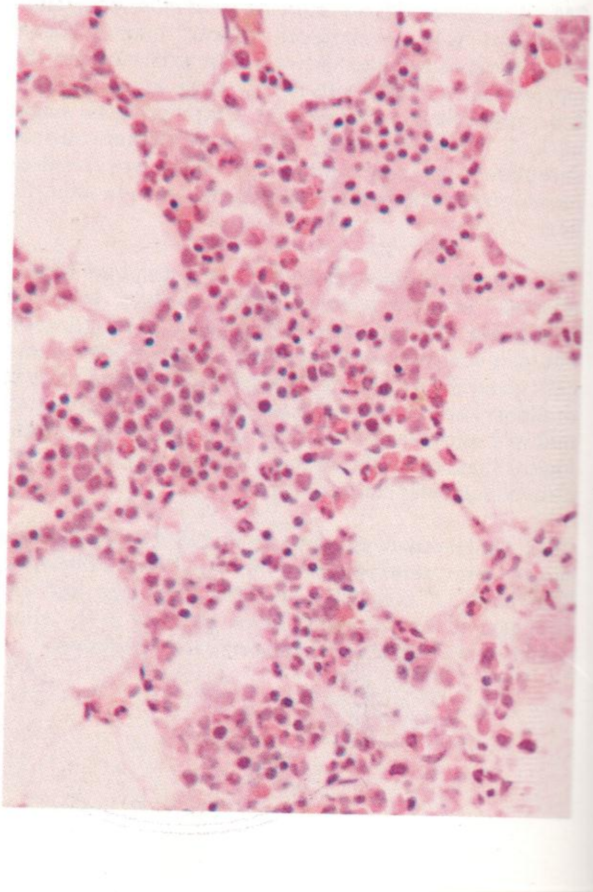

716

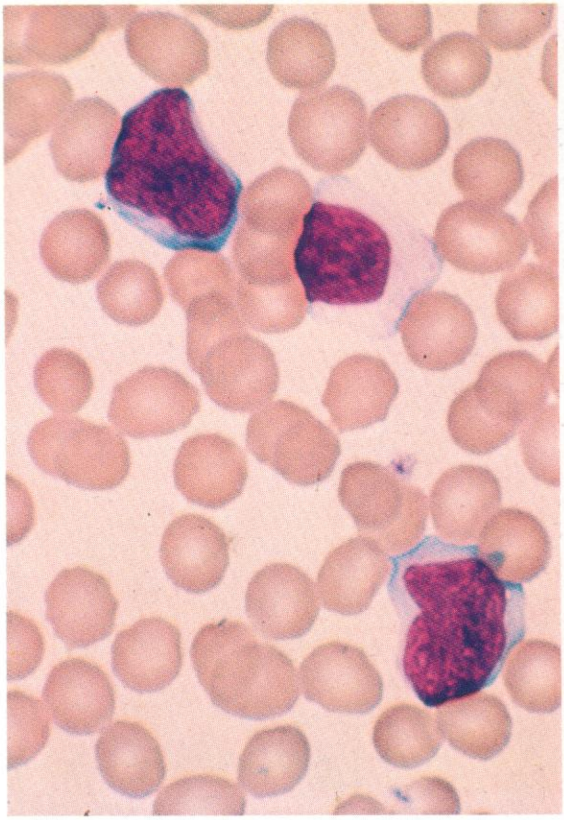

717

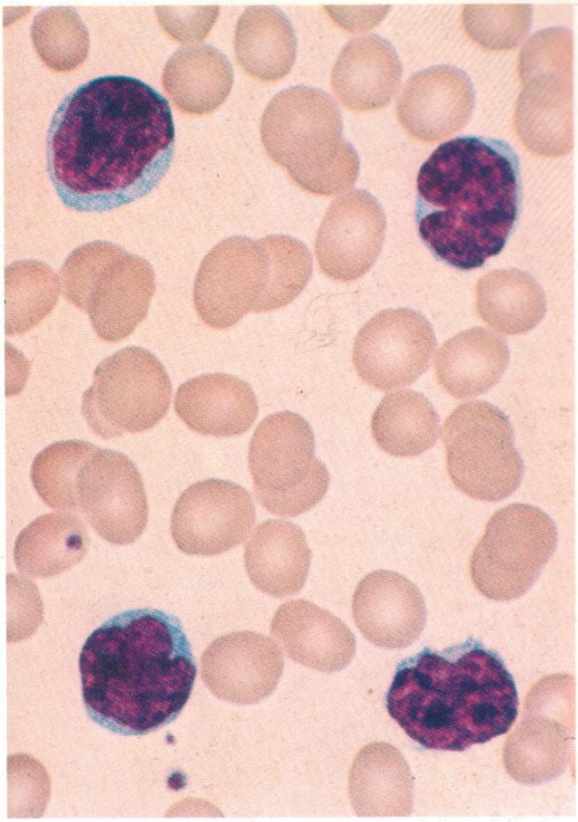

716–718. *Blood smears at stages during the progression of a lymphoblastic lymphoma, convoluted (T-cell) type, to a picture virtually indistinguishable from ALL.*

716. A lymphocyte and two lymphoma cells at a stage when involvement of the blood first occurred, with small numbers of cells.

717. The lymphomatous lymphoblasts now predominate and the total leucocyte count has risen above normal. In this field, as in the preceding one, the twisted and convoluted nuclear outlines of the T lymphoblasts are apparent.

718. A fully leukaemic picture. The T lymphoblasts at this stage tend to lose their previously conspicuous nuclear convolution, and come to resemble the lymphoblasts of primary, *de novo*, T-ALL.

718

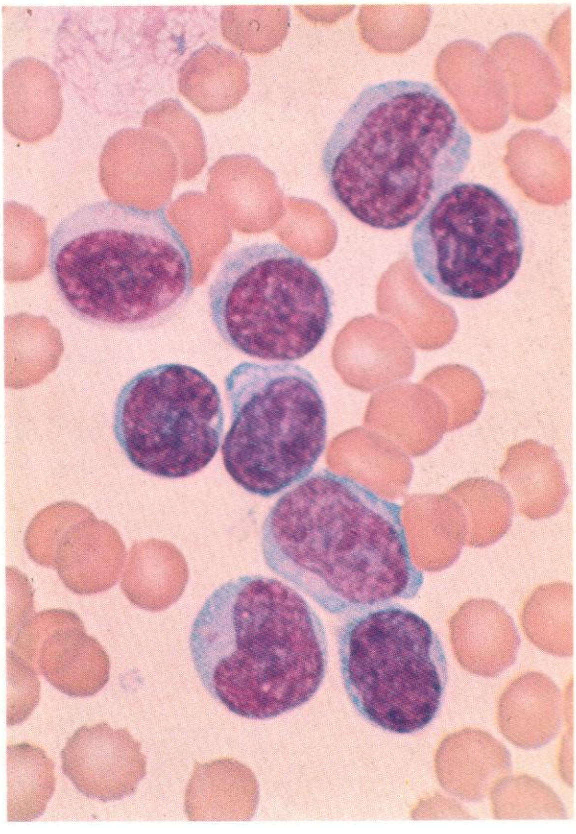

719

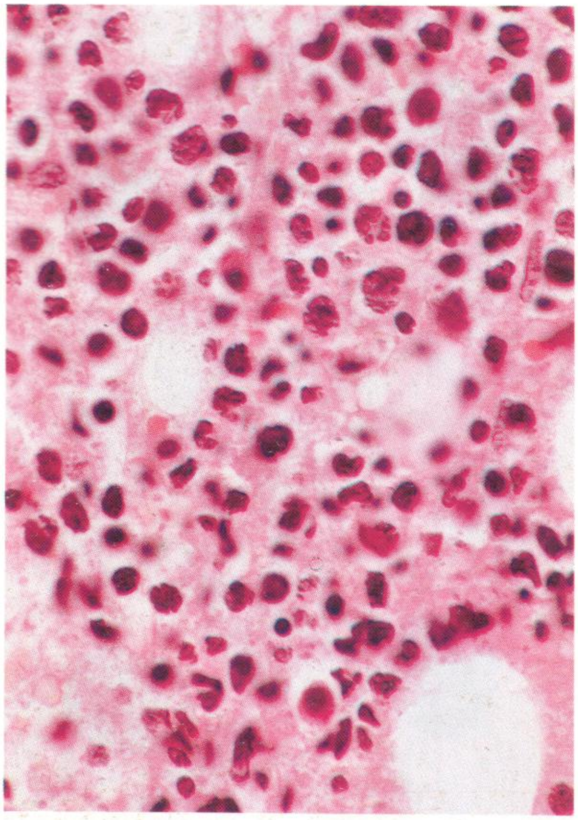

720

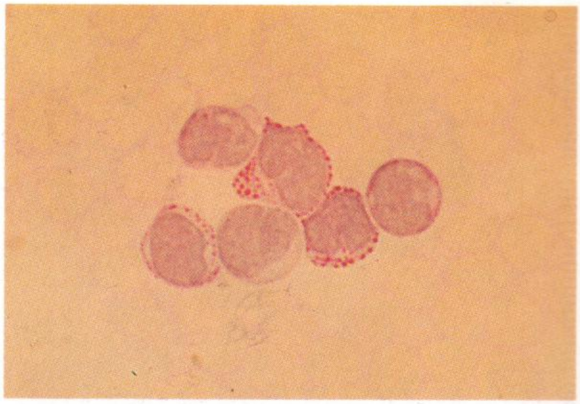

721

722

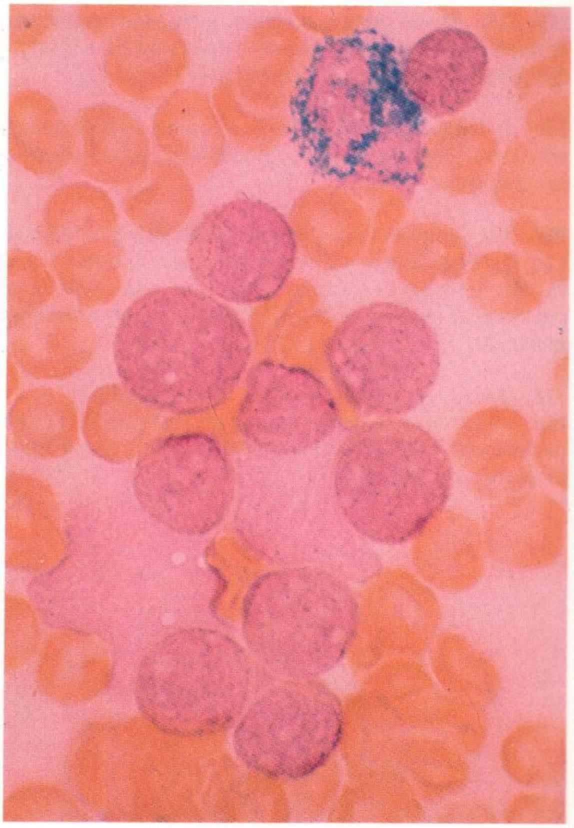

719. A section of bone marrow trephine biopsy from a patient with convoluted T-cell lymphoma, prior to leukaemic progression. There is a scattered diffuse infiltrate with large cells, often showing markedly twisted and convoluted nuclear outlines, but with perhaps 30% of the whole cell population in this field composed of residual normal haemopoietic tissue.

720. The cells from the peripheral blood, during and after the emergence of the leukaemic phase of convoluted T-cell lymphoma, show coarse PAS positivity of the lymphoblastic pattern.

721. Acid phosphatase reaction shows strong localized positivity in most cells.

722. Dual esterase reaction in the same cells shows negativity to BE but a few scattered CE granules only, in the T lymphoblasts.

723

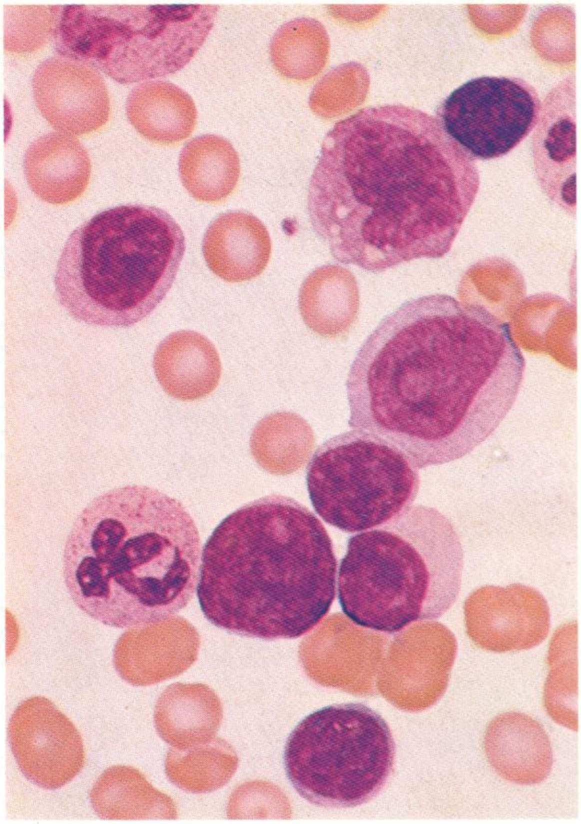

724

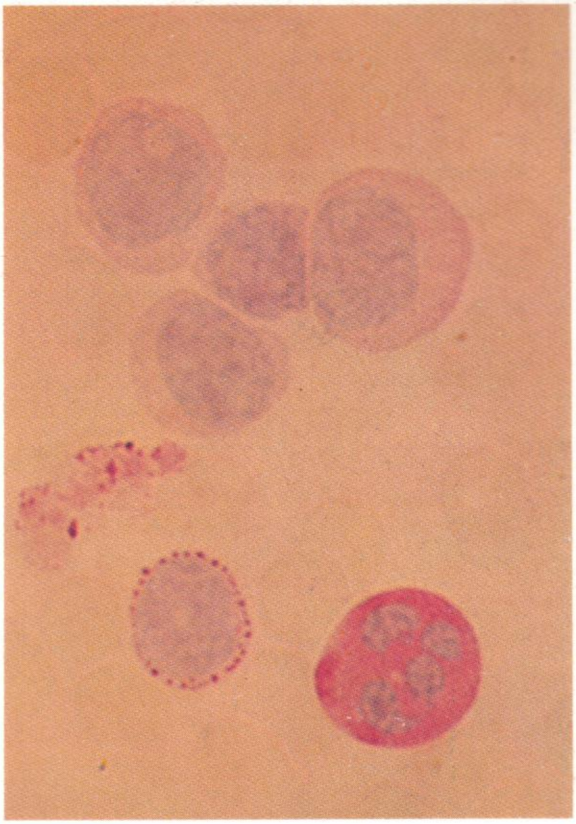

723–725. *Circulating lymphoma cells from a case of follicular lymphoma (mixed small and large FCC tumour, centroblastic/centrocytic type).*

723. Romanowsky stain: a monocyte, two neutrophils and seven lymphoid cells of variable cytology, including a nucleolated centroblast.

724. PAS reaction: variable positivity in centroblasts and centrocytes.

725. Alkaline phosphatase reaction showing positivity in lymphoma cells – a most unusual finding in the peripheral blood. The seven neutrophils present show positivity ranging from + to +++.

725

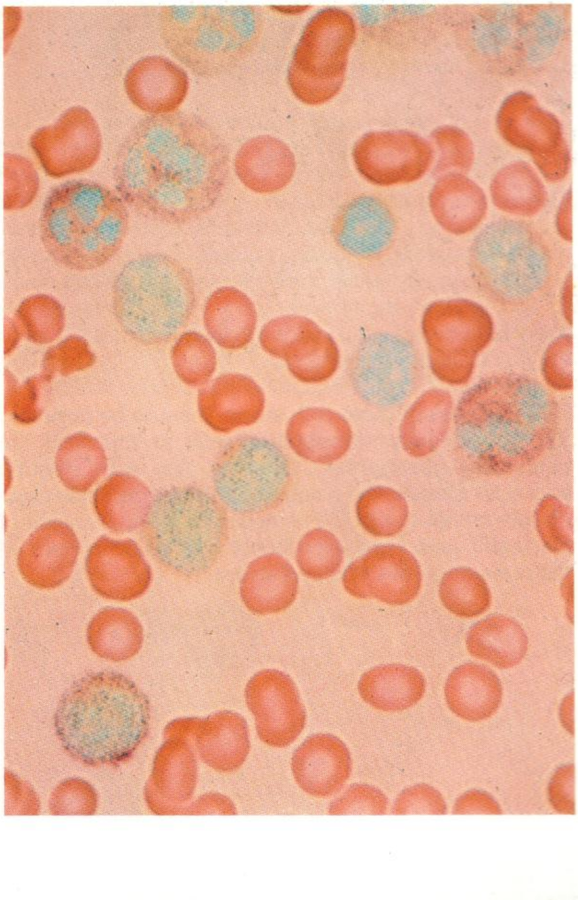

726

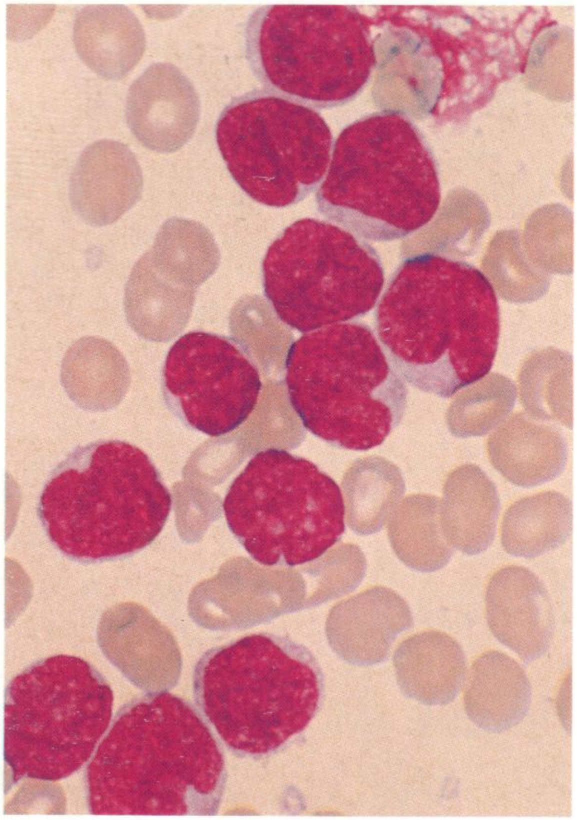

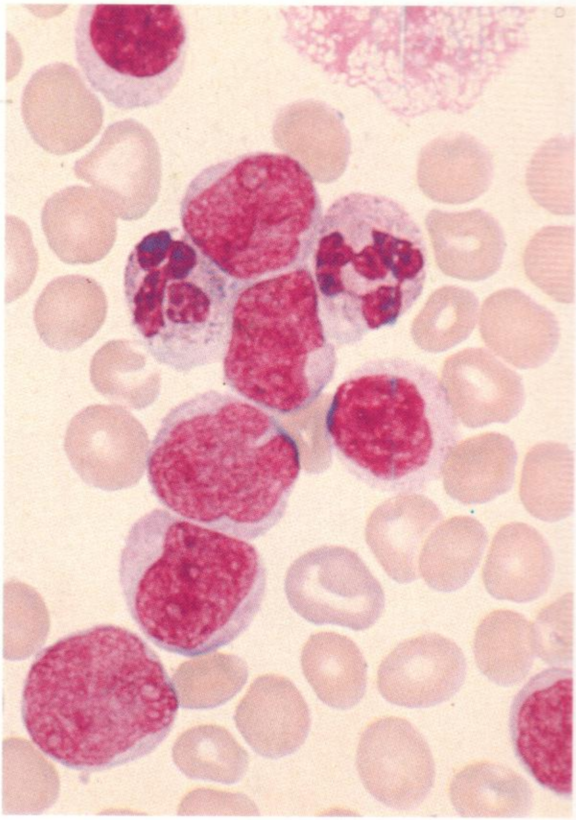

726–733. *Cytological and cytochemical preparations from the peripheral blood buffy coat of a patient with circulating centroblastic lymphoma cells.*

726 and **727**. Romanowsky stains of centroblasts in the buffy coat, accompanied in **727** by two lymphocytes and two neutrophil polymorphs. The distinctive cytological features of centroblasts as seen in smear preparations are well shown; large size, indented or cleaved nuclear outlines, moderately dense nuclear chromatin, one to several, generally small, nucleoli, tending to be disposed at the nuclear membrane, grey rather than deeply basophilic cytoplasm, and a nuclear–cytoplasmic ratio ranging from high to medium.

728. SB stain of these cells shows them to be negative. The two heavily sudanophilic cells in this field are neutrophil polymorphs, and the two with discrete scattered granules of positivity and conspicuous vacuolation are monocytes. The negative cell to the right of the upper monocyte is probably a lymphocyte, but all the remaining cells are centroblasts.

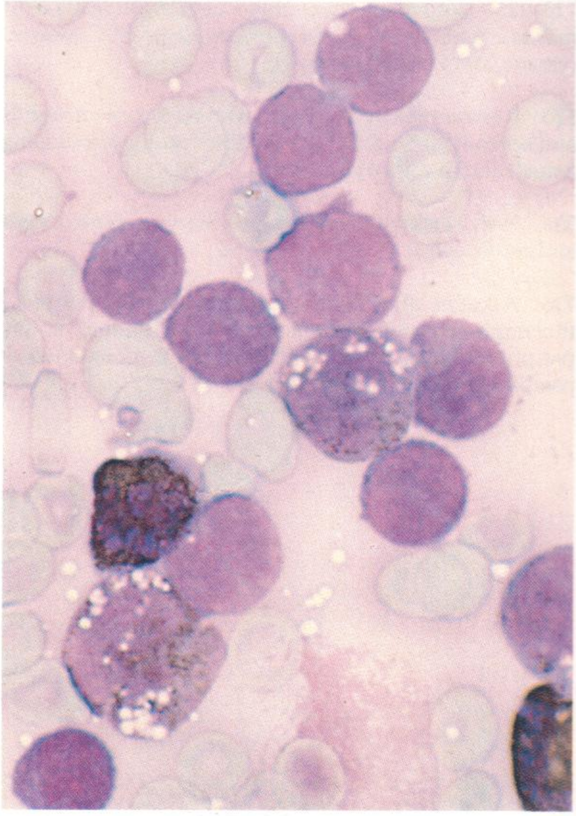

729

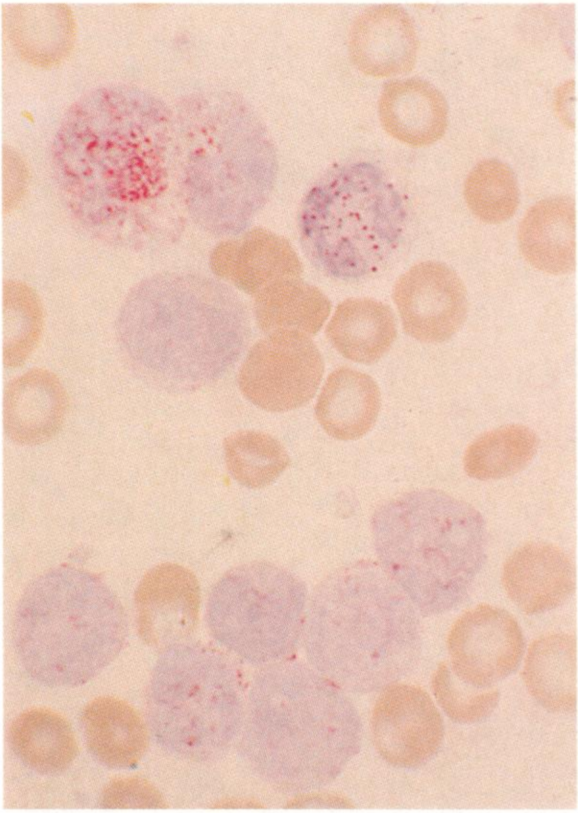

730

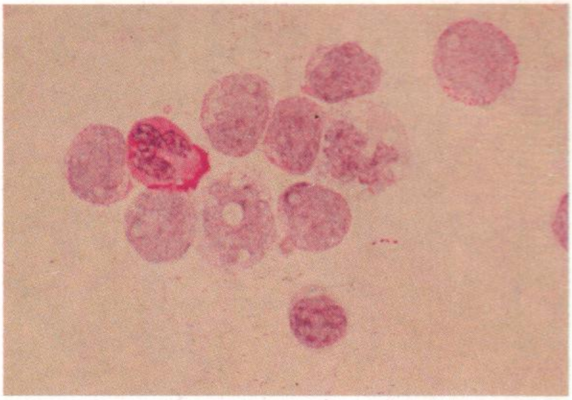

731

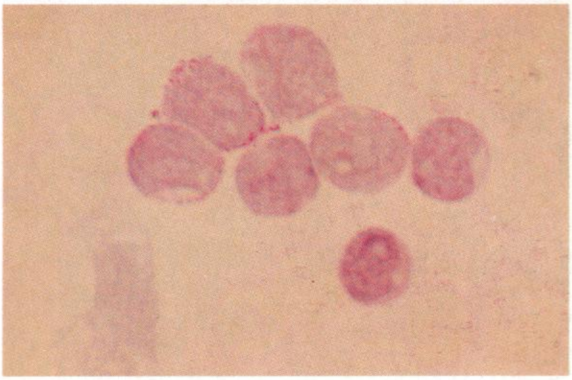

732

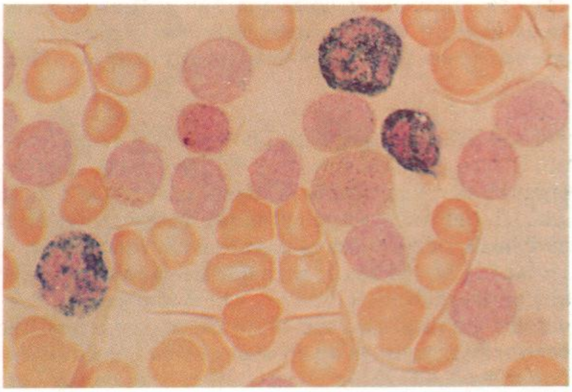

733

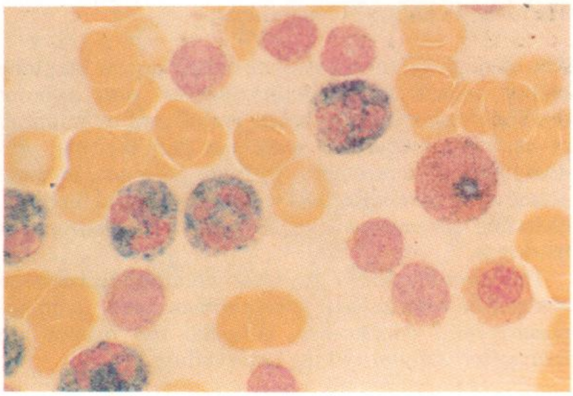

729. Acid phosphatase reaction on the same preparation reveals that most centroblasts have no more than a few scattered granules of positivity, without any paranuclear or other particular localization. The trio of cells at the top of this field are, from left to right, a moderately strongly positive monocyte, a T lymphocyte with a collection of paranuclear granules, and a neutrophil polymorph with the usual scattering of positive granules. The remaining cells are all centroblasts.

730 and **731**. PAS stains for glycogen on these cells show their reactions to be generally less strong than those seen in the earlier example of centroblastic PAS reaction (**705**), here ranging from fine to moderately coarse granular positivity. There is a normally reacting polymorph and a negative lymphocyte in **730**.

732 and **733**. Two fields from a dual esterase stain on the same buffy coat. The first (**732**) shows three CE-positive neutrophil polymorphs and a T lymphocyte with a dot of localized paranuclear reaction, but the remaining centroblasts are essentially negative with no more than a faint non-specific dusting of mixed reaction product. In **733** there are six negatively reacting centroblasts, six positive neutrophils, a negative late normoblast, and, above it, a metamyelocyte with localized CE positivity to one side of the nucleus.

734

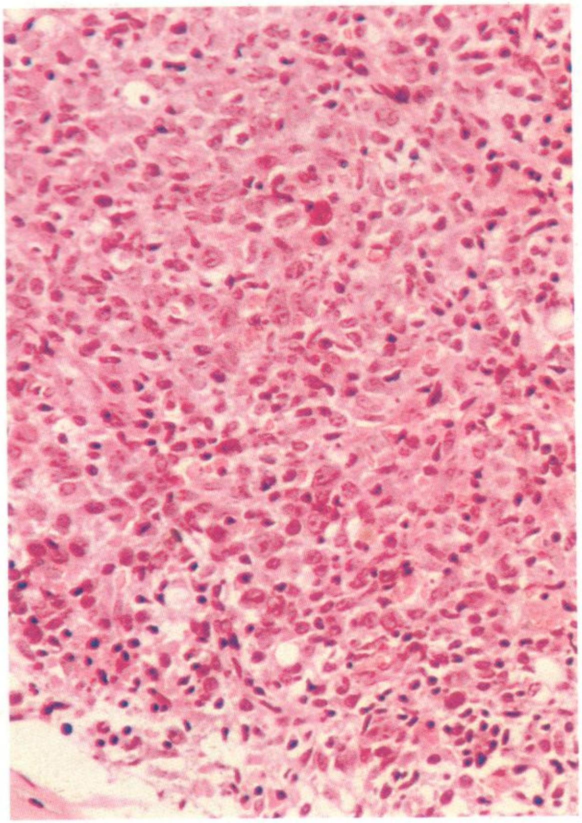

735

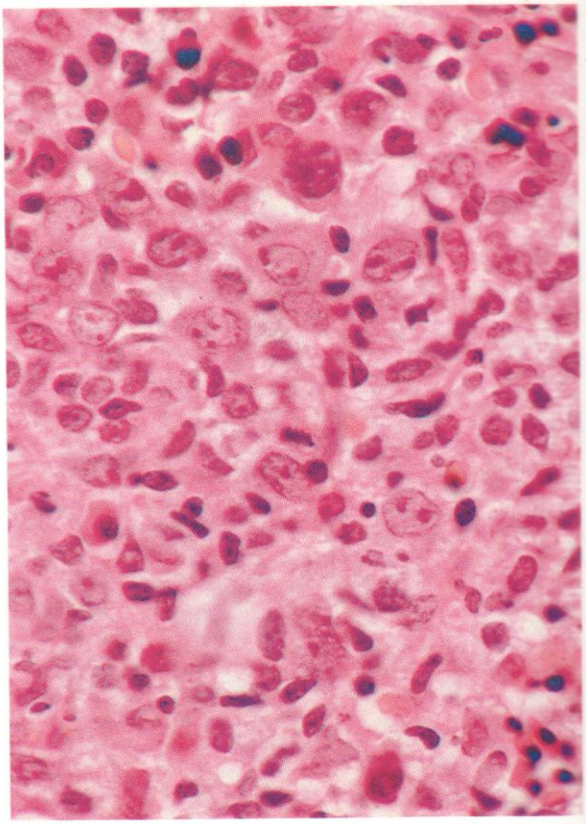

734–736. *Sections of bone marrow trephine biopsies, from patients with nodular follicular centre cell or centrocytic-centroblastic lymphoma and marrow infiltration.*

734 and **735**. Low- and higher-power views, respectively, of a lymphomatous nodule in the bone marrow parenchyma. The nodule occupies most of the field in **734**. The mixed cytology, with the larger centroblasts and smaller and more pachychromatic centrocytes, is visible in **734**, but can be seen much more clearly at the higher magnification of **735**, where the more leptochromatic, vesicular, and often cleaved nuclei of the centroblasts, with their conspicuous peripherally disposed nucleoli, differ clearly from the denser and smaller nuclei of the centrocytes. Occasional normal marrow elements are recognizable.

736. A high-power view of a bone marrow trephine biopsy section from another patient with a more markedly centrocytic follicular lymphoma. A minority of centroblasts can be seen, but with a clear predominance of centrocytes, with the presence, in some areas, of more mature cells with plasmacytoid features, including eccentric nuclei with clock-face chromatin markings.

This case illustrates the close relationship between centrocytic-centroblastic lymphomas and lymphoplasmacytoid lymphomas, although the former are more often nodular and the latter diffuse.

736

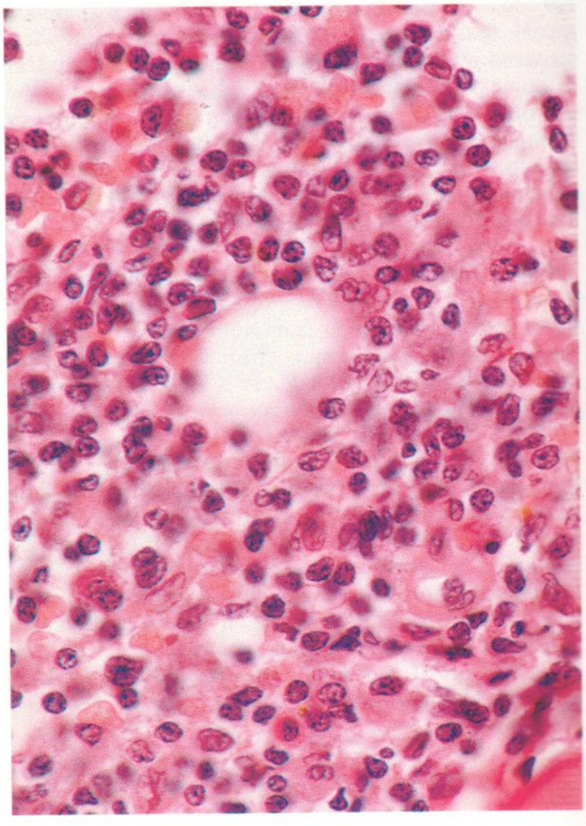

737

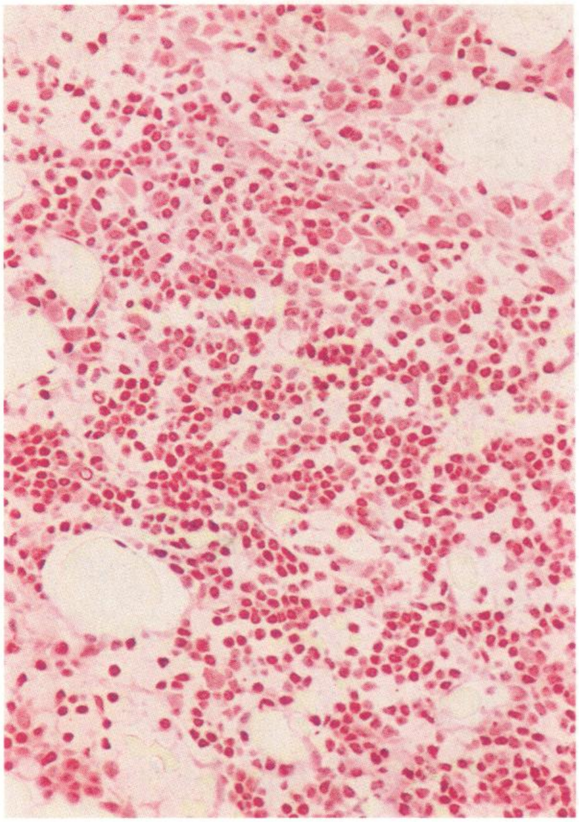

738

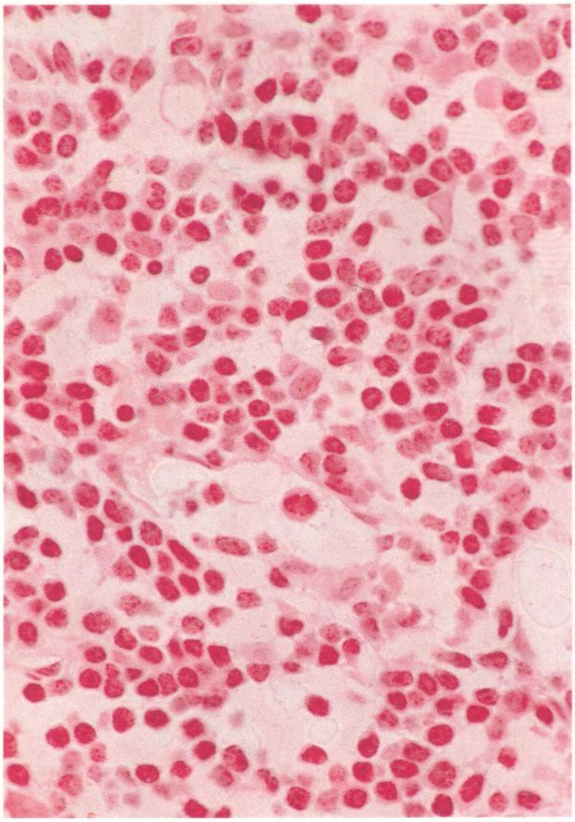

737–739. *Sections of bone marrow trephine biopsies from patients with lymphocytic and lymphocytic–centrocytic lymphomas and marrow infiltration.*

737 and **738**. Respectively low- and higher-power views of a mixed nodular and diffuse lymphocytic infiltrate, a border of less densely infiltrated marrow tissue remaining in the upper third of the field in **737**, which is otherwise largely occupied by a nodular focus of lymphoma. In this field, and more clearly in **738**, the nature of the infiltrating lymphoma cells is apparent as mature small lymphocytes, morphologically indistinguishable from those found infiltrating the marrow in CLL.

739. This paratrabecular nodule of lymphomatous deposit shows rather more pleomorphic cytology, with two or three eosinophils, a few elongated vascular endothelial cells, and an occasional late normoblast, but chiefly a lymphoma cell population of mixed lymphocytes (with small dense nuclei), centrocytes (with more open nuclear chromatin and frequent indentation or cleavage of their nuclear outlines), and lymphoplasmacytoid cells (with eccentric nuclei having clock-face blocks of chromatin).

This case again illustrates the close interrelationship between the various 'low-grade' NHLs.

739

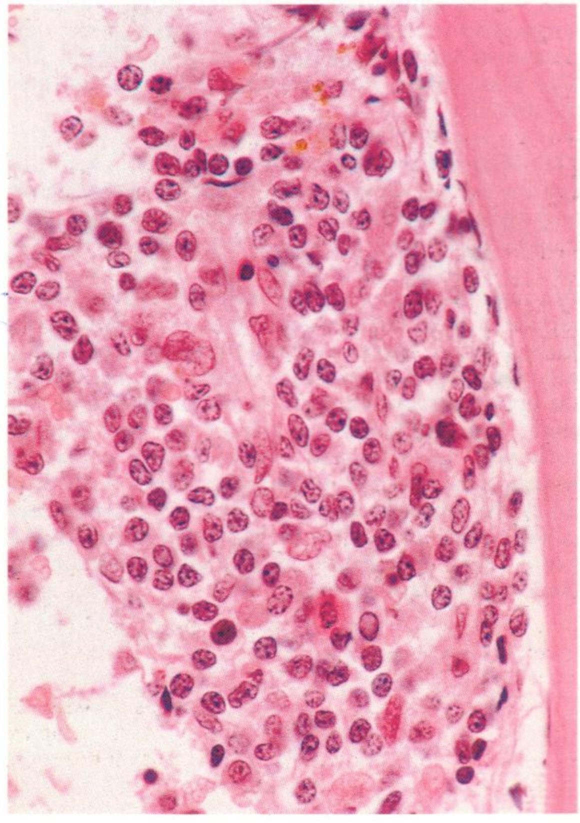

740

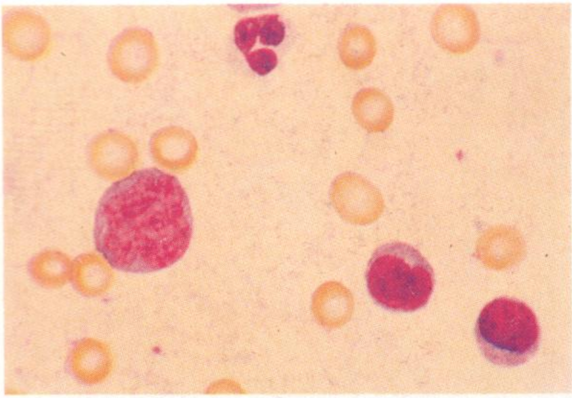

741

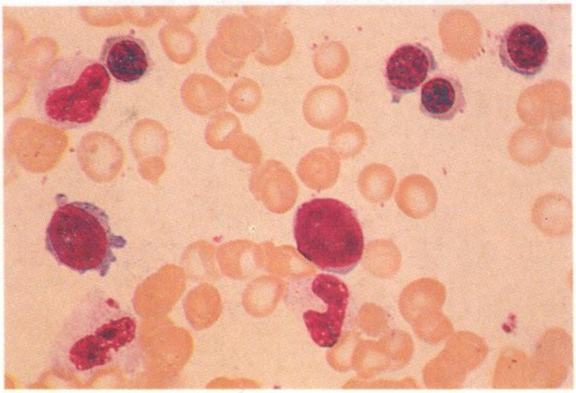

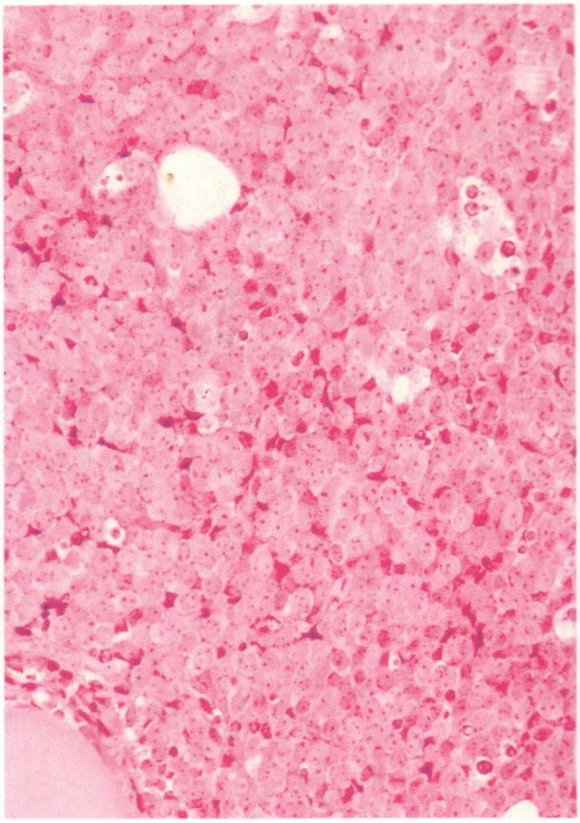

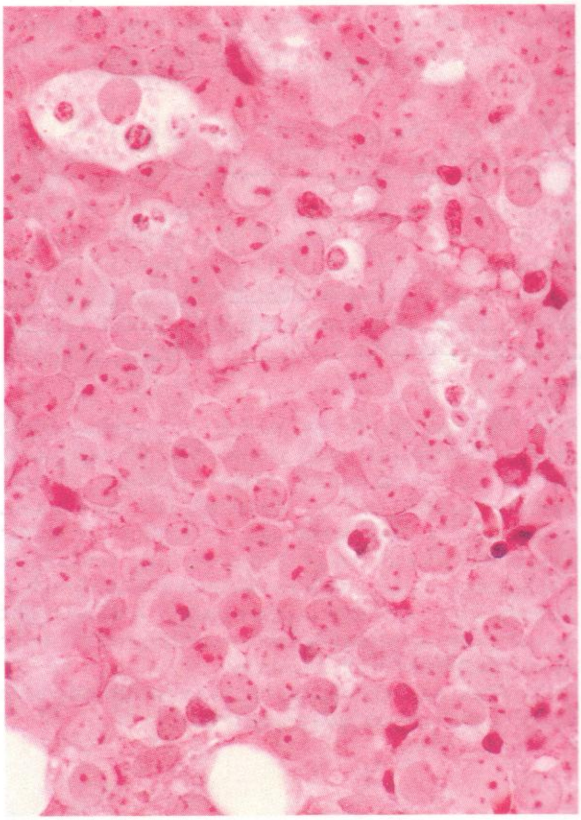

740. A circulating lymphoma cell from a case of lymphoblastic lymphoma, B-cell type, with only occasional lymphoma cells in the peripheral blood. The field also contains two lymphocytes and a segmented neutrophil.

741. Marrow infiltration in the same case: the lymphoma cells show a more lymphoblastic appearance, with higher nuclear–cytoplasmic ratio, than those in the peripheral blood.

742 and **743**. Low- and higher-power views from a section of bone marrow trephine biopsy, taken from a patient with a B-lymphoblastic lymphoma of Burkitt cell type, both showing almost complete replacement of the normal marrow elements by the lymphomatous infiltrate. The lymphoblasts are large and pale-staining, with very leptochromatic nuclei mostly containing several conspicuous small nucleoli. In both fields there are to be seen macrophages containing phagocytosed cellular material, similar to those giving the classical 'starry sky' appearance in histological sections of Burkitt's lymphoma proper.

744

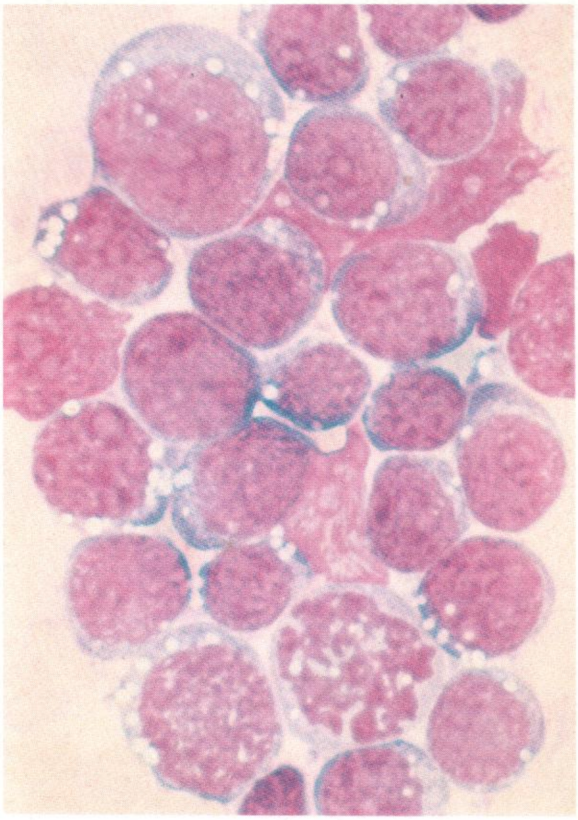

745

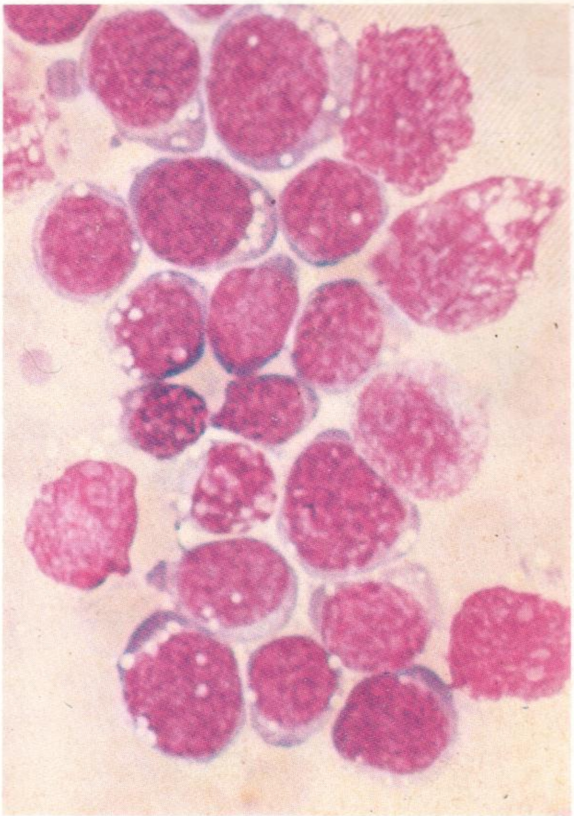

744–747. The first two figures are of Romanowsky stains and the latter two of SB and PAS preparations, respectively, from the bone marrow of a child with Burkitt's lymphoma. An appearance comparable with lymphomatous or acute leukaemic invasion is seen. This type of extensive marrow replacement by tumour is unusual in Burkitt's lymphoma.

The morphology of the cells is unlike that of typical leukaemic lymphoblasts; the nuclear chromatin is coarser and more stranded, and most cells are PAS-negative. The vacuolation, characteristic of the tumour cells in this disease, is well shown, but similar vacuoles may sometimes be seen in acute leukaemias and this feature is not pathognomonic.

746

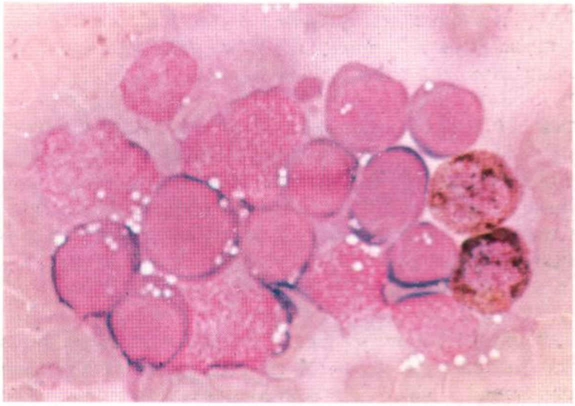

747

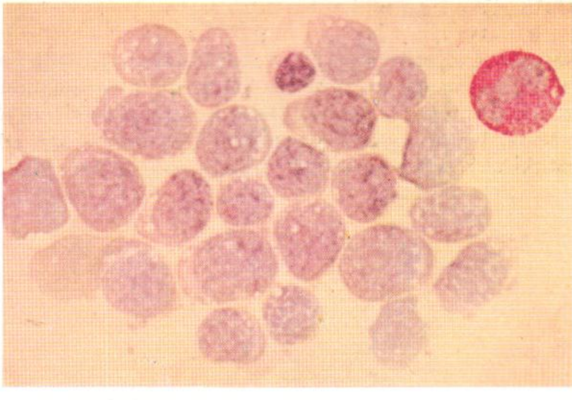

748

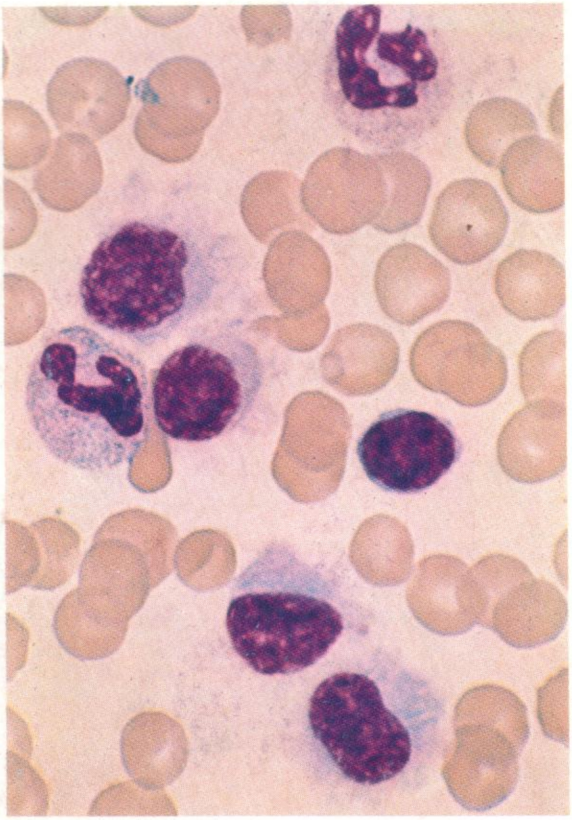

749

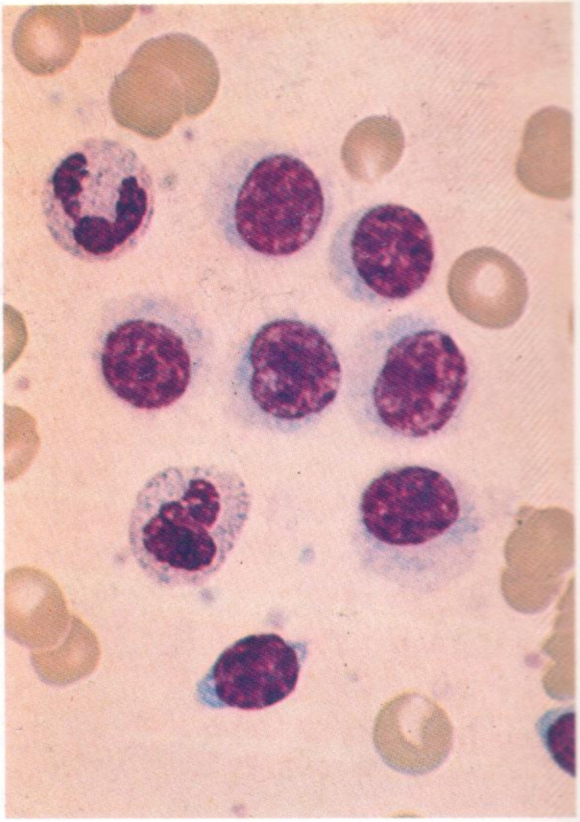

75

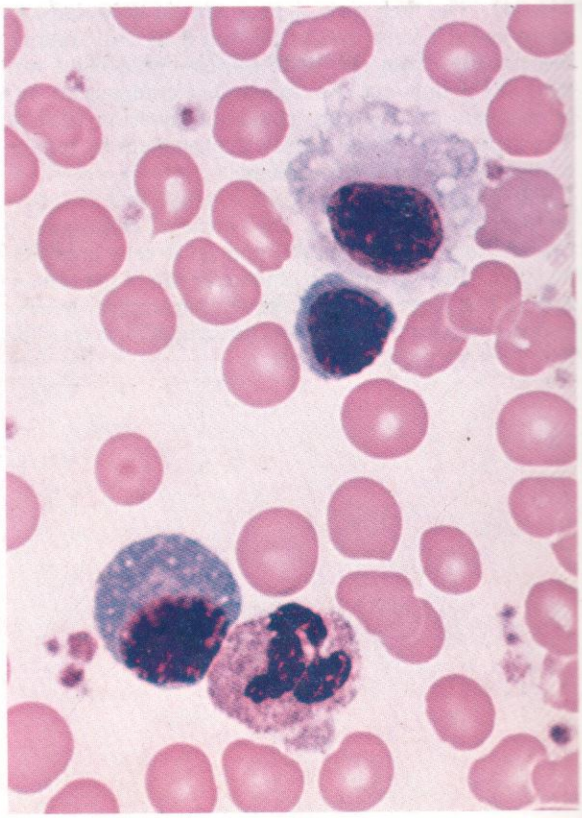

748–761. *Preparations from typical HCL – leukaemic reticulo-endotheliosis (LRE). In all these smears monocytes are conspicuous by their absence.*

748. HCL. Leishman stain of peripheral blood. Two neutrophils, a normal lymphocyte and four hairy cells (HCs), showing the typical eccentric nucleus with moderately coarse chromatin, the pale slate-blue cytoplasm, and the fine surface projections or hairs. A rod-shaped negatively staining inclusion in one of the HCs may represent a ribosome-lamella (R-L) complex.

749. HCL. Leishman stain of peripheral blood from another case. A group of six HCs together with one lymphocyte and two segmented neutrophils. The nuclear staining of the HCs shows the sponge-like or checkerboard pattern often seen.

750. HCL. Leishman stain of another example, with an HC showing the conspicuous cytoplasmic vacuolation which is often a feature of these cells, together with a normal lymphocyte, a neutrophil polymorph and an immunocyte or plasma cell, from a patient with HCL and a virus infection.

751

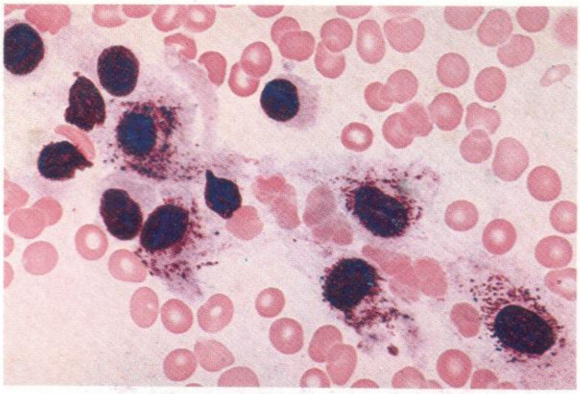

752

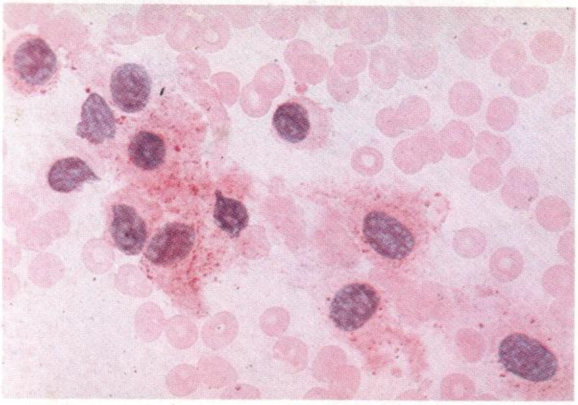

753

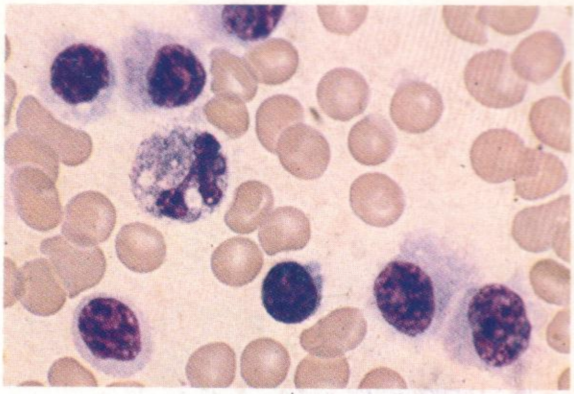

754

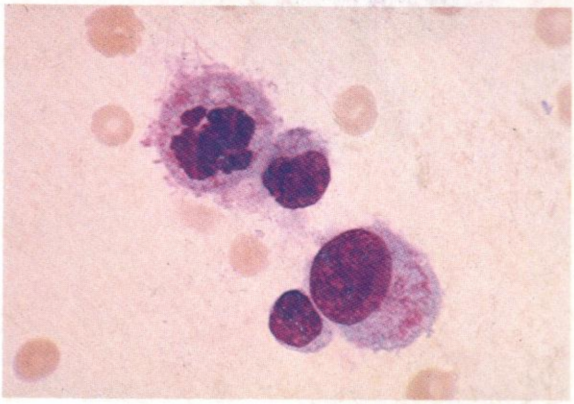

751. HCL. Leishman stain of a bone marrow smear, showing a cluster of HCs with the azurophilic inclusions sometimes present and seen, especially, after short-term culture.

752. Consecutive PAS stain on the same field as in **751**. The tinge and fine granular positivity are typical of HCs.

753 and **754**. HCs in peripheral blood before and after a period of 48 hours in culture, showing increase in cytoplasmic granularity and the occurrence of mitosis.

755. A further example of HCs after 48 hours in culture, showing phagocytosis of red cells and bacteria.

755

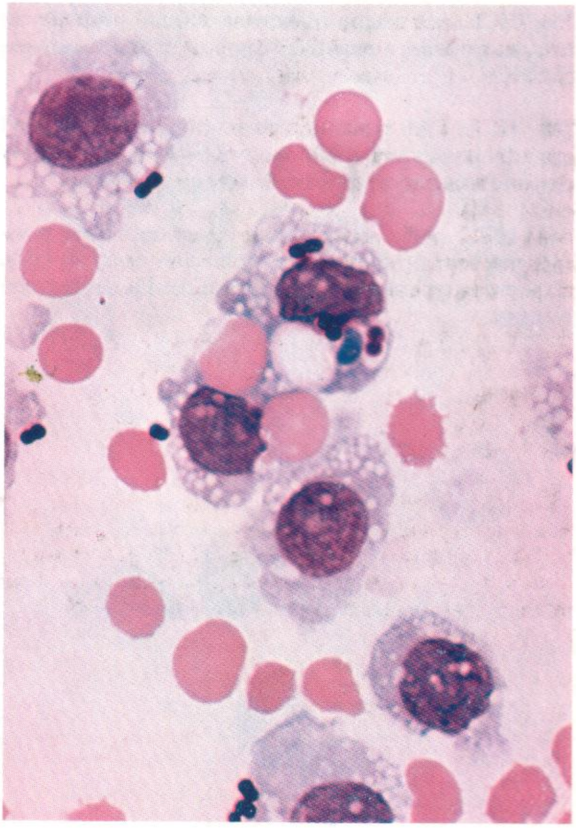

756

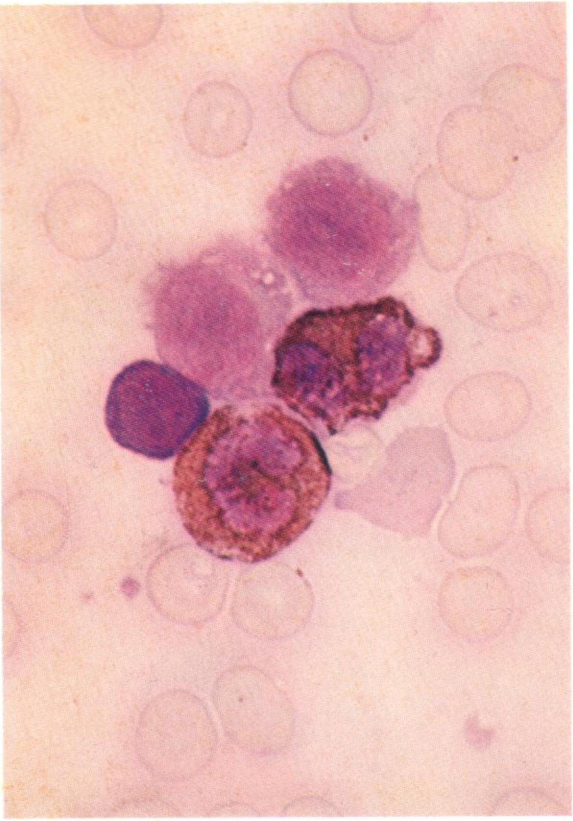

757

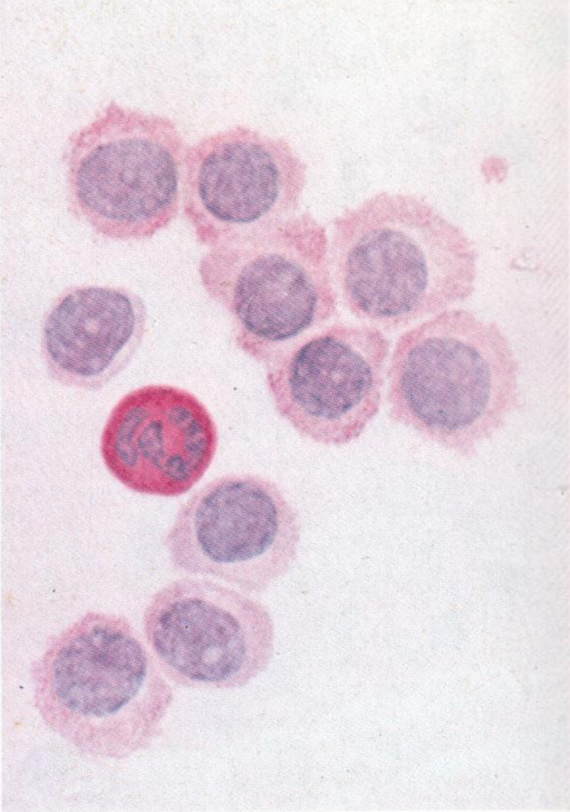

758

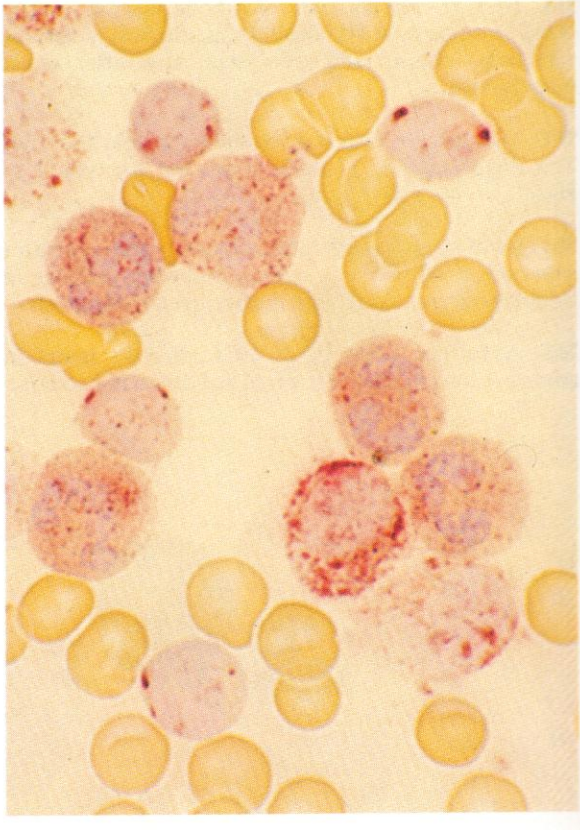

756. HCL. SB reaction, showing normal positivity in two neutrophils, a negative lymphocyte and two negative HCs.

757. HCL. PAS reaction, showing typical diffuse and granular positivity in HCs. A normally reacting neutrophil and a negative lymphocyte complete the field.

758. HCL. Acid phosphatase reaction. Five polymorphs, four probable Tμ lymphocytes and two HCs, all showing typical positivity. That in the HCs is tartrate-resistant.

759

760

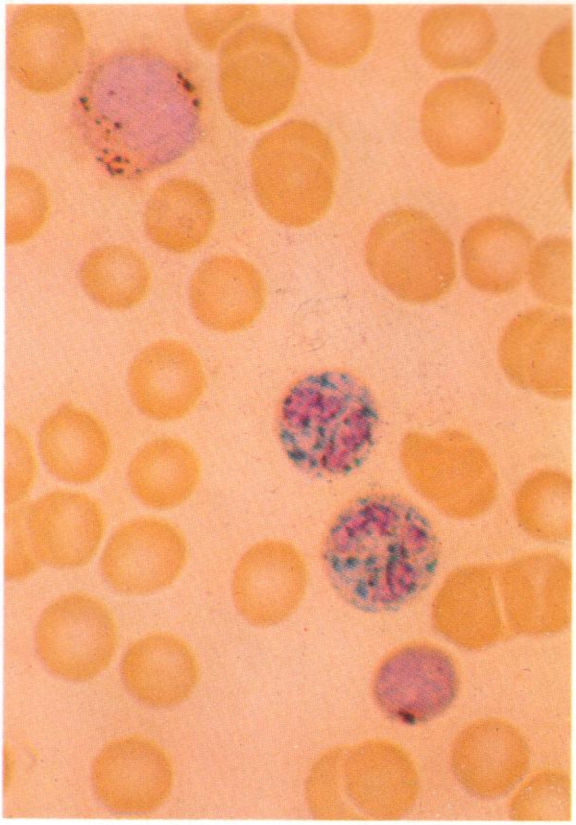

759. A further example of acid phosphatase staining in HCL, showing a neutrophil, two Tμ cells and five HCs, several containing rod-like structures with positive staining, possibly representing R-L complexes. Such inclusions are seen more commonly after acid phosphatase staining than in Romanowsky preparations.

760. Dual esterase reaction in HCL. Two CE-positive neutrophils, a Tμ cell with localized BE positivity, and an HC with granular positivity tending to show a crescentic localization at either side of the nucleus.

761. Alkaline phosphatase reaction in neutrophils in HCL. The score is almost invariably high as in this case where most neutrophils show +++ to ++++ positivity.

761

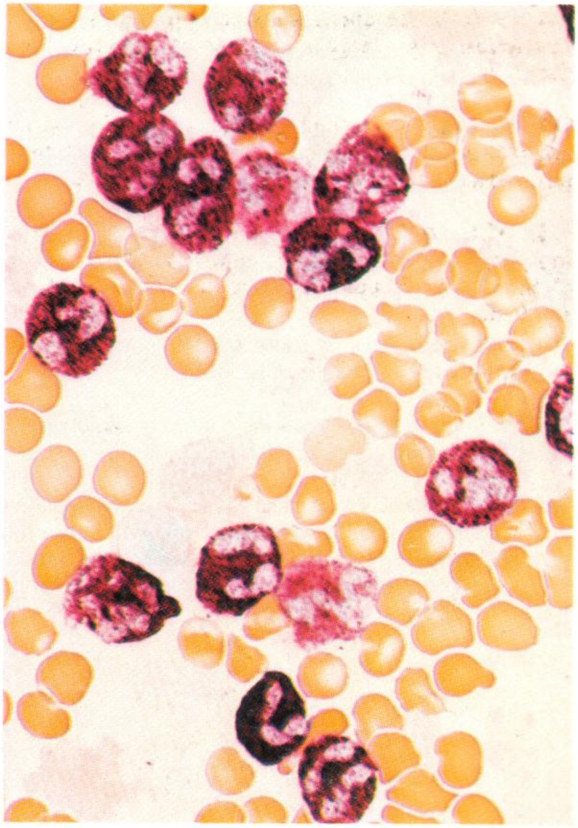

762

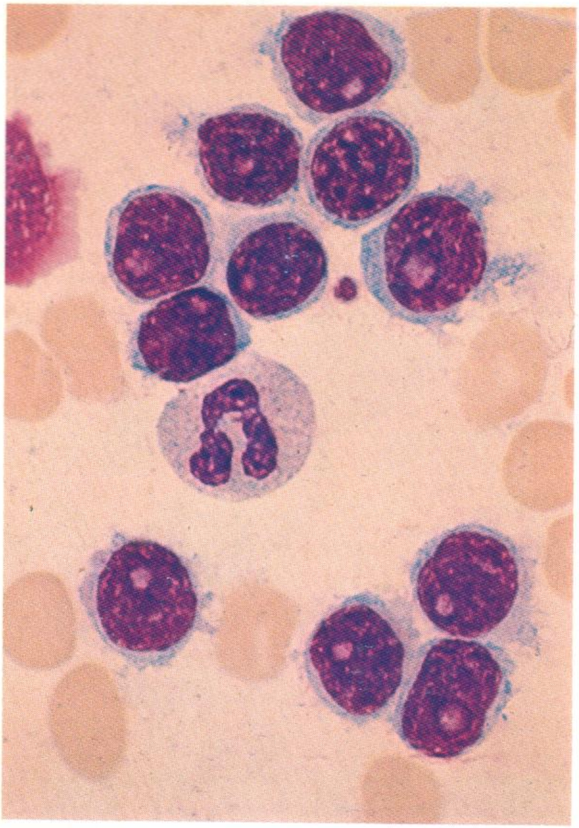

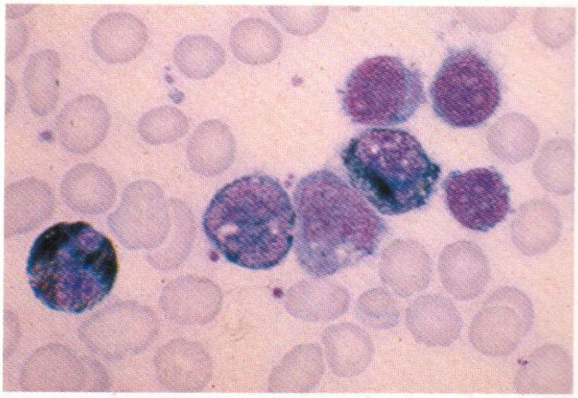

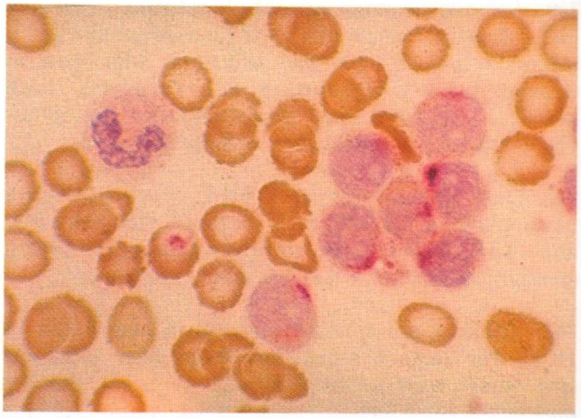

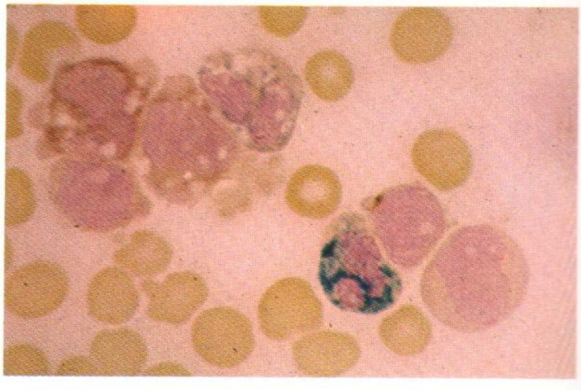

762–776. *An example of atypical HCL (HCL variant), with high leucocytosis, presence of monocytes, normal LAP score and chronic course.*

762. Romanowsky stain, showing more central nuclei, more conspicuous nucleoli, and coarser cytoplasmic projections than usual in HCs.

763. SB stain, showing three negative HCs, two positive neutrophils and two monocytes with variable scattered positive granules.

764. PAS stain showing the usual HC pattern – quite unlike that of, for example, CLL or PLL.

765. Acid phosphatase showing a more markedly polar distribution than in typical HCL.

766. Dual esterase in atypical HCL. Two CE-positive neutrophils, one heavily vacuolated and with only a few positive granules, two BE-positive vacuolated monocytes and three nucleolated HCs, one showing polar BE positivity.

767

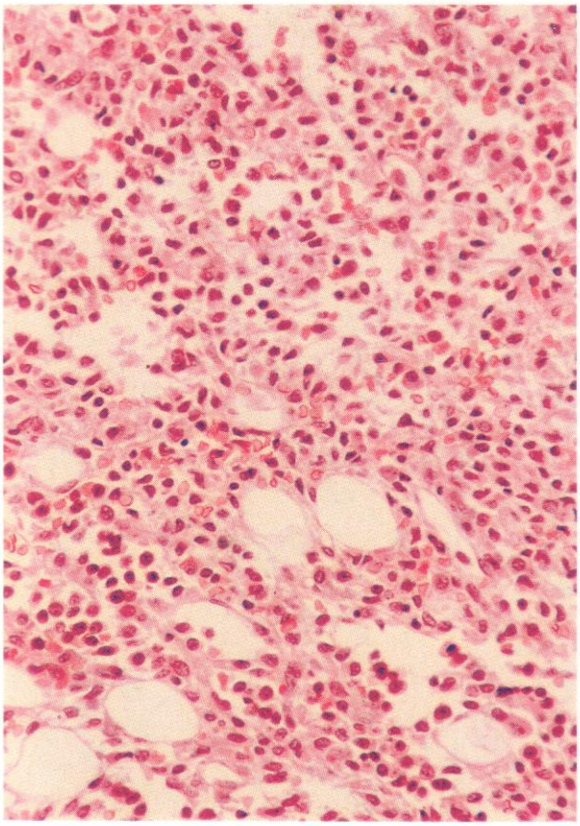

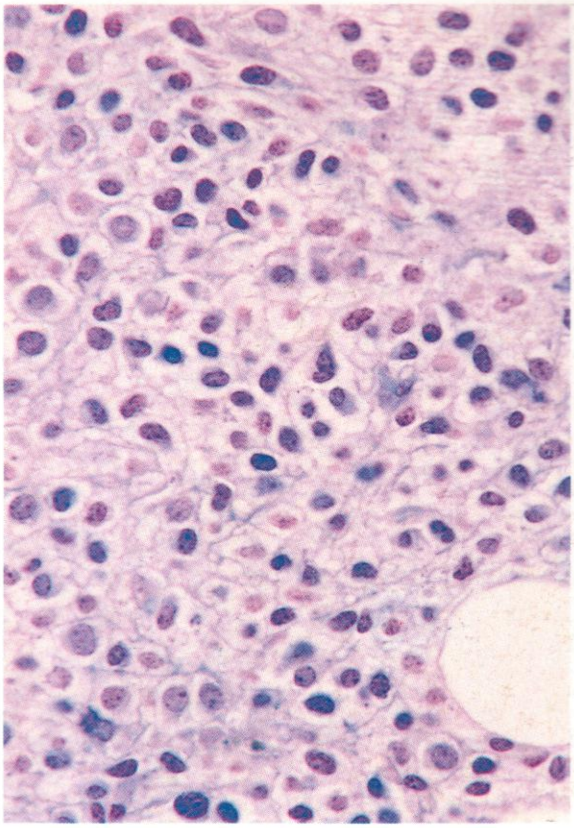

768

767–772. *Various sections of bone marrow trephine biopsies from patients with HCL and marrow infiltration. Marrow involvement in HCL may be irregular and patchy, but where it occurs the HC distribution is diffuse rather than focal.*

767. A low-power view of a bone marrow section heavily infiltrated with HCL. The overall cellularity is around 70% with substantial reduction in the proportion of fat spaces; the cell population can be seen to have two main components, HCs with relatively light-staining nuclei and ample cytoplasm, and erythroblasts with smaller size and densely stained nuclei. One or two megakaryocytes can be discerned, but there is a notable absence of granulocytes, in keeping with the marked peripheral leucopenia almost invariably found in HCL.

768. A Giemsa-stained section from the same biopsy as in **767**, demonstrating more strikingly the wide spacing of HC nuclei and the condensation of peripheral cytoplasmic material, including hairy processes, at the cell interfaces, producing the so-called 'halo' effect.

769. PAS reaction on a thin section from the same preparation as in **767** and **768**, showing cytoplasmic positivity in the HCs, with a recognizably mixed diffuse and granular pattern closely resembling that seen in smear preparations (cf. **757**). There is a positive mast cell towards the top centre.

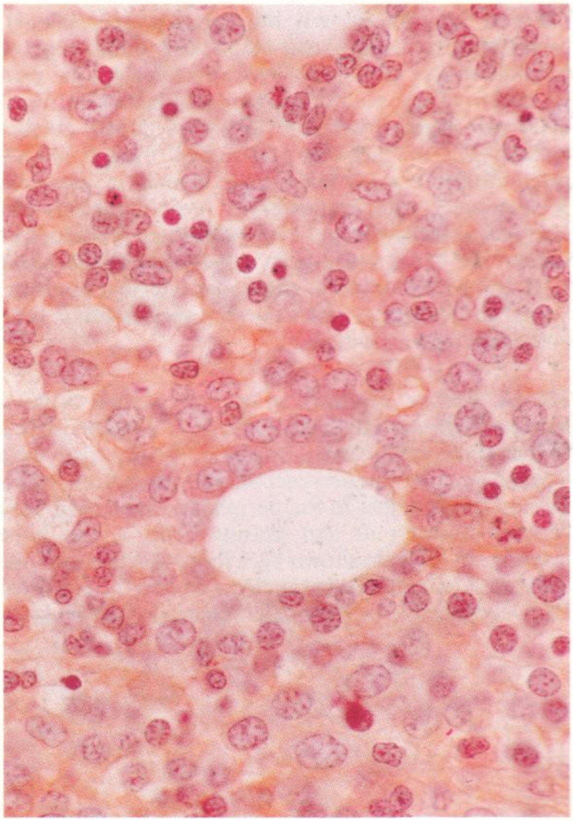

769

770

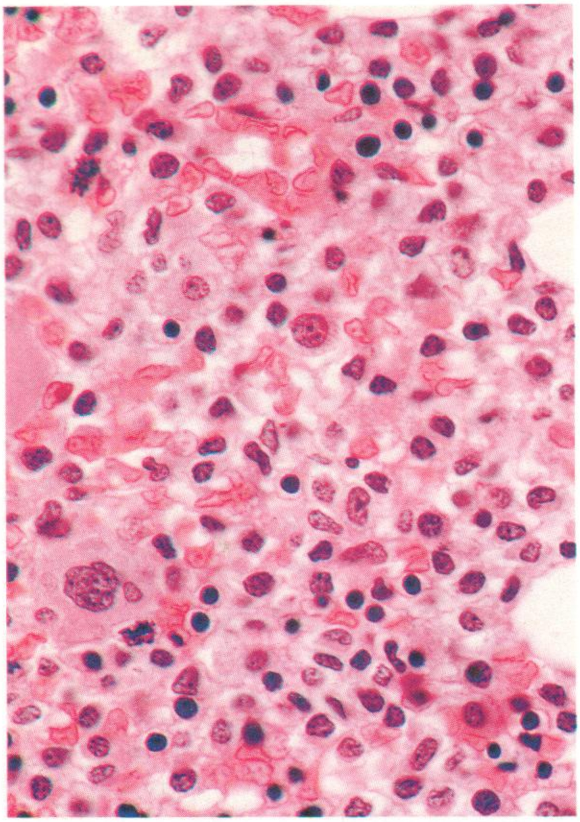

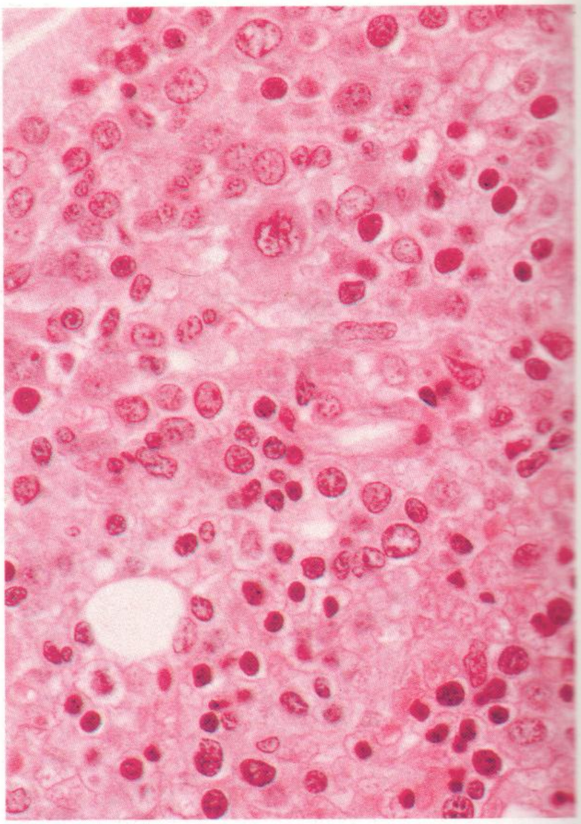

770 and **771**. Thick and thin sections, respectively, from paraffin- and plastic-embedded bone marrow trephine biopsy preparations taken from a patient with HCL during the course of remission-induction treatment with alpha-interferon. In both sections, characteristic HCs are now in a minority, though readily recognizable; normal haemopoietic marrow elements predominate, with erythroblasts most numerous but with megakaryocytes and even occasional granulocytes present. In **770** a tissue mast cell is seen at the lower right and a plasma cell at the upper left near a mitotic figure. In this pair of slides the thin section offers little additional information.

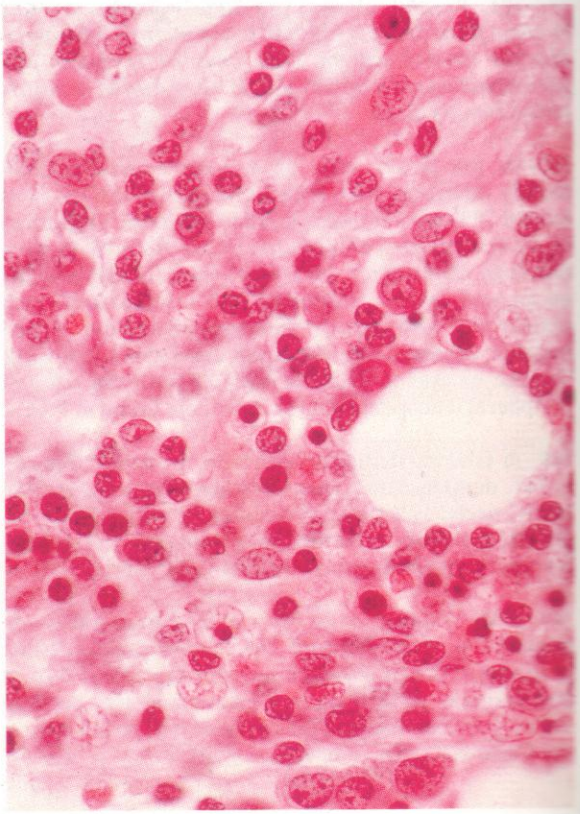

772. A further example of a thin section from a marrow biopsy in HCL, this time from a patient with a concomitant toxoplasma infection, giving rise to a marked immunoblastic reaction with numerous transformed lymphocytes in the peripheral blood, and both lymphoplasmacytoid and plasma cells in the bone marrow. In the field shown here these reactive immune cells predominate, with smaller numbers of scattered HCs recognizable by their paler nuclei and larger size.

773

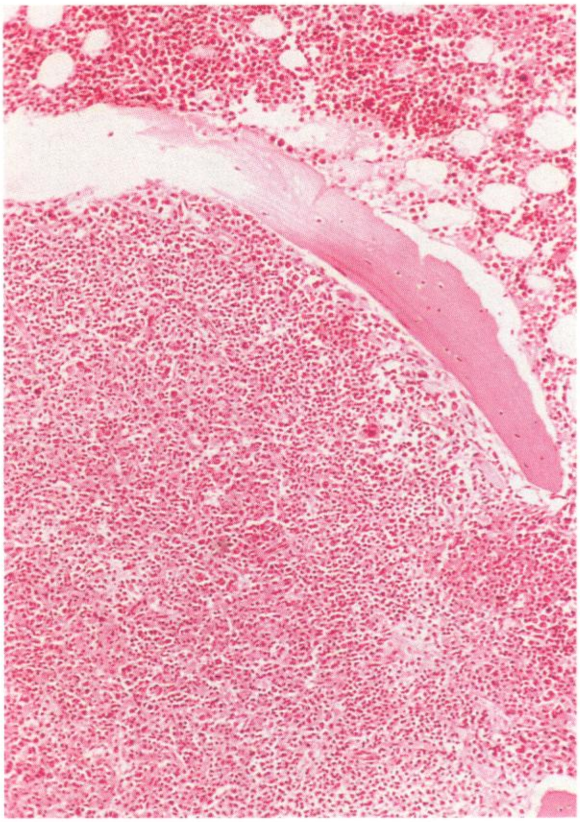

774

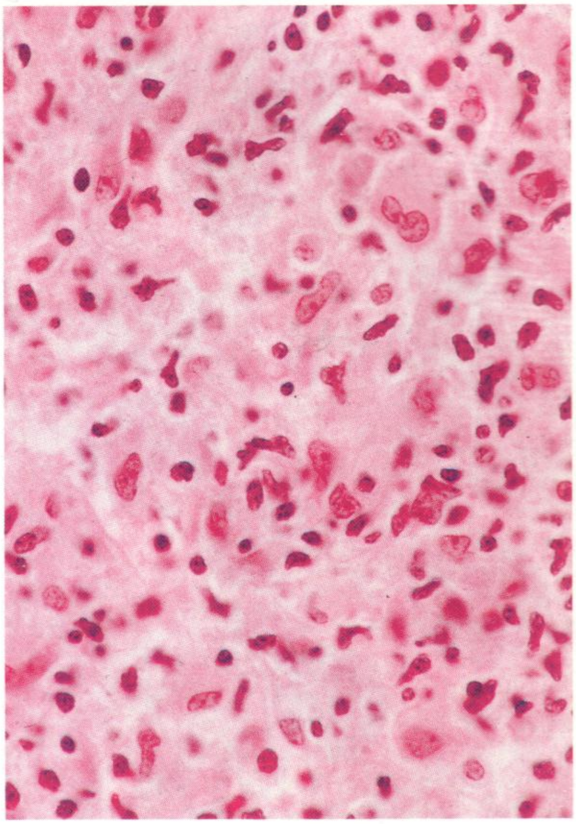

775

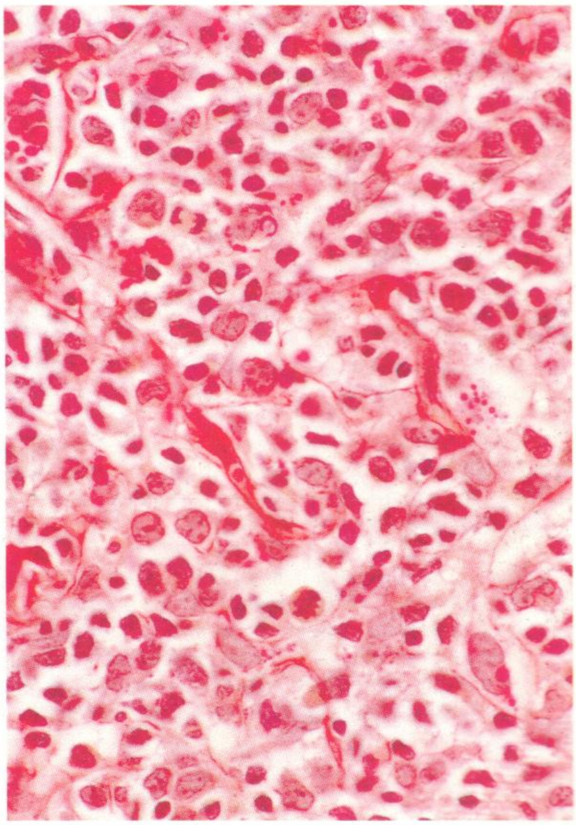

773–775. *Sections of bone marrow trephine biopsy from patients with peripheral T-cell lymphoma and marrow infiltration. This type of lymphoma is morphologically variable, composed of T cells ranging from small mature lymphocytes to large immunoblasts, and classifiable as of either low or high-grade severity. They show a high incidence of bone marrow involvement, mostly diffuse but occasionally with a randomly scattered focal distribution. The histological structure of infiltrates mimics that of the parent lymphoma, with an inflammatory element and prominent vascularity, difficult to distinguish from pleomorphic Hodgkin's disease or various reactive states such as AIL, connective tissue diseases, or immune deficiency syndromes, including AIDS.*

773. A very low-power view of a large focal infiltrate, with relatively normal marrow above the upper trabecular process. To the right, the margin of the focus is not sharp but merges into a zone of diffuse infiltration.

774. A high-power field from a second case of polymorphic peripheral T-cell lymphoma, showing diffuse infiltration with large lymphoma cells, sometimes binucleated and superficially resembling Reed-Sternberg cells, polymorphs with dense twisted nuclei, and elongated vascular endothelial cells, epithelioid histiocytes and occasional fibroblasts.

775. A PAS stain on the same biopsy material as in **774** picks out the PAS-positive vascular endothelial cells and scattered epithelioid histiocytes.

776

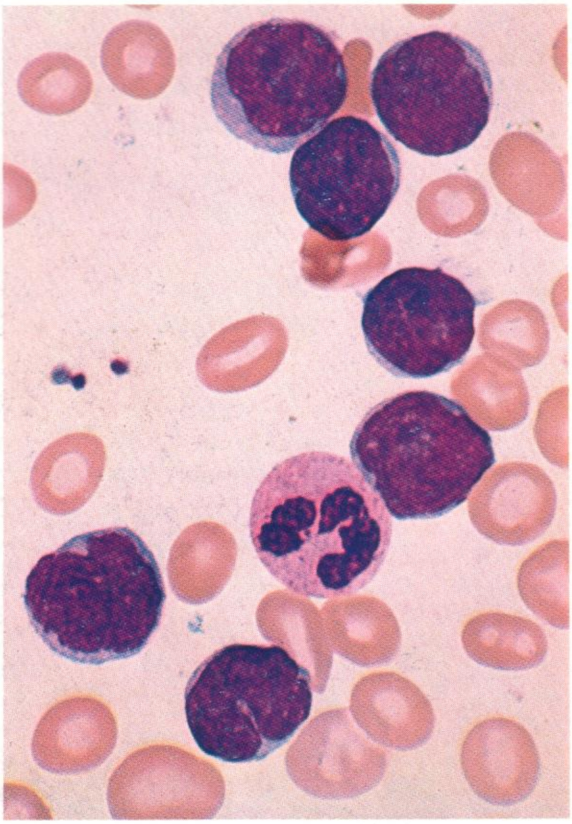

776–788. *Circulating abnormal neoplastic T cells from cases of Sézary's syndrome (SS). This disorder is a variant of mycosis fungoides (MF) with leukaemic involvement of blood and bone marrow, as well as the skin infiltration and the subcutaneous foci of tumour cells and reactive elements known as Pautrier's microabscesses, found in MF. The T cells of SS are usually CD3+, CD4+, and have helper function, although occasionally CD3+, CD8+, suppressor markers and function may be found.*

776. Romanowsky stain: the conspicuous nuclear convolutions shown on electron microscopy (**777**) of the same cells are barely detectable as nuclear creasing by light microscopy.

777. EM preparation from the same case. The circulating Sézary cells show a 'cerebriform' nuclear section, with striking invaginations. Glycogen granules are conspicuous in the cytoplasm.

778. PAS reaction: most cells in this case are negative, but occasionally fine or moderately coarse granular positivity is present. Nucleoli are well shown in some of the neoplastic cells, as is the creased or cleft appearance of some nuclei. The PAS reaction in Sézary cells is quite variable, some cases having much more marked granular positivity.

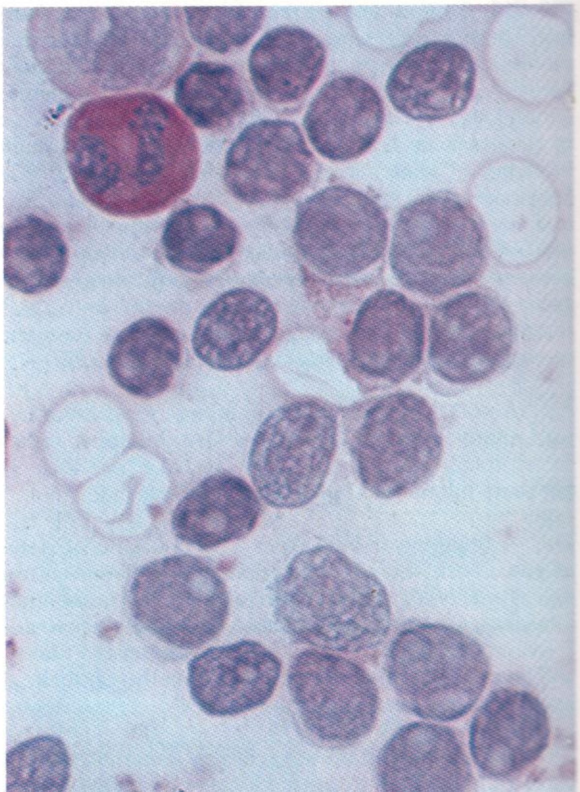

779

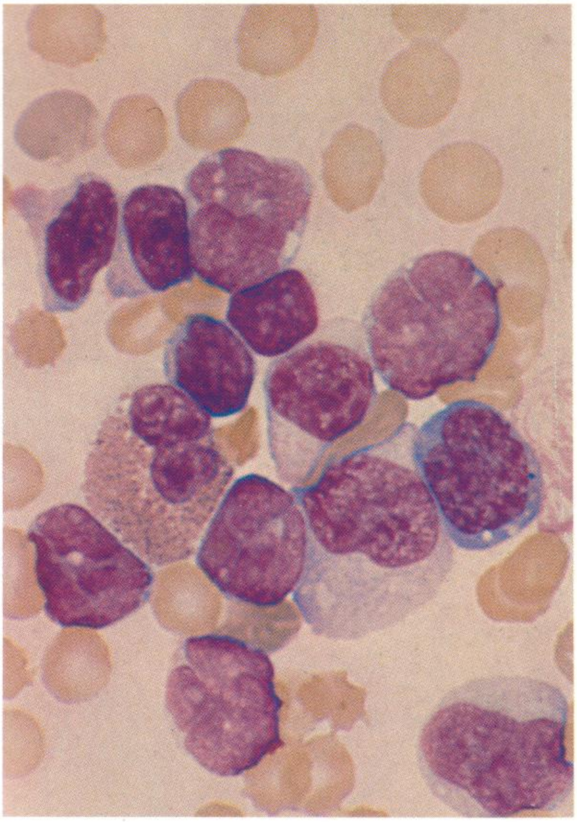

780

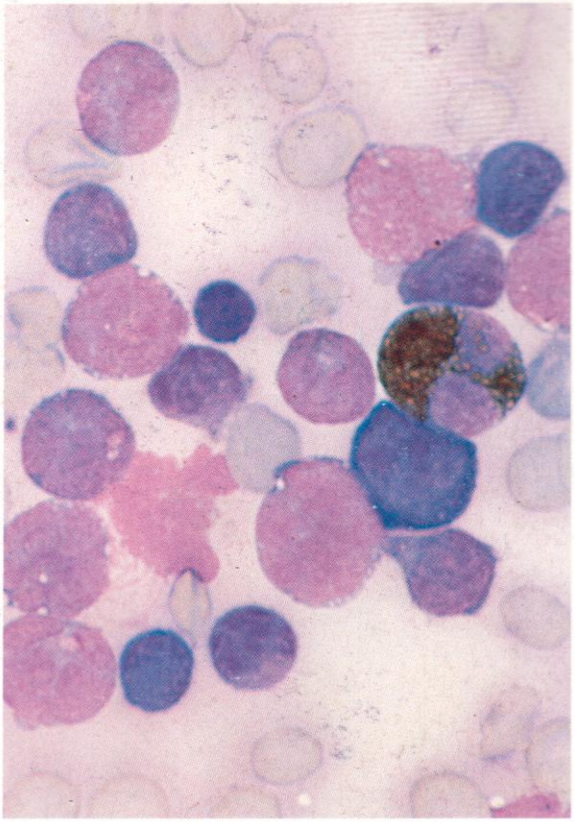

781

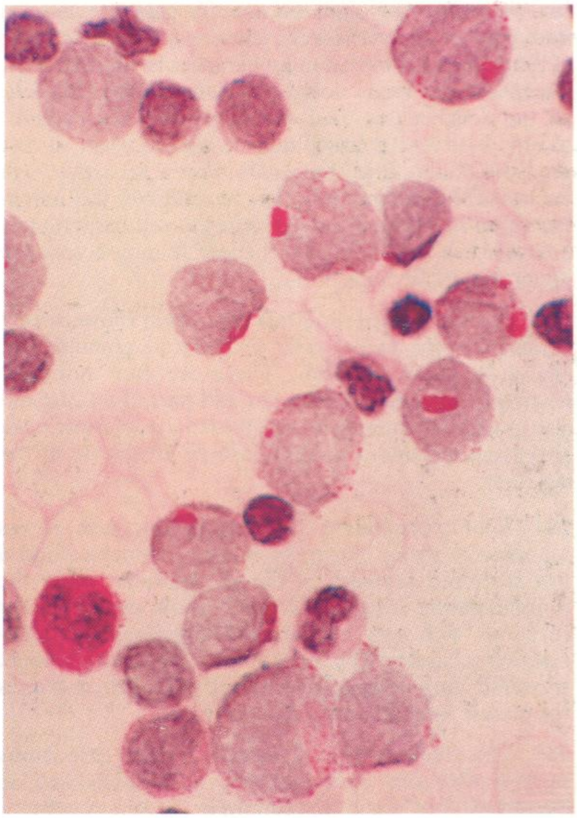

779. Romanowsky stain on a buffy coat preparation from peripheral blood of another patient with SS, showing six Sézary cells with typical high nuclear–cytoplasmic ratio and deeply indented or cleft nuclei, more conspicuous than in the previous case illustrated in **776**. One of these cells shows marked cytoplasmic basophilia, a feature present in only a small minority of Sézary cells. The field in **779** also contains five normal lymphocytes, an eosinophil polymorph and two monocytes.

780. SB stain on the same preparation as in **779**, revealing sudanophilia in only one cell, an eosinophil, while the remaining mixture of the larger Sézary cells and smaller lymphocytes shows negative reactions. Again, one of the Sézary cells shows deep cytoplasmic basophilia.

781. PAS reaction on the same buffy coat preparation shows coarse blocks and/or variable granules of PAS-positive glycogen in most of the Sézary cells, together with the usual dense positivity in a neutrophil polymorph and a less strong, finely granular and diffuse, reaction in a myelocyte and a stab cell. The remaining lymphocytes in this field are negative.

782

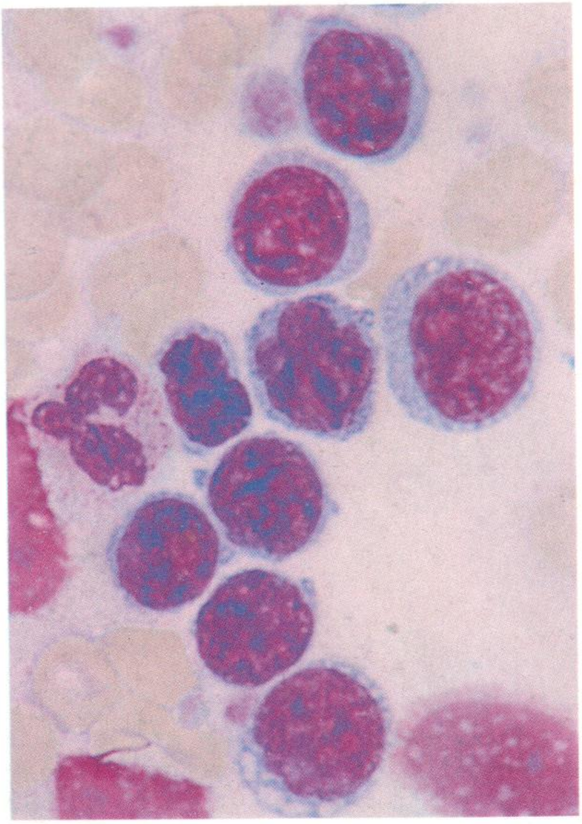

783

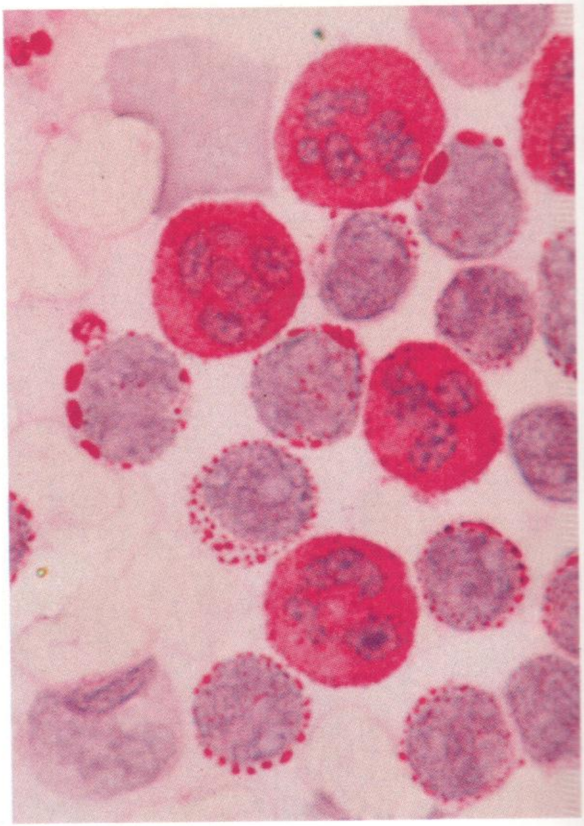

784

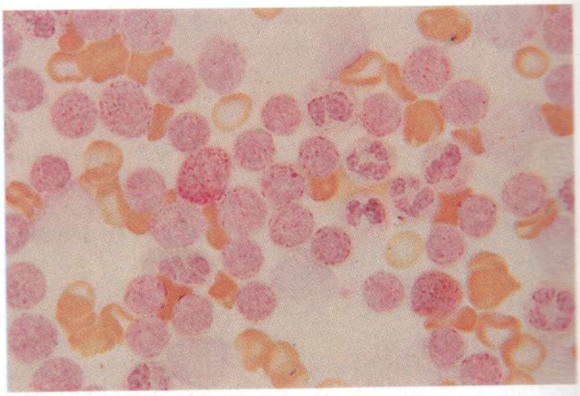

785

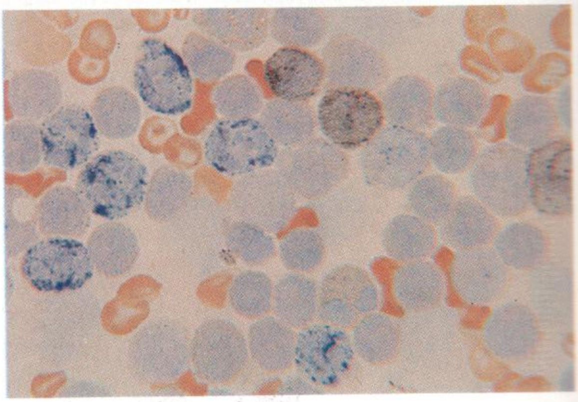

782. Romanowsky stain on a buffy coat preparation from another patient with SS, showing a further example of the range of cytological appearances in this disorder. Except for the single neutrophil polymorph at the left, all the cells in this field are neoplastic Sézary cells, mostly with more basophilic cytoplasm than in the previous illustrations, but again with a generally high nuclear–cytoplasmic ratio. The central cell has indentations of the nuclear outline and the cell immediately below it has a dark line of nuclear folding across the upper part of the nucleus.

783. The PAS reaction in this case again shows strong positivity in the Sézary cells, with coarse granules and blocks in many of them. There are four normally positive neutrophil polymorphs and part of a fifth, and also a negative monocyte with folded cytoplasmic edge at bottom left and a weakly positive myelocyte at the top right.

784. Acid phosphatase reaction in this case shows moderately strong positivity in two monocytes and a few scattered granules in the polymorphs, while the predominating Sézary cells mostly show weak granular reactions with only occasionally the paranuclear disposition characteristic of many T cells. This weak scattered granule pattern without paranuclear dots is the picture most often encountered in SS.

785. This dual esterase stain in the same case shows normal reactions in monocytes, neutrophils and an eosinophil, but negative reactions in the Sézary cells.

786

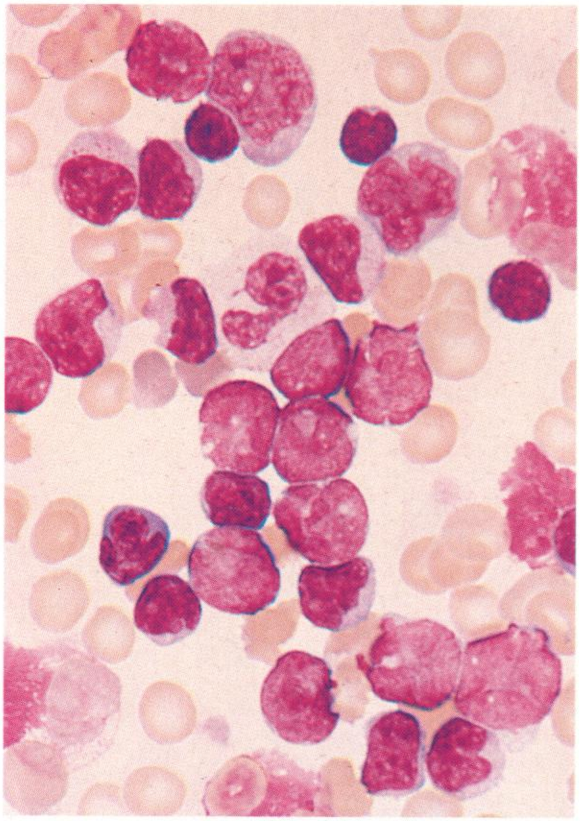

787

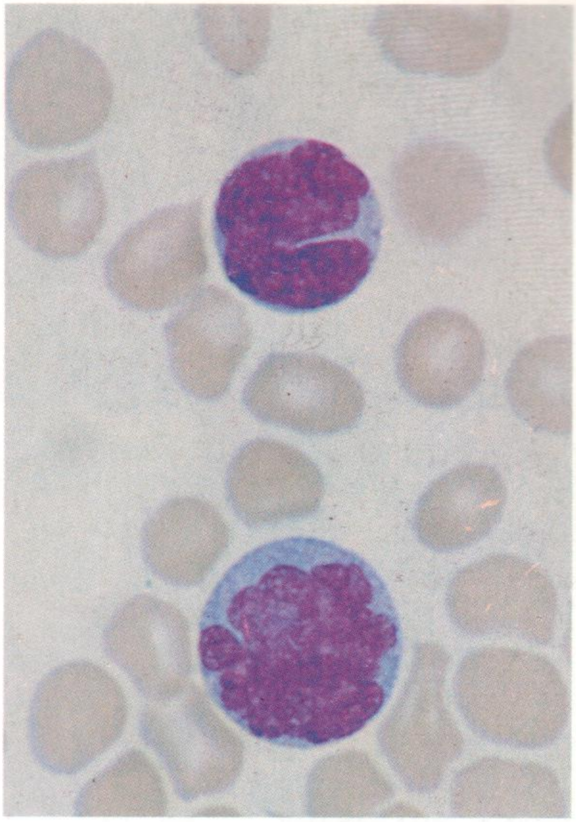

786. Another variant of malignant cell cytology in SS. In this field, from a Romanowsky-stained buffy coat smear, all the cells, apart from a single stab cell above the centre, are either normal lymphocytes or Sézary. The contrast in density of nuclear chromatin is striking, and in this case the deep infolding of the nuclear membrane can be better envisaged than in **782**, perhaps because the blood sample was kept in anticoagulant for some hours before the buffy coat preparation was made, a procedure which tends to exaggerate nuclear membrane irregularities.

787. A high-power view of two Sézary cells from a fresh peripheral blood smear, showing well-marked nuclear infolding but also the existence of multiple small nucleoli, especially in the lower cell, a feature which is not usually conspicuous in Sézary cells.

788. A lower-power view of the same peripheral blood sample as in **787**, showing the usual finding in SS of a positive cell-surface membrane reaction in the neoplastic T cells to an immunocytochemical APAAP stain with the MAb CD4.

788

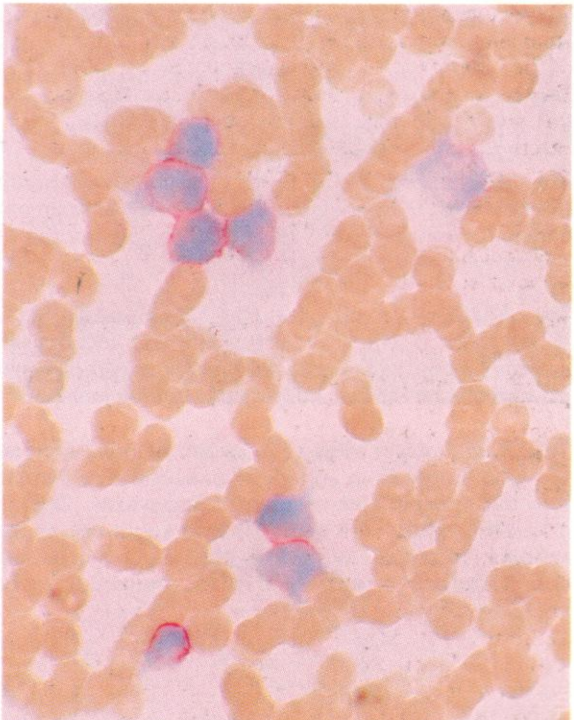

789

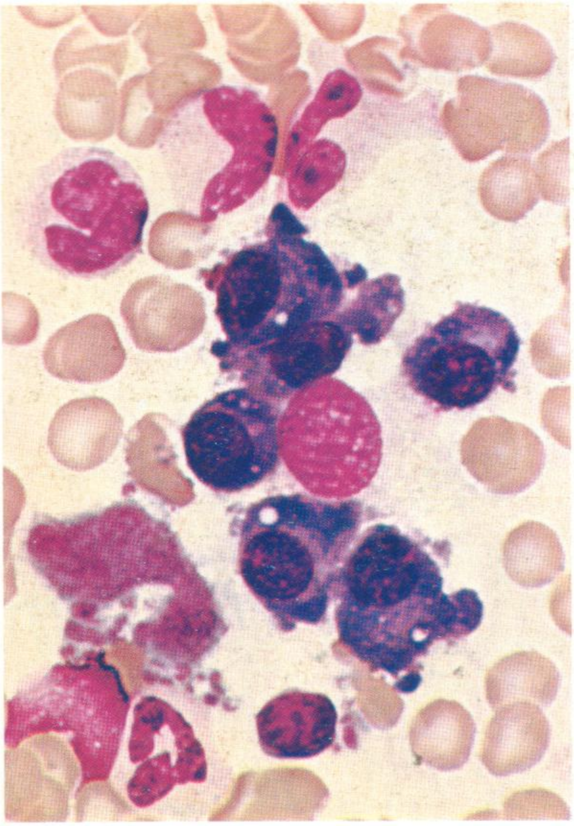

790

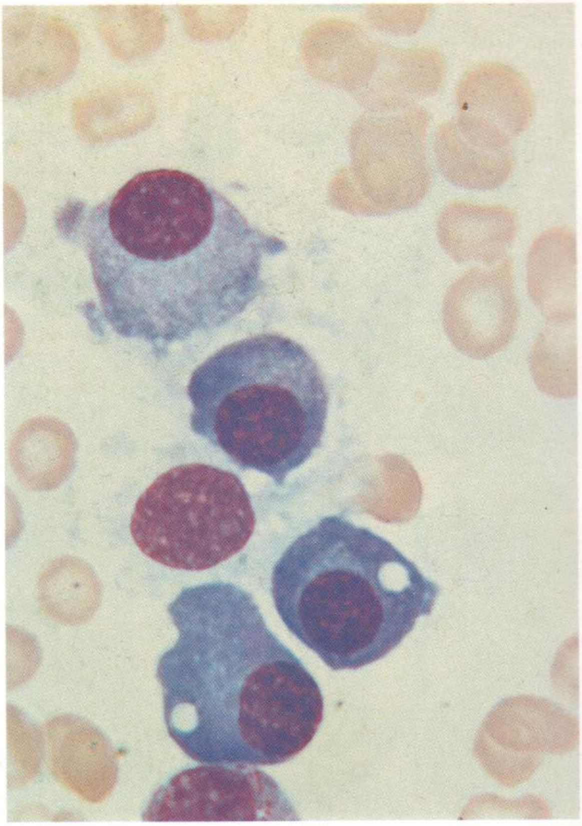

791

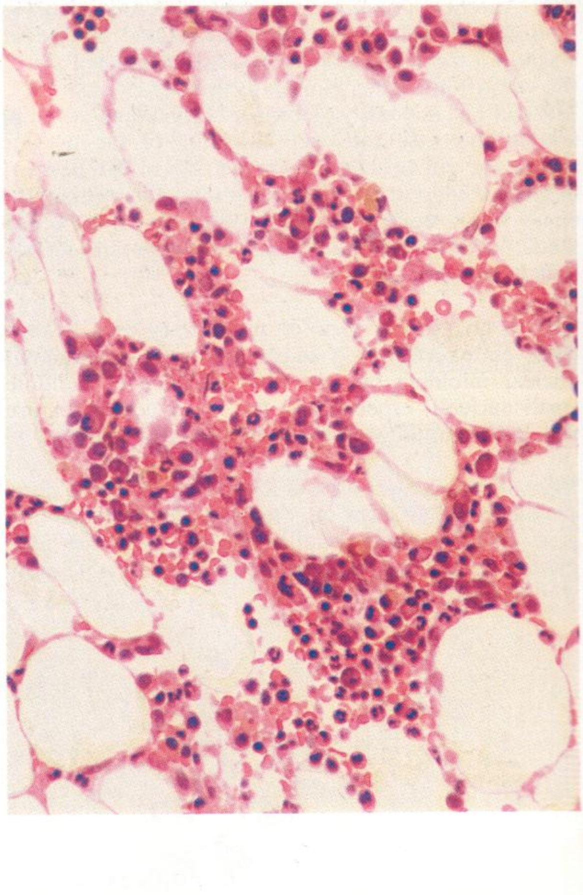

789. A nest of mature plasma cells from the marrow of a patient with cat-scratch disease, showing some reactive plasmacytosis. The vacuolation and tendency to budding and fragmentation of the cytoplasm may indicate enhanced activity. There is a central macrophage nucleus with filmy ill-defined surrounding cytoplasm, a U-shaped residual megakaryocyte nucleus with scattered platelets below it at the lower left, and a fragment containing free iron at the border of the plasma cell to the upper left of the group.

790. Another example of reactive mature plasma cells in the bone marrow of a patient with rheumatoid arthritis, where polyclonal plasmacytosis is commonly associated with the usual hypergammaglobulinaemia.

791. A low-power view of a section of bone marrow trephine biopsy from an elderly patient with a chronic infective process and reactive plasmacytosis. Overall cellularity is low, with many fat spaces, but among the residual haemopoietic marrow cells scattered plasma cells with their eccentric nuclei are frequently to be seen.

792

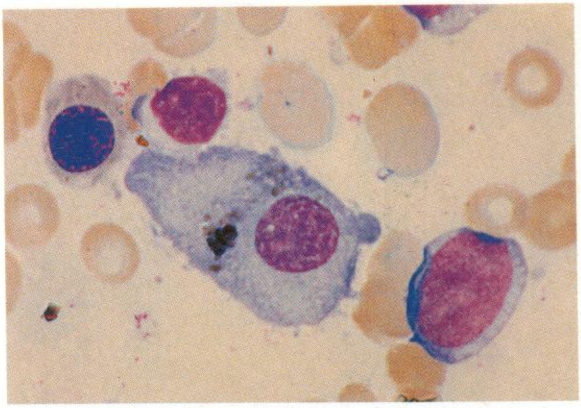

793

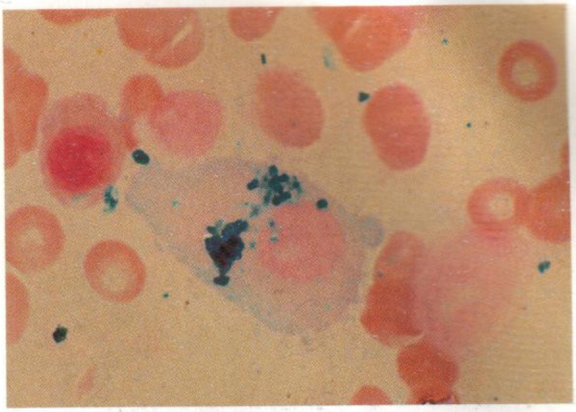

794

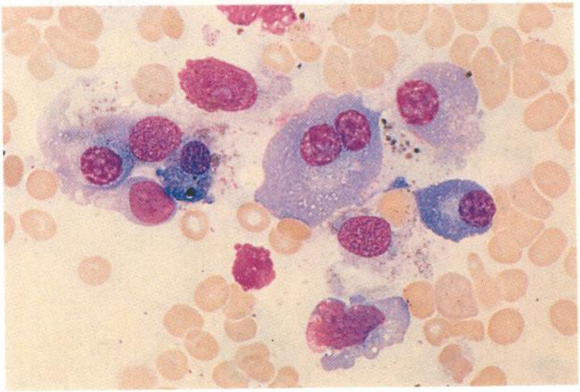

795

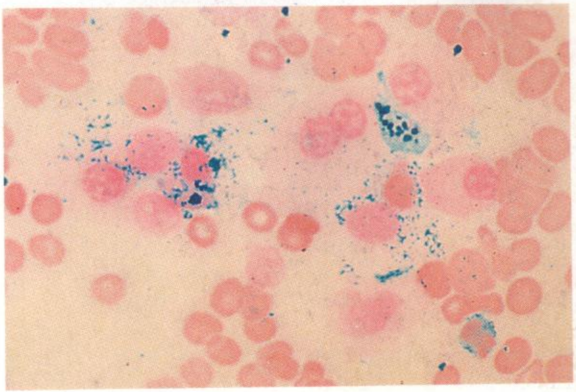

792–797. *A series of paired fields from consecutively stained bone marrow smear preparations to demonstrate the presence of free stainable iron in plasma cells. In each case the first illustration of the pair (**792**, **794** and **796**) shows a Romanowsky-stained field, and the second (**793**, **795** and **797**) the same field after decolorization and restaining by the Prussian blue reaction. The presence of free iron in plasma cells may be a result of transfer of this material from macrophages (two macrophage nuclei are present in **794** and **795**) via cytoplasmic bridges, rather than a consequence of direct phagocytic action, but it appears to be most commonly associated with alcoholism, although it may also be seen in infective hepatitis, as in the present case. The iron has been shown by ultrastructural studies to be located in membrane-bound lysosomal vesicles and not in mitochondria, thus differing from the erythroblastic accumulations in sideroblastic anaemia.*

796

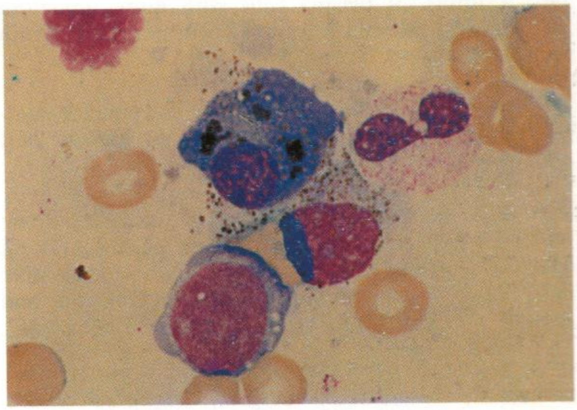

797

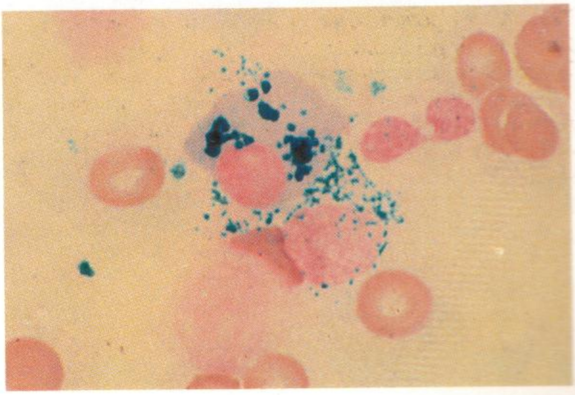

798

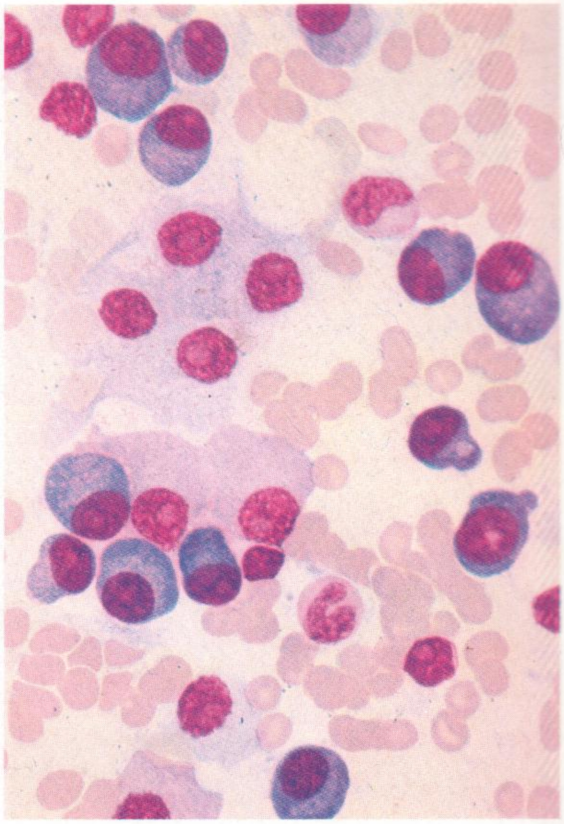

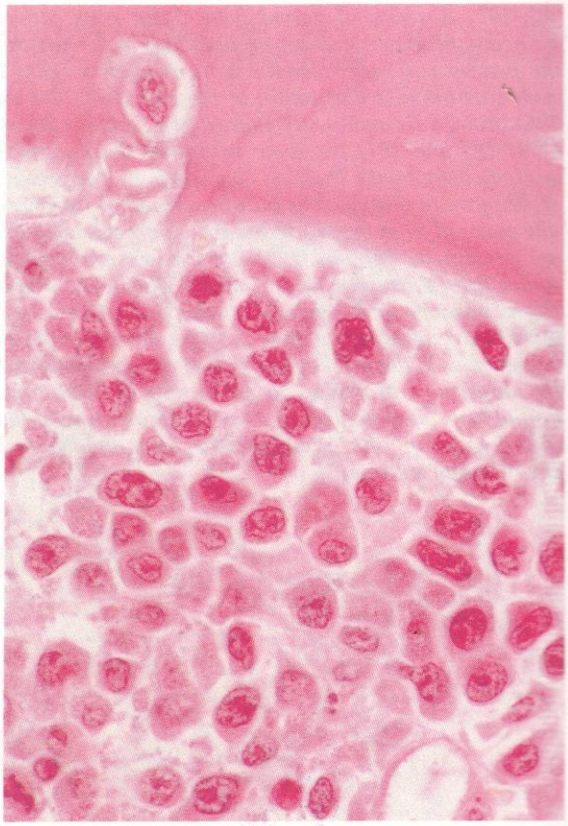

798. A group of plasma cells with more immature features than those in **789** and **790**, from a patient with multiple myeloma.

799. Variability in the size, maturity and general staining characteristics of plasma cells, in the marrow of a patient with multiple myeloma.

800. Bone marrow trephine biopsy in myeloma, showing the predominance of neoplastic plasma cells of variable size and nuclear density, with considerable cytoplasmic fragmentation, and with erosion and cellular infiltration of the trabecular bone at one point.

801
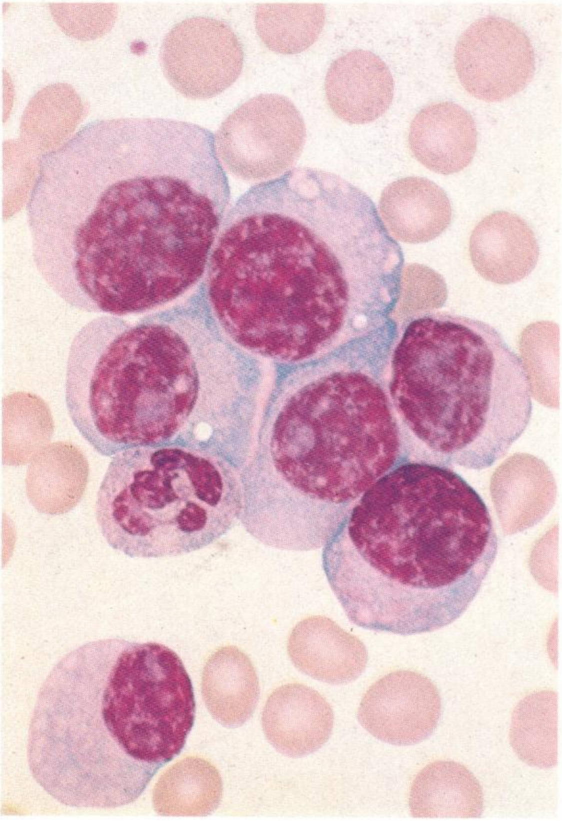

802
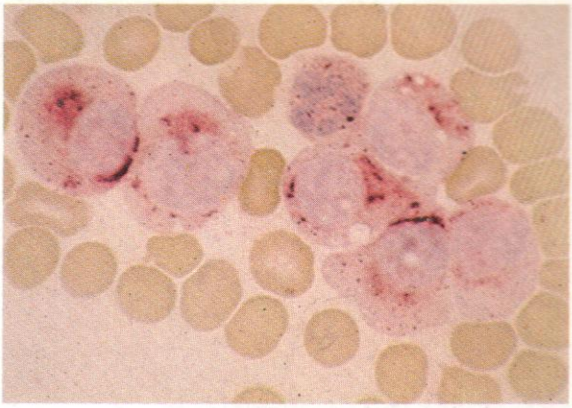

803
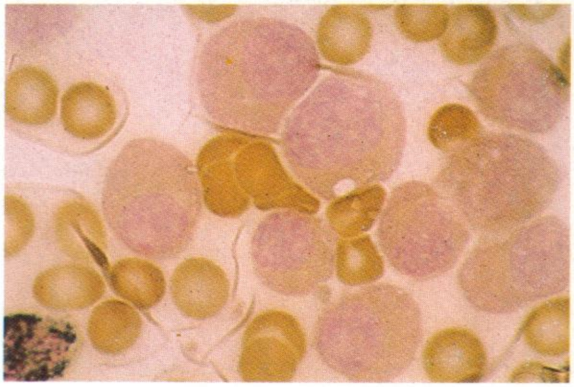

804
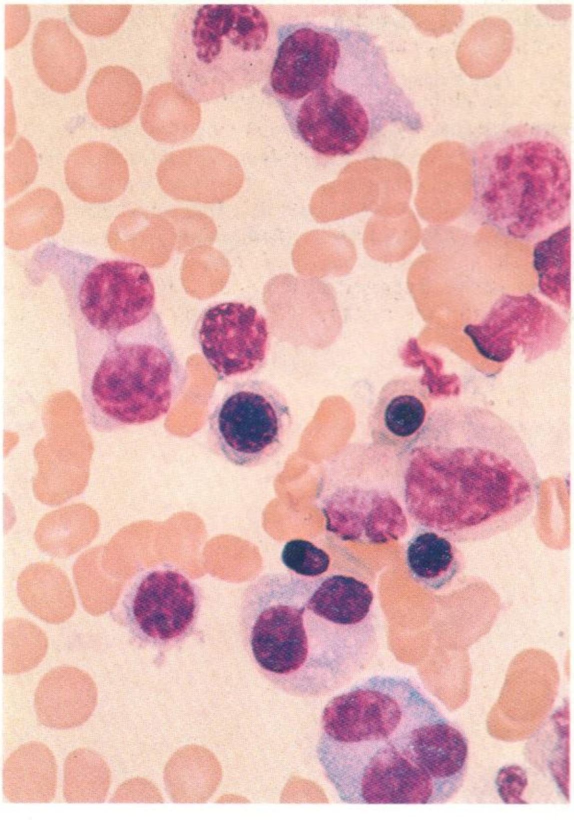

801. Circulating plasma cells from a case of plasma cell leukaemia with predominantly mature non-nucleolated cells. Note absence of rouleaux formation.

802. Acid phosphatase reaction in the same case: there is strong localized positivity, but considerably less intense than usually seen in typical myeloma cells of bone marrow (*see* **825** and **826**).

803. Dual esterase reaction: the same case shows only very weak BE positivity in the plasma cells in comparison with the stronger reaction for BE or CE or both enzymes common in typical myeloma cells of bone marrow (*see* **827**).

804. A remarkable example of internuclear bridging in a case of myeloma. Most myeloma cells had two or three linked nuclei.

805

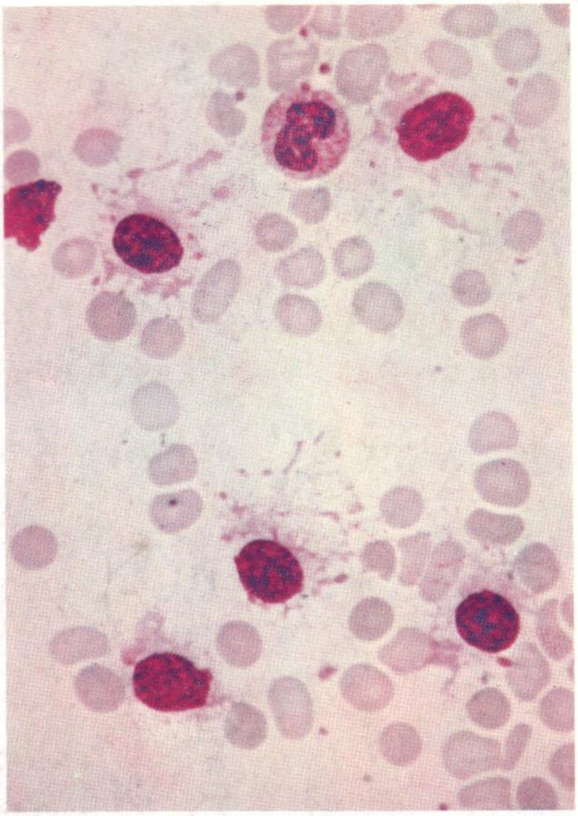

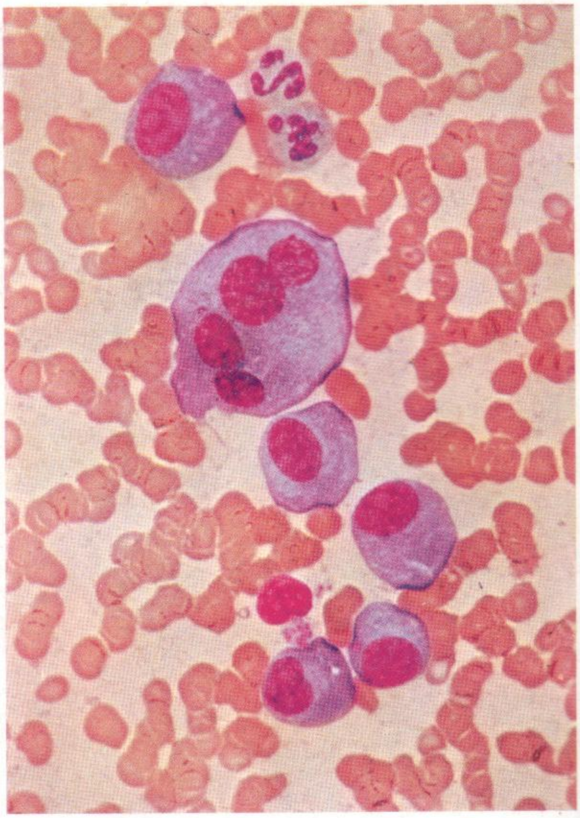

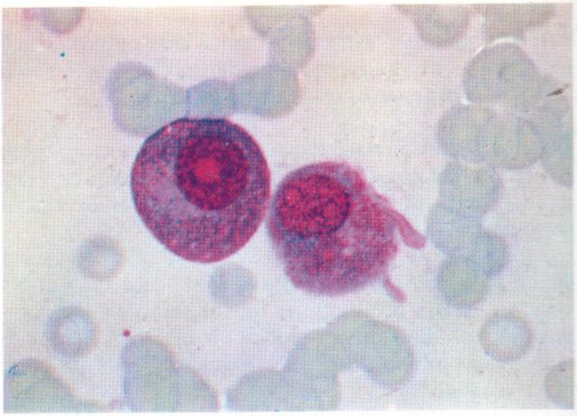

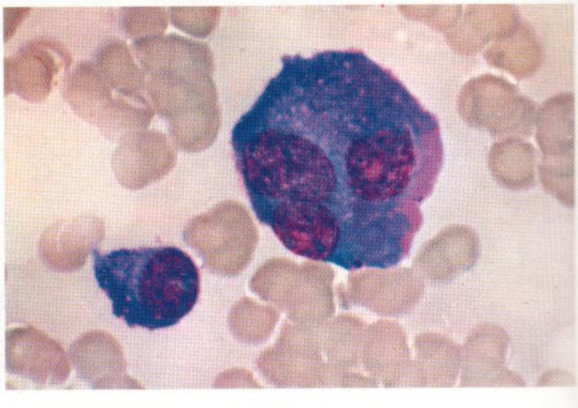

805. Plasma cells in myeloma, showing a remarkable tendency to cytoplasmic disruption.

806. A multinucleated plasma cell in myeloma.

807 and **808**. The development of flaming cells. The smooth eosinophil component which makes up the 'flaming' character in certain plasma cells is usually first seen at the cell periphery. It often contrasts sharply with intense basophilia in the remaining cytoplasm.

809

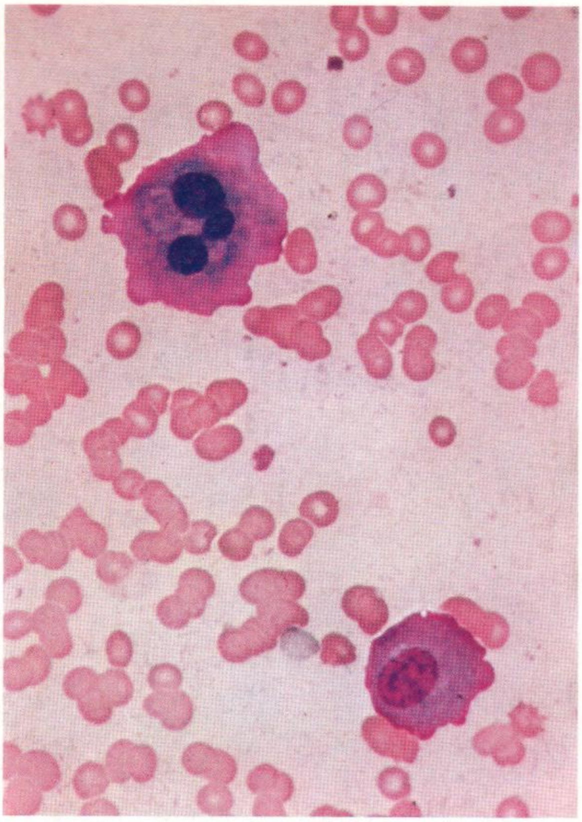

810

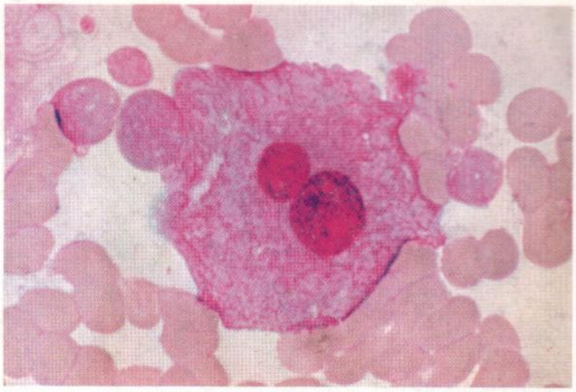

811

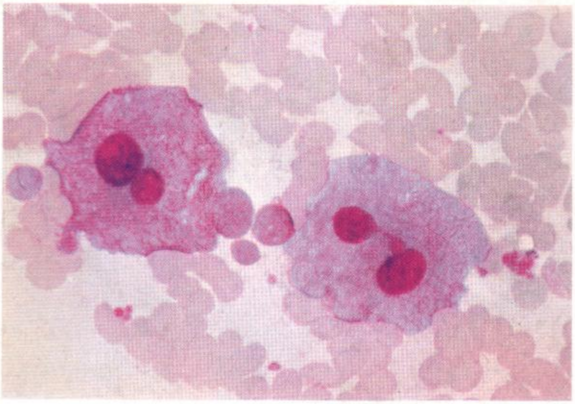

812

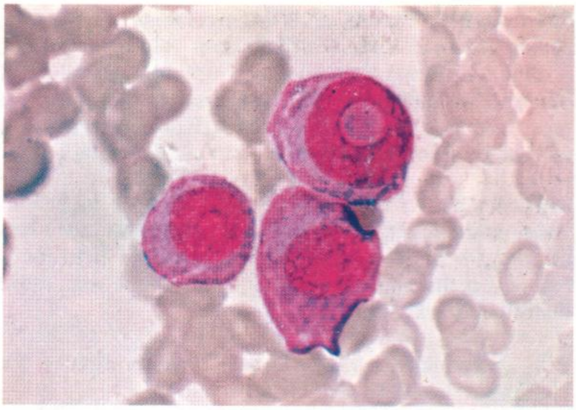

813

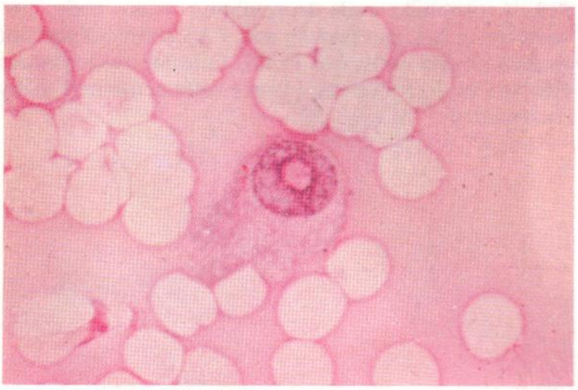

809. A pair of fully developed flaming cells.

810 and **811**. The development of thesaurocytes – large plasma cells with dark, somewhat pycnotic nuclei and extensive fibrillary cytoplasm, sometimes having the appearance of division into compartments. These 'storage cells' usually have 'flaming' characteristics in their remaining cytoplasm.

812 and **813**. Large nuclear inclusions, PAS-positive, occasionally seen in plasma cells in myeloma (and in other conditions). Their significance is unknown; they are less likely than cytoplasmic inclusions to represent secretion or synthesis products.

814

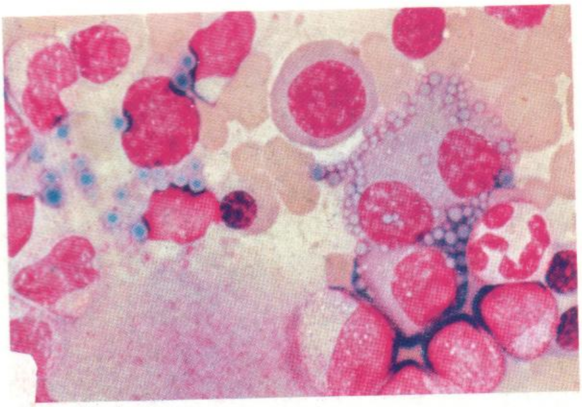

815

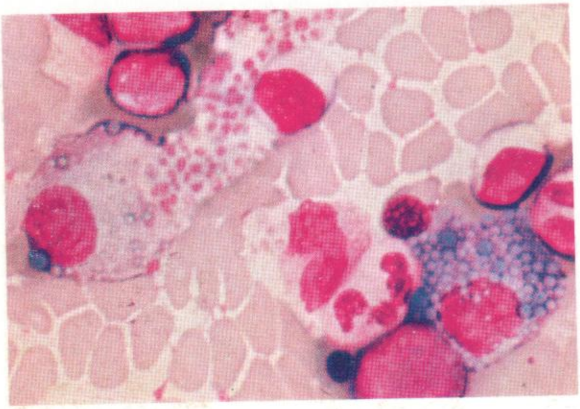

816

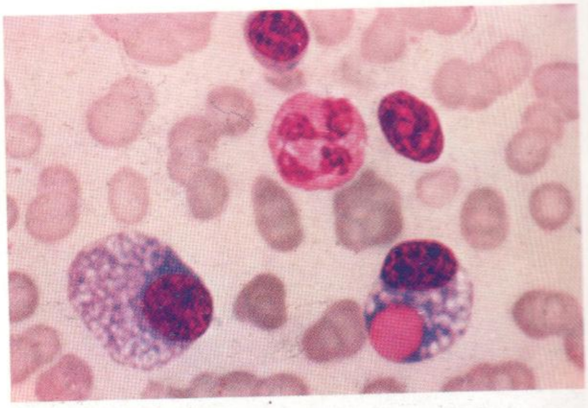

817

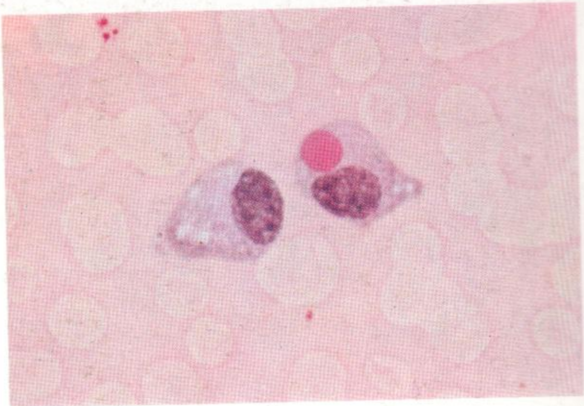

818

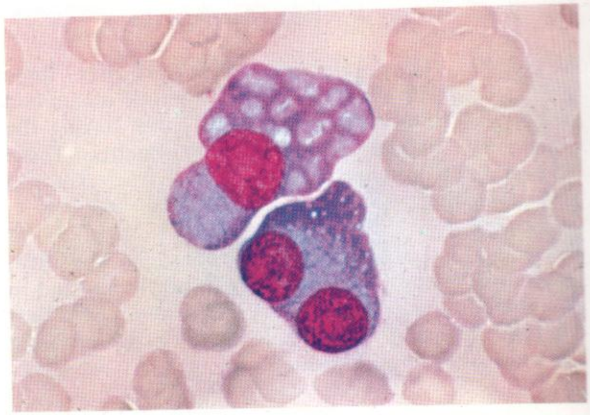

819

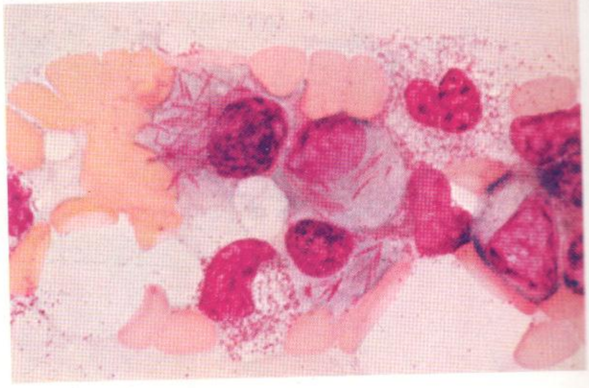

814 and **815**. Plasma cells in myeloma, showing an accumulation of spherical inclusions, bluish in colour, probably representing an abnormal concentration of immunoglobulin precursor. Cells may become full of these bodies (called Russell bodies by some authorities) and are then sometimes referred to as Mott cells.

816 and **817**. Another type of spherical inclusion, eosinophil-staining and PAS-positive, found much less often in smears of plasma cells. This type of inclusion is also given the name Russell body, perhaps with more historical justification.

818. An unusual form of locular degeneration in the cytoplasm of a plasma cell from myeloma.

819. Azurophilic rods (resembling Auer rods, but negative to SB, peroxidase and PAS staining) are not rare in plasma cells, but in this unusual myelomatous case the majority of the plasma cells contained many such rods.

820

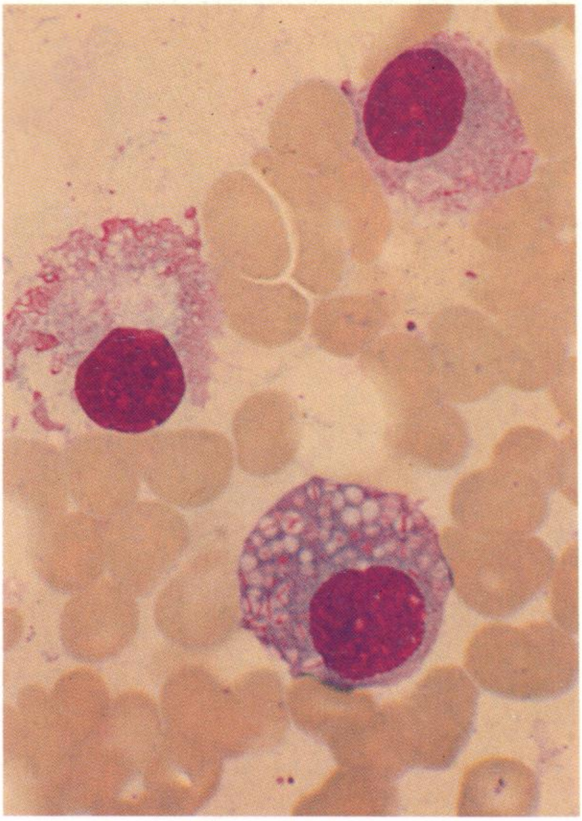

821

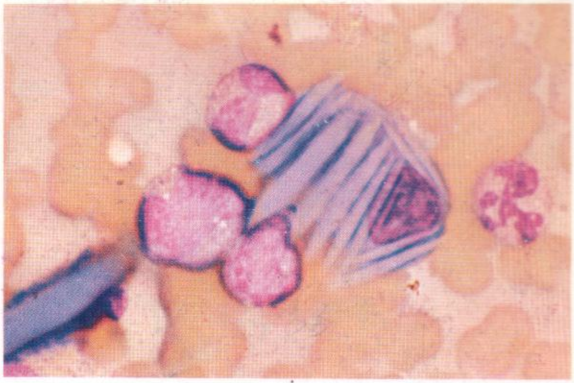

822

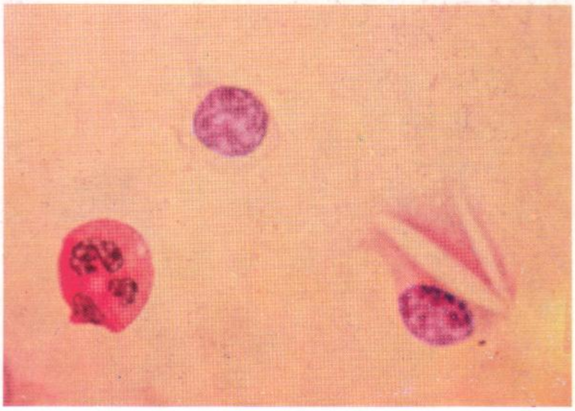

823

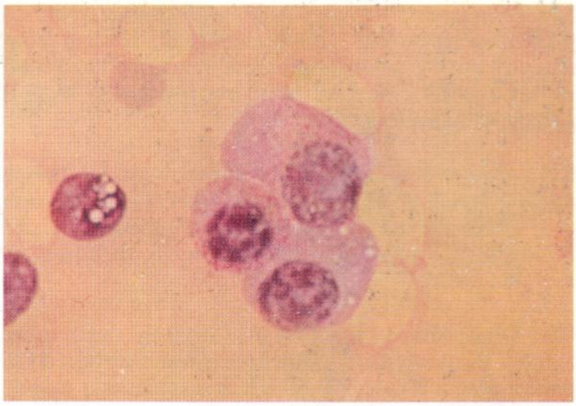

824

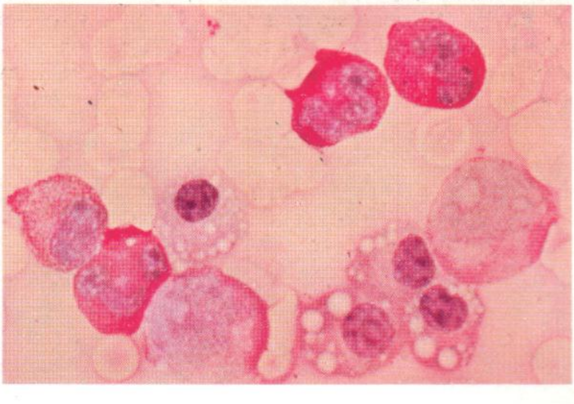

820. Three myeloma cells, two with 'flaming' cell features and the third with multiple small vacuoles often containing azurophilic material, possibly irregular deposits of defective paraprotein within autophagic vacuoles.

821 and **822**. An even more unusual case of myeloma, where nearly all the plasma cells were distorted by large crystalline inclusions, having some resemblance to Charcot-Leyden crystals, and presumably representing the product of disordered synthetic activity in the cells. The cell cytoplasm showed weak PAS positivity, but the inclusions were negative (**822**).

823 and **824**. PAS reactions in plasma cells from cases of multiple myeloma. Reactions range from negative to weakly positive, with occasional granules against a weaker diffuse background of faint positive tinge. The spherical bluish inclusions illustrated in **814** and **815** are PAS-negative.

825

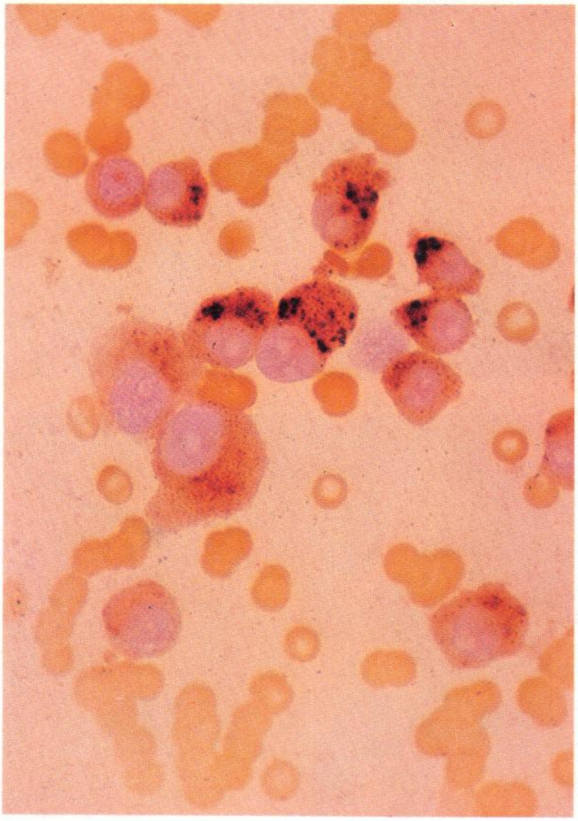

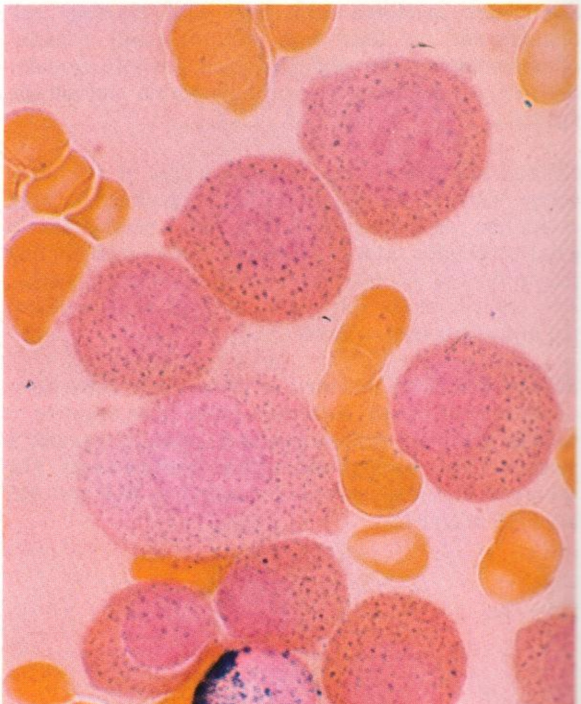

825. The one striking cytochemical characteristic of plasma cells, normal and pathological, is their consistently strong acid phosphatase reaction, illustrated in this general view of a bone marrow smear from a patient with myeloma.

826. A second example of acid phosphatase reaction in myeloma cells. The more sharply particulate deposit arises from the use of naphthol AS-BI phosphoric acid as substrate, compared with α-naphthyl acid phosphate, as used for **825**.

827. Dual esterase reaction in a marrow smear from a patient with myeloma. The cells contain scattered CE positivity in this case, but no BE as is sometimes found.

828

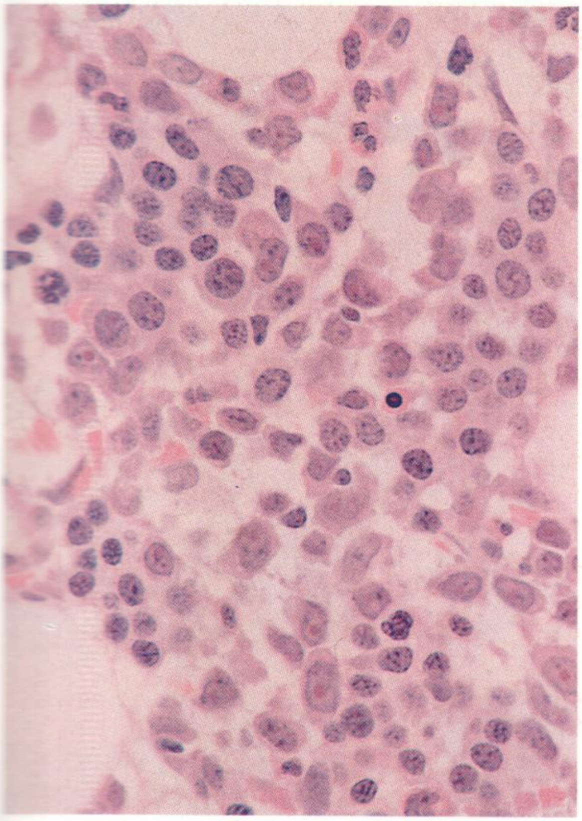

829

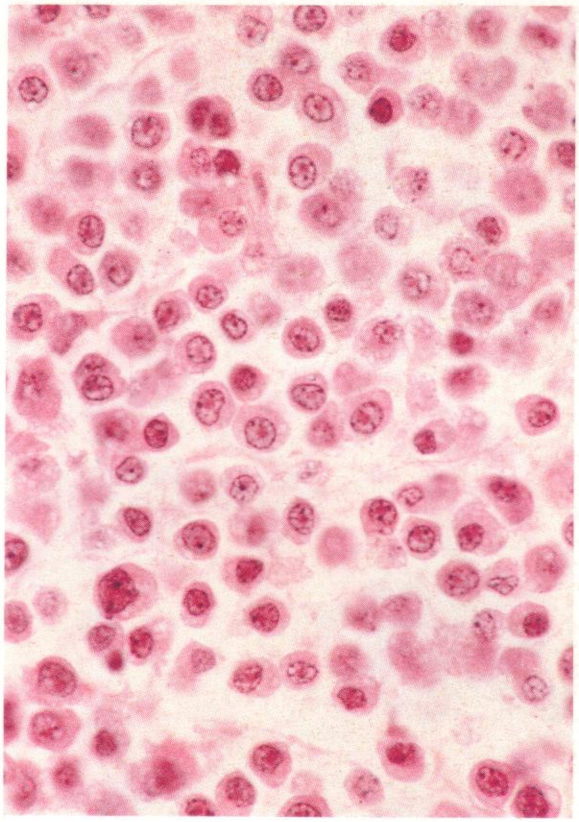

830

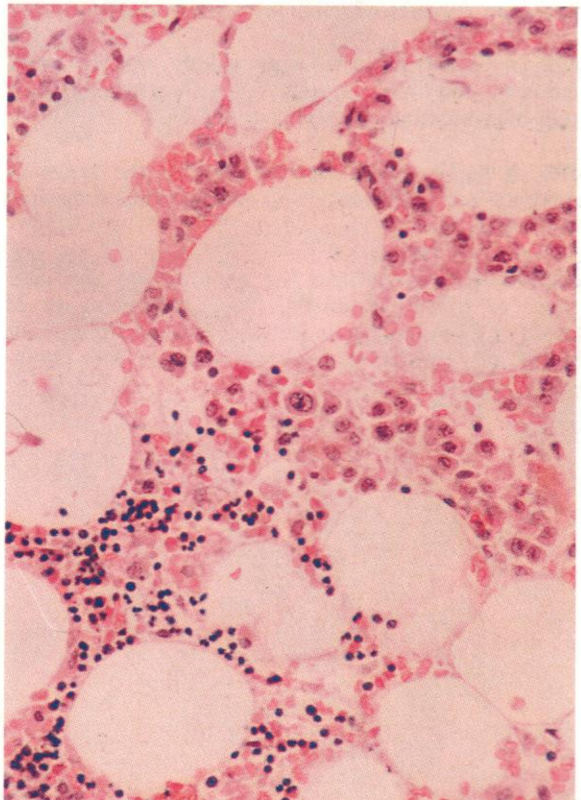

828. Section of bone marrow trephine biopsy from a patient with myeloma, showing typically variable cytology, with differences in cell size and in nuclear chromatin condensation, and with conspicuous pale red intranuclear inclusions in several of the myeloma cells with generally more primitive nuclear patterns. These are presumably the same type of inclusion as shown in **812** and **813**.

829. Another typical example of myeloma cell cytology as seen in histological sections of bone marrow. There are occasional binucleated cells and some variability in maturity, but in general the cell nuclei are more densely chromatic with more conspicuous clock-face markings than in **828**.

830. Myelomatous proliferation is frequently nodular in distribution, and this section from another bone marrow trephine biopsy shows the margin of a focal area of myeloma cell growth, at the upper right, abutting residual normal haemopoietic marrow, with erythroblastic, granulocytic and megakaryocytic components all visible, at the lower left. Overall cellularity in this area is relatively low, with numerous fat spaces.

831

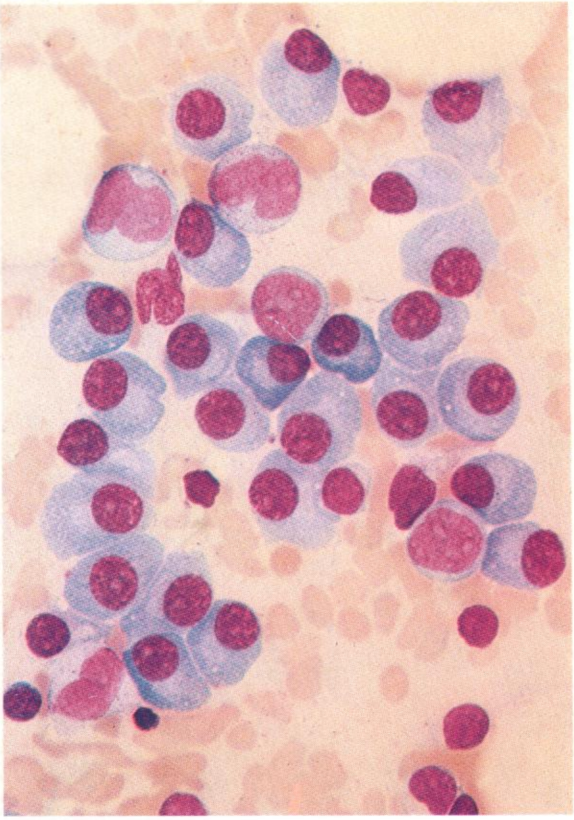

832

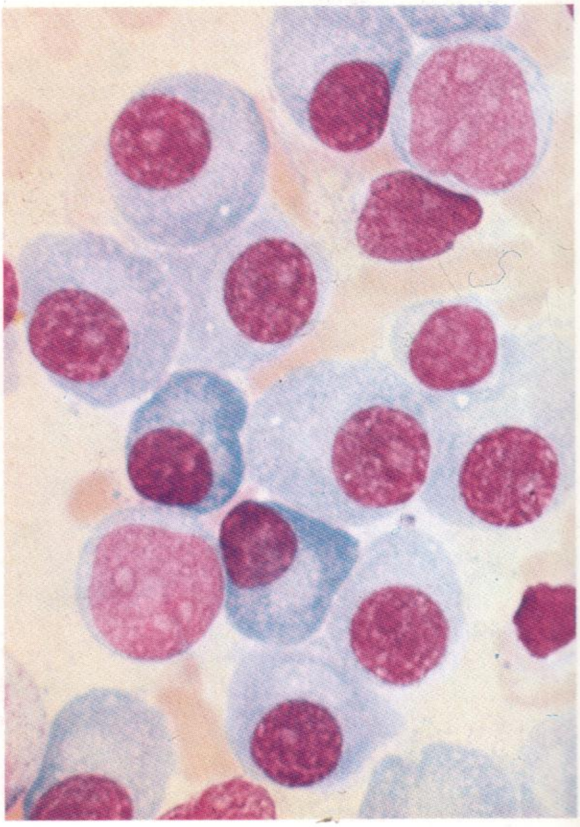

833

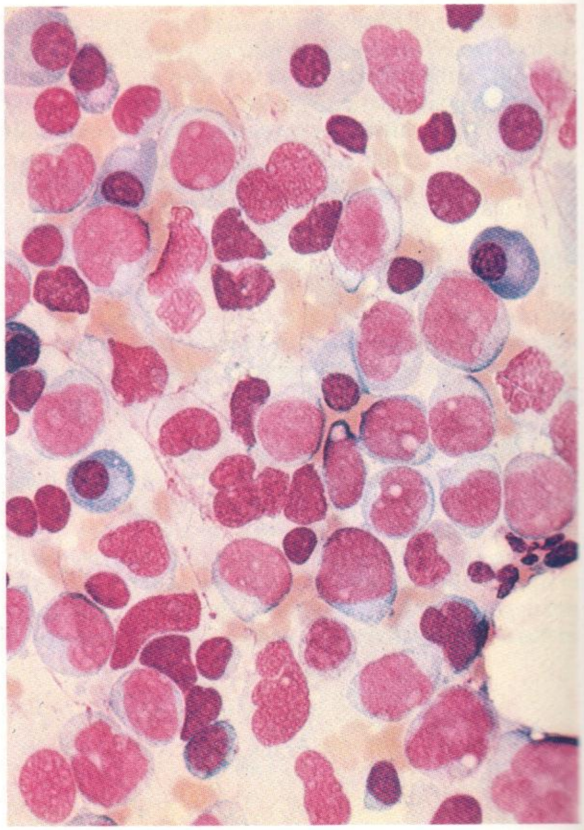

831–833. *Transformation of myeloma to AML.*

831. Myeloma marrow with chiefly mature well-differentiated myeloma cells, but with occasional blast cells of myelomonocytic cytology.

832. A higher-power view to contrast the range of myeloma cell morphology with two nucleolated myeloid blast cells.

833. Marrow smear from the same patient at a later stage of transformation, showing predominance of acute myelomonocytic leukaemia (AMML) blast cells with scanty residual plasma cells and rare later granulocyte stages.

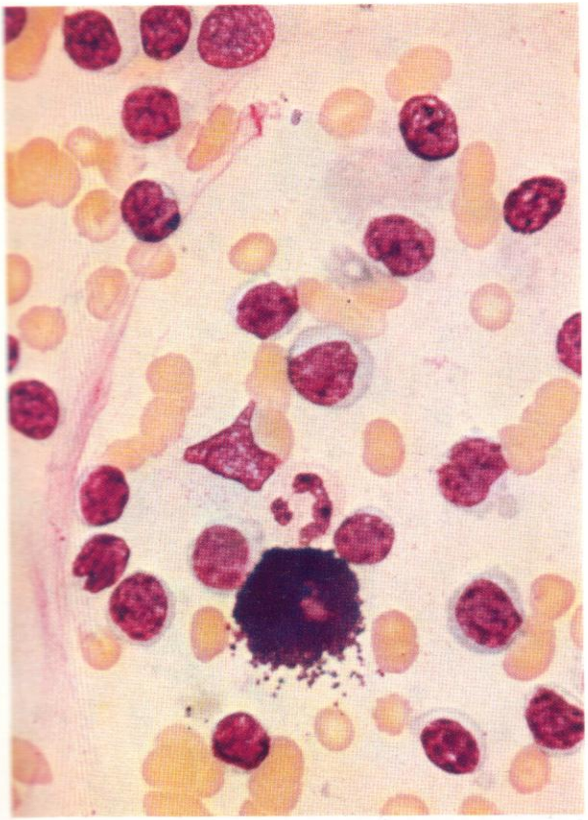

834

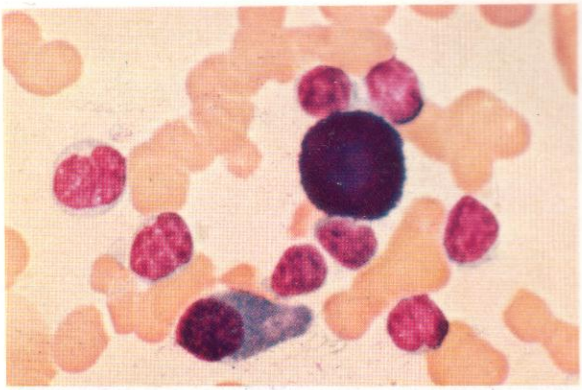

835

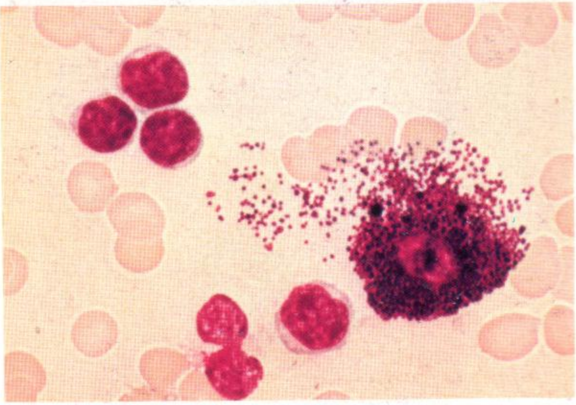

836

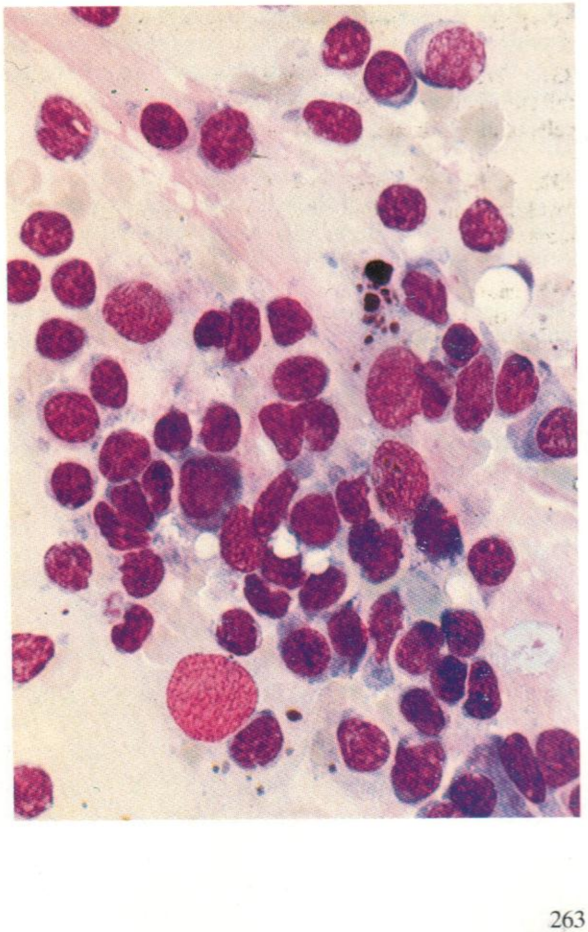

837

834–837. *The marrow picture in Waldenström's macroglobulinaemia is not specific, but appearances such as these are very suggestive and would indicate the need for investigation of the immunoglobulin pattern.*

834. A bone marrow smear from a patient with macroglobulinaemia. Lymphocytes, mostly with disrupting or minimal cytoplasm, predominate. There is also a tissue mast cell present.

835. Another example of bone marrow cytology in macroglobulinaemia. The red cells show conspicuous rouleaux formation, the lymphocytes predominate and have scanty cytoplasm, and there is a plasma cell present as well as a very densely granular tissue mast cell. An alternative name for this last cell, 'basophil ball cell', would here be descriptively apt.

836. Another field from the same preparation, with similar lymphocytes but a disrupted tissue mast cell.

837. The neoplastic cells in this field from the bone marrow of another case show occasional 'lymphoplasmacytoid' features. Phagocytic RE cells are also conspicuous.

838

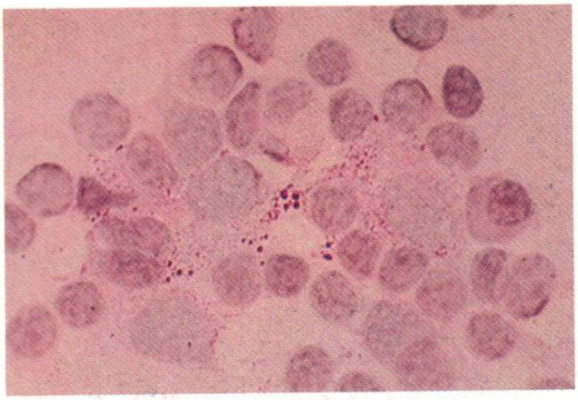

839

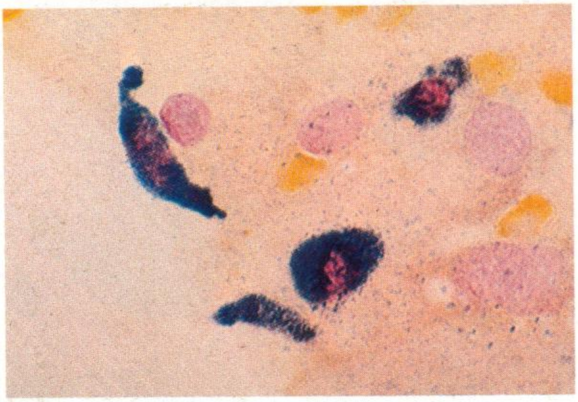

840

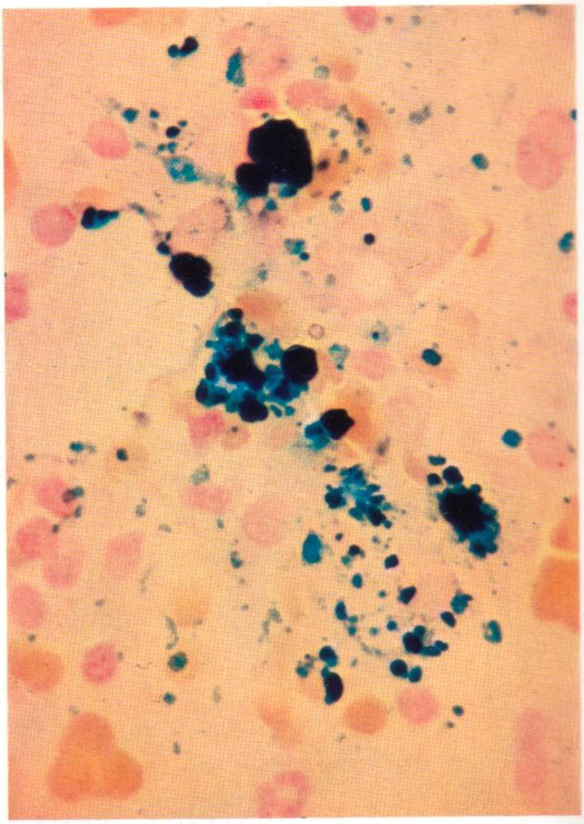

841

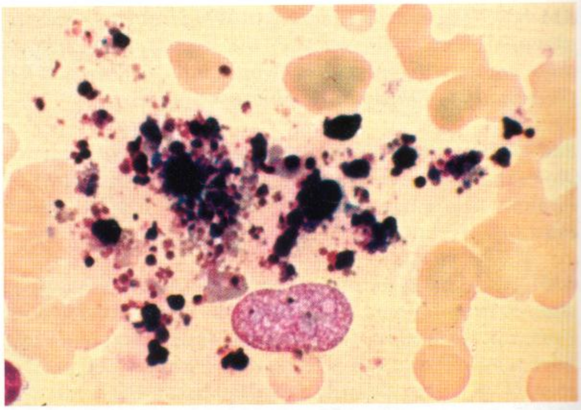

842

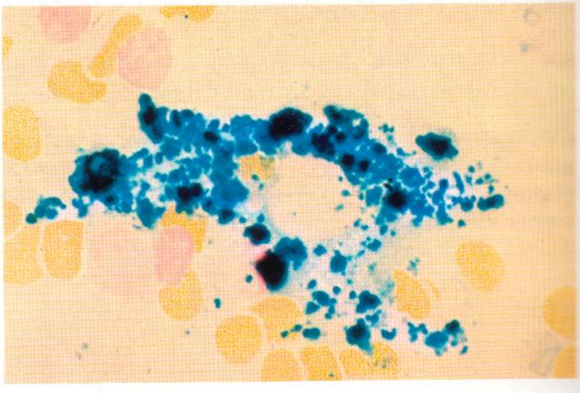

838. PAS stain in macroglobulinaemia: there is scattered granular PAS positivity in the cytoplasm of two RE cells, but the lymphocytes and plasmacytoid cells in this disease show little or no reaction.

839. Dual esterase stain in macroglobulinaemia, showing several tissue mast cells with coarse CE positivity in a marrow fleck. The neoplastic lymphoid cells and RE cells in the fleck show only weak scattered granular positivity to both BE and CE.

840. Free-iron stain on bone marrow smear in macroglobulinaemia. The excessive amount of free iron, both scattered and in macrophages, is evident.

841. Romanowsky stain of marrow from macroglobulinaemia, showing a macrophage heavily laden with iron.

842. A similar cell to that in **841**, stained with the Prussian blue stain for free iron.

843

844

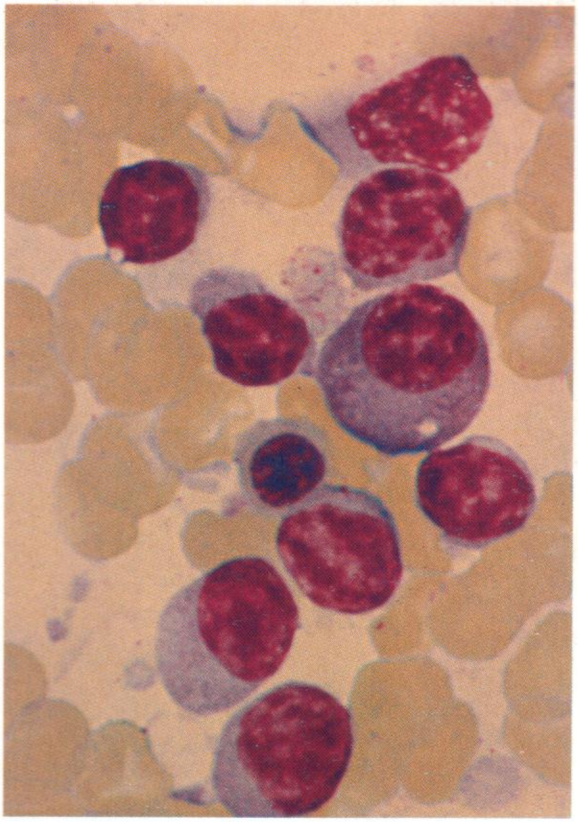

843. A high-power view of a section of bone marrow trephine biopsy from a patient with lymphoplasmacytoid immunocytoma and macroglobulinaemia, providing a clear demonstration of the mixed lymphocytic, plasmacytic, and intermediate cytology of the predominant infiltrating cells. Several binucleated plasma cells can be seen.

844. A smear of bone marrow aspirate from the same case as in **843**, showing the much superior cytological detail of such preparations. There is a central normoblast, but all the remaining cells in this field are of the lymphoplasmacytoid series, with a good sequence of intermediate developmental appearances, from lymphocyte to plasma cell.

845 A low power view of a section of bone marrow trephine biopsy from a case of Waldenström's macroglobulinaemia with lymph node involvement, where lymph node biopsy revealed the histological features of lymphoplasmacytoid immunocytoma. The field shows the edge of a neoplastic nodule, with a marked 'eosinophilic' reaction in the immediately surrounding residual marrow, here seen at the upper part of the field. The tumour cells appear to have generally uniform cytology at low power.

845

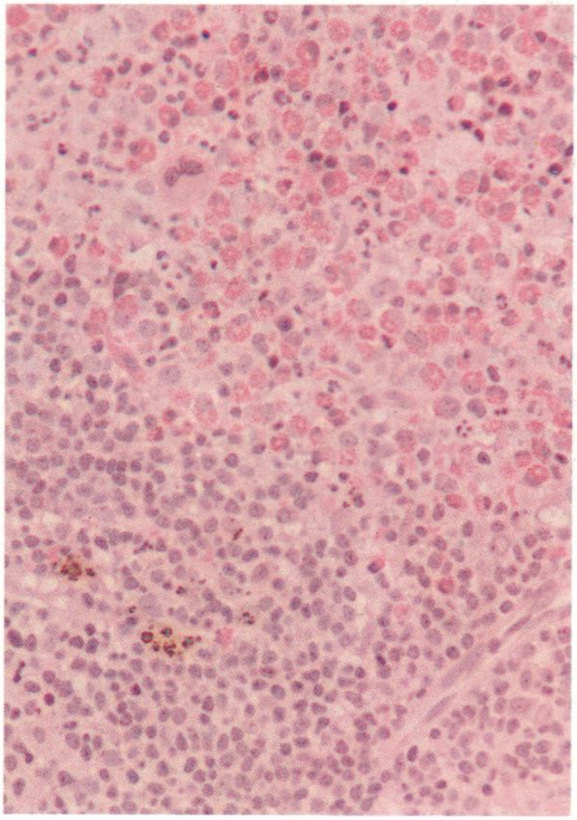

846

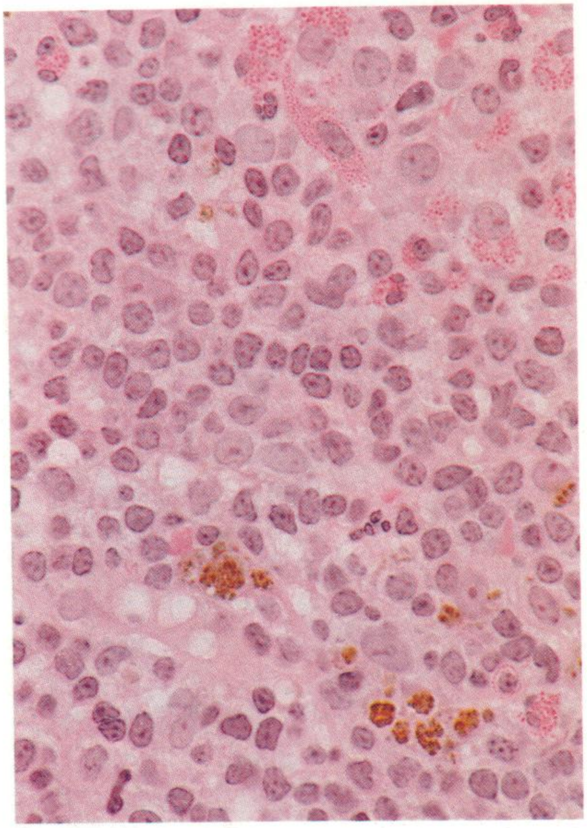

847

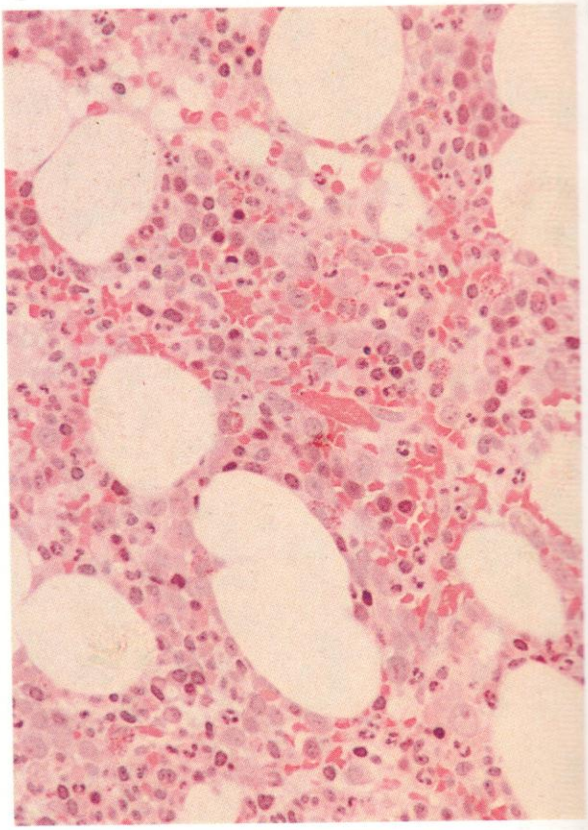

848

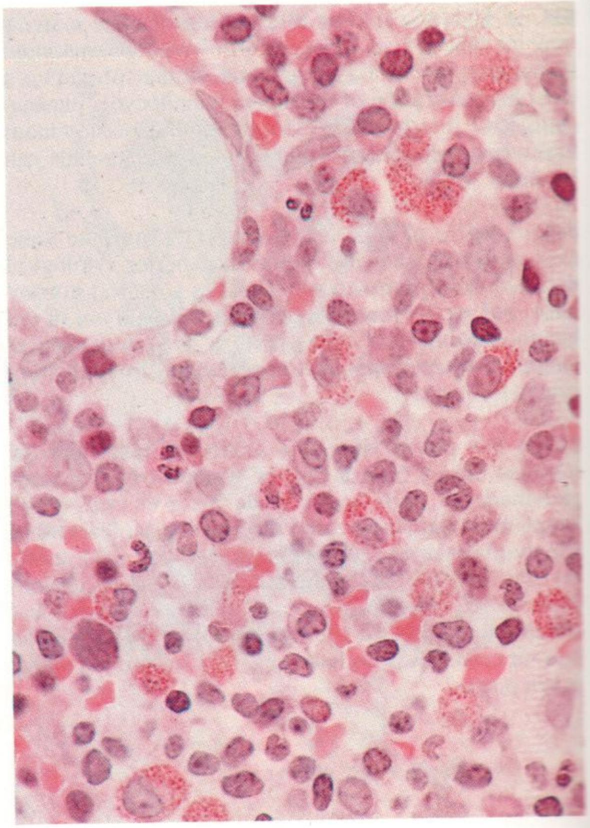

846 A higher power view of the same specimen as in **845**. The infiltrating tumour cells are now seen to range from the predominant mature-looking lymphocytic, centrocytic or plasmacytoid cells, to much less mature larger cells with pale-staining nuclei and occasional nucleoli.

847 and **848**. Thin sections from plastic-embedded trephine biopsy material taken from the bone marrow of another patient with macroglobulinaemia. The low-power view (**847**) illustrates diffuse involvement of residual marrow with lymphoplasmacytoid cells and further 'eosinophilic' mast cells, and also a conspicuous scattered background deposit of amorphous eosinophil deposit, probably representing amyloid material. The higher magnification of **848** reveals quite clearly the lymphoplasmacytoid nature of the infiltrate and the presence of various normal myeloid precursors, and also confirms the presence of numerous tissue mast cells.

849

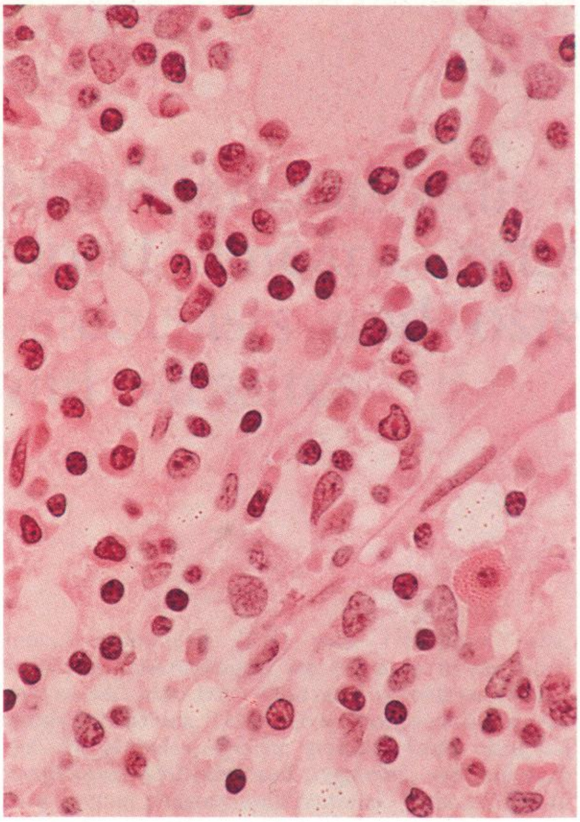

850

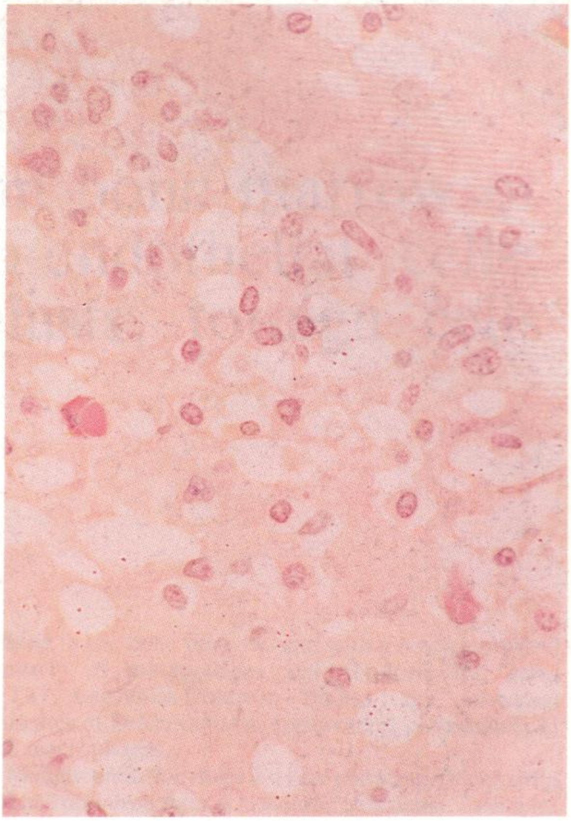

851

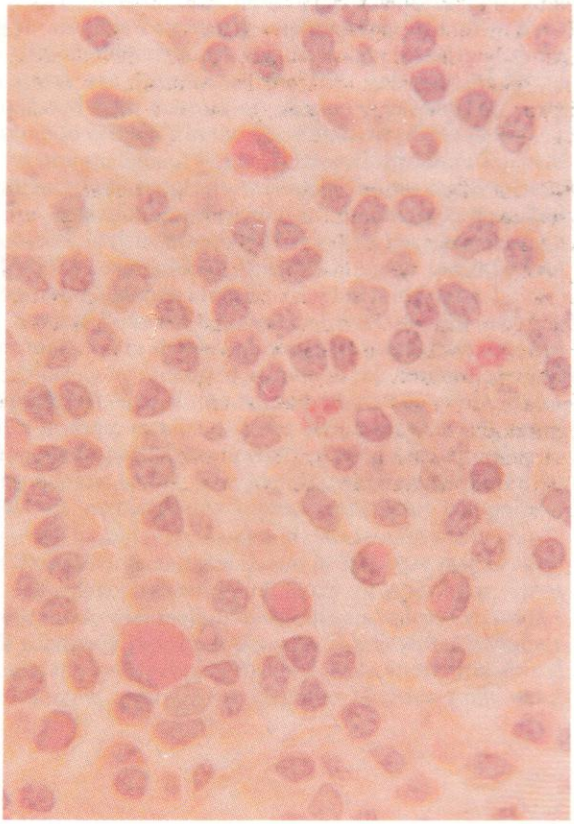

849–851. Sections from a bone marrow trephine biopsy taken from another patient with macroglobulinaemia, **849** stained by H&E, and **850** and **851** by the PAS reaction to show various examples of Dutcher body formation in the neoplastic lymphoplasmacytoid cells. These are PAS-positive nuclear inclusion bodies probably derived from cytoplasmic invaginations. Similar, but generally much smaller, intranuclear inclusions occur in myeloma and less often in reactive plasma cells, but the large inclusions known as Dutcher bodies are seen especially in macroglobulinaemia, where they may be so large, as in **849**, as to cause fragmentation of the nucleus. A PAS-positive body stretching the nuclear membrane and occupying most of the cell is shown in **850**, while in **851** a whole series of these bodies, at various stages of development, appears in the lower part of the field. There is a single PAS-positive polymorph near the top.

Part 4

Miscellaneous cells from bone marrow or blood smears, reticulo-endothelial cells, osteoclasts and osteoblasts, foreign cells and parasites

Reticulo-endothelial (RE) cells (reticulum cells, histiocytes, macrophages) are common in the bone marrow and have been illustrated several times previously in this book. They take up foreign particles, free iron, fat globules, specific granules from disrupted granulocytes, and other cell fragments, and therefore often contain phagocytosed material. Their cytoplasm appears fragile and is readily broken up in the smearing process or stretched out between neighbouring cells – so that the cytoplasmic outlines may be difficult to recognize. They may contain various inclusions – sea-blue histiocyte material, pseudo-Gaucher cell birefringent lipid or blue crystals and grey-green crystals. In certain lipid storage diseases they appear grossly swollen with abnormal fibrillary or globular deposits of lipids.

The nature of this lipid inclusion material in the two main forms of lipidosis, Gaucher's disease and Niemann-Pick's disease, is illustrated in this section and discussed in the accompanying captions.

Glycogen storage disease is also associated with the accumulation of inclusion material, particularly in macrophages, but to a lesser extent in many other haemic cells.

In chronic infective or reactive states involving the bone marrow, ranging from tuberculosis to sarcoidosis, macrophage proliferation may lead to foreign-body giant-cell (or Langhans' cell) formation, with appearances similar to those encountered in the lymph node imprints illustrated in **1098** and **1099**.

Another group of granulomatous states frequently involving the bone marrow are those of the 'histiocytosis X' family, including Hand-Schüller-Christian syndrome, eosinophilic granuloma and Letterer-Siwe disease. All are thought to involve proliferation of Langerhans' cells, prominent in the skin but probably arising in the bone marrow, and with mixed cytological features of macrophages and dendritic RE cells.

The Leishman-Donovan bodies, the protozoal parasites of Leishmaniasis, appear most prominently in RE macrophages.

Malignant histiocytosis is a rare neoplastic state of the RE cell and even rarer is histiocytic leukaemia. Examples of each are illustrated in this section.

Apart from RE cells, most of the other cells illustrated here are less commonly encountered, but they have highly characteristic cytological features, and once these features are appreciated the cells are unlikely to be confused with normal or abnormal variants of more common cell lines in the bone marrow or blood.

A non-malignant form of histiocytic proliferation with enhanced phagocytosis, arising in various opportunistic virus infections, especially in immunocompromised subjects, is virus-associated haemophagocytic syndrome (VAHS); examples of this condition in trephine and aspiration marrow biopsies are illustrated here.

Several different examples of tumour cells invading the marrow are shown. Although an isolated tumour cell may rarely be identified as such in the absence of more typical cell clumps, the feature which allows identification in most instances is the occurrence of cell nests, frequently partially syncytial, of cells not belonging to any haemic series. The identification cannot often go beyond 'metastasizing tumour cells', but comparison with the histology, cytology and cytochemistry of the range of illustrative metastases shown in **980–1024** may provide a suggestive indication of likely origin. Apart from neuroblastoma, medulloblastoma and chemodectoma – all relatively rare tumours with characteristic cytology found in young people – the metastases most often found in marrow aspirates or trephine biopsies from older

patients, usually with leucoerythroblastic anaemia, are from primary malignant tumours of lung, breast, kidney or thyroid, and examples of all these are shown here.

Certain of the more common parasites which may be seen in smears of blood or bone marrow are also illustrated. They are found mostly in tropical or subtropical zones, but their appearance should be recognized by all haematologists; although what may actually be seen under the microscope (as in the photographs here) does not always provide detail comparable with the diagrams and paintings in parasitology texts.

852

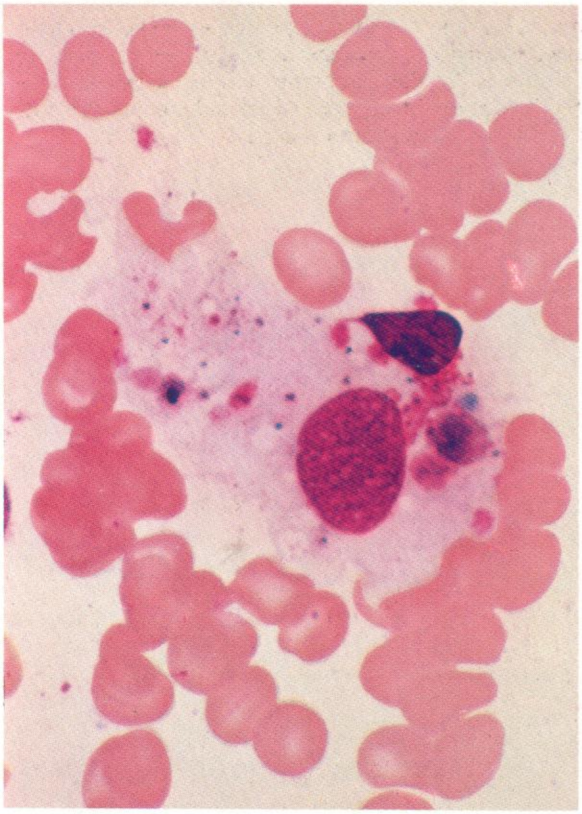

853

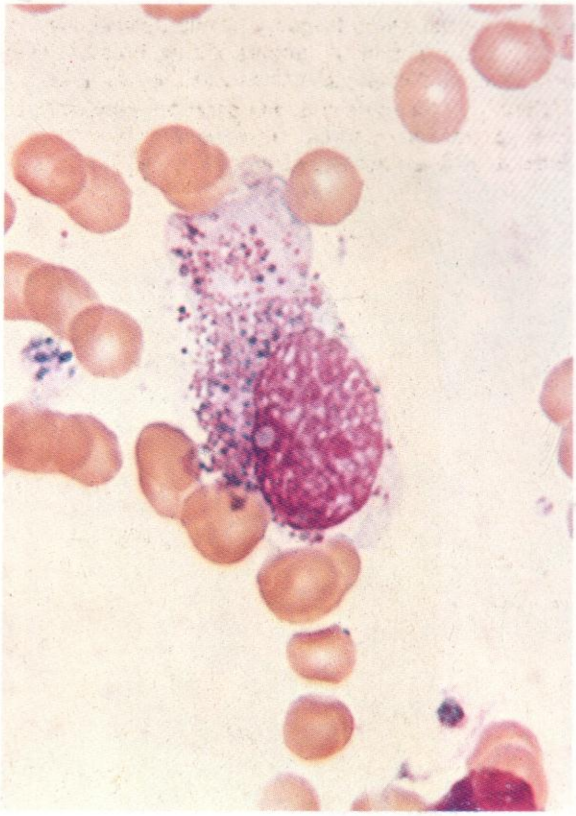

854

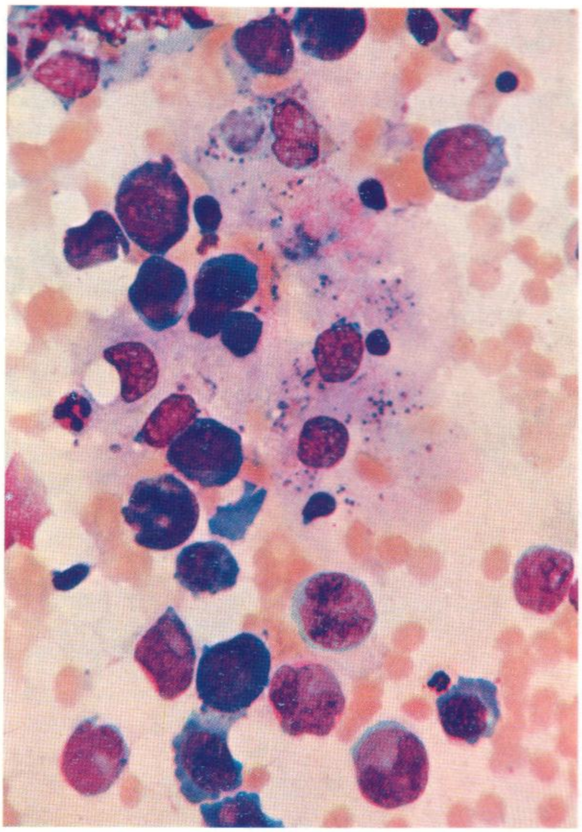

852. A phagocytic reticulo-endothelial (RE) cell containing various particles of cellular debris. These cells are seen only rarely in the peripheral blood, although they may occasionally be found in buffy coat smears in some chronic infective states, as in the monocyte–macrophage sequence in **855–857**, but they are common in bone marrow smears, as here, where they are generally to be found towards the tail of the smear or in marrow flecks. Their thin flattened leptochromatic nuclei, with fine chromatin markings and usually inconspicuous nucleoli, and their extensive fragile cytoplasm, usually with indefinite margins, as shown here, are characteristic.

853. This is probably an RE cell with phagocytosed eosinophil granules from a disrupted myelocyte. The alternative possibility is that it represents a partially smeared degenerating eosinophil myelocyte.

854. A group of RE cells with poorly outlined filmy cytoplasm, from the bone marrow in a case of pernicious anaemia.

855

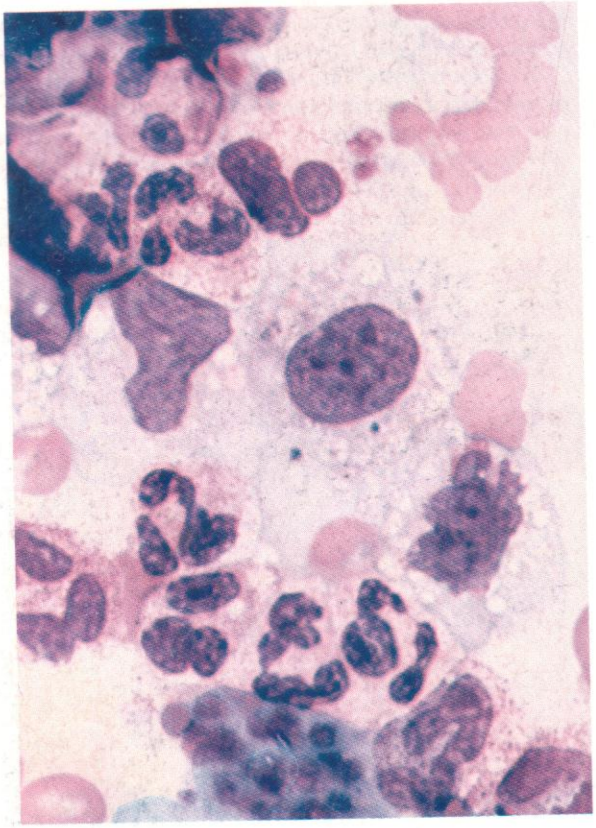

856

857

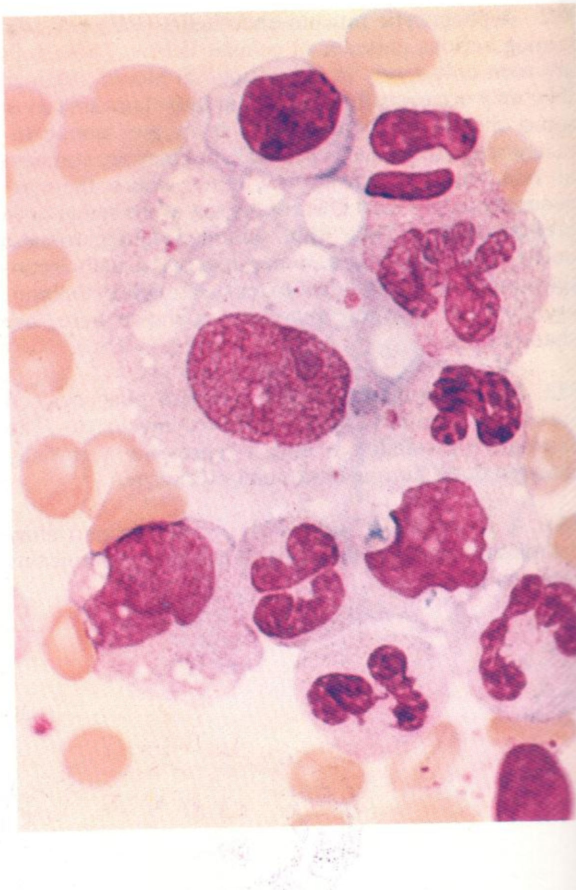

855. A group of three cells of the monocyte–macrophage system in buffy coat of peripheral blood, from a patient with bacterial endocarditis. The middle cell is clearly a macrophage, whereas the contiguous mononuclear cells are still of vacuolated monocytic cytology.

856. A similar macrophage in the buffy coat of this patient, stained to show the free-iron content.

857. Another example of the monocyte–macrophage sequence in peripheral blood. There are lymphocytes at top and bottom of this field, and six neutrophil polymorphs, with three cells showing stages in the monocyte to macrophage transformation, all having phagocytic vacuoles and the uppermost showing the most macrophagic cytology.

858

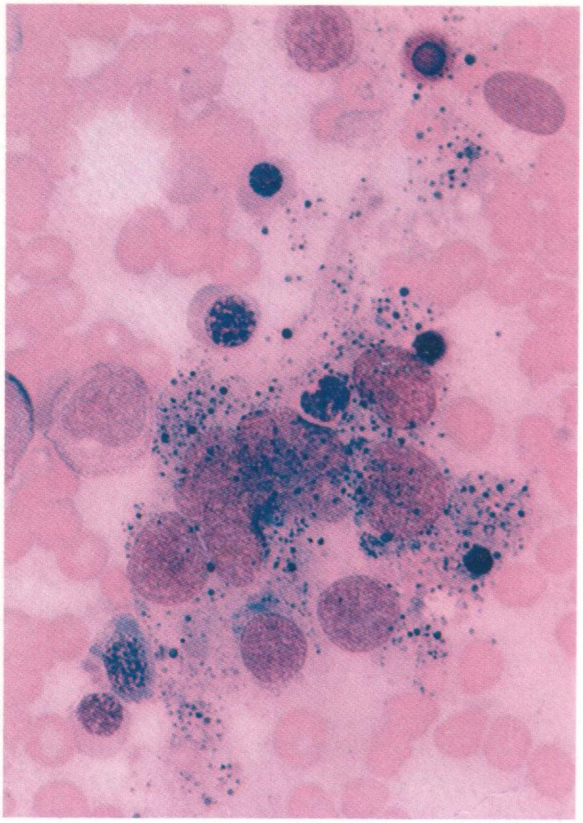

859

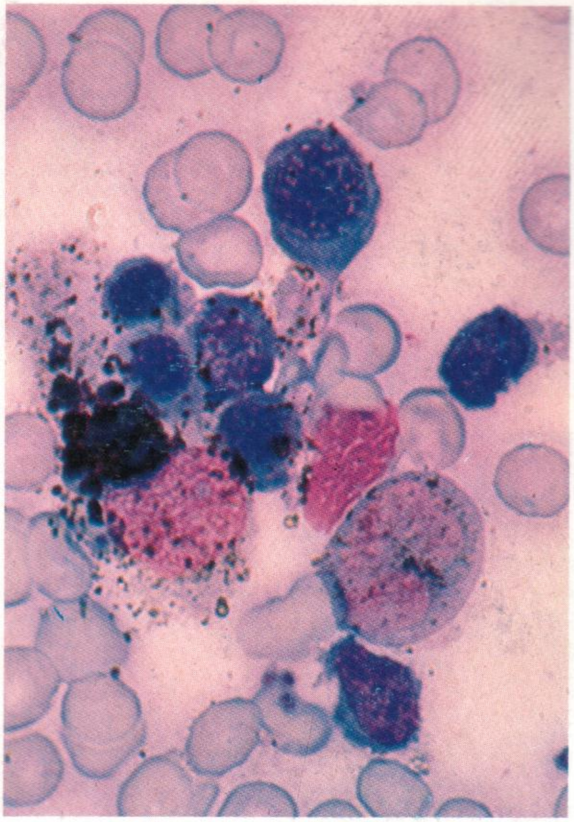

858–891. *Phagocytic RE cells with various cytochemical reactions and inclusions.*

858. Romanowsky stain: a multinucleated RE cell with remnants of several ingested cells, including a polymorph, and multiple granules – most probably iron.

859. SB stain: strong positivity, probably surrounding phagocytosed material, including free-iron particles. There are scattered SB positive granules in a monocyte.

860. PAS reaction: three RE cells, one with scattered PAS-positive granules and the other two with weak PAS reaction but chiefly scattered free-iron particles spreading across the field diagonally.

860

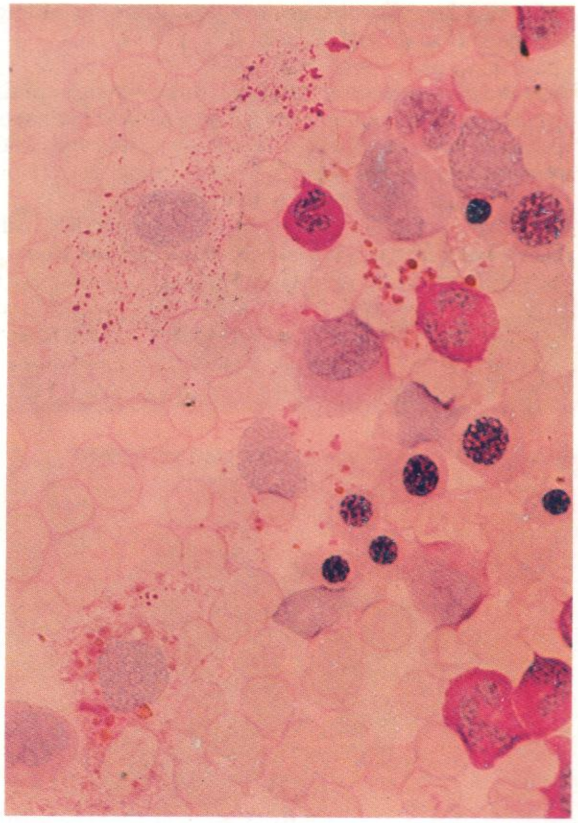

861

862

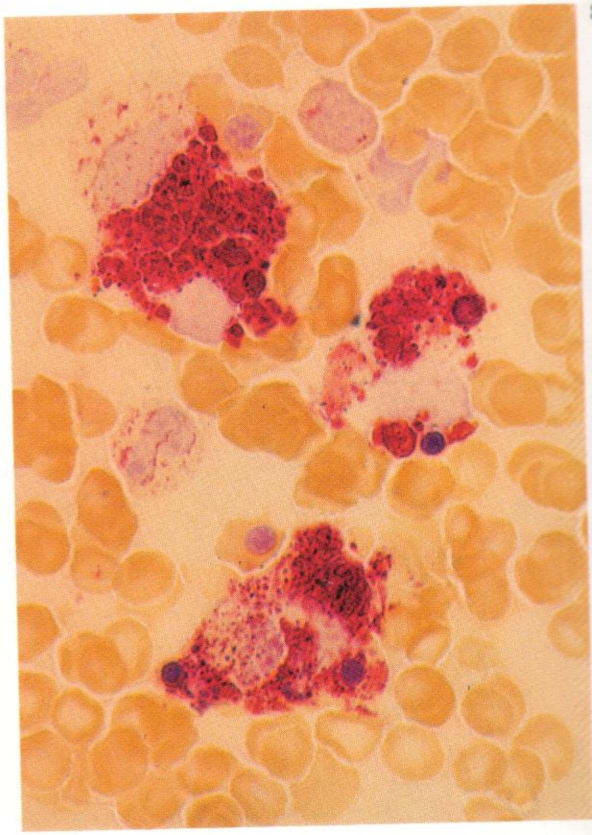

863

861. Alkaline phosphatase reaction, showing strong positivity in a marrow RE cell.

862. Acid phosphatase reaction: three strongly positive RE cells, containing phagocytosed cell remnants and large particles of free iron heavily coated with acid phosphatase.

863. Dual esterase reaction: the phagocytic RE cell shows the typical very strongly positive BE reaction.

864

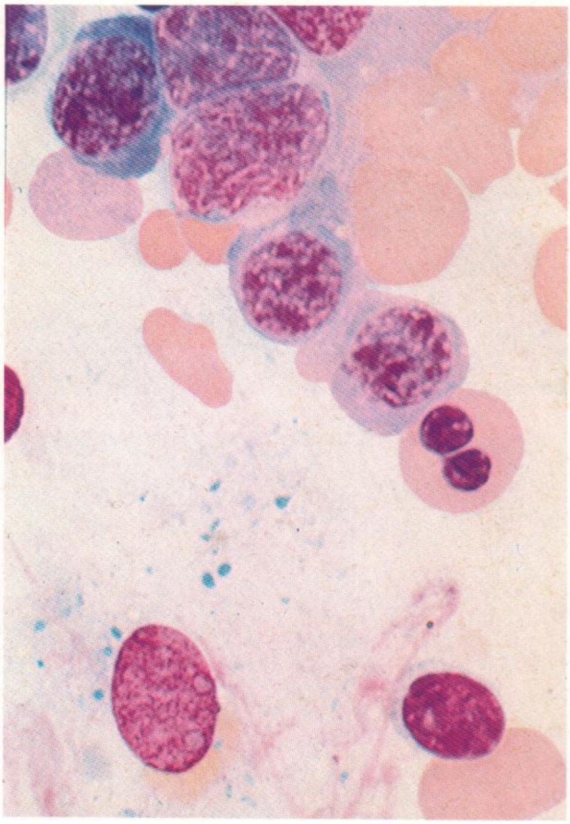

865

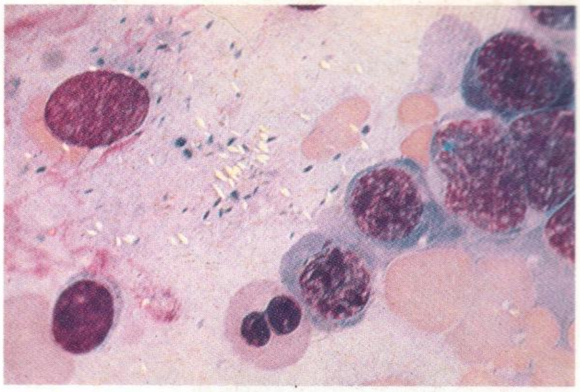

866

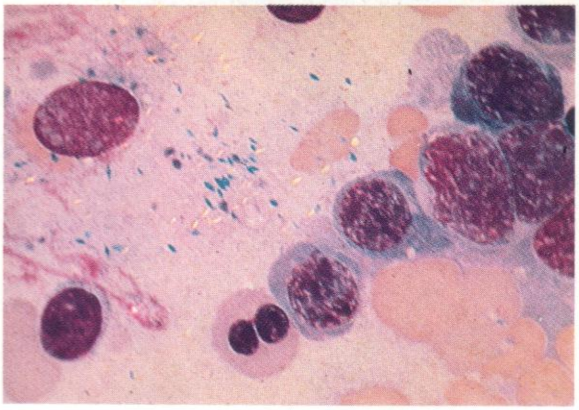

864. Faintly visible blue crystals together with coarser iron granules in a distended RE cell from the marrow in a case of congenital dyserythropoietic anaemia (CDA) type I. RE cells containing such blue crystals, and pseudo-Gaucher cells, RE cells with crumpled swollen cytoplasm, are found not uncommonly in CDA.

865 and **866**. Increased visibility and clear birefringence of these crystals, with reversal of refringence on 90° rotation when the same field as shown in **864** is looked at under polarized light.

867 and **868**. Another Gaucher-like cell with duplicate under polarized light showing refringence. This specimen was from a case of CML, a condition in which the pseudo-Gaucher cell phenomenon is also not infrequent.

867

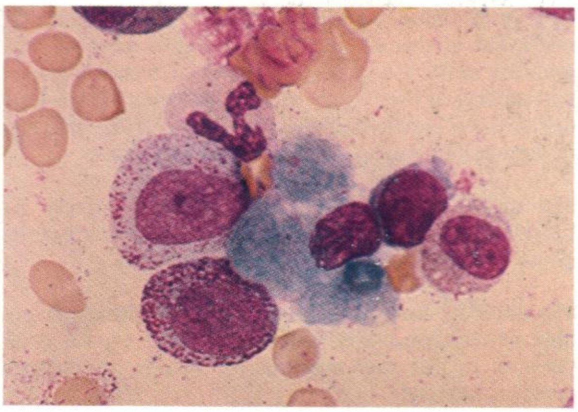

868

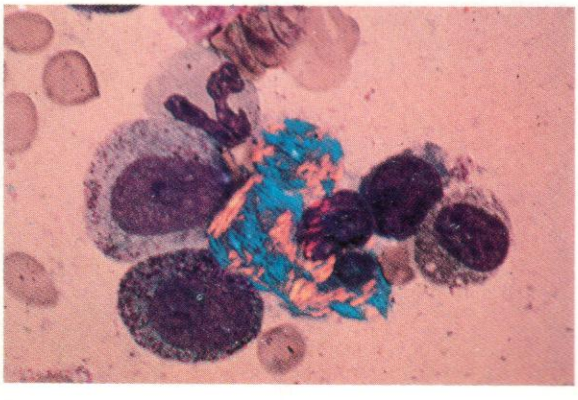

869

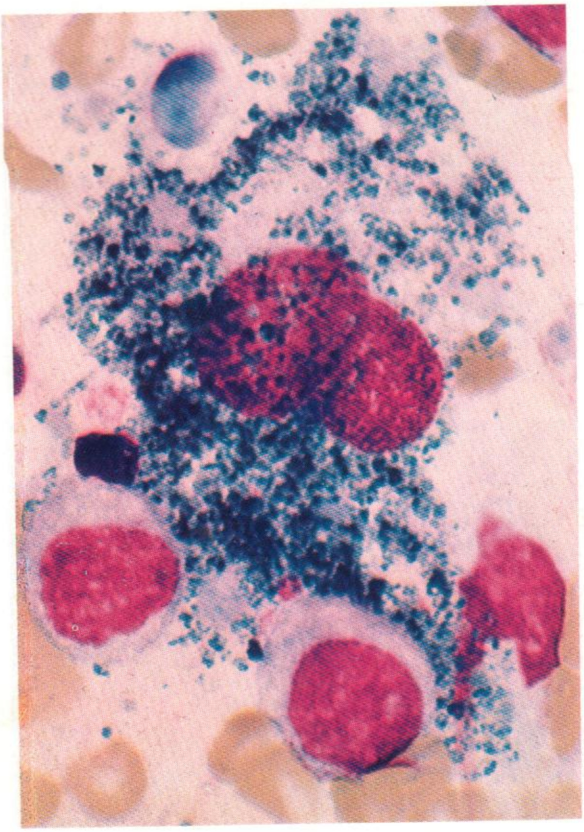

870

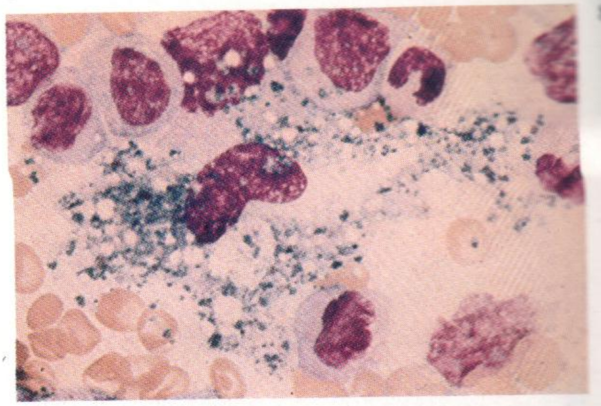

871

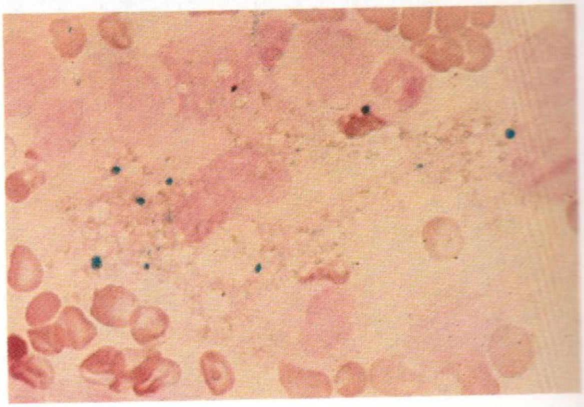

872

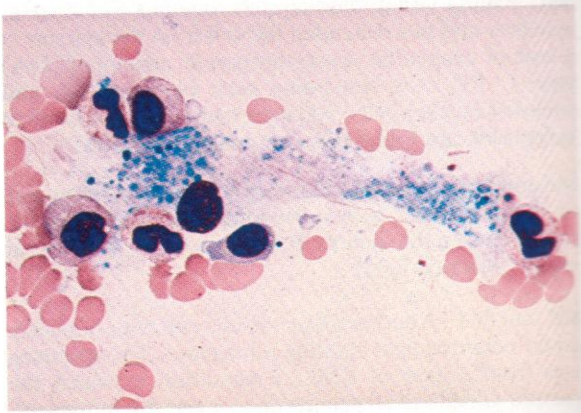

873

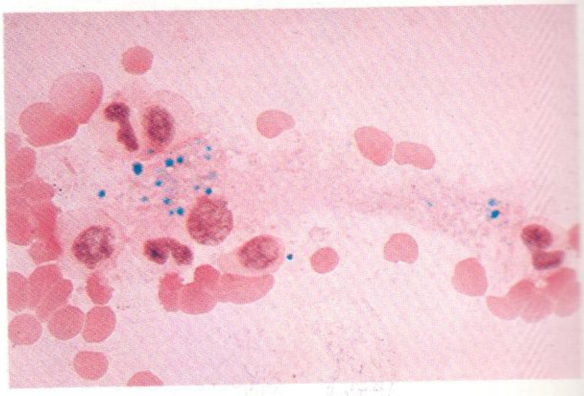

869. A sea-blue histiocyte (SBH): an RE cell, binucleated in this instance, containing a mass of blue granules in the Romanowsky stain. Such cells are seen particularly in the benign genetic disorder of 'sea-blue histiocytosis', and secondarily in myeloid leukaemia and in dysmyelopoietic and dyserythropoietic states.

870 and **871**. An SBH, stained consecutively by Leishman and free-iron stains, to demonstrate that the granular material is chiefly negative for iron.

872 and **873**. An iron-laden macrophage with some sea-blue material similarly stained consecutively for comparison. In this case much of the heavier granularity contains free iron.

874

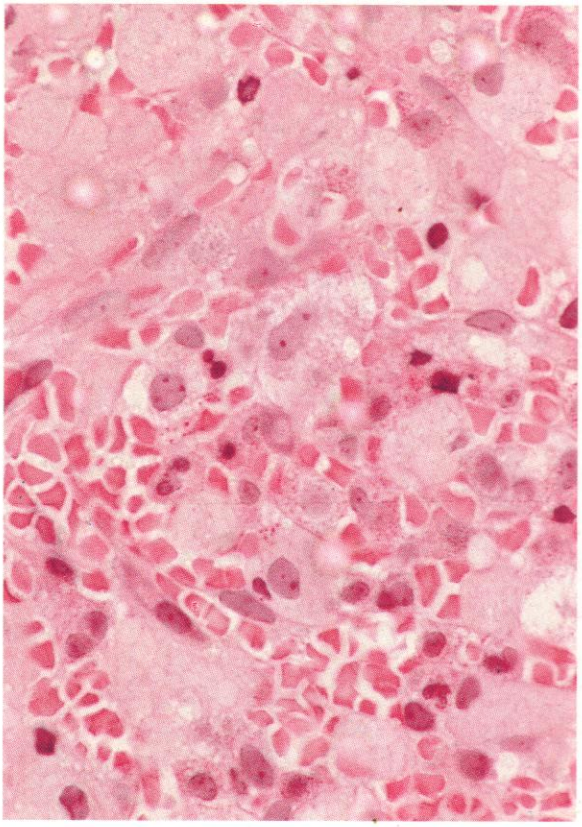

875

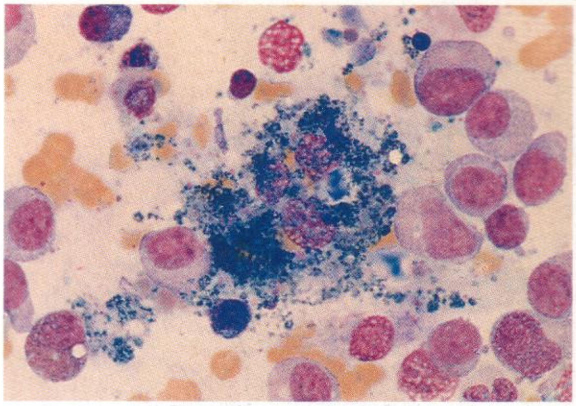

876

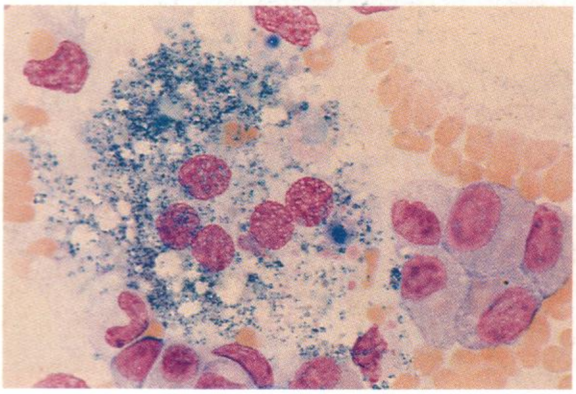

877

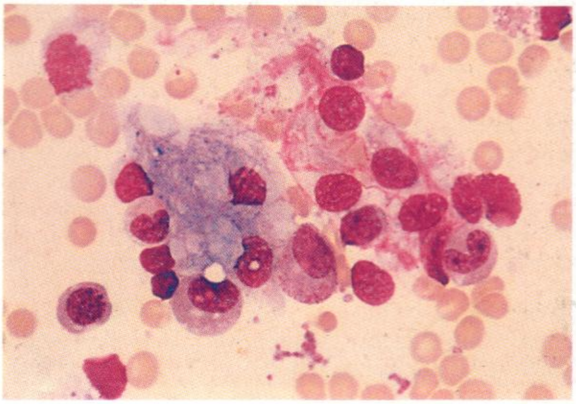

878

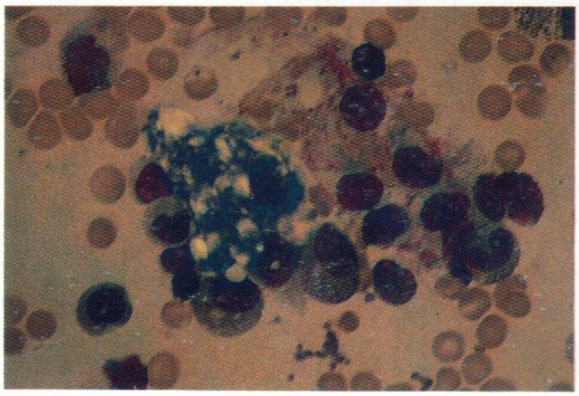

874. A thin section of marrow trephine biopsy from a case of MDS with numerous pseudo-Gaucher cells, histiocytes showing distended granular cytoplasm. Although the H&E stain does not further identify the nature of the granules, these are the same cells as in **875** and **876**, where the granules of many of them are shown to be sea-blue by the use of Romanowsky staining.

875 and **876**. Romanowsky-stained bone marrow smears from the same case as illustrated in **874**, showing SBHs, with neighbouring early myeloid cells having the defective granularity commonly found in the myelodysplastic states. In **875** there are three, and in **876** five, histiocyte or macrophage nuclei visible in the respective sea-blue cell nests.

877 and **878**. Another example of a pseudo-Gaucher cell, in this case from the bone marrow of a child with AML, emerging into remission on chemotherapy. The appearance of the striated and chunky cytoplasmic material is seen under normal microscopic illumination and then under polarized light. The inclusion material is strongly birefringent.

879

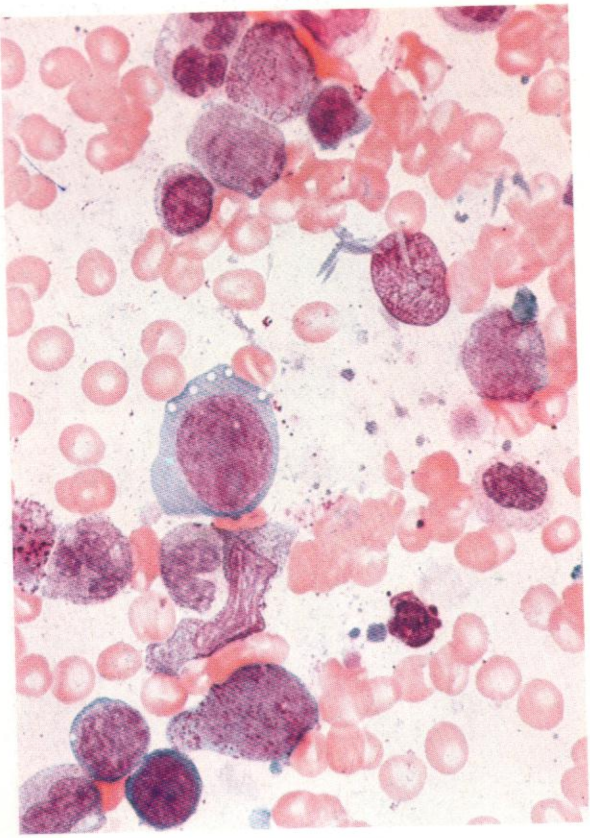

880

881

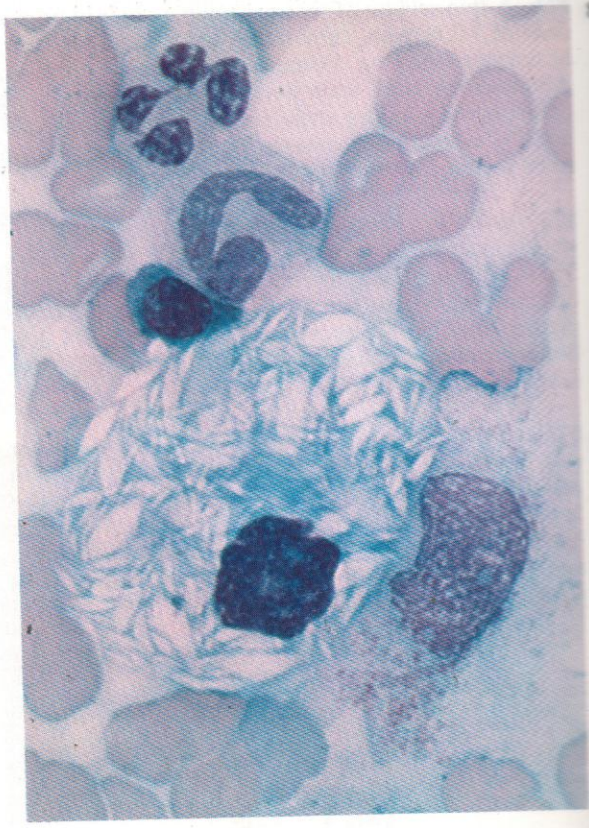

879. Grey-green crystals in a disrupted RE cell. These inclusions occur chiefly in myeloid leukaemias and are not birefringent.

880. Another example of the non-birefringent type of grey-green crystal in a macrophage from the bone marrow of a patient with AML. The flat nucleus and spreading cytoplasm of the macrophage are typical, and the cell contains other phagocytosed material, probably chiefly iron, in addition to the grey-green crystal.

881. A genuine Gaucher cell in the bone marrow of a patient with Gaucher's disease, showing typical coarse onion-skin lipid inclusion material.

882

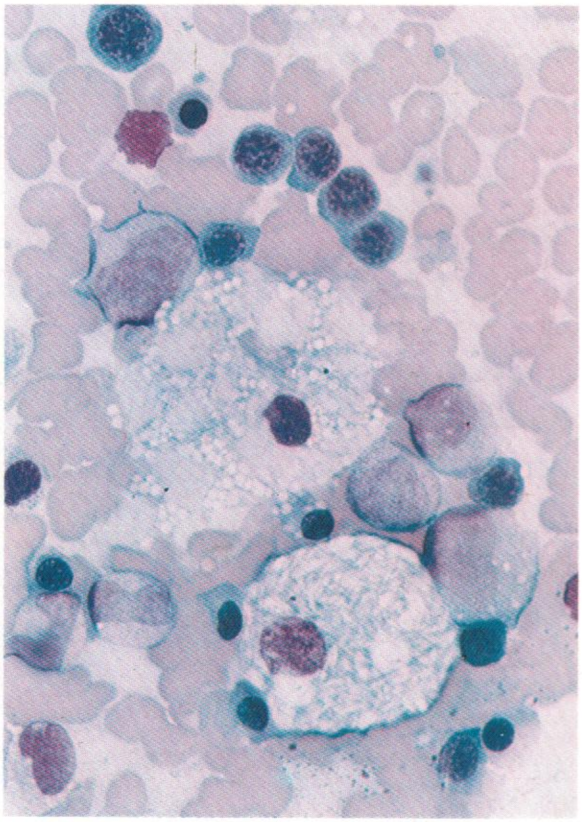

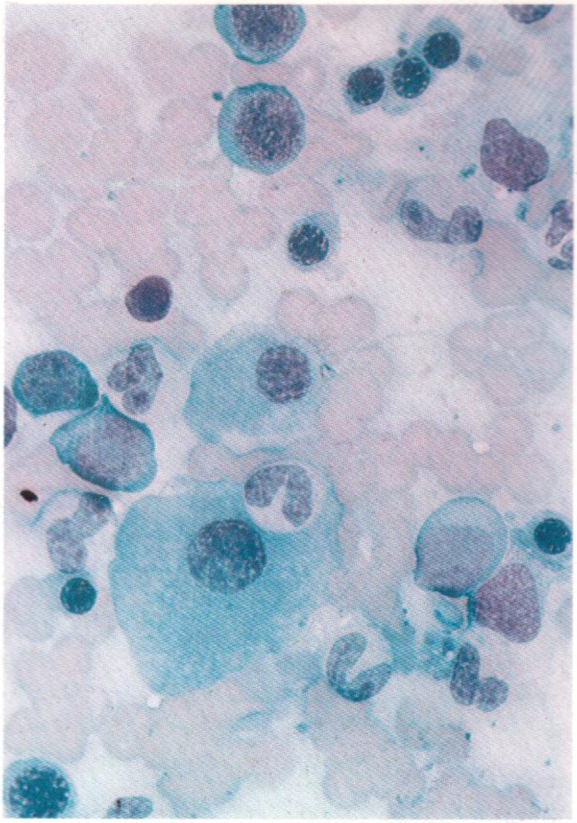

883

882. Two further Gaucher cells in the bone marrow – one typical cell and one heavily vacuolated.

883. Less typical Gaucher cells from the same specimen. The cytoplasm is more granular and less fibrillary.

884 and **885**. Gaucher cells under polarized light: the birefringence is shown in the same cells with the polarizer turned to a 90° angle.

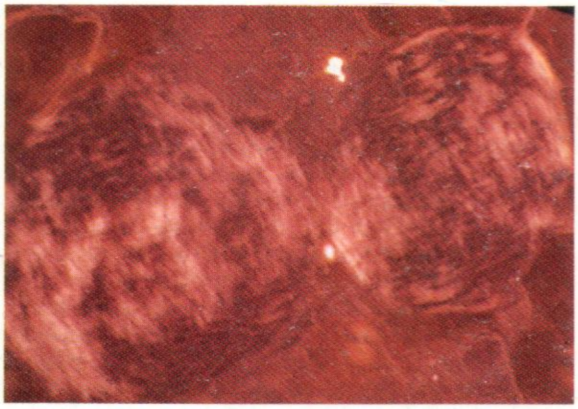

884

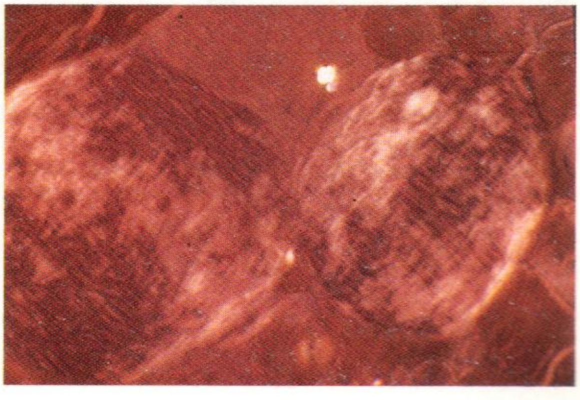

885

886

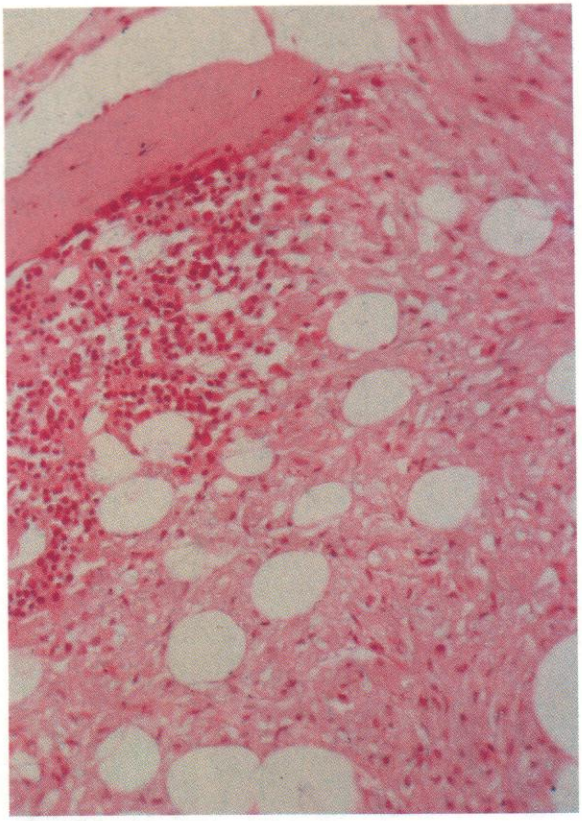

887

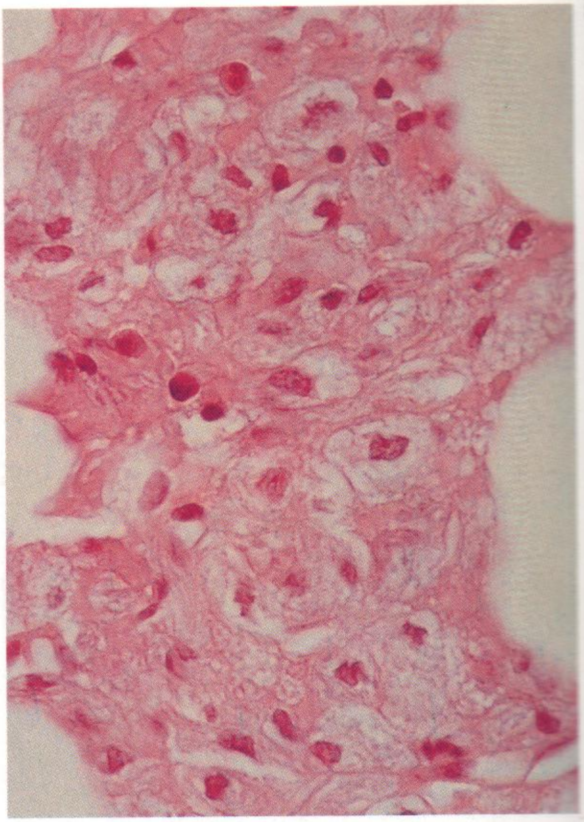

886–889. Marrow trephine sections and aspirate smear from another patient with Gaucher's disease. In the low-power field in **886**, the nodular appearance results from the persistence of normal haemopoietic marrow, with little infiltration in the vicinity of the bony trabeculum at the upper left, but elsewhere the Gaucher cell infiltrate was very extensive in this case. The characteristic histological appearance of these cells in marrow sections stained with H&E is well shown in the higher-power view of **887**, with their ample and swollen cytoplasm, distended with fibrillar material. In the reticulin silver stain of **888** a scattering of interlacing reticulin fibrils, somewhat increased over normal, is revealed, while the accumulated cytoplasmic material has a more granular appearance in this stain and there is even a suggestion of weak argyrophilia in the cytoplasm of some histiocytes. The smear preparation in **889**, with the usual Romanowsky stain, shows the same Gaucher cells as in the preceding sections, here with a mixed fibrillary and granular or foamy appearance.

The striking and highly characteristic appearance of Gaucher cells is due to the accumulation within expanded lysosomes of the lipid glucosyl ceramide, resulting from deficiency of the enzyme glucocerebrosidase.

888

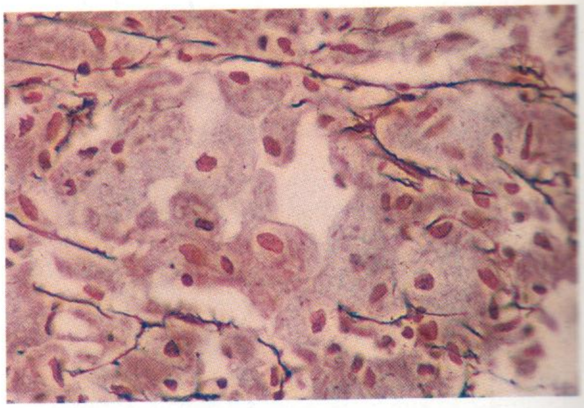

889

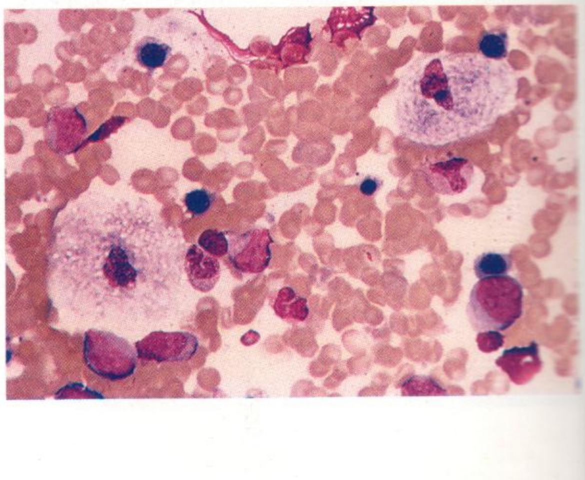

890

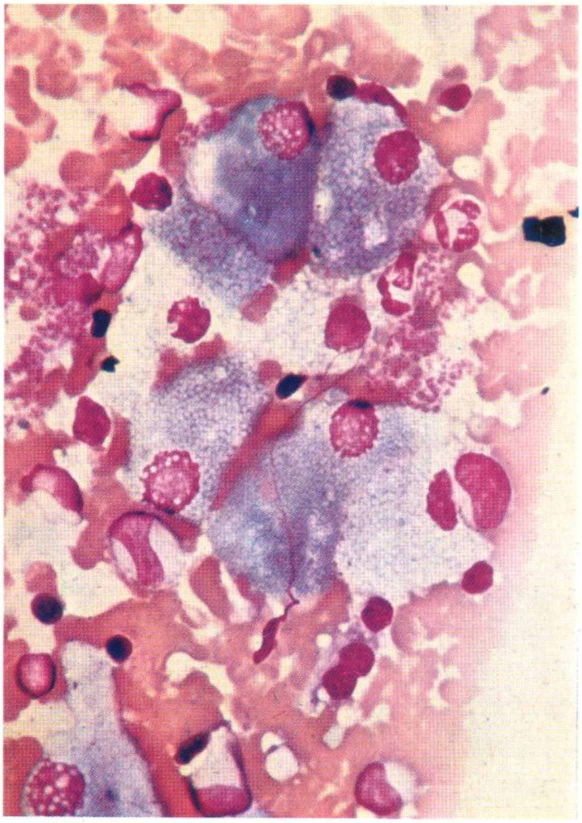

891

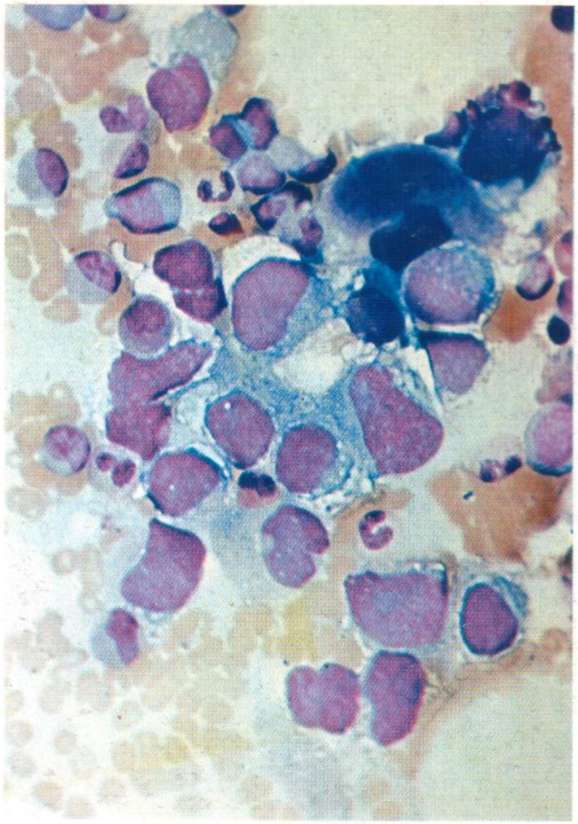

890. RE cells laden with foamy deposits of abnormal lipid in the bone marrow from a patient with Niemann-Pick disease. The lipid in these cells is sphingomyelin.

891. Abnormal cells, probably RE macrophages, with variable reticulated cytoplasmic content of abnormal storage material, from the marrow of a patient with a 'histiocytosis' of the eosinophil granuloma-Hand-Schüller-Christian disease group. These granulomatous conditions, including also Letterer-Siwe disease, are sometimes grouped together under the name 'Histiocytosis X'. They appear to share an origin from Langerhans' cells which probably arise in the bone marrow, typically express CD1 and HLA-DR antigens, and which are characterized by a mixture of features of macrophages and immuno-stimulatory dendritic cells.

892. H&E stain of trephine biopsy bone marrow section from a child with another variant of the same disease group, showing numerous multinucleated histiocytes.

892

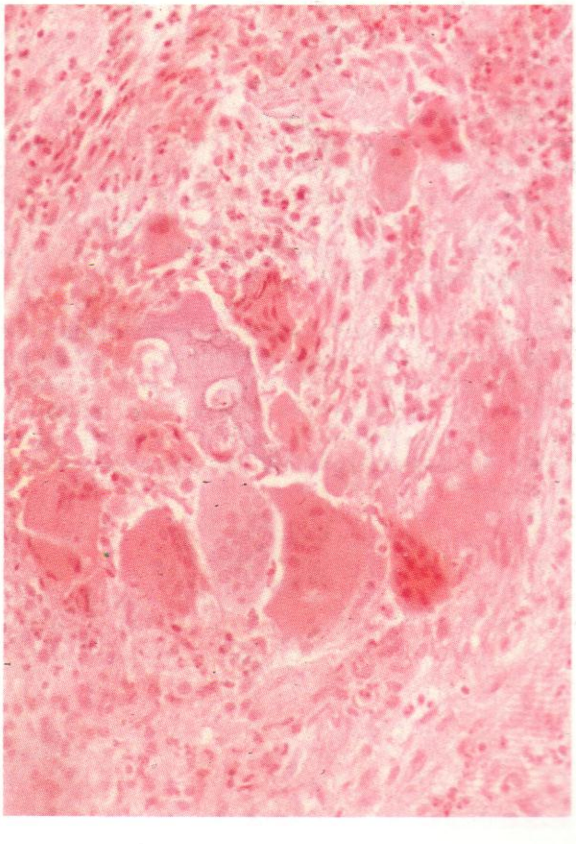

893

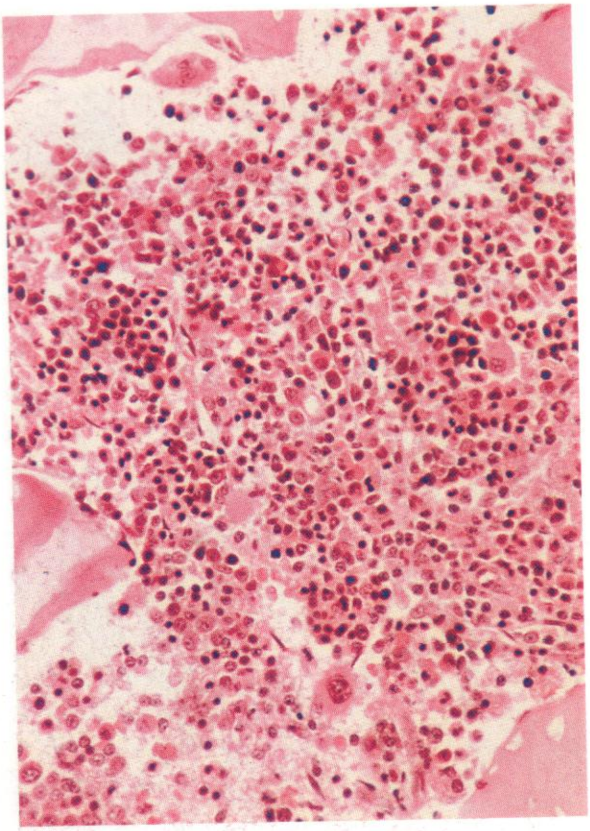

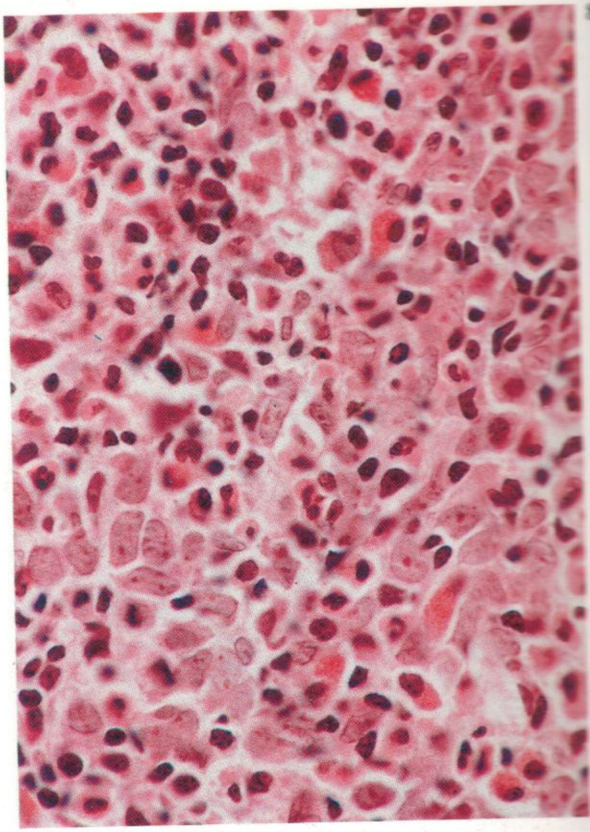

893 and **894**. Low- and higher-power views, respectively, of another example of fibrosing granuloma with eosinophilia in a section of bone marrow trephine biopsy, from a patient with Hodgkin's disease (HD). The granulomas were highly localized in the otherwise normal marrow shown at the lower left part of the field in **893**. The histiocytic proliferation and the eosinophilic reaction are clearly evident in the high-power field of **894**. Granulomas of this sort are not diagnostic of bone marrow involvement – and thus of Stage IV disease – but are suggestive.

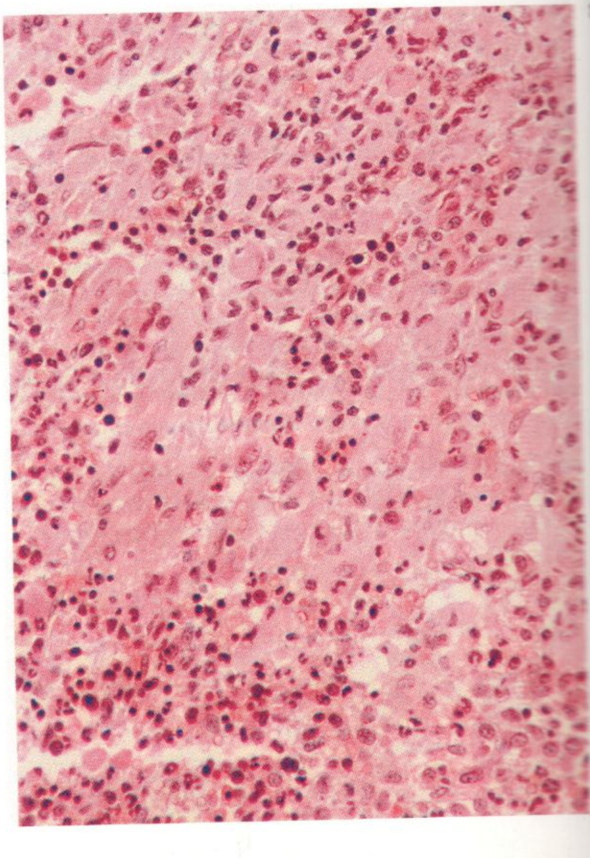

895. Another example of histiocytic proliferation in the bone marrow, with diffuse infiltration throughout the whole section, from a patient with a chronic myelodysplastic state, with refractory anaemia, some increase in blasts and persistent moderately severe thrombocytopenia. The histiocytes appear swollen, with distended cytoplasm.

896

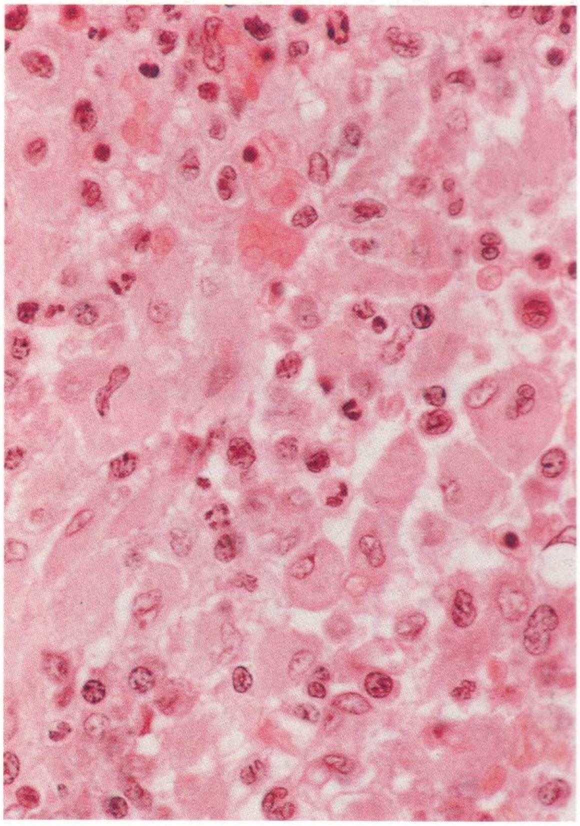

897

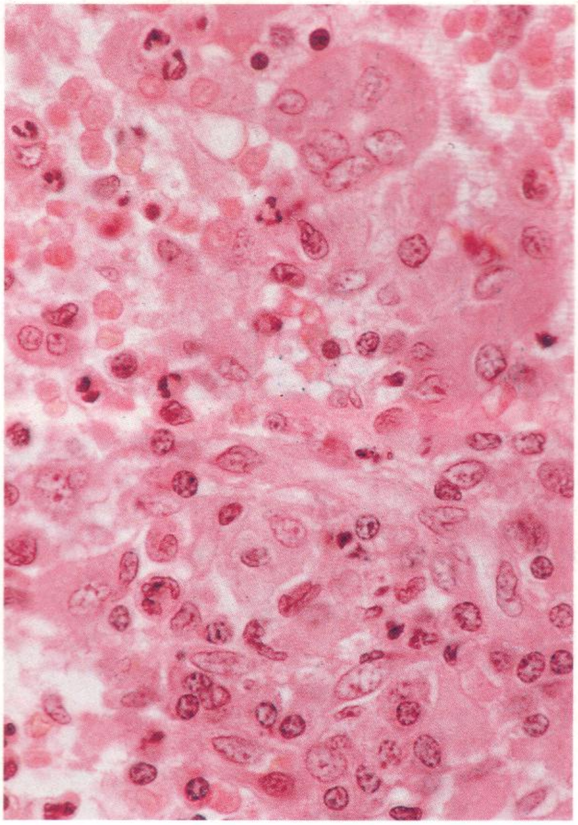

896–898. Further fields from the same trephine biopsy of bone marrow as shown in **895**, with two high-power fields from an H&E stain and one from a Giemsa-stained preparation. The histiocyte cytoplasm here shows some granularity and there is evidence of phagocytic activity, especially in **897**, where there are also several multinucleated histiocytes. In the Giemsa stain a few of the histiocytes show a suggestion of sea-blue inclusion material.

As seen previously, this appearance is not confined to a single specific lysosomal enzyme deficiency as in the main hereditary lipid storage diseases, but appears to occur most often as a manifestation of myelodysplasia and perhaps accompanying increased cell destruction involving especially the granulocyte and thrombocyte lines.

898

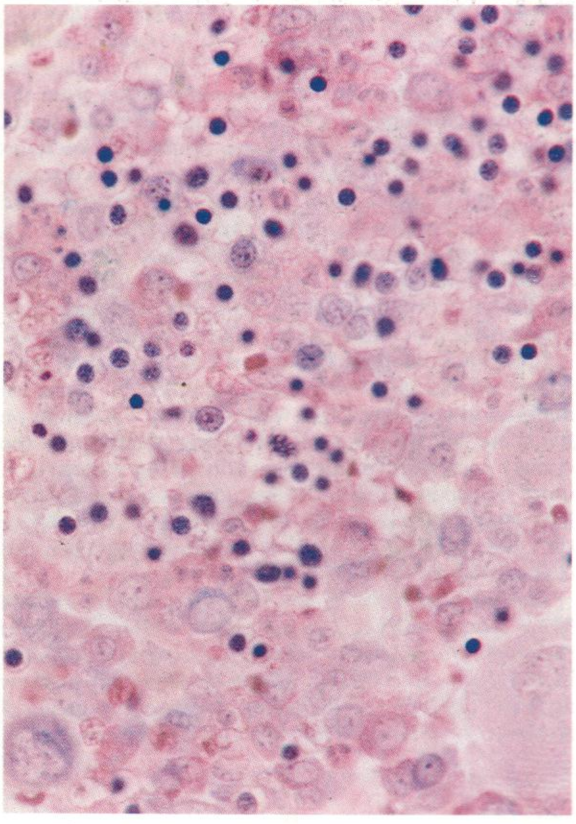

899

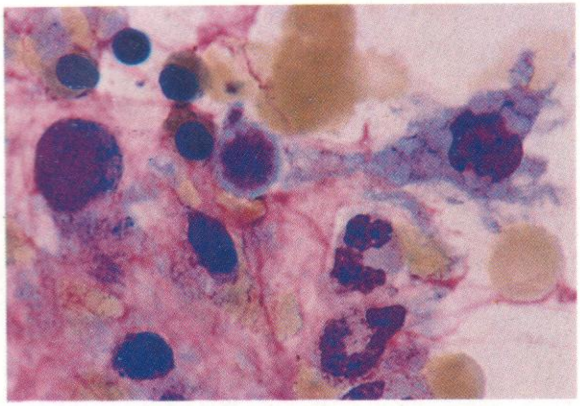

900

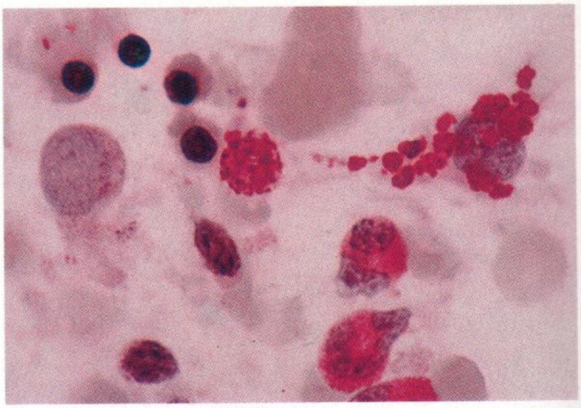

901

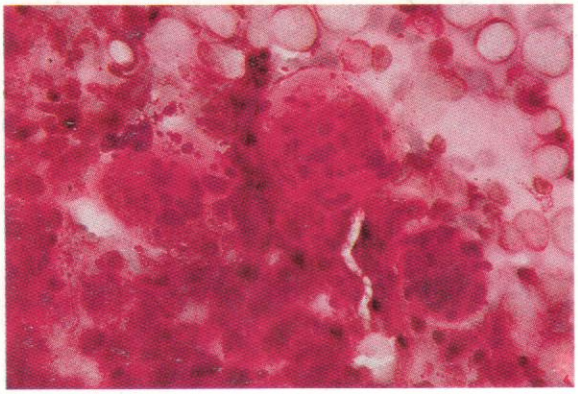

902

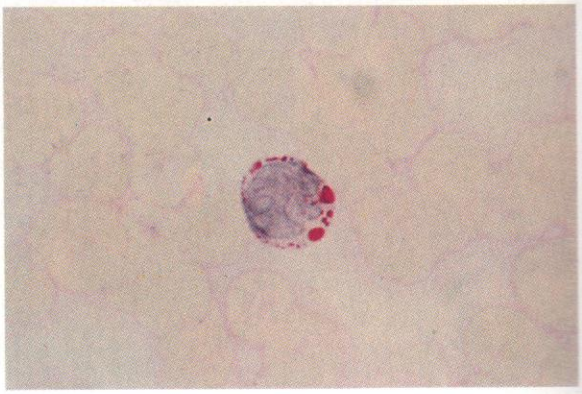

899–904. Smear preparations of bone marrow, and one of buffy coat, from a child with Pompe's disease, glycogen storage disease, type 2. This is another example of a lysosomal storage disease arising from the hereditary deficiency of a single enzyme, in this instance, alpha-1,4-glucosidase. There are commonly vacuoles present in peripheral blood lymphocytes in this disease, but similar vacuoles occur in many other disorders and they are only diagnostically helpful in directing attention to the need for other cytochemical and biochemical investigations and bone marrow studies. In this disease, the PAS reaction gives strong positivity of vacuoles and cytoplasmic granules of a very characteristic kind.

In **899** a Romanowsky stain of a bone marrow fleck shows coarse semi-vacuolated chunks of inclusion material in a macrophage, while in **900** a PAS stain on the same cell reveals typically strong positivity of the chunky inclusions of glycogen-containing material. A more crowded field, including glycogen-laden megakaryocytes, is illustrated in **901**, also a PAS stain, where the megakaryocytes have conspicuous glycogen inclusion bodies.

The lymphocyte with coarse PAS positivity seen in **902** is from a buffy coat preparation, which first raised the possibility of glycogen storage disease as a diagnosis in this case. In **903** and **904**, both from the marrow aspirate, the intensely positive glycogen storage material is shown in a neutrophil polymorph and in an eosinophil.

903

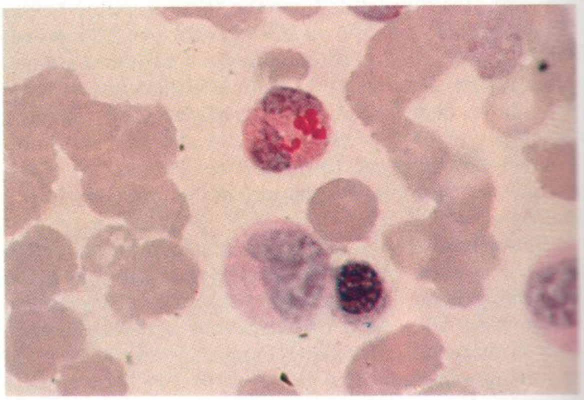

904

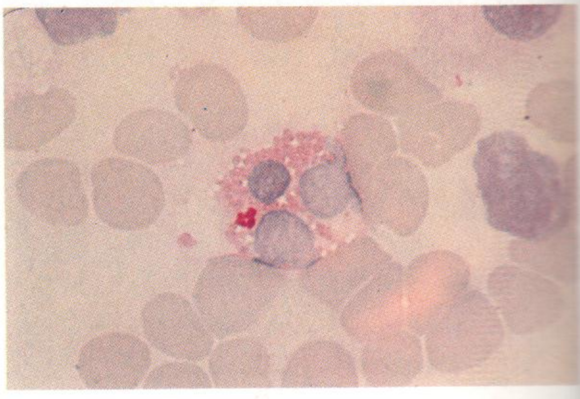

905
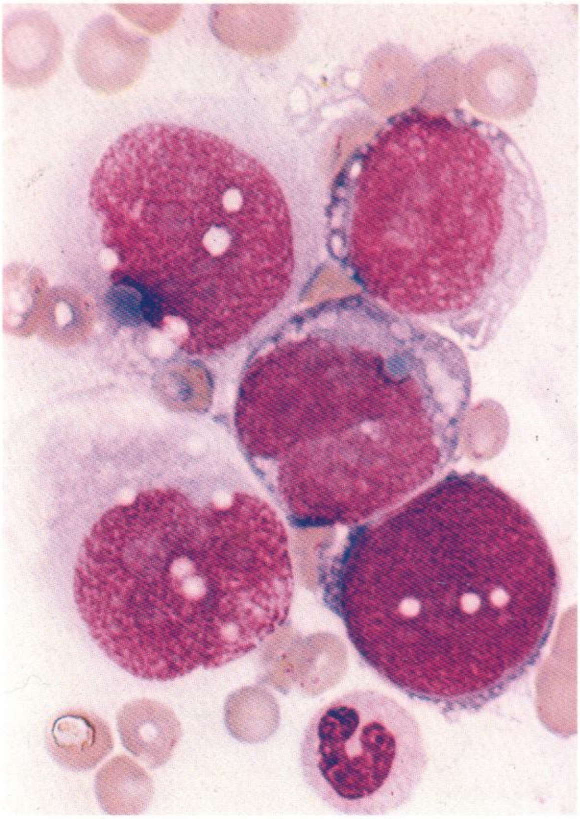

906
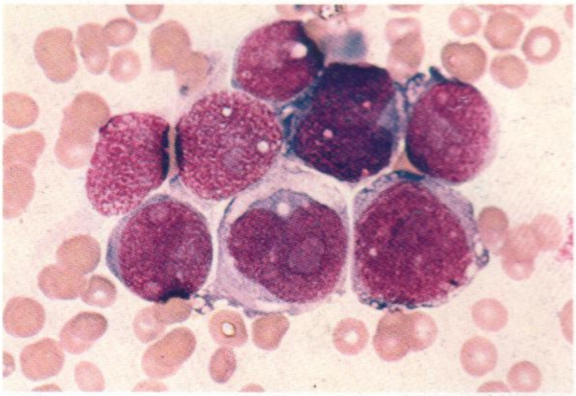

907
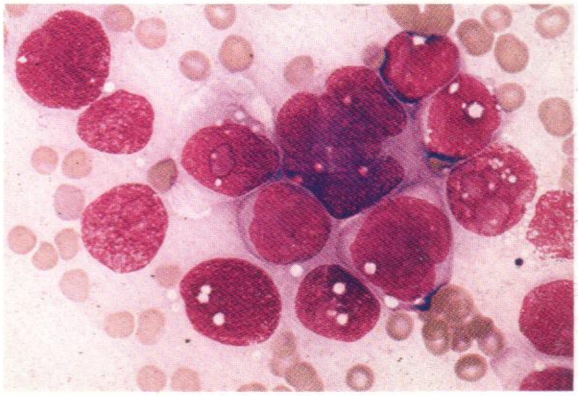

908
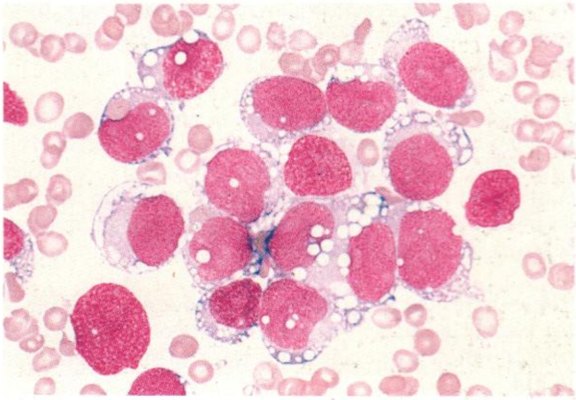

909
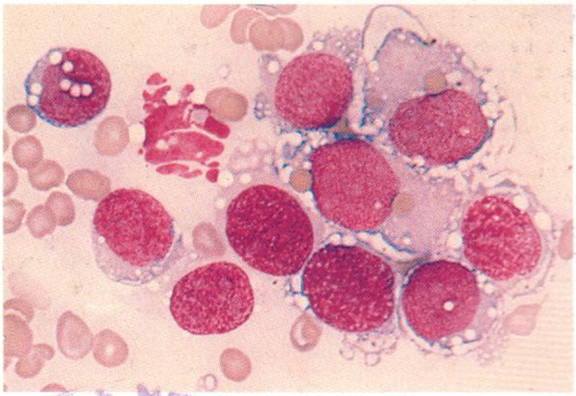

905–921. *Cytology and cytochemistry of bone marrow smears from very uncommon cases of histiocytic leukaemia or leukaemic histiocytosis. The cells involved show many features of activated macrophages, including large size and a marked tendency to spread over the slide surface, very conspicuous formation of cytoplasmic pinocytotic vacuoles and peripheral pseudopodia, with an obvious intense phagocytic activity. Cytochemically, the reactions differ somewhat from those of normal marrow macrophages, with general sudanophobia, unexpectedly strong PAS staining, weak acid and alkaline phosphatases, and almost negative butyrate esterase. These patterns may reflect a neoplastic functional defect or, possibly, enzyme exhaustion following increased phagocytic activity.*

905. Marrow cells from an unusual case of histiocytic leukaemia, showing general cytological similarities to the cells depicted in **891**. Phagocytic inclusions are conspicuous.

906 and **907**. Further fields from the marrow of the same case of histiocytic leukaemia showing cells of primitive cytology, but with scattered vacuoles, occasional multiple nuclei and frequent giant nucleoli.

908 and **909**. Another example of this unusual type of histiocytic leukaemia with blast cells again showing very large size, around 30–40 microns in diameter, irregular and sometimes fragmenting cytoplasmic borders, and coarse vacuolation with occasional erythrophagocytosis.

910

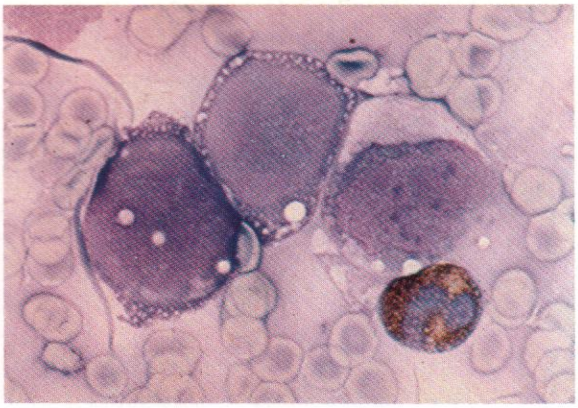

911

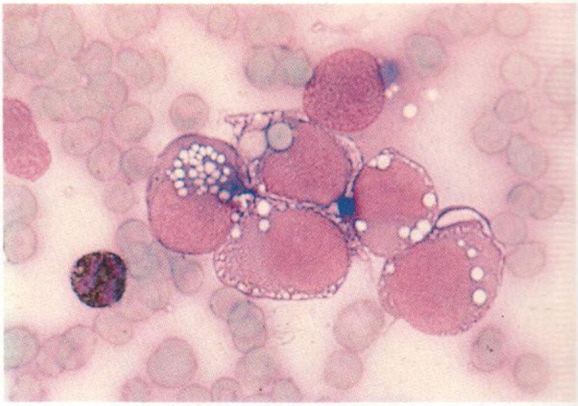

912

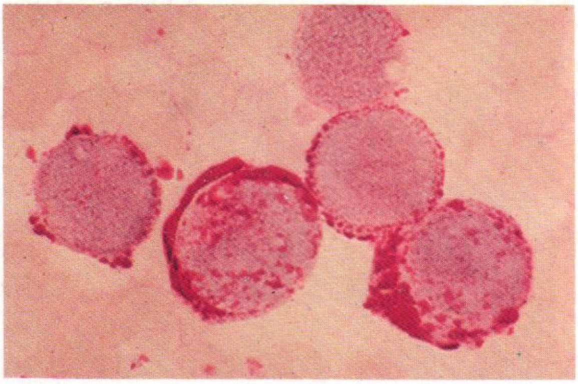

913

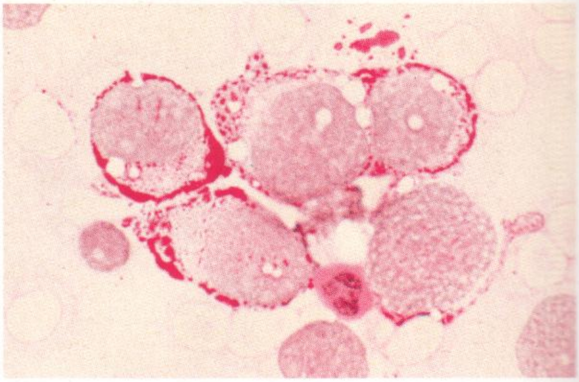

910 and **911**. SB reaction shows these primitive cells to be negative in both cases. There is a positive neutrophil in each of the illustrated fields.

912 and **913**. The PAS reaction shows remarkably strong positivity in virtually every cell in each case. It is clear that many, although not all, of the vacuoles contain glycogen, while the intensity of the stain is emphasized by the relatively weak, though normal, reaction in the neutrophil in **913**.

914 and **915**. Acid phosphatase is moderately strong in the blast cells, scattered over the nucleus, and with local concentration in one cell at the site of an ingested red cell in **914**.

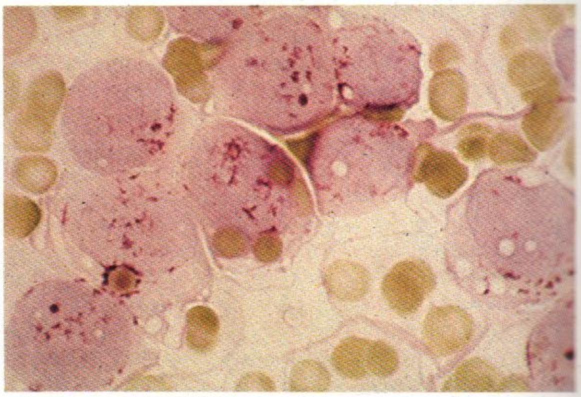

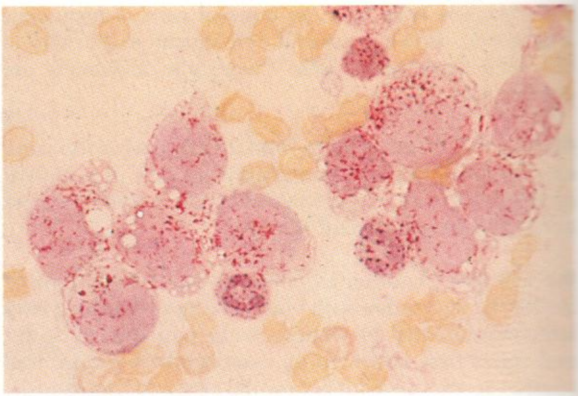

916

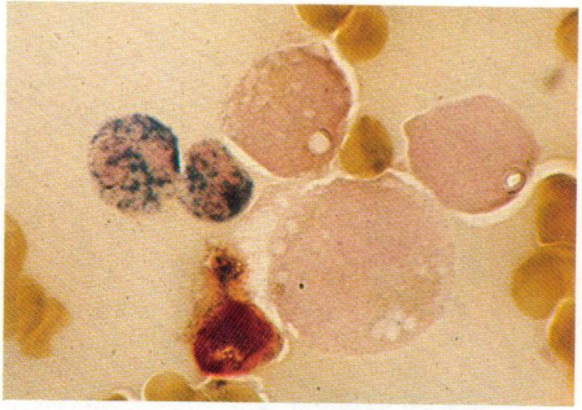

917

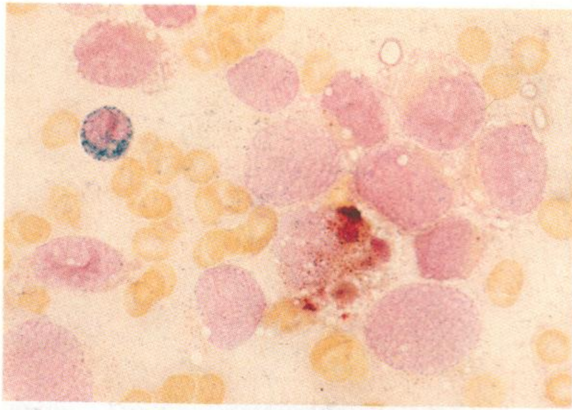

918

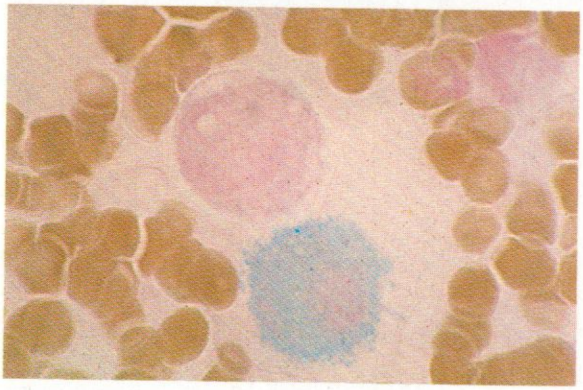

919

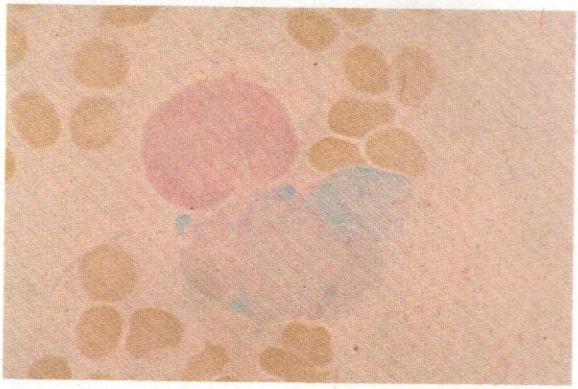

920

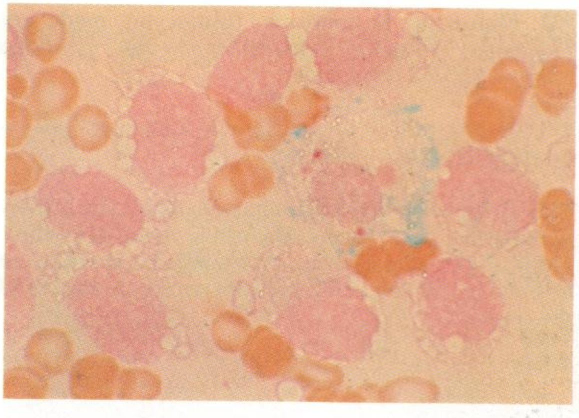

921

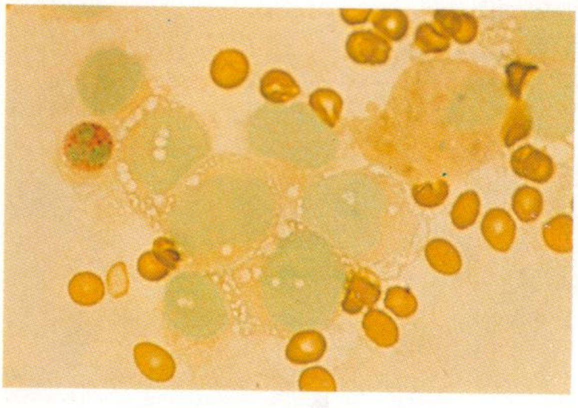

916 and **917**. Dual esterase reaction in smears from each of the two cases of histiocytic leukaemia illustrated on the preceding page. The blast cells are almost entirely negative, with no more than a very weak tinge of butyrate esterase (BE) positivity and a few fine chloro-acetate esterase (CE) granules in **916**. Both fields contain normally reacting CE-positive neutrophils and BE-positive macrophages.

918–920. Free-iron stains showing a positive reaction in some of the primitive histiocytic cells. The positivity is likely to be the result of ingested erythroid cells, and it is noteworthy that the single Fe-positive blast cell among eight which are negative in **920** also contains other cellular debris and has clearly been especially active in phagocytosis.

921. Alkaline phosphatase cytochemistry on a bone marrow smear from the second of the two cases shows a weak tinge of positivity in seven blast cells, a considerably stronger reaction in an eighth, and a neutrophil polymorph with moderate cytoplasmic reaction. Again, the obvious phagocytic activity of the more strongly positive blast cell makes it seem likely that at least part of the alkaline phosphatase activity shown in the histiocytic blast cells is secondary to ingestion of positive neutrophil cytoplasm, although part may be native to these unusual leukaemic cells.

922

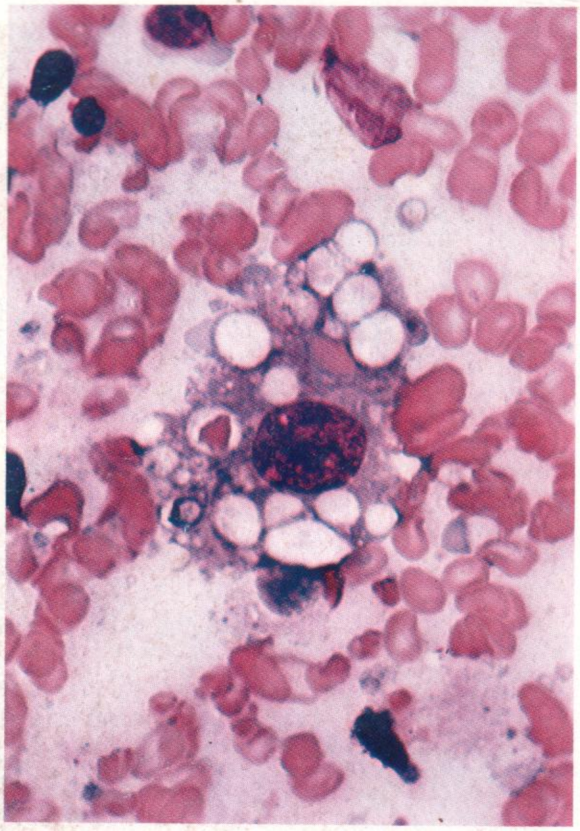

923

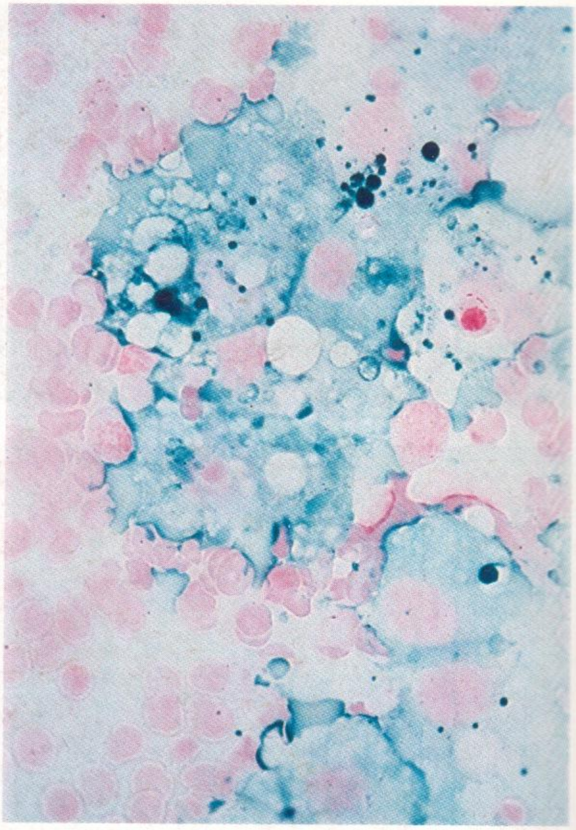

924

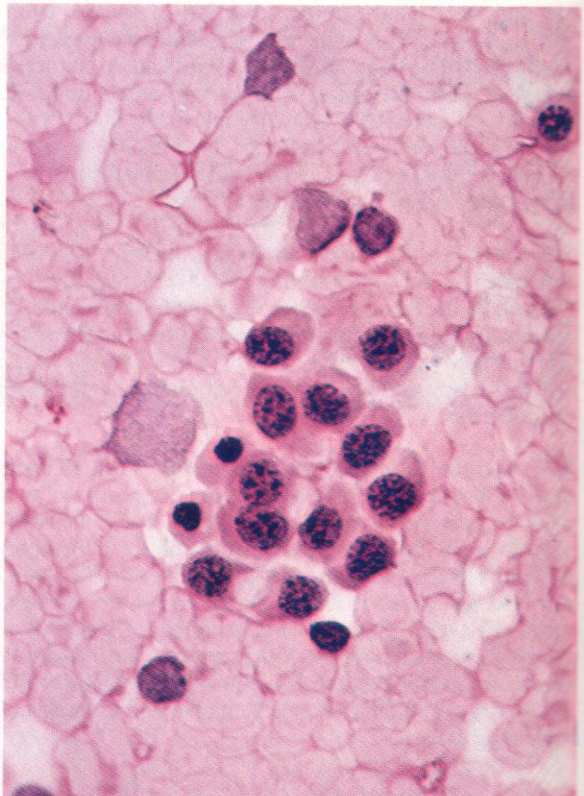

922. Malignant histiocytosis (histiocytic medullary reticulosis) showing erythrophagocytosis by bone marrow RE cell (histiocyte).

923. A free-iron stain on similar malignant phagocytosing RE cells.

924. A further example of increased phagocytic activity in malignant histiocytosis. The whole clump of erythroblasts, showing faint diffuse PAS positivity, is within the cytoplasm of a spread RE cell with nucleus to the left of the clump.

925

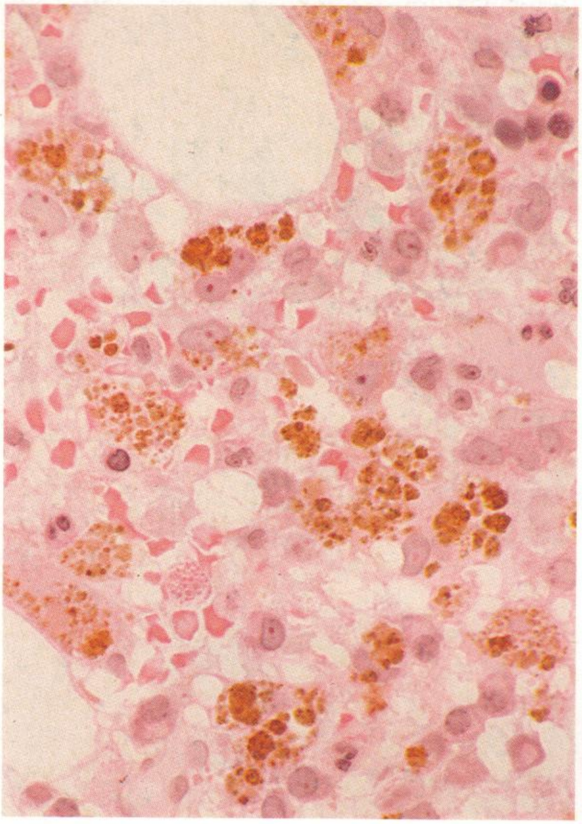

926

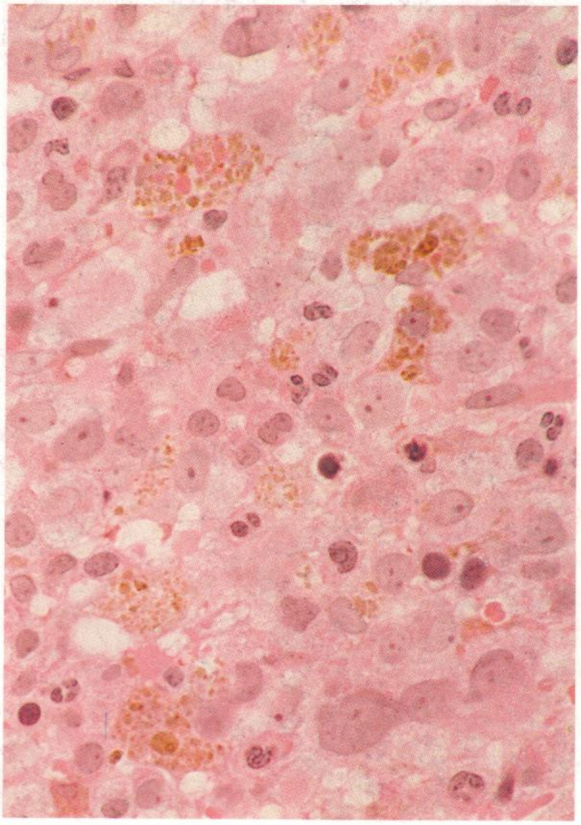

927

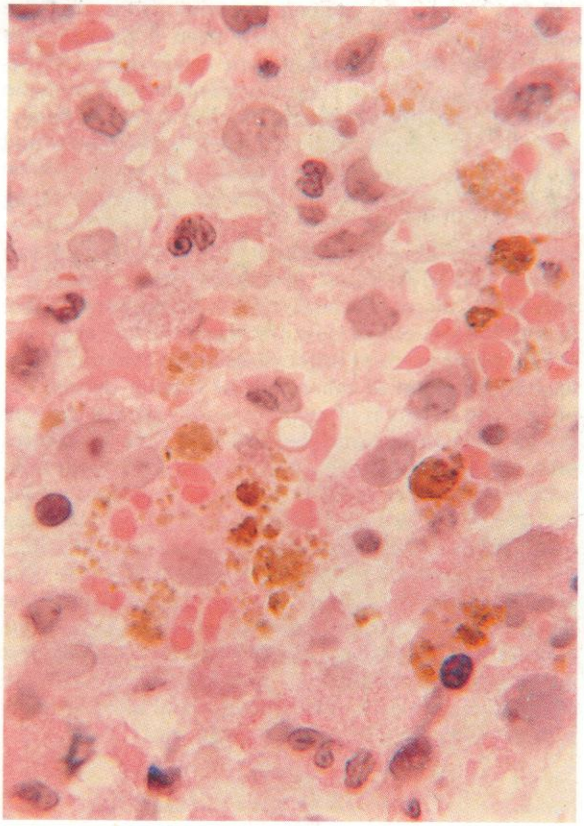

925–927. A series of fields at generally high magnifications, from thin sections of plastic-embedded trephine biopsy material from another patient with malignant histiocytosis. In **925** the extensive accumulation of haemosiderin in many histiocytes is especially noticeable; in the field chosen in **926**, there are again many haemosiderin-laden histiocytes, but the very considerable infiltrate of primitive monocyte–macrophage histiocytes, with palely staining leptochromatic nuclei and conspicuous nucleoli, is also even more clearly evident than in **925**. All these features are visible in the still higher-power view of **927**, where there is also an exceptionally dramatic example of multiple phagocytosis of red cells. Malignant histiocytosis may sometimes be difficult to differentiate from virus-associated haemophagocytic syndrome (**928–939**), especially when, as in the present case, there is extensive haemophagocytosis by more mature histiocytes, either derived from less differentiated precursors or perhaps developing as a reactive component, but the presence of numerous primitive cells strongly suggests the former malignant state.

928

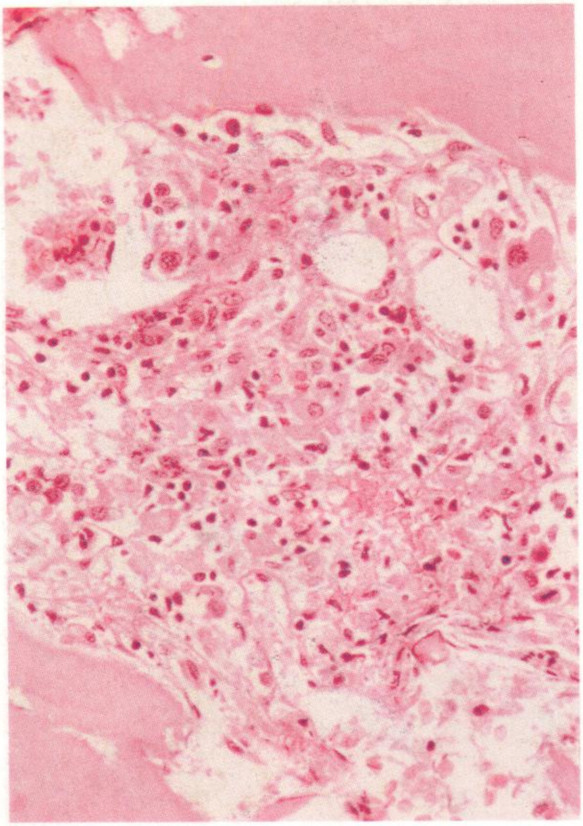

929

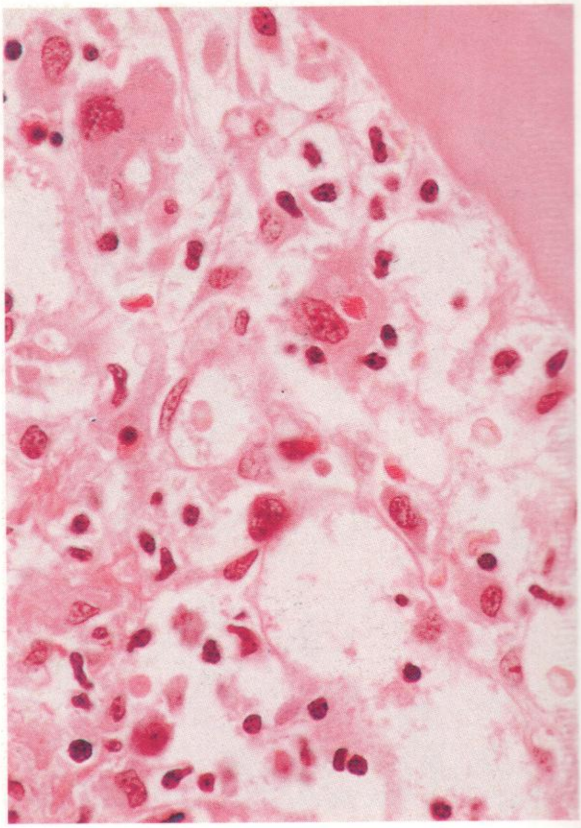

930

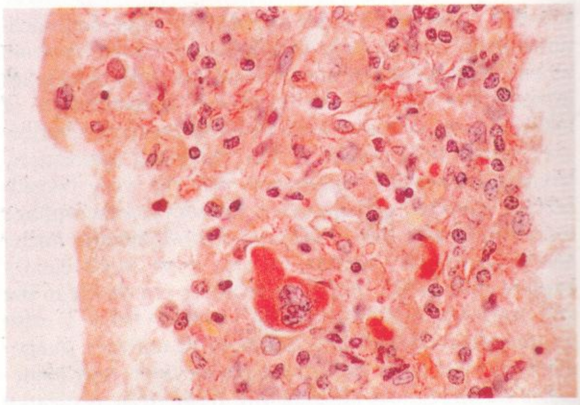

931

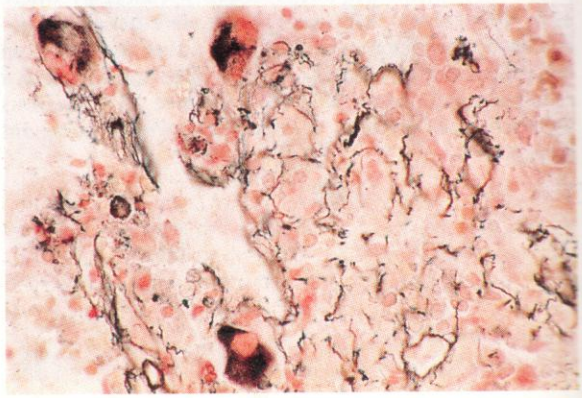

928–931. Variously stained sections from a bone marrow trephine biopsy, taken from a patient with virus associated haemophagocytic syndrome (VAHS). In such patients, there is usually an underlying immune deficiency, and the peripheral blood often shows pancytopenia, sometimes with activated lymphocytes and monocyte-macrophages detectable. The bone marrow varies in cellularity, some decrease commonly being found, as in this specimen, with a reactive increase in reticulin and fibroblastic activity (illustrated in the van Gieson and silver stains of **930** and **931**). There is a widespread increase in histiocytes in the sections, visible in both the low-power view of **928** and the higher-power of **929**, where erythrophagocytosis is also evident. There may be ingestion of other cells or cellular debris, but phagocytic activity is often more readily seen in aspirate smears than in sections (*see* **932–939**). The histiocytes are of generally mature cytology in VAHS, with non-nucleolated nuclei and low nuclear–cytoplasmic ratios, and are to be distinguished from those of malignant histiocytosis, which frequently show nucleoli and high nuclear–cytoplasmic ratios, as in **925–927** above. The distinction may not be easy, however, especially in bone marrow samples, since the more primitive cells of the neoplastic histiocytosis, though generally much less actively phagocytic than the histiocytes of VAHS, are often accompanied by more mature and more strongly phagocytic derived or reactive histiocytes.

932

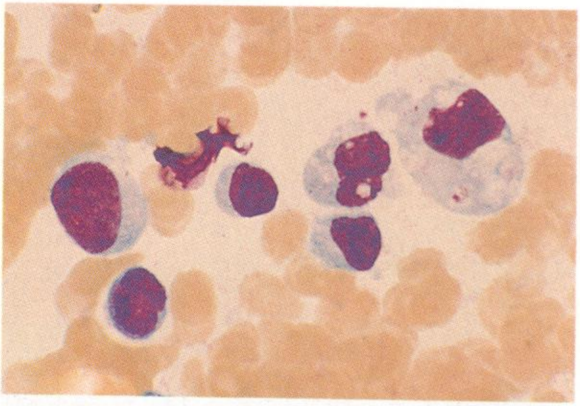

933

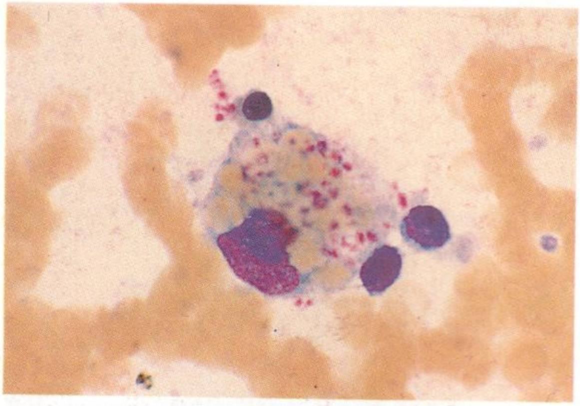

934

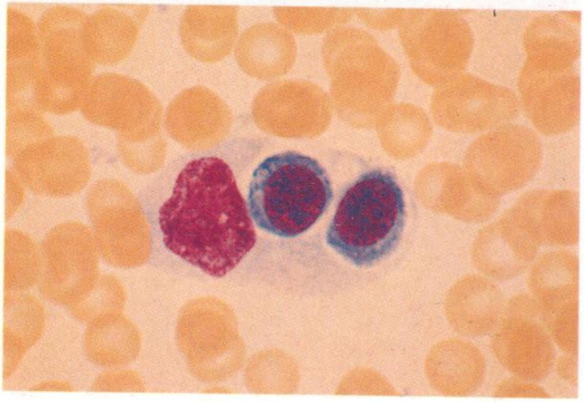

935

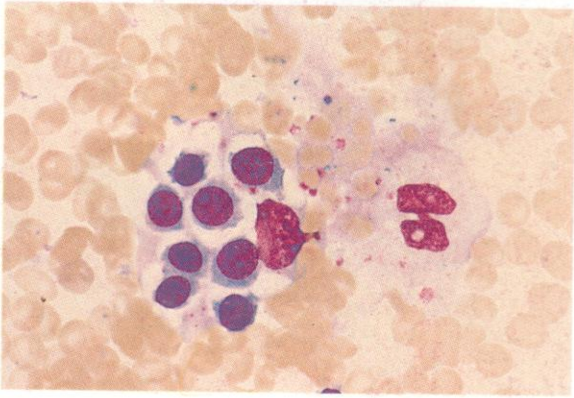

932–935. Examples of reactive lymphocytes and monocytes, and macrophagic phagocytic activity, in Romanowsky-stained smears of bone marrow aspirate from another patient with VAHS and marked peripheral pancytopenia. Various lymphocytes are seen in **932**, that on the left showing activation changes; to the right are two monocytes with progressive transformational change towards macrophages, showing pinocytic vacuoles and ingestion of platelets. In **933** the macrophage contains many ingested red cells and platelets, while the macrophages in **934** and **935** show phagocytosis of two early normoblasts and eight later normoblasts, respectively.

This type of gross and indiscriminate phagocytic activity is more often seen in VAHS than in malignant histiocytosis.

936

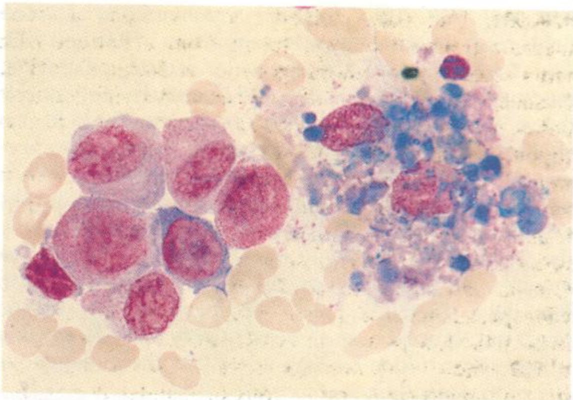

937

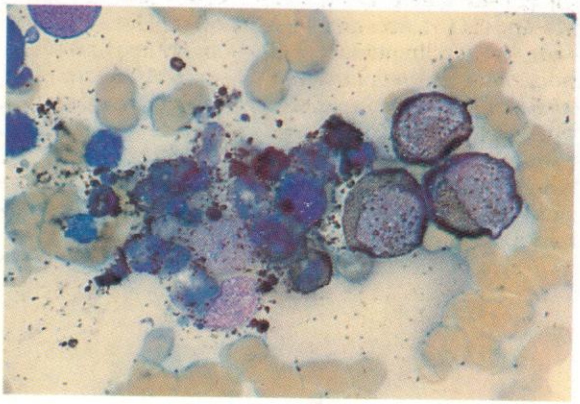

936 and **937**. Further illustrations of massive phagocytosis by marrow macrophages in a patient with refractory anaemia with excess blasts (RAEB) and immune suppression secondary to chemotherapy, later developing VAHS following an opportunistic viral infection. The Romanowsky stain in **936** shows a cell with gross accumulation of granulocyte debris, including dark-staining nuclear remnants and both neutrophil and eosinophil granules. To the left are several somewhat dysplastic myelocytes, a lymphocyte and an early erythroblast. In **937** the SB stain on a similar cell group reveals the strong sudanophilia of the ingested polymorph granules.

938

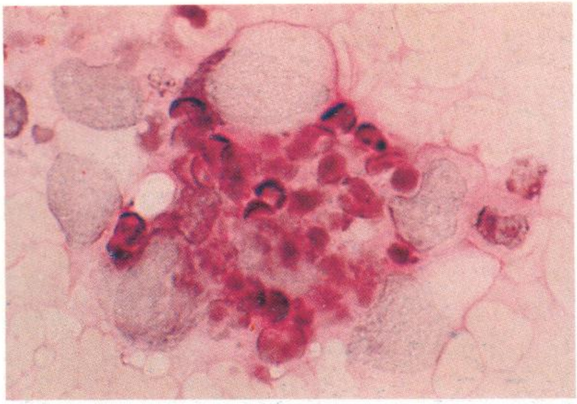

939

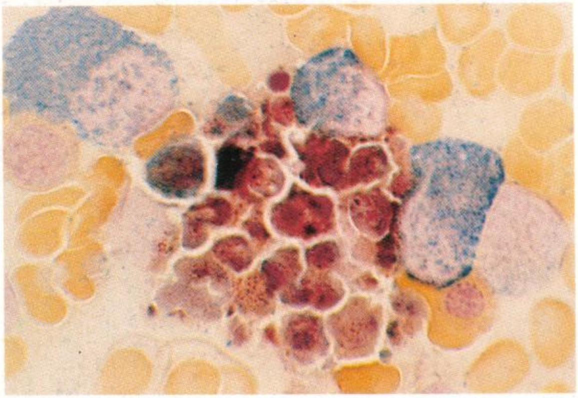

940

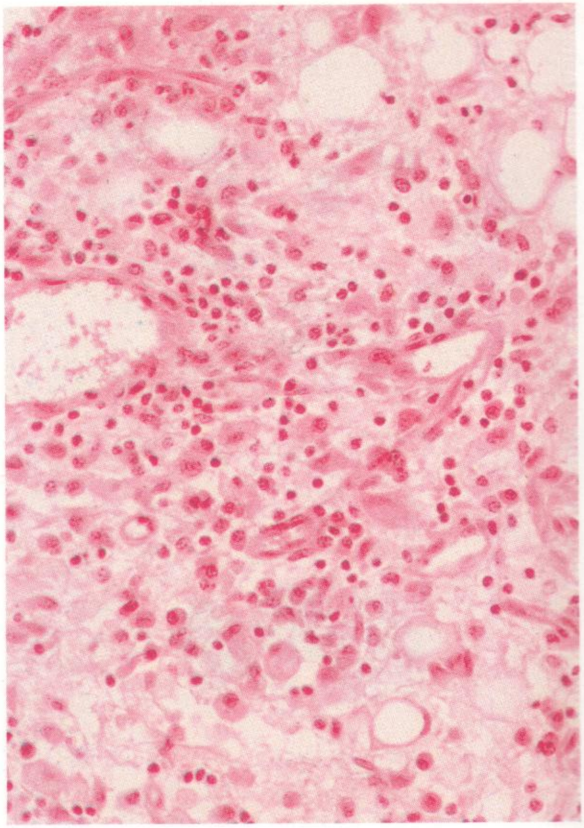

941

938 and **939**. Two further cytochemically stained fields from the same marrow aspirate as in **936** and **937**. The PAS stain in **938** shows a central phagocytic macrophage, again with predominantly polymorph debris having the expected PAS positivity. The field also contains several early, PAS-negative, granulocyte precursors. The dual esterase reaction shown in **939** is unusual, in that the mass of ingested polymorphs appears predominantly BE-positive rather than having the normal CE positivity shown by granulocytes, as manifest for example in the neighbouring myelocytes in this field. Some residual CE reaction can still be made out, however, and it seems likely that this enzyme is being overridden by high activity of the endogenous BE of the engulfing macrophage.

940 and **941**. Low- and higher-power fields, respectively, from a trephine biopsy of bone marrow taken from the same patient at a later stage of disease. The specimen now shows an oedematous marrow stroma with proliferation of fibroblasts and development of fibrosis, perhaps secondary to the earlier chemotherapy, but also with persistent mature cell histiocytic increase and the emergence of some lymphoplasmacytoid reaction to the continuing intractable viral infection.

942

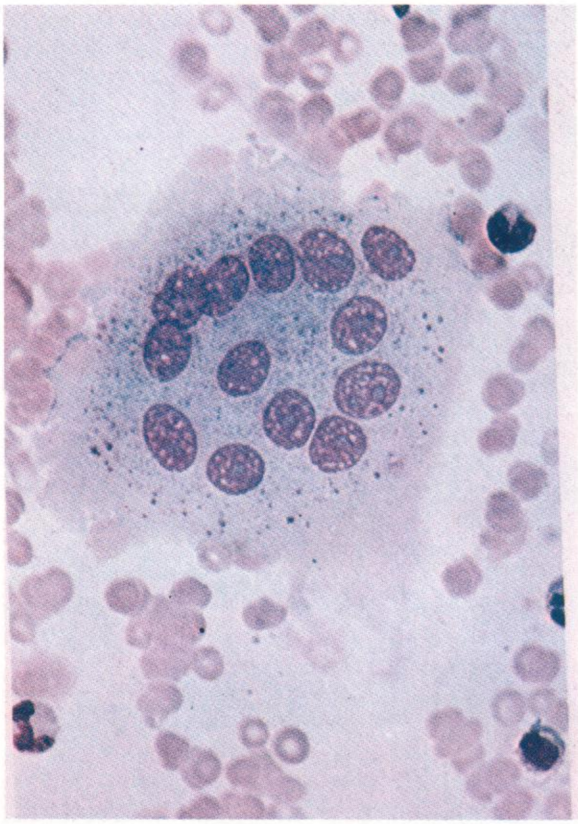

943

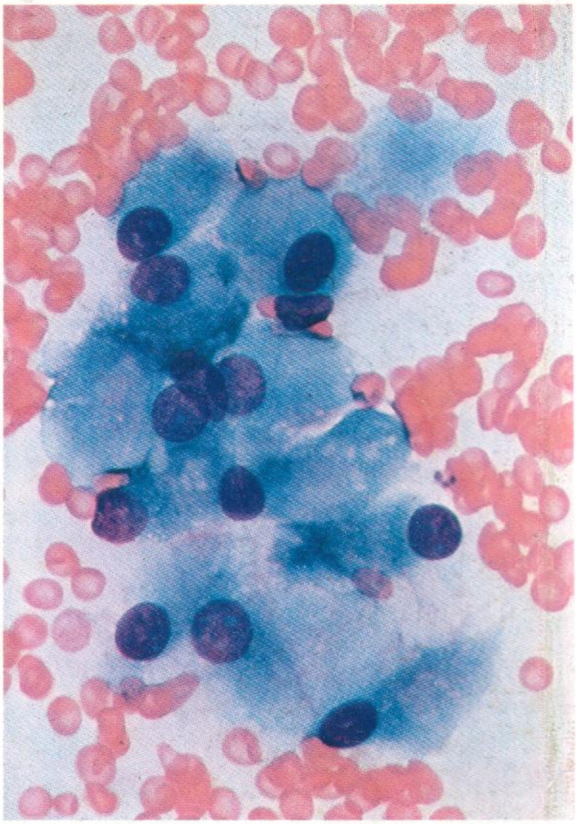

944

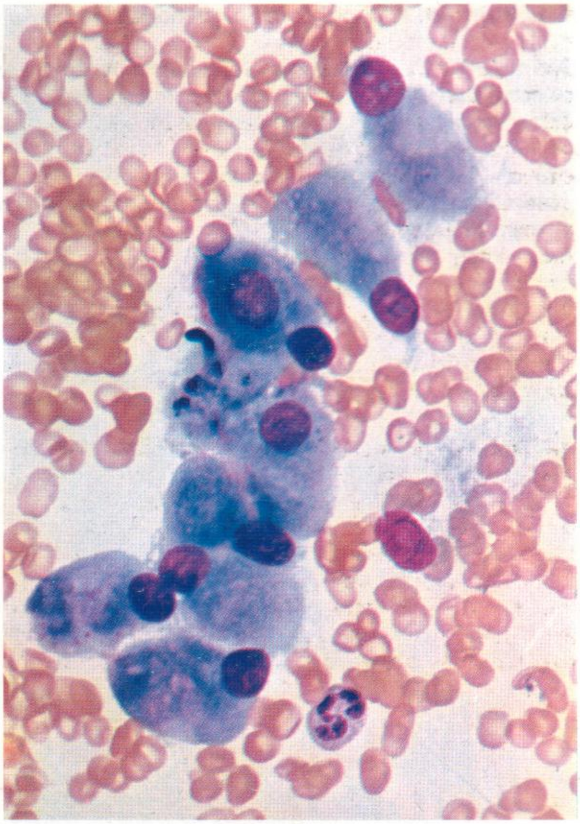

942. An osteoclast from a smear of normal bone marrow. The multiple, discrete, round or oval nuclei, with their single conspicuous nucleoli, and the pale blue, lightly granular cytoplasm are characteristic and prevent confusion with megakaryocytes.

943. A group of osteoblasts, from a smear of normal bone marrow. They have a superficial resemblance to plasma cells, but are larger, do not show the heavy, 'clock-face', nuclear chromatin disposition seen in mature plasma cells, yet have a low nuclear–cytoplasmic ratio, with abundant, rather pale and filmy cytoplasm.

944. A further group of osteoblasts, whose large size is emphasized by the neighbouring segmented neutrophil.

945

946

947

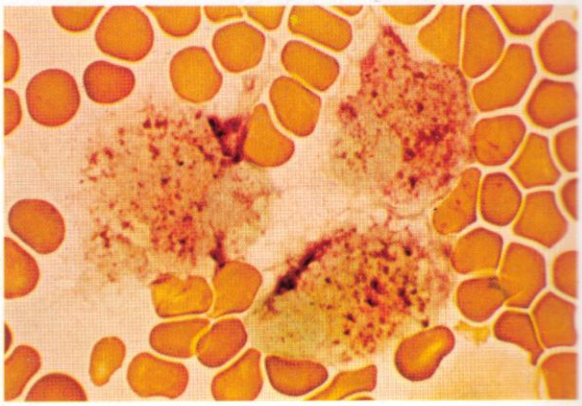

948

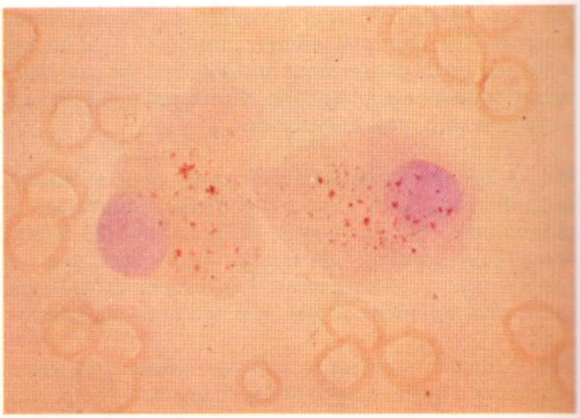

949

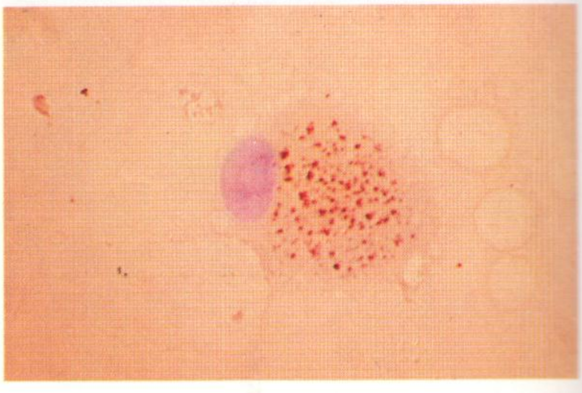

945. Scattered PAS positivity in osteoblasts.

946 and **947**. Strong positivity for alkaline phosphatase in osteoblasts. This provides another differential point from plasma cells, which are negative for this enzyme.

948 and **949**. Weak-to-moderate positivity for acid phosphatase in osteoblasts. This reaction is much stronger in plasma cells.

950

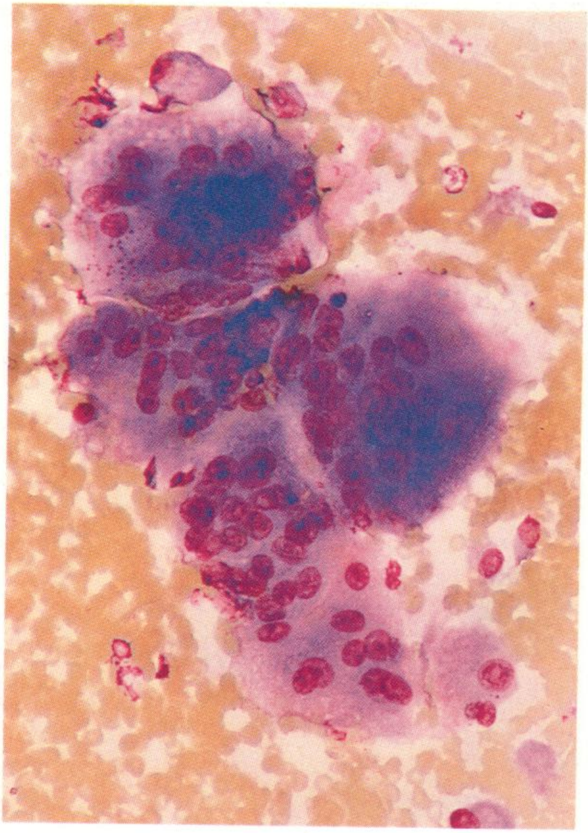

951

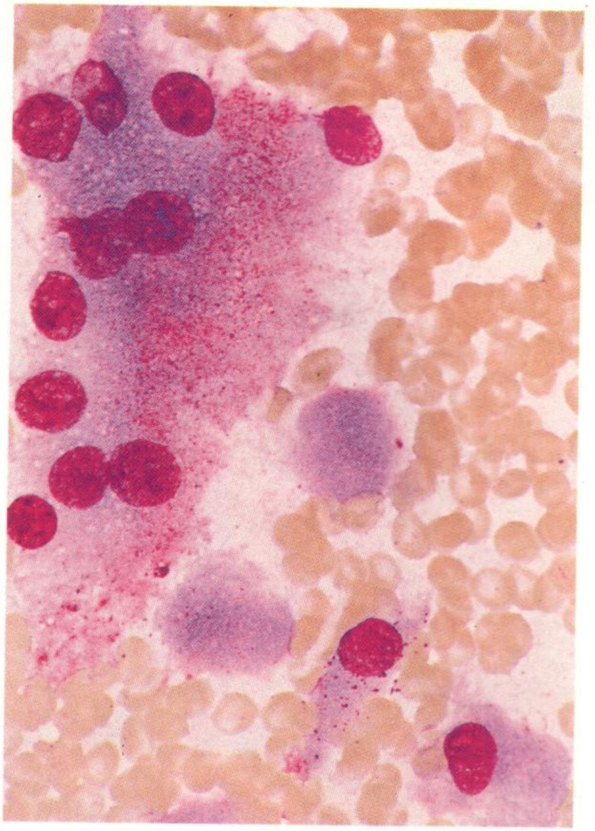

950–952. Low-, intermediate and high-power views, respectively, of mixed osteoblasts and osteoclasts, the former mononucleated and the latter multinucleated, from an otherwise poorly cellular marrow aspirate taken from a patient with Paget's disease. The detailed cytology of the bone remodelling cells can be seen here. There is a similarity between them, especially when the osteoblasts occur in clusters and form syncytia, as they are prone to do when they are very actively proliferating, as in Paget's disease. This appearance is revealed in the predominantly osteoblastic field of **950**. Osteoclasts generally show a lighter blue cytoplasm, with many conspicuous, fine to moderately coarse, red granules; the osteoclast nuclei tend to form a circle or hoop around the periphery of the cell, as seen already in **942** and again in **951**, in contrast to the overlapping nuclei, the more blue than red cytoplasmic granularity, and the frequent separation of mononuclear satellite cells manifest by syncytial osteoblasts as shown in **952**.

952

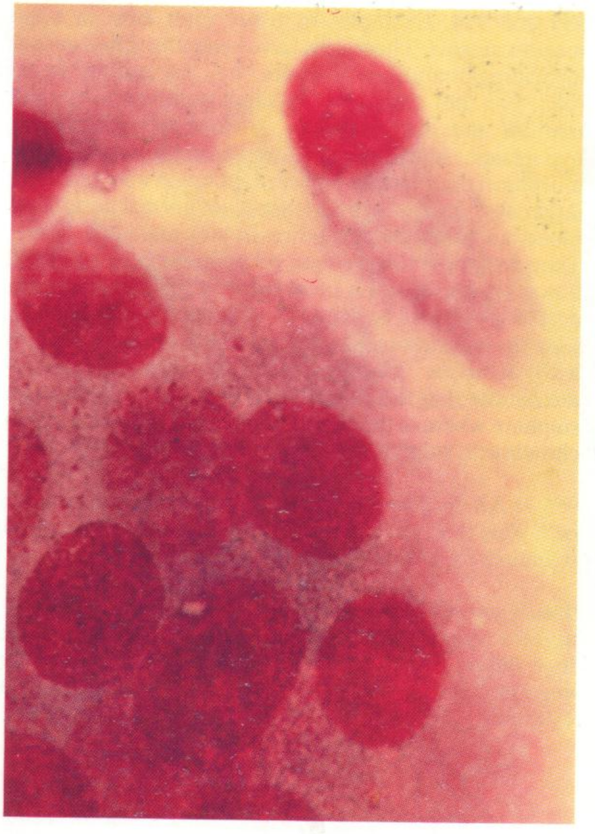

953

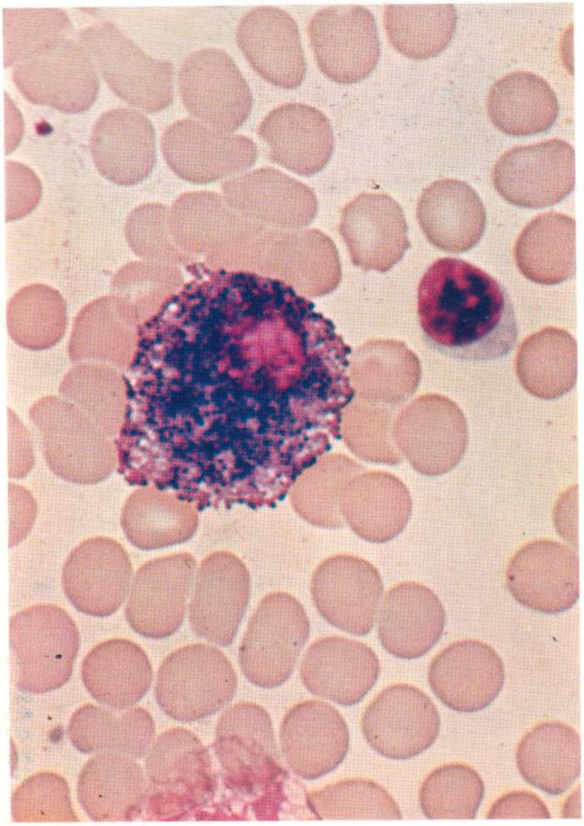

954

953 and **954**. Examples of tissue mast cells in bone marrow smears. These cells have been illustrated earlier in macroglobulinaemia, where they are usually to be seen, but they also occur in small numbers in normal marrow and may show an increase in aplastic and hypoplastic states. They differ from basophil polymorphs in their lack of nuclear lobulation and generally larger size, and in their absence from normal peripheral blood and frequent presence in subcutaneous tissue. They do appear to have their origin in the bone marrow, however, and may be involved in a malignant mastocytosis which may be frankly leukaemic. Like basophils, they show the metachromatic staining of their granules with toluidine blue produced by acid mucopolysaccharides, but this reflects their high content of heparin sulphate whereas the basophil reaction is due chiefly to chondroitin sulphate.

955

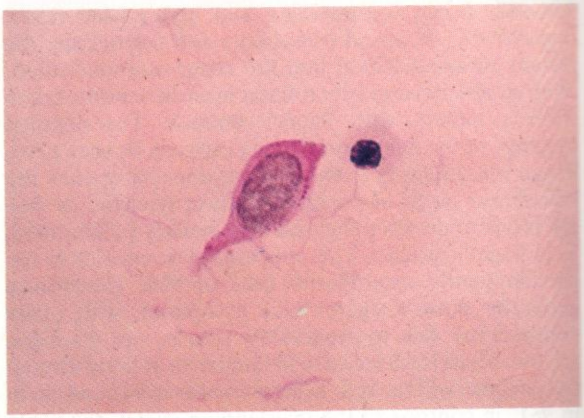

955. PAS reaction shows strong positivity in a mast cell. This reaction generally resembles that of basophil polymorphs, although it is less coarsely granular.

956

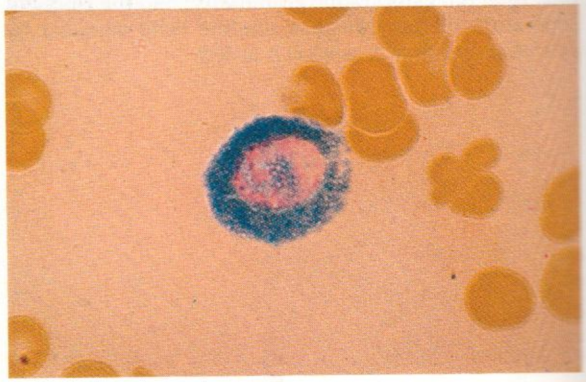

956. Dual esterase reaction showing strong chloroacetate esterase positivity in a mast cell. The reaction here differs from that of basophils, which is essentially negative for all the cytochemically demonstrable esterases.

957

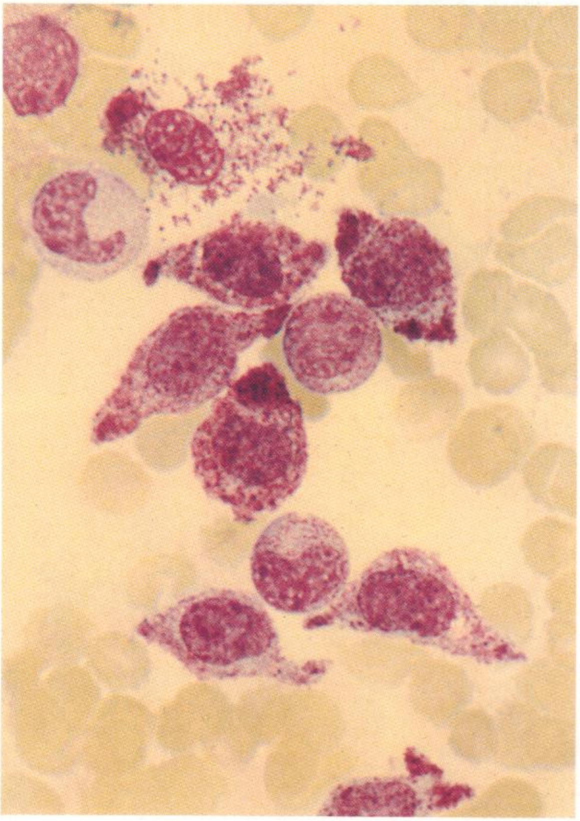

958

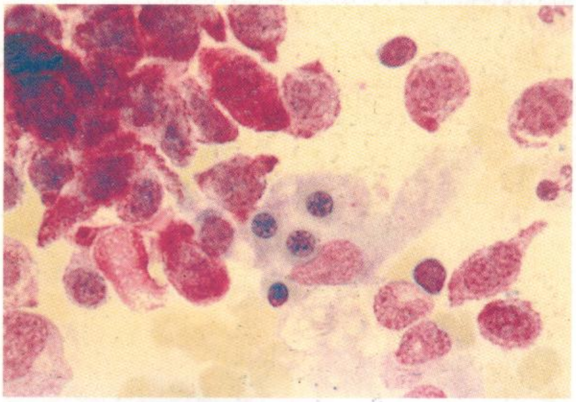

959

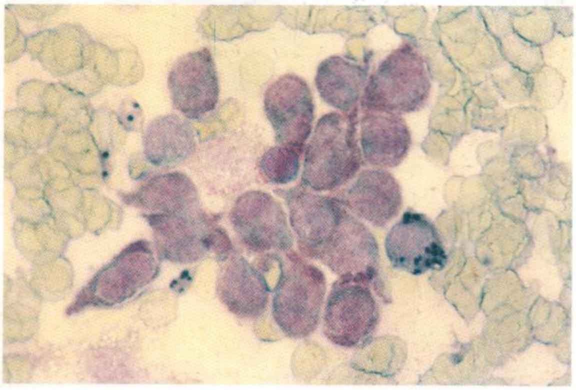

960

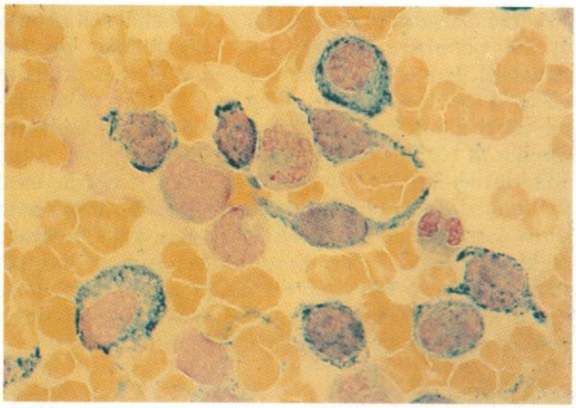

961

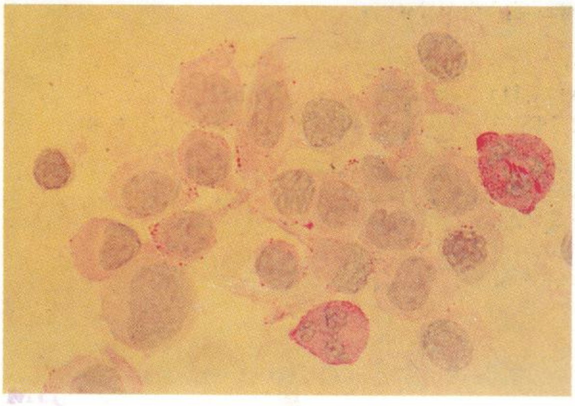

957–961. Cytology and cytochemistry of bone marrow aspirate preparations from a patient with mast cell leukaemia. As can be seen in these illustrations, the neoplastic mast cells tend to have relatively higher nuclear–cytoplasmic ratio than normal mast cells, with often less dense granularity and a patchy disposition of granules. The nucleus is usually round, but may show a degree of indentation, as in some cells in **959** and **961**, while the cytoplasmic outline may be elongated and even spindle-shaped, as in **957** and **960**. There is a particular tendency for malignant mast cells to occur in clumps and in marrow flecks, where they may be mixed with fibroblasts, erythroblasts, megakaryocytes and granulocytes, and may be difficult to recognize except at the edges, as in **958**. The cells may show a metachromatic staining reaction not only with toluidine blue but also with SB, as seen in **959**, where the dark red colour of the mast cell granules contrasts with the black stain of the neutrophil myelocyte at the right and of a few scattered neutrophil granules. The dual esterase reaction of **960** shows strong CE positivity, while the PAS reaction in **961** reveals a weak tinge of positivity in most mast cells, with peripheral granular positivity in many.

Of all the cytochemical reactions, the most helpful in distinguishing neoplastic mast cells from the basophils they may resemble is the esterase reaction, where mast cells are strongly positive for chloroacetate (and also aminocaproate) esterase, for which basophils are negative.

962

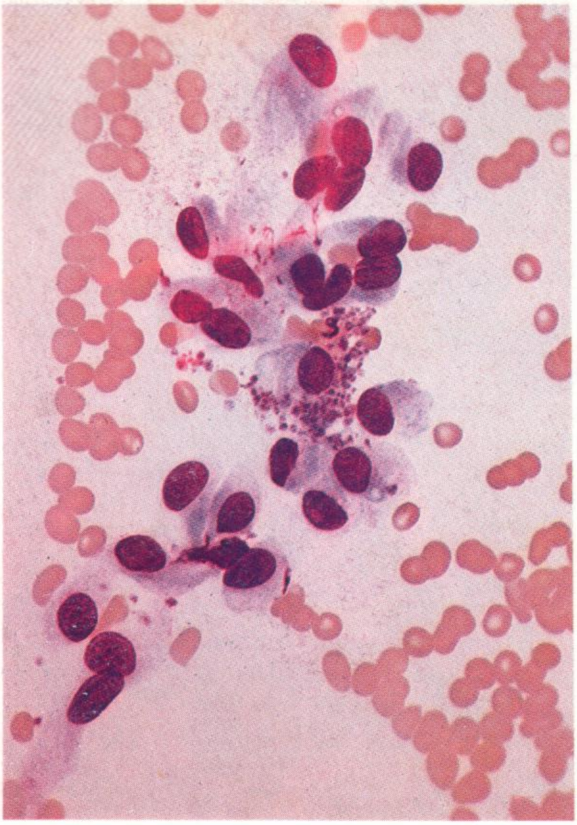

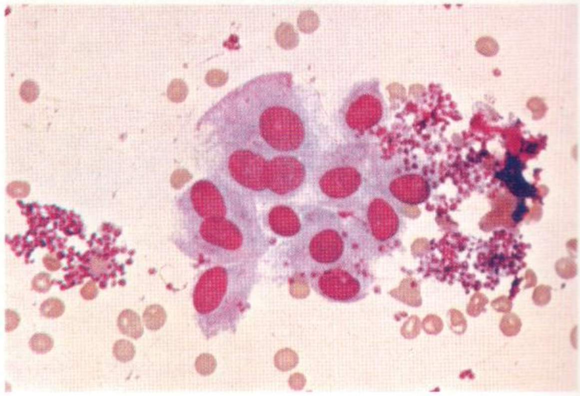

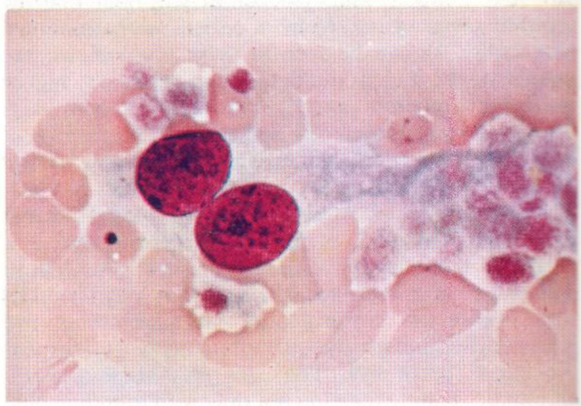

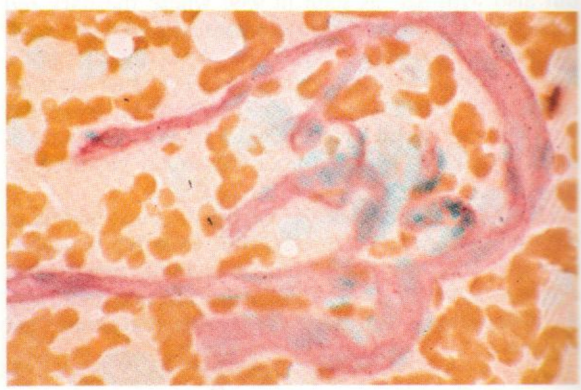

962–966. Examples of vascular endothelial cell clumps in the peripheral blood. The very regular nuclear structure and size and the tendency for these cells to occur in sheets or streaks along the direction of spreading of the film assist in recognition. These cells are foreign to blood, and are lifted from the intima of the vein during insertion or withdrawal of the needle used for collecting the blood sample. The nuclei in **965** both show conspicuous Barr bodies, indicating the presence of the inactive X-chromosomal material of normal female cells. In **966** can be seen alkaline phosphatase positivity in a strand of vascular endothelium, crossing a field of negative immature marrow cells.

57

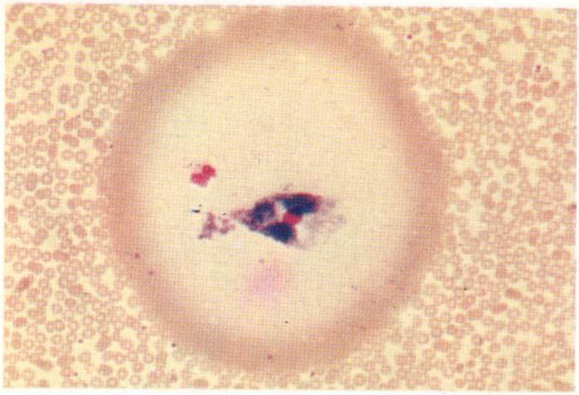

8

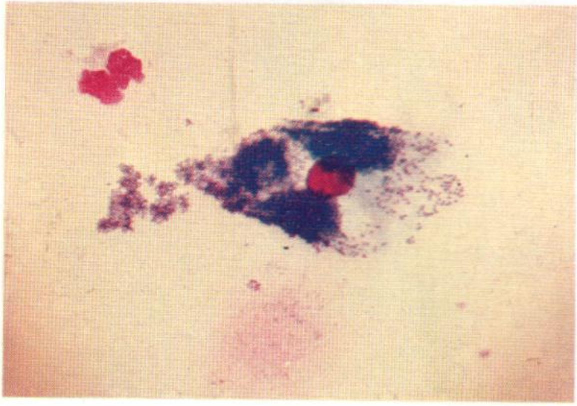

969

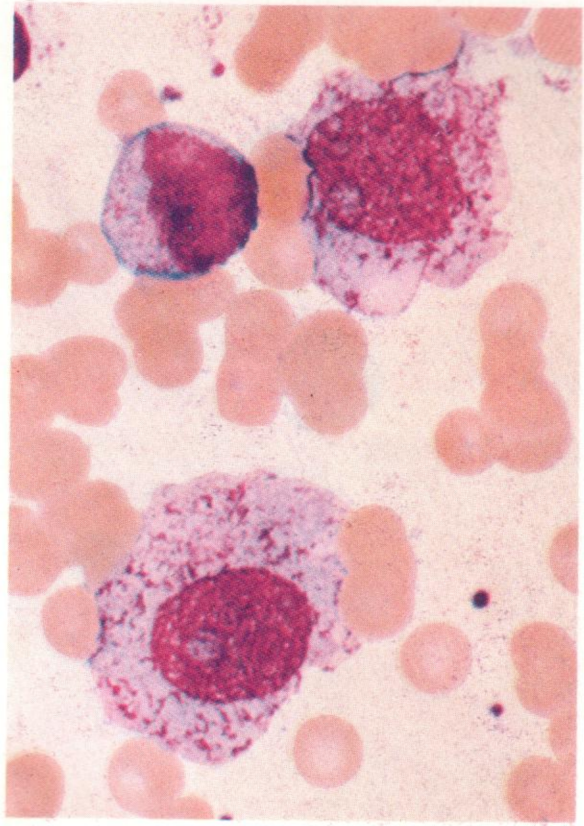

967. Droplet contamination. An artefact produced by coughing over an unfixed blood smear before staining.

968. A higher magnification reveals a cell from the buccal mucosa, with heavy bacterial contamination.

969. One intact promyelocyte and two flattened and partially disrupted promyelocytes, showing exaggerated nucleoli and open nuclear network. This appearance has been known as a 'Ferrata' stage of degeneration.

970. Two buccal mucosal cells with contained bacteria in a bone marrow smear.

970

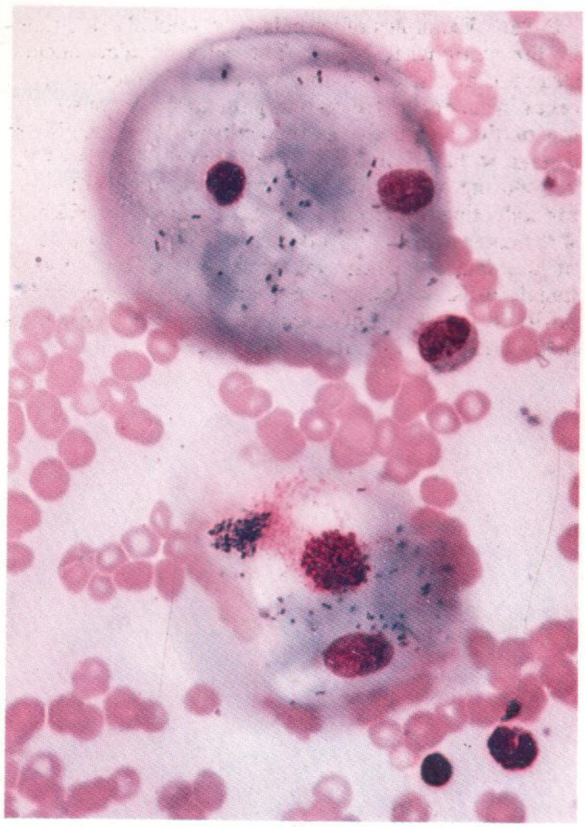

971

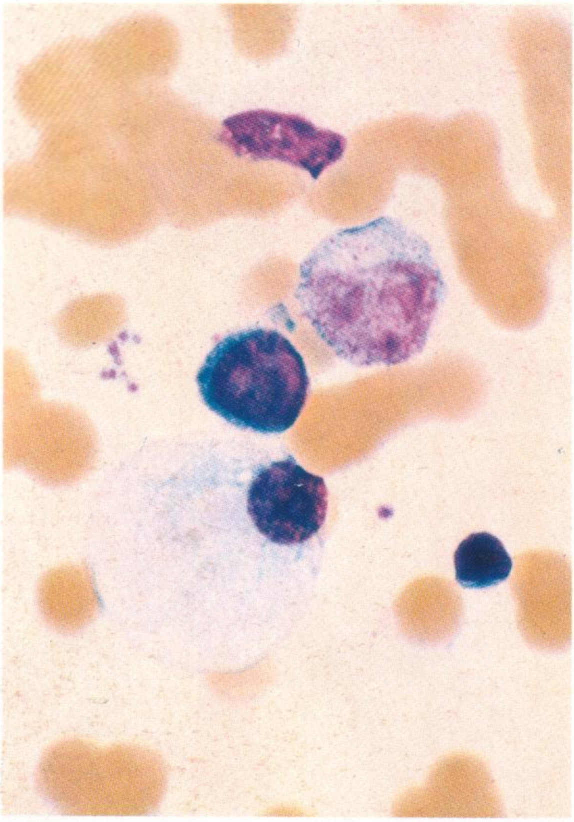

972

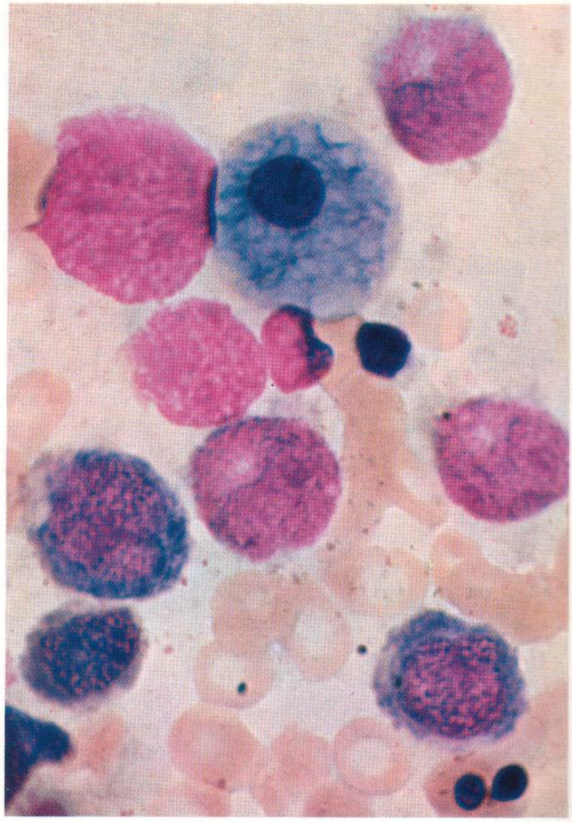

973

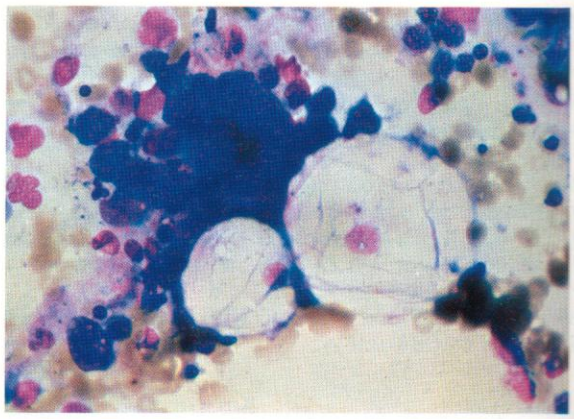

974

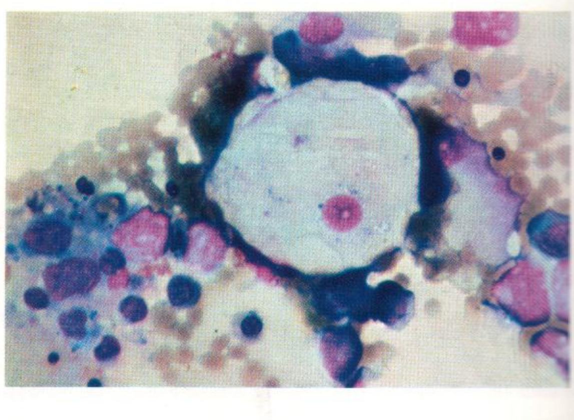

971. A fat-laden RE cell or lipophage from normal bone marrow.

972. A sebaceous skin cell contaminating a marrow smear.

973 and **974**. Stromal fat cells in bone marrow smears.

5
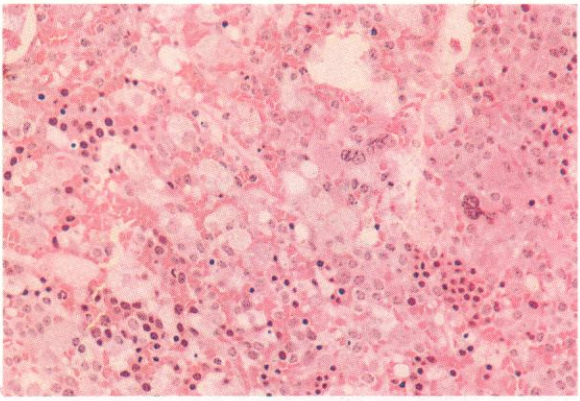

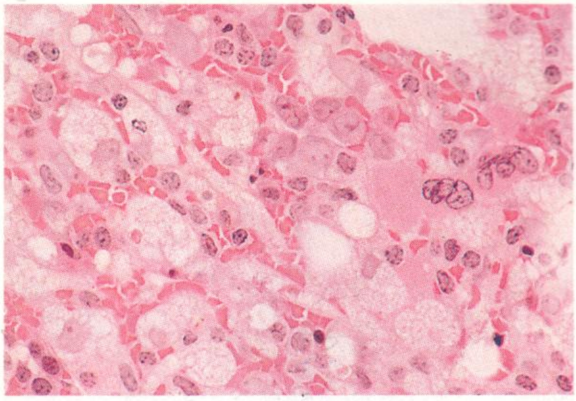
976

7
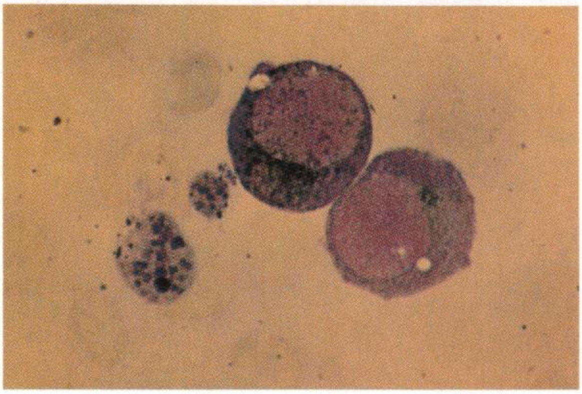

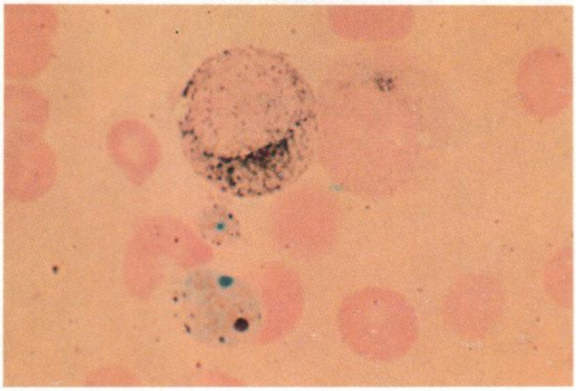
978

975 and **976**. Low- and higher-power views, respectively, of a thin section, stained by H&E, from a bone marrow trephine biopsy taken from a patient with hairy cell leukaemia (HCL) after treatment with alpha-interferon, showing an extensive proliferation of fat-laden foamy macrophages. The low-power field illustrated in **975** contains a pleomorphic cellular admixture, with foamy macrophages, normoblast nests, megakaryocytes and residual hairy cells, while the detailed cytology of all these cell types is seen in **976**. The foamy cells are distended with lipid, no doubt derived from disintegrating hairy cells. They bear a superficial resemblance to the sphingomyelin-laden macrophages of Niemann-Pick disease.

977 and **978**. SB stain and consecutive iron stain on the same field from a marrow aspirate taken from a patient with AML illustrating two cytoplasmic fragments with spurious localization of SB positivity on coarse particles of free iron, probably derived from a disrupted macrophage. The two blast cells present show the expected sudanophilia of early granulocyte precursors.

979. A thin section from a plastic-embedded bone marrow trephine biopsy, showing an artefactual scattering of spherical globules due to the presence of bubbles in the embedding medium. The bubbles are conspicuous and readily recognizable over empty fat spaces, but give rise to confusion when over cellular areas.

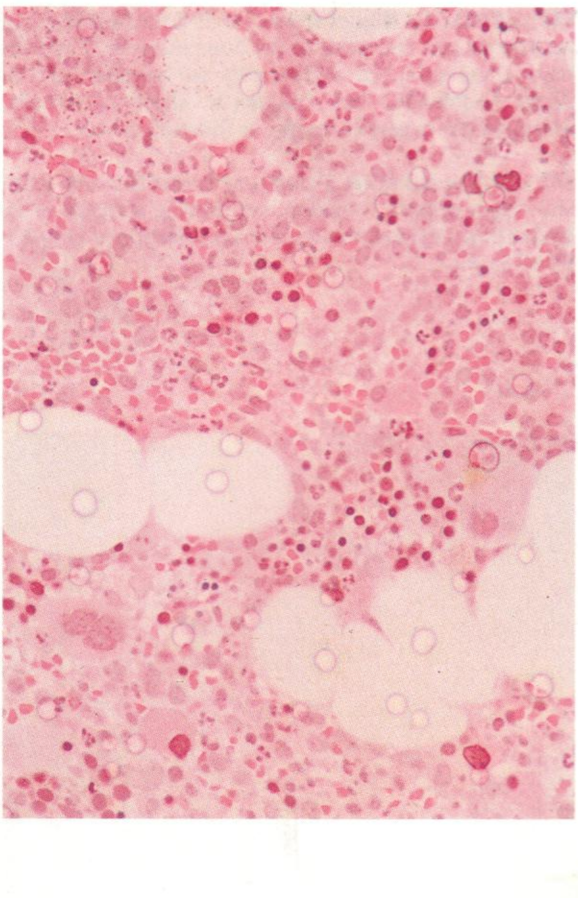
979

980

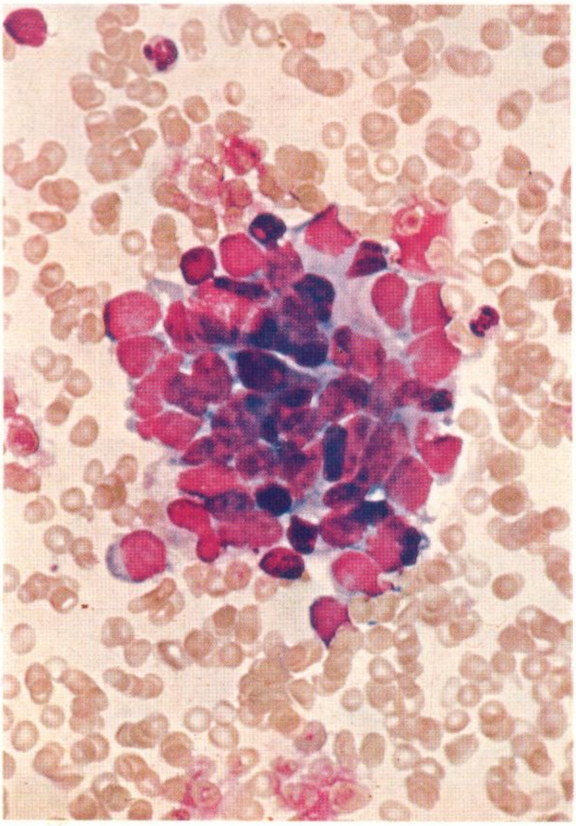

981

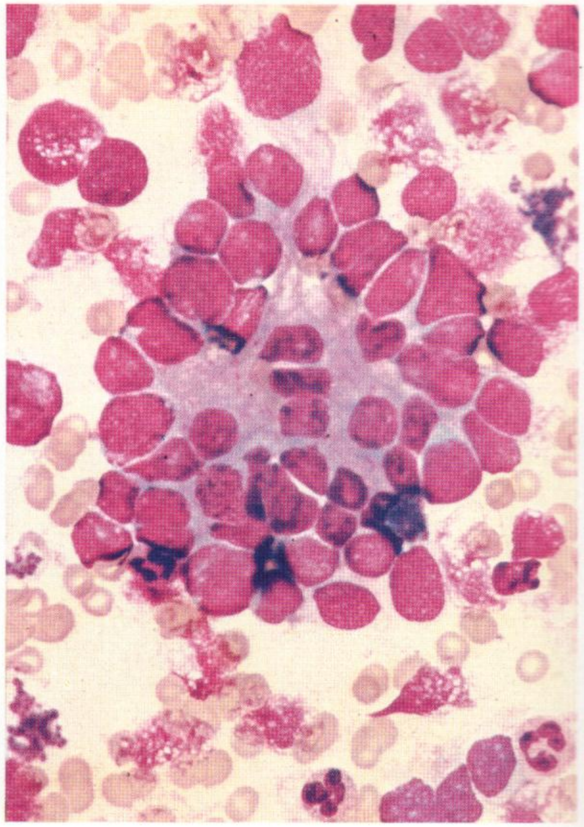

980 and **981**. Examples from two different subjects, of neuroblastoma cell nests in the bone marrow. The cells have a resemblance individually to lymphoblasts of acute leukaemia, but frequently show a whorled arrangement in small clumps, as illustrated here.

982. PAS reaction on a clump of neuroblastoma cells, showing a negative reaction, contrasting with the usual coarse positivity encountered in a proportion of lymphoblasts in ALL.

982

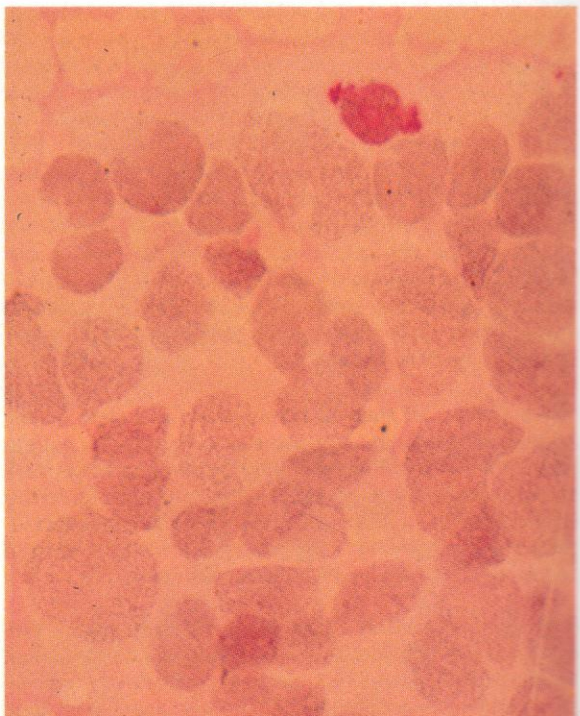

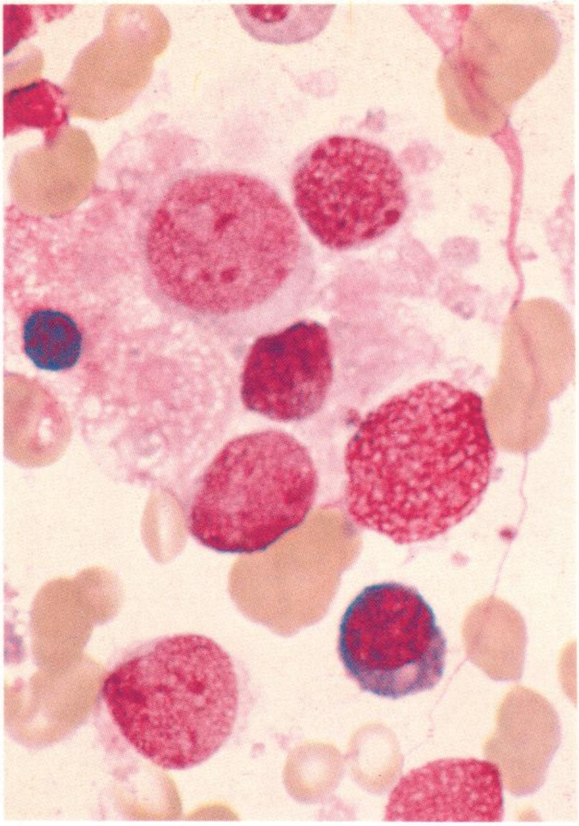

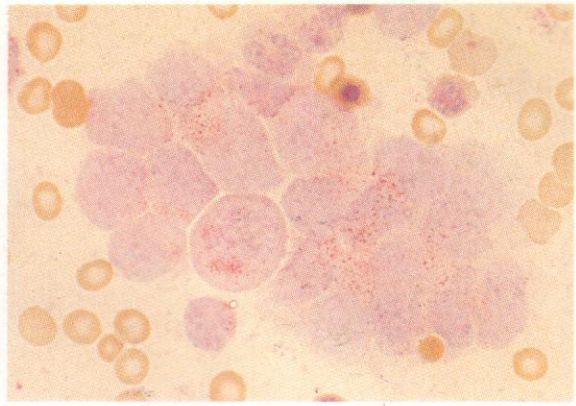

984

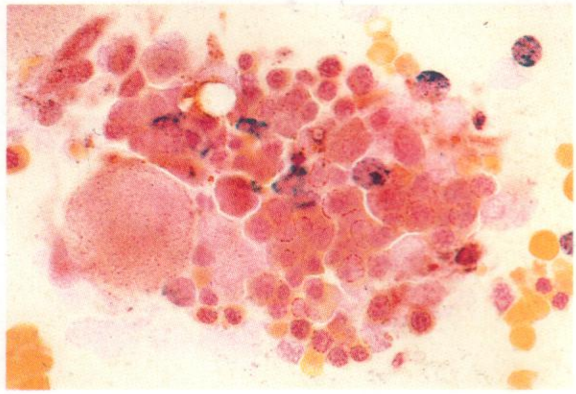

985

983–987. Further cytological and cytochemical features of neuroblastoma cells as seen in bone marrow aspirates. The high-power view of a Romanowsky-stained smear in **983** reveals a clump of neuroblastoma cells with characteristic fine nuclear chromatin containing several dense hyperchromatic spots, but only small and sometimes poorly distinguishable nucleoli. The cytoplasm of these cells is often fragile and easily disrupted, so that the cells may appear as naked nuclei.

In **984** the acid phosphatase reaction in a neuroblastoma cell nest shows the tumour cells to have only very weak positivity, without any sign of the paranuclear concentration seen in T lymphoblasts.

Mixed cell clumps with central neuroblastoma cells and peripheral haemic cells sometimes occur, when they may be confused with normal marrow flecks, especially when dense. Examples are illustrated stained with the dual esterase reaction in **985** and the Prussian blue stain for free iron in **986**. In **985** there is the usual CE positivity in granulocytes and some BE positivity in later normoblasts and a megakaryocyte at the edges of the cell clump, while the neuroblastoma cells show moderately strong, finely granular, BE positivity. There is no detectable free iron in the tumour cell nest seen in **986**, nor in the peripheral normoblasts. This contrasts with the finding of normal quantities of free iron in the marrow fleck of haemopoietic tissue from the same slide, illustrated in **987**, where neuroblastoma cells, if present, are not easily distinguished.

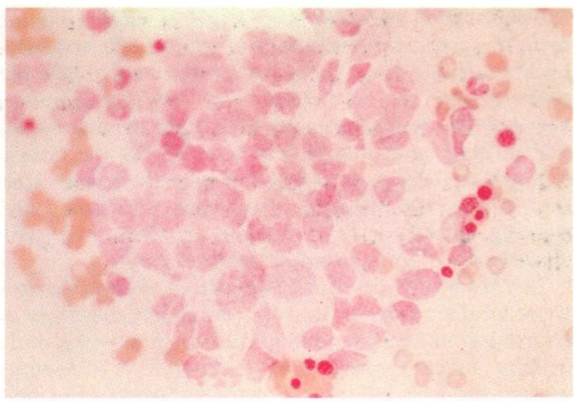

986

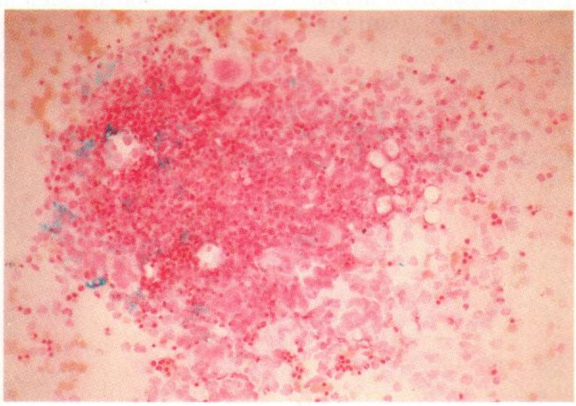

987

988

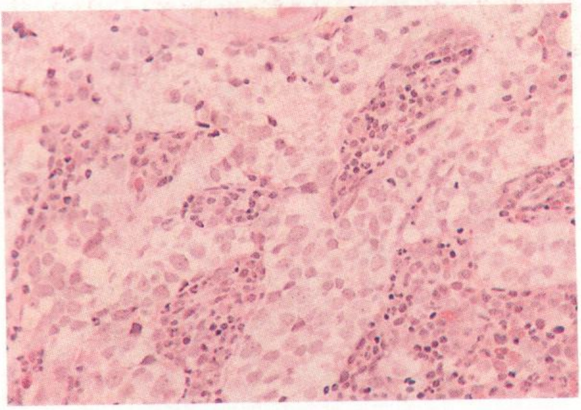

989

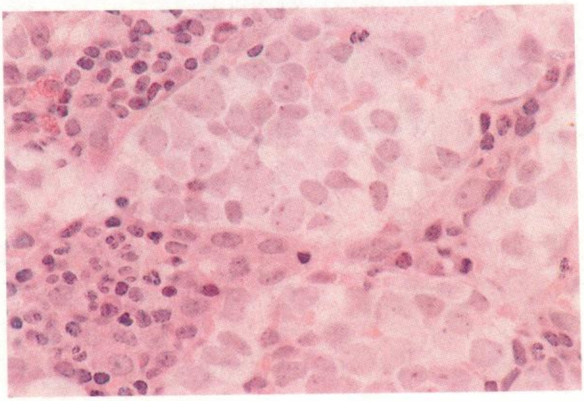

990

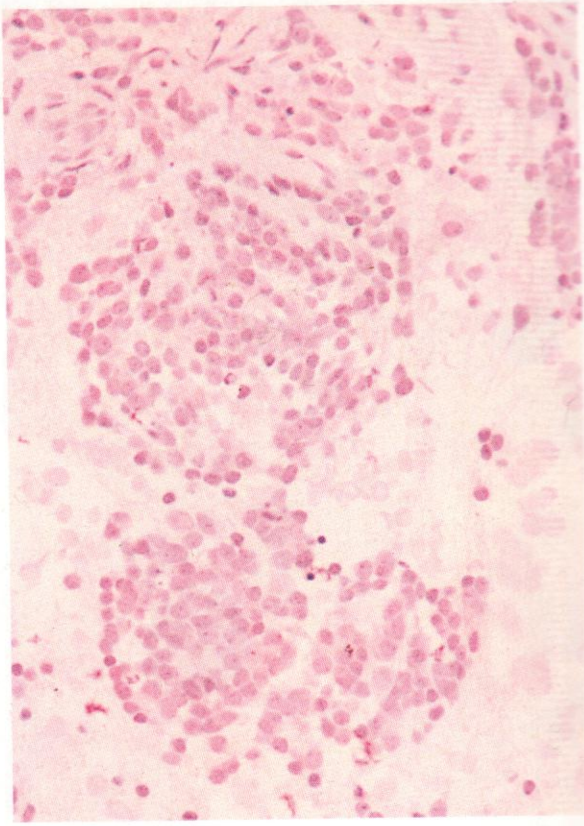

99

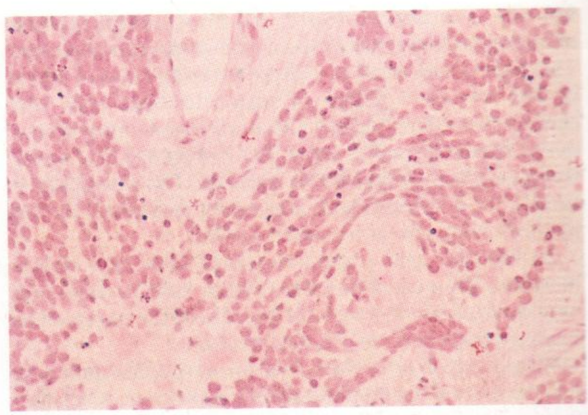

99

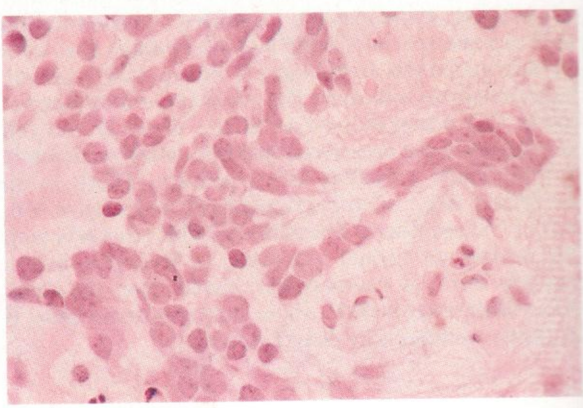

988–992. Thin sections from bone marrow trephine biopsies showing the histological appearance of neuroblastoma infiltration. In the low-power view of **988**, the pale-staining tumour cells form swirling columns between the residual islands of normal haemic tissue, and in the higher-power field seen in **989** the typical features of these cells are well shown: their large size, their flimsy and indefinite cytoplasm, and their pale-staining nuclei without obvious nucleoli but with characteristic hyperchromatic nuclear spots.

In **990** a more heavily infiltrated area of bone marrow from another case is shown, where large clumps of neuroblastoma cells predominate in an otherwise poorly cellular marrow, with scanty residual erythroblasts around the whorled tumour masses. Low- and higher-power views from the same marrow section are seen in **991** and **992**, illustrating the characteristic swirling whorled pattern of growth and infiltration shown by this turnover against a poorly cellular and oedematous, weakly eosinophilic background. The pale nuclei with occasional hyperchromatic dots, and the poorly defined pinkish cytoplasm are again well shown.

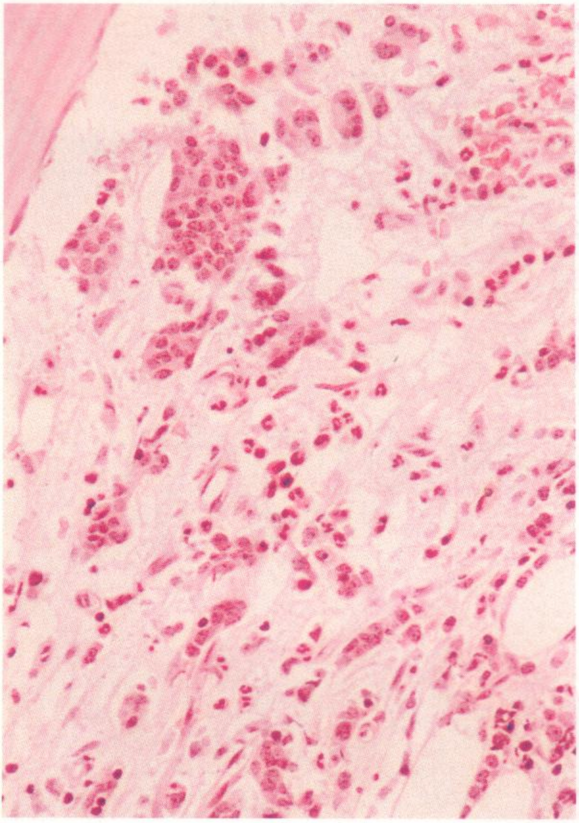

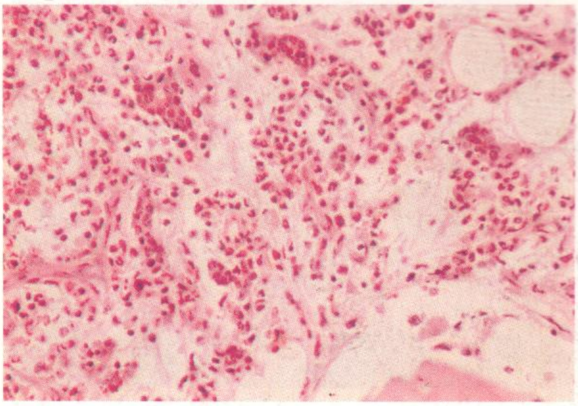

994

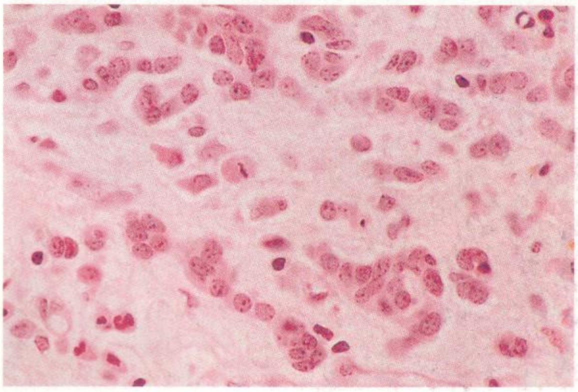

995

993–997. Thin sections from bone marrow trephine biopsies from patients with medulloblastoma invading the marrow. These tumour cells bear some resemblance to neuroblastoma cells, but they are generally more strongly staining, and form smaller cell clumps or chain-like columns of single cells in the bone marrow, and do not usually manifest the swirled or whorled arrangement common in neuroblastoma. The low-power fields of **993** and **994** show these characteristic growth patterns well, with residual normal marrow elements in the background and a sectioned capillary at the left in **994**. The higher magnification of **995** and **996** reveals the moderately dense nuclear chromatin and tendency to form cell chains and small syncytial clumps. In a still higher-power field (**997**), the nuclei of the medulloblastoma cells can be seen to have the same type of hyperchromatic spots as previously shown in neuroblastoma cells.

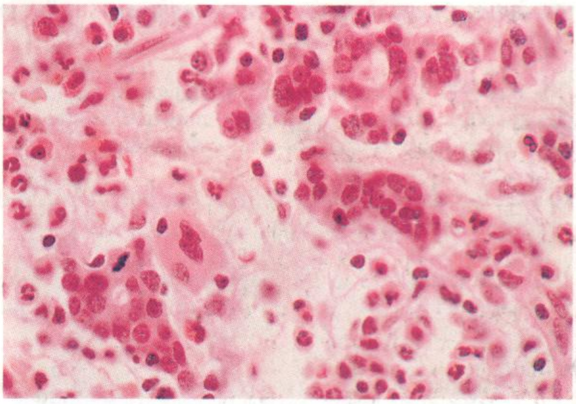

996

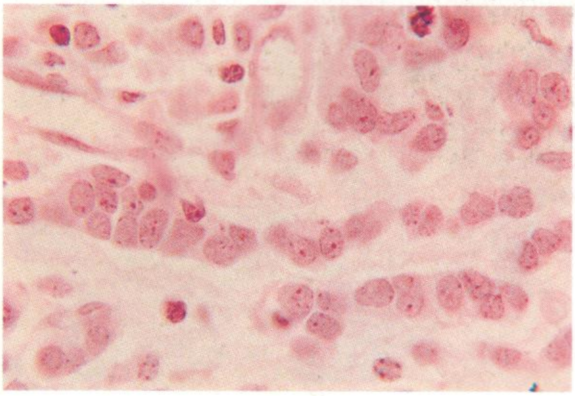

997

998

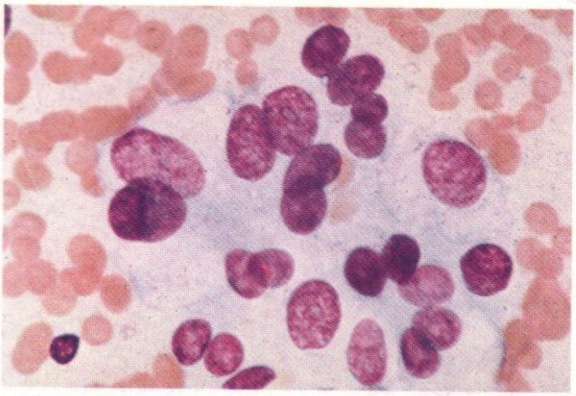

999

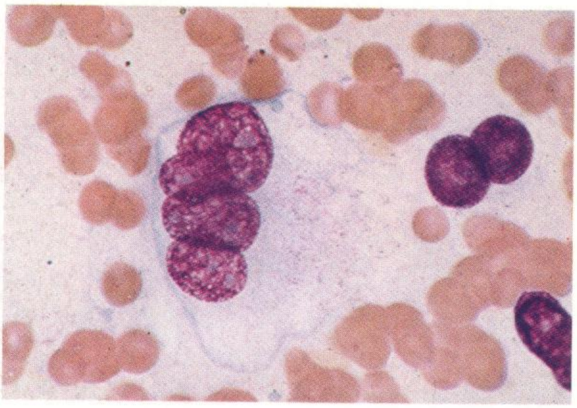

998–1003. *Chemodectoma (paraganglioma) cells in marrow.*

998 and **999**. Leishman stain: the malignant cells show conspicuous nucleoli, sometimes multiple nuclei and generally a large amount of clear cytoplasm.

1000. SB stain with a normally reacting polymorph and negative chemodectoma cells.

1001. PAS reaction in the same preparation showing negative or faint diffusely positive reaction in tumour cells.

1002. Alkaline phosphatase reaction is negative in the tumour cells (in contrast to RE cells). A positive polymorph is present.

1003. Acid phosphatase reaction shows moderately coarse scattered granular positivity in tumour cells.

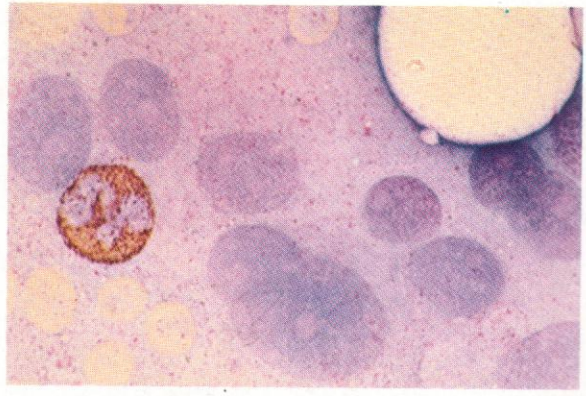

10

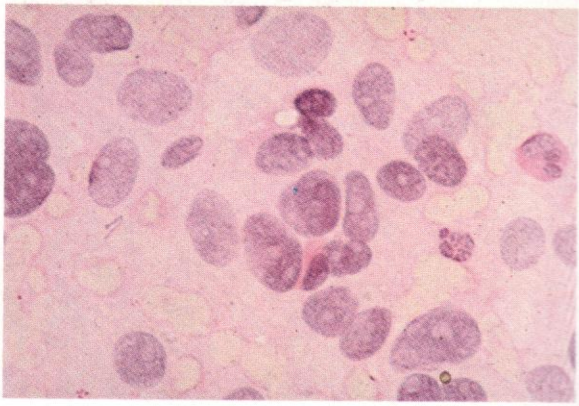

10

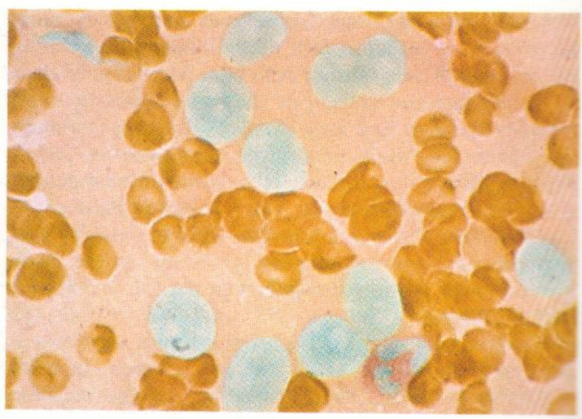

10

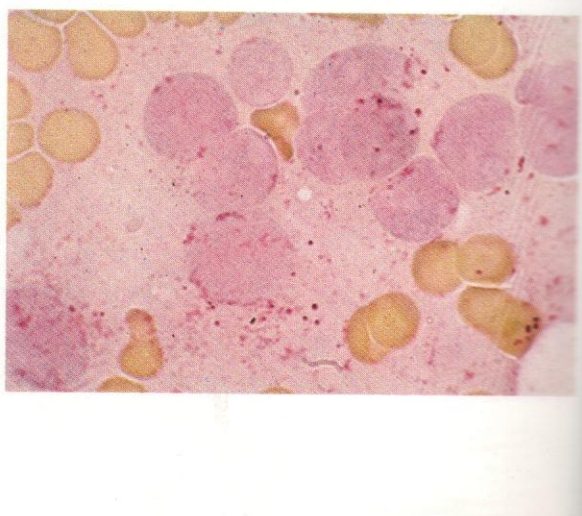

10

04

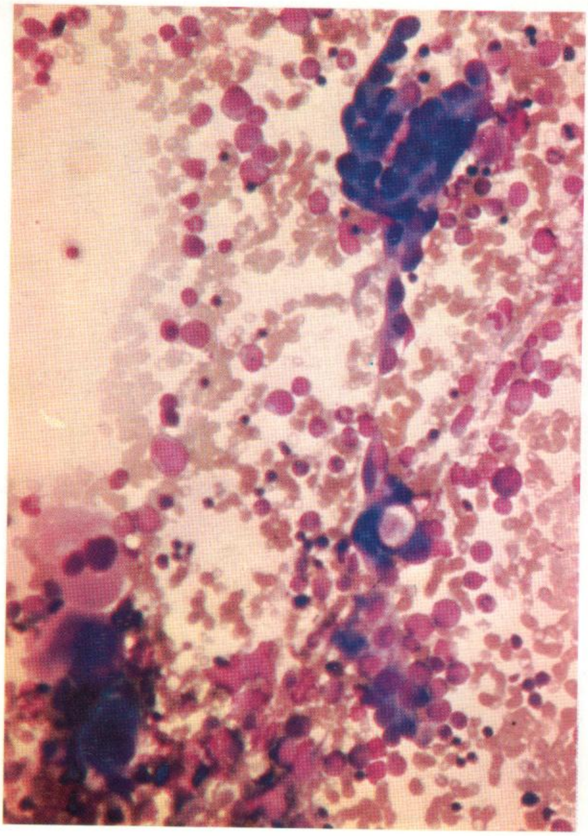

1005

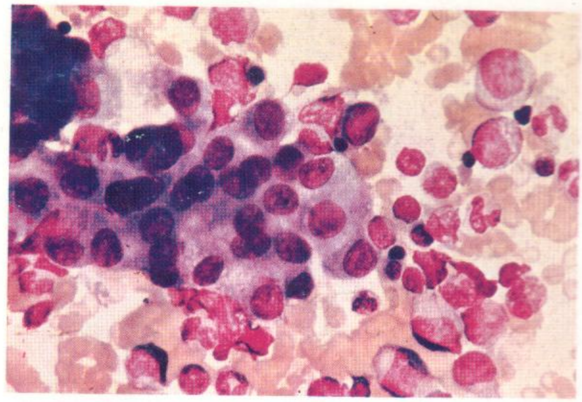

1006

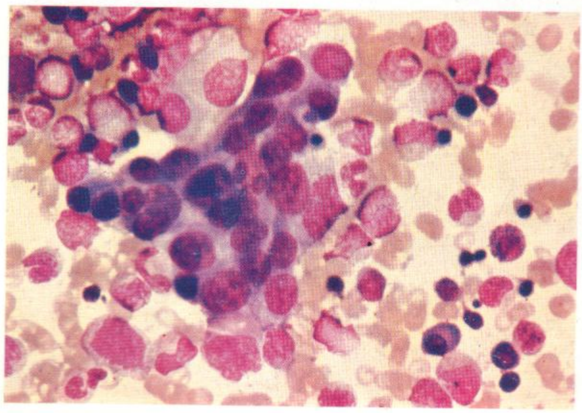

1007

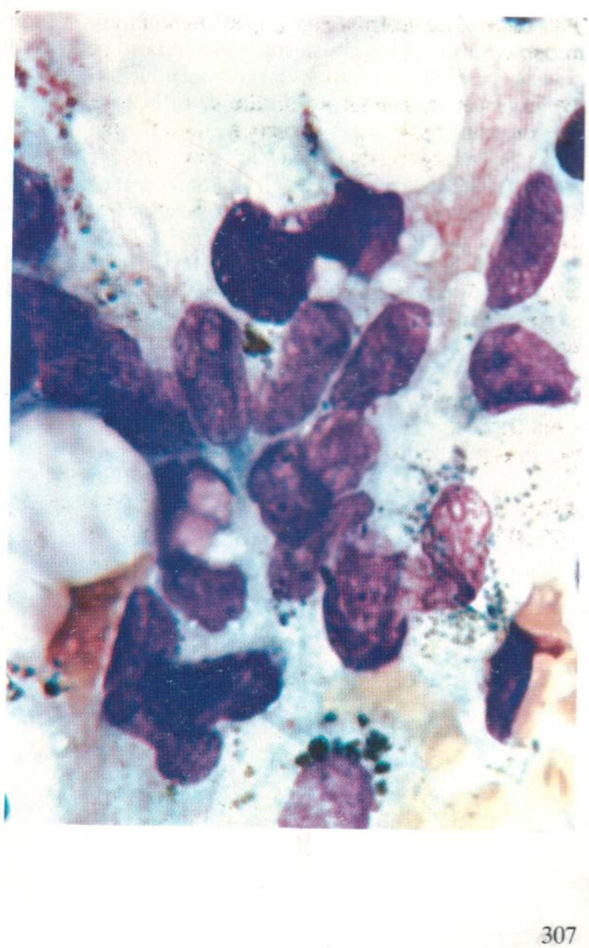

1004. Clumped cells, darkly staining, and unlike any cells normally found in the marrow, allow a diagnosis of tumour cell metastasis to be made. This marrow smear was from a patient with disseminated carcinoma of the stomach.

1005 and **1006**. Cytological detail of cell clumps from the same patient with gastric carcinoma. The tendency to syncytium formation is evident.

1007. A partially syncytial cell clump of secondary deposit from carcinoma of the bronchus in a bone marrow smear.

008

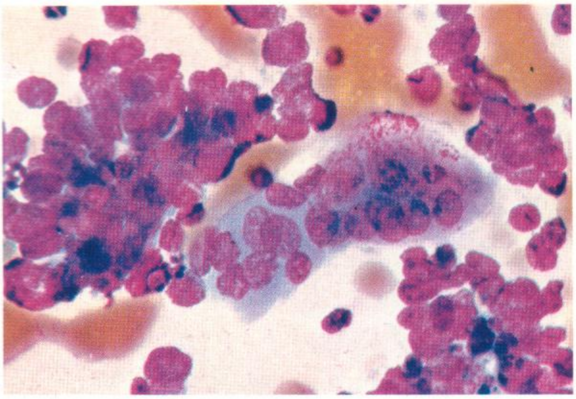

010

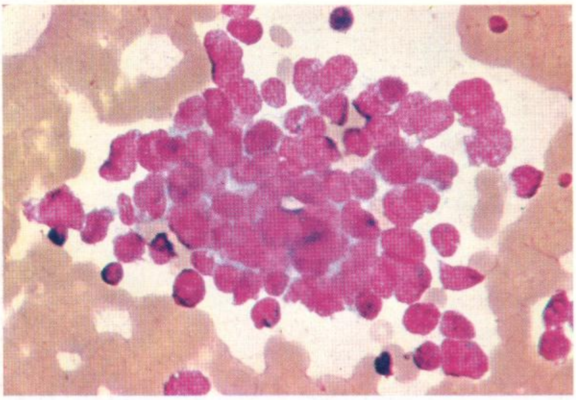

1008. A further example of bronchial carcinoma cells in marrow, showing almost nothing but tumour cells (and clumped erythrocytes). A large multinucleated syncytium is present, perhaps of tumour cells, but possibly an osteoclast.

1009. Bronchial carcinoma cells in marrow from a third patient, here showing a tendency to rosette formation.

1010–1012. Examples of malignant cells in bone marrow aspirates from a patient with disseminated carcinoma of the breast.

1009

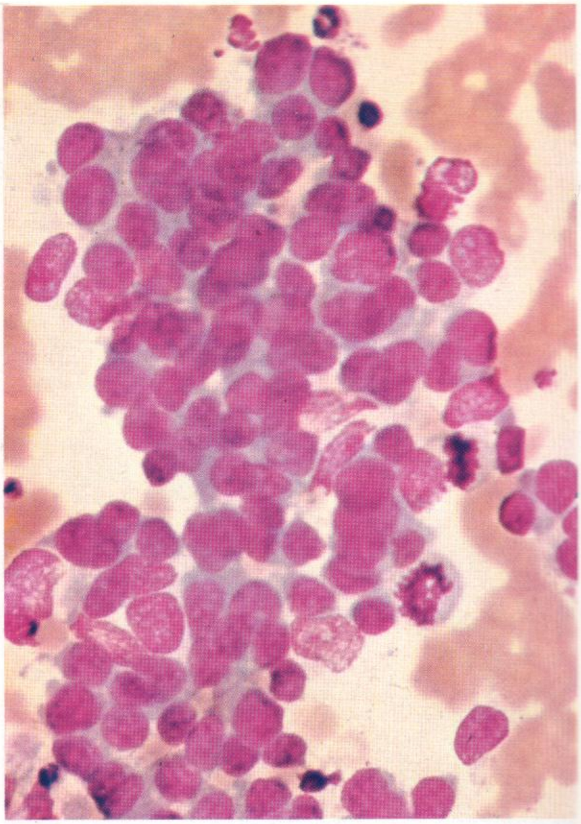

1011

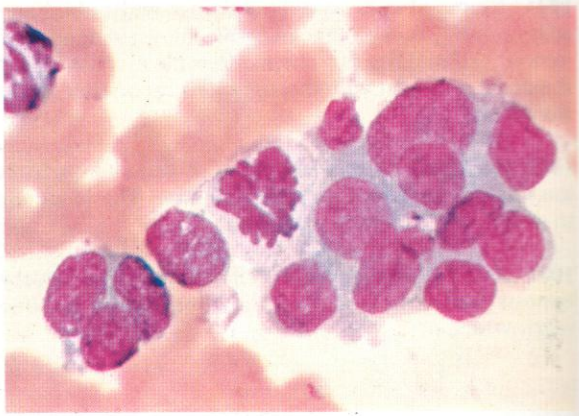

1012

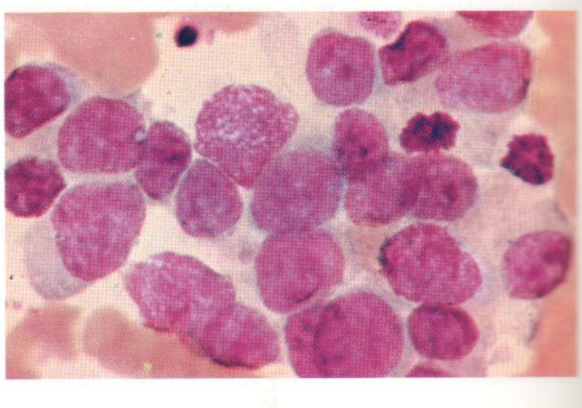

13

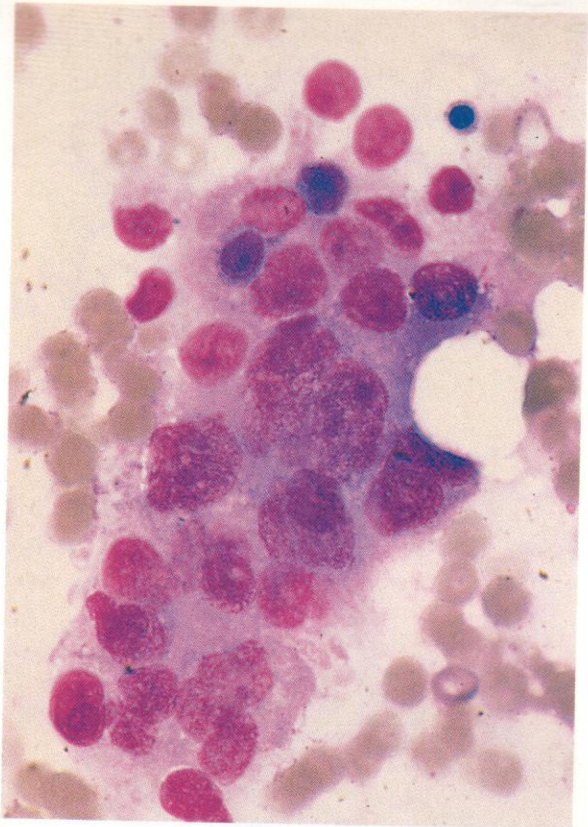

1014

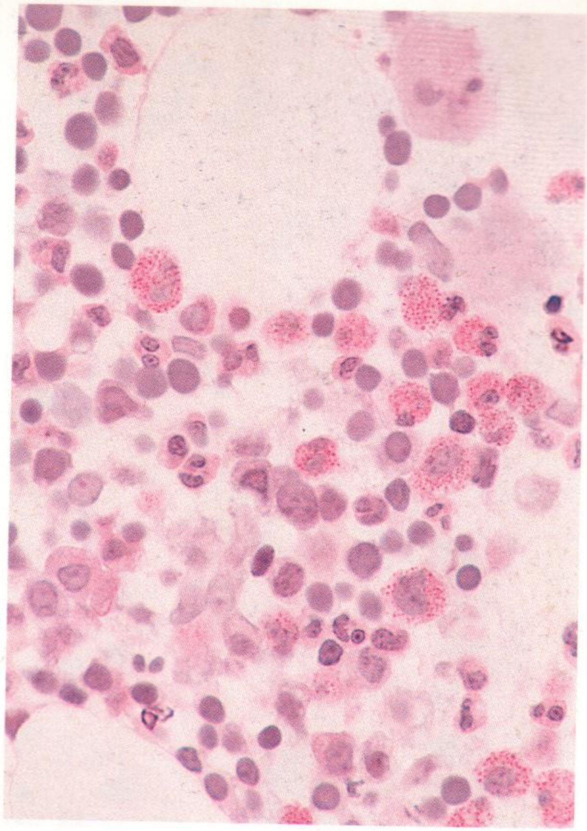

1013. A clump of metastatic tumour cells in a bone marrow aspirate from a patient with breast carcinoma and a leucoerythroblastic anaemia. There is considerable variability in cell size and nuclear configuration.

1014 and **1015**. Two different areas from a section of bone marrow trephine biopsy from the same patient whose marrow aspirate appeared in **1013**. In the first, the area chosen has few tumour cells recognizable with certainty, even at this higher power, although two or three of the larger cells with dark nuclei around the centre of the field may well be carcinoma cells; but the main feature shown is a prominent reactive eosinophilia. In the lower-power view of another area illustrated in **1015** there are several syncytial clumps of carcinoma cells with reactive eosinophils and neutrophils around, though less conspicuous than in **1014**.

1015

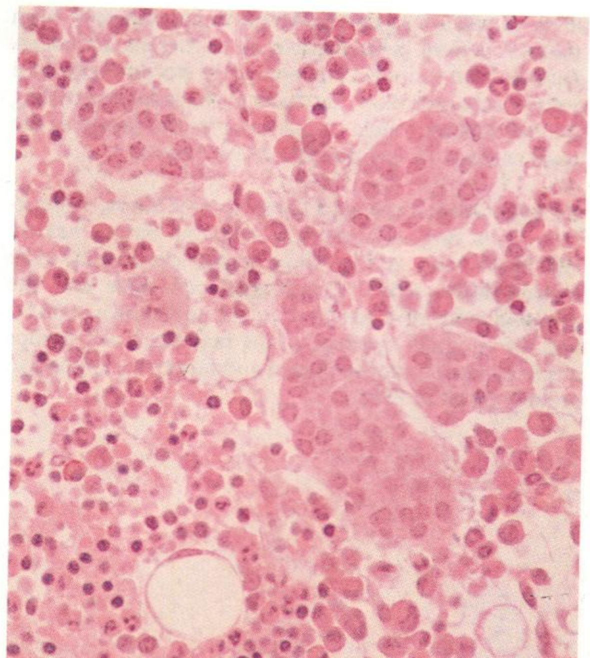

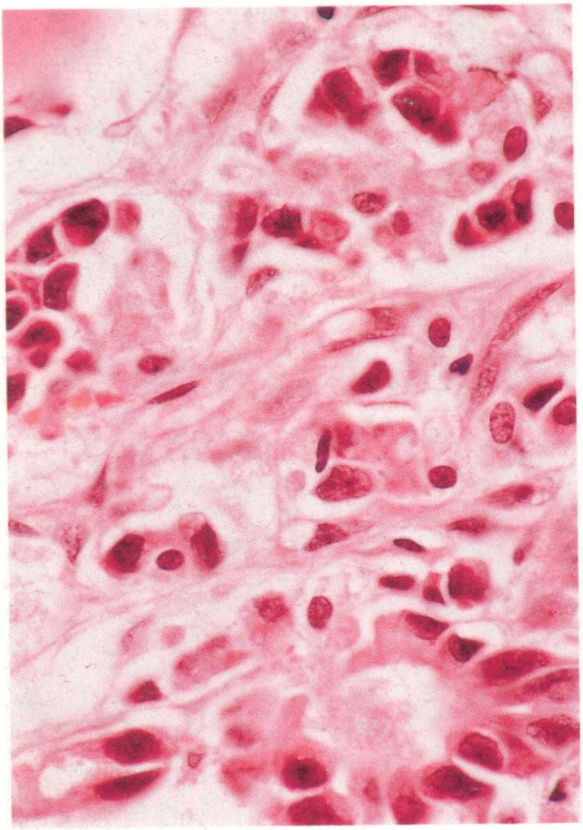

1017

1018

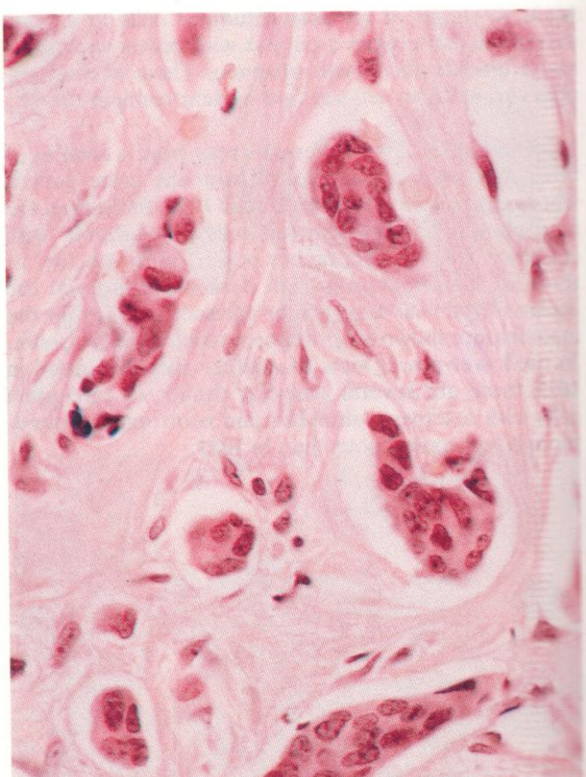

1016. A section of bone marrow trephine biopsy from another patient with metastasis of breast adenocarcinoma. The tumour cells appear to be arranged in a pseudo-acinar fashion, and have perhaps been secreting the eosinophilic mucin which occupies the centre of the lowest acinus. A few fibroblasts are present.

1017 and **1018**. Low- and higher-power views, respectively, of a section of marrow trephine biopsy heavily infiltrated with a fibrosing breast carcinoma. The relative infrequency of epithelial cell nests and the predominance of dense fibrosis are well shown in **1017**, and the irregular cytology of the malignant cell clumps amid the surrounding collagen and fibrocytes appears in greater detail in **1018**.

1019

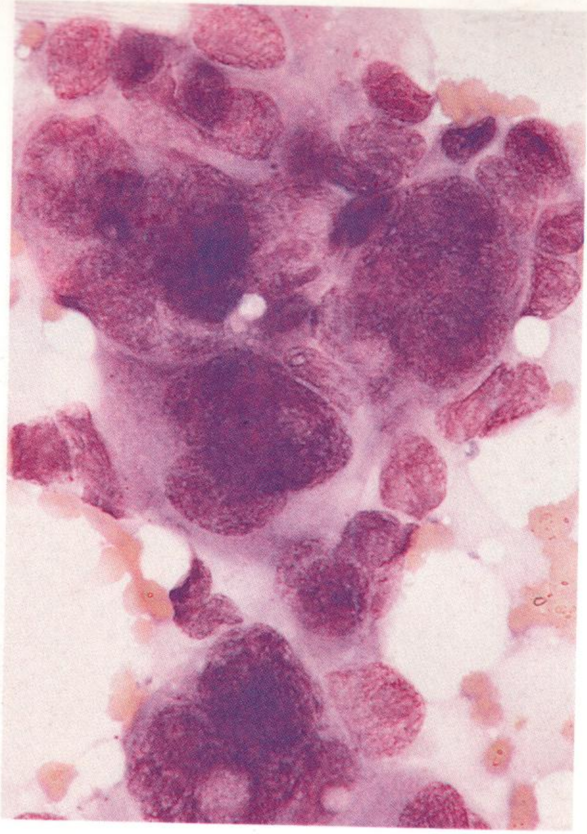

1020

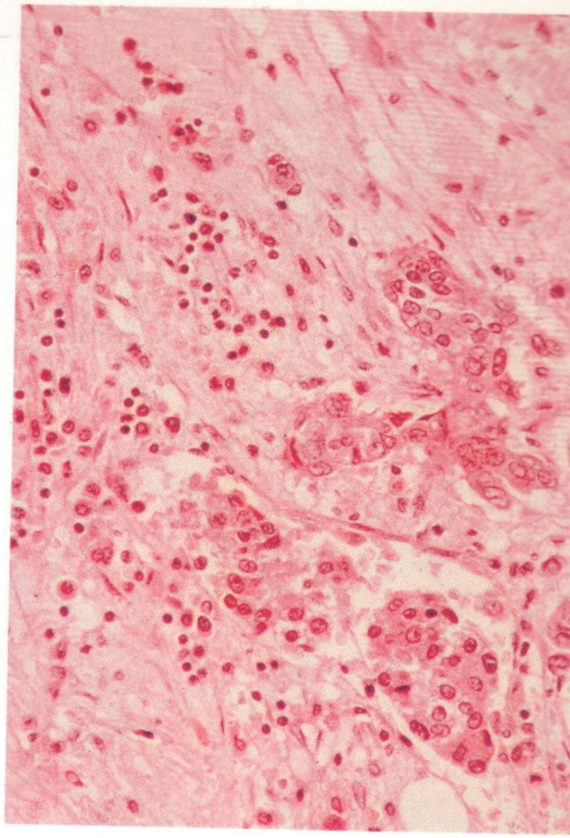

1021

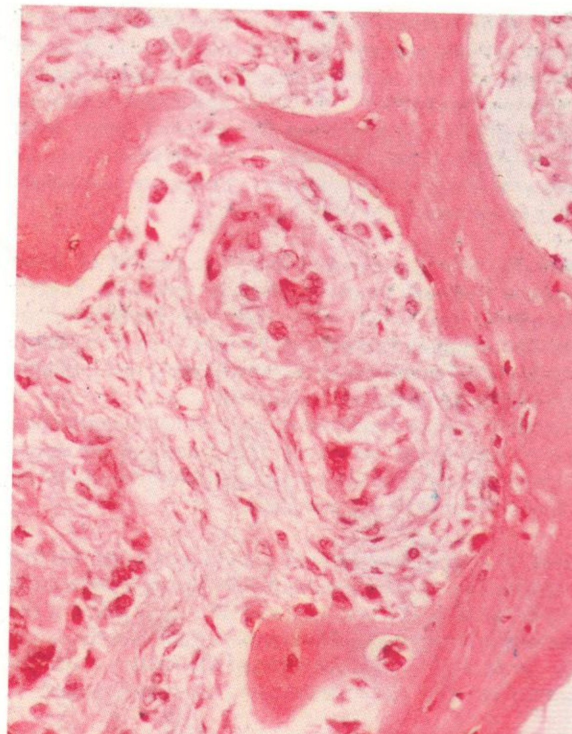

1019. A nest of tumour cells in a bone marrow aspirate from a patient with bronchial carcinoma. There is wide variability in the size of cells and their nuclei in this partially syncytial clump.

1020. A high-power view of tumour metastasis in a bone marrow section, in this case from a patient with a thyroid carcinoma. The cytology of the three components, tumour cells, fibrotic reaction, and residual marrow cells, can be seen in some detail.

1021. A case of bone marrow metastasis from prostatic carcinoma seen in a trephine biopsy section. In this low-power view there is evident erosion of the bony trabeculae and a conspicuous fibrotic reaction around the tumour cell nests.

1022

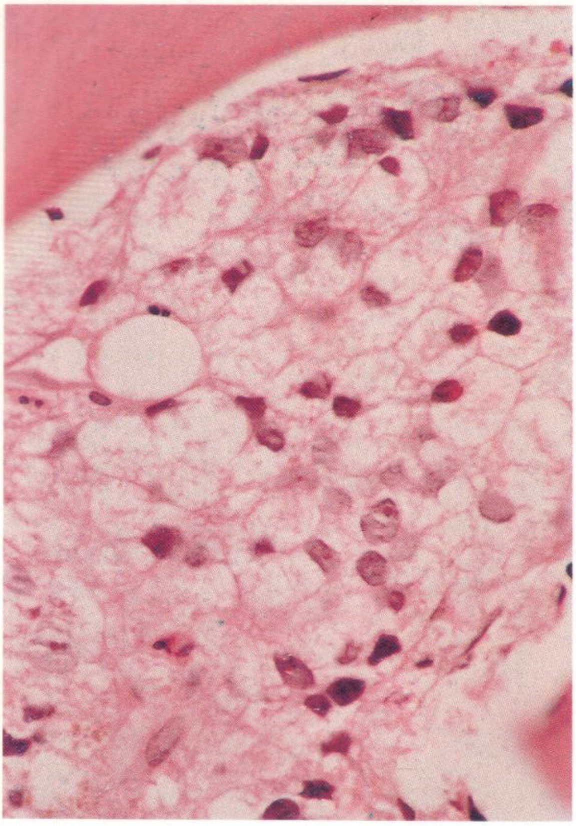

1023

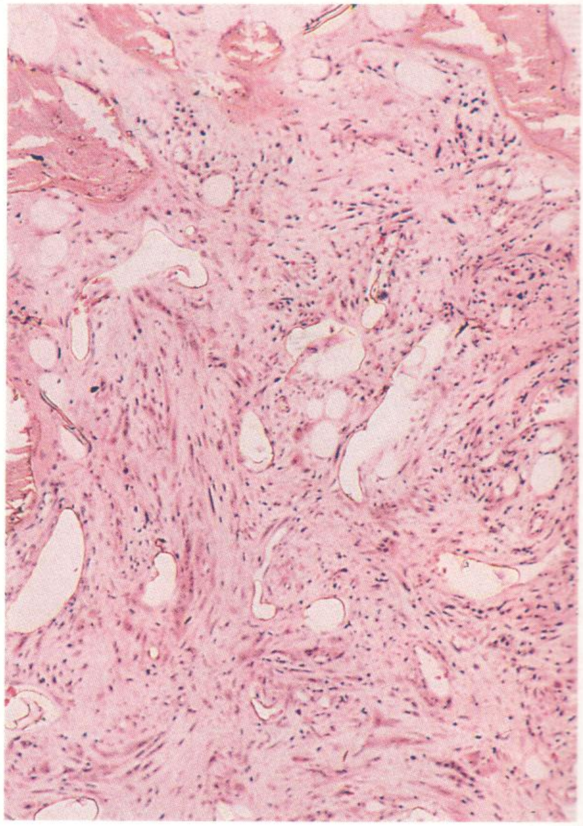

1022. A high-power view of a section from a trephine biopsy of bone marrow, showing metastatic infiltration with tumour cells from a clear-cell carcinoma or hypernephroma of kidney. The field illustrated is almost devoid of residual haemopoietic cells and, apart from the trabecular bone, contains only the polygonal tumour cells with their variable nuclear chromicity and ample clear cytoplasm.

1023. A very low-power view of a section of bone marrow trephine biopsy from a patient with Paget's disease of the bone with malignant fibroblastic or fibrosarcomatous change supervening. The fibroblastic and fibrocytic proliferation is overwhelming and probably represents sarcomatous malignant change. Areas of extensive erosion and destruction of the trabecular bone can be seen at the periphery, particularly at the upper edge, while most of the remaining field is occupied by whorls of fibrosing tumour cells.

1024. A high-power view of a section of bone marrow trephine biopsy from a patient with Ewing's sarcoma of bone, showing the cytology and mitotic activity of the tumour cells, with a multinucleated giant tumour cell at the bottom right. Middle right of the field is a spur of normal marrow tissue penetrating the tumour mass.

1024

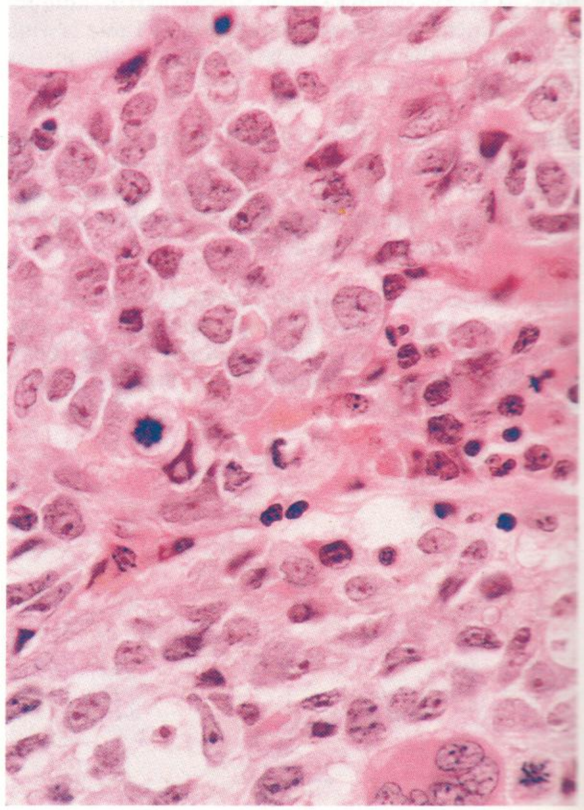

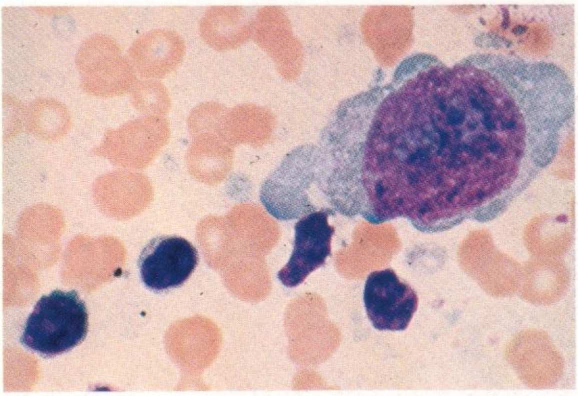

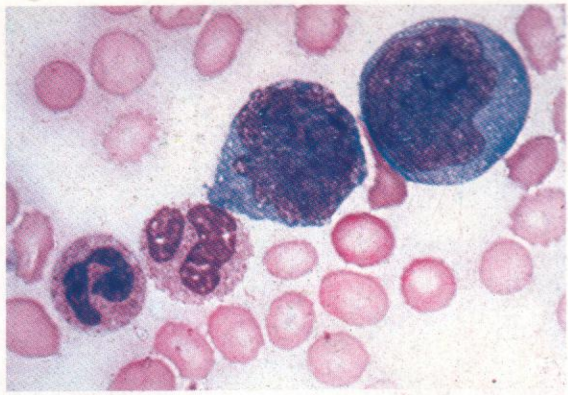

1027

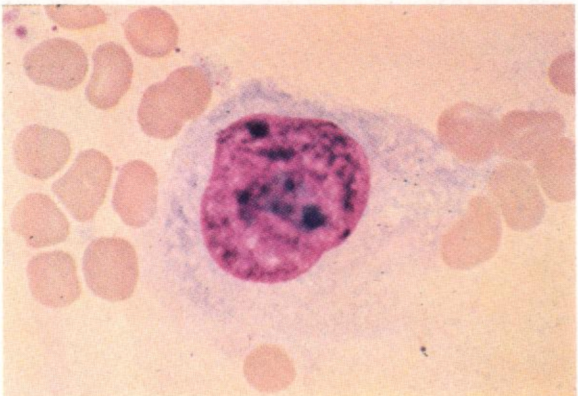

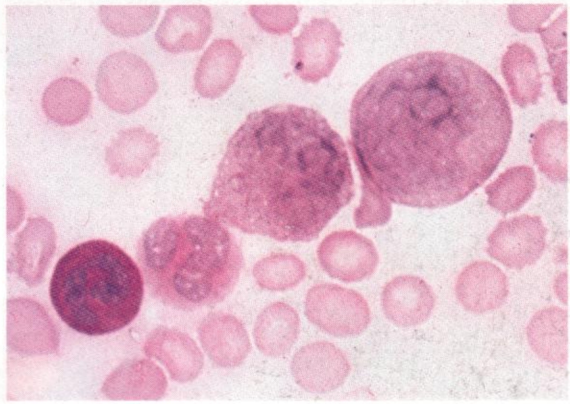

1028

1025–1028. Giant cells (Reed-Sternberg cells) from the bone marrow of a patient with advanced HD. They share the conspicuous large blue nucleoli which are very characteristic of HD giant cells in smears or imprints of lymph nodes. Duplicate Romanowsky and consecutive PAS stains showing the generally weak positivity which most R-S cells manifest are shown in **1027** and **1028**.

1029. Involvement of both marrow and peripheral blood in the terminal stage of HD may produce a leukaemia-like picture. This does not occur commonly, but most examples reported appear to have shown monocytoid primitive cells. Illustrated here is the peripheral blood picture in a terminal leukaemic transformation of HD, where the cells probably belong to the same lineage as R-S cells.

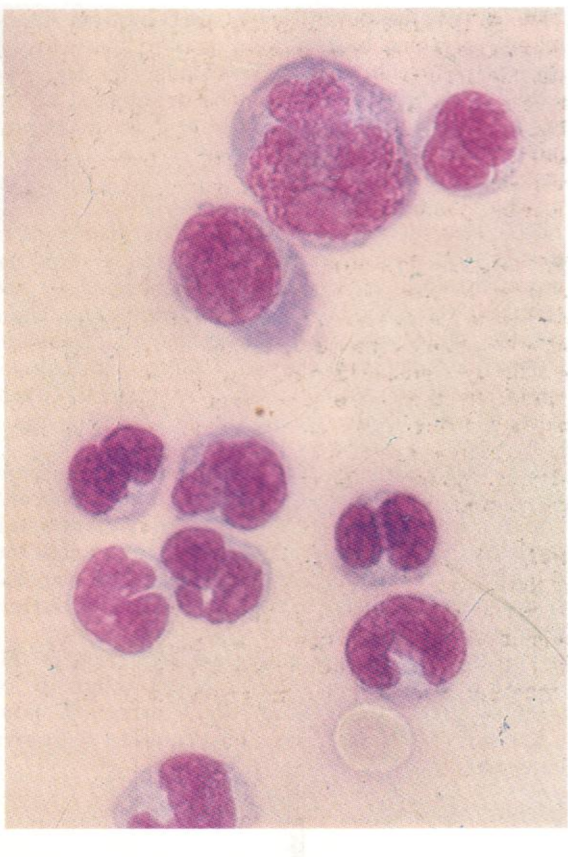

1029

1030

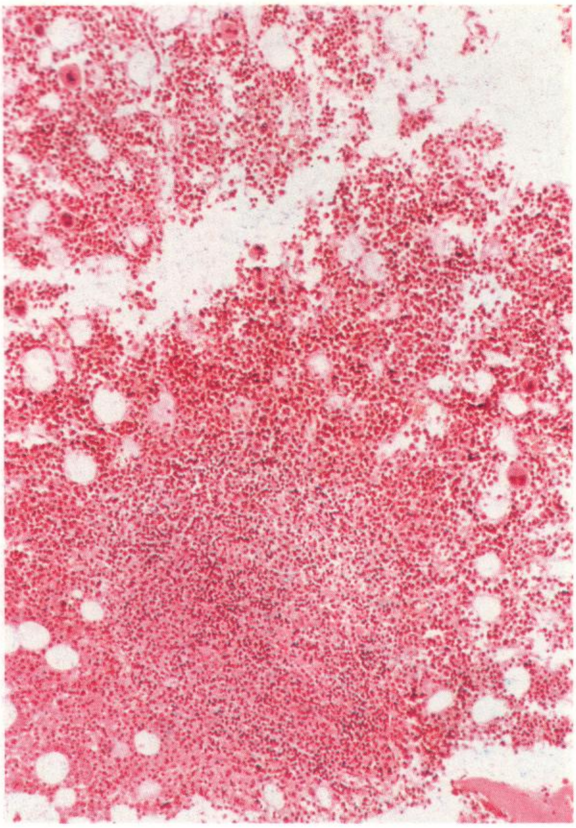

103

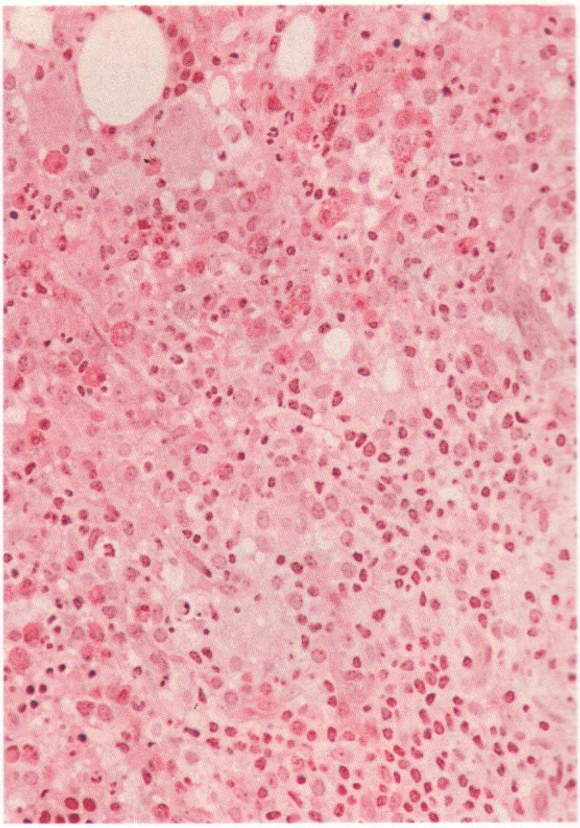

103

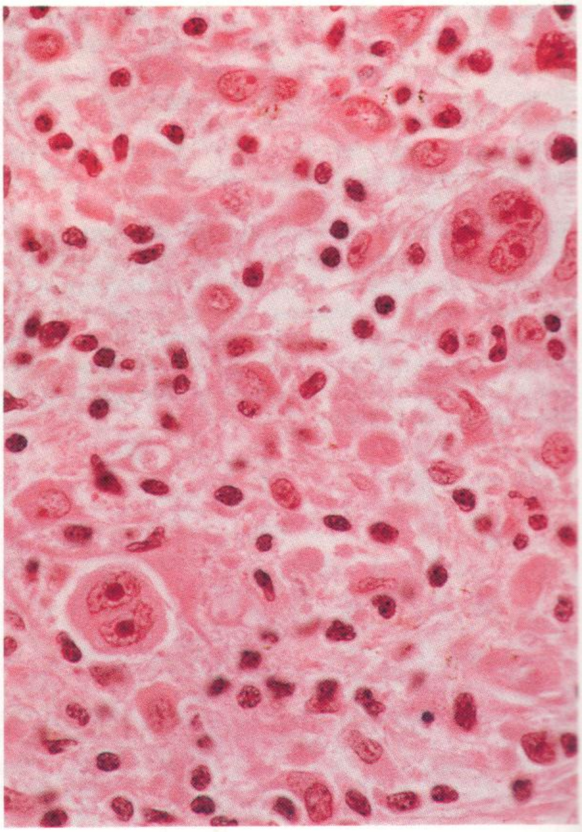

1030. A very low-power view of a section from a bone marrow trephine biopsy, showing a roughly circular nodule of HD infiltrate in the lower half of the field. The nature of the infiltrate cannot be determined at this magnification, of course, but the field illustrates how infiltrative nodules can be detected by section scanning at very low power.

1031. A high-power view of a neighbouring nodule to that in **1030**, from the same section and showing the mixed cytology with numerous Hodgkin's cells and reactive eosinophilia, together with lymphocytes and a considerable fibroblastic reaction; the latter is almost always present in areas of marrow infiltration and is not confined to the nodular sclerosing variant of HD (which does not often involve the marrow).

1032. A high-power field from a section of bone marrow trephine biopsy, taken from a patient with HD and diffuse marrow involvement. The mixed cytology is well shown – including conspicuous large Hodgkin's cells and R-S cells with their characteristic prominent nucleoli, against a background of scattered lymphocytes and less frequent polymorphs and fibroblasts.

The type of marrow infiltration illustrated in this section is most often seen in mixed cellularity or lymphocyte-depleted variants and carries a poor prognostic significance, certainly requiring aggressive chemotherapy.

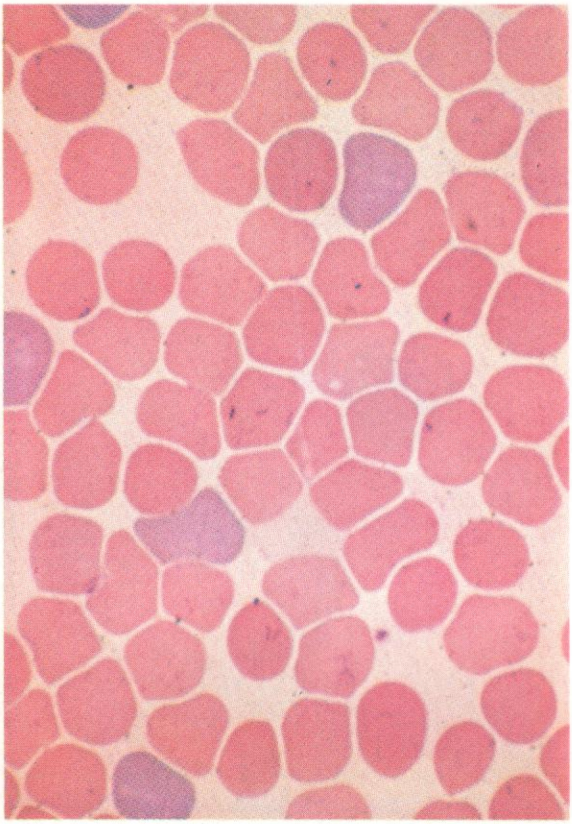

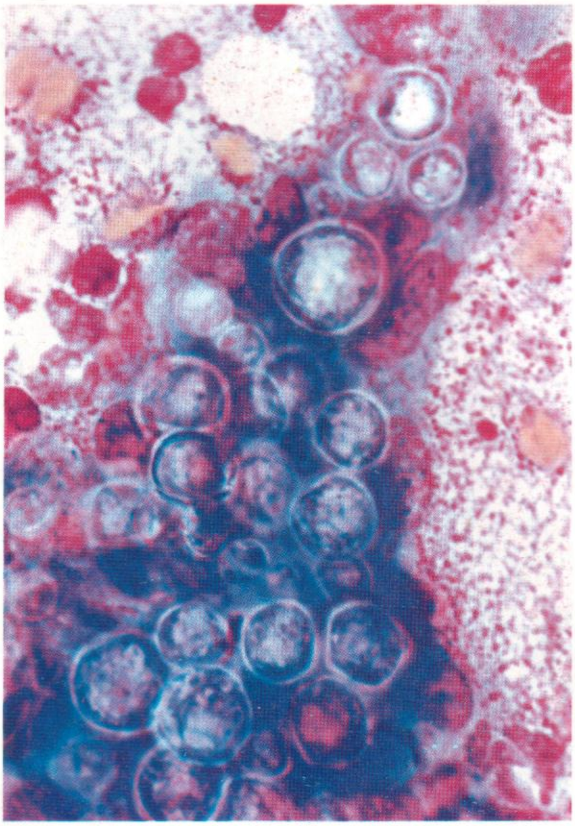

1034

1033. A blood smear in infection with Bartonella bacilliformis. Many erythrocytes contain the organisms, with rod-shaped or sometimes cocco-bacillary form. The disease produced by this organism in man, Bartonellosis, Carrion's disease or Oroya fever, is associated with macrocytosis and haemolytic anaemia, and this smear shows some polychromasia.

1034. Yeast-like bodies of blastomycosis in a spicule of bone marrow, possibly undergoing phagocytosis by RE cells.

1035. An RE cell containing many Leishman-Donovan bodies, from the marrow of a patient with kala-azar. Various other marrow cells, a megakaryocyte, several myelocytes and a late normoblast are also present.

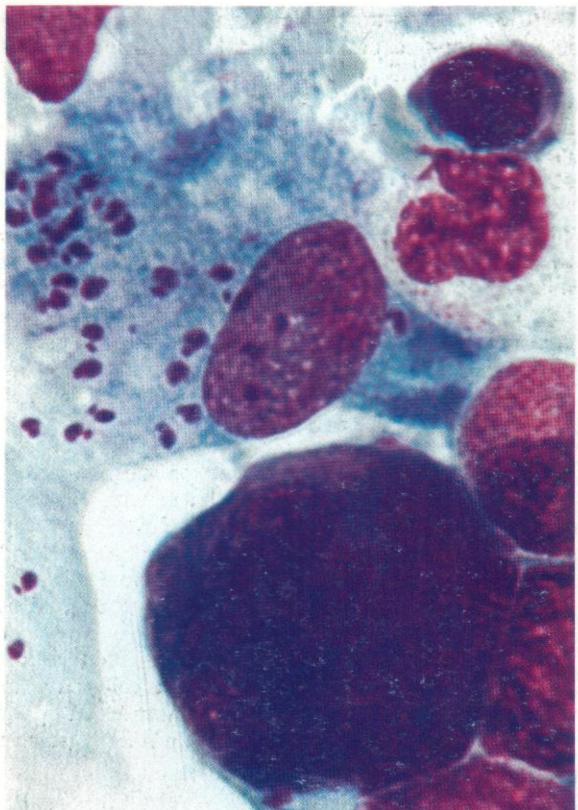

1035

1036

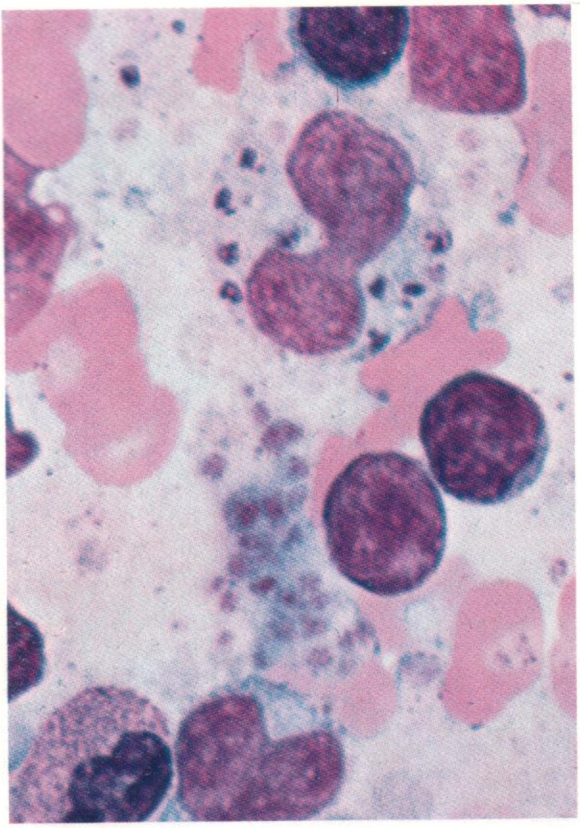

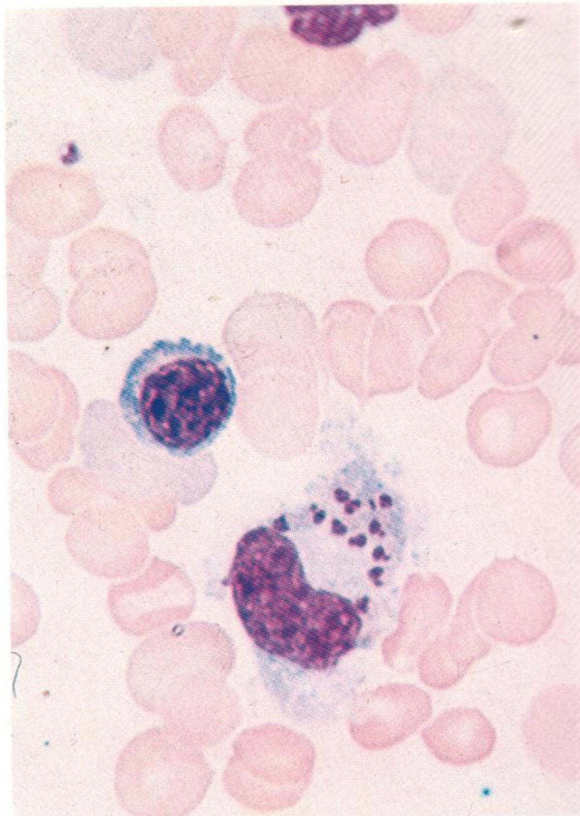

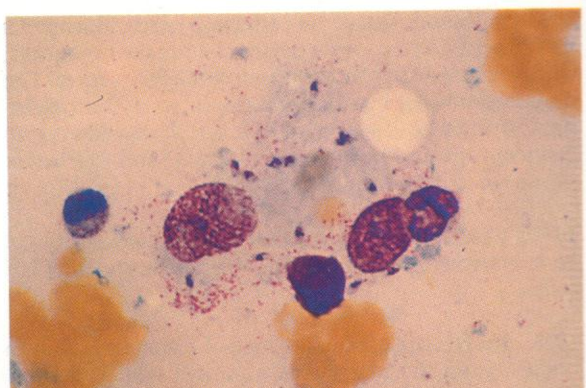

1036. Another example of Leishmania, with organisms within a monocyte and others liberated among the surrounding cells. Below the monocyte is a clump of platelets for comparison with the more sharply and positively staining Leishmania bodies.

1037. Further Leishmania parasites in a monocyte/ macrophage.

1038 and **1039**. Consecutive Romanowsky and PAS reactions on the same field from a smear of bone marrow aspirate taken from a patient with Leishmaniasis. The central pair of macrophages contain between them a dozen parasites, which can be seen in the PAS stain of **1039** to be weakly PAS-positive. There is a necrotic lymphocyte below the macrophages and normally PAS-positive neutrophils to either side.

40

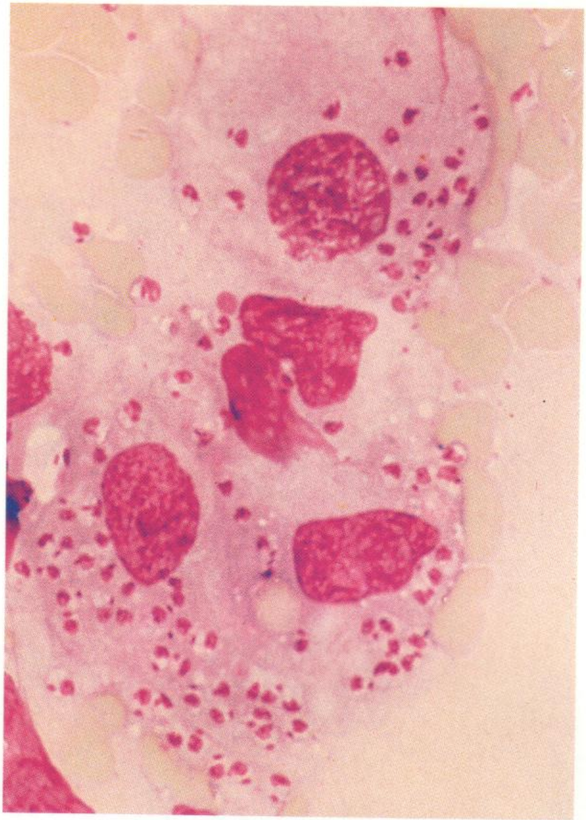

1041

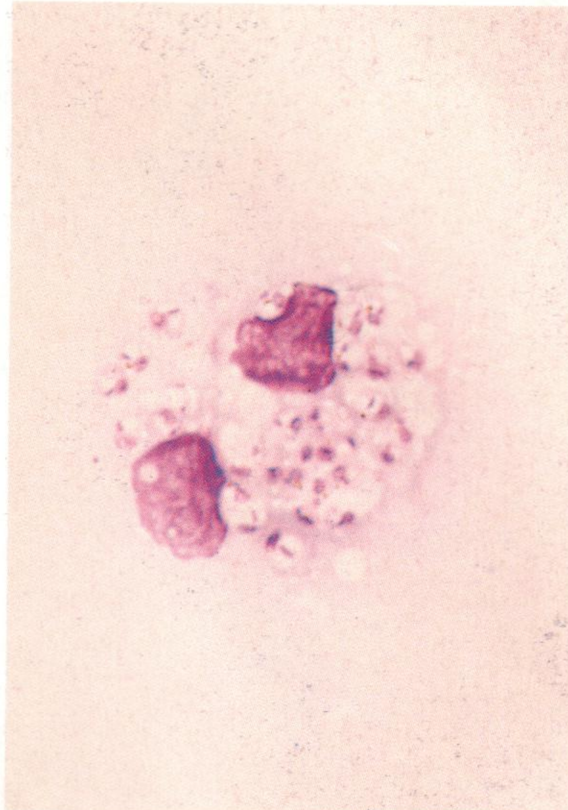

1042

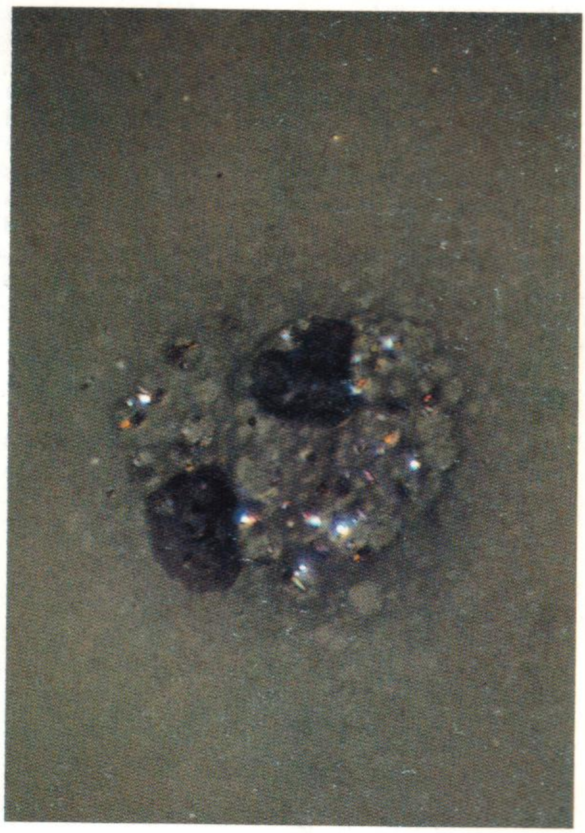

1040. Examples of Leishmania Donovani infantum in a group of macrophages from a bone marrow aspirate taken from an infected Ethiopian child. Parasites may be seen lying free as well as in the macrophages.

1041 and **1042**. Consecutive photographs of a bi-nucleated macrophage containing numerous parasites in a marrow smear from a patient infected with Leishmania Braziliensis, showing the sharp birefringence of the parasites under polarized light.

3

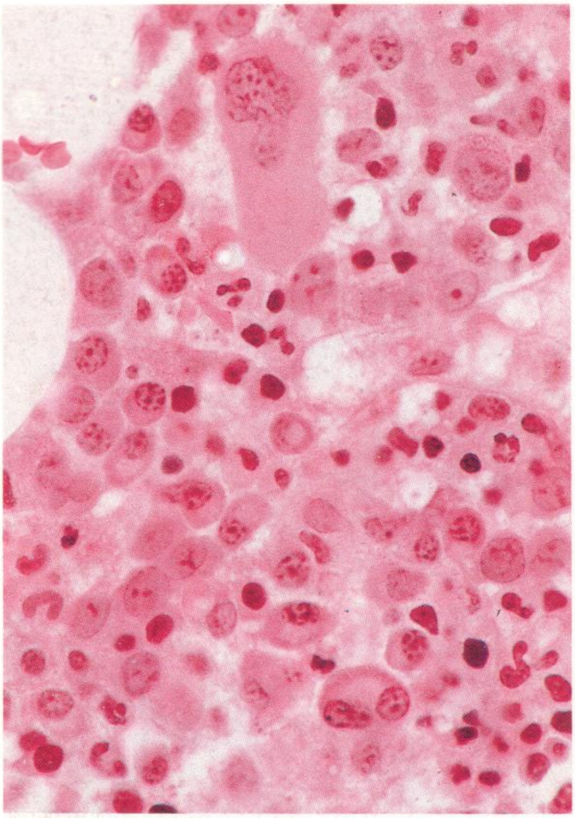

1044

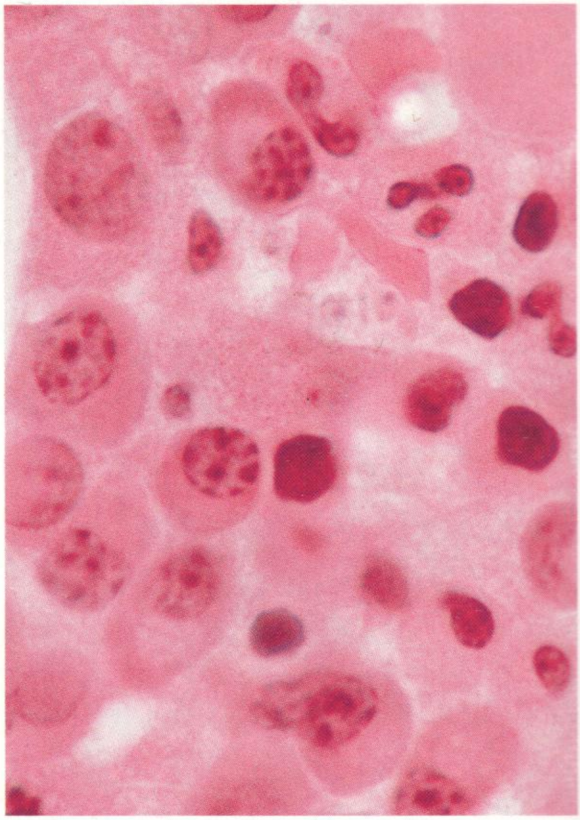

1045

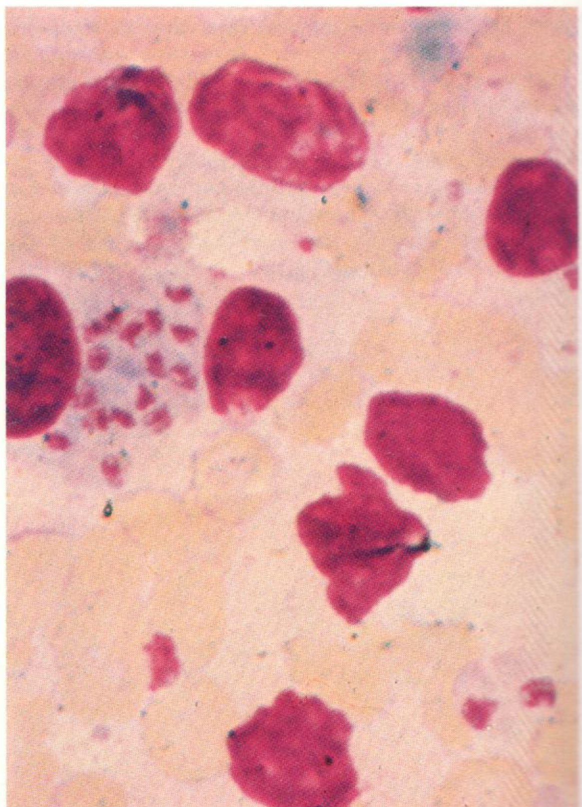

1043 and **1044**. High-power and very high-power views, respectively, of a field from a section of bone marrow trephine biopsy taken from a patient with Leishmaniasis. In **1043** the pleomorphic cytology can be seen, with conspicuous increase in plasma cells and occasional histiocytes among the normal haemopoietic tissue. The Leishmania parasites are difficult to discern in sections of bone marrow, but a group of extracellular parasites can just be distinguished in **1044**, a little to the right and above the centre of the field. The cytology of the predominant plasma cells is also well shown at this magnification.

1045. Toxoplasma within the cytoplasm of a macrophage. Two free organisms are present towards the bottom right, and other single free organisms elsewhere. Their larger size, spindle shape and banded nucleus distinguishes them clearly from Leishmania and from platelets.

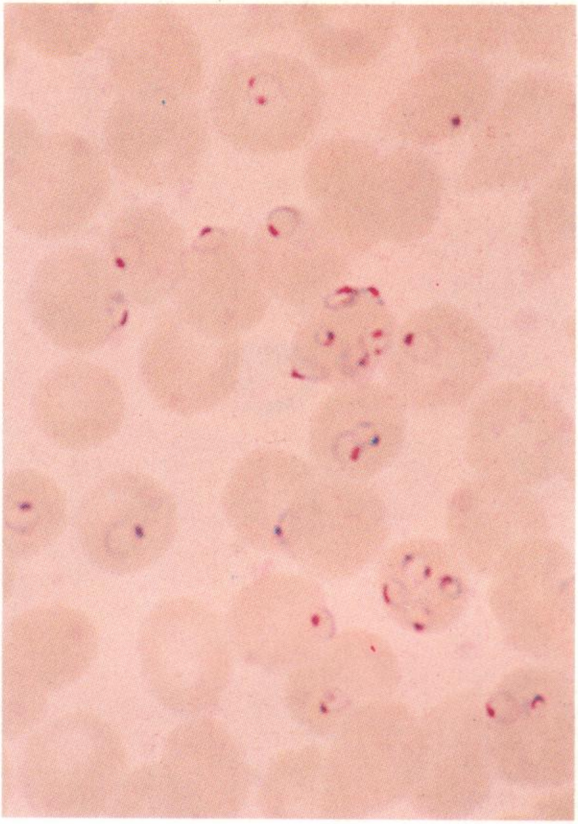

1047

1046–1048. *Plasmodium falciparum infection.*

1046. Ring form trophozoites in erythrocytes. The presence of several rings in a single erythrocyte is strongly suggestive of *P. falciparum*.

1047. Another field showing further ring forms in many red cells. There is also a monocyte in this field.

1048. Crescentic gametocytes, diagnostic of *P. falciparum*. In falciparum malaria the schizonts do not appear in the peripheral blood and only the ring-shaped trophozoites and the crescentic gametocytes are likely to be seen in blood smears.

1048

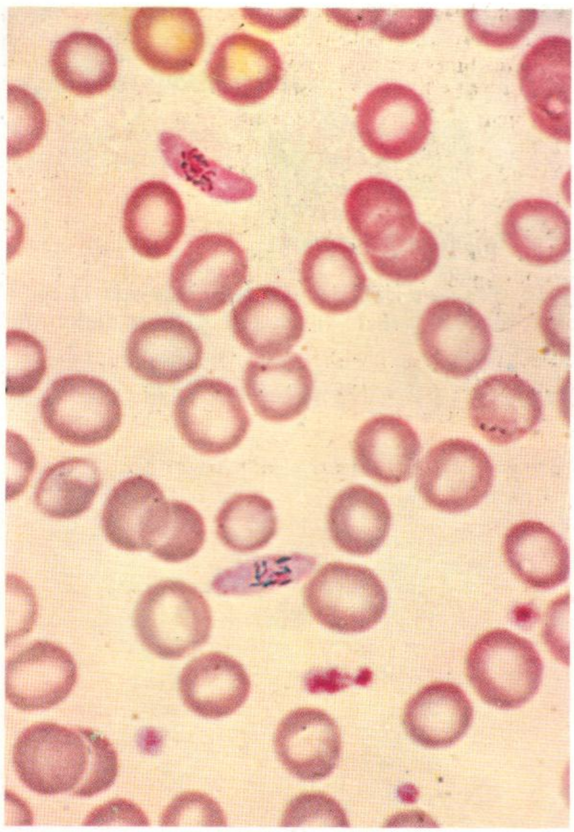

1049

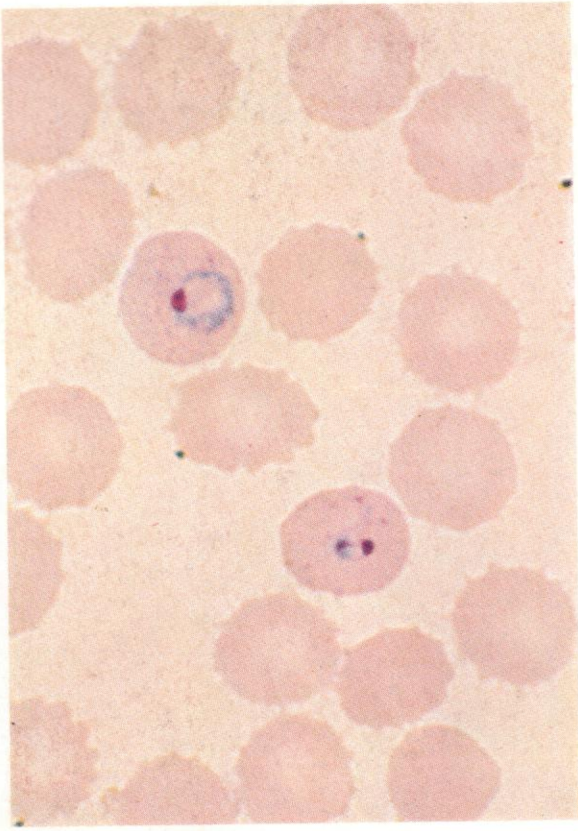

1050

1049–1052. *P. malariae infection*.

1049. Ring-form trophozoites in erythrocytes.

1050. An example of the coarse ring forms found in *P. malariae* infections (and also in *P. vivax* and *P. ovale*, but not in *P. falciparum*).

1051. Maturing trophozoite.

1052. Schizonts containing between six and 12 round merozoites, together with clumps of coarse dark brown pigment.

1051

1052

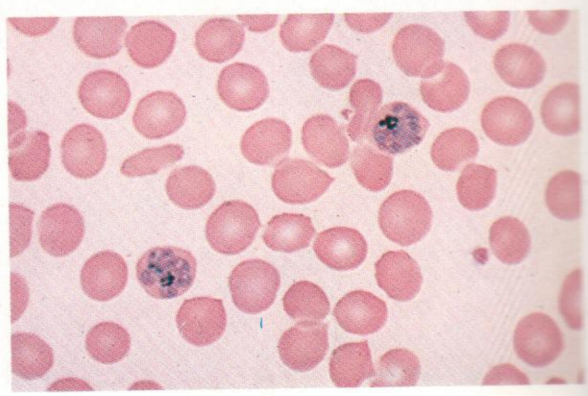

53

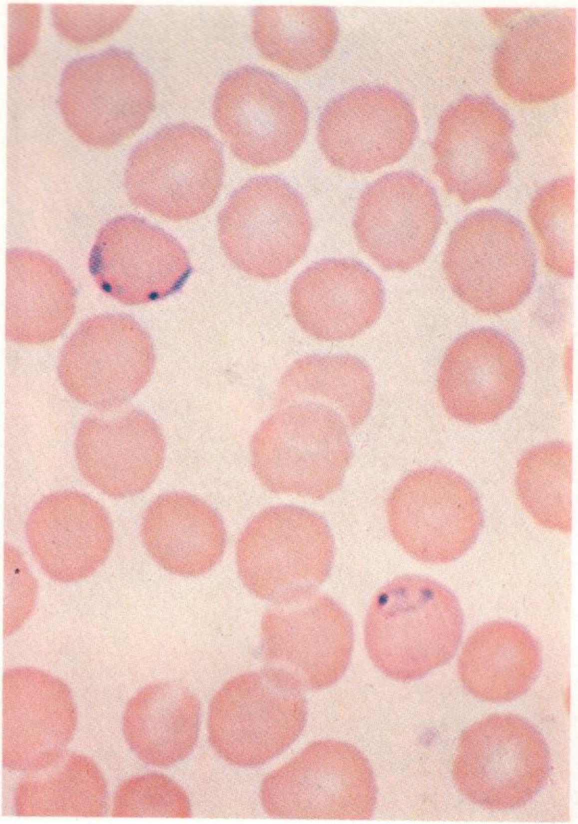

1054

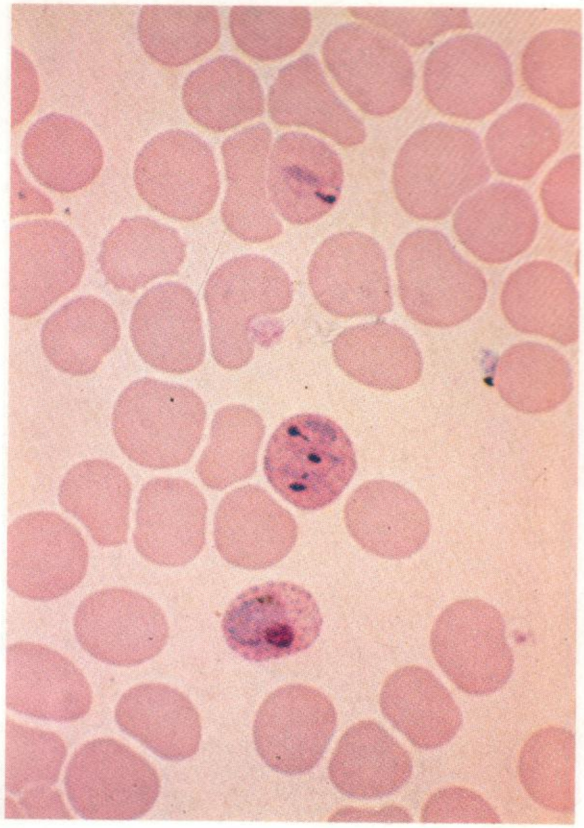

1053. Ring forms in *P. vivax* infection.

1054. Ring-form and more mature trophozoites, from *P. ovale* infection. Schuffner's dots in the erythrocytes are conspicuous, as they may also be in *P. vivax* infections.

1055. A schizont in *P. vivax* infection, containing some 20 merozoites and a quantity of dense brown pigment.

1056. *P. vivax* infection. Ring-form trophozoites, and liberation of merozoites from a fully developed schizont.

1055

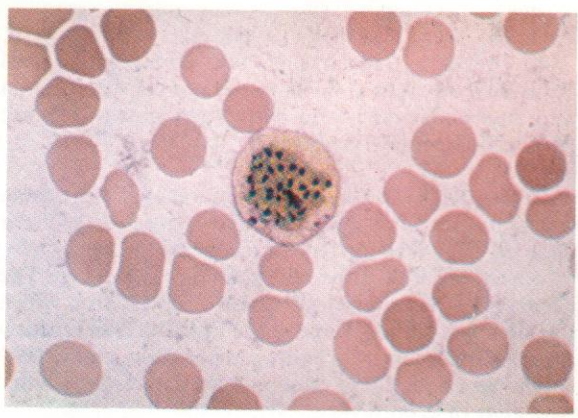

1056

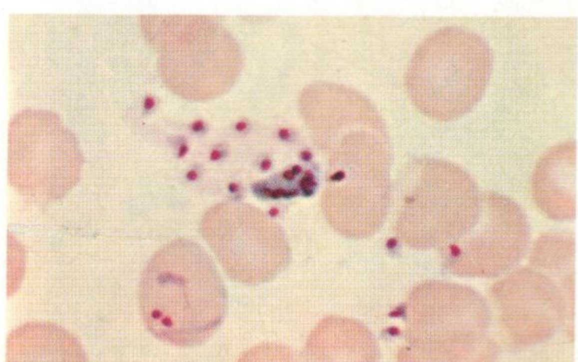

1057

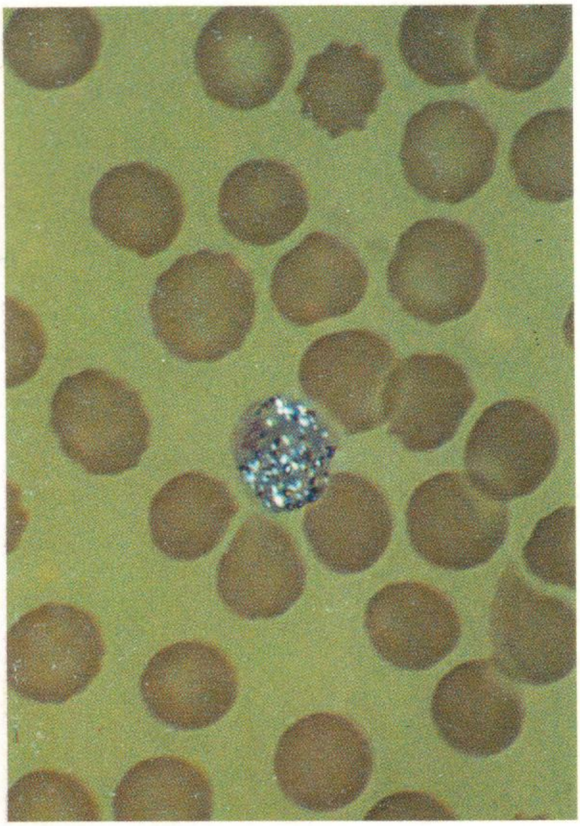

1058

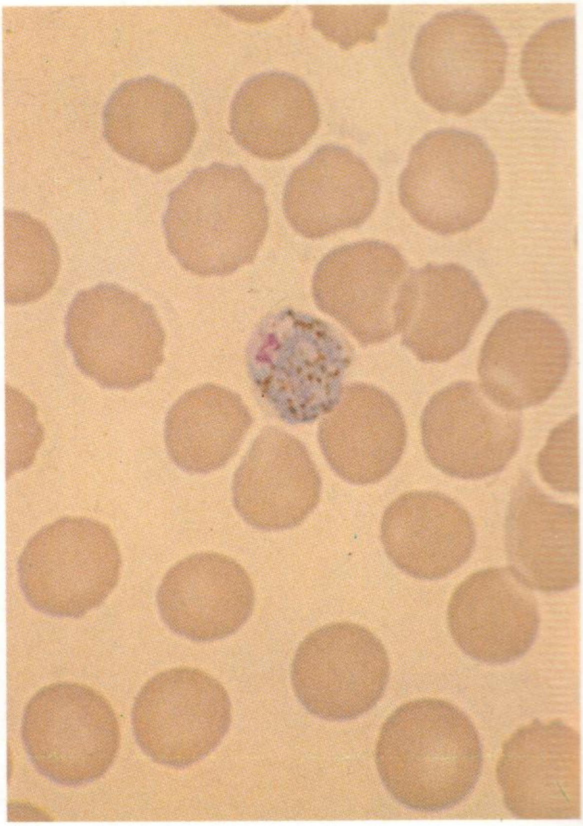

1059

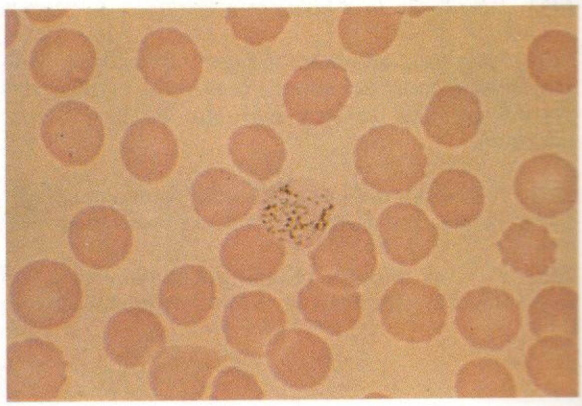

1060

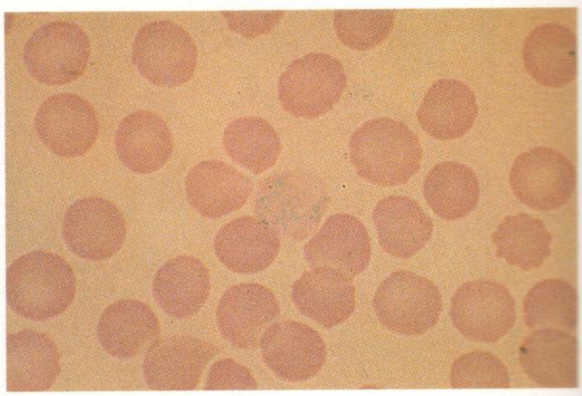

1057 and **1058**. Another example of a schizont in *P. vivax* infection, illustrating the appearance of a Romanowsky-stained smear under normal illumination and then under polarized light. The pigment dots are seen to be strongly birefringent.

1059 and **1060**. Further consecutive stains of the same schizont as shown in the previous two figures. In **1059** the slide has been restained by the Prussian blue reaction for free iron, but little or no blue staining can be seen. The pigment particles do, nevertheless, contain iron which can be rendered accessible to the Prussian blue reaction by prior treatment with hydrogen peroxide, and in **1060** a blue reaction, albeit faint, can be detected after this sequence of exposures.

61

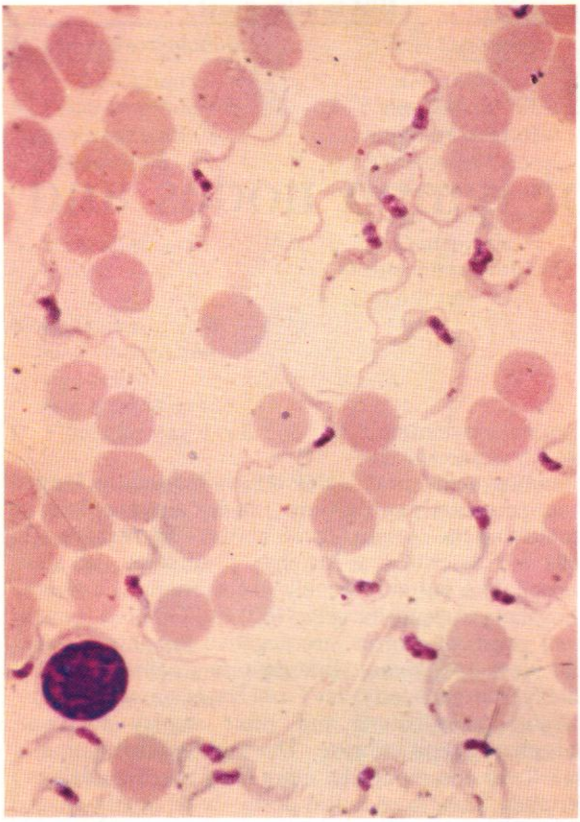

1062

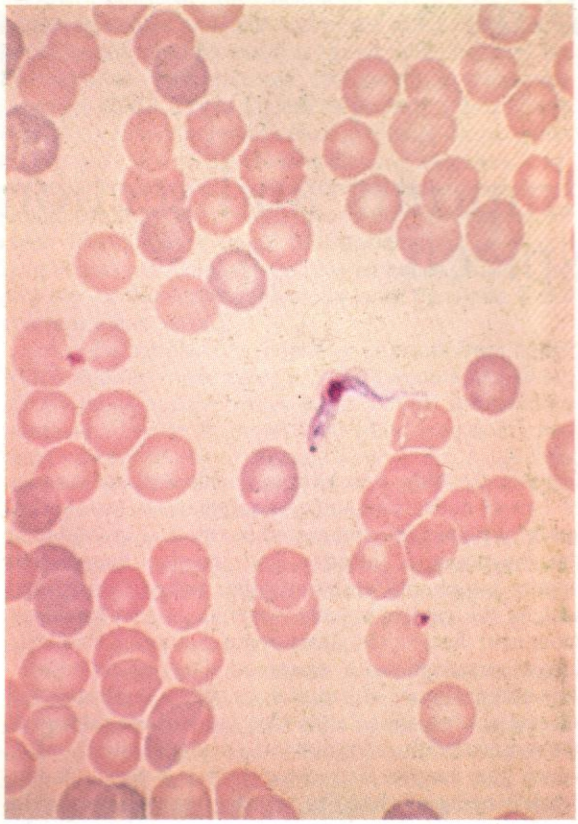

1063

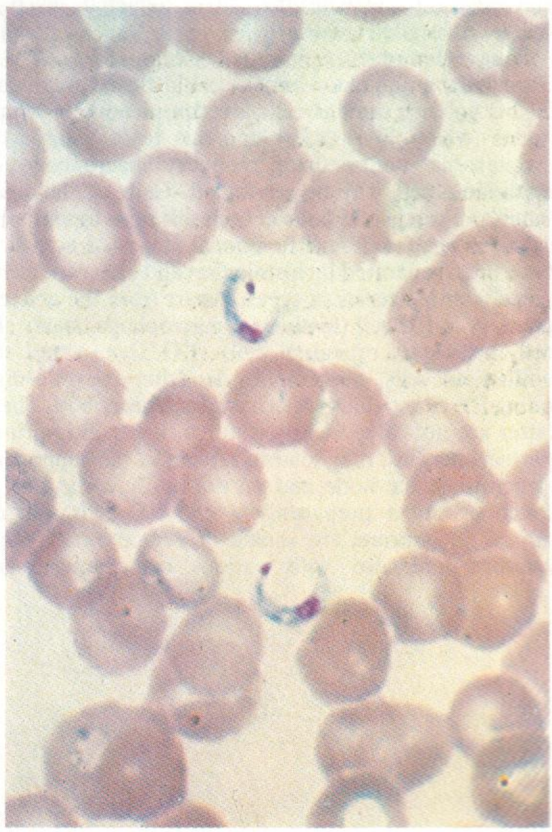

1061. *Trypanosoma gambiense,* the most important species causing African trypanosomiasis. The kinetoplast is much smaller than the central nucleus, the undulating membrane is broad and the contortions of shape variable.

1062. *T. brucei*, present in some areas of Africa, has generally similar morphology.

1063. *T. cruzi,* the cause of Chagas' disease or South American trypanosomiasis, has a much larger kinetoplast, a less conspicuous undulating membrane, and a more fixed horseshoe configuration.

Part 5

Imprints and sections of lymph nodes and spleen

Cytological study of imprint or needle aspirate samples of lymph nodes and spleen complements histological study of biopsy specimens and is especially valuable in the diagnosis of infective and reactive lymphadenopathy, lymphomas and some other metastatic tumours, and, in the case of splenic material, also in lipidoses, malignant histiocytosis and some primarily haematological disorders with extramedullary haemopoiesis. The nomenclature of lymph node cells is confusing and several systems exist. In the illustrations here, certain of the more widely used synonyms are given initially, after which the simple Kiel classification is used chiefly, readers being expected to translate as necessary. The cytological differences between lymphomas, for example, are generally clear in the slides depicted, even if semantic dispute remains.

Phagocytic reticulo-endothelial cells (RE cells) in bone marrow and blood have been illustrated previously in this volume; similar cells are conspicuous in lymph nodes where their development from monocytes through an intermediate monocyte/macrophage or epithelioid cell may be envisaged. Cells of the same family – perhaps the same cells in different topographical sites or at different functional stages of activity – have been separated by histologists and electron microscopists into a series of types. Apart from the actively phagocytic RE cell (histiocyte, macrophage, starry sky cell, histiocytic reticulum cell) (CD11b/c+) and the epithelioid cells, fibroblastic, dendritic and interdigitating RE or reticulum cells have been described. These latter are not often clearly distinguishable in imprints, perhaps because they tend to remain in the supporting structure of the node and do not easily come free in touch or smear preparations. The RE cells that do appear in imprints are shown in Romanowsky preparations and also with various cytochemical and immunocytochemical stains which frequently render them particularly conspicuous. Such stains may help in identifying the variants listed above – fibroblastic RE cells are described as strongly positive for alkaline phosphatase but only weakly so for esterases and acid phosphatase; dendritic cells (CD14+, CD23+), mostly from germinal centres, are negative for phosphatases and weak in esterase; interdigitating cells (CD40+), chiefly from extrafollicular T-cell zones, are negative for alkaline phosphatase and react weakly for acid phosphatase and esterase. The authors' impression is that these criteria are no more than rough guidelines; certainly, the cytochemical positivity of clearly phagocytic RE cells varies widely and is probably much influenced by the nature of the ingested cellular material. The degree of variability of reaction in the cell group as seen in imprints is illustrated in this section.

We have included illustrations of a wide range of malignant disorders affecting lymph nodes, from Hodgkin's disease (HD) and non-Hodgkin's lymphoma (NHL), to secondary metastases from various tumours of non-haemic cell origin. Primary lymph node tumours are often immediately diagnosable with reasonable certainty from imprints made at biopsy, and typical findings for variants of HD and NHL are provided. Histological appearances in lymph node sections are also included, particularly when the structural information they provide is necessary for, or especially relevant to, diagnostic classification. For HD, the conventionally accepted divisions into lymphocyte predominant, nodular sclerosing, mixed cellularity and lymphocyte depleted are followed, while for NHL the Kiel classification is generally used. The table here shows the conditions included in that classification, together with their equivalence to an internationally agreed 'working formulation'.

Classification of NHL

Working Formulation		Kiel Equivalent
Low grade		*Low grade*
A. Small lymphocytic, consistent with CLL. Plasmacytoid	SL	A. Lymphocytic: CLL Lymphoplasmacytic Lymphoplasmacytoid Lymphoepithelioid T-zone lymphoma
B. Follicular, small cleaved	F-SC	B./C. Centrocytic/ centroblastic follicular and diffuse
C. Follicular, mixed small cleaved and large cell	F-M	
Intermediate grade		
D. Follicular, large cell	F-L	D. Centroblastic/centrocytic follicular or diffuse
E. Diffuse, small cleaved	D-SC	E. Centrocytic, diffuse
F. Diffuse, mixed small and large cell +/− sclerosis/epithelioid cells	D-M	F. Centrocytic/centroblastic diffuse
		High grade
G. Diffuse large cell	D-L	G. Centroblastic, diffuse
High grade		
H. Immunoblastic, large cell (plasmacytoid, polymorphous, +/− epithelioid cells)	IB	H. Immunoblastic (B or T) CD 30 (ki−1)+large cell anaplastic, T or B
I. Lymphoblastic, convoluted non-convoluted	LB	I. Lymphoblastic convoluted T-cell unclassified
J. Lymphoblastic, small non-cleaved Burkitt cell type	SNC	J. Lymphoblastic, Burkitt cell type (B-cell)

Miscellaneous: Mycosis fungoides and Sézary syndrome (T-cell), extramedullary plasmacytoma (B-cell), histiocytic and non-classifiable lymphomas.

Descriptions of the histology and cytology of lymphoid tissues and cells and of the reactive and neoplastic conditions illustrated are given in further detail in the captions. Chromosome abnormalities frequently occur in NHL. These include especially t(14;18) and t(11;14) in follicular lymphomas, involving the bcl genes on 18q and 11q with the H-chain locus on 14q; the t(8;14) of Burkitt's lymphoma and lymphoblastic lymphomas of similar cytology, involving c-myc on 8q with the same H-chain locus; and a range of translocations in T-cell lymphomas involving the various tcl genes on 10q, 11p and 14q, or the c-myc gene on 8q, with the alpha T-cell receptor locus on 14q.

Several examples of sections or imprints from nodes with secondary metastases of solid tumours are given, mostly from node biopsies made before the primary tumour had been diagnosed and when lymphoma had been suspected. Since haematologists are frequently involved in the interpretation of such node biopsies, an appropriate range is illustrated here.

Needle biopsy of the spleen may occasionally be diagnostically valuable in conditions such as lipidoses and certain tropical diseases like Leishmaniasis; a few illustrative examples of the appearances of spleen aspirates or imprints are provided.

The occurrence of leukaemic or lymphomatous infiltration in pleura, peritoneum or meninges, may lead to the presence of neoplastic cells in pleural, ascitic or cerebrospinal fluids. The neoplastic cells which may be seen in centrifuged deposits from these fluids look much as they do in buffy coat preparations from blood or in marrow, as illustrated already in earlier sections of this atlas. They are accordingly not shown again here, but some illustrations are given of pleural lining cells, which must be differentiated from neoplastic ones.

1064

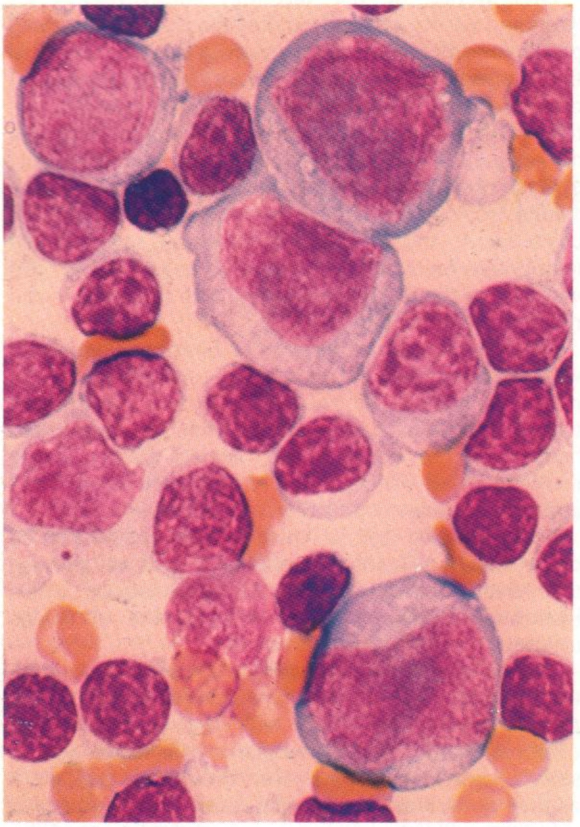

1065

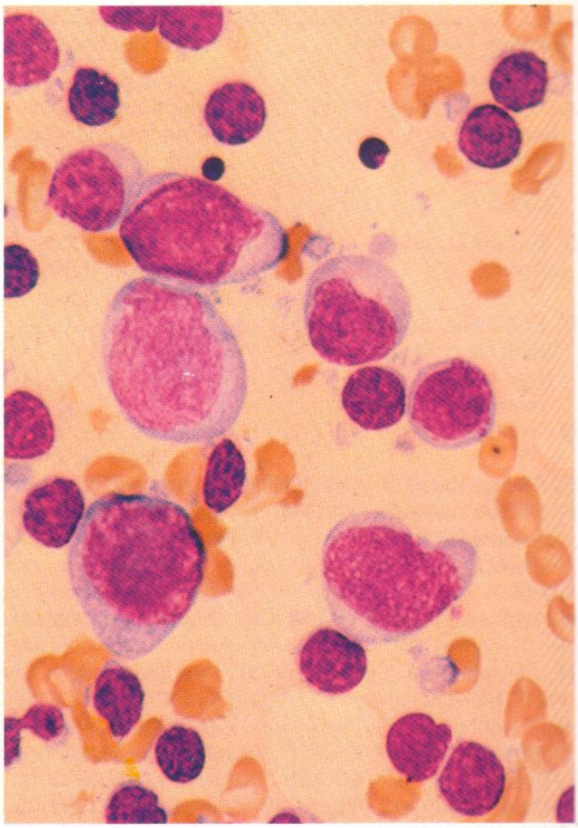

1066

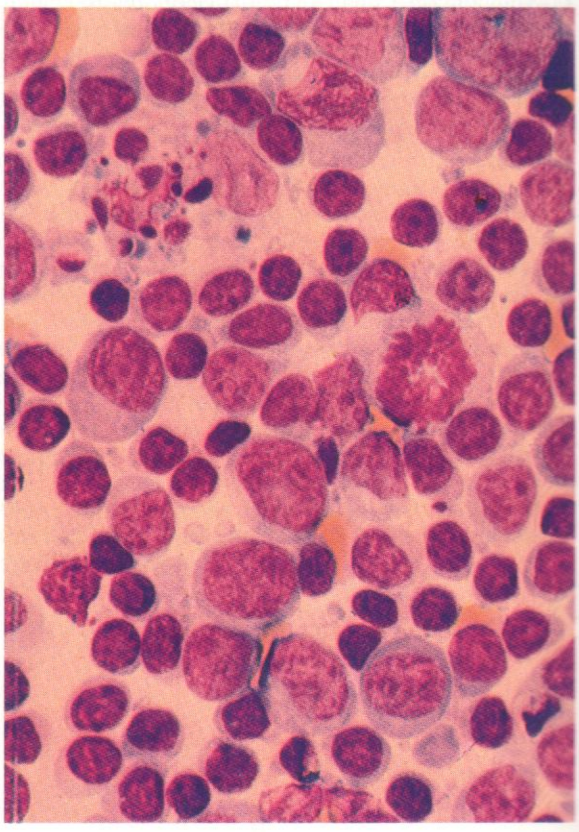

1064. Leishman stain: lymph node imprint: showing three large immunoblasts with ample basophilic cytoplasm, and generally primitive nuclei with nucleoli more centrally than peripherally situated; a somewhat smaller centroblast or large follicular centre cell, top left, with higher nuclear–cytoplasmic ratio but also with cytoplasmic basophilia and three nucleoli more towards the periphery of the nucleus; mature lymphocytes appear above and below the centroblast near the lowest immunoblast; there is a single plasma cell near the central immunoblast and a monocyte/macrophage with a small inclusion at the left of the field. The remaining cells are centrocytes or small follicular centre cells (FCC).

1065. Leishman stain: lymph node imprint: seven immunoblasts illustrate the range of size and cytology in this group. The remaining cells in this field are mostly mature lymphocytes.

1066. Leishman stain: lymph node imprint: a collection of cells from the follicular centre area of a lymph node imprint in reactive hyperplasia secondary to infection. Against a background of small mature lymphocytes are occasional small follicular centre cells (centrocytes) and about a dozen large FCCs or centroblasts with nucleoli and some cytoplasmic basophilia. In the upper right corner are several immunoblasts, and to their left a histiocytic RE cell and a plasma cell.

7

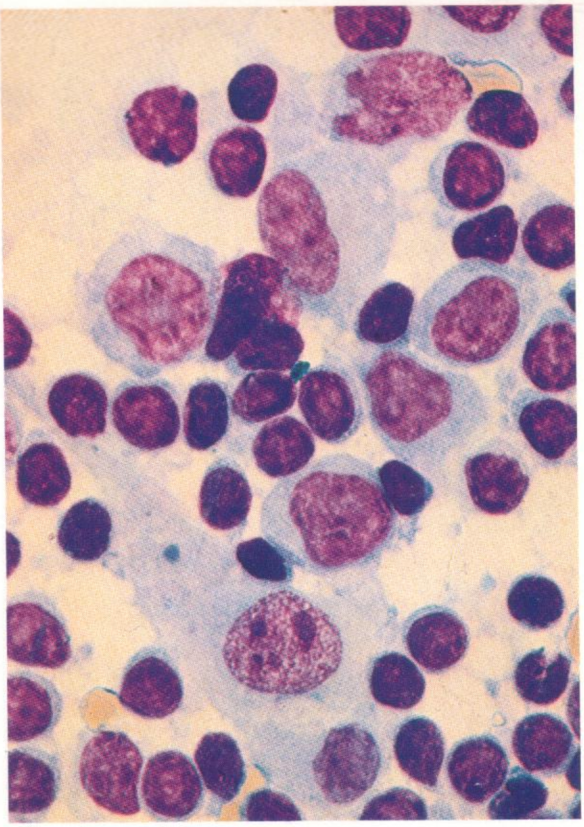

1068

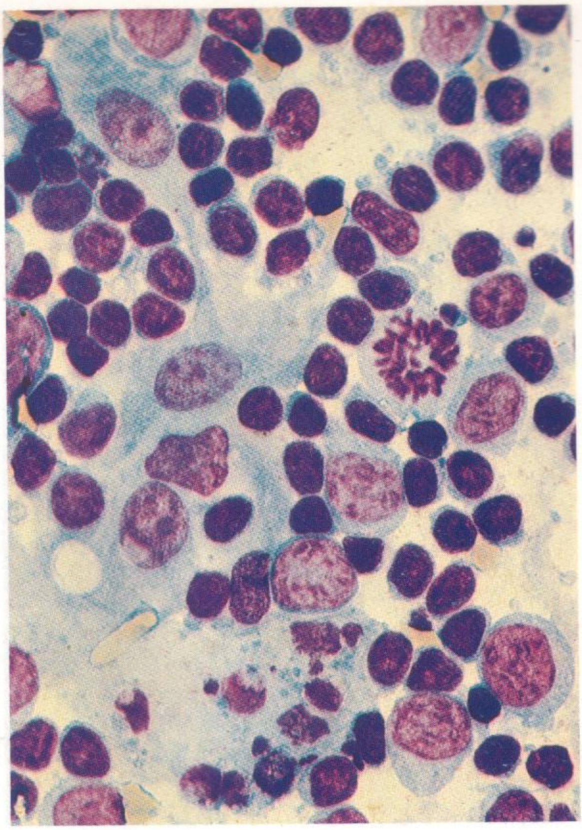

1069

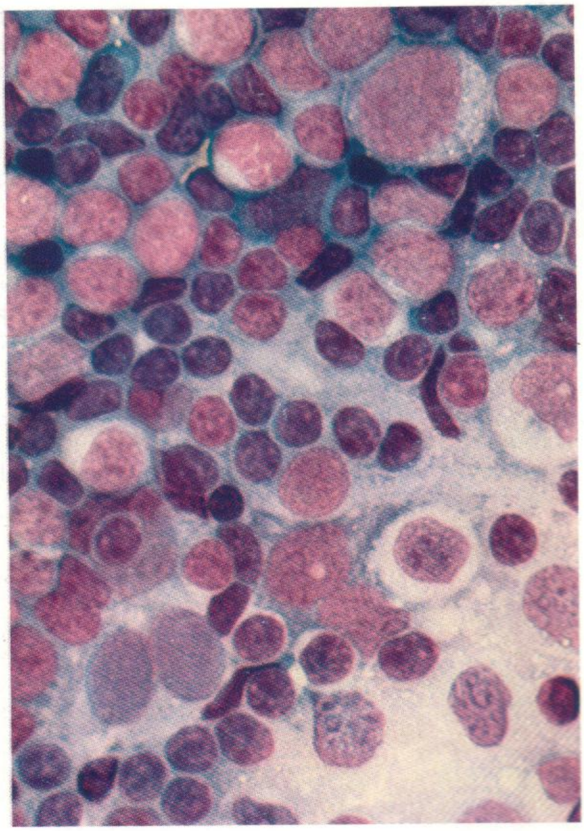

1067. Leishman stain: lymph node imprint: field to illustrate seven large cells involved in a sequence of probable developmental changes along the monocyte-epithelioid cell-macrophage (RE cell) line. The remaining cells in this field are chiefly small lymphocytes.

1068. Leishman stain: lymph node imprint: an example of an epithelioid cell cluster in a lymph node showing a reactive hyperplasia secondary to toxoplasma infection. Around the cluster are chiefly lymphocytes but with a histiocytic RE cell (starry sky cell) at the bottom and six large mononuclear cells, one in mitosis, at the centre and lower right of the field. These cells are probably immunoblasts.

1069. Leishman stain: lymph node imprint: RE cells, perhaps of the interdigitating variety, with little evidence of phagocytosis, but with neighbouring lymphocytes, occupy much of the lower half of this field. Two are binucleated, the left with an adjacent probable tissue mast cell and the right with a more basophilic cytoplasm than usual. The upper half shows a mixture of small lymphocytes with dense nuclei and follicular centre cells or centrocytes with more open nuclei, showing transition towards centroblasts and with a single immunoblast towards the top right corner.

1070

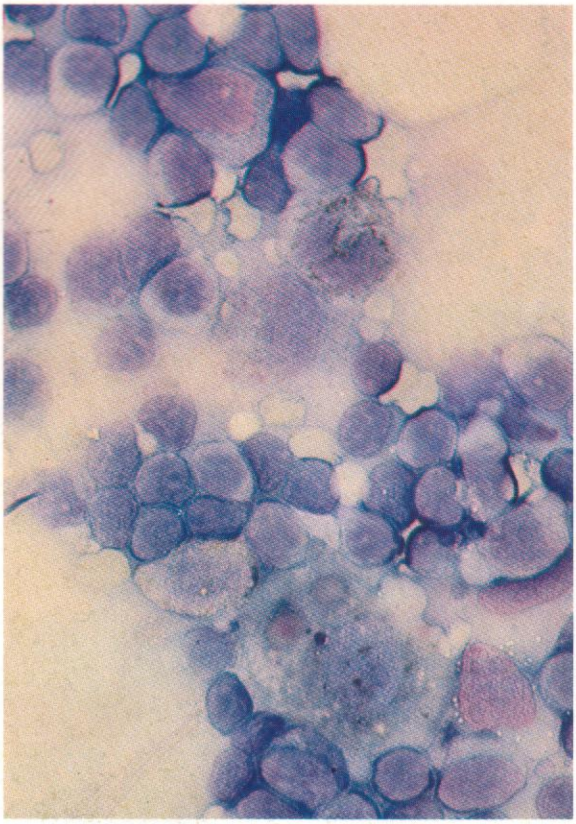

107

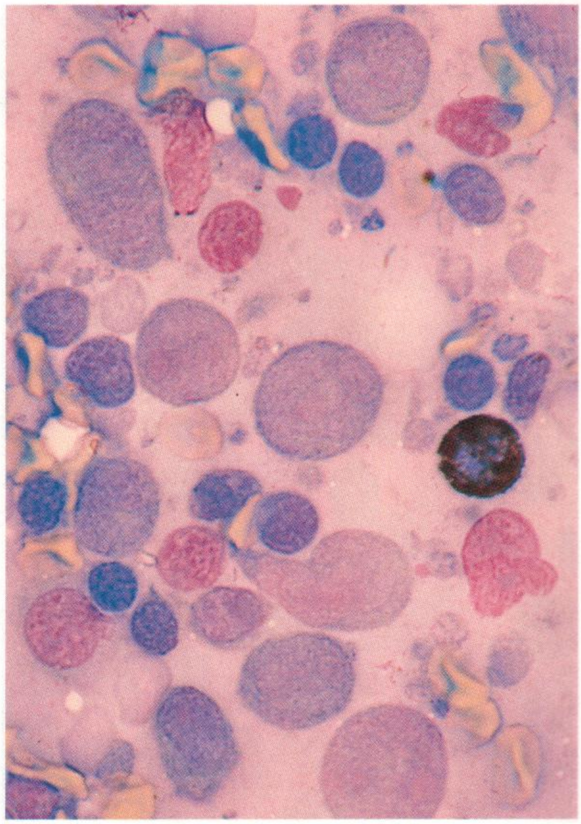

107

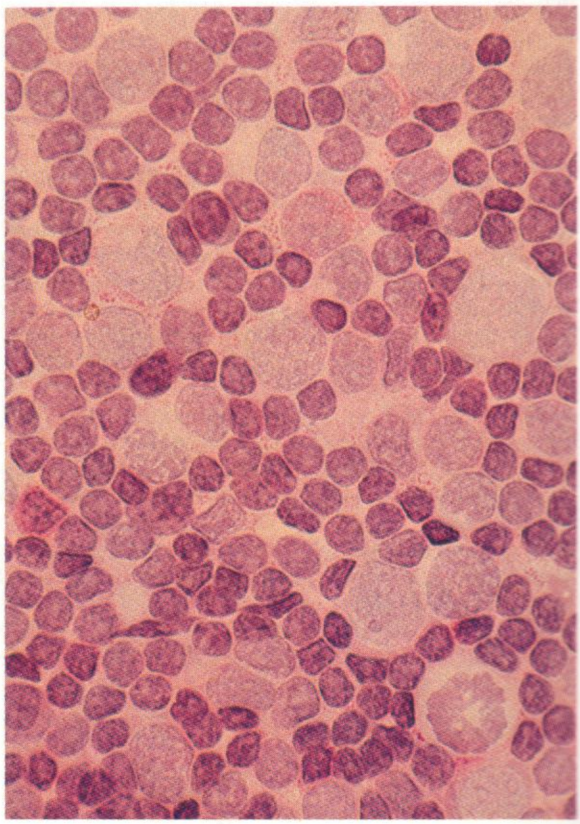

1070. SB stain: lymph node imprint: Sudan black positivity is shown in a histiocytic RE cell and in three cells of the monocyte-macrophage line. All lymphoid elements are negative.

1071. SB stain: lymph node imprint: positivity is shown in a neutrophil polymorph. The remaining cells, including macrophages, centrocytes, centroblasts and immunoblasts, are all SB-negative.

1072. PAS reaction: lymph node imprint: this preparation from the same node as in **1069** shows fine granular positivity in a few mononuclear cells only. One on the left is probably an RE cell of the interdigitating type with granular PAS positivity spreading out in the cytoplasmic prolongations between neighbouring cells. Two other positive cells towards the top of the field are, respectively, a centroblast and a centrocyte. A very occasional lymphocyte also shows detectable granular positivity.

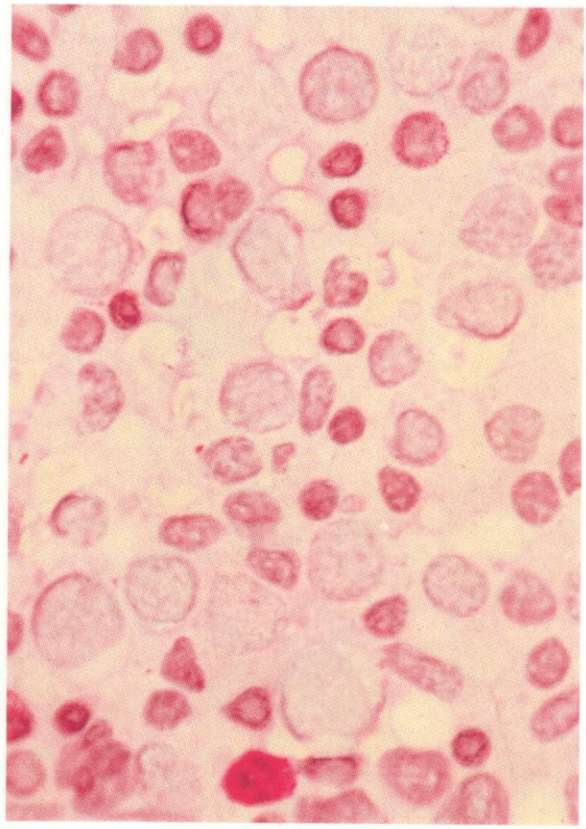

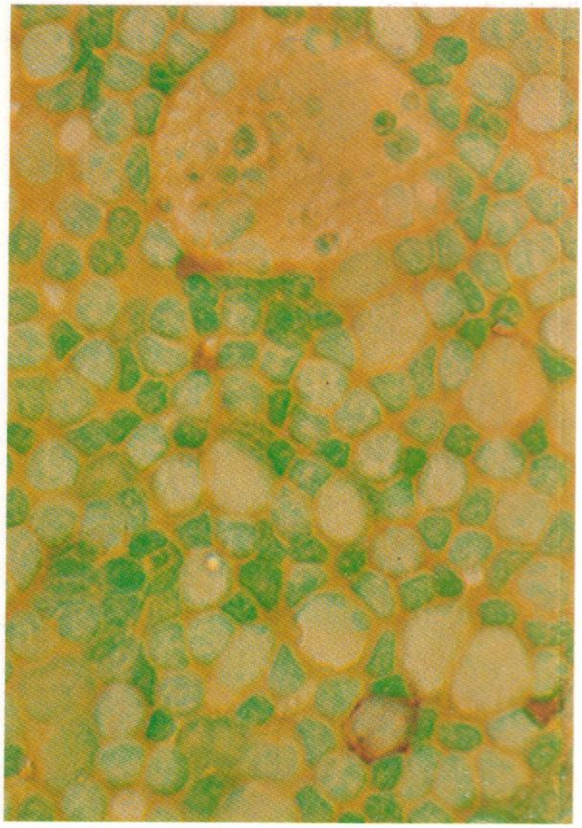

1074

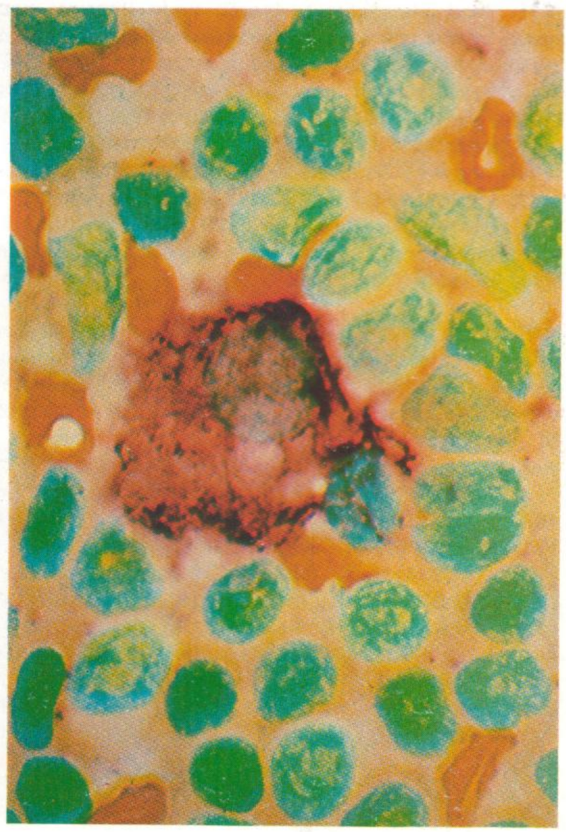

1075

1073. PAS reaction: lymph node imprint: this preparation shows normally positive reactions in neutrophil polymorphs but generally negative reactions in lymphocytes, centrocytes and centroblasts, although there is a single small block of PAS-positive material in one lymphocyte just below the centre of the field, and weak diffuse or finely granular reactions in the narrow cytoplasmic rim of each of two larger cells, probably centroblasts, above the centre.

1074. Alkaline phosphatase: lymph node imprint: this preparation from a reactive node shows lymphocytes, centrocytes, centroblasts and immunoblasts all to be negative for this enzyme, while a single neutrophil polymorph shows ++ positivity and a large phagocytic RE cell is only very weakly positive – despite its obvious past ingestion of various other cell types, probably including a neutrophil.

1075. Alkaline phosphatase: lymph node imprint: strong positivity is manifest in a phagocytic RE cell with ingested cellular remnants: positively reacting fibrils spread out over a neighbouring lymphocyte to give it a spurious appearance of positivity.

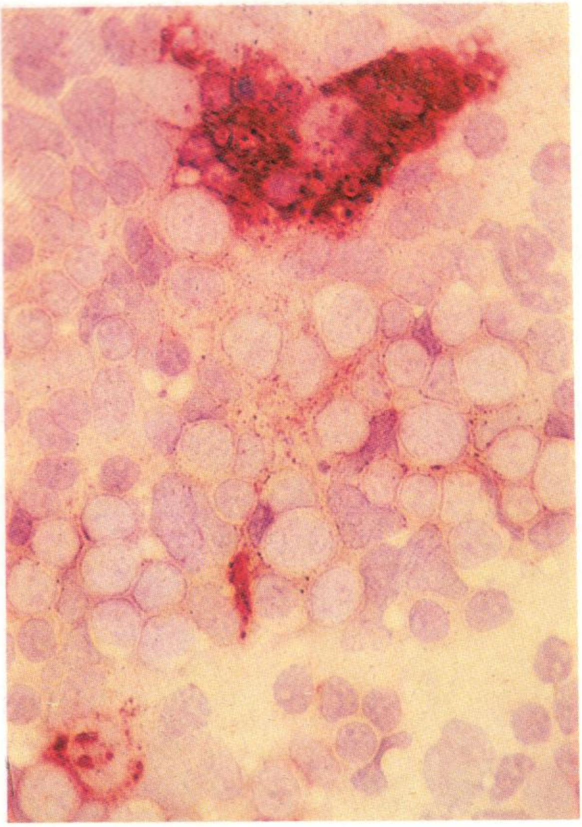

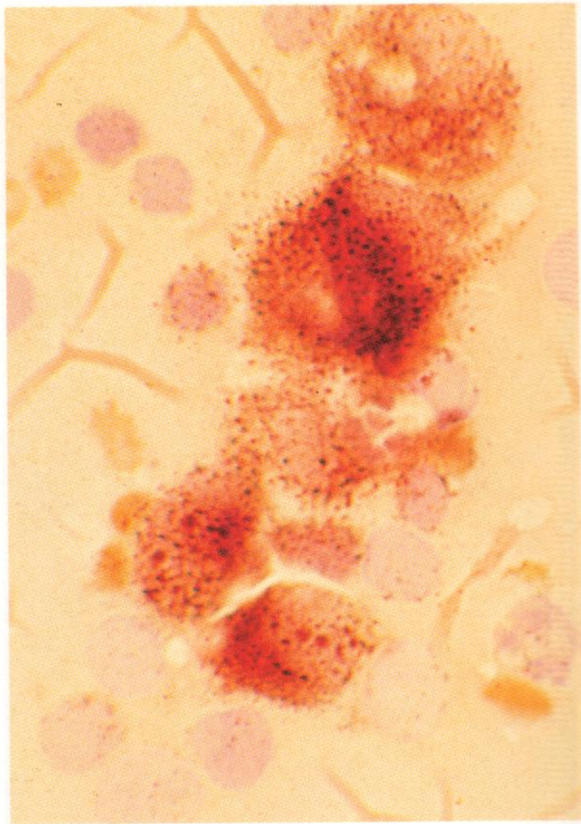

1077

1076. Acid phosphatase: lymph node imprint: very strong positivity is seen in a phagocytic RE cell containing much ingested material, while at the opposite corner of the field a smaller monocyte–macrophage shows less intense but still striking positivity. Most of the remaining cells are of the lymphocyte, centrocyte, centroblast family and show no more than occasional weak granular positivity, but between the cells spreads a network of positively reacting fibrils probably derived from the larger histiocytic RE cell or perhaps from an inconspicuous dendritic RE cell.

1077. Acid phosphatase: lymph node imprint: several strongly positive RE cells of variable size and shape are seen against a background of lymphocytes. These show variable scattered positivity without any clear example of T-cell type focal paranuclear reaction. There is a weakly positive polymorph at the lower right.

1078. Acid phosphatase: lymph node imprint: a phagocytic or histiocytic RE cell with much ingested material (starry sky cell) shows relatively little acid phosphatase positivity in contrast to a more strongly positive monocyte or epithelioid cell. Lymphocytes here show mostly either negative or scattered granular reactions and there are two large mononuclear cells, with variable weak granular positivity, which are probably immunoblasts. At the lower right corner is a positively reacting plasma cell.

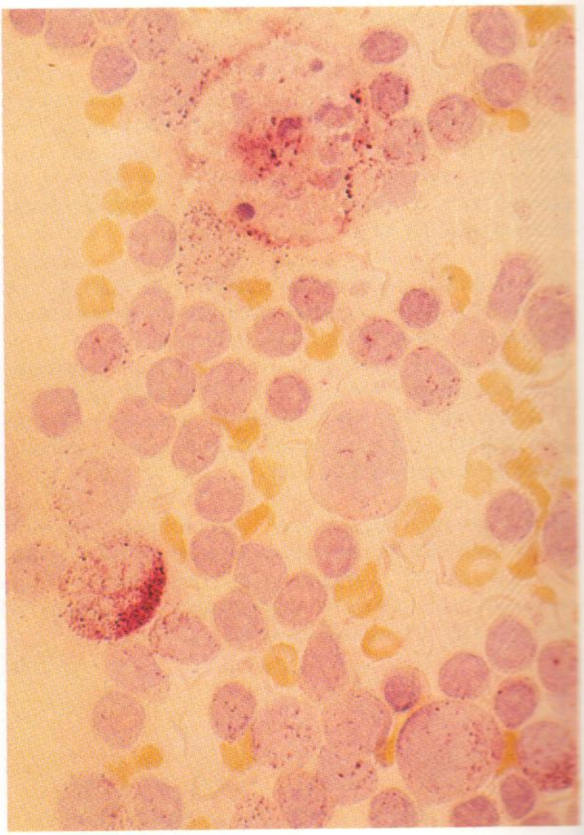

1078

79

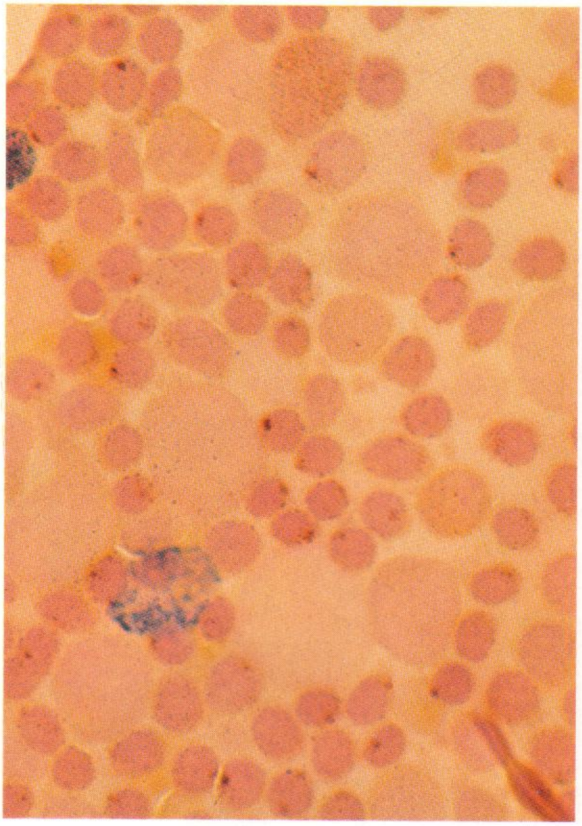

1080

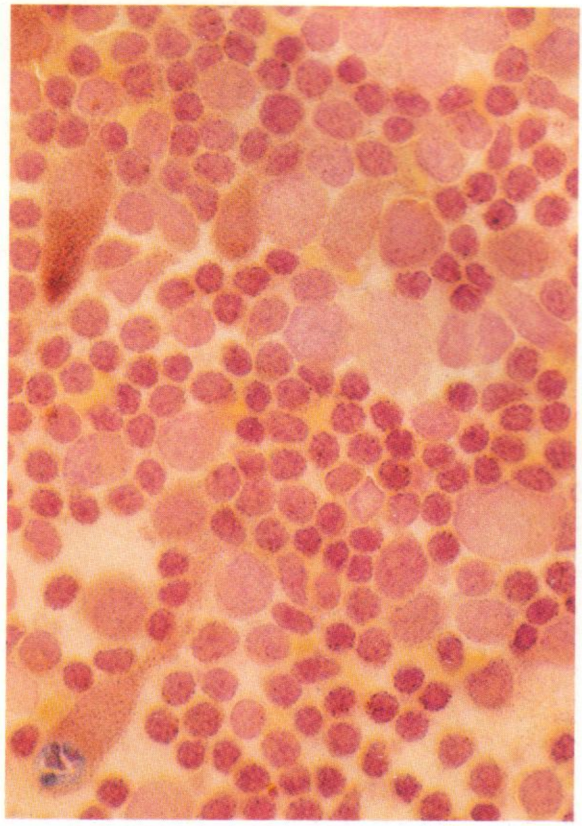

1079. Dual esterase reaction: lymph node imprint: this preparation shows chiefly cortical area Tμ lymphocytes, with strong localized dots of butyrate esterase (BE) positivity, surrounding larger cells of the monocyte–macrophage system, only one of which shows moderately strong BE positivity, the remainder being almost negative with only a few chloroacetate esterase (CE) positive granules. A normally CE-positive polymorph is present.

1080. Dual esterase reaction: lymph node imprint: BE positivity of moderate-to-strong degree in epithelioid cells in this case. One has ingested a CE-positive neutrophil. Most lymphocytes here do not show the localized Tμ type of BE positivity and are presumably chiefly B cells.

1081 and **1082**. Dual esterase reaction: lymph node imprint: these fields from the same case of reactive hyperplasia show strong BE positivity in RE cells probably of the histiocytic or phagocytic variety, weaker reactions in occasional monocyte–macrophage cells, and localized dot-like positivity in certain lymphocytes, presumably of the Tμ subset. A probable dendritic RE cell with long intercellular processes but rather weak BE positivity is also shown in **1082**.

1081

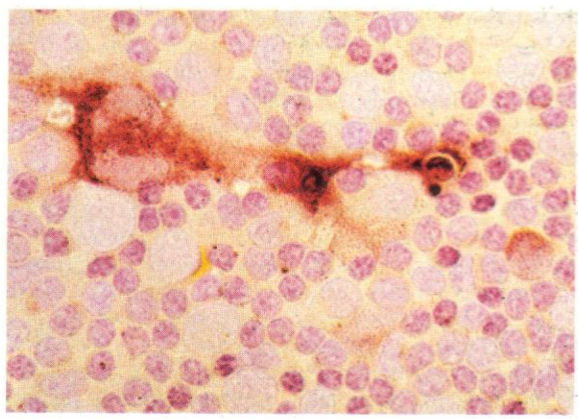

1082

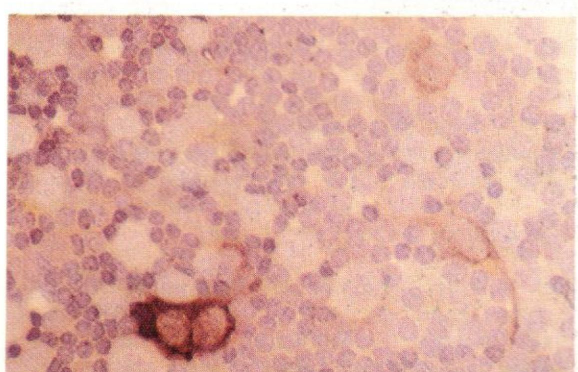

1083

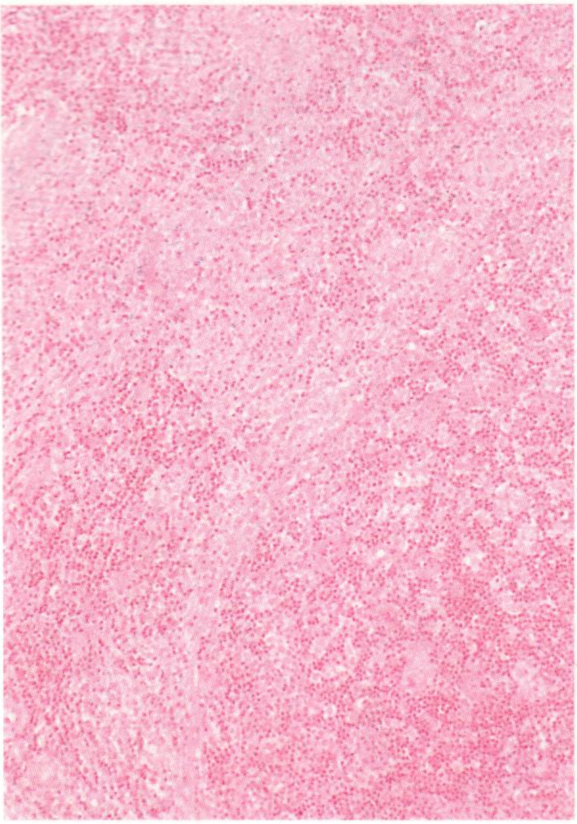

108

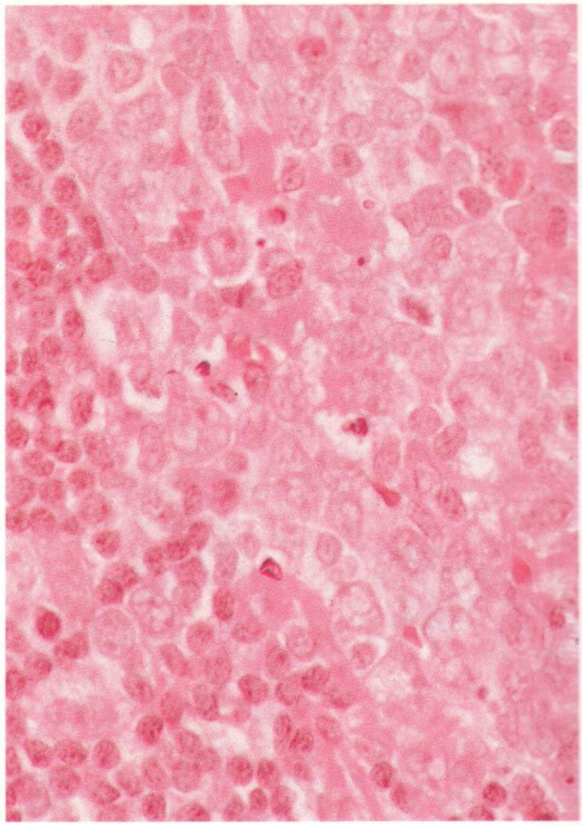

10

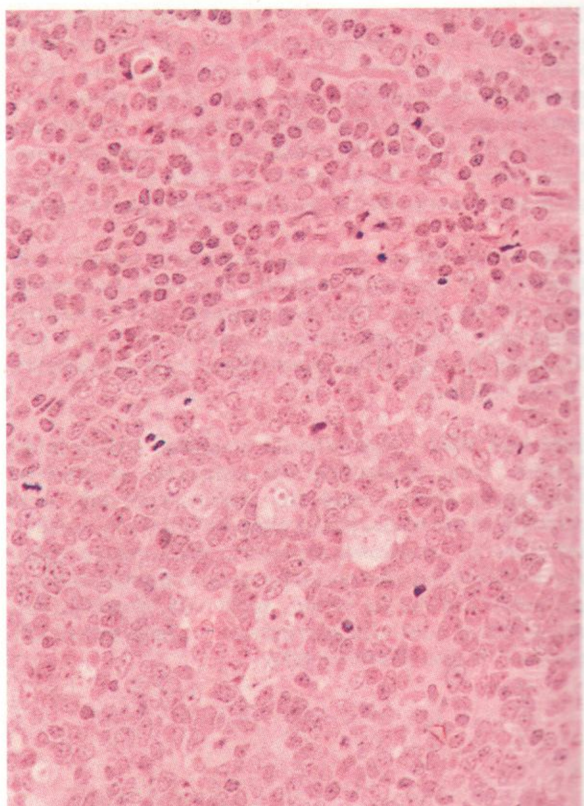

1083–1096. *Sections and imprints from lymph node biopsies taken from patients with toxoplasmosis. The protozoan parasite, although more easily detected in imprints, is not often identifiable in sections, but the histological picture is sufficiently characteristic to suggest the diagnosis in most cases.*

1083. A low-power view of a lymph node section from a patient with toxoplasma infection. The histological picture is a mixed one, with distended sinuses including a marked proliferation of histiocytes, and with further histiocytic hyperplasia in the paracortical areas, but also with follicular hyperplasia and numerous activated B cells appearing as immunoblasts and plasmacytoid cells. In this field the paler areas represent grossly dilated sinuses within the cortex.

1084. A higher-power field from the same area as shown in **1083**, illustrating the paracortical lymphocytes to the left and the dense accumulation of reactive histiocytes in the dilated sinus to the right. The pale vesicular nuclei of the monocytoid histiocytes and the frequent presence of ingested material in their cytoplasm are clearly visible here, while similar large histiocytes are occasionally to be seen among the paracortical cells.

1085. Another high-power field from a different area in the same node, showing the edge of a hyperplastic follicle, sharply demarcated from the parafollicular lymphoid cuff, but with numerous large histiocytes.

1086
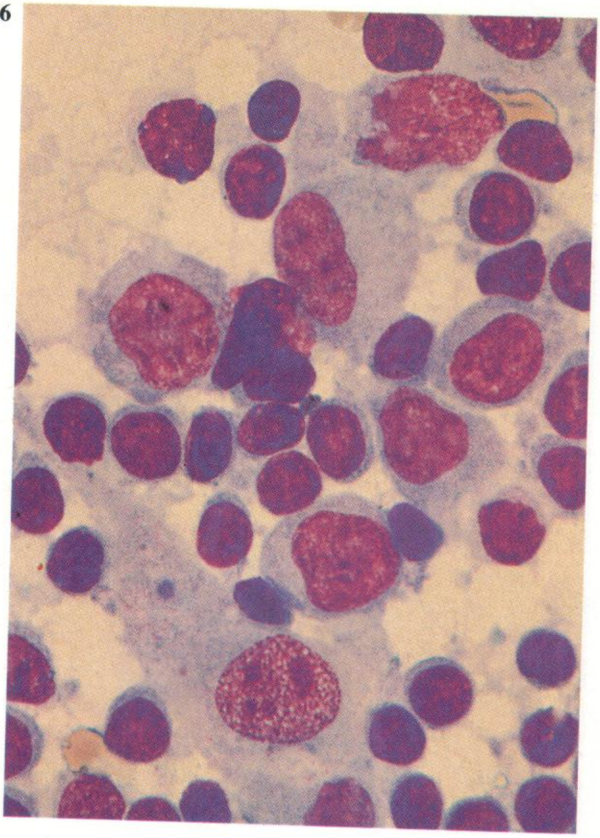

1087
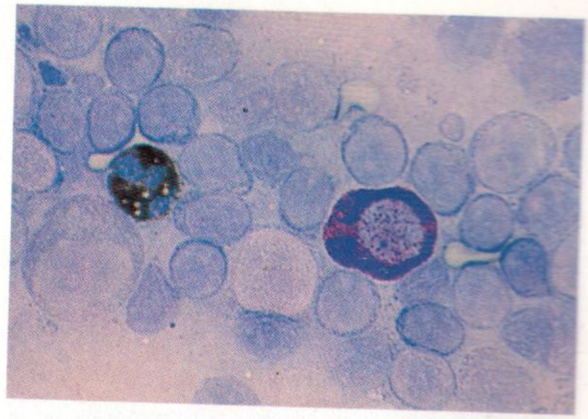

1088
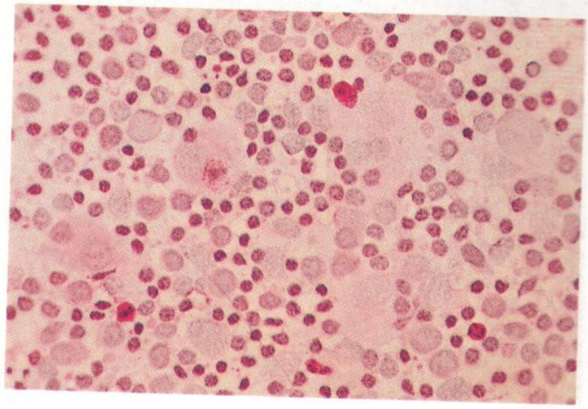

1089
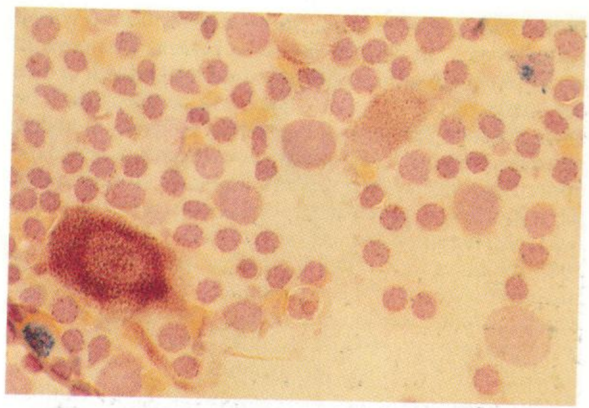

1090
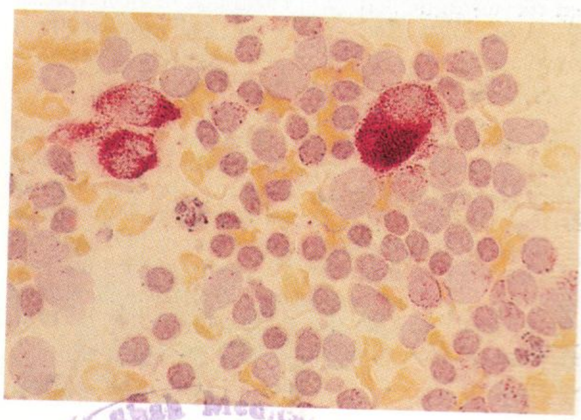

1086–1090. Imprints from a lymph node biopsy taken from another patient with toxoplasma infection, showing the cytology and cytochemistry of the reactive process. The cells in the Romanowsky preparation in **1086** include a macrophage with spreading cytoplasm and several monocytoid cells surrounded by a predominance of lymphocytes. In the SB-stained field shown in **1087** there is a single normally sudanophilic neutrophil and a metachromatically staining tissue mast cell, while all the remaining cells, including immunoblasts and monocytoid macrophages, are SB-negative. The PAS-stained field illustrated at lower power in **1088** again has a mixed cytological content, with a few scattered PAS-positive neutrophils, including one within the cytoplasm of a macrophage, and various lymphocytes, centroblasts and immunoblasts, as well as the conspicuous large monocytoid macrophages. Apart from the neutrophils, most cells here appear PAS-negative, or with no more than a weak cytoplasmic tinge of reactivity, visible in some macrophages. In both the dual esterase and the acid phosphatase reactions shown in **1089** and **1090** the macrophages and their monocytic precursors are picked out by their positive reactions, that for BE contrasting with the CE reaction of neutrophils in **1089**. The majority of the lymphoid elements are negative for both reactions, in conformity with their predominantly B-cell lineage.

1091 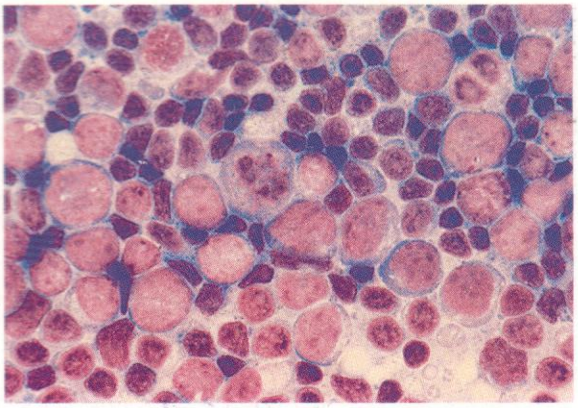

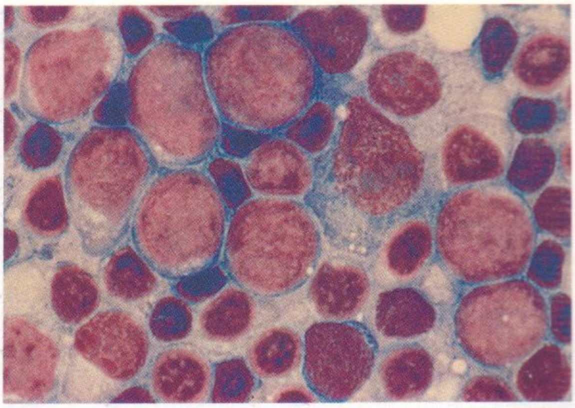 1092

1093 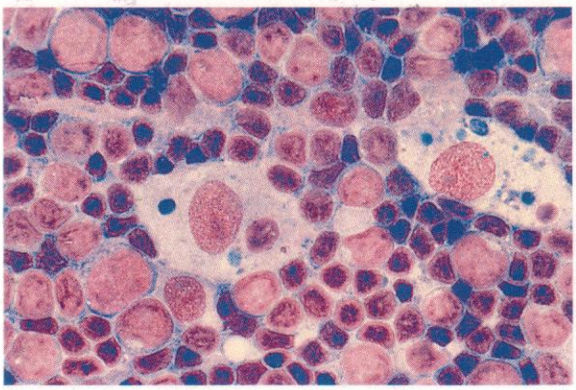

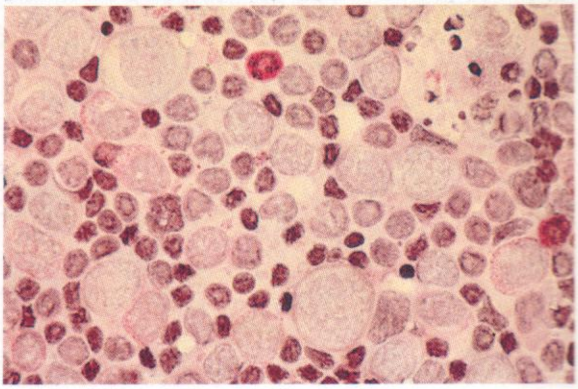 1094

1091–1094. Imprints from another toxoplasmal lymph node biopsy. In **1091** there is a central monocytoid macrophage surrounded by immunoblasts, which in turn are surrounded by lymphocytes and centrocytes. The more detailed cytology of these cells is shown at higher power in **1092**, with two monocytoid macrophages to the upper right, and with eight immunoblasts around and to the left of them, plus a centroblast at mid-bottom of the field, and lymphocytes and centroblasts peripherally. In **1093**, against a similar cytological background, there are two mature macrophages containing ingested material which includes nuclear debris but also elliptical toxoplasma protozoa. The PAS stain in **1094** shows two strongly PAS-positive neutrophils, mostly negative immunoblasts, granular cytoplasmic positivity in three centrocytes to the left of the field and in a centroblast below the right-hand neutrophil, and positivity in a toxoplasma parasite among other cellular debris in a macrophage at the top right corner.

1095 and **1096**. Lymph node imprints, from a patient with recurrence of lymphadenopathy ten years after initial diagnosis of toxoplasmosis. The presence of immunoblastic and monocyte–macrophage proliferation with numerous mitoses, apparent in **1095**, and the multinucleated macrophage with much ingested material, including a probable toxoplasma organism at the extreme right of the cytoplasm, visible in **1096**, confirms persistence or recurrence of the disease.

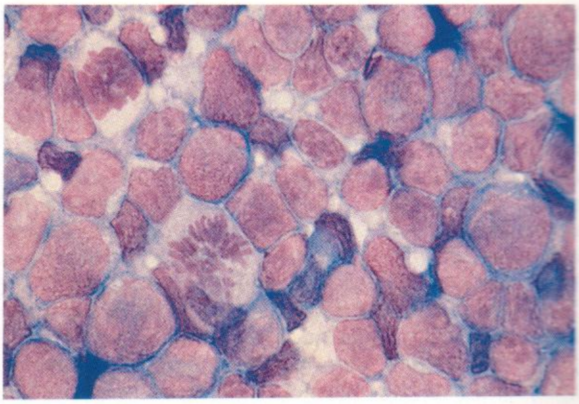 1095

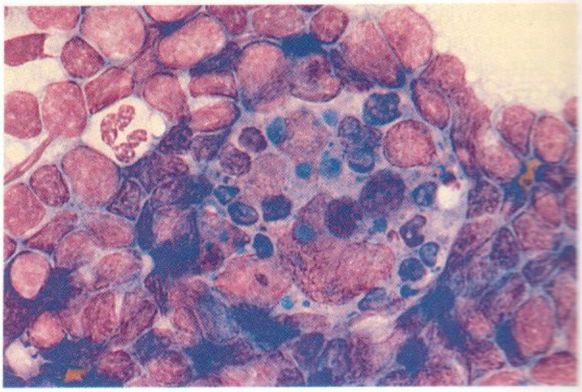 1096

1097

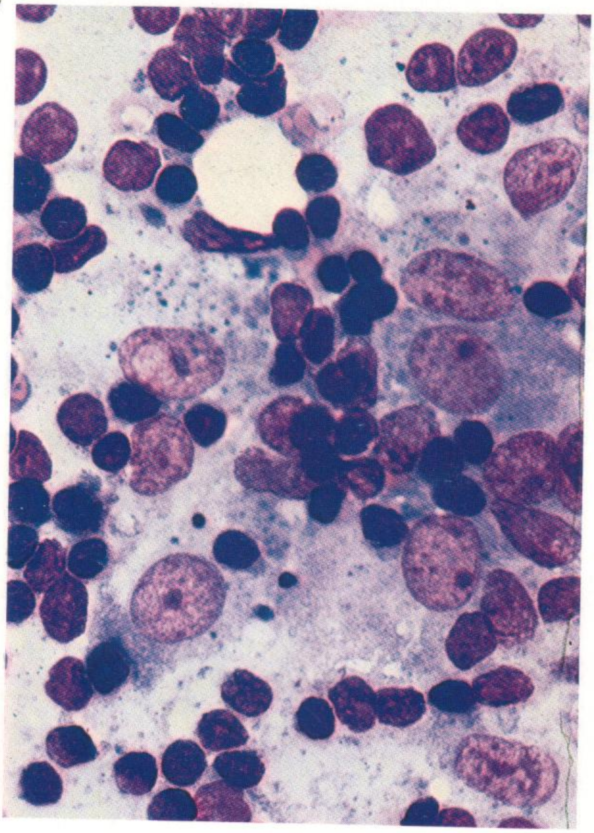

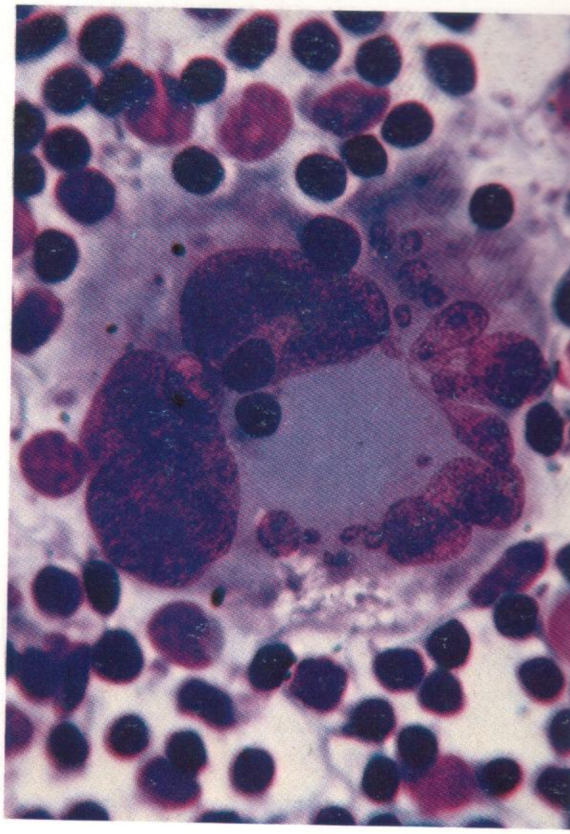

1098

1097–1099. *Leishman stain: lymph node imprints, showing chronic inflammatory changes, including especially the formation of Langhans giant cells.*

1097. A group of epithelioid cells with some phagocytic activity surrounded by lymphocytes and centrocytes from the chronic lymphadenitis of sarcoidosis.

1098. A foreign-body giant cell or Langhans cell from the same condition.

1099. Another example of a Langhans multinucleated giant cell from tuberculous lymphadenitis.

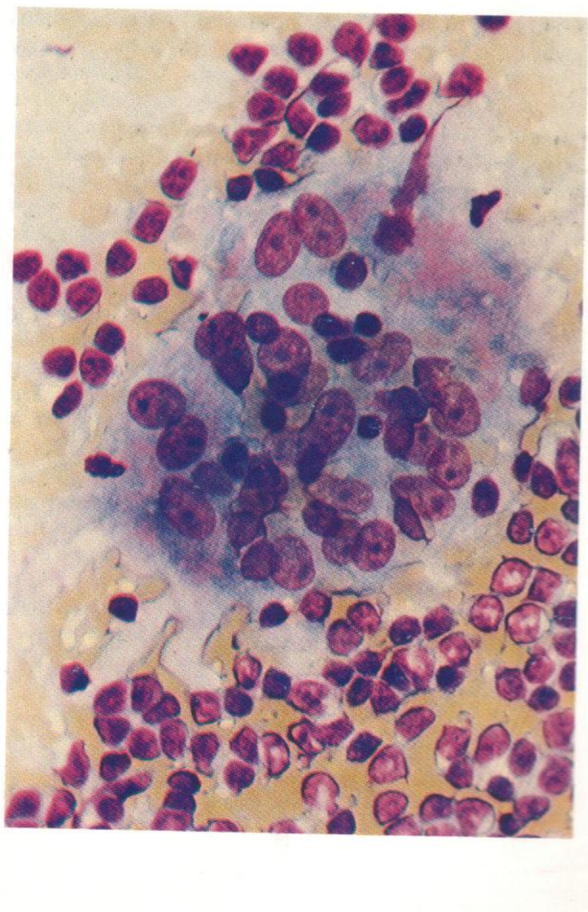

1099

1100

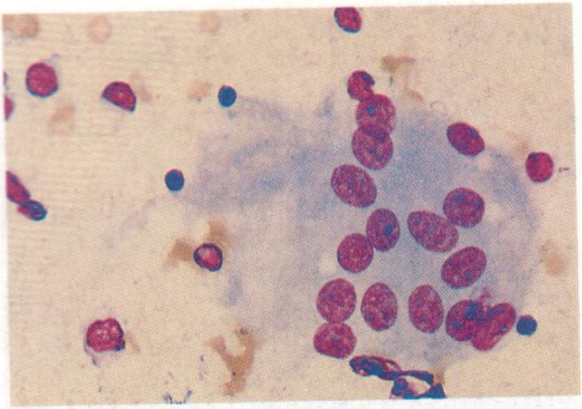

110

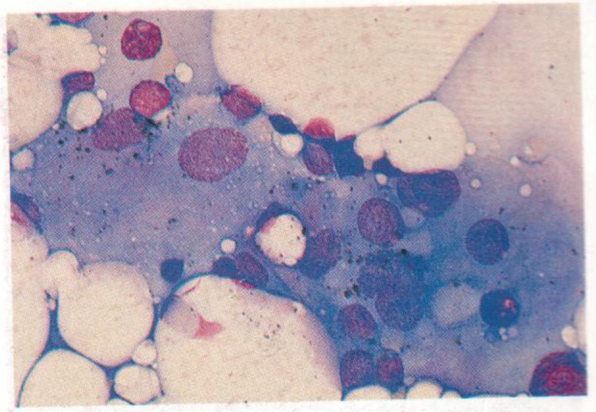

1102

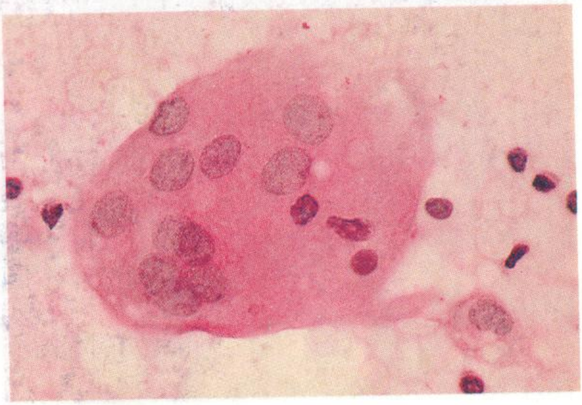

110

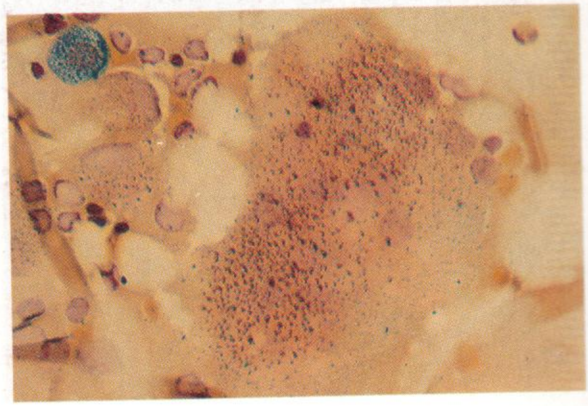

1100–1105. Cytochemical features of typical Langhans giant cells as seen in imprints of a lymph node biopsy from a female patient with chronic granulomatous disease. These cells are probably derived from multiple nuclear divisions without cytokinesis occurring in macrophages. The sequence of stains illustrated here includes, first, a Romanowsky preparation, with flat nuclei of moderate chromatin concentration, without clear nucleoli but with single areas of localized chromatin condensation, usually at the periphery, each probably representing the inactive X chromosome or Barr body. The blue agranular cytoplasm is evidently fragile and easily disrupted. In **1101** the SB stain is essentially negative except for a few scattered granules probably derived from an ingested neutrophil polymorph. The haematoxylin counterstain used in the PAS reaction of **1102** again shows the Barr bodies well, while the cytoplasm has weak diffuse PAS-positivity. The dual esterase reaction of **1103** has a moderately strong granular positivity for BE in the giant cell, with a CE-positive neutrophil top left. In **1104** there is the strong positive acid phosphatase reactivity to be expected in a cell of macrophagic origin, but the alkaline phosphatase stain in **1105** is negative.

110

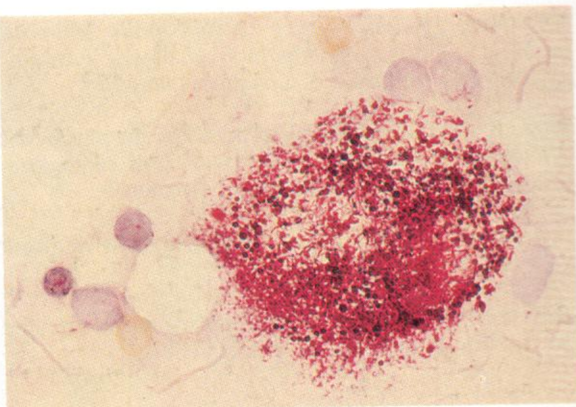

11

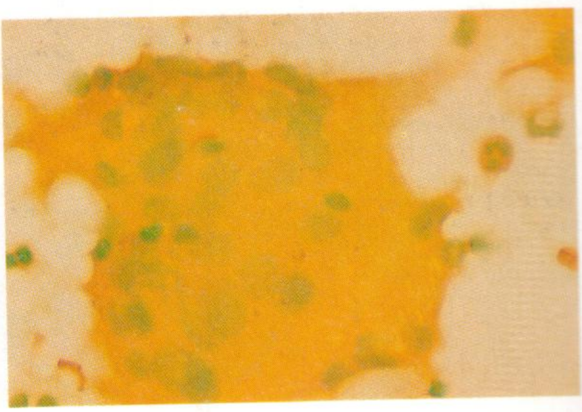

06

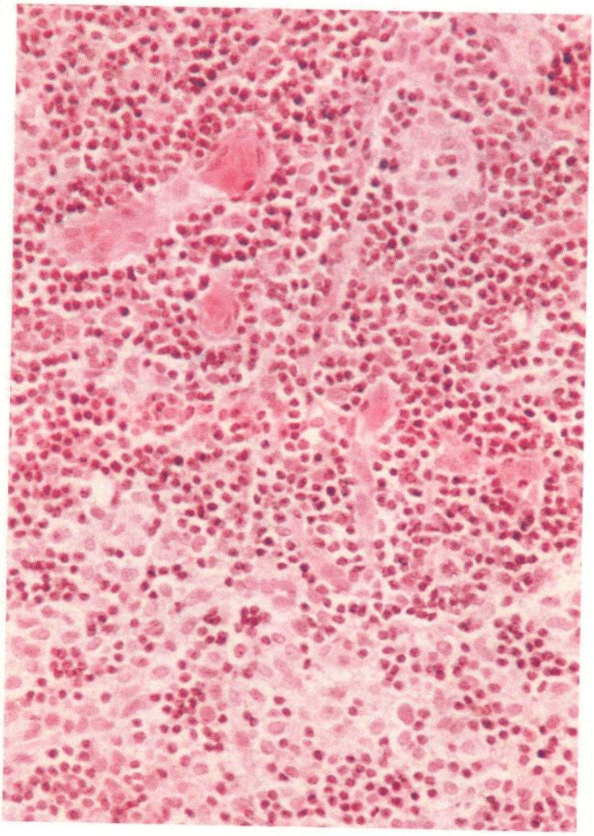

1107

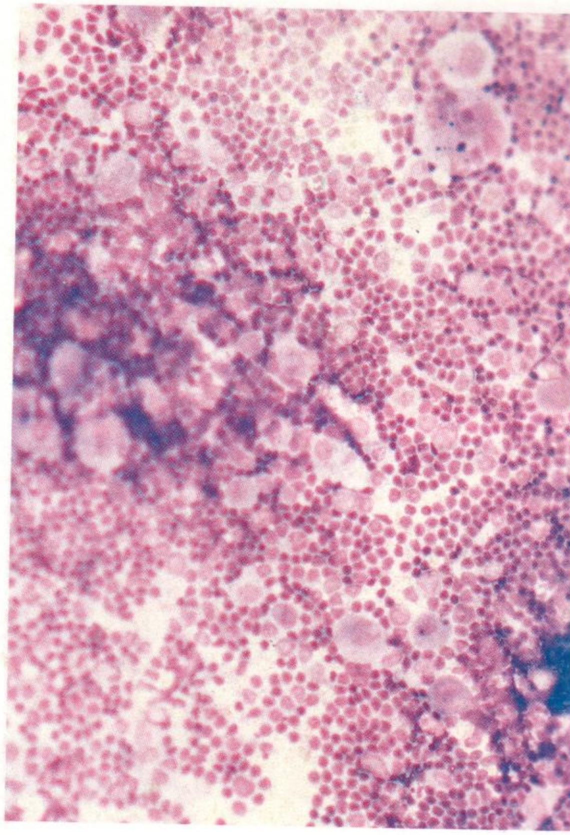

1106–1120. *A section and a sequence of imprints from a lymph node biopsy taken from a patient with Letterer-Siwe syndrome, a form of histiocytosis X, the proliferative mixed granulomatous state involving the nodal equivalent of epidermal Langerhans cells, perhaps related to or derived from dendritic reticulum cells.*

1106. This section shows an area of the cortex with sinus expansion and mononuclear histiocytic or Langerhans cell hyperplasia in the lower part, and several multinucleated giant cells among a preponderance of lymphocytes in the upper part. Although these giant cells bear some resemblance to Langhans foreign body giant cells, they are generally smaller, with fewer and often more centrally placed nuclei.

1107 and **1108**. Imprints from the same node biopsy as in **1106**, showing at low- and higher-power magnification the cytology of the atypical X-histiocytes or Langerhans cells. They tend to occur in clumps, have a more irregular nucleus and more robust cytoplasm than Langhans foreign body giant cells, although with some tendency to extend processes. They often appear to contain phagocytosed material, though less active in this respect than the common histiocyte.

1108

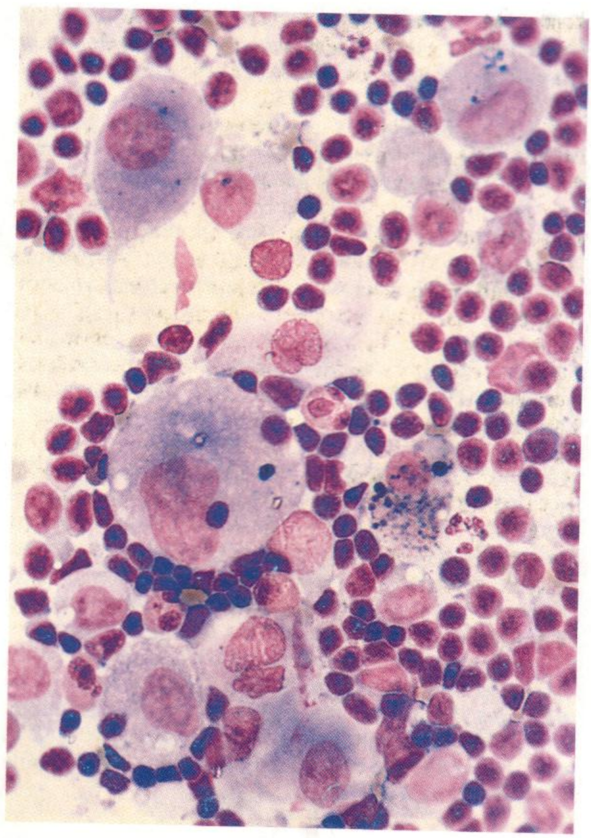

1109

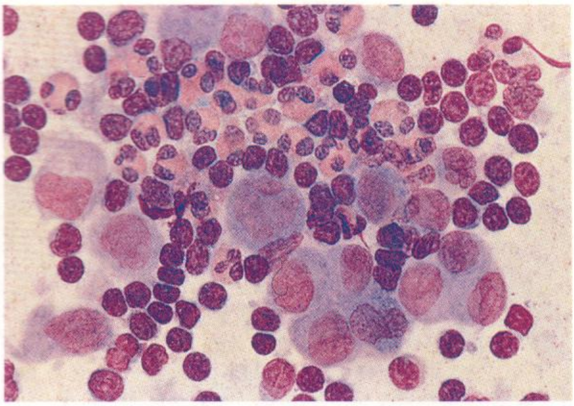

1110

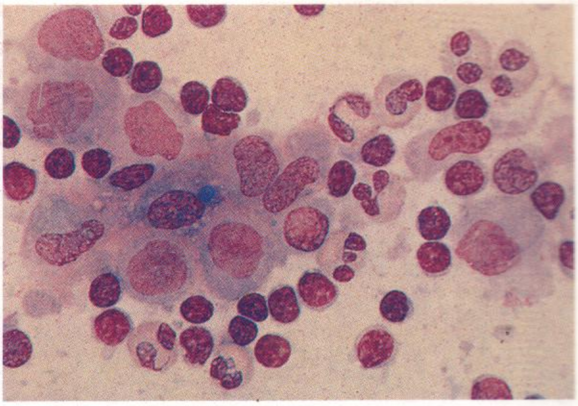

1111

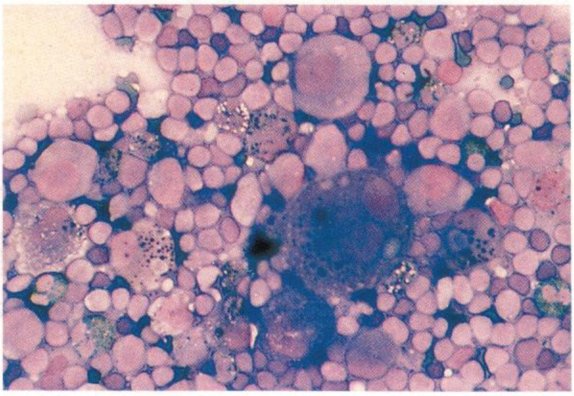

1112

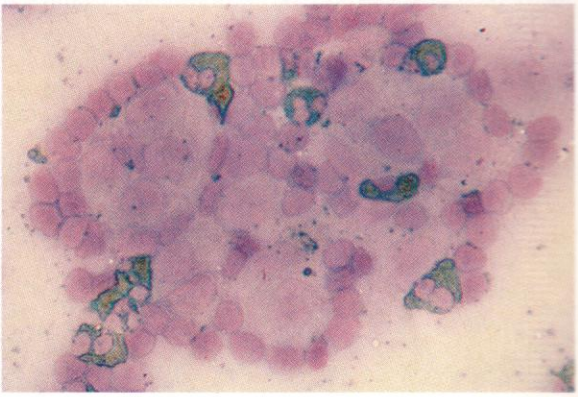

1113

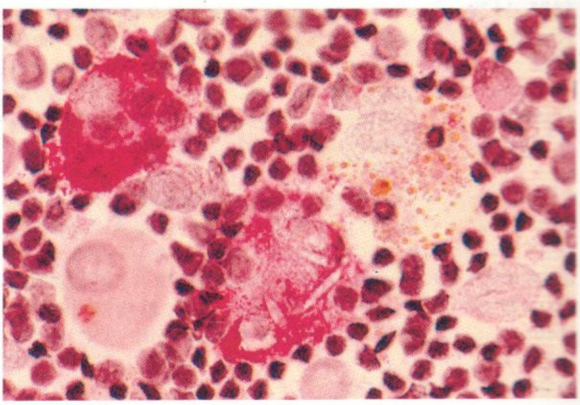

1114

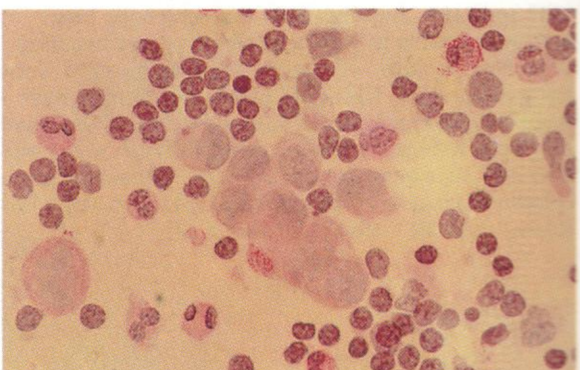

1109–1114. *A sequence of stains of imprints from lymph node biopsies taken from patients with eosinophilic granuloma, another variant of histiocytosis X.*

1109. This Romanowsky-stained preparation shows a nest of eosinophils surrounded by a mixture of large monocytoid Langerhans cells and lymphocytes.

1110. A similar high-power view of the second case shows the more detailed cytology of the Langerhans cells and their close resemblance to monocytoid macrophages.

1111 and **1112**. Low- and higher-power fields, from SB-stained preparations from the two cases, illustrating that the histiocytic cells are generally sudanophobic.

1113 and **1114**. PAS stains from the two cases. In **1113** there are probably six histiocytes present, two (one of them with unstained crystalline inclusions) showing strong PAS-positivity, one containing brownish granules of free iron, one negative except for a small tetrad of positive material, perhaps a phagocytosed starch grain, and the two smaller histiocytes negative. Probably only the last three cells are Langerhans cells, the earlier ones being phagocytic macrophages. The cells from the second case in **1114** are mostly negative, except for weak granular positivity and a diffuse tinge in one large cell to the left of the field. These are probably all Langerhans cells.

1115

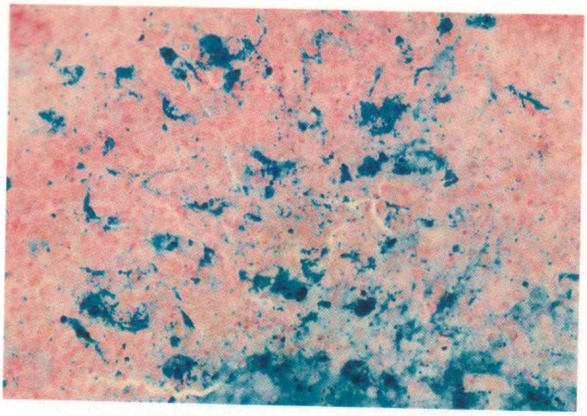

1116

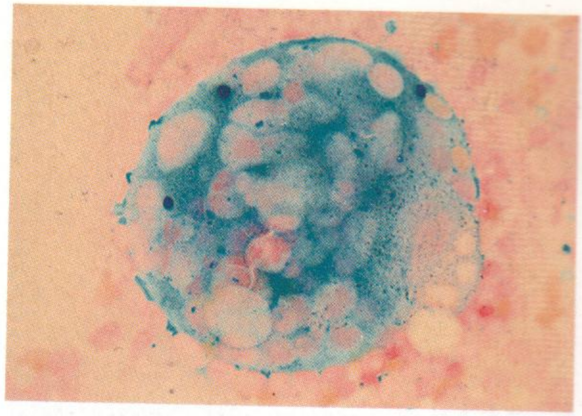

1117

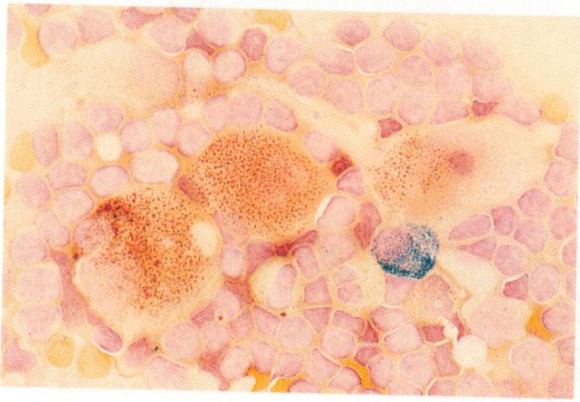

1118

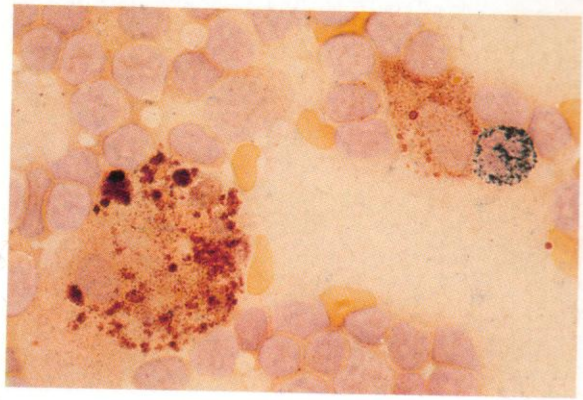

1115–1120. *Further cytochemical stains from the first of these two cases, where, despite the undoubted diagnosis of eosinophilic granuloma, there is an intense concomitant proliferation of phagocytic macrophages in parallel with the proliferation of Langerhans cells.*

1115 and **1116**. The immense amount of free iron demonstrable by the Prussian blue reaction in the lymph node macrophages from this patient is shown in **1115**. This accumulation is no doubt chiefly in phagocytic macrophages, one of which, laden with iron and also much ingested material, including numerous red cells from which the iron is derived, is shown in **1116**.

1117 and **1118**. Different fields from the same dual esterase stain. In each there is a single CE-positive neutrophil and various negative lymphocytes and centrocytes. Three weakly BE-positive large cells, possibly Langerhans cells, are illustrated in **1117**, contrasting with the two much more coarsely BE-positive phagocytic macrophages in **1118**.

1119 and **1120**. Acid and alkaline phosphatase stains, respectively, on the lymph node biopsy material, both fields showing positivity in phagocytic macrophages. Langerhans cells are difficult to identify in these preparations but appear generally negative for both phosphatases.

1119

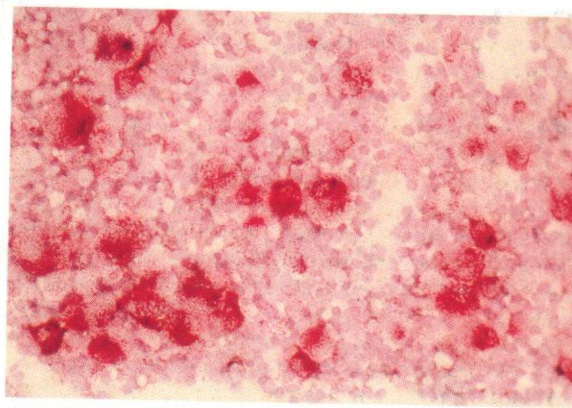

1120

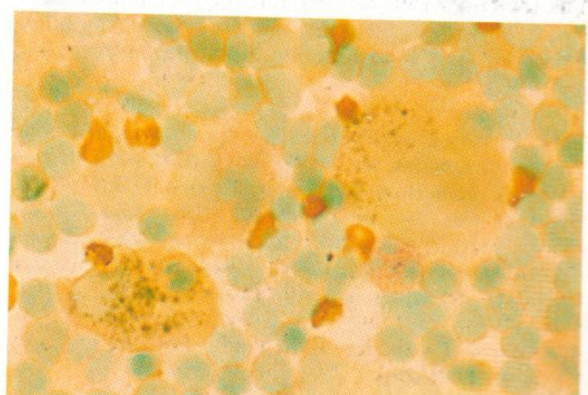

1121

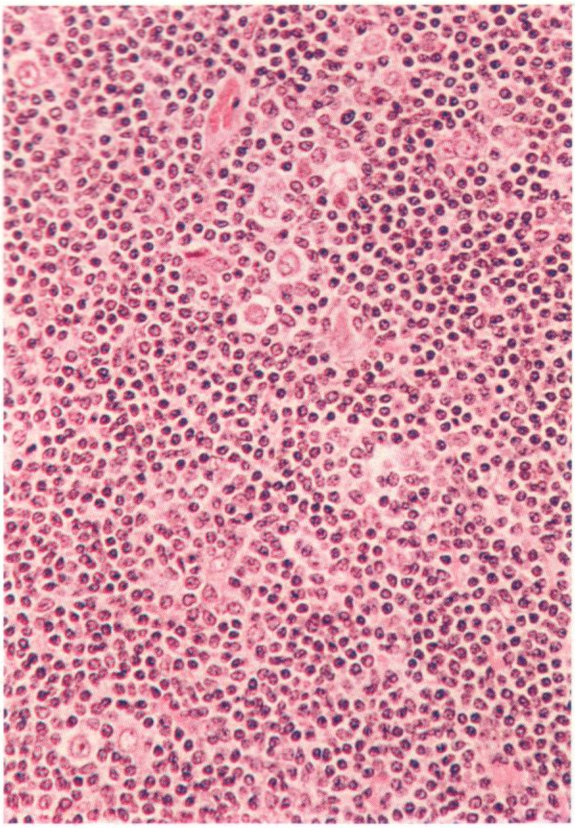

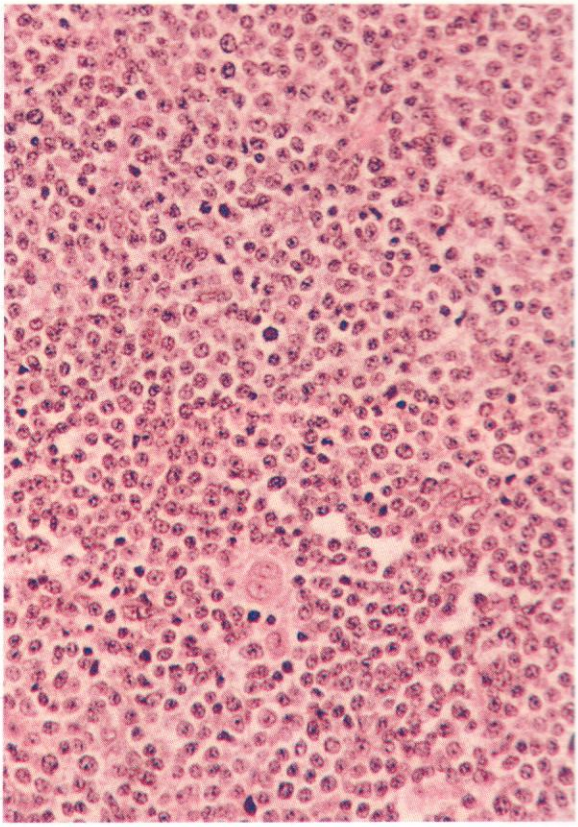

1

1121–1130. *A small selection of lymph node biopsy sections from patients with Hodgkin's disease (HD), to illustrate features of nodal structure relevant to diagnosis of pathological variants, not readily apparent from imprints.*

1121 and **1122**. Both these fields are taken from an example of the lymphocyte predominant variant, where lymphocytes and centrocytes greatly predominate, but where both binucleated Reed-Sternberg (R-S) cells and large mononuclear Hodgkin's cells can be distinguished. These cells, with their conspicuous large single centrally placed nucleoli, are quite numerous and prominent in **1121**, but less frequent though easily enough identified in **1122**. Diagnosis from imprint material may be difficult when R-S and Hodgkin's cells are few, and there may be confusion with lymphocytic non-Hodgkin's lymphoma (NHL) in the interpretation of both imprints and sections.

1123. A very low-power view of a section from a node biopsy, illustrating the coarse bands of fibrosis characteristic of the nodular sclerosing variant of HD (NSHD). Even at this low magnification, occasional R-S or Hodgkin's cells surrounded by an empty space, the so-called lacunar cells, especially found in NSHD, can be made out, as can the presence of eosinophilia.

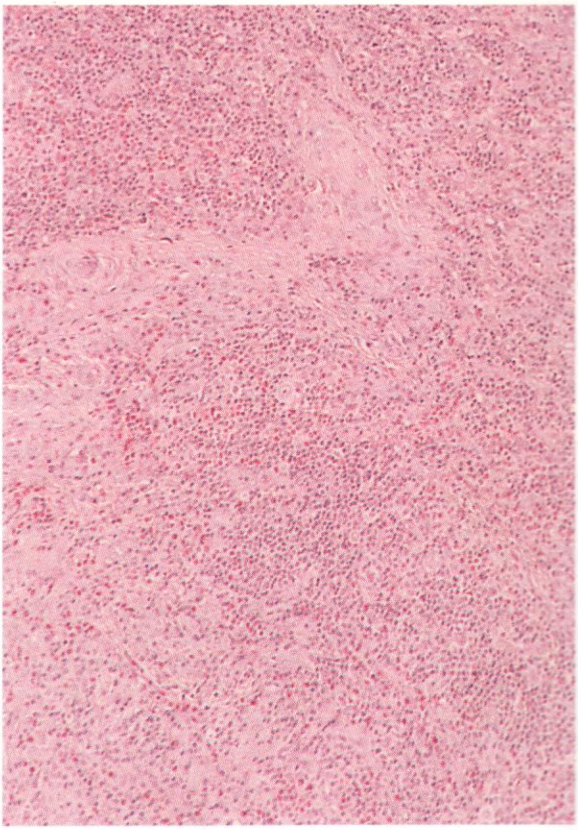

1

24

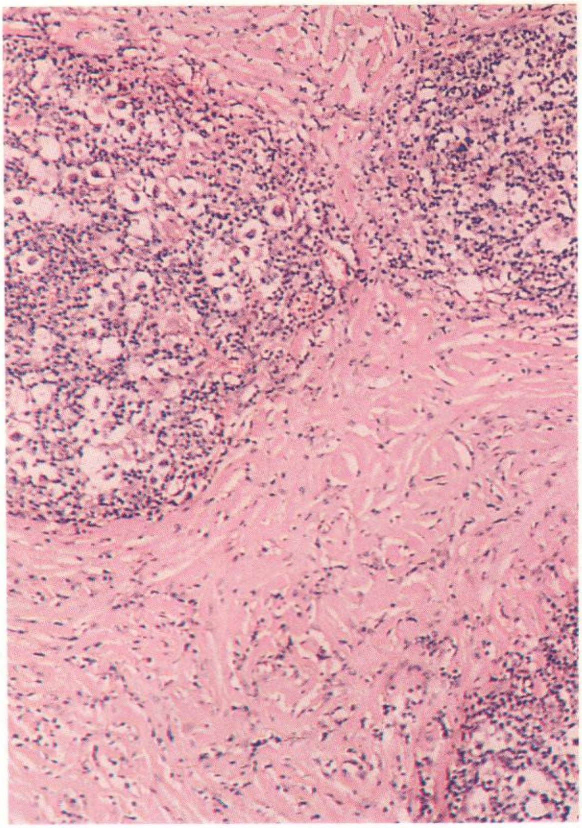

1125

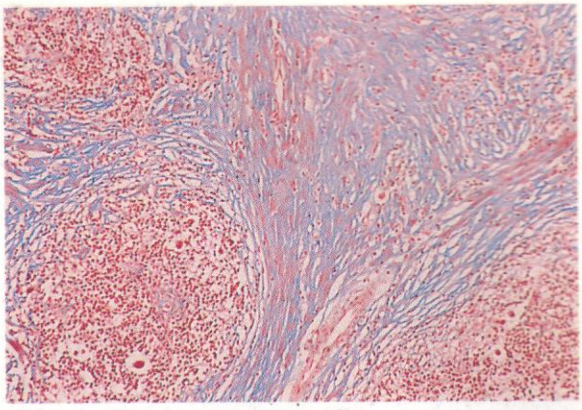

1126

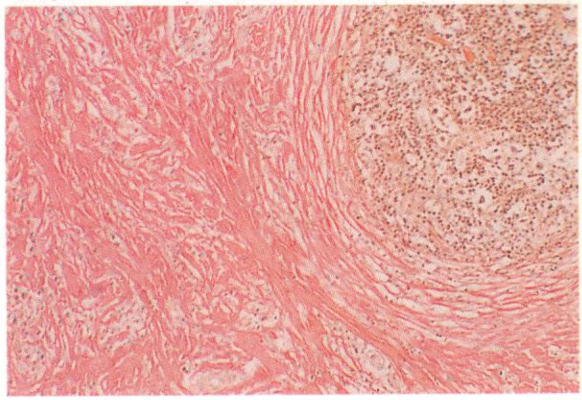

1124–1127. Further illustrations of structural patterns of nodal and cellular architecture in NSHD. In **1124** the H&E stain shows a coarse band of densely fibrotic material separating islands of neoplastic tissue, including a predominance of lacunar cells, conspicuous among the surrounding lymphocytes. In **1125** and **1126** similar fields from sections stained with the Mallory and Ponceau S methods respectively pick out the collagenous tissue with blue and red staining and the neoplastic cell nests with nuclei stained red or brown. The higher-power view of an H&E-stained field in **1127** shows the more detailed cytology of the lacunar cells, with their nucleolated nuclei and well-defined cytoplasm contracted within the lacunar space. These cells are surrounded by lymphocytes with densely chromatic nuclei, interspersed with larger and more lightly staining centrocytes.

1127

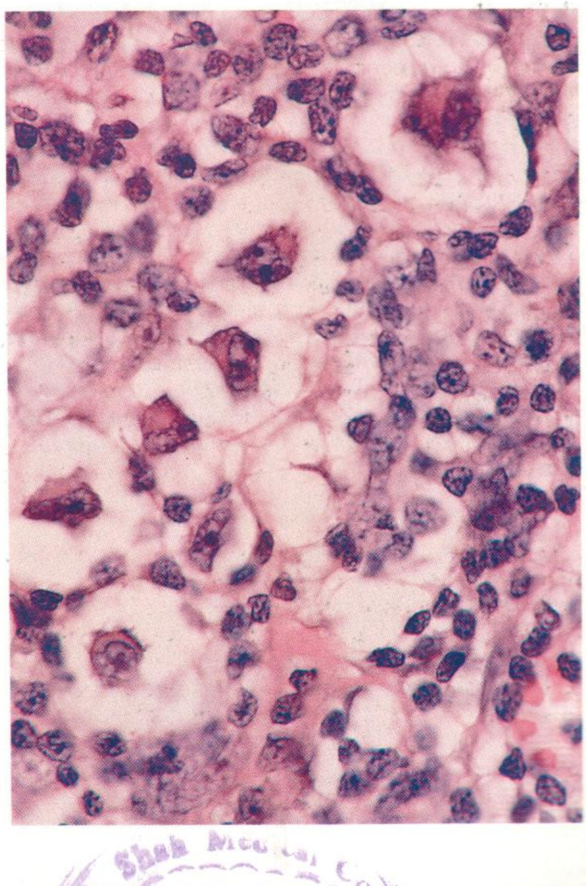

128

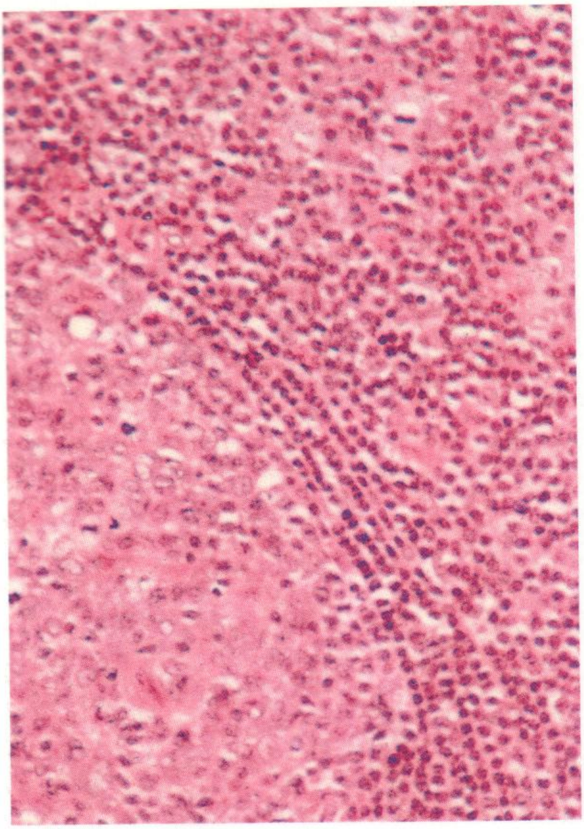

1129

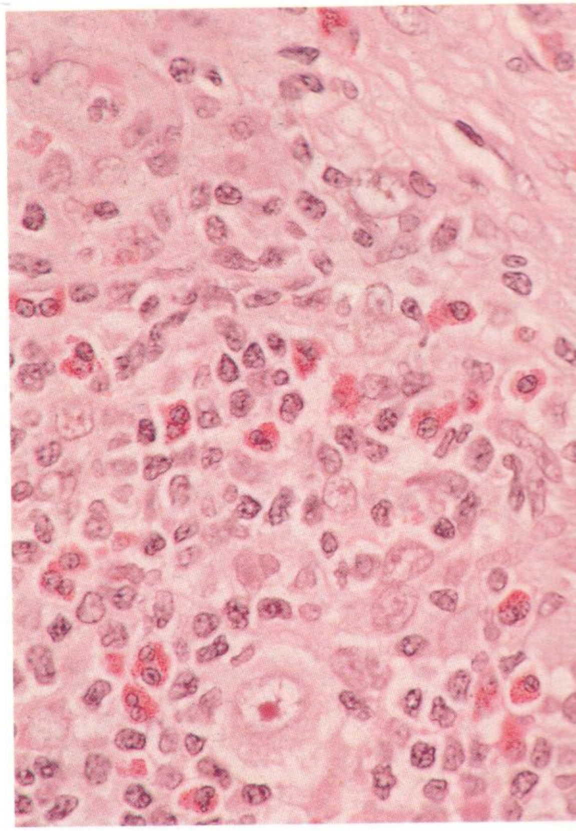

1128–1130. A low-power and two higher-power views of different areas of an H&E-stained section of a lymph node biopsy, from a patient with the mixed cellularity variant of HD (MCHD). The picture is a generally pleomorphic one, with, in **1128**, a pseudofollicular structure produced by an expanding nodule of neoplastic Hodgkin's cells compressing the surrounding lymphocytes into the appearance of a sheath, but with many scattered Hodgkin's and R-S cells also present among the lymphocytes. In **1129** several of these large neoplastic cells can be distinguished, an especially conspicuous one at the lower centre, but there is also a marked eosinophilic infiltration and some fibrotic activity apparent among the neoplastic tissue and the reduced lymphocytic component. Another area of the section, seen in **1130**, has a higher proportion of residual lymphocytes and centrocytes but again a conspicuous proliferation of R-S and Hodgkin's cells.

1130

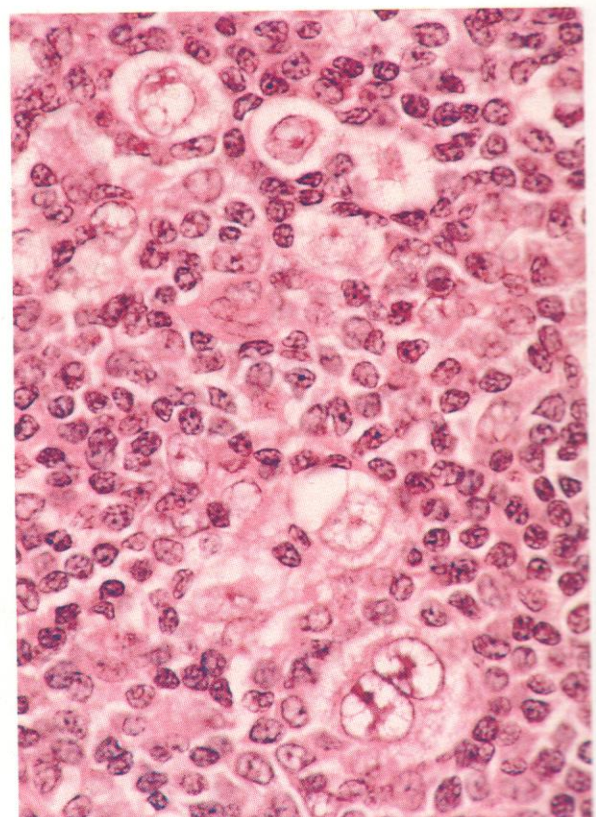

1131

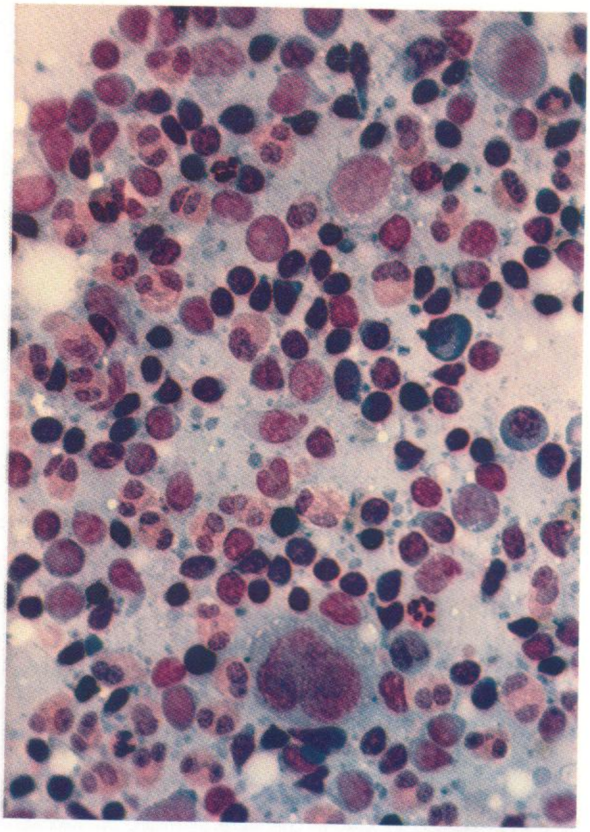

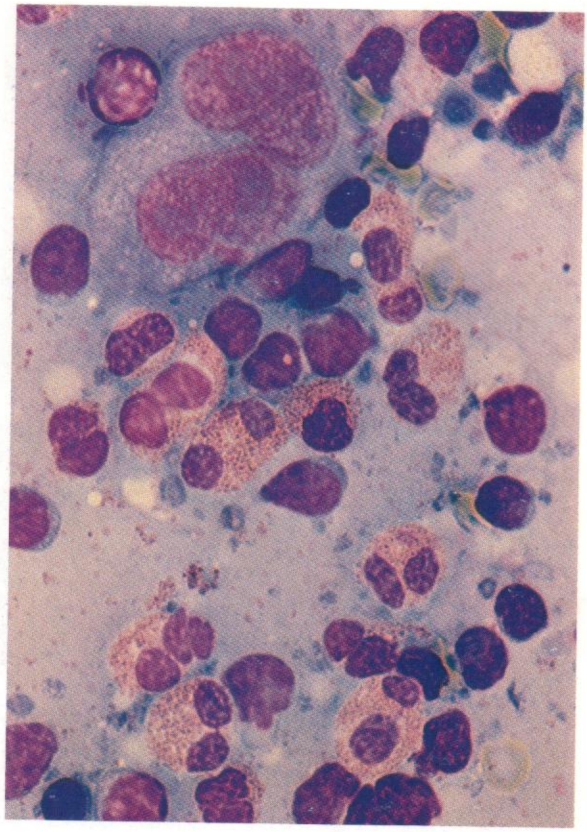

1132

1131–1133. *Leishman stain: lymph node imprints: HD – mixed cellularity.*

1131 and **1132**. Low- and higher-power views, respectively, of the pleomorphic picture commonly seen in node imprints from the disease, especially in the mixed cellularity variant. Lymphocytes, centrocytes, occasional centroblasts and immunoblasts mingle with plasma cells, eosinophil and, sometimes, neutrophil polymorphs, and monocyte–macrophages. There is a single large R-S cell with twisted or overlapping double nucleus and large dark violaceous nucleoli in each figure. The extent of eosinophilia in this example is unusual, but some eosinophils can commonly be found in most imprint preparations from HD.

1133. Another area of the same slide, again showing lymphocytes, centrocytes, centroblasts and an immunoblast (top right), together with a plasma cell and many eosinophils. Centrally, there is a macrophage or RE cell with, on the right, a mononuclear R-S cell or Hodgkin's cell with characteristic nuclear chromatin and nucleoli.

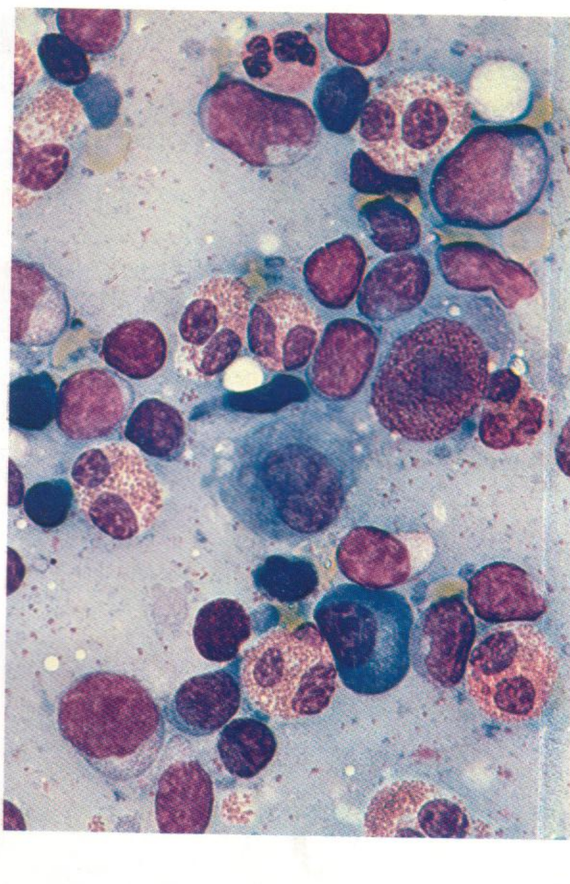

1133

4

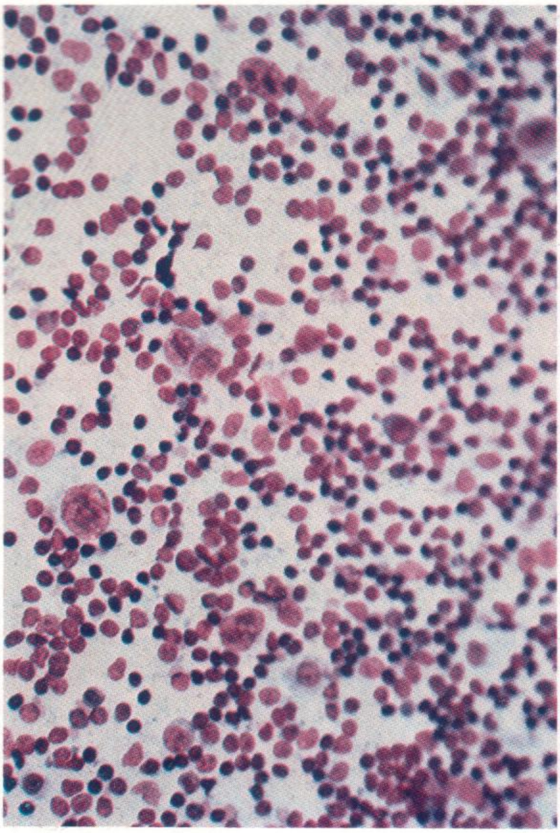

1135

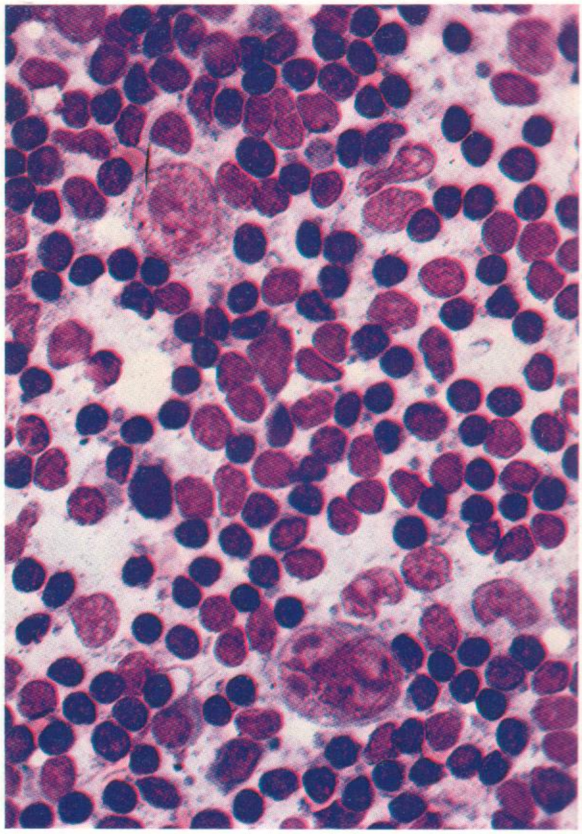

1134–1136. *Leishman stain: lymph node imprints: HD – lymphocyte predominant.*

1134. A low-power view providing a more uniformly lymphocytic and centrocytic background, but with one binucleated R-S cell and several mononuclear Hodgkin's cells. Occasional monocyte–macrophage type cells can be seen.

1135. A higher-power view of the same slide in which all the cell types mentioned above can be more clearly identified.

1136. A still higher magnification of an R-S cell from this specimen, to illustrate the typical reticular nuclear chromatin and the large dark violet nucleoli. The surrounding cells are mostly lymphocytes.

1136

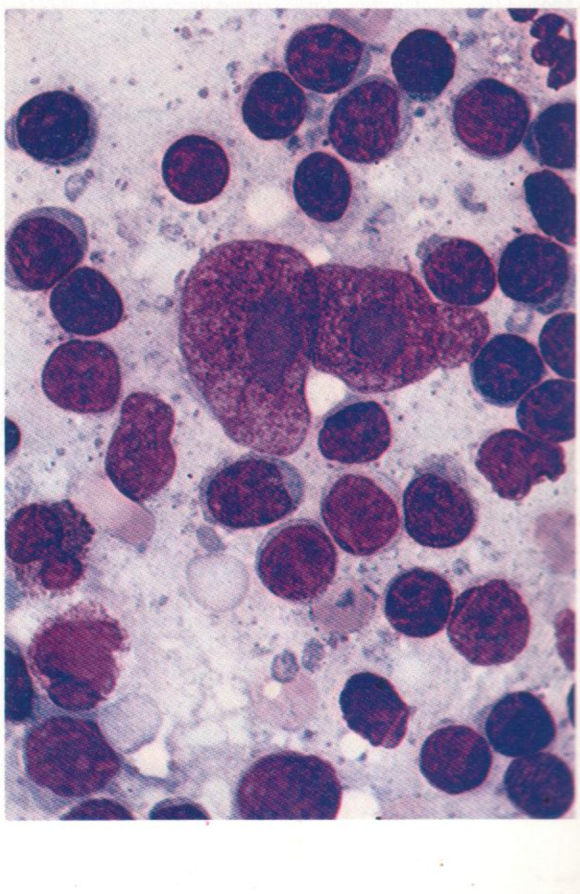

37
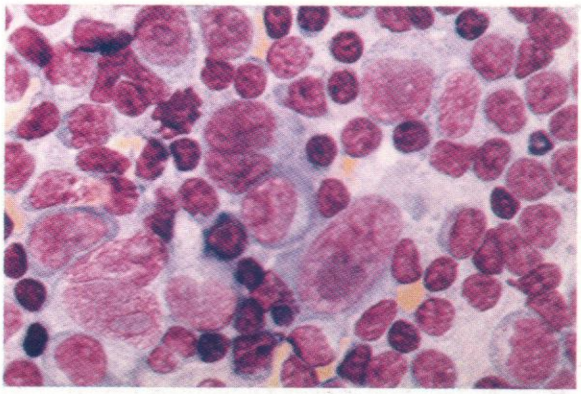

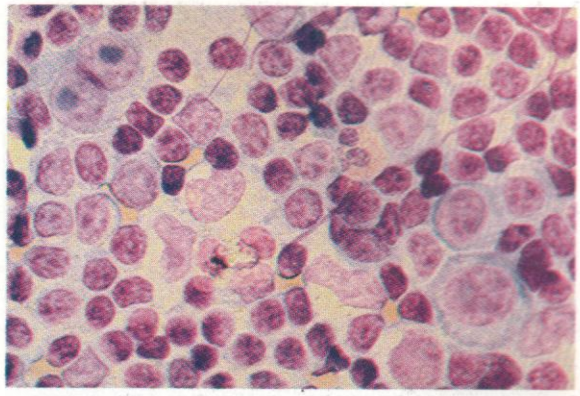
1138

9
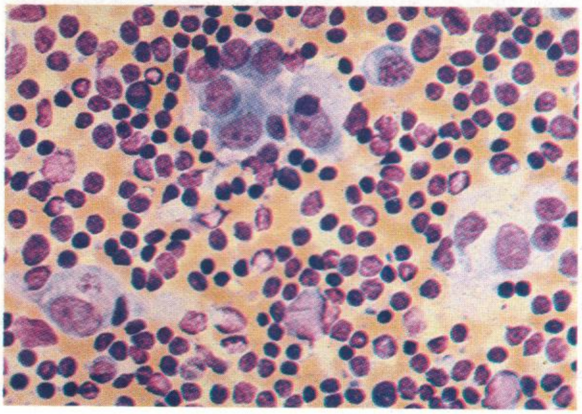

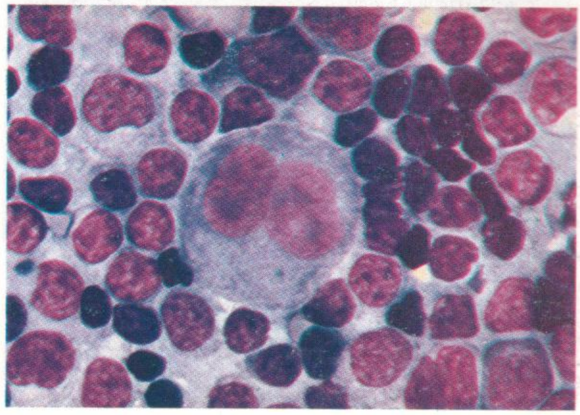
1140

1137–1139. *Leishman stain: lymph node imprint: HD – nodular sclerosing to mixed cellularity – morphological relationships of R-S cells.*

1137. A field showing various binucleated R-S cells and mononuclear Hodgkin's giant cells. A centroblast at the lower right corner and a central immunoblast show morphological similarities to the smaller of the Hodgkin's cells and suggest a possible derivation of the R-S cells from activated B cells.

1138. A second field from the same specimen allows similar parallels to be drawn: the R-S cell in the upper left corner relates to the probable mononuclear Hodgkin's cell in the lower right, and that in turn to the immunoblast above it.

1139. Yet another area in the same slide shows a collection of histiocytic RE cells, some with ingested cell debris, which are clearly morphologically distinct from the R-S and Hodgkin's cells of the previous figures.

1140–1145. *Leishman stain: lymph node imprints: variants of giant cells in HD.*

1140–1142. Typically binucleated R-S cells. There is also a mononuclear Hodgkin's cell in **1142**.

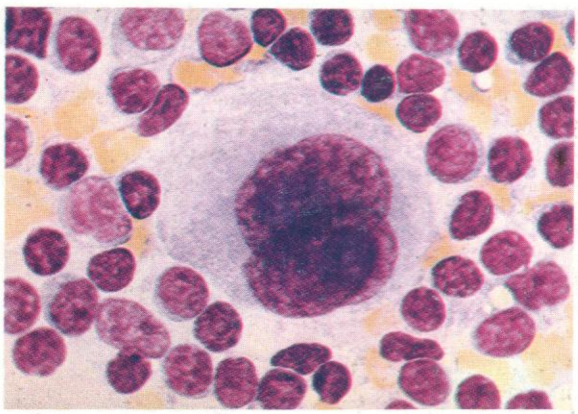
1141

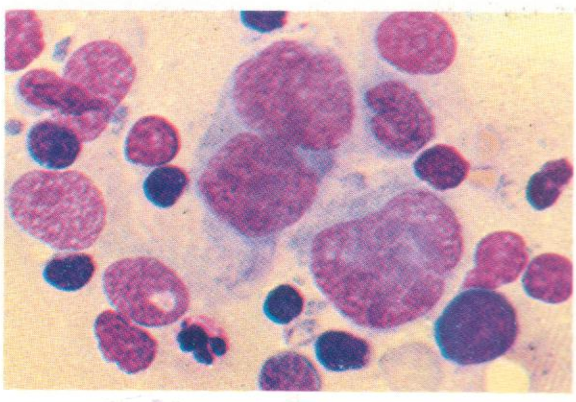
1142

1143

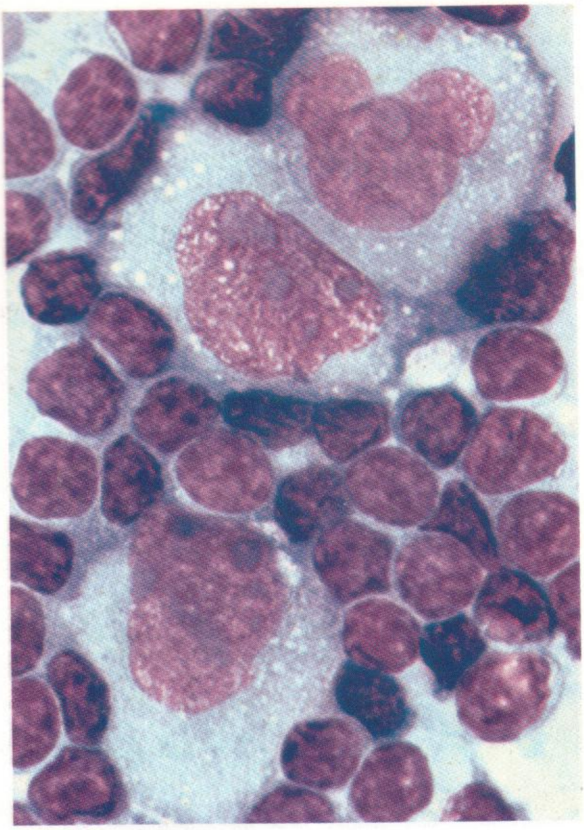

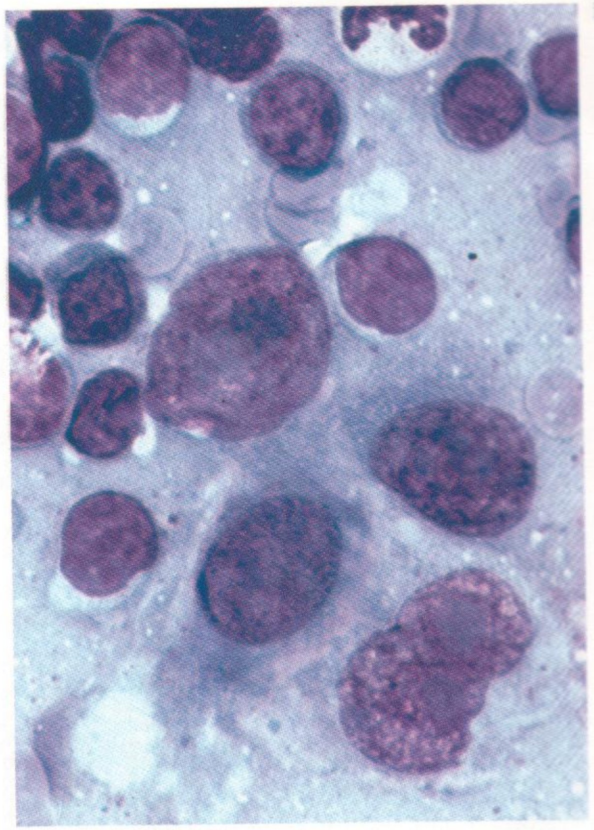

1143 and **1144**. Mononuclear Hodgkin's cells, with characteristic nuclear and nucleolar patterns. In **1144** a pair of these cells, one possibly with overlapping double nucleus, are separated by a pair of RE cells of clearly contrasting nuclear and cytoplasmic morphology.

1145. A mitotic figure in an R-S cell, showing the clearly intact nucleoli surrounded by separated chromosomes. To the left of this cell is a macrophage.

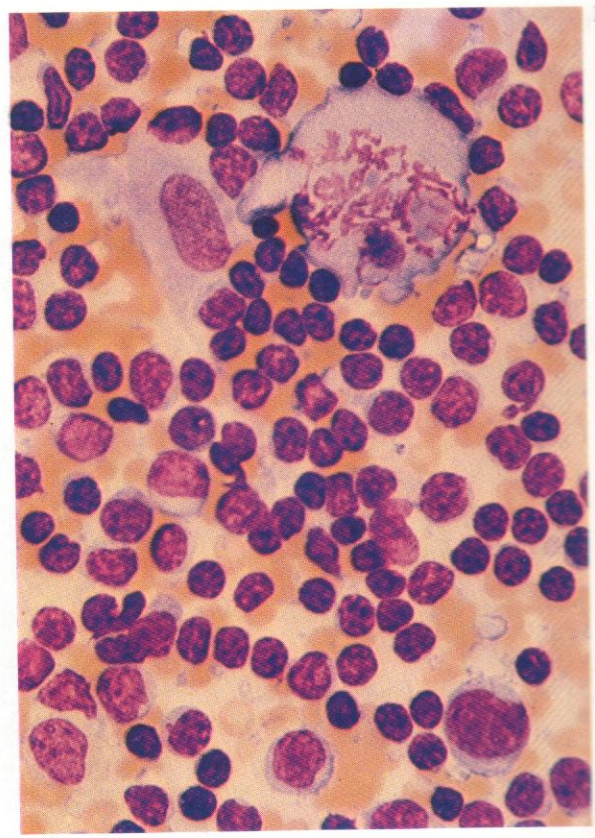

6

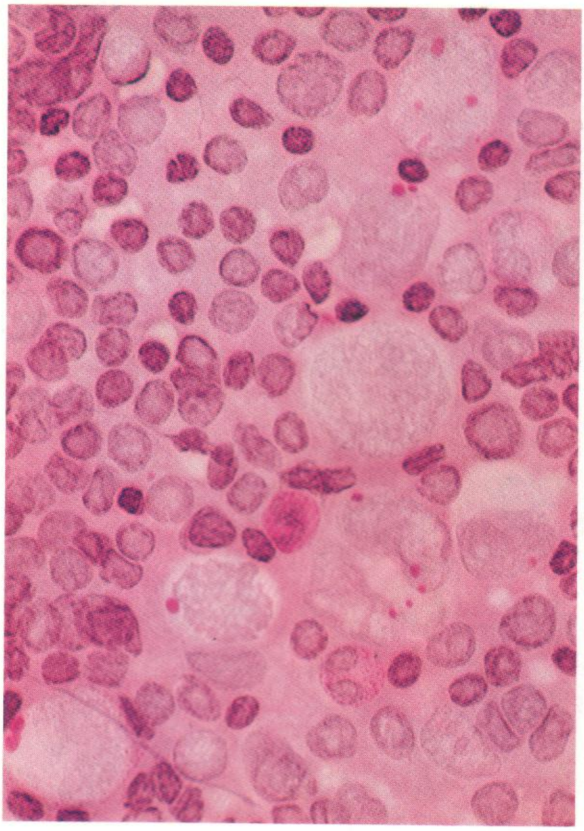

1147

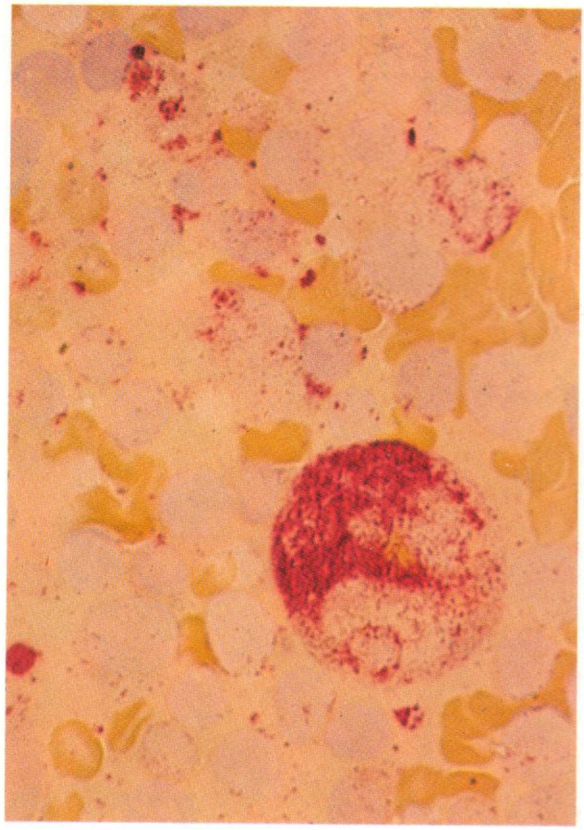

1148

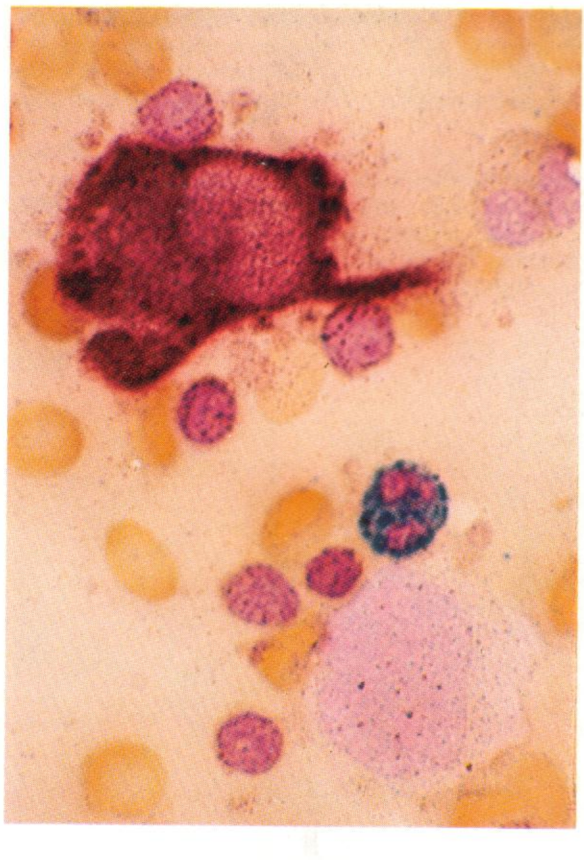

1146. PAS reaction: lymph node imprint: HD. A clearly binucleated R-S cell and five out of six mononuclear Hodgkin's cells, including one in mitosis, show globules or blocks of PAS positivity. Although the giant cells of HD are most often PAS-negative, the appearance of globules of positivity as in this figure, or even coarsely scattered granular positivity, is by no means rare.

1147. Acid phosphatase stain: lymph node imprint: HD. A binucleated R-S cell shows strong positivity.

1148. Dual esterase reaction: lymph node imprint: HD. Hodgkin's cells usually show little esterase positivity, as here, where weakly scattered BE and CE granules are detectable, in sharp contrast to the strong BE positivity in a neighbouring giant RE cell. An eosinophil, a CE-positive neutrophil and variably BE-positive lymphocytes complete the field.

1149

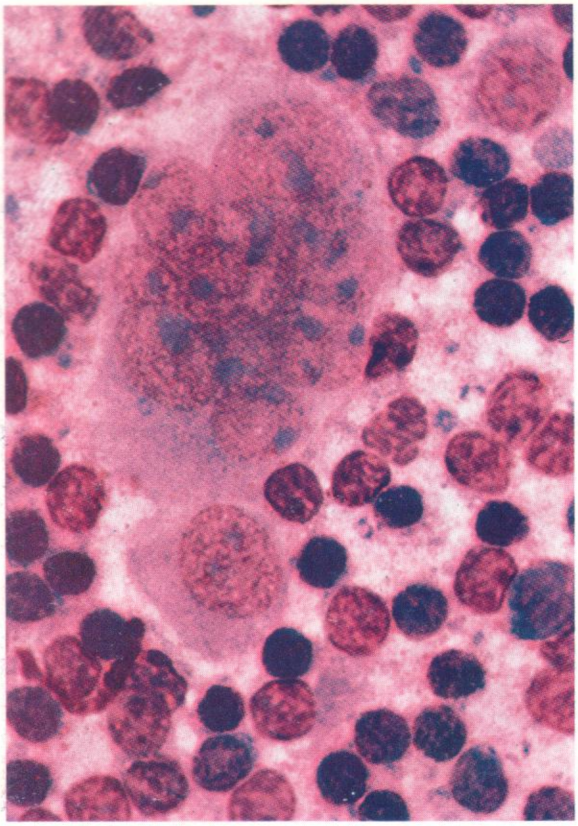

1150

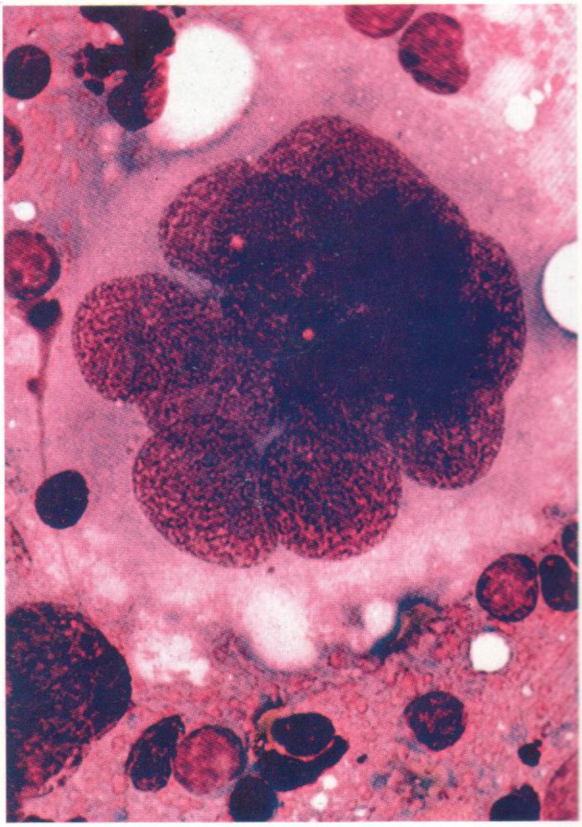

1151

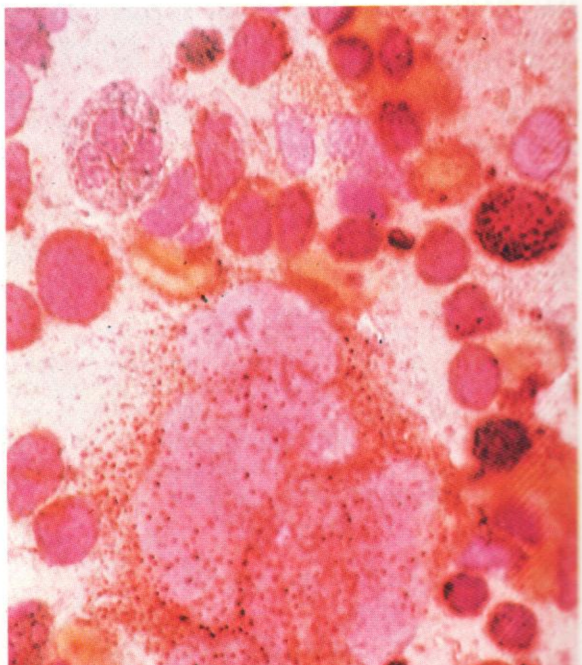

1149 and **1150**. Leishman stain: lymph node imprint: chronic lymphadenitis. Multinucleated giant cells, with flat epithelial-type nuclei and relatively small or inconspicuous nucleoli; not to be mistaken for HD giant cells.

1151. Dual esterase reaction from the same specimen. One of the multinucleated giant cells shows strong BE positivity, unlike R-S cells which are usually negative. Localized dot-like positivity is seen also in some probable T cells and there is CE positivity in several neutrophils and mixed reaction in a plasma cell.

1152 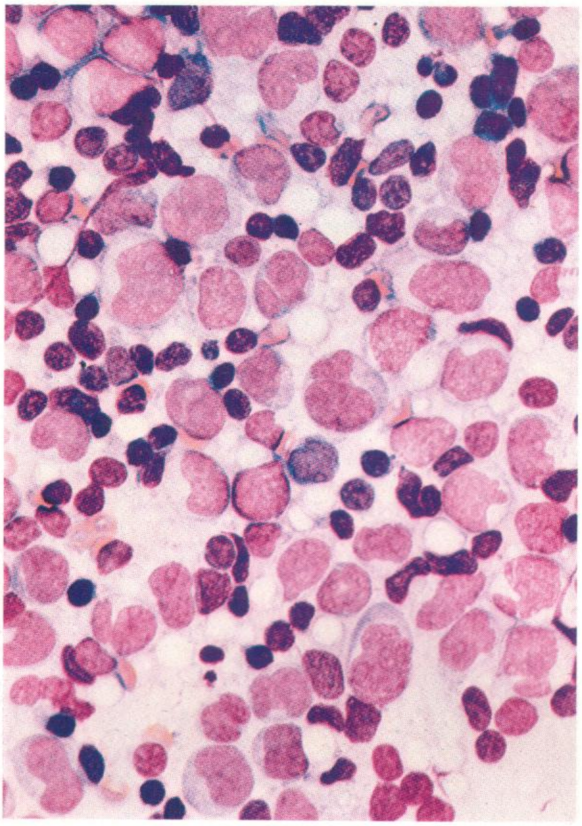

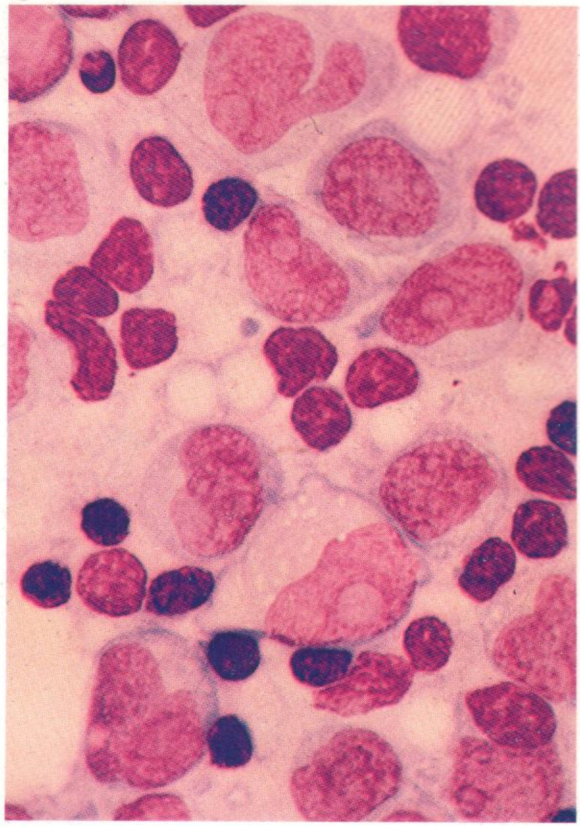 1153

1152–1157. *Lymph node imprints: follicular lymphoma, centrocytic-centroblastic; mixed small and large follicular centre-cell lymphoma.*

1152. Leishman stain: lower-power view of a mixture of centrocytes and centroblasts, with a scattering of mature lymphocytes.

1153. A higher-power view of the same preparation, revealing large single or occasionally multiple nucleoli in the larger cells – centroblasts – which often show indentation or cleaving of the nucleus. The two varieties of small-cell, densely pachychromatic lymphocytes and more lightly stained centrocytes, can be clearly differentiated.

1154. SB reaction in this node imprint shows all the lymphoma cells to be negative. The single positively reacting cell is a neutrophil polymorph.

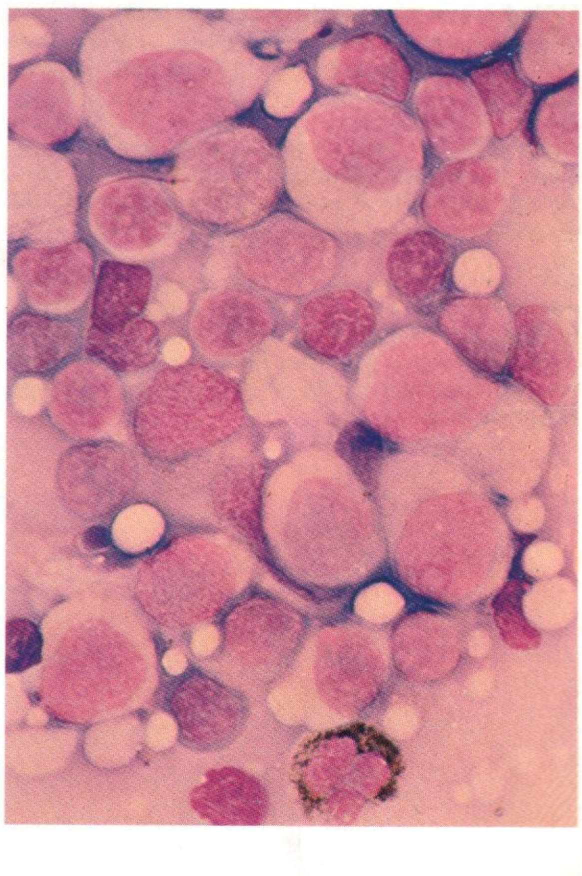 1154

1155

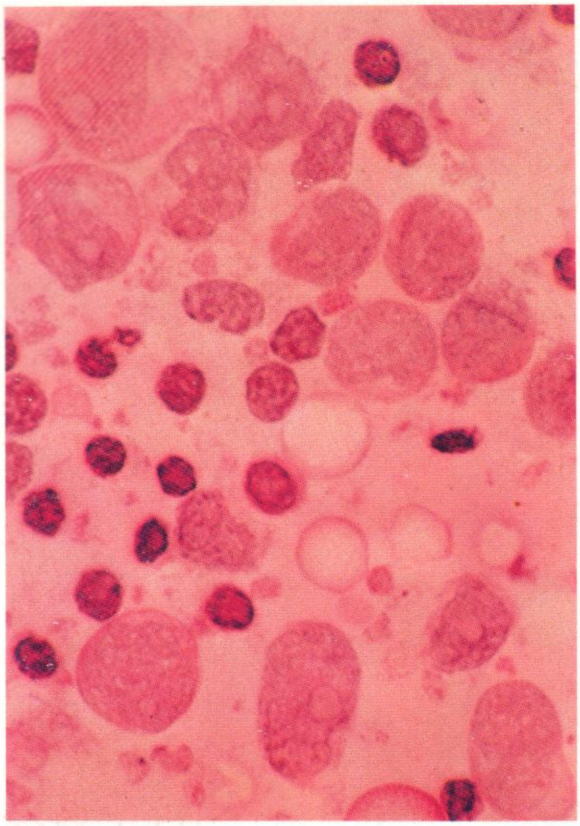

1156

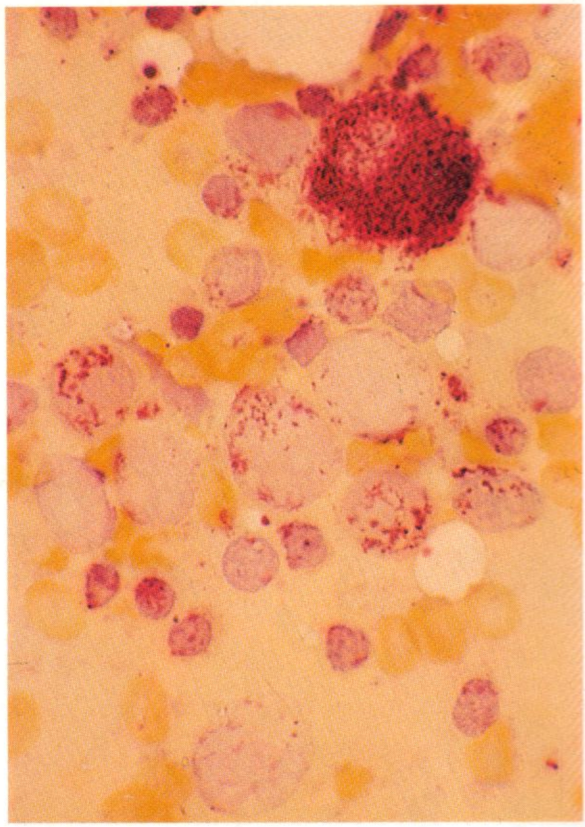

1157

1155. PAS reaction on the same node imprint shows a little positivity in cytoplasmic fragments, and some tinge and fine granular reaction in lymphoma cells.

1156. Acid phosphatase reaction on this specimen shows variable + to +++ positivity in lymphoma cells, scattered and not particularly localized in the paranuclear zone. There is a strongly positive RE cell present.

1157. Dual esterase reaction here shows CE positivity in a neutrophil polymorph and in a tissue mast cell, with BE positivity of modest degree in an RE cell, possibly dendritic, with fine processes extending between neighbouring lymphoma cells. The lymphoma cells are essentially negative.

158

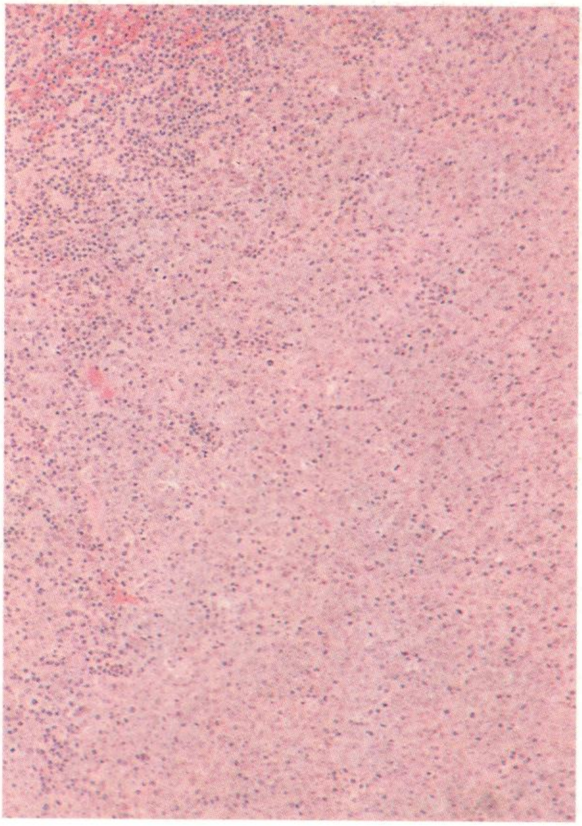

1159

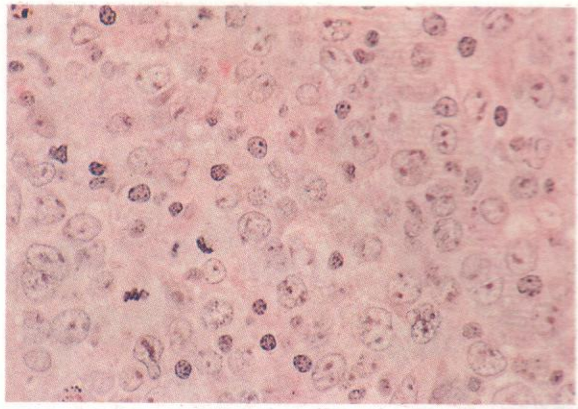

1160

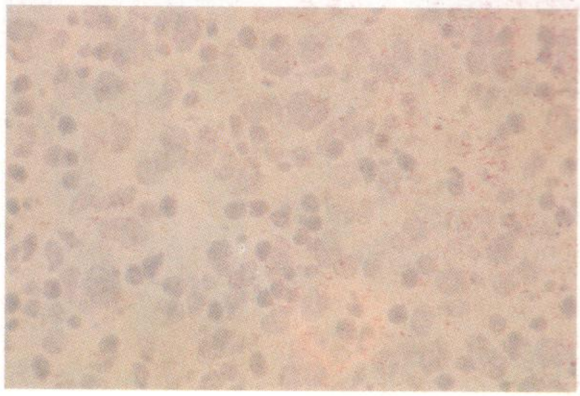

1161

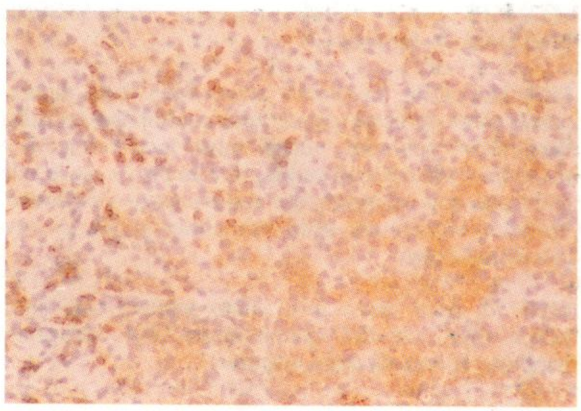

1162

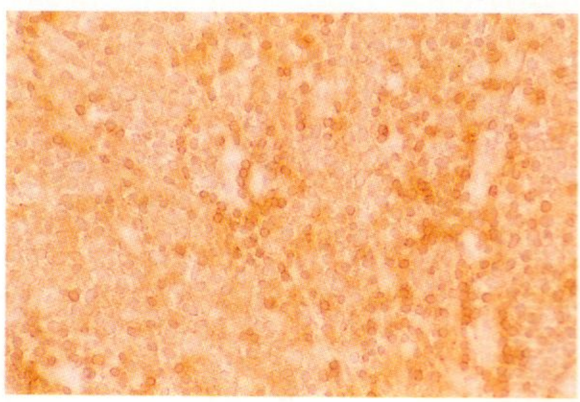

1158–1162. *Lymph node sections from centrocytic-centroblastic malignant lymphoma.*

1158 and **1159**. A very low-power view and a higher-power field from an H&E-stained section. In **1158** most of the field is occupied by part of a nodule of lymphoma cells, with compressed normal parafollicular tissue at the upper and left edges. The tumour appears paler than the predominantly lymphocytic surrounding tissue. The mixed cytology of the follicular tumour is shown in detail in **1159**; the centroblasts have large and palely staining vesicular nuclei with peripheral nucleoli, the centrocytes are smaller with darker nuclei and inconspicuous nucleoli, and there are one or two deeply stained small lymphocytes. Several mitotic figures can be seen.

1160–1162. Immunocytochemical PAP reactions on sections from the same biopsy. A negative control is seen in **1160**, and a reaction with the pan-B MAb CD19 in **1161** – the latter showing strong positivity in more mature residual lymphocytes at the upper left and weaker positivity in the centrocytes and centroblasts comprising the bulk of the tumour follicle in the lower right of the field. The negative T cells, scanty within the tumour tissue but more frequent in the cortical area, stand out clearly. A reaction with the leucocyte common MAb CD45 is seen in **1162** where all the cells in the section show positivity of greater or less intensity.

1163

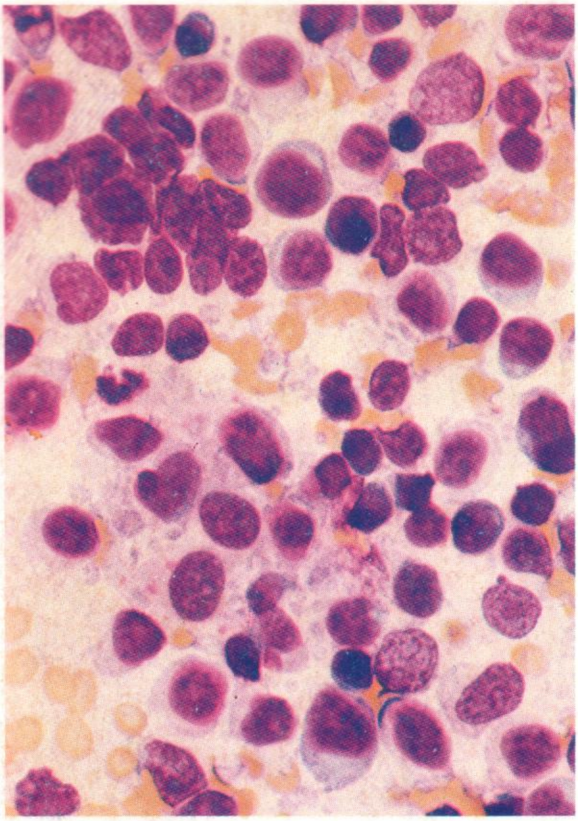

1164

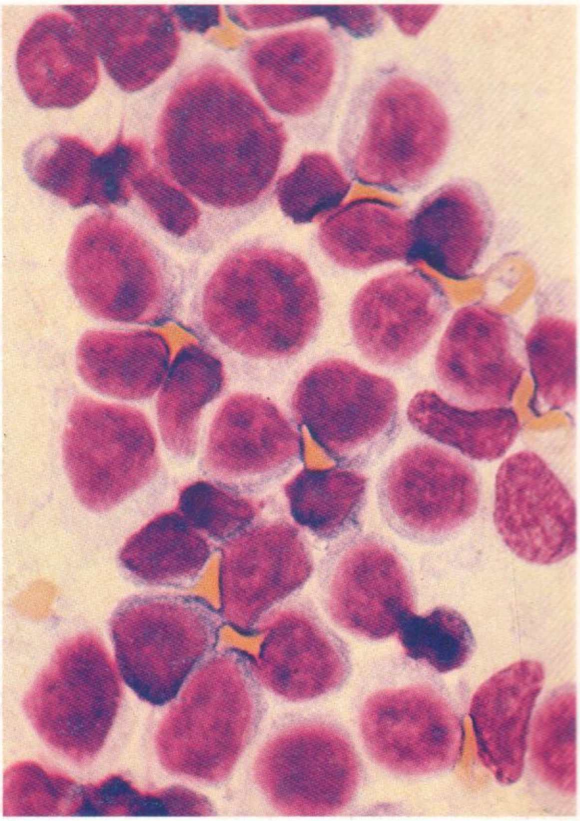

1163–1168. *Lymph node imprints: lymphoblastic lymphoma, B-cell type.*

1163 and **1164**. Leishman stain: low- and higher-power views of the neoplastic lymphoblast tumour cells; they show rounded nuclei with moderately fine chromatin and nucleoli varying in number between one and three or four, mostly not at the nuclear membrane. There is moderately deep basophilia in the narrow cytoplasmic rim.

1165. SB stain: there is a single positive neutrophil polymorph, but the lymphoblasts and occasional lymphocytes are all quite negative.

1165

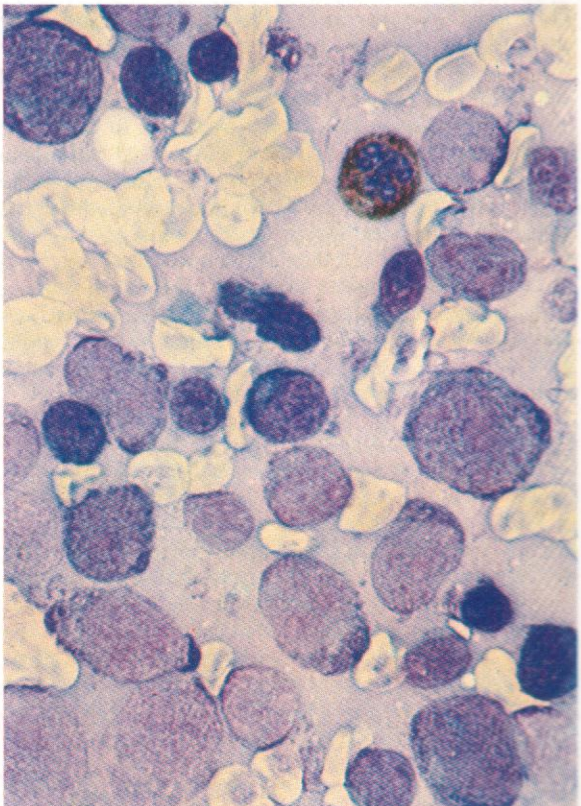

66

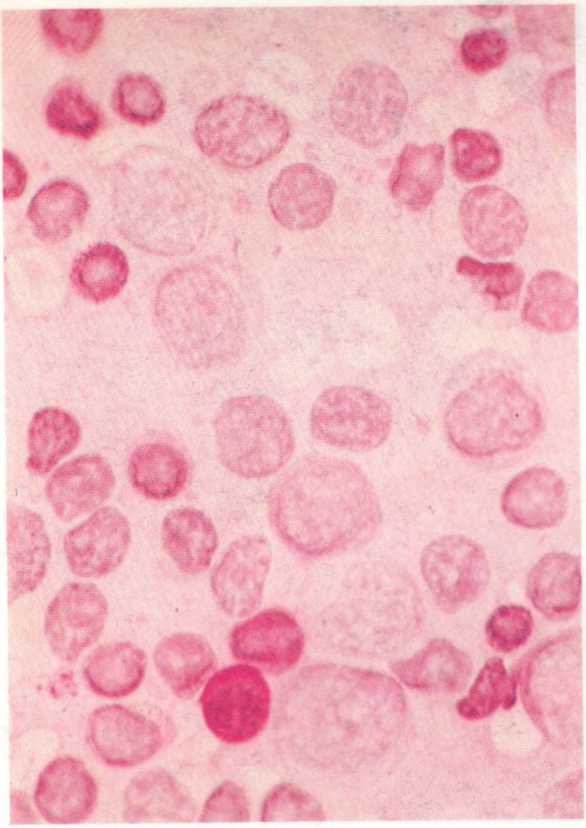

1167

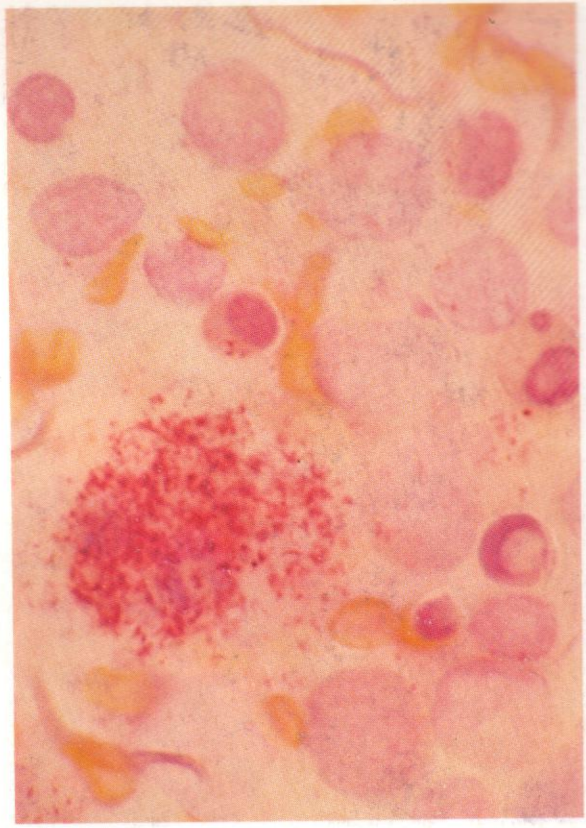

1168

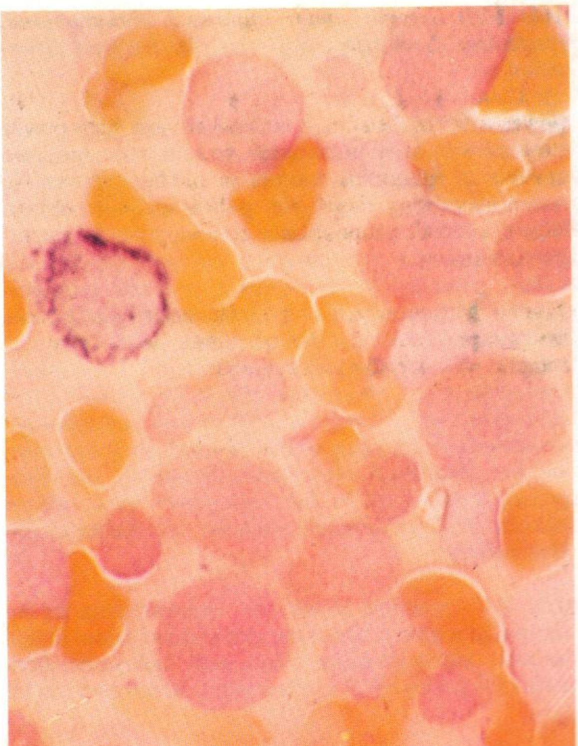

1166. PAS reaction: the blast cells are virtually entirely negative; there is some granular positivity in one lymphocyte and the usual strong reaction in the single neutrophil present.

1167. Acid phosphatase: the blast cells are again negative while a phagocytic RE cell is strongly positive. A few positive granules are seen in a single plasma cell above the RE cell.

1168. Dual esterase: the lymphoblasts show fine scattered BE positivity. A neutrophil polymorph is CE-positive.

1169

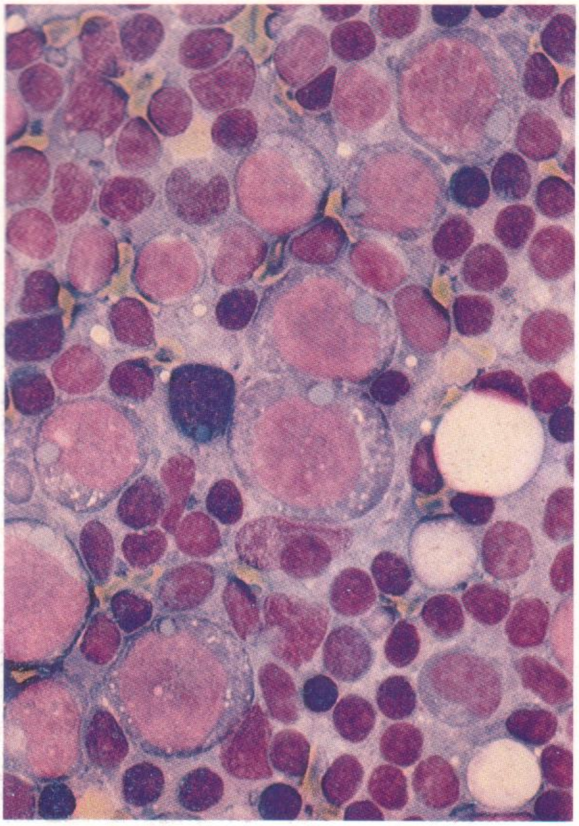

1170

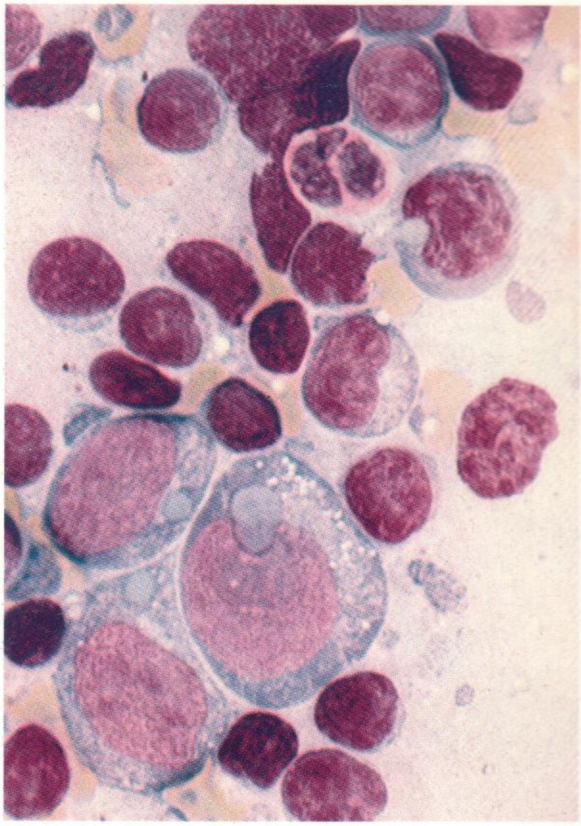

1169–1174. *Lymph node imprints: immunoblastic lymphoma, B-cell type, with some plasmacytoid differentiation.*

1169 and **1170**. Leishman stain: low- and high-power views showing large immunoblastic cells with moderate amounts of basophilic cytoplasm and leptochromatic nuclei containing large but poorly defined central nucleoli. Most immunoblasts contain globular inclusions, staining a greyish-green colour, like Russell bodies, presumably representing secreted immunoglobulin. This feature is only occasionally seen in cases of immunoblastic lymphoma, but when present indicates the secretory B-cell nature of the tumour. Among the surrounding small cells, chiefly lymphocytes and centrocytes, are some with plasmacytic morphology occasionally containing similar Russell-body inclusion material. Scattered cytoplasmic fragments are conspicuous, especially in the high-power view, where multiple small cytoplasmic vacuoles are visible in the immunoblasts.

1171. PAS reaction shows the immunoblasts to be essentially negative, as are the globular inclusions in this instance, although more often such inclusions show weak PAS positivity. A single positive neutrophil can be seen.

1171

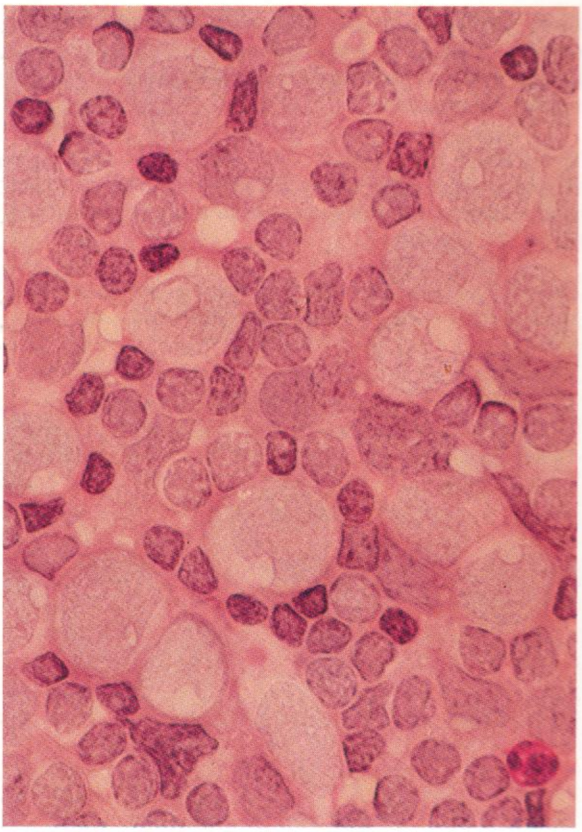

2

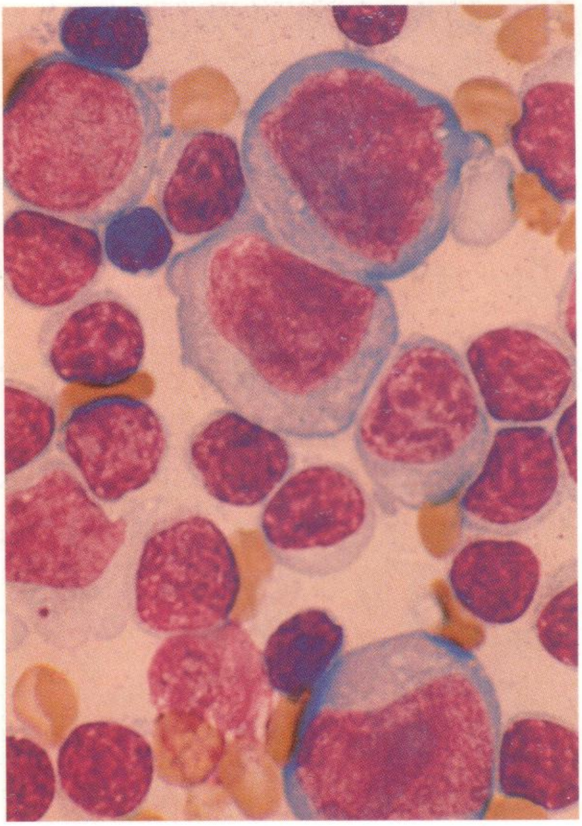

1173

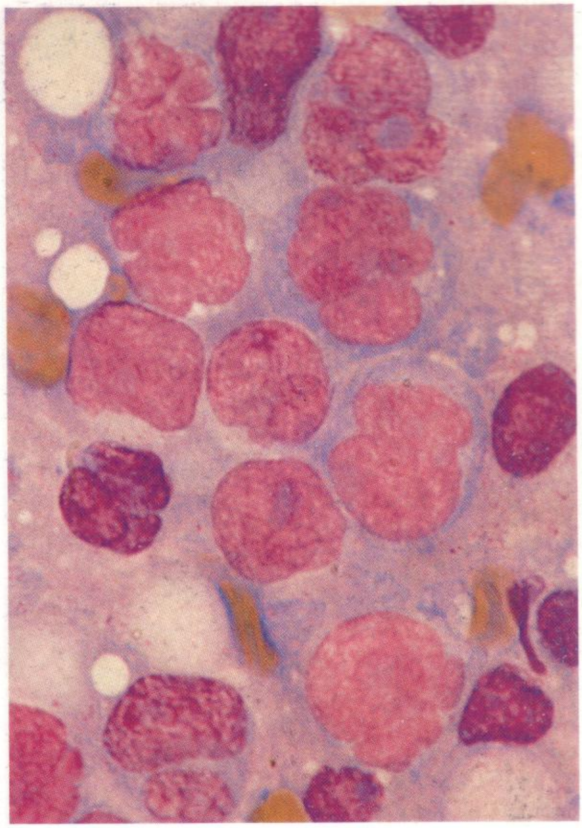

1172–1174. Imprints of lymph node biopsies from another two cases of immunoblastic lymphoma with generally similar cytology but without the globular inclusions seen in the previous case. In the first, the field shown in **1172** again illustrates the characteristic cytology of the immunoblasts and also the presence of lymphoplasmacytoid cells among the lymphocytes and centrocytes; the immunoblasts from the second case, depicted in **1173**, have more irregular nuclear outlines, as may sometimes be seen. The PAS reaction on the cells from this example, shown in **1174**, is more variable in positivity than was the case in **1171**, ranging from negative to quite strongly positive, with fine or coarse granules, as at the top left and lower right, respectively, of this field. An occasional block of PAS positivity was present in the immunoblasts in this case and one such block is seen free from the cytoplasm in the centre of the field. Variable PAS positivity of this kind is not uncommon in immunoblastic lymphoma.

1174

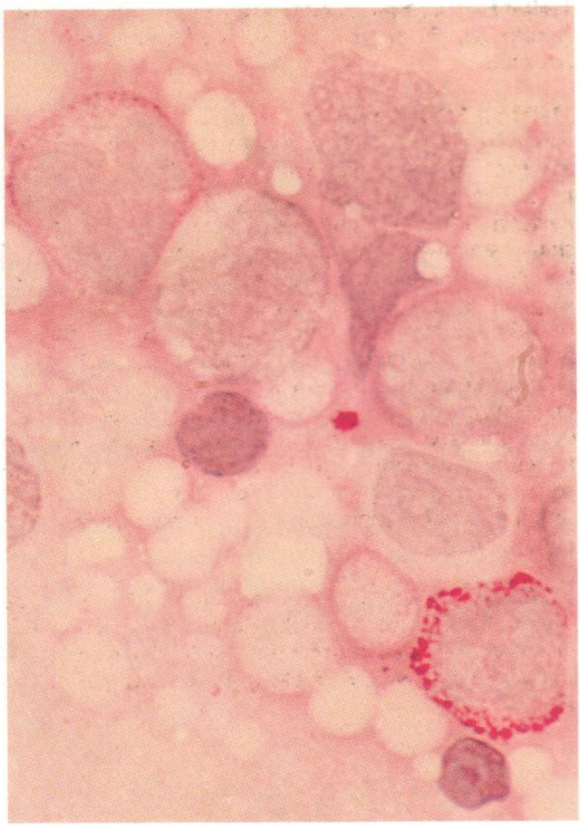

1175

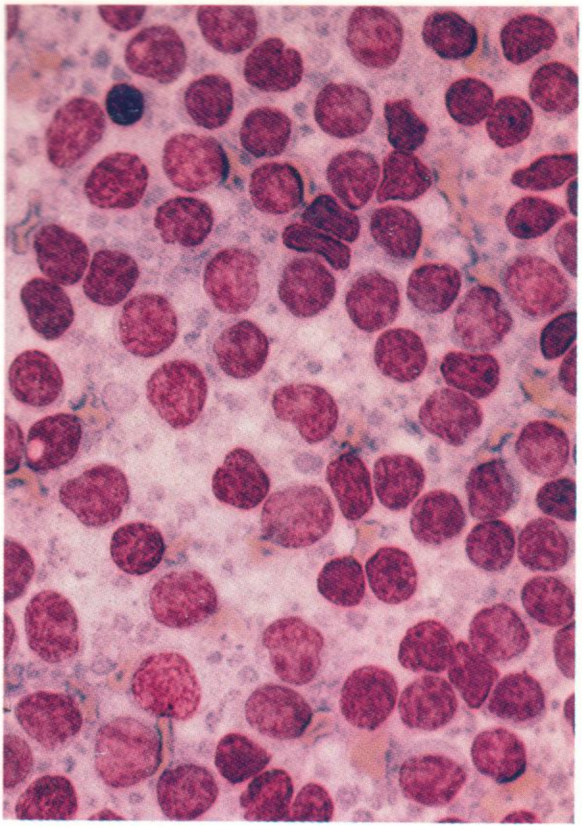

1176

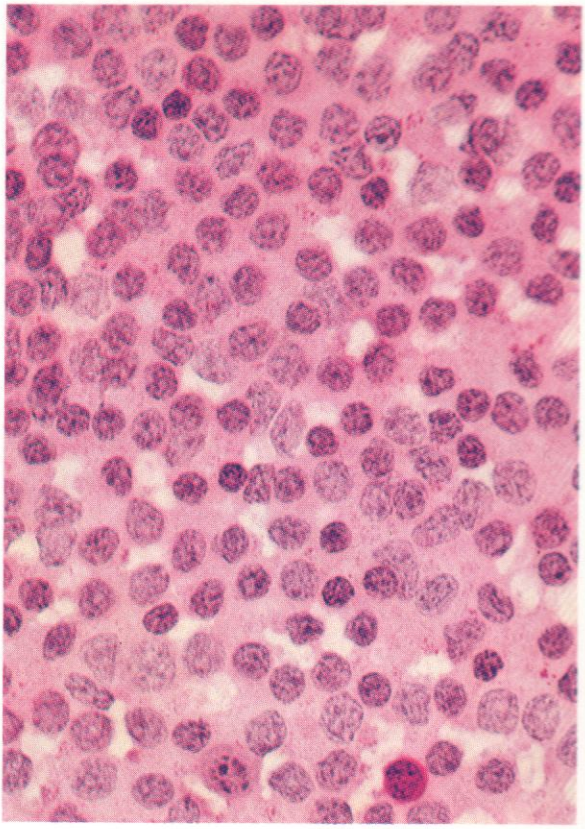

1175–1178. *Lymph node imprints: hairy cell leukaemia (HCL).*

1175. Leishman stain: the specimen is composed almost entirely of hairy cells (HCs). There is gross cytoplasmic fragmentation but there are virtually no normal lymph node elements. A single lymphocyte can be seen near the top left-hand corner.

1176. PAS reaction: there is diffuse or finely granular positivity in the background, which is largely made up of the fragmented cytoplasm of HCs.

1177. Acid phosphatase: most cells show moderately strong granular positivity, and there is also considerable background scattered positivity from cytoplasmic fragmentation. Only four normal lymphocytes can be detected.

1178. Dual esterase: there is strong BE positivity in a histiocytic RE cell, and weaker reaction in the cytoplasmic rim of many HCs and in the scattered fragments of disrupted HC cytoplasm.

1177

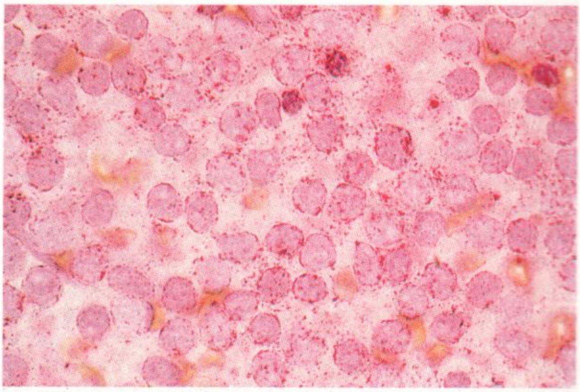

1178

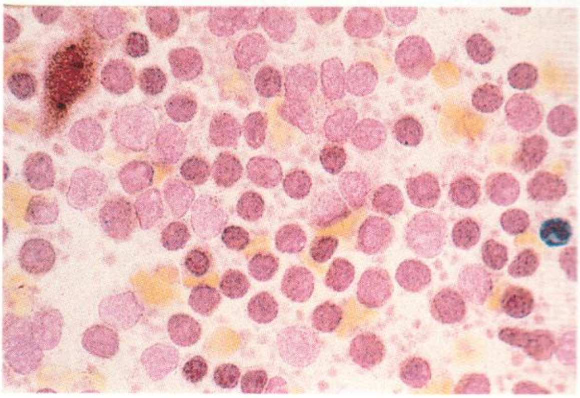

79

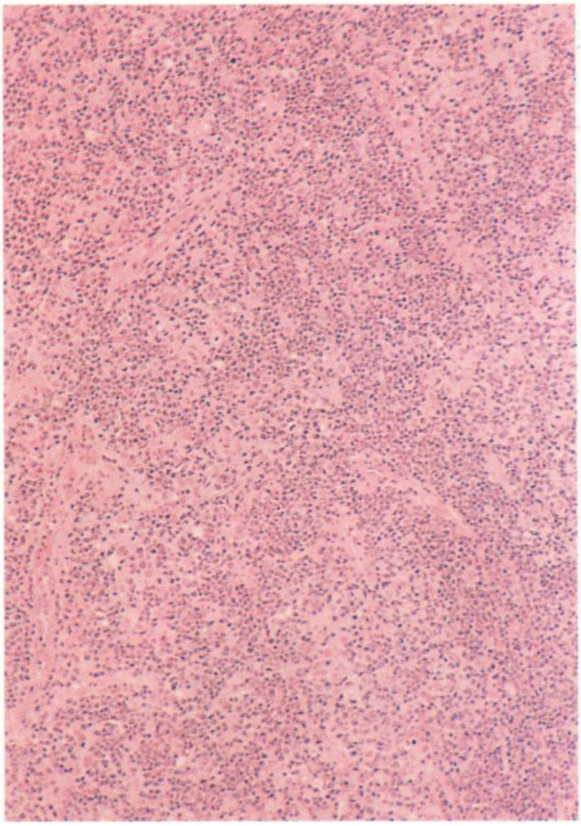

1180

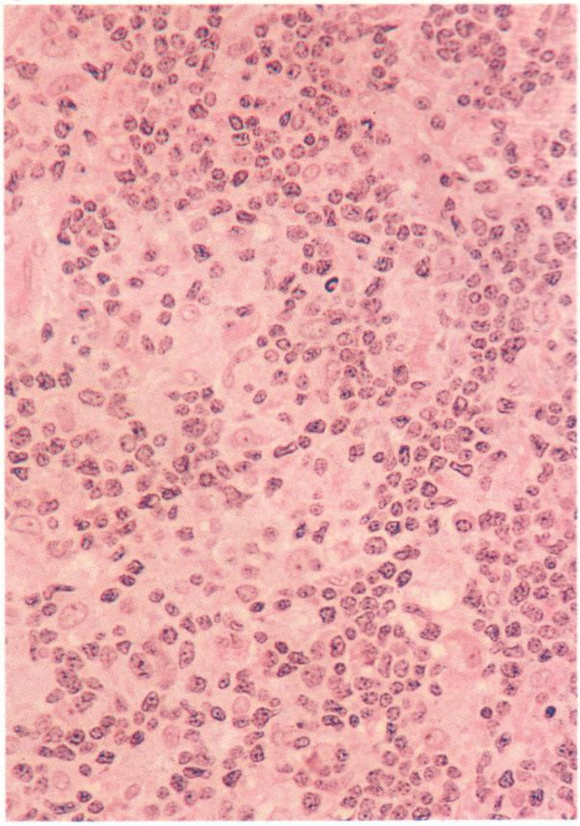

1179–1187. *Sections and imprints of lymph node biopsies from patients with peripheral T-cell lymphomas (Lennert's lymphoma). T-lymphoblastic lymphomas, like T-ALL, which they closely resemble and into which they usually undergo transformation, are regarded as being derived from precursor T cells, but another group of lymphomas with diffuse histological distribution and variable clinical course react with mature T-cell markers, often with CD4, and do not possess TdT. Their morphology is pleomorphic, with the lymphomatous cells either mature T cells or T immunoblasts or, more commonly, a heterogeneous mixture, but with a marked reactive component of epithelioid histiocytes and increased vascularity. The neoplastic T cells may show atypical surface antigen expression, sometimes failing to react with the pan-T marker CD7, for example, but their clonal origin can be confirmed by the demonstration of specific TCR gene rearrangement in Southern blots.*

1179–1181. Successively increasing magnifications of areas from a section of lymph node showing the characteristic features of T-cell lymphoma; the increased vascularity and conspicuous epithelioid cell reaction among the malignant lymphocytes are manifest in **1179** and **1180**, while details of the T-cell and epithelioid-cell cytology are revealed in **1181**.

1181

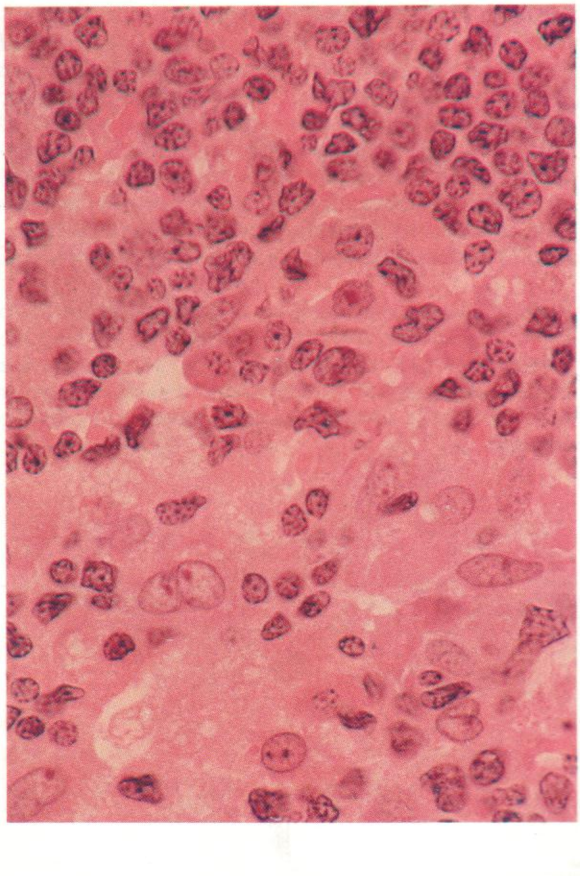

182

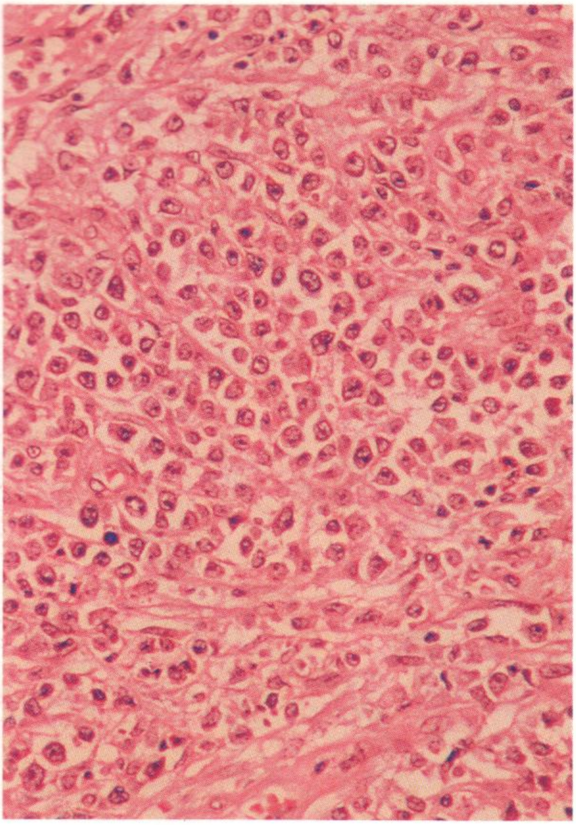

1183

1182 and **1183**. Low- and higher-power views, respectively, of a lymph node section from another case of peripheral T-cell lymphoma, again illustrating the mixed but here chiefly large-cell immunoblastic neoplastic cytology, the marked vascularity and the epithelioid histiocytes, although the last component is less conspicuous in this case than in the previous one. In **1183** there is a multinucleated giant cell, probably of Langhans type and derived from the reactive epithelioid histiocytes, a finding quite common in this kind of lymphoma.

1184. An immunoperoxidase reaction against the MAb CD4, on a section from the same biopsy, showing the presence of the helper phenotypic antigen on the malignant T lymphocytes and immunoblasts. The larger epithelioid cells and the vascular endothelial cells are negative.

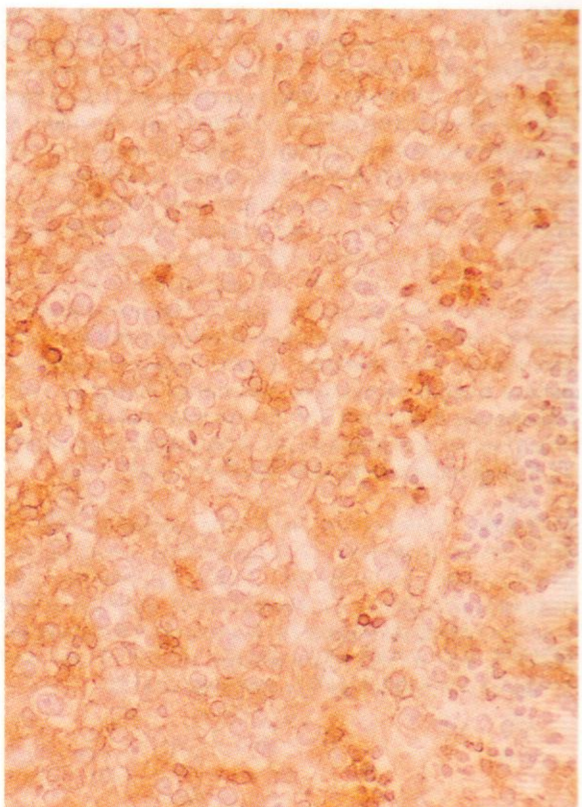

1184

85

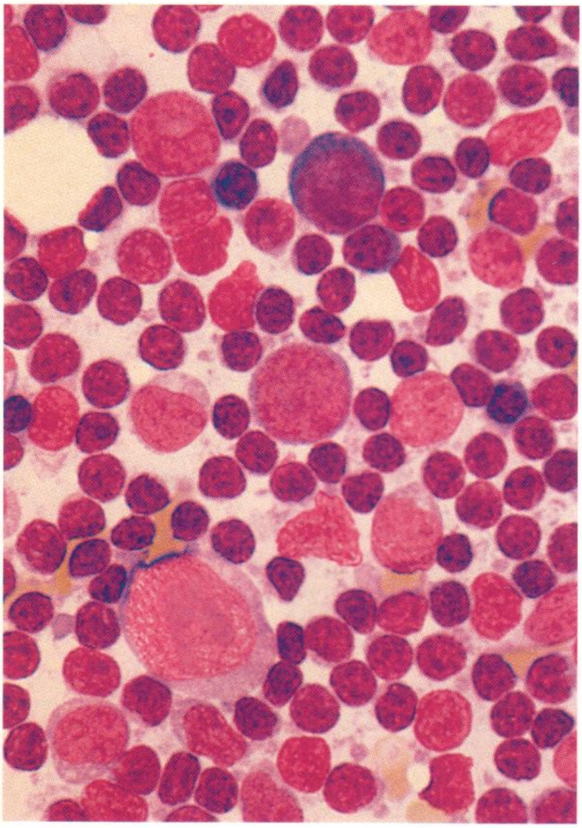

1186

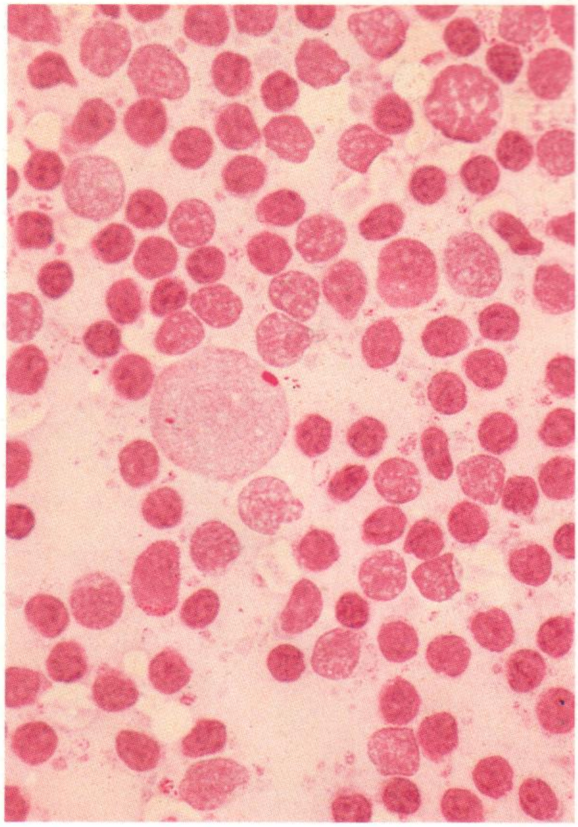

1185–1187. Romanowsky, PAS and acid phosphatase stains on imprints made from a lymph node biopsy from a similar case of peripheral T-cell (Lennert's) lymphoma. In imprints, the feature of increased vascularity cannot, of course, be demonstrated, and the epithelioid histiocytic proliferation is also less easy to appreciate than in sections, because the epithelioid cells tend to adhere to the cut surface of the node and not to be adequately represented in the imprint. The mixed neoplastic T-cell cytology, with a range from mature lymphocytes to immunoblasts, is apparent in **1185**, however, with a generally negative PAS reaction – except for a single block in one immunoblast (shown in **1186**) – but with the strong localized paranuclear acid phosphatase positivity typically found in T cells (as seen in **1187**).

1187

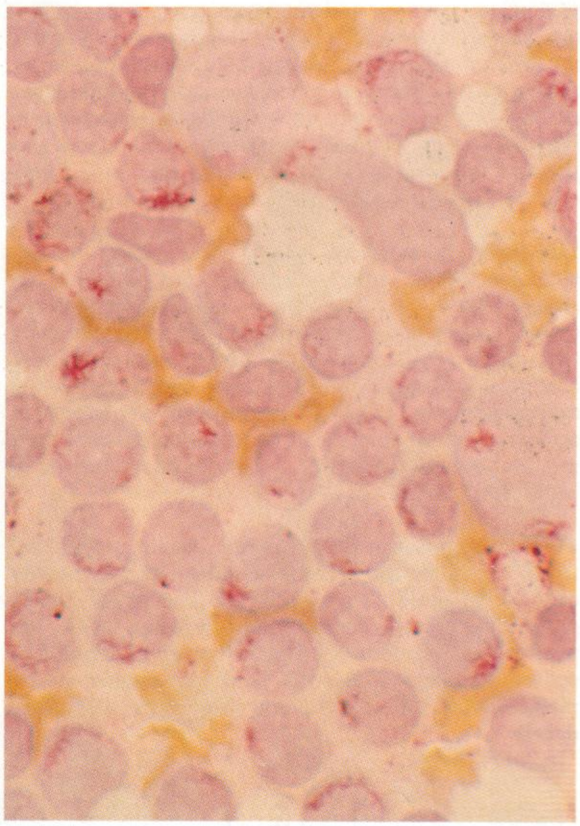

188

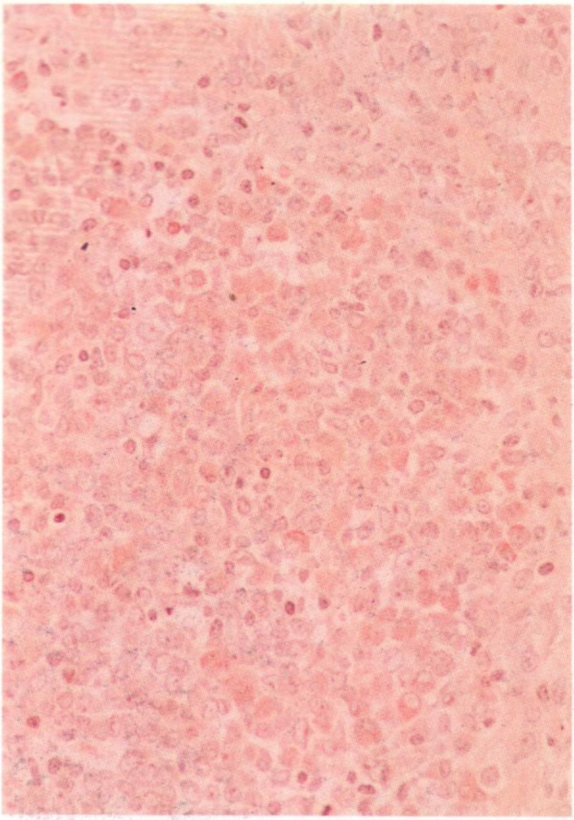

1189

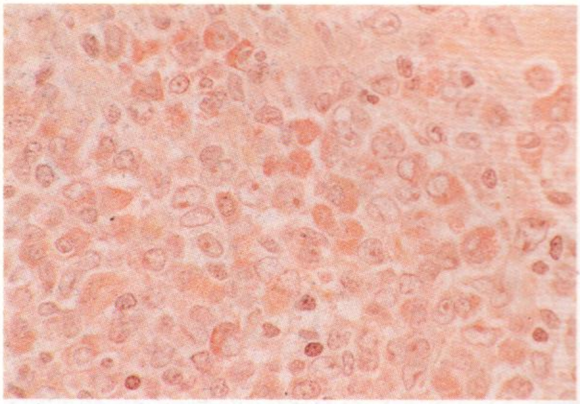

1190

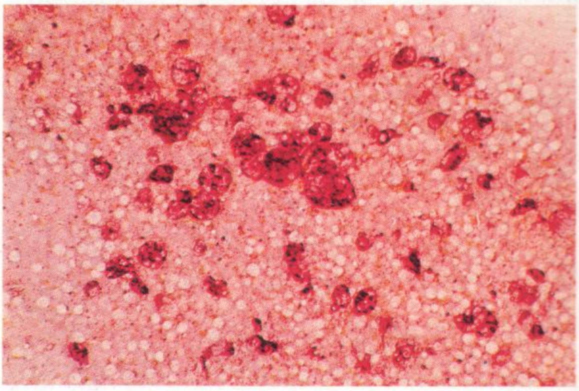

1191

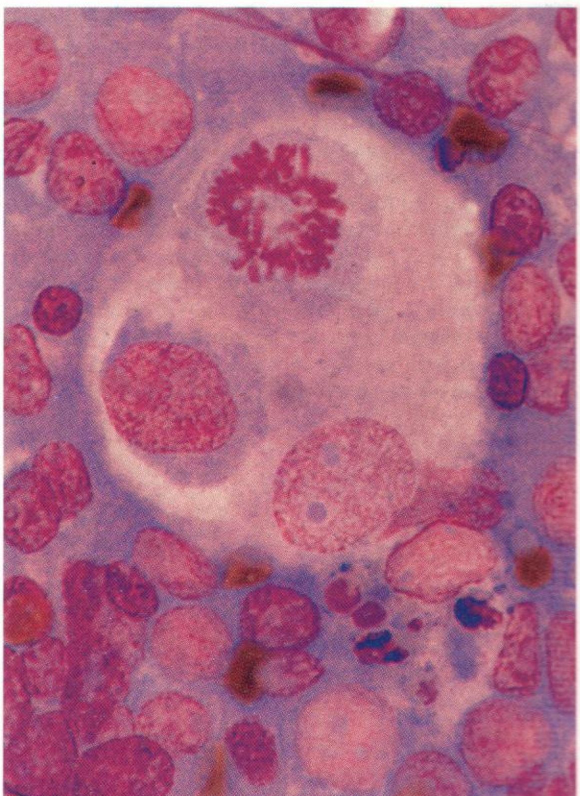

1188–1191. *Sections and an imprint from an example of true histiocytic lymphoma (THL), a localized variant of the generalized systemic disease malignant histiocytosis. Diagnosis usually requires cytochemical or immunocytochemical confirmation of the cell lineage, with acetate or butyrate esterase and acid phosphatase staining, or with positive reactions to CD14, since the neoplastic histiocytes in THL often show little phagocytic activity.*

1188–1190. Sections of lymph node biopsy from a localized nodal enlargement without evidence of generalized disease, showing predominance of histiocytes, demonstrable as such by cytochemical staining for the monocyte–macrophage enzyme alpha-naphthyl acetate esterase, as shown at low- and higher-power magnification in **1188** and **1189**, respectively. In **1190** an acid phosphatase stain on another section from the same material shows the strong positivity characteristic of histiocytes.

1191. A high-power field from an imprint preparation from the same node biopsy, showing an unusual example of multiple phagocytosis. The larger macrophage (histiocyte) contains two ingested cells, one probably a centroblast and the other an unidentifiable cell in metaphase of mitosis, while the smaller macrophage below contains several fragments of cellular debris.

92

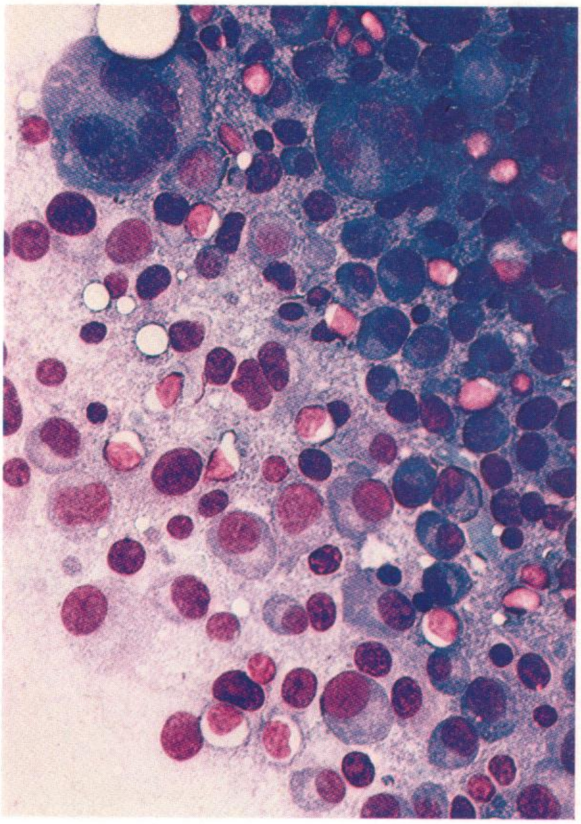

1193

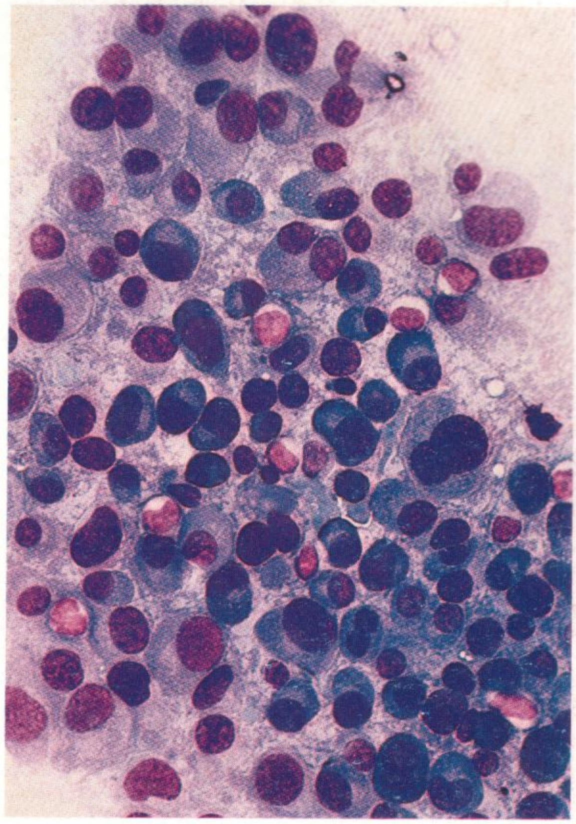

1192–1194. A lymph node imprint: Leishman stain: myeloma. The fields illustrate variable size and staining characteristics of infiltrating plasma cells, occasional marked multinuclearity, and the general contrast between the plasma cell elements and the background centrocytes, with their lighter nuclei and clear cytoplasm. In **1194**, there is an example of a mitotic figure in a myeloma cell with probable polyploidy, while another more normal mitotic figure can be seen in a neighbouring centroblast.

1194

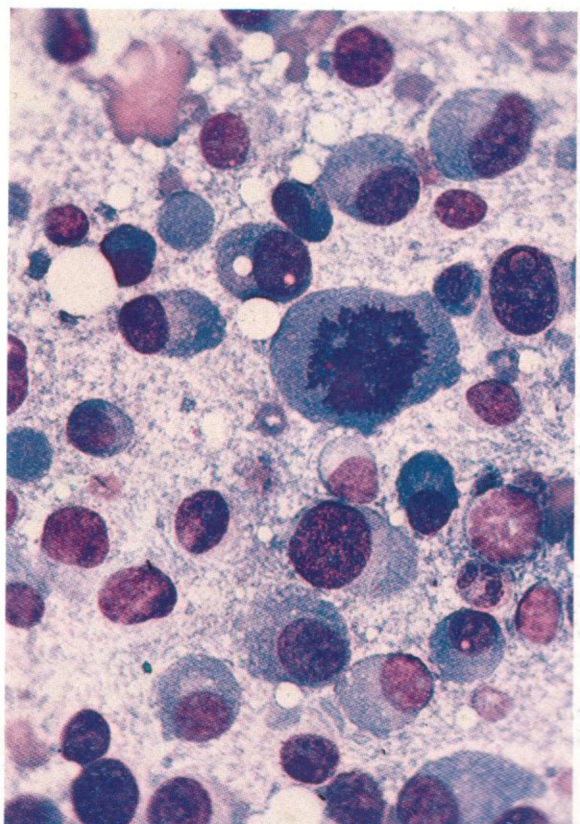

95

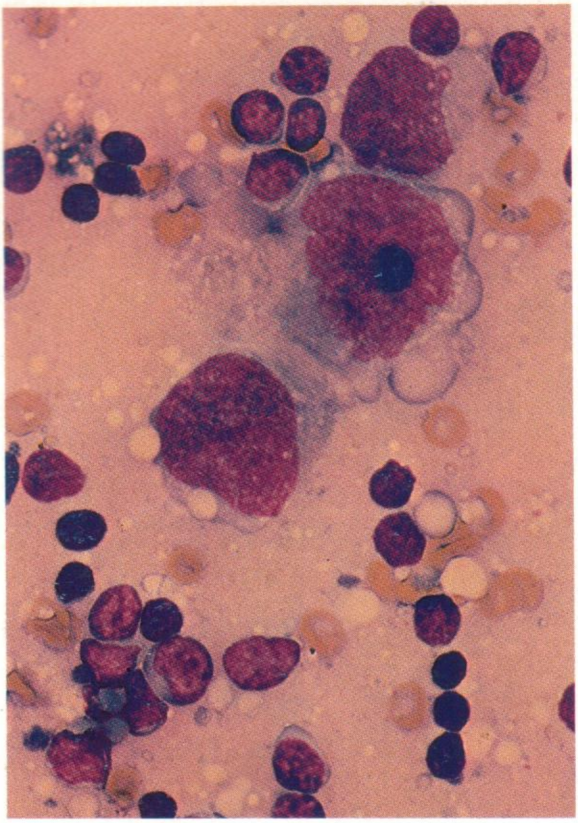

1196

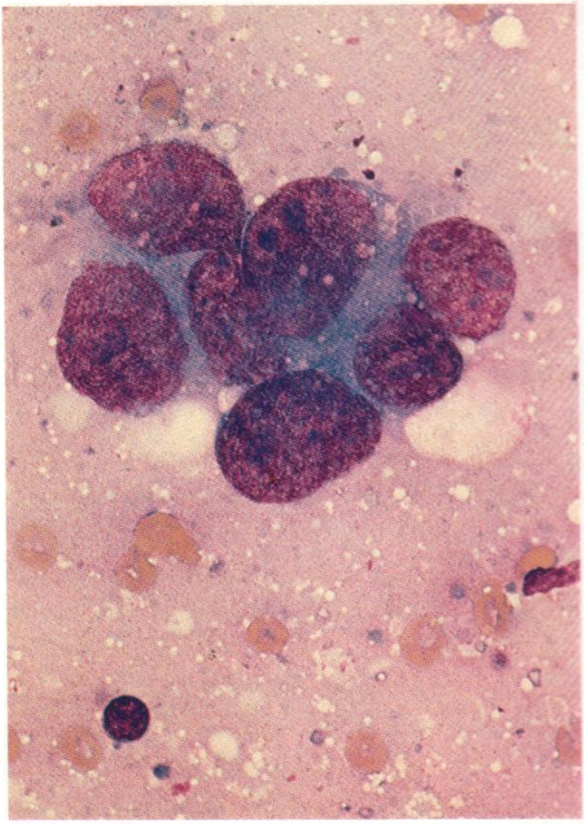

1195–1197. *A lymph node biopsy: imprint preparations, Leishman stain. Node infiltration by testicular teratoma.*

1195. Three large tumour cells among normal and reactive lymph node cells.

1196 and **1197**. Characteristic tumour cell clumps: the cytological structure of these teratoma cells is quite distinct from any normal or lymphomatous component to be found in lymph nodes.

1197

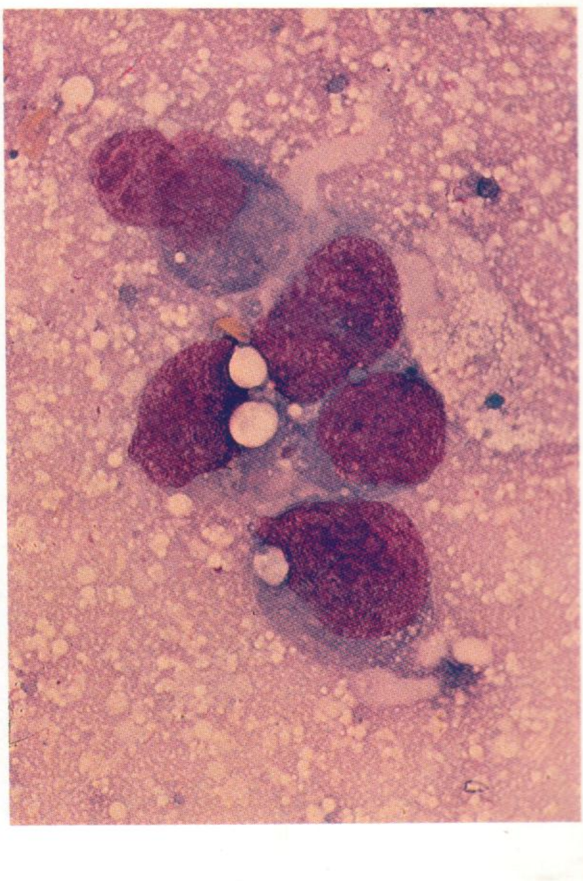

198

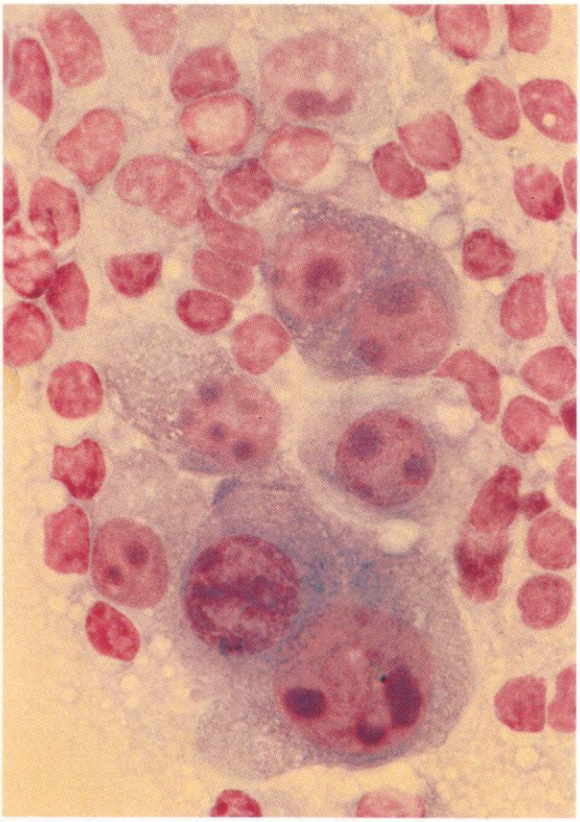

1199

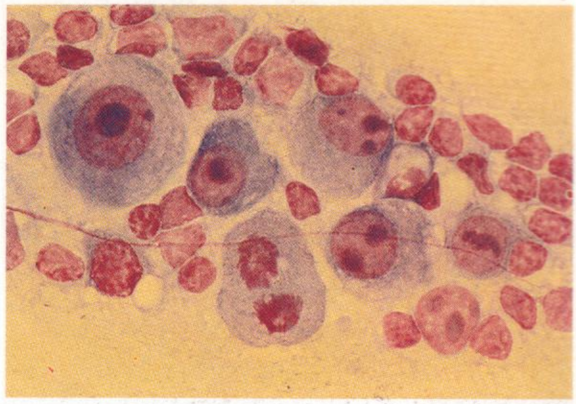

1200

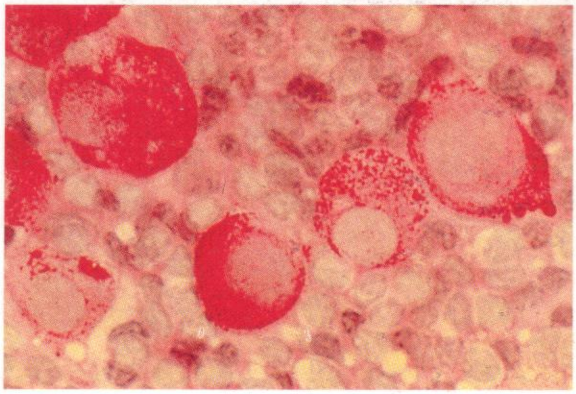

1198–1202. *Lymph node imprints: metastasizing ovarian carcinoma.*

1198 and **1199**. Two fields from the same Romanowsky-stained preparation, to illustrate the striking morphology of the ovarian tumour cells, with variability in size and degree of cytoplasmic basophilia and large deeply staining nucleoli. The cells are unlike any encountered in either normal or lymphomatous lymph nodes.

1200–1202. The cytochemical stains shown here – the PAS reaction in **1200**, an acid phosphatase stain in **1201**, and an alkaline phosphatase stain in **1202** – all show strong positive reactions in the tumour cell cytoplasm, again unlike any cells of haemic origin.

1201

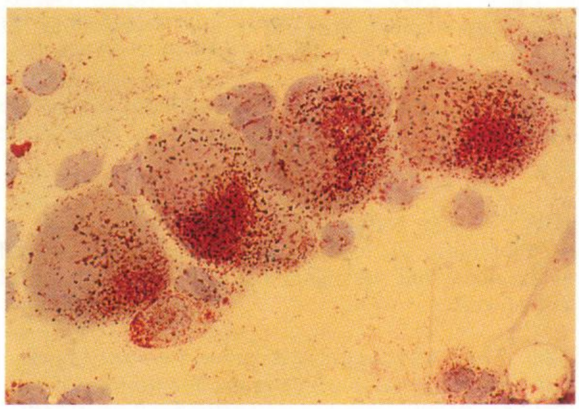

1202

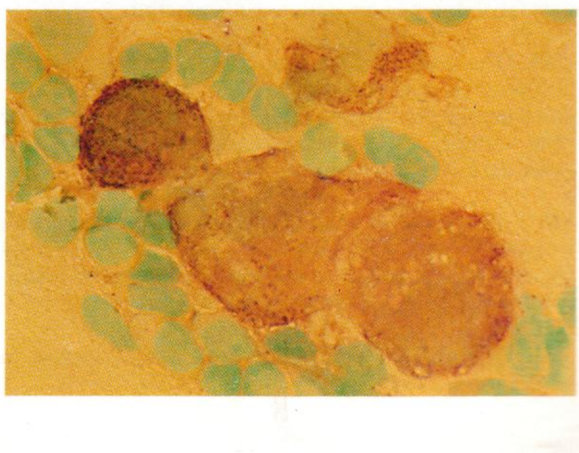

203
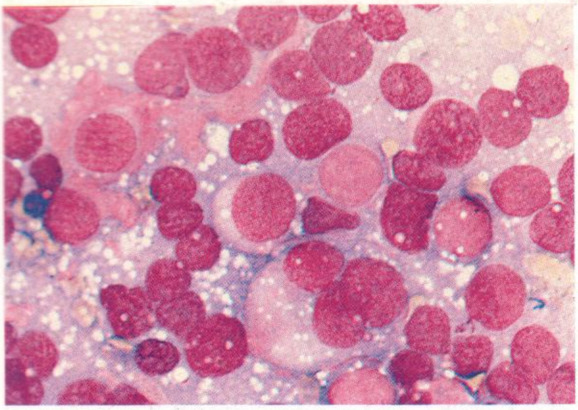

1204
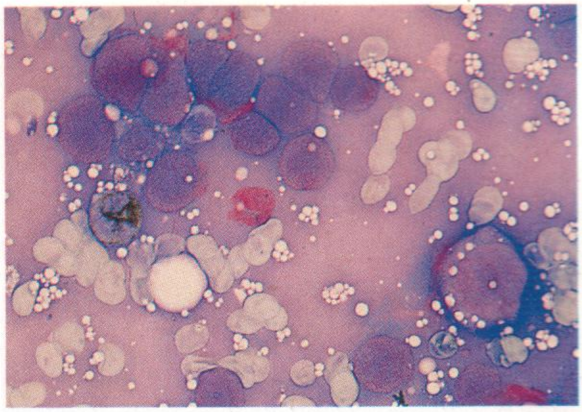

205
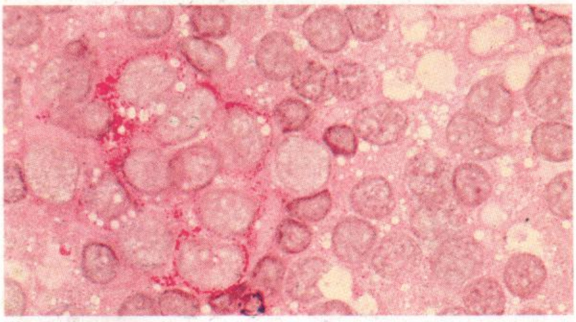

1206
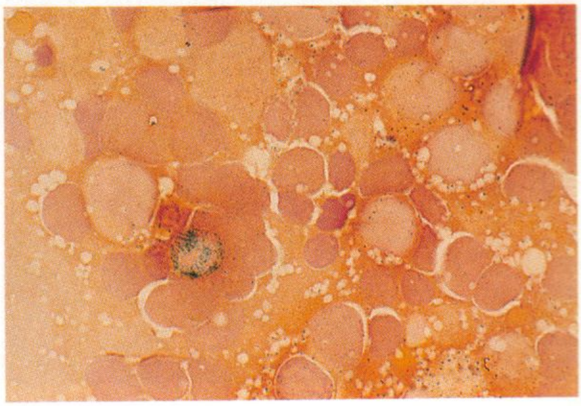

1207
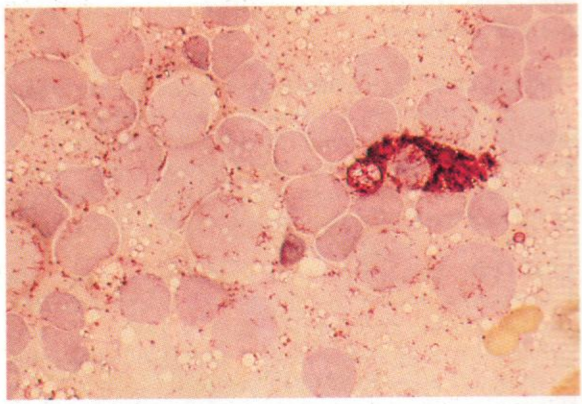

1208
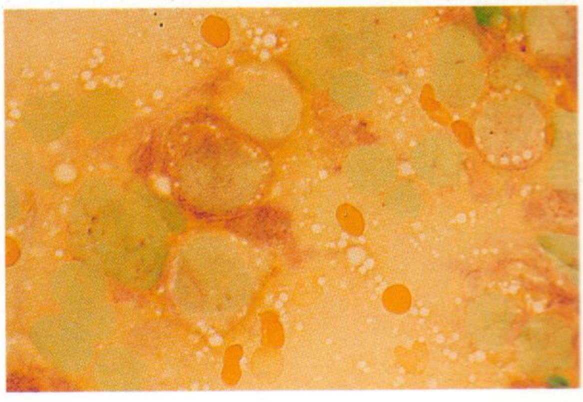

1203–1208. *Lymph node imprints: infiltration with carcinoma lung.*

1203. Romanowsky staining reveals replacement of lymphoid tissue by tumour cells with fragile and generally poorly defined cytoplasm, and with smooth structureless nuclei, occasionally multiple. There are widespread scattered vacuoles, possibly of cytoplasmic origin.

1204. SB stain shows the lung carcinoma cells to be sudanophobic. There is a single SB-positive neutrophil in this field, but the remaining cells are probably all tumour cells.

1205. The PAS reaction here shows a group of tumour cells with moderately strong granular cytoplasmic positivity, surrounded by normal lymphoid cells with darker nuclear staining and negative PAS reaction.

1206. The dual esterase stain in this field reveals CE positivity in a neutrophil and moderately strong BE positivity in the larger, more leptochromatic tumour cells, with generally negative reactions in the occasional small dark lymphoid cells.

1207. The acid phosphatase reaction in this view shows a strongly positive macrophage, but no more than a weak scattered granular reaction in the tumour cells – with little evidence of focal localization.

1208. The alkaline phosphatase reaction is positive in several of the larger neoplastic cells.

9

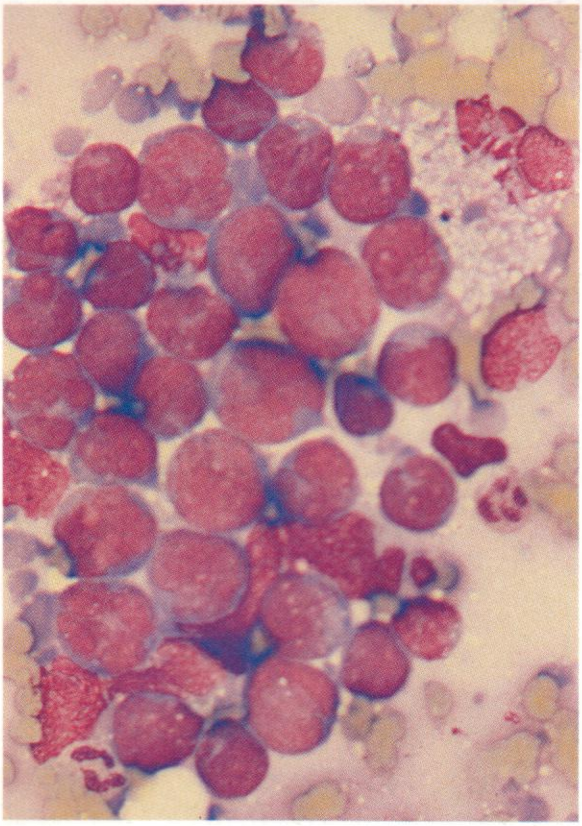

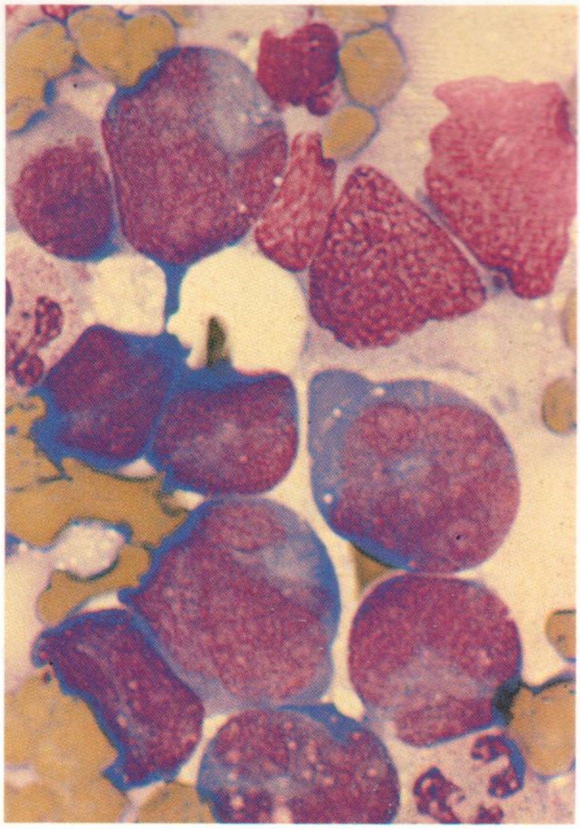

1210

1209 and **1210**. *Lymph node imprints: cervical node with secondary gastric carcinoma.*
Low- and higher-power views, respectively, of a Romanowsky-stained preparation, showing a clump of tumour cells with large size, high nuclear–cytoplasmic ratio, irregularly cleft and indented nuclei with several poorly defined nucleoli, and deeply basophilic cytoplasm. There are two or three degenerating necrobiotic carcinoma cell remnants and two normal neutrophils in each field.

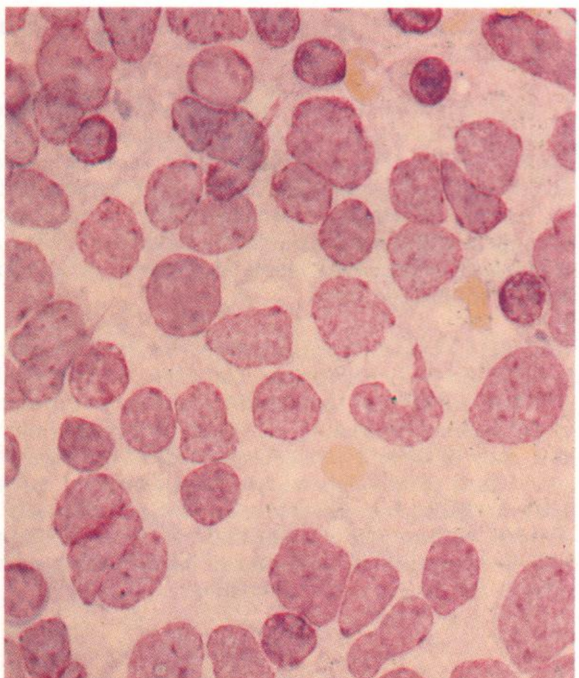

1211

1211. *Neuroblastoma cells in a lymph node imprint.*
The field shown of this Romanowsky-stained preparation contains only two residual lymphocytes, their darkly stained nuclei standing out in contrast to the paler generally leptochromatic nuclei of the preponderating neuroblastoma cells. Although in this area of the lymph node imprint the whorled clumping of neuroblastoma cell nests is not apparent, the cells show very conspicuously the feature of dense chromatin spots, sometimes called chromocentres or karyocentres, within many of the nuclei, characteristic especially of this type of tumour and seen in few others except the related medulloblastoma.

1212

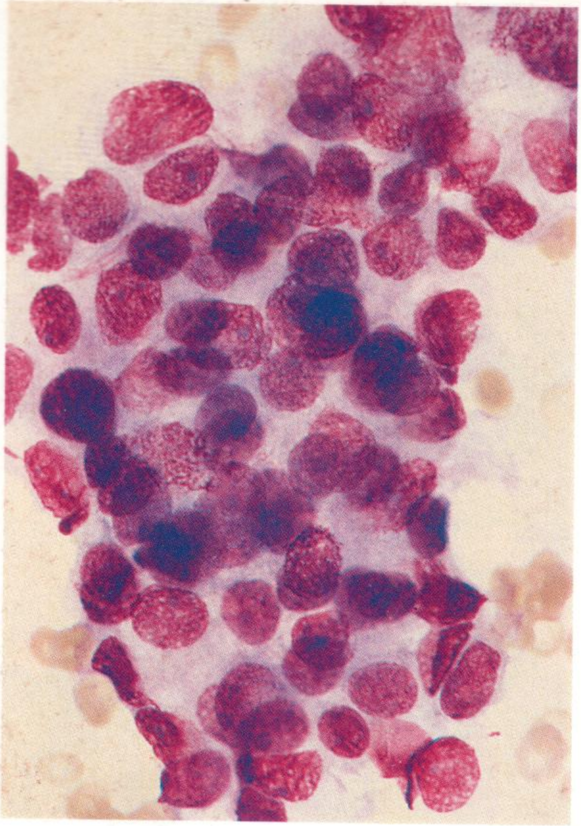

1213

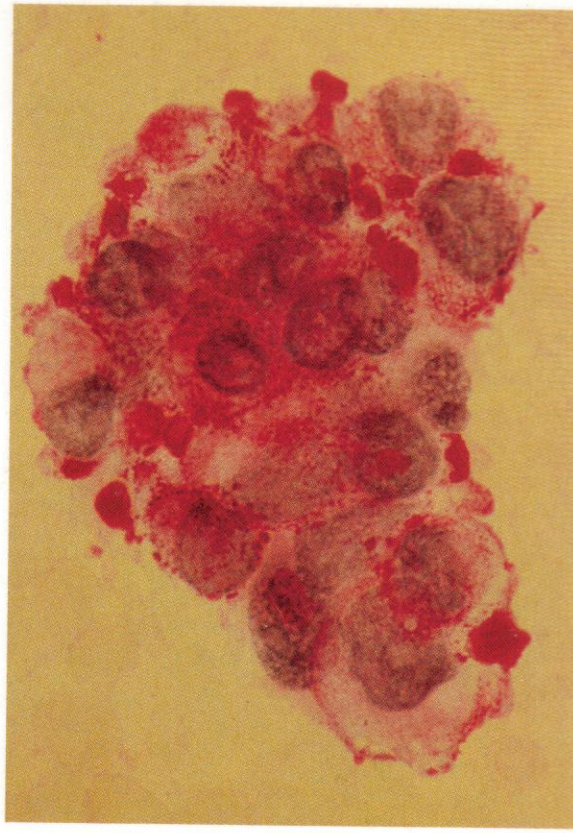

1212–1215. *A clump of breast carcinoma cells in a lymph node imprint.*

1212. In this Romanowsky stain the breast carcinoma cells appear as a largely syncytial clump with over 70 nuclei, many overlapping, and some showing early necrobiotic changes, with an opening and reticulation of the nuclear chromatin. Most nuclei have a smooth and flat appearance, with occasional purple nucleoli visible. A diagnosis of breast carcinoma secondary could not be made from this specimen.

1213–1215. Cytochemical reactions – to the PAS stain in **1213**, to acid phosphatase in **1214**, and to dual esterases in **1215** – all show strong positivity, in the case of the esterase reaction to BE. It is interesting to note that each of these cytochemically stained cell clumps shows more clearly defined cytoplasmic outlines and a less syncytial appearance than in the Romanowsky stain, perhaps because the cytochemical reaction products tend to emphasize the periphery of the cytoplasm, as is notably the case in the PAS reaction.

1214

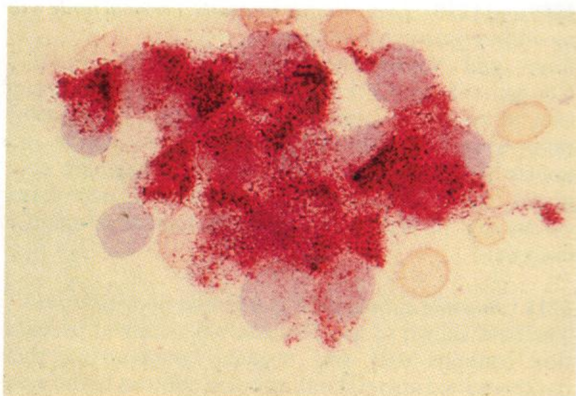

1215

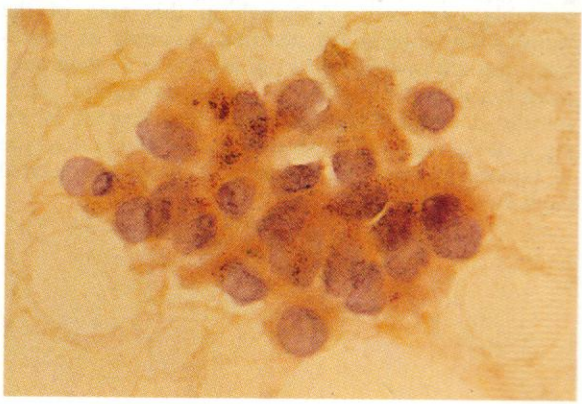

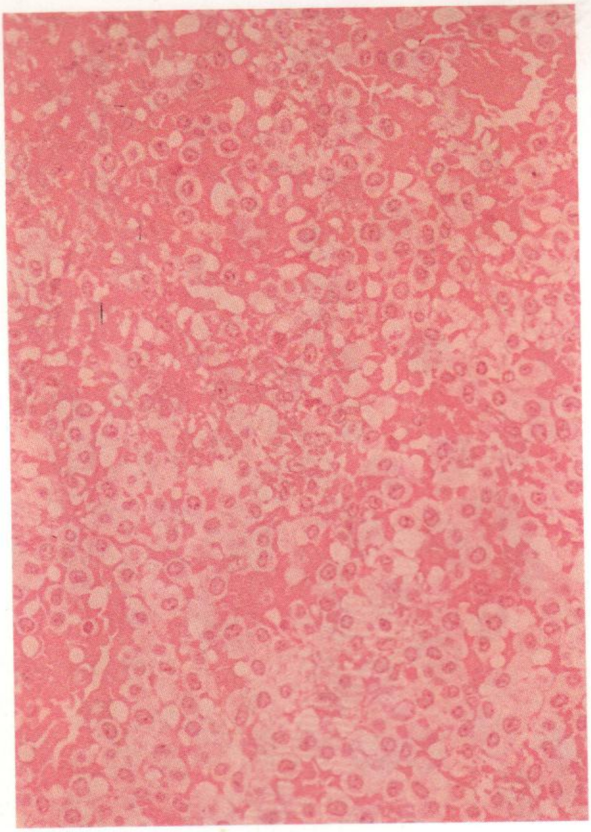

1217

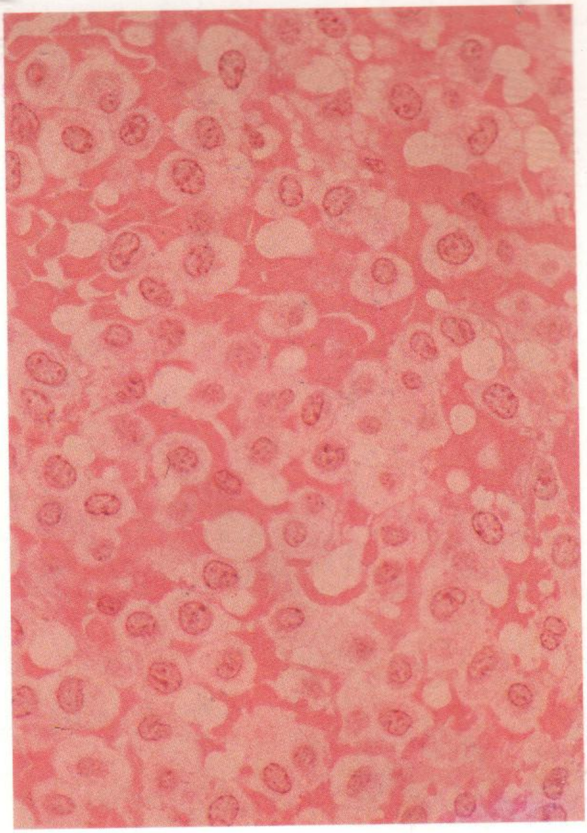

1216–1219. *Sections of spleen from patients with HCL. In this disease the spleen is generally moderately enlarged, with diffuse infiltration with HCs. The splenic follicles, Malpighian bodies, and the whole of the white pulp are much atrophied and often no longer visible, while the red pulp shows a characteristic combination of heavy infiltration with HCs and areas of marked pseudovascular dilatation engorged with red cells, giving an appearance resembling haemangioma. The pseudosinuses are actually lined chiefly by tartrate-resistant acid phosphatase (TRAP)-positive HCs rather than vascular endothelial cells.*

1216 and **1217**. Low- and higher-power fields, respectively, from a thin section, showing an area of diffuse infiltration of splenic cortical tissue with HCs. The typical halated appearance of the HCs, with their centrally placed nuclei, irregularly marked nuclear chromatin, and ample cytoplasm against an eosinophilic background of red cells, is well shown.

1218. A low-power view of a thicker section from the spleen of another case of HCL, more strongly staining with H&E, showing the pseudosinuses engorged with red cells in the upper half of the field and the predominance of HCs in the less vascular lower half.

1218

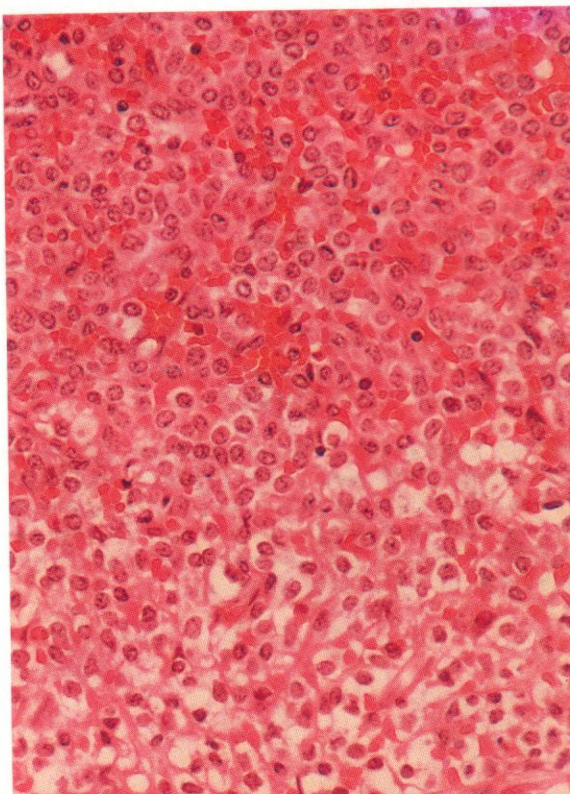

1219

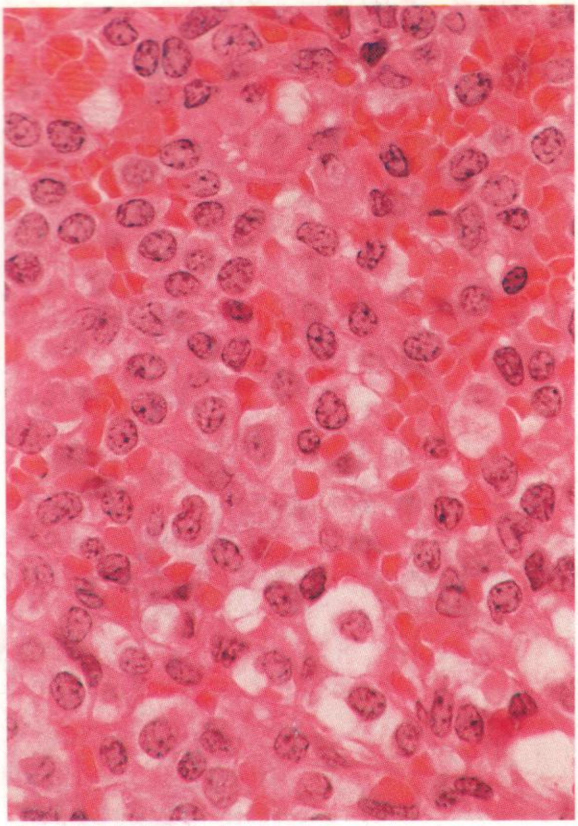

1220

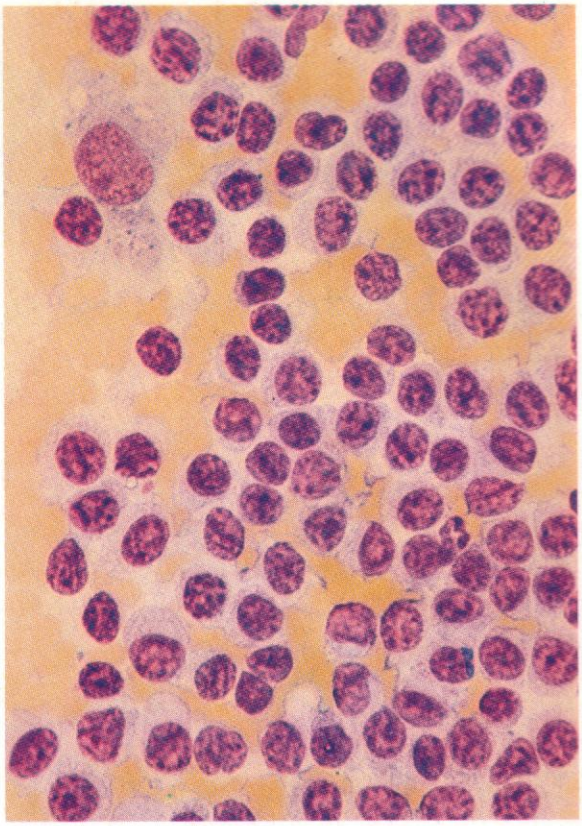

1221

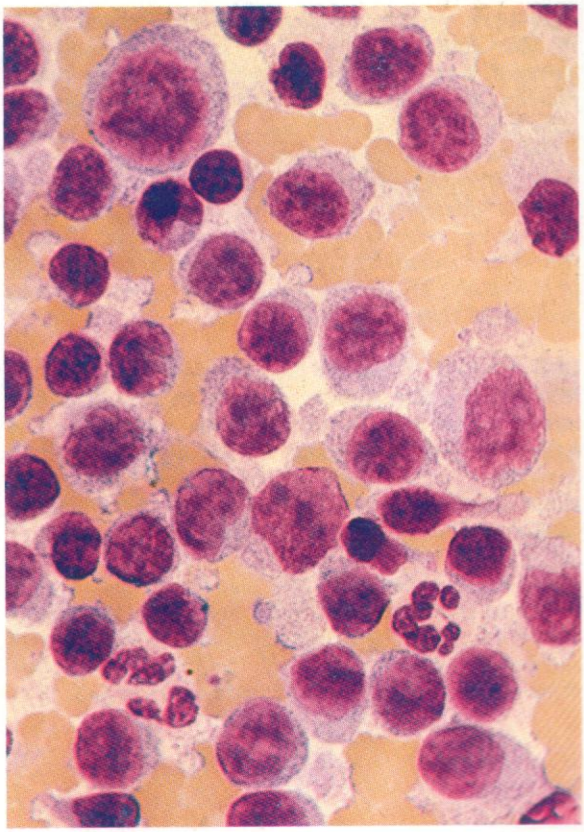

1219. A higher-power view of part of the same field as that shown in **1218**, where the pseudosinuses with their evident lining of HCs, and the characteristic nuclear and cytoplasmic patterns of these cells, are shown in more detail.

1220 and **1221**. *A splenic imprint: HCL: Leishman stain.*

1220. Typical appearances of intact HCs in spleen imprint. The nuclear pattern and moderate amount of greyish cytoplasm suggest the diagnosis, although hairy processes cannot be distinguished. A single RE cell is present, but no monocytes, no granulocytes and almost no normal small lymphocytes.

1221. A spleen imprint from another case of HCL, with rather more variable nuclear patterns and a tendency to cytoplasmic process formation and fragmentation. A few normal lymphocytes and neutrophil polymorphs can be seen and there is a characteristic background of red cells from the congested pulp.

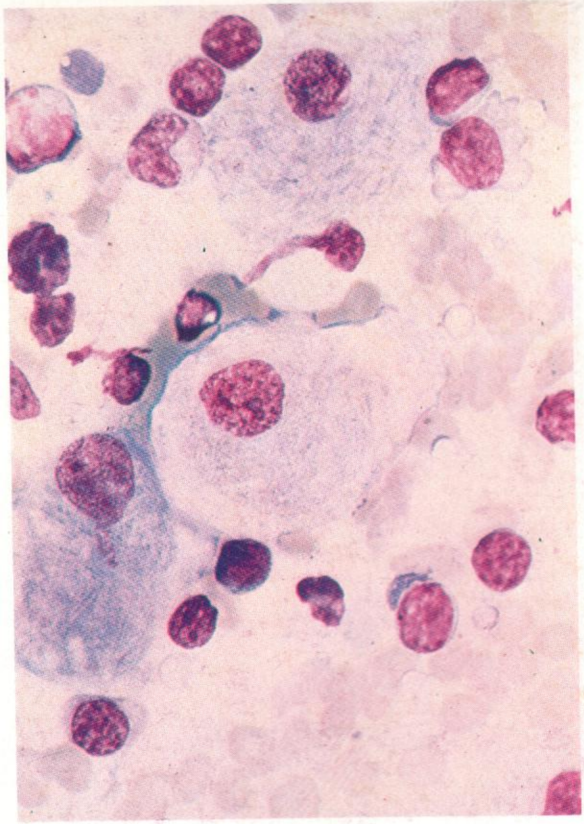

1222–1229. *Splenic imprints: Gaucher's disease. Since one of the most striking clinical features of Gaucher's disease is splenomegaly, and the diagnostic cells may not be found in the bone marrow aspirates or trephine biopsies taken in the course of investigating the accompanying anaemia or cytopenias, this is one of the few haematological conditions for which needle biopsy of the spleen may still be diagnostically valuable.*

1222 and **1223**. Leishman stain: various Gaucher cells show the granular, fibrillar and onion-skin patterns of cytoplasmic lipid inclusion material.

1224. SB stain: two granulocytes show sudanophilia but the two Gaucher cells are essentially negative.

1223

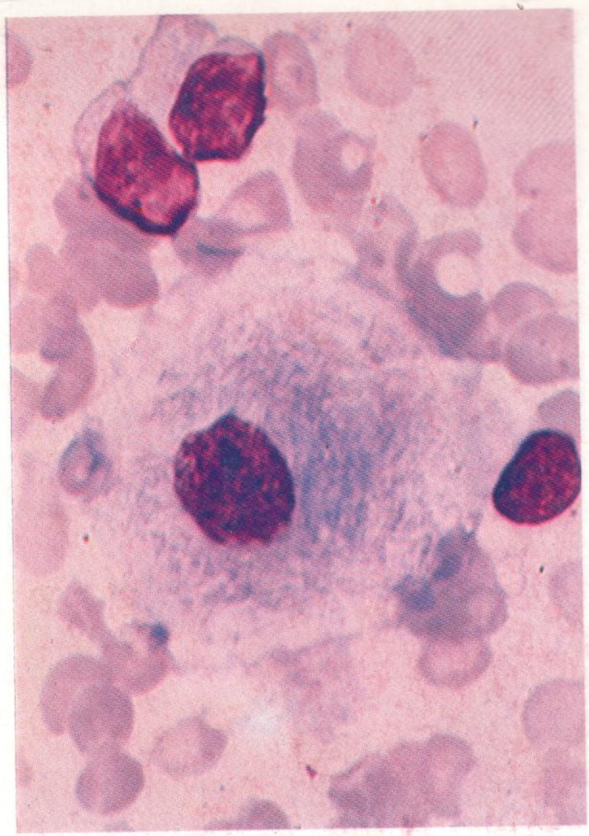

1224

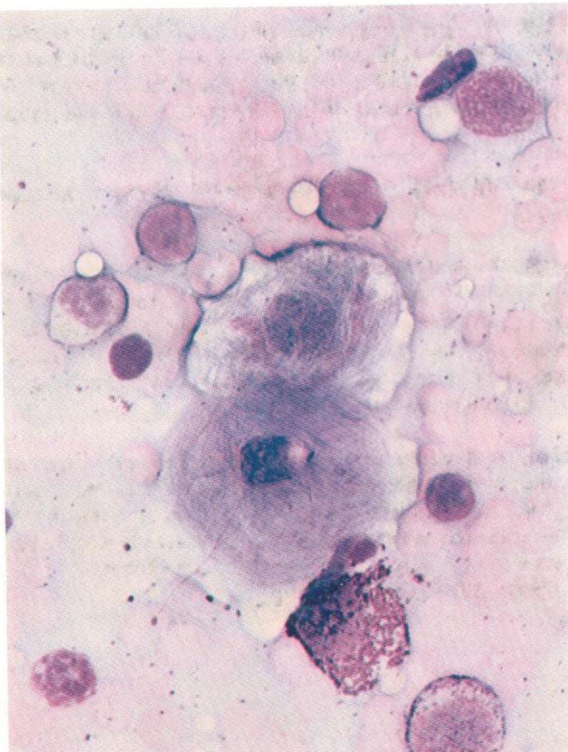

1225

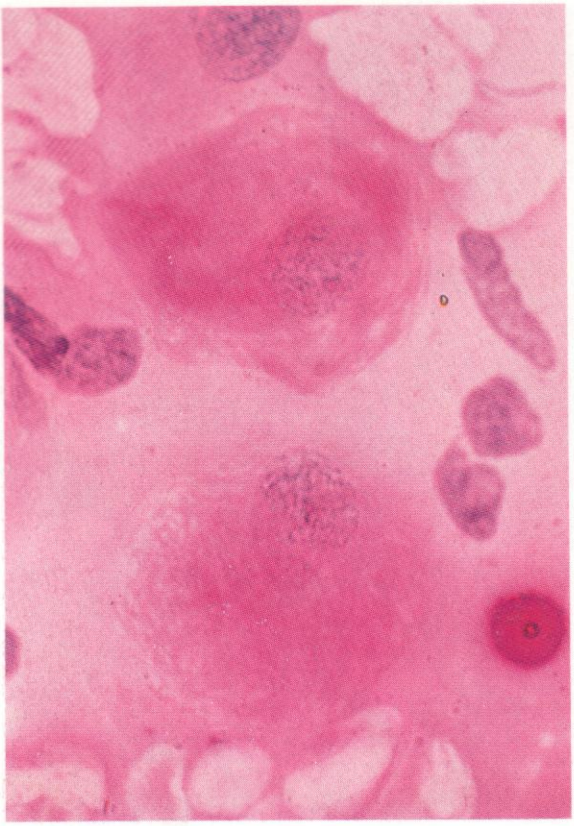

1226

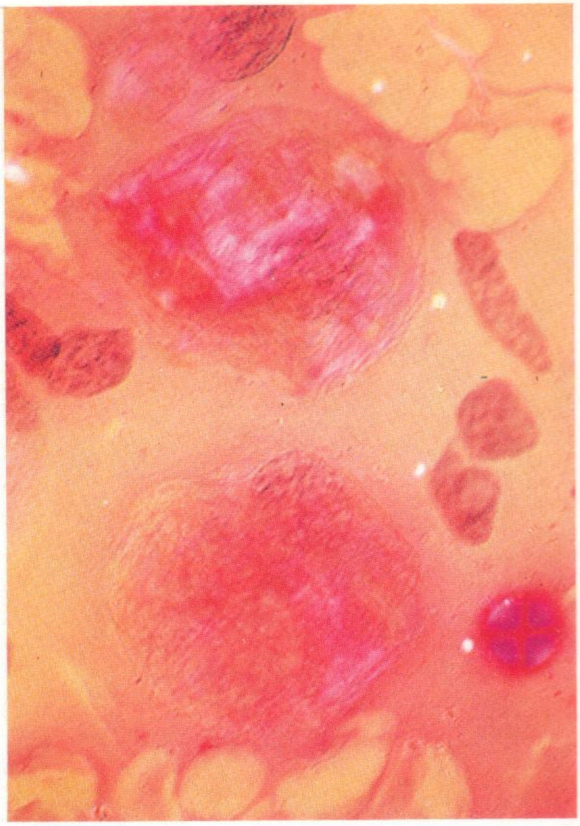

1225 and **1226**. PAS reaction: a consecutive pair of photographs of the same field containing two Gaucher cells; the first shows PAS positivity of diffuse or finely granular disposition and the second, under polarized light, shows the refringence of the fibrillar inclusion material. The brightly refringent PAS-positive 'hot cross bun' structure at the bottom is a starch granule, from surgical glove-powder contamination.

1227. Acid phosphatase: the Gaucher cells show strong positivity.

1227

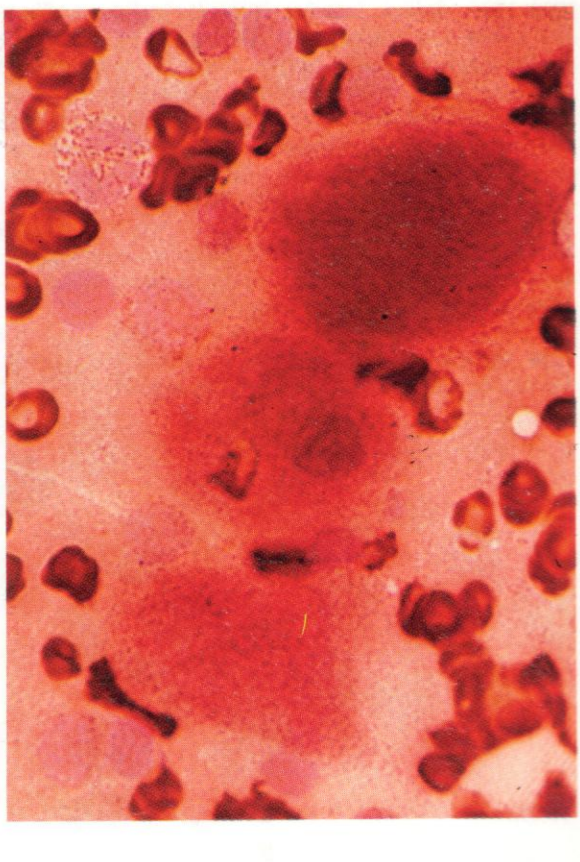

28

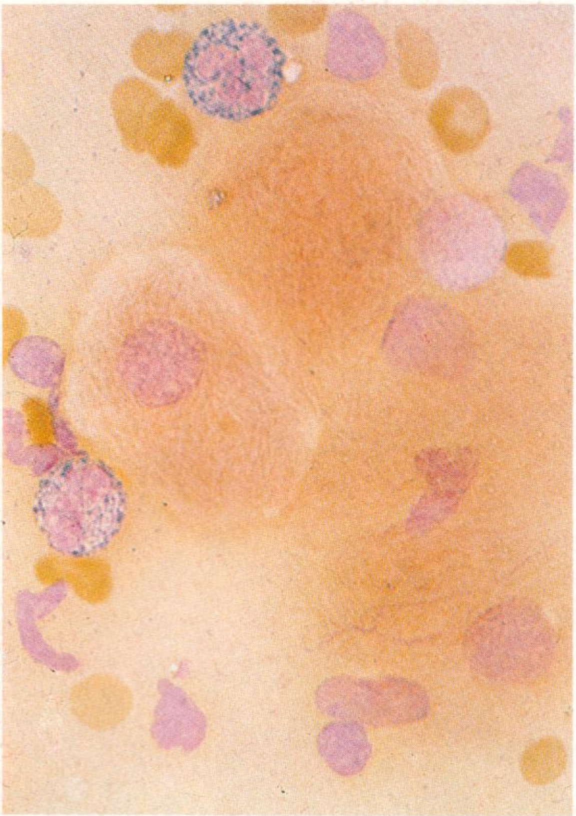

1229

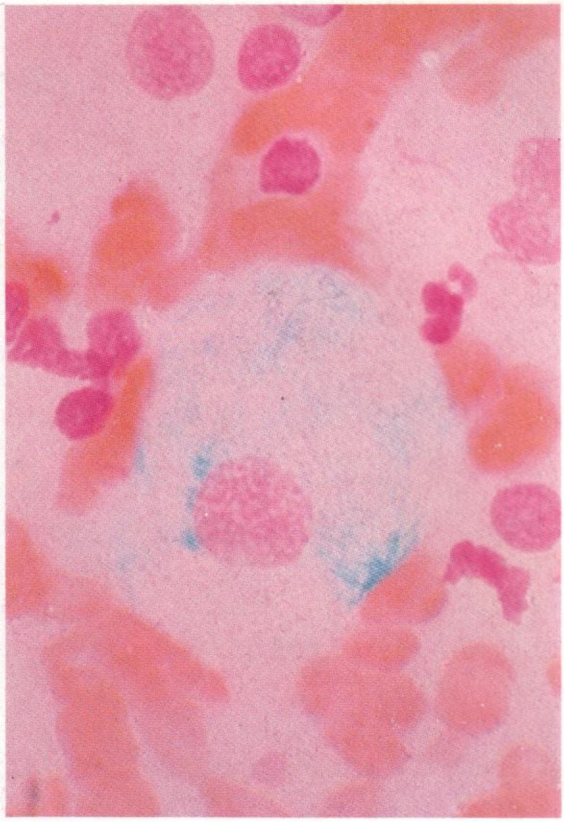

1228. Dual esterase: two neutrophil polymorphs show normal CE positivity, while the group of Gaucher cells show moderately strong BE positivity.

1229. Prussian blue reaction: the Gaucher cell in the centre of the field shows free iron staining of varied intensity in much of the cytoplasm.

1230 and **1231**. Another duplicate pair of photographs of a field showing starch-powder contamination, similar to that appearing in **1225** and **1226**. In this instance, the contamination is very much heavier and is seen in a lymph node imprint from a patient with follicular (centroblastic-centrocytic) lymphoma.

1230

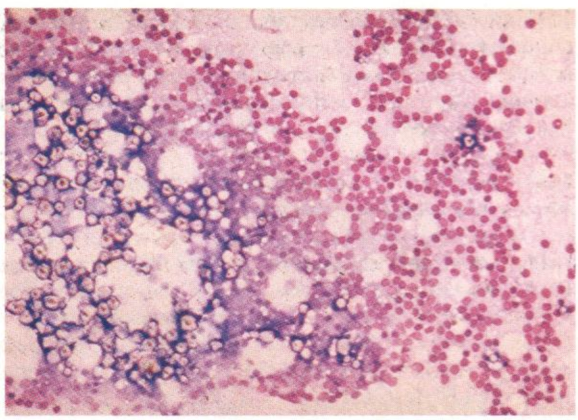

1231

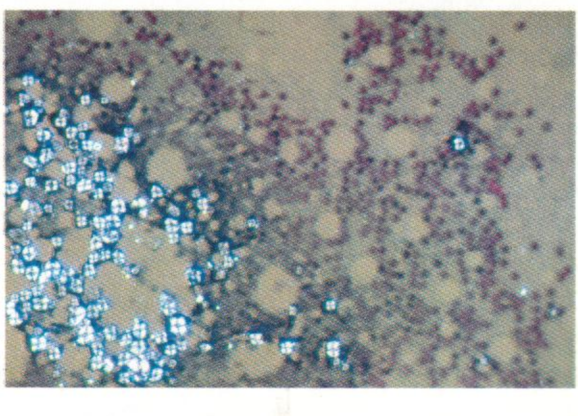

1232

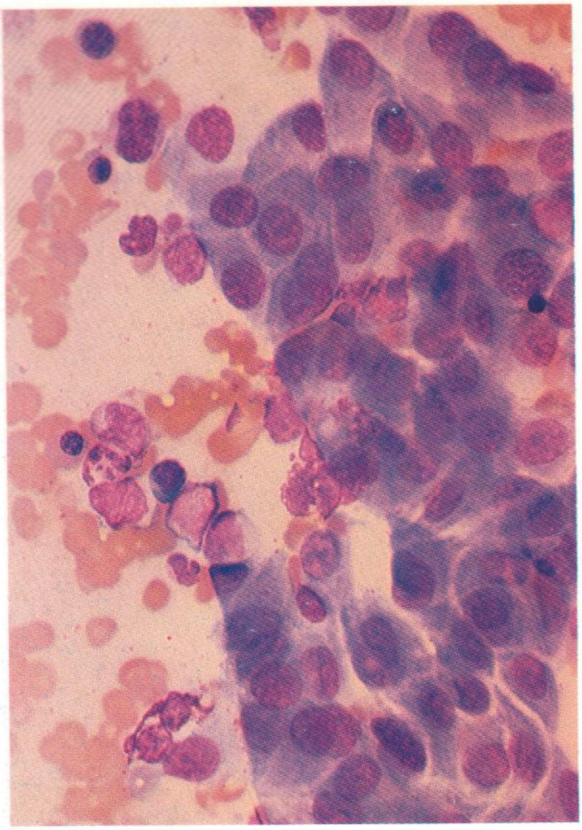

123

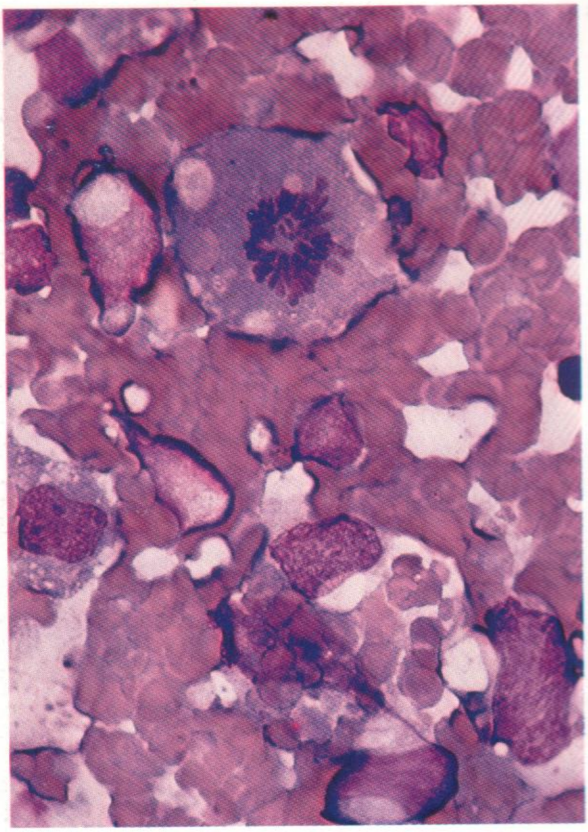

123

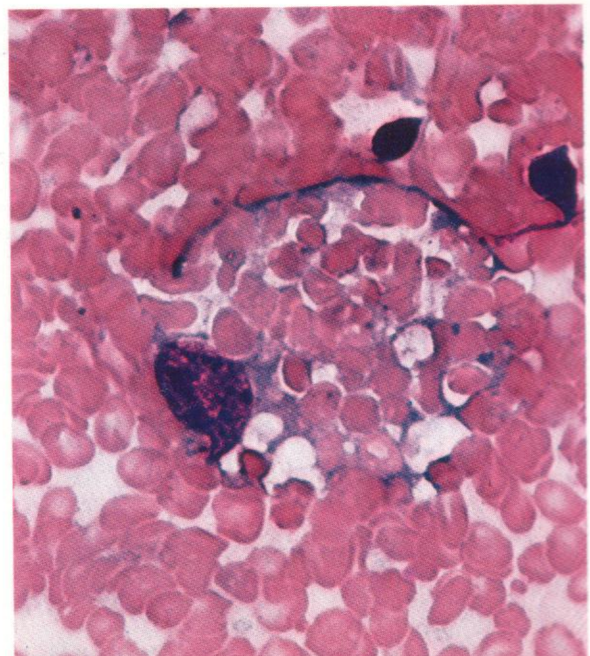

1232. A splenic puncture smear: Leishman stain. A conspicuous cluster of serosal cells, picked up as the needle traverses the peritoneal lining cells of the spleen surface. Their flat epithelial nuclear structure and lanceolate cytoplasm are very characteristic.

1233 and **1234**. Leishman stain: splenic puncture smear. Malignant histiocytosis (histiocytic medullary reticulosis), showing gross phagocytosis of red cells by malignant histiocytic RE cells. In **1233** there is a mitotic figure in one such RE cell, which also contains the remnants of some six or seven erythrocytes, while a second histiocytic RE cell contains within its cytoplasm some 20 erythrocytes. In **1234** a similar cell contains more than 30 erythrocytes.

1235

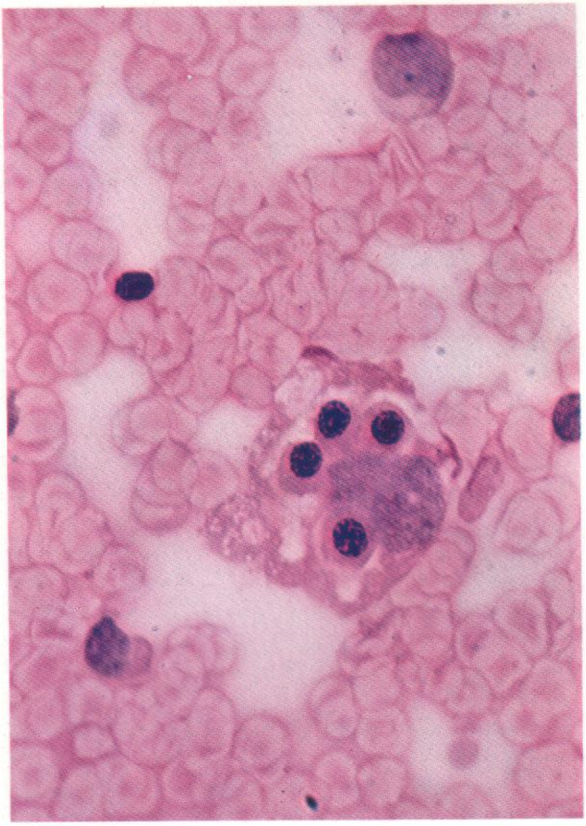

1236

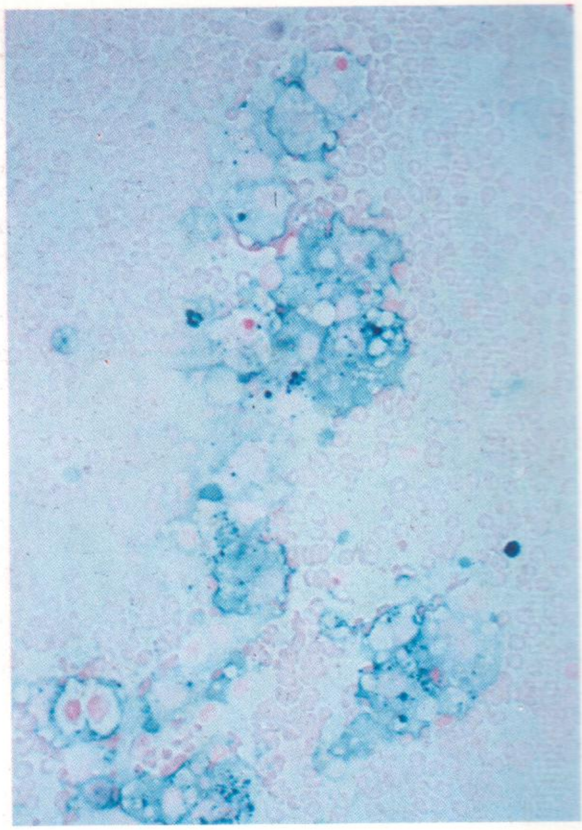

1235. PAS reaction on the same preparation as the previous two figures. The malignant histiocytic RE cell illustrated here contains four erythroblasts and shows PAS positivity in the surrounding cytoplasm.

1236 and **1237**. Prussian blue reaction on the same preparation at low and higher magnification to show the accumulation of free iron in the malignant histiocytes consequent upon the ingestion and breakdown of erythrocytes.

1237

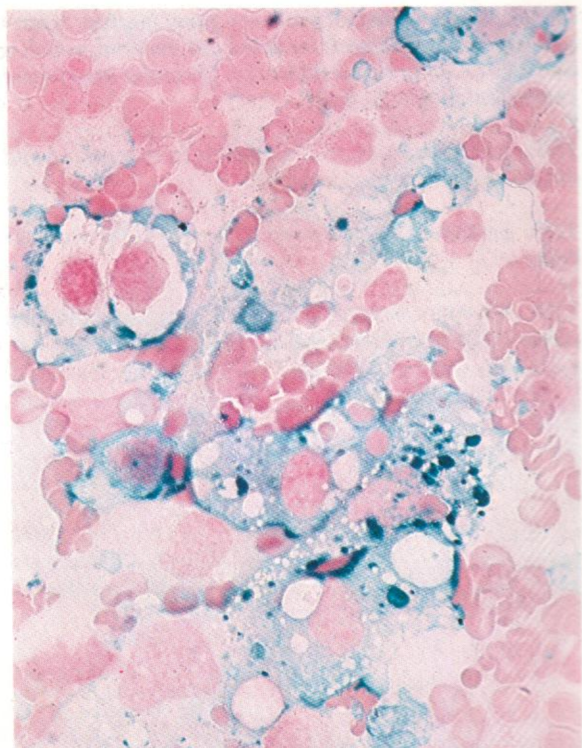

1238

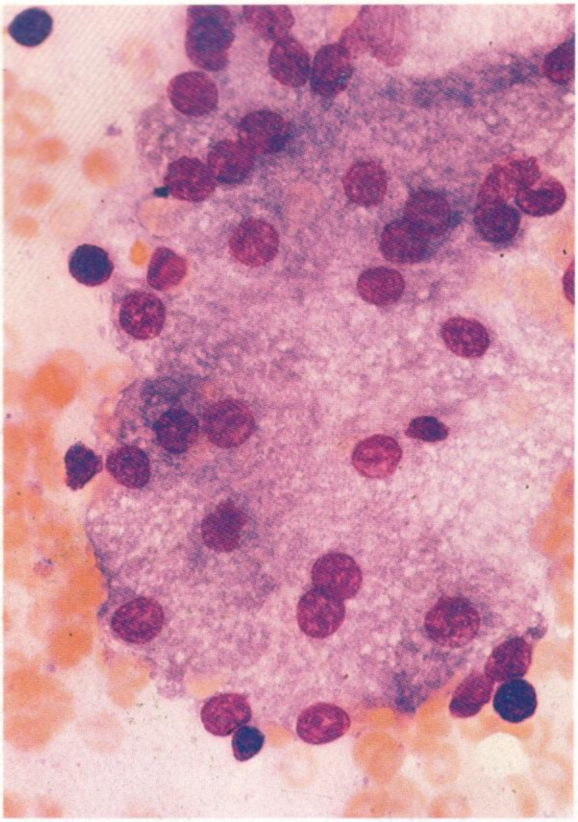

1239

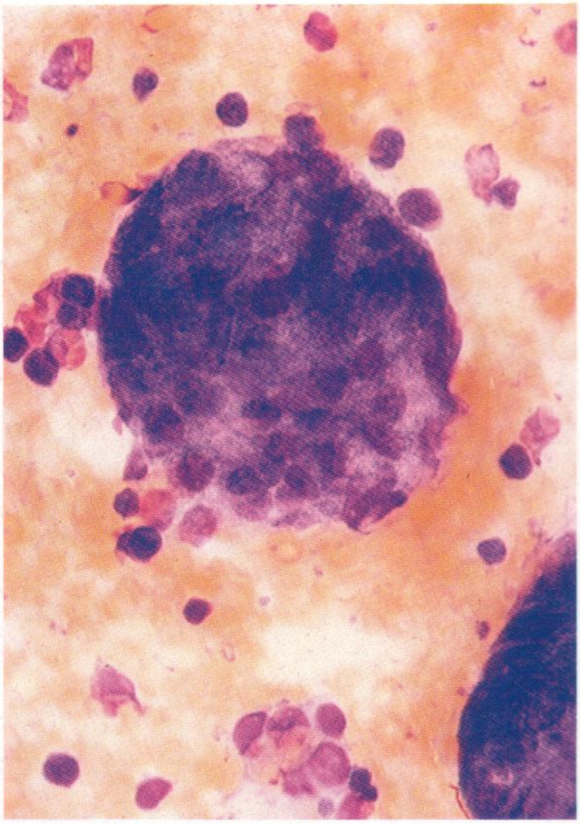

1240

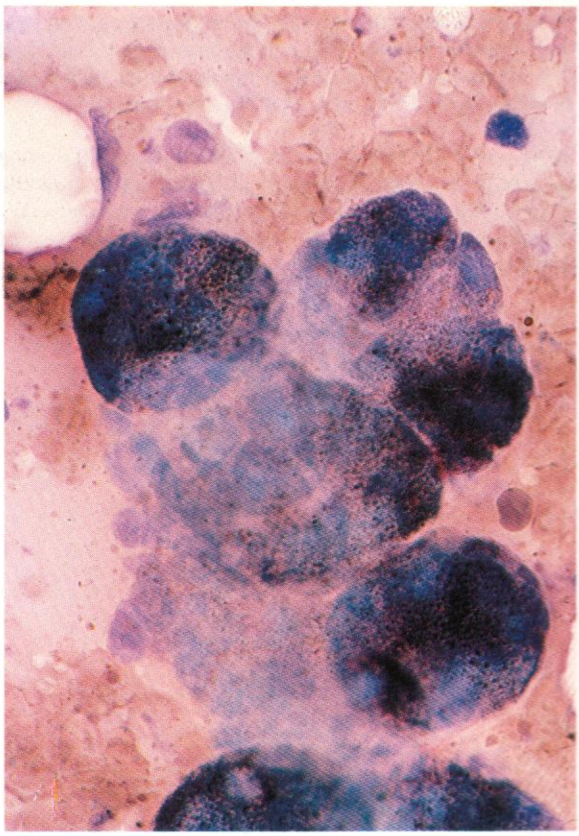

1238–1243. *Submaxillary salivary gland imprint: biopsy of a regional lymph node included this material, which is illustrated here to aid identification of similar unexpected cytological biopsy findings.*

1238. Leishman stain: clump of cells from a spread and disrupted salivary-gland acinus.

1239. Leishman stain: a more compact clump of acinar cells.

1240. SB stain: several clumps of secretory epithelial acinar cells show strong sudanophilia.

1241

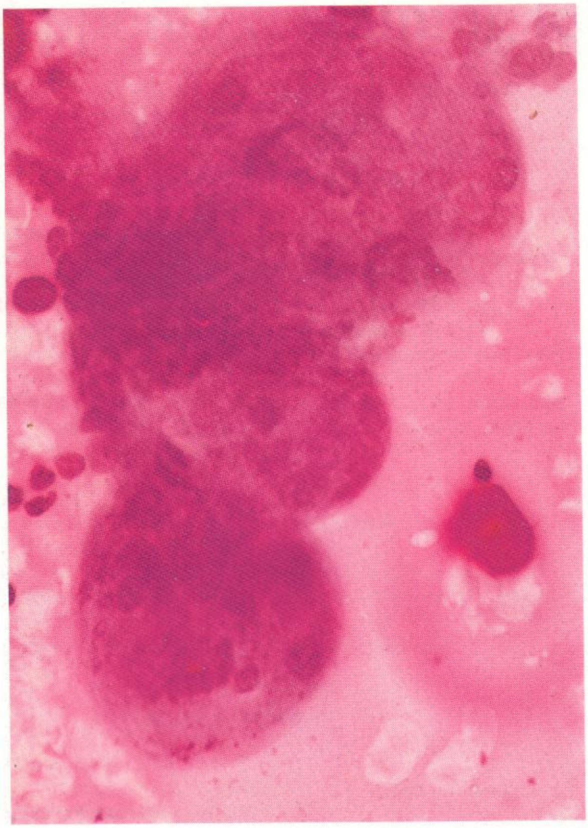

124

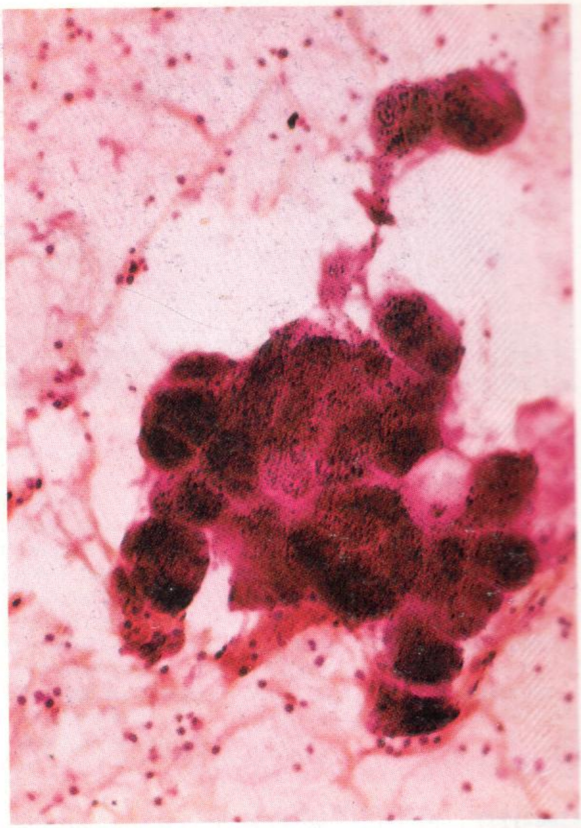

12

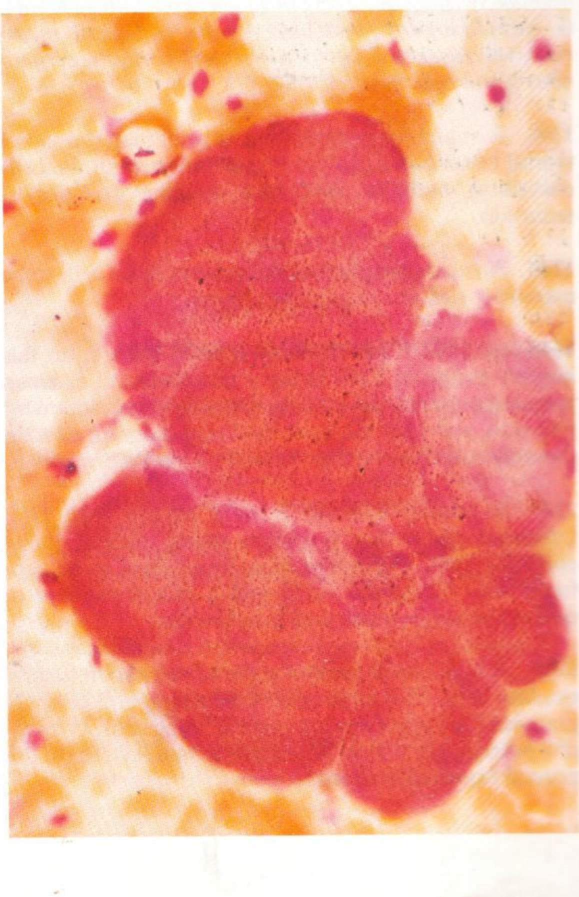

1241. PAS reaction: further acinar cell clumps showing strong PAS positivity of the mucinous secretory content. The very dense PAS-positive material near the cell clumps is starch from surgical gloves.

1242. Acid phosphatase preparation showing strong positivity. The accompanying lymphocytes give some impression of the giant size of these salivary gland cells.

1243. Dual esterase: the acinar columnar epithelial cells show scattered BE positivity.

244

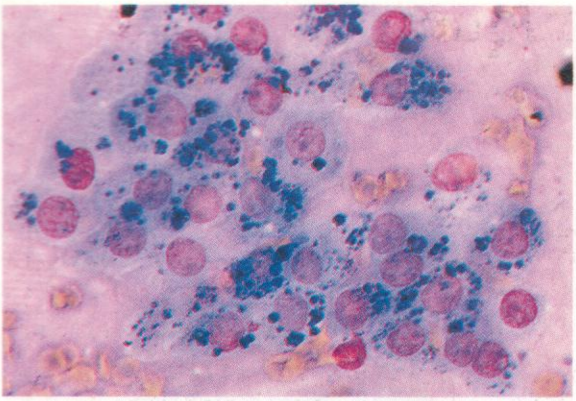

1245

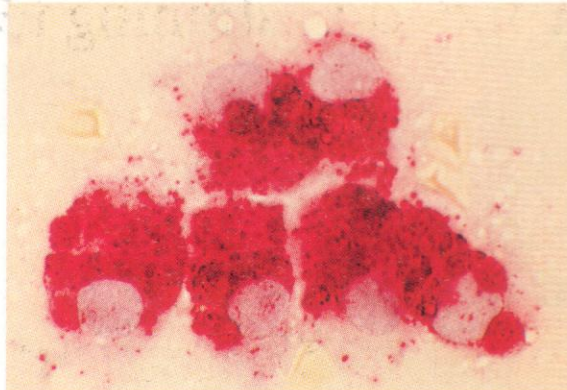

246

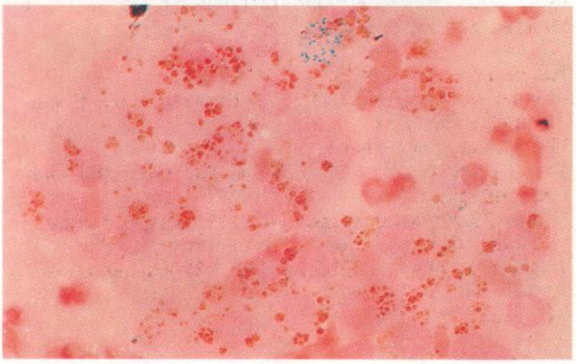

1247

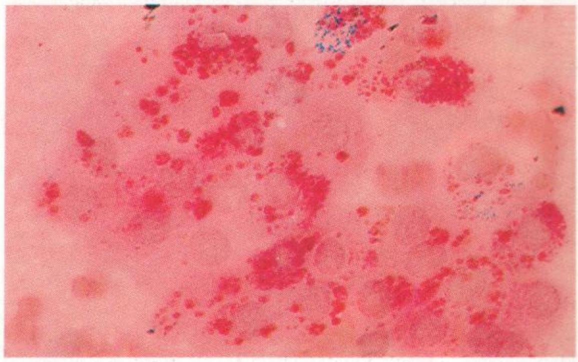

1248

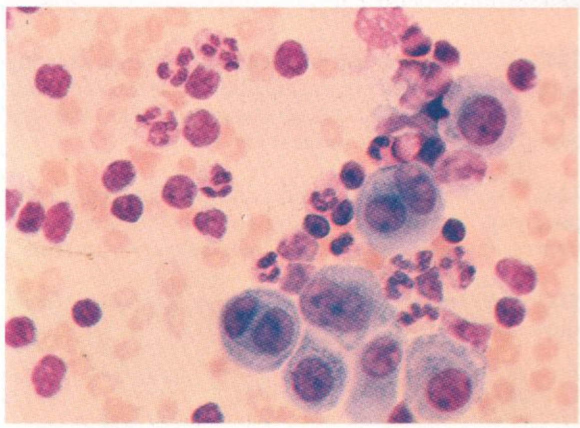

1249

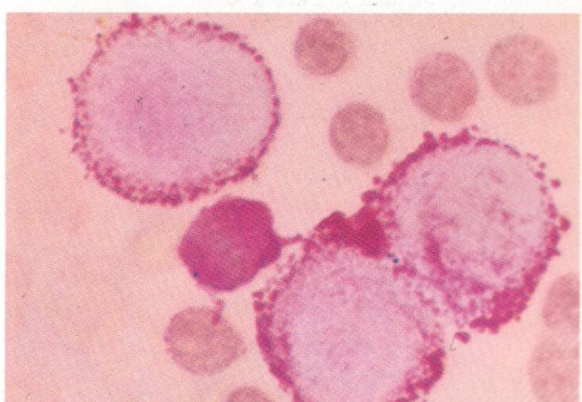

1244–1247. *Imprint preparations from a post-auricular nodular swelling occurring in a patient with t(8;21) AML in haematological remission. A local leukaemic recurrence was suspected, but biopsy revealed only the ceruminous gland cells illustrated here.*

1244. Romanowsky stain of this imprint material shows typical ceruminous glandular epithelium, with the cells containing multiple dark blue staining granules of secretion.

1245. An acid phosphatase stain shows these cells to be extremely rich in cytoplasmic enzyme.

1246 and **1247**. Consecutively stained fields from this imprint material, **1246** being a decolorized Leishman preparation restained with the Prussian blue reaction for free iron, and **1247** the same field rephotographed after the slide had been further stained by the PAS reaction.

1248. A pleural effusion from a patient with HD: Leishman stain: the specimen shows pleural lining epithelial cells, sometimes binucleated (not to be confused with Hodgkin's cells) and a mixed exudate of neutrophil polymorphs and lymphocytes.

1249. A high-power view of a PAS reaction on pleural exudate cells. The large cells with strong and coarsely granular PAS positivity are pleural lining cells. Neutrophil polymorphs and an occasional lymphocyte show the normal expected positivity.

Appendix: staining techniques

ROMANOWSKY STAINS

Purified reagent method (Heyl)

Reagents:
(a) Azure B-thiocyanate (Heyl): 1.5 g. in 200 ml. dimethyl sulphoxide (DMSO).
(b) Eosin Y (G) (Heyl): 0.5 g. in 300 ml. methanol.
(c) Stock stain: Mix (a) and (b) together. Store in dark.
(d) Buffer: 2.38 g. HEPES in 1 l. distilled water (0.01M); pH adjusted to 6.8 with 1N NaOH. Store at +4°C.
(e) Working stain: Add 3 ml. stock stain to 41.5 ml. buffer plus 2.5 ml. DMSO. Fresh working stain should be made up daily.

Technique:
1. Fix air-dried smears for 5 minutes with stock stain.
2. Rinse briefly in distilled water.
3. Cover or immerse in Coplin jar with working stain for 25 – 35 minutes (for blood or bone marrow smears, respectively).
4. Rinse in distilled water for 2 minutes and blot dry.

Leishman

Reagents:
(a) Leishman stain (dry powder): 0.15 g. in 100 ml. methanol.
(b) Phosphate buffer pH 7.2.

Technique:
1. Fix air-dried smears in undiluted Leishman for 3 minutes.
2. Dilute 1:2 with phosphate buffer for 8–10 minutes.
3. Wash in distilled water or phosphate buffer.
4. Blot dry.

N.B. 8–10 minutes staining for peripheral blood smears is quite sufficient, but bone marrow specimens require 10–20 minutes depending on the cellularity.

May–Grünwald–Giemsa

Reagents:
(a) May–Grünwald stain: Prepare 0.3% solution of powder in methanol by grinding with pestle and mortar. Filter after 2–3 days. Before use dilute 1:1 with buffer solution (phosphate buffer, pH 7.2). Diluted solution should be discarded after one day.
(b) Giemsa: Add 0.6 g. Giemsa powder to 50 ml. methanol. Shake to dissolve. Add 25 ml. glycerine. Filter after 2–3 days. Before use dilute 10 ml. stock solution with 90 ml. of phosphate buffer (pH 7.2).

Technique:
Air-dried smears of blood or bone marrow are used. Coplin jars are used throughout.
1. Fix 15 minutes in methanol.
2. Transfer without blotting to diluted May-Grünwald solution: 15 minutes.
3. Drain off stain on filter paper without blotting and transfer to diluted Giemsa solution for 30 minutes.
4. Transfer to phosphate buffer (pH 7.2) and agitate for 10–20 seconds.
5. Remove and blot dry.

FREE IRON STAIN

(after MacFadzean and Davis, 1947)

1. Fix air-dried smears in formalin vapour for 30 minutes.
2. Wash in distilled water for 2 minutes.
3. Immerse in Coplin jar containing equal parts 2% potassium ferrocyanide (Prussian blue) and 2% dilution of pure (37%) hydrochloric acid for 1 hour.
4. Rinse with distilled water.
5. Counterstain with 0.1% nuclear fast red made up in 5% aluminium sulphate solution for 30 minutes.

Staining jars must be iron-free.

SUDAN BLACK B

(after Sheehan and Storey, 1947)

Reagents:
(a) Sudan black B (SB) (Gurr): 0.3 g. in 100 ml. absolute ethanol.
(b) Buffer: Dissolve 16 g. crystalline phenol in 30 ml. absolute ethanol. Add to 100 ml. distilled water in which 0.3 g. hydrated disodium hydrogen phosphate ($Na_2HPO_4 + 12H_2O$) has been dissolved.
(c) Working stain: add 40 ml. buffer to 60 ml. SB solution and filter by suction. Keeps 2–3 months. Store in refrigerator.

Technique:
*1. Fix air-dried smears in formalin vapour for 5–10 minutes.
2. Wash briefly in distilled water and blot dry.
3. Immerse in working stain for 1 hour.
4. Wash off with 70% ethanol.
5. Counterstain with Leishman or MGG.

**40% w/v formaldehyde saturated filter paper in bottom of Coplin jar.*

PAS REACTION

(modified from McManus, 1946)

Reagents:

(a) Periodic acid solution: Dissolve 5 g. periodic acid crystals in 500 ml. distilled water. Store in dark bottle. Keeps for 3 months.

(b) Basic fuchsin: Dissolve 5 g. basic fuchsin in 500 ml. hot distilled water. Filter when cool. Saturate with SO_2 gas by bubbling for 1 hour. Shake with 2 g. activated charcoal in conical flask for few minutes until just clear and filter immediately through Whatman No. 1 filter into a dark bottle. Charcoal extraction should be done in fume cupboard. Solution keeps for 3–6 months depending on how often used.

Technique:

1. Fix air-dried smears for 10 minutes in 10 ml. 40% formalin and 90 ml. ethanol solution.
2. Wash briefly in tap water.
3. Treat with periodic acid solution for 10 minutes.
4. Wash in distilled water and blot dry.
5. Immerse in Schiff's basic fuchsin in Coplin jar for 30 minutes. (Return fuchsin solution to stock bottle immediately after use.)
6. Wash in tap water for 5–10 minutes.
7. Counterstain with aqueous haematoxylin for 10–15 minutes.

   Control smears are exposed to salivary digestion for 30 minutes between stages 2 and 3.

ALKALINE PHOSPHATASE

Reagents:

(a) Stock propanediol buffer, 0.2M: Dissolve 10.5 g. 2-amino-2-methyl propane-(1:3)-diol in 500 ml. distilled water. Store at 4°C; discard after 3 months.

(b) Working buffer, 0.05M: Mix 25 ml. stock buffer with 5 ml. 0.1N HCl and make up to 100 ml. with distilled water.

(c) Substrate, to be made up freshly immediately before use:
Sodium alpha-naphthyl phosphate: 35 mg.
Fast Garnet GBC salt: 35 mg.
Working buffer: 35 ml.

(d) Methyl green: 2% in distilled water, freed from contamination with methyl violet by extraction with chloroform and kept free by storage at room temperature in continuous contact with chloroform.

Technique:

1. Fix air-dried smears in 10% formalin in absolute methanol for 30 seconds (use stopwatch) at 0–5°C.
2. Pour freshly prepared substrate directly on to slides and incubate for 5–10 minutes at room temperature. Substrate must be used within 5 minutes of preparation.
3. Rinse slides in tap water for 10–15 seconds.
4. Counterstain with methyl green for 10–15 seconds.

   Good positive controls are provided by slides from polycythaemia, infection, hairy cell leukaemia or Hodgkin's disease.

PEROXIDASE

Modified Graham-Knoll technique

1. Fix air-dried smears for *30 seconds* (use stopwatch) in 10 ml. 40% formalin and 90 ml. ethanol solution at room temperature.
2. Wash with tap water for 10 seconds and blot dry.
3. Dissolve approx. 250 mg. of benzidine or o-tolidine* in 6 ml. ethanol and dilute with 4 ml. distilled water. Add 0.02 ml. hydrogen peroxide (20 vol.). When solution is complete, pour onto slide without filtration and allow to react for 7 minutes.
4. Wash with tap water for 10 seconds and allow to dry in air.
5. Counterstain with Leishman, diluted immediately with buffer, or use standard May-Grünwald-Giemsa technique for counterstaining.

**N.B. Both these compounds are carcinogenic and should be handled with care.*

Diaminobenzidine (DAB) method for peroxidase

Reagents:

(a) Fixative: Buffered formol acetone (BFA) – Na_2HPO_4 40 mg., KH_2PO_4 200 mg., acetone 90 ml., concentrated formalin 50 ml., distilled water 60 ml. Store at 4°C and use cold for fixation.

(b) Stock phosphate buffer: Dulbecco A, pH 7.3 – NaCl 40 g., KCl 1 g., anhydrous Na_2HPO_4 5.75 g., KH_2PO_4 1 g., distilled water 1 l.

(c) Working buffer: Dilute 1 l. stock buffer with 4 l. distilled water.

(d) Substrate: 3,3′diaminobenzidine (DAB).

(e) Hydrogen peroxide (100 vol.).

(f) Working incubation solution: Dissolve 30 mg. DAB in 60 ml. working buffer and add 120 l. of 100 vol. H_2O_2; use immediately.

(g) Carazzi's aqueous haematoxylin: Dissolve 75 g. potassium aluminium sulphate in 1200 ml. warm distilled water; add 1.5 g. haematoxylin powder dissolved in 300 ml. glycerol by grinding with pestle and mortar; dissolve 0.3 g. sodium iodate in a little water and add gradually.

Technique:

1. Fix air-dried smears in BFA for 45 seconds.
2. Rinse with distilled water and drain dry.
3. Incubate in working substrate solution for 10 minutes.
4. Rinse with distilled water.
5. Counterstain with Carazzi's (or other water-soluble) haematoxylin for 1 minute.
6. Rinse with distilled water and air-dry.

ACID PHOSPHATASE

Reagents:

(a) Naphthol AS-BI phosphoric acid: 10 mg.

(b) Fast garnet GBC salt (Gurr): 10 mg.

(c) Walpole's acetate buffer, 0.1M, pH 5.0: 50 ml.

(d) Filter freshly prepared substrate into Coplin jar.

Technique:

1. Fix air-dried smears in formalin vapour for 4 minutes.
2. Wash briefly in tap water and blot dry.
3. Incubate in substrate solution at 37°C for 1–1½ hours.
4. Wash briefly in tap water.
5. Counterstain with aqueous haematoxylin for 10–15 minutes.

   For assessment of tartrate resistance add 100 mg. L(+) tartaric acid to the substrate.

DUAL ESTERASE

Reagents:

(a) Chloroacetate substrate solution: use at once 0.1M phosphate buffer (pH 8.0): 10 ml.
Alpha-naphthol AS-D chloroacetate: 0.25 mg. (0.7×10^{-4}M) in 0.1 ml. acetone.
Fast blue BB salt: 15 mg. (5×10^{-3}M).

(b) Butyrate substrate solution: use at once 0.1M phosphate buffer (pH 8.0): 10 ml.
Alpha-naphthyl butyrate: 0.5 mg. (2.33×10^{-4}M).
Fast garnet GBC salt: 3 mg. (9×10^{-4}M).
For testing fluoride inhibition, add NaF 1.5 mg./ml. to buffer.

Technique:

1. Fix air-dried smears in formalin vapour for 4 minutes.
2. Wash briefly in distilled water and blot dry.
3. Incubate in freshly prepared chloroacetate substrate solution for 5–15 minutes at room temperature.
4. Wash briefly in distilled water and blot dry.
5. Incubate in freshly prepared butyrate substrate solution for 15–30 minutes, at room temperature and away from light.
6. Wash briefly in distilled water.
7. Counterstain in aqueous haematoxylin for 5 minutes.
8. Wash in distilled water, blot dry and examine.

IMMUNOCYTOCHEMICAL METHODS

Immunoperoxidase – indirect PAP (peroxidase–antiperoxidase) method

Reagents:

(a) Specific primary antibodies, e.g. rabbit anti-human Ig antisera, specific for the different heavy and light chains; mouse monoclonal antibodies.

(b) Appropriate secondary antibodies, e.g. swine anti-rabbit immunoglobulin; goat anti-mouse immunoglobulin.

(c) Appropriate rabbit or mouse antiperoxidase–peroxidase complex.

(d) DAB peroxidase cytochemical reagents. A solution of 5 mg. DAB in 10 ml. tris-saline solution plus 1 drop of 100 vol. hydrogen peroxide is freshly prepared and filtered before use.

Technique:

1. Fix air-dried smears in methanol for 10 minutes to block endogenous peroxidase.
2. Add primary antibody and incubate for 15–30 minutes. A titration effect may be achieved by using concentrations ranging from 1 in 20 to 1 in 500.
3. Wash in tris-saline solution for 5 minutes.
4. Add secondary antibody at 1 in 20 to 1 in 100 for 15–30 minutes.
5. Wash as in 3.
6. Add PAP complex 1 in 20 to 1 in 40 for 15–30 minutes.
7. Wash as in 3.
8. Add DAB substrate and incubate for 10 minutes.
9. Counterstain with aqueous haematoxylin 1 minute, rinse and blot dry.

Immunoalkaline phosphatase – indirect alkaline phosphatase–anti-alkaline phosphatase (APAAP) method

Reagents:

(a) Primary antibodies – any murine monoclonal, for example.

(b) Appropriate secondary antibodies – anti-mouse immunoglobulin in this case.

(c) APAAP complex, consisting of alkaline phosphatase and mouse monoclonal antibody specific for alkaline phosphatase.

(d) Incubation medium for alkaline phosphatase. 2 mg. of naphthol AS-BI (or AS-MX) phosphate are dissolved in 0.2 ml. of N,N-dimethylformamide, to which 9.8 ml. 0.1M Tris-HC1 buffer, pH 8.2, are added. Immediately before use, add 10 mg. Fast Red TR salt (or another suitable diazonium salt) and filter directly on to slides.

When necessary, endogenous alkaline phosphatase activity can be inhibited by adding 0.24 mg./ml. (1 mmol./l.) levamisole to buffer.

Technique for smears and imprints:

1. Fix air-dried smears in buffered formalin-acetone (Na_2HPO_4 20 mg., KH_2PO_4 100 mg., acetone 45 ml., concentrated formalin 25 ml., distilled water 30 ml.) for 30 seconds at room temperature, wash briefly in distilled water and allow to dry.
2. Immerse in Tris-buffered saline (TBS) for 10 minutes, then tip off excess.
3. Add primary mouse monoclonal antibody and incubate in moist chamber for 30 minutes at room temperature. Optimal dilution of MAb in TBS has to be selected for individual MAbs.
4. Wash slides in TBS with three changes, 3 minutes each.
5. Add anti-mouse Ig, diluted 1:25 in TBS, for 15–30 minutes.
6. Wash as in 4 above.
7. Add APAAP complex, diluted 1:50 in TBS, for 15–30 minutes.
8. Wash as in 4 above. Intensity of final staining may be increased by repeating steps 5–8, with reduced incubation times.
9. Add freshly prepared alkaline phosphatase incubation medium for 15–30 minutes.
10. Wash briefly in tap water, rinse in distilled water and allow to dry.
11. Counterstain with haematoxylin for 2 minutes.
12. Mount slides in an aqueous medium such as glycerine jelly or in DPX.

Index

Numbers in light type refer to page numbers in text, those in **bold** to picture and caption numbers.